

Emmanuel N. Saridakis · Ruth Lazkoz ·
Vincenzo Salzano · Paulo Vargas Moniz ·
Salvatore Capozziello · Jose Beltrán Jiménez ·
Mariafelicia De Laurentis · Gonzalo J. Olmo *Editors*

Modified Gravity and Cosmology

An Update by the CANTATA Network

 Springer

Modified Gravity and Cosmology

Emmanuel N. Saridakis · Ruth Lazkoz ·
Vincenzo Salzano · Paulo Vargas Moniz ·
Salvatore Capozziello · Jose Beltrán Jiménez ·
Mariafelicia De Laurentis · Gonzalo J. Olmo
Editors

Modified Gravity and Cosmology

An Update by the CANTATA Network

 Springer

Editors

Emmanuel N. Saridakis
National Observatory of Athens
Athens, Greece

Ruth Lazkoz
University of the Basque Country
Leioa, Spain

Vincenzo Salzano
Institute of Physics, University of Szczecin
Szczecin, Poland

Paulo Vargas Moniz
University of Beira Interior
Covilhã, Portugal

Salvatore Capozziello
Università di Napoli Federico II
Napoli, Italy

Jose Beltrán Jiménez
University of Salamanca
Salamanca, Spain

Mariafelicia De Laurentis
University of Naples Federico II
Napoli, Italy

Gonzalo J. Olmo
University of Valencia
Burjassot, Valencia, Spain

ISBN 978-3-030-83714-3

ISBN 978-3-030-83715-0 (eBook)

<https://doi.org/10.1007/978-3-030-83715-0>

© The Editor(s) (if applicable) and The Author(s), under exclusive license to Springer Nature Switzerland AG 2021, corrected publication 2022

This work is subject to copyright. All rights are solely and exclusively licensed by the Publisher, whether the whole or part of the material is concerned, specifically the rights of translation, reprinting, reuse of illustrations, recitation, broadcasting, reproduction on microfilms or in any other physical way, and transmission or information storage and retrieval, electronic adaptation, computer software, or by similar or dissimilar methodology now known or hereafter developed.

The use of general descriptive names, registered names, trademarks, service marks, etc. in this publication does not imply, even in the absence of a specific statement, that such names are exempt from the relevant protective laws and regulations and therefore free for general use.

The publisher, the authors and the editors are safe to assume that the advice and information in this book are believed to be true and accurate at the date of publication. Neither the publisher nor the authors or the editors give a warranty, expressed or implied, with respect to the material contained herein or for any errors or omissions that may have been made. The publisher remains neutral with regard to jurisdictional claims in published maps and institutional affiliations.

This Springer imprint is published by the registered company Springer Nature Switzerland AG
The registered company address is: Gewerbestrasse 11, 6330 Cham, Switzerland

Preface

The dawn of the twenty-first century came with very positive prospects for gravity, cosmology, and astrophysics. Technological progress made it possible for cosmology to enter to its adulthood and become a precision science, both for its own sake and for being the laboratory of gravity, which can now be accurately tested and investigated in scales different from the earth ones. As a result, the opinion that cosmology is one of the main directions that will lead to progress in physics in the near future is now well established.

“Cosmology and Astrophysics Network for Theoretical Advances and Training Actions” (CANTATA) is a COST European Action established in 2015 in order to contribute to the front of research in the fields of gravity, cosmology, and astrophysics. It involves Institutions from 26 European countries, as well as from 5 countries abroad. CANTATA Collaboration has a variety of interests, which include: (i) the classification and definition of theoretical and phenomenological aspects of gravitational interaction that cannot be enclosed in the standard lore scheme but might be considered as signs of alternative theories of gravity, (ii) the confrontation of the theoretical predictions with observations at both the background and the perturbation levels, (iii) the production of numerical codes to simulate astrophysical and cosmological phenomena, (iv) the construction of self-consistent models at various scales and the investigation of the features capable of confirming or ruling out an effective theory of gravity, and (v) the study of how extended and modified theories of gravity emerge from quantum field theory and how mechanisms produced by the latter may explain cosmological dynamics.

General Relativity and the Λ CDM framework are currently the standard lore and constitute the concordance paradigm. Nevertheless, long-standing open theoretical issues, as well as possible new observational ones arising from the explosive development of cosmology the last two decades, offer the motivation and lead a large amount of research to be devoted in constructing various extensions and modifications.

All extended theories and scenarios are first examined under the light of theoretical consistency, and then are applied to various geometrical backgrounds, such as the cosmological and the spherical symmetric ones. Their predictions at both the

background and perturbation levels, and concerning cosmology at early, intermediate, and late times, are then confronted with the huge amount of observational data that astrophysics and cosmology are able to offer recently. Theories, scenarios, and models that successfully and efficiently pass the above steps are classified as viable and are candidates for the description of Nature.

This work is a review of the recent developments in the fields of gravity and cosmology, presenting the state of the art, highlighting the open problems, and outlining the directions of future research. Its realization was performed in the framework of the CANTATA COST Action.

Athens, Greece
Leioa, Spain
Szczecin, Poland
Covilhã, Portugal
Napoli, Italy
Salamanca, Spain
Napoli, Italy
Burjassot, Spain

Emmanuel N. Saridakis
Ruth Lazkoz
Vincenzo Salzano
Paulo Vargas Moniz
Salvatore Capozziello
Jose Beltrán Jiménez
Mariafelicia De Laurentis
Gonzalo J. Olmo

The original version of the book was revised: The affiliations of the authors Álvaro de la Cruz-Dombriz in chapter 5, Francisco S. N. Lobo in chapter 13 and Sebastian Bahamonde, Konstantinos F. Dialektopoulos, Manuel Hohmann, Jackson Levi Said in chapter 14 have been updated. The incorrect equation (9.13) in chapter 9 has also been updated. Error in reference linking have been corrected in all the chapters. The correction to the book is available at https://doi.org/10.1007/978-3-030-83715-0_39

Acknowledgements

This publication is supported by COST (European Cooperation in Science and Technology) and is based on work from CANTATA COST action CA15117, EU Framework Programme Horizon 2020.

Y. A. is supported by LabEx ENS-ICFP: ANR-10-LABX-0010/ANR-10-IDEX-0001-02 PSL*.

J. B. J. would like to thank David Figueruelo, for his help in compiling and unifying parts of the manuscript.

J. L. B-S, B. K., and J. K. gratefully acknowledge support by the DFG Research Training Group 1620 *Models of Gravity* and the COST Action CA16104. JLBS would like to acknowledge support from the DFG project BL 1553, and the FCT projects PTDC/FISOUT/28407/2017 and PTDC/FIS-AST/3041/2020.

M. B. L.'s work is supported by the Basque Foundation of Science Ikerbasque. She also would like to acknowledge the partial support from the Basque government Grant No. IT956-16 (Spain) and from the project FIS2017-85076-P (MINECO/AEI/FEDER, UE).

G.C. thanks M. Maggiore for useful feedback; his work is supported by the I+D grant FIS2017-86497-C2-2-P of the Spanish Ministry of Science, Innovation and Universities.

J. A. R. C. acknowledges financial support from the MINECO (Spain) Projects No. FIS2016-78859-P (AEI/ FEDER) and No. PID2019-107394GB-I00.

A. d. l. C.-D. acknowledges financial support from NRF Grants No.120390, Reference: BSFP190-416431035, No.120396, Reference: CSRP190405427545, and No 101775, Reference: SFH1507-27131568; Project No. FPA2014-53375-C2-1-P from the Spanish Ministry of Economy and Science, MICINN Project No. PID2019-108655GB-I00, Project No. FIS2016-78859-P from the European Regional Development Fund and Spanish Research Agency (AEI).

A.-C. D. is supported by a Ph.D. contract of the program *FPU 2015* (Spanish Ministry of Economy and Competitiveness) with reference FPU15/05406, and acknowledges further support from the Spanish project No. FIS2017-84440-C2-1-P (MINECO/FEDER,EU), i-LINK1215 (CSIC), and the projects SEJI/2017/042 and PROMETEO/2020/079 (Generalitat Valenciana).

J. M. E. is grateful to M. Zumalacárregui, J. Beltrán, L. Heisenberg, and J. García-Bellido for fruitful discussions and collaborations on topics covered in this contribution; he has been supported by the Spanish FPU Grant No. FPU14/01618, the Research Project FPA2015-68048-03-3P (MINECO-FEDER), and the Centro de Excelencia Severo Ochoa Program SEV- 2016-0597, by NASA through the NASA Hubble Fellowship grant HST-HF2-51435.001-A awarded by the Space Telescope Science Institute, which is operated by the Association of Universities for Research in Astronomy, Inc., for NASA, under contract NAS5-26555, and by the Kavli Institute for Cosmological Physics through an endowment from the Kavli Foundation and its founder Fred Kavli.

N. F. and S. P. thank Louis Perenon for useful discussions; the research of NF is supported by Fundação para a Ciência e a Tecnologia (FCT) through national funds (UID/FIS/04434/2013), by FEDER through COMPETE2020 (POCI-01-0145-FEDER-007672) and by FCT project “DarkRipple—Spacetime ripples in the dark gravitational Universe” with ref. number PTDC/FIS-OUT/29048/2017, and S. P. acknowledges support from the NWO and the Dutch Ministry of Education, Culture and Science (OCW), and also from the D-ITP consortium, a program of the NWO that is funded by the OCW.

L. Á. G. is grateful to Cecília Nagy for generating the figure, to Roberto Casadio for discussions and to David Hobill for collaboration in the subject over many years; he was supported by the Hungarian National Research Development and Innovation Office (NKFIH) in the form of the Grant No. 123996.

L. K. and L. P. thank Levon Pogolian, Alex Zucca, Savvas Nesseris, and George Alestas for their help with the MGCAMB and MGCOSMOMC packages; all the runs were performed in the Hydra Cluster of the Institute of Theoretical Physics (IFT) in Madrid, their research is co-financed by Greece and the European Union (European Social Fund-ESF) through the Operational Programme “Human Resources Development, Education and Lifelong Learning” in the context of the project “Strengthening Human Resources Research Potential via Doctorate Research” (MIS-5000432), implemented by the State Scholarships Foundation (IKY).

J. P. M. and F. S. N. L. acknowledge funding from the Fundação para a Ciência e a Tecnologia (FCT, Portugal) research projects No. UID/FIS/04434/2020, No. PTDC/FIS-OUT/29048/2017, and No. CERN/FIS-PAR/0037/2019; F. S. N. L. additionally acknowledges support from the FCT Scientific Employment Stimulus contract with reference CEECIND/04057/2017.

P. M. M. acknowledges financial support from the project FIS2016-78859-P (AEI/FEDER, UE).

M. M. has received the support of a fellowship from “la Caixa” Foundation (ID 100010434), with fellowship code LCF/BQ/PI19/11690015.

D. F. M. thanks M. Gronke, R. Hagala, A. Hammami, C. Llineares, M. Lima, R. Voivodic, and H. Winther whose collaborations resulted in the articles which this review is based on; his work was partially supported by the Research Council of Norway and the simulations were performed in NOTUR.

G. J. O. is supported by the Spanish project FIS2017-84440-C2-1-P (MINECO/FEDER, EU), the project H2020-MSCA-RISE-2017 Grant FunFiCO-777740, the project PROMETEO/2020/079 (Generalitat Valenciana), and the Edital 006/2018 PRONEX (FAPESQ-PB/CNPQ, Brazil, Grant 0015/2019).

V. P. and A. S. thank Jean-Luc Starck for useful comments.

D. R. G. is funded by the *Atracción de Talento Investigador* programme of the Comunidad de Madrid (Spain) No. 2018-T1/TIC-10431, and acknowledges further support from the Ministerior de Ciencia, Innovación y Universidades (Spain) project No. PID2019-108485GB-I00/AEI/10.13039/501100011033, the FCT projects No. PTDC/FIS-PAR/31938/2017 and PTDC/FIS-OUT/29048/2017, the Spanish project No. FIS2017-84440-C2-1-P (MINECO/FEDER, EU), the project PROMETEO/2020/079 (Generalitat Valenciana), and the Edital 006/2018 PRONEX (FAPESQ-PB/CNPQ, Brazil) Grant No. 0015/2019.

E. N. S is supported in part by the USTC Fellowship for international professors.

I. S. is partially supported by a 2019 “Research and Education” grant from Fondazione CRT. The OAVdA is managed by the Fondazione Clément Fillietroz-ONLUS, which is supported by the Regional Government of the Aosta Valley, the Town Municipality of Nus, and the “Unité des Communes valdôtaines Mont-Émilis”. I. D. S. is funded by European Structural and Investment Funds and the Czech Ministry of Education, Youth and Sports (Project CoGraDS—CZ.02.1.01/0.0/0.0/15003/0000437).

A. W. is supported by the EU through the European Regional Development Fund CoE program TK133 “The Dark Side of the Universe”.

Contents

1	Cosmophysics of Modified Gravity	1
	Ruth Lazkoz	
1.1	Breaking Scientific and Geographic Boundaries Through the Physics of Gravitation During a Societal Plight	1
	References	16
2	General Relativity	17
	José Pedro Mimoso	
	References	24
3	Foundations of Gravity—Modifications and Extensions	27
	Christian G. Böhmer	
3.1	Preliminaries	27
3.2	Matter Couplings	30
3.3	The Einstein–Hilbert Action—Linear Extensions	31
3.4	The Einstein–Hilbert Action—Nonlinear Extensions	35
	References	37
Part I Theories of Gravity		
4	Introduction to Part I	41
	Salvatore Capozziello and Jose Beltrán Jiménez	
5	A Flavour on $f(R)$ Theories: Theory and Observations	43
	Álvaro de la Cruz-Dombriz	
5.1	Historia, Lux Veritatis	43
5.2	Scalar-Tensor Theories	45
	5.2.1 Field Equations of Scalar-Tensor Gravity	46
	5.2.2 Brans–Dicke Theory	47
5.3	Introduction to $f(R)$ Gravity	48
	5.3.1 $f(R)$ Formalisms	50
	5.3.2 $f(R)$ Gravity From a Scalar-Tensor Perspective	52
	5.3.3 Viability	54

5.4	Background Cosmology in the Metric Formulation	59
5.5	Scalar Perturbations: The 1 + 3 Formalism	61
5.5.1	Fluid Sources	62
5.5.2	Geometry	63
5.5.3	Propagation and Constraint Equations	65
5.6	Geodesic Deviation in $f(R)$ Gravity	68
5.6.1	Formalism	68
5.6.2	Past-Directed Null Geodesics and Area Distance in $f(R)$ Gravity	70
5.7	Gravitational Attractiveness in $f(R)$?	71
5.8	Conclusions	73
	References	75
6	Horndeski/Galileon Theories	79
	Prado Martín-Moruno	
6.1	From Brans–Dicke to Horndeski	79
6.2	Background Cosmology	81
6.3	Cosmological Perturbations	84
6.4	Gravitational Waves Constraints	85
	References	86
7	Massive Gravity and Bigravity	89
	Lavinia Heisenberg	
7.1	Massive and Bimetric Gravity	90
7.2	Cosmological Applications	93
	References	94
8	Gravity in Extra Dimensions	97
	Jose A. R. Cembranos	
8.1	Kaluza-Klein Model	97
8.2	Large Extra Dimensions	98
8.2.1	Brane Worlds	98
8.2.2	Universal Extra Dimensions	102
8.2.3	Mixed Models	103
	References	104
9	Non-local Gravity	109
	Gianluca Calcagni	
9.1	UV Nonlocal Gravity	110
9.1.1	Singularity Problem	112
9.1.2	Inflation	114
9.1.3	Dark Energy	115
9.1.4	Gravitational Waves	115
9.2	IR Nonlocal Gravity	117
9.2.1	Singularity Problem	119
9.2.2	Inflation	120
9.2.3	Dark Energy	120

9.2.4	Gravitational Waves	121
	References	121
10	Metric-Affine Gravity	129
	Damianos Iosifidis and Emmanuel N. Saridakis	
10.1	Geometrical Objects: Torsion, Curvature and Non-metricity	130
10.2	Geometrical Meaning of Torsion and Non-metricity	133
10.2.1	Geometrical Meaning of Torsion	133
10.2.2	Geometrical Meaning of Non-metricity	134
10.3	Identities of Non-Riemannian Geometry	135
10.3.1	The Sources of Metric-Affine Gravity	137
10.4	Field Equations of Metric-Affine Gravity	137
10.5	The Differential Form Formulation of Metric-Affine Gravity	138
10.6	Conservation Laws and Hyperfluid Models	139
10.6.1	Hyperfluids in Cosmology	140
	References	142
11	Geometric Foundations of Gravity	143
	Tomi S. Koivisto	
11.1	Metric-Affine Geometry	143
11.2	The Geometrical Trinity	145
11.3	Purified Gravity	148
11.3.1	Field Equations	149
11.3.2	Energy and Entropy	150
11.3.3	On Quantum Theory	152
11.3.4	Matter Coupling	154
11.4	Modified Gravity	156
	References	158
12	Palatini Theories of Gravity and Cosmology	163
	Adrià Delhom and Diego Rubiera-Garcia	
12.1	Smoothing Out Cosmological Singularities	164
12.2	Inflationary Models	166
12.3	Background Evolution, Late-Time Acceleration, and Observational Constraints	168
	References	171
13	Hybrid Metric-Palatini Gravity and Cosmology	177
	Francisco S. N. Lobo	
13.1	Hybrid Metric-Palatini Gravity: The General Formalism	178
13.1.1	Action and Gravitational Field Equations	178
13.1.2	Scalar-Tensor Representation	179
13.2	Hybrid-Gravity Cosmology	182
13.2.1	Background Expansion	182
13.2.2	Cosmological Perturbations	186

13.3	Discussions and Final Remarks	188
	References	189
14	Teleparallel Gravity: Foundations and Cosmology	191
	Sebastian Bahamonde, Konstantinos F. Dialektopoulos, Manuel Hohmann, and Jackson Levi Said	
14.1	Foundations of Teleparallel Gravity	191
14.1.1	Teleparallel Geometry	192
14.1.2	Translation Gauge Theory	193
14.1.3	Local Lorentz Invariance	196
14.1.4	Matter Coupling	196
14.1.5	Teleparallel Equivalent of General Relativity (TEGR)	197
14.2	Teleparallel Gravity Extensions	199
14.2.1	$f(\mathbb{T})$ Gravity	199
14.2.2	New General Relativity and Extensions	200
14.2.3	Higher-Order Derivatives, $f(\mathbb{T}, B, T_G, B_G)$	202
14.2.4	Teleparallel Non-local Theories	203
14.2.5	Horndeski Analog and Subclasses	204
14.2.6	Teleparallel Dark Energy Models	207
14.3	Phenomenology of Teleparallel Gravity	207
14.3.1	$f(\mathbb{T})$ Cosmology and the Power-Law Model	208
14.3.2	Cosmography in $f(\mathbb{T})$ Gravity	209
14.3.3	The Growth Factor	211
14.3.4	The H_0 Tension Problem	213
14.3.5	Inflation in Teleparallel Theories of Gravity	217
14.3.6	Dynamical System in Cosmology for Teleparallel Theories Of Gravity	218
14.3.7	Noether Symmetry Approach in Teleparallel Theories of Gravity	222
14.3.8	Bounce Solutions in Modified Teleparallel Cosmology	226
14.4	What Can Teleparallel Theories Have to Offer? What Are the Open Problems in Teleparallel Theories?	228
	References	231
15	Finsler Gravity	243
	Nicoleta Voicu and Christian Pfeifer	
15.1	Physical Motivations	243
15.1.1	Finsler Geometry in Physics	243
15.1.2	Finsler Gravity	245
15.1.3	Finsler Cosmology	245
15.2	Definition of Finsler Spacetimes	246
15.2.1	Positive Definite Finsler Manifolds	247
15.2.2	Finsler Spacetime	248

15.2.3	Geodesics, Geodesic Deviation and Curvature Scalar	250
15.3	Finslerian Scalars as Physical Fields	252
15.4	Gravitational Dynamics	254
15.4.1	The Kinetic Gas Action on the Tangent Bundle	254
15.4.2	The Finsler Gravity Action	256
15.4.3	Kinetic Gases as Physical Sources for Finsler Gravity	256
	References	257
16	Gravity’s Rainbow	261
	Remo Garattini	
16.1	The Cosmological Constant as a Sturm-Liouville Eigenvalue Problem	262
16.2	From Quantum Mechanics to Quantum Field Theory	265
16.2.1	The Wheeler-DeWitt Equation Distorted by Gravity’s Rainbow	267
16.3	Correspondence of Gravity’s Rainbow with Hořava-Lifshitz Gravity	269
	References	272
17	Quantum Cosmology in Modified Theories of Gravity	275
	Mariam Bouhmadi-López and Prado Martín-Moruno	
17.1	Quantum Cosmology in a Metric Theory	276
17.2	Quantum Cosmology in a Palatini Theory	277
	References	278
Part II Testing Relativistic Effects		
18	Introduction to Part II	281
	Mariafelicia De Laurentis and Gonzalo J. Olmo	
19	Laboratory Constraints	283
	Anne-Christine Davis and Benjamin Elder	
19.1	Chameleons in Laboratory Vacuums	284
19.2	Atom Interferometry	285
19.3	Eöt-Wash	287
19.4	Casimir	287
19.5	Neutron, Atomic and Electron Dipole Moment Tests	288
19.6	The Symmetron	288
19.7	Conclusions	289
	References	290
20	Screening Mechanisms	293
	Philippe Brax	
20.1	Screening	293
20.2	Laboratory Experiments and Quantum Effects	296

20.3	Other Screening Effects	297
	References	298
21	Small-Scale Effects Associated to Non-metricity and Torsion	299
	Adrià Delhom	
21.1	Small-Scale Effects and Gravity	299
21.2	Small-Scale Effects Associated to Non-metricity	300
	21.2.1 Small-Scale Effects in $f(\mathcal{R})$ Theories	303
	21.2.2 Small-Scale Effects in Generic RBGs	306
21.3	Small-Scale Effects Associated with Torsion	307
21.4	Outlook	312
	References	312
22	Stars as Tests of Modified Gravity	317
	Gonzalo J. Olmo, Diego Rubiera-Garcia, and Aneta Wojnar	
22.1	Modified Tolman-Oppenheimer-Volkoff Equations	318
22.2	Modified Lane-Emden Equation	320
	References	322
23	Compact Objects in General Relativity and Beyond	329
	Jose Luis Blázquez-Salcedo, Burkhard Kleihaus, and Jutta Kunz	
23.1	Neutron Stars	330
	23.1.1 Neutron Stars in General Relativity	330
	23.1.2 Neutron Stars in Generalized Theories of Gravity	335
23.2	Black Holes	340
	23.2.1 Black Holes in General Relativity	340
	23.2.2 Black Holes in Generalized Theories of Gravity	341
23.3	Conclusions	345
	References	345
24	Parametrized Post-Newtonian Formalism	357
	Manuel Hohmann	
24.1	Historical Remarks	357
24.2	Parametrized Post-Newtonian Formalism	358
24.3	Comparison to Observations	360
24.4	Extensions and Modifications	361
	24.4.1 Invariant Density Formulation	361
	24.4.2 Broken Diffeomorphism Invariance	362
	24.4.3 Yukawa-Type Couplings	362
	24.4.4 Higher Derivative Orders	363
	24.4.5 Parity-Violating Terms	363
	24.4.6 Screening Mechanisms	363
	24.4.7 Cosmological Background Evolution	364
	24.4.8 Multiple Metrics	364
	24.4.9 Tetrad Formulation	364
	24.4.10 Gauge-Invariant Approach	364

24.5	Post-Newtonian Limit of Particular Theories	365
24.5.1	Scalar-Tensor and $f(R)$ Theories	365
24.5.2	Multi-scalar-Tensor Theories	366
24.5.3	Horndeski Gravity	367
24.5.4	Bimetric and Multimetric Gravity	367
24.5.5	Teleparallel Gravity	367
	References	368
25	Gravitational Waves	375
	Mairi Sakellariadou	
25.1	Tests of General Relativity	375
25.2	Modified Gravity	379
25.3	Quantum Gravity	380
	References	382
26	Gravitational Lensing	385
	László Á. Gergely	
26.1	Deflection of Light in Schwarzschild Geometry	385
26.2	Deflection of Light by Spherically Symmetric, Static Tidal Charged Brane Black Holes	388
26.3	The Lens Equation	390
26.4	Image Positions	392
26.5	Magnification Ratios	393
26.6	Strong Lensing by Spherically Symmetric, Static Tidal Charged Black Holes	393
26.7	Gravitational Lensing by Other Spherically Symmetric, Static Brane Black Holes	394
26.8	Gravitational Lensing in Hořava-Lifshitz Gravity	396
26.9	Gravitational Lensing in $f(R)$ Gravity	397
26.10	Gravitational Lensing in Scalar-Tensor Theories	398
26.11	Gravitational Lensing in Teleparallel Gravity	399
26.12	Gravitational Lensing, Galaxies and Cosmology	399
26.13	Concluding Remarks	400
	References	401
27	Classicalizing Gravity	405
	Roberto Casadio and Andrea Giusti	
27.1	Semiclassical Gravity and Localized Quantum States	405
27.2	Corpuscular Gravity	407
27.3	Gravitational Collapse	410
27.4	Bootstrapping Newton	411
27.5	Quantum Compositeness of Gravity at Cosmological Scales	414
27.6	Outlook	416
	References	416

Part III Cosmology and Observational Discriminators

28 Introduction to Part III 421
 Ruth Lazkoz and Vincenzo Salzano

29 Phenomenological Tests of Gravity on Cosmological Scales 425
 Yashar Akrami and Matteo Martinelli

29.1 Cosmological Tests of Gravity 425

29.1.1 Large Scales and the Linear Regime:
 Phenomenological Departures from GR 426

29.1.2 Cosmological Observables
 and Phenomenological Constraints 429

29.1.3 Einstein-Boltzmann Codes: From Theoretical
 Predictions to Data Analysis 435

29.1.4 Small Scales and Nonlinearities 436

29.2 Existing Constraints and Tensions 437

29.3 Upcoming Surveys and the Road Ahead 442

References 444

30 Relativistic Effects 451
 Camille Bonvin

30.1 Number Counts 451

30.2 Correlation Function 453

30.2.1 Estimators 453

30.2.2 Even and Odd Multipoles 454

30.3 Test of the Equivalence Principle 457

30.4 Conclusions 461

References 462

**31 Cosmological Constraints from the Effective Field Theory
 of Dark Energy** 465
 Noemi Frusciante and Simone Peirone

31.1 The Effective Field Theory for Dark Energy in a Nutshell 465

31.2 Einstein Boltzmann Codes 467

31.3 Cosmological Constraints on Horndeski and GLPV
 Models 469

31.4 Astrophysical Constraints 473

References 475

32 The H_0 Tensions to Discriminate Among Concurring Models 483
 Eleonora Di Valentino

32.1 The Effective Number of Relativistic Degrees of Freedom 486

32.2 Dark Energy Equation of State 486

32.3 Multi-parameters Extension 487

32.4 Early Dark Energy 488

32.5 Interacting Dark Energy 489

32.6 Modified Gravity 490

32.7	More Specific Models	491
32.8	Requirements: Hubble Hunter’s Guide	493
32.9	Standard Sirens	494
	References	495
33	σ_8 Tension. Is Gravity Getting Weaker at Low z?	
	Observational Evidence and Theoretical Implications	507
	Lavrentios Kazantzidis and Leandros Perivolaropoulos	
33.1	The $f\sigma_8$ Tension and Modified Gravity	516
	33.1.1 Observational Evidence	516
	33.1.2 Theoretical Implications	520
33.2	Evolving G_{eff} and the Pantheon SNeIa Dataset	524
33.3	Constraints on Evolving G_{eff} from Low l CMB Spectrum and the ISW Effect	527
33.4	Conclusions	529
	References	530
34	Testing Gravity with Standard Sirens: Challenges and Opportunities	539
	Jose María Ezquiaga	
34.1	Gravitational Wave Propagation Beyond General Relativity	539
34.2	Standard Sirens	541
34.3	The Speed of GWs	543
	34.3.1 Constraints After GW170817	543
34.4	GW Luminosity Distance	545
34.5	GW Oscillations	547
34.6	Future Prospects	549
	34.6.1 Theoretical Challenges	550
	34.6.2 Observational Opportunities	551
	References	553
35	Testing the Dark Universe with Cosmic Shear	557
	Valeria Pettorino and Alessio Spurio Mancini	
35.1	2D, Tomographic and 3D Weak Lensing	558
35.2	Current Data and Forecasts on Horndeski Gravity	561
35.3	Higher-Order Statistics and Lensing Peak Counts	563
35.4	Machine Learning and the Dark Universe	566
	References	567
36	Galaxy Clusters and Modified Gravity	571
	Ippocratis D. Saltas and Lorenzo Pizzuti	
36.1	What Makes Galaxy Clusters Interesting for Testing Gravity?	571
36.2	Consistency Conditions Based on the Mass Profiles of Galaxy Clusters	572
	36.2.1 Generalities	572

36.2.2	Probes Based on Mass Profiles from Galaxy Kinematics and Lensing	573
36.2.3	Probes Based on Thermal and Lensing Mass Profiles	575
36.3	A Brief Discussion on Systematics	577
36.4	Future Outlook	579
	References	580
37	Probing Screening Modified Gravity with Non-linear Structure Formation	583
	David F. Mota	
37.1	Theoretical Models	584
37.1.1	Chameleon- $f(R)$ Gravity	585
37.1.2	Symmetron	586
37.2	Efficiency of Screening Mechanisms	587
37.2.1	Solar System Constraints	588
37.2.2	Simulations	588
37.2.3	Results	589
37.3	Distribution of Fifth Force in Dark Matter Haloes	590
37.4	The Matter and the Velocity Power Spectra	591
37.5	The Dynamical and Lensing Masses	592
37.6	Thermal Versus Lensing Mass Measurements	594
37.6.1	Including the Non-thermal Pressure Component	595
37.7	Modelling Void Abundance in Modified Gravity	597
37.7.1	Linear Power Spectrum	597
37.7.2	Spherical Collapse	600
37.7.3	Void Abundance Function	601
37.7.4	Voids from Simulations	605
37.7.5	Results	606
37.8	Conclusions and Perspectives	610
	References	612
 Part IV Conclusion		
38	The End of the Beginning	617
	Emmanuel N. Saridakis	
	References	624
	Correction to: Modified Gravity and Cosmology	C1
	Emmanuel N. Saridakis, Ruth Lazkoz, Vincenzo Salzano, Paulo Vargas Moniz, Salvatore Capozziello, Jose Beltrán Jiménez, Mariafelicia De Laurentis, and Gonzalo J. Olmo	
	Index	627

Contributors

Yashar Akrami Département de Physique, École Normale Supérieure, Paris, France

Sebastian Bahamonde Laboratory of Theoretical Physics, Institute of Physics, University of Tartu, Tartu, Estonia;
Department of Mathematics, University College London, London, United Kingdom

Jose Luis Blázquez-Salcedo Departamento de Física Teórica and IPARCOS, Universidad Complutense de Madrid, Madrid, Spain

Christian G. Böhrer Department of Mathematics, University College London, London, United Kingdom

Camille Bonvin Department of Physics and Astronomy, University of Hawai'i, Watanabe Hall, Honolulu, HI, USA

Mariam Bouhmadi-López IKERBASQUE, Basque Foundation for Science, Bilbao, Spain;
Department of Theoretical Physics, University of the Basque Country UPV/EHU, Bilbao, Spain

Philippe Brax Institut de Physique Théorique, Université Paris-Saclay, CEA, CNRS, Gif/Yvette Cedex, France

Gianluca Calcagni Instituto de Estructura de la Materia, CSIC, Madrid, Spain

Salvatore Capozziello Dipartimento di Fisica “E. Pancini”, Università di Napoli “Federico II”, Napoli, Italy;
INFN, Sezione di Napoli, Complesso Universitario di Monte S. Angelo, Napoli, Italy;
Laboratory for Theoretical Cosmology, Tomsk State University of Control Systems and Radioelectronics (TUSUR), Tomsk, Russia

Roberto Casadio Dipartimento di Fisica e Astronomia, Università Bologna, Bologna, Italy

Jose A. R. Cembranos Departamento de Física Teórica and IPARCOS, Universidad Complutense de Madrid, Madrid, Spain

Anne-Christine Davis DAMTP, Centre for Mathematical Sciences, University of Cambridge, Cambridge, UK

Álvaro de la Cruz-Dombriz Cosmology and Gravity Group, Department of Mathematics and Applied Mathematics, University of Cape Town, Cape Town, South Africa;

Departamento de Física Fundamental and IUFFyM, Universidad de Salamanca, Salamanca, Spain

Mariafelicia De Laurentis Dipartimento di Fisica “E. Pancini”, Università di Napoli “Federico II”, Napoli, Italy;

Laboratory for Theoretical Cosmology, Tomsk State University of Control Systems and Radioelectronics (TUSUR), Tomsk, Russia;

Istituto Nazionale di Fisica Nucleare (INFN), Sezione di Torino, Torino, Italy

Adrià Delhom Departamento de Física Teórica and IFIC, Centro Mixto Universidad de Valencia - CSIC, Universidad de Valencia, Burjassot, Valencia, Spain

Eleonora Di Valentino Jodrell Bank Center for Astrophysics, School of Physics and Astronomy, University of Manchester, Manchester, UK

Konstantinos F. Dialektopoulos Center for Gravitation and Cosmology, College of Physical Science and Technology, Yangzhou University, Yangzhou, China

Benjamin Elder School of Physics and Astronomy, University of Nottingham, Nottingham, UK;

Department of Physics and Astronomy, University of Hawai’i, Honolulu, HI, USA

Jose María Ezquiaga NASA Einstein Fellow, Kavli Institute for Cosmological Physics and Enrico Fermi Institute, The University of Chicago, Chicago, IL, USA

Noemi Frusciante Researcher, Instituto de Astrofísica e Ciências do Espaço, Faculdade de Ciências da Universidade de Lisboa, Lisboa, Portugal

Remo Garattini Dipartimento di Ingegneria e Scienze Applicate, Università degli Studi di Bergamo, Dalmine, Bergamo, Italy;

Istituto Nazionale di Fisica Nucleare (INFN), Sezione di Milano, Milan, Italy

László Á. Gergely Institute of Physics, University of Szeged, Szeged, Hungary

Andrea Giusti Department of Physics and Astronomy, Bishops University, Sherbrooke, Québec, Canada

Lavinia Heisenberg Institute for Theoretical Physics, ETH Zurich, Zurich, Switzerland

Manuel Hohmann Laboratory of Theoretical Physics, Institute of Physics, University of Tartu, Tartu, Estonia

Damianos Iosifidis Department of Physics, Aristotle University of Thessaloniki, Thessaloniki, Greece

Jose Beltrán Jiménez Departamento de Física Fundamental and IUFFyM, Universidad de Salamanca, Salamanca, Spain

Lavrentios Kazantzidis Department of Physics, University of Ioannina, Ioannina, Greece

Burkhard Kleihaus Institut für Physik, Universität Oldenburg, Oldenburg, Germany

Tomi S. Koivisto Departamento de Física Fundamental and IUFFyM, Universidad de Salamanca, Salamanca, Spain

Jutta Kunz Institut für Physik, Universität Oldenburg, Oldenburg, Germany

Ruth Lazkoz Department of Theoretical Physics, University of the Basque Country UPV/EHU, Leioa, Spain

Francisco S. N. Lobo Instituto de Astrofísica e Ciências do Espaço, Faculdade de Ciências da Universidade de Lisboa, Edifício, Lisbon, Portugal

Matteo Martinelli Instituto de Física UAM-CSI, Madrid, Spain

Prado Martín-Moruno Departamento de Física Teórica and IPARCOS, Universidad Complutense de Madrid, Madrid, Spain

José Pedro Mimoso Instituto de Astrofísica e Ciências do Espaço, Faculdade de Ciências da Universidade de Lisboa, Lisbon, Portugal

David F. Mota Institute of Theoretical Astrophysics, University of Oslo, Oslo, Blindern, Norway

Gonzalo J. Olmo Depto. de Física Teórica and IFIC, Centro Mixto Universidad de Valencia-CSIC, Burjassot, Valencia, Spain;
Departamento de Física, Universidade Federal da Paraíba, João Pessoa, Paraíba, Brazil

Simone Peirone Institute Lorentz, Leiden University, Leiden, The Netherlands

Leandros Perivolaropoulos Department of Physics, University of Ioannina, Ioannina, Greece

Valeria Pettorino AIM, CEA, CNRS, Université Paris-Saclay, Université Paris Diderot, Gif-sur-Yvette, France

Christian Pfeifer Laboratory of Theoretical Physics, Institute of Physics, University of Tartu, Tartu, Estonia

Lorenzo Pizzuti Osservatorio Astronomico della Regione Autonoma Valle d'Aosta, Nus, Italy

Diego Rubiera-Garcia Departamento de Física Teórica and IPARCOS, Universidad Complutense de Madrid, Madrid, Spain

Jackson Levi Said Institute of Space Sciences and Astronomy, University of Malta, Msida, Malta;
Department of Physics, University of Malta, Msida, Malta

Mairi Sakellariadou Theoretical Particle Physics and Cosmology Group, Department of Physics, Kings College London, University of London, Strand, London, UK

Ippocratis D. Saltas CEICO, Institute of Physics of the Czech Academy of Sciences, Prague, Czechia

Vincenzo Salzano Institute of Physics, University of Szczecin, Szczecin, Poland

Emmanuel N. Saridakis National Observatory of Athens, Athens, Greece;
Key Laboratory for Researches in Galaxies and Cosmology, Department of Astronomy, University of Science and Technology of China, Hefei, Anhui, People's Republic of China;
School of Astronomy, School of Physical Sciences, University of Science and Technology of China, Hefei, People's Republic of China

Alessio Spurio Mancini Mullard Space Science Laboratory, University College London, Surrey, UK

Nicoleta Voicu Faculty of Mathematics and Computer Science, Transilvania University, Brasov, Romania

Aneta Wojnar Laboratory of Theoretical Physics, Institute of Physics, University of Tartu, Tartu, Estonia

Conventions¹

Greek small letters α, μ, ν, \dots	Space-time coordinate indices
Latin small letters i, j, k, \dots	Space coordinate indices
Latin capital indices A, B, \dots	Tangent space indices (only in Chaps. 8 and 9)
	D-dimensional coordinate indices)
$g_{\mu\nu}$	Metric tensor
(-+++)	Metric signature
$\Gamma_{\nu\rho}^{\mu}$	Levi-Civita connection
$R_{\nu\alpha\beta}^{\mu} = \partial_{\alpha}\Gamma_{\nu\beta}^{\mu} - \partial_{\beta}\Gamma_{\nu\alpha}^{\mu} + \Gamma_{\sigma\alpha}^{\mu}\Gamma_{\nu\beta}^{\sigma} - \Gamma_{\sigma\beta}^{\mu}\Gamma_{\nu\alpha}^{\sigma}$	Riemann curvature tensor
$R_{\mu\nu} = R_{\mu\alpha\nu}^{\alpha}$	Ricci tensor
$R = R_{\alpha}^{\alpha}$	Ricci scalar
$G_{\mu\nu} = R_{\mu\nu} - \frac{1}{2}g_{\mu\nu}R$	Einstein tensor
∇_{μ}	Covariant derivative
$\square \equiv g^{\mu\nu}\nabla_{\mu}\nabla_{\nu}$	d'Alembertian operator
$2X_{[\alpha\beta]} = X_{\alpha\beta} - X_{\beta\alpha}$	Anti-symmetry
$2X_{(\alpha\beta)} = X_{\alpha\beta} + X_{\beta\alpha}$	Symmetry
$ds^2 = -dt^2 + a^2(t)\left[\frac{dr^2}{1-kr^2} + r^2(d\theta^2 + \sin^2\theta d\phi^2)\right]$	Four-dimensional Friedmann-Lemaître-Robertson-Walker (FLRW) line element
$\tau = \int dt/a(t)$	Conformal time
$\dot{} \equiv \frac{d}{dt}$	Cosmic time derivative
$\prime \equiv \frac{d}{d\tau}$	Conformal time derivative
$ds_{(3)}^2 = \gamma_{ij}dx^i dx^j = \frac{dr^2}{1-kr^2} + r^2 d\theta^2 + r^2 \sin^2\theta d\phi^2$	Maximally symmetric three-dimensional: space-like hyper-surfaces metric

¹ List of notational conventions used in this manuscript, unless otherwise stated.

$\vec{\nabla}_i$	Grad operator on the three-dimensional: space-like hyper-surfaces
$\Delta \equiv \gamma^{ij} \vec{\nabla}_i \vec{\nabla}_j$	Laplacian operator
$ds^2 = -(1 + 2\Psi)dt^2 + a^2(t)(1 - 2\Phi)\gamma_{ij}dx^i dx^j$	Newtonian gauge scalar metric perturbations
$T^{\mu\nu} = \frac{2}{\sqrt{-g}} \frac{\delta \mathcal{L}_m}{\delta g_{\mu\nu}}$	Energy-momentum tensor of the Lagrangian density \mathcal{L}
$\kappa^2 \equiv 8\pi G_N \equiv M_{Pl}^{-2}$	Gravitational constant
$\hbar = c = k_B = 1$	Natural units
$\hat{\Gamma}_{\mu\nu}^\alpha$	General affine connection
$\tilde{\Gamma}_{\mu\nu}^\alpha$	Palatini connection
$\dot{\Gamma}_{\mu\nu}^\alpha$	Teleparallel affine (Weitzenböck) connection
$\diamond_{\mu\nu}^\alpha$	Symmetric teleparallel connection
$\bar{\Gamma}_{\mu\nu}^\alpha$	Chern-Rund linear connection
$\bar{\Gamma}_\nu^\mu$	Canonical nonlinear connection
\circ	Arbitrary object w.r.t. the Levi-Civita connection
$\hat{\circ}$	Arbitrary object w.r.t. the metric affine connection
$\check{\circ}$	Arbitrary object w.r.t. the Palatini connection
\bullet	Arbitrary object w.r.t. the Weitzenböck connection
\diamond	Arbitrary object w.r.t. the symmetric teleparallel connection
$\bar{\circ}$	Arbitrary object w.r.t. the Chern-Rund linear connection
$\bar{\circ}$	Arbitrary object w.r.t. the canonical nonlinear connection
$\omega^A_{B\mu}$	Spin connection
D_μ	Fock-Ivanenko derivative
$T^\mu_{\nu\rho}$	Torsion tensor
$Q_{\alpha\mu\nu} = \nabla_\alpha g_{\mu\nu}$	Non-metricity tensor
$T_\mu = T^\nu_{\nu\mu}$	Torsion vector
$\hat{R}_{\alpha\beta} := \hat{R}^\mu_{\mu\alpha\beta}$	Homothetic curvature

$$\hat{\mathcal{R}}_k^\lambda := \hat{R}_{\mu\nu k}^\lambda g^{\mu\nu} \mathcal{R} \equiv g^{\mu\nu} \mathcal{R}_{\mu\nu} \equiv$$

$$g^{\mu\nu} \left(\check{\Gamma}_{\mu\nu, \alpha}^\alpha - \check{\Gamma}_{\mu\alpha, \nu}^\alpha + \check{\Gamma}_{\alpha\lambda}^\alpha \check{\Gamma}_{\mu\nu}^\lambda - \check{\Gamma}_{\mu\lambda}^\alpha \check{\Gamma}_{\alpha\nu}^\lambda \right)$$

$$e^A{}_\mu$$

$$e_A{}^\mu$$

$$K^\mu{}_{\nu\rho}$$

$$L^\mu{}_{\nu\rho}$$

$$S^\nu{}_\mu{}^\rho$$

$$\mathbb{T}$$

$$\mathbb{Q}$$

$$\epsilon_{\mu\alpha\beta\gamma}$$

Co-Ricci tensor

Palatini curvature

Tetrad (vielbein, coframe)

Frame dual to $e^A{}_\mu$

Contortion tensor

Distortion tensor

Superpotential

Torsion scalar

Non-metricity scalar

Four-dimensional totally antisymmetric: Levi-Civita tensor

Chapter 1

Cosmophysics of Modified Gravity



Ruth Lazkoz

1.1 Breaking Scientific and Geographic Boundaries Through the Physics of Gravitation During a Societal Plight

One of the biggest achievements of Physics has been tailoring a standard cosmological model to describe the Universe quite successfully through a vast multitude of observations. In this architectural miracle the role of buildings bricks and joists is played by exquisite observational data, informing us about different epochs, regions and regimes. Evidence ranges from cosmic microwave background fluctuations to supernovae luminosity distances, along with baryon acoustic oscillations, cluster mass measurements and several other probes. Note that our access to an exquisite profusion of data is a fortunate sign of our times, while that was not certainly the case when the architects of modern cosmology set the foundations of our discipline. They certainly did not work in such gilded stage, as Nobel Laureate James Peebles recalls about his graduate years:

I was very uneasy about going into cosmology because the experimental observations were so modest.

However, our standard cosmological paradigm is a little patchy picture: in general, transitions between different epochs and scales are somewhat poorly depicted. Traditionally, cosmologists have aspired to fitting as much physics as possible into a full-fledged single model, but this goal faces challenges which have recently become quite an issue. In this respect we can mention two that have gathered some attention for different reasons.

Firstly, we witness the discrepancy between reputed teams of cosmologists as to what is the speed at which astronomical bodies are hurtling away from us, unprivileged observers. This results in the so called tension on the current value of the H_0

R. Lazkoz (✉)
Department of Theoretical Physics, University of the Basque Country UPV/EHU,
P.O. Box 644, 48080 Leioa, Spain

© The Author(s), under exclusive license to Springer Nature Switzerland AG 2021
E. N. Saridakis et al. (eds.) *Modified Gravity and Cosmology*,
https://doi.org/10.1007/978-3-030-83715-0_1

parameter (see Chap. 32 by Di Valentino), a concern that has been around us for some years now and that does not cease to be a lively source of controversy, quite the opposite.

Secondly, I wish to add to this very short editor's choice of baffling problems another bold departure from (cosmological) orthodoxy that has been put forward according to reliable evidence coming from *Planck* data: the spatial curvature of the Universe might be non zero [1]. The debate is alive and kicking, although it might be closed by a thoughtful identification of degeneracy-breaking data set, cosmic chronometers, which, perhaps not so anecdotally rely heavily on our understanding on galactic evolution [2].

We may be tempted to regard these two quandaries as astrophysical rather gravitational, but gravity is by all means the dominant interaction on the scales of astrophysical interest, which are revealing to us every day more exquisitely. For this reason, it is clear that these are times when a fluid dialogue between theory and experiment is very much needed. As Albert Einstein had it:

A theory is something nobody believes, except the person who made it. An experiment is something everybody believes, except the person who made it.

It may seem from the previous paragraphs that the routes to test the gravitational interaction are restricted to macroscopic realms where concentrations of mass and/or energy are very significant, but even though full characterizations of effects in some modified gravity scenarios are still lacking, our improved understanding (and in particular beyond Riemannian frameworks) tells us that microscopic experiments might bring surprises (see Chap. 21 by A. Delhom). Just keep in mind that:

We often fail to notice things that we are not expecting. —Lisa Randall

Another possible summary from the preceding paragraphs is that the array of fundamental problems the community is involved is certainly quite vast, and hence I could have easily arranged a different set of questions to tackle rather than the pair up above (even without venturing into the quantum gravity dominion). Yet, in my personal view, the current wide spectrum of enigmas is nothing but a manifestation of our need to improve and extend the standard body of our knowledge in gravity. Fortunately, even though history tells us that early motivations to go beyond General Relativity were more intellectually motivated by Mathematics, it is Physics itself where such explorations find their roots at present (see Chap. 3 by C. Boehmer and references therein). Needless to say that a portion of our readership may benefit from the review Chap. 2 by J. P. Mimoso on basic aspects of General Relativity that acts as a kick-off to this volume.

One of the most tempting routes of modification of General Relativity (GR) has been the possibility that our spacetime has more than four dimensions, with the extra ones inaccessible to low-energy exploration methods (as explained in a much broader context in Chap. 8 J. A. R. Cembranos). But it is well known that if we want to describe our macroscopic experience of the Universe in those scenarios, we have to roll up these extra dimensions. Such operation typically results in specific modifications of the gravitational Lagrangian, which can be found among the many

covered in the huge assortment of possibilities discussed in the present manuscript (endorsed with their physical motivation, definitely).

But extra-dimensional gravity has not been the major operation ground of the European network CANTATA, whose work is celebrated by this and all following chapters. In general, our large team has rather set the focus on other enticing possibilities, those in which the gravitational Lagrangian is modified in a “why not” intellectually legit spirit, thus allowing other degrees of freedom to play a role in the construction of our theoretical settings. Put in a bit rough way: most modifications to be found in the following pages rely on modifying the action by resorting to scalars that can be built with either the metric tensor or different pieces of the affine connection.

Note that I have inconspicuously introduced in my dissertation the two main building blocks of our gravitational theory: differential geometry as its mathematical formulation on one hand, and the Lagrangian as the encoder of its physical content on the other hand. The necessary association among them emerges when we eventually find out how a manifold, furnished with a metric and a connection, dictates how all the particles that live in it move, and conversely, how all the physical manifestations of those particles cipher the metric and the connection. For a less over-scrupulous redemption of this powerful idea the reader can resort to the *ad nauseam* quoted pronouncement by John Archibald Wheeler:

Space-time tells matter how to move; matter tells space-time how to curve.

Let me elaborate further on this by working for a moment on a setting in which Newton’s mechanics (and theory of gravity) is valid, say, Special Relativity (SR). In a covariant fashion, the (vanishing) acceleration we require to describe the motion of massive particles in free fall takes the following form for any observer other than the local inertial one:

$$a^\lambda \equiv \frac{d^2 x^\lambda}{d\tau^2} + \Gamma_{\mu\nu}^\lambda \frac{dx^\mu}{d\tau} \frac{dx^\nu}{d\tau}, \quad (1.1)$$

where $\Gamma_{\mu\nu}^\lambda$, according to usual notation, represents the Christoffel symbol of the second kind, also known as the Levi–Civita connection, which is defined through the usual operation of combining partial derivatives of the metric and contractions (with the metric itself). Note that all the rest of notation used is so standard that explanations can hopefully be waived.

Now, in order to preserve our ability to switch consistently between the physical conclusions of different observers, we need to pinpoint rigorously some key aspects within the broad concept of “variation”. For instance, in this specific problem I have resorted to a definition of acceleration that works the same in all coordinate systems. It turns out that the (mere) partial derivative of the velocity with respect to the proper time does not render a covariant vector which can be interpreted as the acceleration.

This is where the covariant derivative enters the picture and lets us define the acceleration rigorously and (in principle) exactly as above. But this difficulty with derivatives is not just a particular problem of the velocity: partial derivatives in general do not play as good tensor operators, whereas the covariant derivative does

indeed allow for parallel transport of tangent vectors along curves, i.e. it produces derivatives with tensorial nature. In this fashion, the acceleration is nothing but the covariant derivative of the velocity along the curves which the velocity field itself constructs, that is, $a^\mu \equiv u^\mu{}_{;\nu}u^\nu$. Nevertheless, there is a subtle point here, as this geometric route brings us back formally to the geodesics equation, that is, Eq. 1.1, but with the caveat that in this setting $\Gamma_{\mu\nu}^\lambda$ can represent any connection whatsoever, and not necessarily the Levi–Civita one, which is metric compatible and torsion free (and therefore symmetric). Roadmaps to geometric concepts such as the last two, which will be revisited often in this volume, can be found in Chap. 10 by D. Iosifidis and E. N. Saridakis and in Chap. 11 by T. Koivisto).

Before proceeding any further, an apology is in order, though, because I am taking advantage of the many more details other contributions are to offer in this collection to simplify my dissertation, and therefore I am giving myself permission to follow the Nobel Laureate Roger Penrose’s recommendation:

Do not be afraid to skip equations (I do this frequently myself).

The ambitious and broad next step would then to perform experiments to inform us of the motion of test particles, which would then reveal the specific form of the connection through their geometric properties. In this respect, this volume offers deeper insights into the boundless question of how curvature affects the motion of particles (see Chap. 26 by L. Á. Gergely for an overview on gravitational lensing). But in order to paint a master work of art and not a mere sketch, us physicists have to associate the equations of motion governing the pertinent trajectories with a physical framework, that is, we need to match particles and fields.¹

The, perhaps, most elegant way to accomplish this task is the application of the variational principle to an action. The advantage of this method is how (relatively) undemanding it becomes to compare GR and its modifications with other classical field theories (such as Maxwell’s theory). Nevertheless, for the sake of fluidity of this chapter, I feel compelled to write here the so very well-known action

$$S = \int d^4x \sqrt{-g} \left[\frac{1}{2\kappa} R + \mathcal{L}_m \right], \quad (1.2)$$

where, again, standard textbook notation is being used, and therefore $\kappa = 8\pi G/c^4$, R denotes the Ricci scalar, and g is the determinant of the $g_{\mu\nu}$ metric. In the usual manner, I also let \mathcal{L}_m account for any matter fields. Once the degrees of freedom of the action have been established, variation upon them will yield the (relevant) field equations, which will, in turn, be the route to the equations of motion. In this way, the geometric and matter pieces in the above Lagrangian yield the left and right hand side of the Einstein equations:

¹ Not that I pretend by any means to be an unpaired artist of gravitation myself. I rather mean the work of art, that the edifice of gravitational theories represent, will be or has been the result of collective efforts such as our network’s.

$$R_{\mu\nu} - \frac{1}{2}g_{\mu\nu}R = \kappa T_{\mu\nu}. \quad (1.3)$$

The mathematical identity represented by the vanishing covariant derivative of the left hand side, implies the vanishing of the right hand side, and four constraint equations follow. In the particular case that the energy-momentum tensor is that of incoherent matter, a straightforward² calculation can be followed to get exactly the same geodesics equation as above.

In case the reader finds this justification for the use of the variational principle not strong, I can rough out a two-fold additional justification. On one hand, the action provides a most fundamental starting point, in the sense that it offers a link with the underlying high energy physics. On the other hand, it provides precisely the classical equations of motion, and this takes root on Wheeler’s First Moral Principle:

Never make a calculation until you know the answer. Make an estimate before every calculation, try a simple physical argument (symmetry! invariance! conservation!) before every derivation, guess the answer to every paradox and puzzle.

In fact, this can be used as a *mantra* from now on, as any modification of GR we may fancy, must be reducible to it under some restrictions, or in the correct limit, as meekly as GR becomes SR in the absence of gravity, or Newton’s gravity in the weak-field and low-velocity limit. But this would be a reduction pursued along the route of physical properties, whereas we can follow a more mathematical track (or at least one which is not so physically grounded at its onset, which however converges with Physics as it progresses). This route to modify Einstein’s gravity is that offered by considering a non-trivial connection, as it allows to produce two extra fundamental objects with valuable relevant geometric information (see Chap. 11). The first one is the non-metricity tensor:

$$Q_{\alpha\mu\nu} \equiv \nabla_{\alpha}g_{\mu\nu}. \quad (1.4)$$

The second one is the torsion, which stems from the antisymmetric part of the connection:

$$T^{\alpha}_{\mu\nu} \equiv \Gamma^{\alpha}_{\mu\nu} - \Gamma^{\alpha}_{\nu\mu}. \quad (1.5)$$

As explained in more detail in Chap. 10, the respective effects of torsion under parallel transport is to crack parallelograms into pentagons whereas what non-metricity produces are changes in dot products and vector lengths.

If the torsion and non-metricity tensors vanish (that is, if connection is symmetric and metricity holds), the Levi–Civita connection is recovered, and gravity “à la Einstein” is (in which the metric is the only degree of freedom). Conversely, the metric and the connection could be considered as independent objects, whose relations would be given by the field equations. This is the so-called Palatini formalism (see here below).

² Needless to say that in this framework straightforward actually means “inexperienced lecturer mind blowing”.

In addition, and in view of the previous discernment, a general connection $\Gamma_{\mu\nu}^\alpha$ can be decomposed as [3, 4]:

$$\hat{\Gamma}_{\mu\nu}^\alpha = \Gamma_{\mu\nu}^\alpha + K_{\mu\nu}^\alpha + L_{\mu\nu}^\alpha, \quad (1.6)$$

where

$$K_{\mu\nu}^\alpha = \frac{1}{2}T_{\mu\nu}^\alpha + T_{(\mu}{}^\alpha{}_{\nu)} \quad (1.7)$$

is the contortion, and

$$L_{\mu\nu}^\alpha = \frac{1}{2}Q_{\mu\nu}^\alpha - Q_{(\mu}{}^\alpha{}_{\nu)} \quad (1.8)$$

is the disformation.

The Riemann tensor for this general connection turns out to have a too phenomenal look for me to avoiding to portrait it here, and I will restrict myself to just mentioning that, by resorting to some clever tricks, it can be made vanish, thus leading to two equivalent formulations of gravity. These two rely upon the definition of the invariants \mathbb{T} or \mathbb{Q} , obviously related to the torsion and non-metricity. Specifically the corresponding two new settings stem from the Einstein–Hilbert Lagrangian upon the replacements $R \rightarrow -\mathbb{T}$ or $R \rightarrow -\mathbb{Q}$, which lead respectively to the metric teleparallel or symmetric metric teleparallel versions of GR. Full fledged chapters of this volume, namely Chaps. 11 and 14 by S. Bahamonde, K. F. Dialektopoulos, M. Hohmann, J. L. Said, are devoted to these modifications of gravity and the reader is invited to dwell into them.

However, it is not convenient to lose sight of the physical perspective. Let us go back to the need of celebrating the ability of Einstein’s relativity to describe most of the physical behaviours we have access too, and acknowledge at the same time that many puzzles are still standing, and therefore modifications attempting at solving them must have a sensible GR limit. This is, of course, one of the key aspects of one of the most popular ways to modify Einstein’s gospel: the so called scalar-tensor theories. Historically, they originated as an arguably better way to incorporate Mach’s principle into gravitational theory, a trick to make it impossible to gauge away the gravitational field completely, leaving behind a remnant which depends on an universal quantity such as the mass of the whole Universe. Under these rules, the Lagrangian will then typically become dependent on a new quantity, the scalar field ϕ .

In the pioneering presentation of this seductive idea, Brans and Dicke considered

$$S = \int d^4x \sqrt{-g} \left[\frac{\phi}{16\pi} R + \mathcal{L}_\phi(\phi, g_{\mu\nu}, \phi^{;\alpha}) + \mathcal{L}_m \right], \quad (1.9)$$

with a carefully tailored \mathcal{L}_ϕ so that the field equations do not display derivatives of order higher than second. This is important so as to guarantee the theory remains

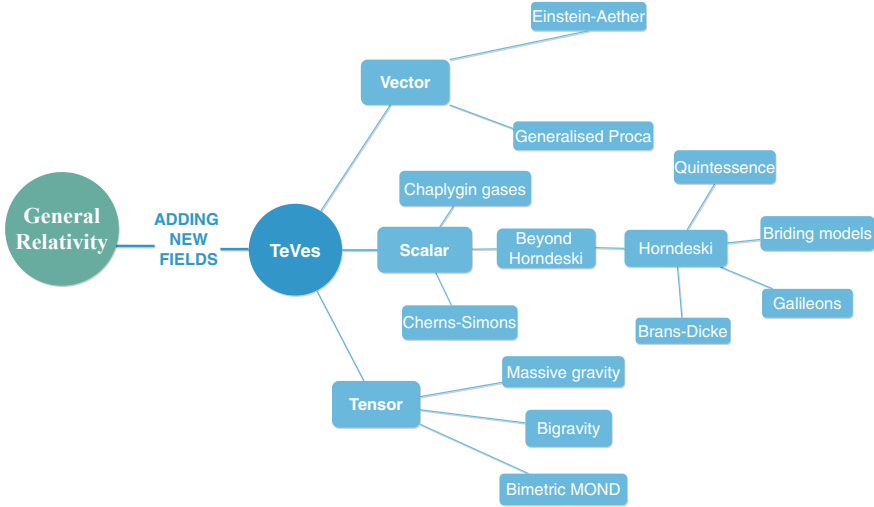


Fig. 1.1 Schematic categorisation of the Tensor-Vector-Scalar (TeVeS) class of theories, arising by adding new fields to General Relativity

ghost free (that is, no Ostrogradski instabilities appear). One can of course consider to replace the ϕR with $f(\phi)R$ by means of an arbitrary function, which again requires a wise choice of the term \mathcal{L}_ϕ to avoid divergences.

More generally, by relaxing some requirements, it is possible to engineer the family of all models with a Lagrangian containing second order derivatives of the field leading to second order equations of motion. These are the so called Horndeski scenarios, which were rediscovered some decades after their first appearance, and were then dubbed Galileon models. In a compact way we can rewrite them as

$$S = \int d^4x \sqrt{-g} \left[\mathcal{L}_H(\phi, g_{\mu\nu}, \phi^{;\alpha}, \phi^{;\alpha}_{;\beta}, R^{\eta\sigma}_{\lambda\tau}) + \mathcal{L}_m \right]. \quad (1.10)$$

This is the right place to invite the reader to have a look at the contribution by P. Martín Moruno in Chap. 6, and references therein, where a more detailed account is offered on scalar-tensor theories such as those defined above and others beyond. In Fig. 1.1 we present a schematic categorisation of the Tensor-Vector-Scalar class of theories, arising by adding new fields to General Relativity.

But unstoppable as curiosity and imagination are, the continuously growing set of generalisations of GR has one subset that stands above all others because of its popularity and (if we may) promises, the $f(R)$ proposal, where the Ricci scalar R is replaced in the original Einstein–Hilbert (plus additions) action:

$$S = \frac{1}{2\kappa} \int d^4x \sqrt{-g} [f(R) + \mathcal{L}_m]. \quad (1.11)$$

With their generality, tractability and flexibility, these scenarios offer chances to reproduce a wide assortment of cosmological kinematics (see the staggering overview in Chap. 5 by Á. de la Cruz-Dombriz). They are constestably able to provide mechanisms to explain either early or late-time acceleration (fitting *customer's* needs) and, in a sense, they represent the simplest general modification of Einstein's gravity than can be thought of. The understanding of the capability of this broad context to reproduce a succession of necessary stages (radiation-like, matter-like, and dark energy-like) has improved over the year along with the restrictions they are subject to. But then one should not be fooled by the potentialities offered by $f(R)$ theories: hardly ever has there been in the history of Physics an one-size fit to all theoretical framework, which is actually a feature that has made our discipline precisely to play its unmatched role in science. From a strictly very personal perspective, it is somewhat frustrating how often we hear/read the claim that these scenarios can always be tweaked so they fit the data, which is quite a too loose statement if one does not provide an accompanying report of the quality of fit and other demanded statistical criteria. At the end of the day, if $f(R)$ theories (and other modified gravity routes) were the "holy grail" there would be no justification to write a volume such as ours. So, brushing aside this perhaps hypercritical tone, we should celebrate modified gravity models as laboratories to tests ideas, predict difficulties and venture solutions. Remember, we get challenged and, as put in the words of Neil de Grasse Tyson,

The Universe is under no obligation to make sense to you.

Let me now, however, briefly sketch other relevant works shaping the section of the volume devoted to research in the theoretical front (that of Working Group (WG)1), so as to offer a tidbit of the high tea menu it represents. Clearly, a simple gaze at the table of contents reveals that the role played by the metric-affine or Palatini formalism is major in modified gravity, in general. It allows to relax the "standard" convention between the metric and the connection, so that the latter can be worked out from first principles [5]. I will make no distinction between the Palatini and the metric-affine formalism, as it is customary in many works, and in some of our chapters, although formally a bit of extra rigour (and a highlight of differences) is in order if fermions are present in the matter Lagrangian [2, 6], which is not really necessary for most cosmological applications.

The metric-affine scheme progresses initially from the construction of a curvature scalar using the connection and the metric tensor as independent quantities, but then it can be enlarged considerably by constructing Lagrangians with other scalar terms built from the symmetric part of the Ricci tensor and its contractions with the metric tensor. These settings offer many new attractive possibilities, such as the removal or smoothing out of cosmological singularities which are generic in GR scenarios, as discussed in Chap. 12 by A. Delhom and D. Rubiera-Garcia). Another remarkable point of the Palatini formulation is that, unlike in the metric approach, second-order field equation are always obtained, even for Lagrangians with terms which are non linear in the scalar curvature or include the above mentioned less standard scalars. A related approach is hybrid-metric Palatini gravity, where the standard R term coming

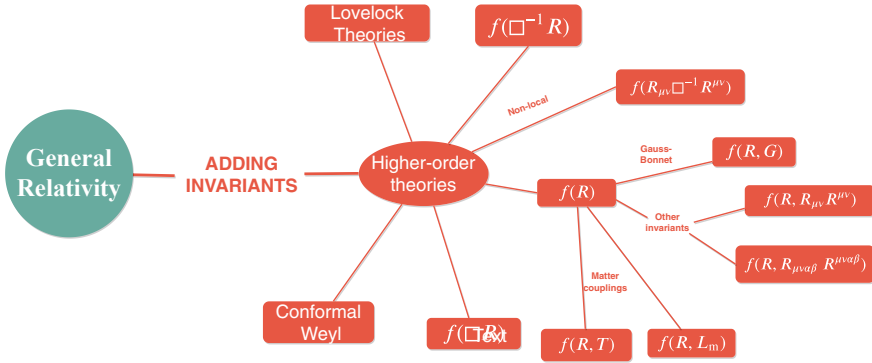


Fig. 1.2 Schematic categorisation of the higher-order class of theories, arising by adding higher-order invariants in the Lagrangian of General Relativity

from the metric connection is added to extra terms depending on an alternative curvature scalar, \mathcal{R} , derived from an independent connection, such terms offering a richer phenomenology as to the evolution of matter inhomogeneities. These and many other aspects are covered in the contribution by F. S. N. Lobo in Chap. 13. In Fig. 1.2 we present a schematic categorisation of the theories, arising by adding higher-order invariants in the Lagrangian of General Relativity.

Alternatively, a (wilder and) completely separate route to describe gravity as a manifestation of geometry can be pursued too: teleparallel gravity and its extensions. These replace curvature with torsion and are build upon a curvature-free connection (therefore flat). Following the recipe I anticipated above, one possible Lagrangian starting point for teleparallel descriptions of gravity is:

$$S = \frac{1}{2\kappa} \int d^4x \sqrt{-g} [f(\mathbb{T}) + \mathcal{L}_m]. \tag{1.12}$$

Among the attractive features of teleparallel gravity we see again the second-order nature of the equations and the broadness of the whole setting, which allows to rewrite many theories built from the metric and the Levi-Civita connection. It is also certainly very appealing that the theory allows to waive the equivalence principle, thus re-framing gravitation as an interaction more similar to other fundamental ones. Many aspects of teleparallel gravity are covered into the sizeable contribution in Chap. 14, where the authors do not forget to acknowledge the absolute need to continue to examine these extensions in the light of observations. Actually, the collection of new features offered by these framework is tremendous, as the possibility of interpreting it as a gauge theory of translations contributes to filling the gap between gravity and other interactions in Nature, or as the intellectually not less challenging question of the definition and characterization of singularities in this alternative formulation of gravitational physics. In Fig. 1.3 we present a schematic categorisation of the theories arising by modifying the geometry of General Relativity.

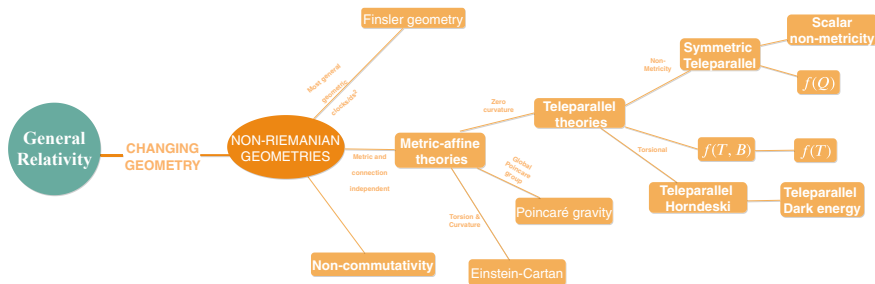


Fig. 1.3 Schematic categorisation of the theories arising by modifying the geometry of General Relativity

Recapitulating, there seem to be two main and disparate ways to manufacture modifications to GR: the addition of new fields on one hand, and geometry based restylings on the other hand. This splitting is largely a matter of convention, as prescriptions to go from one to another can be typically found with manageable techniques (see again Chaps. 5 and 13). But this dual possibility has proved so far more enriching than a source of confusion, and it continues to provide motivation and inspiration.

Nevertheless, this whole collection of possible alternatives to Einstein gravity may seem as if the community was meandering rather than following a straight course. But remembering Roger Penrose’s words again, is just opportune:

Sometimes it’s the detours which turn out to be the fruitful ideas.

In this sense, I also invite specialists to explore the contribution by N. Voicu and C. Pfeifer in Chap. 15 and learn about the possibilities of relativistic extensions of Finsler geometry, with their intrinsic unusual features such as multiple covariant derivatives and matter dynamics.

Perhaps, some readers have noticed the absence of references to the colossal problem of our lack of substantial understanding of gravity at the quantum level. The reason is mainly that it falls beyond the major objectives of the Action. This choice is really not a gesture of contempt, but rather a need to concentrate efforts on an otherwise major attempt, which is to understand gravity at the mainly classical level. Our team however is happy to boast about intrepid representatives which explore the quantum side of gravity through (again) extensions of Einstein’s framework. In this respect see Chap. 9 by G. Calcagni, Chap. 16 by R. Garattini, Chap. 17 by M. Bouhmadi-López and P. Martín-Moruno, and Chap. 27 by R. Casadio and A. Giusti. In Fig. 1.4 we present a schematic categorisation of the theories arising by the use of quantum arguments.

Let me again stress that the two main routes to knowledge about modifications of our understanding of gravity are theory and data analysis, which must act synergistically, as it has been the case of the activities of our Action. This volume is a voracious reflection of that fact, with a carefully tailored choice of contributions at the forefront of the field in its broadest manifestation.

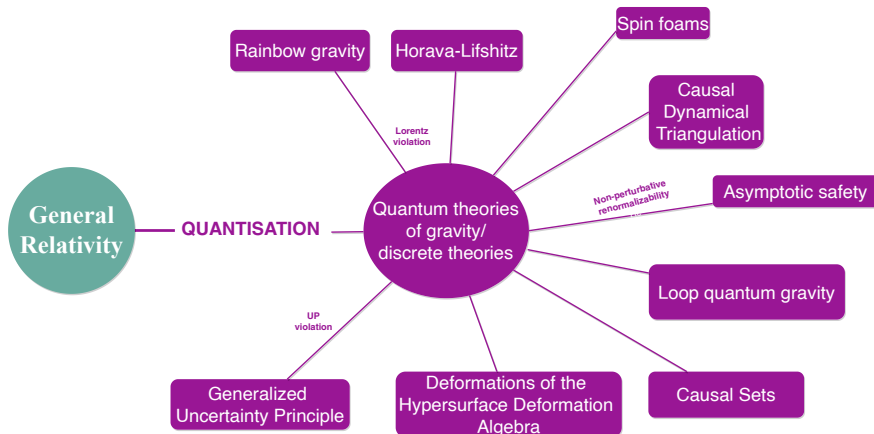


Fig. 1.4 Schematic categorisation of the theories arising by the use of quantum arguments

CANTATA researchers whose theoretical work makes strong contact with observations have contributed to WG2 (testing relativistic effects) an WG3 (observational discriminators) mainly. Their daily research encourages them to reflect pointedly about the questions that these new observational findings pose. This allows these scientists to perform masterly forecasts of constraints to be placed on theoretical frameworks by the coming generation of cosmological observations. Remember in this context the wise words by Vera Rubin:

Science progresses best when observations force us to alter our preconceptions.

One important area of operation where scientists in WG2 of our team have completed proficient works are tests of gravity at scales well below 1 Mpc, that is, non-cosmological ones (clusters are not covered in Part II, but rather in Part III), ranging from earth laboratory tests to orbits around compact objects. Within this domain, screening mechanisms in scalar-tensors theories with a scalar field coupled to matter have gathered a lot of interest. The reason is that the screening treats differently traditional gravity tests and laboratory tests in the sense that it allows effects to evade detection by the former, while revealing to the latter, as if some kind of reward for clever and inspired novel experiments were offered. Several screening mechanisms have been proposed so far [7], and among the most popular we find those with canonical kinetic terms on one hand, such as the chameleon and the symmetron mechanisms, and then a third one on the other, the Vainshtein mechanism, which emerges from derivative non-linearities. In the contribution by Anne-Christine Davies and Benjamin Elder in Chap. 19 the focus is mainly set on tests on chameleon scalar fields through different approaches such as vacuum chambers, atom interferometry, torsion balances, Casimir force searchers and others. The symmetron field is covered as well, but with less extension, as research on this area is more recent. In a wide sense the dynamics of the scalar field is governed by an effective potential:

$$V_{\text{eff}}(\phi) = V(\phi) + (A(\phi) - 1)\rho_m. \quad (1.13)$$

The (square of) the auxiliary function $A(\phi)$ encapsulates the coupling between matter and the scalar field in the form of a conformal rescaling between the metric used to express the matter sector of the action (Jordan metric/frame) and the metric used to render the Einstein equations in the “orthodox” fashion (Einstein metric/frame). Further details can be found in Chap. 20 by P. Brax. But the zoo of screening mechanisms contains more species, and when one lets curiosity (or imagination) run and non canonical kinetic terms enter the picture, we can find other mechanisms such as K-mouflage (see Chap. 20) described in this volume, a screening possibility which has so far not been tightly constrained by gravitational wave observations.

Now, if Earth-based laboratories are at the bottom of the scale ladder of experiments to test modifications of gravity, the solar system is the obvious next: a weak-field limit realm which is typically treated under the parametrized post-Newtonian formalism, an in-between stratagem to wrap-up conjectures about both observations and theories being considered, which connects the former with the latter through a set of parameters. This is explained in detail in the contribution by M. Hohmann in Chap. 24, where both the standard version and some extensions are discussed. In fact, a large class of extensions of GR can be accommodated into the customary formulation, but the community has not stopped there, and broader versions have been devised for cases demanding so. The (well-known) first two parameters of the expansion (γ and β) estimate how mass creates curvature on one hand and the degree of nonlinearity in the superposition law for the gravitational potentials on the other hand. Stringent bounds have been obtained through refined experiments and can offer light on the viability of modifications of gravity with significant impact on those parameters and subsequent ones.

But the prevailing weak-field/strong-field battle in physics explorations demands we also turn our attention (as a team) to representatives of largest curvature and highest densities regimes: compact stars and black holes. Modelling stellar structure is a demanding task in the default GR setting, and modifications of gravity introduce additional difficulties, both from the mathematical and physical perspectives. Hardly any features can be studied from a general formulation and individual investigations are typically the way to go. New knowledge will, for instance, allow to spot (if any) changes in the mass-radius relation of neutron stars, as it will depend on new parameters characterizing the modifications (see Chap. 22 by G. Olmo, D. Rubiera-Garcia, and A. Wojnar). The analogous operates on black holes, in the sense that the famous absence of hair theorem may need a tweak in the presence of additional gravitational degrees of freedom.

These are just some of the surprises that compact objects (whether extreme or not) may have in store. Another is spontaneous scalarization, which consists in the emergence of a non-trivial configuration of a scalar field without sources and which vanishes asymptotically. For this to occur a scalar field must exist which is non-minimally coupled to gravity. This highly nonlinear effect may offer tight limits to the modified scenarios through observations of, for instance, binary systems as discussed in Chap. 23 by J. L. Blázquez-Salcedo, B. Kleihaus, and J. Kunz.

When we move to (much) larger scales we must publicize that efforts of CAN-TATA researchers have served the international effort of the community on the design of future accurate tests of gravity (modified or standard) and the improvement of current ones with their expertise on numerics and computation. Some of our colleagues have made distinguished contributions to large teams expected to lead the design and operation of terrestrial and space-based surveys which will be operating in the near future. A glimpse of the breathtaking future is offered by observations of gravitational waves, which have brought strong implications for modified theories of gravity. At the cosmological background level [8], an additional friction that adds to the Hubble one appears, and this modifies the amplitude of the waves, whereas an effective (anomalous) mass and consequent atypical speed alter the phase, as discussed in Chap. 34 by J. M. Ezquiaga. Notoriously, gravitational waves provides a new observational channel for testing gravity theories which predict a non-null mass for the graviton. In this context we can highlight the closely related massive gravity and bigravity settings, which belong to the field theory framework of gravity and of which a glimpse is offered in Chap. 7 by L. Heisenberg.

But more sophisticated and challenging effects could also arise in the physics of gravitational waves when modified gravity scenarios are considered, as not only additional polarisations emerge (up to four extra ones), but also they could get mixed up and frequency mutations might be produced too; see Chap. 25 by M. Sakellariadou. Actually, the detection of these additional polarisation modes represents a significant technical challenge.

Into the bargain, the absolutely greatest promise of gravitational waves is the cosmological realm. Events that can be regarded as standard sirens [9] (may be able to) probe the redshift evolution of the luminosity distance of the gravitational wave source, which is proportional to the inverse of the amplitude. In principle, it can be different from the electromagnetic luminosity distance of a companion event, and therefore their ratio will offer a test for parameters associated with physics beyond GR and also with dark energy evolution (which is also referred to, sometimes, as “new physics”, as differing from the Λ CDM setting).

Now, along those lines, the scheme which makes currently most sense is to combine those measurements with observations of the large scale structure coming from surveys which will probe the Universe in different scale regimes as compared to the size of the horizon. Further details on this classification are given in the contribution by Y. Akrami and M. Martinelli in Chap. 29, where readers can find a summary of one of the most popular formulations of perturbations valid for the linear regime (that is, for horizon size scales or intermediate scales).

The starting point for this approach is to rewrite the Friedmann-Lemaître-Robertson-Walker metric in the Newtonian gauge as

$$g_{\mu\nu} = \text{diag} \left[-(1 + 2\Phi), a^2(1 - 2\Psi)\delta_{ij} \right], \quad (1.14)$$

where a is the scale factor and Φ and Ψ are the gauge-invariant Bardeen potentials.

One route to progress is making use of the quasi-static approximation, which is valid for the subhorizon linear regime and significant breadth of gravitational

theories. This approach produces a sizeable simplification of the pertinent equations, as the extra degrees of freedom associated with departures from GR can be jumbled up in the (generally) time and space dependent functions μ and η , respectively the effective Newton's constant and the gravitational slip. The second function (that is, η) makes the two Bardeen potentials differ from each other, unlike the GR case, and leads to observable weak lensing effects through the combination of μ and ν ; whereas ν (on its own) affects the growth of structure; see Chap. 33 by L. Kazantzidis and L. Perivolaropoulos.

Related to the previous discussion, one analytic method based on the perturbation theory framework I particularly like to highlight is the Effective Field Theory (EFT) approach, which can capture interesting effects on scales smaller than the intermediate one, and in particular the onset of the transition from GR to a modified gravity regime, which is crucial for the research objectives of our Action. In particular, it depicts physical effects germane to macroscopic scales by integrating out short-distance features, so they appear on long-distance characteristics as extra/perturbative parameters. This chassis supports any dark energy or modified gravity model possessing one additional scalar degree of freedom in the way described in detail in Chap. 31 by N. Frusciante and S. Peirone.

These theoretical developments are, of course, a concoction to make the community ready to take advantage of future large scale structure surveys when they become available. In this respect even though the current constraints are of $\mathcal{O}(1)$, they are expected to get as low as $\mathcal{O}(10^{-1})$, and there is hope that violations of the current observational inference of $\mu(z=0) = \nu(z=0)$ could be detected (see again Chap. 29).

Among the abundance of outputs of future large scale structure surveys we must mention the sensitivity of the clustering of galaxies to the (specific) theory of gravity under play. Effects less tangible than density perturbations and redshift-space distortions will place unprecedented constrains which are obtained by confronting pertinent gauge-invariant quantities (the two Bardeen potentials being among them again) with the information provided by the power spectrum and its multipole expansion, exploring effects which are currently neglected in current surveys; see the contribution of C. Bonvin in Chap. 30. Note that the importance of these studies is twofold. On one hand they vindicate the role of galaxies as concentrations of baryonic (and therefore electromagnetically accessible) concentrations of matter for the study of the Universe, and on the other they offer a fundamental channel to explore the vital role of dark matter. In addition, it is relevant that the interplay between baryons and dark matter [10], which takes place in regions with high matter density, also allows to test the equivalence principle [11]

The teamwork between dark and baryonic matter and its proportions in the Universe can be literarily cast into the dainty mould of these words by one of the clearest minds in gravitation, Arthur S. Eddington:

An ocean traveler has even more vividly the impression that the ocean is made of waves than that it is made of water.

But having stated the paramount importance of galaxies to understand modified theories of gravity the Universe, we cannot forget that the Universe offers us even better laboratories, galaxy clusters. Their ambivalence as both astrophysical and cosmological objects can help us discriminate between gravitational effects and cumbersome astrophysical phenomena as thoroughly covered in Chap. 36 by I. D. Saltas and L. Pizzuti, where prospect of kinematic, thermal and lensing explorations are reviewed yet again resorting to perturbative quantities considered in other contributions, such as the gravitational slip η . Nevertheless, for a flavour on the sort of discriminating criteria clusters can offer when time evolution of scalar fields is addressed, it is worth check the contribution by D. Mota in Chap. 37, which closes those related to WG3.

But then again, going back to cosmological scales, I must stress that studies with perturbative ingredients will necessarily be flawed until some pending disquietudes regarding the cosmological background and its linear perturbations are relieved. The most talked about one being the tension between high and low redshift data estimates of the Hubble constant, H_0 (see Chap. 32 for a state-of-the-art review and a sketch of what lies road ahead). The second actor in this stage play of tensions is the apparent discrepancy in the amplitude of the matter power spectrum as set by σ_8 , the root-mean-square fluctuations in the matter mass density in a comoving sphere of diameter 8 Mpc. Large compilations of redshift-space distortions and other dynamical probes show a statistically significant discrepancy with *Planck* data and would favor an evolving and weaker effective Newton's constant (through μ), and readers can head to the contribution of Chap. 33 for a detailed discussion and review of the topic. Clearly, all complementary routes offered by tests of dynamical features are destined to play a most relevant role, for instance weak lensing. Its very-hard-to-spot effects are again encoded in the Bardeen potentials, and forecasts have been carried out for surveys such as *Euclid* in the theoretical context of Horndeski theories; see Chap. 35 by V. Pettorino and A. S. Mancini.

It should be clear by now to the reader that has come so far, that the route to erudition in this limitless field is grievous, and will unavoidably require all the literature anybody can digest so as to get an exquisite insight on caveats of these scenarios. Such an exercise would undoubtedly lead the candidate to a multifaceted and more thorough understanding of (her/his favourite flavour of) gravity through questions such as whether the correct weak field limit is attainable, whether instabilities occur (a typical pathology of higher order theories), and whether the initial value problem is well posed. Nevertheless, and here comes the crux of the matter, no proficient understanding of a modified gravity framework can be reached without an analysis of the formation (and sustenance) of structures. In this context I cannot but highlight again the key question of whether its cosmological perturbations of the cosmological background are capable of leaving a blueprint agreeable with the currently observed patterns in the cosmic microwave background and the large-scale structure itself. The intimate connection between theory and observations is therefore an unbreakable bond, and the seed sown by our team's work will surely thrive and feed our knowledge hungry community, and, again, as a team, our feeling is that:

This is the way —The Mandalorian

References

1. E. Di Valentino, A. Melchiorri, J. Silk, Planck evidence for a closed Universe and a possible crisis for cosmology. *Nature Astron.* **4**(2), 196–203 (2019). [arXiv:1911.02087](#)
2. S. Vagnozzi, A. Loeb, M. Moresco, *Eppure piatto? The cosmic chronometer take on spatial curvature and cosmic concordance*. [arXiv:2011.11645](#)
3. L. Järv, M. Rünkla, M. Saal, O. Vilson, Nonmetricity formulation of general relativity and its scalar-tensor extension. *Phys. Rev. D* **97**(12), 124025 (2018). [arXiv:1802.00492](#)
4. J.B. Jiménez, L. Heisenberg, T.S. Koivisto, The geometrical trinity of gravity. *Universe* **5**(7), 173 (2019). [arXiv:1903.06830](#)
5. G.J. Olmo, Introduction to Palatini theories of gravity and nonsingular cosmologies (INTECH 2012), pp. 157–184. [arXiv:1212.6393](#)
6. F.W. Hehl, J. McCrea, E.W. Mielke, Y. Ne’eman, Metric affine gauge theory of gravity: Field equations, Noether identities, world spinors, and breaking of dilation invariance. *Phys. Rept.* **258**, 1–171 (1995). [arXiv:gr-qc/9402012](#)
7. J. Khoury, Theories of Dark Energy with Screening Mechanisms. [arXiv:1011.5909](#)
8. E. Belgacem, Y. Dirian, S. Foffa, M. Maggiore, Gravitational-wave luminosity distance in modified gravity theories. *Phys. Rev. D* **97**(10), 104066 (2018). [arXiv:1712.08108](#)
9. R. Gray et al., Cosmological inference using gravitational wave standard sirens: a mock data analysis. *Phys. Rev. D* **101**(12), 122001 (2020). [arXiv:1908.06050](#)
10. M.H. Chan, A universal constant for dark matter-baryon interplay. *Sci. Rep.* **9**(1), 3570 (2019). [arXiv:1902.03786](#)
11. C. Bonvin, F.O. Franco, P. Fleury, A null test of the equivalence principle using relativistic effects in galaxy surveys. *JCAP* **08**, 004 (2020). [arXiv:2004.06457](#)

Chapter 2

General Relativity



José Pedro Mimoso

Modern cosmology stems from Einstein's General Relativity as the fundamental description of gravitation. General Relativity mutates the gravitational force into the curvature of the four-dimensional space-time, which responds to the distribution of mass-energy. It was this revolutionary viewpoint that rendered it possible for the first time to consider the whole Universe (Cosmos) as a single object of study [1].

A few fundamental building blocks underlie Einstein's theory, beginning with the Principle of Relativity, which prescribes that the laws of physics should be the same in all reference frames [2]. This means that there should be no preferred frame, and this is encapsulated in the Principle of General Covariance (also referred to as Diffeomorphism Invariance), by which the equations are tensorial and invariant under coordinate transformations [3]. The Equivalence Principle establishes that there are no local experiments that distinguish free-falling observers from inertial observers, and its weak formulation stands on the equivalence between inertial and gravitational masses. Finally, the theory is expected to recover Newtonian gravity in the weak field limit and slow motion of sources. This is denoted as the Correspondence Principle, in analogy with the corresponding requirement met by quantum theory [2].

In General Relativity [4], the curvature of the spacetime is encoded into the Riemann tensor defined by the Ricci identities $\nabla_{[\gamma}\nabla_{\delta]}X^\alpha = R^\alpha{}_{\beta\gamma\delta}X^\beta$, where X^α is an arbitrary spacetime vector. It follows that

$$R^\alpha{}_{\beta\mu\nu} = \partial_\mu\Gamma^\alpha{}_{\beta\nu} - \partial_\nu\Gamma^\alpha{}_{\beta\mu} + \Gamma^\delta{}_{\beta\nu}\Gamma^\alpha{}_{\delta\mu} - \Gamma^\delta{}_{\beta\mu}\Gamma^\alpha{}_{\delta\nu}, \quad (2.1)$$

where $\Gamma^\alpha{}_{\mu\nu}$ is the affine connection that defines the concept of parallelism in the four-dimensional manifold. However, the further prescription of a metric tensor $g_{\alpha\beta}$ to the space-time both generalises the special-relativistic Minkowski line-element $ds^2 =$

J. P. Mimoso (✉)

Instituto de Astrofísica e Ciências do Espaço, Faculdade de Ciências da Universidade de Lisboa, Edifício C8, Campo Grande, P-1749-016 Lisbon, Portugal

© The Author(s), under exclusive license to Springer Nature Switzerland AG 2021

17

E. N. Saridakis et al. (eds.) *Modified Gravity and Cosmology*,

https://doi.org/10.1007/978-3-030-83715-0_2

$\eta_{\alpha\beta} dx^\alpha dx^\beta = -dt^2 + dx^2 + dy^2 + dz^2$ with $ds^2 = g_{\alpha\beta} dx^\alpha dx^\beta$, and specifies the metric connection

$$\Gamma^\alpha{}_{\beta\gamma} = \frac{1}{2} g^{\alpha\delta} (\partial_\beta g_{\delta\gamma} + \partial_\gamma g_{\delta\beta} - \partial_\delta g_{\beta\gamma}). \quad (2.2)$$

It also means that the spacetime manifold has no torsion [5]. Indeed, the connection is symmetric and this implies that $\Gamma^\alpha{}_{[\mu\nu]} = 0$. The Riemann tensor can then be decomposed into irreducible components

$$R^\alpha{}_{\beta\mu\nu} = C^\alpha{}_{\beta\mu\nu} + \frac{1}{2} (\delta_\mu^\alpha R_{\beta\nu} + g_{\beta\nu} R_\mu^\alpha - \delta_\nu^\alpha R_{\beta\mu} - g_{\beta\mu} R_\nu^\alpha) + \frac{R}{6} (\delta_\nu^\alpha g_{\beta\mu} - \delta_\mu^\alpha g_{\beta\nu}), \quad (2.3)$$

where $C^a{}_{bcd}$ is the traceless conformally invariant Weyl tensor, and the traces $R_{\alpha\beta} = g^{\beta\delta} R_{\alpha\beta\gamma\delta}$, and $R = g^{\alpha\beta} R_{\alpha\beta}$ are, respectively, the Ricci tensor and the Ricci curvature scalar.

Einstein's field equations, which govern the interplay between the spacetime geometry and the non-gravitational fields, can be variationally derived from the fundamental Einstein–Hilbert (EH) action [6]

$$S_{EH} = \int dx^4 \sqrt{-g} \left[\frac{1}{2\kappa^2} (R - 2\Lambda) + \mathcal{L}_m(g_{\mu\nu}, \psi^\alpha) \right], \quad (2.4)$$

where $g_{\mu\nu}$ is the metric of space-time, g the determinant of this metric and R the corresponding Ricci curvature scalar. Additionally, Λ is the cosmological constant, $\mathcal{L}(g_{\mu\nu}, \psi^\alpha)$ represents the Lagrangian of the matter fields generically denoted ψ^α , and κ^2 is the gravitational coupling constant $\kappa^2 = 8\pi G_N/c^4$, with G_N the Newton's constant and c the speed of light set to 1. The stationarity conditions associated with the variational differentiation of the EH action with respect either to the metric or, alternatively, with respect to the metric and the connections in the so-called Palatini formalism, yield the celebrated equations [4, 7]

$$R_{\mu\nu} - \frac{1}{2} g_{\mu\nu} R = \kappa^2 T_{\mu\nu} \quad , \quad (2.5)$$

where $T_{\mu\nu}$ is defined by

$$T^{\mu\nu} \equiv \frac{2}{\sqrt{-g}} \frac{\delta(\sqrt{-g} \mathcal{L}_m)}{\delta g_{\mu\nu}} \quad (2.6)$$

which is the energy-momentum tensor of the matter fields. When we consider a time-like vector field u^α the energy-momentum tensor can be decomposed as

$$T^{\mu\nu} = \rho u^\mu u^\nu + p h^{\mu\nu} + \Pi^{\mu\nu} + 2q^{(\mu} u^{\nu)}, \quad (2.7)$$

where $h_{\mu\nu} = g_{\mu\nu} + u_\mu u_\nu$ is the metric induced on the spatial hypersurfaces orthogonal to u^α , $\Pi_{\mu\nu} = (h_\mu^\gamma h_\nu^\delta - \frac{1}{3}h_{\mu\nu}h^{\gamma\delta})T_{\gamma\delta}$ is a transverse traceless tensor, and $q^\mu = h_\delta^\mu T_\nu^\delta u^\nu$ is a spatial vector field. The quantities ρ and p are defined as $\rho = T_{\mu\nu}u^\mu u^\nu$ and $3p = T_{\mu\nu}h^{\mu\nu}$, and are respectively the energy-density and the pressure of the matter fluid measured by an observer moving with 4-velocity u^α , while the quantities $\Pi^{\mu\nu}$ and q^μ are the anisotropic stress tensor and the heat flow vector.

The diffeomorphism invariance of the action translates into the Bianchi-contracted identities

$$\nabla_\nu T^{\mu\nu} = 0. \quad (2.8)$$

Taking into consideration that $u^\mu \nabla_\mu (\cdot) = (\cdot)^\cdot$, i.e., the dot represents differentiation with respect to the cosmic time t , and that the induced metric $h_{\mu\nu}$ is a projector onto the spatial hypersurfaces, we can make the following decomposition:

$$\nabla_\mu u_\nu = -\dot{u}_\mu u_\nu + \frac{\theta}{3} h_{\mu\nu} + \sigma_{\mu\nu} + \omega_{\mu\nu}, \quad (2.9)$$

where $\dot{u}^\mu = u^\alpha \nabla_\alpha u^\mu$ is the acceleration, $\theta = h^{\mu\alpha} \nabla_\alpha u_\beta h^{\beta\mu}$ is the expansion scalar, $\sigma_{\mu\nu} = 2h_{(\mu}^\alpha \nabla_\alpha u_{\beta} h_{\nu)}^\beta - \frac{1}{3}\theta h_{\mu\nu}$ is the shear, and $\omega_{\mu\nu} = 2h_{[\mu}^\alpha \nabla_\alpha u_{\beta} h_{\nu]}^\beta$ is the vorticity tensor. Thus, the Bianchi identities (2.8) can be cast as

$$\dot{\rho} = -(\rho + p)\theta - \Pi^{\mu\nu}\sigma_{\mu\nu} - q^\mu u_\mu - \nabla_\nu q^\nu \quad (2.10)$$

$$(\rho + p)\dot{u}^\mu = -h^{\mu\beta} \left(\nabla_\beta p + \nabla_\nu \Pi_\beta^\nu + \dot{q}_\beta \right) + \left(\omega_\nu^\mu + \sigma_\nu^\mu - \frac{4}{3}\theta h_\nu^\mu \right) q^\nu. \quad (2.11)$$

The field equations (2.5) are a system of non-linear partial differential equations on the components of the curvature tensor (see, for instance, J. Barrow's contribution in [8]). This implies that the gravitational field is itself also a source of curvature, and that a curved spacetime can thus be a solution of the vacuum field equations. The components of the metric tensor can be perceived as generalising the Newtonian concept of gravitational potential. This is particularly well illustrated by the first exact solution discovered by K. Schwarzschild early in 1916 [9]

$$ds^2 = -\left(1 - \frac{2G_N M}{r}\right) dt^2 + dr^2 \left(1 - \frac{2G_N M}{r}\right)^{-1} + r^2 (d\theta^2 + \sin^2 \theta d\phi^2), \quad (2.12)$$

where one uses the standard spherical coordinates r , θ and ϕ , and where M represents the Misner-Sharp mass $M = 4\pi \int_0^r \rho(u) u^2 du$ [10]. This metric represents the gravitational field of a central, spherical distribution of mass, M , on the exterior vacuum space. Clearly, its coefficients g_{00} and g_{rr} relate to Newton's potential $\Phi(r) = -G_N M/r$, and the discovery of this solution allowed us to confirm both Einstein's explanation of Mercury's perihelium shift, anomalous in the framework of Newtonian celestial mechanics, and the predicted value for the deflection of light rays passing close to the Sun in excess of the Newtonian value. The observational

test of the latter forecast was made one century ago, on 1919, and it was just the first of many empirical successes at the Solar System level.

The piling up of experimental tests was boosted in the early 1960's by the challenge placed by proposals of extended gravity theories such as the Brans–Dicke theory [11]. This led to the development of a systematic scrutiny of the Post-Newtonian effects, through the consideration of a consistent multipolar expansion of the gravitational potentials in the metric, dubbed Parametric Post-Newtonian [12]. Different gravitational theories yield diverse values or dependences on the parameters of the expansion for the competing theories. Experiments on the scale of the Solar System have led to very accurate measurements of these coefficients and to very tight constraints on gravitational theory [12, 13]. It must be emphasised at this point that the theories under scrutiny are mostly theories that share with General Relativity the paradigm set by its underlying principles.

So far, General Relativity has passed the Solar System tests with flying colours. Moreover, its success has also been further vindicated recently by the detection of gravitational waves by LIGO in 2015 [14], and by obtaining the first image of a black hole in 2019 [15]. These were staggering landmarks both in regard to the exquisite precision achieved in these observations, and in regard to the confirmation of precocious predictions made by the theory decades ago.

Aiming at a completely different range of scales, modern cosmology began with the astonishing realisation that the Universe is expanding [1, 16–20] out of an incredibly tiny size [18]. It was necessary to repel the idea that the universe should be static, avoiding gravitational collapse onto itself, which led to the introduction of the much-debated cosmological constant Λ [1, 21–23]. The assumption of a Copernician or cosmological principle by which our location in the Universe is not special, and taking into account the observed uniformity of the distribution of matter at large scales, is reflected in the adoption of the spatially homogeneous and isotropic metric Friedmann–Lemaître–Robertson–Walker (FLRW) metrics

$$ds^2 = a^2(\tau) \left[-d\tau^2 + \frac{dr^2}{1 - kr^2} + r^2 (d\theta^2 + \sin^2 \theta d\phi^2) \right], \quad (2.13)$$

where $a(\tau)$ is termed as the scale factor, $k = 0 \pm 1$ accounts for the three possible curvatures of the spatial hypersurfaces, and τ is the so-called conformal time, which relates to the cosmological time t through $dt = a(\tau)d\tau$. This metric is characterised by the vanishing of the shear $\sigma_{\mu\nu} = 0$, the vorticity $\omega_{\mu\nu} = 0$ and the acceleration $\dot{u}^\mu = 0$. The expansion is the only non-vanishing kinematical quantity, and is $\theta = 3\dot{a}/a$.

In addition, the admissible energy-momentum tensor (2.7) compatible with the assumed symmetries of the spacetime reduces to

$$T^{\mu\nu} = (\rho + p)u^\mu u^\nu + pg^{\mu\nu}, \quad (2.14)$$

usually interpreted as representing a perfect fluid with energy-density ρ , and pressure p measured by the co-moving observer with 4-velocity u^a (such that $u_a u^a = -1$,

under our choice of signature) [24, 25]. Of course the latter energy-momentum tensor can be the sum of several components, i.e., $\rho = \sum_i \rho_{(i)}$, $p = \sum_i p_{(i)}$, with or without mutual interactions [26, 27].

Applying the general Einstein field equations (2.5) in the case of the cosmological FLRW metrics, one obtains the Friedmann equations, namely

$$H^2 + \frac{k}{a^2} = \frac{\kappa^2}{3}\rho + \frac{\Lambda}{3} \quad (2.15)$$

$$\dot{H} + H^2 = -\frac{\kappa^2}{6}(\rho + 3p) + \frac{\Lambda}{3}, \quad (2.16)$$

where we have introduced the so-called Hubble parameter

$$H = \frac{\dot{a}}{a}. \quad (2.17)$$

The cosmological model is fully prescribed when we assume some equation(s) of state. In the simplest scenario it is possible to model the expansion rate of the Universe, and its thermal history [28] as the interplay of two conventional matter sources: incoherent, baryonic matter ($p_b = 0$) and radiation ($p_r = \rho_r/3$)—summing up about 5% of the overall budget of the Universe at the present time, plus two unconventional components dubbed “dark matter” (with $p_{dm} \simeq 0$) and “dark energy” (with $p_{DE} = p_{DE}(\rho_{DE})$). The latter two are motivated, on the one hand, by the process of formation of the large-scale structure (LSS) through gravitational instability, and on the other hand by the unexpected discovery that the Universe at low redshifts is inflating. Structure formation requires about 30% of non-interacting matter, which is collectively denoted by $\rho_m (\equiv \rho_b + \rho_{dm})$. The accelerated expansion of the Universe, revealed by the observation of supernova type Ia (SNIa) [29, 30], demands a repulsive effect that can be simplest fitted by the elusive cosmological constant Λ [31, 32], representing about 70% of the content of the Universe. In the latter case the cosmological constant is interpreted as a matter component of equation of state $p_\Lambda = -\rho_\Lambda$.

It must be remarked at this point that the adoption of the spatially homogeneous and isotropic FLRW models to describe the Universe was questioned in the 1970s [33]. It was pointed out that there are causality issues when one attempts to explain the onset of such a highly symmetrical Universe out of an initial Big-Bang singularity. Another problem would stem from the possibility that topological defects formed during the Early Universe would close it, in contrast with the observations that favour a Universe with flat spatial hypersurfaces of homogeneity. The latter flatness was also a problem, as a Universe filled with matter and radiation required an extreme fine tuning of primordial conditions to fit the observations. It was then devised [34, 35] that a brief stage of early inflation, i.e., of accelerated expansion close to the Planck epoch, would solve the problems under scrutiny (see, for instance, [36], and references therein). This inflationary epoch is thought to be the outcome of primordial quantum conditions still not fully understood. The first

scenarios involved a scalar field, dubbed the inflaton, with the ability to produce a repulsive negative pressure, and hence inducing the accelerated stage of expansion. Moreover the quantum fluctuations of this field can be interpreted as the seeds for the density fluctuations that eventually grow into the observed large scale structure of the Universe. This would naturally happen at the transition between the epoch dominated by radiation and ultra-relativistic matter, and the subsequent epoch dominated by non-relativistic matter. Significantly this enables one to relate the power-spectrum of the CMB to the conditions fulfilled by inflation [37], and thus it is a most relevant building block in regard to the possibility of testing the models of the Early Universe. There is a multitude of proposals and scenarios to promote the inflationary stage. Most of them involve the consideration of one or several scalar fields, but there are also scenarios in which other fields are envisaged [36].

Among the notable successes of this cosmological model, we count the prediction of the abundances of the light elements [38] and of the number of particle species [25], plus the explanation of the Cosmic Microwave Background (CMB) radiation found in 1965 [39, 40]. Moreover, the remarkable observational progress and the judicious combination of different observations, such as CMB [41], Baryonic Acoustic Oscillations (BAO) [42], LSS power spectrum, and weak lensing [43] have led to a best fit that favours a Λ CDM model [41, 44, 45].

One description of the space-time metric which nicely adapts both to the astrophysical and cosmological scales addressed by General Relativity, is the perturbed metric [46, 47]

$$ds^2 = a^2(\tau) \left[-(1 + 2\Psi) d\tau^2 + 2\omega_i d\tau dx^i + [(1 - 2\Phi) \gamma_{ij} + 2h_{ij}] dx^i dx^j \right]. \quad (2.18)$$

In this expression $a^2(\tau)$ is a conformal factor that rescales the whole line element, and which for cosmological purposes is restricted to be only dependent on the so-called conformal time τ . It accounts, of course, for the underlying expansion of the Universe. Φ and Ψ are scalar fields that relate to the Newtonian potential of the isotropic weak-field case. The vector ω_i represents the vorticity, and γ_{ij} is the metric induced on the spatial surfaces, usually the co-moving part of the FLRW metric. Finally, h_{ij} is a symmetric traceless tensor that represents tensor perturbations, and hence relates to the gravitational waves. This form of the metric, denoted the Newtonian longitudinal gauge, is particularly useful when investigating the evolution of perturbations. In the weak-field approximation, we assume $a(\tau)$ is effectively constant and the parameters Φ , Ψ , ω^i and h_{ij} respectively describe the scalar, vector and tensor modes of small perturbations away from Minkowski space-time (in this case the induced 3-metric is $\gamma_{ij} = \delta_{ij}$). When we wish to investigate fluctuations in the cosmological context, we usually set $\omega^i = 0$ due to the fast damping of rotational perturbations, the potentials Ψ and Φ are equal due to the background isotropy, and describe scalar perturbations. The equation for h_{ij} yields the propagation of gravitational waves. The resulting gravitational wave equation corresponds to a spin-2 particle, carrying the gravitational interaction—the graviton. The investigation of the evolution of perturbations into their non-linear regime is a crucial block to contrast the cosmological models with observations [37].

Despite the impressive agreement of General Relativity with most observational data, it has been recognised that it faces difficulties both at the small scales (and high energies), and at the large scales (and small energies). These opposite limits have been dubbed the ultraviolet (UV) and infrared (IR) limits, respectively. In the former case, one recognises the lack of success in building a consistent quantum gravity and in the latter case, we are faced with the tantalising absence of explanation for the existence of enigmatic gravitational components in the large-scale Universe, called dark matter and dark energy problems [48].

In order to address the latter caveats, the investigation of extended gravity theories sharing the same fundamental principles of GR, but otherwise looking for improved field equations, has been a focal point of interest. This endeavour can be traced back to the very first years after GR was put forward, when the efforts to find a Grand Unified Theory (GUT) of all the fundamental forces started [49]. At first the goal was circumscribed to merging gravitation and the electromagnetic field, but the need to encompass the weak and strong nuclear forces further increased the proportions and difficulties of the task. The design of a Grand Unified Theory (GUT) has led to increasingly sophisticated theories of which the theory of Superstring is the present, and most promising paradigm [50, 51].

In regard to the restricted problem of extending GR without the specific consideration of quantum gravity, it is of great importance to be aware of the possible avenues for progress. On the one hand, we have three different alternative, variational derivations of the gravitational equations of motion available: (i) the metric formalism; (ii) Palatini formalism; (iii) metric-affine formalism [52, 53]. In the metric formalism, the action is assumed to be only dependent on the metric tensor, whilst in the Palatini formalism the metric and the connection are taken to be independent degrees of freedom of the curvature. In the metric-affine approach the perspective is similar to the latter, but one no longer assumes the independence between the metric and the affine connection. We still vary the action with respect to both the metric and the affine connection, but the variation with respect to the affine connection yields a constraint to be articulated with the metric equation.

On the other hand, Lovelock's theorem [54] clarifies the assumptions that must be met by the gravitational Lagrangian leading to second-order field equations, when the action is built from the metric tensor. Indeed, in four dimensions the most general Lagrangian density \mathcal{L} built just from the metric and its derivatives that can yield Einstein's field equations reads

$$\mathcal{L} = \eta\sqrt{-g}R - 2\lambda\sqrt{-g} + \gamma\epsilon^{\alpha\beta\mu\nu}R^{\gamma\delta}{}_{\alpha\beta}R_{\gamma\delta\mu\nu} + \xi\sqrt{-g}\left(R^2 - 4R^\mu{}_\nu R^\nu{}_\mu + R^{\alpha\beta}{}_{\mu\nu}R^{\mu\nu}{}_{\alpha\beta}\right) \quad (2.19)$$

where γ and λ are constants and $\epsilon^{\alpha\beta\mu\nu}$ is the completely skew Levi-Civita tensor. Lovelock's theorem [54] states that the third and fourth terms are boundary terms, and therefore do not contribute to the field equations. This reduces the contributing part of the previous Lagrangian only to the necessary terms to build the Einstein-Hilbert action plus a constant term.

By the same token, it becomes apparent which fields and/or couplings can evade the conditions of Lovelock's theorem. It tells us that if one wishes to introduce modifications in the gravitational sector [32, 55], at least one of the following options must be taken:

- Include more fields beyond, or even instead of, the metric tensor;
- Allow for higher-order derivatives in the field equations;
- Work in a space-time with more than four dimensions;
- Break the diffeomorphism invariance.

In the next chapter, as well as in Part I of the present Review, these alternative extensions to General Relativity will be thoroughly addressed.

References

1. A. Einstein, Cosmological considerations in the general theory of relativity. *Sitzungsber. Preuss. Akad. Wiss. Berlin (Math. Phys.)* **1917**, 142–152 (1917)
2. W. Rindler, *Relativity: Special, General, and Cosmological* (2006)
3. J.B. Jiménez, L. Heisenberg, T.S. Koivisto, The geometrical trinity of gravity. *Universe* **5**(7), 173 (2019). [arXiv:1903.06830](https://arxiv.org/abs/1903.06830)
4. A. Einstein, The field equations of gravitation. *Sitzungsber. Preuss. Akad. Wiss. Berlin (Math. Phys.)* **1915**, 844–847 (1915)
5. Y.-F. Cai, S. Capozziello, M. De Laurentis, E.N. Saridakis, $f(T)$ teleparallel gravity and cosmology. *Rept. Prog. Phys.* **79**(10), 106901 (2016). [arXiv:1511.07586](https://arxiv.org/abs/1511.07586)
6. R. d'Inverno, *Introducing Einstein's Relativity* (1992)
7. A. Einstein, On the general theory of relativity. *Sitzungsber. Preuss. Akad. Wiss. Berlin (Math. Phys.)* **1915**, 778–786 (1915). ([Addendum: *Sitzungsber. Preuss. Akad. Wiss. Berlin (Math. Phys.)* 1915, 799 (1915)])
8. J.D. Barrow, A.B. Henriques, M.T.V.T. Lago, M.S. Longair, The Physical, universe: the interface between cosmology, astrophysics and particle physics, in *Proceedings, 12th Autumn School of Physics, Lisbon, Portugal, October 1–5*, Lecture Notes in Physics, vol. 383 (1991), pp. 1–312 (1990)
9. K. Schwarzschild, On the gravitational field of a mass point according to Einstein's theory. *Abh. Konigl. Preuss. Akad. Wissenschaften Jahre 1906, 92, Berlin, 1907* **1916**, 189–196 (1916)
10. C.W. Misner, D.H. Sharp, Relativistic equations for adiabatic, spherically symmetric gravitational collapse. *Phys. Rev.* **136**, B571–B576 (1964)
11. C. Brans, R.H. Dicke, Mach's principle and a relativistic theory of gravitation. *Phys. Rev.* **124**, 925–935 (1961). ([142 (1961)])
12. C.M. Will, *Theory and Experiment in Gravitational Physics* (1993)
13. C.M. Will, The confrontation between general relativity and experiment. *Living Rev. Rel.* **17**, 4 (2014). [arXiv:1403.7377](https://arxiv.org/abs/1403.7377)
14. LIGO Scientific, Virgo Collaboration, B.P. Abbott et al., Observation of gravitational waves from a binary black hole merger. *Phys. Rev. Lett.* **116**(6), 061102 (2016). [arXiv:1602.03837](https://arxiv.org/abs/1602.03837)
15. Event Horizon Telescope Collaboration, K. Akiyama et al., First M87 event horizon telescope results. VI. The shadow and mass of the central black hole. *Astrophys. J.* **875**(1), L6 (2019). [arXiv:1906.11243](https://arxiv.org/abs/1906.11243)
16. A. Friedman, On the curvature of space. *Z. Phys.* **10**, 377–386 (1922). ([*Gen. Rel. Grav.* 31, 1991 (1999)])
17. G. Lemaitre, The expanding universe. *Mon. Not. Roy. Astron. Soc.* **91**, 490–501 (1931)

18. G. Lemaitre, Republication of: the beginning of the world from the point of view of quantum theory. *Nature* **127**, 706 (1931). ([*Gen. Rel. Grav.* 43, 2929 (2011)])
19. E. Hubble, A relation between distance and radial velocity among extra-galactic nebulae. *Proc. Nat. Acad. Sci.* **15**, 168–173 (1929)
20. G. Lemaitre, The expanding universe. *Gen. Rel. Grav.* **29**, 641–680 (1997). ([*Annales Soc. Sci. Bruxelles A* 53, 51 (1933)])
21. W. de Sitter, Einstein’s theory of gravitation and its astronomical consequences. First Paper. *Mon. Not. Roy. Astron. Soc.* **76**, 699–728 (1916)
22. W. de Sitter, Einstein’s theory of gravitation and its astronomical consequences, Second Paper. *Mon. Not. Roy. Astron. Soc.* **77**, 155–184 (1916)
23. W. de Sitter, Einstein’s theory of gravitation and its astronomical consequences, Third Paper. *Mon. Not. Roy. Astron. Soc.* **78**, 3–28 (1917)
24. J. Bernstein, *Kinetic Theory in the Expanding Universe*. Cambridge Monographs on Mathematical Physics. (Cambridge University Press, Cambridge, 1988)
25. E.W. Kolb, M.S. Turner, The early universe. *Front. Phys.* **69**, 1–547 (1990)
26. G.F.R. Ellis, Relativistic cosmology. *Cargese Lect. Phys.* **6**, 1–60 (1973)
27. G.F.R. Ellis, H. van Elst, Cosmological models: cargese lectures. *NATO Sci. Ser. C* **541**(1999), 1–116 (1998). [arXiv:gr-qc/9812046](https://arxiv.org/abs/gr-qc/9812046)
28. G. Gamow, The evolution of the universe. *Nature* **162**(4122), 680–682 (1948)
29. Supernova Cosmology Project Collaboration, S. Perlmutter et al., Measurements of Ω and Λ from 42 high redshift supernovae. *Astrophys. J.* **517**, 565–586 (1999). [arXiv:astro-ph/9812133](https://arxiv.org/abs/astro-ph/9812133)
30. Supernova Search Team Collaboration, A.G. Riess et al., Observational evidence from supernovae for an accelerating universe and a cosmological constant. *Astron. J.* **116**, 1009–1038 (1998). [arXiv:astro-ph/9805201](https://arxiv.org/abs/astro-ph/9805201)
31. E.J. Copeland, M. Sami, S. Tsujikawa, Dynamics of dark energy. *Int. J. Mod. Phys. D* **15**, 1753–1936 (2006). [arXiv:hep-th/0603057](https://arxiv.org/abs/hep-th/0603057)
32. T. Clifton, P.G. Ferreira, A. Padilla, C. Skordis, Modified gravity and cosmology. *Phys. Rept.* **513**, 1–189 (2012). [arXiv:1106.2476](https://arxiv.org/abs/1106.2476)
33. R. Dicke, P. Peebles, The big bang cosmology: enigmas and nostrums (1979)
34. A.H. Guth, The inflationary universe: a possible solution to the horizon and flatness problems. *Adv. Ser. Astrophys. Cosmol.* **3**, 139–148 (1987)
35. A.A. Starobinsky, A new type of isotropic cosmological models without singularity. *Adv. Ser. Astrophys. Cosmol.* **3**, 130–133 (1987)
36. R.H. Brandenberger, Inflationary cosmology: progress and problems, in *IPM School on Cosmology 1999: Large Scale Structure Formation*, vol. 1 (1999). [arXiv:hep-ph/9910410](https://arxiv.org/abs/hep-ph/9910410)
37. E. Bertschinger, Simulations of structure formation in the universe. *Ann. Rev. Astron. Astrophys.* **36**, 599–654 (1998)
38. R.A. Alpher, H. Bethe, G. Gamow, The origin of chemical elements. *Phys. Rev.* **73**, 803–804 (1948)
39. A.A. Penzias, R.W. Wilson, A Measurement of excess antenna temperature at 4080-Mc/s. *Astrophys. J.* **142**, 419–421 (1965)
40. R.H. Dicke, P.J.E. Peebles, P.G. Roll, D.T. Wilkinson, Cosmic black-body radiation. *Astrophys. J.* **142**, 414–419 (1965)
41. Planck Collaboration, P.A.R. Ade et al., Planck 2013 results. I. Overview of products and scientific results. *Astron. Astrophys.* **571**, A1 (2014). [arXiv:1303.5062](https://arxiv.org/abs/1303.5062)
42. SDSS Collaboration, W.J. Percival et al., Baryon acoustic oscillations in the sloan digital sky survey data release 7 Galaxy sample. *Mon. Not. Roy. Astron. Soc.* **401**, 2148–2168 (2010). [arXiv:0907.1660](https://arxiv.org/abs/0907.1660)
43. M. Bartelmann, P. Schneider, Weak gravitational lensing. *Phys. Rept.* **340**, 291–472 (2001). [arXiv:astro-ph/9912508](https://arxiv.org/abs/astro-ph/9912508)
44. P.G. Ferreira, Cosmological tests of gravity. *Ann. Rev. Astron. Astrophys.* **57**, 335–374 (2019). [arXiv:1902.10503](https://arxiv.org/abs/1902.10503)
45. É. Aubourg et al., Cosmological implications of baryon acoustic oscillation measurements. *Phys. Rev. D* **92**(12), 123516 (2015). [arXiv:1411.1074](https://arxiv.org/abs/1411.1074)

46. V.F. Mukhanov, H.A. Feldman, R.H. Brandenberger, Theory of cosmological perturbations. Part 1. Classical perturbations. Part 2. Quantum theory of perturbations. Part 3. Extensions. *Phys. Rept.* **215**, 203–333 (1992)
47. G. Efstathiou, Cosmological perturbations, in *36th Scottish Universities Summer School in Physics, a NATO ASI: Physics of the Early Universe* (1989), pp. 361–463
48. I. Debono, G.F. Smoot, General relativity and cosmology: unsolved questions and future directions. *Universe* **2**(4), 23 (2016). [arXiv:1609.09781](https://arxiv.org/abs/1609.09781)
49. H. Goenner, On the history of unified field theories. *Living Rev. Rel.* **7**, 2 (2004)
50. M.B. Green, J. Schwarz, E. Witten, *Superstring Theory. Vol. 1: Introduction*. Cambridge Monographs on Mathematical Physics, vol. 7 (1988)
51. M.B. Green, J. Schwarz, E. Witten, *Superstring Theory. Vol. 2: Loop Amplitudes, Anomalies and Phenomenology*, vol. 7 (1988)
52. G.J. Olmo, W. Komp, Nonlinear gravity theories in the metric and Palatini formalisms. [arXiv:gr-qc/0403092](https://arxiv.org/abs/gr-qc/0403092)
53. T. Koivisto, M. Hohmann, L. Marzola, An axiomatic purification of gravity. [arXiv:1909.10415](https://arxiv.org/abs/1909.10415)
54. D. Lovelock, The Einstein tensor and its generalizations. *J. Math. Phys.* **12**, 498–501 (1971)
55. P. Avelino et al., Unveiling the dynamics of the universe. *Symmetry* **8**(8), 70 (2016). [arXiv:1607.02979](https://arxiv.org/abs/1607.02979)

Chapter 3

Foundations of Gravity—Modifications and Extensions



Christian G. Böhrmer

3.1 Preliminaries

Shortly after the formulation of General Relativity was completed in 1915, it became clear that this theory could be extended in various different ways. The theory of General Relativity (GR) is formulated using the language of differential geometry, which—in itself—was a relatively new topic of research in mathematics at that time. The geometrical setting used by Einstein consists of a four-dimensional Lorentzian manifold, equipped with a metric structure g and a covariant derivative ∇ , or equivalently, a connection $\hat{\Gamma}$. This derivative is assumed to be metric compatible and torsion free, which then uniquely determines the connection coefficients to be the Christoffel symbol components Γ .

Let us briefly dissect these assumptions to get an immediate idea of how one could modify GR. To begin with one does not have to restrict the geometry to four dimensions. Kaluza and Klein are credited with suggestions along those lines [1, 2]. The use of four dimensions relies on our experience of three spatial dimensions and a sense of time, which acts as the fourth dimension, commonly denoted as the zeroth coordinate. One could now assume that there exist other spatial dimensions that have not yet been observed. Hypothetically, there could also be other time-like dimensions. These initial ideas were motivated by the idea of geometrically unifying the different physical theories known at that time; see [3, 4] for a comprehensive review on so-called unified field theories. It is probably fair to say that String Theory has followed that path, point particles (points are zero dimensional objects) being replaced by strings (strings or curves are one-dimensional objects). Bosonic string theory is formulated in a 26-dimensional Lorentzian manifold, while superstring theory is formulated in 10 dimensions. These extra dimensions are dealt with by compactification, which means ‘rolling up’ those dimensions in such a way that

C. G. Böhrmer (✉)

Department of Mathematics, University College London, Gower Street, London WC1E 6BT, United Kingdom

e-mail: c.boehmer@ucl.ac.uk

© The Author(s), under exclusive license to Springer Nature Switzerland AG 2021

E. N. Saridakis et al. (eds.) *Modified Gravity and Cosmology*,

https://doi.org/10.1007/978-3-030-83715-0_3

they are very small, hence, effectively leading to a four-dimensional space in which Special Relativity and General Relativity are formulated.

The next generalisation concerns the connection $\hat{\Gamma}$ which neither has to be metric compatible nor torsion free. Both, non-metricity and torsion have neat geometrical interpretations [5, 6]; one speaks of an affine connection. Let us consider an infinitesimal parallelogram that is constructed by parallelly transporting two given vectors along each other. There is no a priori guarantee that this process does give a closed parallelogram. Indeed, torsion represents the failure of this infinitesimal parallelogram to close. In order to understand the effect of non-metricity on the manifold, let us consider a null vector u^μ , which means it satisfies $g_{\mu\nu}u^\mu u^\nu = 0$. If the covariant derivative of the metric tensor does not vanish, then this vector may no longer be null when parallelly transported. In particular, the light cone structure would no longer be invariant under parallel transport. However, neither the lack of closed infinitesimal parallelograms nor the non-invariance of the light cone structure under parallel transport are reason enough to discard these geometrical concepts from a physical point of view. In the end, any theoretical model of the gravitational field will make certain predictions that an experiment can either verify or falsify.

The entire discussion up to now was independent of the Einstein field equations; it merely assumed that there exists a gravitational theory that can be formulated using differential geometry. Let us now start making some connections between the mathematical formulation and the physical content of our theories. It is a well-established everyday fact that light travels along straight lines, and so do massive particles in the absence of external forces. In classical physics one would refer to these as Fermat's principle and Newton's first law, respectively. In the context of differential geometry things start to get interesting now, as a manifold equipped with a metric structure and an affine connection gives rise to two distinct curves geodesics and autoparallels. Geodesics are the shortest possible curves between two fixed end points, autoparallels are the straightest possible curves between two points. Geodesics are generally introduced by studying curves \mathcal{C} with tangent vectors $T^\mu = dX^\mu/d\lambda$ such that the quantity

$$s = \int_{\lambda_1}^{\lambda_2} \sqrt{g_{\mu\nu}T^\mu T^\nu} d\lambda, \quad (3.1)$$

is extremised. Here, $X^\mu(\lambda)$ are the local coordinates of the curve and λ is the (affine) parameter of the curve. This yields the familiar geodesic equations

$$\frac{d^2 X^\mu}{d\lambda^2} + \Gamma_{\sigma\tau}^\mu \frac{dX^\sigma}{d\lambda} \frac{dX^\tau}{d\lambda} = 0 \quad \Leftrightarrow \quad \frac{dT^\mu}{d\lambda} + \Gamma_{\sigma\tau}^\mu T^\sigma T^\tau = 0. \quad (3.2)$$

It needs to be emphasised that the geodesic equation, defined via this variational approach, depends on the Christoffel symbol components $\Gamma_{\sigma\tau}^\mu$ only. This follows from the fact that (3.1) is independent of the affine connection—that is, it depends on the metric tensor and the curve.

On the other hand, we can introduce the straightest possible curves or autoparallels. Let us again consider a curve \mathcal{C} with tangent vector T^μ , then the vector V^σ is parallelly transported along this curve if $T^\mu \nabla_\mu V^\sigma = 0$. The notion of parallel transport allows us to consider curves (defined indirectly) whose tangent vectors are parallelly transported along themselves, the tangent vector is kept as parallel as possible along the curve, hence autoparallel. Using the chain rule and the definition of covariant differentiation, the autoparallel equations are given by

$$T^\mu \nabla_\mu T^\sigma = 0 \quad \Leftrightarrow \quad \frac{dT^\mu}{d\lambda} + \hat{\Gamma}_{\sigma\tau}^\mu T^\sigma T^\tau = 0. \quad (3.3)$$

The key difference between (3.2) and (3.3) is that two different connections appear in these equations, while their form is identical. It is clear that (3.3) depends on the symmetric part of the connection, since one can exchange T^σ and T^τ ; however, it is important to state

$$\hat{\Gamma}_{(\sigma\tau)}^\mu \neq \Gamma_{\sigma\tau}^\mu, \quad (3.4)$$

which means that the symmetric part of the affine connection is not the Christoffel symbol. This symmetric part contains the Christoffel symbol, but it also depends on torsion and non-metricity, should these be present.

General Relativity is special in the sense that the shortest possible lines coincide with the straightest possible lines.¹ These considerations have practical implications. By studying the geometric properties of trajectories of test particles one can, in principle, determine whether the connection contains contributions other than those from the Christoffel symbol; see the footnote again.

In its standard formulation, the dynamical variables of General Relativity are the 10 metric functions $g_{\mu\nu}$, which are the solutions of the ten Einstein field equations

$$G_{\mu\nu} := R_{\mu\nu} - \frac{1}{2}R g_{\mu\nu} = \kappa^2 T_{\mu\nu}. \quad (3.5)$$

Here, $G_{\mu\nu}$ is the Einstein tensor, $R_{\mu\nu}$ is the Ricci tensor, R is the Ricci scalar, and $T_{\mu\nu}$ stands for the metric energy-momentum-stress tensor. This is a true tensor equation in the sense that it is valid for all coordinate systems and hence diffeomorphism invariant. In four spacetime dimensions one has four coordinates, which can be arbitrarily changed, which implies that the Einstein field equations can be viewed as six independent equations. When a Hamiltonian analysis is performed on these equations, one finds four primary constraints, thereby reducing the number of propagating degrees of freedom of this theory to two (10 metric components minus four coordinate transformations minus four primary constraints). When General Relativity is introduced in a first course—see for instance [7]—the Einstein field equations are

¹ If the affine connection differs from the Christoffel symbol components by a totally skew-symmetric piece, geodesics and autoparallels would also coincide.

motivated by comparing Newton's equations with geometrical equations, which may describe the same physics.

A more elegant approach, which somewhat lacks physical motivation from first principles, is the variational approach. The field equations can also be derived from the so-called Einstein–Hilbert action

$$S_{\text{EH}} = \frac{1}{2\kappa^2} \int g^{\mu\nu} R_{\mu\nu} \sqrt{-g} d^4x = \frac{1}{2\kappa^2} \int R \sqrt{-g} d^4x, \quad (3.6)$$

$$S_{\text{matter}} = \int \mathcal{L}_{\text{matter}}(g, \phi, \nabla\psi) d^4x = \int L_{\text{matter}}(g, \phi, \nabla\psi) \sqrt{-g} d^4x, \quad (3.7)$$

$$S_{\text{total}} = S_{\text{EH}} + S_{\text{matter}}, \quad (3.8)$$

where one varies with respect to the dynamical variable $g_{\mu\nu}$. Here, g is the determinant of the metric tensor $g_{\mu\nu}$, so that $\sqrt{-g} d^4x$ is the appropriate volume element when integrating over the manifold. The matter fields are denoted by ψ and the matter Lagrangian can depend on derivatives of the matter fields. The gravitational coupling constant κ^2 is given by $\kappa^2 = 8\pi G/c^4$. It is through this variational approach that one can introduce and motivate various gravitational theories, which can be seen as extensions or modifications of the original theory. In the following sections, some of these ideas will be discussed.

3.2 Matter Couplings

Before discussing other gravitational theories, let us briefly mention the issue of matter couplings. This is, of course, of crucial importance as gravity is universal and is the dominant interaction in the macroscopic world [8]. Lagrangians, which describe scalars (spin 0 particles) or spinors (spin 1/2 particles), typically depend on the fields and their first derivatives, thereby giving rise to equations of motion of at most second order. This also holds for Yang–Mills theories; however, we will focus our discussion on scalars and spinors for now. When the scalar or spinor field actions, formulated in Minkowski space, are formulated on an arbitrary manifold, one replaces the Minkowski metric η with an arbitrary metric g . The partial derivatives are replaced with covariant derivatives. In the scalar field case one simply has $\nabla_\mu\phi = \partial_\mu\phi$, while for spinorial fields the covariant derivative also depends on the connection and we have $\nabla_\mu\psi \neq \partial_\mu\psi$, with ψ standing for a spinor field. The immediate consequence of this is that theories in which variations with respect to the connection are considered will contain source terms when spinor fields are taken into account. Since protons, neutrons and electrons are all spin 1/2 particles, this is an important issue to keep in mind. Finally, when considering Yang–Mills theories we recall that the currents which act as the source terms are conserved and couple to the gauge fields. General Relativity can also be formulated as gauge theories; however, it is not in the form of a typical Yang–Mills theory, see [8–10]. The above mentioned approach is often

referred to as the principle of minimal coupling, however, many other coupling terms are in principle possible. There are Pauli-type terms and Jordan–Brans–Dicke-type terms where geometrical quantities like the Riemann tensor or the Ricci tensor couple to the matter fields; these mainly appear in phenomenological models or when models with symmetry breaking are concerned. Note that any coupling term which involves curvature will necessarily vanish in Special Relativity, therefore such terms require strong gravitational fields to affect the theory and to be, in principle, observable.

3.3 The Einstein–Hilbert Action—Linear Extensions

On manifolds where the connection is metric compatible and torsion free, the Einstein–Hilbert action is the unique action that is linear in a curvature scalar, and the Ricci scalar is the unique linear curvature scalar. In more general spaces with torsion and non-metricity, one can also construct the scalar $\varepsilon^{\mu\nu\kappa\lambda}\hat{R}_{\mu\nu\kappa\lambda}$, which does not vanish in general. This term appears in the so-called Palatini action of General Relativity or the Holst action. It becomes important in the context of Loop Quantum Gravity, where it appears in Ashtekar’s choice of variables, which allows the formulation of GR as a Yang–Mills type theory [11–16]. Let us return to the Einstein–Hilbert action (3.8) for now.

The Riemann curvature tensor and the Ricci tensor can be defined by the affine connection $\hat{\Gamma}$ alone, without requiring the metric tensor. To make this explicit, it is often written as $\hat{R}_{\mu\nu}$. Hence, in affine spacetimes the Einstein–Hilbert action can be generalised simply by writing

$$S = \frac{1}{2\kappa^2} \int g^{\mu\nu} \hat{R}_{\mu\nu} \sqrt{-g} d^4x, \quad (3.9)$$

$$S_{\text{matter}} = \int L_{\text{matter}}(g, \phi, \nabla\psi) \sqrt{-g} d^4x, \quad (3.10)$$

$$S_{\text{total}} = S_{\text{EH}} + S_{\text{matter}}. \quad (3.11)$$

One now considers the metric tensor g and the connection $\hat{\Gamma}$ as a priori independent dynamical variables. The matter action also depends on the connection through the covariant derivative; this is completely consistent with the principle of minimal coupling used in General Relativity. This principle states that first one writes all equations covariantly in a four-dimensional Lorentzian manifold, flat Minkowski space, then one replaces all partial derivatives with covariant derivatives and all Minkowski metric tensors with arbitrary metric tensors; see Sect. 3.2.

If we assume that the matter part of the action does not depend on the connection and we make independent variations with respect to the metric and connection, we arrive at Einstein’s theory of General Relativity. This is often referred to as the Palatini variation; however, as we will soon discuss, things become more subtle when geometries are more general.

In many ways the most natural generalisation of General Relativity is constructed when beginning with (3.11) and allowing the matter part of the action to depend on the matter fields, the metric and an independent connection. When we now compute the variations with respect to the metric and the independent connection, we arrive at two sets of field equations. Variations with respect to the metric yield equations that resemble the Einstein field equations, while variations with respect to the connection give a new set of field equations which determine the connection. The source term that appears in the latter is often referred to as the hyper-momentum $\Delta^\lambda{}_{\mu\nu}$, following a commonly used notation [6]. As the affine connection has no symmetries, the hyper-momentum tensor has, in general, 64 independent components in four dimensions.

Let us now discuss how we can connect these different theories back to General Relativity, using a mathematically consistent approach. The perhaps most elegant way to do it is through the introduction of Lagrange multipliers in the total action (3.11), so that this action is subsequently extremised subject to constraints. These constraints are introduced so that the geometrical properties of the manifold are controlled. More explicitly, let us, for the time being, extract General Relativity within the framework of metric affine theories. Recall that the two key geometrical assumptions are a metric compatible and torsion-free covariant derivative. In the language of constraints we would write

$$S_{\text{GR}} = \frac{1}{2\kappa^2} \int \left\{ g^{\mu\nu} \hat{R}_{\mu\nu} + \lambda_{(1)}^{\mu\nu\lambda} T_{\mu\nu\lambda} + \lambda_{(2)}^{\mu\nu\lambda} Q_{\mu\nu\lambda} \right\} \sqrt{-g} d^4x, \quad (3.12)$$

$$S_{\text{total}} = S_{\text{GR}} + S_{\text{matter}}, \quad (3.13)$$

where $T_{\mu\nu\lambda}$ is the torsion tensor and $Q_{\mu\nu\lambda}$ is the non-metricity tensor. Here, $\lambda_{(1)}$ and $\lambda_{(2)}$ are two Lagrange multipliers which ensure that the affine connection will become the usual Christoffel symbol. Clearly, variations with respect to $\lambda_{(1)}$ give $T_{\mu\nu\lambda} = 0$, while variation with respect to $\lambda_{(2)}$ yields $Q_{\mu\nu\lambda} = 0$.

A popular extension of General Relativity is the so-called Einstein–Cartan theory, which was proposed in the 1920s by Cartan; see [5]. Within the above framework, Einstein–Cartan theory is simply defined by

$$S_{\text{EC}} = \frac{1}{2\kappa^2} \int \left\{ g^{\mu\nu} \hat{R}_{\mu\nu} + \lambda_{(2)}^{\mu\nu\lambda} Q_{\mu\nu\lambda} \right\} \sqrt{-g} d^4x, \quad (3.14)$$

$$S_{\text{total}} = S_{\text{EC}} + S_{\text{matter}}. \quad (3.15)$$

The only difference with respect to General Relativity is the possible presence of torsion, which is no longer assumed to be zero. A natural source term for torsion would be fermions; their action depends on the connection, and hence variations with respect to the connection lead to source terms for torsion. A peculiar property of Einstein–Cartan theory is that the field equations for torsion are algebraic; they do not contain derivatives of the torsion tensor. This immediately implies that torsion cannot propagate, and consequently, only regions of spacetime that contain sources of torsion can contain torsion. This is in stark contrast to curvature, a fact well-known

in GR. The Schwarzschild solution, for instance, is a vacuum (source-free) solution of the Einstein field equations, yet contains curvature. Likewise, gravitational waves can propagate through otherwise empty regions of space-time; torsional waves in this sense do not exist in Einstein–Cartan theory.

If we recall that Minkowski space is the setting of Special Relativity, we can of course also include this using the above approach, namely we consider the following theory

$$S_{\text{Mink}} = \frac{1}{2\kappa^2} \int \left\{ g^{\mu\nu} \hat{R}_{\mu\nu} + \lambda_{(0)}^{\mu\nu\lambda\kappa} \hat{R}_{\mu\nu\lambda\kappa} + \lambda_{(1)}^{\mu\nu\lambda} T_{\mu\nu\lambda} + \lambda_{(2)}^{\mu\nu\lambda} Q_{\mu\nu\lambda} \right\} \sqrt{-g} d^4x. \quad (3.16)$$

Minkowski space is the unique space that has vanishing torsion, vanishing non-metricity and is globally flat.

However, what makes this approach, using constraints, particularly useful is the ability to systematically study a variety of theories in a uniform setting; see also [17]. Let us now discuss a theory, which is equivalent to General Relativity but is formulated rather differently. It was noted in the 1920s by Einstein and others that there exists a formulation of General Relativity based solely on the torsion tensor; this theory is now known as the Teleparallel Equivalent of General Relativity (TEGR).

Start as before, within the setting of metric-affine theories where the connection is assumed to be fully independent of the metric, we can define the Teleparallel Equivalent of General Relativity by

$$S_{\text{TEGR}} = \frac{1}{2\kappa^2} \int \left\{ g^{\mu\nu} \hat{R}_{\mu\nu} + \lambda_{(0)}^{\mu\nu\lambda\kappa} \hat{R}_{\mu\nu\lambda\kappa} + \lambda_{(2)}^{\mu\nu\lambda} Q_{\mu\nu\lambda} \right\} \sqrt{-g} d^4x. \quad (3.17)$$

We note that the constraints force the connection to be metric compatible (no non-metricity, $Q_{\mu\nu\lambda} = 0$) and make the manifold *globally* flat, $\hat{R}_{\mu\nu\lambda\kappa} = 0$ everywhere. There is now a conceptual issue to understand: Is the theory so defined non-trivial? This is a natural question to ask, as we know that only Minkowski space satisfies $R_{\mu\nu\lambda\kappa} = 0$ everywhere in the usual GR setting. To answer this, let us begin by introducing the so-called contortion tensor K , defined by

$$\hat{\Gamma}_{\sigma\tau}^{\mu} = \Gamma_{\sigma\tau}^{\mu} + K_{\sigma\tau}^{\mu}. \quad (3.18)$$

The contortion tensor simply contains all the information of the connection that is not part of the Christoffel symbol. In other words, it contains the deviations from the standard GR framework. When we compute the Riemann curvature tensor for the full connection $\hat{\Gamma}_{\sigma\tau}^{\mu}$ and express the result using the Christoffel symbol and the contortion tensor, we arrive at the neat result

$$\hat{R}_{\nu\mu\lambda}^{\kappa} = R_{\nu\mu\lambda}^{\kappa} + \nabla_{\nu}^{\Gamma} K_{\mu\lambda}^{\kappa} - \nabla_{\mu}^{\Gamma} K_{\nu\lambda}^{\kappa} + K_{\nu\rho}^{\kappa} K_{\mu\lambda}^{\rho} - K_{\nu\rho}^{\kappa} K_{\mu\lambda}^{\rho}, \quad (3.19)$$

which means that the curvature tensor splits into two parts: the Levi–Civita part $R_{\nu\mu\lambda}{}^\kappa$, which is constructed using the Christoffel symbols components only, and a second part that depends on the contortion tensor. The notation ∇^Γ stands for the covariant derivative involving the Christoffel symbol components. One normally defines the torsion tensor to be the skew symmetric part of the affine connection $T_{\mu\nu}{}^\kappa = (\hat{\Gamma}_{\mu\nu}{}^\kappa - \hat{\Gamma}_{\nu\mu}{}^\kappa)/2$ so that, in spaces where $Q_{\mu\nu\lambda} = 0$, one has the simple relation

$$T_{\mu\nu}{}^\kappa = \frac{1}{2} \left(K_{\mu\nu}{}^\kappa - K_{\nu\mu}{}^\kappa \right). \quad (3.20)$$

Therefore, there is a linear relation between torsion and contortion. Going back to (3.17), which imposes the constraint $\hat{R}_{\mu\nu\lambda\kappa} = 0$, we can now attempt to understand this condition in view of (3.19). Is it always possible to choose a contortion or torsion tensor for a given curvature tensor $R_{\nu\mu\lambda}{}^\kappa$ such that the full metric-affine curvature vanishes?

The answer to this question is affirmative; this choice can be made but it requires a little bit more mathematics. Let e_μ^A be four linearly independent orthonormal co-vector or co-frame fields, often called tetrads, which allow us to write the metric tensor at any point of the manifold as

$$g_{\mu\nu} = e_\mu^A e_\nu^B \eta_{AB}. \quad (3.21)$$

These fields can be used to define the frame components of any vector via $V^A = e_\mu^A V^\mu$. Moreover, one needs to introduce the spin connection $\hat{\omega}_\mu^A{}_B$, which is defined through the vanishing of the covariant derivative of the tetrad

$$\nabla_\mu e_\nu^A = 0 \quad \Leftrightarrow \quad \partial_\mu e_\nu^A + \hat{\omega}^A{}_{B\mu} e_\nu^B - \hat{\Gamma}_{\mu\nu}^\sigma e_\sigma^A = 0. \quad (3.22)$$

We can now express the complete (Levi–Civita plus torsional contributions) Riemann curvature tensor using either the connection or the spin connection. In the latter case we have

$$\hat{R}^A{}_{B\mu\nu} = \partial_\mu \hat{\omega}^A{}_{B\nu} - \partial_\nu \hat{\omega}^A{}_{B\mu} + \hat{\omega}^A{}_{C\mu} \hat{\omega}^C{}_{B\nu} - \hat{\omega}^A{}_{C\nu} \hat{\omega}^C{}_{B\mu}, \quad (3.23)$$

which now allows us to make the following useful observations. If we choose $\hat{\omega}^A{}_{B\mu} = 0$ everywhere, then $\hat{R}^A{}_{B\mu\nu} = 0$ everywhere. This means that, applying the decomposition (3.18) to the spin connection, we can write

$$\hat{\omega}^A{}_{B\mu} = \omega^A{}_{B\mu} + K_\mu^A{}_B, \quad (3.24)$$

which implies that $\hat{\omega}^A{}_{B\mu} = 0$, or equivalently $\omega^A{}_{B\mu} = -K_\mu^A{}_B$. Therefore, for any Levi–Civita spin connection $\omega^A{}_{B\mu}$ there exists a contortion tensor $K_\mu^A{}_B$ such that $\hat{\omega}^A{}_{B\mu} = 0$. This result was found by Weitzenböck, who noted that this connection can always be constructed, given a tetrad. Putting this result back into (3.19) allows

us to rewrite the complete Ricci scalar in terms of the Levi–Civita part and a torsion part; this gives

$$\hat{R} = 0 \quad \Leftrightarrow \quad R + 2\nabla_\nu^\Gamma K^\lambda{}_\lambda{}^\nu + K_{\nu\rho}{}^\nu K^\lambda{}_\lambda{}^\rho - K_{\nu\rho}{}^\nu K^\lambda{}_\lambda{}^\rho = 0. \quad (3.25)$$

Consequently, we have an alternative formulation of the Einstein–Hilbert action (3.8) using the previous identity, namely

$$S_{\text{EH}} = \frac{1}{2\kappa^2} \int R\sqrt{-g} d^4x \quad \Leftrightarrow \quad S_{\text{TEGR}} = \frac{1}{2\kappa^2} \int \{K_{\nu\rho}{}^\nu K^\lambda{}_\lambda{}^\rho - K_{\nu\rho}{}^\nu K^\lambda{}_\lambda{}^\rho\} e d^4x, \quad (3.26)$$

where we neglected the boundary term that does not contribute to the equations of motion. Here, e denotes the determinant of the tetrad field, which satisfies $e = \sqrt{-g}$ due to (3.21). This is the standard formulation of the Teleparallel Equivalent of General Relativity where the tetrad e^a_μ is the independent dynamical variable and the spin connection vanishes identically [18].

The issue of matter couplings was mentioned earlier, and the Teleparallel Equivalent of General Relativity is a good case study when it comes to matter couplings, especially for spin 1/2 particles. The Lagrangian for a Dirac field contains the term $\nabla\psi$, where, as before, ψ stands for the spinor field. Its covariant derivative depends explicitly on the connection, which is no longer a dynamical variable in the teleparallel formulation. This leads to issues regarding the coupling prescription of Dirac fields; see in particular the series of papers [19–23] and the references given therein. It was pointed out in [23] that this problem is generic and affects all Poincare gauge theories that admit a teleparallel formulation.

3.4 The Einstein–Hilbert Action—Nonlinear Extensions

All theories considered so far were based on an action linear in the curvature scalar as the key ingredient to formulate gravitational theories; however, we already noted in (3.26) that such actions are quadratic in the contortion tensor. From a theoretical point of view it is well motivated to consider more general theories, which depend on other scalars constructed out of the Riemann curvature tensor or the Ricci tensor. There is no reason to exclude terms like $c_1 R_{\mu\nu} R^{\mu\nu}$, for example, in a gravitational action. Alternatively, one can consider theories where an arbitrary function of the Ricci scalar is considered. In the following we will focus on the latter approach.

The key idea of this scheme is to consider the action

$$S_{f(R)} = \frac{1}{2\kappa^2} \int f(R)\sqrt{-g} d^4x, \quad (3.27)$$

$$S_{\text{matter}} = \int L_{\text{matter}}(g, \phi, \nabla\psi)\sqrt{-g} d^4x, \quad (3.28)$$

$$S_{\text{total}} = S_{f(R)} + S_{\text{matter}}, \quad (3.29)$$

where $f(R)$ is a sufficiently regular function of the Ricci scalar. When choosing $f(R) = R$, one recovers General Relativity, while the choice $f(R) = R - 2\Lambda$ introduces the cosmological constant into the field equations. Such a model was studied in the context of cosmology by [24]; however, it was only after the observation of the accelerated expansion of the Universe that models of this type became more mainstream and were subsequently thoroughly studied [25, 26]; for reviews on $f(R)$ gravity the reader is referred to [27–29]. The basic idea underlying this approach is to view General Relativity as the lowest order theory. To see this, recall that Minkowski spacetime is the geometrical framework for Special Relativity that satisfies $R_{\mu\nu\lambda\kappa} = 0$, the space being globally flat. Let us consider a series expansion of $f(R)$ around Minkowski spacetime, then $f(R) = f(0) + f'(0)R + f''(0)R^2/2 + \dots$ so that a term linear in R emerges quite naturally.

However, if one wishes to modify General Relativity for cosmological applications in particular, this expansion might not be ideal. Over very large scales the curvature becomes small, which motivates modifications that contain inverse powers of the Ricci scalar; clearly such terms pose problems when considering Minkowski space. Other models contain nonlinear functions of total derivative terms, like the Gauss–Bonnet term, for example. The Gauss–Bonnet term is related to a topological number, the Euler characteristic of the manifold. However, when any nonlinear function of any topological quantity is added to the action, it will yield some non-trivial field equations. Of course, one can also introduce new couplings between the geometry and the matter, different from the minimal coupling. Theories of this type have also received substantial attention; see in particular [30] for a comprehensive reference of such models. Let us add a small sceptic’s remark: A function f contains uncountably many degrees of freedom, so it is perhaps not too surprising that various models are able to fit a variety of observational data.

Going back to the Teleparallel Equivalent of General Relativity, one could apply the same ideas to the action (3.26) and consider nonlinear models. The scalar that appears in the integrand of S_{TTEGR} is often denoted by \mathbb{T} , so that (3.25) can be written in the convenient form $R = -\mathbb{T} + B$, where B stands for the boundary term. Consequently, one would consider the model

$$S_{f(\mathbb{T})} = \frac{1}{2\kappa^2} \int f(\mathbb{T}) \sqrt{-g} d^4x, \quad (3.30)$$

$$S_{\text{matter}} = \int L_{\text{matter}}(g, \phi, \nabla\psi) \sqrt{-g} d^4x, \quad (3.31)$$

$$S_{\text{total}} = S_{f(\mathbb{T})} + S_{\text{matter}}, \quad (3.32)$$

which was first suggested in [31] and also led to a surge of interest; for reviews see [32, 33]. These models allow for cosmological solutions with accelerated expansion without the need to introduce dark energy. From a conceptual point of view, modified teleparallel theories of gravity are interesting, as these are no longer invariant under local Lorentz transformation in their standard formulation; this means the choice $\omega_{\mu}{}^A{}_B = 0$, where the spin connection vanishes identically. To see this, one only has

to note that neither \mathbb{T} nor B are Lorentz scalars; the combination $R = -\mathbb{T} + B$ is the unique Lorentz scalar that can be constructed, implying that General Relativity and $f(R)$ gravity are both locally Lorentz invariant, while any nonlinear theories based on combinations of \mathbb{T} and B are not; see [34]. We note that a fully invariant formulation of modified teleparallel gravity models has been proposed [35]. It is very interesting to study the degrees of freedom in $f(\mathbb{T})$ gravity in four dimensions; see [36–38]. While in $f(R)$ gravity the extra degree of freedom is easily interpreted as a scalar due to the function f , an analogue interpretation in $f(\mathbb{T})$ cannot be made and the precise meaning of the extra degrees of freedom is an open question in the field.

Breaking local Lorentz invariance can be well motivated by considering physics on very small scales. Quantum theory implies that positions and momenta cannot be measured simultaneously with unlimited accuracy. Consequently, one would expect a certain length scale at which local Lorentz transformations break down.

Let us finish this section with another sceptic’s remark: Once one starts to consider nonlinear theories based on various scalar quantities, motivated either by the geometry or the matter content, one is able to create a plethora of theories. The entirety of such models is so large that it is (practically) impossible to study all of them. Clearly, many of these models can be built to pass a variety of observational tests due to their generality. What appears to be missing at the moment is an overarching guiding principle, which would allow us to restrict our attention to a small class of models based on some neat theoretical argument.

References

1. T. Kaluza, Zum Unitätsproblem der Physik. Sitzungsber. Preuss. Akad. Wiss. Berlin (Math. Phys.) **1921**, 966–972 (1921). [arXiv:1803.08616](https://arxiv.org/abs/1803.08616). [Int. J. Mod. Phys. D **27**(14), 1870001 (2018)]
2. O. Klein, Quantum theory and five-dimensional theory of relativity. (In German and English). Z. Phys. **37**, 895–906 (1926)
3. H.F.M. Goenner, On the history of unified field theories. Living Rev. Relat. **7**, 2 (2004)
4. H.F.M. Goenner, On the history of unified field theories. Part ii. (ca. 1930–ca. 1965). Living Rev. Relat. **17**, 5 (2014)
5. F.W. Hehl, P. Von Der Heyde, G.D. Kerlick, J.M. Nester, General relativity with spin and torsion: foundations and prospects. Rev. Mod. Phys. **48**, 393–416 (1976)
6. F.W. Hehl, J. McCrea, E.W. Mielke, Y. Ne’eman, Metric affine gauge theory of gravity: field equations, Noether identities, world spinors, and breaking of dilation invariance. Phys. Rept. **258**, 1–171 (1995). [arXiv:gr-qc/9402012](https://arxiv.org/abs/gr-qc/9402012)
7. C.G. Böhm, *Introduction to General Relativity and Cosmology*. Essential Textbooks in Physics, vol. 2. (World Scientific (Europe), London, 2016)
8. M. Blagojević, F.W. Hehl (eds.), *Gauge Theories of Gravitation* (World Scientific, Singapore, 2013)
9. Y.N. Obukhov, Poincare gauge gravity: selected topics. Int. J. Geom. Meth. Mod. Phys. **3**, 95–138 (2006). [arXiv:gr-qc/0601090](https://arxiv.org/abs/gr-qc/0601090)
10. R. Aldrovandi, J.G. Pereira, *Teleparallel Gravity*, vol. 173 (Springer, Dordrecht, 2013)
11. A. Ashtekar, New variables for classical and quantum gravity. Phys. Rev. Lett. **57**, 2244–2247 (1986)

12. A. Ashtekar, New Hamiltonian formulation of general relativity. *Phys. Rev. D* **36**, 1587–1602 (1987)
13. J.F.G. Barbero, Real Ashtekar variables for Lorentzian signature space times. *Phys. Rev. D* **51**, 5507–5510 (1995). [arXiv:gr-qc/9410014](https://arxiv.org/abs/gr-qc/9410014)
14. S. Holst, Barbero’s Hamiltonian derived from a generalized Hilbert-Palatini action. *Phys. Rev. D* **53**, 5966–5969 (1996). [arXiv:gr-qc/9511026](https://arxiv.org/abs/gr-qc/9511026)
15. G. Immirzi, Real and complex connections for canonical gravity. *Class. Quant. Grav.* **14**, L177–L181 (1997). [arXiv:gr-qc/9612030](https://arxiv.org/abs/gr-qc/9612030)
16. T. Thiemann, *Modern Canonical Quantum General Relativity*. Cambridge Monographs on Mathematical Physics. (Cambridge University Press, Cambridge, 2007)
17. J.B. Jiménez, L. Heisenberg, T.S. Koivisto, The geometrical trinity of gravity. *Universe* **5**(7), 173 (2019). [arXiv:1903.06830](https://arxiv.org/abs/1903.06830)
18. J.W. Maluf, The teleparallel equivalent of general relativity. *Annalen Phys.* **525**, 339–357 (2013). [arXiv:1303.3897](https://arxiv.org/abs/1303.3897)
19. Yu.N. Obukhov, J.G. Pereira, Metric affine approach to teleparallel gravity. *Phys. Rev. D* **67**, 044016 (2003). [arXiv:gr-qc/0212080](https://arxiv.org/abs/gr-qc/0212080)
20. J.W. Maluf, Dirac spinor fields in the teleparallel gravity: comment on ‘Metric affine approach to teleparallel gravity’. *Phys. Rev. D* **67**, 108501 (2003). [arXiv:gr-qc/0304005](https://arxiv.org/abs/gr-qc/0304005)
21. E.W. Mielke, Consistent coupling to Dirac fields in teleparallelism: comment on ‘Metric-affine approach to teleparallel gravity’. *Phys. Rev. D* **69**, 128501 (2004)
22. Yu.N. Obukhov, J.G. Pereira, Lessons of spin and torsion: reply to ‘Consistent coupling to Dirac fields in teleparallelism’. *Phys. Rev. D* **69**, 128502 (2004). [arXiv:gr-qc/0406015](https://arxiv.org/abs/gr-qc/0406015)
23. M. Leclerc, On the teleparallel limit of Poincare gauge theory. *Phys. Rev. D* **71**, 027503 (2005). [arXiv:gr-qc/0411119](https://arxiv.org/abs/gr-qc/0411119)
24. J.D. Barrow, A.C. Ottewill, The stability of general relativistic cosmological theory. *J. Phys. A* **16**, 2757 (1983)
25. S. Capozziello, Curvature quintessence. *Int. J. Mod. Phys. D* **11**, 483–492 (2002). [arXiv:gr-qc/0201033](https://arxiv.org/abs/gr-qc/0201033)
26. S. Capozziello, S. Carloni, A. Troisi, Quintessence without scalar fields. *Recent Res. Dev. Astron. Astrophys.* **1**, 625 (2003). [arXiv:astro-ph/0303041](https://arxiv.org/abs/astro-ph/0303041)
27. T.P. Sotiriou, V. Faraoni, $f(R)$ Theories Of Gravity. *Rev. Mod. Phys.* **82**, 451–497 (2010). [arXiv:0805.1726](https://arxiv.org/abs/0805.1726)
28. A. De Felice, S. Tsujikawa, $f(R)$ theories. *Living Rev. Rel.* **13**, 3 (2010). [arXiv:1002.4928](https://arxiv.org/abs/1002.4928)
29. S. Nojiri, S.D. Odintsov, Unified cosmic history in modified gravity: from $F(R)$ theory to Lorentz non-invariant models. *Phys. Rept.* **505**, 59–144 (2011). [arXiv:1011.0544](https://arxiv.org/abs/1011.0544)
30. T. Harko, F.S.N. Lobo, *Extensions of $f(R)$ Gravity* (Cambridge University Press, Cambridge, 2018)
31. R. Ferraro, F. Fiorini, Modified teleparallel gravity: inflation without inflaton. *Phys. Rev. D* **75**, 084031 (2007). [arXiv:gr-qc/0610067](https://arxiv.org/abs/gr-qc/0610067)
32. S. Capozziello, M. De Laurentis, Extended theories of gravity. *Phys. Rept.* **509**, 167–321 (2011). [arXiv:1108.6266](https://arxiv.org/abs/1108.6266)
33. Y.-F. Cai, S. Capozziello, M. De Laurentis, E.N. Saridakis, $f(T)$ teleparallel gravity and cosmology. *Rept. Prog. Phys.* **79**(10), 106901 (2016). [arXiv:1511.07586](https://arxiv.org/abs/1511.07586)
34. S. Bahamonde, C.G. Böhmer, M. Wright, Modified teleparallel theories of gravity. *Phys. Rev. D* **92**(10), 104042 (2015). [arXiv:1508.05120](https://arxiv.org/abs/1508.05120)
35. M. Krssak, R.J. van den Hoogen, J.G. Pereira, C.G. Böhmer, A.A. Coley, Teleparallel theories of gravity: illuminating a fully invariant approach. *Class. Quant. Grav.* **36**(18), 183001 (2019). [arXiv:1810.12932](https://arxiv.org/abs/1810.12932)
36. R. Ferraro, M.J. Guzmán, Hamiltonian formalism for $f(T)$ gravity. *Phys. Rev. D* **97**(10), 104028 (2018). [arXiv:1802.02130](https://arxiv.org/abs/1802.02130)
37. R. Ferraro, M.J. Guzmán, Quest for the extra degree of freedom in $f(T)$ gravity. *Phys. Rev. D* **98**(12), 124037 (2018). [arXiv:1810.07171](https://arxiv.org/abs/1810.07171)
38. M. Blagojević, J.M. Nester, Local symmetries and physical degrees of freedom in $f(T)$ gravity: a Dirac Hamiltonian constraint analysis. *Phys. Rev. D* **102**(6), 064025 (2020). [arXiv:2006.15303](https://arxiv.org/abs/2006.15303)

Part I
Theories of Gravity

Chapter 4

Introduction to Part I



Salvatore Capozziello and Jose Beltrán Jiménez

General Relativity has not ceased its outstanding performance to explain gravitational phenomena with exquisite accuracy in an ever increasing range of scales. In this respect, local gravity experiments, Solar System tests and astrophysical objects have played a central role in establishing the fundamental properties of the gravitational interaction, showing no deviations with respect to General Relativity. Cosmology, on the other hand, has traditionally been a driving force for speculations beyond General Relativity, whose only limitation was the imagination of the theoretical cosmologists. In the last two decades, however, the accumulation of precise cosmological measurements has substantially constrained the permitted theories and we have now the means to robustly rule out wide classes of theories. At the same time, these cosmological observations have triggered investigations seeking for theories beyond General Relativity, mainly motivated by the three fundamental missing ingredients of the standard cosmological model: dark matter, dark energy and inflation.

A very distinctive feature of gravity that actually guided Einstein to its original formulation is its intimate relation with inertia, to the point that it is possible to interpret gravity (at least locally) as a purely inertial effect. This is rooted in the

S. Capozziello (✉)

Dipartimento di Fisica “E. Pancini”, Università di Napoli “Federico II”, 80126 Napoli, Italy

INFN, Sezione di Napoli, Complesso Universitario di Monte S. Angelo, Via Cintia Edificio 6, 80126 Napoli, Italy

Laboratory for Theoretical Cosmology, Tomsk State University of Control Systems and Radioelectronics (TUSUR), 634050 Tomsk, Russia

e-mail: capozziello@na.infn.it

J. B. Jiménez

Departamento de Física Fundamental and IUFFyM, Universidad de Salamanca, E-37008 Salamanca, Spain

e-mail: jose.beltran@usal.es

© The Author(s), under exclusive license to Springer Nature Switzerland AG 2021

E. N. Saridakis et al. (eds.) *Modified Gravity and Cosmology*,

https://doi.org/10.1007/978-3-030-83715-0_4

equivalence principle that dictates the universal character of gravity, which in turn lies at the very heart of the possibility to interpret gravity in geometrical terms. We thus arrive at the properties that could be used to *define* gravity from its geometrical side. From a field theory perspective, General Relativity is a theory that describes the interactions of a massless spin-2 particle. It is profoundly remarkable that by starting with a massless spin-2 particle and imposing some reasonable additional assumptions like Lorentz-invariance, it naturally follows that this particle *must* couple universally (at low energies) to matter fields, and its interactions are precisely those of General Relativity. Thus, from the field theory side, the fundamental defining property of gravity could be identified with its massless spin-2 nature. The structure of General Relativity then results as a particular consequence of the strict rules that govern the interactions of massless particles.

The approaches to modifications of General Relativity come in several fashions, which can be broadly divided into those essentially based on adding new fields, and those that fully embrace its geometrical description and hence the modifications are based on modified geometrical scenarios. Definitely, this separation may be regarded as purely conventional and, as a matter of fact, it is not difficult to go from one to the other in some scenarios. This is clearly illustrated by, for example, gravity theories in a Weyl geometry that can equivalently be regarded as a theory with an extra vector field provided by the Weyl non-metricity trace. As it occurs many times, however, the starting point or interpretation of the same theory can serve as motivation and inspiration to explore different modified gravity scenarios. It is nevertheless important to keep in mind the basic properties that make General Relativity special among all gravity theories, so that the modifications can be clearly ascribed to the breaking of one of the fundamental assumptions for General Relativity. This is particularly important in helping us to discern truly modified theories from those that are simply General Relativity in disguise.

Modifying General Relativity is an arduous task, not only for its aforementioned exquisite performance to explain observations, but because its internal structure is tightly constrained by consistency conditions that are ultimately imposed by the massless spin-2 nature of the graviton. This delicate structure causes many (infrared) modifications of General Relativity to be doomed from their very conception, and this has fuelled an intense activity in recent years to find theoretically consistent modifications of General Relativity that in turn could play a role in describing the Universe's dark sector or inflation. This Part will be devoted to disclosing some of the most popular and interesting modifications of gravity that have been explored, as well as their potential interest for cosmology.

Chapter 5

A Flavour on $f(R)$ Theories: Theory and Observations



Álvaro de la Cruz-Dombriz

5.1 Historia, Lux Veritatis

Modifications to the General Theory of Relativity (GR) emerged almost immediately upon its acceptance by the scientific community. By 1919, Weyl had already toyed with the inclusion of higher-order curvature invariants in the usual Einstein–Hilbert action. Probably the first competitor to Einstein’s GR was Nordström’s 1912 conformally flat scalar theory of gravity. In 1937, Dirac showed, by allowing the gravitational coupling G to vary slowly over cosmological time scales, that there was a relationship that naturally emerged, between the cosmological constants and the fundamental physical constants. This idea was further developed by Jordan, a little over a decade later, using a scalar field to describe the gravitational coupling. In his theory, the gravitational scalar field behaved like a matter field, and satisfied a conservation law that was added to the theory [2]. By 1961, these ideas, thanks to Brans and Dicke [1], culminated a complete gravitational theory, containing one scalar field, which, together with the metric tensor, is responsible for the gravitational interaction. The so-called Brans–Dicke theory is indeed considered to be the prototype of alternative theories to GR [3].

While this and other attempts were driven solely by curiosity, the physical motivation for such exercises was yet to come. In the following decades, the strong gravity regime of physics stimulated interest in higher-order theories of gravity, where it was shown that, unlike GR, higher-order theories are renormalisable [4]. Moreover, tak-

The original version of this chapter was revised. The affiliation of the author, Álvaro de la Cruz-Dombriz has been corrected in this chapter. The correction to this chapter is available at https://doi.org/10.1007/978-3-030-83715-0_39.

Á. de la Cruz-Dombriz (✉)

Cosmology and Gravity Group, Department of Mathematics and Applied Mathematics,
University of Cape Town, Rondebosch, Cape Town 7701, South Africa
e-mail: alvaro.delacruzdombriz@uct.ac.za

Departamento de Física Fundamental and IUFFyM, Universidad de Salamanca, Salamanca, Spain

© The Author(s), under exclusive license to Springer Nature Switzerland AG 2021,
corrected publication 2022

43

E. N. Saridakis et al. (eds.) *Modified Gravity and Cosmology*,
https://doi.org/10.1007/978-3-030-83715-0_5

ing the consideration of quantum corrections into account requires the gravitational action to include higher-order curvature invariants [5–8]. In such cases, the modification to GR would be appreciable only at scales either of the order of the Planck length in the primordial Universe [9] or in the neighbourhood of extremely dense objects [10, 11]. Complementary late-time implications (in the low-energy regime) of modified, also dubbed extended, theories of gravity only became a field of interest later in the 20th century, when the revelation that over 75% of the energy density of the Universe may be unknown became evident from several experiments, including Supernovae type Ia [12], large-scale structure power spectra measurements [13] and the study of CMB physics [14], among others.

Thereafter, scalar field considerations towards viable alternatives to GR, which include the aforementioned Brans–Dicke theory as a subclass, developed into branches of research, including scalar fields coupled non-minimally to curvature and induced gravity. Further popularity of the addition of an extra gravitational scalar field stems from the fact that such a field is actually a vital part of theories such as supergravity, superstring and M-theories. Moreover, scalar fields have also been essential in the development of the inflationary paradigm following the increasing support of an inflationary epoch capable of curing several well-known shortcomings of the Cosmological Concordance (Λ CDM) Model with an initial—Big Bang—singularity.

Thus, it became evident that the required dark energy component indicates the existence of either unknown forms of energy density or additional physics, or both. For instance, the Cosmological Concordance Λ CDM Model contains two *dark* forms of energy, namely dark matter and dark energy, as well as a required, physically unexplained, period of rapid inflation. Although Λ CDM paradigm is able to match many observations with high precision, it suffers from several well-known drawbacks [15]. Consequently, there is no a priori epistemological reason—not even a naive invocation to Ockham’s razor!—to dismiss a theory of gravity for which the observed accelerated expansion of the Universe would emerge as a low energy, large-scale geometrical consequence, rather than requiring the ad hoc introduction of exotic dark fluids with no observational ground.

Any extension of GR amounts to making one or more generalisations of the following form: (i) adding extra fields (ii) including higher-order derivatives of the curvature or curvature-related invariants or other invariants and (iii) adding dimensions to the spacetime. These modifications resulted in a plethora of extended gravity theories deserving study [16, 17] and were indeed far much richer than GR in complexity. Without trying to be rigorous, a few paradigmatic examples would include Lovelock theories featuring field equations of second order in the metric [18], Gauss–Bonnet theories [19–21], scalar-tensor theories [1, 22–24], Tensor-Vector-Scalar (TeVeS) [25–27], theories with extra dimensions [28], and Dvali–Gabadadze–Porrati (DGP) [29] theories for gravity.

In this chapter we shall focus on a class of theories, dubbed $f(R)$, that gained popularity after the discovery of the accelerating present epoch of the Universe, but which had been considered originally in the context of inflation [9]. Such theories involve introducing a generic function of the Ricci scalar into the gravitational action from

which the field equations are subsequently derived. Obviously, once field equations are at hand, both theoretical and observational constraints must be carefully studied in order to assess—or dismiss—the validity of classes of models in the context of these theories.

This chapter is organised as follows: first, in Sect. 5.2 we shall provide a detailed review on the foundations of the scalar-tensor theories of gravity, with some emphasis on the Brans–Dicke theory. The underlying idea would be then to present, in Sect. 5.3, the equivalence between $f(R)$ theories and this subclass of scalar-tensor theories; namely, Brans–Dicke gravity. Therein, we shall first revise some of the most relevant formalisms to study such theories. Also, the viability requirements that $f(R)$ theories need to obey to be considered as a viable alternative to Einsteinian gravity will be displayed. Then, in Sect. 5.4, the $f(R)$ cosmological evolution technicalities within the metric formalism when applied to the usual four-dimensional Friedmann–Lemaître–Robertson–Walker geometry will be provided so that the appearance of an effective curvature fluid becomes evident. Subsequently, as a natural step forward, in Sect. 5.5 we shall provide a thorough revision on how the use of $1 + 3$ covariant gauge-invariant variables can be applied to extended theories of gravity, $f(R)$ theories in particular. This route renders the analysis of cosmological scalar perturbations highly transparent, so that the latest large-scale structure data can be rigorously compared against theoretical predictions. A reader still unfamiliar with this technique will surely find this section very enlightening and accessible to follow. The next two Sects. 5.6 and 5.7, are devoted to illustrate two paradigmatic gravitational features of $f(R)$ theories. On the one hand, in Sect. 5.6 the equivalent geodesic deviation equation for these theories is derived, and the consequences for the observer area distance extracted, a fact with relevant cosmological implications in the measure of distances and comparison with eventual data. On the other hand, in Sect. 5.7 we shall briefly address the attractive or repulsive character that these theories exhibit in a cosmological context. This discussion is obviously related to the literature devoted to studying the so-called energy conditions in the context of extended theories of gravity and thus, it may help to shed some light on these controversial issues depending on the authors one follows. Finally, we present our conclusions in Sect. 5.8.

5.2 Scalar-Tensor Theories

In this section we review the action of general scalar-tensor theories, their resulting field equations, and the equivalence between $f(R)$ gravity and scalar-tensor gravity. Although the bulk of the considerations in subsequent sections may be done from a purely metric $f(R)$ fourth-order gravity perspective, viewing such theories from a scalar-tensor framework may offer some insight into the physical dynamics of the resulting effective scalar field potential. Such a comparison proves useful when facing solutions containing singularities.

5.2.1 Field Equations of Scalar-Tensor Gravity

Scalar-tensor theories of gravity include Brans–Dicke, Galileons, $f(R)$, quintessence and Horndeski theories as subclasses. The general Lagrangian for a scalar tensor theory has the form [16],

$$\mathcal{L} = \frac{1}{2\kappa^2} \sqrt{-g} [f(\phi)R - g(\phi)\nabla_\mu\phi\nabla^\mu\phi - 2\lambda(\phi)] + \mathcal{L}_m(\psi, h(\phi)g_{\mu\nu}), \quad (5.1)$$

where f , g , h and λ are all arbitrary functions of the scalar field ϕ and \mathcal{L}_m accounts for the Lagrangian of the matter fields ψ . Moreover, $\kappa^2 = 8\pi G$ holds for the usual gravitational constant and R is the Ricci scalar curvature. The function $h(\phi)$ may be absorbed into the metric following the conformal transformation

$$h(\phi)g_{\mu\nu} \rightarrow g_{\mu\nu}. \quad (5.2)$$

Should that transformation be performed, the resulting frame is known as the Jordan frame. Therein, the scalar field and matter are independent, the motion of test particles follows geodesics, and the weak equivalence principle is satisfied for massless test particles. The effects of this transformation on the arbitrary functions f , g , h and λ , may be absorbed by a suitable redefinition of these functions. For instance, by setting $f(\phi) \rightarrow \phi$, we can write the Lagrangian density as

$$\mathcal{L} = \frac{1}{2\kappa^2} \sqrt{-g} \left[\phi R - \frac{\omega(\phi)}{\phi} \nabla_\mu\phi\nabla^\mu\phi - 2\Lambda(\phi) \right] + \mathcal{L}_m(\psi, g_{\mu\nu}), \quad (5.3)$$

where $\omega(\phi)$ represents an arbitrary function, dubbed the coupling parameter, and the function Λ provides a generalisation of the cosmological constant (in the case where $\omega(\phi)$ is a constant we shall denote it by ω_0). Variation of the corresponding action for (5.3) with respect to the metric tensor leads to the following equations:

$$\phi G_{\mu\nu} + \left[\square\phi + \frac{1}{2} \frac{\omega}{\phi} (\nabla\phi)^2 + \Lambda \right] g_{\mu\nu} - \nabla_\mu\nabla_\nu\phi - \frac{\omega}{\phi} \nabla_\mu\phi\nabla_\nu\phi = \kappa^2 T_{\mu\nu}^{(m)}, \quad (5.4)$$

where, as usual, $T_{\mu\nu}^{(m)}$ holds for the usual stress-energy matter tensor

$$T_{\mu\nu}^{(m)} = \frac{-2}{\sqrt{-g}} \frac{\delta}{\delta g^{\mu\nu}} (\sqrt{-g} \mathcal{L}_m). \quad (5.5)$$

As mentioned above, within the Jordan frame, the scalar field is also an independent dynamical quantity, so variation of the action with respect to ϕ yields the additional field equation

$$(2\omega + 3)\square\phi + \omega'(\nabla\phi)^2 + 4\Lambda - 2\phi\Lambda' = \kappa^2 T^{(m)}, \quad (5.6)$$

where the prime indicates derivatives with respect to the scalar field ϕ and $T^{(m)}$ is just the trace of $T_{\mu\nu}^{(m)}$. Scalar-tensor theories are known to be conformally equivalent to GR. Indeed, under conformal transformations, we may find a metric tensor obeying a set of field equations analogous to the usual Einstein equations. In such equations, the scalar degree of freedom would source a resulting matter field. However, the latter would not couple to the geodesics like ordinary matter.

5.2.2 Brans–Dicke Theory

Brans–Dicke (BD) theories were first studied in an attempt to mathematically include Mach’s principle in a theory consistent with GR. In BD theories, the gravitational coupling stops being constant and takes the form of a scalar field. Such a scalar field is in principle position-dependent and would feel the distance-scaled effects of all the matter contained in the Universe [1, 3]. A renewed interest in this theory emerged thanks to the discovery that string theories contain a low-energy limit given by a BD-type Lagrangian [30]. Moreover, further interest was fuelled by the fact that $f(R)$ theories, which, thanks to the chameleon mechanism [31], are once again contenders as viable candidates for weak field gravity, are dynamically equivalent to BD theories.

The action for BD theories in the Jordan frame, may be obtained from the Lagrangian in (5.3), just by considering $\omega \rightarrow \text{constant}$ provided $\Lambda \rightarrow 0$. Thus (5.3) becomes

$$S_{\text{BD}} = \frac{1}{2\kappa^2} \int d^4x \sqrt{-g} \left[\phi R - \frac{\omega}{\phi} g^{\mu\nu} \nabla_\mu \phi \nabla_\nu \phi - V(\phi) \right] + S_m. \quad (5.7)$$

Here, S_m is the action of any matter fields present, and ω characterises the dimensionless BD parameter. As seen above, ϕ couples directly to the scalar curvature, but not to the matter fields. The potential $V(\phi)$ above, although not constant in general, can be identified as a general form of the *cosmological constant*. Subsequently, the scalar field ϕ can be thought of as possessing an effective mass, defined by derivatives of V with respect to ϕ , as follows:

$$m^2 = \frac{1}{2\omega + 3} \left(\phi \frac{d^2 V}{d\phi^2} - \frac{dV}{d\phi} \right). \quad (5.8)$$

Variation of action (5.7) with respect to the metric yields the following field equations:

$$G_{\mu\nu} = \frac{\kappa^2}{\phi} T_{\mu\nu}^{(m)} + \frac{\omega}{\phi^2} \left(\nabla_\mu \phi \nabla_\nu \phi - \frac{1}{2} g_{\mu\nu} \nabla^\alpha \phi \nabla_\alpha \phi \right) + \frac{1}{\phi} (\nabla_\mu \nabla_\nu \phi - g_{\mu\nu} \square \phi) - \frac{V}{2\phi} g_{\mu\nu}, \quad (5.9)$$

As could be concluded from (5.9), in this theory, the gravitational coupling could be identified as the inverse of the scalar field, $G_{eff} = \frac{G}{\phi}$, or equivalently $\kappa_{eff}^2 = \frac{\kappa^2}{\phi}$, which obviously becomes a function of spacetime. In order to obtain a positive gravitational coupling and to guarantee the attractive character of gravity, we require that $\phi > 0$. If, then, variations of the action (5.9) with respect to ϕ are performed, the equation of motion for the scalar field,

$$\frac{2\omega}{\phi} \square\phi + R - \frac{\omega}{\phi^2} \nabla^\alpha \phi \nabla_\alpha \phi - \frac{dV}{d\phi} = 0, \quad (5.10)$$

is obtained. Using the trace of the field equations (5.9), we may eliminate R in (5.10), resulting in the dynamical equation for the BD scalar field, ϕ :

$$\square\phi = \frac{1}{2\omega + 3} \left[\kappa^2 T^{(m)} + \phi \frac{dV}{d\phi} - 2V \right]. \quad (5.11)$$

With the pertinent redefinitions, this dynamical equation may also be derived from (5.6). The BD parameter remains as a free parameter of the theory. It turns out that values of $\omega = 1$ are consistent with results in string theory, but in order to satisfy local (Solar System) tests of gravity, ω is preferred to be large. In fact, the larger ω is, the more closely BD theory resembles GR. The latest, most stringent constraints on ω value come from the Cassini probe, and was found to satisfy $\omega > 40000$, and it is this fine tuning of ω that renders BD theories unattractive. However, as shall be discussed later, this fine tuning may be avoided altogether, if the mass of the scalar field is large [32, 33].

5.3 Introduction to $f(R)$ Gravity

Our choice to focus on $f(R)$ theories follows intensive research related to cosmological applications of modified gravity theories, and the need for a wider understanding of the consequences and limitations of this class of theories. Such theories have been the subject of extraordinary attention over the last few decades, and this interest gave birth to a plethora of investigations into somewhat simple $f(R)$ models realisations, the cosmological scenarios that they govern, as well as some understanding into the theoretical caveats associated with these theories [3, 34–37]. As mentioned above, $f(R)$ models were originally considered as a means to facilitate the early-time inflationary epoch required in the Big Bang Theory [9]. More recently, such models proved to be able to provide a mechanism to generating a late-time accelerated epoch in the expansion history of the Universe. This theory gives rise to a gravitational field propagated by a spin-2 massless graviton, as well as a massive scalar degree of freedom that couples to density, resulting in an effective long-range *fifth force*, which can indeed facilitate the late-time acceleration observed.

Indeed, these theories result from a straightforward modification of the Einstein–Hilbert action, which has been claimed to be its simplest general stable modification that can be made [4, 5]. In particular, the Ricci scalar R is replaced with a general function of the Ricci scalar, namely:

$$S = \frac{1}{2\kappa^2} \int f(R) \sqrt{-g} d^4x. \quad (5.12)$$

The renewed interest also brought to light the scalar-tensor theory equivalence with $f(R)$ gravity, and that such an action (5.12) was also able to produce the accelerated expansion, which was being sought at the time, c.f. [38]. Early studies were pessimistic about $f(R)$ gravity, arguing that these theories are automatically ruled out since Solar System constraints required that the BD parameter be greater than 40000 [39], as mentioned above, while other results concluded that $f(R) \propto R^n$, i.e., power laws of R , could not produce standard cosmological evolution [40, 41], for both large and small values of the Ricci scalar. Moreover, it was claimed that $f(R)$ theories did not contain a phase of matter-like expansion ($t^{2/3}$, with t cosmic time), when it was found that typically a radiation-like expansion era ($t^{1/2}$) preceded a phase of dark energy expansion [42]. Since then, the understanding of the dynamics of these models and the various general restrictions that can be placed has developed significantly, and several models have been proposed that are able to sustain a period of matter-like expansion (see for example [43–46]) followed by an acceleration. In what follows, we shall provide the field equations, discuss the FLRW solutions corresponding to viable theories, as well as what exactly makes a theory viable in the first place.

Three remarks are pertinent at this stage. First, the generality $f(R)$ theories grant is fairly wide, and their resulting field equations yield rich and interesting phenomenologies, providing ways to reproduce whatever dynamics one desires (c.f. [47, 48] and subsequent efforts), in particular that of Λ CDM in a two-fluid dominated scenario. Second, $f(R)$ theories are also arguably the most straightforward modification to GR that can be made, meaning their solutions are tractable and their exact solutions can give insight into this class of theories, as well as GR. Various viability considerations, which must be satisfied by viable $f(R)$ models, will be discussed in Sect. 5.3.3. Finally, the most attractive advantage is that $f(R)$ theories avoid the Ostrogradsky instability, from which many other higher-order modifications to the gravitational Lagrangian suffer.

The generalised form of the Lagrangian included in Eq. (5.12) supersedes the addition of even higher-order quadratic curvature invariants such as $R^{\mu\nu} R_{\mu\nu}$, $R^{\mu\nu\alpha\beta} R_{\mu\nu\alpha\beta}$ or $\varepsilon^{\mu\nu\sigma\gamma} R_{\mu\nu\alpha\beta} R^{\alpha\beta}{}_{\sigma\gamma}$, which in fact will reduce to a function of R , $f(R)$, when considering a maximally symmetric, four-dimensional spacetime (a transparent proof of this argument may be found in [49], p. 134).

5.3.1 $f(R)$ Formalisms

The governing field equations for a general $f(R)$ theory may be derived by varying the action (5.12) in three different ways, which result in three different formalisms within the $f(R)$ framework. In particular,

1. The so-called *metric formalism* considers the only independent variable to be the metric itself, and the action,

$$S_{met} = \frac{1}{2\kappa^2} \int d^4x \sqrt{-g} f(R) + S_m(g_{\mu\nu}, \psi) \quad (5.13)$$

is varied with respect to the metric alone, yielding the following field equations:

$$f'(R)R_{\mu\nu} - \frac{1}{2}f(R)g_{\mu\nu} - (\nabla_\mu \nabla_\nu - g_{\mu\nu} \square) f'(R) = \kappa^2 T_{\mu\nu}^{(m)}. \quad (5.14)$$

These equations are fourth-order in the metric tensor, as per the usual definition of the Ricci scalar. Matter fluids are described by $T_{\mu\nu}^{(m)}$ as defined in (5.5). Here, ∇_μ is the covariant derivative corresponding to the usual Levi–Civita connection of the metric, $\square = \nabla^\mu \nabla_\mu$, and primes denote differentiation with respect to the Ricci scalar R .

2. In what is known as the *Palatini formalism*, the action from which we begin (5.13) remains the same, however the connection is assumed as being an independent quantity from the metric. Thus the action must then be varied with respect to both quantities independently:

$$S_{Pal} = \frac{1}{2\kappa^2} \int d^4x \sqrt{-g} f(\mathcal{R}) + S_m(g_{\mu\nu}, \psi), \quad (5.15)$$

where the Riemann tensor and the Ricci tensor are constructed with the independent connection, and, in this section, we denote the difference between the metric Ricci scalar, R , and the Ricci scalar constructed with this independent connection as $\mathcal{R} = g^{\mu\nu} \mathcal{R}_{\mu\nu}$. Hence, varying (5.15) with respect to both the metric and the connection yields [50]

$$f'(\mathcal{R})\mathcal{R}_{(\mu\nu)} - \frac{1}{2}f(\mathcal{R})g_{\mu\nu} = \kappa^2 T_{\mu\nu}^{(m)}, \quad (5.16)$$

$$\bar{\nabla}_\gamma (\sqrt{-g} f'(\mathcal{R}) g^{\mu\nu}) - \bar{\nabla}_\sigma (\sqrt{-g} f'(\mathcal{R}) g^{\sigma(\mu}) \delta_\gamma^{\nu)}) = 0. \quad (5.17)$$

Here, $\bar{\nabla}_\mu$ represents the covariant derivative defined with the independent connection used in the variation. The important point is that when $f(\mathcal{R}) = \mathcal{R}$ in the Palatini formalism and when $f(R) = R$ in the metric formalism, both theories

reduce to GR, and produce the same physics. However, they deviate significantly as soon as a more general function f appears in the Lagrangian.

While, in the Palatini formalism, the connection is considered independent from the metric, it does not appear explicitly in the Lagrangian. The Lagrangian density corresponding to the matter fields is independent of the connection itself, and the covariant derivatives of the matter fields are defined as usual with the Levi–Civita connection. In fact it is possible to eliminate the independent connection entirely from the field equations of Palatini $f(R)$ gravity, since the independent connection is not actually related to the geometry. In this sense, the Palatini formalism is still a metric theory [36]. The interested reader is referred to [50] for a further insight.

3. A third and more general (and more complicated as well) approach to the variation of the $f(R)$ action is known as *metric affine $f(R)$* . Herein, the geometric properties of the independent connection manifest in its coupling to the matter fields present in the theory. In this way, both of the aforementioned approaches can be generalised by taking both the metric and the connection to be independent variables, and also allowing the matter to depend explicitly on the connection. The interested reader is referred to [51] for a further insight.

In the following we shall choose the metric approach as the underlying formalism of our chapter. For the Palatini and metric-affine approaches, interested readers may consult the aforementioned references. Thus, retaking (5.14), these field equations can be rearranged to resemble the Einstein field equations with an additional source term, comprising the higher order curvature contributions:

$$R_{\mu\nu} - \frac{1}{2}g_{\mu\nu}R \equiv G_{\mu\nu} = T_{\mu\nu}^{(R)} + \frac{1}{f'(R)}T_{\mu\nu}^{(m)}, \quad (5.18)$$

with

$$T_{\mu\nu}^{(R)} = \frac{1}{f'(R)} \left[(\nabla_\mu \nabla_\nu - g_{\mu\nu} \square) f'(R) + \frac{1}{2}g_{\mu\nu} (f(R) - f'(R)R) \right] \quad (5.19)$$

being an effective stress-energy tensor, which behaves as a source for the resulting geometry. This new source term is usually dubbed the *curvature fluid*, $T_{\mu\nu}^{(R)}$. Definitely, this idea is not to be taken literally, and we should be aware that actually the resulting theory is completely different from GR. However, intuitively, it lends a useful perspective; the vacuum itself contains a source that is generated by the geometry, in an otherwise Einstein-like field. Obviously, when the stress energy tensor for the curvature fluid is exactly zero, we recover GR. Herein, an effective gravitational coupling can then be defined as $G_{eff} \equiv G/f'(R)$. The coupling is required to be positive, in analogy to requiring that the graviton is not a ghost in scalar-tensor gravity, and this amounts to the following condition on the form of $f(R)$:

$$f'(R) > 0, \quad (5.20)$$

which we touch on again later. The trace of the field equations at (5.14) is given by

$$f'(R)R + 3\Box f'(R) - 2f(R) = \kappa^2 T^{(m)}, \quad (5.21)$$

$T^{(m)} = g^{\mu\nu} T_{\mu\nu}^{(m)}$. The trace Eq. (5.21) makes the distinction between $f(R)$ gravity and GR obvious, where for the latter $R = -\kappa^2 T^{(m)}$. Thus, in the $f(R)$ gravity case, a vanishing of ordinary matter sources does not imply a vanishing of Ricci curvature, hinting at the importance of the additional field, $f'(R)$, and the role it plays in the resultant physics of the given universe. In fact, we can interpret the trace equation as being an equation of motion for this emergent scalar degree of freedom, f_R , which is sometimes called the scalaron. For maximally symmetric solutions of the above equation, where we have surfaces of constant curvature ($R = \text{const}$), considering the vacuum scenario, i.e., $T_{\mu\nu}^{(m)} = 0$, Eq. (5.21) reduces to

$$f'(R)R - 2f(R) = 0, \quad (5.22)$$

which is just an algebraic expression for R . When $R = 0$ is a root of the above equation, then the field equations at (5.14) become $R_{\mu\nu} = 0$, corresponding to isotropic, homogeneous and flat Minkowski spacetime. When $R = \text{const}$ is taken to be a root of (5.22), the field equations (5.14) become $R_{\mu\nu} \propto g_{\mu\nu}$. This root gives an interesting and desirable result, as it represents exponential expansion of space-time, similar to the behaviour of a GR universe plus a cosmological constant.

5.3.2 $f(R)$ Gravity From a Scalar-Tensor Perspective

Performing coordinate transformations, normalisations or variable redefinitions are standard techniques in Classical Mechanics. Such techniques usually improve the convenience of computations and the interpretation of results. Finding equivalence between theories is a tool that comes in handy, especially when a novel theory is being investigated. For the sake of definiteness, we can say that two theories are thought of as equivalent if after an appropriate redefinition, or transformation, or renormalisation, either their field equations or the action from which these are derived, are identical. In this case, the dynamics of the equivalent theories are indistinguishable, and previous progress in understanding one theory will shed light on a theory that is found to be a dynamically equivalent and alternative representation to the former.

It is well known that it is possible to recast quadratic modifications to GR in the form of a BD theory, the latter being a subclass of scalar-tensor theories. This equivalence is easily extended to the special case of $f(R)$ gravity [36, 52]. While metric $f(R)$ gravity explicitly seems not to include extra fields in the action, and the Palatini version, though containing an independent connection, is also fundamentally a metric theory, they both may be represented by various forms of a BD theory. Below, the equivalence is discussed in terms of the equivalence of the actions.

Beginning with the action for metric $f(R)$ gravity, as given by (5.12), we introduce an auxiliary field, χ , to the action, which becomes,

$$S_{met} = \frac{1}{2\kappa^2} \int d^4x \sqrt{-g} [f(\chi) + f'(\chi)(R - \chi)] + S_m(g_{\mu\nu}, \psi), \quad (5.23)$$

where $f(R) = f(\chi) + f'(\chi)(R - \chi)$ is an expansion around the Ricci scalar. Varying with respect to χ reveals the following equation:

$$f''(\chi)(R - \chi) = 0. \quad (5.24)$$

Clearly, under the condition that $f''(\chi) \neq 0$, we obtain that $R = \chi$, which of course reproduces the original action. If we identify $f'(\chi)$ as a scalar degree of freedom, and set $f'(\chi) = \phi$ to be a scalar field, we can then define its effective potential:

$$V(\phi) = \chi(\phi)\phi - f(\chi(\phi)). \quad (5.25)$$

This allows us to rewrite the action (5.12) in terms of the scalar field ϕ and its potential as follows:

$$S_{met} = \frac{1}{2\kappa^2} \int d^4x \sqrt{-g} [\phi R - V(\phi)] + S_m(g_{\mu\nu}, \psi), \quad (5.26)$$

which is simply the action of a BD theory in the Jordan frame, with the BD parameter $\omega_0 = 0$, known as *massive dilaton gravity* [53]. Note that this scalar field ϕ is, unlike a matter field, able to violate all the energy conditions [3] (the energy conditions will be specified in Sect. 5.5.1 below). The field equations that result from metric variation of (5.26) are

$$G_{\mu\nu} = \frac{\kappa^2}{\phi} T_{\mu\nu}^{(m)} - \frac{V(\phi)}{2\phi} g_{\mu\nu} + \frac{1}{\phi} (\nabla_\mu \nabla_\nu \phi - g_{\mu\nu} \square \phi), \quad (5.27)$$

$$R = V'(\phi). \quad (5.28)$$

where in order to guarantee that an $f(R)$ theory is dynamically equivalent to a scalar-tensor theory, the condition $f'' \neq 0$ must be satisfied. Following a similar approach as before for the Palatini formalism of $f(R)$ gravity reveals that the Palatini $f(R)$ theory is dynamically equivalent to the BD theory, for which $\omega_0 = -\frac{3}{2}$ [36, 54, 55], as introduced in (5.3).

As mentioned above, the trace of (5.27) may be used to eliminate R , resulting in Eq. (5.11), which provides an equation of motion for the scalar field in terms of its potential in the presence of matter. Such an equation highlights the difference between metric and Palatini $f(R)$ theories, and their induced dynamics. It is clear to see that in the Palatini formalism the emergent scalar field, or scalaron, is not a dynamic variable, whereas in metric $f(R)$ theory the derivatives of the scalar field are non-zero, therefore resulting in an extra scalar degree of freedom [36].

5.3.3 Viability

In this section we shall give a flavour of the required viability constraints on the general $f(R)$ Lagrangians. Given the apparent freedom on the form of the function f , it has become common practice to construct a theory that produces the desired results in the required energy level or time scale. It has been an interesting exercise for many years, given the $f(R)$ cosmological field equations, to find forms for f that are consistent with data (c.f. [43, 56–59]). Even the reverse has been done, where given sets of data, a function, which best suits the data, has been reconstructed [47, 48]. Below we discuss the various considerations, which must be made prior to an $f(R)$ theory being accepted as a potentially viable candidate for the underlying theory of gravity.

Cosmological Dynamics

It is not difficult to find a function, which, in principle, is consistent with the cosmological expansion history observations, in that it can produce late-time acceleration. The point of interest is making sure that other gravitational aspects and other predictions in the cosmological evolution are also respected, especially Big Bang Nucleosynthesis, the temperature anisotropies of the CMB and the expected growth of large-scale structures. Moreover, the theory must provide an inflationary period, which can solve the horizon, flatness and monopole problems. After this a radiation domination phase of the Universe, leading to a matter domination phase, must be present. Finally, the Universe should evolve towards a stable de Sitter type expansion, such that the theory agrees with observations. Note that the transitions between the various phases must be smooth.

Correct Weak-Field Limit

It took some time before consistent results regarding the weak-field limit in $f(R)$ theories of gravity were derived and understood. In 2003, Chiba [60] concluded that, by virtue of the fact that observations required BD theories with $\omega_0 \geq 40000$, $f(R)$ theories must be ruled out, having $\omega_0 = 0$. However, the Parametrised Post Newtonian slip parameter, $\gamma = -\Psi/\Phi$, defined by the ratio of the Newtonian potentials, is determined by both the mass of the scalar field in these theories, as well as the BD parameter, ω_0 . When the mass is small, constraints on ω_0 are equivalent to constraints on γ . However, provided the mass of the scalar field is endowed with the so-called *Chameleon mechanism*, and therefore is able to acquire a large mass locally depending on the environment, then in this regime the mass of the scalar field will dominate over ω_0 , allowing a select class of $f(R)$ theories to survive [31, 61]. Once the scalar is massive and its range short, it will effectively be invisible to experiments performed within both the Newtonian and post Newtonian limits.

Regarding the existence of a Newtonian limit, it was shown in [62] that the existence of a stable Newtonian limit may be ascertained by the existence of a stable ground state of the theory, whether the ground state solution is Minkowski, de Sitter or anti-de Sitter. In order for a function to provide a theory with a stable Newtonian limit, i.e. in the regime for R where Newtonian gravity can be applied, compact objects,

low velocities and relevant curvatures (curvatures much larger than the present background value in an FRLW universe, but smaller than those interior to very compact bodies, e.g., neutrons stars or black holes), the following conditions on $f(R)$ must be met [63]:

$$|f(R) - R| \ll R, \quad (5.29)$$

$$|f_R(R) - 1| \ll 1, \quad (5.30)$$

$$Rf_{RR}(R) \ll 1, \quad (5.31)$$

for $R \gg R(\text{today})$, which guarantee that any deviations from GR to the metric are kept small. Additionally, the Compton wavelength of the scalar field is much smaller than the radius of curvature of the background [63]. These are essential considerations regarding the form of f , and failing the weak-field limit renders a theory worthless.

Instabilities

An important issue that usually constitutes a problem for most of the higher-order theories of gravity is the appearance of ghost fields. These are massive states of negative norm and, in this context, result in the Hamiltonian for a given theory to be unbounded from below.

Classical and quantum stability

If the modified Lagrangian includes higher-order curvature invariants and derivatives, it has been shown that an additional spin-2 ghost field appears [4, 5], resulting in issues with the quantum stability of the theory [64], as well as on a classical level. To ensure the classical and quantum stability of a theory in the physically relevant domain, i.e., $R > 0$, the following requirements on the derivatives of f are crucial:

$$f_R(R) > 0, \quad (5.32)$$

$$f_{RR}(R) > 0. \quad (5.33)$$

Indeed, the condition (5.32) guarantees that gravity is attractive and that the effective gravitational constant is positive. It also ensures that the graviton is not a ghost [63], and a violation of this requirement has been shown to result in the loss of homogeneity and isotropy in regular FLRW models, and the formation of a strong space-like anisotropy curvature singularity [65, 66].

The requirement (5.33) conveys the avoidance of the so-called Dolgov–Kawasaki instability [67], which may occur in very short time scales. Furthermore, related to the latter, a weak sudden singularity can also arise if $f_{RR}(R) = 0$ for a finite value of the scalar curvature. Both problems are discussed below.

The Dolgov–Kawasaki Instability

To summarise its importance, following [67], let us parametrise $f(R) = R + \epsilon g(R)$, such that ϵ is a small positive constant, containing the dimensions of mass squared,

leaving the function $g(R)$ dimensionless. Substituting this into the $f(R)$ trace equation (5.21), we obtain

$$\square R + \frac{g'''}{g''} \nabla^\mu R \nabla_\mu R + \left(\frac{\epsilon g' - 1}{3\epsilon g''} \right) R = \frac{\kappa^2 T^{(m)}}{3\epsilon g''} + \frac{2g}{3g''}, \quad (5.34)$$

assuming $g'' \neq 0$ (to lighten the notation, here primes denote derivatives with respect to R). Now, we may approximate the local metric as an expansion around the Minkowski metric η ,

$$g_{\mu\nu} = \eta_{\mu\nu} + h_{\mu\nu}, \quad (5.35)$$

in a weak-field region, where we can expand the scalar curvature R as

$$R = -\kappa^2 T^{(m)} + R_1, \quad (5.36)$$

where R_1 is a small perturbation around the GR approximation. We may then consider the trace equation to study the dynamics of R_1 , which to a first order gives:

$$\begin{aligned} \ddot{R}_1 - \nabla^2 R_1 - \frac{2\kappa^2 g'''}{g''} \dot{T}^{(m)} \dot{R}_1 + \frac{2\kappa^2 g'''}{g''} \nabla T^{(m)} \cdot \nabla R_1 + \frac{1}{3g''} \left(\frac{1}{\epsilon} - g' \right) R_1 \\ = \kappa^2 \ddot{T}^{(m)} - \kappa^2 \nabla^2 T^{(m)} - \frac{[\kappa^2 T^{(m)} g^2 + 2g]}{3g''}. \end{aligned} \quad (5.37)$$

The coefficient of the last term on the left-hand side is effectively the square of the mass of R_1

$$m^2 \simeq \frac{1}{3\epsilon g''}, \quad (5.38)$$

and is dominated by the term $(\frac{1}{3\epsilon g''})$, since the value of ϵ is very small [67, 68]. Consequently, the introduced perturbation R_1 will remain under control and the corresponding theory will be stable, provided $g'' > 0$ is satisfied, and unstable when the sign of the effective mass square is negative [68]. Thus, in order to protect against the Dolgov–Kawasaki instability, we require that $f_{RR}(R) > 0$. To include the GR limiting case, we require that $f''(R) \geq 0$. Interestingly, because the scalar field in the Palatini formalism is non-dynamical, it does not suffer any Dolgov–Kawasaki instability. Of course, the above considerations only hold in a small neighbourhood confined to local expansion. However, we may derive a condition for the stability of the de Sitter space in $f(R)$ theories of gravity, by assuming a de Sitter background, and considering a general action that includes both $f(R)$ gravity and scalar-tensor gravity, and mixtures of the two [37]. Considering, as we shall do in general in this work, an FLRW metric to describe the background, the following condition for the existence of a stable de Sitter space solution is obtained:

$$\frac{(f_R^0)^2 - 2f^0 f_{RR}^0}{f_R^0 f_{RR}^0} \geq 0, \quad (5.39)$$

where the zero super index denotes the functions to be evaluated at the de Sitter solution R_0 . Indeed, (5.39) is consistent with the stability condition for homogeneous perturbations [36, 69, 70].

Sudden Singularities

There exists another instability issue, which plagues $f(R)$ gravity even at a background level, due to non-linearities. Many, if not all, of the functions that are constructed to effectively produce GR dynamics in the high curvature regime result in scalar fields for which the potentials $V(\phi)$ contain an unprotected singularity [71].

Some of the first considerations of such singularities, in $f(R)$ gravity, were those that occur as density increases inside compact objects. Such singularities were found to be curable by adding UV corrections to the action, specifically of the form R^2 [63], which are in fact the exact forms for f that were considered as inflationary theories.

Furthermore, it was discovered that oscillations in the Ricci scalar in $f(R)$ theories evolving with increasing redshift, or equivalently going back in time, are common in all viable theories of gravity [63]. The oscillations, occurring about the GR limit, were found to increase in frequency and amplitude, and eventually result in a singularity. Interestingly, in the high-energy regime when considering an inflationary period driven by $f(R)$ theory, such oscillations are actually useful in driving gravitational particle production, enabling phases of reheating, the creation of ordinary matter and the transition to the radiation-dominated FLRW stage [9]. However, in the classical context these oscillations may become problematic since

1. The frequency¹ grows rapidly with redshift to exceed the Planck value, rendering the classical description no longer valid [72–74].
2. The amplitude of the linear oscillations also grows quickly with redshift, resulting in an over-abundance of scalarons at early times, while we require its number density to be appropriately small during BBN [73].

Perturbative approaches such that the Ricci scalar is defined by its value in GR plus a perturbation, $R = R_{GR} + \delta R$, were able to isolate an analytic expression for the oscillating part of the Ricci scalar [73]. It was found that the oscillations become asymmetric and eventually evolve towards a singularity, and that an analysis neglecting nonlinear effects will be blind to pathological behaviour.

These singularities have been widely considered in the scalar tensor framework, where the scalar field $f_R(R)$ is identified and examined using the trace of the field equations (5.48), as a damped harmonic oscillator [71],

$$\square f_R = \frac{1}{3}(2f - f_R R) + \frac{\kappa^2}{3}T^{(m)}, \quad (5.40)$$

¹The frequency of oscillations of R would correspond to the rest mass of the scalarons.

where f_R is the first derivative of $f(R)$ with respect to R , and thus, the additional degree of freedom, the scalar field ϕ , which herein for convenience we define as

$$\phi = f_R - 1. \quad (5.41)$$

Considering the above, Eq.(5.40) in terms of ϕ is

$$\square\phi = V'(\phi) - \mathcal{F}, \quad (5.42)$$

where the effective scalar field potential can be determined by

$$V'(\phi) = \frac{dV}{d\phi} = \frac{1}{3}(2f - f_R R), \quad (5.43)$$

and the force \mathcal{F} driving the scalar field ϕ is the trace of the stress-energy tensor $T^{(m)}$. For a perfect fluid with energy density ρ and pressure p , this is

$$\mathcal{F} = \frac{\kappa^2}{3}(\rho - 3p). \quad (5.44)$$

The dynamics of the scalar field is determined by the field's potential, which is obtained by integrating the following equation

$$\frac{dV}{dR} = \frac{dV}{d\phi} \frac{d\phi}{dR} = \frac{1}{3}(2f - f_R R)f_{RR}. \quad (5.45)$$

The minimum of this potential, which we will identify as being located at ϕ_{min} , is the point that corresponds to the de Sitter solution. There also exists, in most, if not all [71] viable cosmological $f(R)$ theories, a point ϕ_{sing} , where the Ricci scalar diverges to infinity, resulting in a curvature singularity. It has been shown that these two points are often easily separated by a finite value of the potential, thus it is possible (and usually highly likely) that the scalar field, in its oscillation about the potential minimum, may verge on the point leading to singularity. Theories that do not protect against this type of eventuality would be disqualified.

This is a useful approach, and has led to an intuition in understanding the occurrence of these singularities, and insight into how to possibly avoid them, however it has also been argued that this approach is not reliable, and should be performed with caution [75].

Cosmological Perturbations in $f(R)$ Gravity

Arranging a function to mimic a desirable cosmological expansion history is straightforward. In principle there is an infinite number of such functions, and finding them is not a problem. In fact, the bigger problem is finding ways to discriminate between them. The study of perturbations around the chosen background cosmology is one of the most powerful methods to break such a degeneracy. Changing the underly-

ing theory of gravity affects the way that perturbations in the density of the matter components and curvature evolve, leaving an impression in the cosmic microwave background and its fluctuation spectrum, as well as in the large-scale structure of galaxies and galaxy clusters. Also, the tensor (gravitational-wave) spectrum may present differences with respect to the usual GR predictions. In this sense, recent investigations, although constraining the range of parameters of viable $f(R)$ models, have stressed the fact that such theories do not violate the gravitational waves signals as per their predicted propagation speed for the tensorial mode. For seminal references on this issue, refer to [76, 77], as well as subsequent literature. Once predictions of these first-order perturbations are at hand, it is required that the perturbation spectrum produced is consistent with both the cosmological perturbation observables and the gravitational-wave signals.

In $f(R)$ theory context, scalar perturbation modes are affected by the subsequent generalisation of the Einstein–Hilbert action. Consequences include a difference in the correlation between the CMB and the large-scale structure, as well as a decrease in the large angle anisotropy of the CMB [17]. The gravitational coupling in $f(R)$ gravity is stronger, resulting in less large-scale structure than in Λ CDM cosmology. Most studies of perturbations in the $f(R)$ gravity context are performed with respect to a quasi-static limit [78, 78–82]. While for specific functions this approximation may be valid in certain regimes, it must be used with caution, and the obtention of the full fourth-order perturbation equations may be useful in order to study intermediate and Superhubble modes (see [83] and references therein).

The Initial Value Problem

In order for any physical theory to be viable it must have the ability to predict the future of a system, given the details of an instance of its past (an initial vector specifying all the quantities present in the theory), including a description of all interactions at play in the system. Technically speaking, it must have a *well-formulated* and *well-posed* initial value problem. This issue has been widely studied in the scalar-tensor framework and in metric $f(R)$ gravity, and it has been discovered that for these type of theories it is a well-formulated initial value problem in the presence of “reasonable” matter, and well-posed in vacuum too [68, 84].

5.4 Background Cosmology in the Metric Formulation

In the late 1960’s Ehlers, Geren and Sachs provided a compelling argument that if an observer measured the relic background radiation of the Universe as isotropic, assuming that the isotropy holds around every point in the Universe, then such a universe must be isotropic and homogeneous, and thus may be described completely as an FLRW spacetime [85]. While the measurements of the CMB from our observer perspective reveal striking isotropy, our modern ability to resolve tiny anisotropies indicate that in fact the real Universe exhibits perturbations about what appears to be a “nearly isotropic” background radiation. The Ehlers–Geren–Sachs (EGS) theorem

was shown to hold for a “nearly” isotropic measurement of the CMB as well [86]. The “almost EGS” theorem is also valid for $f(R)$ gravity, proven for both metric $f(R)$ and scalar tensor theory [87, 88], when the matter content is described by a barotropic equation of state. Thus, according to the above considerations, the usual FLRW space-time constitutes the ideal arena to study the expansion history of such theories.

Once this metric and a matter stress-energy tensor for a perfect fluid, with energy density ρ and pressure p , are substituted in to the $f(R)$ field equations at (5.14), we obtain the following cosmological evolution equations, where the dot indicates derivatives with respect to cosmic time and H is the usual Hubble parameter. The modified Friedmann equation is

$$H^2 = \frac{1}{3f_R} \left[\rho + \frac{1}{2}(Rf_R - f) - 3H\dot{R}f_{RR} \right], \quad (5.46)$$

and the modified Raychaudhuri equation becomes

$$2\dot{H} + 3H^2 = -\frac{1}{f_R} \left[P + 2H\dot{R}f_{RR} + \frac{1}{2}(f - Rf_R) + \dot{R}^2 f_{3R} + \ddot{R}f_{RR} \right]. \quad (5.47)$$

Additionally, we can also extract the trace of the field equations in this space-time, namely the modified trace equation:

$$3\ddot{R}f_{RR} = \rho(1 - 3w) + f_R R - 2f - 9Hf_{RR}\dot{R} - 3f_{3R}\dot{R}^2, \quad (5.48)$$

where $w \equiv p/\rho$ is the equation-of-state parameter for the perfect fluid under consideration (note that one may have the case where the latter can be the sum of several components, i.e. $\rho = \sum_i \rho_{(i)}$, $p = \sum_i p_{(i)}$, each one with its own equation-of-state parameter w_i).

The $f(R)$ cosmological field equations above are manifestly fourth-order in metric derivative, and since the spatial curvature has been settled to zero, we may in fact eliminate the scale factor altogether, in favour of the Hubble parameter being the only dynamical quantity, reducing the order of the equations by one.

In the spirit of the fact that we may identify all the extra terms in the field equations associated with the function $f(R)$ and its derivatives as an effective *curvature fluid*, we may define its effective equation of state, by using the modified Friedmann and Raychaudhuri equations to define its effective density and pressure as

$$\rho_{\text{FLRW}}^R = \frac{1}{2f_R} (Rf_R - f - 6H\dot{R}f_{RR}), \quad (5.49)$$

$$p_{\text{FLRW}}^R = \frac{1}{f_R} \left[\dot{R}^2 f_{3R} + 2H\dot{R}f_{RR} + \ddot{R}f_{RR} + \frac{1}{2}(f - Rf_R) \right]. \quad (5.50)$$

In this interpretation, in a vacuum, the curvature correction is viewed as an effective fluid, which may be useful for gaining certain intuition, but certainly should

not be taken too far. Even considering energy conditions for this effective geometric fluid would be meaningless, since it is well known that such fluids violate all energy conditions in general [3]. The equation of state for this effective fluid may then be written as

$$w_{\text{FLRW}}^R = \frac{p_{\text{FLRW}}^R}{\rho_{\text{FLRW}}^R} = \frac{[\dot{R}^2 f_{3R} + 2H\dot{R}f_{RR} + \ddot{R}f_{RR} + \frac{1}{2}(f - Rf_R)]}{\frac{1}{2}(Rf_R - f - 6H\dot{R}f_{RR})}. \quad (5.51)$$

For our purposes, in the late-time regime, we require negative pressure to the end of generating accelerated expansion; and from this constraint, $w_{\text{FLRW}}^R \approx -1$, we obtain the following relationship between the derivatives of the function f and the Ricci scalar:

$$\frac{f_{3R}}{f_{RR}} \approx \frac{\dot{R}H - \ddot{R}}{\dot{R}^2}. \quad (5.52)$$

5.5 Scalar Perturbations: The 1 + 3 Formalism

In Sect. 5.4 the metric approach to the derivation of the cosmological field equations in $f(R)$ gravity was presented. As the field of modified theories matured, it became clear that their added complexity leads to practical trouble with analysis. Thus, other frameworks from which a space-time can be studied have been considered, such as decomposing the space-time into a set of 1 + 3 covariant variables, as has been briefly mentioned in Sect. 5.2 [89–91].

The advantage of using the 1 + 3 covariant formalism to study FLRW universes is twofold; the first advantage is that this formalism assists the process of conveniently extending the GR 1 + 3 formalism [89] to modified theories, which must be a major consideration when the task of modifying gravity can come with significant complications, and the second is that in this formalism it is clear to track the physical meaning underlying calculations, which is another important consideration since it is easy to lose intuition at the expense of complexity in modified theories. The 1 + 3 formalism was indeed widely studied in the $f(R)$ gravity framework [41, 92–95].

In the following we shall discuss the kinematical approach from the perspective of a fundamental observer having four-velocity u_α , and we present the constraint and propagation equations that may be derived using the Bianchi identities and conservation equations for momentum and energy.

The kinematic set-up is identical to that in GR; the extension to $f(R)$ gravity is performed simply by adding the curvature fluid as an additional fluid component in the energy-momentum tensor. In this context, it is most natural and intuitive to choose what is known as the matter frame, u_α^m , which is comoving with standard matter, representing motion of galaxies and galaxy clusters. The choice is also preferred for the obvious reason that this frame happens to coincide with the one we are in.

5.5.1 Fluid Sources

The first step is to write down the covariant decomposition of the stress energy momentum tensor relative to the 4-velocity. The critical argument that allows this decomposition analysis in fourth-order theories of gravity is the ability to express the modification to GR in $f(R)$ gravity as an additional source term arising from the extra terms involving curvature and the correction f , where the purely matter part is influenced by a factor of $(\frac{1}{f})$, such that the field equations resemble the Einstein field equations, including a curvature fluid, namely

$$\left(R_{\alpha\beta} - \frac{1}{2}g_{\alpha\beta}R \right) = \tilde{T}_{\alpha\beta}^m + T_{\alpha\beta}^{(R)} = T_{\alpha\beta}, \quad (5.53)$$

where $\tilde{T}_{\alpha\beta}^m = \frac{1}{f_R} T_{\alpha\beta}^m$, and as given by Eq. (5.19), give the expressions for the effective matter fluid and the effective curvature fluid respectively. The stress energy momentum tensor is given by (5.53), where, in terms of the individual contributing sources, the total effective energy density for the combined matter and curvature fluid is

$$\rho = \tilde{\rho}_m + \rho^R = T_{\alpha\beta} u^\alpha u^\beta, \quad (5.54)$$

the total effective isotropic pressure is

$$p = \tilde{p}_m + p^R = \frac{1}{3} T_{\alpha\beta} h^{\alpha\beta}, \quad (5.55)$$

the total effective momentum density, or energy flux relative to u^α , is

$$q_\alpha = \tilde{q}_\alpha^m + q_\alpha^R = -T_{\beta\mu} u^\mu h^\beta{}_\alpha, \quad (5.56)$$

and the total effective projected symmetric trace free anisotropic stress tensor is

$$\pi_{\alpha\beta} = \tilde{\pi}_{\alpha\beta}^m + \pi_{\alpha\beta}^R = T_{\mu\nu}^{(m)} h^\mu{}_{(\alpha} h^\nu{}_{\beta)}. \quad (5.57)$$

Here, the tilde denotes the coupling to the f_R field as follows,

$$\tilde{\rho}_m = \frac{\rho_m}{f_R}, \quad \tilde{p}_m = \frac{p_m}{f_R}, \quad \tilde{q}_\alpha^m = \frac{q_\alpha^m}{f_R}, \quad \tilde{\pi}_{\alpha\beta}^m = \frac{\pi_{\alpha\beta}^m}{f_R}. \quad (5.58)$$

Moreover, the following properties hold for q_α and $\pi_{\alpha\beta}$:

$$q_\alpha u^\alpha = 0, \quad \pi^\alpha{}_\alpha = 0, \quad \pi_{\alpha\beta} = \pi_{(\alpha\beta)}, \quad (5.59)$$

$$\pi_{\alpha\beta} u^\beta = 0, \quad q_\alpha = q_{(\alpha)}, \quad \pi_{\alpha\beta} = \pi_{(\alpha\beta)}. \quad (5.60)$$

The physics will be contained in the specification of an equation of state that relates the quantities above. The framework of a perfect fluid is widely used, and it is characterised by the following constraint:

$$q^\alpha = \pi_{\alpha\beta} = 0 \implies T_{\alpha\beta} = \rho u_\alpha u_\beta + p h_{\alpha\beta}. \quad (5.61)$$

Applying the twice-contracted Bianchi identities to the *total* stress energy tensor, $\nabla^\beta T_{\alpha\beta}^{(m)} = 0$, reveals the conservation properties of the effective fluids. The effective matter fluid is not conserved, since

$$\nabla^\beta \tilde{T}_{\alpha\beta}^{(m)} = \frac{\nabla^\beta T_{\alpha\beta}^{(m)}}{f_R} - \frac{f_{RR}}{f_R^2} T_{\alpha\beta}^{(m)} \nabla^\beta R. \quad (5.62)$$

Furthermore, the conservation of the *total* energy-momentum implies

$$\nabla^\beta T_{\alpha\beta}^{(R)} = \frac{f_{RR}}{f_R^2} \tilde{T}_{\alpha\beta}^{(m)} \nabla^\beta R. \quad (5.63)$$

While the standard matter component is still subject to the energy conditions discussed previously, the effective matter and curvature fluids are free to (and in general do) violate the weak energy condition, leaving the natural choice of frame as the energy frame of the standard matter u_m^α , since the thermodynamical properties of standard matter are always preserved.

The Bianchi identities, as applied to the total stress energy momentum tensor, show that as long as the stress energy momentum tensor for standard matter is conserved, $\nabla^\beta T_{\alpha\beta}^{(m)} = 0$, then the total stress energy momentum tensor will satisfy conservation of energy.

5.5.2 Geometry

In the covariant formalism for GR, transpires that it is more useful to use the reverse representation of the Einstein field equations

$$R_{\alpha\beta} = T_{\alpha\beta}^{(m)} - \frac{1}{2} T^{(m)} g_{\alpha\beta}. \quad (5.64)$$

The Curvature Fluid

In order to discuss the ‘‘thermodynamical’’ properties of the curvature fluid, we consider the right-hand side of Eq. (5.53), where the *curvature fluid* in $f(R)$ gravity is given in Eq. (5.19). Should the terms in this equation be decomposed in derivative operators containing space and time parts, we have

$$T_{\alpha\beta}^R = \frac{1}{f_R} \left[\frac{1}{2} g_{\alpha\beta} (f - Rf_R) - \dot{f}_R \left(\frac{1}{3} h_{\alpha\beta} \Theta + \sigma_{\alpha\beta} + \omega_{\alpha\beta} \right) + \frac{1}{3} h_{\alpha\beta} \tilde{\nabla}^2 f_R \right]. \quad (5.65)$$

Now, using Eqs. (5.54)–(5.58) and the above decomposition, we may rewrite the thermodynamical quantities associated with the curvature fluid in terms of the 1 + 3 variables:

$$\rho^R = \frac{1}{f_R} \left[\frac{1}{2} (Rf_R - f) + f_{3R} \tilde{\nabla}^\alpha R \tilde{\nabla}_\alpha R + f_{RR} \tilde{\nabla}^2 R - \Theta f_{RR} \dot{R} \right], \quad (5.66)$$

$$p^R = \frac{1}{f_R} \left[\frac{1}{2} (f - Rf_R) - \frac{2}{3} f_{RR} \tilde{\nabla}^2 R - \frac{2}{3} f_{3R} \tilde{\nabla}^\alpha R \tilde{\nabla}_\alpha R + \frac{2}{3} \Theta f_{RR} \dot{R} + f_{3R} \dot{R}^2 + f_{RR} \ddot{R} - \dot{u}_\mu f_{RR} \tilde{\nabla}^\mu R \right], \quad (5.67)$$

$$q_\alpha^R = -\frac{1}{f_R} \left[f_{3R} \dot{R} \tilde{\nabla}_\alpha R + f_{RR} \tilde{\nabla}_\alpha \dot{R} - \frac{1}{3} \Theta f_{RR} \tilde{\nabla}_\alpha R - \sigma_{\alpha\mu} f_{RR} \tilde{\nabla}^\mu R - \omega_{\alpha\mu} f_{RR} \tilde{\nabla}^\mu R \right], \quad (5.68)$$

$$\pi_{\alpha\beta}^R = \frac{1}{f_R} \left[f_{3R} \tilde{\nabla}_{(\alpha R} \tilde{\nabla}_{\beta)} R + f_{RR} \tilde{\nabla}_{(\alpha} \tilde{\nabla}_{\beta)} R - \sigma_{\alpha\beta} f_{RR} \dot{R} \right]. \quad (5.69)$$

The twice-contracted Bianchi identities are used to obtain evolution equations for ρ^m , ρ^R and q_α^R :

$$\dot{\rho}_m = -\Theta(\rho_m + p_m), \quad (5.70)$$

$$\dot{\rho}^R + \tilde{\nabla}^\alpha q_\alpha^R = -\Theta(\rho^R + p^R) - 2\dot{u}^\alpha q_\alpha^R - \sigma^{\alpha\beta} \pi_{\beta\alpha}^R + \rho_m \frac{f_{RR} \dot{R}}{f_R^2}, \quad (5.71)$$

$$\begin{aligned} \dot{q}_{(\alpha)}^R + \tilde{\nabla}_\alpha p^R + \tilde{\nabla}^\beta \pi_{\alpha\beta}^R &= -\frac{4}{3} \Theta q_\alpha^R - \sigma_\alpha{}^\beta q_\beta^R - (\rho^R + p^R) \dot{u}_\alpha - \dot{u}^\beta \pi_{\alpha\beta}^R \\ &\quad - \eta_{\alpha}{}^{\beta\mu} \omega_\beta q_\mu^R + \rho_m \frac{f_{RR} \tilde{\nabla}_\alpha R}{f_R^2}. \end{aligned} \quad (5.72)$$

We also have the following relation between the acceleration and the energy density and pressure of the standard matter:

$$\tilde{\nabla} p_m = -(\rho_m + p_m) \dot{u}^\alpha, \quad (5.73)$$

coming from the conservation of momentum for standard matter.

Substituting into (5.64) for the total effective energy momentum tensor, we may write the Ricci tensor and Ricci scalar in terms of the thermodynamic quantities of the total effective fluid as

$$R_{\alpha\beta} = \frac{1}{2} (\rho_{tot} + 3p_{tot}) u_\alpha u_\beta + \frac{1}{2} (\rho_{tot} - p_{tot}) h_{\alpha\beta} + 2u_{(\alpha} q_{\beta)}^{tot} + \pi_{\alpha\beta}^{tot}, \quad (5.74)$$

$$R = \rho_{tot} - 3p_{tot}. \quad (5.75)$$

We can also construct the trace equation of the curvature fluid by considering \tilde{T}^m and $T^{(R)}$, the traces of the effective matter and curvature fluids respectively:

$$\tilde{T}^m = \frac{1}{f_R} g^{\alpha\beta} T_{\alpha\beta}^m = \frac{1}{f_R} (3p_m - \rho_m), \quad (5.76)$$

$$T^{(R)} = g^{\alpha\beta} T_{\alpha\beta}^R = \frac{1}{f_R} \left[2(f - Rf_R) - 3 \left(f_{RR} \tilde{\nabla}^2 R + f'_{RR} \tilde{\nabla}^\alpha R \tilde{\nabla}_\alpha R - f_{3R} \dot{R}^2 - f_{RR} \ddot{R} + \dot{u}_\mu f_{RR} \tilde{\nabla}^\mu R - f_{RR} \theta \dot{R} \right) \right], \quad (5.77)$$

by taking the trace of (5.65). If we substitute (5.76) and (5.77) into the equation for the Ricci scalar, (5.75), and considering only the curvature terms, we obtain the trace equation corresponding to the curvature fluid:

$$Rf_R - 2f = -3 \left(f_{RR} \tilde{\nabla}^2 R + f_{3R} \tilde{\nabla}^\alpha R \tilde{\nabla}_\alpha R - f_{3R} \dot{R}^2 - f_{RR} \ddot{R} + \dot{u}_\mu f_{RR} \tilde{\nabla}^\mu R - f_{RR} \theta \dot{R} \right). \quad (5.78)$$

5.5.3 Propagation and Constraint Equations

The complete 1 + 3 decomposition for the Riemann tensor, in terms of both thermodynamic and geometric quantities defined above, is given by

$$R^{\alpha\beta}{}_{\mu\nu} = R_P^{\alpha\beta}{}_{\mu\nu} + R_I^{\alpha\beta}{}_{\mu\nu} + R_E^{\alpha\beta}{}_{\mu\nu} + R_H^{\alpha\beta}{}_{\mu\nu}, \quad (5.79)$$

where

$$R_P^{\alpha\beta}{}_{\mu\nu} = \frac{2}{3}(\rho + 3p - 2\Lambda)u^{[\alpha}u_{[\mu}h^{\beta]}{}_{\nu]} + \frac{2}{3}(\rho + \Lambda)h^{[\alpha}{}_{[\mu}h^{\beta]}{}_{\nu]}, \quad (5.80)$$

$$R_I^{\alpha\beta}{}_{\mu\nu} = -2u^{[\alpha}h^{\beta]}{}_{[\mu}q_{\nu]} - 2u_{[\mu}h^{[\alpha}{}_{\nu]}q^{\beta]} - 2u^{[\alpha}u_{[\mu}\pi^{\beta]}{}_{\nu]} + 2h^{[\alpha}{}_{[\mu}\pi^{\beta]}{}_{\nu]}, \quad (5.81)$$

$$R_E^{\alpha\beta}{}_{\mu\nu} = 4u^{[\alpha}u_{[\mu}E^{\beta]}{}_{\nu]} + 4h^{[\alpha}{}_{\mu}E^{\beta]}{}_{\nu]}, \quad (5.82)$$

$$R_H^{\alpha\beta}{}_{\mu\nu} = 2\eta^{\alpha\beta\gamma}u_{[\mu}H_{\nu]\gamma]} + 2\eta_{\mu\nu\gamma}u^{[\alpha}H^{\beta]\gamma]}. \quad (5.83)$$

Thus, using equations for the decomposition of the Riemann tensor (5.79)–(5.83), we can obtain three sets of propagation and constraint equations, coming from the Einstein equations, and their integrability conditions in the 1 + 3 covariant decomposition.

1. Ricci Identities

The first set of propagation equations result from the Ricci identities for the velocity vector field u^α , namely

$$2\nabla_{[\alpha}\nabla_{\beta]}u^\mu = R_{\alpha\beta}{}^\mu{}_\nu u^\nu. \quad (5.84)$$

From the Ricci identities for the velocity vector field u^α ,

1. *The Raychaudhuri propagation equation* is given by

$$\dot{\Theta} - \tilde{\nabla}_\alpha \dot{u}^\alpha + \frac{1}{3}\Theta^2 - (\dot{u}_\alpha \dot{u}^\alpha) + \sigma_{\alpha\beta}\sigma^{\alpha\beta} - 2\omega_\alpha\omega^\alpha + \frac{1}{2}(\tilde{\rho}_m + 3\tilde{p}_m) = -\frac{1}{2}(\rho^R - 3p^R). \quad (5.85)$$

2. *The vorticity propagation equation* is as before,

$$\dot{\omega}^{(\alpha)} - \frac{1}{2}\eta^{\alpha\beta\mu}\tilde{\nabla}_\beta \dot{u}_\mu = -\frac{2}{3}\Theta\omega^\alpha + \sigma^\alpha{}_\beta\omega^\beta. \quad (5.86)$$

3. *The shear propagation equation* is

$$\dot{\sigma}^{(\alpha\beta)} - \tilde{\nabla}^{(\alpha}\dot{u}^{\beta)} + \frac{2}{3}\Theta\sigma^{\alpha\beta} - \dot{u}^{(\alpha}\dot{u}^{\beta)} + \sigma^{(\alpha}{}_\mu\sigma^{\beta)\mu} + \omega^{(\alpha}\omega^{\beta)} + E^{\alpha\beta} = \frac{1}{2}\pi_R^{\alpha\beta}. \quad (5.87)$$

4. *The (0α) shear divergence constraint* is

$$0 = (C_1)^\alpha = \tilde{\nabla}_\beta\sigma^{\alpha\beta} - \frac{2}{3}\tilde{\nabla}^\alpha\Theta + \eta^{\alpha\beta\nu}\left[\tilde{\nabla}_\beta\omega_\nu + 2\dot{u}_\beta\omega_\mu\right] + q_R^\alpha. \quad (5.88)$$

5. *The vorticity divergence constraint* is

$$0 = (C_2) = \tilde{\nabla}_\alpha\omega^\alpha - \dot{u}_\alpha\omega^\alpha. \quad (5.89)$$

6. *The gravito-magnetic $H_{\alpha\beta}$ constraint* is

$$0 = (C_3)^{\alpha\beta} = H^{\alpha\beta} + 2\dot{u}^{(\alpha\omega^{\beta)} - \eta^{\mu\nu(\alpha}\tilde{\nabla}_\mu\sigma^{\beta)}{}_\nu + \tilde{\nabla}^{(\alpha\omega^{\beta)}. \quad (5.90)$$

2. Twice-Contracted Bianchi Identities

The constraint obtained by projecting parallel to u^α yields

7. *The energy conservation equation:*

$$\dot{\rho} + \tilde{\nabla}_\alpha q^\alpha = -\Theta(\rho + p) - 2\dot{u}_\alpha q^\alpha - \sigma_{\alpha\beta}\pi^{\alpha\beta}, \quad (5.91)$$

and by projecting orthogonally to u^α yields:

8. *The conservation of momentum equation:*

$$\dot{q}^{(\alpha)} + \tilde{\nabla}^\alpha p + \tilde{\nabla}_\beta\pi^{\alpha\beta} = -\frac{4}{3}\Theta q^\alpha - \sigma^\alpha{}_\beta q^\beta - (\rho + p)\dot{u}^\alpha - \dot{u}_\beta\pi^{\alpha\beta} - \eta^{\alpha\beta\mu}\omega_\beta q_\nu. \quad (5.92)$$

Additionally, for a perfect fluid we have

$$\dot{\rho}_m = -\Theta(\rho_m + p_m), \quad (5.93)$$

$$\tilde{\nabla}_\alpha p_m = -(\rho_m + p_m)\dot{u}_\alpha. \quad (5.94)$$

3. Once-Contracted Bianchi Identities

9. *The gravito-electric \dot{E} propagation equation:*

$$\begin{aligned} (\dot{E}^{(\alpha\beta)} + \frac{1}{2}\dot{\pi}^{(\alpha\beta)}) - \eta^{\mu\nu(\alpha}\tilde{\nabla}_\mu H^{\beta)}_\nu + \frac{1}{2}\tilde{\nabla}^{(\alpha}q^{\beta)} \\ = -\frac{1}{2}(\rho + p)\sigma^{\alpha\beta} - \Theta\left(E^{\alpha\beta} + \frac{1}{6}\pi^{\alpha\beta}\right) + 3\sigma^{(\alpha}{}_\mu\left(E^{\beta)\mu} - \frac{1}{6}\pi^{(\beta)\mu}\right) \\ - \dot{u}^{(\alpha}q^{\beta)} + \eta^{\mu\nu(\alpha}\left[2\dot{u}_\mu H^{\beta)}_\nu + \omega_\mu\left(E^{\beta)}_\nu + \frac{1}{2}\pi^{\beta)}_\nu\right)\right]. \end{aligned} \quad (5.95)$$

10. *The gravito-magnetic \dot{H} propagation equation:*

$$\begin{aligned} \dot{H}^{(\alpha\beta)} + \eta^{\mu\nu(\alpha}\tilde{\nabla}_\mu\left(E^{\beta)}_\nu - \frac{1}{2}\pi^{\beta)}_\nu\right) = -\Theta H^{\alpha\beta} + 3\sigma^{(\alpha}{}_\mu H^{\beta)\mu} + \frac{3}{2}\omega^{(\alpha}q^{\beta)} \\ - \eta^{\mu\nu(\alpha}\left[2\dot{u}_\mu E^{\beta)}_\nu - \frac{1}{2}\sigma^{\beta)}{}_\mu q_\nu - \omega_\mu H^{\beta)}_\nu\right]. \end{aligned} \quad (5.96)$$

11. *The gravito-electric divergence constraint:*

$$\begin{aligned} 0 = (C_4)^\alpha = \tilde{\nabla}_\beta\left(E^{\alpha\beta} + \frac{1}{2}\pi^{\alpha\beta}\right) - \frac{1}{3}\tilde{\nabla}^\alpha\rho + \frac{1}{3}\Theta q^\alpha - \frac{1}{2}\sigma^\alpha{}_\beta q^\beta - 3\omega_\beta H^{\alpha\beta} \\ - \eta^{\alpha\beta\mu}\left[\sigma_{\beta\nu}H^\nu{}_\mu - \frac{3}{2}\omega_\beta q_\mu\right]. \end{aligned} \quad (5.97)$$

12. *The gravito-magnetic divergence (div H) constraint:*

$$0 = (C_5)^\alpha = \tilde{\nabla}_\beta H^{\alpha\beta} + (\rho + p)\omega^\alpha + 3\omega_\beta\left(E^{\alpha\beta} - \frac{1}{6}\pi^{\alpha\beta}\right) \quad (5.98)$$

$$+ \eta^{\alpha\beta\mu}\left[\frac{1}{2}\tilde{\nabla}_\beta q_\mu + \sigma_{\beta\nu}(E^\nu{}_\mu + \frac{1}{2}\pi^\nu{}_\mu)\right]. \quad (5.99)$$

We will recover the GR versions of these equations simply by setting $f(R) = R$, resulting in the matter parts being identical to standard matter, and all curvature fluid terms vanishing. In general, we can close the system by specifying the equation of state of the fluid sources, which amounts to choosing restrictions on the thermodynamic quantities. Very relevant for late-time considerations is that of pressureless non-relativistic matter, dust, with $p = q_\alpha = \pi_{\alpha\beta} = 0 \Rightarrow \dot{u}_\alpha = 0$.

Applying the decomposition to $f(R)$ modified gravity theories, for general space-times we get

$$\nabla_\alpha \nabla_\beta f_R = -\dot{f}_R \left(\frac{1}{3} h_{\alpha\beta} \Theta + \sigma_{\alpha\beta} + \omega_{\alpha\beta} \right) + u_\beta u_\alpha \ddot{f}_R + u_\alpha \dot{f}_R \dot{u}_\beta. \quad (5.100)$$

Furthermore, we obtain

$$\square f_R = -\Theta \dot{f}_R - \ddot{f}_R, \quad (5.101)$$

where any terms containing orthogonally projected derivatives have been neglected, since we are only considering isotropic and homogeneous space times.

The kinematics and thermodynamics above, prescribed by Eqs. (5.85)–(5.98), along with (5.70)–(5.72), formalise the physical interaction and evolution of the matter and gravitational fields in $f(R)$ gravity, and completely specify a cosmological model. This approach is invaluable in the investigations into alternative theories to GR, as it sets out a scheme that is both mathematically rigorous and intuitive. It has also been extremely useful in constructing and studying cosmological perturbations [89, 93, 96]. We refer the reader to these three references for a deeper insight about the foundations on the 1 + 3 covariant gauge invariant treatment of scalar perturbations in $f(R)$ gravity.

5.6 Geodesic Deviation in $f(R)$ Gravity

Historically, the geodesic deviation equation (GDE) has played a key role in the realm of gravitational physics and, consequently, in cosmology. Through this equation one could determine the relative geodesic deviation, dubbed η , between two neighbouring geodesics, which is pertinent to deriving important results for cosmologies. This equation can be recast in terms of the set of expansion-normalised dynamical variables and thus allow us to gain some insight into how for $f(R)$ theories it differs from GR predictions. We refer the reader to [97] for further details.

5.6.1 Formalism

The general geodesic deviation equation is given by

$$\frac{\delta^2 \eta^\alpha}{\delta v^2} = -R^\alpha{}_{\beta\sigma\gamma} V^\beta V^\gamma \eta^\sigma, \quad (5.102)$$

where η is the deviation vector, V^α is the normalised tangent vector field, and v is an affine parameter. It is useful to be able to express this deviation in terms of the density by substituting the expressions for the Riemann and Ricci tensors and the Ricci scalar.

Using the Riemann tensor:

$$R_{\alpha\beta\sigma\gamma} = C_{\alpha\beta\sigma\gamma} + \frac{1}{2} (g_{\alpha\sigma} R_{\beta\gamma} - g_{\alpha\gamma} R_{\beta\sigma} + g_{\beta\gamma} R_{\alpha\sigma} - g_{\beta\sigma} R_{\alpha\gamma}) - \frac{R}{6} (g_{\alpha\sigma} g_{\beta\gamma} - g_{\alpha\gamma} g_{\beta\sigma}), \quad (5.103)$$

and the fact that in FLRW space-times $C_{\alpha\beta\sigma\gamma}$, the Weyl tensor, vanishes, upon contracting (5.103) with $V^\beta \eta^\sigma V^\gamma$, we obtain

$$R^\alpha{}_{\beta\sigma\gamma} V^\beta \eta^\sigma V^\gamma = \frac{1}{2} (\eta^\alpha V^\beta V^\gamma R_{\beta\gamma} - V^\alpha V^\beta \eta^\sigma R_{\beta\sigma} + \epsilon R^\alpha{}_{\sigma} \eta^\sigma) - \frac{R}{6} \eta^\alpha \epsilon. \quad (5.104)$$

By writing $E = -V_\alpha u^\alpha$, $\eta_\alpha u^\alpha = \eta_\alpha V^\alpha = 0$, and $\epsilon = V_\alpha^\alpha$, we can simplify the terms of Eq.(5.104) as follows:

$$R^\alpha{}_{\beta\sigma\gamma} \eta^\sigma = \frac{1}{f_R} \left[\eta^\alpha \left(p_m + \frac{f}{2} - \square f_R \right) + (\nabla^\alpha \nabla_\sigma f_R) \eta^\sigma \right], \quad (5.105)$$

$$R_{\beta\sigma} V^\alpha V^\beta \eta^\sigma = \frac{1}{f_R} [(\nabla_\beta \nabla_\sigma f') V^\alpha V^\beta \eta^\sigma], \quad (5.106)$$

$$R_{\beta\gamma} V^\beta V^\gamma \eta^\alpha = \frac{1}{f_R} \left[(\rho_m + p_m) E^2 + \epsilon \left(p_m + \frac{f}{2} - \square f_R \right) + V^\beta V^\gamma \nabla_\beta \nabla_\gamma f_R \right] \eta^\alpha. \quad (5.107)$$

Using Eq. (5.100) and that for FLRW spacetimes, $\omega_{\alpha\beta} = \sigma_{\alpha\beta} = 0$, we can arrive at the following expressions:

$$V^\beta V^\gamma \nabla_\beta \nabla_\gamma f_R = -\frac{1}{3} \dot{f}_R \Theta (\epsilon + E^2) + E^2 \ddot{f}_R, \quad (5.108)$$

$$(\nabla_\beta \nabla_\sigma f') V^\alpha V^\beta \eta^\sigma = 0, \quad (5.109)$$

$$(\nabla^\alpha \nabla_\sigma f') \eta^\sigma = -\frac{1}{3} \dot{f}_R \Theta \eta^\alpha. \quad (5.110)$$

Substituting the above results into Eq. (5.104) gives

$$R^\alpha{}_{\beta\sigma\gamma} V^\beta V^\gamma \eta^\sigma = \frac{1}{2f_R} \left[\frac{f + \rho_m - 2\dot{f}_R \Theta}{3} - \square f_R + p_m \right] \eta^\alpha \epsilon + \frac{1}{2f_R} \left[\rho_m + p_m - \frac{1}{3} \dot{f}_R \Theta + \ddot{f}_R \right] \eta^\alpha E^2. \quad (5.111)$$

We can then identify terms in Eq. (5.111) to be combinations of the curvature fluid density and pressure, from

$$\rho^R + p^R = \frac{1}{f_R} \left[-\frac{1}{3} \dot{f}_R \Theta + \ddot{f}_R \right], \quad (5.112)$$

$$\rho^R + 3p^R = \frac{1}{f_R} [f + \Theta \dot{f}_R + 3\ddot{f}_R] - R, \quad (5.113)$$

such that we may obtain the final result for the geodesic deviation equation in metric $f(R)$ gravity [97]:

$$R^\alpha{}_{\beta\gamma\sigma} V^\beta V^\gamma \eta^\sigma = \frac{1}{2} (\rho_{tot} + p_{tot}) E^2 \eta^\alpha + \left[\frac{R}{6} + \frac{1}{6} (\rho_{tot} + 3p_{tot}) \right] \epsilon \eta^\alpha. \quad (5.114)$$

The result is consistent with what is expected in a homogeneous and isotropic geometry. The tidal force produced will only depend on η^α , and thus only the magnitude of the deviation vector η will change along the geodesic, while its direction is preserved.

Considering only the paths of photons, where $V^\alpha = k^\alpha$, and $k_\alpha k^\alpha = 0$, so $\epsilon = 0$, Eq. (5.114) becomes

$$R^\alpha{}_{\beta\sigma\gamma} k^\beta k^\gamma \eta^\sigma = \frac{1}{2} (\rho_{tot} + p_{tot}) E^2 \eta^\alpha, \quad (5.115)$$

showing the focusing of all families of past directed null geodesics as long as

$$(\rho_{tot} + p_{tot}) > 0. \quad (5.116)$$

Both Eqs. (5.114) and (5.115) will reduce to the GR result when $f(R) = R$.

5.6.2 Past-Directed Null Geodesics and Area Distance in $f(R)$ Gravity

We now consider how the case $V^\alpha = k^\alpha$, $k_\alpha k^\alpha = 0$, $k^0 < 0$ affects Eq. (5.115). Let $\eta^\alpha = \eta e^\alpha$ and $e^\alpha e_\alpha = 1$, and $e_\alpha u^\alpha = e_\alpha k^\alpha = 0$, with a basis e that is parallelly propagated and aligned, such that, $\delta e^\alpha / \delta v = 0 = k^\beta \nabla_\beta e^\alpha$. Equation (5.115) may thus be written as

$$\frac{d^2 \eta}{dv^2} = -\frac{1}{2} (\rho_{tot} + p_{tot}) E^2 \eta. \quad (5.117)$$

Once again, all families of past directed null geodesics will be focused so long that $(\rho_{tot} + p_{tot}) > 0$. When the right-hand side of (5.117) is zero (de Sitter universe in GR), the solution to this equations is the same as that in a flat Minkowski space-time: $\eta(v) = C_1(v) + C_2$. The chain rule gives

$$\frac{d^2}{dv^2} = \left(\frac{dz}{dv} \right)^2 \left[\frac{d^2}{dz^2} - \frac{dz}{dv} \frac{d^2 v}{dz^2} \frac{d}{dz} \right], \quad (5.118)$$

$$\frac{dz}{dv} = E_0 H(1+z). \quad (5.119)$$

Using this and the modified Friedmann and Raychaudhuri expressions, we obtain the following evolution equation for η with redshift, which depends only on the total equation of state:

$$\frac{d^2\eta}{dz^2} + \frac{(7 + 3w_{tot})}{2(1+z)} \frac{d\eta}{dz} + \frac{3(1 + w_{tot})}{2(1+z)^2} \eta = 0. \quad (5.120)$$

We may then infer an expression for the observer area distance $r_0(z)$

$$r_0(z) = \sqrt{\left| \frac{dA_0(z)}{d\Omega} \right|} = \left| \frac{\eta(z')|_{z'=0}}{d\eta(z')/dz'|_{z'=0}} \right|, \quad (5.121)$$

where A_0 is the area of the object, and Ω is the solid angle in the sky. Using the fact that $d/d\ell = E_0^{-1}(1+z)^{-1}d/dv = H(z+1)d/dz$, we can express r_0 in terms of redshift derivatives as

$$r_0(z) = \left| \frac{\eta(z)}{H(0)d\eta(z')}/dz'|_{z'=0} \right|. \quad (5.122)$$

In general, to find the observer distance relation above, we need to resort to numerical integration. For instance, in [97], the GDE was expressed in terms of a set of dynamical systems variables.

5.7 Gravitational Attractiveness in $f(R)$?

In this section we study the positive contributions of the Raychaudhuri equation for time-like geodesics, which guarantee the attractive character of the gravitational interaction in $f(R)$ theories [98]. Following [99], we write the Raychaudhuri equation as

$$\frac{d\theta}{d\tau} = -\frac{1}{3}\theta^2 - \sigma_{\mu\nu}\sigma^{\mu\nu} + \omega_{\mu\nu}\omega^{\mu\nu} - R_{\mu\nu}\xi^\mu\xi^\nu, \quad (5.123)$$

where θ is the expansion, $\sigma_{\mu\nu}$ is the shear, and $\omega_{\mu\nu}$ is the rotation of a congruence of time-like geodesics, generated by the tangent vector field ξ^μ , and τ is an affine parameter.

In GR, assuming the strong energy condition

$$T_{\mu\nu}^{(m)}\xi^\mu\xi^\nu \geq -\frac{1}{2}T^{(m)}, \quad (5.124)$$

implies that $R_{\mu\nu}\xi^\mu\xi^\nu \geq 0$. This is an important statement and results in the attractive nature of the gravitational interaction. It follows that the mean curvature [100], defined by $\mathcal{M}_\xi = -R_{\mu\nu}\xi^\mu\xi^\nu$, must, in every time-like direction, be negative or zero

in GR for fluids for which (5.124) holds. Following [99, 100], the mean curvature in every time-like direction

$$\mathcal{M}_\xi \equiv -R_{\mu\nu}\xi^\mu\xi^\nu \quad (5.125)$$

is negative or zero in GR, provided that the strong energy condition holds. If one chooses a congruence of time-like geodesics whose tangent vector field is locally hypersurface-orthogonal, then $\omega_{\mu\nu} = 0$ for all the congruences. This result enables the use of the Raychaudhuri equation in the singularity theorems. Since the term $\sigma_{\mu\nu}\sigma^{\mu\nu}$ is non-negative, assuming $R_{\mu\nu}\xi^\mu\xi^\nu \geq 0$, then

$$\frac{d\theta}{d\tau} + \frac{1}{3}\theta^2 \leq 0 \rightarrow \theta^{-1}(\tau) \geq \theta_0^{-1} + \frac{1}{3}\tau. \quad (5.126)$$

Inequality (5.126) indicates that a congruence that is initially converging ($\theta_0 \leq 0$) will converge to zero in a finite time. For this reasoning to be true, we require that $R_{\mu\nu}\xi^\mu\xi^\nu \geq 0$ for every non-space-like vector. In particular, for time-like geodesics, we consider this inequality in the late-time cosmological scenario, assuming a de Sitter phase of expansion, and negligible contributions from radiation and dust. In order to have accelerated expansion of time-like geodesics, the Ricci scalar, $R = R_0$, will be approximately constant.

We followed the results [100], from which it can be proved that

$$R_{\mu\nu}\xi^\mu\xi^\nu \geq \frac{f(R_0 - R_0f'(R_0))}{2(1 + f'(R_0))}, \quad (5.127)$$

where we require that the field equations (5.14), with constant scalar curvature and standard matter sources, satisfy the strong energy condition. Thus, the right-hand side of (5.127) must be negative in order to have $R_{\mu\nu}\xi^\mu\xi^\nu < 0$. Equivalently, $\mathcal{M}_\xi > 0$, and this means we need \mathcal{M}_ξ to be bounded from above. Thus the condition for time-like geodesics to diverge at late times becomes:

$$\frac{f(R_0 - R_0f'(R_0))}{2(1 + f'(R_0))} < 0. \quad (5.128)$$

If $1 + f'(R_0) > 0$, we obtain

$$f(R_0) - R_0f'(R_0) < 0. \quad (5.129)$$

If we take Eq. (5.14) in a vacuum ($T = 0$) for constant scalar curvature solutions, the value of R_0 satisfies

$$R_0 = \frac{-2f(R_0)}{1 - f'(R_0)}. \quad (5.130)$$

Although in general this cannot be solved analytically, some $f(R)$ models exist, depending on their parameters, for which a closed solution can be found. Rearranging

the terms in Eq. (5.129), we can find for a given model whether (5.130) implies that $R_0 > 0$. A positive contribution to the Raychaudhuri equation from the space-time geometry \mathcal{M}_ϵ for every time like direction is obtained, when this is true. This is an important theoretical consideration, which may be used to constrain the parameter space of paradigmatic $f(R)$ models.

5.8 Conclusions

Modifying Einsteinian Relativity is currently a popular field of research in many areas of physics, ranging from quantum theories of gravity to astrophysics and cosmology. The so-called $f(R)$ modification is derived by replacing the Ricci scalar, R , in the usual Einstein–Hilbert gravitational action with a general function f , which could in principle be *any* function of R . As illustrated above, this modification can be equivalent to adding an extra scalar field to the theory, which turns out to be the first derivative of $f(R)$, provided the second derivative of f is non-zero.

In fact, at least pertaining to dark energy models, almost all modifications can be generalised under the umbrella of effective field theories. Over the years, it has become understood that only very special models for $f(R)$ are worth studying in a cosmological and astrophysical sense. Indeed, only specific forms for the function can produce satisfactory physical effects, such as reproducing the gravitational field in and around a compact object, accelerating the Universe at late times as well as generating an expansion history similar to the observable Universe and providing a growth of large-scale structures in agreement with observations.

In particular, a generally favoured approach is to assume that the theory already contains General Relativity as a limit. Since one of the most relevant ways to determine the effects of this kind of modification is to examine dynamical changes in gravitating and large-scale systems, the behaviour of the gravitational field in $f(R)$ theories and the interaction between the emergent scalar field and matter have been widely considered in a range of different physical phenomena (see references in the bulk of the text). Degeneracy between $f(R)$ models has been shown to be the biggest bottleneck for these theories, since in principle there are plenty of clever $f(R)$ proposals capable of satisfying the basic theoretical requirements and fitting the available observational—both cosmological and astrophysical—data.

In this realm, one may have general classes of broken power-law models [43, 59], which are designed to reduce to General Relativity in low curvature regimes, and tend to General Relativity plus a cosmological constant when the curvature is large relatively to the local environment. These models also include, within their parameter space, previously considered $f(R)$ *viable* models, so in that sense, they parametrise a vast class of possible modification of the gravitational interaction with the sole addition of a scalar field. The redshift evolution of the Hubble rate and the deceleration parameter, in the class of models considered here, have very similar behaviour to that of the Λ CDM model. In general, deviations in the Hubble parameter begin to develop only at very low redshifts, $0 < z < 1$, while, the deceleration parameter,

showing larger deviations at low redshifts, still converges towards a value of $\frac{1}{2}$ from around a value of $z = 6$, consistent with the Λ CDM parametrisation. The exact behaviour will depend on the choices of model parameters, but this behaviour is typical of all the values that were tested.

Additionally from a theoretical point of view, the sections above devoted to first-order scalar perturbations, when expressed in the $1 + 3$ formalism, show how this formalism allows us to perform a simple treatment of matter power spectra observables after solving second-order coupled equations, instead of fourth-order counterparts, which would be required in the usual metric approach.

Finally, Sects. 5.6 and 5.7 aimed at illustrating how simple geometric calculations, when having promoted the usual GR action to $f(R)$ generalisations, may shed some light on unexpected consequences, provided the Einsteinian paradigm is abandoned. First, in Sect. 5.6 we provided information on how the geodesic deviation equation can be obtained for $f(R)$ theories. We used a $1 + 3$ decomposition, as explained in previous sections, enabling us to render intermediate calculations manageable and determine that the new geometrical contributions contribute to the deviation for both null and time-like geodesics. Consequently, we proved that the additional terms introduced by $f(R)$ theories, together with the standard matter content, impact on the evolution of the geodesic deviation. The well-known fact that extended gravity theories do not need to accomplish the standard energy conditions leads the geodesic deviation equation to exhibit a model-dependent behaviour that may be useful to constrain the viability of classes of models in such theories. Thus, such a result can be used to study the evolution of the deviation for null geodesics in a cosmological background and the subsequent $f(R)$ model-dependent numerical results for the area distance formula to be tested with observational data.

On the other hand, Sect. 5.7 showed how, should usual energy conditions be solely imposed upon the cosmological standard fluids, the capability of additional $f(R)$ terms to provide cosmological acceleration can be studied in a straightforward and systematic approach. With such a tool, this latter analysis can be extended to more involved cosmological scenarios and other alternative gravity theories beyond the concordance model.

With this brief and humble review on $f(R)$ theories we have intended to provide the main milestones for a layman's understanding of the $f(R)$ framework and how the usual predictions, as provided within the concordance gravitational and cosmological scenario, need to be revisited should they be modified in the scalar-tensor frame of gravitational theories. Once this is done, the pieces of analysis above can be easily extended to other more convoluted theories, different cosmological parameters in models therein and physically well-motivated initial and boundary conditions for the problems under study. Obviously, viable models need to be tested against, amongst others, CMB and weak gravitational lensing data, the ISW effect and even gravitational waves in order to place a full set of constraints on the parameter space of broad classes of $f(R)$ models. Only with such a thorough analysis would the class of most likely theories, given observational cosmological data, be determined and duly constrained.

References

1. C. Brans, R.H. Dicke, Mach's principle and a relativistic theory of gravitation. *Phys. Rev.* **124**, 925–935 (1961). ([142 (1961)])
2. T.L.J. Linden, A scalar field theory of gravitation. *Int. J. Theor. Phys.* **5**, 359–368 (1972)
3. V. Faraoni, *Cosmology in Scalar Tensor Gravity*, vol. 139 (Springer, Berlin, 2004)
4. K.S. Stelle, Renormalization of higher derivative quantum gravity. *Phys. Rev. D* **16**, 953–969 (1977)
5. R. Utiyama, B.S. DeWitt, Renormalization of a classical gravitational field interacting with quantized matter fields. *J. Math. Phys.* **3**, 608–618 (1962)
6. N.D. Birrell, P.C.W. Davies, *Quantum Fields in Curved Space*. Cambridge Monographs on Mathematical Physics. (Cambridge University Press, Cambridge, 1984)
7. I.L. Buchbinder, S.D. Odintsov, I.L. Shapiro, *Effective Action in Quantum Gravity* (IOP, Bristol, 1992), 413 p
8. G.A. Vilkovisky, Effective action in quantum gravity. *Class. Quant. Grav.* **9**, 895–903 (1992)
9. A.A. Starobinsky, A new type of isotropic cosmological models without singularity. *Adv. Ser. Astrophys. Cosmol.* **3**, 130–133 (1987)
10. R.H. Brandenberger, A Nonsingular universe, in *International School of Astrophysics, 'D. Chalonge': 2nd Course: Current Topics in Astrofundamental Physics Erice, Italy, September 6–13, 1992*, pp. 102–112. [arXiv:gr-qc/9210014](https://arxiv.org/abs/gr-qc/9210014)
11. M. Aparicio Resco, Á. de la Cruz Dombriz, F.J. Llanes Estrada, V. Zapatero Castrillo, On neutron stars in $f(R)$ theories: small radii, large masses and large energy emitted in a merger. *Phys. Dark Univ.* **13**, 147–161 (2016). [arXiv:1602.03880](https://arxiv.org/abs/1602.03880)
12. SDSS Collaboration, D.J. Eisenstein et al., Detection of the Baryon acoustic peak in the large-scale correlation function of SDSS luminous red galaxies. *Astrophys. J.* **633**, 560–574 (2005). [arXiv:astro-ph/0501171](https://arxiv.org/abs/astro-ph/0501171)
13. Supernova Search Team Collaboration, A.G. Riess et al., Type Ia supernova discoveries at $z > 1$ from the Hubble space telescope: evidence for past deceleration and constraints on dark energy evolution. *Astrophys. J.* **607**, 665–687 (2004). [arXiv:astro-ph/0402512](https://arxiv.org/abs/astro-ph/0402512)
14. WMAP Collaboration, D.N. Spergel et al., Wilkinson microwave anisotropy probe (WMAP) three year results: implications for cosmology. *Astrophys. J. Suppl.* **170**, 377 (2007). [arXiv:astro-ph/0603449](https://arxiv.org/abs/astro-ph/0603449)
15. J. Martin, Everything you always wanted to know about the cosmological constant problem (but were afraid to ask). *Comptes Rendus Physique* **13**, 566–665 (2012). [arXiv:1205.3365](https://arxiv.org/abs/1205.3365)
16. T. Clifton, P.G. Ferreira, A. Padilla, C. Skordis, Modified gravity and cosmology. *Phys. Rept.* **513**, 1–189 (2012). [arXiv:1106.2476](https://arxiv.org/abs/1106.2476)
17. V. Faraoni, S. Capozziello, *Beyond Einstein gravity*, vol. 170 (Springer, Dordrecht, 2011)
18. D. Lovelock, The Einstein tensor and its generalizations. *J. Math. Phys.* **12**, 498–501 (1971)
19. G. Cognola, E. Elizalde, S. Nojiri, S.D. Odintsov, S. Zerbini, Dark energy in modified Gauss-Bonnet gravity: late-time acceleration and the hierarchy problem. *Phys. Rev. D* **73**, 084007 (2006). [arXiv:hep-th/0601008](https://arxiv.org/abs/hep-th/0601008)
20. S. Nojiri, S.D. Odintsov, Modified Gauss-Bonnet theory as gravitational alternative for dark energy. *Phys. Lett. B* **631**, 1–6 (2005). [arXiv:hep-th/0508049](https://arxiv.org/abs/hep-th/0508049)
21. A. de la Cruz-Dombriz, D. Saez-Gomez, On the stability of the cosmological solutions in $f(R, G)$ gravity. *Class. Quant. Grav.* **29**, 245014 (2012). [arXiv:1112.4481](https://arxiv.org/abs/1112.4481)
22. C.H. Brans, Mach's principle and a relativistic theory of gravitation. II. *Phys. Rev.* **125**, 2194–2201 (1962)
23. J. Garcia-Bellido, A.D. Linde, D.A. Linde, Fluctuations of the gravitational constant in the inflationary Brans-Dicke cosmology. *Phys. Rev. D* **50**, 730–750 (1994). [arXiv:astro-ph/9312039](https://arxiv.org/abs/astro-ph/9312039)
24. J.A.R. Cembranos, K.A. Olive, M. Peloso, J.-P. Uzan, Quantum corrections to the cosmological evolution of conformally coupled fields. *JCAP* **0907**, 025 (2009). [arXiv:0905.1989](https://arxiv.org/abs/0905.1989)
25. L.H. Ford, Inflation driven by a vector field. *Phys. Rev. D* **40**, 967 (1989)

26. J. Beltran Jimenez, A.L. Maroto, A cosmic vector for dark energy. *Phys. Rev. D* **78**, 063005 (2008). [arXiv:0801.1486](#)
27. T. Koivisto, D.F. Mota, Vector field models of inflation and dark energy. *JCAP* **0808**, 021 (2008). [arXiv:0805.4229](#)
28. J. Alcaraz, J.A.R. Cembranos, A. Dobado, A.L. Maroto, Limits on the brane fluctuations mass and on the brane tension scale from electron positron colliders. *Phys. Rev. D* **67**, 075010 (2003). [arXiv:hep-ph/0212269](#)
29. G.R. Dvali, G. Gabadadze, M. Porrati, 4-D gravity on a brane in 5-D Minkowski space. *Phys. Lett. B* **485**, 208–214 (2000). [arXiv:hep-th/0005016](#)
30. D. Blaschke, M.P. Dabrowski, Conformal relativity versus Brans-Dicke and superstring theories. *Entropy* **14**, 1978–1996 (2012). [arXiv:hep-th/0407078](#)
31. J. Khoury, A. Weltman, Chameleon cosmology. *Phys. Rev. D* **69**, 044026 (2004). [arXiv:astro-ph/0309411](#)
32. L. Perivolaropoulos, PPN parameter gamma and solar system constraints of massive Brans-Dicke theories. *Phys. Rev. D* **81**, 047501 (2010). [arXiv:0911.3401](#)
33. M. Hohmann, L. Jarv, P. Kuusk, E. Randla, Post-Newtonian parameters γ and β of scalar-tensor gravity with a general potential. *Phys. Rev. D* **88**(8), 084054 (2013). [arXiv:1309.0031](#). [Erratum: *Phys. Rev. D* 89(6), 069901 (2014)]
34. S. Capozziello, S. Nojiri, S.D. Odintsov, Dark energy: the Equation of state description versus scalar-tensor or modified gravity. *Phys. Lett. B* **634**, 93–100 (2006). [arXiv:hep-th/0512118](#)
35. T.P. Sotiriou, V. Faraoni, $f(R)$ theories of gravity. *Rev. Mod. Phys.* **82**, 451–497 (2010). [arXiv:0805.1726](#)
36. T.P. Sotiriou, $f(R)$ gravity and scalar-tensor theory. *Class. Quant. Grav.* **23**, 5117–5128 (2006). [arXiv:gr-qc/0604028](#)
37. T.P. Sotiriou, Curvature scalar instability in $f(R)$ gravity. *Phys. Lett. B* **645**, 389–392 (2007). [arXiv:gr-qc/0611107](#)
38. S.M. Carroll, V. Duvvuri, M. Trodden, M.S. Turner, Is cosmic speed - up due to new gravitational physics? *Phys. Rev. D* **70**, 043528 (2004). [arXiv:astro-ph/0306438](#)
39. B. Bertotti, L. Iess, P. Tortora, A test of general relativity using radio links with the Cassini spacecraft. *Nature* **425**, 374–376 (2003)
40. L. Amendola, D. Polarski, S. Tsujikawa, Are $f(R)$ dark energy models cosmologically viable? *Phys. Rev. Lett.* **98**, 131302 (2007). [arXiv:astro-ph/0603703](#)
41. L. Amendola, D. Polarski, S. Tsujikawa, Power-laws $f(R)$ theories are cosmologically unacceptable. *Int. J. Mod. Phys. D* **16**, 1555–1561 (2007). [arXiv:astro-ph/0605384](#)
42. L. Amendola, R. Gannouji, D. Polarski, S. Tsujikawa, Conditions for the cosmological viability of $f(R)$ dark energy models. *Phys. Rev. D* **75**, 083504 (2007). [arXiv:gr-qc/0612180](#)
43. W. Hu, I. Sawicki, Models of $f(R)$ cosmic acceleration that evade solar-system tests. *Phys. Rev. D* **76**, 064004 (2007). [arXiv:0705.1158](#)
44. S. Nojiri, S.D. Odintsov, Modified $f(R)$ gravity consistent with realistic cosmology: from matter dominated epoch to dark energy universe. *Phys. Rev. D* **74**, 086005 (2006). [arXiv:hep-th/0608008](#)
45. S. Nojiri, S.D. Odintsov, Modified gravity and its reconstruction from the universe expansion history. *J. Phys. Conf. Ser.* **66**, 012005 (2007). [arXiv:hep-th/0611071](#)
46. J.D. Evans, L.M.H. Hall, P. Cailloil, Standard cosmological evolution in a wide range of $f(R)$ models. *Phys. Rev. D* **77**, 083514 (2008). [arXiv:0711.3695](#)
47. A. de la Cruz-Dombriz, A. Dobado, A $f(R)$ gravity without cosmological constant. *Phys. Rev. D* **74**, 087501 (2006). [arXiv:gr-qc/0607118](#)
48. P.K.S. Dunsby, E. Elizalde, R. Goswami, S. Odintsov, D.S. Gomez, On the LCDM Universe in $f(R)$ gravity. *Phys. Rev. D* **82**, 023519 (2010). [arXiv:1005.2205](#)
49. B.S. DeWitt, Dynamical theory of groups and fields. *Conf. Proc. C* **630701**, 585–820 (1964). ([Les Houches Lect. Notes 13, 585 (1964)])
50. G.J. Olmo, Palatini approach to modified gravity: $f(R)$ theories and beyond. *Int. J. Mod. Phys. D* **20**, 413–462 (2011). [arXiv:1101.3864](#)

51. T.P. Sotiriou, S. Liberati, Metric-affine $f(R)$ theories of gravity. *Ann. Phys.* **322**, 935–966 (2007). [arXiv:gr-qc/0604006](#)
52. T. Chiba, $1/R$ gravity and scalar - tensor gravity. *Phys. Lett. B* **575**, 1–3 (2003). [arXiv:astro-ph/0307338](#)
53. J. O’Hanlon, Mach’s principle and a new gauge freedom in Brans-Dicke theory. *J. Phys. A* **5**, 803–811 (1972)
54. P. Teyssandier, P. Tourrenc, The Cauchy problem for the $R + R * *2$ theories of gravity without torsion. *J. Math. Phys.* **24**, 2793 (1983)
55. D. Wands, Extended gravity theories and the Einstein-Hilbert action. *Class. Quant. Grav.* **11**, 269–280 (1994). [arXiv:gr-qc/9307034](#)
56. R. Lazkoz, M. Ortiz-Baños, V. Salzano, $f(R)$ gravity modifications: from the action to the data. *Eur. Phys. J. C* **78**(3), 213 (2018). [arXiv:1803.05638](#)
57. S. Basilakos, S. Nesseris, Conjoined constraints on modified gravity from the expansion history and cosmic growth. *Phys. Rev. D* **96**(6), 063517 (2017). [arXiv:1705.08797](#)
58. L. Jaime, M. Salgado, L. Patino, Cosmology in $\{R\}$ exponential gravity. *Springer Proc. Phys.* **157**, 363–371 (2014). [arXiv:1211.0015](#)
59. V. Miranda, S.E. Joras, I. Waga, M. Quartin, Viable Singularity-Free $f(R)$ Gravity Without a Cosmological Constant. *Phys. Rev. Lett.* **102**, 221101 (2009). [arXiv:0905.1941](#)
60. T. Chiba, T.L. Smith, A.L. Erickcek, Solar System constraints to general $f(R)$ gravity. *Phys. Rev. D* **75**, 124014 (2007). [arXiv:astro-ph/0611867](#)
61. J. Khoury, A. Weltman, Chameleon fields: Awaiting surprises for tests of gravity in space. *Phys. Rev. Lett.* **93**, 171104 (2004). [arXiv:astro-ph/0309300](#)
62. L.M. Sokolowski, Stability of a metric $f(R)$ gravity theory implies the Newtonian limit. *Acta Phys. Polon. B* **39**, 2879–2901 (2008). [arXiv:0810.2554](#)
63. S.A. Appleby, R.A. Battye, A.A. Starobinsky, Curing singularities in cosmological evolution of $F(R)$ gravity. *JCAP* **1006**, 005 (2010). [arXiv:0909.1737](#)
64. J.M. Cline, S. Jeon, G.D. Moore, The Phantom menaced: constraints on low-energy effective ghosts. *Phys. Rev. D* **70**, 043543 (2004). [arXiv:hep-ph/0311312](#)
65. H. Nariai, Gravitational instability of regular model-universes in a modified theory of general relativity. *Prog. Theor. Phys.* **49**, 165–180 (1973)
66. V.T. Gurovich, A.A. Starobinsky, Quantum effects and regular cosmological models. *Sov. Phys. JETP* **50**, 844–852 (1979). [*Zh. Eksp. Teor. Fiz.* **77**, 1683 (1979)]
67. A.D. Dolgov, M. Kawasaki, Can modified gravity explain accelerated cosmic expansion? *Phys. Lett. B* **573**, 1–4 (2003). [arXiv:astro-ph/0307285](#)
68. V. Faraoni, Matter instability in modified gravity. *Phys. Rev. D* **74**, 104017 (2006). [arXiv:astro-ph/0610734](#)
69. V. Faraoni, de Sitter space and the equivalence between $f(R)$ and scalar-tensor gravity. *Phys. Rev. D* **75**, 067302 (2007). [arXiv:gr-qc/0703044](#)
70. V. Faraoni, $f(R)$ gravity: successes and challenges, in *18th SIGRAV Conference Cosenza, Italy, September 22-25* (2008). [arXiv:0810.2602](#)
71. A.V. Frolov, A singularity problem with $f(R)$ dark energy. *Phys. Rev. Lett.* **101**, 061103 (2008). [arXiv:0803.2500](#)
72. S.A. Appleby, R.A. Battye, Do consistent $F(R)$ models mimic General Relativity plus Λ ? *Phys. Lett. B* **654**, 7–12 (2007). [arXiv:0705.3199](#)
73. A.A. Starobinsky, Disappearing cosmological constant in $f(R)$ gravity. *JETP Lett.* **86**, 157–163 (2007). [arXiv:0706.2041](#)
74. S. Tsujikawa, Observational signatures of $f(R)$ dark energy models that satisfy cosmological and local gravity constraints. *Phys. Rev. D* **77**, 023507 (2008). [arXiv:0709.1391](#)
75. L.G. Jaime, L. Patino, M. Salgado, $f(R)$ cosmology revisited. [arXiv:1206.1642](#)
76. J.M. Ezquiaga, M. Zumalacárregui, Dark energy after GW170817: dead ends and the road ahead. *Phys. Rev. Lett.* **119**(25), 251304 (2017). [arXiv:1710.05901](#)
77. P. Creminelli, F. Vernizzi, Dark energy after GW170817 and GRB170817A. *Phys. Rev. Lett.* **119**(25), 251302 (2017). [arXiv:1710.05877](#)

78. P. Zhang, Testing $f(R)$ gravity against the large scale structure of the universe. *Phys. Rev. D* **73**, 123504 (2006). [arXiv:astro-ph/0511218](#)
79. B. Boisseau, G. Esposito-Farese, D. Polarski, A.A. Starobinsky, Reconstruction of a scalar tensor theory of gravity in an accelerating universe. *Phys. Rev. Lett.* **85**, 2236 (2000). [arXiv:gr-qc/0001066](#)
80. G. Esposito-Farese, D. Polarski, Scalar tensor gravity in an accelerating universe. *Phys. Rev. D* **63**, 063504 (2001). [arXiv:gr-qc/0009034](#)
81. S. Tsujikawa, Matter density perturbations and effective gravitational constant in modified gravity models of dark energy. *Phys. Rev. D* **76**, 023514 (2007). [arXiv:0705.1032](#)
82. R. Bean, D. Bernat, L. Pogosian, A. Silvestri, M. Trodden, Dynamics of linear perturbations in $f(R)$ gravity. *Phys. Rev. D* **75**, 064020 (2007). [arXiv:astro-ph/0611321](#)
83. A. de la Cruz-Dombriz, A. Dobado, A.L. Maroto, On the evolution of density perturbations in $f(R)$ theories of gravity. *Phys. Rev. D* **77**, 123515 (2008). [arXiv:0802.2999](#)
84. M. Salgado, The Cauchy problem of scalar tensor theories of gravity. *Class. Quant. Grav.* **23**, 4719–4742 (2006). [arXiv:gr-qc/0509001](#)
85. J. Ehlers, P. Geren, R.K. Sachs, Isotropic solutions of the Einstein-Liouville equations. *J. Math. Phys.* **9**, 1344–1349 (1968)
86. S.J. Stoeger, R. William, R. Maartens, G.F.R. Ellis, proving almost homogeneity of the universe: an almost Ehlers-Geren-Sachs theorem. *Astrophys. J.* **443**, 1 (1995)
87. C.A. Clarkson, A.A. Coley, E.S.D. O’Neill, The Cosmic microwave background and scalar tensor theories of gravity. *Phys. Rev. D* **64**, 063510 (2001). [arXiv:gr-qc/0105026](#)
88. R. Maartens, D.R. Taylor, Fluid dynamics in higher order gravity. *Gen. Rel. Grav.* **26**, 599–613 (1994)
89. G.F.R. Ellis, H. van Elst, Cosmological models: cargese lectures. *NATO Sci. Ser. C* **541**(1999), 1–116 (1998). [arXiv:gr-qc/9812046](#)
90. J. Ehlers, Contributions to the relativistic mechanics of continuous media. *Gen. Rel. Grav.* **25**, 1225–1266 (1993). ([Abh. Akad. Wiss. Lit. Mainz. Nat. Kl. 11, 793 (1961)])
91. R. Maartens, Linearization instability of gravity waves? *Phys. Rev. D* **55**, 463–467 (1997). [arXiv:astro-ph/9609198](#)
92. S. Carloni, A. Troisi, P.K.S. Dunsby, Some remarks on the dynamical systems approach to fourth order gravity. *Gen. Rel. Grav.* **41**, 1757–1776 (2009). [arXiv:0706.0452](#)
93. S. Carloni, P.K.S. Dunsby, A. Troisi, The Evolution of density perturbations in $f(R)$ gravity. *Phys. Rev. D* **77**, 024024 (2008). [arXiv:0707.0106](#)
94. A. Abebe, A. de la Cruz-Dombriz, P.K.S. Dunsby, Large scale structure constraints for a class of $f(R)$ theories of gravity. *Phys. Rev. D* **88**, 004050 (2013). [arXiv:1304.3462](#)
95. A. Abebe, M. Abdelwahab, A. de la Cruz-Dombriz, P.K.S. Dunsby, Covariant gauge-invariant perturbations in multifluid $f(R)$ gravity. *Class. Quant. Grav.* **29**, 135011 (2012). [arXiv:1110.1191](#)
96. H. Kodama, M. Sasaki, Cosmological Perturbation Theory. *Prog. Theor. Phys. Suppl.* **78**, 1–166 (1984)
97. A. de la Cruz-Dombriz, P.K.S. Dunsby, V.C. Busti, S. Kandhai, On tidal forces in $f(R)$ theories of gravity. *Phys. Rev. D* **89**(6), 064029 (2014). [arXiv:1312.2022](#)
98. Á. de la Cruz-Dombriz, P.K.S. Dunsby, S. Kandhai, D. Sáez-Gómez, Theoretical and observational constraints of viable $f(R)$ theories of gravity. *Phys. Rev. D* **93**(8), 084016 (2016). [arXiv:1511.00102](#)
99. F.D. Albareti, J.A.R. Cembranos, A. de la Cruz-Dombriz, A. Dobado, On the non-attractive character of gravity in $f(R)$ theories. *JCAP* **1307**, 009 (2013). [arXiv:1212.4781](#)
100. F.D. Albareti, J.A.R. Cembranos, A. de la Cruz-Dombriz, Focusing of geodesic congruences in an accelerated expanding Universe. *JCAP* **1212**, 020 (2012). [arXiv:1208.4201](#)

Chapter 6

Horndeski/Galileon Theories



Prado Martín-Moruno

6.1 From Brans–Dicke to Horndeski

General Relativity describes gravity as a geometrical property of the spacetime that has its origin in the matter contained therein. This idea is inspired by what is known as Mach's principle, which argues that inertia should be the result of the interaction between bodies. Nevertheless, Brans and Dicke [1] considered that in order to suitably implement this principle, the gravitational constant $\kappa^2 = 8\pi G$ has to depend on the mass distribution and, therefore, can vary with time and position. They assumed that the scalar variable in which the gravitational “constant” depends is a new scalar field serving to determine the local value of G , so $G \propto 1/\phi$, and that the weak equivalence principle should be satisfied. Therefore, they proposed the following Lagrangian density to describe gravity:

$$\mathcal{L} = \phi R - \frac{\omega}{\phi} \phi_{;\nu} \phi^{;\nu} + \mathcal{L}_m, \quad (6.1)$$

where ω is a positive constant, a semicolon denotes covariant derivative, and \mathcal{L}_m is the Lagrangian density of all (minimally coupled) non-gravitational fields. Whereas $G \propto 1/\phi$ is one of the simplest gravitational couplings one could imagine, it is possible to consider more general functions. One can have generalized Brans–Dicke theories of the form

$$\mathcal{L} = F(\phi)R - \phi_{;\nu} \phi^{;\nu} - V(\phi) + \mathcal{L}_m, \quad (6.2)$$

which lead to $G \propto 1/F'(\phi)$. This Lagrangian density is equivalent to allowing the constant ω to be a function of the field, adding a potential term, and then performing

P. Martín-Moruno (✉)
Departamento de Física Teórica and IPARCOS, Universidad Complutense de Madrid,
28040 Madrid, Spain
e-mail: pradomm@ucm.es

a trivial field redefinition in the Brans-Dicke Lagrangian (6.1). With that field redefinition, Lagrangian (6.1) can also be written in the form of (6.2) with $F(\phi) \propto \phi^2$.

On the other hand, even within General Relativity, it is possible to go beyond the minimally coupled canonical scalar field. For example, regarding the applications of scalar fields to describe dark energy, quintessence models, which assume a canonical kinetic term and a potential, have been generalized to K-essence [2], whose Lagrangian is a more general function $K(\phi, \phi_{;\nu} \phi^{;\nu})$. Furthermore, in kinetic braiding models [3] the scalar field Lagrangian is further generalized:

$$\mathcal{L}_\phi = K(\phi, X) + G(\phi, X)\square\phi, \quad (6.3)$$

where we have defined $X = -\phi_{;\nu} \phi^{;\nu}/2$, and $K(\phi, X)$ and $G(\phi, X)$ are arbitrary functions of the field and its kinetic term. Even if this Lagrangian density contains second derivatives of the field, the combination is such that the field equation is second order [3]; therefore, it is free of the Ostrogradski instability [4].

How far can we go in generalizing the scalar-field Lagrangian without introducing higher derivatives in the field equations? Galileon models [5] are shift-symmetric models in flat space, containing second-order derivatives in the Lagrangian and in the equation of motion. When considering these Galileons in a dynamical spacetime, one has to introduce a non-minimal coupling to curvature in order to avoid the introduction of higher order derivatives in the equations [6]. This coupling can be more general than that considered by Brans and Dicke, Eq. (6.2), and entail $\phi^{;\mu} R_{\mu\nu} \phi^{;\nu}$ terms. Dropping the requirement of shift symmetry, Generalized Galileons [7] comprise all models with a Lagrangian containing second-order derivatives of the field and with second-order equations of motion. The Lagrangian density is given by [8]

$$\mathcal{L}_{\text{GG}} = \mathcal{L}_2 + \mathcal{L}_3 + \mathcal{L}_4 + \mathcal{L}_5, \quad (6.4)$$

with

$$\mathcal{L}_2 = K(\phi, X) \quad (6.5)$$

$$\mathcal{L}_3 = -G_3(\phi, X)\square\phi \quad (6.6)$$

$$\mathcal{L}_4 = G_4(\phi, X)R + G_{4,X}(\phi, X) \left[(\square\phi)^2 - \phi_{;\mu\nu} \phi^{;\mu\nu} \right] \quad (6.7)$$

$$\mathcal{L}_5 = G_5(\phi, X)G_{\mu\nu} \phi^{;\mu\nu} - \frac{1}{6}G_{5,X} \left[(\square\phi)^3 + 2\phi_{;\mu}{}^\nu \phi_{;\nu}{}^\alpha \phi_{;\alpha}{}^\mu - 3\phi_{;\mu\nu} \phi^{;\mu\nu} \square\phi \right], \quad (6.8)$$

with $K(\phi, X)$, $G_3(\phi, X)$, $G_4(\phi, X)$, and $G_5(\phi, X)$ being arbitrary functions and a comma representing a derivative. Note that \mathcal{L}_2 is K-essence, $\mathcal{L}_2 + \mathcal{L}_3$ is kinetic braiding (6.3), and the Brans–Dicke theory, given by Lagrangian (6.2), is just a particular case of $\mathcal{L}_2 + \mathcal{L}_4$. Generalized Galileons are equivalent [8] to Horndeski theory [9], which was constructed in 1974, but it was also practically forgotten for almost 40 years. Horndeski Lagrangian density is [9]

$$\begin{aligned}
\mathcal{L}_H = & \delta_{\mu\nu\sigma}^{\alpha\beta\gamma} \left[\kappa_1(\phi, X) \phi^{;\mu}_{;\alpha} R_{\beta\gamma}{}^{\nu\sigma} + \frac{2}{3} \kappa_{1,X}(\phi, X) \phi^{;\mu}_{;\alpha} \phi^{;\nu}_{;\beta} \phi^{;\sigma}_{;\gamma} \right. \\
& + \kappa_3(\phi, X) \phi_{;\alpha} \phi^{;\mu} R_{\beta\gamma}{}^{\nu\sigma} + 2\kappa_{3,X}(\phi, X) \phi_{;\alpha} \phi^{;\mu} \phi^{;\nu}_{;\beta} \phi^{;\sigma}_{;\gamma} \left. \right] \\
& + \delta_{\mu\nu}^{\alpha\beta} \left[F(\phi, X) R_{\alpha\beta}{}^{\mu\nu} + 2F_{,X}(\phi, X) \phi^{;\mu}_{;\alpha} \phi^{;\nu}_{;\beta} + 2\kappa_8(\phi, X) \phi_{;\alpha} \phi^{;\mu} \phi^{;\nu}_{;\beta} \right] \\
& - 6 \left[F_{,\phi}(\phi, X) - X \kappa_8(\phi, X) \right] \phi^{;\mu}_{;\mu} + \kappa_9(\phi, X), \tag{6.9}
\end{aligned}$$

where $\kappa_i(\phi, X)$ are arbitrary functions (we have absorbed an additional $W(\phi)$ function in $F(\phi, X)$) [8], and

$$F_{,X} = 2(\kappa_3 + 2X\kappa_{3,X} - \kappa_{1,\phi}). \tag{6.10}$$

The antisymmetric character of the generalized delta functions in Lagrangian (6.9) is responsible for removing derivatives of an order higher than two from the equations. The dictionary between Lagrangians (6.4) and (6.9) is [8]

$$K = \kappa_9 + 4X \int^X dX' (\kappa_{8,\phi} - 2\kappa_{3,\phi\phi}), \tag{6.11}$$

$$G_3 = 6F_{,\phi} - 2X\kappa_8 - 8X\kappa_{3,\phi} + 2 \int^X dX' (\kappa_8 - 2\kappa_{3,\phi}), \tag{6.12}$$

$$G_4 = 2F - 4X\kappa_3, \tag{6.13}$$

$$G_5 = -4\kappa_1. \tag{6.14}$$

Horndeski Lagrangian is the most general one leading to second-order equations of motion. However, it is worth noting that there are theories leading to higher-order equations of motion that, even so, avoid the Ostrogradski instability [10–12]. These scalar-tensor theories are known as beyond Horndeski.

6.2 Background Cosmology

Focusing our attention on cosmological models, we consider a spatially flat Friedmann-Lemaître-Robertson-Walker metric

$$ds^2 = -dt^2 + a(t)^2 d\mathbf{x}^2, \tag{6.15}$$

where $a(t)$ is the scale factor. Deriving the field equations from the Horndeski Lagrangian and then restricting to this highly symmetric background is equivalent to obtaining the point-like Lagrangian, which is defined in the minisuperspace formed by the scale factor and the homogeneous field, $\{a, \phi\}$, and then deriving the equations of motion. This is

$$L_H = \mathcal{V}_{(3)}^{-1} \int d^3x \mathcal{L}_H, \tag{6.16}$$

with $\mathcal{V}_{(3)}$ the spatial three-volume element. Second derivatives in the point-like Lagrangian obtained from (6.9) can be removed by integrating by parts [13]. That Lagrangian then takes the simple form [13]

$$L_H(\phi, \dot{\phi}, a, \dot{a}) = a^3 \sum_{i=0..3} X_i(\phi, \dot{\phi}) H^i, \quad (6.17)$$

where $H = \dot{a}/a$ is the Hubble parameter, an over-dot represents a derivative with respect to the cosmic time t , and the functions X_i are [13, 14]

$$X_0 = -\bar{Q}_{7,\phi} \dot{\phi} + \kappa_9, \quad (6.18)$$

$$X_1 = -3\bar{Q}_7 + Q_7 \dot{\phi}, \quad (6.19)$$

$$X_2 = 12 F_{,X} X - 12 F, \quad (6.20)$$

$$X_3 = -4 \kappa_{1,X} \dot{\phi}^3, \quad (6.21)$$

where

$$Q_7 = \bar{Q}_{7,\phi} = 6 F_{,\phi} - 3 \dot{\phi}^2 \kappa_8. \quad (6.22)$$

As there is an Einstein–Hilbert term contained in the Horndeski Lagrangian (6.9), we can extract it from (6.17) and express it explicitly:

$$L = L_{EH} + L_H + L_m, \quad (6.23)$$

with

$$L_{EH} = -\frac{3}{\kappa^2} a^3 H^2 \quad \text{and} \quad L_m = -a^3 \rho(a) = -a^3 \sum_i \rho_i(a), \quad (6.24)$$

where $\rho(a)$ is the conserved total energy density, $\rho_i(a)$ corresponds to each cosmic fluid. Therefore, the modified Friedmann equation and the field equation are

$$\frac{3H^2}{\kappa^2} = \sum_{i=0..3} [(i-1)X_i + X_{i,\dot{\phi}} \dot{\phi}] H^i + \rho(a), \quad (6.25)$$

and

$$\sum_{i=0}^3 \left[X_{i,\phi} - 3X_{i,\dot{\phi}} H - iX_{i,\dot{\phi}} \frac{\dot{H}}{H} - X_{i,\dot{\phi}\dot{\phi}} \dot{\phi} - X_{i,\dot{\phi}\dot{\phi}\dot{\phi}} \ddot{\phi} \right] H^i = 0, \quad (6.26)$$

respectively. These equations can also be expressed using the Generalized Galileons functions of Lagrangian density (6.4). These are [8]

$$\sum_i \mathcal{E}_i = 0, \quad (6.27)$$

with

$$\mathcal{E}_2 = 2XK_{,x} - K \quad (6.28)$$

$$\mathcal{E}_3 = 6X\dot{\phi}HG_{3,X} - 2XG_{3,\phi} \quad (6.29)$$

$$\begin{aligned} \mathcal{E}_4 = & -6H^2G_4 + 24H^2X(G_{4,X} + XG_{4,XX}) - 12H\dot{\phi}G_{4,\phi X} \\ & - 6H\dot{\phi}G_{4,\phi} \end{aligned} \quad (6.30)$$

$$\mathcal{E}_5 = 2H^3X\dot{\phi}(5G_{5,X} + 2XG_{5,XX}) - 6H^2X(3G_{5,\phi} + 2XG_{5,\phi X}), \quad (6.31)$$

and

$$\frac{d}{dt}(a^3 J) = a^3 P_{,\phi}, \quad (6.32)$$

with

$$\begin{aligned} J = & \dot{\phi}K_X + 6HXXG_{3,X} - 2\dot{\phi}G_{3,\phi} + 6H^2\dot{\phi}(G_{4,X} + 2XG_{4,XX}) - 12HXXG_{4,\phi X} \\ & + 2H^3X(3G_{5,X} + 2XG_{5,XX}) - 6H^2\dot{\phi}(G_{5,\phi} + XG_{5,\phi X}) \end{aligned} \quad (6.33)$$

and

$$\begin{aligned} P_{,\phi} = & K_{,\phi} - 2X(G_{3,\phi\phi} + \ddot{\phi}G_{3,\phi X}) + 6G_{4,\phi}(2H^2 + \dot{H}) + 6HG_{4,\phi X}(\dot{X} + 2HX) \\ & - 6H^2XG_{5,\phi\phi} + 2H^3X\dot{\phi}G_{5,\phi X}. \end{aligned} \quad (6.34)$$

This field equation shows the special interest of shift-symmetric models. For these models, the equations are invariant under a field redefinition $\phi \rightarrow \phi + c$. Therefore, $\mathcal{P}_{,\phi} = 0$ and there is a conserved quantity, $\Sigma = Ja^3$; therefore, $J(\dot{\phi}, H) = \Sigma a^{-3} \rightarrow 0$ when the scale factor goes to infinity [8]. Any trajectory in the phase space $\dot{\phi}(H, a)$, which can be obtained from condition $J(\dot{\phi}, H) = \Sigma a^{-3}$, will tend to the *tracker solution* $\dot{\phi}_{\text{tracker}}(H)$, obtained from $\Sigma = 0$ [15]. Therefore, any attractor will be a point in the trajectory $J = 0$, approached by any trajectory in the phase space. De Sitter attractors are of particular interest to describe the late-time cosmic acceleration [15]. Many interesting studies have investigated the potential of Horndeski theory to describe the late-time cosmic acceleration [16–21], with emphasis on the prediction of a de Sitter attractor, and early-time cosmic acceleration [8, 22, 23], pointing out the potential avoidance of the Big Bang singularity. It is impossible to include a complete list of references in the present paper.

6.3 Cosmological Perturbations

We have shown how one can study the background cosmic evolution described by Horndeski models. The next step should be, therefore, to investigate the stability of the obtained cosmic models. In order to simplify the study of cosmic perturbations, Bellini and Sawicki introduced four useful functions that encapsulate all the necessary physics in reference [24]. Defining first the effective reduced Planck mass

$$M_*^2 = 2(G_4 - 2XG_{4,X} + XG_{5,\phi} - \dot{\phi}HXG_{5,X}), \quad (6.35)$$

where we remind the reader that M_*^2 is inversely proportional to the gravitational “constant”, these functions are:

Planck-mass run rate, α_m . The rate of evolution of the effective reduced Planck mass is

$$\alpha_m = H^{-1} \frac{d \ln M_*^2}{dt}. \quad (6.36)$$

Kineticity, α_K . The kinetic energy of scalar perturbations arising directly from the action

$$\begin{aligned} H^2 M_*^2 \alpha_K = & 2X(K_{,X} + 2XK_{,XX} - 2G_{3,\phi} - 2XG_{3,\phi X}) \\ & + 12\dot{\phi}XH(G_{3,X} + XG_{3,XX} - 3G_{4,\phi X} - 2XG_{4,\phi XX}) \\ & + 12XH^2(G_{4,X} + 8XG_{4,XX} + 4X^2G_{4,XXX}) \\ & - 12XH^2(G_{5,\phi} + 5XG_{5,\phi X} + 2X^2G_{5,\phi XX}) \\ & + 4\dot{\phi}XH^3(3G_{5,X} + 7XG_{5,XX} + 2X^2G_{5,XXX}). \end{aligned} \quad (6.37)$$

Braiding, α_B . The mixing of the kinetic terms of the scalar and the metric is

$$\begin{aligned} HM_*^2 \alpha_B = & 2\dot{\phi}(XG_{3,X} - G_{4,\phi} - 2XG_{4,\phi X}) \\ & + 8XH(G_{4,X} + 2XG_{4,XX} - G_{5,\phi} - XG_{5,\phi X}) \\ & + 2\dot{\phi}XH^2(3G_{5,X} + 2XG_{5,XX}). \end{aligned} \quad (6.38)$$

Tensor speed excess, α_T . The deviation of the speed of gravitational waves from that of light is

$$M_*^2 \alpha_T = 2X(2G_{4,X} - 2G_{5,\phi} - (\ddot{\phi} - \dot{\phi}H)G_{5,X}). \quad (6.39)$$

Then, the quadratic action for tensor and scalar cosmological perturbations for Horndeski theory can be expressed as [8, 24]

$$S_{(2)} = \int dt d^3x a^3 \left\{ Q_S \left[\dot{\zeta}^2 - \frac{c_S^2}{a^2} (\partial_i \zeta)^2 \right] + Q_T \left[\dot{h}_{ij}^2 - \frac{c_T^2}{a^2} (\partial_k h_{ij})^2 \right] \right\}, \quad (6.40)$$

where h_{ij} and ζ denote the tensor and scalar perturbations, respectively, and

$$Q_S = \frac{2M_*^2(\alpha_K + 3\alpha_B^2/2)}{(2 - \alpha_B)^2} > 0, \quad (6.41)$$

$$c_S^2 = -\frac{(2 - \alpha_B)[\dot{H} - H^2\alpha_B(1 + \alpha_T)/2 - H^2(\alpha_m - \alpha_T)] - H\dot{\alpha}_B + (\rho + p)/M_*^2}{H^2(\alpha_K + 3\alpha_B^2/2)} > 0, \quad (6.42)$$

$$Q_T = \frac{M_*^2}{8} > 0 \quad (6.43)$$

$$c_T = 1 + \alpha_T > 0. \quad (6.44)$$

As stated, these four functions have to be positive to avoid ghost and gradient instabilities.

It can be noted that the four α -functions, together with the function $H(t)/H_0$ and the constant $\Omega_{m,0}$, encapsulate all the cosmic information of Horndeski models [24]. Probably the most useful application of this formalism has been the development of `hi_class`, which is an extension of the Boltzmann code `CLASS` to calculate predictions of Horndeski models [25]. An alternative approach following the dark energy effective field theory (EFT) program [26], which includes Horndeski theory, is the extension of the code `CAMB`, leading to `EFTCAMB` [27].

6.4 Gravitational Waves Constraints

As we have reviewed, we have all the tools needed to investigate the cosmic implications of complicated Horndeski models, but how complicated can those models be? The detection of a gravitational wave signal with an electromagnetic counterpart (GW170817) produced by a binary neutron star merger imposed strong constraints on some of the functions of Horndeski theory. Therefore, that event limited the application of Horndeski models to describe the late-time acceleration of the Universe [28–30]. In particular, the detection of both signals led to [28]

$$|c_T/c - 1| \leq 5 \cdot 10^{-16}, \quad (6.45)$$

where we have explicitly written the speed of light $c = 1$. Therefore, α_T has to vanish during the recent cosmic evolution. (Potential caveats of this result have been pointed out in references [29, 31].) This result can be accommodated in Horndeski theory, requiring

$$G_{4,X} \approx 0, \quad \text{and} \quad G_5 \approx \text{constant}, \quad (6.46)$$

in Lagrangian (6.4). Indeed, such kinds of constraints had already been suggested, taking into account indirect measures of gravitational waves [32]. Introducing the second expression of (6.46) in (6.8) and using the Bianchi identity, we can conclude that (6.8) is just equivalent to a total derivative; therefore, it can be dismissed. The first expression in (6.46) implies that

$$G_4 = F(\phi), \quad (6.47)$$

and therefore we can consider non-minimal coupling to gravity only if it is of the generalized Brans–Dicke form (6.2). Thus, for applications to the late-time cosmic evolution, we can just consider

$$\mathcal{L}_{\text{GG}} = K(\phi, X) - G_3(\phi, X)\square\phi + F(\phi)R. \quad (6.48)$$

Moreover, it is worth noting that the recent values of $F(\phi)$ are also constrained by limits on the potential evolution of the gravitational “constant” [33]. Those constraints have been obtained in the absence of screening mechanisms, which have been argued to be absent in self-accelerating surviving models [29]. Future observational data will reveal to us if the evolution of $F(\phi)$ is constrained in such a way to effectively lead only to GR plus a (potentially non-minimally coupled) scalar field, if generalized Brans–Dicke theory (with kinetic braiding) plays an important role in our Universe, or if we should go beyond the simple scalar field hypothesis by taking into account additional degrees of freedom or even revisiting our assumptions about the spacetime.

References

1. C. Brans, R.H. Dicke, Mach’s principle and a relativistic theory of gravitation. *Phys. Rev.* **124**, 925–935 (1961). ([142(1961)])
2. C. Armendariz-Picon, V.F. Mukhanov, P.J. Steinhardt, Essentials of k essence. *Phys. Rev. D* **63**, 103510 (2001). [arXiv:astro-ph/0006373](https://arxiv.org/abs/astro-ph/0006373)
3. C. Deffayet, O. Pujolas, I. Sawicki, A. Vikman, Imperfect dark energy from kinetic gravity braiding. *JCAP* **1010**, 026 (2010). [arXiv:1008.0048](https://arxiv.org/abs/1008.0048)
4. R.P. Woodard, Avoiding dark energy with $1/r$ modifications of gravity. *Lect. Notes Phys.* **720**, 403–433 (2007). ([astro-ph/0601672])
5. A. Nicolis, R. Rattazzi, E. Trincherini, The Galileon as a local modification of gravity. *Phys. Rev. D* **79**, 064036 (2009). [arXiv:0811.2197](https://arxiv.org/abs/0811.2197)
6. C. Deffayet, G. Esposito-Farese, A. Vikman, Covariant Galileon. *Phys. Rev. D* **79**, 084003 (2009). [arXiv:0901.1314](https://arxiv.org/abs/0901.1314)
7. C. Deffayet, X. Gao, D. Steer, G. Zahariade, From k-essence to generalised Galileons. *Phys. Rev. D* **84**, 064039 (2011). [arXiv:1103.3260](https://arxiv.org/abs/1103.3260)
8. T. Kobayashi, M. Yamaguchi, J. Yokoyama, Generalized G-inflation: inflation with the most general second-order field equations. *Prog. Theor. Phys.* **126**, 511–529 (2011). [arXiv:1105.5723](https://arxiv.org/abs/1105.5723)
9. G.W. Horndeski, Second-order scalar-tensor field equations in a four-dimensional space. *Int. J. Theor. Phys.* **10**, 363–384 (1974)
10. M. Zumalacárregui, J. García-Bellido, Transforming gravity: from derivative couplings to matter to second-order scalar-tensor theories beyond the Horndeski Lagrangian. *Phys. Rev. D* **89**, 064046 (2014). [arXiv:1308.4685](https://arxiv.org/abs/1308.4685)
11. J. Gleyzes, D. Langlois, F. Piazza, F. Vernizzi, *Healthy theories beyond Horndeski*. [arXiv:1404.6495](https://arxiv.org/abs/1404.6495)
12. J. Gleyzes, D. Langlois, F. Piazza, F. Vernizzi, *Exploring gravitational theories beyond Horndeski*. [arXiv:1408.1952](https://arxiv.org/abs/1408.1952)
13. C. Charmousis, E.J. Copeland, A. Padilla, P.M. Saffin, Self-tuning and the derivation of a class of scalar-tensor theories. *Phys. Rev. D* **85**, 104040 (2012). [arXiv:1112.4866](https://arxiv.org/abs/1112.4866)

14. P. Martín-Moruno, N.J. Nunes, F.S.N. Lobo, Horndeski theories self-tuning to a de Sitter vacuum. *Phys. Rev. D* **91**(8), 084029 (2015). [arXiv:1502.03236](#)
15. C. Germani, P. Martín-Moruno, Tracking our Universe to de Sitter by a Horndeski scalar. *Phys. Dark Univ.* **18**, 1–5 (2017). [arXiv:1707.03741](#)
16. F.P. Silva, K. Koyama, Self-Accelerating Universe in Galileon Cosmology. *Phys. Rev. D* **80**, 121301 (2009). [arXiv:0909.4538](#)
17. A. De Felice, S. Tsujikawa, Cosmology of a covariant Galileon field. *Phys. Rev. Lett.* **105**, 111301 (2010). [arXiv:1007.2700](#)
18. A. De Felice, S. Tsujikawa, Generalized Galileon cosmology. *Phys. Rev. D* **84**, 124029 (2011). [arXiv:1008.4236](#)
19. S. Appleby, E.V. Linder, The paths of gravity in Galileon cosmology. *JCAP* **1203**, 043 (2012). [arXiv:1112.1981](#)
20. P. Martín-Moruno, N.J. Nunes, F.S.N. Lobo, Attracted to de Sitter: cosmology of the linear Horndeski models. *JCAP* **1505**(05), 033 (2015). [arXiv:1502.05878](#)
21. P. Martín-Moruno, N.J. Nunes, Attracted to de Sitter II: cosmology of the shift-symmetric Horndeski models. *JCAP* **1509**(09), 056 (2015). [arXiv:1506.02497](#)
22. D.A. Easson, I. Sawicki, A. Vikman, G-Bounce. *JCAP* **1111**, 021 (2011). [arXiv:1109.1047](#)
23. T. Qiu, Y.-T. Wang, G-bounce inflation: towards nonsingular inflation cosmology with Galileon field. *JHEP* **04**, 130 (2015). [arXiv:1501.03568](#)
24. E. Bellini, I. Sawicki, Maximal freedom at minimum cost: linear large-scale structure in general modifications of gravity. *JCAP* **1407**, 050 (2014). [arXiv:1404.3713](#)
25. M. Zumalacárregui, E. Bellini, I. Sawicki, J. Lesgourgues, P.G. Ferreira, `hi_class`: Horndeski in the cosmic linear anisotropy solving system. *JCAP* **1708**(08), 019 (2017). [arXiv:1605.06102](#)
26. G. Gubitosi, F. Piazza, F. Vernizzi, The effective field theory of dark energy. *JCAP* **1302**, 032 (2013). [arXiv:1210.0201](#). [*JCAP*1302,032(2013)]
27. B. Hu, M. Raveri, N. Frusciante, A. Silvestri, Effective field theory of cosmic acceleration: an implementation in CAMB. *Phys. Rev. D* **89**(10), 103530 (2014). [arXiv:1312.5742](#)
28. J.M. Ezquiaga, M. Zumalacárregui, Dark energy after GW170817: dead ends and the road ahead. *Phys. Rev. Lett.* **119**(25), 251304 (2017). [arXiv:1710.05901](#)
29. T. Baker, E. Bellini, P.G. Ferreira, M. Lagos, J. Noller, I. Sawicki, Strong constraints on cosmological gravity from GW170817 and GRB 170817A. *Phys. Rev. Lett.* **119**(25), 251301 (2017). [arXiv:1710.06394](#)
30. P. Creminelli, F. Vernizzi, Dark energy after GW170817 and GRB170817A. *Phys. Rev. Lett.* **119**(25), 215302 (2017). [arXiv:1710.05877](#)
31. C. de Rham, S. Melville, Gravitational rainbows: LIGO and dark energy at its cutoff. *Phys. Rev. Lett.* **121**(22), 221101 (2018). [arXiv:1806.09417](#)
32. J. Beltrá Jiménez, F. Piazza, H. Velten, Evading the vainshtein mechanism with anomalous gravitational wave speed: constraints on modified gravity from binary pulsars. *Phys. Rev. Lett.* **116**(6), 061101 (2016). [arXiv:1507.05047](#)
33. T. Damour, K. Nordvedt, General relativity as a cosmological attractor of tensor scalar theories. *Phys. Rev. Lett.* **70**, 2217–2219 (1993)

Chapter 7

Massive Gravity and Bigravity



Lavinia Heisenberg

The attempt at altering the underlying fundamental theory of gravity relies strongly on abandoning one of the defining properties of General Relativity. Essentially, one either revises the assumed symmetries or the elemental geometries (see, for instance, [1, 2]). General Relativity represents the fundamental theory of a Lorentz invariant local massless spin-2 field in the field-theoretical representation or a (pseudo-) Riemannian manifold with a fully determined connection in the geometrical formulation. Many efforts have been dovetailed into a unified endeavour of Lorentz-breaking theories [3, 4]. A similar undertaking was devoted to non-local theories. Apart from explicitly breaking Locality and Lorentz symmetry, one can alter the intrinsic geometrical properties.

In the geometrical representation one can attribute gravity either to curvature, to torsion or to non-metricity [5]. In this context, models based on an arbitrary function of the curvature scalar $f(R)$ [6, 7], the torsion scalar $f(T)$ [8, 9] and non-metricity scalar $f(Q)$ [10, 11] received some attention. On the other hand, in the field-theoretical formulation, modifying gravity implies the introduction of additional degrees of freedom. These are typically additional scalar, vector or tensor fields. For instance, if one is willing to abandon the gauge symmetry of the massless spin-2 field, this introduces three additional propagating degrees of freedom in massive gravity. Since effective field theories for a 2-form naturally appear in string theory, one can also consider gravity theories in the presence of 2-forms. However, they will be either dual to a scalar field or to a vector field.

The simplest modification of gravity relies on the introduction of a scalar field. Without altering the fundamental symmetries of the spin-2 field, the most general scalar-tensor theories, the Horndeski theories, can successfully be constructed [12].

L. Heisenberg (✉)

Institute for Theoretical Physics, ETH Zurich, Wolfgang-Pauli-Strasse 27, 8093 Zurich, Switzerland

e-mail: lavinia.heisenberg@phys.ethz.ch

Even though they contain derivative self-interactions and non-minimal couplings, they yield second-order equations of motion. An analogue extension of gravity theories follows the idea of introducing an additional vector field into the gravity sector instead of a scalar field. In this way, one can establish the most general vector-tensor theories with derivative self-interactions but still second-order equations of motion. They constitute the generalised Proca theories with genuinely new vector interactions [13, 14], with tremendous implications for astrophysical and cosmological probes beyond the Horndeski case. The rich phenomenology of Horndeski and generalized Proca theories can be merged together in the form of scalar-vector-tensor theories. Furthermore, new effects emerge, due to the presence of genuinely new scalar-vector couplings.

7.1 Massive and Bimetric Gravity

Considering gravity in the field-theoretical framework, a natural theoretical question arises to whether the graviton particle itself could be a massive particle. In the same way as the particles in the standard model acquire a mass, could the spin-2 particle be endowed with a mass term? The construction of a mass term for spin-1 particles is straightforward. One simply uses the inverse Minkowski metric in order to build a Lorentz scalar $A_\mu A_\nu \eta^{\mu\nu}$. The construction of a mass term for the spin-2 field requires the presence of an additional metric. This could be just a reference metric, as in massive gravity [15], or a fully dynamical metric, as in bigravity [16].

The action for ghost-free massive gravity is given by [15]

$$S = S_{\text{mG}} + S_{\text{matter}}, \quad (7.1)$$

with the gravity sector enforced to have the form

$$S_{\text{mG}} = \int d^4x \left[\frac{1}{2\kappa^2} \sqrt{-g} R_g - \frac{m^2}{\kappa^2} \sqrt{-g} \sum_{n=0}^4 \alpha_n e_n \left(\sqrt{g^{-1} f} \right) \right], \quad (7.2)$$

with $\kappa^2 = 1/M_{\text{pl}}^2$ the gravitational constant and M_{pl} the reduced Planck mass. One can generalize the action for ghost-free massive gravity into bigravity by including an Einstein-Hilbert kinetic term $\frac{M_f^2}{2} \sqrt{-f} R_f$ for the reference metric. The two metrics, g and f , are only allowed to interact through potential interactions encoded in the elementary symmetric polynomials $e_n(S)$ of the matrix square root $S_\nu^\mu = (\sqrt{g^{-1} f})_\nu^\mu$, which satisfies $S_\alpha^\mu S_\nu^\alpha \equiv g^{\mu\alpha} f_{\alpha\nu}$. The polynomials take

$$\begin{aligned}
e_0(S) &= 1, \\
e_1(S) &= [S], \\
e_2(S) &= \frac{1}{2} (S]^2 - [S^2]), \\
e_3(S) &= \frac{1}{6} ([S]^3 - 3[S][S^2] + 2[S^3]), \\
e_4(S) &= \det(S).
\end{aligned} \tag{7.3}$$

One can rewrite the ghost-free interactions of massive gravity in terms of a deformed determinant [17]

$$\det(\delta_{\nu}^{\mu} + S_{\nu}^{\mu}) = \sum_{i=0}^4 \frac{-\alpha_i}{i!(4-i)!} \epsilon^{\mu_1 \dots \mu_i \alpha_{i+1} \dots \alpha_4} \epsilon^{\nu_1 \dots \nu_i \alpha_{i+1} \dots \alpha_4} S_{\nu_1}^{\mu_1} \dots S_{\nu_i}^{\mu_i}, \tag{7.4}$$

where the antisymmetric structure of the elementary polynomials becomes transparent

$$\begin{aligned}
e_0[S] &= \epsilon^{\mu\nu\rho\sigma} \epsilon_{\mu\nu\rho\sigma}, \\
e_1[S] &= \epsilon^{\mu\nu\rho\sigma} \epsilon^{\alpha}_{\nu\rho\sigma} S_{\mu\alpha}, \\
e_2[S] &= \epsilon^{\mu\nu\rho\sigma} \epsilon^{\alpha\beta}_{\rho\sigma} S_{\mu\alpha} S_{\nu\beta}, \\
e_3[S] &= \epsilon^{\mu\nu\rho\sigma} \epsilon^{\alpha\beta\kappa}_{\sigma} S_{\mu\alpha} S_{\nu\beta} S_{\rho\kappa}, \\
e_4[S] &= \epsilon^{\mu\nu\rho\sigma} \epsilon^{\alpha\beta\kappa\gamma} S_{\mu\alpha} S_{\nu\beta} S_{\rho\kappa} S_{\sigma\gamma}.
\end{aligned} \tag{7.5}$$

The antisymmetric nature of the interactions together with the square root structure of the fundamental matrix render the Boulware-Deser ghost non-dynamical. In the case of only g being dynamical, five physical degrees of freedom propagate, which can be decomposed into two helicity-2, two helicity-1, and one helicity-0 mode. Promoting f to be dynamical too introduces two additional degrees of freedom, so that bigravity contains seven modes in its spectrum of one massless and one massive graviton.

One can grasp some of the fundamental properties of massive gravity already in the leading order interactions of the decoupling limit, i.e., the limit in which $m \rightarrow 0$, $M_{\text{Pl}} \rightarrow \infty$, while keeping $\Lambda_3 \equiv (M_{\text{Pl}} m^2)^{1/3}$ fixed. Concentrating on the leading-order contributions of the helicity-2 and helicity-0 modes, the decoupling limit Lagrangian simplifies into [18]

$$\mathcal{L} = -\frac{1}{2} h^{\mu\nu} \mathcal{E}_{\mu\nu}^{\alpha\beta} h_{\alpha\beta} + h^{\mu\nu} \sum_{n=1}^3 \frac{a_n}{\Lambda_3^{3(n-1)}} X_{\mu\nu}^{(n)}(\Pi), \tag{7.6}$$

where the helicity-2 mode $h^{\mu\nu}$ couples to the helicity-0 mode through the matrices X 's

$$\begin{aligned}
X_{\mu\nu}^{(1)}(\Pi) &= \epsilon_\mu^{\alpha\rho\sigma} \epsilon_\nu^{\beta\gamma} \Pi_{\alpha\beta}, \\
X_{\mu\nu}^{(2)}(\Pi) &= \epsilon_\mu^{\alpha\rho\gamma} \epsilon_\nu^{\beta\sigma} \Pi_{\alpha\beta} \Pi_{\rho\sigma}, \\
X_{\mu\nu}^{(3)}(\Pi) &= \epsilon_\mu^{\alpha\rho\gamma} \epsilon_\nu^{\beta\sigma\delta} \Pi_{\alpha\beta} \Pi_{\rho\sigma} \Pi_{\gamma\delta},
\end{aligned} \tag{7.7}$$

with the fundamental tensor $\Pi_{\mu\nu} = \partial_\mu \partial_\nu \pi$. One immediate property of the decoupling limit Lagrangian is the absence of any kinetic term for the helicity-0 mode. One can diagonalise the first two interactions $hX^{(1)}$ and $hX^{(2)}$, which yields the appearance of Galileon interactions. They become strongly coupled at an energy scale $E \sim \Lambda_3$. These leading order interactions of the decoupling limit are characterised by the invariance under global field-space Galilean transformations $\pi \rightarrow \pi + b_\mu x^\mu + b$ of the helicity-0 mode and the linearised diffeomorphisms $h_{\mu\nu} \rightarrow h_{\mu\nu} + \partial_{(\mu} \xi_{\nu)}$ up to total derivatives of the helicity-2 mode.

The construction of the potential interactions in terms of the square root and the relative tunings of $[S]^n$ is crucial for the absence of the Boulware-Deser ghost at all orders. In analogy to Galileon interactions, the leading-order interactions in the decoupling limit of massive gravity are not subject to large quantum corrections. Behind this is a non-renormalisation theorem: the classical operators of the decoupling limit Lagrangian are invariant under the aforementioned symmetries only up to total derivatives, whereas the Feynman diagrams generate operators that fulfill these symmetries exactly. Hence, the classical operators and their relative tunings in the high-energy limit remain unrenormalised. This indicates that the quantum corrections to the parameters of the theory (including the graviton mass) will receive small quantum corrections proportional to the graviton mass itself [19]. This property of technical naturalness is one of the most attractive characteristic of the theory. However, it still might be a matter of concern that the specific structure of the potential interactions might receive a detuning from quantum corrections beyond the decoupling limit. This has led to the analysis of the radiative stability of the full theory [20, 21]. It transpires that the graviton loops do indeed destabilize the precise structure of the potential interactions, but in a way that the Boulware-Deser ghost remains harmless below the Planck scale, at least up to one loop [21, 22].

The linear theory of massive gravity suffers from the vDVZ discontinuity [23, 24], which is tightly related to the fact that the helicity-0 mode does not have its own kinetic term. It emerges only after diagonalising its mixing with the helicity-2 mode, which on the other hand results in a direct coupling of the helicity-0 mode to external matter fields. This coupling hinders the recovery of General Relativity in the vanishing mass limit. However, going beyond linear theory brings the rescue, where non-linear interactions for the massive graviton introduce Galileon-type derivative interactions for the helicity-0 mode. In this way, the same Vainshtein mechanism as for the Galileon scalar field cures this discontinuity: in the vicinity of matter, the non-linear interactions for the helicity-0 mode become large and ultimately suppress its coupling to matter. For a successful implementation of the Vainshtein mechanism in massive gravity, see, for instance, [25, 26].

7.2 Cosmological Applications

The first attempt to apply massive gravity to cosmology was pursued in [27]. There, self-accelerated solutions were successfully found in the decoupling limit of massive gravity, where the de Sitter metric was treated as a small perturbation on top of the Minkowski metric. An immediate observation was that the Hubble parameter is set by the graviton mass. As promising as these solutions were for the late-time acceleration, the helicity-1 mode caused worries due to strong coupling issues. Cosmological solutions have then been investigated beyond the decoupling limit in the full theory. Assuming a FLRW Ansatz for the metric $d_s^2 = -N^2 dt^2 + a^2 d\vec{x}^2$, the equations of motion immediately yield the Bianchi identity

$$m^2 \partial_0(a^3 - a^2) = 0, \quad (7.8)$$

which is at the heart of the no-go result for flat FLRW solutions in massive gravity [28]. A similar no-go result is also there for spatially-closed FLRW solutions. On the other hand, open FLRW solutions do exist [29], in which $J = 0$ (that depends on the parameters of massive gravity and the scale factor), even though their perturbations suffer either from strong coupling (the kinetic terms for the vector and scalar modes are proportional to J) or instabilities [30].

Promoting the reference metric to a dynamical metric, as in bigravity, brought some excitements in the cosmological applications of massive gravity [31–36]. A similar FLRW Ansatz can be assumed for the f metric $d_{sf}^2 = -N_f^2 dt^2 + a_f^2 d\vec{x}^2$. In this case, the above Bianchi identity changes into

$$J(H_g - \xi H_f) = 0, \quad (7.9)$$

where $H_g = \dot{a}_g/(N_g a_g)$, $H_f = \dot{a}_f/(N_f a_f)$ and J depends on the scale factors and the parameters of the theory. Hence, there are two branches of solutions.

The first branch, $J = 0$, is characterised by the fact that the ratio of the scale factors is constant, which enforces the potential interactions to contribute in the form of cosmological constants. Unfortunately, linear perturbations reveal that this branch suffers from strong coupling, due to vanishing kinetic terms for the vector and scalar modes. Therefore, this branch of solutions was disregarded quickly in the literature.

A more promising branch is $H_g = \xi H_f$, where the ratio of the scale factor ξ can evolve in time. Two specific evolutions gained much attention in the literature [37]. The infinite branch of solutions, with ξ evolving from infinity to a finite value, suffers from ghost instabilities [38, 39]. The finite branch of solutions, where the ratio evolves from zero to a finite value, is plagued by gradient instabilities [31, 40, 41]. The gradient instabilities could be avoided by fine-tuning the mass $m \gg H$ [38, 42] or imposing $M_g \gg M_f$ [43].

More promising cosmological solutions can be found if the minimal coupling of the matter fields to the g metric is abandoned. Without introducing any ghost degrees of freedom within the decoupling limit, the dark sector can be coupled to an effective

metric [44–47]

$$g_{\mu\nu}^{\text{eff}} = \alpha^2 g_{\mu\nu} + 2\alpha\beta g_{\mu\rho} \left(\sqrt{g^{-1}f} \right)_\nu^\rho + \beta^2 f_{\mu\nu}. \quad (7.10)$$

In this way the constraint equation in massive gravity $J = 0$ becomes

$$m^2 J = \frac{\alpha\beta a_{\text{eff}}^2 \kappa^2}{a^2} p_m, \quad (7.11)$$

where p_m is pressure of the matter field that couples to $g_{\mu\nu}^{\text{eff}}$ and $a_{\text{eff}} = \alpha a + \beta$. Not only is the no-go theorem for flat FLRW solutions circumvented, but all the five physical degrees of freedom have non-vanishing kinetic terms and strong coupling issues are avoided. Similarly, bigravity with doubly coupled matter fields obtains a key change in the constraint equation

$$\left(m^2 J - \frac{\alpha\beta a_{\text{eff}}^2}{M_g^2 a^2} p_m \right) (H_g - \xi H_f) = 0, \quad (7.12)$$

where the first branch of solutions $J = \frac{\alpha\beta a_{\text{eff}}^2}{m^2 M_g^2 a^2} p_m$ is free of ghost and gradient instabilities.

References

1. L. Heisenberg, A systematic approach to generalisations of General Relativity and their cosmological implications. *Phys. Rept.* **796**, 1–113 (2019). [arXiv:1807.01725](#)
2. A. Joyce, B. Jain, J. Khoury, M. Trodden, Beyond the cosmological standard model. *Phys. Rept.* **568**, 1–98 (2015). [arXiv:1407.0059](#)
3. T.P. Sotiriou, Horava-Lifshitz gravity: a status report. *J. Phys. Conf. Ser.* **283**, 012034 (2011). [arXiv:1010.3218](#)
4. T.P. Sotiriou, M. Visser, S. Weinfurter, Quantum gravity without Lorentz invariance. *JHEP* **10**, 033 (2009). [arXiv:0905.2798](#)
5. J.B. Jiménez, L. Heisenberg, T.S. Koivisto, The geometrical trinity of gravity. *Universe* **5**(7), 173 (2019). [arXiv:1903.06830](#)
6. T.P. Sotiriou, V. Faraoni, f(R) theories of gravity. *Rev. Mod. Phys.* **82**, 451–497 (2010). [arXiv:0805.1726](#)
7. A. De Felice, S. Tsujikawa, f(R) theories. *Living Rev. Rel.* **13**, 3 (2010). [arXiv:1002.4928](#)
8. B. Li, T.P. Sotiriou, J.D. Barrow, $f(T)$ gravity and local Lorentz invariance. *Phys. Rev. D* **83**, 064035 (2011). [arXiv:1010.1041](#)
9. Y.-F. Cai, S. Capozziello, M. De Laurentis, E.N. Saridakis, f(T) teleparallel gravity and cosmology. *Rept. Prog. Phys.* **79**(10), 106901 (2016). [arXiv:1511.07586](#)
10. J.B. Jiménez, L. Heisenberg, T. Koivisto, Coincident general relativity. *Phys. Rev. D* **98**(4), 044048 (2018). [arXiv:1710.03116](#)
11. J.B. Jiménez, L. Heisenberg, T.S. Koivisto, S. Pekar, Cosmology in f(Q) geometry. [arXiv:1906.10027](#)
12. G.W. Horndeski, Second-order scalar-tensor field equations in a four-dimensional space. *Int. J. Theor. Phys.* **10**, 363–384 (1974)

13. L. Heisenberg, Generalization of the Proca action. *JCAP* **1405**, 015 (2014). [arXiv:1402.7026](#)
14. J. Beltran Jimenez, L. Heisenberg, Derivative self-interactions for a massive vector field. *Phys. Lett. B* **757**, 405–411 (2016). [arXiv:1602.03410](#)
15. C. de Rham, G. Gabadadze, A.J. Tolley, Resummation of massive gravity. *Phys. Rev. Lett.* **106**, 231101 (2011). [arXiv:1011.1232](#)
16. S. Hassan, R.A. Rosen, Bimetric gravity from ghost-free massive gravity. *JHEP* **1202**, 126 (2012). [arXiv:1109.3515](#)
17. S. Hassan, R.A. Rosen, On non-linear actions for massive gravity. *JHEP* **1107**, 009 (2011). [arXiv:1103.6055](#)
18. C. de Rham, G. Gabadadze, Generalization of the Fierz–Pauli action. *Phys. Rev. D* **82**, 044020 (2010). [arXiv:1007.0443](#)
19. C. de Rham, G. Gabadadze, L. Heisenberg, D. Pirtskhalava, Nonrenormalization and naturalness in a class of scalar-tensor theories. *Phys. Rev. D* **87**(8), 085017 (2013). [arXiv:1212.4128](#)
20. I.L. Buchbinder, D.D. Pereira, I.L. Shapiro, One-loop divergences in massive gravity theory. *Phys. Lett. B* **712**, 104–108 (2012). [arXiv:1201.3145](#)
21. C. de Rham, L. Heisenberg, R.H. Ribeiro, Quantum corrections in massive gravity. *Phys. Rev. D* **88**, 084058 (2013). [arXiv:1307.7169](#)
22. L. Heisenberg, Quantum corrections in massive bigravity and new effective composite metrics. *Class. Quant. Grav.* **32**(10), 105011 (2015). [arXiv:1410.4239](#)
23. H. van Dam, M. Veltman, Massive and massless Yang–Mills and gravitational fields. *Nucl. Phys. B* **22**, 397–411 (1970)
24. V. Zakharov, Linearized gravitation theory and the graviton mass. *JETP Lett.* **12**, 312 (1970)
25. E. Babichev, C. Deffayet, R. Ziour, Recovering general relativity from massive gravity. *Phys. Rev. Lett.* **103**, 201102 (2009). [arXiv:0907.4103](#)
26. E. Babichev, C. Deffayet, R. Ziour, The recovery of general relativity in massive gravity via the Vainshtein mechanism. *Phys. Rev. D* **82**, 104008 (2010). [arXiv:1007.4506](#)
27. C. de Rham, G. Gabadadze, L. Heisenberg, D. Pirtskhalava, Cosmic acceleration and the helicity-0 graviton. *Phys. Rev. D* **83**, 103516 (2011). [arXiv:1010.1780](#)
28. G. D’Amico, C. de Rham, S. Dubovsky, G. Gabadadze, D. Pirtskhalava, A.J. Tolley, Massive cosmologies. *Phys. Rev. D* **84**, 124046 (2011). [arXiv:1108.5231](#)
29. A.E. Gümrükçüoğlu, C. Lin, S. Mukohyama, Open FRW universes and self-acceleration from nonlinear massive gravity. *JCAP* **1111**, 030 (2011). [arXiv:1109.3845](#)
30. A.E. Gümrükçüoğlu, C. Lin, S. Mukohyama, Cosmological perturbations of self-accelerating universe in nonlinear massive gravity. *JCAP* **1203**, 006 (2012). [arXiv:1111.4107](#)
31. D. Comelli, M. Crisostomi, F. Nesti, L. Pilo, FRW cosmology in ghost free massive gravity. *JHEP* **1203**, 067 (2012). [arXiv:1111.1983](#)
32. M. von Strauss, A. Schmidt-May, J. Enander, E. Mörtzell, S. Hassan, Cosmological solutions in bimetric gravity and their observational tests. *JCAP* **1203**, 042 (2012). [arXiv:1111.1655](#)
33. Y. Akrami, T.S. Koivisto, M. Sandstad, Accelerated expansion from ghost-free bigravity: a statistical analysis with improved generality. *JHEP* **1303**, 099 (2013). [arXiv:1209.0457](#)
34. Y. Akrami, T.S. Koivisto, D.F. Mota, M. Sandstad, Bimetric gravity doubly coupled to matter: theory and cosmological implications. *JCAP* **1310**, 046 (2013). [arXiv:1306.0004](#)
35. A.R. Solomon, Y. Akrami, T.S. Koivisto, Linear growth of structure in massive bigravity. *JCAP* **1410**, 066 (2014). [arXiv:1404.4061](#)
36. J. Enander, Y. Akrami, E. Mörtzell, M. Renneby, A.R. Solomon, Integrated Sachs–Wolfe effect in massive bigravity. *Phys. Rev. D* **91**, 084046 (2015). [arXiv:1501.02140](#)
37. F. Könnig, Y. Akrami, L. Amendola, M. Motta, A.R. Solomon, Stable and unstable cosmological models in bimetric massive gravity. *Phys. Rev. D* **90**, 124014 (2014). [arXiv:1407.4331](#)
38. A. De Felice, A.E. Gümrükçüoğlu, S. Mukohyama, N. Tanahashi, T. Tanaka, Viable cosmology in bimetric theory. *JCAP* **1406**, 037 (2014). [arXiv:1404.0008](#)
39. G. Cusin, R. Durrer, P. Guarato, M. Motta, Gravitational waves in bigravity cosmology. *JCAP* **1505**(05), 030 (2015). [arXiv:1412.5979](#)
40. D. Comelli, M. Crisostomi, L. Pilo, Perturbations in massive gravity cosmology. *JHEP* **1206**, 085 (2012). [arXiv:1202.1986](#)

41. D. Comelli, M. Crisostomi, L. Pilo, FRW cosmological perturbations in massive bigravity. *Phys. Rev. D* **90**(8), 084003 (2014). [arXiv:1403.5679](#)
42. A. De Felice, T. Nakamura, T. Tanaka, Possible existence of viable models of bi-gravity with detectable graviton oscillations by gravitational wave detectors. *PTEP* **2014**, 043E01 (2014). [arXiv:1304.3920](#)
43. Y. Akrami, S.F. Hassan, F. Könnig, A. Schmidt-May, A.R. Solomon, Bimetric gravity is cosmologically viable. *Phys. Lett. B* **748**, 37–44 (2015). [arXiv:1503.07521](#)
44. C. de Rham, L. Heisenberg, R.H. Ribeiro, On couplings to matter in massive (bi-)gravity. *Class. Quant. Grav.* **32**, 035022 (2015). [arXiv:1408.1678](#)
45. J. Enander, A.R. Solomon, Y. Akrami, E. Mörtzell, Cosmic expansion histories in massive bigravity with symmetric matter coupling. *JCAP* **1501**, 006 (2015). [arXiv:1409.2860](#)
46. A.R. Solomon, J. Enander, Y. Akrami, T.S. Koivisto, F. Könnig, E. Mörtzell, Cosmological viability of massive gravity with generalized matter coupling. [arXiv:1409.8300](#)
47. Y. Akrami, P. Brax, A.-C. Davis, V. Vardanyan, Neutron star merger GW170817 strongly constrains doubly coupled bigravity. *Phys. Rev. D* **97**(12), 124010 (2018). [arXiv:1803.09726](#)

Chapter 8

Gravity in Extra Dimensions



Jose A. R. Cembranos

A large amount of present extensions of standard physics agree on the existence of additional spatial dimensions. However, the idea is quite old, since it dates back to almost one hundred years ago, when Kaluza and Klein [1, 2] tried to unify General Relativity proposed by Einstein [3] with classic electromagnetism completed by Maxwell half a century before [4].

The existence of extra dimensions is interesting from different theoretical points of view, but it also introduces new problems or questions. The most basic one is why they have not been observed yet. The answer to this question may be very different, and depending on this answer, the phenomenology of the extra dimensions varies in a broad range. We will briefly summarise the main extra dimensional models following the classification introduced in [5].

8.1 Kaluza-Klein Model

The first historical approach to this subject requires very small extra dimensions. If the additional dimensions are compactified within a very small size, of the order of the Planck length ($1/M_{Pl}$), their effects are negligible. This hypothesis was presented in the original models proposed by Kaluza (1917) and Klein (1926) [1, 2, 6]. There, each field has a Kaluza-Klein (KK) tower of states associated with it. This tower is the result of the factorisation of the wave functions associated with these fields that depend in one part on the ordinary $1 + 3$ dimensions, and in another one depending on the coordinates of the extra dimensions.

J. A. R. Cembranos (✉)

Departamento de Física Teórica and IPARCOS, Universidad Complutense de Madrid,
28040 Madrid, Spain
e-mail: cembra@ucm.es

The effect of such factorisation is that every field propagating in these types of compact extra dimensions with periodic boundary conditions has an infinite numerable number of states of growing mass. In the most simple case, with a flat extra space of toroidal topology: T^δ ($\delta = D - 4 \geq 1$), the mass square of the KK towers depends quadratically on δ integer numbers weighted with the compactification radius of each toroid:

$$m_n^2 = \sum_{i=1}^{\delta} \frac{n_i^2}{R_i^2}. \quad (8.1)$$

Within these types of models, the scales are of the order of the standard four-dimensional Planck mass M_{Pl} , and the standard model particles are interpreted as the zero KK modes, whose mass needs to be explained by an other mechanism, such as the Higgs mechanism within the standard model.

On the other hand, the metric associated with the bulk space is interpreted by a $1 + 3$ observer as a KK tower of spin-2 (gravitons), $\delta - 1$ KK towers associated with $U(1)$ gauge bosons (graviphotons) and $\delta(\delta - 1)/2$ KK escalar towers (graviscalars) [7]. This division depends on the characteristics of the extra space.

The mode with spin-2 and zero mass has exactly the same coupling as the ordinary graviton, whereas the higher mass states can be interpreted as massive gravitons with five degrees of freedom each. On the other hand, the graviphotons have an associated algebra related to the isometries of the extra space, but they do not couple (linearly) to the zero KK modes. Finally, the graviscalars are coupled to the zero KK modes through their trace of the energy-momentum tensor. Indeed, the zero modes of these graviscalars can be identified with the Goldstone bosons (GBs) associated with dilations. Sometimes, they are called dilatons, while at other times they are called radions. In any case, in order to have a viable model, these radions need to be stabilized with an important mass in order to fix the size of the extra dimensions.

8.2 Large Extra Dimensions

In the above models, with small additional dimensions at the Planck scale, physics remains unchanged up to very high energies. However, in the late 1980s several works started to study the possibilities of large extra dimensions compactified with sizes much larger than $\sim 1/M_{Pl}$, or even with non-compact extra dimensions.

8.2.1 Brane Worlds

A brane world is characterised by the fact that the standard model content is confined to propagate within a manifold of three spatial dimensions. This manifold is called

brane. It has a fundamental origin in some string-inspired models [8]. On the contrary, it has also studied the possibility that standard model particles can be confined in a region of the extra space through effective actions [9].

ADD Model

The first proposal of large extra dimensions was introduced by Arkani-Hamed, Dimopoulos and Dvali [10]. The ADD brane world model is characterised by the fact that the brane is neglected as a source of gravity and the background geometry is assumed to be Minkowski. The gravitational field is the only one that propagates in the δ extra dimensions that are typically supposed to be toroidal and with the same radius, R_B .

One of the most distinctive features of this hypothesis is the following relation between the fundamental mass scale of gravity in D dimensions, M_F , and the standard four-dimensional Planck mass $M_{Pl} = \frac{1}{\kappa} = \frac{1}{\sqrt{8\pi G}}$:

$$M_{Pl}^2 = V_\delta M_F^{2+\delta}, \quad (8.2)$$

where V_δ is the volume of the compactified extra space. For instance, $V_\delta = (2\pi R_B)^\delta$ for the commented toroidal case. In this sense, the Planck mass is not fundamental but just the effective scale of gravity in $1 + 3$ dimensions.

Equation (8.2) implies that it is possible to reduce M_F up to the electroweak scale if the extra space is large enough. In particular, inverse radii of an order between $R_B^{-1} \sim 10^{-3}$ eV and 10 MeV provide this effect for a number of extra dimensions between $\delta \sim 2$ and 7 respectively.

On the other hand, the interaction among the fields confined within the brane is not modified. The only modifications are introduced in the coupling with the gravitational interaction. The metric can be linearized in the following way:

$$g_{AB} = \eta_{AB} + \frac{4\sqrt{\pi}}{M_F^{1+\delta/2}} h_{AB}, \quad (8.3)$$

in order to expand h_{AB} in KK modes. They are labelled with δ integer numbers (n) in order to specify the KK spectrum introduced in Eq. (8.1). In this model, the typical mass differences are so tiny, $\Delta m \sim R_B^{-1} \sim 10^{-9} - 10$ MeV, that the spectrum can be assumed continuous at very high energies ($E \gg R_B^{-1}$). Therefore, the multiplicity of KK gravitons for a given energy scales as $N(E) \sim (ER_B)^\delta$.

The most important consequence of reducing the fundamental scale of gravity M_F is that new gravitational effects can be observable at this new energy scale. This fact can be understood trivially in the D -dimensional theory, or in an effective $1 + 3$ -dimensional theory, since the production cross-section for the real production of KK gravitons ($m_n \leq E$) is proportional to

$$\sigma_{KK} \sim \frac{1}{M_{Pl}^2} (ER_B)^\delta \sim \frac{E^\delta}{M_F^{\delta+2}}, \quad (8.4)$$

where we have taken into account that every KK graviton couples in the same way to the brane content:

$$\mathcal{L} = -\frac{2\sqrt{\pi}}{M_{Pl}} h_{\mu\nu}^{(n)} T_{SM}^{\mu\nu}. \quad (8.5)$$

Here, $T_{SM}^{\mu\nu}$ is the conserved energy-momentum tensor of the fields contained within the brane. These KK gravitons are unstable with a lifetime given approximately by $\tau_n \simeq M_{Pl}^2/m_n^3$ [7]. It means that they can be considered stable for collider phenomenology, giving a typical missing energy signal.

An infinite KK tower leads to divergent virtual effects even at tree level. Indeed, KK graviton radiative effects generate new four-body interactions among standard model particles that need to be regularised (except for $\delta = 1$) [7, 11, 12]. Finally, higher KK radiative corrections introduce modifications to different observables, such as anomalous moments, or electroweak precision parameters that also demand regularisation [13].

RS Model

Immediately after the ADD model became popular, Randall and Sundrum (RS) started the study of the phenomenology of similar scenarios when the gravity of the brane is taken into account [14, 15]. The RS models of gravity are built in a 1 + 4-dimensional anti-de Sitter. The extra dimension can be compactified (RS1) or can be infinite (RS2). In the first case, the additional dimension is typically assumed to have a S^1/Z_2 orbifold topology. In both models the metric can be written as:

$$G_{MN} = \begin{pmatrix} \tilde{g}_{\mu\nu}(x, y) & 0 \\ 0 & -1 \end{pmatrix} = \begin{pmatrix} e^{-2k|y|} \eta_{\mu\nu} & 0 \\ 0 & 1 \end{pmatrix}, \quad (8.6)$$

where $y \in [-R_B\pi, R_B\pi]$, R_B being the size of the extra dimension in the compact case, whereas it is $R_B \rightarrow \infty$ for the RS2 model. The k parameter is related to the non-singular part of the curvature scalar associated with the bulk space: $R_{(5)}(y \neq 0, y \neq R_B\pi) = -20k^2$.

From the (1 + 4)-dimensional action, the relation: $M_{Pl} = [(M_F^3/k)(1 - e^{-2k\pi R_B})]^{1/2}$, can be obtained on the positive tension brane. It implies that all the physically relevant scales of the model are of the same order: $k \sim M_F \sim M_P$.

For the compactified model (RS1), in addition to the 3-brane with positive tension placed at $y = 0$, it is necessary to introduce another 3-brane at $y = \pi R_B$ with opposite tension in order to have a consistent solution to the Einstein Equations in 1 + 4 dimensions.

In principle, it was proposed that the standard particle content was placed in the 3-brane with negative tension. The reason is that the above metric generates a natural hierarchy between typical physical scales on the 3-brane and the Planck scale. In this case: $M_{Pl} = [(M_F^3/k)(e^{2k\pi R_B} - 1)]^{1/2}$, which means that the Planck mass is exponentially related with the typical scale of the model. The original idea was to fix this scale at the order of the electroweak scale ($M_F \sim 1$ TeV), so the radius of the extra dimension needs to be stabilized to be $k R_B \sim \mathcal{O}(10)$. This is the most studied scenario from a phenomenological point of view.

As it happens in the ADD model, the most important phenomenological consequence is the potential extreme reduction of the scale at which one can be sensitive to new gravitational effects, typically at the order of M_F . By linearly expanding the metric over the RS background:

$$g_{\mu\nu} = e^{-2ky} \left(\eta_{\mu\nu} + \frac{4\sqrt{\pi}}{M_F^{3/2}} h_{\mu\nu} \right), \quad (8.7)$$

and by using a proper decomposition of the gravitational field in KK modes, it is possible to obtain the following interaction term for KK gravitons, with the energy-momentum tensor of the fields placed on the negative tension 3-brane:

$$\mathcal{L} = -\frac{2\sqrt{\pi}}{M_{Pl}} T_{SM}^{\mu\nu} \left(h_{\mu\nu}^{(0)}(x) - e^{2k\pi R_B} \sum_{n \neq 0} h_{\mu\nu}^{(n)}(x) \right). \quad (8.8)$$

In this case, the masses of the KK gravitons read:

$$m_n = kx_n e^{-kR_B\pi}, \quad (8.9)$$

where x_n are the roots of the Bessel function $J_1(x)$. Therefore, KK gravitons may have quite light masses, which can be proved in colliders by the observation of resonances. In such a case, the cleanest signal at hadron colliders, such as the LHC, could be an excess in Drell-Yan processes ($q\bar{q}, gg \rightarrow h^{(1)} \rightarrow l^+l^-$) [16, 17]. These light gravitons can also be produced directly, together with a single photon or jet. It is interesting to note that the RS1 model predicts a mono-energetic photon, whereas the ADD model does not.

The commented phenomenology is associated with the RS1 model. The RS2 model is characterised by an infinite extra dimension and it contains a continuum of KK gravitons [15]. A summary of the RS model phenomenology can be found, for example, in [18].

Brane Dynamics

In addition to KK states, brane worlds introduce another set of very distinctive states. The dynamics of the brane itself can be parameterised by δ functions or fields, depending on the 1 + 3 coordinates. A 1 + 3 observer identifies these fields as new scalar (or pseudo-scalar) modes. These scalars are called branons: π^α , and their leading coupling with the brane content is suppressed by the brane tension $\tau \equiv f^4$, which quantifies the flexibility of the brane [19–23]:

$$S_B = \int_{M_4} d^4x \sqrt{g} \left[-f^4 + \mathcal{L}_{SM} + \frac{1}{2} g^{\mu\nu} \delta_{\alpha\beta} \partial_\mu \pi^\alpha \partial_\nu \pi^\beta - \frac{1}{2} M_{\alpha\beta}^2 \pi^\alpha \pi^\beta + \frac{1}{8f^4} (4\delta_{\alpha\beta} \partial_\mu \pi^\alpha \partial_\nu \pi^\beta - M_{\alpha\beta}^2 \pi^\alpha \pi^\beta \tilde{g}_{\mu\nu}) T_{SM}^{\mu\nu} \right], \quad (8.10)$$

where the branon mass matrix $M_{\alpha\beta}^2$ is determined by the local geometry of the bulk space where the brane is located (see [9] for a particular example). Branons have zero mass only in highly symmetric bulk spaces.

A parity transformation in the extra space introduces a change of sign for the branon fields. The above Lagrangian (8.10) preserves this extra dimensional parity or brane parity. If this symmetry is exact, branons interact by pairs with the particles confined into the brane and become stable. As they are generically massive and weakly coupled, they are natural dark matter candidates.

Independent of their cosmological impact, branons can be searched for at colliders [21, 24–31]. Like many other dark matter candidates, their typical signatures include missing energy or missing transverse momenta signals [21, 25–29]. On the other hand, as happens with KK gravitons, branon radiative corrections generate new couplings among SM particles. The leading terms are given by four-particle interactions. In addition, two-loop effects contribute to precision observables, such as anomalous magnetic moments [30, 31].

With respect to the cosmological role of branon fields, they can achieve the required abundance of cold dark matter with the standard freeze-out mechanism [32, 33] or non-thermally [34], in very much the same way as axions [35–37] or other bosonic degrees of freedom [38–41]. This fact opens up the possibility for searching for branons through CMB and large-scale structure data [42–45], but also with direct dark matter experiments [27], or indirectly through the analysis of cosmic rays. Indeed, two branons can annihilate contributing to the astrophysical flux of different particles. A series of studies have shown the possibilities for detecting branons through photons, neutrinos, positrons and antiprotons [46–55].

8.2.2 *Universal Extra Dimensions*

Motivated by the success of the brane world models discussed above, other extra dimension models without the existence of branes have also attracted important attention. In the Universal Extra Dimensional case there are no branes, and every field can propagate in the entire bulk space.

In such a case, due to the translation invariance in the extra space, the associated momenta, i.e., the KK number n , is conserved, at least at tree level. This implies that a vertex with N particles with KK numbers: n_1, n_2, \dots, n_N , can be non-zero only if:

$$n = n_1 + n_2 \dots + n_{N-1} + n_N = 0. \quad (8.11)$$

Although the total KK number is not conserved due to radiative corrections, the K -parity: $(-1)^{|n|}$ is [56]. This implies that at least, one of the lightest KK states is stable. This state is very interesting from a cosmological or astrophysical approach, since this mode is a natural candidate for dark matter [57–59]. On the contrary, for collider physics, the sensitivity of the different experiments is reduced, since the lightest KK excitations need to be produced by pairs. In any case, within this frame-

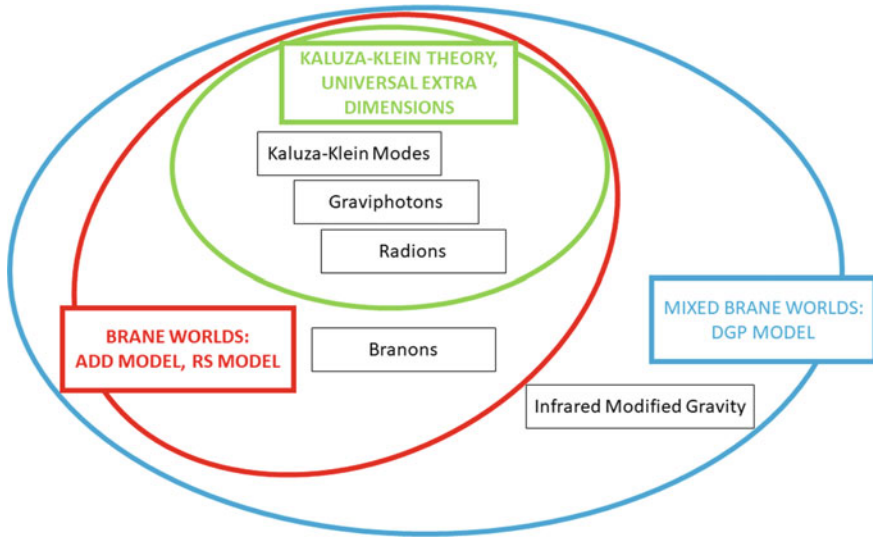


Fig. 8.1 Schematic representation of the basic phenomenology associated with the different extra dimensional models discussed within this chapter

work, the expected degenerate spectrum of the first KK modes provides a distinctive phenomenology both for collider and astrophysics searches [60, 61] (Fig. 8.1).

8.2.3 Mixed Models

Finally, we cannot finish this brief summary about extra dimensional models without commenting about what we will call mixed models. All of them are built with the presence of 3-branes, but they do not restrict the standard model particles to propagate within such a brane. On the contrary, part of the standard model content may have access to the bulk space. In other models, the situation is even more involved, and different manifolds are available for different fields.

For example, standard model gauge bosons (W^\pm and Z) can propagate in the entire bulk space and the zero modes can mix with their excited KK states. These effects also depend on the Higgs field that can propagate in the bulk space, on the branes, or on a combination of both [62, 63].

On the other hand, the fields can have kinetic terms in different domains. For example, a field that has access to the bulk space can also have a kinetic term defined on the brane. An important detail of such terms is that they are naturally produced by radiative corrections, due to translational invariance breaking in the extra space. This effect has been proved when the fields that propagate in the extra dimensions couple to the fields that are confined to the brane [64].

An interesting model motivated by the above discussion is the one proposed by Dvali, Gabadadze and Porrati (DGP) [65]. The action of this model does not only introduce the scalar curvature associated with the bulk space, but also the scalar curvature of the metric induced on the brane:

$$S_G = \frac{M_F^3}{16\pi} \int_{M_5} d^5 Y \sqrt{G} R_D + \frac{M_{Pl}^2}{16\pi} \int_{M_4} d^4 x \sqrt{g} R. \quad (8.12)$$

This model is able to produce an accelerated expansion without introducing a cosmological constant or any other type of dark energy. Newtonian gravity can be approximately maintained with a non-compact extra dimension. Indeed, the Newton force does not suffer modifications at low distances but at large ones.

It has been argued that the branch of the model associated with this accelerated phase is unstable [66] and in conflict with present observations related to baryon acoustic oscillations, the anisotropies of the cosmic microwave background and type Ia supernovae [67]. In any case, the DGP model has attracted a lot of attention due to its relation to massive gravity and the avoidance of the vDVZ discontinuity due to non-perturbative effects.

References

1. T. Kaluza, Zum Unitätsproblem der Physik. Sitzungsber. Preuss. Akad. Wiss. Berlin (Math. Phys.) **1921**, 966–972 (1921). [arXiv:1803.08616](https://arxiv.org/abs/1803.08616). Int. J. Mod. Phys. D **27**(14), 1870001 (2018)
2. O. Klein, Quantum theory and five-dimensional theory of relativity. (In German and English). Z. Phys. **37**, 895–906 (1926)
3. A. Einstein, The field equations of gravitation. Sitzungsber. Preuss. Akad. Wiss. Berlin (Math. Phys.) **1915**, 844–847 (1915)
4. J.C. Maxwell, A dynamical theory of the electromagnetic field. Phil. Trans. Roy. Soc. Lond. **155**, 459–512 (1865)
5. J.A.R. Cembranos, *Ph.D. thesis: Lagrangianos efectivos en teorías con dimensiones extras*
6. D. Bailin, A. Love, Kaluza-Klein theories. Rept. Prog. Phys. **50**, 1087–1170 (1987)
7. T. Han, J.D. Lykken, R.-J. Zhang, On Kaluza-Klein states from large extra dimensions. Phys. Rev. D **59**, 105006 (1999). [arXiv:hep-ph/9811350](https://arxiv.org/abs/hep-ph/9811350)
8. I. Antoniadis, N. Arkani-Hamed, S. Dimopoulos, G.R. Dvali, New dimensions at a millimeter to a Fermi and superstrings at a TeV. Phys. Lett. B **436**, 257–263 (1998). [arXiv:hep-ph/9804398](https://arxiv.org/abs/hep-ph/9804398)
9. A.A. Andrianov, V.A. Andrianov, P. Giacconi, R. Soldati, Domain wall generation by fermion selfinteraction and light particles. JHEP **07**, 063 (2003). [arXiv:hep-ph/0305271](https://arxiv.org/abs/hep-ph/0305271)
10. N. Arkani-Hamed, S. Dimopoulos, G.R. Dvali, Phenomenology, astrophysics and cosmology of theories with submillimeter dimensions and TeV scale quantum gravity. Phys. Rev. D **59**, 086004 (1999). [arXiv:hep-ph/9807344](https://arxiv.org/abs/hep-ph/9807344)
11. G.F. Giudice, R. Rattazzi, J.D. Wells, Quantum gravity and extra dimensions at high-energy colliders. Nucl. Phys. B **544**, 3–38 (1999). [arXiv:hep-ph/9811291](https://arxiv.org/abs/hep-ph/9811291)
12. J.L. Hewett, Indirect collider signals for extra dimensions. Phys. Rev. Lett. **82**, 4765–4768 (1999). [arXiv:hep-ph/9811356](https://arxiv.org/abs/hep-ph/9811356)
13. G.F. Giudice, A. Strumia, Constraints on extra dimensional theories from virtual graviton exchange. Nucl. Phys. B **663**, 377–393 (2003). [arXiv:hep-ph/0301232](https://arxiv.org/abs/hep-ph/0301232)
14. L. Randall, R. Sundrum, A Large mass hierarchy from a small extra dimension. Phys. Rev. Lett. **83**, 3370–3373 (1999). [arXiv:hep-ph/9905221](https://arxiv.org/abs/hep-ph/9905221)

15. L. Randall, R. Sundrum, An Alternative to compactification. *Phys. Rev. Lett.* **83**, 4690–4693 (1999). [arXiv:hep-th/9906064](#)
16. H. Davoudiasl, J.L. Hewett, T.G. Rizzo, Phenomenology of the Randall-Sundrum Gauge hierarchy model. *Phys. Rev. Lett.* **84**, 2080 (2000). [arXiv:hep-ph/9909255](#)
17. B.C. Allanach, K. Odagiri, M.A. Parker, B.R. Webber, Searching for narrow graviton resonances with the ATLAS detector at the Large Hadron Collider. *JHEP* **09**, 019 (2000). [arXiv:hep-ph/0006114](#)
18. H. Davoudiasl, J.L. Hewett, T.G. Rizzo, Experimental probes of localized gravity: on and off the wall. *Phys. Rev. D* **63**, 075004 (2001). [arXiv:hep-ph/0006041](#)
19. A. Dobado, A.L. Maroto, The dynamics of the Goldstone bosons on the brane. *Nucl. Phys. B* **592**, 203–218 (2001). [arXiv:hep-ph/0007100](#)
20. J.A.R. Cembranos, A. Dobado, A.L. Maroto, Brane skyrmions and wrapped states. *Phys. Rev. D* **65**, 026005 (2002). [arXiv:hep-ph/0106322](#)
21. J. Alcaraz, J.A.R. Cembranos, A. Dobado, A.L. Maroto, Limits on the brane fluctuations mass and on the brane tension scale from electron positron colliders. *Phys. Rev. D* **67**, 075010 (2003). [arXiv:hep-ph/0212269](#)
22. J.A.R. Cembranos, A. Dobado, A.L. Maroto, Dark geometry. *Int. J. Mod. Phys. D* **13**, 2275–2280 (2004). [arXiv:hep-ph/0405165](#)
23. J.A.R. Cembranos, A.L. Maroto, Disformal scalars as dark matter candidates: branon phenomenology. *Int. J. Mod. Phys.* **31**(1415), 1630015 (2016). [arXiv:1602.07270](#)
24. P. Brax, C. Burrage, Constraining disformally coupled scalar fields. *Phys. Rev. D* **90**(10), 104009 (2014). [arXiv:1407.1861](#)
25. L3 Collaboration, P. Achard et al., Search for branons at LEP. *Phys. Lett. B* **597**, 145–154 (2004). [arXiv:hep-ex/0407017](#)
26. J.A.R. Cembranos, A. Dobado, A.L. Maroto, Branon search in hadronic colliders. *Phys. Rev. D* **70**, 096001 (2004). [arXiv:hep-ph/0405286](#)
27. J.A.R. Cembranos, J.L. Diaz-Cruz, L. Prado, Impact of DM direct searches and the LHC analyses on branon phenomenology. *Phys. Rev. D* **84**, 083522 (2011). [arXiv:1110.0542](#)
28. G. Landsberg, Searches for extra spatial dimensions with the CMS detector at the LHC. *Mod. Phys. Lett. A* **30**(15), 1540017 (2015). [arXiv:1506.00024](#)
29. C.M.S. Collaboration, V. Khachatryan et al., Search for new phenomena in monophoton final states in proton-proton collisions at $\sqrt{s} = 8$ TeV. *Phys. Lett. B* **755**, 102–124 (2016). [arXiv:1410.8812](#)
30. J.A.R. Cembranos, A. Dobado, A.L. Maroto, Dark matter clues in the muon anomalous magnetic moment. *Phys. Rev. D* **73**, 057303 (2006). [arXiv:hep-ph/0507066](#)
31. J.A.R. Cembranos, A. Dobado, A.L. Maroto, Branon radiative corrections to collider physics and precision observables. *Phys. Rev. D* **73**, 035008 (2006). [arXiv:hep-ph/0510399](#)
32. J.A.R. Cembranos, A. Dobado, A.L. Maroto, Brane world dark matter. *Phys. Rev. Lett.* **90**, 241301 (2003). [arXiv:hep-ph/0302041](#)
33. J.A.R. Cembranos, A. Dobado, A.L. Maroto, Cosmological and astrophysical limits on brane fluctuations. *Phys. Rev. D* **68**, 103505 (2003). [arXiv:hep-ph/0307062](#)
34. A.L. Maroto, The Nature of branon dark matter. *Phys. Rev. D* **69**, 043509 (2004). [arXiv:hep-ph/0310272](#)
35. J. Preskill, M.B. Wise, F. Wilczek, Cosmology of the invisible axion. *Phys. Lett.* **120B**, 127–132 (1983)
36. L.F. Abbott, P. Sikivie, A cosmological bound on the invisible axion. *Phys. Lett.* **120B**, 133–136 (1983)
37. M. Dine, W. Fischler, The not so harmless axion. *Phys. Lett.* **120B**, 137–141 (1983)
38. J.A. Frieman, A.H. Jaffe, Cosmological constraints on pseudoNambu-Goldstone bosons. *Phys. Rev. D* **45**, 2674–2684 (1992)
39. W. Hu, R. Barkana, A. Gruzinov, Cold and fuzzy dark matter. *Phys. Rev. Lett.* **85**, 1158–1161 (2000). [arXiv:astro-ph/0003365](#)
40. J.A.R. Cembranos, C. Hallabrin, A.L. Maroto, S.J.N. Jareno, Isotropy theorem for cosmological vector fields. *Phys. Rev. D* **86**, 021301 (2012). [arXiv:1203.6221](#)

41. J.A.R. Cembranos, A.L. Maroto, S.J. Núñez Jareño, Perturbations of ultralight vector field dark matter. *JHEP* **02**, 064 (2017). [arXiv:1611.03793](#)
42. J.A.R. Cembranos, A.L. Maroto, S.J. Núñez Jareño, Cosmological perturbations in coherent oscillating scalar field models. *JHEP* **03**, 013 (2016). [arXiv:1509.08819](#)
43. J.A.R. Cembranos, A.L. Maroto, S.J. Núñez-Jareño, H. Villarrubia-Rojo, Constraints on an harmonic corrections of fuzzy dark matter. *JHEP* **08**, 073 (2018). [arXiv:1805.08112](#)
44. P. Brax, J.A.R. Cembranos, P. Valageas, Impact of kinetic and potential self-interactions on scalar dark matter. *Phys. Rev. D* **100**(2), 023526 (2019). [arXiv:1906.00730](#)
45. P. Brax, P. Valageas, J.A.R. Cembranos, Fate of scalar dark matter solitons around supermassive galactic black holes. [arXiv:1909.02614](#)
46. J.A.R. Cembranos, L.E. Strigari, Diffuse MeV Gamma-rays and galactic 511 keV line from decaying WIMP dark matter. *Phys. Rev. D* **77**, 123519 (2008). [arXiv:0801.0630](#)
47. J.A.R. Cembranos, A. de la Cruz-Dombriz, V. Gammaldi, A.L. Maroto, Detection of branon dark matter with gamma ray telescopes. *Phys. Rev. D* **85**, 043505 (2012). [arXiv:1111.4448](#)
48. J.A.R. Cembranos, A. de la Cruz-Dombriz, A. Dobado, R.A. Lineros, A.L. Maroto, Photon spectra from WIMP annihilation. *Phys. Rev. D* **83**, 083507 (2011). [arXiv:1009.4936](#)
49. J.A.R. Cembranos, V. Gammaldi, A.L. Maroto, Possible dark matter origin of the gamma ray emission from the galactic center observed by HESS. *Phys. Rev. D* **86**, 103506 (2012). [arXiv:1204.0655](#)
50. J.A.R. Cembranos, V. Gammaldi, A.L. Maroto, Spectral study of the HESS J1745–290 Gamma-Ray source as dark matter signal. *JCAP* **1304**, 051 (2013). [arXiv:1302.6871](#)
51. J.A.R. Cembranos, V. Gammaldi, A.L. Maroto, Neutrino fluxes from dark matter in the HESS J1745–290 source at the galactic center. *Phys. Rev. D* **90**(4), 043004 (2014). [arXiv:1403.6018](#)
52. J.A.R. Cembranos, V. Gammaldi, A.L. Maroto, Antiproton signatures from astrophysical and dark matter sources at the galactic center. *JCAP* **1503**(03), 041 (2015). [arXiv:1410.6689](#)
53. A. Weltman et al., *Fundamental Physics with the Square Kilometre Array*. [arXiv:1810.02680](#)
54. J.A.R. Cembranos, Á. De La Cruz-Dombriz, V. Gammaldi, M. Méndez-Isla, *SKA-Phase I sensitivity for synchrotron radio emission from multi-TeV Dark Matter candidates*. [arXiv:1905.11154](#)
55. J.A.R. Cembranos, A. de la Cruz-Dombriz, P.K.S. Dunsby, M. Mendez-Isla, Analysis of branon dark matter and extra-dimensional models with AMS-02. *Phys. Lett. B* **790**, 345–353 (2019). [arXiv:1709.09819](#)
56. T.G. Rizzo, Probes of universal extra dimensions at colliders. *Phys. Rev. D* **64**, 095010 (2001). [arXiv:hep-ph/0106336](#)
57. H.-C. Cheng, J.L. Feng, K.T. Matchev, Kaluza-Klein dark matter. *Phys. Rev. Lett.* **89**, 211301 (2002). [arXiv:hep-ph/0207125](#)
58. G. Servant, T.M.P. Tait, Is the lightest Kaluza-Klein particle a viable dark matter candidate? *Nucl. Phys. B* **650**, 391–419 (2003). [arXiv:hep-ph/0206071](#)
59. K. Kong, K.T. Matchev, Precise calculation of the relic density of Kaluza-Klein dark matter in universal extra dimensions. *JHEP* **01**, 038 (2006). [arXiv:hep-ph/0509119](#)
60. J.A.R. Cembranos, J.L. Feng, L.E. Strigari, Exotic collider signals from the complete phase diagram of minimal universal extra dimensions. *Phys. Rev. D* **75**, 036004 (2007). [arXiv:hep-ph/0612157](#)
61. J.A.R. Cembranos, J.L. Feng, L.E. Strigari, Resolving cosmic gamma ray anomalies with dark matter decaying now. *Phys. Rev. Lett.* **99**, 191301 (2007). [arXiv:0704.1658](#)
62. M. Masip, A. Pomarol, Effects of SM Kaluza-Klein excitations on electroweak observables. *Phys. Rev. D* **60**, 096005 (1999). [arXiv:hep-ph/9902467](#)
63. T.G. Rizzo, J.D. Wells, Electroweak precision measurements and collider probes of the standard model with large extra dimensions. *Phys. Rev. D* **61**, 016007 (2000). [arXiv:hep-ph/9906234](#)
64. F. del Aguila, M. Perez-Victoria, J. Santiago, Bulk fields with general brane kinetic terms. *JHEP* **02**, 051 (2003). [arXiv:hep-th/0302023](#)
65. G.R. Dvali, G. Gabadadze, M. Porrati, 4-D gravity on a brane in 5-D Minkowski space. *Phys. Lett. B* **485**, 208–214 (2000). [arXiv:hep-th/0005016](#)

66. D. Gorbunov, K. Koyama, S. Sibiryakov, More on ghosts in DGP model. *Phys. Rev. D* **73**, 044016 (2006). [arXiv:hep-th/0512097](https://arxiv.org/abs/hep-th/0512097)
67. W. Fang, S. Wang, W. Hu, Z. Haiman, L. Hui, M. May, Challenges to the DGP model from horizon-scale growth and geometry. *Phys. Rev. D* **78**, 103509 (2008). [arXiv:0808.2208](https://arxiv.org/abs/0808.2208)

Chapter 9

Non-local Gravity



Gianluca Calcagni

Quantum gravity is a collective name labelling all those theoretical frameworks combining quantum mechanics and the gravitational force in a consistent way. On one hand, there are approaches that quantise gravity as a fundamental force, or they embed it in a unified theory of elementary interactions. In this case, new physics is expected to emerge at short, ultraviolet (UV) scales of the order of the Planck length ℓ_{Pl} . On the other hand, quantum gravity may also indicate an effective field theory with infrared (IR) corrections manifesting themselves at large scales. This does not mean that the first group of theories is unobservable; on the contrary, Planckian scales may show up in the sky if quantum corrections were not negligible when cosmological inflation took place. Several examples of this amplification mechanism in quantum gravity exist [1].

Here we review a specific candidate of both of the above groups (theories or models with UV or IR corrections): nonlocal gravity. The latter is a field theory endowed with nonlocal form factors. A covariant nonlocal form factor $\gamma(\square)$ can be alternatively described either as an operator with infinitely many derivatives or as the convolution with an integral kernel [2]. For a generic field φ ,

$$\gamma(\square) \varphi(x) = \int d^D y F(y-x) \varphi(y), \quad F(z) = \int \frac{d^D k}{(2\pi)^D} e^{ik \cdot z} \gamma(-k^2), \quad (9.1)$$

The original version of this chapter was revised. The incorrect equation (9.13) has been corrected in this chapter. The correction to this chapter is available at https://doi.org/10.1007/978-3-030-83715-0_39

G. Calcagni (✉)
Instituto de Estructura de la Materia, CSIC, Serrano 121, 28006 Madrid, Spain
e-mail: g.calcagni@csic.es

© The Author(s), under exclusive license to Springer Nature Switzerland AG 2021,
corrected publication 2022

E. N. Saridakis et al. (eds.) *Modified Gravity and Cosmology*,
https://doi.org/10.1007/978-3-030-83715-0_9

where $\square = \nabla_M \nabla^M$ is the Laplace–Beltrami operator. Since the derivative description can be misleading when the counting of degrees of freedom and the Cauchy problem of the theory are considered [3, 4], we prefer the name *nonlocal*, without a hyphen, in order to stress the uniqueness and originality of the dynamical properties of these theories with respect to local theories.

As is well known, quantum field theory (QFT) is nonlocal at the quantum level because loop corrections to the bare propagator typically contain non-polynomial functions of momentum. In general, the quantum effective action contains nonlocal modifications that, in the case of gravity, may leave an imprint on the IR. This IR nonlocality is an effective description of a certain regime of a fundamentally local theory. In contrast, UV nonlocality refers to theories that are fundamentally nonlocal already at the classical level. Historically, UV nonlocality is as old as IR nonlocality. QFT pioneers such as Wataghin [5] and Yukawa [6, 7] considered nonlocality as a means to give particles a finite radius and, thus, to cure the infinities of their self-energy [8]. Nowadays, fundamental nonlocality is invoked for roughly the same reason (to remove the classical singularities of General Relativity and to improve its renormalizability at the quantum level), as well as others such as preservation of unitarity (absence of ghosts and conservation of probability). In the following, we first review UV nonlocal theories and their phenomenology, followed by IR nonlocal models. Note that, strictly speaking, IR nonlocal models are not models of quantum gravity because, despite their loose motivation from nonlocal corrections found in quantum theories, they do not arise from the latter.

9.1 UV Nonlocal Gravity

UV nonlocal gravity, or nonlocal quantum gravity, is a perturbative quantum field theory of the gravitational force, such that the bare action and its classical dynamics are endowed with nonlocal operators of a certain form. The foundations of fundamentally nonlocal QFT have been set by Efimov and collaborators in the case of a scalar field [9–14], while gauge and gravitational theories were considered about a decade later by Krasnikov and Kuz'min [15, 16]. Since then, a surge of interest in classical and quantum nonlocal scalar field theory, gauge theory and gravity, as well as in singularity resolution and cosmology in nonlocal gravity, has been taking place and is gradually increasing [3, 4, 17–67]. The bare (classical) action of the theory in D dimensions is

$$S = \frac{1}{2\kappa_D^2} \int d^D x \sqrt{|g|} [R - 2\Lambda + R\gamma_0(\square)R + R_{MN}\gamma_2(\square)R^{MN} + R_{MNKL}\gamma_4(\square)R^{MNKL} + \mathcal{V}(\mathcal{R})], \quad (9.2)$$

where the form factors $\gamma_{0,2,4}(\square)$ are certain functions of the Laplace–Beltrami operator \square and $\mathcal{V}(\mathcal{R})$ is a “potential” term made of local curvature operators. When

$\gamma_{0,2,4} = 0$, one recovers the Einstein–Hilbert action, while when $\gamma_{0,2,4} = \text{const.}$, one gets fourth-order Stelle gravity and its generalisations [68–72]. To study non-trivial form factors, one can use the generic parametrisation

$$\gamma(\square) = \frac{e^{\text{H}(\square)} - 1}{\square} \simeq \frac{\text{H}(\square)}{\square} = c_0 + c_1 \square + \dots, \quad (9.3)$$

where the function $\text{H}(\square)$ depends on the dimensionless combination $\ell_*^2 \square$ and ℓ_* is a fixed length scale, presumably $O(\ell_{Pl})$. Assuming that $\text{H}(0) = 0$, then by construction the $1/\square$ operator does not carry any of the field-redefinition issues that we will discuss in Sect. 9.2 because it is absorbed by the $O(\square)$ term of $\text{H}(\square) = c_0 \square + c_1 \square^2 + \dots$.

The choice of form factors $\gamma_{0,2,4}$ is not unique but the UV properties of the theory greatly reduce the possibilities. The absence of extra degrees of freedom at the linearized tree level around Minkowski spacetime requires

$$\gamma_0(\square) = -\frac{(D-2)(e^{\text{H}_0} - 1) + D(e^{\text{H}_2} - 1)}{4(D-1)\square} + \gamma_4(\square), \quad \gamma_2(\square) = \frac{e^{\text{H}_2} - 1}{\square} - 4\gamma_4(\square), \quad (9.4)$$

which reduce to the relation $2\gamma_0(\square) + \gamma_2(\square) + 2\gamma_4(\square) = 0$ when $\text{H}_1 = \text{H}_2$. Renormalisability of the theory constrains the form factor $\gamma_4(\square)$ to have the same (or lower in the number of derivatives) asymptotic UV behaviour as the other two form factors $\gamma_{0,2}(\square)$. Since $\gamma_4(\square)$ does not appear in the graviton propagator, the minimal choice compatible with unitarity corresponds to $\gamma_4(\square) = 0$, but a non-vanishing form factor affects the admissible metric solutions of the theory. In particular, Ricci-flat spacetimes with $R_{MNKL} \neq 0$ are not classical solutions if $\gamma_4 \neq 0$.

Two classes of form factors have been widely studied in the literature:

- *Exponential-monomial form factors*, which include the *minimal form factor* [20, 33]

$$\gamma(\square) = \frac{e^{-\ell_*^2 \square} - 1}{\square}, \quad (9.5)$$

and the *Krasnikov form factor* [15]

$$\gamma(\square) = \frac{e^{\ell_*^4 \square^2} - 1}{\square}. \quad (9.6)$$

When linearizing in the metric $g_{MN} = g_{MN}^{(0)} + h_{MN}$ and expanding around the background $g_{MN}^{(0)}$, the minimal form factor produces a kinetic term $\sim h_{MN} \square \exp(-\ell_*^2 \square) h^{MN}$, where the kinetic operator is called Wataghin form factor [5] and is typically found in string field theory.

- *Asymptotically polynomial form factors*. Here, $\exp[\text{H}(z)]$ is such that: (i) it is an entire function; (ii) it has no zeros in the whole complex plane, hence $\text{H}(z)$ is also entire; (iii) it is real and positive on the real axis; (iv) $\text{H}(0) = 0$ ($\gamma(z)$ is non-singular); (v) in a suitable conical region \mathcal{C} , $\exp[\text{H}_\infty(z)] :=$

$\lim_{|z| \rightarrow +\infty} \exp[H(z)] = |z|^n$, where n is a natural number that depends on the order of local derivative operators in the action, on the spacetime dimension D and on the renormalisability of the theory; (vi) in the conical region \mathcal{C} , $\lim_{|z| \rightarrow +\infty} \{\exp[H(z)] / \exp[H_\infty(z)] - 1\} z^n = 0$ for all $n \in \mathbb{N}$, hence the name asymptotically polynomial. Two representatives of this class are the *Kuz'min form factor* [16]

$$H(\square) = H_{\text{Kuz}}(\square) := \alpha \left[\ln(-\ell_*^2 \square) + \Gamma(0, -\ell_*^2 \square) + \gamma_E \right], \quad (9.7)$$

where $\alpha \geq 3$, and the *Tomboulis form factor* [18, 26]

$$H(\square) = H_{\text{Tom}}(\square) := \frac{1}{2} \left\{ \ln p^2(\square) + \Gamma[0, p^2(\square)] + \gamma_E \right\}, \quad (9.8)$$

where $\Gamma(0, x)$ is the upper incomplete gamma function with its first argument vanishing, $\gamma_E \approx 0.577$ is the Euler–Mascheroni constant and $p(z)$ is a real polynomial of degree n with $p(0) = 0$.

Exponential-monomial form factors are simpler but asymptotically polynomial form factors are especially well behaved at the quantum level. Within the above choices, and depending on the spacetime dimension D and the local potential $\mathcal{V}(\mathcal{R})$, the theory is super-renormalisable (only one-loop divergences survive and one must add a finite number of operators to absorb them) or finite (no divergences, all beta functions vanish), tree-level unitary (no classical instabilities, no ghost modes) and perturbative unitary (conservation of probability). The job of the nonlocal form factors in gravity is, on one hand, to modify the renormalisation properties of the theory and, on the other hand, to guarantee unitarity. In contrast, higher-order local gravity is renormalisable but non-unitary.

Particle physics places a lower bound on the energy scale of the theory, $E_* = 1/\ell_* > 1 - 3 \text{ TeV}$ [38]. Above that scale, interesting physical effects are obtained, which we describe in the following.

9.1.1 Singularity Problem

The infinities of General Relativity are not supposed to survive in a renormalisable theory of gravitation. However, this statement depends on the background and on the specific form of the Lagrangian. Consider first the question about the fate of black-hole singularities. There are two diametrically opposed claims in the literature of UV nonlocal gravity: singularities do not disappear just because the dynamics is nonlocal [22, 53, 59, 67] or they actually do [48, 54, 56, 57, 62, 63]. There is no contradiction between these views, since the former holds in theories with $\gamma_4(\square) = 0$, while the latter holds when $\gamma_4(\square) \neq 0$.

In the $\gamma_4 = 0$ case, Ricci-flat spacetimes are not only exact vacuum solutions of the theory [45], but they are also stable against perturbations of linear order [53, 59]

or even arbitrary order [67], if they are stable in General Relativity. Any Ricci-flat stable vacuum solution of Einstein gravity is also a solution of nonlocal gravity and, consequently, the Schwarzschild metric is also a stable solution. This implies that singular solutions exist in the theory. However, the issue of whether such black holes are physical or not is still open and it depends on the matter distribution (calculated in the sense of generalised functionals) associated with them. A matter distribution incompatible with the singularity at $r = 0$ could indicate that the vacuum solution is purely mathematical.

In the $\gamma_4 \neq 0$ case, Ricci-flat metrics are not solutions to the theory because the Riemann tensor does not vanish therein. Finding alternative exact solutions is difficult, both because the equations of motion are complicated and because in theories with higher-order curvature terms there is no Birkhoff theorem guaranteeing the uniqueness of spherically symmetric solutions. Still, one can look at linearised perturbations of the Minkowski background and, in particular, at the Newton potential. The latter is the static potential $\Phi(\mathbf{x})$ in $(D - 1)$ -dimensional flat space defined by the Green equation

$$\gamma(\nabla^2)\Phi(\mathbf{x}) = \delta^{D-1}(\mathbf{x}). \quad (9.9)$$

When $\gamma(\nabla^2) = \nabla^2 \exp(-\ell_*^2 \nabla^2)$, Φ is regular near the origin $r := |\mathbf{x}| = 0$ [17, 19] (see also [20, 25, 48]; all these papers work in $D = 4$ dimensions):

$$\Phi(r) = -\frac{1}{4\pi^{\frac{D-1}{2}} r^{D-3}} \left[\Gamma\left(\frac{D-3}{2}\right) - \Gamma\left(\frac{D-3}{2}, \frac{r^2}{4\ell_*^2}\right) \right] \quad (9.10)$$

$$\stackrel{D=4}{=} -\frac{\operatorname{erf}\left(\frac{r}{2\ell_*}\right)}{4\pi r}, \quad (9.11)$$

where $\Gamma(\nu, z)$ is the upper incomplete gamma function of order ν and erf is the error function. Near the origin,

$$\Phi(r) = -\frac{1}{(D-3)2^{D-2}\pi^{\frac{D-1}{2}}\ell_*^{D-3}} + O(r^2) \stackrel{D=4}{=} -\frac{1}{4\pi^{\frac{3}{2}}\ell_*} + O(r^2), \quad (9.12)$$

i.e., the Newton potential tends to a non-zero constant. Consistently, in the limit $\ell_* \rightarrow 0$ one recovers the local potential singular at $r = 0$. A general no-go theorem is that the theory with the Riemann–Riemann term does not allow any metric potential of the form $1/r^\alpha$ with $\alpha > 0$ [57].

The nonlocal generalization of the Schwarzschild black-hole $D = 4$ linearised line element features this potential in its 00 and rr components [56]:

$$ds^2 = -[1 + 2\Phi(r)]dt^2 + [1 - 2\Phi(r)]dr^2 + r^2 d\Omega^2, \quad (9.13)$$

where $d\Omega^2$ is the angular line element. Although this line element represents a linear perturbation of the Minkowski background, one can argue that it is sufficient to assess the microscopic properties of spherically symmetric solutions, since in

the UV nonlocal gravity is weak, due to asymptotic freedom [62]. The linear size $r_{\text{nonlocal}} \simeq 2\ell_*$ of the nonlocal region is larger than the Schwarzschild radius of black holes in General Relativity, while the interior is regular and described by an effective Euclidean field theory [56, 62].

Therefore, black holes are non-singular in the theory with $\gamma_4 \neq 0$ [56, 57]. These results were generalised to non-singular rotating black holes (the counter part of the Kerr metric in General Relativity) [54] and charged black holes (the counter part of the Reissner–Nordström metric in General Relativity) [63].

The Big Bang is another singularity that nonlocality could smear out. Friedmann–Lemaître–Robertson–Walker (FLRW) classical solutions to the equations of motion typically have a bouncing scale factor $a(t)$, as shown in a toy model with pure Ricci-scalar Lagrangian ($\gamma_2 = 0 = \gamma_4$) [20, 23, 30, 40]. Also, the Kasner metric with scale factor $a(t) = t^{p_i}$ ($i = 1, 2, 3$) is not a solution of the theory, neither with $\gamma_4 = 0$ [33] nor with $\gamma_4 \neq 0$ [58]. In the first case, it was shown that the Belinsky–Khalatnikov–Lifshitz singularity is replaced by an anisotropic bounce [33].

In the theory with $\gamma_2 \neq 0$ and $\gamma_4 = 0$, a bouncing profile $a(t)$ is an approximate solution of the full equations of motion valid both at very early times (when, roughly, the cosmological horizon scale is near the asymptotically free UV fixed point) and at late times. This profile can be described by the effective Friedmann equation [33]

$$H^2 = \frac{\kappa^2}{3} \rho_{\text{eff}} := \frac{\kappa^2}{3} \rho \left[1 - \left(\frac{\rho}{\rho_*} \right)^\beta \right], \quad (9.14)$$

where $H := \dot{a}/a$ is the Hubble parameter (not to be confused with the form factor H), $\kappa^2 = 8\pi G_N$ with G_N the four-dimensional Newton's constant, ρ is the total energy density of the Universe content, $\rho_* \leq \rho_{\text{Pl}}$ is the critical energy density at which the bounce occurs, ρ_{Pl} is the Planck energy density, and $\beta > 0$ is a real parameter. The exponent β is determined by plugging the profile $a(t)$ found under the provision of asymptotic freedom (weak coupling in the UV) into (9.14) for a given energy density profile $\rho(a)$. Since this fit is generally rather good, one can conclude that the asymptotic bouncing solution is also reasonably valid at intermediate times, and that the bouncing accelerating scenario of the theory is well described by the effective Friedmann equation (9.14).

The presence of non-singular solutions does not guarantee the removal of infinities at the classical level unless such solutions are typical. As an example where nonlocal operators are not enough to make the dynamics singularity-free, we cite a scalar-tensor nonlocal theory with both bouncing and singular solutions [22]. In that case, conformal invariance seems to play a more pivotal role than nonlocality in the resolution of the Big Bang. This is confirmed in the finite versions of nonlocal quantum gravity, where the beta functions vanish and, therefore, there is no conformal anomaly, conformal invariance holds at the quantum level and, trivially, classical singularities are removed by a conformal transformation [44].

9.1.2 Inflation

The realization of early-universe acceleration in UV nonlocal gravity is anticipated by the observation that de Sitter cosmology (exponential scale factor, constant H) is a solution of the theory. Its stability and the absence of extra propagating degrees of freedom therein was checked both at the linear order [51, 52] and at all perturbative orders [67].

On a less formal side, acceleration is automatically implemented by the non-singular scale factors $a(t)$ discussed above. All these solutions realize a geodesically complete inflationary scenario because they accelerate near the bounce. Geometry can drive an early acceleration era both in a toy model with pure Ricci-scalar Lagrangian ($\gamma_2 = 0 = \gamma_4$) [23, 30, 40] and the minimal theory with $\gamma_2 \neq 0 = \gamma_4$ in the asymptotically free regime [21, 33]. The model is compatible with observations, since it yields the local Starobinsky action in the limit of small ℓ_* [35].

9.1.3 Dark Energy

The cosmological constant problem has not been addressed yet in this class of theories beyond some preliminary considerations [24].

9.1.4 Gravitational Waves

The golden age of gravitational-wave (GW) observations, from those emitted by small-redshift astrophysical compact objects [73, 74] to the inflationary tensor spectrum generated in the early Universe [75], has been among the most notable achievements of General Relativity. To date, the predictions of Einstein gravity related to GWs, small ripples of spacetime propagating through cosmological scales, have been confirmed, and no evidence of new physics has been found. While with the available LIGO-Vigro data we are closing in on many models beyond General Relativity, new astrophysical and cosmological constraints have been devised to be tested in near-future experiments such as KAGRA, LISA or DECIGO. One of the observables we can use to discriminate among different cosmological models is the luminosity distance of standard sirens, which are sources of both photons (light) and gravitons (GWs) that will become gradually available when populating the catalogue of GWs [76].

Quantum gravity is among the things that could happen beyond General Relativity and, although most theories of quantum gravity predict too small effects to be detected, some could generate a non-negligible signal [77, 78]. Unfortunately, nonlocal quantum gravity is among the candidates failing to produce such a signal [67]. The intuitive reason, common to many other (albeit not all) quantum gravities,

is that nonlocal corrections are confined to Planckian scales. Still, it is instructive to see the details of the result, because on one hand they introduce the basics of luminosity distance and, on the other hand, they are an example of how to extract predictions from the theory and pitch them against observations. The smoking gun of nonlocal quantum gravity cannot be found in other GW observables either, such as the amplitude of the primordial stochastic GW background [79], which we will not discuss here.

We first consider General Relativity in four dimensions. The linearised propagation equation of GWs on a FLRW background is $\square h = 0$, where $h(t, \mathbf{x}) = h_{+, \times}(t, \mathbf{x})$ is the amplitude of either tensor polarisation mode [80]. From the solution of this equation, or from a simple scaling argument, one can recast the GW amplitude in terms of the redshift $z := 1/a - 1$ and a physical observable, the luminosity distance of an optical source

$$d_L^{\text{EM}} = (1+z) \int_0^z \frac{dz}{H}. \quad (9.15)$$

It turns out that, up to coefficients [81],

$$\frac{1}{d_L^{\text{GW}}} := h = \frac{1}{d_L^{\text{EM}}}, \quad (9.16)$$

where we defined the GW luminosity distance as the inverse of the amplitude. Therefore, for a standard siren in General Relativity $d_L^{\text{GW}}/d_L^{\text{EM}} = 1$.

In UV nonlocal gravity, the linearized perturbation equation is [26, 82]

$$\square \tilde{h} = 0, \quad \tilde{h} := e^H h. \quad (9.17)$$

Using the same scaling argument as in General Relativity, with h replaced by \tilde{h} , for entire form factors we have

$$\tilde{h} = \frac{1}{d_L^{\text{GW}}} \implies h = e^{-H} \frac{1}{d_L^{\text{GW}}}. \quad (9.18)$$

We can estimate the nonlocal correction in the right-hand side for the minimal form factor (9.5), $H(\square) = -\ell_*^2 \square = \ell_*^2 (\partial_t^2 + 3H\partial_t)$ in the homogeneous approximation and, crudely, an approximately constant Hubble parameter $H \simeq H_0$, so that $z \simeq e^{-H_0(t-t_0)} - 1$ and $d_L \simeq (z+1)z/H_0 \simeq [e^{-2H_0(t-t_0)} - e^{-H_0(t-t_0)}]/H_0$. Since $e^{-H(\square)} e^{nH_0 t} = e^{-n(n+3)(\ell_* H_0)^2} e^{nH_0 t}$, at large redshift $h \simeq H_0 e^{-10(\ell_* H_0)^2} e^{2H_0(t-t_0)}$, while at small redshift $z \simeq -H_0(t-t_0) \ll 1$ one has $h \simeq H_0 e^{-3(\ell_* H_0)^2} e^{2H_0(t-t_0)}$. Overall,

$$h \simeq \frac{e^{-c(\ell_* H_0)^2}}{d_L^{\text{GW}}}, \quad c = O(1) - O(10). \quad (9.19)$$

The binary neutron star merger GW170817 is the first known example of standard siren [74]. If propagation of electromagnetic waves was affected in the same way by

the form factor, then the ratio between the luminosity distance d_L^{GW} measured by an interferometer and the luminosity distance d_L^{EM} measured for the optical counter-part would be equal to 1, as in General Relativity. However, even if light was not affected by nonlocality, we would have

$$\frac{d_L^{\text{GW}}}{d_L^{\text{EM}}} \simeq 1 + c(\ell_* H_0)^2, \quad (9.20)$$

and, for $\ell_* = \ell_{Pl}$, the right-hand side would be of the order of $1 + 10^{-120}$, an effect completely unobservable compared with the estimated error $\Delta d_L/d_L \sim 0.001 - 0.1$ of present and future interferometers [83–86]. For a power-law expansion $a = (t/t_0)^p$, $d_L \propto (t_0/t)^{2p}(t_0 - t)$, and one can show that, again, the correction in the ratio (9.20) is of the order of $(\ell_*/t_0)^2 \sim 10^{-120}$. Increasing ℓ_* to particle-physics scales does not magnify this correction enough, since it is governed by the cosmological scale $H_0^{-1} \sim t_0 \sim 10^{17}$ s.

9.2 IR Nonlocal Gravity

At the level of the quantum effective action in perturbative gravity, one can add all admissible higher-order curvature terms featuring four derivatives. These terms, of the form $\mathcal{R}^l \square^{-n} \mathcal{R}^m$, where \mathcal{R} is a generic curvature tensor, are such that $n = m + l - 2 \geq 0$, so that the effective action is decorated with inverse powers of the Laplace–Beltrami operator \square [87]. Since in momentum space $\square^{-n} \rightarrow (-k^2)^{-n}$, these terms can dominate in the IR (small momenta). However, one cannot expand perturbative one-loop corrections from light particles, which have been calculated and take the well-known logarithmic form $\ln(-\square)$ [88–95], to get \square^{-n} operators with a cosmological impact, since loop corrections are valid in the UV, while the latter are an IR effect (deviations from General Relativity at large scales) [96]. Therefore, the main motivation to consider Lagrangians of the form $f(\square^{-n} R)$ is phenomenological. Although there may still be high-energy scenarios justifying them [96–98], they are not strictly necessary, since here the focus is on IR divergences that could generate an effective mass dynamically.

The operator $1/\square$ admits an integral representation via the solution of the Green equation

$$\square_x \mathcal{K}(x - x') = \frac{\delta^D(x - x')}{\sqrt{|g|}}. \quad (9.21)$$

The kernel \mathcal{K} is nothing but the representation of the form factor $1/\square$.

Nonlocal field redefinitions $\varphi(x) \rightarrow \tilde{\varphi}(x) = \gamma(\square)\varphi(x)$ do not change the spectrum of the theory in the case of form factors $\gamma(\square) = c_0 + c_1 \square + O(\square^2)$ with $c_0 \neq 0$, i.e., those with trivial kernel. However, the operator $1/\square$ does not enjoy this property and nonlocal field redefinitions are defined up to a harmonic function

λ , $\bar{\varphi}(x) = \square^{-1}\varphi(x) + \lambda(x)$, where $\square\lambda(x) = 0$. This delicate point must be dealt with carefully, since dynamical solutions do not admit $\lambda = 0$ in general.

In (9.21), one must specify a contour prescription for the Green function \mathcal{K} . However, even if the causal (retarded) propagator $\mathcal{K}_{\text{ret}}(x - y)$ is used to define the \square^{-1} operator, the variation of an action with \square^{-1} operators acting on the fields always gives rise to the even combination $\mathcal{K}_{\text{ret}}(x - y) + \mathcal{K}_{\text{ret}}(y - x) =: \mathcal{K}_{\text{ret}}(x - y) + \mathcal{K}_{\text{adv}}(x - y)$. The retarded Green function is not even, and changing the sign to its argument gives the advanced Green function $\mathcal{K}_{\text{ret}}(y - x) = \mathcal{K}_{\text{adv}}(x - y)$, which is anti-causal. Therefore, the equations of motion for the field expectation values on in-out states (obtained from the variation of the quantum effective action) in theories with nonlocalities of the type \square^{-1} are acausal [97, 99, 100]. However, in-in expectation values obey equations of motion obtained in the Schwinger–Keldysh formalism, which automatically give the retarded propagator. Considered in this way, IR nonlocal theories are causal [97, 99].

A class of models with such peculiarities is

$$\mathcal{L} = \frac{1}{2\kappa_D^2} [R + \mathcal{R} f(\square^{-n}\mathcal{R})], \quad (9.22)$$

with different choices of parameters and operators. The best studied candidates in $D = 4$ dimensions are the Deser–Woodard model [101], nonlocal massive gravity [102] and the Maggiore–Mancarella model [103]:

- *Deser–Woodard* (or $f(\square^{-1}R)$) *model* ($\mathcal{R} = R$, $n = 1$, f arbitrary) [100, 101, 104–120]:

$$\mathcal{L} = \frac{1}{2\kappa^2} R [1 - f(\square^{-1}R)]. \quad (9.23)$$

When $f = \mathbb{1}$ and $\mathcal{L} \propto R - R\square^{-1}R$, one obtains an approximation of the first IR nonlocal model of this type, due to Wetterich [121].

- *Nonlocal massive gravity* (or *RT model*), where an $\mathcal{R} = R$, $n = 1$ correction arises at the level of the equations of motion [99, 102, 118, 122–126]:

$$G_{\mu\nu} - \frac{m^2}{3}(g_{\mu\nu}\square^{-1}R)^T = \kappa^2 T_{\mu\nu}, \quad (9.24)$$

where T indicates the transverse part of the tensor. This version of the theory improves a previous one [127] with unstable cosmological evolution [122].

- *Maggiore–Mancarella* (or $R\square^{-2}R$, or *RR model*) ($\mathcal{R} = R$, $n = 2$, $f = \mathbb{1}$) [96, 97, 103, 118, 124, 125, 128–130]:

$$\mathcal{L} = \frac{1}{2\kappa^2} R \left(1 - \frac{m^2}{6} \frac{1}{\square^2} R \right). \quad (9.25)$$

- *Other models*: with the Ricci tensor ($\mathcal{R} = R_{\mu\nu}$, $f = \mathbb{1}$), $R_{\mu\nu}\square^{-1}R^{\mu\nu}$ model ($n = 1$) [131, 132], $R_{\mu\nu}\square^{-1}G^{\mu\nu}$ model ($n = 1$) [98, 133–135] and $R_{\mu\nu}\square^{-2}R^{\mu\nu}$ model

($n = 2$) [100, 136]; conformal extension with $\mathcal{R} = R$, $n = 1$ [137], similar to Wetterich's early proposal [121]; new Deser–Woodard model [138, 139].

The Deser–Woodard model [101] does not contain any extra scale, while the massive-gravity model [102, 122, 127] and the Maggiore–Mancarella model [103] feature a mass scale m . Furthermore, while the Deser–Woodard and the Maggiore–Mancarella models have simple actions and complicated equations of motion, massive gravity has simple equations of motion and a possibly complicated non-linear action, which is still unknown. Finally, the massive-gravity model and the Maggiore–Mancarella model give the same linearized equations on Minkowski background but they differ on other backgrounds or at the non-linear level, the second model deviating more strongly from Λ CDM [128].

Auxiliary fields can be introduced so that, for instance in the $\mathcal{R} = R$ case, the Lagrangian $\tilde{\mathcal{L}} \propto R [1 + f(\phi)] + \psi(\square\phi - R)$ replicates on shell the dynamics of the original system (9.22) [104]. However, this version is not completely equivalent to the former because the equation of motion $\square\phi - R = 0$ of the Lagrange multiplier ψ is used to obtain ϕ as a nonlocal function of R . The problem is that the solution of this relation is of the form

$$\phi = \square^{-1}R + \lambda, \quad (9.26)$$

where λ is a scalar mode obeying the homogeneous equation $\square\lambda = 0$ [107]. This extra mode is responsible for extending the space of solutions to dynamics not admitted by the original nonlocal system [107]. Also, it makes an otherwise immaterial ghost degree of freedom dynamical. Integrating by parts,

$$\psi\square\phi \rightarrow -\partial_\mu\psi\partial^\mu\phi = -\frac{1}{4}\partial_\mu(\psi + \phi)\partial^\mu(\psi + \phi) + \frac{1}{4}\partial_\mu(\psi - \phi)\partial^\mu(\psi - \phi).$$

Suitable conditions on f , found along the same lines of ghost constraints in $f(R)$ or higher-order theories, remove this ghost [111].

All these models can be recovered in a unified way as the integer-order limit of the action [140]

$$S = \frac{1}{2\kappa^2} \int d^4x \sqrt{|g|} [R + \ell_*^2 G_{\mu\nu} (-\ell_*^2 \square)^{\gamma-2} R^{\mu\nu}], \quad (9.27)$$

where $0 < \gamma < 1$. This theory has been built as a perturbative quantum field theory of gravity realizing a change of spacetime spectral dimension across scales. While renormalizability and unitarity are difficult to achieve simultaneously, unitarity is generally preserved in the above range of γ . Therefore, it may be possible to recover the phenomenology of IR nonlocal gravity while at the same time avoiding stability problems.

9.2.1 Singularity Problem

IR nonlocal models have been considered in the early Universe only recently. The Deser–Woodard mode admits bouncing solutions, thus removing the Big-Bang singularity [120].

9.2.2 Inflation

Given that the generalisation $\mathcal{L} \propto F(R) + \mathcal{R} f(\square^{-n} \mathcal{R})$ of the total Lagrangian (9.23) contains both local and nonlocal higher-order curvature terms, there is the possibility to unify early-time (inflation) and late-time (dark energy) acceleration. For instance, the local term $F(R)$ and the nonlocal term $R f(\square^{-n} R)$ can drive, respectively, inflation and dark energy. In both cases, acceleration is sustained by the scalar fields hidden in the dynamics and made explicit by, respectively, a local ($\phi = F'(R)$) or nonlocal (9.26) field redefinition. However, unification scenarios require a certain degree of engineering of the functions F and f [104].

Both the massive-gravity and the Maggiore–Mancarella models are compatible with observations of the cosmic microwave background (CMB) multipole spectrum [97, 124, 129].

9.2.3 Dark Energy

All the IR nonlocal models listed above are endowed with self-accelerating late-time solutions without a cosmological constant, where the role of dark energy is played by a nonlocal curvature component with an effective phantom equation of state (effective barotropic index $w < -1$).

Since the field redefinition (9.26) entails a non-trivial homogeneous solution, the Deser–Woodard model in its nonlocal form (9.23) differs from its “localised” form obtained via such a field transformation. Therefore, predictions are frame-dependent. The Deser–Woodard model was mainly studied in its localised form. Since $R = 0$ during the radiation epoch, $O(\square^{-1} R)$ terms start to grow only after the onset of matter domination and do not spoil early-universe constraints, which makes this model a viable candidate for dark energy. Functions f fitting late-time observations can be extracted by data [108, 109]. For instance, the Λ CDM model is reproduced when

$$f(\phi) = c \left[\tanh \left(\sum_{l=0}^3 c_l \phi^l \right) - 1 \right], \quad (9.28)$$

for certain numerical coefficients c and c_l [108]. The form of f is completely *ad hoc* and not especially attractive, but it does not involve fine tuning. Depending on the

data set of structure-evolution observations and on the type of analysis, the Deser–Woodard model is favoured [114, 115] or comparable [119] with respect to standard General Relativity. However, the model does not pass Solar-System tests, due to failure of its screening mechanism [118]. The new Deser–Woodard model seems able to avoid this issue [138, 139].

The localised version of the Maggiore–Mancarella model gives a viable dark-energy evolution with $m = O(H_0)$ [97, 103, 124, 125, 128] and is compatible with structure formation [97, 124, 125, 129]. Unfortunately, the lack of a screening mechanism leads to non-negligible deviations in Solar-System tests, which rule the model out [118, 129].

The massive-gravity model passes a battery of observational tests [123] and, in fact, it is indistinguishable from Λ CDM with present data [125]. Since it is compatible also with Solar-System tests [118], it is a stronger candidate than the Deser–Woodard and the Maggiore–Mancarella models and, perhaps, the only survivor of the three.

Finally, the $n = 2$, $\mathcal{R} = R_{\mu\nu}$ model is unviable, due to instabilities in tensor perturbations [100, 136].

9.2.4 Gravitational Waves

IR nonlocal gravity could leave an imprint in GW propagation [76, 97, 116]. In particular, the ratio of the gravitational and electromagnetic luminosity distance for a standard siren fits the parametrisation

$$\frac{d_L^{\text{GW}}}{d_L^{\text{EM}}} \simeq \Xi_0 + \frac{1 - \Xi_0}{(1+z)^n}, \quad (9.29)$$

where Ξ_0 and n are constants. The Mancarella–Maggiore model (RR model, under strong pressure by Solar-System tests) predicts $\Xi_0 \approx 0.970$ and $n \approx 2.5$ [116], while for nonlocal massive gravity (RT model) $\Xi_0 \approx 0.934$ and $n \approx 2.6$ when setting the initial conditions in the radiation-domination era [76]. These values are within the sensitivity of LISA, for which an $O(1\%)$ relative error on Ξ_0 has been estimated [76]. Setting instead the initial conditions during inflation, one can get even larger deviations from General Relativity (around $\Xi_0 \sim 1.5$) while respecting other constraints [126].

References

1. G. Calcagni, *Classical and Quantum Cosmology Graduate Texts in Physics* (Springer, Berlin, 2017)
2. A. Pais, G.E. Uhlenbeck, On field theories with non-localized action. *Phys. Rev.* **79**, 145–165 (1950)

3. G. Calcagni, L. Modesto, G. Nardelli, Initial conditions and degrees of freedom of non-local gravity. *JHEP* **05**, 087 (2018). [arXiv:1803.00561](https://arxiv.org/abs/1803.00561). [Erratum: *JHEP*05,095(2019)]
4. G. Calcagni, L. Modesto, G. Nardelli, Non-perturbative spectrum of non-local gravity. *Phys. Lett. B* **795**, 391–397 (2019). [arXiv:1803.07848](https://arxiv.org/abs/1803.07848)
5. G. Wataghin, Bemerkung über die Selbstenergie der Elektronen. *Z. Phys.* **88**(1–2), 92–98 (1934)
6. H. Yukawa, On the radius of the elementary particle. *Phys. Rev.* **76**, 300–301 (1949)
7. H. Yukawa, Quantum theory of non-local fields. part i. free fields. *Phys. Rev.* **77**, 219–226 (1950)
8. W. Pauli, Die allgemeinen Prinzipien der Wellenmechanik, in *Handbuch der Physik*, vol. XXIV/1, (1933), p. 83, <https://www.springer.com/gp/book/9783642525650>
9. G.V. Efimov, Analytic properties of Euclidean amplitudes. *Sov. J. Nucl. Phys.* **4**(2), 309–315 (1967). [*Yad. Fiz.*4,no.2,432(1966)]
10. G.V. Efimov, Non-local quantum theory of the scalar field. *Commun. Math. Phys.* **5**(1), 42–56 (1967)
11. V.A. Alebastrov, G.V. Efimov, A proof of the unitarity of S-matrix in a nonlocal quantum field theory. *Commun. Math. Phys.* **31**(1), 1–24 (1973)
12. V.A. Alebastrov, G.V. Efimov, Causality in quantum field theory with nonlocal interaction. *Commun. Math. Phys.* **38**(1), 11–28 (1974)
13. G.V. Efimov, Quantization of non-local field theory. *Int. J. Theor. Phys.* **10**(1), 19–37 (1974)
14. G.V. Efimov, *Nonlocal Interactions of Quantized Fields* (Nauka, Moscow, 1977). (in Russian)
15. N.V. Krasnikov, Nonlocal gauge theories. *Theor. Math. Phys.* **73**, 1184–1190 (1987). [*Teor. Mat. Fiz.*73,235(1987)]
16. Yu.V. Kuzmin, The convergent nonlocal gravitation (in Russian). *Sov. J. Nucl. Phys.* **50**, 1011–1014 (1989). [*Yad. Fiz.*50,1630(1989)]
17. A.A. Tseytlin, On singularities of spherically symmetric backgrounds in string theory. *Phys. Lett. B* **363**, 223–229 (1995). [arXiv:hep-th/9509050](https://arxiv.org/abs/hep-th/9509050)
18. E.T. Tomboulis, *Superrenormalizable gauge and gravitational theories*. [arXiv:hep-th/9702146](https://arxiv.org/abs/hep-th/9702146)
19. W. Siegel, *Stringy gravity at short distances*. [arXiv:hep-th/0309093](https://arxiv.org/abs/hep-th/0309093)
20. T. Biswas, A. Mazumdar, W. Siegel, Bouncing universes in string-inspired gravity. *JCAP* **0603**, 009 (2006). [arXiv:hep-th/0508194](https://arxiv.org/abs/hep-th/0508194)
21. J. Khoury, Fading gravity and self-inflation. *Phys. Rev. D* **76**, 123513 (2007). [arXiv:hep-th/0612052](https://arxiv.org/abs/hep-th/0612052)
22. G. Calcagni, G. Nardelli, Non-local gravity and the diffusion equation. *Phys. Rev. D* **82**, 123518 (2010). [arXiv:1004.5144](https://arxiv.org/abs/1004.5144)
23. T. Biswas, T. Koivisto, A. Mazumdar, Towards a resolution of the cosmological singularity in non-local higher derivative theories of gravity. *JCAP* **1011**, 008 (2010). [arXiv:1005.0590](https://arxiv.org/abs/1005.0590)
24. J.W. Moffat, Ultraviolet complete quantum gravity. *Eur. Phys. J. Plus* **126**, 43 (2011). [arXiv:1008.2482](https://arxiv.org/abs/1008.2482)
25. L. Modesto, J.W. Moffat, P. Nicolini, Black holes in an ultraviolet complete quantum gravity. *Phys. Lett. B* **695**, 397–400 (2011). [arXiv:1010.0680](https://arxiv.org/abs/1010.0680)
26. L. Modesto, Super-renormalizable quantum gravity. *Phys. Rev. D* **86**, 044005 (2012). [arXiv:1107.2403](https://arxiv.org/abs/1107.2403)
27. T. Biswas, E. Gerwick, T. Koivisto, A. Mazumdar, Towards singularity and ghost free theories of gravity. *Phys. Rev. Lett.* **108**, 031101 (2012). [arXiv:1110.5249](https://arxiv.org/abs/1110.5249)
28. S. Alexander, A. Marciano, L. Modesto, The hidden quantum groups symmetry of super-renormalizable gravity. *Phys. Rev. D* **85**, 124030 (2012). [arXiv:1202.1824](https://arxiv.org/abs/1202.1824)
29. L. Modesto, Super-renormalizable multidimensional quantum gravity. *Astron. Rev.* **8**(2), 4–33 (2013). [arXiv:1202.3151](https://arxiv.org/abs/1202.3151)
30. T. Biswas, A.S. Koshelev, A. Mazumdar, S.Yu. Vernov, Stable bounce and inflation in non-local higher derivative cosmology. *JCAP* **1208**, 024 (2012). [arXiv:1206.6374](https://arxiv.org/abs/1206.6374)
31. F. Briscese, A. Marcianò, L. Modesto, E.N. Saridakis, Inflation in (super-)renormalizable gravity. *Phys. Rev. D* **87**(8), 083507 (2013). [arXiv:1212.3611](https://arxiv.org/abs/1212.3611)

32. L. Modesto, Super-renormalizable Gravity, in *Proceedings, 13th Marcel Grossmann Meeting on Recent Developments in Theoretical and Experimental General Relativity, Astrophysics, and Relativistic Field Theories (MG13): Stockholm, Sweden, 1–7 July 2012* (2015), pp. 1128–1130. [arXiv:1302.6348](#)
33. G. Calcagni, L. Modesto, P. Nicolini, Super-accelerating bouncing cosmology in asymptotically-free non-local gravity. *Eur. Phys. J. C* **74**(8), 2999 (2014). [arXiv:1306.5332](#)
34. L. Modesto, S. Tsujikawa, Non-local massive gravity. *Phys. Lett. B* **727**, 48–56 (2013). [arXiv:1307.6968](#)
35. F. Briscese, L. Modesto, S. Tsujikawa, Super-renormalizable or finite completion of the Starobinsky theory. *Phys. Rev. D* **89**(2), 024029 (2014). [arXiv:1308.1413](#)
36. T. Biswas, A. Conroy, A.S. Koshelev, A. Mazumdar, Generalized ghost-free quadratic curvature gravity. *Class. Quant. Grav.* **31**, 015022 (2014). [arXiv:1308.2319](#). [Erratum: *Class. Quant. Grav.* **31**, 159501(2014)]
37. L. Modesto, *Multidimensional finite quantum gravity*. [arXiv:1402.6795](#)
38. T. Biswas, N. Okada, Towards LHC physics with nonlocal Standard Model. *Nucl. Phys. B* **898**, 113–131 (2015). [arXiv:1407.3331](#)
39. L. Modesto, L. Rachwal, Super-renormalizable and finite gravitational theories. *Nucl. Phys. B* **889**, 228–248 (2014). [arXiv:1407.8036](#)
40. A. Conroy, A.S. Koshelev, A. Mazumdar, Geodesic completeness and homogeneity condition for cosmic inflation. *Phys. Rev. D* **90**(12), 123525 (2014). [arXiv:1408.6205](#)
41. S. Talaganis, T. Biswas, A. Mazumdar, Towards understanding the ultraviolet behavior of quantum loops in infinite-derivative theories of gravity. *Class. Quant. Grav.* **32**(21), 215017 (2015). [arXiv:1412.3467](#)
42. L. Modesto, L. Rachwal, Universally finite gravitational and gauge theories. *Nucl. Phys. B* **900**, 147–169 (2015). [arXiv:1503.00261](#)
43. P. Donà, S. Giaccari, L. Modesto, L. Rachwal, Y. Zhu, Scattering amplitudes in super-renormalizable gravity. *JHEP* **08**, 038 (2015). [arXiv:1506.04589](#)
44. L. Modesto, M. Piva, L. Rachwal, Finite quantum gauge theories. *Phys. Rev. D* **94**(2), 025021 (2016). [arXiv:1506.06227](#)
45. Y.-D. Li, L. Modesto, L. Rachwal, Exact solutions and spacetime singularities in nonlocal gravity. *JHEP* **12**, 173 (2015). [arXiv:1506.08619](#)
46. E.T. Tomboulis, Renormalization and unitarity in higher derivative and nonlocal gravity theories. *Mod. Phys. Lett. A* **30**(03n04), 1540005 (2015)
47. S. Talaganis, A. Mazumdar, High-energy scatterings in infinite-derivative field theory and ghost-free gravity. *Class. Quant. Grav.* **33**(14), 145005 (2016)
48. J. Edholm, A.S. Koshelev, A. Mazumdar, Behavior of the Newtonian potential for ghost-free gravity and singularity-free gravity. *Phys. Rev. D* **94**(10), 104033 (2016). [arXiv:1604.01989](#)
49. S. Giaccari, L. Modesto, Nonlocal supergravity. *Phys. Rev. D* **96**(6), 066021 (2017). [arXiv:1605.03906](#)
50. L. Modesto, L. Rachwal, *Finite Conformal Quantum Gravity and Nonsingular Spacetimes*. [arXiv:1605.04173](#)
51. T. Biswas, A.S. Koshelev, A. Mazumdar, Consistent higher derivative gravitational theories with stable de Sitter and anti-de Sitter backgrounds. *Phys. Rev. D* **95**(4), 043533 (2017). [arXiv:1606.01250](#)
52. A.S. Koshelev, K. Sravan Kumar, L. Modesto, L. Rachwal, Finite quantum gravity in dS and AdS spacetimes. *Phys. Rev. D* **98**(4), 046007 (2018). [arXiv:1710.07759](#)
53. G. Calcagni, L. Modesto, Stability of Schwarzschild singularity in non-local gravity. *Phys. Lett. B* **773**, 596–600 (2017). [arXiv:1707.01119](#)
54. A.S. Cornell, G. Harmen, G. Lambiase, A. Mazumdar, Rotating metric in nonsingular infinite derivative theories of gravity. *Phys. Rev. D* **97**(10), 104006 (2018). [arXiv:1710.02162](#)
55. J. Edholm, Revealing infinite derivative gravity’s true potential: The weak-field limit around de Sitter backgrounds. *Phys. Rev. D* **97**(6), 064011 (2018). [arXiv:1801.00834](#)
56. L. Buoninfante, A.S. Koshelev, G. Lambiase, A. Mazumdar, Classical properties of non-local, ghost- and singularity-free gravity. *JCAP* **1809**(09), 034 (2018). [arXiv:1802.00399](#)

57. A.S. Koshelev, J. Marto, A. Mazumdar, Schwarzschild $1/r$ -singularity is not permissible in ghost free quadratic curvature infinite derivative gravity. *Phys. Rev. D* **98**(6), 064023 (2018). [arXiv:1803.00309](#)
58. A.S. Koshelev, J. Marto, A. Mazumdar, Towards resolution of anisotropic cosmological singularity in infinite derivative gravity. *JCAP* **1902**, 020 (2019). [arXiv:1803.07072](#)
59. G. Calcagni, L. Modesto, Y.S. Myung, Black-hole stability in non-local gravity. *Phys. Lett. B* **783**, 19–23 (2018). [arXiv:1803.08388](#)
60. S. Giaccari, L. Modesto, *Causality in Nonlocal Gravity*. [arXiv:1803.08748](#)
61. F. Briscese, L. Modesto, Cutkosky rules and perturbative unitarity in Euclidean nonlocal quantum field theories. *Phys. Rev. D* **99**(10), 104043 (2019). [arXiv:1803.08827](#)
62. L. Buoninfante, A.S. Koshelev, G. Lambiase, J. Marto, A. Mazumdar, Conformally-flat, non-singular static metric in infinite derivative gravity. *JCAP* **1806**(06), 014 (2018). [arXiv:1804.08195](#)
63. L. Buoninfante, G. Harmsen, S. Maheshwari, A. Mazumdar, Nonsingular metric for an electrically charged point-source in ghost-free infinite derivative gravity. *Phys. Rev. D* **98**(8), 084009 (2018). [arXiv:1804.09624](#)
64. L. Buoninfante, G. Lambiase, A. Mazumdar, Ghost-free infinite derivative quantum field theory. *Nucl. Phys. B* **944**, 114646 (2019). [arXiv:1805.03559](#)
65. F. Briscese, L. Modesto, Nonlinear stability of Minkowski spacetime in nonlocal gravity. *JCAP* **1907**(07), 009 (2019). [arXiv:1811.05117](#)
66. L. Buoninfante, G. Lambiase, M. Yamaguchi, Nonlocal generalization of Galilean theories and gravity. *Phys. Rev. D* **100**(2), 026019 (2019). [arXiv:1812.10105](#)
67. F. Briscese, G. Calcagni, L. Modesto, Nonlinear stability in nonlocal gravity. *Phys. Rev. D* **99**(8), 084041 (2019). [arXiv:1901.03267](#)
68. K.S. Stelle, Renormalization of higher derivative quantum gravity. *Phys. Rev. D* **16**, 953–969 (1977)
69. K.S. Stelle, Classical gravity with higher derivatives. *Gen. Rel. Grav.* **9**, 353–371 (1978)
70. I.L. Buchbinder, S.D. Odintsov, I.L. Shapiro, *Effective action in quantum gravity* (Bristol, UK, IOP, 1992), p. 413p
71. M. Asorey, J.L. Lopez, I.L. Shapiro, Some remarks on high derivative quantum gravity. *Int. J. Mod. Phys. A* **12**, 5711–5734 (1997). [arXiv:hep-th/9610006](#)
72. F.d.O. Salles, I.L. Shapiro, Do we have unitary and (super)renormalizable quantum gravity below the Planck scale? *Phys. Rev. D* **89**(8), 0840454 (2014). [arXiv:1401.4583](#). [Erratum: *Phys. Rev. D* **90**, no.12, 129903 (2014)]
73. LIGO Scientific, Virgo Collaboration, B.P. Abbott et al., Observation of gravitational waves from a binary black hole merger. *Phys. Rev. Lett.* **116**(6), 061102 (2016). [arXiv:1602.03837](#)
74. LIGO Scientific, Virgo, Fermi-GBM, Integral, B.P. Abbott et al., Gravitational waves and gamma-rays from a binary neutron star merger: GW170817 and GRB 170817A. *Astrophys. J.* **848**(2), L13 (2017). [arXiv:1710.05834](#)
75. Planck Collaboration, Y. Akrami et al., *Planck 2018 results. I. Overview and the cosmological legacy of Planck*. [arXiv:1807.06205](#)
76. LISA Cosmology Working Group Collaboration, E. Belgacem et al., Testing modified gravity at cosmological distances with LISA standard sirens. *JCAP* **1907**(07), 024 (2019). [arXiv:1906.01593](#)
77. G. Calcagni, S. Kuroyanagi, S. Marsat, M. Sakellariadou, N. Tamanini, G. Tasinato, Gravitational-wave luminosity distance in quantum gravity. *Phys. Lett. B* **798**, 135000 (2019). [arXiv:1904.00384](#)
78. G. Calcagni, S. Kuroyanagi, S. Marsat, M. Sakellariadou, N. Tamanini, G. Tasinato, Quantum gravity and gravitational-wave astronomy. *JCAP* **1910**(10), 012 (2019). [arXiv:1907.02489](#)
79. G. Calcagni, S. Kuroyanagi, *Stochastic gravitational-wave background in quantum gravity*. [arXiv:2012.00170](#)
80. V.F. Mukhanov, H.A. Feldman, R.H. Brandenberger, Theory of cosmological perturbations. Part 1. Classical perturbations. Part 2. Quantum theory of perturbations. Part 3. Extensions. *Phys. Rep.* **215**, 20–3333 (1992)

81. M. Maggiore, *Gravitational Waves. Vol. 1: Theory and Experiments* Oxford Master Series in Physics. (Oxford University Press, Oxford, 2007)
82. V.A. Kostelecky, S. Samuel, Collective physics in the closed bosonic string. *Phys. Rev. D* **42**, 1289–1292 (1990)
83. N. Dalal, D.E. Holz, S.A. Hughes, B. Jain, Short grb and binary black hole standard sirens as a probe of dark energy. *Phys. Rev. D* **74**, 063006 (2006). [arXiv:astro-ph/0601275](#)
84. S. Nissanke, D.E. Holz, S.A. Hughes, N. Dalal, J.L. Sievers, Exploring short gamma-ray bursts as gravitational-wave standard sirens. *Astrophys. J.* **725**, 496–514 (2010). [arXiv:0904.1017](#)
85. S. Camera, A. Nishizawa, Beyond concordance cosmology with magnification of gravitational-wave standard sirens. *Phys. Rev. Lett.* **110**(15), 151103 (2013). [arXiv:1303.5446](#)
86. N. Tamanini, C. Caprini, E. Barausse, A. Sesana, A. Klein, A. Petiteau, Science with the space-based interferometer eLISA. III: probing the expansion of the Universe using gravitational wave standard sirens. *JCAP* **1604**(04), 002 (2016). [arXiv:1601.07112](#)
87. V.P. Frolov, G.A. Vilkovisky, Quantum gravity removes classical singularities and shortens the life of black holes, in *The Second Marcel Grossmann Meeting on the Recent Developments of General Relativity (In Honor of Albert Einstein) Trieste, Italy, 5–11 July 1979* (1979), p. 0455
88. A.O. Barvinsky, G.A. Vilkovisky, The generalized Schwinger-Dewitt technique in Gauge theories and quantum gravity. *Phys. Rep.* **119**, 1–74 (1985)
89. I.L. Shapiro, Effective action of vacuum: semiclassical approach. *Class. Quant. Grav.* **25**, 103001 (2008). [arXiv:0801.0216](#)
90. A.O. Barvinsky, G.A. Vilkovisky, Beyond the Schwinger-Dewitt technique: converting loops into trees and in-in currents. *Nucl. Phys. B* **282**, 163–188 (1987)
91. A.O. Barvinsky, G.A. Vilkovisky, Covariant perturbation theory. 2. Second order in the curvature. General algorithms. *Nucl. Phys. B* **333**, 471–511 (1990)
92. A.O. Barvinsky, Yu.V. Gusev, G.A. Vilkovisky, V.V. Zhytnikov, The Basis of nonlocal curvature invariants in quantum gravity theory. (Third order.). *J. Math. Phys.* **38**, 3525–3542 (1994). [arXiv: gr-qc/9404061](#)
93. A.O. Barvinsky, Y.V. Gusev, G.A. Vilkovisky, V.V. Zhytnikov, Asymptotic behaviors of the heat kernel in covariant perturbation theory. *J. Math. Phys.* **35**, 3543–3559 (1994). [arXiv:gr-qc/9404063](#)
94. E.V. Gorbar, I.L. Shapiro, Renormalization group and decoupling in curved space. *JHEP* **02**, 021 (2003). [arXiv:hep-ph/0210388](#)
95. E.V. Gorbar, I.L. Shapiro, Renormalization group and decoupling in curved space. 2. The Standard model and beyond. *JHEP* **06**, 004 (2006). [arXiv:hep-ph/0303124](#)
96. M. Maggiore, Perturbative loop corrections and nonlocal gravity. *Phys. Rev. D* **93**(6), 063008 (2016). [arXiv:1603.01515](#)
97. E. Belgacem, Y. Dirian, S. Foffa, M. Maggiore, Nonlocal gravity. Conceptual aspects and cosmological predictions. *JCAP* **1803**(03), 002 (2018). [arXiv:1712.07066](#)
98. A.O. Barvinsky, Nonlocal action for long distance modifications of gravity theory. *Phys. Lett. B* **572**, 109–116 (2003). [arXiv:hep-th/0304229](#)
99. S. Foffa, M. Maggiore, E. Mitsou, Apparent ghosts and spurious degrees of freedom in non-local theories. *Phys. Lett. B* **733**, 76–83 (2014). [arXiv:1311.3421](#)
100. Y.-L. Zhang, K. Koyama, M. Sasaki, G.-B. Zhao, Acausality in nonlocal gravity theory. *JHEP* **03**, 039 (2016). [arXiv:1601.03808](#)
101. S. Deser, R.P. Woodard, Nonlocal cosmology. *Phys. Rev. Lett.* **99**, 111301 (2007). [arXiv:0706.2151](#)
102. M. Maggiore, Phantom dark energy from nonlocal infrared modifications of general relativity. *Phys. Rev. D* **89**(4), 043008 (2014). [arXiv:1307.3898](#)
103. M. Maggiore, M. Mancarella, Non-local gravity and dark energy. *Phys. Rev. D* **90**, 023005 (2014). [arXiv:1402.0448](#)
104. S. Nojiri, S.D. Odintsov, Modified non-local-F(R) gravity as the key for the inflation and dark energy. *Phys. Lett. B* **659**, 821–826 (2008). [arXiv:0708.0924](#)
105. T. Koivisto, Dynamics of nonlocal cosmology. *Phys. Rev. D* **77**, 123513 (2008). [arXiv:0803.3399](#)

106. T.S. Koivisto, Newtonian limit of nonlocal cosmology. *Phys. Rev. D* **78**, 123505 (2008). [arXiv:0807.3778](#)
107. N.A. Koshelev, Comments on scalar-tensor representation of nonlocally corrected gravity. *Grav. Cosmol.* **15**, 220–223 (2009). [arXiv:0809.4927](#)
108. C. Deffayet, R.P. Woodard, Reconstructing the distortion function for nonlocal cosmology. *JCAP* **0908**, 023 (2009). [arXiv:0904.0961](#)
109. E. Elizalde, E.O. Pozdeeva, S.Y. Vernov, Reconstruction procedure in nonlocal models. *Class. Quant. Grav.* **30**, 035002 (2013). [arXiv:1209.5957](#)
110. E. Elizalde, E.O. Pozdeeva, S.Y. Vernov, Y.-L. Zhang, Cosmological solutions of a nonlocal model with a perfect fluid. *JCAP* **1307**, 034 (2013). [arXiv:1302.4330](#)
111. S. Deser, R.P. Woodard, Observational viability and stability of nonlocal cosmology. *JCAP* **1311**, 036 (2013). [arXiv:1307.6639](#)
112. S. Dodelson, S. Park, Nonlocal gravity and structure in the universe. *Phys. Rev. D* **90**, 043535 (2014). [arXiv:1310.4329](#). [Erratum: *Phys. Rev. D* **98**, no.2, 029904(2018)]
113. S. Park, A. Shafieloo, Growth of perturbations in nonlocal gravity with non- Λ CDM background. *Phys. Rev. D* **95**(6), 064061 (2017). [arXiv:1608.02541](#)
114. H. Nersisyan, A.F. Cid, L. Amendola, Structure formation in the Deser-Woodard nonlocal gravity model: a reappraisal. *JCAP* **1704**(04), 046 (2017). [arXiv:1701.00434](#)
115. S. Park, Revival of the Deser-Woodard nonlocal gravity model: comparison of the original non-local form and a localized formulation. *Phys. Rev. D* **97**(4), 044006 (2018). [arXiv:1711.08759](#)
116. E. Belgacem, Y. Dirian, S. Foffa, M. Maggiore, Modified gravitational-wave propagation and standard sirens. *Phys. Rev. D* **98**(02), 023510 (2018). [arXiv:1805.08731](#)
117. S. Park, R.P. Woodard, Exciting the scalar ghost mode through time evolution. *Phys. Rev. D* **99**(2), 024014 (2019). [arXiv:1809.06841](#)
118. E. Belgacem, A. Finke, A. Frassino, M. Maggiore, Testing nonlocal gravity with Lunar Laser Ranging. *JCAP* **1902**, 035 (2019). [arXiv:1812.11181](#)
119. L. Amendola, Y. Dirian, H. Nersisyan, S. Park, Observational constraints in nonlocal gravity: the Deser-Woodard case. *JCAP* **1903**(03), 045 (2019). [arXiv:1901.07832](#)
120. C.-Y. Chen, P. Chen, S. Park, Primordial bouncing cosmology in the Deser-Woodard nonlocal gravity. *Phys. Lett. B* **796**, 112–116 (2019). [arXiv:1905.04557](#)
121. C. Wetterich, Effective nonlocal Euclidean gravity. *Gen. Rel. Grav.* **30**, 159–172 (1998). [arXiv:gr-qc/9704052](#)
122. S. Foffa, M. Maggiore, E. Mitsou, Cosmological dynamics and dark energy from nonlocal infrared modifications of gravity. *Int. J. Mod. Phys. A* **29**, 1450116 (2014). [arXiv:1311.3435](#)
123. S. Nesseris, S. Tsujikawa, Cosmological perturbations and observational constraints on non-local massive gravity. *Phys. Rev. D* **90**(2), 024070 (2014). [arXiv:1402.4613](#)
124. Y. Dirian, S. Foffa, M. Kunz, M. Maggiore, V. Pettorino, Non-local gravity and comparison with observational datasets. *JCAP* **1504**(04), 044 (2015). [arXiv:1411.7692](#)
125. Y. Dirian, S. Foffa, M. Kunz, M. Maggiore, V. Pettorino, Non-local gravity and comparison with observational datasets. II. Updated results and Bayesian model comparison with Λ CDM. *JCAP* **1605**(5), 068 (2016). [arXiv:1602.03558](#)
126. E. Belgacem, Y. Dirian, A. Finke, S. Foffa, M. Maggiore, Nonlocal gravity and gravitational-wave observations. *JCAP* **1911**(11), 022 (2019). [arXiv:1907.02047](#)
127. M. Jaccard, M. Maggiore, E. Mitsou, Nonlocal theory of massive gravity. *Phys. Rev. D* **88**(4), 044033 (2013). [arXiv:1305.3034](#)
128. Y. Dirian, S. Foffa, N. Khosravi, M. Kunz, M. Maggiore, Cosmological perturbations and structure formation in nonlocal infrared modifications of general relativity. *JCAP* **1406**, 033 (2014). [arXiv:1403.6068](#)
129. A. Barreira, B. Li, W.A. Hellwing, C.M. Baugh, S. Pascoli, Nonlinear structure formation in Nonlocal Gravity. *JCAP* **1409**(09), 031 (2014). [arXiv:1408.1084](#)
130. H. Nersisyan, Y. Akrami, L. Amendola, T.S. Koivisto, J. Rubio, Dynamical analysis of $R \frac{1}{\square} R$ cosmology: impact of initial conditions and constraints from supernovae. *Phys. Rev. D* **94**(4), 043531 (2016). [arXiv:1606.04349](#)

131. P.G. Ferreira, A.L. Maroto, A few cosmological implications of tensor nonlocalities. *Phys. Rev. D* **88**(12), 123502 (2013). [arXiv:1310.1238](#)
132. H. Nersisyan, Y. Akrami, L. Amendola, T.S. Koivisto, J. Rubio, A.R. Solomon, Instabilities in tensorial nonlocal gravity. *Phys. Rev. D* **95**(4), 043539 (2017). [arXiv:1610.01799](#)
133. A.O. Barvinsky, On covariant long-distance modifications of Einstein theory and strong coupling problem. *Phys. Rev. D* **71**, 084007 (2005). [arXiv:hep-th/0501093](#)
134. A.O. Barvinsky, Dark energy and dark matter from nonlocal ghost-free gravity theory. *Phys. Lett. B* **710**, 12–16 (2012). [arXiv:1107.1463](#)
135. A.O. Barvinsky, Serendipitous discoveries in nonlocal gravity theory. *Phys. Rev. D* **85**, 104018 (2012). [arXiv:1112.4340](#)
136. G. Cusin, S. Foffa, M. Maggiore, M. Mancarella, Nonlocal gravity with a Weyl-square term. *Phys. Rev. D* **93**(4), 043006 (2016). [arXiv:1512.06373](#)
137. G. Cusin, S. Foffa, M. Maggiore, M. Mancarella, Conformal symmetry and nonlinear extensions of nonlocal gravity. *Phys. Rev. D* **93**(8), 083008 (2016). [arXiv:1602.01078](#)
138. S. Deser, R.P. Woodard, Nonlocal Cosmology II - Cosmic acceleration without fine tuning or dark energy. *JCAP* **1906**(06), 034 (2019). [arXiv:1902.08075](#)
139. J.-C. Ding, J.-B. Deng, Structure formation in the new Deser-Woodard nonlocal gravity model. *JCAP* **1912**(12), 054 (2019). [arXiv:1908.11223](#)
140. G. Calcagni, *Scalar and gravity quantum field theories with fractional operators*. [arXiv:2102.03363](#)

Chapter 10

Metric-Affine Gravity



Damianos Iosifidis and Emmanuel N. Saridakis

Probably one of the most beautiful characteristics of General Relativity (GR) is its clear geometric interpretation. Having been acquainted with this idea of geometrization of gravity, theories that incorporate geometrical notions are of particular interest and well motivated. Let us recall that in Einstein's Gravity, the fundamental field is the metric $g_{\mu\nu}$ and the connection is in some sense a secondary object, since it can be obtained by the former and its derivatives (the Levi-Civita connection). One is then dealing with the familiar Riemannian geometry [1], where the metric of the manifold completely determines its structure. In this case the connection is by definition symmetric (torsionless) and metric compatible (the metric is covariantly constant), and is the unique Levi-Civita connection.

From the above discussion it becomes clear what would be the most natural way to extend the geometry, and this is of course the relaxation of the Riemannian constraints. In other words, by starting with a general affine connection that admits both torsion and non-metricity (see definitions in what follows), one enriches the geometric arena and is in the realm of the so-called non-Riemannian geometry [2]. The underlying gravity theory formulated in such generalised geometry is the Metric-

D. Iosifidis (✉)

Department of Physics, Aristotle University of Thessaloniki, 54124 Thessaloniki, Greece
e-mail: diosifid@auth.gr

E. N. Saridakis

National Observatory of Athens, Athens, Greece
e-mail: msaridak@noa.gr

Key Laboratory for Researches in Galaxies and Cosmology, Department of Astronomy,
University of Science and Technology of China, Hefei, Anhui 230026,
People's Republic of China

School of Astronomy, School of Physical Sciences, University of Science and Technology
of China, Hefei 230026, People's Republic of China

© The Author(s), under exclusive license to Springer Nature Switzerland AG 2021

E. N. Saridakis et al. (eds.) *Modified Gravity and Cosmology*,

https://doi.org/10.1007/978-3-030-83715-0_10

Affine Gravity (MAG) [3]. As we noted above in the non-Riemannian arena of MAG the manifold apart from curvature is also endowed with torsion and non-metricity. In this space, vectors rotate (torsion) and experience a length change (non-metricity) when moved from one point of the manifold to another. Both of those degrees of freedom (i.e. torsion and non-metricity) are beautifully encoded into the general affine connection $\hat{\nabla}$. By restricting the general connection in certain ways, one obtains the teleparallel equivalents [4–7] that are elaborated in great detail in subsequent chapters.

Going back to the MAG framework, the fundamental variables in this case are both the metric and the affine connection (note that in the equivalent differential form formalism of MAG the independent fields are the frame e^A and the linear connection $\hat{\omega}^A_B$ one forms [3]). The field equations are obtained by varying independently with respect to both. The relation between the metric and the connection may be found only after solving the associated field equation. In what follows we briefly discuss the geometric and physical setup of Metric-Affine Theories. It is also worth mentioning that MAG is a gauge theory of gravity. More precisely, when expressed in the language of differential forms it is clear that MAG is the gauge theory of the $GL(4, \mathbb{R})$ group [3]. It also offers interesting possibilities for the quantisation of Gravity [8]. For further details on the matter of MAG, see, for instance, [3, 9–13].

10.1 Geometrical Objects: Torsion, Curvature and Non-metricity

The structure of a given manifold is completely determined once a metric tensor g and an affine-connection with coefficients $\hat{\Gamma}$ is given. The manifold is then denoted as $(\mathcal{M}, g, \hat{\Gamma})$. Geometrically speaking, the above two notions of metric and connection serve different purposes and are, in general, unrelated. The metric is needed in order to define distances, dot products between vector fields, and also define mappings among covariant and contravariant tensor fields. On the other hand, the connection defines parallel transport of tensor fields (through covariant differentiation) and allows to compare vectors living at different vector spaces. In a general setting, the affine-connection possesses both torsion and non-metricity, namely it is neither symmetric nor metric compatible. This generalized geometrical setup is known as non-Riemannian Geometry [2]. As we have mentioned, this non-Riemannian geometry offers a playground for the Metric-Affine Theories to be constructed. It is therefore appropriate to discuss some basic concepts of non-Riemannian geometries, that will help delve into the Metric-Affine framework.

Let us start with some basic concepts of non-Riemannian geometry. Firstly, in our conventions, the covariant derivative of, say, a $(1, 1)$ type tensor reads

$$\hat{\nabla}_\alpha A^\mu{}_\nu = \partial_\alpha A^\mu{}_\nu - \hat{\Gamma}^\lambda{}_{\nu\alpha} A^\mu{}_\lambda + \hat{\Gamma}^\mu{}_{\lambda\alpha} A^\lambda{}_\nu. \quad (10.1)$$

Considering the commutator of two covariant derivatives and acting it on a scalar, it follows that

$$2\hat{\nabla}_{[\mu}\hat{\nabla}_{\nu]}\phi = -\hat{T}^{\lambda}_{\mu\nu}\hat{\nabla}_{\lambda}\phi, \quad (10.2)$$

where

$$\hat{T}^{\lambda}_{\mu\nu} := -2\hat{\Gamma}^{\lambda}_{[\mu\nu]} \quad (10.3)$$

is the torsion tensor, which as seen from the above equation is defined as the anti-symmetric part of the affine-connection. Out of the torsion tensor we can construct the torsion vector according to

$$\hat{T}_{\mu} := \hat{T}^{\lambda}_{\lambda\mu}, \quad (10.4)$$

which exists for arbitrary space dimension- n . For $n = 4$ in particular we can also define the torsion pseudo-vector

$$\hat{A}_{\mu} := \epsilon_{\mu\alpha\beta\gamma}\hat{T}^{\alpha\beta\gamma}, \quad (10.5)$$

where $\epsilon_{\mu\alpha\beta\gamma}$ is the 4-dimensional totally antisymmetric Levi-Civita tensor.

Acting now, with the antisymmetrized covariant derivative on a vector field u^{μ} we obtain

$$[\hat{\nabla}_{\alpha}, \hat{\nabla}_{\beta}]u^{\mu} = 2\hat{\nabla}_{[\alpha}\hat{\nabla}_{\beta]}u^{\mu} = \hat{R}^{\mu}_{\nu\alpha\beta}u^{\nu} - \hat{T}^{\nu}_{\alpha\beta}\hat{\nabla}_{\nu}u^{\mu}, \quad (10.6)$$

where

$$\hat{R}^{\mu}_{\nu\alpha\beta} := 2\partial_{[\alpha}\hat{\Gamma}^{\mu}_{|\nu|\beta]} + 2\hat{\Gamma}^{\mu}_{\rho[\alpha}\hat{\Gamma}^{\rho}_{|\nu|\beta]} \quad (10.7)$$

is the usual Riemann or Curvature tensor and the horizontal bars around an index denote that this index is left out of the (anti)-symmetrization. It is worth mentioning that in general (non-Riemannian Geometries), the only symmetry of the Riemann tensor is antisymmetry in its last two indices, as seen from (10.7). Without the use of any metric, we can construct the two independent contractions

$$\hat{R}_{\nu\beta} := \hat{R}^{\mu}_{\nu\mu\beta}, \quad (10.8)$$

$$\hat{R}_{\alpha\beta} := \hat{R}^{\mu}_{\mu\alpha\beta}. \quad (10.9)$$

Expression (10.8) defines as usual the Ricci tensor, while expression (10.9) defines the homothetic curvature (the field strength of the Weyl vector) it is of purely non-Riemannian origin and it is anti-symmetric. Note that in our discussion so far, no metric was involved. If we enrich the geometrical structure with a metric we can form yet another contraction,

$$\hat{\mathcal{R}}^{\lambda}_{\kappa} := \hat{R}^{\lambda}_{\mu\nu\kappa}g^{\mu\nu}, \quad (10.10)$$

which is often called, ‘‘co-Ricci’’ tensor, and in general is different from the Ricci tensor (10.8) (in General Relativity we have that $\hat{\mathcal{R}}_{\kappa}^{\lambda} = -\hat{R}^{\lambda}_{\kappa}$). However, the Ricci scalar is still uniquely defined since

$$\hat{R} := \hat{R}_{\mu\nu}g^{\mu\nu} = -\hat{\mathcal{R}}_{\mu\nu}g^{\mu\nu} \quad (10.11)$$

$$\hat{\hat{R}}_{\mu\nu}g^{\mu\nu} = 0. \quad (10.12)$$

Having introduced a metric tensor on a manifold the latter is not, in general, covariantly constant. A metric is said to be compatible with a given connection, if and only if its covariant derivative with respect to this connection vanishes, i.e. $\hat{\nabla}_{\alpha}g_{\mu\nu} \equiv 0$. Hence, it is exactly this deviation from the compatibility condition, defines the non-metricity tensor

$$\hat{Q}_{\alpha\mu\nu} = \hat{\nabla}_{\alpha}g_{\mu\nu}. \quad (10.13)$$

We can then contract the above in two independent ways, to get the two non-metricity vectors

$$\hat{Q}_{\alpha} := \hat{Q}_{\alpha\mu\nu}g^{\mu\nu}, \quad \hat{Q}_{\nu} = \hat{Q}_{\alpha\mu\nu}g^{\alpha\mu}. \quad (10.14)$$

The former goes by the name Weyl vector, and the latter is the second independent vector that can be extracted from non-metricity. The general non-Riemannian space that has all of its geometrical objects unconstrained is often denoted as L_n , and is the playground of general Metric-Affine Theories. As a last note, let us mention that with the above definitions it is trivial to show that the affine connection can be decomposed according to [14] (see also [3, 11]),

$$\hat{\Gamma}^{\lambda}_{\mu\nu} = \Gamma^{\lambda}_{\mu\nu} + \frac{1}{2}g^{\alpha\lambda}(-\hat{Q}_{\mu\nu\alpha} - \hat{Q}_{\nu\alpha\mu} + \hat{Q}_{\alpha\mu\nu}) + \frac{1}{2}g^{\alpha\lambda}(\hat{T}_{\nu\alpha\mu} + \hat{T}_{\mu\alpha\nu} - \hat{T}_{\alpha\mu\nu}), \quad (10.15)$$

where

$$\Gamma^{\lambda}_{\mu\nu} = \frac{1}{2}g^{\lambda\kappa}(g_{\kappa\nu,\mu} + g_{\mu\kappa,\nu} - g_{\mu\nu,\kappa}),$$

represents the usual Levi-Civita connection, and the combination

$$\hat{L}_{\alpha\mu\nu} + \hat{K}_{\alpha\mu\nu} = \frac{1}{2}(-\hat{Q}_{\mu\nu\alpha} - \hat{Q}_{\nu\alpha\mu} + \hat{Q}_{\alpha\mu\nu}) + \frac{1}{2}(\hat{T}_{\nu\alpha\mu} + \hat{T}_{\mu\alpha\nu} - \hat{T}_{\alpha\mu\nu}) \quad (10.16)$$

is known as the distortion tensor, measuring how much the affine connection deviates from the Riemannian Levi-Civita connection. This decomposition allows one to split any object into its Riemannian part, plus non-Riemannian contributions.

Let us now touch upon the geometrical interpretation of the geometrical objects. Since the role of curvature is widely known, we shall concentrate on the notion of torsion and non-metricity.

10.2 Geometrical Meaning of Torsion and Non-metricity

10.2.1 Geometrical Meaning of Torsion

Let us examine the geometric effect of torsion with the following simple example. Consider two curves $\mathcal{C} : x^\mu = x^\mu(\lambda)$ and $\tilde{\mathcal{C}} : \tilde{x}^\mu = \tilde{x}^\mu(\lambda)$ with associated tangent vectors

$$u^\mu = \frac{dx^\mu}{d\lambda} \quad \text{and} \quad \tilde{u}^\mu = \frac{d\tilde{x}^\mu}{d\lambda} \quad (10.17)$$

respectively. Now, let $d\tilde{x}^\mu$ represent a displacement of u^α along $\tilde{\mathcal{C}}$ and obtain u'^α which in first order is given by

$$u'^\alpha = u^\alpha + (\partial_\mu u^\alpha) d\tilde{x}^\mu, \quad (10.18)$$

but recalling that u^α is parallel transported along $\tilde{\mathcal{C}}$, it follows that

$$\frac{d\tilde{x}^\mu}{d\lambda} \hat{\nabla}_\mu u^\alpha = 0 = \frac{d\tilde{x}^\mu}{d\lambda} \partial_\mu u^\alpha + \hat{\Gamma}^\alpha_{\nu\mu} \frac{d\tilde{x}^\mu}{d\lambda} u^\nu,$$

or

$$(\partial_\mu u^\alpha) d\tilde{x}^\mu = -\hat{\Gamma}^\alpha_{\nu\mu} u^\nu \tilde{u}^\mu d\lambda, \quad (10.19)$$

which when placed against (10.18) gives

$$u'^\alpha = u^\alpha - \hat{\Gamma}^\alpha_{\nu\mu} u^\nu \tilde{u}^\mu d\lambda. \quad (10.20)$$

Following the exact same procedure, but now for a dx^μ -displacement of \tilde{u}^α along \mathcal{C} , we acquire

$$\tilde{u}'^\alpha = \tilde{u}^\alpha - \hat{\Gamma}^\alpha_{\nu\mu} \tilde{u}^\nu u^\mu d\lambda = \tilde{u}^\alpha - \hat{\Gamma}^\alpha_{\mu\nu} \tilde{u}^\mu u^\nu d\lambda. \quad (10.21)$$

From the last two we obtain

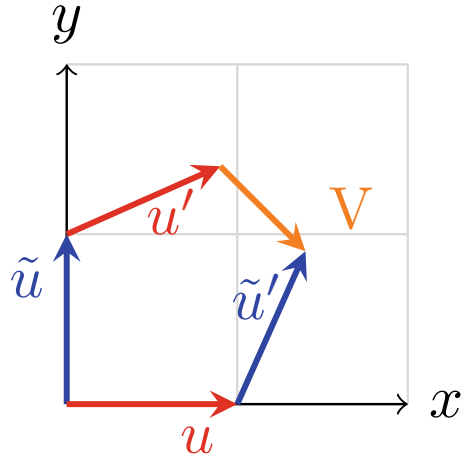
$$(\tilde{u}'^\alpha + u'^\alpha) - (u^\alpha + \tilde{u}'^\alpha) = -\hat{T}^\alpha_{\mu\nu} \tilde{u}^\mu u^\nu d\lambda. \quad (10.22)$$

Notice now that for the infinitesimal parallelogram to exist, the vectors $(\tilde{u}^\alpha + u'^\alpha)$ and $(u^\alpha + \tilde{u}'^\alpha)$ should be equal, and as is clear from the above, this is not true in the presence of torsion. Defining the vector that shows this deviation as $\hat{V}^\alpha d\lambda = (\tilde{u}^\alpha + u'^\alpha) - (u^\alpha + \tilde{u}'^\alpha)$, the latter can also be written as

$$\hat{V}^\alpha = -\hat{T}^\alpha_{\mu\nu} \tilde{u}^\mu u^\nu, \quad (10.23)$$

which represents how much the parallelogram has been cracked. This is definitely true for small displacements in the directions of \tilde{u}^μ and u^ν which themselves are

Fig. 10.1 Representation of torsion in 2 dimensions



computed at the starting point of the path. Hence, simply put, the presence of torsion cracks parallelograms into pentagons, as illustrated in Fig. 10.1 (in a 2-dim flat space).

10.2.2 Geometrical Meaning of Non-metricity

Let us explore the geometric property of non-metricity. We consider a differential manifold, and we assume that a metric and a connection are also given for this manifold. Moreover, we consider two vectors a^μ and b^μ on this manifold. Defining their inner product $a \cdot b = a^\mu b^\nu g_{\mu\nu}$ let us parallel transport both vectors along a given curve $\mathcal{C} : x^\mu = x^\mu(\lambda)$. We have

$$\frac{\hat{D}}{d\lambda}(a \cdot b) = \frac{dx^\alpha}{d\lambda}(\hat{\nabla}_\alpha a^\mu)b_\mu + \frac{dx^\alpha}{d\lambda}(\hat{\nabla}_\alpha b^\nu)a_\nu + \frac{dx^\alpha}{d\lambda}(\hat{\nabla}_\alpha g_{\mu\nu})a^\mu b^\nu. \quad (10.24)$$

Now, since a^μ and b^μ are parallel transported along the curve, it follows that

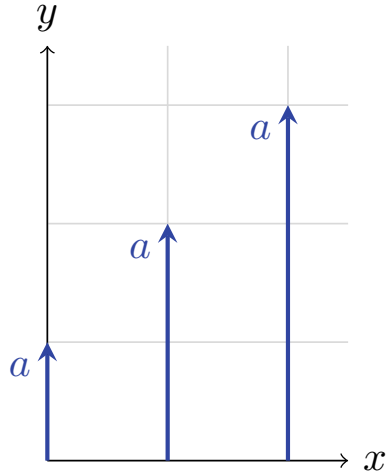
$$\frac{dx^\alpha}{d\lambda}(\hat{\nabla}_\alpha a^\mu) = 0, \quad \frac{dx^\alpha}{d\lambda}(\hat{\nabla}_\alpha b^\nu) = 0, \quad (10.25)$$

and thus

$$\frac{\hat{D}}{d\lambda}(a \cdot b) = \hat{Q}_{\alpha\mu\nu} \frac{dx^\alpha}{d\lambda} a^\mu b^\nu, \quad (10.26)$$

which tells us that the inner product of two vectors changes when we parallel transport them along a curve. Note that, for $b^\mu = a^\mu$ the above becomes

Fig. 10.2 Representation of non-metricity in 2 dimensions



$$\frac{\hat{D}}{d\lambda}(|a|^2) = \hat{Q}_{\alpha\mu\nu} \frac{dx^\alpha}{d\lambda} a^\mu a^\nu, \tag{10.27}$$

which signals a length change of the vectors magnitude when we parallel transport it along a given curve. Therefore, in a space with non-metricity, dot products and lengths of vectors change under parallel transport (for more concrete examples on the geometrical meaning of both, as well as non-metricity, see [11]). Figure 10.2 illustrates a two-dimensional example of a vector dragged along the x -axis in the presence of non-metricity.

10.3 Identities of Non-Riemannian Geometry

Many (if not all) of the identities that are familiar from GR generalise and receive further contributions from torsion and non-metricity when passing to a non-Riemannian background. Let us start with the generalised Bianchi identities for a torsionful, non-metric connection. These identities are also known as Weitzenböck identities. The first one we obtain by taking the covariant derivative of the Riemann tensor and antisymmetrise in three indices, which results in [10, 14]

$$\hat{\nabla}_{[\rho} \hat{R}^\alpha_{|\beta|\mu\nu]} = -\hat{R}^\alpha_{\beta\lambda[\rho} \hat{T}^\lambda_{\mu\nu]}, \tag{10.28}$$

where the vertical bars around an index indicate that this index is left out of the (anti-)symmetrisation. The above constitute the generalised differential Bianchi identities in a non-Riemannian setup. Another identity comes about by applying the com-

mutator of two covariant derivatives on the metric tensor. Then, using the definitions of curvature, torsion and non-metricity, one can easily show [10, 14]

$$\hat{R}_{(\alpha\mu)\beta\nu} = -\hat{\nabla}_{[\beta}\hat{Q}_{\nu]\alpha\mu} + \hat{T}_{\beta\nu}^{\lambda}\hat{Q}_{\lambda\alpha\mu}, \quad (10.29)$$

which shows that in the presence of non-metricity, the curvature tensor is no longer antisymmetric in its first two indices. If we contract the latter with $g^{\alpha\beta}$ and employ the Leibniz rule we get the relation

$$\hat{R}_{\mu\nu} + \hat{\hat{R}}_{\mu\nu} = -\hat{\nabla}_{\lambda}\hat{Q}_{\nu\mu}^{\lambda} + \hat{Q}_{\nu\alpha\beta}\hat{Q}_{\mu}^{\alpha\beta} + \hat{\nabla}_{\nu}\hat{Q}_{\mu} - \hat{Q}_{\nu\mu\alpha}\hat{Q}^{\alpha} + 2\hat{T}_{\alpha\beta\nu}\hat{Q}_{\mu}^{\beta\alpha}. \quad (10.30)$$

showing that the third contraction $\hat{\hat{R}}_{\mu\nu}$ of the curvature is not completely independent from the Ricci tensor. In addition, using the definition of the Riemann tensor and antisymmetrizing in its last three indices, we easily obtain [10, 14]

$$\hat{R}_{[\beta\mu\nu]}^{\alpha} = \hat{\nabla}_{[\beta}\hat{T}_{\mu\nu]}^{\lambda} - \hat{T}_{[\beta\mu}^{\lambda}\hat{T}_{\nu]\lambda}^{\alpha}, \quad (10.31)$$

which is the analogue of the algebraic Bianchi identity in a non-Riemannian geometry. Notice that the Riemannian geometry identity $\hat{R}_{[\beta\mu\nu]}^{\alpha} = 0$ is spoiled now by the presence of torsion only. It should be clear by now that apart from the antisymmetry in the last two indices, the Riemann tensor possesses no other symmetry in a generalized geometry. In particular, in $\hat{R}_{\alpha\beta\mu\nu}$ one cannot interchange the set of indices $\alpha\beta$ with $\mu\nu$ that is $\hat{R}_{\alpha\beta\mu\nu} \neq \hat{R}_{\mu\nu\alpha\beta}$. However, a thing that is never mentioned in the literature is that there is a certain identity that measures the difference between the aforementioned two Riemann tensors. Indeed, starting with a general tensor identity holding for arbitrary type $(0, 4)$ tensors and applying it to the Riemann tensor, after using the identities we derived above, it follows that [10]

$$\begin{aligned} \hat{R}_{\mu\nu\kappa\lambda} - \hat{R}_{\kappa\lambda\mu\nu} &= \hat{\nabla}_{[\lambda}\hat{Q}_{\kappa]\nu\mu} + \nabla_{[\nu}\hat{Q}_{\lambda]\kappa\mu} + \hat{\nabla}_{[\kappa}\hat{Q}_{\mu]\lambda\nu} + \hat{\nabla}_{[\mu}\hat{Q}_{\nu]\lambda\kappa} + \hat{\nabla}_{[\mu}\hat{Q}_{\lambda]\nu\kappa} + \hat{\nabla}_{[\nu}\hat{Q}_{\kappa]\lambda\mu} \\ &\quad - \frac{3}{2}\left(g_{\mu\alpha}\hat{T}_{[\nu\lambda}^{\beta}\hat{T}_{\kappa]\beta}^{\alpha} + g_{\nu\alpha}\hat{T}_{[\mu\lambda}^{\beta}\hat{T}_{\kappa]\beta}^{\alpha} + g_{\kappa\alpha}\hat{T}_{[\lambda\mu}^{\beta}\hat{T}_{\nu]\beta}^{\alpha} + g_{\lambda\alpha}\hat{T}_{[\kappa\mu}^{\beta}\hat{T}_{\nu]\beta}^{\alpha}\right) \\ &\quad + \frac{1}{2}\left(\hat{T}_{\lambda\kappa}^{\alpha}\hat{Q}_{\alpha\nu\mu} + \hat{T}_{\nu\lambda}^{\alpha}\hat{Q}_{\alpha\kappa\mu} + \hat{T}_{\kappa\mu}^{\alpha}\hat{Q}_{\alpha\lambda\nu} + \hat{T}_{\mu\nu}^{\alpha}\hat{Q}_{\alpha\lambda\kappa} + \hat{T}_{\mu\lambda}^{\alpha}\hat{Q}_{\alpha\nu\kappa} + \hat{T}_{\nu\kappa}^{\alpha}\hat{Q}_{\alpha\lambda\mu}\right) \\ &\quad - \frac{3}{2}\left(g_{\mu\alpha}\hat{\nabla}_{[\nu}\hat{T}_{\lambda\kappa]}^{\alpha} + g_{\nu\alpha}\hat{\nabla}_{[\mu}\hat{T}_{\lambda\kappa]}^{\alpha} + g_{\kappa\alpha}\hat{\nabla}_{[\lambda}\hat{T}_{\mu\nu]}^{\alpha} + g_{\lambda\alpha}\hat{\nabla}_{[\kappa}\hat{T}_{\mu\nu]}^{\alpha}\right), \quad (10.32) \end{aligned}$$

and we see that the symmetry $\hat{R}_{\mu\nu\kappa\lambda} = \hat{R}_{\kappa\lambda\mu\nu}$ only holds when both torsion and non-metricity vanish. This last identity clearly shows that when one is working in the general Metric-Affine framework, with a generic affine connection, things get quite serious computationally!

10.3.1 The Sources of Metric-Affine Gravity

As we have noted, in the general Metric-Affine Gravity (MAG) framework, the action is a functional of the metric, the frame and the independent affine connection and the matter fields. More precisely, the matter sector of general MAG Theories reads¹

$$S_{\text{matter}}[g, e, \hat{\Gamma}, \phi] = \int d^4x \sqrt{-g} \mathcal{L}_{\text{matter}}(g, \hat{\Gamma}, \phi) \quad (10.33)$$

where ϕ collectively denotes the matter fields. One then defines as usual the metrical (symmetric) energy-momentum tensor by the metric variation of the matter part

$$T_{\alpha\beta} := -\frac{2}{\sqrt{-g}} \frac{\delta S_{\text{matter}}}{\delta g^{\alpha\beta}} = -\frac{2}{\sqrt{-g}} \frac{\delta(\sqrt{-g} \mathcal{L}_{\text{matter}})}{\delta g^{\alpha\beta}}. \quad (10.34)$$

In MAG, the connection naturally couples to matter, so we now also have the variation

$$\hat{\Delta}_\lambda{}^{\mu\nu} := -\frac{2}{\sqrt{-g}} \frac{\delta S_{\text{matter}}}{\delta \hat{\Gamma}^\lambda{}_{\mu\nu}} = -\frac{2}{\sqrt{-g}} \frac{\delta(\sqrt{-g} \mathcal{L}_{\text{matter}})}{\delta \hat{\Gamma}^\lambda{}_{\mu\nu}}, \quad (10.35)$$

which is the hypermomentum tensor [15] and encompasses the microscopic characteristics of matter, such as spin, dilation and shear [3]. Additionally, there is also the canonical energy-momentum tensor given by

$$t_C^\mu = \frac{1}{\sqrt{-g}} \frac{\delta S_{\text{matter}}}{\delta e^C{}_\mu}, \quad (10.36)$$

which is not symmetric in general. The above three currents ($T_{\alpha\beta}$, $\hat{\Delta}_\lambda{}^{\mu\nu}$, t_C^μ) represent the sources of MAG [3, 16], which produce spacetime curvature, torsion and non-metricity through the field equations of MAG.

10.4 Field Equations of Metric-Affine Gravity

Let us now proceed with the field equations of MAG theories. A fairly general class of theories consists of a gravitational Lagrangian constructed out of curvature, torsion and non-metricity,² i.e., $\mathcal{L} = \mathcal{L}(g_{\mu\nu}, \hat{R}^\alpha{}_{\beta\gamma\rho}, \hat{T}^\lambda{}_{\mu\nu}, \hat{Q}_{\alpha\mu\nu})$. After all, these are

¹ The independent geometrical variables are truly two, since it can be shown that the metric field equations are redundant and are related to the ones coming from the connection and the frame [3]. In other words, the set of field equations for $(e, \hat{\Gamma})$ and $(g, \hat{\Gamma})$ are fully equivalent, and it is a matter of personal preference, which one to solve.

² And on the metric $g_{\mu\nu}$ obviously.

the three covariant geometrical objects building up a non-Riemannian Geometry. Then, adding some matter fields, the general action reads

$$S[g, \hat{\Gamma}, \phi] = \frac{1}{2\kappa^2} \int d^4x \sqrt{-g} \mathcal{L}(g_{\mu\nu}, \hat{R}^\alpha_{\beta\gamma\rho}, \hat{T}^\lambda_{\mu\nu}, \hat{Q}_{\alpha\mu\nu}) + S_m. \quad (10.37)$$

Defining now the field excitations

$$\hat{\Omega}_\lambda^{\mu\alpha\nu} := \frac{\partial \mathcal{L}}{\partial \hat{R}^\lambda_{\mu\alpha\nu}}, \quad \hat{V}_\lambda^{\mu\nu} := -2 \frac{\partial \mathcal{L}}{\partial \hat{T}^\lambda_{\mu\nu}}, \quad \hat{W}^{\alpha\mu\nu} := -\frac{\partial \mathcal{L}}{\partial \hat{Q}_{\alpha\mu\nu}}, \quad (10.38)$$

we vary independently with respect to g, Γ and ϕ to obtain

$$-2 \frac{\hat{V}_\alpha(\sqrt{-g} \hat{\Omega}_\lambda^{\mu\alpha\nu})}{\sqrt{-g}} + 2 \hat{\Omega}_\lambda^{\mu\alpha\nu} \hat{T}_\alpha + \frac{1}{2} \hat{\Omega}_\lambda^{\mu\gamma\delta} \hat{T}^\nu_{\gamma\delta} + 2 \hat{W}^{\mu\nu}_\lambda + \hat{V}^{\mu\nu}_\lambda = \kappa^2 \hat{\Delta}_\lambda^{\mu\nu}, \quad (10.39)$$

$$-\frac{1}{2} g_{\mu\nu} \mathcal{L} + \frac{\partial \mathcal{L}}{\partial g^{\mu\nu}} + \frac{1}{\sqrt{-g}} (\hat{T}_\alpha - \hat{V}_\alpha) \sqrt{-g} \frac{\partial \mathcal{L}}{\partial \hat{Q}_\alpha^{\mu\nu}} = \kappa^2 T_{\mu\nu}, \quad (10.40)$$

$$\frac{\delta S_m}{\delta \phi} = 0. \quad (10.41)$$

The above field equations cover a fairly wide spectrum of Metric-Affine Theories of Gravity. Notice that we chose to present them in a coordinate-based formalism (our basic variables were $g_{\mu\nu}$ and $\hat{\Gamma}^\lambda_{\alpha\beta}$), but one can just as well work with the equivalent differential forms formalism [3] and regard as fundamental gravitational fields the coframe e^A and linear connection $\hat{\omega}^A_B$ 1-forms, as we briefly discuss below.

10.5 The Differential Form Formulation of Metric-Affine Gravity

The true gauge character of MAG is most transparent when using its exterior differential form formulation. In such a formalism, the independent gauge potentials are the orthonormal coframe e^A , the linear connection $\hat{\omega}^A_B$ and the metric η_{AB} and the associated gauge field strengths are the torsion, curvature and non-metricity

$$\hat{T}^A := \hat{D}e^A \quad (10.42)$$

$$\hat{R}^A_B := d\hat{\omega}^A_B + \hat{\omega}^A_C \wedge \hat{\omega}^C_B \quad (10.43)$$

$$\hat{Q}_{AB} := \hat{D}\eta_{AB} \quad (10.44)$$

respectively. Here, \hat{D} represents the gauge exterior covariant derivative. Equations (10.42) and (10.43) are often referred to as Cartan's first and second structure equations. Note that torsion and curvature are 2-forms while non-metricity is an 1-form. For instance, in components, torsion is expanded as

$$\hat{T}^A = \frac{1}{2} \hat{T}^A_{\mu\nu} dx^\mu \wedge dx^\nu. \quad (10.45)$$

Acting on the above three field strengths with \hat{D} , we easily obtain the Bianchi identities (see, for instance, [3])

$$\hat{D}\hat{T}^A = \hat{R}^A_B \wedge e^B \quad (10.46)$$

$$\hat{D}\hat{R}^A_B = 0 \text{ or } \hat{D}\hat{R}^{AB} = \hat{R}^A_C \wedge \hat{Q}^{CB} \quad (10.47)$$

$$\hat{D}\hat{Q}_{AB} = 2\hat{R}_{(AB)}, \quad (10.48)$$

which are just the identities (10.31), (10.28) and (10.30), expressed in the language of differential forms. In this formulation, the field equations are obtained by varying with respect to the three gauge fields e^A , $\hat{\omega}^A_B$, η_{AB} . However, it can be shown [3] that the field equations obtained by varying with respect to the metric are not independent from the field equations coming from the coframe and the linear connection and therefore, as independent fields can be regarded only the latter two.

10.6 Conservation Laws and Hyperfluid Models

As one may have guessed, in a general MAG framework the familiar conservation law for the energy momentum tensor of matter no longer applies. In this case, the diffeomorphism along with the GL (local general linear group) invariance of the matter action, yield [3, 16–19]

$$\frac{1}{\sqrt{-g}} \left(\hat{T}_\mu - \hat{\nabla}_\mu \right) (\sqrt{-g} t^\mu_\alpha) = \frac{1}{2} \hat{\Delta}^{\lambda\mu\nu} \hat{R}_{\lambda\mu\nu\alpha} - \frac{1}{2} \hat{Q}_{\alpha\mu\nu} T^{\mu\nu} - \hat{T}_{\nu\alpha\mu} t^{\mu\nu}, \quad (10.49)$$

$$t^\mu_\lambda = T^\mu_\lambda - \frac{1}{2\sqrt{-g}} \left(\hat{T}_\nu - \hat{\nabla}_\nu \right) (\sqrt{-g} \hat{\Delta}^{\mu\nu}_\lambda), \quad (10.50)$$

provided that the matter fields satisfy their field equations (i.e. the on-shell condition $\frac{\delta S_m}{\delta \phi} = 0$ holds). The above constitute the conservation laws for energy-momentum and hyper-momentum currents in MAG. Notice that, combining the above one can get the divergence of the energy momentum tensor [19]

$$\begin{aligned} \sqrt{-g}(2\hat{\nabla}_\mu T^\mu_\alpha - \hat{\Delta}^{\lambda\mu\nu}\hat{R}_{\lambda\mu\nu\alpha}) + (\hat{T}_\mu - \hat{\nabla}_\mu)(\hat{T}_\nu - \hat{\nabla}_\nu)(\sqrt{-g}\hat{\Delta}_\alpha^{\mu\nu}) \\ - \hat{T}^\lambda_{\mu\alpha}(\hat{T}_\nu - \hat{\nabla}_\nu)(\sqrt{-g}\hat{\Delta}_\lambda^{\mu\nu}) = 0. \end{aligned} \quad (10.51)$$

The above conservation laws combined with the field equations of MAG along with making a proper ansatz for the sources, constitute a complete setup for the study of the effects of MAG theories.

10.6.1 Hyperfluids in Cosmology

The question then arises what is the current status of non-Riemannian Cosmology? The answer is that it is not quite so clear at the moment. There are many interesting works, see, for instance, [20], but almost all of them depend on specific ansatz that restricts the underlying structure. For a historical review regarding the chronological ordering of such investigations, see [21] and references therein (some inflationary scenarios in MAG were recently discussed in [22]). However, as we pointed out, most of these works make some restrictive assumptions about the form of torsion and non-metricity (like the assumption that the geometry is of Weyl-Cartan type) and thus cannot give an adequate description of the effects of torsion and non-metricity. Perhaps the reason why the role of non-Riemannian degrees of freedom in cosmology has been obscure so far is because a complete cosmological hyperfluid model was lacking.

A development in this direction was the model of the unconstrained hyperfluid [23], which is described by the energy tensors

$$\hat{\Delta}_{\alpha\mu\nu} = \hat{J}_{\alpha\mu}u_\nu, \quad (10.52)$$

where $T^{\mu\nu}$ is the usual energy-momentum tensor of perfect fluid and $J_{\mu\nu}$ is the hyper-momentum density of the hyperfluid [23] (another interesting model was developed in [18]). Even though the above model is certainly interesting, it has some serious limitations, since when applied to cosmology it cannot produce any torsional degrees of freedom and only allows for a restricted form of non-metricity. As a result it does not allow confident conclusions, about the effects of torsion and non-metricity.

A model taking into account all the non-Riemannian degrees of freedom in cosmology (two for torsion and three for non-metricity) was only recently developed [19]. This is the model of the Perfect Cosmological Hyperfluid, which is the most general non-Riemannian fluid that is compatible with the Cosmological Principle. In this model the energy tensors read

$$t_{\mu\nu} = T_{\mu\nu} = \rho u_\mu u_\nu + p h_{\mu\nu} \quad (10.53)$$

$$\hat{\Delta}_{\alpha\mu\nu} = \phi h_{\mu\alpha}u_\nu + \chi h_{\nu\alpha}u_\mu + \psi u_\alpha h_{\mu\nu} + \omega u_\alpha u_\mu u_\nu + \epsilon_{\alpha\mu\nu\kappa}u^\kappa \zeta, \quad (10.54)$$

where $T^{\mu\nu}$ again has the usual expression (corresponding to a perfect fluid with energy density ρ and pressure p) and the above form of the hyper-momentum is the most general one that is allowed in an FLRW universe (i.e. the most general form compatible with the Cosmological Principle). Finally, $h_{\mu\nu} = g_{\mu\nu} + u_\mu u_\nu$ is the projection operator. The functions $\phi, \chi, \psi, \omega, \zeta$ can only depend on time and are associated with the microscopic characteristics of matter (have a purely non-Riemannian origin). These five fields are the sources for the two torsional [24] and three non-metricity [25] degrees of freedom that span a homogeneous cosmological background [19].

The most straightforward application of the Perfect Hyperfluid Model is to consider the Einstein-Hilbert action and the presence of such a fluid in an FLRW background. Then, the modified Friedmann equations in the presence of hyperfluid induced torsion and non-metricity, read [19]

$$H^2 = -H \left[\frac{3}{2}X - \frac{1}{2}Y + Z + V \right] - \frac{1}{2}(\dot{X} + \dot{Y}) - \frac{1}{2}(X - Y)(Z + V) + XY + W^2 + \frac{\kappa^2}{3}\rho_m, \quad (10.55)$$

$$\dot{H} + H^2 = -\frac{\kappa^2}{6}[\rho_m + 3p_m] + \dot{Y} + H(Y + Z + V) - Y(V + Z), \quad (10.56)$$

with ρ_m and p_m the energy density and pressure of usual matter, and where X, Y, Z, V, W are given by the decomposition of (10.16)

$$\hat{L}_{\alpha\mu\nu} + \hat{K}_{\alpha\mu\nu} = X(t)h_{\mu\alpha}u_\nu + Y(t)h_{\nu\alpha}u_\mu + Z(t)u_\alpha h_{\mu\nu} + V(t)u_\alpha u_\mu u_\nu + \epsilon_{\alpha\mu\nu\kappa} u^\kappa W(t), \quad (10.57)$$

and in this case, they are linearly related to the sources $\phi, \chi, \psi, \omega, \zeta$, see [19]. The above modified Friedmann equations combined with the conservation laws of the perfect hyperfluid

$$\begin{aligned} \dot{\rho}_m + 3H(\rho_m + p_m) &= -\frac{1}{2}u^\mu u^\nu (\chi \hat{R}_{\mu\nu} + \psi \hat{\mathcal{R}}_{\mu\nu}), \quad (10.58) \\ -\delta_\lambda^\mu \frac{\partial_\nu(\sqrt{-g}\phi u^\nu)}{\sqrt{-g}} - u^\mu u_\lambda \frac{\partial_\nu(\sqrt{-g}(\phi + \chi + \psi + \omega)u^\nu)}{\sqrt{-g}} &+ \left[\left(\hat{T}_\lambda - \frac{\hat{Q}_\lambda}{2} \right) u^\mu - \hat{\nabla}_\lambda u^\mu \right] \chi + \\ + \left[\left(\hat{T}^\mu - \frac{\hat{Q}^\mu}{2} + \hat{Q}^\mu \right) u_\lambda - g^{\mu\nu} \hat{\nabla}_\nu u_\lambda \right] \psi &+ u^\mu u_\lambda (\dot{\chi} + \dot{\psi}) - (\phi + \chi + \psi + \omega)(\dot{u}^\mu u_\lambda + u^\mu \dot{u}_\lambda) = 0, \quad (10.59) \end{aligned}$$

constitute a cosmological model where all the non-Riemannian degrees of freedom are taken into account in a minimal way (with this terminology we mean that we do not go beyond the Einstein-Hilbert action as far as the gravitational part of the action is concerned). In a sense, these represent the most natural generalisation of the Friedmann equations in MAG. The cosmological implications of the latter are currently under investigation. For an analytic review on the various other non-Riemannian models that have been considered in the literature, see [21].

References

1. L.P. Eisenhart, *Riemannian Geometry* (Princeton University Press, Princeton, 1997)
2. L.P. Eisenhart, *Non-Riemannian Geometry* (Courier Corporation, 2012)
3. F.W. Hehl, J. McCrea, E.W. Mielke, Y. Ne'eman, Metric affine gauge theory of gravity: field equations, Noether identities, world spinors, and breaking of dilation invariance. *Phys. Rept.* **258**, 1–171 (1995). [arXiv:gr-qc/9402012](https://arxiv.org/abs/gr-qc/9402012)
4. R. Aldrovandi, J.G. Pereira, *Teleparallel Gravity*, vol. 173 (Springer, Dordrecht, 2013)
5. J.M. Nester, H.-J. Yo, Symmetric teleparallel general relativity. *Chin. J. Phys.* **37**, 113 (1999). [arXiv:gr-qc/9809049](https://arxiv.org/abs/gr-qc/9809049)
6. J. Beltrán Jiménez, L. Heisenberg, T.S. Koivisto, Teleparallel Palatini theories. *JCAP* **1808**, 039 (2018). [arXiv:1803.10185](https://arxiv.org/abs/1803.10185)
7. J.B. Jiménez, L. Heisenberg, D. Iosifidis, A. Jiménez-Cano, T.S. Koivisto, General teleparallel quadratic gravity. *Phys. Lett. B* **805**, 135422 (2020). [arXiv:1909.09045](https://arxiv.org/abs/1909.09045)
8. R. Percacci, *Towards Metric-Affine Quantum Gravity* (2020). [arXiv:2003.09486](https://arxiv.org/abs/2003.09486)
9. F.W. Hehl, A. Macias, Metric affine gauge theory of gravity. 2. Exact solutions. *Int. J. Mod. Phys. D* **8**, 399–416 (1999). [arXiv:gr-qc/9902076](https://arxiv.org/abs/gr-qc/9902076)
10. D. Iosifidis, *Metric-Affine Gravity and Cosmology/Aspects of Torsion and non-Metricity in Gravity Theories*. Ph.D. thesis, Thessaloniki U. (2019). [arXiv:1902.09643](https://arxiv.org/abs/1902.09643)
11. D. Iosifidis, Exactly solvable connections in metric-affine gravity. *Class. Quant. Grav.* **36**(8), 085001 (2019). [arXiv:1812.04031](https://arxiv.org/abs/1812.04031)
12. Yu.N. Obukhov, E.J. Vlachynsky, W. Esser, F.W. Hehl, Effective Einstein theory from metric affine gravity models via irreducible decompositions. *Phys. Rev. D* **56**, 7769–7778 (1997)
13. V. Vitagliano, T.P. Sotiriou, S. Liberati, The dynamics of metric-affine gravity. *Ann. Phys.* **326**, 1259–1273 (2011). [arXiv:1008.0171](https://arxiv.org/abs/1008.0171). [Erratum: *Ann. Phys.* 329, 186 (2013)]
14. J.A. Schouten, *Ricci-Calculus: An Introduction to Tensor Analysis and Its Geometrical Applications*, vol. 10 (Springer Science & Business Media, 2013)
15. F.W. Hehl, G.D. Kerlick, P. von der Heyde, On hypermomentum in general relativity i. The notion of hypermomentum. *Zeitschrift fuer Naturforschung A* **31**(2), 111–114 (1976)
16. Y.N. Obukhov, D. Puetzfeld, Conservation laws in gravity: a unified framework. *Phys. Rev. D* **90**(2), 024004 (2014). [arXiv:1405.4003](https://arxiv.org/abs/1405.4003)
17. Y.N. Obukhov, D. Puetzfeld, Conservation laws in gravitational theories with general nonminimal coupling. *Phys. Rev. D* **87**(8), 081502 (2013). [arXiv:1303.6050](https://arxiv.org/abs/1303.6050)
18. O.V. Babourova, B.N. Frolov, Perfect hypermomentum fluid: variational theory and equations of motion. *Int. J. Mod. Phys. A* **13**, 5391–5407 (1998). [arXiv:gr-qc/0405124](https://arxiv.org/abs/gr-qc/0405124)
19. D. Iosifidis, *Cosmological Hyperfluids, Torsion and Non-Metricity*. [arXiv:2003.07384](https://arxiv.org/abs/2003.07384)
20. D. Puetzfeld, A cosmological model in Weyl-Cartan space-time. 1. Field equations and solutions. *Class. Quant. Grav.* **19**, 3263–3280 (2002). [arXiv:gr-qc/0111014](https://arxiv.org/abs/gr-qc/0111014)
21. D. Puetzfeld, Status of non-Riemannian cosmology. *New Astron. Rev.* **49**, 59–64 (2005). [arXiv:gr-qc/0404119](https://arxiv.org/abs/gr-qc/0404119)
22. K. Shimada, K. Aoki, K.-I. Maeda, Metric-affine gravity and inflation. *Phys. Rev. D* **99**(10), 104020 (2019). [arXiv:1812.03420](https://arxiv.org/abs/1812.03420)
23. Y.N. Obukhov, On a model of an unconstrained hyperfluid. *Phys. Lett. A* **210**, 163–167 (1996). [arXiv:gr-qc/0008014](https://arxiv.org/abs/gr-qc/0008014)
24. M. Tsamparlis, Cosmological principle and torsion. *Phys. Lett. A* **75**, 27–28 (1979)
25. A.V. Minkevich, A.S. Garkun, Isotropic cosmology in metric - affine gauge theory of gravity. [arXiv:gr-qc/9805007](https://arxiv.org/abs/gr-qc/9805007)

Chapter 11

Geometric Foundations of Gravity



Tomi S. Koivisto

11.1 Metric-Affine Geometry

Gravity theories are naturally considered in a geometrical setting. In the original formulation of General Relativity, in terms of coordinates x^μ of spacetime and a metric tensor $g_{\mu\nu}$ defined on them, the setting is a (pseudo-)Riemannian space. Cartan's work provided a more suitable, coordinate-independent, framework for the geometrical approach to theories of gravity. There, local frames are described by a set of vectors \mathbf{e}_A whose components e_A^μ are known as the vierbein $\mathbf{e}_A = e_A^\mu \partial_\mu$. Unless the frame field is degenerate, it has an inverse, the coframe one-form \mathbf{e}^A , which is dual to the frame with respect to the inner product $\mathbf{e}^A \cdot \mathbf{e}_B = \delta_B^A$. The relationship of the frames at different points in spacetime can be specified by referring to the concept of parallel transport. This is determined by the connection $\hat{\omega}_A^B$ which is a one-form, $\hat{\omega}_A^B = \hat{\omega}_A^B{}_\mu dx^\mu$. We denote by \hat{D} the covariant derivative associated with this connection.

To translate tensorial objects from the frame formulation into the coordinate formulation, the projections by the frame and the coframe are used. It should, however, be taken into account that the connection $\hat{\gamma}_A^B$ is not a tensor but has an inhomogeneous transformation rule. If we consider a general linear transformation $\Lambda^A{}_B$ with the inverse $\Lambda_A{}^B$, we have $\mathbf{e}^A \rightarrow \Lambda^A{}_B \mathbf{e}^B$ and $\mathbf{e}_A \rightarrow \Lambda_A{}^B \mathbf{e}_B$ but $\hat{\gamma}_A^B \rightarrow \Lambda_A{}^C \hat{\gamma}_C^D \Lambda^B{}_D - d\Lambda_A^B$. The connection describing the corresponding parallel transport in the tensor formalism is called $\hat{\Gamma}^\alpha{}_{\mu\nu}$, and is defined by $\hat{\Gamma}^\alpha{}_{\mu\nu} = e_A^\alpha \hat{D}_\mu e^A{}_\nu = -e^A{}_\nu \hat{D}_\mu e_A{}^\alpha$. In the Riemannian formulation of General Relativity the connection was not an independent field, but was rather given as

T. S. Koivisto (✉)

Departamento de Física Fundamental and IUFFyM, Universidad de Salamanca, 37008 Salamanca, Spain

e-mail: t.s.koivisto@astro.uio.no

© The Author(s), under exclusive license to Springer Nature Switzerland AG 2021

E. N. Saridakis et al. (eds.) *Modified Gravity and Cosmology*,

https://doi.org/10.1007/978-3-030-83715-0_11

143

$$\Gamma^\alpha{}_{\mu\nu} = g^{\alpha\lambda} \left(g_{\lambda(\mu,\nu)} - \frac{1}{2} g_{\mu\nu,\lambda} \right). \quad (11.1)$$

However, in hindsight, “[...] it seems of secondary importance, in some sense, that some particular $\hat{\Gamma}$ field can be deduced from a Riemannian metric” [1].

There are two gauge-invariant properties of a generic connection. These are the curvature two-form and the torsion two-form, defined as

$$\hat{\mathbf{R}}_A{}^B = \hat{\mathbf{D}}\hat{\omega}_A{}^B = d\hat{\omega}_A{}^B + \hat{\gamma}_A{}^C \wedge \hat{\omega}_C{}^B, \quad (11.2)$$

$$\hat{\mathbf{T}}^A = \hat{\mathbf{D}}e^A = de^A + \hat{\omega}_A{}^B \wedge e_B, \quad (11.3)$$

respectively. By construction, these satisfy the Bianchi identities $\hat{\mathbf{D}}\hat{\mathbf{R}}_A{}^B = 0$ and $\hat{\mathbf{D}}\hat{\mathbf{T}}^A = \hat{\mathbf{R}}_B{}^A \wedge e^B$. From the definition of the affine connection $\hat{\Gamma}^\alpha{}_{\mu\nu}$, it follows that the corresponding objects in the tensor formulation are

$$\hat{R}^\alpha{}_{\beta\mu\nu} = 2\partial_{[\mu}\hat{\Gamma}^\alpha{}_{\nu]\beta} - 2\hat{\Gamma}^\alpha{}_{[\mu|\lambda|}\hat{\Gamma}^\lambda{}_{\nu]\beta} = -e^A{}_\beta \hat{R}_A{}^B{}_{\mu\nu} e_B{}^\alpha, \quad (11.4)$$

$$\hat{T}^\alpha{}_{\mu\nu} = 2\hat{\Gamma}^\alpha{}_{[\mu\nu]} = \hat{T}^A{}_{\mu\nu} e_A{}^\alpha. \quad (11.5)$$

These objects have a clear geometrical interpretation. By using the identity

$$[\hat{\nabla}_\mu, \hat{\nabla}_\nu]V^\alpha = \hat{R}^\alpha{}_{\beta\mu\nu} V^\beta - \hat{T}^\lambda{}_{\mu\nu} \hat{\nabla}_\lambda V^\alpha, \quad (11.6)$$

one may see that when a vector V^μ is parallel transported around a closed loop, torsion describes the displacement of the vector, and curvature describes the change of the vector. These concepts do not require a metric, but are the properties solely of the connection.

If a metric structure $g_{\mu\nu}$ is also available, it is possible to refer to concepts such as lengths and angles. Then we may define the contraction $\hat{R}_{\alpha\beta\mu\nu} = g_{\alpha\lambda} \hat{R}^\lambda{}_{\beta\mu\nu}$ and see that the metric curvature $\hat{R}_{[\alpha\beta]\mu\nu}$ describes the rotation of the vector that is parallel-transported around a closed loop, and the non-metric curvature $\hat{R}_{(\alpha\beta)\mu\nu}$ describes the change of the magnitude of the components of the vector; in particular, the piece $g^{\alpha\beta} \hat{R}_{\alpha\beta\mu\nu}$ describes an overall rescaling, and the rest of the symmetric components describe the shape distortions. The presence of non-metric curvature implies that that the inner products are not conserved by the connection. The incompatibility of the two structures can be quantified by the non-metricity defined as $\hat{Q}_{\alpha\mu\nu} = \hat{\nabla}_\alpha g_{\mu\nu}$. Note that even if the affine geometry is integrable, $\hat{R}^\alpha{}_{\beta\mu\nu} = 0$, $\hat{T}^\alpha{}_{\mu\nu} = 0$, it can be incompatible with the metric geometry, $\hat{Q}_{\alpha\mu\nu} \neq 0$. The geometric interpretation of the invariants is illustrated in Fig. 11.1.

The generic connection can be decomposed, with respect to a given metric, as

$$\hat{\Gamma}^\alpha{}_{\mu\nu} = \Gamma^\alpha{}_{\mu\nu} + \hat{K}^\alpha{}_{\mu\nu} + \hat{L}^\alpha{}_{\mu\nu}, \quad (11.7)$$

where the contributions of the torsion and the non-metricity,

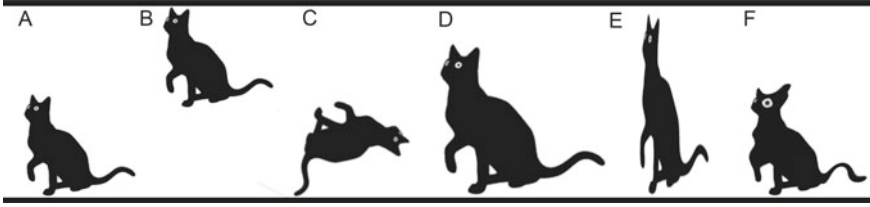


Fig. 11.1 Exploring the metric-affine space wherein $\mathbf{a} \hat{\mathbf{R}}_A^B = \hat{\mathbf{T}}^A = 0$, $\mathbf{b} \hat{\mathbf{T}}^A \neq 0$, $\mathbf{c} \mathbf{R}_A^B \neq 0$, $\mathbf{d} \hat{\mathbf{R}}_A^A \neq 0$, $\mathbf{e} \hat{\mathbf{R}}_A^B \neq 0$ for $A = B$, and $\mathbf{f} \hat{\mathbf{R}}_A^B - \delta_B^A \hat{\mathbf{R}}_C^C \neq 0$.

$$\hat{\mathbf{K}}^\alpha{}_{\mu\nu} = \frac{1}{2} \hat{\mathbf{T}}^\alpha{}_{\mu\nu} - \hat{\mathbf{T}}_{(\mu\nu)}^\alpha, \tag{11.8}$$

$$\hat{\mathbf{L}}^\alpha{}_{\mu\nu} = \frac{1}{2} \hat{\mathbf{Q}}^\alpha{}_{\mu\nu} - \hat{\mathbf{Q}}_{(\mu\nu)}^\alpha, \tag{11.9}$$

are called the contortion and the disformation, respectively. These two tensors can be related to the corresponding one-forms with latin indices. The contortion one-form $\hat{\mathbf{K}}_A^B$ could be defined via $\hat{\mathbf{K}}_B^A \wedge \mathbf{e}^B = \hat{\mathbf{T}}^A$. The disformation one-form is given by $\hat{\mathbf{L}}_{AB} = \frac{1}{2} \hat{\mathbf{D}}\eta_{AB} - \mathbf{e}_{[A} \cdot \hat{\mathbf{D}}\eta_{B]C} \mathbf{e}^C$, where η_{AB} is the tangent space metric, whose covariant derivative is related to the non-metricity one-form $\hat{\mathbf{Q}}_{AB}$ as $\hat{\mathbf{D}}\eta_{AB} = 2(\hat{\mathbf{Q}}_{AB} + \hat{\gamma}_{(AB)})$. Finally, we may note that defining the Levi-Civita one-form ω_A^B via $\omega_B^A \wedge \mathbf{e}^B = -d\mathbf{e}^A$, we can display the decomposition

$$\hat{\gamma}_A^B = \omega_A^B + \hat{\mathbf{K}}_A^B + \hat{\mathbf{L}}_A^B, \tag{11.10}$$

which is just the rewriting of (11.7).

11.2 The Geometrical Trinity

In the standard description of General Relativity, the tangent space is endowed with the Minkowski metric η_{AB} , and the spacetime metric is then its projection $g_{\mu\nu} = e^A{}_\nu e^B{}_\nu \eta_{AB}$. The Einstein-Hilbert action can then be cast in the well-known equivalent forms

$$S_{\text{GR}} = \frac{1}{2\kappa^2} \int \epsilon_{ABCD} \mathbf{R}^{AB} \wedge \mathbf{e}^C \wedge \mathbf{e}^D = \frac{1}{2\kappa^2} \int d^4x \sqrt{-g} g^{\beta\nu} R^\alpha{}_{\beta\alpha\nu}. \tag{11.11}$$

It is also possible to consider the Einstein-Palatini action that does not impose $\hat{\Gamma}^\alpha{}_{\mu\nu} = \Gamma^\alpha{}_{\mu\nu}$ but obtains this (up to an undetermined but irrelevant piece of torsion) as a dynamical condition. It is very interesting to consider further alternatives, from the viewpoint of the decomposition of the geometric elements we found above in (10.15).

We split the connection $\hat{\omega}_A{}^B = \omega_A{}^B + \hat{x}_A{}^B$ into the metrical part $\omega_A{}^B$ and the rest that we'll call the distortion $\hat{x}_A{}^B$, and we can now split the curvature

$$\hat{\mathbf{R}}_A{}^B = \hat{\mathbf{D}}\hat{\omega}_A{}^B = d\hat{\omega}_A{}^B + \hat{\omega}_A{}^C \wedge \hat{\omega}_C{}^B = \mathbf{R}_A{}^B + \hat{\mathbf{D}}\hat{x}_A{}^B + \hat{x}_A{}^C \wedge \hat{x}_C{}^B \quad (11.12)$$

Therefore, if one imposes teleparallelism, i.e. $\hat{\mathbf{R}}_A{}^B = 0$, it appears that the action

$$S_{\text{GR}_{\parallel}} = -\frac{1}{2\kappa^2} \int \epsilon_{ABCD} \hat{x}^{AE} \wedge \hat{x}_E{}^B \wedge \mathbf{e}^C \wedge \mathbf{e}^D, \quad (11.13)$$

is equivalent to (11.11) up to a total derivative [2]. This change of geometrical variables opens new perspectives on Einstein's theory. In particular, the equivalence of the formulations has been established in two extensively studied cases, which we shall now review.

In the case of metric teleparallelism, one imposes metric-compatibility. Then, (11.13) becomes the action of TEGR (read: the metric Teleparallel Equivalent of General Relativity¹ [3, 4];),

$$S_{\text{TEGR}} := S_{\mathring{\text{GR}}} = -\frac{1}{2\kappa^2} \int \epsilon_{ABCD} \mathring{\mathbf{K}}^{AE} \wedge \mathring{\mathbf{K}}_E{}^B \wedge \mathbf{e}^C \wedge \mathbf{e}^D = -\frac{1}{2\kappa^2} \int d^4x \sqrt{-g} \mathbb{T}. \quad (11.14)$$

We have introduced the torsion scalar

$$\mathbb{T} = -\mathring{T}_{\alpha\mu\nu} \left(\frac{1}{4} \mathring{T}^{\alpha\mu\nu} + \frac{1}{2} \mathring{T}^{\mu\alpha\nu} - g^{\alpha\nu} \mathring{T}^{\lambda\mu}{}_{\lambda} \right). \quad (11.15)$$

In the case of symmetric teleparallelism, one precludes torsion. Then, (11.13) becomes the action of $\mathring{\text{GR}}$ (read: the symmetric Teleparallel Equivalent of General Relativity [5, 6]),

$$S_{\text{STEGR}} := S_{\mathring{\text{GR}}} = -\frac{1}{2\kappa^2} \int \epsilon_{ABCD} \mathring{\mathbf{L}}^{AE} \wedge \mathring{\mathbf{L}}_E{}^B \wedge \mathbf{e}^C \wedge \mathbf{e}^D = -\frac{1}{2\kappa^2} \int d^4x \sqrt{-g} \mathbb{Q}, \quad (11.16)$$

where we have introduced the non-metricity scalar [7]

$$\mathbb{Q} := \frac{1}{2} \mathring{Q}^{\alpha\mu\nu} \left(\mathring{L}^{\alpha}{}_{\mu\nu} - \mathring{L}^{\alpha}{}_{\nu\mu} \right), \quad (11.17)$$

which may be defined in terms of the Weyl connection

¹ It is a convention to denote quantities in this geometry (with some exceptions like that of the frame and the coframe) with the bullets on top of them; and another convention is to drop the epithet "metric" when referring to the special case with metric-compatible connection.

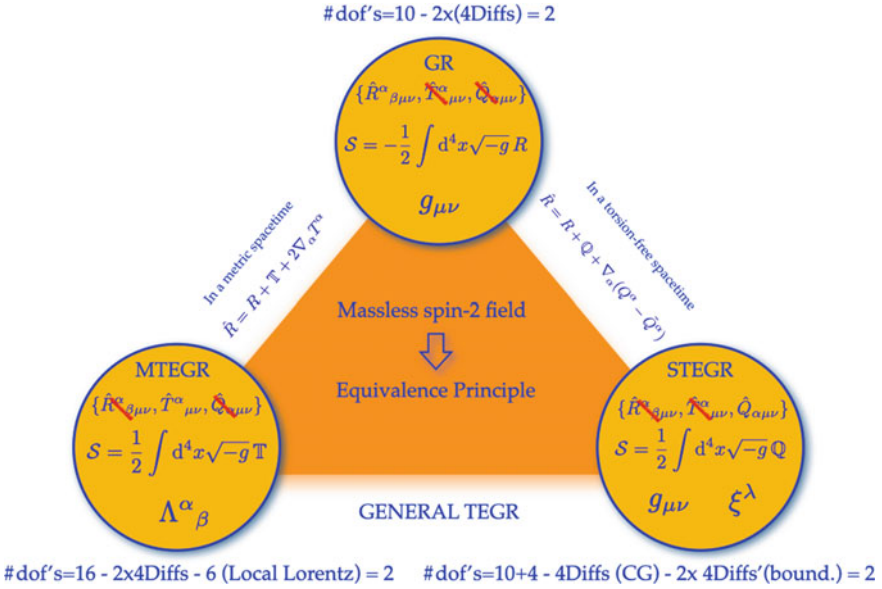


Fig. 11.2 A schematic illustration of the geometrical trinity

$$\bar{L}^{\alpha}_{\mu\nu} = \frac{1}{2} Q^{\alpha} g_{\mu\nu} - \delta^{\alpha}_{(\mu} Q_{\nu)}, \quad Q_{\alpha} = g_{\mu\nu} Q^{\alpha\mu\nu}. \tag{11.18}$$

A technical remark is that the connection in each of the three cases (11.11, 11.14, 11.16) can be either restricted to the desired form a priori or by the use of Lagrange multipliers, with the same result in each case. We also emphasise that in each of the three cases either of the two given forms of the action can equally well be taken as the definition of the theory, since teleparallel theories admit a consistent Palatini formulation [7, 8]. The geometrical trinity is schematically presented in Fig. 11.2.

At the conceptual level, (11.11) most naturally describes gravity as geometry, (11.14) as force, and (11.16) as inertia. Consider, for example, the equation of motion for the trajectory $x^{\alpha}(\tau)$ of a test particle,

$$\ddot{x}^{\alpha} + \Gamma^{\alpha}_{\mu\nu} \dot{x}^{\mu} \dot{x}^{\nu} = 0, \tag{11.19}$$

which in the standard Riemannian context is seen as the statement that the particle moves along the geodesics, coinciding with the shortest path as measured by the metric. The coordinate system wherein $\Gamma^{\alpha}_{\mu\nu} = 0$ is taken to be freely falling. The very same equation (11.19) can be rewritten in terms of the metric teleparallel connection and contortion,

$$\ddot{x}^{\alpha} + \dot{\Gamma}^{\alpha}_{\mu\nu} \dot{x}^{\mu} \dot{x}^{\nu} = \dot{K}^{\alpha}_{\mu\nu} \dot{x}^{\mu} \dot{x}^{\nu} = F^{\alpha}, \tag{11.20}$$

where in the Weitzenböck frame the left hand side describes the gravitational force F^α that tends to displace the particle, and is orthogonal to the four-velocity, $F^\alpha \dot{x}_\alpha = 0$. Now we cannot, in general, find a frame wherein $\mathring{\Gamma}^\alpha_{\mu\nu}$ would vanish, but there is a frame $\ddot{x}^\mu = 0$ wherein the inertial and gravitational forces exactly cancel each other out. In symmetric teleparallel geometry, the equation reads

$$\ddot{x}^\alpha + \mathring{\Gamma}^\alpha_{\mu\nu} \dot{x}^\mu \dot{x}^\nu = \mathring{L}^\alpha_{\mu\nu} \dot{x}^\mu \dot{x}^\nu = I^\alpha. \quad (11.21)$$

Now we can choose the coincident gauge $\mathring{\Gamma}^\alpha_{\mu\nu} = 0$, where the deviation of the trajectory from straight lines is seen to be solely due to the inertial effects described by the left hand side. The latter are not appropriately interpreted as forces, since $I_\alpha \dot{x}^\alpha = -\frac{1}{2} \mathring{Q}_{\alpha\mu\nu} \dot{x}^\alpha \dot{x}^\mu \dot{x}^\nu \neq 0$. Instead, the disformation describes the apparent change of magnitudes, i.e. rescalings of units of measurements, due to the non-preservation of the metric. The frame $\ddot{x}^\alpha = 0$ is simply the inertial frame of the particle, coinciding with what we call below the canonical frame.

Though these are merely matters of interpretation at the level of classical dynamics, the different formulations of the action principle can lead to very different results in calculations of the quantum theory, energetics, or thermodynamics of gravity. In particular, the framework of (11.16) has recently lead to some interesting new results, which we would like to review in the following.

11.3 Purified Gravity

Let us first have a closer look at the action principle (11.16). As a direct consequence of (11.12), we have, in the absence of curvature and torsion,

$$g^{\mu\nu} \mathring{R}^\alpha_{\mu\alpha\nu} = \mathbb{Q} + \nabla_\mu \left(\mathring{Q}^\mu - \mathring{Q}^\mu_{\alpha\alpha} \right). \quad (11.22)$$

Thus, the action (11.16) differs from (11.11) by a total derivative. In fact, it can be regarded as the minimal covariantisation of Einstein's original action principle [9]. Noting that a symmetric teleparallel connection $\mathring{\Gamma}^\alpha_{\mu\nu}$ can always be expressed in terms of a 4×4 matrix Λ^μ_{ν} that has an inverse Λ_ν^μ as

$$\mathring{\Gamma}^\alpha_{\mu\nu} = \Lambda_\lambda^\alpha \partial_\mu \Lambda^\lambda_{\nu}, \quad (11.23)$$

since the most general flat linear connection must be obtained by a general linear transformation of the vanishing connection, we can choose the gauge in which this connection vanishes, $\mathring{\Gamma}^\alpha_{\mu\nu} = 0$. It is straightforward to see that in this gauge we have

$$\mathbb{Q} = 2 g^{\mu\nu} \Gamma^\alpha_{\beta[\mu} \Gamma^\beta_{\alpha]\nu}, \quad (11.24)$$

where the left-hand side is the Einstein Lagrangian [9]. The action (11.16) thus combines the desired properties of both Hilbert's and Einstein's formulations, since it is a scalar and quadratic in first derivatives. Next, let us note that since we also require the connection to be free of torsion, the matrix $\Lambda^\alpha{}_\mu$ in (11.23) has to reduce to a Jacobian of a coordinate transformation, i.e. $\Lambda^\alpha{}_\mu = \xi^\alpha{}_{,\mu}$ for some ξ^α . Thus the connection is always of the form [7, 8]

$$\hat{\Gamma}^\alpha{}_{\mu\nu} = \frac{\partial x^\alpha}{\partial \xi^\lambda} \frac{\partial^2 \xi^\lambda}{\partial x^\mu \partial x^\nu}, \quad (11.25)$$

that is, a (passive) translation of the vanishing connection. This proves that purified gravity is the unique framework that provides the minimal covariantisation of the Einstein Lagrangian and the canonical gauge theory of translation.

11.3.1 Field Equations

Let us now consider the field equations. For that it is convenient to introduce the non-metricity conjugate, defined as

$$P^\alpha{}_{\mu\nu} = -\frac{1}{2}L^\alpha{}_{\mu\nu} + \frac{1}{4}(Q^\alpha - Q^\lambda{}_{\alpha\lambda})g_{\mu\nu} - \frac{1}{4}\delta_{(\mu}^\alpha Q_{\nu)}. \quad (11.26)$$

The field equations derived by the variation with respect to the metric are

$$\hat{\tau}^\mu{}_\nu = T^\mu{}_\nu + \hat{t}^\mu{}_\nu, \quad (11.27)$$

where $T^\mu{}_\nu$ is the energy-momentum tensor of matter, defined as usual by

$$T_{\mu\nu} = \frac{-2}{\sqrt{-g}} \frac{\delta S_{\text{matter}}}{\delta g^{\mu\nu}}, \quad (11.28)$$

where S_{matter} is the action for the matter fields, and

$$\hat{\tau}^\mu{}_\nu = \frac{2\kappa^2}{\sqrt{-g}} \hat{\nabla}_\alpha \left(\sqrt{-g} \hat{P}^{\alpha\mu}{}_\nu \right), \quad (11.29)$$

$$\hat{t}^\mu{}_\nu = \frac{\kappa^2}{2} \mathbb{Q} \delta_\nu^\mu - \kappa^2 \hat{P}^\mu{}_{\alpha\beta} \hat{Q}_\nu{}^{\alpha\beta}. \quad (11.30)$$

It is interesting to note that $\hat{t}^\mu{}_\nu$ is the canonical current according to Noether's theorem [10], and indeed Einstein had proposed this pseudotensor to describe the energy-momentum of the gravitational field [9]. Likewise, one finds that $2\hat{\nabla}_\alpha (\sqrt{-g} \hat{P}^{\alpha\mu}{}_\nu) = \hat{\nabla}_\alpha \hat{H}^{\alpha\mu}{}_\nu$, and for the object $\hat{H}^{\alpha\mu}{}_\nu = \hat{H}^{[\alpha\mu]}{}_\nu$,

$$\mathring{H}^{\mu\nu}{}_{\alpha} = \kappa^2 \sqrt{-g} \left(\mathring{Q}^{[\mu\nu]}{}_{\alpha} - \mathring{Q}^{[\mu} \delta_{\alpha}^{\nu]} + \mathring{Q}^{\beta[\mu}{}_{\beta} \delta_{\alpha}^{\nu]} \right), \quad (11.31)$$

for which $\mathring{H}^{\alpha\mu}{}_{\nu}$ is what is known as the Einstein energy-momentum complex. Thus, we have arrived at the covariant version of the canonical energy-momentum split. In addition to the usual metric-covariant conservation law

$$\nabla_{\mu} \mathring{\tau}^{\mu}{}_{\nu} = \nabla_{\mu} \left(T^{\mu}{}_{\nu} + \mathring{t}^{\mu}{}_{\nu} \right) = 0, \quad (11.32)$$

we now also have the covariant form of the usual conservation law

$$\mathring{\nabla}_{\mu} \left(\sqrt{-g} \mathring{\tau}^{\mu}{}_{\nu} \right) = \mathring{\nabla}_{\mu} \left(\sqrt{-g} T^{\mu}{}_{\nu} + \sqrt{-g} \mathring{t}^{\mu}{}_{\nu} \right) = 0, \quad (11.33)$$

from which it is directly seen that $2\mathring{\nabla}_{\alpha}(\sqrt{-g}\mathring{P}^{\alpha\mu}{}_{\nu}) = \mathring{\nabla}_{\alpha}\mathring{H}^{\alpha\mu}{}_{\nu}$, but it can also be derived as the equation of motion for the connection which, we recall, is now an independent variable.

11.3.2 Energy and Entropy

We should note that the field equation (11.27) now possesses two gauge invariances: one may transform only the metric or both the metric and the connection. In fact, this is related to the unique property of the quadratic action (11.16), which is that the translational gauge connection decouples from it at the linear order [7]. Now, however, the split into $\mathring{t}^{\mu}{}_{\nu}$ and $\mathring{\tau}^{\mu}{}_{\nu}$ is not invariant under independent transformations of the connection or of the metric. This introduces an ambiguity into the definition of the gravitational energy-momentum and related quantities. This situation is the same as in GR, where the results depend arbitrarily on the coordinate frame, and in TEGR, where the results depend arbitrarily on the local Lorentz frame. Recently, a possible resolution was proposed by suggesting that the canonical frame of purified gravity should be defined by the vanishing of the energy-momentum associated with the metric field [11]. This is the natural consequence of the interpretation of gravitation as fundamentally an inertial phenomenon, despite its alternative descriptions as force or geometry. Let us emphasise that the proposed prescription, which is nothing but the minimal covariant version of the canonical prescription, uniquely determines any physical quantity of interest.

The energy-momentum of any gravity-matter system according to Noether's theorem can in our case be determined from the integral, which after applying the Gauss theorem becomes

$$E_{\mu} = \int d^2x H^{i0}{}_{\mu} n_i, \quad (11.34)$$

where n_i is the outward normal vector of the surface of the volume under consideration. The energy of the system can be also determined in the Euclidean path integral

approach wherein, in the saddle point approximation, the partition function $Z(\beta)$ is given by the exponential of the Euclidean action. At the leading (on-shell) order we have

$$-\log Z(\beta) \approx \frac{\kappa^2}{2} \int d^3x \sqrt{-g} \left(\dot{Q}^\alpha - \dot{Q}_\mu^{\alpha\mu} \right) n_\alpha + \int d^4x \sqrt{-g} \left(L_{\text{matter}} - \frac{1}{2} T \right), \quad (11.35)$$

where for the gravitational sector we have again used the Gauss theorem, and written the contribution from the matter sector in terms of the Lagrangian L_{matter} and the trace of the matter energy-momentum tensor T . The partition function is considered a function of the inverse temperature β , while the energy E_0 and entropy S of the system are given by

$$\langle E_0 \rangle = -\frac{\partial}{\partial \beta} \log Z, \quad S = \beta \langle E_0 \rangle + \log Z, \quad (11.36)$$

respectively. The formulae (11.34) and (11.35) are to be evaluated in the canonical frame specified by $i^\mu{}_\nu = 0$, but they are valid in any coordinate system. Notice that both the universal expressions have been reduced to integrals over the boundaries of spatial and spacetime volumes, respectively, and that the path integral needs the introduction of neither a surface nor a counter term.

It is highly nontrivial that the above expressions (11.34) and (11.35) yield results that are consistent with each other, with the first law of thermodynamics, and with the area law of black hole thermodynamics. We omit the details of the calculations but we will report the results in the two most important cases with horizons: the black hole spacetime and the cosmological spacetime [11]. Consider first a black hole described by the metric

$$ds^2 = -f(r)dt^2 + f^{-1}(r)dr^2 + r^2 d\Omega_2^2, \quad (11.37)$$

where Ω_2 is the metric on the unit 2-sphere. Recall that the temperature is $\beta^{-1} = -f'(r)/4\pi$ and the horizon radius r_+ is the largest r for which $f(r) = 0$. Let us consider a charged black hole, described by $f(r) = 1 - 2m/r + q/r^2$. When the charge is $q \neq 0$ we need to also take into account the electromagnetic field that supports the solution. The formula (11.34) then gives $E_\mu = (m - q^2/(2r_+))\delta_\mu^0$. The canonical energy thus reduces to the expected $E_0 = m$ in the case of the Schwarzschild black hole, whilst a charged black hole with the same mass, together with the surrounding electromagnetic field, has less total energy, in the extremal case $E_0 \rightarrow m/2$. From (11.35) we obtain, by direct calculation, that $-\log Z \approx \pi r_+^2 + \beta q^2/(2r_+)$. This is precisely the consistent result for which (11.36) implies that $E_0 = (m - q^2/(2r_+))$, $S = \pi r_+^2$. In the case of de Sitter space, we may consider the line element (11.37) where now $f(r) = 1 - 2r^2/r_+^2$. Then, we find vanishing energy-momentum from (11.34), $E_\mu = 0$. Using (11.35) and (11.36), we obtain consistently that $E_0 = 0$, $S = \pi r_+^2$.

It is important to note that the canonical frame wherein $\hat{i}^\mu{}_\nu = 0$ is reached only with a non-trivial connection for the form of the metric (11.37). The results computed in any other frame would describe the measurement of a non-inertial observer, and their physical interpretation would thus be very difficult. The correct results that were quoted above can also be computed with a vanishing connection by simply transforming into the coincident gauge. After such a transformation one finds the metric in the form

$$g_{\mu\nu} = \eta_{\mu\nu} + [f(r) - 1] \ell_\mu \ell_\nu, \quad (11.38)$$

where

$$\ell_\mu dx^\mu = dt + \delta_{ij} \frac{x^i}{r} dx^j, \quad r^2 = \delta_{ij} x^i x^j. \quad (11.39)$$

It is clear to see that now $\hat{i}^\mu{}_\nu = 0$ and the formulae (11.34) and (11.35) yield the energy-momentum and the entropy as quoted above for the two physical systems. In contrast, if we consider the coordinate system (11.37) in the coincident gauge, we are not in the canonical frame where the energy-momentum of the metric field would vanish, but instead we obtain from (11.30) that, for example $\hat{i}^0{}_0 = -(1/\kappa r)^2$, meaning that there appears to be nonzero (in fact, negative) energy due to the gravitational field. Now we have $\mathbb{Q} = -1/r^2$, and therefore the action is positive, but divergent. In particular, there is a logarithmic divergence at $r \rightarrow \infty$, which is fully consistent with the interpretation that this frame is non-inertial. In precisely such a case we might expect to find spurious effects that do not vanish even infinitely far away from the sources. Note that these effects are now completely independent of the actual mass of the black hole, but vanish when the gravitational coupling is set to vanish.

11.3.3 On Quantum Theory

It may be useful to consider the analogy of purified gravity and massive electromagnetism. The action (11.16) is manifestly a mass term for the connection, and the metric could thus be considered as a field restoring the broken symmetry, in analogy to Stueckelberg's version of Proca's theory. Perhaps the analogy is complete in that there is also a (canonical) kinetic term for the connection, though at the classical level we may neglect the field strength of the connection. The reason is that since the connection is massive, it interacts only at finite distances. To wit, the range of the force is of the order of the Planck length, $\sim 10^{-35}$ meters. It is interesting to consider that though at the macroscopic level the gauge field of purified gravity does not propagate, gravity should become impure as microscopic distances approaching the Planck scale are probed. One might even speculate that such ripples of spacetime at its tiniest scales could eventually vindicate the idea of Clifford's visionary geometric theory of gravity according to which matter is nothing but a disturbance in the spatial

curvature, so that matter in motion can be understood as a simple variation in space of these wave-like disturbances.

To elaborate on the analogy of GR with massive vector field theory, let us consider the strength tensor $F_{\mu\nu}$ and the excitation tensor density $H^{\mu\nu}$ sourced by matter current density T^μ (usually denoted J^μ). The premetric form of the equations is then

$$\mathring{\nabla}_\mu H^{\mu\nu} = T^\mu + \mathring{t}^\mu, \quad \mathring{\nabla}_{[\alpha} F_{\mu\nu]} = 0. \quad (11.40)$$

The difference with massless electromagnetism is that the field also sources itself through the term \mathring{t}^μ . For the theory to be predictive, one has to specify the constitutive relations that determine the forms of the extensive $H^{\mu\nu}$ and \mathring{t}^μ in terms of the intensive quantities. In the case of Proca, the constitutive relations involve a metric, $H^{\mu\nu} = \sqrt{-g}F^{\mu\nu}$ and $\mathring{t}^\mu = m^2 A^\mu$, where m is the mass of the gauge potential A_μ , whose existence one deduces from the second premetric equation (11.40). As we have seen, the equations of motion in purified gravity are

$$\mathring{\nabla}_\mu \mathring{H}^{\mu\nu}{}_\alpha = T^\mu{}_\alpha + \mathring{t}^\mu{}_\alpha, \quad F^{\alpha\beta}{}_{\mu\nu} = 0. \quad (11.41)$$

The different number of indices in the first equations (11.41) with respect to that of (11.40) only reflects that the latter is deduced from the conservation of the electric charge, whereas the former is deduced from the conservation of the four translational charges, but the form of the equations is exactly the same. The question arises as to whether the analogy of theories is complete, the second equation in (11.41) then being a valid approximation only at super-Planckian length scales, the full theory only being subject to $\mathring{\nabla}_{[\rho} F^{\alpha\beta}{}_{\mu\nu]} = 0$. Though massive Abelian gauge theories are renormalisable even without the Higgs mechanism [12], from the perspective of purified gravity it is natural to consider a spontaneous emergence of the Planck scale, since one wants to recover scale invariance at the most fundamental level of physics. The idea of the metric as a Goldstone boson of spontaneous symmetry breaking goes back to at least Isham, Salam and Sthraheedee [13], and has been previously discussed in various different contexts [13–23]. However, the analogy with massive gauge theory and the Planck mass as the rationale of teleparallelism are very recent theoretical advances [24].

Even regardless of those, we should recall the results of 11.3.2, which we believe could be highly relevant in view of the eventual reconciliation of gravity and quantum physics. In the canonical approach to quantum gravity, the notorious problem of time might be taken into reconsideration from the perspective wherein besides the conventional ADM Hamiltonian formalism, we also have available the unique consistent definition of localisable energy in a gravitational system. The other main approach to quantisation, the path integral formalism, can obviously also be reconsidered from a more promising starting point, since the action (11.16) in the canonical frame is well-defined without the addition of boundary terms or counter terms. We already took advantage of this in the zeroth order approximation to Euclidean quantum gravity by determining the entropy of charged black holes and the de Sitter Universe by

a considerably simplified calculation compared to the standard ones. It could also be mentioned that the origin of the otherwise mysterious simplifications that have been found to occur in the perturbative quantum gravity calculations via the famous technique dubbed the double copy [25] can presumably be traced back to the realisation of a translation gauge theory in the framework of purified gravity [8].

11.3.4 Matter Coupling

Having seen that the geometrical trinity encloses an infinite theory space of equivalent formulations, the question may have arisen whether the geometry of spacetime can be decided by experiments, or whether it is merely a matter of convention. Considering solely a theory of a vacuum, the latter may well be the case, but by taking into account matter besides the gravitational field(s), criteria could be found that distinguish the “physical” geometry. Matter particles in the Standard Model are described by spin-half fields, whose gravitational coupling is intriguing and, especially in metric-affine geometries, often an issue of some controversy [26–28]. We present in careful detail what we find to be the most reasonable approach.

Consider the Hermitean Dirac action for a (for simplicity, massless) spinor ψ

$$S_D = -\frac{1}{2} \int d^4x \sqrt{-g} \left[\left(i\bar{\psi}\gamma^\mu \hat{\nabla}_\mu \psi \right) + \left(i\bar{\psi}\gamma^\mu \hat{\nabla}_\mu \psi \right)^\dagger \right], \quad (11.42)$$

where $\gamma^\mu = \gamma^A e_A{}^\mu$ are the Dirac matrices satisfying the Clifford algebra $\gamma^{(A}\gamma^{B)} = -\eta^{AB}$, and $\bar{\psi} = \psi^\dagger \gamma^0$ is the conjugate spinor. Let us denote the spinor covariant derivative as $\hat{\nabla}_\mu \psi = \partial_\mu \psi + \hat{\Gamma}_\mu \psi$. Without making any assumptions about the geometry or the connection $\hat{\Gamma}_\mu$, we obtain the equation of motion for the spinor

$$\left[2\gamma^\mu \partial_\mu + \frac{1}{\sqrt{-g}} \partial_\mu (\sqrt{-g} \gamma^\mu) + \gamma^\mu \hat{\Gamma}_\mu - \gamma^0 \hat{\Gamma}_\mu^\dagger \gamma^0 \gamma^\mu \right] \psi = 0. \quad (11.43)$$

The equation of motion for the spinor conjugate is the same, with $\hat{\Gamma}_\mu \rightarrow -\hat{\Gamma}_\mu$, $\psi \rightarrow \bar{\psi}$. Now we should deduce how to present the connection (10.15) for fermions.

To extend the Lorentz algebra of the rotation generators r_{AB}

$$[r_{AB}, r_{CD}] = 2 (\eta_{D[A} r_{B]C} - \eta_{C[A} r_{B]D}), \quad (11.44a)$$

to the general linear algebra, we need to also introduce the shear generators q_{AB} , entailing the additional commutation relations

$$[q_{AB}, q_{CD}] = 2 (\eta_{C(A} r_{B)D} + \eta_{D(A} r_{B)C}), \quad (11.44b)$$

$$[q_{AB}, r_{CD}] = 2 (\eta_{C(A} q_{B)D} - \eta_{D(A} q_{B)C}). \quad (11.44c)$$

It is clear to see that the generators can be represented as

$$r_{AB} = 2x_{[A}\partial_{B]} + \Delta_{[AB]}, \quad q_{AB} = 2x_{(A}\partial_{B)} + \Delta_{(AB)}, \quad (11.45)$$

where the vectors are called the orbital parts, while the Δ_{ab} , the form of which depends on the fields we are acting upon, are called the matrix parts of the generators. The infinitesimal transformations of the fields are nothing but their Lie derivatives along the Killing vectors of the group, in the case at hand given by (11.45). For example, the Lie Derivative \mathfrak{L}_X of a vector V along X is

$$(\mathfrak{L}_X V)^\mu = X^\alpha \partial_\alpha V^\mu - V^\alpha \partial_\alpha X^\mu. \quad (11.46)$$

Quite intuitively, the first term gives the orbital action and the second term gives the matrix part. From the 16 Killing vectors X we now have, it is easy to obtain the matrix components $\Delta_{AB\mu}^\nu = -2\eta_{\mu A}\delta_B^\nu$ and check that (11.45) then generates the correct rotations and shear transformations of any vector V , taking into account its argument. Now, for a spinor ψ , the Lie derivative is given as

$$\mathfrak{L}_X \psi = X^A \nabla_A \psi - \frac{1}{4} \nabla_A X_B \gamma^A \gamma^B \psi. \quad (11.47)$$

In the case that one antisymmetrises the above, $\gamma^A \gamma^B \rightarrow \gamma^{[A} \gamma^{B]}$, it is called the Kosmann lift. We obtain

$$\Delta_{AB}^{\frac{1}{2}} = -\frac{1}{2} \gamma_A \gamma_B = \eta_{AB} - \frac{1}{2} \gamma_{[A} \gamma_{B]}. \quad (11.48)$$

We can now plug the decomposition (10.15) into this spinor basis. We get

$$\hat{\omega} = -\frac{1}{4} \eta^{AB} \hat{D} \eta_{AB} + \frac{1}{4} \left(\omega_{AB} + \hat{\mathbf{K}}_{AB} - e_{[A} \cdot \hat{D} \eta_{B]C} e^C \right) \gamma^{[A} \gamma^{B]}. \quad (11.49)$$

In particular, it should be noted that non-metricity enters not only into the Weyl part, but also into the Lorentz part, since though $\hat{\mathbf{Q}}_{[AB]} = 0$, $\hat{\mathbf{L}}_{[AB]} \neq 0$. If one adopts the Kosmann lift, only the trace part is dropped.

Now we can return to the equation of motion (11.43). First let us remark that although now, the Clifford algebra is dictating that $\mathcal{Q}_\alpha^{\mu\nu} = \hat{\nabla}_\alpha \gamma^{(\mu} \gamma^{\nu)}$, the parallel transport does not preserve the matrices $\hat{\nabla}_\mu \gamma^\alpha = \hat{\mathcal{Q}}_{\mu\beta}{}^\alpha \gamma^\beta$; the matrices nevertheless are invariant with respect to the metric-covariant derivative, as usual. In the following, it is more transparent to write (11.49) in a coordinate system,

$$\hat{\Gamma}_\mu = -\frac{1}{4} \hat{\mathcal{Q}}_\mu + \frac{1}{4} \left(\omega_{\alpha\beta\mu} + \hat{\mathbf{K}}_{\alpha\beta\mu} - \hat{\mathcal{Q}}_{[\alpha\beta]\mu} \right) \gamma^{[\alpha} \gamma^{\beta]}, \quad (11.50)$$

noting, though, that $\omega_{\alpha\beta\mu} = e^A{}_\alpha e^B{}_\beta \omega_{AB\mu}$ is not a tensor. We immediately see that the trace part decouples from the action (11.42). This reflects the scale invariance of

massless spinors. However, the possible imaginary part of the trace would remain, leaving us with a U(1) gauge field to contemplate the geometric unification of gravitation and electromagnetism [29, 30] (a gravitoelectroweak extension was considered in [23]).

The property of Lorentz generators that $\gamma^0(\gamma^{[\mu}\gamma^{\nu]})^\dagger\gamma^0 = -\gamma^{[\mu}\gamma^{\nu]}$ is readily checked. Only a few more lines of Clifford algebra is required to show that the combination appearing in (11.43) reduces to

$$\{\gamma^\mu, \gamma^{[\alpha}\gamma^{\beta]}\} = -2i\epsilon^{\alpha\beta\mu\nu}\gamma_\nu\gamma^5. \quad (11.51)$$

Wrapping up the final result then we have

$$\gamma^\mu\partial_\mu\psi + \frac{1}{2\sqrt{-g}}\partial_\mu(\sqrt{-g}\gamma^\mu)\psi - \frac{1}{4}(\omega_{\alpha\beta\mu} + \hat{K}_{\alpha\beta\mu})i\epsilon^{\alpha\beta\mu\nu}\gamma_\nu\gamma^5\psi = 0. \quad (11.52)$$

All the non-metricity has disappeared. We mention that the Dirac equation has also been considered written directly in terms of the connection (11.49) [31–33]. However, that equation (which features non-metricity) does not follow from the Hermitean action (11.42) of a unitary theory. A derivation in an index-free formalism [34] seems to agree with our conclusion.

This is one of the most important arguments supporting purified gravity. In a generic Teleparallel Equivalent of General Relativity (11.13), there is both torsion and non-metricity. Whereas the latter does not appear in the spinor connection $\hat{\omega}$, the presence of the former should be stringently constrained. The case of TEGR is obviously ruled out, since there, matter would couple only to the Weitzenböck connection - so actually the right hand side in (11.20) is an ad hoc non-minimal coupling. In contrast, for the case of TEGR, Eq.(11.21) is exactly what the theory predicts. Even when the spacetime connection vanishes, $\hat{\Gamma}^\alpha{}_{\mu\nu} = 0$, matter moves along the metric geodesics, i.e. following the connection $\Gamma^\alpha{}_{\mu\nu}$, due to the peculiar property of fermions. In this way, causal structure is filtered into the reality of material objects “from nothing”.

Finally we comment on the case of gauge fields, where the same conclusion follows much more directly: promoting the kinetic term of (for simplicity, the Abelian) gauge field A_μ into manifest general linear covariance, $F_{\mu\nu} = 2\partial_{[\mu}A_{\nu]} \rightarrow 2\hat{\nabla}_{[\mu}A_{\nu]} = F_{\mu\nu} - \hat{T}^\alpha{}_{\mu\nu}A_\alpha$, makes no difference unless the $\hat{\nabla}_\mu$ has torsion that would spoil the gauge invariance.

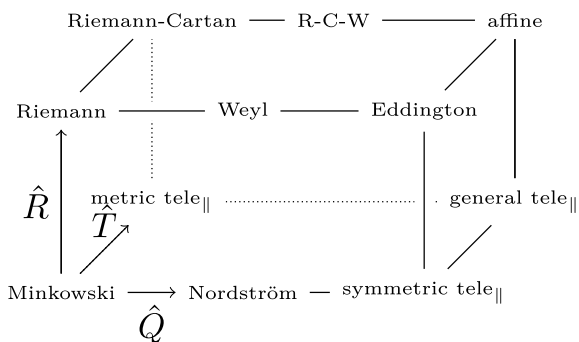
11.4 Modified Gravity

The results above suggest that the complementary perspectives to the theory of General Relativity could be very useful in unifying gravity with quantum mechanics and the other fundamental interactions of nature. The geometrical trinity also provides fresh starting points for building new extended theories of gravity. A plethora of

such theories have been proposed, motivated by the cosmological observations that cannot be explained by General Relativity without invoking exotic matter and energy components. Many of the extended gravity theories are also based on introducing additional fields into the gravitational sector [35]. Indeed, in the Riemannian corner of the trinity the only viable purely gravitational non-trivial modification is the well-known $f(R)$ theory, which is in fact is a scalar-tensor theory discussed in Chap. 5. Some of the limitations in generalising the action are due to the higher-derivative property of the curvature of the connection $\Gamma^\alpha_{\mu\nu} = g^{\alpha\beta}(g_{\beta(\mu,\nu)} - g_{\mu\nu,\beta}/2)$. While theories with an independent connection avoid this, the degrees of freedom in the connection can introduce ghosts unless they are suitably eliminated by symmetries. In any case, in the framework of metric-affine theories, where the connection is independent of the metric, there are at least in principle many new possibilities for extensions, as we learned in Chap. 10.

An obvious generalisation of Einstein’s theory in this framework is to consider more general curvature invariants in the action than the scalar R . Along the lines of $f(R)$ models, we can consider actions defined by a function $f(\hat{R})$. We recall from Chap. 10 that these theories have a very interesting structure, where the scalar \hat{R} does not introduce additional dynamics but can be determined algebraically from the trace of the field equations as a function of the matter fields. While such models could account for the accelerating expansion of the background Universe, they fail to reproduce the observed matter power spectrum [36] (see [37]). In Chap. 13 the hybrid metric-Palatini theories were introduced, which interpolate between the $f(\hat{R})$ and $f(R)$ models [38–44], and which (barring [45]) can also be recast as scalar-tensor theories. In the metric-affine context it is also possible to consider, without introducing higher derivatives, more generic curvature invariants than the Ricci scalar of the connection, such as in the so called Ricci-based models [46]. Such models do not reduce to simple scalar-tensor theories, but there is some evidence that they usually contain pathological degrees of freedom, at least unless one restricts to symmetric connections [47]. The latter case is labeled “Eddington” in Fig. 11.3 since symmetric affine connections had been utilised in, e.g., Born-Infeld type constructions of gravity [48]. Delhom and Rubiera-Garcia have reviewed some of the many cosmological applications of these models.

Fig. 11.3 Special cases of metric-affine geometries are obtained by switching on/off the curvature \hat{R}^A_B and/or the torsion \hat{T}^A and/or the non-metricity \hat{Q}_{AB} . The labels in the box refer to spacetime geometries in the context of gravity theories



As special cases of generic metric-affine formulations, the metric and the symmetric teleparallel geometries provide novel starting points for generalisation. As an example, it is natural to consider the nonlinear generalisation of (11.16),

$$S_{f(\mathbb{Q})} = -\frac{1}{2\kappa^2} \int d^4x \sqrt{-g} f(\mathbb{Q}), \quad (11.53)$$

which clearly reduces to (11.16) when $f = \mathbb{Q}$. The cosmological background equations of the $f(\mathbb{Q})$ models [49, 50] contain the same solutions as the extensively studied $f(\mathbb{T})$ models [7], but the evolution of cosmological perturbations and, consequently, the predicted large-scale structure of the Universe, can be considerably different [51]. The dark energy problem was also considered in the generalisation of the model with non-minimal matter couplings at cosmological scales [52–54], and the models might be relevant for dark matter at galactic scales as well [55, 56]. However, an action of the form (11.53) was shown to propagate two extra scalar degrees in the general cosmological background, but one of those decouples at the limit of de Sitter space [51]. This degree of freedom thus appears to be strongly coupled, which could be a problem for the viability of the model. Dialektopoulos classified the cosmological Noether symmetries as an action that can be an arbitrary function of the six invariants [57]. The special 5-parameter quadratic case had been dubbed Newer General Relativity [7]. Gravitational waves were recently considered in this quadratic theory [58, 59], although Conroy had analysed in detail the full spectrum of symmetric teleparallel gravity, including the ghost-free and singularity-free ultra-violet completions inspired by string field theory [60]. Some of the interesting classes of extensions in symmetric teleparallel gravity are models of conformal gravity [61, 62].

Modified gravity in the metric teleparallel corner of Fig. 11.3 has attracted considerable attention and was described in Chapter 14. Additionally, whilst investigations most often focus on astrophysical and cosmological phenomenology, some studies considering the theoretical consistency of teleparallel modified gravity have pointed out generic problems related to strong coupling [51, 63], formulation of the Cauchy problem [64, 65] and ghosts [7, 66]. In fact, in our opinion there still remains the open question that we could now pose as a theoretical challenge: *are there any consistent teleparallel modified gravity models that do not have a metric equivalent?*

References

1. A. Einstein, *The Meaning of Relativity*. Routledge Classics Series (Routledge, 2015)
2. J.B. Jiménez, L. Heisenberg, D. Iosifidis, A. Jiménez-Cano, T.S. Koivisto, General teleparallel quadratic gravity. *Phys. Lett. B* **805**, 135422 (2020). [arXiv:1909.09045](https://arxiv.org/abs/1909.09045)
3. R. Aldrovandi, J.G. Pereira, *Teleparallel Gravity*, vol. 173 (Springer, Dordrecht, 2013)
4. J.W. Maluf, The teleparallel equivalent of general relativity. *Ann. Phys.* **525**, 339–357 (2013). [arXiv:1303.3897](https://arxiv.org/abs/1303.3897)

5. J.M. Nester, H.-J. Yo, Symmetric teleparallel general relativity. *Chin. J. Phys.* **37**, 113 (1999). [arXiv:gr-qc/9809049](#)
6. M. Adak, M. Kalay, O. Sert, Lagrange formulation of the symmetric teleparallel gravity. *Int. J. Mod. Phys. D* **15**, 619–634 (2006). [arXiv:gr-qc/0505025](#)
7. J.B. Jiménez, L. Heisenberg, T. Koivisto, Coincident general relativity. *Phys. Rev. D* **98**(4), 044048 (2018). [arXiv:1710.03116](#)
8. J. Beltrán Jiménez, L. Heisenberg, T.S.. Koivisto, Teleparallel Palatini theories. *JCAP* **1808**, 039 (2018). [arXiv:1803.10185](#)
9. A. Einstein, *HAMILTONsches Prinzip und allgemeine Relativitätstheorie, Sitzungsberichte der Königlich Preußischen Akademie der Wissenschaften (Berlin), Seite 1111-1116* (1916)
10. E. Noether, Invariante variationsprobleme. *Nachrichten von der Gesellschaft der Wissenschaften zu Göttingen, Mathematisch-Physikalische Klasse* **1918**, 235–257 (1918)
11. J.B. Jiménez, L. Heisenberg, T.S. Koivisto, *The canonical frame of purified gravity*. [arXiv:1903.12072](#)
12. H. Ruegg, M. Ruiz-Altaba, The Stueckelberg field. *Int. J. Mod. Phys. A* **19**, 3265–3348 (2004). [arXiv: hep-th/0304245](#)
13. C.J. Isham, A. Salam, J.A. Strathdee, Nonlinear realizations of space-time symmetries, Scalar and tensor gravity. *Ann. Phys.* **62**, 98–119 (1971)
14. R. Percacci, The Higgs phenomenon in quantum gravity. *Nucl. Phys. B* **353**, 271–290 (1991). [arXiv:0712.3545](#)
15. R. Percacci, Gravity from a Particle Physicists’ perspective. *PoS ISFTG*, 011(2009). [arXiv:0910.5167](#)
16. C. Pagani, R. Percacci, Quantum gravity with torsion and non-metricity. *Class. Quant. Grav.* **32**(19), 195019 (2015). [arXiv:1506.02882](#)
17. R. Tresguerres, E.W. Mielke, Gravitational Goldstone fields from affine gauge theory. *Phys. Rev. D* **62**, 044004 (2000). [arXiv:gr-qc/0007072](#)
18. M. Leclerc, The Higgs sector of gravitational gauge theories. *Ann. Phys.* **321**, 708–743 (2006). [arXiv: gr-qc/0502005](#)
19. A. Tiemblo, R. Tresguerres, Gauge theories of gravity: the nonlinear framework. *Recent Res. Devel. Phys.* **5**, 1255 (2004). [arXiv: gr-qc/0510089](#)
20. S.A. Ali, S. Capozziello, Nonlinear realization of the local conform-affine symmetry group for gravity in the composite fiber bundle formalism. *Int. J. Geom. Meth. Mod. Phys.* **4**, 1041–1074 (2007). [arXiv:0705.4609](#)
21. H.F. Westman, T.G. Zlosnik, An introduction to the physics of Cartan gravity. *Ann. Phys.* **361**, 330–376 (2015). [arXiv:1411.1679](#)
22. T. Zlosnik, F. Urban, L. Marzola, T. Koivisto, Spacetime and dark matter from spontaneous breaking of Lorentz symmetry. *Class. Quant. Grav.* **35**(23), 235003 (2018). [arXiv:1807.01100](#)
23. T. Koivisto, M. Hohmann, T. Zlosnik, The general linear Cartan Khronon. *Universe* **5**(6), 153 (2019). [arXiv:1905.02967](#)
24. T. Koivisto, M. Hohmann, L. Marzola, *An Axiomatic Purification of Gravity*. [arXiv:1909.10415](#)
25. C. Cheung, *TASI Lectures on Scattering Amplitudes*, in *Proceedings, Theoretical Advanced Study Institute in Elementary Particle Physics : Anticipating the Next Discoveries in Particle Physics (TASI 2016): Boulder, CO, USA, June 6-July 1, 2016*, pp. 571–623 (2018). [arXiv:1708.03872](#)
26. J.W. Maluf, Dirac spinor fields in the teleparallel gravity: comment on ‘Metric affine approach to teleparallel gravity’. *Phys. Rev. D* **67**, 108501 (2003). [arXiv: gr-qc/0304005](#)
27. Y.N. Obukhov, J.G. Pereira, Lessons of spin and torsion: reply to ‘Consistent coupling to Dirac fields in teleparallelism’. *Phys. Rev. D* **69**, 128502 (2004). [arXiv: gr-qc/0406015](#)
28. E.W. Mielke, Consistent coupling to Dirac fields in teleparallelism: comment on ‘Metric-affine approach to teleparallel gravity’. *Phys. Rev. D* **69**, 128501 (2004)
29. T. Koivisto, An integrable geometrical foundation of gravity. *Int. J. Geom. Meth. Mod. Phys.* **15**, 1840006 (2018). [arXiv:1802.00650](#)
30. B. Janssen, A. Jiménez-Cano, Projective symmetries and induced electromagnetism in metric-affine gravity. *Phys. Lett. B* **786**, 462–465 (2018). [arXiv:1807.10168](#)

31. M. Adak, T. Dereli, L.H. Ryder, Dirac equation in space-times with nonmetricity and torsion. *Int. J. Mod. Phys. D* **12**, 145–156 (2003). [arXiv: gr-qc/0208042](#)
32. M. Adak, T. Dereli, L.H. Ryder, Possible effects of spacetime non-metricity on neutrino oscillations. *Phys. Rev. D* **69**, 123002 (2004). [arXiv: gr-qc/0303080](#)
33. M. Adak, Ö. Sert, M. Kalay, M. Sari, Symmetric teleparallel gravity: some exact solutions and spinor couplings. *Int. J. Mod. Phys. A* **28**, 1350167 (2013). [arXiv:0810.2388](#)
34. J.B. Formiga, C. Romero, Dirac equation in non-Riemannian geometries. *Int. J. Geom. Meth. Mod. Phys.* **10**, 1320012 (2013). [arXiv:1210.1615](#)
35. L. Heisenberg, A systematic approach to generalisations of General Relativity and their cosmological implications. *Phys. Rep.* **796**, 1–113 (2019). [arXiv:1807.01725](#)
36. T. Koivisto, The matter power spectrum in $f(r)$ gravity. *Phys. Rev. D* **73**, 083517 (2006). [arXiv:astro-ph/0602031](#)
37. T. Koivisto, Viable Palatini- $f(R)$ cosmologies with generalized dark matter. *Phys. Rev. D* **76**, 043527 (2007). [arXiv:0706.0974](#)
38. T. Harko, T.S. Koivisto, F.S.N. Lobo, G.J. Olmo, Metric-Palatini gravity unifying local constraints and late-time cosmic acceleration. *Phys. Rev. D* **85**, 084016 (2012). [arXiv:1110.1049](#)
39. I. Leanizbarrutia, F.S.N. Lobo, D. Saez-Gomez, Crossing SNe Ia and BAO observational constraints with local ones in hybrid metric-Palatini gravity. *Phys. Rev. D* **95**(8), 084046 (2017). [arXiv:1701.08980](#)
40. M. Vargas dos Santos, J.S. Alcaniz, D.F. Mota, S. Capozziello, Screening mechanisms in hybrid metric-Palatini gravity. *Phys. Rev. D* **97**(10), 104040 (2018). [arXiv:1712.03831](#)
41. B. Dănilă, T. Harko, F.S.N. Lobo, M.K. Mak, Spherically symmetric static vacuum solutions in hybrid metric-Palatini gravity. *Phys. Rev. D* **99**(6), 064028 (2019). [arXiv:1811.02742](#)
42. A. Wojnar, Polytropic stars in Palatini gravity. *Eur. Phys. J. C* **79**(1), 51 (2019). [arXiv:1808.04188](#)
43. K.A. Bronnikov, *Spherically symmetric black holes and wormholes in hybrid metric-Palatini gravity*. [arXiv:1908.02012](#)
44. J. L. Rosa, S. Carloni, J.P.S. Lemos, *The cosmological phase space of generalized hybrid metric-Palatini theories of gravity*. [arXiv:1908.07778](#)
45. L. Amendola, K. Enqvist, T. Koivisto, Unifying Einstein and Palatini gravities. *Phys. Rev. D* **83**, 044016 (2011). [arXiv:1010.4776](#)
46. V.I. Afonso, G.J. Olmo, D. Rubiera-Garcia, Mapping Ricci-based theories of gravity into general relativity. *Phys. Rev. D* **97**(2), 021503 (2018). [arXiv:1801.10406](#)
47. J. Beltrán Jiménez, A. Delhom, *Ghosts in metric-affine higher order curvature gravity*. [arXiv:1901.08988](#)
48. J. Beltran Jimenez, L. Heisenberg, G.J. Olmo, D. Rubiera-Garcia, Born–Infeld inspired modifications of gravity. *Phys. Rep.* **727**, 1–129 (2018). [arXiv:1704.03351](#)
49. J. Lu, X. Zhao, G. Chee, Cosmology in symmetric teleparallel gravity and its dynamical system. *Eur. Phys. J. C* **79**(6), 530 (2019). [arXiv:1906.08920](#)
50. R. Lazkoz, F.S.N. Lobo, M. Ortiz-Baño, V. Salzano, *Observational constraints of $f(Q)$ gravity*. [arXiv:1907.13219](#)
51. J.B. Jiménez, L. Heisenberg, T.S. Koivisto, S. Pekar, *Cosmology in $f(Q)$ geometry*. [arXiv:1906.10027](#)
52. T. Harko, T.S. Koivisto, F.S.N. Lobo, G.J. Olmo, D. Rubiera-Garcia, Coupling matter in modified Q gravity. *Phys. Rev. D* **98**(8), 084043 (2018). [arXiv:1806.10437](#)
53. T. Harko, T.S. Koivisto, G.J. Olmo, F.S.N. Lobo, R.-G. Diego, *Novel couplings between non-metricity and matter, in 15th Marcel Grossmann Meeting on Recent Developments in Theoretical and Experimental General Relativity, Astrophysics, and Relativistic Field Theories (MG15) Rome, Italy, July 1-7, 2018* (2019). [arXiv:1901.00805](#)
54. Y. Xu, G. Li, T. Harko, S.-D. Liang, $f(Q, T)$ gravity. *Eur. Phys. J. C* **79**(8), 708 (2019). [arXiv:1908.04760](#)
55. M. Milgrom, *Noncovariance at low accelerations as a route to MOND*. [arXiv:1908.01691](#)
56. F. D’Ambrosio, M. Garg, L. Heisenberg, *Non-linear extension of non-metricity scalar for MOND*. [arXiv:2004.00888](#)

57. K.F. Dialektopoulos, T.S. Koivisto, S. Capozziello, Noether symmetries in symmetric teleparallel cosmology. *Eur. Phys. J. C* **79**(7), 606 (2019). [arXiv:1905.09019](#)
58. M. Hohmann, C. Pfeifer, J.L. Said, U. Ualikhanova, Propagation of gravitational waves in symmetric teleparallel gravity theories. *Phys. Rev. D* **99**(2), 024009 (2019). [arXiv:1808.02894](#)
59. I. Soudi, G. Farrugia, V. Gakis, J. Levi Said, E..N. Saridakis, Polarization of gravitational waves in symmetric teleparallel theories of gravity and their modifications. *Phys. Rev. D* **100**(4), 044008 (2019). [arXiv:1810.08220](#)
60. A. Conroy, T. Koivisto, The spectrum of symmetric teleparallel gravity. *Eur. Phys. J. C* **78**(11), 923 (2018). [arXiv:1710.05708](#)
61. D. Iosifidis, T. Koivisto, *Scale transformations in metric-affine geometry*. [arXiv:1810.12276](#)
62. V. Gakis, M. Krššák, J. Levi Said, E..N. Saridakis, Conformal gravity and transformations in the symmetric teleparallel framework. *Phys. Rev. D* **101**(6), 064024 (2020). [arXiv:1908.05741](#)
63. J. B. Jiménez and K. F. Dialektopoulos, *Non-Linear Obstructions for Consistent New General Relativity*. [arXiv:1907.10038](#)
64. W.-H. Cheng, D.-C. Chern, J.M. Nester, Canonical analysis of the one parameter teleparallel theory. *Phys. Rev. D* **38**, 2656–2658 (1988)
65. R. Ferraro, M.J. Guzmán, Hamiltonian formalism for f(T) gravity. *Phys. Rev. D* **97**(10), 104028 (2018). [arXiv:1802.02130](#)
66. T. Koivisto, G. Tsimperis, *The spectrum of teleparallel gravity*. [arXiv:1810.11847](#)

Chapter 12

Palatini Theories of Gravity and Cosmology



Adrià Delhom and Diego Rubiera-Garcia

In the Palatini formulation, the metricity (or Riemannian) postulate, which renders the affine connection as a secondary object completely determined by the metric, is abandoned to view metric and connection as equally fundamental fields in describing the gravitational interaction. Indeed, whether the affine structure is determined by the metric one or otherwise is a fundamental question in the understanding of the gravitational interaction as a manifestation of a curved spacetime, whose associated phenomenology has begun to be unravelled very recently. A large family of Palatini theories of gravity can be nicely accommodated by considering those Lagrangian densities built out of the (symmetric part of the) Ricci tensor and its contractions with the metric. More specifically, such theories are constructed as traces of powers of the object $M^\mu{}_\nu \equiv g^{\mu\alpha} R_{\alpha\nu}$ and include, as particular examples, GR itself, $f(R)$ theories, Ricci-squared theories $f(R, R_{\mu\nu} R^{\mu\nu})$, or Born-Infeld-inspired theories of gravity [1, 2].

An Einstein-frame representation for this family of theories can be conveniently introduced as

$$G^\mu{}_\nu(q) = \frac{\kappa^2}{|\Omega|^{1/2}} \left[T^\mu{}_\nu - \left(\mathcal{L}_G + \frac{T}{2} \right) \delta^\mu{}_\nu \right], \quad (12.1)$$

where the independent connection Γ is Levi-Civita of the auxiliary metric $q_{\mu\nu}$ (that is, $\nabla_\alpha(\sqrt{-q}q^{\mu\nu}) = 0$), $T^\mu{}_\nu$ represents the energy-momentum tensor of the matter

A. Delhom (✉)

Departamento de Física Teórica and IFIC, Centro Mixto Universidad de Valencia - CSIC,
Universidad de Valencia, 46100 Burjassot Valencia, Spain
e-mail: adria.delhom@uv.es

D. Rubiera-Garcia

Departamento de Física Teórica and IPARCOS, Universidad Complutense de Madrid, E-28040
Madrid, Spain
e-mail: drubiera@ucm.es

fields (with T its trace) and $|\Omega|$ is the determinant of the *deformation* matrix Ω , which relates the auxiliary and spacetime metrics as $q_{\mu\nu} = g_{\mu\alpha}\Omega^\alpha{}_\nu$ and can always be written on-shell as a function of the matter fields and (possibly) the spacetime metric itself (and so does the gravitational Lagrangian \mathcal{L}_G). This (projectively-invariant) class of theories, dubbed as *Ricci-based gravities* (RBGs) features a number of relevant properties: second-order field equations and absence of ghost-like instabilities (with the projective symmetry requirement playing a key role in incorporating this feature [3, 4]), and reduction to GR equations in vacuum,¹ which ensures their compatibility with Solar System observations and the propagation of gravitational waves at the speed of light in vacuum. In high-energy density environments, however, the dynamics encoded in the new couplings engendered by the matter fields yield relevant deviations from GR results that can be exploited, in particular, in cosmological scenarios, which we review in this section for different kinds of RBG theories.

For completeness, we will write down the modified Friedmann equations for isotropic cosmologies and for the isotropic branch of solutions of $\Omega^\mu{}_\nu$ of the form $\Omega^\mu{}_\nu = \text{diag}(\Omega_0, \Omega_x, \Omega_x, \Omega_x)$. Assuming a FLRW metric of the form $ds_g^2 = -dt^2 + a^2(t)d\vec{x}^2$ we will have $ds_q^2 = -\Omega_0 dt^2 + \tilde{a}^2(t)d\vec{x}^2$ with $\tilde{a}^2 = \Omega_x a^2$. By using (12.1) and the fact that $M^\mu{}_\nu$ is also diagonal $M^\mu{}_\nu = \text{diag}(M, M_x, M_x, M_x)$, we arrive at the following modified Friedman equation

$$6H^2 = \frac{3\frac{\Omega_0}{\Omega_x}M_x - M_0}{\left[1 - 3(\rho + p)(\partial_\rho \log \sqrt{\Omega_x} + c_s^2 \partial_p \log \sqrt{\Omega_x})\right]^2}, \quad (12.2)$$

where M_i and Ω_i can be written in terms of ρ and p by using the field equations of the theory [5].

12.1 Smoothing Out Cosmological Singularities

A great deal of activity within this context is based upon the removal or smoothing out of cosmological singularities encountered in GR. While it is known that within GR the singularities cannot be avoided for matter fields that satisfy the energy conditions, this is not the case in Palatini RBGs. This can be traced back to Einstein-frame representation (12.1) of RBGs, where the matter fields become non-linearly interacting. Presumably, if one couples matter that satisfies the energy conditions to an RBG, it is plausible that in the passage to the Einstein frame the modified matter sector violates some of the energy conditions. Thus, the removal of cosmological singularities can be understood in light of the equivalence between RBGs and GR with non-linearly modified matter sectors that have recently been introduced in a series of works [1, 2, 6–9].

¹ Although the equations for the deformation matrix $\Omega^\mu{}_\nu$ are non-linear, and there might be several branches of solutions, there always exists a branch which recovers GR in vacuum [5].

The main focus of research on smoothing cosmological singularities has been the finding of bounces replacing the Big Bang singularity. One of the first works builds an $f(R)$ action such that the corresponding cosmological evolution matches that predicted by Loop Quantum Cosmology with a scalar field, i.e., a singularity-free bouncing cosmology [10]. The existence of such an action explicitly demonstrated the covariance of LQC at the background evolution level. The next obvious step was to perform an analysis allowing conditions to be found that a generic Palatini $f(R)$ has to satisfy in order to describe such non-singular bouncing cosmologies. This was done in [11], where it was found that for flat models either the condition $f_R = 0$ or $\kappa^2 \rho + (Rf_R - f)/2 = 0$ (with $w > -1$) have to be satisfied at some point in the evolution in order to find a bounce (here ρ is the energy density of the total or the dominant sector at the bounce phase).

In the non-flat universe case the discussion is more involved, although bouncing solutions can be found under quite generic conditions. The particular case of $R + R^2/R_P$ (with R_P being Planck's curvature) is also analysed, finding bouncing solutions for flat as well as non-flat universes. Also adding torsion, a Nieh-Yan term and a dynamical Immirzi field to quadratic $f(R)$ gravity yields bouncing solutions in some branch of the theory [12]. After finding such bouncing solutions one must guarantee their stability against perturbations. A general formalism for computing the evolution of perturbations in $f(R)$ models was devised in [13], with the result that solutions with $f_R = 0$ at the bounce have an unstable behaviour in a flat universe with dust, although the behaviour can improve in the non-flat case. Nonetheless, it is noticed that the relation between Jordan and Einstein frames becomes ill-defined at $f_R = 0$, and that the perturbation expansion is not valid at the bounce, which implies that the unstable behaviour could be due to the breakdown of the perturbative expansion. A non-perturbative analysis is therefore necessary.

Moving on from $f(R)$, Eddington-inspired Born-Infeld (EiBI) gravity has been the pivotal point of many discussions of bouncing solutions and their perturbations. A cosmological bounce was indeed shown to arise within this theory for a radiation fluid in the early work of [14]. In several subsequent works [15–17], linear perturbations on a cosmological background were studied. It was found that that linear tensor perturbations are singular for the EiBI parameter $\epsilon < 0$ [15], but that they can be stable for $\epsilon > 0$ and a time-varying equation of state parameter w [16].

The evolution of a universe driven by a perfect fluid within this model was investigated in [18], finding that for $w > 0$ there is a non-singular initial state of finite size at which $H = 0$. For $w = 0$, the Universe approaches a de Sitter evolution at high energy densities (early times). Other bouncing cosmologies can be found in power-law extensions of the fundamental object defining EiBI gravity [19] or in elementary polynomial extensions [20], where for $-2/3 < w \leq 0$ a quasi de Sitter inflationary phase can also be achieved.

As shown in [19, 21], in all Palatini-type models tensorial perturbations propagate upon the auxiliary metric $q_{\mu\nu}$ (and not $g_{\mu\nu}$), which entails that for all these power-law type extensions of EiBI gravity, a severe instability is found for bouncing solutions ($\epsilon < 0$) due to a strong coupling problem that yields a diverging speed of propagation.

A milder instability is found for loitering solutions ($\epsilon > 0$, which interpolate with an asymptotic Minkowski past) due to the vanishing of the propagation speed.

It is, moreover, seen that such instabilities might be cured by adding higher-derivative terms to the pure EiBI theory and its power-law extensions, and that for elementary polynomial extensions the propagation speed remains non-vanishing, thus solving the problem [21]. A combination of EiBI+ $f(R)$ has also been investigated in [22]. This allows selection of the parameters in R^n -type terms (but not other terms such as those of $Tr[(R^\mu{}_\nu)^n]$) of the curvature expansion of the EiBI Lagrangian. It is seen that bouncing solutions are robust against such modifications of the coefficients for $\epsilon < 0$, while for $\epsilon > 0$ the robustness is lost. It is also shown that these modifications can account for an inflationary stage without the need of extra degrees of freedom. Similar results are found for an $f(|\Omega|)$ extension in [23]. The stability of an Einstein static universe filled with a perfect fluid within EiBI has also been studied in [24]. There is no spatially flat Einstein universe and it is seen that scalar perturbations are unstable in Einstein closed universe, while Einstein open universes could be stable if $\epsilon < 0$ and $\omega < -1$.

The possibility of resolving other cosmological singularities than the Big Bang within Palatini theories such as future cosmological singularities has also been investigated. It has been shown in [25] that for the spacetime metric the Big Rip and Little Rip singularities driven by phantom dark energy are not cured, but some other phantom dark energy-related singularities occurring in GR are smoothed out. For the auxiliary metric, only a past type IV singularity persists on a tiny region of the parameter space, while all the other singularities disappear. Furthermore, bound structures are found to be destroyed near Big Rip and Little Rip singularities, while they can remain bounded at sudden, Big Freeze and type IV singularities. Moreover, by exploiting the cosmographic approach, it is concluded that EiBI is a good alternative that smoothes curvature singularities occurring in GR [25].

Recently, a modified Wheeler-DeWitt equation was derived from the EiBI Hamiltonian, and it is seen that quantum effects could avoid the Big Rip singularity when it is sourced either by phantom dark energy or by a phantom scalar field [26, 27]. Additionally, future singularities within the quadratic $f(R)$ model have been investigated by finding a new type of sewn singularities, where the first derivative of the potential (in scalar-tensor representation) has a discontinuity. However, the model appears to be disfavoured as compared to Λ CDM regarding Ω_γ [28].

12.2 Inflationary Models

Inflation in the quadratic $f(R)$ model has been considered in several works. In [29] it was shown that the new corrections to GR modify the kinetic-energy dominated epoch of the inflationary regime, constraining the kinetic energy density of the scalar field to be sub-Planckian, while the potential-energy dominated epoch is not affected by these corrections. Since Palatini $f(R)$ models have no extra propagating degrees of freedom, one way to trigger inflation is to consider non-minimal couplings.

With this ingredient, several potentials such as quadratic, quasi-scale invariant Coleman-Weinberg, induced gravity model, or Higgs-type, were considered within the slow roll inflationary paradigm, all of which turn out to be viable models when compared to Planck's data [30]. The predictions of these models deviate from those of their metric counterparts in the preheating era in terms of resonance bands and transfer of energy from the scalar field to fluctuations [31], as well as in the number of e-folds [32, 33]. The quadratic $f(R)$ model also yields a suppression of the tensor-scalar-ratio and the tensor spectral index [34], which are compatible with Planck's data [35]. Further analysis of this question [36] shows that, for Higgs inflation, the reduction of the number of e-folds and smaller spectral index is channelled through tachyonic production of Higgs excitation, while preheating occurs almost instantaneously in such a way that almost all of the background energy density at the end of inflation is turned into radiation. Though in both the metric and the Palatini formulations the Universe evolves into a slow-roll inflationary era, discriminating them could be possible via a stochastic background of primordial gravitational waves in future high-frequency detectors. These conclusions also hold when the inflation potential is considered a periodic function of the inflaton field [37]. On the other hand, $f(R)$ models with $\alpha R^m - \beta/R^n$ terms are able to generate an inflationary epoch, although this cannot be followed by a radiation era [38].

Regarding EiBI gravity, in [39] it was coupled to a scalar field with a quadratic potential, where it was shown to provide a natural precursor of inflation. This is due to the fact that the maximal pressure state (MPS) of the Universe in this theory, though being non-singular, is unstable and evolves to an inflationary period. The tensor-to-scalar ratio within this theory is smaller than in GR [40, 41], while tensor perturbations give similar results to standard chaotic inflation [42]; however, if the attractor of the model does not account for 60 e-folds, then the perturbations near the MPS have to be taken into account in explaining the behaviour of low-angular modes. High- k modes show a similar behaviour to those in the attractor regime, but low- k modes are enhanced with respect to standard inflation, which could serve as a discriminator.

Furthermore, potentials with asymptotic form ϕ^{2+2n} are seen to allow for a non-singular initial state for $n \leq 0$, leading to an inflationary epoch for $-1 \leq n \leq 2$ [43]. In [44] a large (though constrained) value of ϵ is considered to analyse the behaviour of scalar and tensor perturbations within the strong gravity regime of the ϕ^2 model. The scalar power spectrum receives little corrections, while the tensor power spectrum, as well as the tensor-to-scalar ratio, can be suppressed significantly with respect to GR+ ϕ^2 . The correction to the spectral index also fits well with observations, and therefore, although the ϕ^2 model is ruled out within GR, it is not within EiBI gravity. An inflationary model for EiBI coupled to a Born-Infeld-like scalar field has also been considered in [45], for which a particular form of the kinetic term is chosen, and it is seen to satisfactorily fit late-time acceleration for any sign of ϵ .

Different behaviours for the early Universe may arise for the different sign of ϵ , but only a particular example is treated. As shown in [46], inflation in EiBI gravity can also be induced by gravitating dust, with a graceful exit naturally provided by the dilution of the matter density. Reheating can be implemented if it is assumed that the

dust components conform an unstable chain that ends by decaying in radiation, with two coexisting dust components being the minimum amount of components that give predictions compatible with observations. This scenario is predictive thanks to the dependence of background evolution in the sound speed and, in particular, it predicts no primordial gravitational waves, therefore it could be ruled out if B-modes are found within the CMB. By contrast to Palatini $\alpha R^m - \beta/R^n$ models, EiBI+ $f(R)$ gravity for an FLRW background can generate an inflationary epoch followed by a radiation era, as shown in [47], using a dynamical systems approach. There it is seen how an initial radiation-dominated epoch can be followed by inflation and evolve into radiation-dominated, matter-dominated and accelerated expansion eras. Similar conclusions apply for a Bianchi I cosmology within this theory.

In [22] it is shown that the fact that an inflationary stage without extra degrees of freedom can be achieved in EiBI+ $f(R)$ can be traced back to the possibility introduced by the $f(R)$ term to modify the R^n coefficients of the curvature expansion of the EiBI Lagrangian. Other models such as $R + (R_{\mu\nu}R^{\mu\nu})^n$ corrections have also been shown to account for an inflationary epoch if $n > 3/4$ [48], although they have not received much attention in the literature regarding the inflationary scenario. It has also been argued in [16] that bouncing models in EiBI gravity can by themselves account for the solution of the typical problems solved by inflation (without actually having an inflationary phase). Particularly, if the contracting branch lasts long enough, this could solve the horizon problem, as well as the size age and entropy problems. Given that the Universe meets the maximum density after the contracting branch, the flatness problem can also be alleviated. If the bounce occurs at a scale below Grand Unification, the monopole problem can also be solved. Furthermore, a matter-bounce scenario can generate a nearly scale-invariant primordial spectrum.

12.3 Background Evolution, Late-Time Acceleration, and Observational Constraints

The first relevant cosmological application of Palatini theories of gravity was a possible explanation of late-time accelerated expansion without the need of a cosmological constant, driven by the simple inverse model $R - \alpha^2/R$ [49]. It was shown that the Palatini formulation of this theory is free from ghosts, and when coupled to dust it approaches a de Sitter Universe exponentially fast at late times. Shortly after its birth, however, this model was ruled out as an explanation for cosmic speed-up due to the appearance of new matter interactions that were not in agreement with observations [50]. Moreover, the approach employed in [50] was criticized later in [51] on the basis that field re-definitions may not be allowed in curved spacetime.

Cosmologically accelerated solutions at late-times without dark energy have been implemented in other Palatini models. The FLRW cosmology of a generic Palatini $f(R)$ and the possibility of using generic $f(R)$ infrared corrections to GR (beyond the μ^4/R one) as an explanation of the cosmic speed-up problem was devised in

[52, 53]. In [48], explicit solutions for the models R^n , $\ln(R)$, and $\sinh^{-1}(R)$ were found, and it is explicitly seen that $f(R)$ corrections that grow at low curvatures in the Palatini formalism lead to cosmic speed-up. Moreover, corrections to GR of the form $f(R_{\mu\nu}R^{\mu\nu})$ were analysed in [48] and, in particular, $(R_{\mu\nu}R^{\mu\nu})^n$ corrections were shown to account for cosmic speed-up for $n < 0$. Indeed, after much effort it was shown that in (Palatini-type) infrared modifications to GR that account for late-time acceleration, the behaviour of low-curvature $f(R)$ corrections to GR aimed at explaining the cosmic speed-up (with μ^4/R as a particular case) inevitably leads to instabilities in the hydrogen atom, forcing its fundamental state to decay after a short time and thus being incompatible with experiments [54]. In the same work it was also shown that ultraviolet $f(R)$ corrections to GR do not introduce these instabilities, and thus are still not excluded.

Palatini $f(R)$ and $f(R^{\mu\nu}R_{\mu\nu})$ cosmological models have also been confronted with different sets of observational data. For the model $R + \lambda_1 \exp(R/\lambda_2)$, the CMB, the matter power spectrum [55] and linear perturbations [56] have been considered. For the CMB it is shown that the integrated Sachs-Wolfe effect receives significant corrections for intermediate multipole moments $l \sim (10, 500)$, recovering the Λ CDM behaviour for both larger and smaller l 's. The matter power spectrum picks up oscillatory corrections for high momentums, leading to effective pressure fluctuations and a diminished growth of small-scale density perturbations [55]. In [56], WMAP, SNLS and SDSS data are used to constrain Palatini $\alpha(-R)^\beta$ corrections to GR, being able to substantially reduce the parameter space by demanding small departures from Λ CDM. The matter power spectrum was also computed for this model in [57], where the observational constraints were found to favour values of the parameter close to Λ CDM. For the model $\alpha(-R)^\beta$, constraints to (α, β) parameters are obtained from CMB data, with a best fit of $\alpha = -3.6$ and $\beta = 0.09$, and the predictions of this model lying within 1σ from Λ CDM model predictions [58].

R^n models were analysed in [59], finding that super-horizon density perturbations evolve as in GR, but sub-horizon evolutions differ from it. Later on, by studying the evolution of the deceleration parameter, it was seen that positive values of n representing ultraviolet corrections to GR are very suppressed by cosmographic constraints [60]. The model $\sqrt{R^2 - R_0^2}$ has been confronted with data from type Ia supernovae, CMB, BAO and large-scale structure formation [61]. Using both separate and combined analysis, similar results to the Λ CDM for the best fit of $R_0 \sim (6.3 \pm 0.2)H_0^2$ are obtained, although inconsistencies with the age of the quasar APM 08279+5255 are found. A generalisation of the form $(R^n - R_0^n)^{1/n}$ was later analysed in [62], with the same data plus data from gas mass fraction, in galaxy clusters. The best fits are $n = 0.98 \pm 0.08$ and $R_0 \sim (4.4 \pm 0.4)H_0^2$, being also close to Λ CDM (note that for $n = 1$ this model is exactly GR+ Λ with $R_0 = 2\Lambda$), but the same problem for the quasar APM 08279+5255 arises.

The quadratic + inverse $f(R)$ model was compared to SNIa data using the SNLS catalogue of 115 SNIa in [63] and the Union2.1 catalogue of 580 SNIa [64], whose best fit has large confidence intervals, with the conclusion that there is too much degeneracy in the space of parameters to fit them all by just considering SNIa data

[65]. We point out that the analysis of the Hubble drift (the relation between the Hubble parameter and the redshift) of this model gives a different prediction for large z as compared to Λ CDM paradigm [66].

Corrections of the form β/R^n , $\alpha \ln(R) - \beta$, which are able to generate phase transitions corresponding to the radiation-matter-dark energy dominated eras, were constrained with SNIa and BAO data in [38]. For the model including Ricci-squared corrections $R + F(R_{\mu\nu}R^{\mu\nu})$, the background evolution is obtained by interpreting the corrections to GR as an effective stress-energy tensor [67]. A particular power-law model $F = \alpha(R_{\mu\nu}R^{\mu\nu})^\beta$ is then confronted to SNIa luminosity distance and CMB shift parameter data, leading to a preferred small positive value for β at 95% confidence level, but with the standard Λ CDM lying in the 68% confidence level. Late-time matter density perturbations growth is also analysed within the model, finding similar results to $f(R)$, having also an effective scale-dependent sound-speed-like term in the equations.

Cosmographic approaches have also been used to constraint these models. This is the case with $f(R)$ models using power-law forms [68], while an analysis of more general models can be found at [69]. Via the cosmographic approach, for $R +$ power-law and $R +$ logarithmic models, their parameters are fitted using CMB, SNIa and BAO data, together with Hubble parameter estimations, finding that these models can be made compatible with the right sequence of cosmological eras but with large confidence intervals [70].

Linear scalar perturbations in the matter-dominated era and large-scale structure formation within EiBI gravity are studied in [71]. The growth rate deviates (it is suppressed for $\epsilon > 0$ and enhanced for $\epsilon < 0$) from Λ CDM at early times (high energy-densities) and the deviation increases with k , but as the Universe expands, it quickly approaches the Λ CDM prediction.

The early-times deviations are insignificant if one takes into account the tightest constraints on ϵ . The influence of the integrated SW effect on the CMB power spectrum is seen to have no deviations from Λ CDM. In [72], BBN data was used to constrain the free parameter of EiBI, finding the bound $\epsilon \leq 6 \times 10^8 \text{ m}^5 \text{ kg}^{-1} \text{ s}^{-2}$ (where $\epsilon > 0$ was assumed), although it is much weaker than other bounds from astrophysical scenarios, nuclear physics or high-energy experiments [73–76]. FRWL solutions in a model combining an EiBI + $f(R)$ were found in [47] by means of a dynamical systems analysis with several choices for $f(R)$ (quadratic, inverse, power-law), finding a plethora of accelerated/decelerated solutions.

Additionally, a hybrid version of EiBI gravity was introduced in [77], where it was found to reproduce both late-time acceleration and flat rotation curves. In [78] it was also shown that in this theory dark matter effects are relevant at the linearized cosmological level, which agrees with observations on large scales.

Cosmological effects were also analysed in [79], finding that although the growth of structure occurs as in Λ CDM, if the theory is demanded to produce cosmic accelerated expansion then the gravitational potentials grow (and some combinations diverge), leading to an enhancement of the integrated Sachs-Wolfe effect that does not match the data. However, if the theory is not demanded to reproduce dark energy effects but dark matter effects only, then the entire evolution is indistinguishable from

Λ CDM cosmology. In [80], WMAP7, BAO and SNIa data are used to conclude that the model cannot be used as an explanation for both dark energy and dark matter either. In [81] an analysis of Bianchi I cosmology is made within this theory, finding that the isotropic solution is an attractor, according with the data, but the decay of the shears is damped-oscillations-like.

Cosmological models corresponding to gravity theories with non-minimal matter-curvature couplings have also been analysed. For instance, in $f(R, T)$ gravity, using quadratic and inverse forms for the $f(R)$ sector, de Sitter type solutions at late times are found [82]. Other non-minimal couplings of the form $f(R) + F(R)L_\phi$, as considered in [83], were used in [84] in the more general class of models $f(R, \phi)$ to find that the amplitude of vector and tensor perturbations gets modulated by a factor depending on f_R , and also that a damping term appears for gravitational waves. Scalar perturbations get a more complex modification, and it is also seen that an effective pressure gradient appears when the expansion of the Universe is driven by non-linear curvature terms, which is problematic when compared to structure formation data.

Considering models including torsion in $f(R)$ theories, their incorporation within this framework yields hard equations to crack [85], although some preliminary ideas were considered in [86, 87]. For instance, the torsional degrees of freedom can be treated as a scalar field, in such a way that a cosmological toy model can be constructed, where torsion dynamically determines a relation between the amounts of dark matter and dark energy at present times [88].

Finally, accelerated cosmologies can also be found in a two-parameter scalar-tensor theory with derivative coupling of the scalar field to the curvature scalar and to the Ricci tensor [89]. More general models can be considered: for instance, assuming an anisotropic deformation matrix in general RBG theories yields the result that when the spacetime metric describes a standard FLRW metric, the auxiliary one describes a Bianchi type-I [90].

References

1. V.I. Afonso, C. Bejarano, J. Beltran Jimenez, G.J. Olmo, E. Orazi, The trivial role of torsion in projective invariant theories of gravity with non-minimally coupled matter fields. *Class. Quant. Grav.* **34**(23), 235003 (2017). [arXiv:1705.03806](https://arxiv.org/abs/1705.03806)
2. J. Beltran Jimenez, L. Heisenberg, G.J. Olmo, D. Rubiera-Garcia, Born-Infeld inspired modifications of gravity. *Phys. Rept.* **727**, 1–129 (2018). [arXiv:1704.03351](https://arxiv.org/abs/1704.03351)
3. J. Beltrán Jiménez, A. Delhom, Ghosts in metric-affine higher order curvature gravity. *Eur. Phys. J. C* **79**(8), 1–7 (2019). [arXiv:1901.08988](https://arxiv.org/abs/1901.08988)
4. J.B. Jiménez, A. Delhom, Instabilities in metric-affine theories of gravity with higher order curvature terms. *Eur. Phys. J. C* **80**(6), 585 (2020). [arXiv:2004.11357](https://arxiv.org/abs/2004.11357)
5. J.B. Jiménez, D. de Andrés, A. Delhom, Anisotropic deformations in a class of projectively-invariant metric-affine theories of gravity. *Class. Quant. Grav.* **37**(22), 225013 (2020). [arXiv:2006.07406](https://arxiv.org/abs/2006.07406)
6. V.I. Afonso, G.J. Olmo, E. Orazi, D. Rubiera-Garcia, Mapping nonlinear gravity into General Relativity with nonlinear electrodynamics. *Eur. Phys. J. C* **78**(10), 866 (2018). [arXiv:1807.06385](https://arxiv.org/abs/1807.06385)

7. V.I. Afonso, G.J. Olmo, E. Orazi, D. Rubiera-Garcia, Correspondence between modified gravity and general relativity with scalar fields. *Phys. Rev. D* **99**(4), 044040 (2019). [arXiv:1810.04239](#)
8. V.I. Afonso, G.J. Olmo, D. Rubiera-Garcia, Mapping Ricci-based theories of gravity into general relativity. *Phys. Rev. D* **97**(2), 021503 (2018). [arXiv:1801.10406](#)
9. A. Delhom, G.J. Olmo, E. Orazi, Ricci-Based Gravity theories and their impact on Maxwell and nonlinear electromagnetic models. *JHEP* **11**, 149 (2019). [arXiv:1907.04183](#)
10. G.J. Olmo, P. Singh, Effective Action for Loop Quantum Cosmology a la Palatini. *JCAP* **0901**, 030 (2009). [arXiv:0806.2783](#)
11. C. Barragan, G.J. Olmo, H. Sanchis-Alepuz, Bouncing Cosmologies in Palatini $f(R)$ Gravity. *Phys. Rev. D* **80**, 024016 (2009). [arXiv:0907.0318](#)
12. F. Bombacigno, G. Montani, Big bounce cosmology for Palatini R^2 gravity with a Nieh-Yan term. *Eur. Phys. J. C* **79**(5), 405 (2019). [arXiv:1809.07563](#)
13. T.S. Koivisto, Bouncing Palatini cosmologies and their perturbations. *Phys. Rev. D* **82**, 044022 (2010). [arXiv:1004.4298](#)
14. M. Banados, P.G. Ferreira, Eddington's theory of gravity and its progeny. *Phys. Rev. Lett.* **105**, 011101 (2010). [arXiv:1006.1769](#). [Erratum: *Phys. Rev. Lett.* 113, no. 11, 119901(2014)]
15. C. Escamilla-Rivera, M. Banados, P.G. Ferreira, A tensor instability in the Eddington inspired Born-Infeld Theory of Gravity. *Phys. Rev. D* **85**, 087302 (2012). [arXiv:1204.1691](#)
16. P.P. Avelino, R.Z. Ferreira, Bouncing Eddington-inspired Born-Infeld cosmologies: an alternative to Inflation? *Phys. Rev. D* **86**, 041501 (2012). [arXiv:1205.6676](#)
17. K. Yang, X.-L. Du, Y.-X. Liu, Linear perturbations in Eddington-inspired Born-Infeld gravity. *Phys. Rev. D* **88**, 124037 (2013). [arXiv:1307.2969](#)
18. I. Cho, H.-C. Kim, T. Moon, Universe Driven by Perfect Fluid in Eddington-inspired Born-Infeld Gravity. *Phys. Rev. D* **86**, 084018 (2012). [arXiv:1208.2146](#)
19. S.D. Odintsov, G.J. Olmo, D. Rubiera-Garcia, Born-Infeld gravity and its functional extensions. *Phys. Rev. D* **90**, 044003 (2014). [arXiv:1406.1205](#)
20. J. Beltran Jimenez, L. Heisenberg, G.J. Olmo, Infrared lessons for ultraviolet gravity: the case of massive gravity and Born-Infeld. *JCAP* **1411**, 004 (2014). [arXiv:1409.0233](#)
21. J. Beltran Jimenez, L. Heisenberg, G.J. Olmo, D. Rubiera-Garcia, On gravitational waves in Born-Infeld inspired non-singular cosmologies. *JCAP* **1710**(10), 029 (2017). [arXiv:1707.08953](#). [Erratum: *JCAP*1808,no.08,E01(2018)]
22. A.N. Makarenko, S. Odintsov, G.J. Olmo, Born-Infeld- $f(R)$ gravity. *Phys. Rev. D* **90**, 024066 (2014). [arXiv:1403.7409](#)
23. A.N. Makarenko, S.D. Odintsov, G.J. Olmo, D. Rubiera-Garcia, Early-time cosmic dynamics in $f(R)$ and $f(|\dot{\Omega}|)$ extensions of Born-Infeld gravity. *TSPU Bull.* **12**, 158–163 (2014). [arXiv:1411.6193](#)
24. S.-L. Li, H. Wei, Stability of the Einstein static universe in Eddington-inspired Born-Infeld theory. *Phys. Rev. D* **96**(2), 023531 (2017). [arXiv:1705.06819](#)
25. M. Bouhmadi-López, C.-Y. Chen, P. Chen, Eddington-Born-Infeld cosmology: a cosmographic approach, a tale of doomsdays and the fate of bound structures. *Eur. Phys. J. C* **75**, 90 (2015). [arXiv:1406.6157](#)
26. M. Bouhmadi-López, C.-Y. Chen, P. Chen, On the Consistency of the Wheeler-DeWitt Equation in the Quantized Eddington-inspired Born-Infeld Gravity. *JCAP* **1812**(12), 032 (2018). [arXiv:1810.10918](#)
27. I. Albarran, M. Bouhmadi-López, C.-Y. Chen, P. Chen, Quantum cosmology of Eddington-Born-Infeld gravity fed by a scalar field: The big rip case. *Phys. Dark Univ.* **23**, 100255 (2019). [arXiv:1811.05041](#)
28. A. Stachowski, M. Szydłowski, A. Borowiec, Starobinsky cosmological model in Palatini formalism. *Eur. Phys. J*
29. X.-H. Meng, P. Wang, R^{*2} corrections to the cosmological dynamics of inflation in the Palatini formulation. *Class. Quant. Grav.* **21**, 2029–2036 (2004). ([gr-qc/0402011](#))
30. I. Antoniadis, A. Karam, A. Lykkas, K. Tamvakis, Palatini inflation in models with an R^2 term. *JCAP* **1811**(11), 028 (2018). [arXiv:1810.10418](#)

31. C. Fu, P. Wu, H. Yu, Inflationary dynamics and preheating of the nonminimally coupled inflaton field in the metric and Palatini formalisms. *Phys. Rev. D* **96**(10), 103542 (2017). [arXiv:1801.04089](#)
32. J.P.B. Almeida, N. Bernal, J. Rubio, T. Tenkanen, Hidden Inflaton Dark Matter. *JCAP* **1903**, 012 (2019). [arXiv:1811.09640](#)
33. A. Racioppi, Coleman-Weinberg linear inflation: metric vs. Palatini formulation. *JCAP* **1712**(12), 041 (2017). [arXiv:1710.04853](#)
34. V.-M. Enckell, K. Enqvist, S. Rasanen, L.-P. Wahlman, Inflation with R^2 term in the Palatini formalism. *JCAP* **1902**, 022 (2019). [arXiv:1810.05536](#)
35. I. Antoniadis, A. Karam, A. Lykkas, T. Pappas, K. Tamvakis, Rescuing Quartic and Natural Inflation in the Palatini Formalism. *JCAP* **1903**, 005 (2019). [arXiv:1812.00847](#)
36. J. Rubio, E.S. Tomberg, Preheating in Palatini Higgs inflation. *JCAP* **1904**(4), 021 (2019). [arXiv:1902.10148D](#)
37. R. Jinno, K. Kaneta, K.-Y. Oda, S.C. Park, Hillclimbing inflation in metric and Palatini formulations. *Phys. Lett. B* **791**, 396–402 (2019). [arXiv:1812.11077](#)
38. S. Fay, R. Tavakol, S. Tsujikawa, $f(R)$ gravity theories in Palatini formalism: Cosmological dynamics and observational constraints. *Phys. Rev. D* **75**, 063509 (2007). ([astro-ph/0701479])
39. I. Cho, H.-C. Kim, T. Moon, Precursor of Inflation. *Phys. Rev. Lett.* **111**, 071301 (2013). [arXiv:1305.2020](#)
40. I. Cho, N.K. Singh, Tensor-to-scalar ratio in Eddington-inspired Born-Infeld inflation. *Eur. Phys. J. C* **74**(11), 3155 (2014). [arXiv:1408.2652](#)
41. I. Cho, N.K. Singh, Scalar perturbation produced at the pre-inflationary stage in Eddington-inspired Born-Infeld gravity. *Eur. Phys. J. C* **75**(6), 240 (2015). [arXiv:1412.6344](#)
42. I. Cho, H.-C. Kim, Inflationary tensor perturbation in Eddington-inspired born-infeld gravity. *Phys. Rev. D* **90**(2), 024063 (2014). [arXiv:1404.6081](#)
43. H.-C. Kim, Origin of the universe: A hint from Eddington-inspired Born-Infeld gravity. *J. Korean Phys. Soc.* **65**(6), 840–845 (2014). [arXiv:1312.0703](#)
44. I. Cho, N.K. Singh, Primordial Power Spectra of EiBI Inflation in Strong Gravity Limit. *Phys. Rev. D* **92**(2), 024038 (2015). [arXiv:1506.02213](#)
45. S. Jana, S. Kar, Born-Infeld cosmology with scalar Born-Infeld matter. *Phys. Rev. D* **94**(6), 064016 (2016). [arXiv:1605.00820](#)
46. J. Beltran Jimenez, L. Heisenberg, G.J. Olmo, C. Ringeval, Cascading dust inflation in Born-Infeld gravity. *JCAP* **1511**, 046 (2015). [arXiv:1509.01188](#)
47. D.K. Banik, S.K. Banik, K. Bhuyan, Dynamical system approach to Born-Infeld $f(R)$ gravity in Palatini formalism. *Phys. Rev. D* **97**(12), 124041 (2018)
48. G. Allemandi, A. Borowiec, M. Francaviglia, Accelerated cosmological models in Ricci squared gravity. *Phys. Rev. D* **70**, 103503 (2004). ([hep-th/0407090])
49. D.N. Vollick, $1/R$ Curvature corrections as the source of the cosmological acceleration. *Phys. Rev. D* **68**, 063510 (2003). ([astro-ph/0306630])
50. E.E. Flanagan, Palatini form of $1/R$ gravity. *Phys. Rev. Lett.* **92**, 071101 (2004). ([astro-ph/0308111])
51. D.N. Vollick, On the Dirac field in the Palatini form of $1/R$ gravity. *Phys. Rev. D* **71**, 044020 (2005). ([gr-qc/0409068])
52. X. Meng, P. Wang, Cosmological evolution in $1/r$ -gravity theory. *Class. Quant. Grav.* **21**, 951–960 (2004). ([astro-ph/0308031])
53. S. Nojiri, S.D. Odintsov, The Minimal curvature of the universe in modified gravity and conformal anomaly resolution of the instabilities. *Mod. Phys. Lett. A* **19**, 627–638 (2004). ([hep-th/0310045])
54. G.J. Olmo, Hydrogen atom in Palatini theories of gravity. *Phys. Rev. D* **77**, 084021 (2008). [arXiv:0802.4038](#)
55. B. Li, M.C. Chu, CMB and Matter Power Spectra of Early $f(R)$ Cosmology in Palatini Formalism. *Phys. Rev. D* **74**, 104010 (2006). ([astro-ph/0610486])
56. B. Li, K.C. Chan, M.C. Chu, Constraints on $f(R)$ Cosmology in the Palatini Formalism. *Phys. Rev. D* **76**, 024002 (2007). ([astro-ph/0610794])

57. T. Koivisto, The matter power spectrum in $f(r)$ gravity. *Phys. Rev. D* **73**, 083517 (2006). ([astro-ph/0602031])
58. M. Amarzguoui, O. Elgaroy, D.F. Mota, T. Multamaki, Cosmological constraints on $f(r)$ gravity theories within the palatini approach. *Astron. Astrophys.* **454**, 707–714 (2006). ([astro-ph/0510519])
59. S. Lee, Palatini $f(R)$ Cosmology. *Mod. Phys. Lett. A* **23**, 1388–1396 (2008). [arXiv:0801.4606](#)
60. N. Pires, J. Santos, J.S. Alcaniz, Cosmographic constraints on a class of Palatini $f(R)$ gravity. *Phys. Rev. D* **82**, 067302 (2010). [arXiv:1006.0264](#)
61. M.S. Movahed, S. Baghran, S. Rahvar, Consistency of $f(R) = \sqrt{R^2 - R_0^2}$ Gravity with the Cosmological Observations in Palatini Formalism. *Phys. Rev. D* **76**, 044008 (2007). [arXiv:0705.0889](#)
62. S. Baghran, M.S. Movahed, S. Rahvar, Observational tests of a two parameter power-law class modified gravity in Palatini formalism. *Phys. Rev. D* **80**, 064003 (2009). [arXiv:0904.4390](#)
63. S.N.L.S. Collaboration, P. Astier et al., The Supernova Legacy Survey: Measurement of Ω_M , Ω_Λ and w from the first year data set. *Astron. Astrophys.* **447**, 31–48 (2006). ([astro-ph/0510447])
64. R. Amanullah et al., Spectra and light curves of six type Ia supernovae at $0.511 < Z < 1.12$ and the union2 compilation. *Astrophys. J.* **716**, 712–738 (2010). [arXiv:1004.1711](#)
65. P. Pinto, L. Del Vecchio, L. Fatibene, M. Ferraris, Extended cosmology in Palatini $f(R)$ -theories. *JCAP* **1811**(11), 044 (2018). [arXiv:1807.00397](#)
66. L. Del Vecchio, L. Fatibene, S. Capozziello, M. Ferraris, P. Pinto, S. Camera, Hubble drift in Palatini $f(R)$ -theories. *Eur. Phys. J. Plus* **134**(1), 5 (2019). [arXiv:1810.10754](#)
67. B. Li, J.D. Barrow, D.F. Mota, The Cosmology of Ricci-Tensor-Squared gravity in the Palatini variational approach. *Phys. Rev. D* **76**, 104047 (2007). [arXiv:0707.2664](#)
68. S. Capozziello, R. D’Agostino, O. Luongo, Kinematic model-independent reconstruction of Palatini $f(R)$ cosmology. *Gen. Rel. Grav.* **51**(1), 2 (2019). [arXiv:1806.06385](#)
69. S. Capozziello, R. D’Agostino, O. Luongo, Extended gravity cosmography. *Int. J. Mod. Phys. D* **28**(10), 1930016 (2019). [arXiv:1904.01427](#)
70. F.A. Teppa Pannia, S.E. Perez Bergliaffa, N. Manske, Cosmography and the redshift drift in Palatini $f(R)$ theories. *Eur. Phys. J. C* **79**(3), 267 (2019). [arXiv:1811.08176](#)
71. X.-L. Du, K. Yang, X.-H. Meng, Y.-X. Liu, Large Scale Structure Formation in Eddington-inspired Born-Infeld Gravity. *Phys. Rev. D* **90**, 044054 (2014). [arXiv:1403.0083](#)
72. P.P. Avelino, Eddington-inspired Born-Infeld gravity: astrophysical and cosmological constraints. *Phys. Rev. D* **85**, 104053 (2012). [arXiv:1201.2544](#)
73. P.P. Avelino, Eddington-inspired Born-Infeld gravity: nuclear physics constraints and the validity of the continuous fluid approximation. *JCAP* **1211**, 022 (2012). [arXiv:1207.4730](#)
74. P.P. Avelino, Probing gravity at sub-femtometer scales through the pressure distribution inside the proton. *Phys. Lett. B* **795**, 627–631 (2019). [arXiv:1902.01318](#)
75. A.D.I. Latorre, G.J. Olmo, M. Ronco, Observable traces of non-metricity: new constraints on metric-affine gravity. *Phys. Lett. B* **780**, 294–299 (2018). [arXiv:1709.04249](#)
76. A. Delhom, V. Miralles, A. Peñuelas, *Effective interactions in Ricci-Based Gravity models below the non-metricity scale*. [arXiv:1907.05615](#)
77. M. Banados, Eddington-Born-Infeld action for dark matter and dark energy. *Phys. Rev. D* **77**, 123534 (2008). [arXiv:0801.4103](#)
78. C. Skordis, Eddington-Born-Infeld theory and the dark sector. *Nucl. Phys. Proc. Suppl.* **194**, 338–343 (2009)
79. M. Banados, P.G. Ferreira, C. Skordis, Eddington-Born-Infeld gravity and the large scale structure of the Universe. *Phys. Rev. D* **79**, 063511 (2009). [arXiv:0811.1272](#)
80. A. De Felice, B. Gumjudpai, S. Jhingan, Cosmological constraints for an Eddington-Born-Infeld field. *Phys. Rev. D* **86**, 043525 (2012). [arXiv:1205.1168](#)
81. D.C. Rodrigues, Evolution of Anisotropies in Eddington-Born-Infeld Cosmology. *Phys. Rev. D* **78**, 063013 (2008). [arXiv:0806.3613](#)
82. J. Wu, G. Li, T. Harko, S.-D. Liang, Palatini formulation of $f(R, T)$ gravity theory, and its cosmological implications. *Eur. Phys. J. C* **78**(5), 430 (2018). [arXiv:1805.07419](#)

83. G. Allemandi, A. Borowiec, M. Francaviglia, S.D. Odintsov, Dark energy dominance and cosmic acceleration in first order formalism. *Phys. Rev. D* **72**, 063505 (2005). ([gr-qc/0504057])
84. T. Koivisto, H. Kurki-Suonio, Cosmological perturbations in the Palatini formulation of modified gravity. *Class. Quant. Grav.* **23**, 2355–2369 (2006). ([astro-ph/0509422])
85. A.V. Minkevich, A.S. Garkun, *Isotropic cosmology in metric - affine gauge theory of gravity*. gr-qc/9805007
86. F.W. Hehl, A. Macias, Metric affine gauge theory of gravity. 2. Exact solutions. *Int. J. Mod. Phys. D* **8**, 399–416 (1999). ([gr-qc/9902076])
87. S. Capozziello, S. Vignolo, Metric-affine $f(R)$ -gravity with torsion: An Overview. *Annalen Phys.* **19**, 238–248 (2010). [arXiv:0910.5230](https://arxiv.org/abs/0910.5230)
88. S. Capozziello, R. Cianci, C. Stornaiolo, S. Vignolo, $f(R)$ gravity with torsion: The Metric-affine approach. *Class. Quant. Grav.* **24**, 6417–6430 (2007). [arXiv:0708.3038](https://arxiv.org/abs/0708.3038)
89. D. Gal'tsov, S. Zhidkova, Ghost-free Palatini derivative scalar-tensor theory: Desingularization and the speed test. *Phys. Lett. B* **790**, 453–457 (2019)
90. A. Delhom, J. de Andres, J.B. Jimenez, Anisotropic deformations in projectively invariant metric-affine theories of gravity. *Class. Quantum Gravity* **37**(22), 225013 (2020)

Chapter 13

Hybrid Metric-Palatini Gravity and Cosmology



Francisco S. N. Lobo

Given the success of General Relativity (GR) at relatively short scales (such as the Solar System, stellar models, or compact binary systems), the idea that modified dynamics could arise at larger scales has been investigated in much detail over recent years. Theories in which the gravitational action consists of more general combinations of curvature invariants than the pure Einstein-Hilbert term have been investigated with special emphasis [1]. From these investigations it was soon noticed that the usual metric formulation of alternative theories of gravity is generically different from its Palatini (or metric-affine) counterpart (see [2] for a recent review on the Palatini approach). Whereas the metric approach typically leads to higher-order derivative equations, in the Palatini formulation the resulting field equations are always second-order. The appealing character of the second-order equations of the Palatini formalism, however, is accompanied by certain algebraic relations between the matter fields and the affine connection, which is now determined by a set of equations coupled to the matter fields and the metric.

The case of $f(R)$ theories is particularly useful to illustrate the differences between these two approaches. In the metric formulation, the object $\phi \equiv df/dR$ behaves as a dynamical scalar field, which satisfies a second-order equation with self-interactions that depend on the form of the Lagrangian $f(R)$. In order to have an impact at large astrophysical and cosmological scales, the scalar field ϕ should have a very low mass, implying a long interaction range. It is well known, however, that light scalars do have an impact at shorter scales, where their presence is strongly

The original version of this chapter was revised. The affiliation of the author, Francisco S. N. Lobo has been corrected from “Facultade” to “Faculdade”. The correction to this chapter is available at https://doi.org/10.1007/978-3-030-83715-0_39

F. S. N. Lobo (✉)

Instituto de Astrofísica e Ciências do Espaço, Faculdade de Ciências da Universidade de Lisboa, Edifício C8, Campo Grande, 1749-016 Lisbon, Portugal

© The Author(s), under exclusive license to Springer Nature Switzerland AG 2021, corrected publication 2022

177

E. N. Saridakis et al. (eds.) *Modified Gravity and Cosmology*,
https://doi.org/10.1007/978-3-030-83715-0_13

constrained by laboratory and Solar System observations unless some kind of screening mechanism is invoked. In the Palatini case, a scalar-tensor representation is also possible, but with the scalar field satisfying an algebraic rather than a differential equation. It is then found that the scalar ϕ turns out to be an algebraic function of the trace of the stress-energy tensor of the matter, $\phi = \phi(T)$, which may lead, in models of late-time cosmic speed-up, to undesired gradient instabilities at various contexts, as has been shown by studies of cosmological perturbations [3, 4] and atomic physics [5, 6].

In this chapter we will review the *hybrid* variation of $f(R)$ gravity, in which the (purely metric) Einstein-Hilbert action is supplemented with (metric-affine) correction terms constructed à la Palatini [7, 8]. Given that the metric and Palatini $f(R)$ theories allow the construction of simple extensions of GR with interesting properties and, at the same time, suffer from different types of drawbacks, it proves interesting to establish bridges between these two seemingly disparate approaches, hoping to find ways to cure or improve their individual deficiencies. For that purpose, in a number of works [1, 7–12] a hybrid combination of metric and Palatini elements to construct the gravity Lagrangian was considered, and it was found that viable models sharing properties of both formalisms are possible. An interesting aspect of these theories is the possibility to generate long-range forces without entering into conflict with local tests of gravity and without invoking any kind of screening mechanism (which would, however, require that at the present time the cosmological evolution reduces to GR).

The possibility of expressing these hybrid $f(R)$ metric-Palatini theories using a scalar-tensor representation simplifies the analysis of the field equations and the construction of solutions. In some sense, considering a theory like $R + f(\mathcal{R})$ means that one retains all the positive results of GR, represented by the Einstein-Hilbert part of the action R , while the further “gravitational budget” is endowed in the metric-affine $f(\mathcal{R})$ component, where \mathcal{R} is the Palatini curvature scalar constructed in terms of an independent connection. In fact, it is well known that metric-affine and purely metric formalisms coincide in GR, i.e., considering the action R . On the contrary, the two formalisms lead to different results considering more generic functions $f(\mathcal{R})$.

13.1 Hybrid Metric-Palatini Gravity: The General Formalism

We start our considerations by providing the general features of the theory. More specifically, we present the action and the field equations both in the so-called hybrid metric-Palatini gravity and its equivalent scalar-tensor representations in both the Jordan and the Einstein frames.

13.1.1 Action and Gravitational Field Equations

The action of the hybrid metric-Palatini gravity is specified as [8, 9]

$$S = \frac{1}{2\kappa^2} \int d^4x \sqrt{-g} [R + f(\mathcal{R})] + S_m, \quad (13.1)$$

where S_m is the matter action, $\kappa^2 \equiv 8\pi G$, R is the Einstein-Hilbert term, $\mathcal{R} \equiv g^{\mu\nu} \check{\mathcal{R}}_{\mu\nu}$ is the Palatini curvature, defined in terms of an independent connection $\check{\Gamma}_{\mu\nu}^\alpha$ as

$$\mathcal{R} \equiv g^{\mu\nu} \check{\mathcal{R}}_{\mu\nu} \equiv g^{\mu\nu} \left(\check{\Gamma}_{\mu\nu,\alpha}^\alpha - \check{\Gamma}_{\mu\alpha,\nu}^\alpha + \check{\Gamma}_{\alpha\lambda}^\alpha \check{\Gamma}_{\mu\nu}^\lambda - \check{\Gamma}_{\mu\lambda}^\alpha \check{\Gamma}_{\alpha\nu}^\lambda \right), \quad (13.2)$$

which generates the Ricci curvature tensor $\mathcal{R}_{\mu\nu}$ as

$$\mathcal{R}_{\mu\nu} \equiv \check{\Gamma}_{\mu\nu,\alpha}^\alpha - \check{\Gamma}_{\mu\alpha,\nu}^\alpha + \check{\Gamma}_{\alpha\lambda}^\alpha \check{\Gamma}_{\mu\nu}^\lambda - \check{\Gamma}_{\mu\lambda}^\alpha \check{\Gamma}_{\alpha\nu}^\lambda. \quad (13.3)$$

Now, varying the action (13.1) with respect to the metric, one obtains the following gravitational field equation

$$G_{\mu\nu} + F(\mathcal{R}) \mathcal{R}_{\mu\nu} - \frac{1}{2} f(\mathcal{R}) g_{\mu\nu} = \kappa^2 T_{\mu\nu}, \quad (13.4)$$

where the matter stress-energy tensor is defined, as usual, through

$$T_{\mu\nu} \equiv -\frac{2}{\sqrt{-g}} \frac{\delta(\sqrt{-g} \mathcal{L}_m)}{\delta(g^{\mu\nu})}. \quad (13.5)$$

Varying the action with respect to the independent connection $\check{\Gamma}_{\mu\nu}^\alpha$, it is then found as the solution to the resulting equation of motion that $\check{\Gamma}_{\mu\nu}^\alpha$ is compatible with the metric $F(\mathcal{R})g_{\mu\nu}$, conformally related to the physical metric $g_{\mu\nu}$, with the conformal factor given by $F(\mathcal{R}) \equiv df(\mathcal{R})/d\mathcal{R}$. This implies the following relation:

$$\mathcal{R}_{\mu\nu} = R_{\mu\nu} + \frac{3}{2} \frac{1}{F^2(\mathcal{R})} F(\mathcal{R})_{,\mu} F(\mathcal{R})_{,\nu} - \frac{1}{F(\mathcal{R})} \nabla_\mu F(\mathcal{R})_{,\nu} - \frac{1}{2} \frac{1}{F(\mathcal{R})} g_{\mu\nu} \nabla_\alpha \nabla^\alpha F(\mathcal{R}). \quad (13.6)$$

13.1.2 Scalar-Tensor Representation

In a similar manner to the pure metric and Palatini approaches [13, 14], the action (13.1) for the hybrid metric-Palatini theory can be represented as that of a scalar-tensor theory by introducing an auxiliary field A , such that

$$S = \frac{1}{2\kappa^2} \int d^4x \sqrt{-g} [\Omega_A R + f(A) + f_A(\mathcal{R} - A)] + S_m, \quad (13.7)$$

where $f_A \equiv df/dA$ and a coupling constant Ω_A has been included for generality, where $\Omega_A = 1$ reduces to the original hybrid metric-Palatini theory [8]. Now, rearranging the terms and defining $\phi \equiv f_A$, $V(\phi) = Af_A - f(A)$, Eq. (13.7) becomes

$$S = \frac{1}{2\kappa^2} \int d^4x \sqrt{-g} [\Omega_A R + \phi \mathcal{R} - V(\phi)] + S_m, \quad (13.8)$$

which is equivalent to our original starting point (13.1).

In order to obtain the equations of motion, one varies the action (13.8) with respect to the metric, the scalar ϕ and the connection, which leads to the following field equations:

$$\Omega_A R_{\mu\nu} + \phi \mathcal{R}_{\mu\nu} - \frac{1}{2} (\Omega_A R + \phi \mathcal{R} - V) g_{\mu\nu} = \kappa^2 T_{\mu\nu}, \quad (13.9)$$

$$\mathcal{R} - V_\phi = 0, \quad (13.10)$$

$$\check{\nabla}_\alpha (\sqrt{-g} \phi g^{\mu\nu}) = 0, \quad (13.11)$$

respectively.

The solution of Eq. (13.11) implies that the independent connection is the Levi-Civita connection of a metric $h_{\mu\nu} = \phi g_{\mu\nu}$. This implies that the relation (13.6) between the tensors $\mathcal{R}_{\mu\nu}$ and $R_{\mu\nu}$ reduces to

$$\mathcal{R}_{\mu\nu} = R_{\mu\nu} + \frac{3}{2\phi^2} \partial_\mu \phi \partial_\nu \phi - \frac{1}{\phi} \left(\nabla_\mu \nabla_\nu \phi + \frac{1}{2} g_{\mu\nu} \nabla_\alpha \nabla^\alpha \phi \right), \quad (13.12)$$

which can be inserted in the action (13.8) to eliminate the independent connection and to obtain the following scalar-tensor representation, ultimately arriving at:

$$S = \frac{1}{2\kappa^2} \int d^4x \sqrt{-g} \left[(\Omega_A + \phi) R + \frac{3}{2\phi} \partial_\mu \phi \partial^\mu \phi - V(\phi) \right] + S_m. \quad (13.13)$$

In the limit $\Omega_A \rightarrow 0$, the theory (13.13) presents the Palatini- $f(\mathcal{R})$ gravity, and in the limit $\Omega_A \rightarrow \infty$ the metric $f(R)$ gravity [15]. Apart from these singular cases, the more generic theories with a finite Ω_A thus lie in the ‘‘hybrid’’ regime, which from this perspective provides a unique interpolation between the two a priori completely distinct classes of gravity theories. In fact, we have arrived at Brans-Dicke type of theories specified by the non-trivial coupling function

$$\omega_{BD} = \frac{3\phi}{2\phi - 2\Omega_A}, \quad (13.14)$$

which generalises the $\omega_{BD} = 0$ and $\omega_{BD} = -3/2$ cases, which in turn correspond to the scalar-tensor representations of the metric $f(R)$ and the Palatini- $f(\mathcal{R})$ gravities [16], respectively.

Using Eqs. (13.12) and (13.10) in Eq. (13.9), the metric field equation can be written as

$$(\Omega_A + \phi)R_{\mu\nu} = \kappa^2 \left(T_{\mu\nu} - \frac{1}{2}g_{\mu\nu}T \right) + \frac{1}{2}g_{\mu\nu} (V + \nabla_\alpha \nabla^\alpha \phi) + \nabla_\mu \nabla_\nu \phi - \frac{3}{2\phi} \partial_\mu \phi \partial_\nu \phi, \quad (13.15)$$

or equivalently as

$$(\Omega_A + \phi)G_{\mu\nu} = \kappa^2 T_{\mu\nu} + \nabla_\mu \nabla_\nu \phi - \nabla_\alpha \nabla^\alpha \phi g_{\mu\nu} - \frac{3}{2\phi} \nabla_\mu \phi \nabla_\nu \phi + \frac{3}{4\phi} \nabla_\lambda \phi \nabla^\lambda \phi g_{\mu\nu} - \frac{1}{2}V g_{\mu\nu}, \quad (13.16)$$

from which it is seen that the spacetime curvature is generated by both the matter and the scalar field. The scalar field equation can be manipulated in two different ways that illustrate further how the hybrid models combine physical features of the $\omega_{BD} = 0$ and $\omega_{BD} = -3/2$ scalar-tensor models.

First, tracing Eq. (13.9) with $g^{\mu\nu}$, we find $-\Omega_A R - \phi \mathcal{R} + 2V = \kappa^2 T$, and using Eq. (13.10), it takes the following form:

$$2V - \phi V_\phi = \kappa^2 T + \Omega_A R. \quad (13.17)$$

Similar to the Palatini ($\omega_{BD} = -3/2$) case, this equation tells us that the field ϕ can be expressed as an algebraic function of the scalar $X \equiv \kappa^2 T + \Omega_A R$, i.e., $\phi = \phi(X)$. In the pure Palatini case, however, ϕ is just a function of T . The right-hand side of Eq. (13.15), therefore, besides containing new matter terms associated with the trace T and its derivatives, also contains the curvature R and its derivatives. Thus, this theory can be seen as a higher-derivative theory in both matter and metric fields. However, such an interpretation can be avoided if R is replaced in Eq. (13.17) with the relation

$$R = \mathcal{R} + \frac{3}{\phi} \nabla_\mu \nabla^\mu \phi - \frac{3}{2\phi^2} \partial_\mu \phi \partial^\mu \phi \quad (13.18)$$

together with $\mathcal{R} = V_\phi$. It is then found that the scalar field is governed by the second-order evolution equation that becomes, when $\Omega_A = 1$,

$$-\nabla_\mu \nabla^\mu \phi + \frac{1}{2\phi} \partial_\mu \phi \partial^\mu \phi + \frac{\phi[2V - (1 + \phi)V_\phi]}{3} = \frac{\phi \kappa^2}{3} T, \quad (13.19)$$

which is an effective Klein-Gordon equation. This last expression shows that, unlike in the Palatini ($\omega_{BD} = -3/2$) case, the scalar field is dynamical. The theory is therefore not affected by the microscopic instabilities that arise in Palatini models with infrared corrections [2].

Finally, we can make a conformal transformation into the Einstein frame of these theories. Thus, considering the following conformal rescaling $\tilde{g}_{\mu\nu} \equiv (\phi + \Omega_A) g_{\mu\nu}$, the Einstein frame Lagrangian becomes

$$\tilde{\mathcal{L}} = \tilde{R} + \frac{3\Omega_A}{2\phi} \frac{\tilde{g}^{\alpha\beta} \phi_{,\alpha} \phi_{,\beta}}{(\phi + \Omega_A)^2} - (\phi + \Omega_A)^2 V(\phi). \quad (13.20)$$

This can be further put into its canonical form by introducing the rescaled field ψ as $\phi = \Omega_A \tan^2 \left[\psi / (2\sqrt{3}) \right]$. Thus, the vacuum theory then becomes a canonical scalar theory with a very specific potential (stemming, of course, from the original function $f(\mathcal{R})$) in the Einstein frame.

13.2 Hybrid-Gravity Cosmology

In order to explore the cosmology of the metric-Palatini gravitational theories, we employ the scalar-tensor formulation derived above (13.13):

$$S = \frac{1}{2\kappa^2} \int d^4x \sqrt{-g} \left[(\Omega_A + \phi) R + \frac{3}{2\phi} (\partial\phi)^2 - 2\kappa^2 V(\phi) \right] + S_m, \quad (13.21)$$

where

$$\kappa^2 V(\phi) = \frac{1}{2} [r(\phi)\phi - f(r(\phi))], \quad r(\phi) \equiv f'^{-1}(\phi). \quad (13.22)$$

In this section, we first write down the cosmological equations in the formulation (13.21) and then have a brief look at the phase space of exact solutions for these equations (we refer the reader to the recent phase space analysis for the most complete global analysis of the cosmological dynamics of these theories [12]). Then we will analyse the formation of cosmological large-scale structure in these models.

13.2.1 Background Expansion

The flat Friedmann-Lemaître-Robertson-Walker metric is defined as

$$ds^2 = -dt^2 + a^2(t) (dx^2 + dy^2 + dz^2), \quad (13.23)$$

where the rate of time-evolution of the scale factor $a(t)$ is parameterised by the Hubble parameter $H = \dot{a}/a$, and the overdot denotes a derivative with respect to cosmic time t . In the following we will mainly be interested in accelerating dark energy-like dynamics; for a study of Einstein static spaces, see Ref. [10].

The Friedmann Equations

The Friedmann equations that govern the evolution of H can be written in terms of an effective energy density and pressure, respectively, in the following manner

$$3H^2 = \kappa^2 \rho_{\text{eff}} , \quad (13.24)$$

$$\dot{H} = -\frac{\kappa^2}{2} (\rho_{\text{eff}} + p_{\text{eff}}) , \quad (13.25)$$

where for the theory defined by the action (13.21) we obtain the following effective source terms

$$(\Omega_A + \phi) \kappa^2 \rho_{\text{eff}} = -\frac{3}{4\phi} \dot{\phi}^2 + \kappa^2 V(\phi) - 3H\dot{\phi} + \kappa^2 \rho_m , \quad (13.26)$$

$$(\Omega_A + \phi) \kappa^2 p_{\text{eff}} = -\frac{3}{4\phi} \dot{\phi}^2 - \kappa^2 V(\phi) + \ddot{\phi} + 2H\dot{\phi} + \kappa^2 p_m , \quad (13.27)$$

respectively. The conservation equations for the matter component and the scalar field are

$$\dot{\rho}_m + 3H(\rho_m + p_m) = 0 , \quad (13.28)$$

$$\ddot{\phi} + 3H\dot{\phi} - \frac{\dot{\phi}^2}{2\phi} + \frac{1}{3}\phi R - \frac{2}{3}\kappa^2 \phi V'(\phi) = 0 . \quad (13.29)$$

Recalling that $R = 6(2H^2 + \dot{H})$ and using Eqs. (13.24) and (13.25), we can rewrite the Klein-Gordon equation as

$$\ddot{\phi} + 3H\dot{\phi} - \frac{\dot{\phi}^2}{2\phi} + U'(\phi) + \frac{\kappa^2 \phi}{3\Omega_A} (\rho_m - 3p_m) = 0 , \quad (13.30)$$

where for notational simplicity, $U'(\phi)$ is defined by

$$U'(\phi) \equiv \frac{2\kappa^2 \phi}{3\Omega_A} [2V(\phi) - (\Omega_A + \phi) V'(\phi)] . \quad (13.31)$$

Note that as a consistency check we can verify that the Klein-Gordon equation together with the matter conservation, allows one to derive Eq. (13.25) from (13.24). By combining Eqs. (13.29) and (13.30), we find that

$$2V(\phi) - V'(\phi)\phi = \frac{1}{2} (\Omega_A R + \kappa^2 T) \equiv \frac{1}{2} X . \quad (13.32)$$

The solution for $\phi = \phi(X = 0)$ gives us the natural initial condition for the field in the early Universe. The asymptotic value of the field in the far future may then be deduced by studying the minima of the function $U(\phi)$ defined by Eq. (13.31).

Dynamical System Analysis

The cosmological dynamics can be analysed by taking into account a suitable dynamical system. Consider the following dimensionless variables

$$\Omega_m \equiv \frac{\kappa^2 \rho_m}{3H^2}, \quad x \equiv \phi, \quad y = x_{,N}, \quad z = \frac{\kappa^2 V}{3H^2}, \quad (13.33)$$

where $N = \log a$ is the e -folding time. The Friedmann equation (13.24) can then be rewritten as

$$\Omega_A + x + y - z + \frac{y^2}{4x} = \Omega_m. \quad (13.34)$$

Due to this constraint, the number of independent degrees of freedom is three instead of four. We choose to span our phase space by the triplet $\{x, y, z\}$, so that the autonomous system of equations reads as

$$x_{,N} = y, \quad (13.35)$$

$$y_{,N} = \frac{2x+y}{8\Omega_A x} \left\{ (3w_m - 1)y^2 + 4x[(3w_m - 1)y - 3(1+w_m)z] - 4x^2(1 - 3w_m - 2u(x)z) + 4\Omega_A [3x(w_m - 1)y + y^2 - x^2(2 - 6w_m - 4u(x)z)] \right\}, \quad (13.36)$$

$$z_{,N} = \frac{z}{4\Omega_A x} \left\{ (3w_m - 1)y^2 + 4x[(3w_m - 1)y - 3(1+w_m)z] + 4\Omega_A x(3 + 3w_m + u(x)y) + 4x^2(3w_m - 1 + 2u(x)z) \right\}, \quad (13.37)$$

respectively, with $w_m \equiv p_m/\rho_m$ the matter equation-of-state parameter. Additionally, we have defined $u(x) \equiv V'(\phi)/V(\phi)$. The relevant fixed points appear in this system. In particular, we have the matter-dominated fixed point where $x = y = z = 0$ and $w_{\text{eff}} = w_m$, and the de Sitter fixed point described by $w_{\text{eff}} = -1$ and

$$x_* = (2 - \Omega_A u_*)/u_*, \quad y_* = 0, \quad z_* = 2/u_*. \quad (13.38)$$

We denote the asymptotic values corresponding to this fixed point by a subscript star. In particular, the asymptotic value of the field x_* is solved from the first equation in (13.38) once the form of the potential is given. As expected, this value corresponds to the minimum of the effective potential (13.31), $U'(x_*) = 0$. To construct a viable model, the potential should be such that we meet the two requirements:

- The matter-dominated fixed point should be a saddle point and the de Sitter fixed point an attractor. Then we naturally obtain a transition to acceleration following standard cosmological evolution.
- At the present epoch the field value should be sufficiently close to zero, in order to avoid conflict with the Solar System tests of gravity [1, 8].

Note that the simplest metric $f(R)$ theories that provide acceleration fail in both predicting a viable structure formation era and the Solar System as we observe it. On

the other hand, it can be argued that the Palatini- $f(\mathcal{R})$ models can be ruled out as a dark energy alternative by considering their structure formation or implications to microphysics, if such a theory is regarded as consistent in the first place. As shown here and explored further below, hybrid metric-Palatini gravity models exist that are free of these problems.

To summarise: the field goes from ϕ_i to ϕ_* , where the former is given by $2V(\phi_i) = V'(\phi_i)\phi_i$ and the latter by $2V(\phi_*) = (\Omega_A + \phi_*)V'(\phi_*)$. We just need a suitable function $V(\phi)$, i.e., a form of $f(\mathcal{R})$ in such a way that the slope will be downwards and ϕ_* near the origin. We refer the reader to [12] for a more complete and detailed phase space analysis of the cosmological background dynamics.

On Cosmological Solutions

As a specific simple example, let us consider in more detail the specific case of the de Sitter solution in vacuum when $\Omega_A = 1$. For this case, the modified Friedmann equations take the form

$$3H^2 = \frac{1}{1+\phi} \left[\kappa^2 \rho_m + \frac{V}{2} - 3\dot{\phi} \left(H + \frac{\dot{\phi}}{4\phi} \right) \right], \quad (13.39)$$

$$2\dot{H} = \frac{1}{1+\phi} \left[-\kappa^2(\rho_m + p_m) + H\dot{\phi} + \frac{3}{2} \frac{\dot{\phi}^2}{\phi} - \ddot{\phi} \right], \quad (13.40)$$

and the scalar field equation (13.19) becomes

$$\ddot{\phi} + 3H\dot{\phi} - \frac{\dot{\phi}^2}{2\phi} + \frac{\phi}{3}[2V - (1+\phi)V_\phi] = -\frac{\phi\kappa^2}{3}(\rho_m - 3p_m). \quad (13.41)$$

Furthermore, consider a model that arises by demanding that matter and curvature satisfy the same relation as in GR. Taking

$$V(\phi) = V_0 + V_1\phi^2, \quad (13.42)$$

the trace equation automatically implies $R = -\kappa^2 T + 2V_0$ [8, 9]. As $T \rightarrow 0$ with the cosmic expansion, this model naturally evolves into a de Sitter phase, which requires $V_0 \sim \Lambda$ for consistency with observations. If V_1 is positive, the de Sitter regime represents the minimum of the potential [1, 8]. The effective mass for local experiments, $m_\phi^2 = 2(V_0 - 2V_1\phi)/3$, is then positive and small as long as $\phi < V_0/V_1$. For sufficiently large V_1 one can make the field amplitude small enough to be in agreement with Solar System tests. It is interesting that the exact de Sitter solution is compatible with dynamics of the scalar field in this model [1, 8, 9].

The accelerating dynamics that drive the hybrid metric-Palatini gravitational theory towards its general relativistic limits today have indeed been realised in several specific models [8, 9, 17, 18]. Our preliminary phase space analysis confirmed the existence of de Sitter attractor solutions, and the recent study of cosmology in terms of dynamical system analysis extends this result to more general models [12]. Ana-

lytic solutions were also presented in Ref. [9] as well as in Ref. [11], using a Nöether symmetry technique. A designer approach was formulated by Lima [17] to reconstruct precisely the standard Λ CDM expansion history by a nontrivial hybrid metric-Palatini model, and finally, two families of models were constrained by confronting their predictions with a combination of cosmic microwave background, supernovae Ia and baryonic acoustic oscillations background data [18].

13.2.2 Cosmological Perturbations

To understand the implications of these models on the cosmological structure formation, we derive the perturbation equations and analyse them in some specific cases of interest. This paves the way for a detailed comparison of the predictions with the cosmological data on large-scale structure and the cosmic microwave background. For generality, we will keep the parameter Ω_A in the formulae in this section.

Field Equations and Conservation Laws

Consider the Newtonian gauge [19], which can be parameterised by the two gravitational potentials Φ and Ψ ,

$$ds^2 = -(1 + 2\Psi) dt^2 + a^2(t) (1 - 2\Phi) d\vec{x}^2. \quad (13.43)$$

As a matter source we consider a perfect fluid, with the background equation of state w and with density perturbation $\delta = \delta\rho_m/\rho_m$, pressure perturbation $\delta p_m = c_s^2 \delta\rho_m$ and velocity perturbation v .

The 0-0 part of the field equations is given by

$$\begin{aligned} & -\frac{k^2}{a^2} \Phi - 3 \left(H - \frac{\dot{\phi}}{2(\Omega_A + \phi)} \right) \dot{\Phi} - 3 \left(H^2 + \frac{H\dot{\phi}}{F} - \frac{\dot{\phi}^2}{4\phi(\Omega_A + \phi)} \right) \Psi \\ & = \frac{1}{2F} \left[\kappa^2 \delta\rho_m + \left(\frac{3}{4\phi^2} \dot{\phi}^2 + V'(\phi) - 3H^2 - \frac{k^2}{a^2} \right) \varphi - 3 \left(H + \frac{\dot{\phi}}{2\phi} \right) \dot{\varphi} \right], \end{aligned} \quad (13.44)$$

where we have denoted $\varphi = \delta\phi$. The Raychaudhuri equation for the perturbations reads

$$\begin{aligned} & \left[6(H^2 + 2\dot{H}) - 2\frac{k^2}{a^2} + \frac{6}{F} \left(\ddot{\phi} - \frac{\dot{\phi}^2}{\phi^2} + H\dot{\phi} \right) \right] \Psi - 3 \left(2H - \frac{\dot{\phi}}{F} \right) (\dot{\Phi} + \dot{\Psi}) + 6\ddot{\Phi} = \\ & \frac{1}{F} \left\{ \kappa^2 (\delta\rho_m + 3\delta p_m) + \left[6H^2 + 6\dot{H} + 3\frac{\ddot{\phi}}{\phi^2} - 2V'(\phi) + \frac{k^2}{a^2} \right] \varphi + 3 \left(H - \frac{2\dot{\phi}}{\phi} \right) \dot{\varphi} + 3\ddot{\varphi} \right\}. \end{aligned} \quad (13.45)$$

The 0- i equation is

$$\left(H + \frac{\dot{\phi}}{2(\Omega_A + \phi)} \right) \Phi - \dot{\Phi} = \frac{1}{2(\Omega_A + \phi)} \left[\kappa^2 (\rho_m + p_m) a v_m + \left(H + \frac{3\dot{\phi}}{2\phi} \right) \varphi + \dot{\varphi} \right]. \quad (13.46)$$

Note that the set of perturbed field equations is completed by the off-diagonal spatial piece:

$$\Psi - \Phi = -\frac{\varphi}{\mathbb{F}}. \quad (13.47)$$

Assuming a perfect fluid, the continuity and Euler equations for the matter component are

$$\dot{\delta} + 3H(c_s^2 - w)\delta = (1+w)\left(3\dot{\Phi} + \frac{k^2}{a}v\right), \quad (13.48)$$

$$\ddot{v} + (1 - 3c_a^2)Hv = \frac{1}{a}\left(\Psi + \frac{c_s^2}{1+w}\delta\right), \quad (13.49)$$

respectively. The linear part of the Klein-Gordon equation is then compatible with the above system, which for completeness, is given by

$$\begin{aligned} \ddot{\varphi} + \left(3H + \frac{1}{\phi}\right)\dot{\varphi} + \left(\frac{k^2}{a^2} + \frac{\dot{\phi}^2}{2\phi^2} - \frac{2}{3}V''(\phi)\right)\varphi = \left(2\ddot{\Phi} + 6H\dot{\Phi} - \frac{3}{2\phi}\dot{\phi}^2\right)\Psi \\ + \dot{\phi}(\dot{\Psi} + 3\dot{\Phi}) - \frac{\phi}{3}\delta R. \end{aligned} \quad (13.50)$$

This completes the presentation of the field equations and the conservation laws.

Matter-dominated Cosmology

In this subsection, we consider the formation of structure in the matter-dominated Universe, where $w = c_s^2 = 0$, and assume scales deep inside the Hubble radius. This so-called quasi-static approximation is well-known in the literature, having been applied to scalar-tensor theories since early studies [20], and which more recently has been generalised to a wide variety of coupled dark sector models [21]. In this limit the spatial gradients are more important than the time derivatives and, consequently, the matter density perturbations are much stronger than the gravitational potentials. Combining the continuity and the Euler equation at this quasi-static subhorizon limit, one obtains

$$\ddot{\delta} = -2H\dot{\delta} - \frac{k^2}{a^2}\Psi. \quad (13.51)$$

We then need to solve the gravitational potential. Let us define $\Pi = a^2\rho_m\delta/k^2$ and write the field equations and the Klein-Gordon equation at this limit in a very simple way as

$$(\Omega_A + \phi)\Phi = \varphi - \Pi, \quad (13.52)$$

$$(\Omega_A + \phi)(\Psi - \Phi) = -\varphi, \quad (13.53)$$

$$-2(\Omega_A + \phi)\Psi = \Pi + \varphi, \quad (13.54)$$

$$3\varphi = -2\phi(\Psi - 2\Phi). \quad (13.55)$$

We immediately see that one of the equations is (as expected) redundant, and that the Ψ is (as usual) proportional to Π , where now the proportionality is given as a function of the field ϕ . Our result is

$$\ddot{\delta} + 2H\dot{\delta} = 4\pi G_{\text{eff}}\rho_m\delta, \quad (13.56)$$

with

$$G_{\text{eff}} \equiv \frac{\Omega_A - \frac{1}{3}\phi}{\Omega_A (\Omega_A + \phi)} G_N. \quad (13.57)$$

This shows that instabilities can be avoided in the evolution of the matter inhomogeneities, in contrast to the Palatini- $f(\mathcal{R})$ models and some matter-coupled scalar field models (recall that our theory can be mapped into such in the Einstein frame). Equation (13.56) provides a very simple approximation to track the growth of structure accurately within the linear regime during matter-dominated cosmology.

Vacuum Fluctuations

The propagation of the scalar degree of freedom in vacuum is also a crucial consistency check on the theory. Setting $\rho_m = 0$, consider the curvature perturbation in the uniform-field gauge ζ , which in terms of the Newtonian gauge perturbations is given by $\zeta = -\Phi - H\varphi/\dot{\phi}$. After somewhat more tedious algebra than in the previous case, we obtain the exact (linear) evolution equation [1, 9].

$$\ddot{\zeta} + \left\{ 3H - 2 \left[\frac{\ddot{\phi} + 2\dot{H}(\Omega_A + \phi) - \frac{\dot{\phi}^2}{F}}{\dot{\phi} + 2H(\Omega_A + \phi)} \right] + \frac{\phi}{\dot{\phi}^2} \left[\frac{2\ddot{\phi}\dot{\phi}}{\phi} + \frac{\dot{\phi}^3(\Omega_A + \phi)^3\phi}{1 - \phi^3(\Omega_A + \phi)^3} \right] \right\} \dot{\zeta} = -\frac{k^2}{a^2}\zeta. \quad (13.58)$$

The friction term depends on the perturbation variable we consider, but the perturbations at small scales still propagate with the speed of light, as in canonical scalar field theory. This also excludes gradient and tachyon instabilities in the graviscalar sector. Now, Eq. (13.58) can be used to study the generation of fluctuations in hybrid metric-Palatini-inflation. Construction of specific models and their observational tests are left for forthcoming studies; let us only note in passing that the Einstein-frame formulation (13.20) might present a convenient starting point for this: in fact, we note that the quadratic \mathcal{R}^2 curvature correction results in an interesting generalisation of the Starobinsky inflation in the hybrid metric-Palatini context, where the parameter Ω_A controls the flow along the so-called alpha attractor.

13.3 Discussions and Final Remarks

In this work we have presented a hybrid metric-Palatini framework for modified theories of gravity, and we have tested the new theories it entails, using a number of theoretical consistency checks and observational constraints. Having established the

theoretical consistency and interest on the hybrid metric-Palatini family of theories, we considered applications in which these theories provide gravitational alternatives to dark energy [1, 9]. As shown by the post-Newtonian analysis [1, 8], hybrid theories are promising in this respect, as they can avoid the local gravity constraints but modify the cosmological dynamics at large scales. Cosmological perturbations have also been analysed in these models up to the linear order [8, 9, 17], and the results imply that the formation of large-scale structure in the aforementioned accelerating cosmologies is viable although it exhibits subtle features that might be detectable in future experiments.

At an effective level, the hybrid theory modifications involve both (the trace of) the matter stress energy and (the Ricci scalar of) the metric curvature, and from this point of view it appears appealing to speculate on the possible relevance of these theories to both the problems of dark energy and dark matter, in a unified theoretical framework and without distinguishing a priori matter and geometric sources. Various aspects of dark-matter phenomenology, from astronomical to galactic and extragalactic scales, have also been discussed [7, 22, 23]. The generalised virial theorem can acquire, in addition to the contribution from the baryonic masses, effective contributions of geometrical origin to the total gravitational potential energy [7, 22], which may account for the well-known virial theorem mass discrepancy in clusters of galaxies. In the context of galactic rotation curves, the scalar-field modified relations between the various physical quantities such as tangential velocities of test particles around galaxies, Doppler frequency shifts and stellar dispersion velocities were derived [7, 23]. More recently, observational data of stellar motion near the Galactic centre were compared with simulations of the hybrid gravity theory, which turned out to be particularly suitable to model star dynamics.

To conclude, whilst the physics of the metric and the Palatini versions of $f(R)$ gravity have been uncovered in exquisite detail in a great variety of different contexts [16, 24–27], those studies largely wait to be extended for the hybrid version of the theory. We believe the results this far, as reported in this work, provide compelling motivation for the further exploration of these particular theories.

References

1. T. Harko, F.S.N. Lobo, *Extensions of $f(R)$ Gravity* (Cambridge University Press, Cambridge, 2018)
2. G.J. Olmo, Palatini approach to modified gravity: $f(R)$ theories and beyond. *Int. J. Mod. Phys. D* **20**, 413–462 (2011). [arXiv:1101.3864](https://arxiv.org/abs/1101.3864)
3. T. Koivisto, The matter power spectrum in $f(r)$ gravity. *Phys. Rev. D* **73**, 083517 (2006). [arXiv:astro-ph/0602031](https://arxiv.org/abs/astro-ph/0602031)
4. T. Koivisto, H. Kurki-Suonio, Cosmological perturbations in the palatini formulation of modified gravity. *Class. Quant. Grav.* **23**, 2355–2369 (2006). [arXiv:astro-ph/0509422](https://arxiv.org/abs/astro-ph/0509422)
5. G.J. Olmo, Violation of the equivalence principle in modified theories of gravity. *Phys. Rev. Lett.* **98**, 061101 (2007). [arXiv:gr-qc/0612002](https://arxiv.org/abs/gr-qc/0612002)
6. G.J. Olmo, Hydrogen atom in Palatini theories of gravity. *Phys. Rev. D* **77**, 084021 (2008). [arXiv:0802.4038](https://arxiv.org/abs/0802.4038)

7. S. Capozziello, T. Harko, F.S.N. Lobo, G.J. Olmo, Hybrid modified gravity unifying local tests, galactic dynamics and late-time cosmic acceleration. *Int. J. Mod. Phys. D* **22**, 1342006 (2013). [arXiv:1305.3756](#)
8. T. Harko, T.S. Koivisto, F.S.N. Lobo, G.J. Olmo, Metric-Palatini gravity unifying local constraints and late-time cosmic acceleration. *Phys. Rev. D* **85**, 084016 (2012). [arXiv:1110.1049](#)
9. S. Capozziello, T. Harko, T.S. Koivisto, F.S.N. Lobo, G.J. Olmo, Cosmology of hybrid metric-Palatini $f(X)$ -gravity. *JCAP* **1304**, 011 (2013). [arXiv:1209.2895](#)
10. C.G. Böhmer, F.S.N. Lobo, N. Tamanini, Einstein static Universe in hybrid metric-Palatini gravity. *Phys. Rev. D* **88**(10), 104019 (2013). [arXiv:1305.0025](#). [*Phys. Rev. D* **88**, 104019 (2013)]
11. A. Borowiec, S. Capozziello, M. De Laurentis, F.S.N. Lobo, A. Paliathanasis, M. Paoletta, A. Wojnar, Invariant solutions and Noether symmetries in hybrid gravity. *Phys. Rev. D* **91**(2), 023517 (2015). [arXiv:1407.4313](#)
12. S. Carloni, T. Koivisto, F.S.N. Lobo, Dynamical system analysis of hybrid metric-Palatini cosmologies. *Phys. Rev. D* **92**(6), 064035 (2015). [arXiv:1507.04306](#)
13. G.J. Olmo, The Gravity Lagrangian according to solar system experiments. *Phys. Rev. Lett.* **95**, 261102 (2005). [arXiv:gr-qc/0505101](#)
14. G.J. Olmo, Post-Newtonian constraints on $f(R)$ cosmologies in metric and Palatini formalism. *Phys. Rev. D* **72**, 083505 (2005). [arXiv:gr-qc/0505135](#)
15. T.S. Koivisto, Cosmology of modified (but second order) gravity. *AIP Conf. Proc.* **1206**, 79–96 (2010). [arXiv:0910.4097](#)
16. S. Capozziello, M. De Laurentis, Extended theories of gravity. *Phys. Rept.* **509**, 167–321 (2011). [arXiv:1108.6266](#)
17. N.A. Lima, Dynamics of Linear Perturbations in the hybrid metric-Palatini gravity. *Phys. Rev. D* **89**(8), 083527 (2014). [arXiv:1402.4458](#)
18. N.A. Lima, V.S. Barreto, Constraints on hybrid metric-palatini gravity from background evolution. *Astrophys. J.* **818**(2), 186 (2016). [arXiv:1501.05786](#)
19. C.-P. Ma, E. Bertschinger, Cosmological perturbation theory in the synchronous and conformal Newtonian gauges. *Astrophys. J.* **455**, 7–25 (1995). [arXiv:astro-ph/9506072](#)
20. B. Boisseau, G. Esposito-Farese, D. Polarski, A.A. Starobinsky, Reconstruction of a scalar tensor theory of gravity in an accelerating universe. *Phys. Rev. Lett.* **85**, 2236 (2000). [arXiv:gr-qc/0001066](#)
21. T.S. Koivisto, E.N. Saridakis, N. Tamanini, Scalar-Fluid theories: cosmological perturbations and large-scale structure. *JCAP* **1509**, 047 (2015). [arXiv:1505.07556](#)
22. S. Capozziello, T. Harko, T.S. Koivisto, F.S.N. Lobo, G.J. Olmo, The virial theorem and the dark matter problem in hybrid metric-Palatini gravity. *JCAP* **1307**, 024 (2013). [arXiv:1212.5817](#)
23. S. Capozziello, T. Harko, T.S. Koivisto, F.S.N. Lobo, G.J. Olmo, Galactic rotation curves in hybrid metric-Palatini gravity. *Astropart. Phys.* **50–52**, 65–75 (2013). [arXiv:1307.0752](#)
24. S. Capozziello, Curvature quintessence. *Int. J. Mod. Phys. D* **11**, 483–492 (2002). [arXiv:gr-qc/0201033](#)
25. A. De Felice, S. Tsujikawa, $f(R)$ theories. *Living Rev. Rel.* **13**, 3 (2010). [arXiv:1002.4928](#)
26. F.S.N. Lobo, The dark side of gravity: modified theories of gravity. [arXiv:0807.1640](#)
27. S. Nojiri, S.D. Odintsov, Unified cosmic history in modified gravity: from $F(R)$ theory to Lorentz non-invariant models. *Phys. Rept.* **505**, 59–144 (2011). [arXiv:1011.0544](#)

Chapter 14

Teleparallel Gravity: Foundations and Cosmology



Sebastian Bahamonde, Konstantinos F. Dialektopoulos, Manuel Hohmann, and Jackson Levi Said

14.1 Foundations of Teleparallel Gravity

Teleparallel Gravity theories have received growing attention during the last decade. Their most distinguishing feature is the use of a different geometric setting compared to General Relativity, which features a flat (curvature-free) connection, and torsion instead of curvature. This section gives a brief introduction to the mathematical background and foundations of Teleparallel Gravity. Section 14.1.1 gives an overview of the geometric setting and dynamical field content. Its relation to a gauge theory of

The original version of this chapter was revised. The affiliations of authors, Sebastian Bahamonde, Konstantinos F. Dialektopoulos, Manuel Hohmann, Jackson Levi Said have been updated. The correction to this chapter is available at https://doi.org/10.1007/978-3-030-83715-0_39

S. Bahamonde (✉)

Laboratory of Theoretical Physics, Institute of Physics, University of Tartu, W. Ostwaldi 1, 50411 Tartu, Estonia

Department of Mathematics, University College London, Gower Street, WC1E 6BT London, United Kingdom

e-mail: sbahamonde@ut.ee

K. F. Dialektopoulos

Center for Gravitation and Cosmology, College of Physical Science and Technology, Yangzhou University, Yangzhou 225009, China

e-mail: kdialekt@gmail.com

M. Hohmann

Laboratory of Theoretical Physics, Institute of Physics, University of Tartu, W. Ostwaldi 1, 50411 Tartu, Estonia

e-mail: manuel.hohmann@ut.ee

J. L. Said

Institute of Space Sciences and Astronomy, University of Malta, Msida MSD 2080, Malta

e-mail: jackson.said@um.edu.mt

Department of Physics, University of Malta, Msida MSD 2080, Malta

© The Author(s), under exclusive license to Springer Nature Switzerland AG 2021, corrected publication 2022

191

E. N. Saridakis et al. (eds.) *Modified Gravity and Cosmology*,

https://doi.org/10.1007/978-3-030-83715-0_14

translations is explained in Sect. 14.1.2. Local Lorentz invariance is discussed in Sect. 14.1.3. Section 14.1.4 briefly elucidates how matter couples to the teleparallel geometry. Finally, Sect. 14.1.5 gives an account of the most simple Teleparallel Gravity theory, which is equivalent to General Relativity at the level of its field equations. The notation used here and in the following sections on Teleparallel Gravity is summarized in the Convention Table in the beginning of the book.

14.1.1 Teleparallel Geometry

The most important, distinguishing feature of Teleparallel Gravity [1] is its use of an affine connection, whose connection coefficients will be denoted by $\dot{\Gamma}^\mu_{\nu\rho}$, and which is different from the Levi-Civita connection of the metric $g_{\mu\nu}$. This connection is chosen to be flat, in the sense that has vanishing curvature

$$\dot{R}^\mu_{\nu\alpha\beta} = \partial_\alpha \dot{\Gamma}^\mu_{\nu\beta} - \partial_\beta \dot{\Gamma}^\mu_{\nu\alpha} + \dot{\Gamma}^\mu_{\rho\alpha} \dot{\Gamma}^\rho_{\nu\beta} - \dot{\Gamma}^\mu_{\rho\beta} \dot{\Gamma}^\rho_{\nu\alpha} \equiv 0, \quad (14.1)$$

where we denote quantities related to the teleparallel connection with a bullet to distinguish them from their Levi-Civita counterparts. For instance, $\dot{\nabla}_\mu$ denotes the teleparallel covariant derivative, while ∇_μ denotes the Levi-Civita covariant derivative. The flatness of the connection allows a path-independent parallel transport, hence maintaining a notion of being parallel at a distance, which is the reason for calling it “teleparallel” [2]. Further, the teleparallel connection is metric compatible, so that its non-metricity tensor vanishes,

$$\dot{Q}_{\rho\mu\nu} = \dot{\nabla}_\rho g_{\mu\nu} = \partial_\rho g_{\mu\nu} - \dot{\Gamma}^\sigma_{\mu\rho} g_{\sigma\nu} - \dot{\Gamma}^\sigma_{\nu\rho} g_{\mu\sigma} \equiv 0, \quad (14.2)$$

while its torsion

$$\dot{T}^\rho_{\mu\nu} = \dot{\Gamma}^\rho_{\nu\mu} - \dot{\Gamma}^\rho_{\mu\nu} \quad (14.3)$$

is allowed to be non-vanishing. In Teleparallel Gravity, the torsion takes the role of the gravitational field strength, in contrast to General Relativity, where this role is attributed to the Levi-Civita curvature.

There are different, equivalent possibilities to implement the teleparallel connection as a dynamical field. In the original formulation by Einstein [2], the only fundamental dynamical field is a tetrad (or vielbein) field $e^A = e^A_\mu dx^\mu$. Here and in the remainder of this section, capital Latin letters $A, B = 0, \dots, 3$ denote Lorentz indices. The tetrad defines both the metric

$$g_{\mu\nu} = \eta_{AB} e^A_\mu e^B_\nu \quad (14.4)$$

and the coefficients

$$\dot{\Gamma}^\mu_{\nu\rho} = e^A_\nu \partial_\rho e^A_\nu \quad (14.5)$$

of the teleparallel affine connection, where $\eta_{AB} = \text{diag}(-1, 1, 1, 1)$ is the Minkowski metric and $e_A = e_A^\mu \partial_\mu$ is the inverse tetrad satisfying $e_A^\mu e_{A'}^\nu = \delta_{AA'}^\nu$ and $e_A^\mu e_B^\mu = \delta_B^A$. This particular choice of the connection is known as the Weitzenböck connection, and it belongs to a family of flat, metric compatible connections. The constituents of this family can be expressed in terms of the connection one-forms $\dot{\omega}^A_B = \dot{\omega}^A_{B\mu} dx^\mu$ of a flat Lorentz spin connection via the relation

$$\dot{\Gamma}^\mu_{\nu\rho} = e_A^\mu (\partial_\rho e^A_\nu + \dot{\omega}^A_{B\rho} e^B_\nu). \quad (14.6)$$

Here, flatness corresponds to vanishing curvature of the spin connection,

$$\dot{R}^A_{B\alpha\beta} = \partial_\alpha \dot{\omega}^A_{B\beta} - \partial_\beta \dot{\omega}^A_{B\alpha} + \dot{\omega}^A_{C\alpha} \dot{\omega}^C_{B\beta} - \dot{\omega}^A_{C\beta} \dot{\omega}^C_{B\alpha} \equiv 0, \quad (14.7)$$

while metric compatibility follows from the antisymmetry $\dot{\omega}^{(AB)}_\mu \equiv 0$. In the covariant formulation of teleparallel gravity theories [3], the spin connection is promoted to a dynamical field, and its flatness must be imposed either through Lagrange multipliers in the gravitational action or by explicitly allowing only for flat connections and accordingly restricting the variation with respect to the spin connection in the derivation of the Euler-Lagrange equations [4]. Yet another possibility to ensure the flatness of the spin connection is to consider it as a dependent quantity $\dot{\omega}^A_{B\mu} = \Lambda^A_C \partial_\mu \Lambda_B^C$ derived from a local Lorentz transformation Λ^A_B , and to promote the latter to a fundamental dynamical field next to the tetrad [5, 6].

Another implementation of teleparallel geometry is the Palatini approach, which considers as fundamental fields the metric $g_{\mu\nu}$ and the affine connection coefficients $\dot{\Gamma}^\rho_{\mu\nu}$, and enforces metric compatibility and flatness of the connection via Lagrange multipliers [7].

14.1.2 Translation Gauge Theory

One argument that is commonly mentioned in favour of Teleparallel Gravity is its possible interpretation as a gauge theory of translations. Various approaches and realisations of this gauge theory have been studied [8]. It was first found in the non-covariant formulation of Teleparallel Gravity that the tetrad allows for a gauge symmetry, which can be related to infinitesimal translations, and that imposing this symmetry leads to an action equivalent to the Einstein-Hilbert action [9, 10]. Relaxing the condition of local Lorentz invariance yields a more general class of theories [11]. A more sophisticated approach relates Teleparallel Gravity to higher gauge theory, and generalisations of Cartan geometry [12]. Cartan geometry has also been suggested as a possible interpretation of the non-standard nature of translational gauge transformations, which act not only on an internal space, is usual in gauge theory, but also on the underlying spacetime manifold [13]. This interpretation has been contrasted with a formulation making use of a principal bundle of translations [14].

Despite their differences, the aforementioned approaches have in common that the tetrad field is related to a gauge potential of translations, while the spin connection is related to an external Lorentz gauge symmetry. However, for a more fundamental understanding of how the tetrad and spin connection in the covariant formulation of Teleparallel Gravity arise, it is helpful to take a step backwards and view Teleparallel Gravity in the more general context of Poincaré gauge theory, and even more generally in the context of metric-affine gravity [15, 16]. We therefore briefly review their description in terms of gauge connections.

We denote by FM the general linear frame bundle of the spacetime manifold M . The fiber $F_x M$ at a point $x \in M$ is the set of all frames, i.e., ordered bases of the tangent space $T_x M$. Any frame can be expressed by a bijective linear map $f : \mathbb{R}^4 \rightarrow T_x M$. Given coordinates (x^μ) on M , we can introduce coordinates (x^μ, f_A^μ) on FM , where the frame f maps an element $v \in \mathbb{R}^4$ with components v^A to $v^A f_A^\mu \partial_\mu \in T_x M$. Note that FM is a principal bundle: the group $H_0 = \text{GL}(4, \mathbb{R})$ acts from the right on the fibres of FM . Writing the matrix components of an element $\Lambda \in H_0$ as Λ^A_B , the action reads

$$(x^\mu, f_A^\mu) \mapsto (x^\mu, f_A^\mu) \cdot \Lambda = (x^\mu, f_B^\mu \Lambda^B_A) \quad (14.8)$$

in the coordinates we used.

A frame allows expressing tensor fields in a basis that is different from the coordinate basis. Changing the frame changes the basis, while keeping the point fixed at which the tensor field is evaluated. In order to incorporate translations as well, one considers a larger bundle, which may be constructed as follows. Let $G_0 = \text{GA}(4, \mathbb{R}) = \mathbb{R}^4 \rtimes \text{GL}(4, \mathbb{R})$ be the general affine group. The group H_0 , being a subgroup of G_0 , acts on G_0 by left multiplication: given $\tilde{\Lambda} \in H_0$ and $(\Lambda, v) \in G_0$, one has

$$\tilde{\Lambda} \cdot (\Lambda, v) = (\tilde{\Lambda}\Lambda, \tilde{\Lambda}v). \quad (14.9)$$

This action gives rise to an associated bundle $AM = FM \times_{H_0} G_0$, which we call the affine frame bundle. To understand the geometry of AM , recall that for each $x \in M$ the elements of the fiber $A_x M$ are given by equivalence classes

$$[\tilde{f}, (\Lambda, v)] = [\tilde{f} \cdot \tilde{\Lambda}^{-1}, \tilde{\Lambda} \cdot (\Lambda, v)], \quad (14.10)$$

where $\tilde{f} \in F_x M$ is a frame at x and $(\Lambda, v) \in G_0$, and equivalence is given by the simultaneous action of $\tilde{\Lambda} \in H_0$ on both of these objects, following the equation above. One can see that every such equivalence class is defined by a frame $f = \tilde{f} \cdot \Lambda$, as well as a tangent vector $y = \tilde{f}v$, or in components

$$f_A^\mu = \tilde{f}_B^\mu \Lambda^B_A \quad \text{and} \quad y^\mu = v^A \tilde{f}_A^\mu, \quad (14.11)$$

since these combinations are invariant under the application of $\tilde{\Lambda}$. Hence, the affine frame bundle has the structure

$$AM = TM \times_M FM, \quad (14.12)$$

or in other words, every element of AM consists of a base point $x \in M$, a vector $y \in T_x M$ and a frame $f \in F_x M$. Coordinates on AM thus take the form (x^μ, y^μ, f_A^μ) . One finds that AM is a principal G_0 -bundle, where the right action is given by

$$(x^\mu, y^\mu, f_A^\mu) \mapsto (x^\mu, y^\mu, f_A^\mu) \cdot (\Lambda, v) = (x^\mu, y^\mu + f_A^\mu v^A, f_B^\mu \Lambda^B_A) \quad (14.13)$$

for $(\Lambda, v) \in G_0$.

The bundle AM is the arena for the gauge theory we model. The gauge connection is given by a one-form $\hat{\mathbf{A}} \in \Omega^1(AM, \mathfrak{g}_0)$ on AM , taking values in the Lie algebra \mathfrak{g}_0 of G_0 . Since this Lie algebra splits as $\mathfrak{g}_0 = \mathfrak{h}_0 \oplus \mathfrak{z}$ into the homogeneous part \mathfrak{h}_0 and translations $\mathfrak{z} \cong \mathbb{R}^4$, the same holds for the gauge connection $\hat{\mathbf{A}} = \hat{\omega} + \mathbf{e}$. Using the canonical matrix and vector representations of these Lie algebras, it turns out that the most general one-form connection can be written in the form

$$\hat{\omega}^A_B = f^{-1A}{}_\mu (f_B{}^\nu \hat{\Omega}^\mu{}_{\nu\rho} dx^\rho + df_B^\mu), \quad (14.14a)$$

$$\mathbf{e}^A = f^{-1A}{}_\mu (E^\mu{}_\nu dx^\nu + \hat{\Omega}^\mu{}_{\nu\rho} y^\nu dx^\rho + dy^\mu) \quad (14.14b)$$

in our chosen coordinates, where $E^\mu{}_\nu$ and $\hat{\Omega}^\mu{}_{\nu\rho}$ are functions of x only. This form is a consequence of the demand that $\hat{\mathbf{A}}$ is a principal connection.

Finally, to obtain the gauge fields on the spacetime manifold M , we need to choose a *gauge*; this corresponds to choosing a section $\sigma : M \rightarrow AM$. In our coordinates this section can be expressed as

$$\sigma : x \mapsto (x^\mu, \sigma^\mu, \sigma_A{}^\mu). \quad (14.15)$$

The section allows us to take the pullbacks

$$\sigma^* \hat{\omega}^A_B = \hat{\omega}^A_{B\mu} dx^\mu = \sigma^{-1A}{}_\mu (\sigma_B{}^\nu \hat{\Omega}^\mu{}_{\nu\rho} + \partial_\rho \sigma_B^\mu) dx^\rho, \quad (14.16a)$$

$$\sigma^* \mathbf{e}^A = e^A{}_\mu dx^\mu = \sigma^{-1A}{}_\mu (E^\mu{}_\rho + \hat{\Omega}^\mu{}_{\nu\rho} \sigma^\nu + \partial_\rho \sigma^A) dx^\rho. \quad (14.16b)$$

Here we have already suggestively identified these pullbacks with the tetrad $e^A{}_\mu$ and teleparallel spin connection $\hat{\omega}^A_{B\mu}$. To justify this identification and to resort to more familiar notation, we introduce new coordinates

$$(x^\mu, y^\mu, f_A^\mu) \mapsto (x^\mu, \xi^A, f_A^\mu) = (x^\mu, f^{-1A}{}_\mu y^\mu, f_A^\mu), \quad (14.17)$$

and accordingly replace $\sigma^\mu = \sigma^A \sigma_A{}^\mu$. Then the tetrad (14.16b) becomes

$$\sigma^* \mathbf{e}^A = e^A{}_\mu dx^\mu = (B^A{}_\rho + \hat{\omega}^A_{B\rho} \sigma^B + \partial_\rho \sigma^A) dx^\rho, \quad (14.18)$$

where $B^A{}_\rho = \sigma^{-1 A}{}_\mu E^\mu{}_\rho$. This is the form most commonly encountered in the literature [1]. Note that changing the section $\sigma^A{}_\mu$ simply corresponds to a change of the Lorentz frame, while a change of σ^A can be interpreted as a translation gauge transformation. Finally, calculating the torsion yields

$$\hat{T}^A{}_{\mu\nu} dx^\mu \wedge dx^\nu = de^A + \hat{\omega}^A{}_B \wedge e^B = (\partial_\mu B^A{}_\nu + \hat{\omega}^A{}_{B\mu} B^B{}_\nu + \partial_\mu \hat{\omega}^A{}_{B\nu} \sigma^B + \hat{\omega}^A{}_{C\mu} \hat{\omega}^C{}_{B\nu} \sigma^B) dx^\mu \wedge dx^\nu. \quad (14.19)$$

In the teleparallel geometry the spin connection has vanishing curvature (14.7), and so the two terms involving σ^B vanish. The torsion then becomes the field strength of the translation gauge potential $B^A{}_\mu$.

14.1.3 Local Lorentz Invariance

When the concept of teleparallelism was introduced, the only dynamical field was the tetrad $e^A{}_\mu$, which has 16 components. It was believed that gravity is described by the 10 components of the metric, while the additional six components could be attributed to the electromagnetic field strength [2]. However, this turned out not to be the case, and it was realised that these additional components are related to local Lorentz transformations $e^A{}_\mu \mapsto \Lambda^A{}_B e^B{}_\mu$ instead. Further, it was found that in general Teleparallel gravity theories are not invariant under such local Lorentz transformations, due to the presence of the Weitzenböck connection $\hat{\Gamma}^\rho{}_{\mu\nu} = e_A{}^\rho \partial_\nu e^A{}_\mu$: in order to solve the field equations of such theories, one cannot choose an arbitrary tetrad corresponding to a particular metric, but only specific tetrads are allowed [17–21]. This means that the extra components present in the tetrad cannot be regarded as pure gauge degrees of freedom. This fact raised a debate regarding the nature of the additional degrees of freedom, whether they might be acausal or even superluminal, or whether some of them can be absorbed by a remnant gauge symmetry that is still present despite the otherwise broken Lorentz symmetry [22–30].

In order to resolve the aforementioned issues, a covariant formulation of Teleparallel Gravity theories was developed, which features the flat Lorentz spin connection $\hat{\omega}^A{}_{B\mu}$ as an additional dynamical field [3, 4, 31, 32]. In the covariant formulation, local Lorentz transformations take the form

$$e^A{}_\mu \mapsto \Lambda^A{}_B e^B{}_\mu, \quad \hat{\omega}^A{}_{B\mu} \mapsto \Lambda^A{}_C (\Lambda^{-1})^D{}_B \hat{\omega}^C{}_{D\mu} + \Lambda^A{}_C \partial_\mu (\Lambda^{-1})^C{}_B, \quad (14.20)$$

and thus act on both the tetrad and the spin connection. The teleparallel connection (14.6), and hence also its torsion (14.3), are invariant under this combined transformation. It thus follows that any action constructed from the (in any case invariant) metric, the torsion and their derivatives are locally Lorentz invariant.

Note that the spin connection (14.16a) also naturally arises in the gauge theory approach shown in Sect. 14.1.2. In this picture, local Lorentz transformations are simply transformations of the Lorentz part $\sigma^A{}_\mu$ of the section defining the gauge.

14.1.4 Matter Coupling

An important issue in Teleparallel Gravity is the question about how to couple matter to the teleparallel geometry. The most commonly considered procedure is given by the minimal coupling prescription, according to which the metric $g_{\mu\nu}$ in the matter action is chosen to be the metric (14.4) obtained from the tetrad. This prescription is sufficient for bosonic fields, which couple to the metric only, without direct coupling to a spin connection. This differs from the case of fermions, where a spin connection must be specified. The question about a consistent coupling of fermions and the proper choice of the spin connection is a highly topic [16, 33–37]. We will not enter this debate here, and assume that fermions couple to the metric geometry through the spin connection associated with the Levi-Civita connection only. Following this assumption, the matter action does not depend on the teleparallel spin connection, but only on the tetrad. For the variation with respect to the tetrad we may write

$$\delta_e S_{\text{matter}} = - \int d^4x e T_A^\mu \delta e^A{}_\mu. \quad (14.21)$$

The quantity T_A^μ introduced here is the matter energy-momentum tensor, which we also write in the form $T_{\mu\nu} = e^A{}_\mu g_{\mu\nu} T_A{}^\rho$.¹ Demanding that the matter action is invariant under local Lorentz transformations, which is equivalent to demanding that it depends only on the metric obtained from the tetrad, then implies that the energy-momentum tensor is symmetric, $T_{[\mu\nu]} = 0$ [38].

14.1.5 Teleparallel Equivalent of General Relativity (TEGR)

An interesting feature of Teleparallel Gravity is that it allows for an alternative formulation of General Relativity, in which gravity is mediated by torsion instead of curvature [39]. One possibility to derive the action for the Teleparallel Equivalent of General Relativity (TEGR) is by starting from the Einstein-Hilbert action

$$S_{\text{GR}} = \frac{1}{2\kappa^2} \int d^4x \sqrt{-g} R, \quad (14.22)$$

where $\kappa^2 = 8\pi G$, and by rewriting the Ricci scalar in terms of the torsion of the teleparallel connection. For this purpose, we introduce the contortion tensor

$$\dot{K}{}^\rho{}_{\mu\nu} = \dot{\Gamma}{}^\rho{}_{\mu\nu} - \Gamma{}^\rho{}_{\mu\nu} = \frac{1}{2} \left(\dot{T}{}^\rho{}_{\mu\nu} + \dot{T}{}^\rho{}_{\nu\mu} - \dot{T}{}^\rho{}_{\mu\nu} \right) \quad (14.23)$$

¹ While $T_{\mu\nu}$ refers to the energy-momentum tensor, $\dot{T}{}^\rho{}_{\mu\nu}$ refers to the torsion tensor which is not related.

as the difference between the teleparallel and Levi-Civita connection coefficients. By making use of this relation, one can write the Riemann curvature tensor of the Levi-Civita connection in the form

$$R^\mu{}_{\nu\rho\sigma} = \dot{R}^\mu{}_{\nu\rho\sigma} - \nabla_\rho \dot{K}^\mu{}_{\nu\sigma} + \nabla_\sigma \dot{K}^\mu{}_{\nu\rho} - \dot{K}^\mu{}_{\tau\rho} \dot{K}^\tau{}_{\nu\sigma} + \dot{K}^\mu{}_{\tau\sigma} \dot{K}^\tau{}_{\nu\rho}, \quad (14.24)$$

keeping in mind that the curvature of the teleparallel connection vanishes, $\dot{R}^\mu{}_{\nu\rho\sigma} \equiv 0$, while the curvature of the Levi-Civita connection does not vanish in general. Taking the appropriate contractions, and using the antisymmetry $\dot{K}^{(\mu\nu)\rho} = 0$, the Ricci scalar reads

$$R = -2\nabla_\mu \dot{K}^{\mu\nu}{}_\nu + \dot{K}^{\rho\mu}{}_\mu \dot{K}^{\nu}{}_\rho{}^\nu - \dot{K}^{\rho\mu\nu} \dot{K}^{\rho\nu\mu} = -\mathbb{T} + 2\nabla_\mu \dot{T}^{\nu\mu} = -\mathbb{T} + B. \quad (14.25)$$

Here we introduced the torsion scalar \mathbb{T} , which can be written in the form

$$\mathbb{T} = \frac{1}{2} \dot{T}^\rho{}_{\mu\nu} \dot{S}^{\mu\nu}{}_\rho = \frac{1}{4} \dot{T}^{\mu\nu\rho} \dot{T}_{\mu\nu\rho} + \frac{1}{2} \dot{T}^{\mu\nu\rho} \dot{T}_{\rho\nu\mu} - \dot{T}^\mu{}_{\mu\rho} \dot{T}^{\nu\rho}{}_\nu, \quad (14.26)$$

where we used the superpotential

$$\dot{S}^{\mu\nu}{}_\rho = \dot{K}^{\mu\nu}{}_\rho - \delta_\rho^\mu \dot{T}^{\sigma\nu}{}_\sigma + \delta_\rho^\nu \dot{T}^{\sigma\mu}{}_\sigma. \quad (14.27)$$

Finally, the last term in the expression (14.25) is a total divergence, and thus appears as a boundary term in the action, which does not contribute to the field equations. Omitting this term and using the fact that the determinants of the metric and the tetrad are related by

$$e = \sqrt{-g}, \quad (14.28)$$

the TEGR action finally reads

$$S_{\text{TEGR}} = -\frac{1}{2\kappa^2} \int d^4x e \mathbb{T}. \quad (14.29)$$

Variation of this action, together with a matter action, with respect to the tetrad, and transforming the resulting Lorentz index into a spacetime index, yields the field equations

$$\nabla_\rho \dot{S}_{(\mu\nu)}{}^\rho - \frac{1}{2} \dot{S}_{(\mu}{}^{\rho\sigma} \dot{T}_{\nu)\rho\sigma} + \frac{1}{2} \mathbb{T} g_{\mu\nu} = \kappa^2 T_{\mu\nu}. \quad (14.30)$$

The right-hand side is given by the energy-momentum tensor (14.21). The left-hand side of these field equations is most easily understood by realising the geometric identity

$$\nabla_\rho \dot{S}_{(\mu\nu)}{}^\rho - \frac{1}{2} \dot{S}_{(\mu}{}^{\rho\sigma} \dot{T}_{\nu)\rho\sigma} + \frac{1}{2} \mathbb{T} g_{\mu\nu} = R_{\mu\nu} - \frac{1}{2} R g_{\mu\nu} = G_{\mu\nu}, \quad (14.31)$$

and so it turns out that the field equations indeed agree with those of General Relativity, as one would expect. An interesting property of the action (14.29) is the fact that the teleparallel spin connection $\dot{\omega}^A{}_{B\mu}$ enters only in the form of a boundary term [40]. This can be seen from the relation (14.25) between the Ricci scalar of the Levi-Civita connection and the torsion scalar. The left-hand side is independent of the teleparallel spin connection, and so its variation $\delta_\omega R$ vanishes. This implies

$$\delta_\omega \mathbb{T} = 2\delta_\omega \nabla_\mu \dot{T}_\nu{}^{\nu\mu} = 2\nabla_\mu \delta_\omega \dot{T}_\nu{}^{\nu\mu}, \quad (14.32)$$

so that variation of the TEGR action with respect to the teleparallel spin connection yields a boundary term only. One consequence is that the teleparallel spin connection drops out of the field equations, as can be seen from the identity (14.25). From this, further follows that the theory is invariant not only under the local Lorentz transformations (14.20), but also under the pure tetrad transformations $e^A{}_\mu \mapsto \Lambda^A{}_B e^B{}_\mu$. This invariance, which does not hold for general teleparallel theories, as discussed in the following section, is one reason why Teleparallel Gravity was originally developed without appealing to a non-trivial spin connection, and the viability of the covariant formulation of TEGR has been challenged [41].

14.2 Teleparallel Gravity Extensions

Even if Λ CDM has passed most of the observational tests with flying colours, General Relativity (GR), and thus the Teleparallel Equivalent of GR (TEGR) as well, contain some shortcomings. Motivated mostly by the accelerated expansion of the Universe, many people initiated the hunt for a modification of gravity. In the same way as in the curvature case, the literature abounds different theories of Teleparallel Gravity, that introduce new degrees of freedom to describe several phenomena.

Either by introducing scalar fields to the TEGR Lagrangian, or by generalising it to an arbitrary function of the torsion scalar, i.e. $f(\mathbb{T})$, by introducing non-localities, non-linear boundary terms and other topological invariants, there has been a great plethora of models studied. In this section we will give a brief review on the most well-known modifications.

14.2.1 $f(\mathbb{T})$ Gravity

In the curvature case, the most straightforward modification, and maybe the simplest one, is the so-called $f(R)$ gravity. As the name witnesses, it is a generalisation of the Einstein-Hilbert action to an arbitrary function of the Ricci scalar that offers richer phenomenology [42–45] by introducing a new scalar degree of freedom [46–48]. In the same spirit, $f(\mathbb{T})$ theory was proposed almost a decade ago [19, 49–51] and its

action reads

$$\mathcal{S}_{f(\mathbb{T})} = \frac{1}{2\kappa^2} \int d^4x \, ef(\mathbb{T}) + \mathcal{S}_{\text{matter}}. \quad (14.33)$$

It is worth mentioning that even though at the level of field equations GR and TEGR are totally equivalent theories, the same does not happen for $f(R)$ and $f(\mathbb{T})$ theories. As already discussed in the previous section, $R = -\mathbb{T} + B$ (14.25), where $B = -2\partial_\alpha(e\dot{T}^{\mu\alpha}_\mu)/e$ is a boundary term, that in TEGR does not contribute to the field equations. However, the arbitrary function $f(\mathbb{T})$ is non-linear and thus the two theories are no longer equivalent.

Varying the action (14.33) with respect to the tetrad e^A_μ we get its field equations that read

$$f_{\mathbb{T}}\partial_\nu(e\dot{S}_A^{\mu\nu}) + e\left(f_{\mathbb{T}\mathbb{T}}\dot{S}_A^{\mu\nu}\partial_\nu\mathbb{T} - f_{\mathbb{T}}\dot{T}^B_{\nu A}\dot{S}_B^{\nu\mu} + f_{\mathbb{T}}\dot{\omega}^B_{A\nu}\dot{S}_B^{\nu\mu} + \frac{1}{2}fe_A^\mu\right) = \kappa^2eT_A^\mu, \quad (14.34)$$

with $f_{\mathbb{T}}$ and $f_{\mathbb{T}\mathbb{T}}$ being respectively the first, and second-order derivatives of f with respect to \mathbb{T} and $T_\mu^\nu = e^A_\mu T_A^\nu$ is the energy-momentum tensor of the matter fields. As one can immediately notice, the equations for the tetrad are of second order, in contrast with those in $f(R)$ gravity. For the unimodular formulation of $f(\mathbb{T})$ gravity, where the determinant of the tetrad is kept constant, one can check [52].

Variation of (14.33) with respect to the spin connection [4, 53, 54] gives the antisymmetric part of the tetrad equations (14.34), meaning

$$f_{\mathbb{T}\mathbb{T}}\dot{S}_{[AB]}^\nu\dot{T}_\nu = 0 \quad (14.35)$$

There was a period when it was believed that $f(\mathbb{T})$ gravity violates local Lorentz invariance [17, 18]. Indeed, if one considers the theory with the tetrad being the only variable, the discussion is constrained on a very specific class of frames where the spin connection vanishes. That is why the existence of *good* and *bad tetrads* was proposed [20], referring to tetrads in the same equivalence class that solve and do not solve respectively the field equations. An illuminating example is that the diagonal tetrad in spherical symmetry

$$e^A_\mu = \text{diag}(A, B, r, r \sin \theta), \quad (14.36)$$

corresponding to the metric $g_{\mu\nu} = \text{diag}[A^2(r), B^2(r), r^2, r^2 \sin^2 \theta]$, is a bad tetrad, not satisfying the field equations (14.34) with a vanishing spin connection for $f_{\mathbb{T}\mathbb{T}} \neq 0$, while the non-diagonal tetrad associated to the same metric

$$e^A_\mu = \begin{pmatrix} A & 0 & 0 & 0 \\ 0 & B \cos \phi \sin \theta & r \cos \phi \cos \theta & -r \sin \phi \sin \theta \\ 0 & -B \cos \theta & r \sin \theta & 0 \\ 0 & B \sin \phi \sin \theta & r \sin \phi \cos \theta & r \cos \phi \sin \theta \end{pmatrix}, \quad (14.37)$$

is a good tetrad. The problem was resolved when the covariant formulation of $f(\mathbb{T})$ gravity was proposed [3], where both the tetrad $e^A{}_\mu$ and the spin connection $\dot{\omega}^A{}_{B\mu}$ are determined by the field equations (14.34). For a more detailed study about tetrads in spherical symmetry in Teleparallel theories, see [55].

14.2.2 New General Relativity and Extensions

This modification of TEGR is the first one, and it was proposed by Hayashi and Shirafuji in [11]. The torsion tensor can be decomposed into its three irreducible parts as

$$\dot{T}_{\lambda\mu\nu} = \frac{2}{3}(\dot{i}_{\lambda\mu\nu} - \dot{i}_{\lambda\nu\mu}) + \frac{1}{3}(g_{\lambda\mu}\dot{v}_\nu - g_{\lambda\nu}\dot{v}_\mu) + \epsilon_{\lambda\mu\nu\rho}\dot{a}^\rho, \quad (14.38)$$

where $\dot{v}_\mu = \dot{T}^\lambda{}_{\lambda\mu}$, $\dot{a}_\mu = \frac{1}{6}\epsilon_{\mu\nu\sigma\rho}\dot{T}^{\nu\sigma\rho}$, and $\dot{i}_{\lambda\mu\nu} = \frac{1}{2}(\dot{T}_{\lambda\mu\nu} + \dot{T}_{\mu\lambda\nu}) + \frac{1}{6}(g_{\nu\lambda}\dot{v}_\mu + g_{\nu\mu}\dot{v}_\lambda) - \frac{1}{3}g_{\lambda\mu}\dot{v}_\nu$.

Contracting these components, one can construct the following scalars up to quadratic order

$$T_{\text{ten}} = \dot{i}_{\lambda\mu\nu}\dot{i}^{\lambda\mu\nu}, \quad T_{\text{ax}} = \dot{a}_\mu\dot{a}^\mu, \quad T_{\text{vec}} = \dot{v}_\mu\dot{v}^\mu. \quad (14.39)$$

The torsion scalar \mathbb{T} is equal to

$$\mathbb{T} = \frac{3}{2}T_{\text{ax}} + \frac{2}{3}T_{\text{ten}} - \frac{2}{3}T_{\text{vec}}, \quad (14.40)$$

and an immediate generalisation of this, with arbitrary coefficients, is the action of the New General Relativity, i.e.

$$\mathcal{S}_{\text{NGR}} = \frac{1}{2\kappa^2} \int d^4x e (c_1 T_{\text{ax}} + c_2 T_{\text{vec}} + c_3 T_{\text{ten}}). \quad (14.41)$$

For completeness we should mention that there are two more quadratic scalars that one can construct from the torsion tensor,

$$P_1 = \dot{v}_\mu\dot{a}^\mu \quad \text{and} \quad P_2 = \epsilon_{\mu\nu\rho\sigma}\dot{i}^{\lambda\mu\nu}\dot{i}_\lambda{}^{\rho\sigma}. \quad (14.42)$$

However, both of them are parity violating and we do not consider them here. For more details one can check Ref. [56], where the authors argue that the parity violating sector could play a crucial role for the well-posedness of the Cauchy problem. It is not clear whether these parity violating scalars can play a fully consistent role in gravitational theories.

The theory (14.41) has been studied and constrained since its proposal in Refs. [23, 57, 58]. In greater detail, Solar System tests were studied [11], singularities of Schwarzschild-like spacetimes in [59], axially symmetric solutions in [60] and its weak-field limit in [61]. More recently, in [62] the propagation of gravitational waves was studied, as well as its Hamiltonian analysis was considered in [5, 63, 64]. Finally, the linearized theory was studied in [65], where the author shows that in order for the theory to be viable, the 2-form field has to feature a gauge symmetry so that it describes a massless Kalb–Ramond field. However, cubic order interactions show [66] that the above gauge symmetry of the 2-form is not preserved at higher orders.

Beyond the NGR theory, extensions of different kinds were considered as well. In [67] it was found that it is possible to construct a conformally invariant theory considering a quadratic Lagrangian based on the tensorial and axial part of torsion, which has the following form,

$$\mathcal{S}_{\text{Conformal-TG}} = \frac{1}{2\kappa^2} \int d^4x e \left(\frac{3}{2} T_{\text{ax}} + \frac{2}{3} T_{\text{ten}} \right)^2. \quad (14.43)$$

Note that the vectorial part of the torsion tensor does not appear in this theory. Specifically, in [68] a generalisation of NGR by nine functions of the d’Alembertian operator was considered and the authors show that it can accommodate the ghost- and singularity-free structure that was realised in the metric theories [69–71]. In addition, in the same spirit with $f(\mathbb{T})$, a straightforward generalisation of NGR is the $f(T_{\text{ax}}, T_{\text{vec}}, T_{\text{ten}})$ theory proposed in [72]. Apart from richer phenomenology compared to $f(\mathbb{T})$ gravity, this theory provides us with the ability to study conformal transformations of teleparallel theories in a simple way. In particular, the quadratic scalars constructed by the irreducible parts of the torsion tensor (14.39) transform under the conformal transformation of the tetrad $\tilde{e}^A{}_\mu = \Omega e^A{}_\mu$ (or of the metric $\tilde{g}_{\mu\nu} = \Omega^2 g_{\mu\nu}$), with Ω being the conformal factor, as

$$T_{\text{ax}} = \Omega^2 \tilde{T}_{\text{ax}}, \quad T_{\text{ten}} = \Omega^2 \tilde{T}_{\text{ten}}, \quad T_{\text{vec}} = \Omega^2 \tilde{T}_{\text{vec}} + 6\Omega v^\mu \tilde{\partial}_\mu \Omega + 9\tilde{g}^{\mu\nu} \tilde{\partial}_\mu \Omega \tilde{\partial}_\nu \Omega. \quad (14.44)$$

Obviously, unlike the $f(R)$ case [42], in modified teleparallel theories there cannot be an Einstein frame because of the way T_{vec} transforms. More studies on conformal transformations in the teleparallel framework can be found in Refs. [73, 74].

14.2.3 Higher-Order Derivatives, $f(\mathbb{T}, B, T_G, B_G)$

In the $f(\mathbb{T})$ theory only the torsion scalar takes part in the action, and since it contains only first derivatives of the tetrads, the resulting equations are of second order. This is not a necessity though (if you can ignore or screen out ghosts), and thus the field equations can be of higher order as well; as is in $f(R)$.

One of the most well-studied theories include, in addition to the torsion scalar, the boundary term $B = -2\partial_\alpha(e\dot{T}^{\mu\alpha}{}_\mu)/e$. The action of this theory [75–77] reads

$$\mathcal{S}_{f(\mathbb{T}, B)} = \frac{1}{2\kappa^2} \int d^4x e f(\mathbb{T}, B) + \mathcal{S}_{\text{matter}} \quad (14.45)$$

and varying this with respect to the tetrad we take the field equations

$$\begin{aligned} 2ee_A{}^\nu \square f_B - 2ee_A{}^\mu \nabla^\nu \nabla_\mu f_B + eBf_B e_A{}^\nu + 4e(\partial_\mu f_B + \partial_\mu f_{\mathbb{T}}) \dot{S}_A{}^{\mu\nu} + \\ + 4\partial_\mu(e\dot{S}_A{}^{\mu\nu})f_{\mathbb{T}} - 4ef_{\mathbb{T}}\dot{T}^\lambda{}_{\mu A}\dot{S}_\lambda{}^{\nu\mu} - efe_A{}^\lambda = 2\kappa eT_A{}^\nu. \end{aligned} \quad (14.46)$$

It is interesting to notice that such theories are much more general than the $f(R)$ theories, since the last ones are just a subclass when $f(\mathbb{T}, B) = f(-\mathbb{T} + B) = f(R)$. In addition to these, theories with higher derivative terms of the torsion scalar, e.g. $\nabla^2\mathbb{T}$, $\square\mathbb{T}$, etc., where also proposed [78].

Last but not least, theories with higher-order invariants were also considered in the literature. An interesting example is the inclusion of the Gauss-Bonnet invariant,

$$\mathcal{G} = R^2 - 4R_{\mu\nu}R^{\mu\nu} + R^{\alpha\beta\mu\nu}R_{\alpha\beta\mu\nu}. \quad (14.47)$$

Its teleparallel version reads, as with the Ricci scalar,

$$\mathcal{G} = -T_{\mathcal{G}} + B_{\mathcal{G}}, \quad (14.48)$$

where $T_{\mathcal{G}}$ is the teleparallel Gauss-Bonnet term and $B_{\mathcal{G}}$ its boundary term. Such theories have an action of the form

$$\mathcal{S}_{f(\mathbb{T}, T_{\mathcal{G}})} = \frac{1}{2\kappa^2} \int d^4x e f(\mathbb{T}, T_{\mathcal{G}}), \quad (14.49)$$

or even more complicated functions like $f(\mathbb{T}, B, T_{\mathcal{G}}, B_{\mathcal{G}})$. Such theories present some interesting features in cosmology [79–82]. Other theories considering non-minimal couplings between matter and gravity have also been considered in Teleparallel Gravity. One example for this is the so-called $f(\mathbb{T}, T)$ gravity, where T is the trace of the energy-momentum tensor [83]. This theory is analogous to the famous $f(R, T)$ gravity considered in the GR framework [84]. Other theories based on Lagrangian like $f_1(\mathbb{T}) + f_2(\mathbb{T})(1 + \lambda\mathcal{L}_m)$, where \mathcal{L}_m is the matter Lagrangian density and λ is a constant, have been studied in [85]. Furthermore, a more general theory concerning $f(\mathbb{T}, B, \mathcal{L}_m)$ gravity has also been studied in order to connect and generalise these kind of theories [86].

14.2.4 Teleparallel Non-local Theories

Apart from adding new degrees of freedom, modifications can be done in the foundations of a theory, like violating general covariance, locality, abandoning the equivalence principle, etc. In the Riemannian geometry, the first non-local proposal came a bit more than a decade ago, with the introduction of a *distortion function* $f(\square^{-1}R)$ of the inverse d'Alembertian operator acting on the Ricci scalar. The action of that theory reads

$$\mathcal{S}_{\text{non-local}} = \frac{1}{2\kappa^2} \int d^4x \sqrt{-g} R (1 + f(\square^{-1}R)). \quad (14.50)$$

The argument of f can be expressed using the retarded Green's function $G(x, x')$ as

$$\square^{-1}F(x) = \int d^4x' e(x') F(x') G(x, x'). \quad (14.51)$$

The motivation came clearly from high energies, since such terms arise in quantum loop corrections and they are also considered as possible solution to the black hole information paradox [87, 88]. It was seen however, that even at larger scales, such non-local terms can unify the inflation with the late-time acceleration era and they have been proven ghost-free and stable.

Based on that, it was natural to study what the effect of such terms would be in the teleparallel framework. That is why the teleparallel non-local (TNL) theory

$$\mathcal{S}_{\text{TNL}} = -\frac{1}{2\kappa^2} \int d^4x e \mathbb{T} + \frac{1}{2\kappa^2} \int d^4x e \mathbb{T} f(\square^{-1}\mathbb{T}). \quad (14.52)$$

was proposed in [89]. The authors show that the theory is consistent with cosmological data from SNe Ia + BAO + CC + H_0 observations. A generalisation of (14.52) was proposed in [90], where they also introduced the effect of the d'Alembertian operator on the boundary term B . The action of that theory is

$$\mathcal{S}_{\text{TNL}} = -\frac{1}{2\kappa^2} \int d^4x e \mathbb{T} + \frac{1}{2\kappa^2} \int d^4x e (\xi \mathbb{T} + \chi B) f(\square^{-1}\mathbb{T}, \square^{-1}B). \quad (14.53)$$

A localised version of this has been studied, introducing scalar fields. In addition, using symmetries, a classification of the distortion function has been done.

14.2.5 Horndeski Analog and Subclasses

Horndeski theory is the most general scalar tensor theory (with a single scalar field) that leads to second-order field equations in four dimensions [91, 92]. Most of the modified theories of gravity can be mapped onto its action; from Brans-Dicke [93],

extended quintessence [94, 95], kinetic gravity braiding [96] to $f(R)$ [42]. However, there is no physical requirement that forces us to use the Levi-Civita connection as the fundamental connection to formulate the theory, and thus we have the freedom to build the theory in any affine geometry. For this reason, in [97] S. Bahamonde, K. F. Dialektopoulos and J. Levi Said formulated the BDLS theory, that is the teleparallel analog of the Horndeski gravity.

In greater detail, they wanted to build a theory which has the properties: i. leads to second order field equations; ii. the scalar invariants are not parity violating; and iii. only quadratic contractions of the torsion tensor are included. In that way, BDLS action reads

$$\mathcal{S}_{\text{BDLS}} = \frac{1}{2\kappa^2} \int d^4x e \mathcal{L}_{\text{Tele}} + \frac{1}{2\kappa^2} \sum_{i=2}^5 \int d^4x e \mathcal{L}_i, \quad (14.54)$$

where

$$\mathcal{L}_{\text{Tele}} = G_{\text{Tele}}(\phi, X, \mathbb{T}, T_{\text{ax}}, T_{\text{vec}}, I_2, J_1, J_3, J_5, J_6, J_8, J_{10}), \quad (14.55)$$

and

$$\mathcal{L}_2 := G_2(\phi, X), \quad (14.56)$$

$$\mathcal{L}_3 := G_3(\phi, X) \square \phi, \quad (14.57)$$

$$\mathcal{L}_4 := G_4(\phi, X) (-\mathbb{T} + B) + G_{4,X}(\phi, X) \left[(\square \phi)^2 - \phi_{;\mu\nu} \phi^{;\mu\nu} \right], \quad (14.58)$$

$$\mathcal{L}_5 := G_5(\phi, X) \mathcal{G}_{\mu\nu} \phi^{;\mu\nu} - \frac{1}{6} G_{5,X}(\phi, X) \left[(\square \phi)^3 + 2\phi_{;\mu}{}^\nu \phi_{;\nu}{}^\alpha \phi_{;\alpha}{}^\mu - 3\phi_{;\mu\nu} \phi^{\mu\nu} (\square \phi) \right]. \quad (14.59)$$

where comma denotes the partial derivative, semi-colon the covariant derivative with respect to the Levi-Civita connection, and \square the associated d'Alembertian operator. The scalars that appear in the (14.55) are

$$I_2 = \dot{\mathbf{v}}^\mu \partial_\mu \phi, \quad J_1 = \dot{\mathbf{a}}^\mu \dot{\mathbf{a}}^\nu \partial_\mu \phi \partial_\nu \phi, \quad J_3 = \dot{\mathbf{v}}_\mu \dot{\mathbf{t}}^{\mu\lambda\nu} \partial_\lambda \phi \partial_\nu \phi, \quad J_5 = \dot{\mathbf{t}}^{\sigma\mu\nu} \dot{\mathbf{t}}^{\alpha\beta\gamma} \partial_\sigma \phi \partial_\mu \phi \partial_\nu \phi \partial_\alpha \phi \partial_\beta \phi \partial_\gamma \phi, \quad (14.60)$$

$$J_6 = \dot{\mathbf{t}}^{\sigma\mu\nu} \dot{\mathbf{t}}_{\sigma}{}^{\kappa\lambda} \partial_\mu \phi \partial_\nu \phi \partial_\kappa \phi \partial_\lambda \phi, \quad J_8 = \dot{\mathbf{t}}^{\sigma\mu\nu} \dot{\mathbf{t}}_{\sigma\mu}{}^\alpha \partial_\nu \phi \partial_\alpha \phi, \quad J_{10} = \epsilon^\mu{}_{\nu\rho\sigma} \dot{\mathbf{a}}^\nu \dot{\mathbf{t}}^{\alpha\sigma\rho} \partial_\mu \phi \partial_\alpha \phi, \quad (14.61)$$

all the rest they are either parity violating or can be obtained combining these [97–99].

Obviously, because of the existence of G_{Tele} in the action, this theory contains much more phenomenology compared to its curvature analog. Specifically, it contains the curvature analog as a subclass when $G_{\text{Tele}} = 0$. Its relation with various known theories is depicted in Fig. 14.1.

The curvature case of Horndeski was severely constrained [100, 101] after the observation of GW170817 and its companion GW170817A [102], since the speed of the gravitational waves is constrained to the value of the speed of light

$$\left| \frac{c_g}{c} - 1 \right| \gtrsim 10^{-15}. \quad (14.62)$$

That is another reason the BDLS theory is worth studying. In [98] the authors study the tensor mode perturbations on a flat FLRW background and they show that the models that survive the above constraint (14.62) are given by

$$\begin{aligned} \mathcal{L} = & \tilde{G}_{\text{tele}}(\phi, X, \mathbb{T}, T_{\text{vec}}, T_{\text{ax}}, I_2, J_1, J_3, J_6, J_8 - 4J_5, J_{10}) + G_2(\phi, X) + G_3(\phi, X)\square\phi, \\ & + G_4(\phi, X) + G_{4,X} \left[(\square\phi)^2 - \phi_{;\mu\nu}\phi^{;\mu\nu} + 4J_5 \right] + G_5(\phi)\mathcal{G}_{\mu\nu}\phi^{;\mu\nu} - 4J_5G_{5,\phi}, \end{aligned} \quad (14.63)$$

meaning that many models that were eliminated in the curvature case, like quartic and quintic Galileons, the Fab-Four and more, will survive in the teleparallel framework because of the appearance of the J_5 scalar.

14.2.6 Teleparallel Dark Energy Models

All the scalar torsion theories in four dimensions with a single scalar field are subclasses of the BDLS theory [103–111]. The first one with a non-minimal coupling between the scalar field and the torsion scalar was proposed in [103] under the name teleparallel dark energy, and its action reads

$$S_{\text{TDE}} = \int d^4x e \left[\frac{\mathbb{T}}{2\kappa^2} + \frac{1}{2}\xi\mathbb{T}\phi^2 + \frac{1}{2}\nabla_\mu\phi\nabla^\mu\phi - V(\phi) \right]. \quad (14.64)$$

Such models present interesting cosmological behaviour, not necessarily the same compared to $f(\mathbb{T})$ models [112, 113]. There are similar to the $\xi R\phi^2$ models in the Riemannian geometry and such models will be discussed in detail in Sect. 14.3. Moreover, in [114], a generalisation of the above theory with an extra term $\chi B\phi^2$ was considered. This theory contains the theory with the coupling $\xi R\phi^2$ as a special case for the case $\chi = -\xi$. Apart from these ones, in a recent series of papers [31, 115–117] the most general scalar-torsion theories have been presented in their covariant formulation, as well as theories involving kinetic and derivative couplings of the scalar field with torsion.

14.3 Phenomenology of Teleparallel Gravity

After formulating a possible well-motivated gravitational theory, it is then important to see its viability in terms of its confrontations with observations. It is well-known that GR works very well at Solar System scales, therefore, any meaningful theory must not deviate too much from these predictions at this scale of phenomenology. The easiest way to verify if a modified theory passes these constraints is by computing the

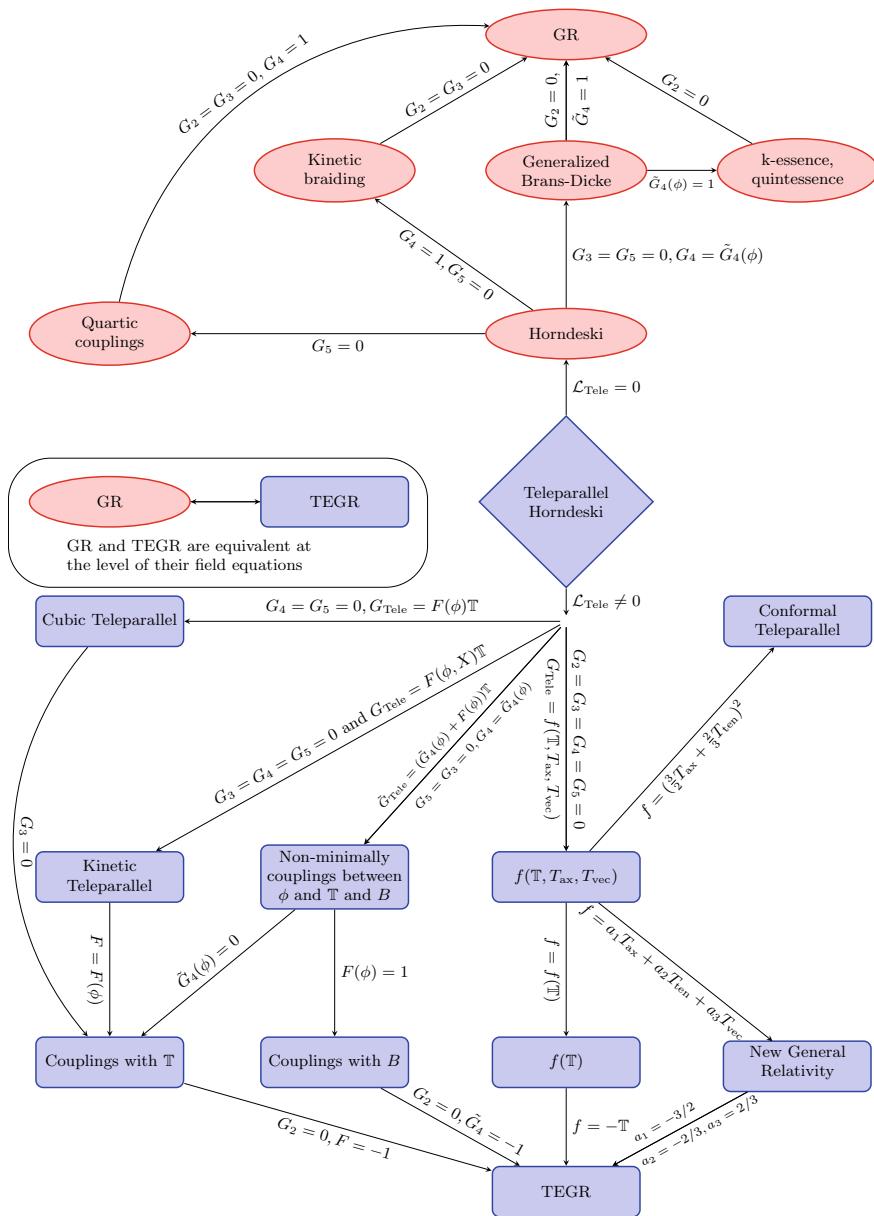


Fig. 14.1 Relationship between BDLs and various theories

so-called *post-Newtonian parameters* (PPN). Basically, these parameters measure the weak-field approximation of a theory with the corresponding post-Newtonian terms. For a detailed review about this method, see Ref. [118]. Usually, this method is constructed for theories concerning the metric but since Teleparallel Gravity uses tetrads, a different approach is needed as discussed in [119]. These parameters already put some constraints on different modified gravity models. In the context of Teleparallel Gravity, it was found that the PPN parameters of both $f(\mathbb{T})$ gravity and teleparallel dark energy (see Sect. 14.2) are exactly the same as GR, therefore, these theories automatically pass all the Solar System observations [120–122], as confirmed in [123–125]. If one further generalises $f(\mathbb{T})$ to $f(T_{\text{ax}}, T_{\text{vec}}, T_{\text{ten}})$ or teleparallel dark energy with an extra coupling between the boundary term and the scalar field as $\chi B\phi^2$, the PPN parameters γ and β deviate from GR, constraining these models [122, 126, 127]. These studies were further generalised to more general teleparallel scalar tensor theories such as $f(\mathbb{T}, X, Y, \phi)$ and Teleparallel Horndeski in [128, 129], finding again that only α and β can differ from GR. For the general $f(\mathbb{T}, B)$ gravity scenario, the precise form of this deviation is investigated in [130, 131], where the solar system tests and gravitomagnetic effects are probed against current observations. Moreover, in [132] the stability of theory and its thermodynamics are probed. One of the strongest bounds coming from these PPN parameters are the observations from Cassini, which is $|\gamma - 1| \lesssim 2 \cdot 10^{-5}$ and also, using the lunar laser ranging experiments, $|\beta - 1| \lesssim 2 \cdot 10^{-4}$ [118].

There are other new observational bounds that one needs to take into account for constructing a coherent theory. For example, in Ref. [133], it was found that the speed of the propagation of gravitational waves c_g is very close to the speed of light $|c/c_g - 1| \lesssim 3 \cdot 10^{-15}$. The theories $f(\mathbb{T})$, $f(\mathbb{T}, T_G)$ and $f(\mathbb{T}, B)$ predict that $c_g = c$ [134, 135], so that they are not observationally constrained through this test. Furthermore, there are only two propagating modes in both $f(\mathbb{T})$ and $f(\mathbb{T}, T_G)$ gravity [135, 136], exactly like GR. On the other hand, as in $f(R)$ gravity, $f(\mathbb{T}, B)$ exhibits an extra polarisation mode (longitudinal or breathing mode) [135]. Further generalisations such as Teleparallel Horndeski predicts a different speed of the gravitational waves, and hence, the theory needs to be constrained for a certain type of them. However, one notices that the number of theories respecting $c_g = c$ is larger than in standard Horndeski gravity. Furthermore, the coupling functions $G_4(\phi, X)$ and $G_5(\phi)$ that were highly constrained in the standard version of Horndeski, can now be restored in its teleparallel analogue [98].

The majority of the work produced in modified Teleparallel Gravity has been done in the context of cosmology. There are several works regarding this for different kinds of theories. Some important results in these theories are:

- The possibility of explaining the acceleration of the Universe without evoking a cosmological constant (see, for example, Sects. 14.3.6 and 14.3.7).
- The possibility of roughly describing the evolution of the observed Universe eras (see, for example, Sect. 14.3.6) and crossing of the phantom divide line [114].
- The possibility of reducing the tension for the value of the H_0 parameter and the growing $f\sigma_8$ tension (see Sect. 14.3.4).

- The existence of cosmological bouncing solutions (see Sect. 14.3.8).
- The possibility of avoiding dark matter for describing the galactic rotation curves [137].

In the following sections, we will briefly describe some of these results, and also some techniques used for studying cosmology in these theories.

14.3.1 $f(\mathbb{T})$ Cosmology and the Power-Law Model

The framework that Teleparallel Gravity offers in the form of its $f(\mathbb{T})$ gravity formulation can be investigated against cosmological observations, where tensions appear to be growing with Λ CDM [138–140]. The analysis takes the good tetrad $e^a{}_\mu = (1, a(t), a(t), a(t))$ for a homogeneous and isotropic universe (this reproduces the standard FLRW metric in its Cartesian coordinates form). By choosing the Lagrangian density to take the form $-\mathbb{T} + F(\mathbb{T})$, the resulting field equations turn out to be [3, 49, 141]

$$H^2 = \frac{\kappa^2}{3} (\rho + \rho_{\text{DE}}), \quad (14.65)$$

$$2\dot{H} = -\kappa^2 (\rho + p + \rho_{\text{DE}} + p_{\text{DE}}), \quad (14.66)$$

where $\kappa^2 := 8\pi G$, and the effect of the extension to theTEGR Lagrangian is to act as an exotic fluid with components

$$\rho_{\text{DE}} = \frac{1}{2\kappa^2} (2\mathbb{T}F_{\mathbb{T}} - F), \quad (14.67)$$

$$p_{\text{DE}} = \frac{1}{2\kappa^2} \left[\frac{F - \mathbb{T}F_{\mathbb{T}} + 2\mathbb{T}^2 F_{\mathbb{T}\mathbb{T}}}{1 + F_{\mathbb{T}} + 2\mathbb{T}F_{\mathbb{T}\mathbb{T}}} \right]. \quad (14.68)$$

Together, these fluid properties satisfy the continuity equation

$$\dot{\rho}_{\text{DE}} + 3H(\rho_{\text{DE}} + p_{\text{DE}}) = 0, \quad (14.69)$$

as well as make up the effective EoS

$$w_{\text{DE}} = -\frac{F/\mathbb{T} - F_{\mathbb{T}} + 2\mathbb{T}F_{\mathbb{T}\mathbb{T}}}{(1 + F_{\mathbb{T}} + 2\mathbb{T}F_{\mathbb{T}\mathbb{T}})(F/\mathbb{T} - 2F_{\mathbb{T}})}, \quad (14.70)$$

which returns a constant $w_{\text{DE}} = -1$ for the appearance of a cosmological constant through the condition $F_{\mathbb{T}} = 0$. Here, we assume that $F(\mathbb{T}) \neq 0$, so that gravity is indeed modified by $f(\mathbb{T})$ gravity.

Finally, using the EoS in Eq. (14.70), it follows that $F/\mathbb{T} - F_{\mathbb{T}} + 2\mathbb{T}f_{\mathbb{T}\mathbb{T}} = 0$ has solutions $F(\mathbb{T}) = c_1\sqrt{\mathbb{T}} + c_2$, where the first part plays no role in the cosmic

dynamics in four dimensions, while the second part plays the role of the cosmological constant [142–144]. Thus, this case is neglected since it reduces to Λ CDM.

14.3.2 Cosmography in $f(\mathbb{T})$ Gravity

Cosmography offers a model independent way in which to determine viable models of gravity through standard candle data (such as SNeIa) [145]. That is, by using the Hubble diagram, gravitational Lagrangians can be constrained in their parameter space by using expansion data. In Refs. [146–148], this is considered for the following parameters: Hubble ($H = \dot{a}/a$), deceleration ($q = -\frac{1}{a} \frac{d^2 a}{dt^2} H^{-2}$), jerk ($j = \frac{1}{a} \frac{d^3 a}{dt^3} H^{-3}$), and snap ($s = \frac{1}{a} \frac{d^4 a}{dt^4} H^{-4}$). These cosmographic parameters can then be correlated with the Hubble diagram by considering the Taylor expansion of the scale factor about present time, $a_0 = 1$, together with the luminosity distance relation

$$H(z) = \left[\frac{d}{dz} \left(\frac{d_L(z)}{1+z} \right) \right]^{-1}, \quad (14.71)$$

and redshift relation $a = (1+z)^{-1}$, which result in the Hubble cosmographic relations

$$H(z) \simeq H_0 \left[1 + H^{(1)} z + \frac{H^{(2)}}{2} z^2 + \frac{H^{(3)}}{6} z^3 \right], \quad (14.72)$$

where

$$H^{(1)} = 1 + q_0, \quad H^{(2)} = j_0 - q_0^2, \quad H^{(3)} = 3q_0^2 + 3q_0^3 - j_0(3 + 4q_0) s_0, \quad (14.73)$$

with $(H, q, j, s) = (H_0, q_0, j_0, s_0)$ are all determined at current times. This expansion is considered up to fourth-order derivatives, due to the lack of accuracy of the cosmological data beyond that point [149, 150]. Fitting each of these parameters, using the Hubble diagram, it is then straightforward to infer an $F(\mathbb{T})$ model by using the modified Friedmann equations in Eqs. (14.65)–(14.66). To do this, consider $f(\mathbb{T}) = -\mathbb{T} + F(\mathbb{T})$, so that we can impose the following constraints: (i) the effective gravitational constant must be equal to Newton's constant at present times [148]

$$\left. \frac{df}{dz} \right|_{z=0} = 1, \quad (14.74)$$

which emerges by considering again the Friedmann equation in Eq. (14.65) as $H^2 = \kappa^2(\rho - 2F/(3\kappa^2))/(6F_{\mathbb{T}})$ and recognising the effective coupling parameter, $G_{\text{eff}} = G/f_{\mathbb{T}}$ ($f_{\mathbb{T}} = df/d\mathbb{T}$). The requirement can then be written as $G_{\text{eff}}|_{z=0} = G \Rightarrow f_{\mathbb{T}}|_{z=0} = 1$. This means that at current time we recover TEGR. (ii) The second constraint is an evaluation of the Friedmann equation in Eq. (14.65) at current times,

such that the present value of the Lagrange density must be

$$f(\mathbb{T}(z))\Big|_{z=0} = 6H_0^2 (\Omega_{M0} - 2) , \quad (14.75)$$

where Ω_{M0} is the present value of the matter density parameter.

In Refs. [146–148], various $f(\mathbb{T})$ models were considered, but we focus on the power-law model here. This can be represented by [151]

$$f(\mathbb{T}) = \alpha\mathbb{T} + \beta\mathbb{T}^n , \quad (14.76)$$

where α, β, n are arbitrary constants, and the constraints on the Lagrangian density result in the relations

$$\alpha = \frac{(2 - \Omega_{M0})n - 1}{n - 1} , \quad \beta = \frac{(\Omega_{M0} - 1)T_0^{1-n}}{1 - n} . \quad (14.77)$$

While the parameter β is used, it can be made dimensionless by taking the transformation $\beta \rightarrow \beta_0/T_0^n$. To preserve TEGR for Solar System scale physics and the astrophysics regime, the α parameter can be set to -1 so that this is recovered as a first approximation. The best-fit cosmographic parameters then give $n = -0.011$ [147]. The result is an expansion rate very close to Λ CDM but not exactly equal. Along a similar vein, in [152] cosmography was used to reconstruct various $f(\mathbb{T})$ gravity Lagrangians by imposing conditions in the jerk parameter.

This analysis relies heavily on the assumption that higher-order contributions, which have much less accurate observational data, are sub-dominant, which may not always hold. Also, this analysis has only been applied to the popular $F(\mathbb{T})$ extension to TEGR. It would be interesting to explore other avenues of Teleparallel Gravity such as, for example, the ones presented in Sect. 14.2.

Along a similar rationale, in [153, 154] the $f(\mathbb{T})$ Lagrangian is reconstructed against phenomenological data, achieving very interesting constraints on viable models.

14.3.3 The Growth Factor

The inflationary epoch rendered an early Universe that was nearly uniform. It was small quantum fluctuations that then resulted in the seeds of structure formation. Over the cosmic timescale, these seeds then grew into the structure we can observe today. This effect was amplified during the early matter-dominated phase of the Universe, where density perturbations were intensified by gravity. The growth factor can propagate how this growth changes between different theories of gravity.

To explore this aspect of cosmology, the evolution of linear scalar perturbations must be considered, which at the level of the metric appear as

$$ds^2 = a^2(\tau) \left[- (1 + 2\Psi) d\tau^2 + (1 - 2\Phi) \gamma_{ij} dx^i dx^j \right], \quad (14.78)$$

where the spatial metric is chosen to be the Cartesian coordinate system. The problem then becomes, what perturbed tetrad to consider? One approach is given in Ref. [155], but the resulting field equations turn out to restrict the $f(\mathbb{T})$ Lagrangian to its TEGR value which is not allowable with a good tetrad. It was later in Refs. [142, 156–159] that the correct good tetrad was studied. In perturbation theory, a good tetrad must adhere to the already discussed conditions for being a good tetrad up to perturbative order (see Sect. 14.2.1 for further details). This is ultimately represented by

$$e^a{}_{\mu} = (\delta_b^a + \chi^a{}_b) \bar{e}^b{}_{\mu}, \quad (14.79)$$

where $\bar{e}^b{}_0 = \delta_0^b$ and $\bar{e}^b{}_i = a\delta_i^b$, and the scalar perturbations are given by

$$\chi_{ab} = \begin{pmatrix} \phi & \partial_i w \\ \partial_i \tilde{w} & \delta_{ij} \psi + \partial_i \partial_j h + \epsilon_{ijk} \partial^k \tilde{h} \end{pmatrix} \quad (14.80)$$

where w and \tilde{w} are 2 scalar degrees of freedom (DoFs) of mass dimension and h and \tilde{h} are parity-violating terms. To obtain the correct scalar perturbations in the Newtonian gauge, the setting $w = -\tilde{w}$ and $h = 0$ [142] needs to be taken, while \tilde{h} vanishes naturally at the level of the metric. Using this tetrad setting, the correct scalar perturbations at the level of the metric are obtained, as in Eq. (14.78) (in cosmic time rather than conformal time). We consider only the scalar perturbations in this work, but interesting results have also been obtained for tensor perturbations in Refs. [134, 156, 158–163]. The end result indeed appears in the linear perturbations of the torsion scalar as

$$\mathbb{T} = 6H^2 - 12H (\dot{\psi} + H\phi), \quad (14.81)$$

which means that the scalar perturbations have an effect in the $F(\mathbb{T})$ gravity section, while, the matter perturbations are taken by considering only dust ($p = 0 = \delta p$). The density perturbations, $\delta\rho$, can then be encapsulated in the so-called gauge invariant fractional matter perturbation given by

$$\delta_m = \frac{\delta\rho_m}{\rho_m} - 3Hv, \quad (14.82)$$

where v is the magnitude of the velocity of the fluid, $v^i = u^i/u^0$ [164]. This regime is best studied by going into the Fourier domain and considering subhorizon modes where $\phi \sim \psi$. By combining the $f(\mathbb{T})$ field equations, the following linear matter evolution equation is obtained in Ref. [142]

$$\ddot{\delta}_m + 2H\dot{\delta}_m - 4\pi G_{\text{eff}}\rho_m\delta_m = 0, \quad (14.83)$$

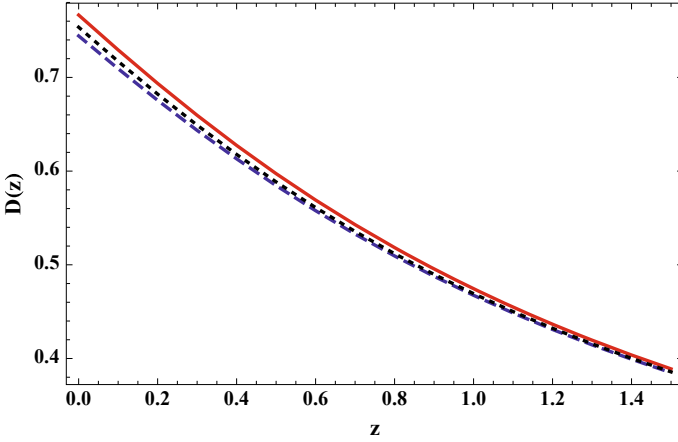


Fig. 14.2 Matter perturbation evolution for Λ CDM (solid red line), power-law $F(\mathbb{T})$ (dashed blue line), and constant dark energy EoS in GR (dotted black line) [142]

where $G_{\text{eff}} = G/(-1 + F_{\mathbb{T}})$ is the effective gravitational constant. This is generalised in Ref. [157] to include the Lagrangians formed with arbitrary combinations of the contraction of the stress-energy tensor, $T = T^{\mu}_{\nu}$.

To probe the growth of matter density perturbations, Ref. [142] defines the variable

$$g(a) := \frac{D(a)}{a}, \quad (14.84)$$

which is defined this way to avoid scale factor dependence during matter-dominated eras, and where the reasonable initial conditions $g(a_i) = 1$, $(dg/d \ln a)|_{a=a_i} = 0$ are chosen. Here, $D(a) := \delta_m(a)/\delta_m(a_i)$ (for some reference scale factor a_i) is the growth factor.

Considering again the power-law model with $F(\mathbb{T}) = \beta \mathbb{T}^n$, the growth factor as a function of redshift can be solved numerically and turns out to give the evolution depicted in Fig. 14.2. Given that $F_{\mathbb{T}} > 0$ for the power-law, it follows that the growth factor will be dampened due to the effective gravitational constant relation. The main result of this is that over-dense perturbations grow slower when compared with GR. In Ref. [159], it was also found that the vector perturbations are well-behaved for sub-horizon modes. These results are confirmed in Refs. [156, 158], where it is also noted that the cause of the lack of extra propagating DoFs could be the symmetric nature of the background cosmology.

14.3.4 The H_0 Tension Problem

The discrepancy between model-independent measurements of the current value of the Hubble parameter [139, 140] and those inferred from the CMB using flat Λ CDM [138, 165] is now corroborated by an overwhelming wealth of evidence. The H_0 tension problem then points to the necessity of new physics beyond flat Λ CDM, such as modified gravity within the Teleparallel Gravity regime [166].

To explore this possibility in Teleparallel Gravity, we need to consider again the perturbations in Eq. (14.79). However, in this scenario the contributions of matter and radiative pressures are not neglected even at perturbative level [167, 168]. Also, the gravitational potentials ϕ and ψ are no longer equal. As already discussed in Refs. [158, 162], the following modified Poisson equation is derived

$$k^2\psi = 4\pi G_{\text{eff}}a^2\delta\rho, \quad (14.85)$$

where we have transformed to Fourier space. By keeping to the power-law model, Ref. [162] explores this possibility in terms of the H_0 problem as well as the growing $f\sigma_8$ tension. In this work, the authors show that the H_0 tension can be reduced in conjunction with reducing the $f\sigma_8$ tension. As they show in Fig. 14.3, a consistent cosmological setup can be constructed for a small value of index n .

One of the principal motivations for exploring modified gravity in cosmology is to better explain the appearance of dark energy without modifying the matter content of the Universe. This entails reinterpreting the Friedmann equation as an effective equation in which the modified gravity component acts as a separate contribution to cosmic evolution beyond GR. This can easily be done by writing [167]

$$\frac{H^2(z, \mathbf{r})}{H_0^2} = \Omega_{m0}(1+z)^3 + \Omega_{r0}(1+z)^4 + \Omega_{F0}y(z, \mathbf{r}), \quad (14.86)$$

where $\Omega_{F0} = 1 - \Omega_{m0} - \Omega_{r0}$ is the $F(\mathbb{T})$ density parameter at current times, and

$$y(z, \mathbf{r}) = \frac{1}{\mathbb{T}_0\Omega_{F0}}(F - 2\mathbb{T}F_{\mathbb{T}}), \quad (14.87)$$

represent the background evolution of the $F(\mathbb{T})$ model. In the right panel of Fig. 14.3, the $n - \Omega_{F0}$ plane is shown, where Ref. [162] reports promising results for small values of n .

Along a similar vein, the authors of Ref. [170] confront the growth of structure in the Universe by using several cosmological probes. The study involves three $F(\mathbb{T})$ models, but we highlight the results for the power-law model here. In their analysis, they use growth rate data for $f\sigma_8$ that has been verified for internal robustness [171], which differs from some other approaches where inconsistencies can arise due to overlaps between separate studies. The second data set used in this study is the updated Hubble expansion through the cosmic chronometric method [172], while

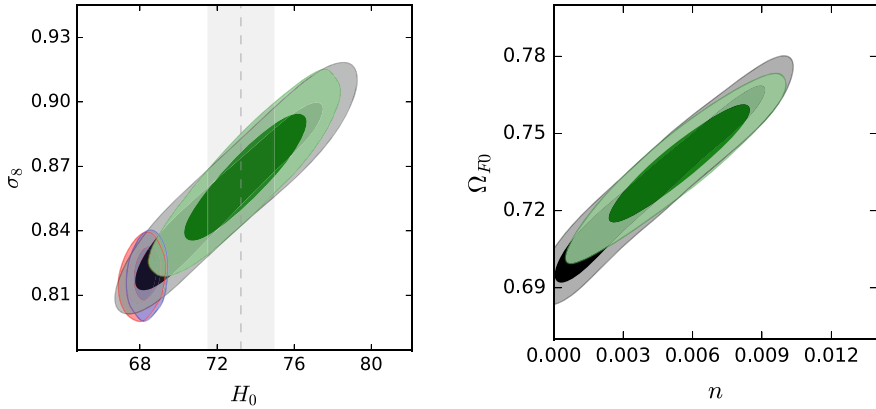


Fig. 14.3 The comparison of Λ CDM with the $f(\mathbb{T})$ gravity power-law model as reported in Ref. [162]. Left panel: Plot of the $\sigma_8 - H_0$ parameter space comparing the Λ CDM model in red (blue) for CMB+BAO (CMB+BAO+ H_0) data respectively. Additionally, we present the results for the power-law $f(\mathbb{T})$ model in black (green) for the same data, where the vertical gray band corresponds to $H_0 = 73.24 \pm 1.74 \text{ km s}^{-1}$ [169]. The extended model has best fit index parameter $n = 0.0043^{+0.0033}_{-0.0039}$ ($0.0054^{0.0020}_{0.0020}$) [161] (more details here about the data used). Right panel: 68% and 95% confidence levels for CMB+BAO (CMB+BAO+ H_0) data in black (green) [161]

the third is the latest standard candle data in Ref. [173]. These three data sets are used in a joint analysis for the power-law $F(\mathbb{T})$ model resulting in the likelihood plots shown in Fig. 14.4.

In this work, the authors use the Akaike Information Criterion (AIC) [174], Bayesian Information Criterion (BIC) [175] and Deviance Information Criterion (DIC) [176] to compare the different models. The power-law is favoured using the AIC and BIC comparisons when compared to Λ CDM. While not performing best using the DIC to compare the models, it still fares relatively well compared to other prominent models in the literature.

Another important contribution to the reduction of the H_0 tension are Refs. [177–179], where Hubble data is interpreted as a stochastic process such that the various model ansatz choices must reproduce. By taking this approach, the authors determine a region for acceptable Lagrangian forms for the $F(\mathbb{T})$ model. While this region is model-independent and goes up to $z = 2.4$, various models can be constrained against cosmic data. In Ref. [179], Gaussian processes are used on Hubble data which is interpreted as being sourced by stochastic processes. Here, the authors reconstruct values of the arbitrary Lagrangian through the Friedmann equation and then use Gaussian processes to determine the best fit for this function. The result is a model independent reconstruction of the Lagrangian $\mathbb{F}(T)$ (except for the assumption that Λ CDM dominates at current times, which resonates with the results from cosmography in Sect. 14.3.2). These values, together with their 1 and 2 σ errors are shown in Fig. 14.5, which depicts the allowable regions in which all cosmological models must predict values for the arbitrary Lagrangian.

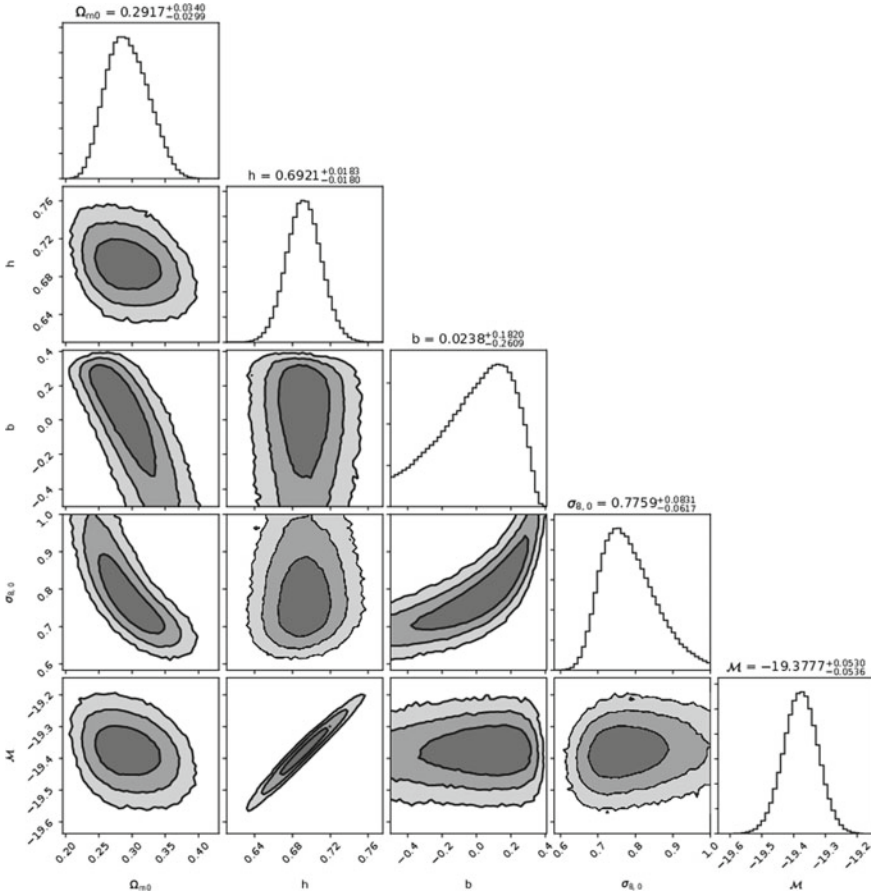


Fig. 14.4 The 1σ , 2σ and 3σ likelihood contours for the $F(\mathbb{T})$ power-law model (with $F(\mathbb{T}) = \alpha(\mathbb{T})^b$) [170]

There has also been a growing body of work of confronting observations within other extensions of Teleparallel Gravity, such as [180], where Pantheon data is used in $f(\mathbb{T}, B)$ gravity. In this work, the H_0 tension problem is also confronted with new constraints on literature models within this framework of gravity.

14.3.5 Inflation in Teleparallel Theories of Gravity

The first modification of Teleparallel Gravity was introduced in [51], with the aim of studying inflation. In this paper, the authors found that for a Born-Infeld $f(\mathbb{T})$ gravity model, it is possible to cure the horizon problem without an inflation field,

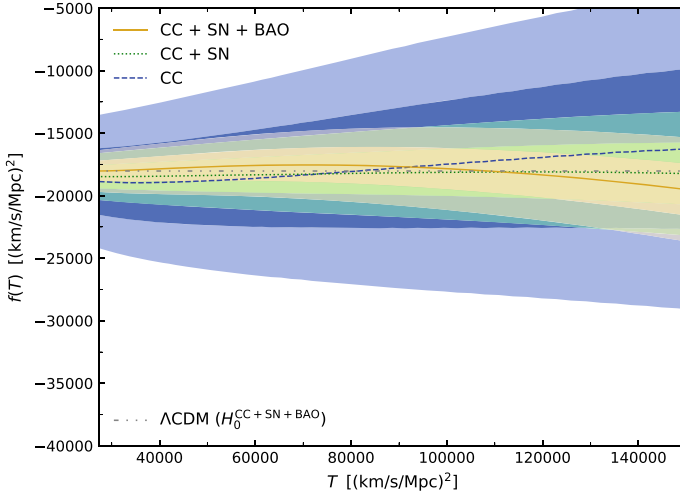


Fig. 14.5 The regions are produced by a model-independent reconstruction from Hubble data with 1 and 2 σ error regions coming from the Gaussian process method (the present matter density parameter is imposed to be $\Omega_{m0} = 0.302$). The blues regions represent cosmic chronometer data, green includes also supernova data, while orange represents the inclusion of baryonic acoustic data [179]

and describe a de-Sitter expansion. This paper was the crucial starting point for investigating cosmology in the context of Teleparallel Gravity. So far, the majority of the inflationary models in modified teleparallel theories have been carried out in $f(\mathbb{T})$ gravity. By performing a 3+1 decomposition for the tetrad, the cosmic inflationary perturbations for $f(\mathbb{T})$ were computed in [112]. Similar to the Starobinsky inflationary model $R + \alpha R^2$, in [181] it was found that the case $-\mathbb{T} + \alpha \mathbb{T}^2$ behaves differently since in this case, a de-Sitter solution occurs (not a quasi de-Sitter). This means that in the teleparallel version of the Starobinsky model, only eternal de Sitter inflation is possible. In [182] it was further found that these models can have good agreements with a hot big bang nucleosynthesis, and also that the system evolves towards a flat FLRW universe naturally, even if we start with a non-flat one. Later in [183], it was found that power-law and intermediate inflationary models in $f(\mathbb{T})$ gravity are compatible with Planck measurements, and that a self-interacting quartic potential $V(\phi) \propto \phi^4$, which has an interesting reheating process is viable in $f(\mathbb{T})$ inflation. Further, the standard inflationary model is not observationally compatible with this kind of potential. After introducing a suitable scale factor, it was found that depending on a parameter, $f(\mathbb{T})$ gravity can have a graceful exit inflation or can have a bounce [184]. In that study it was obtained that the problem of a large tensor-to-scalar ratio is not present in the bouncing models. The standard logamediate inflation is not compatible with observations but in [185] it was concluded that in $f(\mathbb{T})$ gravity, this model can be compatible with Planck observations. Finally, in [186] it was found that a super inflation scenario can be achieved in $f(\mathbb{T})$ gravity.

Concerning extensions to $f(\mathbb{T})$ gravity, in [187], the authors introduced a coupling between a Maxwell field and the torsion scalar, $I(\mathbb{T})F_{\mu\nu}F^{\mu\nu}$, finding the possibility of generating large-scale magnetic fields from inflation. In $f(\mathbb{T}, T_G)$ gravity, there was obtained a model that unifies inflation with dark energy with a super inflation mechanism [188]. A unimodular $f(\mathbb{T})$ gravity model was also analysed in the context of inflation, finding another alternative inflationary models with, graceful inflationary exit [189].

The first study related to inflation in the context of teleparallel scalar tensor theories was done in [190], where an extended $f(\mathbb{T})$ plus an inflation field with a kinetic, a potential term and an interaction term was introduced. In this work, it was found that a possible warm-inflation model is compatible with the Planck data. Later in [191], a similar model was studied, finding a reheating process, with the scalar field being responsible to reheat the Universe after the inflationary era. In [192], another scalar tensor model concerning two non-minimally couplings with the scalar field, one with the torsion scalar $F(\phi)\mathbb{T}$ and the other with a vector field $G(\phi)F_{\mu\nu}F^{\mu\nu}$, was considered in the context of anisotropic inflation, obtaining that in the strong coupling regime, the anisotropy shear to expansion ratio has a different value than its standard form. The constant-roll inflation in $f(\mathbb{T})$, minimally coupled with a scalar field, was analysed in [193], allowing the theory to have a wide range of viability in terms of observations. In [194] the authors studied slow-roll inflation in a more general teleparallel scalar-tensor theory, with a canonical scalar field non-minimally coupled to torsion with a Galileon-type field $G(\phi, X)\square\phi$ and a monomial scalar field potential $V \propto \phi^n/n$. This theory is a particular case of the BDLS theory (see Sect. 14.2.5). Based on Planck 2018 data for both the spectral index n_s and the tensor-to-scalar ratio r , standard inflation with monomial scalar field potential with $n \geq 2$ is ruled out. However, in this teleparallel version, $n = 2$ (chaotic quadratic inflation) is in agreement with data and $n = 1$ and $n = 2/3$ are even more favoured than previous models. In a model with non-minimally couplings between a scalar field and both the boundary term and the torsion scalar, it was shown that the scalar field does not source linear scalar perturbations, unless the coupling functions satisfy certain conditions [195]. Only in these situations, can one have successful Higgs inflationary models. Finally, considering more exotic models, a tachyonic teleparallel one explaining inflation and agreeing with the current observational Planck limits was studied in [196]. Further, it was also found in [197] that by extending the study with a boundary term non-minimally coupled with the scalar field, accelerated expansion and scaling solutions are attained.

14.3.6 *Dynamical System in Cosmology for Teleparallel Theories Of Gravity*

When one starts modifying or extending the Einstein field equations, the cosmological equations become more involved to solve. The FLRW equations can be written

as an autonomous system of differential equations, and for this, they can be recast as a dynamical system. Mathematicians have studied these systems for a long time, giving an easy way to understand the dynamics of a model and how the stability of their critical points behave. Hence, this is a powerful mathematical technique, which is very useful for studying cosmology in modified theories of gravity. For a detailed review about dynamical systems, both mathematically and in terms of cosmology, see [198–201].

There are several works in modified Teleparallel Gravity that use dynamical systems in the context of cosmology. The first work for $f(\mathbb{T})$ cosmology was presented in [202], where the authors studied a power-law $f(\mathbb{T})$ finding one critical point behaving as a late-time attractor and another two describing matter and radiation eras as saddle points. Later, in [203], a logarithmic $f(\mathbb{T})$ cosmology was studied, finding a de-Sitter late-time attractor. In [204–206], it was also found that by introducing an interaction between the dark fluids and considering a power law $f(\mathbb{T})$, it is possible to get tracker cosmological solutions. Other dynamical system studies concerning more general approaches for $f(\mathbb{T})$ cosmology have been done. For example, in [207] the authors used the nullcline method to study the bifurcation phenomenon to study the global dynamical properties of the dynamical system. In [208], it was found that there are three conditions which ensure that $f(\mathbb{T})$ cosmology could roughly describe the cosmological history of the evolution of the Universe. Using non-standard dimensionless variables, Hohmann et al. [209] found de-Sitter fixed points, accelerated expansion, crossing the phantom divide, and finite time singularities in $f(\mathbb{T})$ cosmology. They also found some bounce solutions in this model. Finally, in [210], the authors were able to rewrite the $f(\mathbb{T})$ dynamical system as a one dimensional one by using the fact that \mathbb{T} depends only on the Hubble parameter as $\mathbb{T} = 6H^2$ in flat FLRW. Doing this, they found that it is possible to reconstruct the whole history of the Universe starting from a big bang singularity and finalising in an accelerating expansion. In addition, they also found some other exotic solutions, such as cosmological bounce and turnaround, the phantom-divide crossing, the Big Brake and the Big Crunch, and also they found that it may exhibit various singularities.

Let us now briefly review the dynamical system of $-\mathbb{T} + F(\mathbb{T})$ (TEGR plus $F(\mathbb{T})$) cosmology described by the modified flat FLRW equations (14.65) and (14.66). For a universe composed of two fluids with effective energy density described by $\rho = \rho_{\text{rad}} + \rho_{\text{m}}$, where the first fluid represents a radiation fluid and the second one a pressureless fluid, one can introduce the following dimensionless variables

$$x = -\frac{F(\mathbb{T})}{6H^2}, \quad y = \frac{\mathbb{T}F_{\mathbb{T}}}{3H^2}, \quad \Omega_{\text{rad}} = z = \frac{\kappa^2 \rho_{\text{rad}}}{3H^2}, \quad \Omega_{\text{m}} = \frac{\kappa^2 \rho_{\text{m}}}{3H^2}, \quad (14.88)$$

to then rewrite the first FLRW equation (14.65) as follows

$$\Omega_{\text{m}} = 1 - x - y - z, \quad (14.89)$$

which gives a constraint and reduces the dynamical system to be a 3 dimensional one. By introducing $N = \log(a)$, the dynamical system for this model becomes

$$\frac{dx}{dN} = -(2x + y) \frac{z + 3 - 3x - 3y}{2my - 2 + y}, \quad (14.90)$$

$$\frac{dy}{dN} = 2my \frac{z + 3 - 3x - 3y}{2my - 2 + y}, \quad (14.91)$$

$$\frac{dz}{dN} = -4z - 2z \frac{z + 3 - 3x - 3y}{2my - 2 + y}, \quad (14.92)$$

where we have introduced the quantity

$$m = \frac{\mathbb{T} F_{\mathbb{T}\mathbb{T}}}{F_{\mathbb{T}}}. \quad (14.93)$$

In order to close the dynamical system, one needs to assume a form for $F(\mathbb{T})$. The easiest case is to assume that $m = \text{constant}$, which closes the dynamical system and includes two kind of $F(\mathbb{T})$, one behaving as a power-law $F(\mathbb{T}) = C_1 \mathbb{T}^{m+1}/(m + 1) + C_2$ when $m \neq -1$ and also including a logarithmic case $F(\mathbb{T}) = C_1 \log(\mathbb{T}) + C_2$ for $m = -1$. We will assume this case for simplicity. For other kinds of $F(\mathbb{T})$, see the papers mentioned before. The dark energy state parameter (14.70) in the dimensionless variables reads

$$w_{\text{DE}} = -\frac{x + y/2 - my}{(1 - y/2 - my)(x + y)}. \quad (14.94)$$

For $m = \text{constant}$, one finds that the dynamical system (14.90)–(14.92) has three critical points. The first critical point is $P_1 = (x, y, z) = (0, 0, 0)$ which is the origin of the phase space and represents a matter-dominated era, since $\Omega_m = 1$. This critical point has three eigenvalues with different signs, $\{3, -1, -3m\}$, so that, this point is always a saddle point. This behaviour is expected for describing the standard matter-dominated era, since it is known that this point needs to be represented by a point which attracts trajectories in some directions but repels them along others. The second critical point is $P_2 = (x, y, z) = (0, 0, 1)$, representing a universe dominated by radiation, $\Omega_{\text{rad}} = 1$. This point has also three eigenvalues $\{4, 1, -4m\}$ but now depending if $m > 0$, the point is saddle, and if $m < 0$ the point is unstable. This again has the correct cosmological behaviour, since it is known that there was a radiated-dominated era at some point of the history of the Universe but after this era, this era changed to be a matter-dominated era. This is then achieved by having either an unstable or a saddle point for P_2 (neglecting inflation). The final point is represented by the critical line $P_3 = (x, 1 - x, 0)$ whose cosmological behaviour is representing an accelerating universe with an effective state parameter of -1 , which denotes a de-Sitter accelerating expansion. This critical line has three eigenvalues $\{0, -4, -3\}$. Since one of them is zero, one cannot study its stability property with the standard linear stability theory since it is a non-hyperbolic point, and this method fails for analysing such points. Other stability methods can then be used, such as Lyapunov functions or centre manifold theory. See [198] for a detailed description about these methods. If one uses the second mentioned method, one needs to first shift the critical

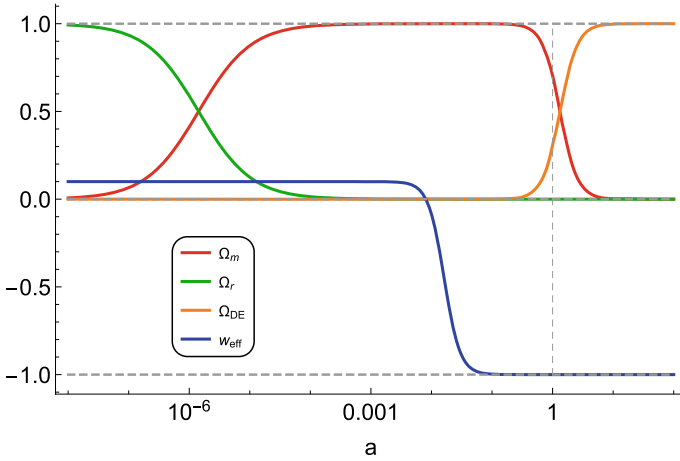


Fig. 14.6 Evolution of energy density matter Ω_m , radiation Ω_{rad} and dark energy Ω_{DE} for a $f(\mathbb{T}) = -\mathbb{T} + \frac{C_1}{m+1} \mathbb{T}^{m+1}$ model with $m = 0.1$

point to the origin, then introduce new variables in such a way that one can diagonalise the Jacobian matrix associated with the dynamical system. After doing this, the centre manifold can then be constructed according to the theorem described in Sect. 2.4 in [198]. By doing this for our dynamical system, we find that the leading term in the dynamical system is reduced to the centre manifold $\dot{z} = -4z + \mathcal{O}(z^2)$, which tells us that the point P_3 is always stable. Thus, the critical line P_3 represents a late-time accelerating attractor behaving as a de-Sitter. Then, $-\mathbb{T} + F(\mathbb{T})$ cosmology can describe a transition from radiation- to matter-dominated eras, finalising in a dark energy era with a de-Sitter accelerating expansion of the Universe. This analysis would be valid for both logarithmic and power-law kinds of $F(\mathbb{T})$. As an example, Fig. 14.6 shows the evolution of the relative energy density of matter Ω_m , radiation Ω_{rad} and dark energy Ω_{DE} related to the modifications coming from $F(\mathbb{T})$ for the case where $m = 0.1$, which represents a power-law type of $F(\mathbb{T})$. One can notice that the evolution of the Universe is roughly described as one expected from our Universe, starting from a radiation-dominated era, then passing to a matter dominated era and finalising in a dark energy dominated era.

Other different modified Teleparallel Gravity cosmological models extending $f(\mathbb{T})$ gravity have also been analysed using dynamical systems techniques. In the papers [211–213], a $f(\mathbb{T}, B)$ gravity model including the boundary term B , which connects the Ricci scalar computed with the Levi-Civita connection and the torsion scalar, was analysed, finding scaling solutions, a matter epoch of the Universe, and that two accelerated phases can be recovered describing de-Sitter universes. Later, using non-minimally torsion-matter theories like $f_1(\mathbb{T}) + f_2(\mathbb{T})\mathcal{L}_m$, with \mathcal{L}_m being the matter density Lagrangian, some scaling decelerated solutions, dark-matter dominated, or dark-energy dominated accelerated solutions were found. Further generalisations such as $f(\mathbb{T}, B, \mathcal{L}_m)$ also found similar results [86]. Other models with

higher-order torsion invariants such as $f(\mathbb{T}, T_G)$ found scaling solutions and found past, present and future singularities, depending on the parameters of the theory [82]. In two recent papers [214, 215], the authors studied the dynamical system of a teleparallel Lovelock gravity theory and string-inspired theories finding a rich phenomenology that can also describe a late-time acceleration of the Universe. Further higher-order derivative torsion theories such as $f(\mathbb{T}, (\nabla\mathbb{T})^2, \square\mathbb{T})$ or non-local theories $\mathbb{T}f(\square^{-1}\mathbb{T})$ found vacuum de-Sitter solutions and phantom divide line crossing in agreement with observations [78, 216]. Regarding higher dimensional models, in [217] the authors used dynamical systems to find that $f(\mathbb{T})$ gravity in eleven dimensions can give rise to an early inflationary epoch driven by the presence of extra dimensions without other matter sources.

In [113], the authors analysed the first teleparallel scalar-tensor theory using dynamical system techniques. He analysed a model called teleparallel dark energy (see Sect. 14.2), which is constructed by a non-minimally coupling between the torsion scalar \mathbb{T} and a scalar field ϕ as $(1 + \xi\phi^2)\mathbb{T}$, with ξ being a constant, finding that these models contain certain similarities to Elko spinor dark energy models. In a non-minimally coupled model between the Ricci scalar and a scalar field, it is possible to find scaling solutions but in teleparallel dark energy, this cannot be achieved [113]. However, if the coupling is changed to $F(\phi)\mathbb{T}$ scaling solutions can be obtained [218]. Further, in [219] the authors analysed the phase space of this model, finding similar results as standard quintessence models but having an additional late-time solution behaving as de-Sitter without any fine-tuning. They also found that the crossing of the phantom divide line is possible for this model. In a series of two papers, Skugoreva et al. [220, 221] also studied this model, giving a detailed comparison between it with the standard non-minimally coupled case constructed from the Ricci scalar, finding that in teleparallel dark energy the presence of oscillatory behaviors is more frequent [220, 221]. If one uses the teleparallel dark energy model and adds an additional coupling between dark matter and dark energy, is a deceleration to acceleration phase transition via a Z_2 symmetry breaking results [222]. Another proposed teleparallel model was introduced in [114] by adding a new coupling $\chi B\phi^2$, where χ is a constant and B is the boundary term. Clearly, the standard Ricci case non-minimally coupled with the scalar field is recovered by setting $\chi = -\xi$. The authors studied the case where only a boundary term coupling exists, and they found that the evolution of the model evolves towards a late-time accelerating attractor without any fine-tuning. They also found the possibility of the crossing of the phantom divide line in this model. Later, in [223], it was found that using this coupling, one can also get scaling solutions. Other more exotic models have been also proposed, such as tachyonic teleparallel models [197, 218, 224–227] finding scaling solutions, alleviating the coincidence problem without fine-tuning, obtaining a late-time accelerating attractor and also finding a field-matter-dominated era. Moreover, quintom models concerning two scalar fields (one phantom and the other canonical), non-minimally coupled two both the torsion scalar and the boundary term, have also been studied using the dynamical system, finding similar results to the other models obtaining the correct picture of the history of the Universe [107].

As discussed in this section, the correct use of recasting the FLRW equations into a dynamical system form helps in understanding the main behaviour of the system without the need for analytically solving the equations directly. In the next section, a different approach that is related to obtain analytical cosmological solutions will be presented.

14.3.7 Noether Symmetry Approach in Teleparallel Theories of Gravity

The Einstein field equations are a system of ten partial differential equations and certain symmetries need to be assumed (such as spherical or cylindrical symmetries) in order to find analytical solutions. When they are modified, usually, the equations become even more involved, and for this reason, it is not so easy to find analytical solutions in those models (even for the maximally symmetric cases). One useful tool to obtain analytical solutions for a certain Lagrangian is Noether's symmetry approach, which allows us to reduce dynamics for a certain model by using their symmetries and conserved quantities from the Noether theorem. This allows us to get an exact integration of a system because their symmetries are first integrals.

The procedure to get analytical solutions using Noether's theorem is quite simple, but in practice it sometimes becomes a hard task. First, the point-like canonical Lagrangian associated with the studied action in the examined geometry needs to be written down. After this, Noether's theorem is used which can be stated in two parts [228–230]:

Theorem 1 (Noether's theorem part one) *Let q^i be some generalised coordinates in the configured space $\mathcal{Q} = \{q^i\}$ of a non-higher derivative order Lagrangian $L = L(t, q^i, \dot{q}^i)$ whose tangent space is $\mathcal{T}\mathcal{Q} = \{q^i, \dot{q}^i\}$ with dots representing differentiation with respect to the time coordinate. The existence of a Noether symmetry that leaves the Euler Lagrange equations $E_i(L) = 0$ associated with the Lagrangian invariant under the transformations $\bar{t} = t + \epsilon\xi(t, q^i)$ and $\bar{q}^i = q^i + \epsilon\eta^i(t, q^k)$, with ϵ being a parameter, implies the existence of a function $g(t, q^k)$ which satisfies the condition*

$$\mathbf{X}^{[1]}L + L \frac{d\xi}{dt} = \frac{dg}{dt}, \quad (14.95)$$

where $\mathbf{X}^{[1]}$ is the first prolongation of the generator vector field given by

$$\mathbf{X}^{[1]} = \xi(t, q^i) \frac{\partial}{\partial t} + \eta^i(t, q^i) \frac{\partial}{\partial q^i} + \dot{\eta}^i(t, q^i) \frac{\partial}{\partial \dot{q}^i} = \mathbf{X} + \dot{\eta}^i(t, q^i) \frac{\partial}{\partial \dot{q}^i}, \quad (14.96)$$

and \mathbf{X} is the Noether symmetry vector.

Theorem 2 (Noether's theorem part two) *For any Noether symmetry vector \mathbf{X} associated with the Lagrangian $L = L(t, q^i, \dot{q}^i)$, there corresponds a function called the*

Noether integral of the Euler Lagrange equations, which is given by

$$I = \left(\dot{q}^i \frac{\partial L}{\partial \dot{q}^i} - L \right) - \eta^i \frac{\partial L}{\partial \dot{q}^i} + g \quad (14.97)$$

and is the first integral of the equations of motion $dI/dt = 0$.

Using this theorem, one can get the conserved quantities related to the symmetries of a certain theory. This method has been used in TG in the context of cosmology and also in the case of spherically symmetric spacetimes. It is important to mention that different authors have used an incomplete version of Noether's theorem just by considering the uncompleted Noether's condition $\mathbf{X}L = 0$ instead of the complete Noether's condition (14.95). This method is also correct but it does not give all the possible symmetries of a model. The first work related to this method in teleparallel theories was done in [231] for vacuum $f(\mathbb{T})$ cosmology, finding power-law $f(\mathbb{T}) = c_1 \mathbb{T}^n$ solutions using the incomplete Noether's condition and then finding power-law analytical cosmological solutions $a(t) \propto t^{2n-3}$. Some days later, independently, other authors found the same results in [232]. Using the complete Noether's condition, a more detailed analysis was carried out in [233] and [234] in $f(\mathbb{T})$ cosmology, obtaining similar cosmological solutions to the first work. In [235] the authors added a minimally coupled scalar field, obtaining $f(\mathbb{T}) \propto \mathbb{T}^{3/4}$ with a potential $V(\phi) \propto \phi^2$. One of the first non-trivial spherically symmetric solutions in $f(\mathbb{T})$ theories was found using Noether's symmetry approach in [236]. Among these solutions, one of them behaves similarly to the Schwarzschild solution. For $f(\mathbb{T}, B)$ gravity, in [77], several types of power-law cosmological solutions were obtained, along with a new logarithmic boundary term solution $f(\mathbb{T}, B) = -\mathbb{T} + (1/3)B \log B$, which admits a new cosmological solution $a(t) = (c_2 e^{C_1 t} + 3C_3(t + c_4))^{1/3}$. The authors also made a comparison between the symmetries found in $f(\mathbb{T})$, $f(R)$ and $-\mathbb{T} + f(B)$ gravity. Further, in [237], new spherically symmetric exact solutions were found in $f(\mathbb{T}, B)$ gravity. The modified teleparallel Gauss-Bonnet theory $f(\mathbb{T}, T_G)$ [79] and then the extended case with the boundary terms $f(\mathbb{T}, B, T_G, B_G)$ [238] also found different kinds of analytical power-law types of gravity solutions for f , with some non-trivial scale factors behaving as a combination of exponential with power-laws or hyperbolic functions.

Later, using Noether's symmetry approach for a generalised non-local teleparallel theory $(\xi \mathbb{T} + \chi B)f(\square^{-1} \mathbb{T}, \square^{-1} B)$ and without assuming any condition, the authors found that the non-local coupling functions are constrained from the symmetries to be either linear combination or exponential [90]. It is interesting to remark that some non-local theories were using exponential non-local coupling functions by hand to get renormalisable theories, but in [90], this result appears directly from the symmetries of the theory. Regarding teleparallel scalar tensor theories, there have been a large amount of papers on different theories, such as teleparallel dark energy or its extended version to non-minimally coupling $F(\phi)\mathbb{T}$ [239, 240], adding non-minimal couplings with the boundary term and the scalar field [241, 242], or adding vector fields [243, 244], or with a fermionic field [245], or even adding an

unusual coupling $F(\phi, \partial_\mu \phi \partial^\mu \phi) \mathbb{T}$ [246]. In these works, new wormhole spherically symmetric solutions and also non-trivial cosmological solutions were found in flat FLRW and in Bianchi models concerning different non-trivial scale factors, along with different types of coupling functions $F(\phi)$ between both the torsion scalar and the boundary term B . Therefore, the teleparallel community has used Noether's symmetry approach in many different works in order to get cosmological and spherically symmetric solutions.

As an example, following [234], let us here briefly review the simplest non-trivial modified TG case, which is vacuum $f(\mathbb{T})$ gravity in flat FLRW cosmology. The canonical point-like Lagrangian for $f(\mathbb{T})$ gravity in the minisuperspace of flat FLRW can be found by considering the canonical variables a, \mathbb{T} in the action (14.33) and then using $\mathbb{T} = 6H^2$ in flat FLRW cosmology. This lets us rewrite the action using Lagrange multipliers to then finally obtain the following point-like Lagrangian

$$L = a^3 (f(\mathbb{T}) - \mathbb{T} f'(\mathbb{T})) + 6a\dot{a}^2 f_{\mathbb{T}}. \quad (14.98)$$

Now, we replace the above point-like Lagrangian into Noether's condition (14.95), finding a set of partial differential equations for Noether's vector, and also depending on the function $f(\mathbb{T})$. For this model, there are seven differential equations

$$a^3 (f_{\mathbb{T}} \mathbb{T} - f) \xi_{,\mathbb{T}} = g_{,\mathbb{T}}, \quad 3a^2 \eta_1 (f_{\mathbb{T}} \mathbb{T} - f) + a^3 f_{\mathbb{T}\mathbb{T}} \mathbb{T} \eta_2 + a^3 (f_{\mathbb{T}} \mathbb{T} - f) \xi_{,t} = g_{,t}, \quad (14.99)$$

$$\xi_{,a} = 0, \quad \xi_{,\mathbb{T}} = 0, \quad \eta_{1,\mathbb{T}} = 0, \quad 12f_{\mathbb{T}} a \eta_{1,t} + a^3 (f_{\mathbb{T}} \mathbb{T} - f) \xi_{,a} = g_{,a}, \quad (14.100)$$

$$f_{\mathbb{T}} \eta_1 + f_{\mathbb{T}\mathbb{T}} \mathbb{T} \eta_2 + 2f_{\mathbb{T}} a \eta_{1,a} - f_{\mathbb{T}} a \xi_{,t} = 0, \quad (14.101)$$

where $\eta^i \partial q_i = \eta_1(t, a, \mathbb{T}) \partial_a + \eta_2(t, a, \mathbb{T}) \partial_{\mathbb{T}}$. We now need to solve the above system of partial differential equations to get the symmetries of the model. It is easy to see from (14.100) that Noether's vector is constrained to $\xi = \xi(t)$, $\eta_1 = \eta_1(a)$ and $g = g(t)$. If one uses these conditions into (14.101), one gets $\eta_2 = f_{\mathbb{T}} S(a, \mathbb{T}) / f_{\mathbb{T}\mathbb{T}}$ with $S(a, \mathbb{T})$ being an arbitrary function that must be of the form $S(a, \mathbb{T}) = M(a) + N(\mathbb{T})$ due to (14.99). Considering all of these equations, one finds that $g = \text{constant}$, and then the above system for $f(\mathbb{T}) \neq e^{c_1 \mathbb{T}}$ is reduced to be

$$\frac{f_{\mathbb{T}} \mathbb{T}}{f_{\mathbb{T}} \mathbb{T} - f} = \frac{n}{n-1}, \quad (14.102)$$

$$N = c + \xi_{,t}, \quad 2\eta_{1,a} + \frac{\eta_1}{a} + M = c, \quad 3\frac{\eta_1}{a} + \frac{n}{n-1} M = m, \quad \frac{n}{1-n} N - \xi_{,t} = m, \quad (14.103)$$

where m, n and c are constants. This yields the power-law solution $f(\mathbb{T}) = f_0 \mathbb{T}^n$ with Noether's vector and Noether's integral for $n \neq 3/2$ and $n \neq 1/2$ being equal to

$$\begin{aligned}
X &= \left(\frac{3C}{2n-1} t \right) \partial_t + \left(Ca + c_3 a^{1-\frac{3}{2n}} \right) \partial_a \\
&+ \left[\frac{1}{n} \left((c-m)n + 3c_3 a^{-\frac{3}{2n}} \right) + \frac{3C}{2n-1} + c \right] \mathbb{T} \partial_{\mathbb{T}}, \quad (14.104)
\end{aligned}$$

$$I = \left(\frac{3C}{2n-1} t \right) \mathcal{H} - 12 f_0 n \left(Ca^2 + c_3 a^{2-\frac{3}{2n}} \right) \mathbb{T}^{n-1} \dot{a}, \quad (14.105)$$

with \mathcal{H} being the Hamiltonian and c_i some integration constants. The other cases $n = 3/2$ and $n = 1/2$ have different Noether's symmetries. Finally, if one assumes the power-law $f(\mathbb{T}) = f_0 \mathbb{T}^n$ obtained by the symmetries, it is easy to find from the modified FLRW equations (14.65)–(14.66) with $\rho = p = 0$, that $a(t) \propto t^{2n-3}$ is an analytical solution of the system. Thus, even in vacuum, $f(\mathbb{T})$ power-law admits power-law $a(t)$ solutions. In this way, one is not putting the function $f(\mathbb{T})$ by hand, instead, the symmetries of the model based on Noether's theorem are choosing the form of the function. One can follow the other branch of Noether's equation and find that exponential $f(\mathbb{T}) = f_0 e^{c_1 \mathbb{T}}$ are also part of the symmetries of the model. For this case, one can obtain de-Sitter cosmological solutions from the modified FLRW equations.

14.3.8 Bounce Solutions in Modified Teleparallel Cosmology

One key problem in General Relativity is the existence of both cosmological and black hole singularities. The Λ CDM model, which is based on GR, states that the Universe started from an unnatural initial big bang cosmological singularity and this cannot be alleviated without evoking new physics. This means that the cosmological equations break down at $t = 0$ and some divergences in the curvature appears. In other words, there exists a singularity due to the incompleteness of the geodesic deviation equation. Possible solutions for this in cosmology are the so-called *bouncing cosmological solutions*, which essentially are solutions describing a contraction of the Universe until a minimum non-zero radius to then describing an expanded Universe passing through a bounce. This means that generically, there needs to be a model starting with a contracting universe whose Hubble parameter is $H < 0$, then passing to a continuous bounce with $H = 0$, to then finalising in an expansion with $H > 0$. There are several types of bounce solutions. Some of them have a different evolution, for example, exhibiting a discontinuity in the Hubble parameter. These solutions do not appear in GR, but it is possible to achieve them if either exotic matter or modified gravity are introduced. The simplest way to achieve this in GR is by introducing a quintom scalar field model with two scalar fields. The first scalar field behaves as a standard canonical scalar field and the other one has an incorrect sign in the kinetic term, and then behaves as a ghost scalar field. It is unclear how physical it is to introduce these kind of exotic scalar fields, due to the possible existence of instabilities. If one modifies GR, on the other hand, it is possible to obtain bouncing

solutions without introducing such exotic elements. Basically, the method is very simple, a form of the scale factor (or the Hubble parameter) is assumed, which can describe bounces. Then, a reconstruction technique can be used to get a model (or a theory) that has these kind of solutions. For a more detailed description about bouncing cosmological solutions, see [247].

In the context of TG, the first study that found bouncing cosmological solutions was conducted in $f(\mathbb{T})$ gravity [248]. To achieve this scenario, it is necessary to first check the existence of bounce solutions at the background level and then study the evolution of perturbations through the bounce. Let us here briefly review what happens at the background level. For the perturbation study, see more details in [248]. One type of bouncing cosmological solution can be described by having the following scale factor

$$a(t) = a_0 \left(1 + \frac{3}{2} \sigma t^2 \right)^{1/3}, \quad (14.106)$$

where $\sigma > 0$ and a_0 are constants. The first parameter determines how fast the bounce is, whereas a_0 is the scale factor evaluated at the bouncing point. The Hubble parameter then behaves as

$$H(t) = \frac{\sigma t}{1 + \frac{3}{2} \sigma t^2}, \quad (14.107)$$

with the time varying from $-\infty$ to $+\infty$. Figure 14.7 shows the behaviour of the above Hubble parameter achieving the expected bounce scenario, starting from a matter contraction, then following with a bounce (static) and finalising in an expansion. If we assume a pressureless matter, from the conservation equation the energy density becomes $\rho = C_1/(3\sigma t^2 + 2)$. Since $\mathbb{T} = 6H^2$, we can then find that $t = t(\mathbb{T})$, and we can then use this expression for the first flat FLRW equation (14.65), to then solve this differential equation for $f(\mathbb{T})$, yielding

$$f(\mathbb{T}) = \mathbb{T} + \frac{1}{2} C_1 \kappa^2 \sqrt{\frac{\mathbb{T}}{\sigma}} \arcsin \left(\sqrt{\frac{\mathbb{T}}{\sigma}} \right) + \frac{C_1 \kappa^2}{2} \left(1 + \sqrt{1 - \frac{\mathbb{T}}{\sigma}} \right). \quad (14.108)$$

The scale factor (14.106) that gives the Hubble parameter (14.107) describing a bouncing cosmological solution is a solution of the above form of $f(\mathbb{T})$ gravity, which is a GR term plus some correction terms, depending on the scalar torsion. There are other works finding other kinds of bounce solutions in the context of modified TG. In [249], different types of non-singular bounce solutions were found in $f(\mathbb{T})$, such as Λ CDM with a bounce in the past, with the scale factor behaving as $a(t) \propto \sinh[\sqrt{t^2 + \tau^2}/t_0]$ or future bounces with Quasi-rip and Little-rip behaviours. In [250] some superbounce solutions in $f(\mathbb{T})$ gravity that have a ekpyrotic contracting phase preventing large anisotropies are found. The authors also made some comparisons between other modified models starting from GR, such as $f(R)$ and $f(\mathcal{G})$ gravity. Later, it was found that in $f(\mathbb{T})$ gravity it is possible to have a bounce inflation model with a graceful decelerated exit [184]. Using dynamical systems techniques, in [209], the authors also found the possibility of bounces and turnaround

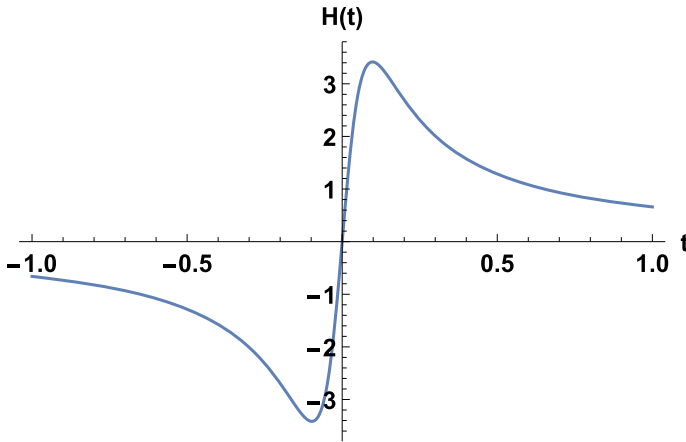


Fig. 14.7 Hubble parameter versus time for the model (14.107) with $\sigma = 70$, in units where $\kappa^2 = 1$, describing a bounce behaviour

solutions in $f(\mathbb{T})$ gravity but the impossibility of cyclic and oscillating universes. In [251], the authors studied a model with $f(\mathbb{T})$ and a scalar field to then perform perturbations for the bounce inflationary models, finding that it is difficult to obtain a stable bounce inflation solution, since there are many conditions that the models need to satisfy in order to have this property, though, they were able to show that a combination of power-law types of $f(\mathbb{T})$ can achieve these stable bounce inflation solutions. If one understands the cosmological singularities as a break down of GR at very high energies, then some studies have argued that Loop quantum cosmology could alleviate them. Some works like [252–254] have also found bounces in a toy model in $f(\mathbb{T})$ gravity, assuming Loop quantum cosmological considerations. Further generalisations to $f(\mathbb{T})$ gravity, such as considering the teleparallel Gauss-Bonnet invariant $T_{\mathcal{G}}$ in the so-called $f(\mathbb{T}, T_{\mathcal{G}})$ gravity, have also been used to analyse possible bounce solutions, finding five types of them [255, 256]. In [257] the case of Born-Infeld gravity was studied. These kind of theories are achieved from $f(\mathbb{T})$ gravity with $f(\mathbb{T}) = \frac{\lambda}{2\kappa^2} \left(\left(1 + \frac{\mathbb{T}}{2\lambda} \right)^{1/2} - 1 \right)$, with λ being a parameter of the theory that becomes important at high energies. In this paper, the author found that at high energy regimes, the big bang singularity is absent, and either a de-Sitter inflationary stage of geometrical character or a bounce is present. Later, in [258], they showed that this behaviour is only valid for a certain region of the parameter space, and other singularities such as Big Rip, Big Bang, Big Freeze, and Sudden singularities can emerge. It is interesting to mention that recently, in [259], a regular Schwarzschild black hole solution was found in this theory. In this context, the central Schwarzschild curvature singularity is replaced by an infinitely long cosmic string related to the parameter λ .

As was seen in the previous example and also in the papers mentioned here, it is not so complicated to get bouncing cosmological solutions in modified TG.

It is important to emphasise that in standard GR, this cannot be achieved without introducing matter that violates the energy conditions.

14.4 What Can Teleparallel Theories Have to Offer? What Are the Open Problems in Teleparallel Theories?

Teleparallel theories give an alternative starting point for understanding gravity compared with the standard curvature-based approach to gravity used in GR. Some interesting features about them compared to GR are:

- *Modified teleparallel theories are broader than standard modified theories starting from GR:*

We have seen that theories equivalent to GR, scalar-tensor gravity, Horndeski theory, $f(R)$ and Gauss-Bonnet gravity based on the teleparallel geometry exist as subclasses of more general families of Teleparallel Gravity theories. In this spirit, Teleparallel Gravity may be used to formulate broader classes of theories than could be constructed by using only the metric and its Levi-Civita connection. This should not be too surprising, since any theory of the latter type can be rewritten into teleparallel language by using the relations (14.4), (14.23) and (14.24) to replace the metric, its Levi-Civita connection and the corresponding curvature by the tetrad and the contortion, and hence the torsion. This teleparallel formulation then gives rise to further extensions and generalisations by splitting off boundary terms or including additional terms that have no equivalent expression in terms of the metric geometry only. An easy example would be to take the case of $f(R)$ and $f(\mathbb{T})$ gravity. If we start by formulating a theory from GR, then torsion is zero and it is not possible to derive a similar theory to $f(\mathbb{T})$. On the other hand, if we start from TG, we can generalise $f(\mathbb{T})$ to $f(\mathbb{T}, B)$ and then we can formulate a teleparallel equivalent version of $f(R)$ by considering $f(\mathbb{T}, B) = f(-\mathbb{T} + B) = f(R)$.

- *It is easy to get second-order field equations, since torsion contains only first-order derivatives:*

Since most physical phenomena are described by up to second-order field equations, it is expected that gravity will not have a behaviour different to this. Moreover, higher-order field equations often lead to ghost instabilities. In Teleparallel Gravity it is easy to get second order field equations because the torsion tensor contains only first-order derivatives of the tetrad, in contrast with the Riemann tensor that contains second-order derivatives in the metric. This means that in modifications like $f(\mathbb{T})$ or even more complicated ones like $f(T_{\text{ax}}, T_{\text{vec}}, T_{\text{ten}})$, BDLs, etc., the field equations will be of second order, unlike in, e.g., $f(R)$ theory where they are fourth-order in all cases beyond GR. In principle, one could construct a theory with infinite contractions of the torsion tensor and still get second-order field equations.

- *Similarity to Yang-Mills theory—possible connections to gauge theory and particle physics:*
The TEGR action in Eq. (14.29) has an obvious similarity with a Yang-Mills type action, since it is quadratic in the first-order derivatives of the tetrad, the latter being the fundamental dynamical field of the theory. This means that has more in common with actions encountered in particle physics than it is the case for the Einstein-Hilbert action. Furthermore, the potential interpretation as a gauge theory of translations makes it more similar to theories describing the other fundamental interactions in Nature, hence paving a potential road map towards a unification of gravity and other forces. While still being non-renormalisable, it may provide an alternative and possibly more promising starting point for constructing a UV complete theory.
- *The possibility of formulating the theory without the equivalence principle:* In GR, gravitation is characterised by curvature through the Ricci scalar, which then acts on particles through the geodesic equation. TG is wholly different in that the geometric torsion that is produced to expressed gravity, acts through a Lorentz force-type equation. In this way, we recover the original concept of gravitation as a force similar to the other fundamental forces of Nature. While the equations turn out to be equivalent for TEGR, they differ for modifications to this model. Coupled with the potential of being described as a gauge theory of translations, TG does not rely on the weak equivalence principle in that it would survive a violation [1, 260]. However, in these settings, the Newtonian limits remain intact resulting in a more natural weak-field limit compared with GR.
- *Defining a gravitational energy-momentum tensor:*
TG offers the possibility of describing gravitation as a gauge current [1, 5, 6]. Then, by separating inertial and gravitation, it may become possible to define an energy-momentum tensor for gravitation. However, this feature of the theory may require selection of a Lorentz frame, which would limit the applicability of this result [261, 262].
- *The regularity of the TEGR action. One does not need to introduce a Gibbons-Hawking-York boundary term:*
One may argue that the TEGR action in Eq. (14.29) is a more natural formulation of the dynamics of GR than the Einstein-Hilbert action, since the latter also contains second order derivatives of the metric. The latter mandates the inclusion of a Gibbons-Hawking-York boundary term in order to possess a well-defined variational problem and Hamiltonian formulation, which is not the case for TEGR. While this does not affect the classical equations of motion, it may affect the quantum behavior and thermodynamics of black holes. Further, it was found in [263] that the black hole entropy is more naturally expressed as a volume integral in TEGR than in GR.
- *Torsional or Curvature-based Gravity:*
TEGR is dynamically equivalent to GR in that the identical field equations emerge due to the respective Lagrangian densities being equal up to a boundary term. However, the action may contain further information, such as the renormalisability of the theory, as well as the symmetries of the theory. Moreover, modifications to

TEGR offer a much richer avenue to construct new theories, due to the second-order nature of the torsion scalar [264].

Although teleparallel theories have attained a lot of attention in the past ten years, the community effort is still not comparable to that in GR. For this reason, there are several open problems/questions that have not been addressed properly in the literature. Some of these open problems are:

- *Confrontation with cosmological data:* Teleparallel theories have shown great promise for consistently describing observations at cosmic scales while also satisfying Solar System and astrophysical-scale physics [105, 134, 160–163, 167, 170, 265–268]. Further work needs to be done in this direction to better understand the explaining power of the theory in its various manifestations.
- *Gravitational Waves:* A strong effort has been made in regards to understanding the cosmological consequences of gravitational waves in $f(\mathbb{T})$ gravity [134, 162, 163, 269]. However, there remains many other contexts in which TG has shown promise, and more than this, further work is needed in the astrophysical context. In Refs. [62, 135, 136, 270], it is shown that $f(\mathbb{T})$ gravity contains only two propagating modes, while other variants of TG can provide more. It would be interesting to investigate further the waveform for astrophysical events, which would entail obtaining further information about the $3 + 1$ formalism of the theory and performing simulations of astrophysical events. Ultimately, it is crucial to understand how current and future observatories can be exploited to test TG.
- *The Galactic Rotation Curve Problem:* $f(\mathbb{T})$ gravity has shown positive results for describing the rotation curves without the requirement of adding dark matter [137]. Weak lensing tests have also contributed to constraints on one of the potential models of the theory [271]. However, further analysis needs to be done on considering more cosmologically inspired models, as well as increasing the breadth of the analysis. One possibility is to use the SPARC (Spitzer Photometry and Accurate Rotation Curves) obtained in Ref. [272].
- *Teleparallel quantum gravity:* The majority of quantum gravity approaches have been attempted with GR as the starting point, but not so many have been initiated from TG. For example, the loop quantum corrections of the TEGR action (14.29) are not so well-known. One of the first attempts was done in [273]. In GR, this has been studied with a lot of effort, even obtaining corrections of an action with $\sum_{i=1}^{70} R^i$ [274]. This has been studied within the asymptotic safety approach to quantum gravity [275] that has not also been applied to Teleparallel Gravity. Another interesting route would be to formulate a teleparallel version of loop quantum gravity, since both formulations use a similar mathematical language.
- *What are singularities in Teleparallel Gravity?:* Hawking and Penrose proposed a way to define singularities in GR, which is based on the incompleteness of the geodesic equation. Then, a simple way to quantify these singularities is by defining some invariants such as the Kretschmann scalar $K \equiv R^{\mu\nu\alpha\sigma} R_{\mu\nu\alpha\sigma}$. In TG, it is not clear whether the Hawking-Penrose theorem would be the same, or if one would need to define different invariants to check if there are singularities. Then, it is still open as to how a singularity in the context of TG can be defined.

References

1. R. Aldrovandi, J.G. Pereira, *Teleparallel Gravity*, vol. 173 (Springer, Dordrecht, 2013)
2. A. Einstein, Riemann-Geometrie mit Aufrechterhaltung des Begriffes des Fernparallelismus. Sitzber. Preuss. Akad. Wiss. **17**, 217–221 (1928)
3. M. Krššák, E.N. Saridakis, The covariant formulation of $f(T)$ gravity. *Class. Quant. Grav.* **33**(11), 115009 (2016). [arXiv:1412.8383](#)
4. A. Golovnev, T. Koivisto, M. Sandstad, On the covariance of teleparallel gravity theories. *Class. Quant. Grav.* **34**(14), 145013 (2017). [arXiv:1701.06271](#)
5. D. Blixt, M. Hohmann, C. Pfeifer, Hamiltonian and primary constraints of new general relativity. *Phys. Rev. D* **99**(8), 084025 (2019). [arXiv:1811.11137](#)
6. D. Blixt, M. Hohmann, C. Pfeifer, On the gauge fixing in the Hamiltonian analysis of general teleparallel theories. *Universe* **5**(6), 143 (2019). [arXiv:1905.01048](#)
7. J. Beltrán Jiménez, L. Heisenberg, T.S. Koivisto, Teleparallel Palatini theories. *JCAP* **1808**, 039 (2018). [arXiv:1803.10185](#)
8. M. Blagojević, F.W. Hehl (eds.), *Gauge Theories of Gravitation* (World Scientific, Singapore, 2013)
9. K. Hayashi, T. Nakano, Extended translation invariance and associated gauge fields. *Prog. Theor. Phys.* **38**, 491–507 (1967). ([354(1967)])
10. Y.M. Cho, Einstein Lagrangian as the Translational Yang-Mills Lagrangian. *Phys. Rev. D* **14**, 2521 (1976). ([393(1975)])
11. K. Hayashi, T. Shirafuji, New general relativity. *Phys. Rev. D* **19**, 3524–3553 (1979). ([409(1979)])
12. J.C. Baez, D.K. Wise, Teleparallel gravity as a higher gauge theory. *Commun. Math. Phys.* **333**(1), 153–186 (2015). [arXiv:1204.4339](#)
13. M. Fontanini, E. Huguet, M. Le Delliou, Teleparallel gravity equivalent of general relativity as a gauge theory: translation or Cartan connection? *Phys. Rev. D* **99**(6), 064006 (2019). [arXiv:1811.03810](#)
14. J.G. Pereira, Y.N. Obukhov, Gauge structure of teleparallel gravity. *Universe* **5**(6), 139 (2019). [arXiv:1906.06287](#)
15. M. Blagojević, *Gravitation and Gauge Symmetries*. Series in High Energy Physics, Cosmology and Gravitation (CRC Press, 2001)
16. Yu.N. Obukhov, J.G. Pereira, Metric affine approach to teleparallel gravity. *Phys. Rev. D* **67**, 044016 (2003). [arXiv:gr-qc/0212080](#)
17. B. Li, T.P. Sotiriou, J.D. Barrow, $f(T)$ gravity and local Lorentz invariance. *Phys. Rev. D* **83**, 064035 (2011). [arXiv:1010.1041](#)
18. T.P. Sotiriou, B. Li, J.D. Barrow, Generalizations of teleparallel gravity and local Lorentz symmetry. *Phys. Rev. D* **83**, 104030 (2011). [arXiv:1012.4039](#)
19. R. Ferraro, F. Fiorini, Non trivial frames for $f(T)$ theories of gravity and beyond. *Phys. Lett. B* **702**, 75–80 (2011). [arXiv:1103.0824](#)
20. N. Tamanini, C.G. Boehmer, Good and bad tetrads in $f(T)$ gravity. *Phys. Rev. D* **86**, 044009 (2012). [arXiv:1204.4593](#)
21. N. Tamanini, C.G. Böhrer, Definition of Good Tetrads for $f(T)$ Gravity, in *Proceedings, 13th Marcel Grossmann Meeting on Recent Developments in Theoretical and Experimental General Relativity, Astrophysics, Relativistic Field Theories (MG13): Stockholm, Sweden, July 1-7, 2012*, pp. 1282–1284 (2015). [arXiv:1304.0672](#)
22. W. Kopczynski, Problems with metric-teleparallel theories of gravitation. *J. Phys. A: Math. General* **15**, 493–506 (1982)
23. W.-H. Cheng, D.-C. Chern, J.M. Nester, Canonical analysis of the one parameter teleparallel theory. *Phys. Rev. D* **38**, 2656–2658 (1988)
24. J.M. Nester, Is there really a problem with the teleparallel theory? *Class. Q. Gravity* **5**, 1003–1010 (1988)
25. H. Chen, J.M. Nester, H.-J. Yo, Acausal PGT modes and the nonlinear constraint effect. *Acta Phys. Polon. B* **29**, 961–970 (1998)

26. Y.C. Ong, K. Izumi, J.M. Nester, P. Chen, Problems with propagation and time evolution in $f(T)$ gravity. *Phys. Rev. D* **88**, 024019 (2013). [arXiv:1303.0993](#)
27. R. Ferraro, F. Fiorini, Remnant group of local Lorentz transformations in *mathcal{f}(T)* theories. *Phys. Rev. D* **91**(6), 064019 (2015). [arXiv:1412.3424](#)
28. P. Chen, K. Izumi, J.M. Nester, Y.C. Ong, Remnant symmetry, propagation and evolution in $f(T)$ gravity. *Phys. Rev. D* **91**(6), 064003 (2015)
29. C. Bejarano, R. Ferraro, F. Fiorini, M.J. Guzmán, Reflections on the covariance of modified teleparallel theories of gravity. *Universe* **5**, 158 (2019). [arXiv:1905.09913](#)
30. R. Ferraro, M.J. Guzmán, Pseudoinvariance and the extra degree of freedom in $f(T)$ gravity. *Phys. Rev. D* **101**(8), 084017 (2020). [arXiv:2001.08137](#)
31. M. Hohmann, L. Järvi, U. Ualikhanova, Covariant formulation of scalar-torsion gravity. *Phys. Rev. D* **97**(10), 104011 (2018). [arXiv:1801.05786](#)
32. M. Krssak, R.J. van den Hoogen, J.G. Pereira, C.G. Böhm, A.A. Coley, Teleparallel theories of gravity: illuminating a fully invariant approach. *Class. Quant. Grav.* **36**(18), 183001 (2019). [arXiv:1810.12932](#)
33. J.W. Maluf, Dirac spinor fields in the teleparallel gravity: comment on ‘Metric affine approach to teleparallel gravity’. *Phys. Rev. D* **67**, 108501 (2003). [arXiv:gr-qc/0304005](#)
34. E.W. Mielke, Consistent coupling to Dirac fields in teleparallelism: comment on ‘Metric-affine approach to teleparallel gravity’. *Phys. Rev. D* **69**, 128501 (2004)
35. Yu.N. Obukhov, J.G. Pereira, Lessons of spin and torsion: reply to ‘Consistent coupling to Dirac fields in teleparallelism’. *Phys. Rev. D* **69**, 128502 (2004). [arXiv:gr-qc/0406015](#)
36. J.B. Formiga, Comment on ‘‘Metric-affine approach to teleparallel gravity.’’ *Phys. Rev. D* **88**(6), 068501 (2013). [arXiv:1306.4964](#)
37. J. Beltran Jimenez, L. Heisenberg, T. Koivisto, The coupling of matter and spacetime geometry. [arXiv:2004.04606](#)
38. Y.N. Obukhov, G.F. Rubilar, Invariant conserved currents in gravity theories with local Lorentz and diffeomorphism symmetry. *Phys. Rev. D* **74**, 064002 (2006). [arXiv:gr-qc/0608064](#)
39. J.W. Maluf, The teleparallel equivalent of general relativity. *Ann. Phys.* **525**, 339–357 (2013). [arXiv:1303.3897](#)
40. M. Krššák, Holographic renormalization in teleparallel gravity. *Eur. Phys. J. C* **77**(1), 44 (2017). [arXiv:1510.06676](#)
41. J.W. Maluf, S.C. Ulhoa, J.F. da Rocha-Neto, *Difficulties of Teleparallel Theories of Gravity with Local Lorentz Symmetry*. [arXiv:1811.06876](#)
42. T.P. Sotiriou, V. Faraoni, $f(R)$ theories of gravity. *Rev. Mod. Phys.* **82**, 451–497 (2010). [arXiv:0805.1726](#)
43. S. Nojiri, S.D. Odintsov, Introduction to modified gravity and gravitational alternative for dark energy. *eConf C0602061*, 06 (2006). [arXiv:hep-th/0601213](#). [*Int. J. Geom. Meth. Mod. Phys.* **4**, 115(2007)]
44. A. De Felice, S. Tsujikawa, $f(R)$ theories. *Living Rev. Rel.* **13**, 3 (2010). [arXiv:1002.4928](#)
45. S. Nojiri, S.D. Odintsov, Unified cosmic history in modified gravity: from $F(R)$ theory to Lorentz non-invariant models. *Phys. Rept.* **505**, 59–144 (2011). [arXiv:1011.0544](#)
46. Y.S. Myung, Propagating degrees of freedom in $f(R)$ gravity. *Adv. High Energy Phys.* **2016**, 3901734 (2016). [arXiv:1608.01764](#)
47. C.P.L. Berry, J.R. Gair, Linearized $f(R)$ gravity: gravitational radiation and solar system tests. *Phys. Rev. D* **83**, 104022 (2011). [arXiv:hep-th/0601213](#). [*Int. J. Geom. Meth. Mod. Phys.* **4**, 115(2007)]
48. S. Capozziello, C. Corda, M.F. De Laurentis, Massive gravitational waves from $f(R)$ theories of gravity: potential detection with LISA. *Phys. Lett. B* **669**, 255–259 (2008). [arXiv:0812.2272](#)
49. G.R. Bengochea, R. Ferraro, Dark torsion as the cosmic speed-up. *Phys. Rev. D* **79**, 124019 (2009). [arXiv:0812.1205](#)
50. R. Ferraro, F. Fiorini, On born-infeld gravity in Weitzenböck spacetime. *Phys. Rev. D* **78**, 124019 (2008). [arXiv:0812.1981](#)
51. R. Ferraro, F. Fiorini, Modified teleparallel gravity: inflation without inflation. *Phys. Rev. D* **75**, 084031 (2007). [arXiv:gr-qc/0610067](#)

52. S.B. Nassur, C. Ainamon, M.J.S. Houndjo, J. Tossa, Unimodular $f(T)$ gravity. *Eur. Phys. J. Plus* **131**(12), 420 (2016). [arXiv:1602.03172](#)
53. M. Krssak, *Variational Problem and Bigravity Nature of Modified Teleparallel Theories*. [arXiv:1705.01072](#)
54. M. Hohmann, L. Järv, M. Krššák, C. Pfeifer, Teleparallel theories of gravity as analogue of nonlinear electrodynamics. *Phys. Rev. D* **97**(10), 104042 (2018). [arXiv:1711.09930](#)
55. M. Hohmann, L. Järv, M. Krššák, C. Pfeifer, Modified teleparallel theories of gravity in symmetric spacetimes. *Phys. Rev. D* **100**(8), 084002 (2019). [arXiv:1901.05472](#)
56. F. Mueller-Hoissen, J. Nitsch, Teleparallelism - a viable theory of gravity? *Phys. Rev. D* **28**, 718–728 (1983)
57. W. Kopczynski, Problems with metric-teleparallel theories of gravitation. *J. Phys. Math. General* **15**, 493–506 (1982)
58. J.M. Nester, Is there really a problem with the teleparallel theory? *Class Quant. Gravity* **5**, 1003–1010 (1988)
59. T. Kawai, N. Toma, Singularities of “Schwarzschild Like” space-time in new general relativity. *Prog. Theor. Phys.* **83**, 1 (1990)
60. M. Fukui, K. Hayashi, Axially symmetric solutions of new general relativity. *Prog. Theor. Phys.* **66**, 1500 (1981)
61. M. Fukui, J. Masukawa, Weak field approximation of new general relativity. *Prog. Theor. Phys.* **73**, 973 (1985)
62. M. Hohmann, M. Krššák, C. Pfeifer, U. Ualikhanova, Propagation of gravitational waves in teleparallel gravity theories. *Phys. Rev. D* **98**(12), 124004 (2018). [arXiv:1807.04580](#)
63. A. Okolow, J. Swiezewski, Hamiltonian formulation of a simple theory of the teleparallel geometry. *Class. Quant. Grav.* **29**, 045008 (2012). [arXiv:1111.5490](#)
64. Y.C. Ong, J.M. Nester, Counting components in the Lagrange multiplier formulation of teleparallel theories. *Eur. Phys. J. C* **78**(7), 568 (2018). [arXiv:1709.00068](#)
65. T. Ortín, *Gravity and Strings Cambridge Monographs on Mathematical Physics* (Cambridge University Press, Cambridge, 2004)
66. J.B. Jiménez, K.F. Dialektopoulos, *Non-Linear Obstructions for Consistent New General Relativity*. [arXiv:1907.10038](#)
67. J.W. Maluf, F.F. Faria, Conformally invariant teleparallel theories of gravity. *Phys. Rev. D* **85**, 027502 (2012). [arXiv:1110.3095](#)
68. T. Koivisto, G. Tsimperis, *The spectrum of teleparallel gravity*. [arXiv:1810.11847](#)
69. A. Conroy, T. Koivisto, The spectrum of symmetric teleparallel gravity. *Eur. Phys. J. C* **78**(11), 923 (2018). [arXiv:1710.05708](#)
70. L. Heisenberg, A systematic approach to generalisations of general relativity and their cosmological implications. *Phys. Rep.* **796**, 1–113 (2019). [arXiv:1807.01725](#)
71. T. Biswas, E. Gerwick, T. Koivisto, A. Mazumdar, Towards singularity and ghost free theories of gravity. *Phys. Rev. Lett.* **108**, 031101 (2012). [arXiv:1110.5249](#)
72. S. Bahamonde, C.G. Böhrer, M. Krššák, New classes of modified teleparallel gravity models. *Phys. Lett. B* **775**, 37–43 (2017). [arXiv:1706.04920](#)
73. K. Bamba, S.D. Odintsov, D. Sáez-Gómez, Conformal symmetry and accelerating cosmology in teleparallel gravity. *Phys. Rev. D* **88**, 084042 (2013). [arXiv:1308.5789](#)
74. R.-J. Yang, Conformal transformation in $f(T)$ theories. *EPL* **93**(6), 60001 (2011). [arXiv:1010.1376](#)
75. S. Bahamonde, C.G. Böhrer, M. Wright, Modified teleparallel theories of gravity. *Phys. Rev. D* **92**(10), 104042 (2015). [arXiv:1508.05120](#)
76. S. Bahamonde, M. Zubair, G. Abbas, Thermodynamics and cosmological reconstruction in $f(T, B)$ gravity. *Phys. Dark Univ.* **19**, 78–90 (2018). [arXiv:1609.08373](#)
77. S. Bahamonde, S. Capozziello, Noether symmetry approach in $f(T, B)$ teleparallel cosmology. *Eur. Phys. J. C* **77**(2), 107 (2017). [arXiv:1612.01299](#)
78. G. Otalora, E.N. Saridakis, Modified teleparallel gravity with higher-derivative torsion terms. *Phys. Rev. D* **94**(8), 084021 (2016). [arXiv:1605.04599](#)

79. S. Capozziello, M. De Laurentis, K.F. Dialektopoulos, Noether symmetries in Gauss-Bonnet-teleparallel cosmology. *Eur. Phys. J. C* **76**(11), 629 (2016). [arXiv:1609.09289](#)
80. S. Bahamonde, C.G. Böhrer, Modified teleparallel theories of gravity: Gauss-Bonnet and trace extensions. *Eur. Phys. J. C* **76**(10), 578 (2016). [arXiv:1606.05557](#)
81. G. Kofinas, E.N. Saridakis, Teleparallel equivalent of Gauss-Bonnet gravity and its modifications. *Phys. Rev. D* **90**, 084044 (2014). [arXiv:1404.2249](#)
82. G. Kofinas, G. Leon, E.N. Saridakis, Dynamical behavior in $f(t, t_g)$ cosmology. *Class. Quant. Gravity* **31**(17), 175011 (2014). [arXiv:1404.7100](#)
83. T. Harko, F.S.N. Lobo, G. Otalora, E.N. Saridakis, $f(T, \text{mathcal{T}})$ gravity and cosmology. *JCAP* **1412**, 021 (2014). [arXiv:1405.0519](#)
84. T. Harko, F.S.N. Lobo, S. Nojiri, S.D. Odintsov, $f(R, T)$ gravity. *Phys. Rev. D* **84**, 024020 (2011). [arXiv:1104.2669](#)
85. T. Harko, F.S.N. Lobo, G. Otalora, E.N. Saridakis, Nonminimal torsion-matter coupling extension of $f(T)$ gravity. *Phys. Rev. D* **89**, 124036 (2014). [arXiv:1404.6212](#)
86. S. Bahamonde, Generalised nonminimally gravity-matter coupled theory. *Eur. Phys. J. C* **78**(4), 326 (2018). [arXiv:1709.05319](#)
87. J.F. Donoghue, General relativity as an effective field theory: the leading quantum corrections. *Phys. Rev. D* **50**, 3874–3888 (1994). [arXiv:gr-qc/9405057](#)
88. S.B. Giddings, Black hole information, unitarity, nonlocality. *Phys. Rev. D* **74**, 106005 (2006). [arXiv:hep-th/0605196](#)
89. S. Bahamonde, S. Capozziello, M. Faizal, R.C. Nunes, Nonlocal teleparallel cosmology. *Eur. Phys. J. C* **77**(9), 628 (2017). [arXiv:1709.02692](#)
90. S. Bahamonde, S. Capozziello, K.F. Dialektopoulos, Constraining generalized non-local cosmology from noether symmetries. *Eur. Phys. J. C* **77**(11), 722 (2017). [arXiv:1708.06310](#)
91. G.W. Horndeski, Second-order scalar-tensor field equations in a four-dimensional space. *Int. J. Theor. Phys.* **10**, 363–384 (1974)
92. T. Kobayashi, M. Yamaguchi, J. Yokoyama, Generalized G-inflation: inflation with the most general second-order field equations. *Prog. Theor. Phys.* **126**, 511–529 (2011). [arXiv:1105.5723](#)
93. C. Brans, R.H. Dicke, Mach’s principle and a relativistic theory of gravitation. *Phys. Rev.* **124**, 925–935 (1961). ([142(1961)])
94. F. Perrotta, C. Baccigalupi, S. Matarrese, Extended quintessence. *Phys. Rev. D* **61**, 023507 (1999). [arXiv:astro-ph/9906066](#)
95. E.J. Copeland, M. Sami, S. Tsujikawa, Dynamics of dark energy. *Int. J. Mod. Phys. D* **15**, 1753–1936 (2006). [arXiv:hep-th/0603057](#)
96. C. Deffayet, O. Pujolas, I. Sawicki, A. Vikman, Imperfect dark energy from kinetic gravity braiding. *JCAP* **1010**, 026 (2010). [arXiv:1008.0048](#)
97. S. Bahamonde, K.F. Dialektopoulos, J.L. Said, *Can Horndeski Theory be recast using Teleparallel Gravity?*. [arXiv:1904.10791](#)
98. S. Bahamonde, K.F. Dialektopoulos, V. Gakis, J.L. Said, *Reviving Horndeski Theory using Teleparallel Gravity after GW170817*. [arXiv:1907.10057](#)
99. M. Hohmann, Disformal transformations in scalar-torsion gravity. *Universe* **5**(7), 167 (2019). [arXiv:1905.00451](#)
100. C.D. Kreisch, E. Komatsu, Cosmological constraints on Horndeski gravity in light of GW170817. *JCAP* **1812**(12), 030 (2018). [arXiv:1712.02710](#)
101. Y. Gong, E. Papantonopoulos, Z. Yi, Constraints on scalar-tensor theory of gravity by the recent observational results on gravitational waves. *Eur. Phys. J. C* **78**(9), 738 (2018). [arXiv:1711.04102](#)
102. LIGO Scientific, Virgo Collaboration, B.P. Abbott et al., GW170817: observation of gravitational waves from a binary neutron star inspiral. *Phys. Rev. Lett* **119**(16), 161101 (2017). [arXiv:1710.05832](#)
103. C.-Q. Geng, C.-C. Lee, E.N. Saridakis, Y.-P. Wu, “Teleparallel” dark energy. *Phys. Lett. B* **704**, 384–387 (2011). [arXiv:1109.1092](#)

104. G. Kofinas, E. Papantonopoulos, E.N. Saridakis, Self-gravitating spherically symmetric solutions in scalar-torsion theories. *Phys. Rev. D* **91**(10), 104034 (2015). [arXiv:1501.00365](#)
105. C.-Q. Geng, C.-C. Lee, E.N. Saridakis, Observational constraints on teleparallel dark energy. *JCAP* **1201**, 002 (2012). [arXiv:1110.0913](#)
106. M. Zubair, S. Bahamonde, M. Jamil, Generalized second law of thermodynamic in modified teleparallel theory. *Eur. Phys. J. C* **77**(7), 472 (2017). [arXiv:1604.02996](#)
107. S. Bahamonde, M. Marciu, P. Rudra, Generalised teleparallel quintom dark energy non-minimally coupled with the scalar torsion and a boundary term. *JCAP* **1804**(04), 056 (2018). [arXiv:1802.09155](#)
108. L. Jarv, A. Toporensky, General relativity as an attractor for scalar-torsion cosmology. *Phys. Rev. D* **93**(2), 024051 (2016). [arXiv:1511.03933](#)
109. G. Kofinas, Hyperscaling violating black holes in scalar-torsion theories. *Phys. Rev. D* **92**(8), 084022 (2015). [arXiv:1507.07434](#)
110. D. Horvat, S. Ilijić, A. Kirin, Z. Narančić, Nonminimally coupled scalar field in teleparallel gravity: Boson stars. *Class. Quant. Grav.* **32**(3), 035023 (2015). [arXiv:1407.2067](#)
111. M. Jamil, D. Momeni, R. Myrzakulov, Stability of a non-minimally conformally coupled scalar field in F(T) cosmology. *Eur. Phys. J. C* **72**, 2075 (2012). [arXiv:1208.0025](#)
112. Y.-P. Wu, C.-Q. Geng, Primordial fluctuations within teleparallelism. *Phys. Rev. D* **86**, 104058 (2012). [arXiv:1110.3099](#)
113. H. Wei, Dynamics of teleparallel dark energy. *Phys. Lett. B* **712**, 430–436 (2012). [arXiv:1109.6107](#)
114. S. Bahamonde, M. Wright, Teleparallel quintessence with a nonminimal coupling to a boundary term. *Phys. Rev. D* **92**(8), 084034 (2015). [arXiv:1508.06580](#). [Erratum: *Phys. Rev. D* **93**, no.10, 109901 (2016)]
115. M. Hohmann, Scalar-torsion theories of gravity I: general formalism and conformal transformations. *Phys. Rev. D* **98**(6), 064002 (2018). [arXiv:1801.06528](#)
116. M. Hohmann, C. Pfeifer, Scalar-torsion theories of gravity II: $L(T, X, Y, \phi)$ theory. *Phys. Rev. D* **98**(6), 064003 (2018). [arXiv:1801.06536](#)
117. M. Hohmann, Scalar-torsion theories of gravity III: analogue of scalar-tensor gravity and conformal invariants. *Phys. Rev. D* **98**(6), 064004 (2018). [arXiv:1801.06531](#)
118. C.M. Will, The confrontation between general relativity and experiment. *Living Rev. Rel.* **17**, 4 (2014). [arXiv:1403.7377](#)
119. J. Hayward, Scalar tetrad theories of gravity. *Gen. Rel. Grav.* **13**, 43–55 (1981)
120. Z.-C. Chen, Y. Wu, H. Wei, Post-Newtonian approximation of teleparallel gravity coupled with a scalar field. *Nucl. Phys. B* **894**, 422–438 (2015). [arXiv:1410.7715](#)
121. J.-T. Li, Y.-P. Wu, C.-Q. Geng, Parametrized post-Newtonian limit of the teleparallel dark energy model. *Phys. Rev. D* **89**(4), 044040 (2014). [arXiv:1312.4332](#)
122. U. Ualikhanova, M. Hohmann, *Parameterized post-Newtonian limit of general teleparallel gravity theories*. [arXiv:1907.08178](#)
123. L. Iorio, N. Radicella, M.L. Ruggiero, Constraining f(T) gravity in the Solar System. *JCAP* **1508**(08), 021 (2015). [arXiv:1505.06996](#)
124. L. Iorio, E.N. Saridakis, Solar system constraints on f(T) gravity. *Mon. Not. Roy. Astron. Soc.* **427**, 1555 (2012). [arXiv:1203.5781](#)
125. G. Farrugia, J.L. Said, M.L. Ruggiero, Solar system tests in f(T) gravity. *Phys. Rev. D* **93**(10), 104034 (2016). [arXiv:1605.07614](#)
126. H. Mohseni Sadjadi, Parameterized post-Newtonian approximation in a teleparallel model of dark energy with a boundary term. *Eur. Phys. J. C* **77**(3), 191 (2017)
127. E.D. Emtsova, M. Hohmann, Post-Newtonian limit of scalar-torsion theories of gravity as analogue to scalar-curvature theories. *Phys. Rev. D* **101**(2), 024017 (2020). [arXiv:1909.09355](#)
128. K. Flathmann, M. Hohmann, Post-Newtonian limit of generalized scalar-torsion theories of gravity. *Phys. Rev. D* **101**(2), 024005 (2020). [arXiv:1910.01023](#)
129. S. Bahamonde, K.F. Dialektopoulos, M. Hohmann, J. Levi Said, *Post-Newtonian limit of Teleparallel Horndeski gravity*. [arXiv:2003.11554](#)

130. G. Farrugia, J. Levi Said, A. Finch, Gravitoelectromagnetism, solar system test and weak-field solutions in $f(T, B)$ gravity with observational constraints. *Universe* **6**(2), 34 (2020). [arXiv:2002.08183](#)
131. S. Capozziello, M. Capriolo, L. Caso, Weak field limit and gravitational waves in $f(T, B)$ teleparallel gravity. *Eur. Phys. J. C* **80**(2), 156 (2020). [arXiv:1912.12469](#)
132. A. Pourbagher, A. Amani, Thermodynamics and stability of $f(T, B)$ gravity with viscous fluid by observational constraints. *Astrophys. Space Sci.* **364**(8), 140 (2019). [arXiv:1908.11595](#)
133. LIGO Scientific, Virgo, Fermi-GBM, INTEGRAL Collaboration, B.P. Abbott et al., Gravitational waves and gamma-rays from a binary neutron star merger: GW170817 and GRB 170817A. *Astrophys. J.* **848**(2), L13 (2017). [arXiv:1710.05834](#)
134. Y.-F. Cai, C. Li, E.N. Saridakis, L. Xue, $f(T)$ gravity after GW170817 and GRB170817A. [arXiv:1801.05827](#)
135. G. Farrugia, J.L. Said, V. Gakis, E.N. Saridakis, Gravitational waves in modified teleparallel theories. *Phys. Rev. D* **97**(12), 124064 (2018). [arXiv:1804.07365](#)
136. K. Bamba, S. Capozziello, M. De Laurentis, S. Nojiri, D. Sáez-Gómez, No further gravitational wave modes in $F(T)$ gravity. *Phys. Lett. B* **727**, 194–198 (2013). [arXiv:1309.2698](#)
137. A. Finch, J.L. Said, Galactic rotation dynamics in $f(T)$ gravity. *Eur. Phys. J. C* **78**(7), 560 (2018). [arXiv:1806.09677](#)
138. Planck Collaboration, N. Aghanim et al., *Planck 2018 results. VI. Cosmological parameters*. [arXiv:1807.06209](#)
139. A.G. Riess, S. Casertano, W. Yuan, L.M. Macri, D. Scolnic, Large magellanic cloud cepheid standards provide a 1% foundation for the determination of the hubble constant and stronger evidence for physics beyond Λ CDM. *Astrophys. J.* **876**(1), 85 (2019). [arXiv:1903.07603](#)
140. K.C. Wong et al., *HOLiCOW XIII. A 2.4% measurement of H_0 from lensed quasars: 5.3 σ tension between early and late-Universe probes*. [arXiv:1907.04869](#)
141. Y.-F. Cai, S. Capozziello, M. De Laurentis, E.N. Saridakis, $f(T)$ teleparallel gravity and cosmology. *Rept. Prog. Phys.* **79**(10), 106901 (2016). [arXiv:1511.07586](#)
142. R. Zheng, Q.-G. Huang, Growth factor in $f(T)$ gravity. *JCAP* **1103**, 002 (2011). [arXiv:1010.3512](#)
143. E.V. Linder, Einstein's other gravity and the acceleration of the Universe. *Phys. Rev. D* **81**, 127031 (2010). [arXiv:1005.3039](#). [Erratum: *Phys. Rev. D* **82**, 109902(2010)]
144. G. Farrugia, J.L. Said, Stability of the flat FLRW metric in $f(T)$ gravity. *Phys. Rev. D* **94**(12), 124054 (2016). [arXiv:1701.00134](#)
145. Á. de la Cruz Dombriz, Towards new constraints in extended theories of gravity: cosmography and gravitational-wave signals from neutron stars. *Galaxies* **6**(1), 28 (2018)
146. A. Aviles, A. Bravetti, S. Capozziello, O. Luongo, Cosmographic reconstruction of $f(\text{mathcal{T}})$ cosmology. *Phys. Rev. D* **87**(6), 064025 (2013). [arXiv:1302.4871](#)
147. S. Capozziello, V.F. Cardone, H. Farajollahi, A. Ravanpak, Cosmography in $f(T)$ -gravity. *Phys. Rev. D* **84**, 043527 (2011). [arXiv:1108.2789](#)
148. S. Capozziello, R. D'Agostino, O. Luongo, *Extended Gravity Cosmography*. [arXiv:1904.01427](#)
149. N. Suzuki, D. Rubin, C. Lidman, G. Aldering, R. Amanullah et al., The hubble space telescope cluster supernova survey: v. improving the dark energy constraints $z > 1$ and building an early-type-hosted supernova sample. *Astrophys. J.* **746**, 85 (2012). [arXiv:1105.3470](#)
150. A.G. Riess et al., Cepheid calibrations of modern type Ia supernovae: implications for the hubble constant. *Astrophys. J. Suppl.* **183**, 109–141 (2009). [arXiv:0905.0697](#)
151. R. Myrzakulov, Accelerating universe from $f(t)$ gravity. *Eur. Phys. J. C* **71**, 1752 (2011)
152. S. Chakrabarti, J.L. Said, K. Bamba, On reconstruction of extended teleparallel gravity from the cosmological jerk parameter. *Eur. Phys. J. C* **79**(6), 454 (2019). [arXiv:1905.09711](#)
153. W. El Hanafy, G. Nashed, Phenomenological reconstruction of $f(T)$ teleparallel gravity. *Phys. Rev. D* **100**(8), 083535 (2019). [arXiv:1910.04160](#)
154. W. El Hanafy, E.N. Saridakis, $f(T)$ cosmology: From Pseudo-Bang to Pseudo-Rip. [arXiv:2011.15070](#)

155. S.-H. Chen, J.B. Dent, S. Dutta, E.N. Saridakis, Cosmological perturbations in $f(T)$ gravity. *Phys. Rev. D* **83**, 023508 (2011). [arXiv:1008.1250](#)
156. K. Izumi, Y.C. Ong, Cosmological perturbation in $f(T)$ gravity revisited. *JCAP* **1306**, 029 (2013). [arXiv:1212.5774](#)
157. G. Farrugia, J.L. Said, Growth factor in $f(T, \mathit{mathcal{T}})$ gravity. *Phys. Rev. D* **94**(12), 124004 (2016). [arXiv:1612.00974](#)
158. A. Golovnev, T. Koivisto, Cosmological perturbations in modified teleparallel gravity models. *JCAP* **1811**(11), 012 (2018). [arXiv:1808.05565](#)
159. Y.-P. Wu, C.-Q. Geng, Matter density perturbations in modified teleparallel theories. *JHEP* **11**, 142 (2012). [arXiv:1211.1778](#)
160. R.C. Nunes, S. Pan, E.N. Saridakis, New observational constraints on $f(T)$ gravity from cosmic chronometers. *JCAP* **1608**(08), 011 (2016). [arXiv:1606.04359](#)
161. R.C. Nunes, Structure formation in $f(T)$ gravity and a solution for H_0 tension. [arXiv:1802.02281](#)
162. R.C. Nunes, S. Pan, E.N. Saridakis, New observational constraints on $f(T)$ gravity through gravitational-wave astronomy. *Phys. Rev. D* **98**(10), 104055 (2018). [arXiv:1810.03942](#)
163. R.C. Nunes, M.E.S. Alves, J.C.N. de Araujo, Forecast constraints on $f(T)$ gravity with gravitational waves from compact binary coalescences. [arXiv:1905.03237](#)
164. S. Dodelson, *Modern Cosmology* (Academic, 2003)
165. B.O.S.S. Collaboration, S. Alam et al., The clustering of galaxies in the completed SDSS-III Baryon oscillation spectroscopic survey: cosmological analysis of the DR12 galaxy sample. *Mon. Not. Roy. Astron. Soc.* **470**(3), 2617–2652 (2017). [arXiv:1607.03155](#)
166. D. Wang, D. Mota, Can $f(T)$ gravity resolve the H_0 tension?. [arXiv:2003.10095](#)
167. S. Nesseris, S. Basilakos, E.N. Saridakis, L. Perivolaropoulos, Viable $f(T)$ models are practically indistinguishable from Λ CDM. *Phys. Rev. D* **88**, 103010 (2013). [arXiv:1308.6142](#)
168. A. El-Zant, W. El Hanafy, S. Elgammal, H_0 tension and the phantom regime: a case study in terms of an infrared $f(t)$ gravity. *Astrophys. J.* **871**(2), 210 (2019). [arXiv:1809.09390](#)
169. A.G. Riess, S. Casertano, W. Yuan, L. Macri, J. Anderson, J.W. MacKenty, J.B. Bowers, K.I. Clubb, A.V. Filippenko, D.O. Jones, B.E. Tucker, New parallaxes of galactic cepheids from spatially scanning the hubble space telescope: implications for the hubble constant. *Astrophys. J.* **855**, 136 (2018). [arXiv:1801.01120](#)
170. F.K. Anagnostopoulos, S. Basilakos, E.N. Saridakis, Bayesian analysis of $f(T)$ gravity using $f\sigma_8$ data. [arXiv:1907.07533](#)
171. B. Sagredo, S. Nesseris, D. Sapone, Internal robustness of growth rate data. *Phys. Rev. D* **98**(8), 083543 (2018). [arXiv:1806.10822](#)
172. H. Yu, B. Ratra, F.-Y. Wang, Hubble parameter and baryon acoustic oscillation measurement constraints on the hubble constant, the deviation from the spatially flat LCDM model, the deceleration-acceleration transition redshift. *Spatial Curvature. Astrophys. J.* **856**(1), 3 (2018). [arXiv:1711.03437](#)
173. D.M. Scolnic et al., The complete light-curve sample of spectroscopically confirmed SNe Ia from Pan-STARRS1 and cosmological constraints from the combined pantheon sample. *Astrophys. J.* **859**(2), 101 (2018). [arXiv:1710.00845](#)
174. H. Akaike, A new look at the statistical model identification. *IEEE Trans. Autom. Control* **19**, 716–723 (1974)
175. G. Schwarz, Estimating the dimension of a model. *Ann. Stat.* **6**, 461–464 (1978)
176. K.P. Burnham, D.R. Anderson, Multimodel inference: understanding aic and bic in model selection. *Sociolog. Methods Res.* **33**(2), 261–304 (2004)
177. Y.-F. Cai, M. Khurshudyan, E.N. Saridakis, Model-independent reconstruction of $f(T)$ gravity from Gaussian Processes. *Astrophys. J.* **888**, 62 (2020). [arXiv:1907.10813](#)
178. S.-F. Yan, P. Zhang, J.-W. Chen, X.-Z. Zhang, Y.-F. Cai, E.N. Saridakis, Interpreting cosmological tensions from the effective field theory of torsional gravity. *Phys. Rev. D* **101**(12), 121301 (2020). [arXiv:1909.06388](#)
179. R. Briffa, S. Capozziello, J. Levi Said, J. Mifsud, E.N. Saridakis, Constraining Teleparallel Gravity through Gaussian Processes. [arXiv:2009.14582](#)

180. C. Escamilla-Rivera, J. Levi Said, Cosmological viable models in $f(T,B)$ gravity as solutions to the H_0 tension. [arXiv:1909.10328](#)
181. K. Bamba, S. Nojiri, S.D. Odintsov, Trace-anomaly driven inflation in $f(T)$ gravity and in minimal massive bigravity. *Phys. Lett. B* **731**, 257–264 (2014). [arXiv:1401.7378](#)
182. G.G.L. Nashed, W. El Hanafy, A built-in inflation in the $f(T)$ -cosmology. *Eur. Phys. J. C* **74**, 3099 (2014). [arXiv:1403.0913](#)
183. K. Rezaeadeh, A. Abdolmaleki, K. Karami, Power-law and intermediate inflationary models in $f(T)$ -gravity. *JHEP* **01**, 131 (2016). [arXiv:1509.08769](#)
184. K. Bamba, G.G.L. Nashed, W. El Hanafy, S.K. Ibraheem, Bounce inflation in $f(T)$ cosmology: a unified inflaton-quintessence field. *Phys. Rev. D* **94**(8), 083513 (2016). [arXiv:1604.07604](#)
185. K. Rezaeadeh, A. Abdolmaleki, K. Karami, Logamediate inflation in $f(T)$ teleparallel gravity. *Astrophys. J.* **836**(2), 228 (2017). [arXiv:1702.07877](#)
186. A.I. Keskin, Viable super inflation scenario from $F(T)$ modified teleparallel gravity. *Eur. Phys. J. C* **78**(9), 705 (2018)
187. K. Bamba, C.-Q. Geng, L.-W. Luo, Generation of large-scale magnetic fields from inflation in teleparallelism. *JCAP* **1210**, 058 (2012). [arXiv:1208.0665](#)
188. A.I. Keskin, Super inflation mechanism and dark energy in $F(T, T_G)$ gravity. *Astrophys. Space Sci.* **362**(3), 50 (2017)
189. K. Bamba, S.D. Odintsov, E.N. Saridakis, Inflationary cosmology in unimodular $F(T)$ gravity. *Mod. Phys. Lett. A* **32**(21), 1750114 (2017). [arXiv:1605.02461](#)
190. M. Jamil, D. Momeni, R. Myrzakulov, Warm intermediate inflation in $F(T)$ gravity. *Int. J. Theor. Phys.* **54**(4), 1098–1112 (2015). [arXiv:1309.3269](#)
191. P. Goodarzi, H. Mohseni Sadjadi, Reheating in a modified teleparallel model of inflation. *Eur. Phys. J. C* **79**(3), 193 (2019). [arXiv:1808.01225](#)
192. H. Abedi, M. Wright, A.M. Abbassi, Nonminimal coupling in anisotropic teleparallel inflation. *Phys. Rev. D* **95**(6), 064020 (2017)
193. A. Awad, W. El Hanafy, G.G.L. Nashed, S.D. Odintsov, V.K. Oikonomou, Constant-roll Inflation in $f(T)$ Teleparallel Gravity. [arXiv:1710.00682](#)
194. M. Gonzalez-Espinoza, G. Otalora, N. Videla, J. Saavedra, Slow-roll inflation in generalized scalar-torsion gravity. [arXiv:1904.08068](#)
195. S. Raatikainen, S. Rasanen, Higgs inflation and teleparallel gravity. *JCAP* **12**(12), 021 (2019). [arXiv:1910.03488](#)
196. A. Rezaei Akbarieh, Y. Izadi, Tachyon inflation in teleparallel gravity. *Eur. Phys. J. C* **79**(4), 366 (2019). [arXiv:1812.06649](#)
197. S. Bahamonde, M. Marciu, J.L. Said, Generalized tachyonic teleparallel cosmology. *Eur. Phys. J. C* **79**(4), 324 (2019). [arXiv:1901.04973](#)
198. S. Bahamonde, C.G. Böhrer, S. Carloni, E.J. Copeland, W. Fang, N. Tamanini, Dynamical systems applied to cosmology: dark energy and modified gravity. *Phys. Rep.* **775–777**, 1–122 (2018). [arXiv:1712.03107](#)
199. D.K. Arrowsmith, C.M. Place, *An Introduction to Dynamical Systems* (Cambridge University Press, 1990)
200. A.A. Coley, *Dynamical Systems and Cosmology* (Kluwer Academic Publishers, Dordrecht, Boston, London, 2003)
201. J. Wainwright, G.F.R. Ellis, *Dynamical Systems in Cosmology* (Cambridge University Press, 1997)
202. P. Wu, H.W. Yu, The dynamical behavior of $f(T)$ theory. *Phys. Lett. B* **692**, 176–179 (2010). [arXiv:1007.2348](#)
203. Y. Zhang, H. Li, Y. Gong, Z.-H. Zhu, Notes on $f(T)$ theories. *JCAP* **1107**, 015 (2011). [arXiv:1103.0719](#)
204. M. Jamil, D. Momeni, R. Myrzakulov, Attractor solutions in $f(T)$ cosmology. *Eur. Phys. J. C* **72**, 1959 (2012). [arXiv:1202.4926](#)
205. M. Jamil, K. Yesmakhanova, D. Momeni, R. Myrzakulov, Phase space analysis of interacting dark energy in $f(T)$ cosmology. *Central Eur. J. Phys.* **10**, 1065–1071 (2012). [arXiv:1207.2735](#)

206. S.K. Biswas, S. Chakraborty, Interacting dark energy in $f(T)$ cosmology?: a dynamical system analysis. *Int. J. Mod. Phys. D* **24**(7), 155004 (2015). [arXiv:1504.02431](#)
207. C.-J. Feng, X.-Z. Li, L.-Y. Liu, Bifurcation and global dynamical behavior of the $f(T)$ theory. *Mod. Phys. Lett. A* **29**(7), 1550046, 1450033 (2014). [arXiv:1403.4328](#)
208. B. Mirza, F. Oboudiat, Constraining $f(T)$ gravity by dynamical system analysis. *JCAP* **1711**(11), 011 (2017). [arXiv:1704.02593](#)
209. M. Hohmann, L. Jarv, U. Ualikhanova, Dynamical systems approach and generic properties of $f(T)$ cosmology. *Phys. Rev. D* **96**(4), 043508 (2017). [arXiv:1706.02376](#)
210. A. Awad, W. El Hanafy, G.G.L. Nashed, E.N. Saridakis, Phase portraits of general $f(T)$ cosmology. *JCAP* **1802**(02), 052 (2018). [arXiv:1710.10194](#)
211. L. Karpathopoulos, S. Basilakos, G. Leon, A. Paliathanasis, M. Tsamparlis, Cartan symmetries and global dynamical systems analysis in a higher-order modified teleparallel theory. *Gen. Rel. Grav.* **50**(7), 79 (2018). [arXiv:1709.02197](#)
212. A. Paliathanasis, de Sitter and Scaling solutions in a higher-order modified teleparallel theory. *JCAP* **1708**(08), 027 (2017). [arXiv:1706.02662](#)
213. A. Paliathanasis, Cosmological evolution and exact solutions in a fourth-order theory of gravity. *Phys. Rev. D* **95**(6), 064062 (2017). [arXiv:1701.04360](#)
214. P. A. González, S. Reyes, Y. Vásquez, Teleparallel Equivalent of Lovelock Gravity, Generalizations and Cosmological Applications. [arXiv:1905.07633](#)
215. S. Bahamonde, M. Marciu, S.D. Odintsov, P. Rudra, String-inspired Teleparallel Cosmology. [arXiv:2003.13434](#)
216. K. Bamba, D. Momeni, M.A. Ajmi, Phase space description of nonlocal teleparallel gravity. *Eur. Phys. J. C* **78**(9), 771 (2018). [arXiv:1711.10475](#)
217. C.G. Böhrer, F. Fiorini, P. González, Y. Vásquez, $D = 11$ cosmologies with teleparallel structure. *Phys. Rev. D* **100**(8), 084007 (2019). [arXiv:1908.03680](#)
218. G. Otalora, Scaling attractors in interacting teleparallel dark energy. *JCAP* **1307**, 044 (2013). [arXiv:1305.0474](#)
219. C. Xu, E.N. Saridakis, G. Leon, Phase-space analysis of teleparallel dark energy. *JCAP* **1207**, 005 (2012). [arXiv:1202.3781](#)
220. M.A. Skugoreva, E.N. Saridakis, A.V. Toporensky, Dynamical features of scalar-torsion theories. *Phys. Rev. D* **91**, 044023 (2015). [arXiv:1412.1502](#)
221. M.A. Skugoreva, A.V. Toporensky, S.Y. Vernov, Global stability analysis for cosmological models with nonminimally coupled scalar fields. *Phys. Rev. D* **90**, 064044 (2014). [arXiv:1404.6226](#)
222. H. Mohseni Sadjadi, Onset of acceleration in a universe initially filled by dark and baryonic matters in a nonminimally coupled teleparallel model. *Phys. Rev. D* **92**(12), 123538 (2015). [arXiv:1510.02085](#)
223. M. Marciu, Dynamical properties of scaling solutions in teleparallel dark energy cosmologies with nonminimal coupling. *Int. J. Mod. Phys. D* **26**(09), 1750103 (2017)
224. G. Otalora, Cosmological dynamics of tachyonic teleparallel dark energy. *Phys. Rev. D* **88**, 063505 (2013). [arXiv:1305.5896](#)
225. A. Banijamali, E. Ghasemi, Dynamical characteristics of a non-canonical scalar-torsion model of dark energy. *Int. J. Theor. Phys.* **55**(8), 3752–3760 (2016)
226. B. Fazlpour, A. Banijamali, Dynamics of generalized tachyon field in teleparallel gravity. *Adv. High Energy Phys.* **2015**, 283273 (2015). [arXiv:1408.0203](#)
227. B. Fazlpour, A. Banijamali, Non-minimally coupled tachyon field in teleparallel gravity. *JCAP* **1504**(04), 030 (2015). [arXiv:1410.4446](#)
228. E. Noether, Invariant variation problems. *Gott. Nachr.* **1918**, 235–257 (1918). [arXiv:physics/0503066](#). [Transp. Theory Statist. Phys.1,186(1971)]
229. K.F. Dialektopoulos, S. Capozziello, Noether Symmetries as a geometric criterion to select theories of gravity. *Int. J. Geom. Meth. Mod. Phys.* **15**(supp01), 1840007 (2018). [arXiv:1808.03484](#)
230. A. Paliathanasis, Symmetries of Differential equations and Applications in Relativistic Physics. Ph.D. thesis, Athens U. (2014). [arXiv:1501.05129](#)

231. H. Wei, X.-J. Guo, L.-F. Wang, Noether symmetry in $f(t)$ theory. *Phys. Lett. B* **707**, 298–304 (2012). [arXiv:1112.2270](#)
232. K. Atazadeh, F. Darabi, $f(T)$ cosmology via Noether symmetry. *Eur. Phys. J. C* **72**, 2016 (2012). [arXiv:1112.2824](#)
233. H. Mohseni Sadjadi, Generalized Noether symmetry in $f(T)$ gravity. *Phys. Lett. B* **718**, 270–275 (2012). [arXiv:1210.0937](#)
234. S. Basilakos, S. Capozziello, M. De Laurentis, A. Paliathanasis, M. Tsamparlis, Noether symmetries and analytical solutions in $f(T)$ -cosmology: a complete study. *Phys. Rev. D* **88**, 103526 (2013). [arXiv:1311.2173](#)
235. M. Jamil, D. Momeni, R. Myrzakulov, Noether symmetry of $F(T)$ cosmology with quintessence and phantom scalar fields. *Eur. Phys. J. C* **72**, 2137 (2012). [arXiv:1210.0001](#)
236. A. Paliathanasis, S. Basilakos, E.N. Saridakis, S. Capozziello, K. Atazadeh, F. Darabi, M. Tsamparlis, New Schwarzschild-like solutions in $f(T)$ gravity through Noether symmetries. *Phys. Rev. D* **89**, 104042 (2014). [arXiv:1402.5935](#)
237. S. Bahamonde, U. Camci, Exact spherically symmetric solutions in modified teleparallel gravity. *Symmetry* **11**(12), 1462 (2019). [arXiv:1911.03965](#)
238. S. Bahamonde, U. Camci, S. Capozziello, Noether symmetries and boundary terms in extended Teleparallel gravity cosmology. *Class. Quant. Grav.* **36**(6), 065013 (2019). [arXiv:1807.02891](#)
239. M. Sharif, I. Shafique, Noether symmetries in a modified scalar-tensor gravity. *Phys. Rev. D* **90**(8), 084033 (2014)
240. Y. Kucukakca, Scalar tensor teleparallel dark gravity via Noether symmetry. *Eur. Phys. J. C* **73**(2), 2327 (2013). [arXiv:1404.7315](#)
241. G. Gecim, Y. Kucukakca, Scalar-tensor teleparallel gravity with boundary term by Noether symmetries. *Int. J. Geom. Meth. Mod. Phys.* **15**(09), 1850151 (2018). [arXiv:1708.07430](#)
242. S. Bahamonde, U. Camci, S. Capozziello, M. Jamil, Scalar-tensor teleparallel wormholes by noether symmetries. *Phys. Rev. D* **94**(8), 084042 (2016). [arXiv:1608.03918](#)
243. H. Motavalli, A. Rezaei Akbarieh, Teleparallel gravity with scalar and vector fields. *Astrophys. Space Sci.* **363**(10), 200 (2018)
244. B. Tajahmad, Noether symmetries of a modified model in teleparallel gravity and a new approach for exact solutions. *Eur. Phys. J. C* **77**(4), 211 (2017). [arXiv:1610.08099](#)
245. Y. Kucukakca, Teleparallel dark energy model with a fermionic field via Noether symmetry. *Eur. Phys. J. C* **74**(10), 3086 (2014). [arXiv:1407.1188](#)
246. B. Tajahmad, Studying the intervention of an unusual term in $f(T)$ gravity via the Noether symmetry approach. *Eur. Phys. J. C* **77**(8), 510 (2017). [arXiv:1701.01620](#)
247. R. Brandenberger, P. Peter, Bouncing cosmologies: progress and problems. *Found. Phys.* **47**(6), 797–850 (2017). [arXiv:1603.05834](#)
248. Y.-F. Cai, S.-H. Chen, J.B. Dent, S. Dutta, E.N. Saridakis, Matter bounce cosmology with the $f(T)$ gravity. *Class. Quant. Grav.* **28**, 215011 (2011). [arXiv:1104.4349](#)
249. A.V. Astashenok, Effective dark energy models and dark energy models with bounce in frames of $F(T)$ gravity. *Astrophys. Space Sci.* **351**, 377–383 (2014). [arXiv:1308.0581](#)
250. S.D. Odintsov, V.K. Oikonomou, E.N. Saridakis, Superbounce and loop quantum ekpyrotic cosmologies from modified gravity: $F(R)$, $F(G)$ and $F(T)$ theories. *Ann. Phys.* **363**, 141–163 (2015). [arXiv:1501.06591](#)
251. T. Qiu, K. Tian, S. Bu, Perturbations of bounce inflation scenario from $f(T)$ modified gravity revisited. *Eur. Phys. J. C* **79**(3), 261 (2019). [arXiv:1810.04436](#)
252. J. Haro, J. Amorós, Viability of the matter bounce scenario in $F(T)$ gravity and Loop Quantum Cosmology for general potentials. *JCAP* **1412**(12), 031 (2014). [arXiv:1406.0369](#)
253. J. Amorós, J. de Haro, S.D. Odintsov, Bouncing loop quantum cosmology from $F(T)$ gravity. *Phys. Rev. D* **87**, 104037 (2013). [arXiv:1305.2344](#)
254. J. De Haro, J. Amorós, Bouncing cosmologies via modified gravity in the ADM formalism: application to Loop Quantum Cosmology. *Phys. Rev. D* **97**(6), 064014 (2018). [arXiv:1712.08399](#)

255. A. de la Cruz-Dombriz, G. Farrugia, J.L. Said, D. Sáez-Chillón Gómez, Cosmological bouncing solutions in extended teleparallel gravity theories. *Phys. Rev. D* **97**(10), 104040 (2018). [arXiv:1801.10085](#)
256. A. de la Cruz-Dombriz, G. Farrugia, J.L. Said, D. Saez-Gomez, Cosmological reconstructed solutions in extended teleparallel gravity theories with a teleparallel Gauss-Bonnet term. *Class. Quant. Grav.* **34**(23), 235011 (2017). [arXiv:1705.03867](#)
257. F. Fiorini, Nonsingular Promises from born-infeld gravity. *Phys. Rev. Lett.* **111**, 041104 (2013). [arXiv:1306.4392](#)
258. M. Bouhmadi-Lopez, C.-Y. Chen, P. Chen, Cosmological singularities in Born-Infeld determinantal gravity. *Phys. Rev. D* **90**, 123518 (2014). [arXiv:1407.5114](#)
259. C.G. Boehmer, F. Fiorini, The regular black hole in four dimensional Born-Infeld gravity. *Class. Quant. Grav.* **36**, 12 (2019). [arXiv:1901.02965](#)
260. E. Knox, Newton-Cartan theory and teleparallel gravity: the force of a formulation. *Stud. Hist. Philos. Mod. Phys.* **42**, 264–275 (2011)
261. J.B. Jiménez, L. Heisenberg, T.S. Koivisto, The canonical frame of purified gravity. [arXiv:1903.12072](#)
262. T. Koivisto, M. Hohmann, T. Zlosnik, The general linear Cartan Khronon. *Universe* **5**(6), 153 (2019). [arXiv:1905.02967](#)
263. F. Hammad, D. Dijamco, A. Torres-Rivas, D. Bérubé, Noether charge and black hole entropy in teleparallel gravity. *Phys. Rev. D* **100**(12), 124040 (2019). [arXiv:1912.08811](#)
264. R. Ferraro, $f(R)$ and $f(T)$ theories of modified gravity. *AIP Conf. Proc.* **1471**, 103–110 (2012). [arXiv:1204.6273](#)
265. R.C. Nunes, A. Bonilla, S. Pan, E.N. Saridakis, Observational Constraints on $f(T)$ gravity from varying fundamental constants. *Eur. Phys. J. C* **77**(4), 230 (2017). [arXiv:1608.01960](#)
266. V.K. Oikonomou, E.N. Saridakis, $f(T)$ gravitational baryogenesis. *Phys. Rev. D* **94**(12), 124005 (2016). [arXiv:1607.08561](#)
267. S. Capozziello, G. Lambiase, E.N. Saridakis, Constraining $f(T)$ teleparallel gravity by Big Bang Nucleosynthesis. *Eur. Phys. J. C* **77**(9), 576 (2017). [arXiv:1702.07952](#)
268. S. Basilakos, S. Nesseris, F. Anagnostopoulos, E. Saridakis, Updated constraints on $f(T)$ models using direct and indirect measurements of the Hubble parameter. *JCAP* **08**, 008 (2018). [arXiv:1803.09278](#)
269. C. Li, Y. Cai, Y.-F. Cai, E.N. Saridakis, The effective field theory approach of teleparallel gravity, $f(T)$ gravity and beyond. *JCAP* **10**, 001 (2018). [arXiv:1803.09818](#)
270. H. Abedi, S. Capozziello, Gravitational waves in modified teleparallel theories of gravity. [arXiv:1712.05933](#)
271. Z. Chen, W. Luo, Y.-F. Cai, E.N. Saridakis, New test on general relativity and $f(T)$ torsional gravity from galaxy-galaxy weak lensing surveys. *Phys. Rev. D* **102**(10), 104044 (2020). [arXiv:1907.12225](#)
272. F. Lelli, S.S. McGaugh, J.M. Schombert, M.S. Pawlowski, One law to rule them all: the radial acceleration relation of galaxies. *Astrophys. J.* **836**, 152 (2017). [arXiv:1610.08981](#)
273. M. Dupuis, F. Girelli, A. Osumanu, W. Wieland, First-order formulation of teleparallel gravity and dual loop gravity. *Class. Quant. Grav.* **37**(8), 085023 (2020). [arXiv:1906.02801](#)
274. K.G. Falls, D.F. Litim, J. Schröder, Aspects of asymptotic safety for quantum gravity. *Phys. Rev. D* **99**(12), 126015 (2019). [arXiv:1810.08550](#)
275. M. Niedermaier, M. Reuter, The asymptotic safety scenario in quantum gravity. *Living Rev. Rel.* **9**, 5–173 (2006)

Chapter 15

Finsler Gravity



Nicoleta Voicu and Christian Pfeifer

This chapter summarises some recent developments in the application of Finsler geometry as the extended geometry of spacetime. As original sources, we refer to the articles [1–3].

15.1 Physical Motivations

Finsler geometry appears in the description of physical systems, as a suitable mathematical tool at various stages. We will briefly discuss the appearance of Finsler geometry in physics and motivate the formulation of a consistent extension of General Relativity based on Finsler geometry.

15.1.1 Finsler Geometry in Physics

In physics, Finsler geometry naturally appears in the study of dispersion relations, as the most general geometric realization of the clock postulate of General Relativity

N. Voicu

Faculty of Mathematics and Computer Science, Transilvania University, Iuliu Maniu Str. 50,
500091 Brasov, Romania
e-mail: nico.voicu@unitbv.ro

C. Pfeifer (✉)

Laboratory of Theoretical Physics, Institute of Physics, University of Tartu, W. Ostwaldi 1,
50411 Tartu, Estonia
e-mail: christian.pfeifer@ut.ee

and as a minimal modification of the Ehlers-Pirani-Schild (EPS) axiomatic approach to spacetime geometry.

A *dispersion relation* is a constraint that the position x and the four-momentum p of a particle have to satisfy, so that the particle is physically viable. Technically, the dispersion relation is described by a Hamilton function H , depending on x and p (i.e., defined on the point particle phase space, or the cotangent bundle of spacetime). The level sets $H(x, p) = \text{const}$ represent the dispersion relation and the Hamilton equations of motion $\dot{x}^\mu = \partial_{p_\mu} H$ and $\dot{p}_\mu = -\partial_{x^\mu} H$ determine the particle trajectory. Dispersion relations lead to a Finslerian spacetime geometry, when the Hamilton function is mapped to a Finsler function via the Helmholtz action. This procedure has been pointed out in [4] for general dispersion relations and has been applied to the κ -Poincaré dispersion relation used in quantum gravity [5, 6], as well as to weak premetric-, or minimal standard model extension electrodynamics [7]. The resulting Finsler geometries are candidates to extend the geometry of spacetime beyond pseudo-Riemannian (Lorentzian) one. Non-quadratic dispersion relations, resulting in a non-pseudo-Riemannian Finsler geometry, are used in the study of physical fields and waves propagating through media [8–10], they emerge in the context of quantum gravity phenomenology from quantum deformations of the Poincaré algebra [5, 11] and in the study of non-local Lorentz invariant physics, such as in the standard model extension or the very special relativity framework [12, 13].

One of the fundamental pillars of Special and General Relativity is the *clock postulate*: “The time which passes for an observer between two events is given by the length of its worldline connecting these two events”. To realize this physical axiom, mathematically the spacetime manifold must be equipped with a length measure for curves. The most general geometric length measure for curves is given by a generic Finsler length measure. Among all possible Finsler length measures, the one induced by a Lorentzian metric is singled out by demanding invariance under local Lorentz transformations. Relaxing the symmetry demand, more general length measures can be obtained, for example, the one found by Bogoslovsky in the study of transformations that leave the massless wave equation invariant [14]. Later, field theories built upon this symmetry were summarised under the name Very Special/Very General Relativity [13, 15, 16]. Further interesting length measures can be identified as they appear in the description of point particle trajectories in certain physical situations, such as, for example: the Randers length measure [17], describing a particle in an electromagnetic field as well as the Zermelo navigation problem and the influence of wind on a physical system in general [8, 10, 18], or m -th root length measures, which describe the point particle limit of quantisable bi-hyperbolic field equations [4]—and, in particular for $m = 4$, the propagation of light on the basis of premetric or area metric electrodynamics [19].

In their *axiomatic approach to spacetime geometry*, Ehlers, Pirani and Schild deduce a pseudo-Riemannian (more precisely, Lorentzian) spacetime geometry from a set of physical demands [20]. One of the axioms is, however, of a rather technical mathematical nature than is physically necessary. It states that for a sufficiently small neighborhood V for every $p \in V$, the map $g_p : p \mapsto t_e t_a$, which associates the product between the emission time t_e and the return time t_a of radar echo between

any particle worldline passing through V (but not through p) and p , must be at least twice differentiable. Tavakol and van den Bergh demonstrated that if one relaxes this demand and only requires g_p to be differentiable once, the EPS spacetime axiomatic leads to a Finslerian spacetime geometry [21]. The EPS axiomatic has been reviewed from a Finsler spacetime perspective in [22].

15.1.2 Finsler Gravity

The natural appearance in physics and its close relation to Special and General Relativity make Finsler geometry one of the candidates for a description of the gravitational interaction, beyond General Relativity. It has the potential to shed light on the shortcomings of Einstein's theory of gravity, such as dark energy and dark matter [23–26], from a geometric point of view.

The idea to use Finsler geometry as geometry of spacetime has been long known in the literature - and is ongoing [1, 18, 27–30]. The difficulty in the construction of a consistent theory of Finsler gravity is, on the one hand, to find a precise definition of Finsler spacetimes, and on the other hand, to prove that Finsler spacetime geometry realises the threefold role of the geometry of spacetime: encoding a causal structure, via the identification of causal (time-like and lightlike) directions, encoding the description of observers and their measurements, and encoding the gravitational interaction and its dynamics. In particular, the coupling between Finsler geometry and physical matter is a point of debate in the literature. The question is whether a scalar, or a tensor Finsler gravitational field equation on the tangent bundle, should be employed in order to determine the (scalar) Finsler function - or, accordingly, the Finsler metric tensor, and how the matter source side term for the respective equation can be constructed. Another possibility is that instead of giving dynamics to the Finsler function as a whole, to give dynamics to various tensor fields on the base manifold, which then compose a Finsler length element [31]. Recently, strong arguments in favour of a scalar field equation—sourced by a kinetic gas—have been given [1, 3].

Indeed, it is possible to realise this threefold role of the geometry of spacetime in physics with Finsler geometry [2]. The existence of a causal structure is ensured by the definition of Finsler spacetime, which we will discuss in Sect. 15.2; observers and their time and length measurements can be constructed with the help of a radar experiment [7, 32], and we will present the description of the gravitational field in term of Finsler geometry, directly sourced by a kinetic gas, in Sect. 15.4.

15.1.3 Finsler Cosmology

Applying the cosmological principle to Finsler spacetime geometry restricts our study to Finsler spacetime geometries that are spatially homogeneous and isotropic [33]. On

these spacetime geometries, the dark energy phenomenology becomes particularly visible. Finsler geometry can address the dark energy issue on two levels: in the description of light propagation and through modified gravitational dynamics.

The accelerated expansion of the Universe reveals itself by extracting the so-called deceleration parameter from the magnitude-redshift relation of distant supernovae. A negative deceleration parameter implies an accelerated expansion of the Universe. The precise prediction of the deceleration parameter depends on the redshift, induced by the background geometry, and on the magnitude of the light signal observed at a distance from its emission. Using a Finslerian spacetime geometry, the redshift differs from the one obtained on the basis of General Relativity, due to Finslerian deformation of the light cone structure. The general Finslerian redshift formula has been obtained in [34]. Explicit expressions for the deceleration parameter have been derived for several Finsler geometry models, such as Randers geometry, $4th$ -root geometry and general Finsler perturbations of Friedmann-Lemaître-Robertson-Walker geometry [35]. A future perspective is to determine the coefficients in the deceleration parameter, obtained in the perturbative approach, from the observed value of this parameter.

To fully address dark energy with Finsler geometry, the kinematic analysis of the magnitude-redshift relation does not suffice. It is furthermore necessary to derive the Finslerian version of the Friedmann equations in order to predict the evolution of the Universe. For the earlier mentioned scalar field equation coupled to a kinetic gas, this task is work in progress—only preliminary results in the context of the so-called Very General Relativity exist [16]. For other strategies to determine a Finslerian length element dynamically, more progress has already been made. For example, in Randers geometries, which are Finsler geometries built from a Lorentzian metric g and a 1-form B on spacetime, resembling dark energy can be obtained in a geometric manner [31]; this is achieved by determining the Lorentzian metric g via the usual Einstein equations and coupling the additional 1-form via the Finslerian geodesic deviation equation. More generally, in the context of non-Lorentz invariant cosmological models, it has been shown that there exist Finsler models which predict a cosmological bounce [36] and that Finsler-inspired generalized geometries give a geometric picture of scalar tensor cosmologies [37].

The aforementioned results merely represent an incomplete excerpt of the literature on the explicit applications of Finsler geometry in cosmology.

15.2 Definition of Finsler Spacetimes

Before defining Finsler spacetimes, we briefly recall the definition of classical, positive definite Finsler spaces, which are straightforward generalisations of Riemannian ones. The idea of equipping a manifold with a non-quadratic length measure for vectors—accordingly, of curves—goes back to Riemann himself [38], but only Finsler analysed such spaces systematically [39]. Since then, Finsler geometry became an established field in mathematics [40].

Roughly speaking, a Finslerian manifold, respectively a Finslerian spacetime, is a smooth manifold M equipped with a length measure for curves $L(x, \dot{x})$, where the function L is just 2-homogeneous in the tangent vectors \dot{x} (i.e., not necessarily quadratic, as in the case of pseudo-Riemannian manifolds).

We introduce the following notations on the tangent bundle TM of a connected, orientable smooth manifold M . Any local coordinate chart (U, x^μ) on M induces a local coordinate chart (TU, x^μ, \dot{x}^μ) on TM as follows. For an element $(x, \dot{x}) \in TU$, (x^μ, \dot{x}^μ) are given by the coordinates (x^μ) of the point $x \in U$ and the decomposition $\dot{x} = \dot{x}^\mu \partial_\mu|_x$ of the vector $\dot{x} \in T_x M$ in the natural local basis. If there is no risk of confusion, we will sometimes omit the indices on the coordinate representation, i.e., we write briefly (x, \dot{x}) for (x^μ, \dot{x}^μ) . The natural coordinate bases of the tangent and cotangent spaces of M are denoted by $(\partial_\mu = \frac{\partial}{\partial x^\mu}, \dot{\partial}_\mu = \frac{\partial}{\partial \dot{x}^\mu})$ and $(dx^\mu, d\dot{x}^\mu)$, respectively.

15.2.1 Positive Definite Finsler Manifolds

A Finslerian manifold (M, F) is a smooth n -dimensional manifold M equipped with a continuous *Finsler norm* $F : TM \rightarrow (0, \infty); (x, \dot{x}) \mapsto F(x, \dot{x})$, which satisfies:

- (1) F is positively 1-homogeneous in $\dot{x} : F(x, \ell\dot{x}) = \ell F(x, \dot{x}), \forall \ell \in \mathbb{R}^+$.
- (2) F is smooth on $TM \setminus \{0\}$.
- (3) The Finsler metric, defined by the Hessian of $L := F^2$ with respect to \dot{x}^μ ,

$$g_{\mu\nu}^F = \frac{1}{2} \dot{\partial}_\mu \dot{\partial}_\nu L,$$

is positive definite.

As a consequence of the above axioms, F obeys (pointwise) the triangle inequality: $F(x, \dot{x} + \dot{\tilde{x}}) \leq F(x, \dot{x}) + F(x, \dot{\tilde{x}})$. Moreover, the length measure for curves $\gamma : [a, b] \rightarrow M, \tau \mapsto \gamma(\tau)$ on M :

$$S[\gamma] = \int_a^b F(\gamma(\tau), \dot{\gamma}(\tau)) d\tau \tag{15.1}$$

is independent of the choice of the parameter τ along γ .

Riemannian geometry is obtained as a particular case, for $F(x, \dot{x}) = \sqrt{g_{\mu\nu}(x)\dot{x}^\mu \dot{x}^\nu}$ i.e., for quadratic functions $L(x, \dot{x}) = g_{\mu\nu}(x)\dot{x}^\mu \dot{x}^\nu$ in \dot{x} , where $g_{\mu\nu}$ define a Riemannian metric. In this case, $g_{\mu\nu} = g_{\mu\nu}^F$ only depend on the point x (which is not true for general Finsler metrics).

The geometry of a Finsler manifold can be derived from the Finsler function F and the Finsler metric g^F , in very close analogy to the derivation of the geometry of a Riemannian manifold from its metric g .

15.2.2 Finsler Spacetime

Changing from positive definite Finsler manifolds to Lorentzian Finsler spaces, there arises the problem that, typically, the Finsler function can not be smooth everywhere on $TM \setminus \{0\}$, due to the existence of non-trivial zero length vectors, i.e., null vectors. We have to carefully impose further restrictions upon L in order to ensure the existence of a well-defined causal structure. To formulate the definition in a precise way, we need the notion of conic subbundle.

Let $\overset{\circ}{TM} := TM \setminus \{0\}$ be the tangent bundle without the zero section $x \mapsto (x, 0)$. A conic subbundle of TM is a non-empty open submanifold $\mathcal{Q} \subset \overset{\circ}{TM}$, with $\pi_{TM}(\mathcal{Q}) = M$, possessing the so-called *conic property*: if $(x, \dot{x}) \in \mathcal{Q}$, then, for any $\ell > 0$: $(x, \ell \dot{x}) \in \mathcal{Q}$ [18].

Definition 1 By a Finsler spacetime we will understand in the following a pair (M, L) , where M is a smooth n -dimensional manifold and the Finsler Lagrangian $L : \mathcal{A} \rightarrow \mathbb{R}$ is a smooth function on a conic subbundle $\mathcal{A} \subset \overset{\circ}{TM}$, such that:

- L is positively homogeneous of degree two with respect to \dot{x} : $L(x, \lambda \dot{x}) = \lambda^2 L(x, \dot{x})$ for all $\lambda \in \mathbb{R}^+$;
- on \mathcal{A} , the vertical Hessian of L , called L -metric, is non-degenerate,

$$g_{\mu\nu}^L = \frac{1}{2} \frac{\partial^2 L}{\partial \dot{x}^\mu \partial \dot{x}^\nu}; \tag{15.2}$$

- there exists a conic subbundle $\mathcal{T} \subset \mathcal{A}$ such that on \mathcal{T} : $L > 0$, has Lorentzian signature $(+, -, -, -)$ and, on the boundary $\partial\mathcal{T}$, L can be continuously extended as $L|_{\partial\mathcal{T}} = 0$.¹

This is a refined version of the definition of Finsler spacetimes in [1] and basically covers, if one chooses $\mathcal{A} = \mathcal{T}$, the improper Finsler spacetimes defined in [22].

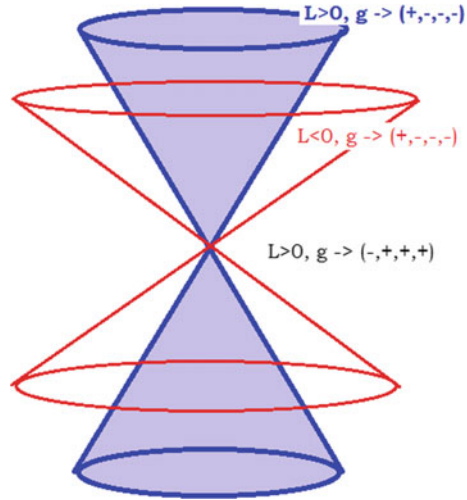
The non-degeneracy, respectively the signature condition on g^L , are well defined, i.e., they do not depend on the choice of the local chart on TM . Moreover, the 2-homogeneity of L implies: $L(x, \dot{x}) = g_{\mu\nu}^L(x, \dot{x}) \dot{x}^\mu \dot{x}^\nu$.

We notice the presence of four conic subbundles of TM :

- \mathcal{A} , called the set of *admissible vectors*, is the subbundle where L is defined, smooth and g^L is nondegenerate.
- $\mathcal{N} = L^{-1}(0)$ is the set of *null or lightlike vectors*.
- $\mathcal{A}_0 = \mathcal{A} \setminus \mathcal{N}$ is the set of admissible, non-lightlike vectors; it is the subset of TM where L can be used for homogenizing geometric objects.
- \mathcal{T} is a maximally connected conic subbundle where $L > 0$, the L metric exists and has Lorentzian signature $(+, -, -, -)$. This will be interpreted as the set of *future*

¹ It is possible to equivalently formulate this property with the opposite sign of L and the metric g^L of signature $(-, +, +, +)$. We fixed the signature and sign of L here to simplify the discussion.

Fig. 15.1 The local causal structure of a bi-metric Finsler spacetime



pointing time-like vectors, which are allowed as tangent vectors to the trajectories of physical observers. The fibres $\mathcal{T}_x := \mathcal{T} \cap T_x M$ are convex cones.

We note that $\mathcal{T} \subset \mathcal{A}_0 \subset \mathcal{A}$, but \mathcal{N} is not necessarily contained in \mathcal{A} .

The set

$$\mathcal{O} := \{(x, \dot{x}) \in \mathcal{T} \mid L(x, \dot{x}) = 1\},$$

of normalized future-directed time-like vectors, is called the *observer space* and is interpreted as the set of admissible 4-velocities of massive particles.

Our definition includes large classes of Finsler spacetimes according to the older definitions. It allows, for example, Finsler spacetime geometries of:

- Randers type: $L = \epsilon(\sqrt{|g_{\mu\nu}\dot{x}^\mu\dot{x}^\nu|} + A_\sigma\dot{x}^\sigma)^2$, where $\epsilon = \text{sign}(\sqrt{|g_{\mu\nu}\dot{x}^\mu\dot{x}^\nu|} + A_\sigma\dot{x}^\sigma)$;
- Bogoslovsky/Kropina type $L = \epsilon|g_{\mu\nu}\dot{x}^\mu\dot{x}^\nu|^{1-q}(A_\sigma(x)\dot{x}^\sigma)^{2q}$, $\epsilon = \text{sign}(g_{\mu\nu}\dot{x}^\mu\dot{x}^\nu)$;
- polynomial m -th root type $L = \epsilon|P|^{\frac{2}{m}}$, where $P = G_{\mu_1 \dots \mu_m}(x)\dot{x}^{\mu_1} \dots \dot{x}^{\mu_m}$, $\epsilon = \text{sign}(P)$.

To illustrate the interesting causal structures, which can be described geometrically in terms of Finsler geometry, Fig. 15.1 presents the situation for a polynomial 4-th root metric $L(x, \dot{x}) = \epsilon\sqrt[4]{|(g_{\mu\nu}\dot{x}^\mu\dot{x}^\nu)(h_{\sigma\rho}\dot{x}^\sigma\dot{x}^\rho)|}$ (where g and h are Lorentzian metrics). Such bimetric geometries naturally appear in the study of birefringent crystals. The null set \mathcal{N}_x of L at $x \in M$ is the union of two cones; the set \mathcal{T}_x is the interior of the sharper cone (in blue). We notice that g^L is allowed to change signature on TM ; but, on \mathcal{T} , the sign of L and the signature of g^L must agree. L is, obviously, not smooth on \mathcal{N} ; yet, it can be proven, [29, 30], that the geodesic equation coefficients admit a C^∞ -smooth prolongation to \mathcal{N} .

A particularly important class of Finsler spacetime metrics is represented by the ones with cosmological symmetry, i.e., spatial homogeneity and isotropy. Denoting by $(t, r, \theta, \varphi, \dot{t}, \dot{r}, \dot{\theta}, \dot{\varphi})$ the coordinates on TM induced by the local spherical coordinates (t, r, θ, φ) on the spacetime manifold M , the most general cosmologically symmetric Finsler-Lagrange function $L : TM \rightarrow \mathbb{R}$ is locally described as, [30, 33, 35], as:

$$L = L(t, \dot{t}, w), \text{ where } w^2 := \frac{\dot{r}^2}{1 - kr^2} + r^2\dot{\theta}^2 + r^2\dot{\varphi}^2 \sin^2 \theta.$$

This implies that the cosmological models for the most studied Finsler geometries in the literature take the form:

- Randers type: $L = \epsilon\sqrt{|-n(t)\dot{t}^2 + a(t)w^2|} + A_r(t)\dot{t}$;
- Bogoslovsky/Kropina type: $L = \epsilon| -n(t)\dot{t}^2 + a(t)w^2 |^{1-q} (A_r(t)\dot{t})^{2q}$;
- polynomial 4-th root type: $L = \epsilon|a(t)\dot{t}^4 + b(t)\dot{t}^3w + c(t)\dot{t}^2w^2 + d(t)\dot{t}w^3 + e(t)w^4|^{\frac{1}{4}}$.

Generically they have more degrees of freedom than just the scale factor of the Friedmann-Lemaître-Robertson-Walker metric.

15.2.3 Geodesics, Geodesic Deviation and Curvature Scalar

Arc length parametrised geodesics $\gamma : s \mapsto \gamma(s)$ of (M, L) are characterized by the Euler-Lagrange equations of (15.1). On \mathcal{A} , these will take the form:

$$\ddot{\gamma}^\mu + 2\bar{\bar{\Gamma}}^\mu(\gamma, \dot{\gamma}) = 0,$$

where the geodesic coefficients $\bar{\bar{\Gamma}}^\mu = \bar{\bar{\Gamma}}^\mu(x, \dot{x})$ are given by: $2\bar{\bar{\Gamma}}^\mu = \frac{1}{2}g^{L\mu\nu}(\dot{x}^\sigma L_{,\sigma\nu} - L_{,\nu})$. In turn, $\bar{\bar{\Gamma}}^\mu$ define the coefficients $\bar{\bar{\Gamma}}^\mu{}_\nu := \partial_\nu \bar{\bar{\Gamma}}^\mu$ of the canonical *nonlinear connection*. The latter defines an adapted basis $\{\delta_\mu, \dot{\partial}_\mu\}$ of the tangent spaces $T_{(x,\dot{x})}TM$, with

$$\delta_\mu = \partial_\mu - \bar{\bar{\Gamma}}^\nu{}_\mu \dot{\partial}_\nu.$$

The elements of the adapted basis transform under manifold induced coordinate transformations as if they were vectors on the base manifold M (more technically, they define a splitting of the tangent spaces of TM into horizontal and vertical parts: $T_{(x,\dot{x})}TM = H_{(x,\dot{x})}TM \oplus V_{(x,\dot{x})}TM$).

The nonlinear connection and the L -metric g are the only necessary ingredients for our gravitational field Lagrangian. Yet, in order to handle tensors on \mathcal{A} , we will need a notion of covariant differentiation - given by an affine connection on $\mathcal{A} \subset TM$. In the literature, there are multiple such examples, all of which project onto the Levi-Civita connection in the pseudo-Riemannian case. In the following, we will use the so-called Chern-Rund linear connection, locally defined by

$$D_{\delta_\sigma} \delta_\nu = \bar{\Gamma}^\mu{}_{\nu\sigma} \delta_\mu, \quad D_{\delta_\sigma} \dot{\partial}_\nu = \bar{\Gamma}^\mu{}_{\nu\sigma} \dot{\partial}_\mu, \quad D_{\dot{\partial}_\sigma} \delta_\nu = D_{\dot{\partial}_\sigma} \dot{\partial}_\nu = 0,$$

where $\bar{\Gamma}^\mu{}_{\nu\sigma} := \frac{1}{2} g^{L\mu\rho} (\delta_\sigma g_{\nu\rho}^L + \delta_\nu g_{\sigma\rho}^L - \delta_\rho g_{\nu\sigma}^L)$. The difference

$$P^\mu{}_{\sigma\nu} = \dot{\partial}_\sigma \bar{\Gamma}^\mu{}_{\nu\sigma} - \bar{\Gamma}^\mu{}_{\nu\sigma}$$

defines the so-called *Landsberg tensor* on \mathcal{A} ; we will denote by $P_\mu = P^\nu{}_{\mu\nu}$ its trace.

It is worth noticing that the derivative operator $\nabla := \dot{x}^\mu D_{\delta_\mu}$ of vector fields on TM , called the dynamical covariant derivative, actually only depends on $\bar{\Gamma}^\mu{}_\nu$ (i.e., on the nonlinear connection only).

Let $c = (\gamma, \dot{\gamma})$ be the lift of a Finsler geodesic γ to TM . Its tangent vector \dot{c} can be expressed in the adapted basis as $\dot{c} = \dot{\gamma}^\mu \delta_\mu$, i.e., it is horizontal. If V is a deviation vector field on spacetime, then the geodesic deviation equation is:

$$(\nabla \nabla \hat{V})_{|(\gamma, \dot{\gamma})} = \mathbf{R}(\dot{\gamma}, \hat{V}),$$

where $\hat{V} = V^\mu \delta_\mu$ is the canonical horizontal lift of V . The geodesic deviation operator $\mathbf{R} = R^\mu{}_\nu dx^\nu \otimes \delta_\mu$ is derived from the curvature of the nonlinear connection as

$$R^\mu{}_\nu = R^\mu{}_{\nu\sigma} \dot{x}^\sigma, \quad R^\mu{}_{\nu\sigma} \dot{\partial}_\mu = [\delta_\nu, \delta_\sigma] = (\delta_\sigma \bar{\Gamma}^\mu{}_\nu - \delta_\nu \bar{\Gamma}^\mu{}_\sigma) \dot{\partial}_\mu.$$

The non-homogenized Finsler Ricci scalar R is defined as its trace

$$R = R^\mu{}_\mu = R^\mu{}_{\mu\sigma} \dot{x}^\sigma. \quad (15.3)$$

The curvature tensors appearing here are defined solely in terms of the canonical nonlinear connection. The Finsler linear connections, which one may define, are not entering here.

In the particular case when $L = g_{\mu\nu}(x) \dot{x}^\mu \dot{x}^\nu$, where $g_{\mu\nu}(x)$ are the components of a Lorentzian metric, the geometry of (M, L) becomes essentially the geometry of the pseudo-Riemannian spacetime manifold (M, g) .

The L -metric becomes the Lorentzian metric g , the nonlinear connection coefficients and the nonlinear curvature tensor become the Christoffel symbols $\Gamma^\mu{}_{\nu\rho}(x)$ and the Riemann curvature tensor $r^\mu{}_{\nu\rho\sigma}$ of the Levi-Civita connection of g , up to a contraction with a velocity \dot{x} . Yet, the Finslerian Ricci scalar becomes $R(x, \dot{x}) = -r_{\nu\sigma}(x) \dot{x}^\nu \dot{x}^\sigma$ and is not equal to the Riemannian Ricci scalar $r = r_{\mu\nu} g^{\mu\nu}$ in this case.

In the following, when constructing an action for Finsler gravity, we will need to work with 0-homogeneous objects in \dot{x} . On \mathcal{A}_0 we can introduce the 0-homogenized Ricci scalar

$$R_0 = \frac{1}{L} R. \quad (15.4)$$

15.3 Finslerian Scalars as Physical Fields

By a *Finslerian scalar*, we will understand in the following a function $\Phi : TM \rightarrow \mathbb{R}$, $\Phi = \Phi(x, \dot{x})$, homogeneous of some degree k in \dot{x} . As physical fields, we have in mind two such examples:

- (1) The Finsler-Lagrange function $L : TM \rightarrow \mathbb{R}$ of a Finsler spacetime manifold, obeying $L(x, \ell\dot{x}) = \ell^2 L(x, \dot{x})$, $\ell > 0$.
- (2) The 1-particle distribution function ϕ of a kinetic gas. Typically, $\phi = \phi(x, \dot{x})$ is understood as a function on the observer space \mathcal{O} . Equivalently, we can understand it as a function on the entire TM , setting $\phi(x, \ell\dot{x}) := \phi(x, \dot{x})$ for $\ell > 0$ (and $\phi(x, 0) = 0$).

As we want to apply the standard tools of variational calculus, [41], we need to understand homogeneous functions $\Phi : TM \rightarrow \mathbb{R}$ as *sections* of some fibred manifold. Naively, Φ can be understood as a section of $TM \times \mathbb{R}$. Yet, this description is problematic for the calculus of variations machinery, since, due to the \dot{x} -homogeneity requirement, variations $\delta\Phi$ cannot be compactly supported on TM (since, imposing that $\delta\Phi(x, \dot{x}) = 0$ for some (x, \dot{x}) will force $\delta\Phi(x, \ell\dot{x}) = 0$ for all $\ell > 0$).

The solution comes from considering the so-called positive (or oriented) projective tangent bundle PTM^+ , obtained by treating each half-line $\{(x, \ell\dot{x}) \mid \ell > 0\}$ as a single point. Intuitively, PTM^+ can be interpreted as the *space of directions* over M ; more precisely, PTM^+ is a set of equivalence classes $PTM^+ := \{[(x, \dot{x})]_{\sim} \mid (x, \dot{x}) \in TM\}$, where:

$$(x, \dot{x}) \sim (x, u) \Leftrightarrow u = \ell\dot{x} \text{ for some } \ell > 0.$$

The set PTM^+ is an orientable seven-dimensional manifold. Moreover, the slit tangent bundle $\overset{\circ}{TM} = TM \setminus \{0\}$ is a principal bundle over PTM^+ , with fibre \mathbb{R}_+^* and projection:

$$\pi^+ : \overset{\circ}{TM} \rightarrow PTM^+, \quad (x, \dot{x}) \mapsto [(x, \dot{x})].$$

Local coordinates on PTM^+ . Coordinate charts on PTM^+ can be taken of the form $U_\mu = \{[(x^0, \dots, x^3, \dot{x}^0, \dots, \dot{x}^\mu, \dots, \dot{x}^3)] \mid \dot{x}^\mu \text{ has constant sign}\}$. An element $[(x, \dot{x})] \in U_\mu$ will have the coordinates (x^μ, u^i) , where $u^i = \frac{\dot{x}^i}{\dot{x}^\mu}$, for all $i \in \{0, \dots, 3\}$, $i \neq \mu$.

But, working in coordinates (x^μ, u^i) is usually inconvenient. Fortunately, for $[(x, \dot{x})] \in U_\mu$, one can introduce *homogeneous coordinates*, which are nothing but the coordinates (x^μ, \dot{x}^μ) of the representative $(x, \dot{x}) \in TM$. In these coordinates, the calculations (including differentiation and integration) are identical to those on TM . It simply has to be ensured that the involved geometric objects are well-defined objects on PTM^+ . This can be seen as follows:

- Functions $f^+ = f^+(x^\mu, \dot{x}^\mu)$ and vector fields $X^+ = X^+(x^\mu, \dot{x}^\mu)$ are well-defined on PTM^+ if and only if they are 0-homogeneous in \dot{x} .
- Differential forms $\rho^+ = \rho^+(x^\mu, \dot{x}^\mu)$ are well-defined on PTM^+ if and only if they are 0-homogeneous in \dot{x} and π^+ -horizontal, i.e., $\mathring{i}_\mathbb{C} \rho^+ = 0$, where $\mathbb{C} = \dot{x}^\mu \partial_\mu$ is the generator of the fibres of the principal bundle $(TM, \pi^+, PTM^+, \mathbb{R}_+^*)$.

We will denote by a superscript $+$ objects on PTM^+ , to distinguish them from their TM -correspondents (which have the same coordinate expression), e.g.: $f = f^+ \circ \pi^+, \rho = (\pi^+)^* \rho^+$.

The space of directions PTM^+ has one more property, which is particularly important when dealing with kinetic gases. Integrals on *compact* subsets V of the observer space $\mathcal{O} \subset TM$ can be understood as integrals on compact subsets $V^+ := \pi^+(V)$ of PTM^+ :

$$\int_V \rho = \int_{V^+} \rho^+,$$

where $\rho := (\pi^+)^* \rho^+$; this is possible since the restriction $\pi^+ : V \rightarrow V^+$ is a diffeomorphism. This allows us to express action integrals on PTM^+ as action integrals on \mathcal{O} and vice-versa.

Construction of the configuration bundle. Now, having described the space of directions PTM^+ , it remains to describe the homogeneous functions $L, \phi : TM \rightarrow \mathbb{R}$ as sections of some bundle Y sitting over PTM^+ .

- The 0-homogeneous function ϕ poses no problems, since $\phi(x, \dot{x})$ can be identified as a function $\phi^+([x, \dot{x}])$ on PTM^+ . Hence, in this case, $Y = PTM^+ \times \mathbb{R}$. Briefly: we can equivalently understand ϕ either as a function on \mathcal{O} , or as a function on (a subset of) PTM^+ .
- The situation is more complicated in the case of L - which, because of its non-zero homogeneity degree, cannot be understood as a function on PTM^+ . Still, we will be able to describe L as a section of a fibred manifold sitting over PTM^+ , as follows. We start from the remark that (\mathbb{R}_+^*, \cdot) is a Lie group, acting on both \mathring{TM} and \mathbb{R} :

$$\cdot : \mathring{TM} \times \mathbb{R}_+^* \rightarrow \mathring{TM}, \quad (x, \dot{x}) \cdot \ell = (x, \ell \dot{x}), \quad * : \mathbb{R}_+^* \times \mathbb{R} \rightarrow \mathbb{R}, \quad \ell * z = \ell^2 z.$$

The 2-homogeneity of L can be understood as *equivariance* under these actions. This points out to the associated bundle to the principal bundle \mathring{TM} , with fibre \mathbb{R} (and base PTM^+)

$$Y := (\mathring{TM} \times \mathbb{R})_{j\sim}$$

where the equivalence relation \sim is given by: $(x, \dot{x}, L) \sim (x, \ell \dot{x}, \ell^2 L)$, $\ell \in \mathbb{R}_+^*$. The set Y is a fibred manifold over PTM^+ , with projection: $\pi : Y \rightarrow$

PTM^+ , $[(x, \dot{x}, L)] \rightarrow [(x, \dot{x})]$. Using homogeneous local coordinates (x^μ, \dot{x}^μ) on PTM^+ , the local coordinates on Y will be simply (x^μ, \dot{x}^μ, L) . Then, Finsler-Lagrange functions $L = L(x, \dot{x})$ are in one-to-one correspondence with sections γ of Y :

$$L \mapsto \gamma : PTM^+ \rightarrow Y, \quad \gamma([(x, \dot{x})]) = [x, \dot{x}, L(x, \dot{x})]. \quad (15.5)$$

or, in local coordinates, $\gamma : (x^\mu, \dot{x}^\mu) \mapsto (x^\mu, \dot{x}^\mu, L(x^\mu, \dot{x}^\mu))$.

Having constructed the configuration bundle Y , the gravitational field Lagrangian will be understood as a 7-form $\Lambda = \mathcal{L}(x, \dot{x}, L, DL, \dots, D^k L)d(Vol)$ on a jet bundle $J^k Y$. The corresponding action is constructed by substituting $L = L(x, \dot{x})$ into Λ (i.e., pulling back this 7-form to PTM^+ by sections $J^k \gamma$) and integrating over arbitrary compact domains $V^+ \subset PTM^+$. A similar construction holds for ϕ .

15.4 Gravitational Dynamics

The mathematical construction presented in the previous section lays the foundation to construct consistent Finslerian theories of gravity and matter fields. Since the geometry of Finsler spacetimes is described on the tangent bundle, it is necessary to also describe physically viable matter on the same level, so that the matter can actually determine the geometry dynamically. The construction of such a matter-geometry coupling has for long been an open issue. A natural candidate for such coupling is the kinetic description of gases. By using Finsler geometry to describe kinetic gases, we constructed for the first time a coupling between a Finsler geometric description of gravity and physical matter, which naturally lives on the tangent bundle [3, 42].

15.4.1 The Kinetic Gas Action on the Tangent Bundle

The properties of a large system of P (interacting or non-interacting), particles can be encoded into the so-called 1-particle distribution function (1PDF) $\phi = \phi(x, \dot{x})$ [43, 44], which is a 0-homogeneous real scalar function defined on TM - hence equivalently on PTM^+ , or on the observer space \mathcal{O} . It is defined by the particle number counting integral

$$N(\sigma) := \int_{\sigma} \phi \Omega,$$

which gives the number of particles intersecting an arbitrary oriented six-dimensional hypersurface $\sigma \subset \mathcal{O}$, i.e., it counts the intersection of tangent bundle particle trajectories $c = (\gamma, \dot{\gamma})$ with σ . The volume form Ω is canonically determined from the Finsler-Lagrange function L , see [3].

Since in all physical realistic situations, there will be particles of maximal velocity, we can assume that the restriction of the 1PDF to the observer space $\phi_x(\cdot) = \phi(x, \cdot)$ is compactly supported.

For collisionless gases, the 1PDF satisfies the *Liouville equation*

$$\frac{\dot{x}^\mu}{\sqrt{L}} \delta_\mu \phi = 0, \quad (15.6)$$

which can be derived from the demand that the number of particles is constant between two different hypersurfaces, that are transversal to particle trajectories. In the following, we will see that the Liouville equation can be understood as an energy-momentum conservation equation.

The action of the kinetic gas is

$$S_{\text{gas}} = \int_V \phi \Sigma = \int_D \left(\int_{\mathcal{O}_x} \phi \Sigma_x \right) d^4x, \quad (15.7)$$

where the compact subset $V \subset \mathcal{O}$ is generated by the flow of particle worldlines from a given hypersurface σ_0 for a finite flow parameter. The second equal sign above is justified as follows. Taking into account that $\phi(x, \cdot)$ is compactly supported, the integral of $\phi \Sigma$ on V can be understood as an integral on $\bigcup_{x \in D} \mathcal{O}_x$, where $D = \pi(V)$ and $\mathcal{O}_x = \mathcal{O} \cap T_x M$ is the set of unit time-like directions at x ; in this way, the latter expression of S_{gas} is well defined and equal to an integral on a corresponding domain $V^+ \subset PTM^+$. The volume forms Σ on V and Σ_x on \mathcal{O}_x are, again, canonically determined by the Finsler Lagrangian L and can be found in [3].

The action (15.7) is invariant under coordinate transformations on TM induced from coordinate transformations on M . As a consequence of this invariance, we can identify the *energy-momentum distribution tensor* Θ of the gas on \mathcal{O} as

$$\Theta^\mu{}_\nu = \phi \frac{\dot{x}^\mu \dot{x}_\nu}{L}.$$

It satisfies an averaged conservation equation

$$\int_{\mathcal{O}_x} D_{\delta_\mu} \Theta^\mu{}_\nu \Sigma_x = 0. \quad (15.8)$$

For a collisionless gas, we see that even a pointwise conservation equation holds, since

$$D_{\delta_\mu} \Theta^\mu{}_\nu = \frac{\dot{x}^\mu \dot{x}_\nu}{L} D_{\delta_\mu} \phi = \frac{\dot{x}^\mu \dot{x}_\nu}{L} \delta_\mu \phi = 0$$

is precisely the Liouville equation. The other way around, demanding that (15.8) holds pointwise, the Liouville equation is implied.

The usual fluid energy-momentum tensor density T of the kinetic gas on the base manifold M is obtained by averaging Θ over the unit time-like directions:

$$T^\mu{}_\nu(x) := \int_{\mathcal{O}_x} \Theta^\mu{}_\nu(x, \dot{x}) \Sigma_x = \int_{\mathcal{O}_x} \phi \frac{\dot{x}^\mu \dot{x}_\nu}{L} \Sigma_x. \tag{15.9}$$

It is worth noting that in the particular case where L is pseudo-Riemannian, the operator D_{δ_μ} becomes the usual Levi-Civita covariant derivative \cdot_μ and it can be pulled out of the integral. Hence, in this case, averaged conservation law (15.8) becomes equivalent to the usual covariant conservation law.

15.4.2 The Finsler Gravity Action

One of the first Finsler gravitational field equations proposed as a generalization of the Einstein vacuum equations was suggested by Rutz [28] as the vanishing of the Finsler Ricci scalar

$$R_0 = 0.$$

This equation represents the vanishing of the trace of the geodesic deviation operator, a method suggested by Pirani to find the Einstein vacuum equations.

We proved that the Rutz equation has one drawback, namely that it cannot be derived from an action. The variational completion algorithm [45] revealed that the closest Finsler gravity equation, which can be derived from an action, must be obtained from the action on PTM^+

$$S_{\text{grav}} = \int_{V^+} R_0^+ \Sigma^+ = \int_V R_0 \Sigma,$$

where actually, since we assume $V^+ \subset PTM^+$ to be compact, it can be equivalently expressed on $V \subset \mathcal{O}$; see [1], where the 1PDF of the kinetic gas action is defined, too. After this preparation it is straightforward to derive the coupled Finsler spacetime gravitational dynamics.

15.4.3 Kinetic Gases as Physical Sources for Finsler Gravity

The combined action for a kinetic gas coupled to a Finslerian spacetime geometry, which encodes gravity, is

$$S = \frac{2}{\kappa^2} \int_V R_0 \Sigma + \int_V \phi \Sigma.$$

Variation with respect to the Finsler-Lagrange function L yields [3]

$$3R_0 - \frac{1}{2}g^{\mu\nu}R_{\cdot\mu\nu} + g^{\mu\nu}[(\nabla P_\mu)_{\cdot\nu} + D_{\delta_\nu}P_\mu - P_\mu P_\nu] = \kappa^2\phi. \quad (15.10)$$

The corresponding vacuum equation, setting $\phi = 0$, has already been discussed in [30]. Its completion through the addition of a viable consistent physical matter coupling has only been achieved recently.

Equation (15.10) determines the geometry of spacetime, i.e., the gravitational field, directly from the 1PDF of a kinetic gas. It takes into account the influence of the generally nontrivial velocity distribution over the different gas particles. In contrast, in the general relativistic coupling between a system of P particles and gravity in terms of the energy-momentum tensor, the velocity distribution of the particles is averaged out. Hence, we expect that the Finslerian description of the gravitational field of kinetic gases gives a more accurate result than its general relativistic description.

The future application of the gravitational field equation is expected to highly improve the understanding of systems that are described by gravitating fluids, such as the Universe as a whole in cosmology, ordinary and neutron stars, as well as accretion disks of black holes, by replacing the averaged gravitating fluid by the more accurate and finer notion of a kinetic gas.

References

1. M. Hohmann, C. Pfeifer, N. Voicu, Finsler gravity action from variational completion. *Phys. Rev. D* **100**(6), 064035 (2019). [arXiv:1812.11161](#)
2. C. Pfeifer, Finsler spacetime geometry in Physics. *Int. J. Geom. Methods Mod. Phys.* **16**(supp02), 1941004 (2019). [arXiv:1903.10185](#)
3. M. Hohmann, C. Pfeifer, N. Voicu, Relativistic kinetic gases as direct sources of gravity. *Phys. Rev. D* **101**, 024062 (2020). [arXiv:1910.14044](#)
4. D. Raetzl, S. Rivera, F.P. Schuller, Geometry of physical dispersion relations. *Phys. Rev. D* **83**, 044047 (2011). [arXiv:1010.1369](#)
5. G. Amelino-Camelia, L. Barcaroli, G. Gubitosi, S. Liberati, N. Loret, Realization of doubly special relativistic symmetries in Finsler geometries. *Phys. Rev. D* **90**(12), 25030 (2014). [arXiv:1407.8143](#)
6. I.P. Lobo, C. Pfeifer, Reaching the Planck scale with muon lifetime measurements. *Phys. Rev. D* **103**, 106025 (2021). [arXiv:2011.10069](#)
7. N. Gürlebeck, C. Pfeifer, Observers' measurements in premetric electrodynamics: time and radar length. *Phys. Rev. D* **97**(8), 084043 (2018). [arXiv:1801.07724](#)
8. G.W. Gibbons, C.M. Warnick, The geometry of sound rays in a wind. *Contemp. Phys.* **52**, 197–209 (2011). [arXiv:1102.2409](#)
9. T. Yajima, H. Nagahama, Finsler geometry of seismic ray path in anisotropic media. *Proc. R. Soc. A: Math., Phys. Eng. Sci.* **465**(2106), 1763–1777 (2009)
10. S. Markvorsen, A Finsler geodesic spray paradigm for wildfire spread modelling. *Nonlinear Anal.: R. World Appl.* **28** (2016)
11. L. Barcaroli, L.K. Brunkhorst, G. Gubitosi, N. Loret, C. Pfeifer, Curved spacetimes with local κ -Poincaré dispersion relation. *Phys. Rev. D* **96**(8), 084010 (2017). [arXiv:1703.02058](#)
12. A. Kostelecky, Riemann-Finsler geometry and Lorentz-violating kinematics. *Phys. Lett. B* **701**, 137–143 (2011). [arXiv:1104.5488](#)

13. A.G. Cohen, S.L. Glashow, Very special relativity. *Phys. Rev. Lett.* **97**, 021601 (2006). [arXiv:hep-ph/0601236](#)
14. G. Bogoslovsky, A special-relativistic theory of the locally anisotropic space-time. *Il Nuovo Cim. B Ser.* **11**(40), 99 (1977)
15. G.W. Gibbons, J. Gomis, C.N. Pope, General very special relativity is Finsler geometry. *Phys. Rev. D* **76**, 081701 (2007). [arXiv:0707.2174](#)
16. A. Fuster, C. Pabst, C. Pfeifer, Berwald spacetimes and very special relativity. *Phys. Rev. D* **98**(8), 084062 (2018). [arXiv:1804.09727](#)
17. G. Randers, On an asymmetrical metric in the four-space of general relativity. *Phys. Rev.* **59**, 195–199 (1941)
18. M.A. Javaloyes, M. Sánchez, On the definition and examples of cones and Finsler spacetimes. [arXiv:1805.06978](#)
19. R. Punzi, M.N. Wohlfarth, F.P. Schuller, Propagation of light in area metric backgrounds. *Class. Quant. Grav.* **26**, 035024 (2009). [arXiv:0711.3771](#)
20. J. Ehlers, F. Pirani, A. Schild, Republication of: the geometry of free fall and light propagation. *Gen. Relativ. Gravit.* **44**, 06 (2012)
21. R. Tavakol, Geometry of spacetime and Finsler geometry. *Int. J. Mod. Phys.-IJMPA* **24**(04), 1678–1685 (2009)
22. A. Bernal, M.Á. Javaloyes, M. Sánchez, Foundations of Finsler spacetimes from the observers' viewpoint. *Universe* **6**(4), 55 (2020). [arXiv:2003.00455](#)
23. D. Clowe, M. Bradac, A.H. Gonzalez, M. Markevitch, S.W. Randall, C. Jones, D. Zaritsky, A direct empirical proof of the existence of dark matter. *Astrophys. J.* **648**, L109–L113 (2006). [arXiv:astro-ph/0608407](#)
24. E. Corbelli, P. Salucci, The extended rotation curve and the dark matter halo of M33. *Mon. Not. Roy. Astron. Soc.* **311**, 441–447 (2000). [arXiv:astro-ph/9909252](#)
25. P.J.E. Peebles, B. Ratra, The Cosmological constant and dark energy. *Rev. Mod. Phys.* **75**, 559–606 (2003). [arXiv:astro-ph/0207347](#) (592(2002))
26. A.G. Riess, Supernova Search Team Collaboration et al., Observational evidence from supernovae for an accelerating universe and a cosmological constant. *Astron. J.* **116**, 1009–1038 (1998). [arXiv:astro-ph/9805201](#)
27. J.K. Beem, Indefinite finsler spaces and timelike spaces. *Can. J. Math.* **22**(5), 1035–1039 (1970)
28. S. Rutz, A Finsler generalisation of Einstein's vacuum field equations. *Gen. Relativ. Gravit.* **25**(01), 1139–1158 (1993)
29. C. Pfeifer, M.N.R. Wohlfarth, Causal structure and electrodynamics on Finsler spacetimes. *Phys. Rev. D* **84**, 044039 (2011). [arXiv:1104.1079](#)
30. C. Pfeifer, M.N.R. Wohlfarth, Finsler geometric extension of Einstein gravity. *Phys. Rev. D* **85**, 064009 (2012). [arXiv:1112.5641](#)
31. S. Basilakos, A.P. Kouretsis, E.N. Saridakis, P. Stavrinos, Resembling dark energy and modified gravity with Finsler-Randers cosmology. *Phys. Rev. D* **88**, 123510 (2013). [arXiv:1311.5915](#)
32. C. Pfeifer, Radar orthogonality and radar length in Finsler and metric spacetime geometry. *Phys. Rev. D* **90**(6), 064052 (2014). [arXiv:1408.5306](#)
33. M. Hohmann, C. Pfeifer, N. Voicu, Cosmological Finsler spacetimes. *Universe* **6**(5), 65 (2020). [arXiv:2003.02299](#)
34. W. Hasse, V. Perlick, Redshift in Finsler spacetimes. *Phys. Rev. D* **100**(2), 024033 (2019). [arXiv:1904.08521](#)
35. M. Hohmann, C. Pfeifer, Geodesics and the magnitude-redshift relation on cosmologically symmetric Finsler spacetimes. *Phys. Rev. D* **95**(10), 104021 (2017). [arXiv:1612.08187](#)
36. G. Minas, E.N. Saridakis, P.C. Stavrinos, A. Triantafyllopoulos, Bounce cosmology in generalized modified gravities. *Universe* **5**, 74 (2019). [arXiv:1902.06558](#)
37. S. Ikeda, E.N. Saridakis, P.C. Stavrinos, A. Triantafyllopoulos, Cosmology of Lorentz fiber-bundle induced scalar-tensor theories. *Phys. Rev. D* **100**(12), 124035 (2019). [arXiv:1907.10950](#)
38. B. Riemann, über die Hypothesen, welche der Geometrie zu Grunde liegen. *Abhandlungen der Königlich Gesellschaft der Wissenschaften zu Göttingen* **13** (1867)

39. P. Finsler, Über Kurven und Flächen in allgemeinen Räumen. Ph.D. thesis, Georg-August Universität zu Göttingen (1918)
40. D. Bao, S.-S. Chern, Z. Shen, *An Introduction to Finsler-Riemann Geometry* (Springer, New York, 2000)
41. D. Krupka, *Introduction to Global Variational Geometry* (Springer, Berlin, 2015)
42. M. Hohmann, C. Pfeifer, N. Voicu, The kinetic gas universe. *Eur. Phys. J. C* **80**(9), 809 (2020). [arXiv:2005.13561](https://arxiv.org/abs/2005.13561)
43. J. Ehlers, *General-Relativistic Kinetic Theory Of Gases* (Springer, Berlin Heidelberg, Berlin, Heidelberg, 2011), pp. 301–388
44. L. Rezzolla, O. Zanotti, *Relativistic Hydrodynamics* (Oxford University Press, Oxford, 2013)
45. N. Voicu, D. Krupka, Canonical variational completion of differential equations. *J. Math. Phys.* **56**(4), 043507 (2015). <https://doi.org/10.1063/1.4918789>

Chapter 16

Gravity's Rainbow



Remo Garattini

According to Quantum Mechanics, Zero Point Energy (ZPE) is the lowest possible energy that a quantum mechanical system may have. Unlike in classical mechanics, quantum systems constantly fluctuate in their lowest energy state as described by the Heisenberg uncertainty principle. The same behaviour appears also in Quantum Field Theory and, if one wishes to also apply the quantum world to General Relativity, one should obtain a quantum theory of the gravitational field, better known as *Quantum Gravity*. Unfortunately, such a theory is still lacking. However, there is no barrier to searching for a possible ZPE candidate, even if it is well known that every ZPE calculation is plagued by divergences. Usually, the divergences are kept under control with the help of a regularisation and renormalisation procedure. In ordinary gravity the computation of ZPE for quantum fluctuations of the *pure gravitational field* can be extracted by rewriting the Wheeler-DeWitt equation (WDW) [1] in a form that looks like an expectation value computation [2, 3]. Its derivation is a consequence of the Arnowitt-Deser-Misner (ADM) decomposition [4] of spacetime based on the following line element

$$ds^2 = g_{\mu\nu}(x) dx^\mu dx^\nu = (-N^2 + N_i N^i) dt^2 + 2N_j dt dx^j + g_{ij} dx^i dx^j, \quad (16.1)$$

where N is the *lapse* function and N_i the *shift* function. In terms of the ADM variables, the four-dimensional scalar curvature R can be decomposed in the following way

$$R = {}^{(3)}R + K_{ij} K^{ij} - (K)^2 - 2\nabla_\mu (K u^\mu + a^\mu), \quad (16.2)$$

R. Garattini (✉)

Dipartimento di Ingegneria e Scienze Applicate, Università degli Studi di Bergamo,
Viale Marconi, 524044 Dalmine, Bergamo, Italy

Istituto Nazionale di Fisica Nucleare (INFN), Sezione di Milano, Milan, Italy
e-mail: remo.garattini@unibg.it

where

$$K_{ij} = -\frac{1}{2N} [\partial_t g_{ij} - N_{i|j} - N_{j|i}] \quad (16.3)$$

is the second fundamental form, $K = g^{ij} K_{ij}$ is its trace, ${}^{(3)}R$ is the three-dimensional scalar curvature and $\sqrt{\gamma}$ is the three-dimensional determinant of the metric. The last term in (16.2) represents the boundary terms contribution where the four-velocity u^μ is the timelike unit vector normal to the spacelike hypersurfaces ($t=\text{constant}$) denoted by Σ_t and $a^\mu = u^\alpha \nabla_\alpha u^\mu$ is the acceleration of the timelike normal u^μ . Thus

$$\mathcal{L}[N, N_i, g_{ij}] = \sqrt{-g} (R - 2\Lambda) = \frac{N}{2\kappa} \sqrt{g} [K_{ij} K^{ij} - K^2 + {}^{(3)}R - 2\Lambda - 2\nabla_\mu (K u^\mu + a^\mu)] \quad (16.4)$$

represents the gravitational Lagrangian density where $\kappa = 8\pi G$ with G the Newton's constant, and for the sake of generality we have also included a cosmological constant Λ . After a Legendre transformation, the WDW equation simply becomes

$$\mathcal{H}\Psi = \left[(2\kappa) G_{ijkl} \pi^{ij} \pi^{kl} - \frac{\sqrt{g}}{2\kappa^2} ({}^{(3)}R - 2\Lambda) \right] \Psi = 0, \quad (16.5)$$

where G_{ijkl} is the super-metric and where the conjugate super-momentum π^{ij} is defined as

$$\pi^{ij} = \frac{\delta \mathcal{L}}{\delta (\partial_t g_{ij})} = (g^{ij} K - K^{ij}) \frac{\sqrt{g}}{2\kappa}. \quad (16.6)$$

Note that $\mathcal{H} = 0$ represents the classical constraint that guarantees the invariance under time reparametrisation. The other classical constraint represents the invariance by spatial diffeomorphism and it is described by $\pi_{|j}^{ij} = 0$, where the vertical stroke “|” denotes the covariant derivative with respect to the 3D metric g_{ij} . It is interesting to note that formally, the WDW equation can be transformed into an eigenvalue equation. Let us see how, with a concrete example.

16.1 The Cosmological Constant as a Sturm-Liouville Eigenvalue Problem

The Friedmann-Lemaître-Robertson-Walker (FLRW) line element is defined as

$$ds^2 = -N^2 dt^2 + a^2(t) d\Omega_3^2, \quad (16.7)$$

describing a homogeneous, isotropic and closed universe, where

$$d\Omega_3^2 = g_{ij} dx^i dx^j \quad (16.8)$$

is the line element on the three-sphere, N is the lapse function and $a(t)$ denotes the scale factor. Let us consider a very simple mini-superspace model described by the metric of Eq. (16.7). In this background the Einstein-Hilbert action in $(3 + 1)$ -dim becomes

$$S = -\frac{3\pi}{4G} \int_I \left[\dot{a}^2 a - a + \frac{\Lambda}{3} a^3 \right] dt, \quad (16.9)$$

where Λ is the cosmological constant. In Eq. (16.9), we have integrated every degree of freedom except the scale factor. In addition we have computed the volume associated with the three-sphere, namely $V_3 = 2\pi^2$, and we have set $N = 1$. The canonical momentum reads

$$\pi_a = \frac{\delta S}{\delta \dot{a}} = -\frac{3\pi}{2G} \dot{a} a, \quad (16.10)$$

and the resulting Hamiltonian density is

$$\mathcal{H} = \pi_a \dot{a} - \mathcal{L} = -\frac{G}{3\pi} - \frac{3\pi}{4G} a + \frac{3\pi}{4G} \frac{\Lambda}{3} a^3. \quad (16.11)$$

Following the canonical quantization prescription, we promote π_a to a momentum operator, setting

$$\pi_a^2 \rightarrow -a^{-q} \left[\frac{\partial}{\partial a} a^q \frac{\partial}{\partial a} \right], \quad (16.12)$$

where we have introduced a factor order ambiguity q . The generalisation to $k = 0, -1$ is straightforward. The WDW equation for such a metric is

$$\begin{aligned} H\Psi(a) &= \left[-a^{-q} \left(\frac{\partial}{\partial a} a^q \frac{\partial}{\partial a} \right) + \frac{g\pi^2}{4G^2} \left(a^2 - \frac{\Lambda}{3} a^4 \right) \right] \Psi(a), \\ &= \left[-\frac{\partial^2}{\partial a^2} - \frac{q}{a} \frac{\partial}{\partial a} + \frac{9\pi^2}{4G^2} \left(a^2 - \frac{\Lambda}{3} a^4 \right) \right] \Psi(a) = 0. \end{aligned} \quad (16.13)$$

It represents the quantum version of the invariance with respect to time reparametrisation. If we define the following reference length $a_0 = \sqrt{3/\Lambda}$, then Eq. (16.13) assumes the familiar form of a one-dimensional Schrödinger equation for a particle moving in the potential

$$U(a) = \frac{9\pi^2}{4G^2} \left[\left(\frac{a}{a_0} \right)^2 - \left(\frac{a}{a_0} \right)^4 \right], \quad (16.14)$$

with zero total energy. The potential $U(a)$ resembles a potential well, which is unbounded from below. When $0 < a < a_0$, Eq. (16.14) implies $U(a) > 0$, which is the classically forbidden region, while for $a > a_0$, one gets $U(a) < 0$, which is the classically allowed region. It is interesting to note that for the special case of the operator ordering $q = -1$, exact solutions can be determined [5]. Even if the

WDW equation (16.13) has a zero-energy eigenvalue, it also has a hidden structure. Indeed, Eq. (16.13) has the structure of a Sturm-Liouville eigenvalue problem with the cosmological constant as the eigenvalue. We ask the reader to recall that a Sturm-Liouville differential equation is defined by

$$\frac{d}{dx} \left(p(x) \frac{dy(x)}{dx} \right) + q(x) y(x) + \lambda w(x) y(x) = 0, \quad (16.15)$$

while the normalisation is defined by

$$\int_a^b dx w(x) y^*(x) y(x). \quad (16.16)$$

In the case of the FLRW model we have the following correspondence

$$\begin{aligned} p(x) &\rightarrow a^q(t), \\ q(x) &\rightarrow \left(\frac{3\pi}{2G} \right)^2 a^{q+2}(t), \\ w(x) &\rightarrow a^{q+4}(t), \\ y(x) &\rightarrow \Psi(a), \\ \lambda &\rightarrow \frac{\Lambda}{3} \left(\frac{3\pi}{2G} \right)^2, \end{aligned} \quad (16.17)$$

and the normalisation becomes

$$\int_0^\infty da a^{q+4} \Psi^*(a) \Psi(a). \quad (16.18)$$

It is a standard procedure to convert the Sturm-Liouville problem (16.15) into a variational problem of the form¹

$$F[y(x)] = \frac{-\int_a^b dx y^*(x) \left\{ \frac{d}{dx} \left[p(x) \frac{d}{dx} \right] + q(x) \right\} y(x)}{\int_a^b dx w(x) y^*(x) y(x)}, \quad (16.20)$$

with a boundary condition to be specified. If $y(x)$ is an eigenfunction of (16.15), then

¹ Actually the standard variational procedure prefers the following form

$$F[y(x)] = \frac{-[y^*(x) p(x) \frac{d}{dx} y(x)]_a^b + \int_a^b dx p(x) \left[\frac{d}{dx} y(x) \right]^2 - q(x) y(x)}{\int_a^b dx w(x) y^*(x) y(x)}, \quad (16.19)$$

with appropriate boundary conditions.

$$\lambda = \frac{-\int_a^b dx y^*(x) \left\{ \frac{d}{dx} \left[p(x) \frac{d}{dx} \right] + q(x) \right\} y(x)}{\int_a^b dx w(x) y^*(x) y(x)}, \quad (16.21)$$

is the eigenvalue, otherwise

$$\lambda_1 = \min_{y(x)} \frac{-\int_a^b dx y^*(x) \left\{ \frac{d}{dx} \left[p(x) \frac{d}{dx} \right] + q(x) \right\} y(x)}{\int_a^b dx w(x) y^*(x) y(x)}. \quad (16.22)$$

The minimum of the functional $F[y(x)]$ corresponds to a solution of the Sturm-Liouville problem (16.15) with the eigenvalue λ . In the mini-superspace approach with a FLRW background,² one finds

$$\frac{\int \mathcal{D}a a^q \Psi^*(a) \left[-\frac{\partial^2}{\partial a^2} - \frac{q}{a} \frac{\partial}{\partial a} + \frac{9\pi^2}{4G^2} a^2 \right] \Psi(a)}{\int \mathcal{D}a a^{q+4} \Psi^*(a) \Psi(a)} = \frac{3\pi^2}{4G^2}. \quad (16.23)$$

Note that the original WDW Eq. (16.13) is always preserved. This means that the cosmological constant, in this approach, represents the degree of degeneracy of the original eigenvalue $E = 0$. It is immediate to generalise the quantum mechanical problem into a problem of quantum field theory with the help of Eq. (16.5).

16.2 From Quantum Mechanics to Quantum Field Theory

The Sturm-Liouville problem represented by the functional (16.20) can be generalised to describe a problem of quantum field theory. Indeed to this purpose, one can write

$$\frac{1}{V} \frac{\int \mathcal{D}[g_{ij}] \Psi^*[g_{ij}] \int_{\Sigma} d^3x \hat{\Lambda}_{\Sigma} \Psi[g_{ij}]}{\int \mathcal{D}[g_{ij}] \Psi^*[g_{ij}] \Psi[g_{ij}]} = \frac{1}{V} \frac{\langle \Psi | \int_{\Sigma} d^3x \hat{\Lambda}_{\Sigma} | \Psi \rangle}{\langle \Psi | \Psi \rangle} = -\frac{\Lambda}{\kappa}, \quad (16.24)$$

where we have integrated over the hypersurface Σ and we have defined

$$V = \int_{\Sigma} d^3x \sqrt{g} \quad (16.25)$$

as the volume of the hypersurface Σ with

$$\hat{\Lambda}_{\Sigma} = (2\kappa) G_{ijkl} \pi^{ij} \pi^{kl} - \sqrt{g}^{(3)} R / (2\kappa). \quad (16.26)$$

² For applications of this procedure to Varying Speed of Light Cosmology (VSL), see [6]. For applications to the Generalized Uncertainty Principle (GUP), see [7] and finally, for applications to Inflation, see [8].

In this form, Eq. (16.24) can be used to compute Zero Point Energy (ZPE) provided that Λ/κ is considered as an eigenvalue of $\hat{\Lambda}_\Sigma$. Nevertheless, solving Eq. (16.24) is a quite impossible task, therefore we are oriented to use a variational approach with trial wave functionals. The related boundary conditions are dictated by the choice of the trial wave functionals, which, in our case, are of the Gaussian type; this choice is justified by the fact that ZPE should be described as a good candidate of the “*vacuum state*”. However, if we change the form of the wave functionals we also change the corresponding boundary conditions and therefore the description of the vacuum state. It is better to observe that the obtained eigenvalue Λ/κ , is far to be a constant, so it will be dependent on some parameters and therefore it will be considered more like a “*dynamical cosmological constant*”. Usually, when we compute Eq. (16.24) to one loop or higher loops, ultra-violet (UV) divergences appear. In ordinary gravity, to take under control such divergencies we need a regularisation/renormalisation scheme [2, 3]. Basically, we find that the one loop evaluation on a spherically symmetric background is represented by the following expression

$$\rho_i = -\frac{1}{4\pi^2} \int_{\sqrt{m_i^2(r)}}^{+\infty} d\lambda_i \lambda_i^2 \sqrt{\lambda_i^2 - m_i^2(r)}; \quad i = 1, 2, \quad (16.27)$$

where $i = 1, 2$ represents the two modes of the TT tensor. Of course, the expression (16.27) is divergent. The divergence can be kept under control, adopting the zeta function regularization scheme so that the integral in (16.27) becomes

$$\rho_i(\varepsilon, \mu) = -\frac{1}{4\pi^2} \mu^{2\varepsilon} \int_{\sqrt{m_i^2(r)}}^{+\infty} d\lambda_i \frac{\lambda_i^2}{(\lambda_i^2 - m_i^2(r))^{\varepsilon - \frac{1}{2}}}; \quad i = 1, 2. \quad (16.28)$$

The integration has to be meant in the range where $\lambda_i^2 - m_i^2(r) \geq 0$ and the additional mass parameter μ has been introduced in order to restore the correct dimension for the regularised quantities. Following the same steps as in [2, 3], we obtain

$$\rho_i(\varepsilon, \mu) = \frac{m_i^4(r)}{64\pi^2} \left[\frac{1}{\varepsilon} + \ln \left(\frac{4\mu^2}{m_i^2(r) \sqrt{e}} \right) \right], \quad i = 1, 2. \quad (16.29)$$

In order to renormalise the divergent ZPE, we write

$$\frac{\Lambda}{8\pi G} \rightarrow \frac{\Lambda_0}{8\pi G} + \frac{\Lambda^{div}}{8\pi G} = \frac{\Lambda_0}{8\pi G} + \frac{m_1^4(r) + m_2^4(r)}{64\pi^2 \varepsilon}. \quad (16.30)$$

Thus, the renormalisation is performed via the absorption of the divergent part into the re-definition of the bare classical constant Λ . The remaining finite value for the cosmological constant reads

$$\frac{\Lambda_0(\mu)}{8\pi G} = \sum_{i=1}^2 \rho_i(\mu) = \frac{1}{64\pi^2} \sum_{i=1}^2 m_i^4(r) \ln \left(\frac{4\mu^2}{m_i^2(r) \sqrt{e}} \right) = \rho_{eff}^{TT}(\mu, r). \quad (16.31)$$

To avoid the dependence on the arbitrary mass scale μ in Eq. (16.31), we adopt the renormalisation group equation and we impose that

$$\frac{1}{8\pi G} \mu \frac{\partial \Lambda_0(\mu)}{\partial \mu} = \mu \frac{d}{d\mu} \rho_{eff}^{TT}(\mu, r). \tag{16.32}$$

Solving it, we find that the renormalised constant Λ_0 should be treated as a running one in the sense that it varies, provided that the scale μ is changing³

$$\frac{\Lambda_0(\mu, r)}{8\pi G} = \frac{\Lambda_0(\mu_0, r)}{8\pi G} + \frac{m_1^4(r) + m_2^4(r)}{32\pi^2} \ln \frac{\mu}{\mu_0}. \tag{16.33}$$

It is interesting to note that the whole regularisation/renormalisation procedure can be avoided if we consider appropriate distortions of General Relativity; one good candidate is represented by Gravity's Rainbow.

16.2.1 The Wheeler-DeWitt Equation Distorted by Gravity's Rainbow

We refer the reader to Ref. [9] for details, even if a brief outline will be presented. As a first step, one has to introduce two arbitrary functions $g_1(E/E_P)$ and $g_2(E/E_P)$, which have the following property [10]

$$\lim_{E/E_P \rightarrow 0} g_1(E/E_P) = 1 \quad \text{and} \quad \lim_{E/E_P \rightarrow 0} g_2(E/E_P) = 1. \tag{16.34}$$

For a spherically symmetric line element, we can write the *rainbow* version as

$$ds^2 = -\frac{N^2(r)}{g_1^2(E/E_P)} dt^2 + \frac{dr^2}{\left(1 - \frac{b(r)}{r}\right) g_2^2(E/E_P)} + \frac{r^2}{g_2^2(E/E_P)} \left(d\theta^2 + \sin^2 \theta d\phi^2\right), \tag{16.35}$$

where N is the lapse function and $b(r)$ is subject to the only condition $b(r_t) = r_t$. Following Ref. [9], one can write the distorted classical constraint in the following way

$$\mathcal{H} = (2\kappa) \frac{g_1^2(E/E_P)}{g_2^3(E/E_P)} \tilde{g}_{ijkl} \tilde{\pi}^{ij} \tilde{\pi}^{kl} - \frac{\sqrt{\tilde{g}}}{2\kappa g_2(E/E_P)} \left({}^{(3)}\tilde{R} - \frac{2\Lambda_c}{g_2^2(E/E_P)} \right) = 0, \tag{16.36}$$

where we have used the following property on ${}^{(3)}R$

$${}^{(3)}R = g^{ij} {}^{(3)}R_{ij} = g_2^2(E/E_P) {}^{(3)}\tilde{R}, \tag{16.37}$$

³ Note that the same procedure can be applied also to a $f(R)$ theory [6].

and where

$$G_{ijkl} = \frac{1}{2\sqrt{\gamma}} (g_{ik}g_{jl} + g_{il}g_{jk} - g_{ij}g_{kl}) = \frac{\tilde{G}_{ijkl}}{g_2(E/E_P)}. \quad (16.38)$$

The symbol “ \sim ” indicates the quantity computed in absence of the rainbow’s functions $g_1(E/E_P)$ and $g_2(E/E_P)$. The corresponding vacuum expectation value (16.24) becomes

$$\frac{g_2^3(E/E_P)}{\tilde{V}} \frac{\langle \Psi | \int_{\Sigma} d^3x \tilde{\Lambda}_{\Sigma} | \Psi \rangle}{\langle \Psi | \Psi \rangle} = -\frac{\Lambda}{\kappa}, \quad (16.39)$$

with

$$\tilde{\Lambda}_{\Sigma} = (2\kappa) \frac{g_1^2(E/E_P)}{g_2^3(E/E_P)} \tilde{G}_{ijkl} \tilde{\pi}^{ij} \tilde{\pi}^{kl} - \frac{\sqrt{\tilde{g}}^{(3)} \tilde{R}}{(2\kappa) g_2(E/E_P)}. \quad (16.40)$$

Extracting the TT tensor contribution from Eq. (16.39), we find

$$\hat{\Lambda}_{\Sigma}^{\perp} = \frac{g_2^3(E/E_P)}{4\tilde{V}} \int_{\Sigma} d^3x \sqrt{\tilde{g}} \tilde{G}^{ijkl} \left\{ (2\kappa) \frac{g_1^2(E/E_P)}{g_2^3(E/E_P)} \tilde{K}^{-1\perp}(x, x)_{ijkl} + \frac{1}{(2\kappa) g_2(E/E_P)} \left[\tilde{\Delta}_L^m \tilde{K}^{\perp}(x, x) \right]_{ijkl} \right\}, \quad (16.41)$$

with the prescription that the corresponding eigenvalue equation transforms as

$$\left(\hat{\Delta}_L^m h^{\perp} \right)_{ij} = E^2 h_{ij}^{\perp} \quad \rightarrow \quad \left(\tilde{\Delta}_L^m \tilde{h}^{\perp} \right)_{ij} = \frac{E^2}{g_2^2(E/E_P)} \tilde{h}_{ij}^{\perp}, \quad (16.42)$$

in order to re-establish the correct way of transformation of the perturbation. $\tilde{\Delta}_L^m$ is the modified Lichnerowicz operator [9], defined as

$$\left(\tilde{\Delta}_L^m h^{\perp} \right)_{ij} = \left(\tilde{\Delta}_L h^{\perp} \right)_{ij} - 4R_i^k h_{kj}^{\perp} + {}^{(3)}R h_{ij}^{\perp}, \quad (16.43)$$

where $\tilde{\Delta}_L$ is the Lichnerowicz operator defined by

$$\left(\tilde{\Delta}_L h \right)_{ij} = \Delta h_{ij} - 2{}^{(3)}R_{ikjl} h^{kl} + {}^{(3)}R_{ik} h_j^k + {}^{(3)}R_{jk} h_i^k \quad \Delta = -\nabla^a \nabla_a. \quad (16.44)$$

Finally, the propagator $K^{\perp}(x, x)_{iakl}$ will transform as

$$K^{\perp}(\vec{x}, \vec{y})_{iakl} \rightarrow \frac{1}{g_2^4(E/E_P)} \tilde{K}^{\perp}(\vec{x}, \vec{y})_{iakl}. \quad (16.45)$$

Thus the total one-loop energy density for the graviton for the distorted GR becomes

$$\frac{\Lambda}{8\pi G} = -\frac{1}{2\tilde{V}} \sum_{\tau} g_1(E/E_P) g_2(E/E_P) \left[\sqrt{E_1^2(\tau)} + \sqrt{E_2^2(\tau)} \right], \quad (16.46)$$

and can be rearranged to give

$$\frac{\Lambda}{8\pi G} = -\frac{1}{3\pi^2} \sum_{i=1}^2 \int_{E^*}^{+\infty} E_i g_1(E/E_P) g_2(E/E_P) \frac{d}{dE_i} \sqrt{\left(\frac{E_i^2}{g_2^2(E/E_P)} - m_i^2(r) \right)^3} dE_i, \quad (16.47)$$

where E^* is the value that annihilates the argument of the root. It is easy to see that if $g_1(E) = g_2(E) = 1$, one recovers the expression (16.27) with a different normalisation factor. It is clear that not every choice of the rainbow's functions will produce a finite integral. This is the case for the following choice on the range $[E^*, +\infty)$

$$g_1(E/E_P) = 1 - \eta(E/E_P)^n \quad \text{and} \quad g_2(E/E_P) = 1, \quad (16.48)$$

where η is a dimensionless parameter and n is an integer [11, 12, 12]. An interesting and promising choice seems to be

$$g_1(E/E_P) = \sum_{i=0}^n \beta_i \frac{E^i}{E_P^i} \exp\left(-\alpha \frac{E^2}{E_P^2}\right), \quad g_2(E/E_P) = 1; \quad \alpha > 0, \beta_i \in \mathbb{R}. \quad (16.49)$$

The use of a ‘‘Gaussian’’ form is dictated by the possibility of doing a comparison with NCG models [13]. That one could obtain a finite result from a one-loop calculation modifying gravity in the high energy sector is not a surprise. Indeed, as shown by Hořava, a modification of Einstein gravity motivated by the Lifshitz theory in solid state physics [13, 14] allows the theory to be power-counting UV renormalisable with the prescription to recover General Relativity in the infrared (IR) limit.

16.3 Correspondence of Gravity's Rainbow with Hořava-Lifshitz Gravity

Following [13, 15] one finds that the Hamiltonian constraint for a FRLW background in Hořava-Lifshitz gravity becomes

$$H = \pi_a^2 + \frac{(3\lambda - 1)}{\kappa^2} 24\pi^4 a^4(t) \left[\frac{6}{a^2(t)} - \frac{12\kappa b}{a^4(t)} - \frac{24\kappa^2 c}{a^6(t)} - 2\Lambda \right] = 0, \quad (16.50)$$

where

$$\begin{aligned} 3g_2 + g_3 &= b, \\ 9g_4 + 3g_5 + g_6 &= c \end{aligned} \tag{16.51}$$

and

$$\begin{aligned} g_0\kappa^{-1} &\equiv 2\Lambda, \\ g_1 &\equiv -1. \end{aligned} \tag{16.52}$$

General Relativity is recovered when $b = c = 0$, which does not necessarily mean that all the couplings are vanishing. The potential part is obtained by imposing the “projectability” condition, which is a weak version of the invariance with respect to time reparametrisations, namely that the lapse function is just a function of time, i.e., $N = N(t)$ [16]. Such a condition also allows for a significant reduction of terms in the potential, since it eliminates the spatial derivatives of N . In this case, and neglecting parity-violating terms, the potential part of the action becomes [17]

$$\begin{aligned} \mathcal{L}_P = N\sqrt{g} \{ &g_0\kappa^{-1} + g_1R + \kappa [g_2R^2 + g_3R^{ij}R_{ij}] \\ &+ \kappa [g_4R^3 + g_5RR^{ij}R_{ij} + g_6R^i_kR^j_kR^k_i \\ &+ g_7R\nabla^2R + g_8\nabla_iR_{jk}\nabla^iR^{jk}] \}, \end{aligned} \tag{16.53}$$

where the couplings g_a ($a = 0 \dots 8$) are all dimensionless and running, and moreover we can set $g_1 = -1$. Let us mention here that the scenario described by the distorted potential Lagrangian (16.53), in the specific case of FLRW geometry, could be considered to arise equivalently in the framework of $f(R)$ gravity, with R the three-dimensional scalar curvature [18]. Indeed, if one starts from the Lagrangian

$$\mathcal{L}_{f(R)} = N\sqrt{g}f(R) \tag{16.54}$$

with

$$\begin{aligned} f(R) &= g_0\kappa^{-1} + g_1R - \frac{\kappa b}{3}R^2 - \frac{\kappa^2 c}{9}R^3, \\ &= 2\Lambda + R \left(1 - 2\pi b \frac{R}{R_0} - 4\pi^2 c \frac{R^2}{R_0^2} \right), \end{aligned} \tag{16.55}$$

and b and c given by (16.51), one will obtain the same equations as those extracted from \mathcal{L}_P in (16.53). Lastly, note that we have used the definitions (16.52), while we have furthermore set

$$R_0 \equiv \frac{6\pi}{G^2} = \frac{6}{l_p^2}. \tag{16.56}$$

Note that a direct correspondence arises if we allow the energy E to evolve depending on t . In this case, we find that the classical Hamiltonian constraint reduces to

$$\mathcal{H} = \tilde{\pi}_a^2 + \frac{12(3\lambda - 1)\pi^4 a^4(t)}{\kappa^2} \left[g_2^2(E(a(t))/E_P) \frac{6}{a^2(t)} - 2\Lambda \right] = 0, \quad (16.57)$$

and if we assume that and we use the definition (16.56), we find

$$\begin{aligned} g_2^2(E(a(t))/E_P) \frac{6}{a^2(t)} &= \frac{6}{a^2(t)} \left[1 - \frac{2\kappa b}{a^2(t)} - \frac{4\kappa^2 c}{a^4(t)} \right] \\ &= 1 - \frac{16bR}{R_0} - \frac{256cR^2}{R_0^2}. \end{aligned} \quad (16.58)$$

Although at first site identification (16.58) seems to be imposed *ad hoc*, it can be supported by invoking the dispersion relation of a massless graviton, which (see the appendix of Ref. [15] for details) for a FLRW background, acquires the form

$$E^2 = \frac{k^2}{a^2(t)}, \quad (16.59)$$

with k the constant dimensionless radial wavenumber. Thus, when Gravity's Rainbow comes into play, we find

$$\frac{E^2}{g_2^2(E(a(t))/E_P)} = \frac{k^2}{a^2(t)}. \quad (16.60)$$

Since the dispersion relation (16.60) is valid at the Planck scale too, we can write

$$\frac{E^2}{g_2^2(E(a(t))/E_P)} \rightarrow \frac{E_P^2}{g_2^2(E_P/E_P)} = E_P^2 = \frac{k^2}{a_P^2}. \quad (16.61)$$

Hence, Eq. (16.58) becomes

$$\begin{aligned} g_2^2(E(a(t))/E_P) &= 1 - \frac{16b\pi R}{R_0} - \frac{256c\pi^2 R^2}{R_0^2} \\ &= 1 - c_1 \frac{E^2(a(t))}{E_P^2} - c_2 \frac{E^4(a(t))}{E_P^4}. \end{aligned} \quad (16.62)$$

Therefore, we deduce that

$$E^2 = R/6k^2 \quad (16.63)$$

with

$$E_P^2 = G^{-1}, \quad c_1 = 16b\pi \quad \text{and} \quad c_2 = 256c\pi^2. \quad (16.64)$$

To summarise, the connection between Gravity's Rainbow and Hořava-Lifshitz gravity offers an interesting opportunity to investigate the possible quantum nature of General Relativity. This opportunity is also corroborated by the fact that, in this

analysis, it is the pure gravitational field and its fluctuations that come into play. Since the quantum fluctuations are represented by the graviton, and it is the only particle present in absence of matter fields, we can argue that it is the graviton itself that is able to distort the gravitational field. From a certain point of view this is not surprising, since gravity is nonlinear. As a consequence of such a distortion, some of the usual divergencies that naturally appear in quantum field theory can be kept under control. This property is also present in Hořava-Lifshitz gravity. Note that the correspondence between the two theories is established through the examination of their Wheeler-De Witt equations. However, although we have explicitly shown this in the case of two physically interesting spacetimes, namely the FLRW and the spherically symmetric ones (see [15] for further details), and thus we have a strong indication that this correspondence is not an artifact of the spacetime symmetries but rather it arises from the features of the two theories, a general proof (or disproof) in the case of arbitrary metrics is still needed. It is interesting to mention that Gravity's Rainbow, in the FLRW background, generates Hořava-Lifshitz gravity under a specific form of $f({}^{(3)}R)$ theory. A similar result was pointed out in [19], where a connection between the rainbow's functions and a specific $f({}^{(3)}R)$ form seems to be evident. These issues reveal that the bridge between Gravity's Rainbow and Hořava-Lifshitz gravity could be much richer, and deserves further investigation.

References

1. B.S. DeWitt, Quantum theory of gravity. 1: the canonical theory. *Phys. Rev.* **160**, 1113–1148 (1967)
2. R. Garattini, Casimir energy and the cosmological constant. *TSPU Bull.* **44N7**, 72–80 (2004). [arXiv:gr-qc/0409016](#)
3. G. Amelino-Camelia, F. D'Andrea, G. Mandanici, Group velocity in noncommutative spacetime. *JCAP* **0309**, 006 (2003). [arXiv:hep-th/0211022](#)
4. R.L. Arnowitt, S. Deser, C.W. Misner, The dynamics of general relativity. *Gen. Rel. Grav.* **40**, 1997–2027 (2008). [arXiv:gr-qc/0405109](#)
5. A. Vilenkin, Quantum cosmology and the initial state of the universe. *Phys. Rev. D* **37**, 888 (1988)
6. S. Capozziello, R. Garattini, The cosmological constant as an eigenvalue of $f(R)$ -gravity hamiltonian constraint. *Class. Quant. Grav.* **24**, 1627–1646 (2007). [arXiv:gr-qc/0702075](#)
7. R. Garattini, M. Faizal, Cosmological constant from a deformation of the Wheeler-DeWitt equation. *Nucl. Phys. B* **905**, 313–326 (2016). [arXiv:1510.04423](#)
8. R. Garattini, M. Sakellariadou, Does gravity's rainbow induce inflation without an inflaton? *Phys. Rev. D* **90**(4), 043521 (2014). [arXiv:1212.4987](#)
9. R. Garattini, G. Mandanici, Modified dispersion relations lead to a finite zero point gravitational energy. *Phys. Rev. D* **83**, 084021 (2011). [arXiv:1102.3803](#)
10. J. Magueijo, L. Smolin, *Class. Quant. Grav.* Gravity's rainbow **21**, 1725–1736 (2004). [arXiv:gr-qc/0305055](#)
11. Y. Ling, Rainbow universe. *JCAP* **0708**, 017 (2007). [arXiv:gr-qc/0609129](#)
12. Y. Ling, X. Li, H.-B. Zhang, Thermodynamics of modified black holes from gravity's rainbow. *Mod. Phys. Lett. A* **22**, 2749–2756 (2007). [arXiv:gr-qc/0512084](#)
13. R. Garattini, P. Nicolini, A Noncommutative approach to the cosmological constant problem. *Phys. Rev. D* **83**, 064021 (2011). [arXiv:1006.5418](#)

14. P. Horava, Membranes at quantum criticality. *JHEP* **03**, 020 (2009). [arXiv:0812.4287](#)
15. R. Garattini, E.N. Saridakis, Gravity's rainbow: a bridge towards Hořava-Lifshitz gravity. *Eur. Phys. J. C* **75**(7), 343 (2015). [arXiv:1411.7257](#)
16. P. Horava, Quantum gravity at a lifshitz point. *Phys. Rev. D* **79**, 084008 (2009). [arXiv:0901.3775](#)
17. R. Garattini, Casimir energy, the cosmological constant and massive gravitons. *J. Phys. Conf. Ser.* **33**, 215–220 (2006). [arXiv:gr-qc/0510062](#)
18. R. Garattini, Distorting general relativity: gravity's rainbow and $f(R)$ theories at work. *JCAP* **1306**, 017 (2013). [arXiv:1210.7760](#)
19. G.J. Olmo, Palatini actions and quantum gravity phenomenology. *JCAP* **1110**, 018 (2011). [arXiv:1101.2841](#)

Chapter 17

Quantum Cosmology in Modified Theories of Gravity



Mariam Bouhmadi-López and Prado Martín-Moruno

Singularities are commonplace in gravitational theories. In particular, singularities tend to form at the beginning of the Universe through the Big Bang or during gravitational collapse, like in black holes. Curvature becomes increasingly large as one approaches those singularities, which indicates that the new physics could come into play near them. Therefore, quantum gravitational effects are usually expected to cure spacetime singularities and this effect is intrinsic to any gravitational theory, in particular to any modified or extended theory of gravity. In the next few pages we will give a brief account of quantum cosmology in modified theories of gravity within the metric and the Palatini approach. Please bear in mind that so far there is no consensus on how a fundamental theory encapsulating gravity and quantum physics should be constructed, and it is still currently a very active area of research. However, it is expected that a fundamental quantum theory of gravity is necessary, such that some pathologies within gravitational theories at high energy scales can be resolved, such as the non-renormalisability of the theory or the appearance of singularities (in case that those pathologies are also present in the new theory).

One of the promising approaches to tackle this issue is based on the quantum geometrodynamics in which the Wheeler-DeWitt (WDW) equation describes the quantum state of the Universe as a whole through its wave function [1]. Alterna-

M. Bouhmadi-López (✉)

IKERBASQUE, Basque Foundation for Science, 48011 Bilbao, Spain

Department of Theoretical Physics, University of the Basque Country UPV/EHU,

P.O. Box 644, 48080 Bilbao, Spain

e-mail: mariam.bouhmadi@ehu.es

P. Martín-Moruno

Departamento de Física Teórica and IPARCOS, Universidad Complutense de Madrid,

28040 Madrid, Spain

e-mail: pradomm@ucm.es

© The Author(s), under exclusive license to Springer Nature Switzerland AG 2021

E. N. Saridakis et al. (eds.) *Modified Gravity and Cosmology*,

https://doi.org/10.1007/978-3-030-83715-0_17

tive approaches to quantum gravity include path integrals, loop quantum gravity and string theory, but they will not be covered here. The WDW equation in General Relativity (GR) is deduced through the Hamiltonian constraint defined by the Einstein equation. Therefore, as it is natural whenever the gravitational action, or equivalently the equation of motions are modified, we expect to get a new modified WDW equation. In addition, if the solution to the WDW equation satisfies the DeWitt (DW) boundary condition [1], that is, it vanishes at the classical singularity, we may claim that the singularity is expected to be avoidable through quantum effects. We expect, this condition, in principle, to be independent of the WDW equation. In the coming subsections, we will briefly summarise how this approach can be applied to some modified theories of gravity.

17.1 Quantum Cosmology in a Metric Theory

As this extensive review shows, there are plenty of metric theories. The simplest—and in many aspect best-suited for observations of the early- and the late-universe—is the $f(R)$ metric approach, which, for example, describes perfectly the early inflationary era through the Starobinsky model [2]. The Starobinsky inflationary model was quantised about thirty years ago. To this end, it was necessary to obtain the correct modified WDW equation for a homogeneous and isotropic universe after introducing at the classical level a proper Lagrange multiplier that takes into account the relation between the size of the Universe, i.e., the scalar factor, and the curvature as measured through the scalar curvature [3]. We remind readers at this point that an $f(R)$ metric theory (different from GR) has a further degree of freedom, named the scalaron. It is therefore not surprising that for a homogeneous and isotropic universe, the WDW equation in this case has two degrees of freedom, even for an empty universe. A quantum approach for a more general class of higher-derivative theories was analysed in the references [4, 5].

In addition, dark energy singularities in this type of theories have been recently analysed: (i) the Big Rip singularity in the framework of $f(R)$ quantum geometrodynamics and invoking the DeWitt criterion has been analysed in [6], where the existence was shown of solutions to the WDW equation that vanishes when approaching the singularity, i.e., fulfilling this condition; similarly, (ii) the Little Sibling of the Big Rip in the framework of $f(R)$ quantum geometrodynamics was analysed in [7]. For a recent review on dark energy singularities, please see [8]. It is very important to highlight that this equation is always hyperbolic for any $f(R)$ -cosmology, even if the classical model mimics a phantom expansion.

17.2 Quantum Cosmology in a Palatini Theory

Likewise, there is a plethora of extended theories of gravity within the Palatini approach; here we will focus on the Eddington-inspired-Born-Infeld (EiBI) scenario proposed in [9] which is appealing for several theoretical aspects: (i) it reduces to GR in vacuum, unlike $f(R)$ metric theories, and deviates from it when matter fields are included. (ii) Due to the structure of the gravitational action (there is a square root in front of the linear combination that involves the curvature of spacetime), the curvature scale and the energy scale seem to be bounded from above (at least when the strong energy condition is fulfilled) and the Big Bang singularity is naturally avoided in the EiBI gravity [9]. (iii) The theory is simple in the sense that it only contains one free additional parameter, the Born-Infeld constant, as compared with GR. (iv) This scenario is free of ghost instabilities because the theory is constructed through a Palatini variational principle; i.e., the connection is different from the Levi-Civita connection. The interested reader can see [10] to check the conditions that Palatini higher-order theories have to satisfy to avoid those instabilities. In fact, the idea of including the Born-Infeld structure into the gravitational theory was proposed in [11] but within a metric variational principle inducing, in principle, ghost degrees of freedom, due to the higher-order derivative terms in the field equations. The EiBI theory, however, is formulated via the Palatini variational principle. The field equations only contain up to second-order derivatives, and consequently no ghost is present in the theory. The applications and several properties of the EiBI gravity have been studied widely in the literature; see [12] for a nice review on the topic. Some approaches to quantise EiBI gravity have been proposed in [13–18].

In fact, in [14, 17] instantons were analysed showing, for example, that $O(4)$ -symmetric regular instanton solutions can deviate from those of GR, and in particular the singular Vilenkin instanton and the Hawking-Turok instanton (in GR) can be regular under certain conditions. Moreover, in [13, 15, 16, 18] the modified WDW equation in the EiBI scenario was analysed. In fact, this involves a very careful analysis of the classical Hamiltonian, and in particular of the primary and secondary constraints. It can be shown that the total Hamiltonian is a first class constraint. After identifying the independent constraints of the theory and using the Poisson brackets of all those constraints, one can identify any gauge degree of freedom of the theory and fix it. Finally, the quantisation of the system requires a proper use of Dirac brackets and the promotion of the first class constraint of the total Hamiltonian as a restriction on the Hilbert space, where the wave function of the Universe is defined. This approach has been used in several EiBI models with several kinds of matter contents: perfect fluids, standard scalar field as well as phantom scalar fields, and it has been shown successfully that cosmological singularities are removed at the quantum level.

In summary, modified theories of gravity in many cases need to be quantised like GR, and at the same time they offer a splendid new arena to further explore the most suitable or even the correct path to get a consistent quantum gravity theory. In this sense, there is still a lot of interesting and important work to be carried on.

References

1. C. Kiefer, *Quantum Gravity*, International Series of Monographs on Physics (OUP Oxford, 2007)
2. A.A. Starobinsky, A new type of isotropic cosmological models without singularity. *Adv. Ser. Astrophys. Cosmol.* **3**, 130–133 (1987)
3. A. Vilenkin, Classical and quantum cosmology of the starobinsky inflationary model. *Phys. Rev. D* **32**, 2511 (1985)
4. S.W. Hawking, J.C. Luttrell, Higher derivatives in quantum cosmology. I: the isotropic case. *Nucl. Phys. B* **247**, 250 (1984). (*Adv. Ser. Astrophys. Cosmol.* **3**, 256 (1987))
5. G.T. Horowitz, Quantum cosmology with a positive definite action. *Phys. Rev. D* **31**, 1169 (1985). (*Adv. Ser. Astrophys. Cosmol.* **3**, 292 (1987))
6. A. Alonso-Serrano, M. Bouhmadi-López, P. Martín-Moruno, $f(R)$ quantum cosmology: avoiding the big rip. *Phys. Rev. D* **98**(10), 104004 (2018). [arXiv:1802.03290](https://arxiv.org/abs/1802.03290)
7. T.B. Vasilev, M. Bouhmadi-López, P. Martín-Moruno, Classical and quantum fate of the little sibling of the big rip in $f(R)$ cosmology. *Phys. Rev. D* **100**(8), 084016 (2019). [arXiv:1907.13081](https://arxiv.org/abs/1907.13081)
8. M. Bouhmadi-López, C. Kiefer, P. Martín-Moruno, Phantom singularities and their quantum fate: general relativity and beyond-a CANTATA COST action topic. *Gen. Rel. Grav.* **51**(10), 135 (2019). [arXiv:1904.01836](https://arxiv.org/abs/1904.01836)
9. M. Banados, P.G. Ferreira, Eddington's theory of gravity and its progeny. *Phys. Rev. Lett.* **105**, 011101 (2010). [arXiv:1006.1769](https://arxiv.org/abs/1006.1769). (Erratum: *Phys. Rev. Lett.* **113**(11), 119901 (2014))
10. J. Beltrán Jiménez, A. Delhom, Ghosts in metric-affine higher order curvature gravity. [arXiv:1901.08988](https://arxiv.org/abs/1901.08988)
11. S. Deser, G.W. Gibbons, Born-Infeld-Einstein actions? *Class. Quant. Grav.* **15**, L35–L39 (1998). [arXiv:hep-th/9803049](https://arxiv.org/abs/hep-th/9803049)
12. J.B. Jimenez, L. Heisenberg, G.J. Olmo, D. Rubiera-Garcia, Born-Infeld inspired modifications of gravity. *Phys. Rept.* **727**, 1–129 (2018). [arXiv:1704.03351](https://arxiv.org/abs/1704.03351)
13. M. Bouhmadi-López, C.-Y. Chen, Towards the quantization of Eddington-inspired-Born-Infeld theory. *JCAP* **1611**, 023 (2016). [arXiv:1609.00700](https://arxiv.org/abs/1609.00700)
14. F. Arroja, C.-Y. Chen, P. Chen, D.-H. Yeom, Singular instantons in Eddington-inspired-Born-Infeld gravity. *JCAP* **1703**, 044 (2017). [arXiv:1612.00674](https://arxiv.org/abs/1612.00674)
15. I. Albarran, M. Bouhmadi-López, C.-Y. Chen, P. Chen, Doomsdays in a modified theory of gravity: a classical and a quantum approach. *Phys. Lett. B* **772**, 814–818 (2017). [arXiv:1703.09263](https://arxiv.org/abs/1703.09263)
16. M. Bouhmadi-López, C.-Y. Chen, P. Chen, On the consistency of the wheeler-dewitt equation in the quantized Eddington-inspired Born-Infeld gravity. *JCAP* **1812**(12), 032 (2018). [arXiv:1810.10918](https://arxiv.org/abs/1810.10918)
17. M. Bouhmadi-López, C.-Y. Chen, P. Chen, D.-H. Yeom, Regular instantons in the Eddington-inspired-Born-Infeld gravity: lorentzian wormholes from bubble nucleations. *JCAP* **1810**, 056 (2018). [arXiv:1809.06579](https://arxiv.org/abs/1809.06579)
18. I. Albarran, M. Bouhmadi-López, C.-Y. Chen, P. Chen, Quantum cosmology of Eddington-Born-Infeld gravity fed by a scalar field: the big rip case. *Phys. Dark Univ.* **23**, 100255 (2019). [arXiv:1811.05041](https://arxiv.org/abs/1811.05041)

Part II
Testing Relativistic Effects

Chapter 18

Introduction to Part II



Mariafelicia De Laurentis and Gonzalo J. Olmo

The confrontation of gravitation theories with experimental and observational data is a fundamental step in the scientific process. The analysis of relativistic effects is not only necessary but essential for this purpose. Laboratory tests typically search for fifth force effects in the form of short range interactions, which can introduce departures from Newton's law via Yukawa-type corrections mediated by some kind of massive degree of freedom. In some cases this may require going beyond the linearized approximation due to the existence of screening mechanisms that may hide these (chameleon) interactions, which poses severe experimental challenges for current technologies such as atomic interferometry, torsion balance experiments, Casimir force, dipole moment tests, ... Screening mechanisms can also be constrained via Lunar ranging, by measuring cosmic filaments, and by probing the nonlinear regime of cosmological perturbations.

The effects of modified gravitational dynamics may also arise via nonlinearities induced by the stress-energy densities rather than by new propagating degrees of freedom, thus leading to new phenomena, which do not involve fifth force interactions. This can have nontrivial effects even in scenarios involving elementary par-

M. De Laurentis

Istituto Nazionale di Fisica Nucleare (INFN), Sezione di Torino, Via P. Giuria 1,

I-10125 Torino, Italy

e-mail: mariafelicia.delarentis@unina.it

Dipartimento di Fisica "E. Pancini", Università di Napoli "Federico II", 80126 Napoli, Italy

Laboratory for Theoretical Cosmology, Tomsk State University of Control Systems and

Radioelectronics (TUSUR), 634050 Tomsk, Russia

G. J. Olmo (✉)

Depto. de Física Teórica and IFIC, Centro Mixto Universidad de Valencia-CSIC, 46100 Burjassot, Valencia, Spain

Departamento de Física, Universidade Federal da Paraíba, João Pessoa, Paraíba 58051-900, Brazil

© The Author(s), under exclusive license to Springer Nature Switzerland AG 2021

281

E. N. Saridakis et al. (eds.) *Modified Gravity and Cosmology*,

https://doi.org/10.1007/978-3-030-83715-0_18

ticles if one focuses on aspects not related to curvature but to non-metricity and/or torsion. However, from an effective field theory perspective, such new interactions could fit naturally in an extended matter framework; the universality of certain couplings could reveal an underlying geometric structure, thus showing that elementary particle experiments could complement astrophysical tests to unveil modified gravity effects. The possibility of having new gravitational physics induced by nonlinearities in the matter sector may also have an impact on the structural properties of self-gravitating systems. In very low mass stars, where the equation of state of the gas is well understood, modifications in the Newtonian dynamics can change the threshold for sustained hydrogen burning reactions, offering new observables in the search for departures from the predictions of GR. In compact objects such as neutron stars, on the other hand, these interactions could lead to new degeneracies with the matter sector, complicating even more the quest for the properties of the nuclear matter equation of state. In order to break such degeneracies, it is important to identify observables that may lead to universal relations able to tell different gravity theories apart. Some of these relations involve the moment of inertia, asteroseismology, quasi-normal modes, etc, and it has been shown that massive scalar degrees of freedom could manifest themselves clearly in sufficiently separated binary systems and in quasi-normal modes spectra.

Orbital motions and lensing are also key probes for modifications of gravity. The parametrised post-Newtonian formalism developed in the 1970s allows us to confront very different types of theories with observations by just computing certain key coefficients in the appropriate limit and gauge choice. This formalism must be extended in order to accommodate new theories, which do not quite fit within this original framework.

Beyond stellar objects and the slow motion limit, strong gravity effects, such as gravitational waves and strong lensing, typically involving black holes, also offer a glimpse of potentially new gravitational phenomena, including the quantum regime.

Chapter 19

Laboratory Constraints



Anne-Christine Davis and Benjamin Elder

Dark energy is a cosmological phenomenon per se [1]. In this chapter we will describe attempts to detect effects of the physics of modified gravity, motivated by dark energy and the cosmological constant problem, in the laboratory. Classical effects of modified gravity can be tested by fifth force searches, where new classical interactions could influence the motion of test masses [2]. The quantum nature of the modifications can also be probed using the Casimir effect [3], atom [4, 5] and neutron [6] interferometry, the neutron energy levels in vacuum [7], atomic spectra [8, 9] and the electron magnetic moment [10]. For a recent review, see [11]. We will restrict our attention to scalar-tensor theories with a coupling between a scalar field and matter.

Laboratory tests of gravity have a long history, and the need to make cosmological theories of dark energy and modified gravity compatible with laboratory and Solar System tests was a key motivation for the introduction of screening mechanisms. Screening allows for modified gravity theories to evade traditional tests of gravity, whilst still modifying gravity cosmologically. However, carefully designed laboratory experiments can allow the effects of the scalar field to be unscreened. The additional level of precision and control that we have in the laboratory then means that these measurements tend to be extremely constraining for cosmological modified gravity theories. Laboratory tests probe the theory in the nonlinear regime, unlike cosmological tests where the linear regime is easiest to test. Probing

A.-C. Davis (✉)

DAMTP, Centre for Mathematical Sciences, University of Cambridge,
Cambridge CB3 0WA, UK
e-mail: a.c.davis@damtp.cam.ac.uk

B. Elder

School of Physics and Astronomy, University of Nottingham, Nottingham NG7 2RD, UK
e-mail: Benjamin.Elder@nottingham.ac.uk

Department of Physics and Astronomy, University of Hawai'i, Watanabe Hall, 2505,
Correa Road, Honolulu, HI 96822, USA

the nonlinear regime necessitates a case-by-case analysis, since a model independent parameterised description is not yet available for laboratory tests.

Laboratory experiments are most effective at constraining theories, which screen through a chameleon-like mechanism, i.e., *thin-shell* theories. Thin-shell theories have the advantage that the scalar field responds rapidly to changes in density, meaning that even if the effects of the scalar are screened in the Solar System they can be unscreened by a laboratory vacuum chamber. Other theories, notably Galileons [12], do not have this property and are therefore not as tightly constrained by laboratory tests, so in this chapter we restrict our attention to thin-shell theories.

In this section we will first describe how a thin-shell scalar behaves in a laboratory vacuum, and then go on to detail the laboratory experiments, which currently are the most constraining for chameleon models. For convenience's sake, we focus on the prototypical chameleon model [13, 14]

$$V_{\text{eff}}(\phi) = \frac{\Lambda^{4+n}}{\phi^n} + \frac{\beta}{M_{Pl}}\phi\rho_m + \dots, \quad (19.1)$$

where ρ_m is the ambient matter density, $M_{Pl} \equiv (8\pi G)^{-1/2}$, and the \dots includes a cosmological constant piece, as chameleons do not lead to self-acceleration. The coupling of the chameleon field ϕ to matter may be understood as originating from a coupling function $A(\phi) = e^{\beta\phi/M_{Pl}}$, which rescales the metric between the Jordan and Einstein frames.

19.1 Chameleons in Laboratory Vacuums

The chameleon scalar field changes its mass $m \equiv \frac{d^2}{d\phi^2} V_{\text{eff}}(\phi)$ as a function of the local matter density ρ_m . We consider here an idealised vacuum chamber, which is spherical with internal radius L , internal density ρ_{vac} and walls of density ρ_{wall} and thickness T . If $T > 1/m(\rho_{\text{wall}})$, then the field has sufficient room to minimise its effective potential within the vacuum chamber walls. This greatly simplifies our calculations, as it guarantees that the interior of the vacuum chamber is effectively shielded from external objects. Whilst the condition $T > 1/m(\rho_{\text{wall}})$ needs to be checked experiment by experiment, and model by model, in general we find that this is satisfied for chameleon models of interest if $T \gtrsim 1$ mm.

In the interior of the vacuum chamber the density is much smaller than within the walls, therefore inside the vacuum chamber the chameleon field will try to reach the minimum of its effective potential in this lower density ρ_{vac} . This is only possible if there is sufficient room for the scalar field to do so, that is, if $L > 1/m(\rho_{\text{vac}})$. If this condition is not met, then the chameleon takes a value such that its Compton wavelength is of the order of the size of the vacuum chamber $L \approx 1/m(\rho_{\text{vac}})$. In general, one needs to compute the chameleon profile inside the vacuum chamber numerically [15, 16].

Whether or not an object is screened depends on the value of the scalar field in the interior of the object ϕ_{obj} , and the background value that the scalar would take if the source were absent, ϕ_{vac} . The advantage of performing experiments in laboratory vacua is that the difference $|\phi_{\text{vac}} - \phi_{\text{obj}}|$ can be very large. Furthermore, the range of the chameleon force inside the vacuum chamber is approximately $1/m_{\text{vac}}$, which can stretch to \sim cm scales, making it far easier to detect the fifth force in vacuum than in the atmosphere.

In large parts of the chameleon parameter space, very small (but dense) objects like neutrons, atomic nuclei and silica microspheres can be unscreened in vacua with $L \sim 10$ cm and $\rho_{\text{vac}} \sim 10^{-17}$ g/cm³, which makes them excellent test masses. In the following sub-sections we review the most constraining experiments for chameleon models. These constraints are summarised in Fig. 19.1.

19.2 Atom Interferometry

Atom interferometry is a well-established technique to measure the external forces acting on a single atom [18]. It functions in a manner somewhat analogous to the classic double slit experiment. The atom's wave function is split into two parts, which are sent along different trajectories and then overlapped again at a later point in time. Any difference in the quantum mechanical phase that is accumulated along the paths results in interference at the end point.

This process is accomplished in the following manner. First, a small cloud of cold atoms are placed in free-fall inside a vacuum chamber. The atoms are then subjected to a pulse of laser light, the frequency and duration of which are chosen such that each atom has a 50% probability of absorbing a photon and its momentum and being kicked into an excited state. This splits the wavefunction of each individual atom into two wavepackets, travelling along slightly different trajectories. A short time T later, a second laser pulse is timed such that atoms in the ground state have a 100% probability of absorbing a photon, and the atoms in the excited state have a 100% probability of undergoing stimulated emission. This reverses the relative motion of the wavepackets, so that they overlap after another T seconds. At that time, a third 50% pulse recombines and interferes the wavepackets, and the relative phase accumulated along the two paths may be measured by counting the numbers of atoms in the ground and excited states.

Relative phase differences may be due to a difference in the accumulated action along each path, or from differences in the phase inherited from the photon at each photon absorption and stimulated emission event. If the atoms experience a constant acceleration along the direction of the laser pulses, then the total phase difference is particularly simple, and the probability to find the atoms in the initial state is

$$P \propto \cos^2(akT^2), \quad (19.2)$$

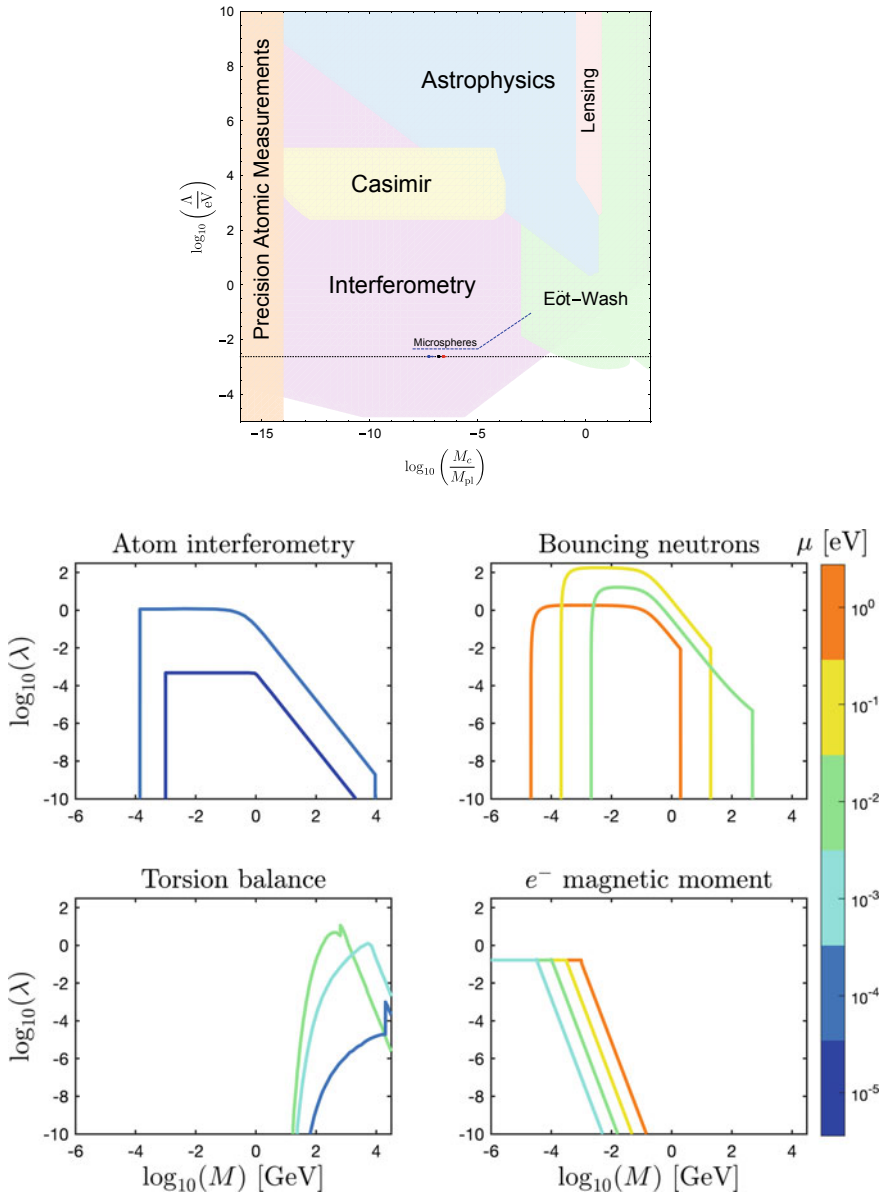


Fig. 19.1 **Upper:** Experimental constraints on the chameleon self-coupling Λ and coupling to matter $M_c = \frac{M_{\text{Pl}}}{\beta}$, for the chameleon potential $V(\phi) = \Lambda^5/\phi$ [17]. Shaded regions are ruled out. **Lower:** Constraints on the symmetron parameters μ, λ, M . The area below each curve is ruled out. The symmetron has three parameters (as opposed to two parameters for the simplest chameleon model), hence bounds are plotted separately for improved readability. The constraints deriving from measurements of the electron’s magnetic moment extend into other regions of parameter space as well; see [10] for details. Some caution is warranted in interpreting constraints on exceedingly large or small values of λ ; again, see [10] for a discussion

where k is the photon momentum, T is the time between laser pulses (so that $2T$ is the duration of the experiment), and a is the constant acceleration.

The acceleration a includes all external forces acting on the atom, including Newtonian gravity and any new fifth forces. To constrain the latter, the experiment is performed with an *in-vacuum* source mass near the atoms. The experiment is performed twice, with the source mass nearby and again with the source mass far away, such that the force due to the source mass may be isolated. After subtracting out the ordinary Newtonian gravitational force, any leftover signal would be due to new interactions, such as chameleons.

The source mass is typically sufficiently large that it will be screened, but the atomic nuclei are small enough that, as discussed in the previous subsection, they are unscreened over a large range of the parameter space [15, 19, 20], making them sensitive probes of the chameleon field. Experiments searching for chameleon accelerations with atom interferometry have reached a sensitivity of $\approx 10^{-8}g$ [4, 5, 21, 22], where $g \equiv GM_{\text{Earth}}/R_{\text{Earth}}$ is the gravitational acceleration at the surface of the Earth.

19.3 Eöt-Wash

Torsion balance experiments have a long history of searching for fifth forces and modifications of gravity. The underlying principle is to have one or more test masses suspended, and to look for deflections of the test masses towards source masses by measuring the torsion in the suspension of the test masses. Commonly, the source and test masses are arranged so that the inverse-square contribution to the total force is cancelled, and the experiment is only sensitive to deviations from standard gravity.

The current best constraints come from the Eöt-Wash experiment [23], which uses circular disks for the masses. The disks have holes bored into them and are arranged one above the other, so that if there are no modifications to gravity then there is expected to be no net torque between the two plates. Recent constraints on fifth forces are discussed in [24, 25].

19.4 Casimir

The Casimir force is an effect predicted by quantum electrodynamics, which is absent in classical physics. It is the force that arises between two parallel plates, placed in vacuum, due to the quantum fluctuations of the electromagnetic field in the space between the plates. This force scales as d^{-4} , where d is the distance between the plates, and therefore is most easily detected when the plates are placed close together. Current experiments probe sub-mm and sub-micron distance scales [26]. If fifth forces exist they could also be detected by an experiment searching for Casimir effects. These experiments are particularly sensitive to screening through the thin-

shell effect, as close to the surface of a source the field is changing rapidly, giving rise to potentially detectable forces. The chameleon force (per unit area) between two plates scales as [27]

$$\frac{F_{\text{cham}}}{A} \propto d^{-\frac{2n}{n+2}}. \quad (19.3)$$

The experimental challenge for such a search is to make the two plates perfectly smooth and to keep the plates perfectly parallel. In practice it may be easier to search for the Casimir effect between a plate and a sphere. Current searches for the Casimir force are most constraining for chameleon models with $n = -4$ and $n = -6$, when Λ_c is fixed to the dark energy scale. Further sensitivity to the chameleon could be obtained by varying the density of the gas between the two plates [28], or by using a sphere and plate experiment, which enables different distances to be investigated, as in [29].

19.5 Neutron, Atomic and Electron Dipole Moment Tests

New fifth forces would also change the quantum energy spectrum of ultra-cold neutrons in the gravitational potential of the Earth. A spectroscopic technique based on the Rabi resonance method has been used to constrain the parameters of popular dark energy models [30].

As previously discussed, atomic nuclei can be unscreened in a laboratory vacuum. The nuclei can be considered as the source of a chameleon field that is probed by the orbiting electrons. If the unscreened chameleon force is very strong then this could cause measurable perturbations to atomic energy levels. The most precise measurements currently are of the structure of hydrogenic atoms. Shifts to the lowest energy levels due to a chameleon force can occur and are discussed in [8, 9]. In [9], constraints were imposed on the coupling of the chameleon to matter and also to photons. Similarly, fifth forces induce additional quantum corrections to the electron dipole moment, which also leads to constraints [10].

19.6 The Symmetron

The symmetron is another quintessential example of a screened modification to gravity [31]. The symmetron is similar to the chameleon in that it has a canonical kinetic term, and its screening is through terms that are nonlinear in the field. However, the difference between the models is that while the chameleon screens because mass varies depending on its environment, the symmetron screens primarily because the strength of its coupling to matter is allowed to vary dynamically. This is possible thanks to the symmetron's spontaneous symmetry breaking potential, which con-

tains a coupling to matter such that regions of high density restore the symmetry, effectively shutting off the coupling to matter.

To see this concretely, the symmetron effective potential is

$$V_{\text{eff}}(\phi) = \frac{1}{2} \left(-\mu^2 + \frac{\rho}{M^2} \right) \phi^2 + \frac{\lambda}{4!} \phi^4, \quad (19.4)$$

where μ is the bare mass of the symmetron, M the energy scale controlling strength of the coupling to matter, and λ the dimensionless constant controlling the self-interactions of the field. The form of the coupling to matter also means that the symmetron fifth force experienced by a test particle is $\mathbf{F} = \phi \nabla \phi / M^2$. Note that the strength of the force is scaled by the local field value consequently, in dense regions where $\rho > \mu^2 M^2$, the field is driven to $\phi \rightarrow 0$ and the fifth force shuts off.

As can be seen from Eq. (19.4) the mass of the symmetron in the symmetry broken phase is approximately μ . Unlike the chameleon, therefore, the symmetron does not have the ability to adjust its mass in the low density environment of a laboratory vacuum chamber. If the Compton wavelength of the symmetron is larger than the size of the vacuum chamber, $\mu L \ll 1$, the field is not able to vary within the chamber and so no fifth force can be present. Conversely, if the Compton wavelength of the symmetron is smaller than the distances probed in the experiment (for example, the distance between test and source masses), then the fifth force will be exponentially suppressed by the Yukawa term e^{-md} , where m is the symmetron mass and d the distance between two objects. This means that any experiment is only sensitive to symmetron models whose masses fall between these two limits.

Constraints on the symmetron model have recently been computed for all of the experiments described above, and the bounds are summarised in Fig. 19.1. Casimir constraints are very recent [32] and use a sphere and plate, with the experiment probing two different distances by a clever set-up similar to that described in [29]. As the full details of that experiment are not yet available, those constraints are not presently included.

19.7 Conclusions

In summary, laboratory tests of gravity contain a wealth of information about dark energy and modifications to gravity. The rich phenomenology of screened theories in particular leads us to look for new physics in novel and sometimes surprising ways. As these experiments probe the nonlinear regime, there is no model-independent way to connect these constraints to the parametrised linear and quasi-linear theories used to obtain cosmological constraints. However, once a model is specified, that connection can be made clear.

References

1. P. Brax, What makes the Universe accelerate? a review on what dark energy could be and how to test it. *Rept. Prog. Phys.* **81**(1), 016902 (2018)
2. D.J. Kapner, T.S. Cook, E.G. Adelberger, J.H. Gundlach, B.R. Heckel, C.D. Hoyle, H.E. Swanson, Tests of the gravitational inverse-square law below the dark-energy length scale. *Phys. Rev. Lett.* **98**, 021101 (2007). [arXiv:hep-ph/0611184](#)
3. S.K. Lamoreaux, Demonstration of the Casimir force in the 0.6 to 6 micrometers range. *Phys. Rev. Lett.* **78**, 5–8 (1997). (Erratum: *Phys. Rev. Lett.* **81**, 5475 (1998))
4. P. Hamilton, M. Jaffe, P. Haslinger, Q. Simmons, H. Müller, J. Khoury, Atom-interferometry constraints on dark energy. *Science* **349**, 849–851 (2015). [arXiv:1502.03888](#)
5. D.O. Sabulsky, I. Dutta, E.A. Hinds, B. Elder, C. Burrage, E.J. Copeland, Experiment to detect dark energy forces using atom interferometry. *Phys. Rev. Lett.* **123**(6), 061102 (2019). [arXiv:1812.08244](#)
6. H. Lemmel, P. Brax, A.N. Ivanov, T. Jenke, G. Pignol, M. Pitschmann, T. Potocar, M. Wellenzohn, M. Zawisky, H. Abele, Neutron Interferometry constrains dark energy chameleon fields. *Phys. Lett. B* **743**, 310–314 (2015). [arXiv:1502.06023](#)
7. V.V. Nesvizhevsky et al., Measurement of quantum states of neutrons in the earth’s gravitational field. *Phys. Rev. D* **67**, 102002 (2003). [arXiv:hep-ph/0306198](#)
8. P. Brax, C. Burrage, Atomic precision tests and light scalar couplings. *Phys. Rev. D* **83**, 035020 (2011). [arXiv:1010.5108](#)
9. L.K. Wong, A.-C. Davis, One-electron atoms in screened modified gravity. *Phys. Rev. D* **95**(10), 104010 (2017). [arXiv:1703.05659](#)
10. P. Brax, A.-C. Davis, B. Elder, L.K. Wong, Constraining screened fifth forces with the electron magnetic moment. *Phys. Rev. D* **97**(8), 084050 (2018). [arXiv:1802.05545](#)
11. P. Brax, C. Burrage, A.-C. Davis, Laboratory constraints. *Int. J. Mod. Phys. D* **27**(15), 1848009 (2018)
12. A. Nicolis, R. Rattazzi, E. Trincherini, The Galileon as a local modification of gravity. *Phys. Rev. D* **79**, 064036 (2009). [arXiv:0811.2197](#)
13. J. Khoury, A. Weltman, Chameleon fields: awaiting surprises for tests of gravity in space. *Phys. Rev. Lett.* **93**, 171104 (2004). [arXiv:astro-ph/0309300](#)
14. P. Brax, C. van de Bruck, A.-C. Davis, J. Khoury, A. Weltman, Detecting dark energy in orbit: the cosmological chameleon. *Phys. Rev. D* **70**, 123518 (2004). [arXiv:astro-ph/0408415](#)
15. B. Elder, J. Khoury, P. Haslinger, M. Jaffe, H. Müller, P. Hamilton, Chameleon dark energy and atom interferometry. *Phys. Rev. D* **94**(4), 044051 (2016). [arXiv:1603.06587](#)
16. S. Schlögel, S. Clesse, A. Füzfa, Probing modified gravity with atom-interferometry: a numerical approach. *Phys. Rev. D* **93**(10), 104036 (2016). [arXiv:1507.03081](#)
17. C. Burrage, J. Sakstein, A compendium of chameleon constraints. *JCAP* **1611**(11), 045 (2016). [arXiv:1609.01192](#)
18. A. Peters, K.Y. Chung, S. Chu, Measurement of gravitational acceleration by dropping atoms. *Nature* **400**(6747), 849–852 (1999)
19. C. Burrage, E.J. Copeland, E. Hinds, Probing dark energy with atom interferometry. [arXiv:1408.1409](#)
20. C. Burrage, E.J. Copeland, Using atom interferometry to detect dark energy. *Contemp. Phys.* **57**(2), 164–176 (2016). [arXiv:1507.07493](#)
21. C. Burrage, A. Kuribayashi-Coleman, J. Stevenson, B. Thrussell, Constraining symmetron fields with atom interferometry. *JCAP* **1612**, 041 (2016). [arXiv:1609.09275](#)
22. M. Jaffe, P. Haslinger, V. Xu, P. Hamilton, A. Upadhye, B. Elder, J. Khoury, H. Müller, Testing sub-gravitational forces on atoms from a miniature, in-vacuum source mass. *Nat. Phys.* **13**, 938 (2017). [arXiv:1612.05171](#)
23. E.G. Adelberger, B.R. Heckel, A.E. Nelson, Tests of the gravitational inverse square law. *Ann. Rev. Nucl. Part. Sci.* **53**, 77–121 (2003). [arXiv:hep-ph/0307284](#)
24. A. Upadhye, Dark energy fifth forces in torsion pendulum experiments. *Phys. Rev. D* **86**, 102003 (2012). [arXiv:1209.0211](#)

25. A. Upadhye, Symmetron dark energy in laboratory experiments. *Phys. Rev. Lett.* **110**(3), 031301 (2013). [arXiv:1210.7804](#)
26. S.K. Lamoreaux, W.T. Buttler, Thermal noise limitations to force measurements with torsion pendulums: applications to the measurement of the Casimir force and its thermal correction. *Phys. Rev. E* **71**, 036109 (2005). [arXiv:quant-ph/0408027](#)
27. P. Brax, C. van de Bruck, A.-C. Davis, D.F. Mota, D.J. Shaw, Detecting chameleons through Casimir force measurements. *Phys. Rev. D* **76**, 124034 (2007). [arXiv:0709.2075](#)
28. P. Brax, C. van de Bruck, A.C. Davis, D.J. Shaw, D. Iannuzzi, Tuning the mass of chameleon fields in Casimir force experiments. *Phys. Rev. Lett.* **104**, 241101 (2010). [arXiv:1003.1605](#)
29. Y.J. Chen, W.K. Tham, D.E. Krause, D. Lopez, E. Fischbach, R.S. Decca, Stronger limits on hypothetical Yukawa interactions in the 30–8000 nm range. *Phys. Rev. Lett.* **116**(22), 221102 (2016). [arXiv:1410.7267](#)
30. P. Brax, G. Pignol, D. Roulier, Probing strongly coupled chameleons with slow neutrons. *Phys. Rev. D* **88**, 083004 (2013). [arXiv:1306.6536](#)
31. K. Hinterbichler, J. Khoury, Symmetron fields: screening long-range forces through local symmetry restoration. *Phys. Rev. Lett.* **104**, 231301 (2010). [arXiv:1001.4525](#)
32. B. Elder, V. Vardanyan, Y. Akrami, P. Brax, A.-C. Davis, R.S. Decca, Classical symmetron force in Casimir experiments. *Phys. Rev. D* **101**(6), 064065 (2020). [arXiv:1912.10015](#)

Chapter 20

Screening Mechanisms



Philippe Brax

20.1 Screening

Quintessence models are meant to reproduce the late-time acceleration of the Universe, using a scalar field sufficient for this one particular problem. Requiring that the equation of state of the scalar field model is close to -1 implies that the mass of the scalar must be of the order of the Hubble rate. This would not be a problem if the scalar field were decoupled from matter. However, the scalar couples to gravity and standard model particles too. This induces at one loop a coupling between the scalar and matter, which is logarithmically divergent. In the absence of symmetry reasoning, this coupling is not naturally vanishing and should be considered as a new parameter of quintessence models.

The coupling between matter and the scalar can be embodied using a conformal rescaling between the Jordan metric and the Einstein one. The Jordan metric $\tilde{g}_{\mu\nu}$ is the one that is used to write down the matter action. The Einstein metric $g_{\mu\nu}$ is the one where the Einstein equation takes a natural form. The simplest relation between them is

$$\tilde{g}_{\mu\nu} = A^2(\phi)g_{\mu\nu}, \quad (20.1)$$

and the coupling is then identified with

$$\beta = m_{\text{Pl}} \frac{\partial \ln A(\phi)}{\partial \phi}. \quad (20.2)$$

In the Solar System, the Cassini bound on fifth forces implies that $\beta^2 \leq 10^{-5}$ which would exclude metric $f(R)$ theories as their $\beta = 1/\sqrt{6}$ is fixed. This is not the case

P. Brax (✉)

Institut de Physique Théorique, Université Paris-Saclay, CEA, CNRS,
91191 Gif/Yvette Cedex, France

when the chameleon mechanism is at play. Indeed, in the presence of matter, the dynamics of the scalar is governed by the effective potential

$$V_{\text{eff}}(\phi) = V(\phi) + (A(\phi) - 1)\rho_m, \quad (20.3)$$

where ρ_m is the conserved matter density and $V(\phi)$ is the potential of the scalar model. When the effective potential admits a density-dependent minimum for which the mass of the scalar at the minimum, i.e., the second derivative of the effective potential at the minimum, is larger than the Hubble rate, then the minimum is a cosmological tracker. In this case the model is a chameleon model. For large curvature $f(R)$ theories, the minimum is a tracker and they are chameleon models. In this case and for static configurations, screening occurs when the mass of the scalar field inside a dense body is so large that its Yukawa suppression in e^{-mr} from each point inside the body prevents any radiation of the field outside the body. Only a thin shell of mass ΔM can in fact generate a scalar field outside the body and hence contribute to a fifth force. The mass of the thin shell is given by

$$\frac{\Delta M}{M} = \frac{|\phi_\infty - \phi_c|}{2\beta_\infty \Phi_N m_{\text{Pl}}}, \quad (20.4)$$

where ϕ_c is the value of the field at the minimum associated with the density ρ_c of the body. Outside, the density is ρ_∞ and the associated minimum is ϕ_∞ . The coupling in the vacuum outside is β_∞ and Φ_N is the Newton potential at the surface of the body, e.g., 10^{-6} for the Sun. Screening occurs when $\Delta M \lesssim M$. In this situation, the scalar interaction between two bodies contributes an extra factor $2\beta_A\beta_B$ between bodies A and B . If they are not screened, then $\beta_{A,B} = \beta_\infty$. If the bodies are screened then $\beta_A = \beta_\infty \frac{\Delta M_A}{M_A}$. In particular, the Sun, the Earth and the Moon must be screened to pass Solar System tests of gravitation. The Lunar Ranging experiment has constrained the difference between the accelerations of the Moon and the Earth towards the Sun at the 10^{-13} level. This implies that

$$\beta_\oplus \leq 10^{-6}, \quad \beta_\odot \leq 10^{-9}. \quad (20.5)$$

and for an unscreened satellite the Cassini bound only requires $\beta_\infty\beta_\odot \leq 10^{-5}$, which is always satisfied when $\beta_\infty = \mathcal{O}(1)$. This formalism has been successfully applied to the case of Hybrid-Metric Palatini theories [1] where the first derivative f_{R_g} of the function $f(\hat{R})$ of the Palatini curvature that parameterises the deviation from General Relativity must be less than 10^{-4} . This result is similar to the bound on f_{R_g} in large curvature metric models.

Screening operates differently when the density of the compact objects is not constant. For instance, in the case of stars on the Red Giant Branch, checks must be made as to whether the field can really stay at the minimum of the effective potential when the density evolves. For this, one must compare the chameleon time $t_\phi = 1/m_\phi$ where m_ϕ is the mass at the putative minimum and the collapse time $t_{\text{ast}} = \frac{1}{(G_N\rho)^{1/2}}$

for a star of average density ρ . When $t_\phi \ll t_{\text{ast}}$, the field tracks the evolution of the density all the way to the Red Giant formation. Different chameleon models with different couplings to matter have been considered in [2], where the effects of the chameleon are found to be small.

For compact objects such as neutron stars, the coupling between the scalar field and gravity cannot be neglected, resulting in modified Tolman-Oppenheimer-Volkov equations. In this case an instability occurs due to the unboundedness from below of the effective potential when the density falls below the pressure deep inside the star, i.e.,

$$\rho < 3p. \quad (20.6)$$

When this is not the case, the effects of modified gravity are almost degenerate with a change of the equation of state of matter in the neutron star. This has been observed in [3], where it has been suggested that the degeneracy can be lifted using the relationship between the reduced moment of inertia $\bar{I} = I/G_N^2 M^3$ and the compactness $C = G_N M/R$ of the star, which does not depend on the equation of state.¹

Another astrophysical probe of screening can be found on astrophysical scales: cosmic filaments. Indeed, the constraints from the Solar System such as the Lunar Ranging experiment, lead to (20.5), which in turn implies for typical models such as the Hu-Sawicki $f(R)$ model that the mass of the scalar field on cosmological scales is typically larger than $10^2 H_0$, where H_0 is the Hubble rate now. This implies that the range of the scalar interaction is shorter than a few Mpc. Filaments of sizes between 1 and 20 Mpc are particularly suited to see effects of screened modified gravity. Indeed, it has been shown in [4], using the N-body simulations generated by the ISIS and RAMSES codes, that filaments are shorter and denser than in the Λ CDM model. Overall they are good candidates to observe sizeable differences with the standard model of cosmology on astrophysical scales. A similar type of observables probing the nonlinear to the quasi-linear regime of cosmological perturbations on scales between 0.1 and 10 Mpc is the power spectrum of the Lyman- α flux decrement. Lyman- α clouds at high redshifts absorb the light emitted by distant quasars. For the Hu-Sawicki $f(R)$ model the deviations from the standard model are small. On the other hand, for models subject to another type of screening mechanism, i.e., K-mouflage, this can be more significant. K-mouflage operates when the gravitational acceleration $|\nabla\Phi_N|$ is large enough. Typically this happens in scalar models of the K-essence type where the kinetic terms are a function $K(X)$, which is nonlinear and where $X = -\frac{(\partial\phi)^2}{2M^4}$ with M taken to be the dark energy scale $M \simeq 10^{-3}$ eV. The coupling to matter β is typically required to be less than 0.1 to satisfy the Solar System tests. In this context, a precise comparison of K-mouflage screened models and the Lyman- α effects will require dedicated numerical simulations of the intergalactic medium in the presence of modified gravity [5]. On larger scales, the effects of screening necessitate the study of cosmological perturbations beyond leading order. This has been performed in [6], where effects on the higher-order statistics of the

¹ Here, R is the radius where the pressure vanishes and M is the mass of the star within this radius.

density contrast of matter have been investigated. These tools will be of relevance with the advent of large-scale surveys in the next decade.

20.2 Laboratory Experiments and Quantum Effects

Screened models of the chameleon type could induce large effects in laboratory experiments. The prime example is the Casimir effect, whereby two metallic plates are attracted due to the quantum fluctuations of the photon field. Scalar fields can induce a classical force between screened plates, as they are very dense, due to the particular profile of the scalar field in the vacuum between the plates. A particularly relevant model in this context is the symmetron, whose potential and coupling functions read

$$V(\phi) = -\frac{\mu^2}{2}\phi^2 + \frac{\lambda}{4}\phi^4, \quad A(\phi) = 1 + \frac{\phi^2}{2\Lambda^2}. \quad (20.7)$$

This Higgs-like models has a Z_2 breaking transition in the presence of matter. Between plates the field vanishes when the distance between the plates is small enough, $d \lesssim \frac{\pi}{\mu}$. When the distance is large enough, a soliton-like solution can be found involving elliptic Jacobi functions. These solutions allow for an exact calculation of the classical Casimir force between two plates for symmetrons [7]. Another consequence of the symmetron phase transition is that starting in the symmetric phase, corresponding to a vanishing field and lowering the density in the presence of boundaries, e.g., plates, can result in the spontaneous appearance of domain walls interpolating between the two vacua at $\phi = \pm \frac{\mu}{\sqrt{\lambda}}$. These domain walls could be triggered in dedicated experiments by removing the gas inside a chamber. A probe of the existence of domain walls in an experimental cavity could be obtained by monitoring the trajectories of neutral particles across the domain walls. Their crossing time of the cavity would be affected by the scalar force induced by the domain wall. This has been investigated in [8].

So far we have only considered the classical interaction mediated by a scalar field between matter particles or objects. In fact, coupled scalar fields also mediate a quantum interaction, which manifests itself when the coupling function $A(\phi)$ has a non-vanishing second derivative. The force acting on a body separated from another one by a distance L is given by

$$F = \int d^3x \partial_L J < A >_J, \quad (20.8)$$

where $J(x)$ is the matter density of all the objects and the derivative is taken by moving one object with respect to the other one. The quantum average $< A >_J$ is the average of the quantum operator in the presence of the source J . This formal results can be loop-expanded. The tree level force is the classical interaction that we have already presented. The first correction occurs at one loop and reads

$$F_{1\text{-loop}} = \frac{1}{2} \int d^3x \partial_L J A'' \Delta_J(x, x), \quad (20.9)$$

involving the second derivative of the coupling function $A(\phi)$ and the Feynman propagator in the presence of the source J evaluated at coinciding points. This formulation allows one to calculate the quantum contribution to the Casimir effect from light scalars. In particular, one retrieves that for a nearly massless scalar between two plates where the coupling is nearly infinite, as they are very dense, the quantum force for a scalar is one half of the photon case. These results have been exploited in [9]—in particular for symmetron models. One-loop effects can also induce a scalar correction to the magnetic moment of the electron. This happens when the usual photon propagator between two electron lines coupled to a photon is replaced by the scalar field propagator. The constraints thus obtained are particularly stringent for the symmetron [10].

20.3 Other Screening Effects

We have dealt with the chameleon screening mechanisms and touched upon the K-mouflage screening. There is a good reason for selecting these effects: they have not been tightly constrained by the speed of gravitons as deduced from the LIGO/VIRGO experiments. Indeed, in all these models the speed of gravitons is equal to the speed of light. This is not the case for models such as the quartic and quintic Galileons, where the speed of the gravitons deviate significantly from unity when the scalar field is responsible for the acceleration of the Universe. The cubic Galileon, whose leading nonlinear term in its Lagrangian is $\square\phi(\partial\phi)^2$, is not affected by these constraints. The induced modification of gravity is locally reduced by the Vainshtein mechanism, whereby the nonlinear terms dominate inside the Vainshtein radius and Newtonian gravity is retrieved. In this context, it is highly relevant that inside clusters of galaxies, where the density profile is not constant, the Vainshtein screening could be lifted, resulting in a discrepancy between the two Newtonian potentials. Although no significant deviation from General Relativity can be inferred from data using this effect yet, it has to be noted that for certain relaxed clusters the violation of the Vainshtein mechanism inside the cluster could help in resolving the tension between lensing and X-ray cluster data [11].

Finally, new screening mechanisms have been proposed in [12], where in a 5d scenario with a warped bulk, the dark sector lives on the IR brane and the standard model on the UV brane. At low energy the two scalars are coupled via a bulk scalar. At high energy the bulk scalar can decay into gravitons, leading to a finite width for its propagator. This imaginary part operates at high energy, larger than the energy of the IR brane, and induces a complete decoupling of the two branes [12].

References

1. M. Vargas dos Santos, J.S. Alcaniz, D.F. Mota, S. Capozziello, Screening mechanisms in hybrid metric-Palatini gravity. *Phys. Rev. D* **97**(10), 104010 (2018). [arXiv:1712.03831](#)
2. S. Najafi, M.T. Mirtorabi, Z. Ansari, D.F. Mota, Red giant evolution in modified gravity. *JCAP* **1902**, 011 (2019). [arXiv:1802.04001](#)
3. P. Brax, A.-C. Davis, R. Jha, Neutron stars in screened modified gravity: chameleon versus dilaton. *Phys. Rev. D* **95**(8), 083514 (2017). [arXiv:1702.02983](#)
4. A. Ho, M. Gronke, B. Falck, D.F. Mota, Probing modified gravity in cosmic filaments. *Astron. Astrophys.* **619**, A122 (2018). [arXiv:1807.07287](#)
5. P. Brax, P. Valageas, Lyman- α power spectrum as a probe of modified gravity. *JCAP* **1901**, 049 (2019). [arXiv:1810.06661](#)
6. A. Aviles, J.L. Cervantes-Cota, D.F. Mota, Screenings in modified gravity: a perturbative approach. *Astron. Astrophys.* **622**, A62 (2019). [arXiv:1810.02652](#)
7. P. Brax, M. Pitschmann, Exact solutions to nonlinear symmetron theory: one- and two-mirror systems. *Phys. Rev. D* **97**(6), 064015 (2018). [arXiv:1712.09852](#)
8. C. Llinares, P. Brax, Detecting coupled domain walls in laboratory experiments. *Phys. Rev. Lett.* **122**(9), 091102 (2019). [arXiv:1807.06870](#)
9. P. Brax, S. Fichet, Quantum chameleons. *Phys. Rev. D* **99**(10), 104049 (2019). [arXiv:1809.10166](#)
10. P. Brax, A.-C. Davis, B. Elder, L.K. Wong, Constraining screened fifth forces with the electron magnetic moment. *Phys. Rev. D* **97**(8), 084050 (2018). [arXiv:1802.05545](#)
11. V. Salzano, D.F. Mota, S. Capozziello, M. Donahue, Breaking the Vainshtein screening in clusters of galaxies. *Phys. Rev. D* **95**(4), 044038 (2017). [arXiv:1701.03517](#)
12. P. Brax, S. Fichet, P. Tanedo, The warped dark sector. [arXiv:1906.02199](#)

Chapter 21

Small-Scale Effects Associated to Non-metricity and Torsion



Adrià Delhom

21.1 Small-Scale Effects and Gravity

The fact that the gravitational coupling constant is so weak compared to the other fundamental couplings may suggest that gravity plays a negligible role in physical scenarios where other fundamental forces are present, unless Planck scale processes are involved. This is actually not true, due to the fact that, unlike the other forces, the *charge* that sources the gravitational field is additive, and there are scenarios where the presence of a huge amount of mass/energy makes gravity the dominant force at macroscopic scales, as in astrophysical or cosmological processes. Nonetheless, one could expect that in microscopic experiments, where the amounts of mass/energy are much smaller, gravity indeed plays a negligible role.

However, the fact that the charges corresponding to the other interactions are not additive allows looking for special set-ups, where the strength of the other interactions can be tuned to be smaller than possible gravitational effects occurring in some microscopic systems. Given that gravity is still unknown at small scales (in the UV), it is then interesting to characterise what kind of effects due to gravity could appear in microscopic systems.

Keeping with metric theories, the only gravitational effects that can appear are those due to the spacetime curvature (i.e., the coupling to the graviton), thus pushing those effects all the way up to the Planck scale. However, when metric-affine gravity theories are explored, the phenomenology becomes much richer due to the fact that they allow for non-Riemannian geometries, which brings new effects that could be relevant even in processes where other interactions play a central role. We mention here that in the present chapter, and similarly to Chap. 10, “non-Riemannian” may refer to both departure from the Levi-Civita connection as well as from *metricity*.

A. Delhom (✉)

Depto. de Física Teórica and IFIC, Centro Mixto Universidad de Valencia-CSIC,
Burjassot 46100, Valencia, Spain
e-mail: adria.delhom@uv.es

From the geometrical perspective, this fact is related to the non-Riemannian geometric objects that arise within the metric-affine formalism, namely the *torsion* and *non-metricity* tensors, defined respectively by $\mathcal{T}^\alpha{}_{\mu\nu} = 2\hat{\Gamma}^\alpha{}_{[\mu\nu]}$ and $\mathcal{Q}_{\alpha\mu\nu} = \nabla_\alpha g_{\mu\nu}$. These objects can generate new effective interactions within the matter sector due to the coupling between matter and geometry, and such interactions will be suppressed by the length scale at which the geometry deviates from a metric one. Below that scale, there could in principle be propagation of the non-Riemannian geometrical features in the whole spacetime, and non-metricity and torsion would play a central role in the description of gravity.

From the field theory perspective, there are two different cases: when these new fields $\mathcal{T}^\alpha{}_{\mu\nu}$ and $\mathcal{Q}_{\alpha\mu\nu}$ do not propagate any extra degrees of freedom, they can be algebraically solved in terms of the matter fields and (possibly) their derivatives and the metric tensor, which allows to integrate them out of the action and obtain these new effective interactions that will be suppressed by a universal energy, related to the geometrical length scale mentioned above. In the case that they propagate new degrees of freedom, they are usually assumed to be massive, so that they can also be integrated out by producing similar effects that will be now suppressed by the mass scale of the corresponding new particles that have been integrated out. This mass scale would characterise the scale at which the particles associated with torsion and/or non-metricity propagate and their effects become non-perturbative. While the theories of propagating torsion and non-metricity are not well developed to date, we will see below that the new geometry-related effective interactions that arise in metric-affine theories of gravity can be constrained by observations, which allow us to set a bound to the scale at which non-Riemannian features can play a nontrivial role in the description of gravity.

21.2 Small-Scale Effects Associated to Non-metricity

In general, metric-affine theories of gravity are not well understood, due to the difficulty in solving their dynamics, and the role played by non-metricity in the microscopic regime is not yet fully characterised. However, there is a broad class of metric-affine theories dubbed as Ricci-Based Gravities (RBGs) where small-scale perturbative effects associated to non-metricity are currently understood. The class comprises all metric-affine gravity theories with diffeomorphism and projective symmetries, where the action is an arbitrary scalar function of the Ricci tensor and the metric (see e.g. [1]). A generic RBG action reads:

$$S_{\text{RBG}} = \frac{1}{2\kappa^2} \int d^4x \sqrt{-g} F(g^{ab}, \mathcal{R}_{(ab)}, \Lambda_{\text{RBG}}), \quad (21.1)$$

where $\kappa^2 = 8\pi G_N = M_{Pl}^{-2}$, \mathcal{R}_{ab} is the Ricci tensor of the independent affine connection $\hat{\Gamma}^a{}_{bc}$, and Λ_{RBG} is a high-energy scale parametrising departures from it. We

stress that the energy scale Λ_{RBG} need not to be related to the cosmological constant. Examples of widely explored gravity theories that fall within the RBG are, for instance, GR, as well as the extensions $f(\mathcal{R})$, Ricci-squared, $f(\mathcal{R}, \mathcal{R}^{(ab)}\mathcal{R}_{(ab)})$, the Eddington-inspired Born-Infeld gravity, and the majority of the metric-affine curvature-based models of the literature. For consistency with experimental data, F is also required to recover GR at low energy scales, i.e., in the limit $E/\Lambda_{\text{RBG}} \rightarrow 0$. Note also that projective symmetry requires that only the symmetric part of the Ricci tensor appears in the action, thus guaranteeing the absence of ghostly degrees of freedom [1, 2]. The field equations derived from (21.1) imply that the connection is non-dynamical and that it is the Levi-Civita connection of some symmetric 2-tensor q_{ab} , usually called *auxiliary metric*. By performing a field redefinition and integrating out metric and connection, it can be shown that these theories admit an Einstein-frame representation in terms q_{ab} . In the process, one can see that there exists an on-shell relation between the spacetime metric and this auxiliary metric given by $g_{ab} = q_{ac}(\Omega^{-1})^c_b$ and where the *deformation matrix* is defined as

$$\sqrt{\Omega}(\Omega^{-1})^a_b = \frac{\partial F}{\partial \mathcal{R}_{(ac)}} g_{cb}, \quad (21.2)$$

being $\Omega = \det(\Omega^a_b)$. It is in general possible to write the deformation matrix as a combination of one of the metrics, the matter fields and their derivatives, and as shown in [3], due to the non-linearities of the equations for the deformation matrix, they usually admit several solutions. Noteworthy, there is always one solution that connects with GR at low energies and for which the deformation matrix satisfies the same symmetries than the metric g_{ab} . In this branch, the deformation matrix will satisfy (at least) the same internal symmetries as the stress energy tensor, and the metric q_{ab} will also share the symmetries of satisfied by the metric g_{ab} . This is strictly true if the matter sector does not couple to the connection. For matter fields that do couple to the connection, even for the branch that recovers GR at low energies, the dependence of the deformation matrix on the matter fields can be more general [1, 4, 5]. However, this will only imply that the spacetime, as a function of the auxiliary metric and matter fields, will have more general combinations of matter fields that may in general have other symmetries than those of the stress-energy tensor.

In vacuum, the deformation matrix is trivial and all RBG theories exactly reproduce the dynamics of vacuum GR. Nonetheless, in the presence of matter the deformation matrix becomes nontrivial and introduces nonlinear modifications in the matter sector of the Einstein-frame, which couples to q_{ab} . In fact, in this frame, the field equations can be written as

$$\mathcal{G}^a_b(q) = \kappa^2 \tilde{T}^a_b \quad (21.3)$$

where \tilde{T}^a_b is the stress-energy tensor of the Einstein-frame matter sector.

The fact that the equations for the auxiliary metric are formally identical to those for the spacetime metric in GR puts forward that the role played by q_{ab} in RBG theories is analogous to the role of g_{ab} in GR. The auxiliary metric is the object that accounts for the usual effects associated with gravity: a long-range force mediated

by a massless spin-2 field. Thus q_{ab} accounts for the gravitational force due to *total* amounts of matter-energy and propagates gravitational waves. However, in the presence of matter fields, there arise new effects that depend on *local* amounts of energy density, and which have their origin in the gravitational sector. Indeed, due to the nontrivial form of the deformation matrix, the spacetime metric picks up corrections that depend on local amounts of energy-density. This can be explicitly seen by writing the deformation perturbatively as

$$(\Omega^{-1})^a_b = \delta^a_b + \frac{1}{\Lambda_Q^4} \left(\alpha T \delta^a_b + \beta T^a_b \right) + \mathcal{O}(\Lambda_Q^{-8}), \quad (21.4)$$

where α , β are model-dependent dimensionless parameters that are completely specified once we choose a particular RBG Lagrangian, and $\Lambda_Q = \sqrt{M_{Pl} \Lambda_{\text{RBG}}}$ is a high-energy scale whose meaning will be explained later in detail. Notice that the requirement that GR must be recovered at low energies requires the zeroth order term in the expansion to be δ^a_b (actually it suffices to be proportional to δ^a_b , in which case it would only affect the normalisation of the fields). As a consequence, in vacuum, all RBG theories are exactly GR.

The above expansion for the deformation matrix allows us to write

$$g_{ab} = q_{ab} + \frac{1}{\Lambda_Q^4} \left(\alpha T q_{ab} + \beta T_{ab} \right) + \mathcal{O}(\Lambda_Q^{-8}) \quad (21.5)$$

$$Q_{abc} = \frac{1}{\Lambda_Q^4} \left[\alpha (\nabla_a T) q_{bc} + \beta (\nabla_a T_{bc}) \right] + \mathcal{O}(\Lambda_Q^{-8}), \quad (21.6)$$

where $Q_{abc} \equiv \nabla_a g_{bc}$ is the non-metricity tensor, and notice that we defined the auxiliary metric such that its covariant derivative vanishes on-shell [4, 5]. Although the above expansion is only valid below the scale Λ_Q , the general form of the deformation matrix suggests that these effects will also generally have a non-perturbative counterpart. Indeed, here we can see how the scale Λ_Q is the scale at which non-perturbative corrections to GR related to the non-Riemannian nature of the underlying spacetime arise within the RBG framework. Below that scale the non-metricity tensor has perturbative effects and becomes suppressed by $(E/\Lambda_Q)^4$, although it plays a fundamental role in the non-perturbative behaviour of these theories, as is apparent from (21.6). From here, we can see that the spacetime metric, besides taking into account the typical effects of gravity, is also point-wise sensitive to the distribution of energy density, which represents a distinctive feature of RBG theories among other modified gravities.

Thus, in the RBG frame, we see that the spacetime metric accounts for two different effects of gravitational origin: a long-range force mediated by a spin-2 field associated with gravitational waves, and new effects controlled by the energy scale Λ_Q that depend upon the local distribution of energy-density, and which can be associated with a non-dynamical non-metricity tensor sourced by matter-energy density which occurs within RBGs, as seen in (21.6). Given that all matter fields

couple to the metric, an expansion of the spacetime metric in powers of $1/\Lambda_Q$ also allows us to interpret these non-metricity related effects as perturbative interactions within the RBG frame.

From the point of view of the Einstein frame, however, these new effects related to non-metricity are translated into nonlinear interactions within the matter sector whose fields propagate in a General Relativistic spacetime. The fact that these new effects become more relevant the higher the energy-density scale of the process or, as viewed in the Einstein frame, that they introduce higher-dimensional operators (we are referring to the mass-dimension of the new field operators that describe these nonlinear interactions) in the matter Lagrangian, already points out that they can be relevant at high-energy microscopic processes. Let us illustrate this with some results in this direction available in the literature.

21.2.1 Small-Scale Effects in $f(\mathcal{R})$ Theories

The first context in which the physical implications of these effective interactions were found was that of Palatini $f(\mathcal{R})$ theories (see, e.g., [6]). Let us review these results within the general framework of RBG theories developed above. To that end, we must first look at the form of the deformation matrix within metric-affine $f(\mathcal{R})$ theories, which is given by

$$\Omega^a_b = f_{\mathcal{R}} \delta^a_b, \quad (21.7)$$

being \mathcal{R} (and thus $f_{\mathcal{R}}$), an on-shell function of the stress-energy tensor trace obtained from the trace of the metric field equations $\mathcal{R} f_{\mathcal{R}} - 2f = \kappa^2 T$. Given a particular model of $f(\mathcal{R})$, we will be able to write the corresponding deformation matrix only in terms of the trace of the stress-energy tensor, which implies that the β coefficient in (21.8) will vanish for all $f(\mathcal{R})$ models, having an on-shell parametrisation for an arbitrary $f(\mathcal{R})$ of the form

$$(\Omega^{-1})^a_b \Big|_{f(\mathcal{R})} = \delta^a_b + \frac{\alpha}{\Lambda_Q^4} T \delta^a_b + \mathcal{O}(\Lambda_Q^{-8}). \quad (21.8)$$

Once a particular $f(\mathcal{R})$ is chosen, then the algebraic equation $\mathcal{R} f_{\mathcal{R}} - 2f = \kappa^2 T$ can be solved for $\mathcal{R}(T)$, leading to the function $f_{\mathcal{R}}(T)$ that fixes the dimensionless α coefficient. This deformation matrix introduces new interactions in the matter sector due to the coupling between the metric and all the matter fields. For instance, a spin 1/2 field is coupled to an $f(\mathcal{R})$ theory that will be described by the Lagrangian

$$\begin{aligned} \mathcal{L}_{1/2} = & \sqrt{-q} \left[\frac{i}{2} (\bar{\psi} \gamma_q^\mu \nabla_\mu \psi - (\nabla_\mu \bar{\psi}) \gamma_q^\mu \psi) - \bar{\psi} m \psi \right] \\ & + \sqrt{-q} \frac{3\alpha}{2\Lambda_Q^4} T \left[\frac{i}{2} (\bar{\psi} \gamma_q^\mu \nabla_\mu \psi - (\nabla_\mu \bar{\psi}) \gamma_q^\mu \psi) - 2\bar{\psi} m \psi \right] + \mathcal{O}(\Lambda_Q^{-8}), \end{aligned} \quad (21.9)$$

where $\{\gamma_q^\mu, \gamma_q^\nu\} = 2q^{\mu\nu}$. This Lagrangian describes a fermion field with contact interactions with all matter fields through the trace of the stress-energy tensor. Notice that the perturbative expansion breaks down at the scale Λ_Q , where the interactions described by the above Lagrangian become non-unitary, and non-perturbative effects are expected to dominate.

The fact that matter fields in metric-affine $f(\mathcal{R})$ theories develop new contact interactions below Λ_Q was first noticed in the context of $\mathcal{R} - \Lambda_{\text{RBG}}^4/\mathcal{R}$ by Flanagan in [7] (where originally μ was written instead of Λ_{RBG}). For that particular model we have the relation

$$f_{\mathcal{R}} = 1 + \frac{4\Lambda_{\text{RBG}}^4}{-\kappa^2 T \pm \sqrt{\kappa^4 T^2 + 12\Lambda_{\text{RBG}}^4}},$$

which after the constant re-scaling of the auxiliary metric $q_{\mu\nu} \rightarrow 3/4q_{\mu\nu}$ leads to the dimensionless coefficient $\alpha = \mp 1/4\sqrt{3}$. We can then derive with the form of the stress-energy tensor for a spin 1/2 from (21.9) and use the above value of α to obtain

$$\begin{aligned} \mathcal{L}_{1/2} = & \sqrt{-q} \left[\frac{i}{2} (\bar{\psi}\gamma_q^\mu \nabla_\mu \psi - (\nabla_\mu \bar{\psi})\gamma_q^\mu \psi) - \bar{\psi}m\psi \right] \\ & + \sqrt{-q} \left\{ \pm \frac{\sqrt{3}}{16\Lambda_Q^4} [\bar{\psi}\gamma_q^\mu \nabla_\mu \psi - (\nabla_\mu \bar{\psi})\gamma_q^\mu \psi]^2 \mp \frac{\sqrt{3}m^2}{2\Lambda_Q^4} (\bar{\psi}\psi)^2 \right. \\ & \left. \pm i \frac{5\sqrt{3}m}{16\Lambda_Q^4} [\bar{\psi}\gamma_q^\mu \nabla_\mu \psi - (\nabla_\mu \bar{\psi})\gamma_q^\mu \psi] (\bar{\psi}\psi) \right\} + \mathcal{O}(\Lambda_Q^{-8}). \end{aligned} \quad (21.10)$$

As Flanagan pointed out in [7], these effective interactions would have physical implications for the spin 1/2 sector of the Standard Model. Indeed, the value that the energy scale Λ_Q should take for $\mathcal{R} - \Lambda_{\text{RBG}}^4/\mathcal{R}$ to account for late-time acceleration (i.e., $\Lambda_Q = \sqrt{M_{\text{Pl}}\Lambda_{\text{RBG}}} \sim 10^{-3}eV$) was seen to be incompatible with experimental data on, for instance, electron-electron scattering experiments, which rules out the model as an alternative explanation for dark energy [7]. Shortly afterwards, two remarks to the work by Flanagan were made by Vollick.

Firstly, in [8] it was argued that the two frames admitted by $f(\mathcal{R})$ theories were not physically equivalent, due to the fact that the mapping between frames may become singular in some spacetime regions (here we call these frames the RBG and Einstein frames, since we discuss $f(\mathcal{R})$ as a subset of theories of the RBG class, although traditionally, within $f(\mathcal{R})$ theories they were called Jordan and Einstein ones respectively). However, since a field re-definition is known to leave physics invariant, both frames should be equivalent at least where the field re-definition is well defined. Vollick also argued [9] that there is no proof that field re-definitions leave the S-matrix invariant in curved spacetimes.

Secondly, Vollick in [9] also discussed how Flanagan did not consider the potential role played by torsion by assuming that the spin connection is given by the Levi-Civita connection, which is not consistent with the metric-affine formalism. Indeed,

the corresponding modifications to include torsion were introduced, and as expected, the coupling between the fermion fields and the connection led to a non-propagating torsion field that is algebraic in the fermion fields and can be integrated out to produce further four-fermion effective interactions. However, given that the coupling constant for the interactions was the Planck scale, rather than Λ_Q , they are negligible compared to the ones in Flanagan's analysis. Even if they were characterised by the same scale, since the non-metricity related interaction terms contain powers of the derivatives of the fields, the dependence on the momenta of the different interaction terms when calculating decay rates or cross-sections will be different than that of the torsion-related interactions. Thus, cancellation between the different terms cannot take place and Vollick's result would presumably still apply. Hence, in this case the interactions do not contain derivatives of the fields, which implies that the contribution to the cross-sections will grow with a different power, although from the field theory perspective it appears that the result can be generalised in a rather straightforward manner, because as far as we know there is still no rigorous proof.

These effective interactions were also used by Olmo in [10] to derive corrections to the hydrogen atom behaviour in general metric-affine $f(\mathcal{R})$ theories. In order to do so, the non-relativistic limit of the modified Dirac equation that resulted from taking into account these new interactions in a general Palatini $f(\mathcal{R})$ theory was computed. Then it was shown that while UV $f(\mathcal{R})$ corrections to GR were perfectly compatible with the observed behaviour of the hydrogen atom (provided that the UV scale is high enough), IR $f(\mathcal{R})$ corrections characterised by an IR scale that accounted for late-time acceleration generically have dramatic consequences for the stability of atomic systems [10]. The particular cases of $\mathcal{R} + \mathcal{R}^2/R_p$ and $\mathcal{R} - \Lambda_{\text{RBG}}^4/\mathcal{R}$ were analysed, and while in the first case the hydrogen atom was perfectly stable, $1/\mathcal{R}$ modifications were seen to introduce a potential well in the outskirts of the atom to which the electron in the ground state would tunnel in a short time. Indeed, the stability of the ground state of the hydrogen atom in a universe described by $\mathcal{R} - \Lambda_{\text{RBG}}^4/\mathcal{R}$ was found to be of around 12 minutes if μ is chosen to account for late-time acceleration, in clear contradiction with observations. These previous results from particle physics reasoning ruling out Palatini $\mathcal{R} - \Lambda_{\text{RBG}}^4/\mathcal{R}$ as a candidate for explaining late-time acceleration, were confirmed in a different physical system.

Other sources of incompatibility with data of $f(\mathcal{R})$ theories with corrections that grow at low curvature are also potential violations of the Einstein Equivalence Principle (EEP, see [11–13] for a rigorous definition). In an earlier work [14], Olmo pointed out that the corrections induced by the non-minimal interactions introduce effects in atomic-like systems that cannot in general be removed by a suitable choice of freely falling coordinates, thus not recovering (locally) the Minkowski metric and introducing potential violations of the EEP. While these violations would be negligible for UV $f(\mathcal{R})$ corrections (i.e., those that become relevant at high curvatures), they would introduce observable violations of the EEP in $f(\mathcal{R})$ theories with IR corrections (i.e., corrections that become relevant at low curvatures), such as the $\mathcal{R} - \Lambda_{\text{RBG}}^4/\mathcal{R}$ model.

Finally, another interesting consequence of the effective interactions within the $f(\mathcal{R})$ framework is that due to these corrections, the gravitational potential in New-

tonian limit picks up energy-density dependent corrections [15–18]. As also pointed out in [14], this dependence allows for the possibility of having different external gravitational fields sourced by extended objects with the same total mass and symmetries but a different mass-density distribution.

21.2.2 *Small-Scale Effects in Generic RBGs*

The characteristic microscopic effects of RBG theories have also been used to constrain other gravity theories within the RBG class that lie beyond $f(\mathcal{R})$. Particularly, Eddington-inspired Born-Infeld (EiBI) theories have been constrained by means of these effective interactions in the contexts of astrophysics, nuclear physics and high-energy particle physics experiments. Furthermore, some effects related to the behaviour of collapsing matter have been studied. Particularly in [19, 20], Pani et al. and Avelino first showed how these non-minimal couplings can have effects in astrophysical scenarios in both the relativistic and non-relativistic regimes.

As shown previously by Bañados and Ferreira [21], in the non-relativistic regime of the theory, the Poisson equation picks up a correction due to these new effective interactions, leading to the result that non-interacting collapsing particles produce a pressure-less star that is seen to be stable under linear radial perturbations, instead of black holes [19]. In the relativistic regime, though black holes (or wormholes) may form after collapse, it is found that the modifications introduced by the effective matter couplings give birth to a plethora of compact objects that do not exist within GR [19]. Indeed, the non-perturbative effects of these new interactions are also responsible for the existence of wormhole solutions in EiBI when coupled to a free Maxwell field.

The first constraints to EiBI were derived by Avelino in [20], also by exploiting the modified Poisson equation in the non-relativistic limit, which implies a constraint in the energy scale of EiBI due to the mere existence of compact objects of radius R . Avelino also used the modified Poisson equation in a nuclear physics context to constrain the EiBI energy scale by assuming that the corrections due to these effective interactions were smaller than electromagnetic effects inside atomic nuclei [22]. Later, he also showed how measurements of the pressure distribution inside the proton, which get modifications due to these new effective interactions, could further constrain the EiBI energy scale by using nuclear physics data [23].

A systematic analysis of the effect of these effective interactions without the use of the non-relativistic approximation has been carried out in [24, 25]. Concretely, in [24] we developed the framework presented above to describe these new effective interactions for a generic RBG theory when coupled to a free spin 1/2 field. There, the $\mathcal{O}(\Lambda_Q^{-4})$ terms in (21.8) were used to set general bounds to the RBG parameter space, using data from $e^+e^- \rightarrow e^+e^-$ collisions at LEP. Notice that while in the $f(\mathcal{R})$ case only the α parameter is non-vanishing, in a general RBG model there will also feature the β parameter. However, in high energy processes, since the α terms are on-shell-proportional to some power of the particle mass, they are negligible in

front of the β terms that are typically proportional to some power of the momentum of the particles. Thus, the β terms will be the dominant corrections in any tree-level process at a scale above the mass of all the particles involved.

In [24] the authors used data of e^+e^- collisions at $\sqrt{s} = 207$ GeV in LEP, in order to extract a bound, by making the following assumptions: i) neglect the influence of post-Newtonian corrections in experiments carried out in LEP (i.e., assuming $q_{\mu\nu} \approx \eta_{\mu\nu}$) ii) neglect the α -dependent terms, i.e., the α term is suppressed by a factor $m_e/\sqrt{s} \sim 10^{-5}$ with respect to β -dependent terms, where s is the characteristic energy scale of LEP e^+e^- , and iii) neglect the torsion corrections. The last approximation was based on arguments in [26], where it was explained that torsion effects would only be relevant in scenarios with strong magnetic fields, such as neutron stars, due to the need of a high spin-density for torsion effects to be observable. Indeed, within RBGs, although non-metricity related effects are suppressed by Λ_Q , torsion sourced by fermions is suppressed by the Planck mass, which further justifies the approximation. Under these three assumptions, the bound $\Lambda_Q \geq \beta^{1/4} 0.6$ TeV was obtained [24].

This bound is valid for generic RBG models, and it was also particularised for the EiBI case, for which $\beta = 1$, obtaining the most stringent constraints for this theory to date. Recently, the method has been extended to arbitrary spin fields in [25], and using data from $\gamma e^- \rightarrow \gamma e^-$ collisions, a similar bound for β/Λ_Q^4 was obtained. Moreover, X-Ray $\gamma\gamma \rightarrow \gamma\gamma$ collisions were analysed, obtaining a much milder bound due to the fact that photon-photon scattering experiments that are available are performed in the keV range.

21.3 Small-Scale Effects Associated with Torsion

The torsion tensor was first introduced by Cartan in [27–30], and shortly after that, Einstein tried to unify—without success—gravity and electromagnetism by using this brand new geometrical object. Already, Cartan had the intuition that torsion had to be related with matter spin. Inspired by the work of Utiyama [31], Kibble [32] and Sciama [33, 34] realized that the gauge theory of the Poincaré group naturally features a tetrad and an affine connection as the gauge fields of translations and Lorentz rotations respectively.

The simplest Lagrangian for these gauge fields was found to be $\sqrt{-g}\mathcal{R}$ (note that we have here traded the natural gauge variables used in the original work, which were vierbein and spin connection, for the metric and affine connection in order to be consistent with the rest of the text), i.e., the metric-affine/Palatini Lagrangian for General Relativity. We mention that we prefer to use the name Einstein-Cartan-Sciama-Kibble (ECKS), standing for this minimal version of Poincaré gauge theory, since the name metric-affine/Palatini GR could cause confusion (the different names have historical roots, particularly in the different approaches, namely gauge vs. metric-affine approaches). Although the above Lagrangian leads to a vanishing non-metricity, it was seen to lead to a nontrivial torsion tensor if matter fields couple

to the affine connection, as is the case for spin 1/2 fields. Indeed, this coupling leads to a non-vanishing hyper-momentum (or spin-density), which sources torsion, and which for spin 1/2 fields was seen to be

$$\Delta_{\mu\alpha\beta} = \sqrt{-g} \frac{i}{2} \epsilon_{\mu\alpha\beta\sigma} \bar{\psi} \gamma^\sigma \gamma_5 \psi. \quad (21.11)$$

Actually, spin 1/2 fields couple minimally only to the pseudo-vector part of the torsion tensor, defined by

$$S^\mu = \epsilon^{\mu\alpha\beta\gamma} \mathcal{T}_{\alpha\beta\gamma}, \quad (21.12)$$

since the standard kinetic term of Dirac fields has a hidden interaction term of the form $-1/8 S^\mu \bar{\psi} \gamma_\mu \gamma_5 \psi$. Then, by separating the torsion contribution from the metric ones in the gravitational Lagrangian, and integrating out the torsion tensor generated by (21.11), they arrived at the well known effective operator

$$\bar{\psi} \gamma_\mu \gamma_5 \psi \bar{\psi} \gamma^\mu \gamma_5 \psi \quad (21.13)$$

that describes torsion-induced four-fermion interactions within minimal Poincaré gauge theory.

As we see, similar to the case of non-metricity in RBG theories, torsion in metric-affine GR does not propagate and is algebraic in the matter fields, although instead of being sourced by energy density, it is sourced by spin density (or hyper-momentum). As in the case for the non-metricity related effective interactions in RBGs, the effective interactions resulting from integrating out the torsion tensor also have implications in the behaviour of matter fields.

In the review by Hehl et al. [35] it is emphasized that within minimal Poincaré gauge theory, torsion only exists in the bulk of matter fields with non-vanishing spin density, and it was estimated that the effects of torsion within these theories could become relevant right before singularity formation in gravitational collapse, close to the Big Bang, or in some quantum gravity processes; situations where the number of spin 1/2 particles per unit volume is expected to reach the critical value $n = m/\kappa\hbar^2$, where m is the particle mass. These effective interactions have been suggested as mechanisms for singularity avoidance in early Universe cosmology [36].

The idea of treating torsion as an external classical field, or as a new propagating degree of freedom that can be quantised, has also been treated in the literature. To do that, one needs to go beyond the metric-affine GR action, which can be done in several ways. Since it is a very extensive topic, and the main results have already been presented in different works, we will only give here a brief summary of such results. The interested reader is referred to the review by Saphiro [37] and references therein.

The possible parity-preserving couplings of the torsion field to a scalar, and also to spin 1/2 fields, are explored. There are four different couplings for a real scalar field, an extra one for complex scalar field, five couplings for scalar-pseudoscalar couplings, and two couplings for fermion fields. With the minimal coupling prescrip-

tion, only one of these couplings appear, which is the coupling between torsion and fermions through the spin connection given in (21.12). Starting from the classical theory given by minimally-coupled scalar and spin 1/2 fields in a curved background with torsion, it is seen that two non-minimal couplings must be added: the well known $\xi_1 R\phi^2$, and a general version of the minimal coupling between fermions and torsion given by $\eta_1 \bar{\psi} S^\mu \gamma_\mu \gamma_4 \psi$ (notice the arbitrary coefficient). If an extra Yukawa interaction between the fermion and scalar is added, renormalisability requires the addition of an interaction term between the torsion pseudo-vector and the scalar of the form $\xi_4 S^\mu S_\mu \phi^2$.

The renormalisation group (RG) equations that give the running of the masses and matter couplings are identical to their flat spacetime version. Moreover, the running of the couplings to curvature and of the vacuum parameters not related to torsion are not influenced by torsion couplings. However, in general, the running of torsion couplings might be influenced by the other couplings present in the theory. For the η_1 parameter, it is seen that its running is always positive, thus making the interaction between spinors and torsion stronger in the UV for different choices of matter sector, but the running is seen to be not relevant physically. For a non-minimally coupled massless scalar field, it is seen that the non-minimal couplings to torsion modify the potential in such a way that spontaneous symmetry breaking can always be achieved either at the classical or at the quantum level. Additionally, first-order phase transitions might be induced by such non-minimal couplings. Also, anomalies were studied in the presence of torsion, finding that the anomaly cancellation that takes place within the Standard Model is respected by the non-minimal couplings for weak external torsion fields. However, the leptonic current picks up a correction due to curvature and torsion. This correction could induce anisotropies in the polarisation of light that comes from distant galaxies, although the current constraints in the coupling parameter make this effect un-observable.

The possibility of propagating torsion has been mainly studied for its pseudo-vector part from an effective field theory approach. As shown in [38], this pseudo-vector carries four degrees of freedom encoded in a scalar and a spin-1 field. However, if both fields propagate, the Hamiltonian would not be bounded below, thus restricting the parameters of the effective theory. The case of the pseudo-scalar field is treated within [38], showing that it can induce interaction between torsion and minimally-coupled gauge fields due to the chiral anomaly. Several bounds on the torsion mass and the coupling to gauge fields are obtained in that reference. For the case of the spin-1 field, we refer the reader again to the review [37].

Due to an extra gauge symmetry for the torsion pseudo-vector that is broken at low energies by the fermionic mass terms, the pseudo-vector is found to be massive, with a mass that is required to be higher than fermion masses due to non-renormalisability of the theory. Notice that, given its non-renormalisability, it only makes sense as an effective field theory below the torsion mass. If the torsion mass was of the order of the most massive fermion or lower, this would have important corrections to the Standard Model that have not been observed, thus ruling out the possibility. However, one has to keep in mind that these results only apply to a theory of the torsion pseudo-vector, and general theories including the full tensor have not yet been well understood

in the quantum regime. Hence, below the torsion mass, it introduces new contact interactions between fermion fields described again by (21.13). If η^2/M_S^2 is taken as the coupling constant of such an effective operator, the bound $M_S > 1.4\eta$ TeV was found from axial-axial $eeqq$ interactions.

The influence of the torsion pseudo-vector in forward-backward asymmetries has also been discussed in [39]. Following a different approach, and concerned with the fact that the four-fermion interactions are non-renormalisable and become non-unitary in the UV, Boos and Hehl recently suggested in [26] that by adding suitable kinetic terms to the gauge fields of the Poincaré group, which are given by the square of torsion and curvature tensors, new propagating gravitational degrees of freedom related to the affine sector will appear that mediate these interactions. These new degrees of freedom could be understood as gauge bosons of the Poincaré group in close analogy to the W and Z bosons of the electroweak model that gave a more fundamental explanation of Fermi's effective theory for β -decay.

The non-relativistic counterpart of these effective interactions has also been widely treated in the literature. First, Hehl suggested that in the geometric optics approximation, torsion could modify the trajectories of particles with non-vanishing spin-density in [40] (note that in [40] the approximation was called semi-classical but we prefer to call it "geometric optics" to avoid confusion with semi-classical gravity). Later in [41, 42], Audretsch confirmed Hehl's claim by two different methods, showing how in the geometric optics approximation a free spin 1/2 particle, as well as the spin vector, do not propagate along metric geodesics, but instead they follow geodesics of the connection $\Gamma^{*\alpha}_{\mu\nu} = \Gamma(g)^{\alpha}_{\mu\nu} + 3/2 g^{\alpha\sigma} \mathcal{T}_{[\sigma\mu\nu]}$, which can be written in terms of the metric connection and the contortion tensor. From a field theory perspective, since the contortion tensor is sourced by the spin 1/2 field hyper-momentum, it is seen how the effect of the effective interaction of (21.13) in the macroscopic regime is that of a self-force that pushes objects with spin-density away from metric geodesics. Audretsch also showed that the spin vector would precess around the trajectory. After some years, Nomura et al. [43] confirmed previous results using the Fock-Papapetrou method.

More recently, Cembranos et al. made a revision of all the previous work about spin 1/2 particle trajectories. In this revision, they found that the WKB method used by Audretsch is cleaner than the others regarding the derivation of the trajectories and spin precession. Also, by using the Raychaudhuri equations for spin 1/2 particles, they also showed the existence of a new parameter that characterises the difference between the accelerations felt between spin 1/2 particle trajectories and minimal-length trajectories (i.e., metric geodesics), as measured by local observers, which could be employed to detect torsion effects. However, they also concluded that in order to observe the effects, huge magnetic fields that align the spins of a large amount of spin 1/2 particles should be present. Concretely, they propose that a difference in the angles of incidence of photons and neutrinos coming from the same neutron star could be an interesting situation, in which the deviation of the neutrino geodesics with respect to the photon ones due to these torsion effects could become observable.

Recently, Obukhov et al. [44] derived the Foldy-Whitehouse Hamiltonian for a minimally-coupled spin 1/2 field without taking any weak-field limit. They showed

how the gravitational moments played a major role in building a covariant extension of the Dirac Lagrangian that features intrinsic dipole moments (induced by Noether charges) in a systematic way. They also show that, contrary to electromagnetism, anomalous gravito-electric and gravito-magnetic moments cannot be introduced for a Dirac particle in a covariant way (see, e.g., [45] an analogy between gravity and Maxwell's theory in the weak-field limit in the context of gravitoelectromagnetism). There have also been many attempts to observe torsion in the lab due to these high-energy/small-scale effects. Two main classes of experiments involving torsion can be distinguished: those which regard torsion as a background field, and those which understand it as an extra field described by an effective Lagrangian. We will here give a brief taste of the current status of the field. The interested reader is referred to the broad reviews on the topic by Ni [46, 47]. The first observational tests that tried to observe a background torsion field were proposed by Audretsch and Lammerzahl [48], by means of neutron interferometry, and Hughes-Drever type experiments also proposed by Lammerzahl [49]. Assuming minimal coupling to fermions, the bound $|S_i| < 10^{-31}$ GeV was found for the norm of the spatial component of the torsion pseudo-vector. Later, Mohanty and Sarkar [50] used measurements on CPT violation parameters in Kaon systems also allowed to constrain the temporal component to be $|S_0| < 10^{-26}$ GeV.

Singh and Ryder [51] have shown how the pseudo-vectorial torsion could also have observable effects in spectroscopy experiments due to a correction of the energy levels by a spin-rotation coupling. Indeed, in experiments with nuclear spins freely precessing in the bulk of a constant magnetic field, the measurements on the Zeeman frequencies for different nuclei allowed setting bounds to the spatial part of the torsion pseudo-vector of the order of $|S_i| |\cos \theta| \leq 8.1 \times 10^{-31}$ GeV, with θ being the angle between S_i and the magnetic field, as shown by Obukhov et al. in [44].

The possibility of constraining torsion [52] and background non-metricity [53] (see also [54, 55] for Lorentz Violating effects linked to non-metricity in metric-affine bumblebee gravity) by constraints on Lorentz violation parameters has also been discussed. Besides the observables named above, torsion effects were seen to potentially induce Weak Equivalence Principle violation by Ni [46], and universality of free-fall experiments, was also used to constrain torsion gradients by Duan et al. [56]. From the effective field theory perspective, the possibility of discovering torsion at CERN was discussed by deAlmeida et al. in [57]. Indeed, using data on Drell-Yang and $t\bar{t}$ processes at LHC, a possible non-universal coupling between torsion and fermions was severely constrained by Sapiro et al. [58], and also lower bounds on the torsion mass $M_S \geq \mathcal{O}(\text{TeV})$ for a coupling constant of the order of $\eta_1 \sim 10^{-1}$ (remember that minimal coupling is given by $\eta_1 = 1/8$). Constraints to in-matter torsion (such as that of ECKS theory) were first placed in neutron spin rotation experiments using liquid ^4He by Lehnert et al. [59].

21.4 Outlook

As a final remark we would like to mention that although much work has been done, especially in characterising the effects of torsion in metric-affine gravities, the implications of the possible non-minimal couplings to matter are not yet fully explored. Regarding non-metricity, only the consequences through the nontrivial modifications that it induces in the metric tensor in a limited class of metric-affine theories are fairly understood, and an understanding of the effects of the possible non-minimal couplings to matter is lacking. Additionally, even though we have an effective theory for the torsion pseudo-vector, such a construction for the full torsion is still lacking, and for the non-metricity tensor we do not even have an effective theory for any of its irreducible components.

There are also questions on which we should reflect further that stem from the fact that although non-metricity and torsion are geometrical, in most cases (if not all) they can be treated just as extra fields added to the Lagrangian with no relation to geometry at all, and especially in the cases where they do not propagate, they are apparently not distinguishable from just a bunch of irrelevant operators. Do geometrical fields have a different physical behaviour than non-geometrical ones? And if so, is there any canonical way in which the demarcation can be made? The only remainder that we have (for instance in non-metricity related couplings in RBGs) is that these interactions may be interpreted as having geometrical origin comes from their *universality* in the sense that all the effective operators are characterised by the same coupling $1/\Lambda_Q$. Thus it would be important to understand whether geometrical fields have further implications that are not apparent from the pure field theory perspective, or if the geometrical interpretation is just a convenient tool that allows us to gain insight about the behavior of gravitational theories. In this sense, it has been recently argued that although classical GR can be described in three different geometrical ways involving only torsion, only non-metricity or only curvature; the field theory description is the unique theory of a unitary and Lorentz invariant massless spin-2 field, thus implying that the field theory point of view is in some sense a more fundamental one [60]. On the other hand, it is also acknowledgeable that many central results in GR (such as, for instance, the singularity theorems, or the positivity of mass) are only fully understood in geometrical terms, and as far as the author knows, there is no straightforward translation to the field theory language for these results. We thus encourage the interested readers to reflect further on this issues.

References

1. J.B. Jiménez, A. Delhom, Instabilities in metric-affine theories of gravity with higher order curvature terms. *Eur. Phys. J. C* **80**(6), 585 (2020). [arXiv:2004.11357](https://arxiv.org/abs/2004.11357)
2. J. Beltrán Jiménez, A. Delhom, *Ghosts in Metric-affine Higher Order Curvature Gravity*. [arXiv:1901.08988](https://arxiv.org/abs/1901.08988)

3. J.B. Jiménez, D. de Andrés, A. Delhom, Anisotropic deformations in a class of projectively-invariant metric-affine theories of gravity. *Class. Quant. Grav.* **37**(22), 225013 (2020). [arXiv:2006.07406](#)
4. V.I. Afonso, C. Bejarano, J. Beltran Jimenez, G.J. Olmo, E. Orazi, The trivial role of torsion in projective invariant theories of gravity with non-minimally coupled matter fields. *Class. Quant. Grav.* **34**(23), 235003 (2017). [arXiv:1705.03806](#)
5. J. Beltran Jimenez, L. Heisenberg, G.J. Olmo, D. Rubiera-Garcia, Born–Infeld inspired modifications of gravity. *Phys. Rept.* **727**, 1–129 (2018). [arXiv:1704.03351](#)
6. G.J. Olmo, Palatini approach to modified gravity: $f(R)$ theories and beyond. *Int. J. Mod. Phys. D* **20**, 413–462 (2011). [arXiv:1101.3864](#)
7. E.E. Flanagan, Palatini form of $1/R$ gravity. *Phys. Rev. Lett.* **92**, 071101 (2004). [arxiv:astro-ph/0308111](#)
8. D.N. Vollick, On the viability of the Palatini form of $1/R$ gravity. *Class. Quant. Grav.* **21**, 3813–3816 (2004). [arxiv:gr-qc/0312041](#)
9. D.N. Vollick, On the Dirac field in the Palatini form of $1/R$ gravity. *Phys. Rev. D* **71**, 044020 (2005). [arxiv:gr-qc/0409068](#)
10. G.J. Olmo, Hydrogen atom in Palatini theories of gravity. *Phys. Rev. D* **77**, 084021 (2008). [arXiv:0802.4038](#)
11. K.S. Thorne, C.M. Will, Theoretical frameworks for testing relativistic gravity. I. Foundations. *Astrophys. J.* **163**, 595–610 (1971)
12. C.M. Will, The confrontation between general relativity and experiment. *Living Rev. Rel.* **17**, 4 (2014). [arXiv:1403.7377](#)
13. C.M. Will, *Theory and Experiment in Gravitational Physics* (Cambridge University Press, 2 edn., 2018)
14. G.J. Olmo, Violation of the equivalence principle in modified theories of gravity. *Phys. Rev. Lett.* **98**, 061101 (2007). [arxiv:gr-qc/0612002](#)
15. G. Allemandi, M. Francaviglia, M.L. Ruggiero, A. Tartaglia, Post-Newtonian parameters from alternative theories of gravity. *Gen. Rel. Grav.* **37**, 1891–1904 (2005). [arxiv:gr-qc/0506123](#)
16. G.J. Olmo, The Gravity Lagrangian according to solar system experiments. *Phys. Rev. Lett.* **95**, 261102 (2005). [arxiv:gr-qc/0505101](#)
17. G.J. Olmo, Post-Newtonian constraints on $f(R)$ cosmologies in metric and Palatini formalism. *Phys. Rev. D* **72**, 083505 (2005). [arxiv:gr-qc/0505135](#)
18. T.P. Sotiriou, The Nearly Newtonian regime in non-linear theories of gravity. *Gen. Rel. Grav.* **38**, 1407–1417 (2006). [arxiv:gr-qc/0507027](#)
19. P. Pani, T. Delsate, V. Cardoso, Eddington-inspired Born-Infeld gravity. Phenomenology of non-linear gravity-matter coupling. *Phys. Rev.* **85**, 084020 (2012). [arXiv:1201.2814](#)
20. P.P. Avelino, Eddington-inspired Born-Infeld gravity: astrophysical and cosmological constraints. *Phys. Rev. D* **85**, 104053 (2012). [arXiv:1201.2544](#)
21. M. Banados, P.G. Ferreira, Eddington’s theory of gravity and its progeny. *Phys. Rev. Lett.* **105**, 011101 (2010). [arXiv:1006.1769](#). Erratum: *Phys. Rev. Lett.* **113**, no. 11, 119901 (2014)
22. P.P. Avelino, Eddington-inspired Born-Infeld gravity: nuclear physics constraints and the validity of the continuous fluid approximation. *JCAP* **1211**, 022 (2012). [arXiv:1207.4730](#)
23. P.P. Avelino, Probing gravity at sub-femtometer scales through the pressure distribution inside the proton. *Phys. Lett. B* **795**, 627–631 (2019). [arXiv:1902.01318](#)
24. A.D.I. Latorre, G.J. Olmo, M. Ronco, Observable traces of non-metricity: new constraints on metric-affine gravity. *Phys. Lett. B* **780**, 294–299 (2018). [arXiv:1709.04249](#)
25. A. Delhom, V. Miralles, A. Peñuelas, *Effective Interactions in Ricci-Based Gravity Models Below the Non-metricity Scale*. [arXiv:1907.05615](#)
26. J. Boos, F.W. Hehl, Gravity-induced four-fermion contact interaction implies gravitational intermediate W and Z type gauge bosons. *Int. J. Theor. Phys.* **56**(3), 751–756 (2017). [arXiv:1606.09273](#)
27. E. Cartan, *C.R. Acad. Sci. (Paris)* **174**, 593 (1922)
28. E. Cartan, *Ann. Ec. Norm. Sup.* **40**, 325 (1923)
29. E. Cartan, *Ann. E c. Norm. Sup.* **41**, 1 (1924)

30. E. Cartan, *Ann. Ec. Norm. Sup.* **42**, 17 (1925)
31. R. Utiyama, Invariant theoretical interpretation of interaction. *Phys. Rev.* **101**, 1597–1607 (1956). (157 (1956))
32. T.W.B. Kibble, Lorentz invariance and the gravitational field. *J. Math. Phys.* **2**, 212–221 (1961). (168 (1961))
33. D.W. Sciama, *On the Analogy Between Charge and Spin in General Relativity* (1962)
34. D.W. Sciama, The physical structure of general relativity. *Rev. Mod. Phys.* **36**, 463–469 (1964). (Erratum: *Rev. Mod. Phys.* **36**, 1103 (1964))
35. F.W. Hehl, P. Von Der Heyde, G.D. Kerlick, J.M. Nester, General relativity with spin and torsion: foundations and prospects. *Rev. Mod. Phys.* **48**, 393–416 (1976)
36. N.J. Poplawski, Cosmology with torsion: an alternative to cosmic inflation. *Phys. Lett. B* **694**, 181–185 (2010). [arXiv:1007.0587](https://arxiv.org/abs/1007.0587). Erratum: *Phys. Lett. B* **701**, 672 (2011)
37. I.L. Shapiro, Physical aspects of the space-time torsion. *Phys. Rept.* **357**, 113 (2002). [arxiv:hep-th/0103093](https://arxiv.org/abs/hep-th/0103093)
38. S.M. Carroll, G.B. Field, Consequences of propagating torsion in connection dynamic theories of gravity. *Phys. Rev. D* **50**, 3867–3873 (1994). [arxiv:gr-qc/9403058](https://arxiv.org/abs/gr-qc/9403058)
39. A.S. Belyaev, I.L. Shapiro, The Action for the (propagating) torsion and the limits on the torsion parameters from present experimental data. *Phys. Lett. B* **425**, 246–254 (1998). [arxiv:hep-ph/9712503](https://arxiv.org/abs/hep-ph/9712503)
40. F. Hehl, How does one measure torsion of space-time? *Phys. Lett. A* **36**(3), 225–226 (1971)
41. H. Rumpf, Quasiclassical limit of the Dirac equation and the equivalence principle in the Riemann–Cartan geometry. *NATO Sci. Ser. B* **58**, 93–104 (1980)
42. J. Audretsch, Dirac electron in space-times with torsion: spinor propagation, spin precession, and nongeodesic orbits. *Phys. Rev. D* **24**, 1470–1477 (1981)
43. K. Nomura, T. Shirafuji, K. Hayashi, Spinning test particles in space-time with torsion. *Prog. Theor. Phys.* **86**, 1239–1258 (1991)
44. Y.N. Obukhov, A.J. Silenko, O.V. Teryaev, Spin-torsion coupling and gravitational moments of Dirac fermions: theory and experimental bounds. *Phys. Rev. D* **90**(12), 124068 (2014). [arXiv:1410.6197](https://arxiv.org/abs/1410.6197)
45. B. Mashhoon, *Gravitoelectromagnetism: A Brief Review*. [arxiv:gr-qc/0311030](https://arxiv.org/abs/gr-qc/0311030)
46. W.-T. Ni, Searches for the role of spin and polarization in gravity. *Rept. Prog. Phys.* **73**, 056901 (2010). [arXiv:0912.5057](https://arxiv.org/abs/0912.5057)
47. W.-T. Ni, Searches for the role of spin and polarization in gravity: a five-year update. *Int. J. Mod. Phys. Conf. Ser.* **40**, 1660010 (2016). [arXiv:1501.07696](https://arxiv.org/abs/1501.07696)
48. J. Audretsch, C. Lammerzahl, Neutron interference: general theory of the influence of gravity, inertia and space-time torsion. *J. Phys. A Math. Gen.* **16**, 2457–2477 (1983)
49. C. Lammerzahl, Constraints on space-time torsion from Hughes-Drever experiments. *Phys. Lett. A* **228**, 223 (1997). [arxiv:gr-qc/9704047](https://arxiv.org/abs/gr-qc/9704047)
50. S. Mohanty, U. Sarkar, Constraints on background torsion field from K physics. *Phys. Lett. B* **433**, 424–428 (1998). [arxiv:hep-ph/9804259](https://arxiv.org/abs/hep-ph/9804259)
51. P. Singh, L.H. Ryder, Einstein-cartan-dirac theory in the low-energy limit. *Class. Quantum Grav.* **14**, 3513–3525 (1997)
52. V.A. Kostelecky, N. Russell, J. Tasson, New Constraints on Torsion from Lorentz Violation. *Phys. Rev. Lett.* **100**, 111102 (2008). [arXiv:0712.4393](https://arxiv.org/abs/0712.4393)
53. J. Foster, V.A. Kostelecký, R. Xu, Constraints on nonmetricity from bounds on lorentz violation. *Phys. Rev. D* **95**(8), 084033 (2017). [arXiv:1612.08744](https://arxiv.org/abs/1612.08744)
54. A. Delhom, J.R. Nascimento, G.J. Olmo, A.Y. Petrov, P.J. Porfírio, *Quantum Corrections in Weak Metric-affine Bumblebee Gravity*. [arXiv:1911.11605](https://arxiv.org/abs/1911.11605)
55. A. Delhom, J.R. Nascimento, G.J. Olmo, A.Y. Petrov, P.J. Porfírio, *Metric-affine Bumblebee Gravity: Quantum Aspects*. [arXiv:2010.06391](https://arxiv.org/abs/2010.06391)
56. X.-C. Duan, M.-K. Zhou, X.-B. Deng, H.-B. Yao, C.-G. Shao, J. Luo, Z.-K. Hu, Test of the universality of free fall with atoms in different spin Orientations. *Phys. Rev. Lett.* **117**, 023001 (2016). [arXiv:1503.00433](https://arxiv.org/abs/1503.00433)

57. F.M.L. de Almeida Jr., A.A. Nepomuceno, Torsion discovery potential and its discrimination at CERN LHC. *Phys. Rev.* **79**, 014029 (2009). [arXiv:0811.0291](https://arxiv.org/abs/0811.0291)
58. A.S. Belyaev, I.L. Shapiro, M.A.B. do Vale, Torsion phenomenology at the LHC. *Phys. Rev. D* **75**, 034014 (2007). [arxiv:hep-ph/0701002](https://arxiv.org/abs/hep-ph/0701002)
59. R. Lehnert, W.M. Snow, H. Yan, A first experimental limit on in-matter torsion from neutron spin rotation in liquid ${}^4\text{He}$. *Phys. Lett. B* **730**, 353–356 (2014). [arXiv:1311.0467](https://arxiv.org/abs/1311.0467). Erratum: *Phys. Lett. B* **744**, 415 (2015)
60. J.B. Jiménez, L. Heisenberg, T.S. Koivisto, The geometrical trinity of gravity. *Universe* **5**(7), 173 (2019). [arXiv:1903.06830](https://arxiv.org/abs/1903.06830)

Chapter 22

Stars as Tests of Modified Gravity



Gonzalo J. Olmo, Diego Rubiera-Garcia, and Aneta Wojnar

Compact stars, both individual and in binary mergers, represent suitable scenarios to test General Relativity (GR) in its strong-field regime and to eventually find any deviations from its predictions. This is so because compact stars are the objects (excluding black holes) where the largest curvatures and higher densities can be reached in Nature [1]. To model stellar structure within modified theories of gravity in order to be able to explore possible new physics, one has to address several additional difficulties associated with the mathematical structure of these theories or to the new dynamics introduced by them within this context [2]. In this sense, in addition to the well-known troubles with the higher-order equations of motion and propagation of ghost-like instabilities introduced by many such theories, finding theoretically consistent models of stellar structure beyond GR requires additional improvements on a case-by-case basis. This is well illustrated in theories such as $f(R)$ and, more generally, scalar-tensor theories. In such cases, the fact that the scalar field contributes to the mass of the star beyond its surface [3] introduces important technical difficulties, in particular regarding the consistency of their weak-field and

G. J. Olmo

Depto. de Física Teórica and IFIC, Centro Mixto Universidad de Valencia-CSIC,
46100 Burjassot, Valencia, Spain

Departamento de Física, Universidade Federal da Paraíba, João Pessoa, Paraíba
58051-900, Brazil

D. Rubiera-Garcia (✉)

Departamento de Física Teórica and IPARCOS, Universidad Complutense de Madrid,
28040 Madrid, Spain
e-mail: drubiera@ucm.es

A. Wojnar

Laboratory of Theoretical Physics, Institute of Physics, University of Tartu, W. Ostwaldi 1,
50411 Tartu, Estonia
e-mail: aneta.wojnar@cosmo-ufes.org

slow-motion limit with Solar System experiments and also with respect to how to perform the right matching to an external Schwarzschild solution, which has been the source of a heated debate in the literature [4–9]. As another example, those theories inducing additional dependences on the local energy density of the matter fields are known to be potentially problematic in the description of stellar surfaces [10–12], requiring a more careful analysis of the physical description at the matching surface with the external solution [13].

22.1 Modified Tolman-Oppenheimer-Volkoff Equations

Gravitational theories extending GR typically modify the Tolman-Oppenheimer-Volkoff (TOV) equations of hydrostatic equilibrium

$$p' = -(\rho + p) \frac{m(r) + 4\pi pr^3}{r[r - 2m(r)]} \quad (22.1)$$

$$m(r) = 4\pi \int_0^r d\tilde{r} \tilde{r}^2 \rho(\tilde{r}) \quad (22.2)$$

where ρ and p are the energy density and pressure of a perfect fluid as the matter source, respectively, while $m(r)$ is the mass function. In a typical case, such modifications will consist of additional terms/contributions to these equations.

One of the most characteristic and observationally accessible predictions of models of compact stars within these theories corresponds to the mass-radius relations of neutron stars as compared to those of GR. Such relations are obtained once a given equation of state (EOS) relating energy density and pressure $p = p(\rho)$ inside the different layers of a neutron star is given, which allows for the resolution of Eqs.(22.1) and (22.2) and their extensions within modified gravity, typically via numerical methods. Since the EOS of dense matter at the supernuclear densities reached in the innermost region of neutron stars is unknown, the mass-radius relations in GR largely depend on the assumptions on the EOS derived from extrapolations of laboratory nuclear physics. Therefore, the EOS of dense matter can be constrained via observations of neutron stars masses and radii [14], among other quantities, or via observations derived from gravitational wave astronomy [15].

Furthermore, for every modified theory of gravity chosen, such mass-radius relations will also depend on the extra gravitational parameter(s) that appear in the gravitational sector [16]. Since tracking the full mass-radius curve with measurements of enough neutron stars masses and radii is a hard task, the focus is placed instead on the predictions of any such gravitational models on the maximum available mass for a given EOS, and their comparison with the reported measurements of several neutron stars with masses around $2M_\odot$ [17–20]. In this sense, since the TOV equations of $f(R)$ gravity are known in closed form [3], several $f(R)$ models have been thoroughly studied in the literature, including the quadratic one, $f(R) = R + \alpha R^2$

[21–26] (also considering the effects of anisotropies [27]), cubic [28], exponential [29], logarithmic [30, 31], power-law [28, 32], Hu-Sawicki [21], and others [33], using both perturbative and non-perturbative analyses, and dealing with the definition of the measurable mass in these theories. The hyperonic puzzle, namely, the fact that the presence of hyperons in realistic EOS at the neutron star’s core tends to soften it, and decrease the maximum mass perhaps even below the $2M_{\odot}$ has also been addressed within these theories [34].

Beyond $f(R)$ gravity, the mass-radius relations as well as other aspects of the phenomenology of compact stars have been studied within many other theories of gravity, such as in the more general scalar-tensor theories [35–38] where, in particular, evidence for scalarised solutions has been found [39–41]. Further theories with additional scalar fields include the Horndeski and beyond Horndeski families, and their degenerate higher-order scalar-tensor (DHOST) extensions [42–44]. The list of modified theories with other assumptions/dynamics beyond GR investigated within this context is varied, and includes Proca theories [45], Einstein-dilaton-Gauss-Bonnet gravity [46–50], massive gravity [51–53] and bigravity [54, 55], Rainbow’s gravity [56], teleparallel gravity [57–59], mimetic gravity [60, 61], theories breaking the Lorentz invariance [62–65] or the conservation of the energy-momentum tensor [66–69, 69–73], $f(\mathcal{R})$ gravity in metric-affine spaces [74–77], or Eddington-inspired Born-Infeld gravity [10], among many others. The parameter(s) of any such theories are typically experimentally/observationally constrained by Solar System experiments [78], cosmological observations [79], fundamental physics, etc., thus restricting the space of parameters one can play with.

The main observation regarding the phenomenology of such modified gravity models for neutron stars is a modification of the mass-radius relations in the sense of producing larger masses and smaller radii, or the other way round, depending on the specific combinations of parameters and EOS, though some specific models have more involved behaviours. However, regarding the maximum allowed mass for a given EOS, and within experimental/observational constraints of every theory from different sources (when available), most such models yield meagre increases that may be typically smaller than the observational errors of current capabilities to measure neutron stars’ masses and radii. This yields a bottleneck for testing these theories via these observations, unless significant improvements in the precision of these probes are obtained in the near future [80].

There are some exceptions to this general rule, with several models yielding significant increases of the maximum mass. In turn, this might be able to bring back to life some cases of soft EOS unable to reach the $2M_{\odot}$ observational threshold within GR. On the other hand, this offers the possibility of further constraining these theories and testing their observational viability as compared to GR, should heavier neutron stars be detected in the future.

While these are examples of static stars studied within modified theories of gravity, the addition of rotation has several interesting effects and modifications to the above picture. It is indeed known that in GR the presence of rotation may raise the maximum available mass for a given EOS by a factor up to $\sim 15\% - 20\%$ as compared to the

static case [81] and, overall, a similar conclusion can be reached for modified gravity, as has been investigated for several specific models.

However, an even more interesting aspect of the corresponding rotating structure models arises from the consideration of the moment of inertia and other associated quantities, which, being also observationally accessible, typically show much larger increases in their values when moving from GR to modified gravity than in the case of maximum masses. This has been explored and confirmed for several theories, including $f(R)$ [82–84], scalar-tensor theories [39, 85–88], the Horndeski family [89–91], and so on [92], also including anisotropic contributions [93]. Though this analysis is more readily performed for the slowly-rotating case, where the effects of rotation can be simulated via a small perturbation upon a static, spherically symmetric star [94], the case of rapidly and differentially rotating stars has a particular interest for the analysis of tidal deformability and universal (I-love-Q) relations [95–99], as well as for the generation of gravitational waves out of binary neutron star mergers [100–106] in order to place constraints on these theories.

22.2 Modified Lane-Emden Equation

In addition to neutron stars, the case of non-relativistic stars (such as white, brown and red dwarfs) is also of interest. In this case, $p \ll \rho$, the TOV equations can be reduced down to their Newtonian counterpart, namely, the Poisson equation, which is called Lane-Emden equation on its dimensionless form. Moreover, different types of non-relativistic stars can be well modelled using polytropic EOS, $p = K\rho^{\frac{n+1}{n}}$, according to specific values of the polytropic constant K and index n . Despite central densities and curvatures being much weaker than in their relativistic counterparts, this scenario has the advantage of removing the large uncertainty in the EOS ascribed to dense matter inside neutron stars and, therefore, the degeneracy in the predictions of the corresponding models.

The main prediction of many modified gravity models for non-relativistic stars is the weakening/strengthening of the gravitational force inside astrophysical bodies, as given by the presence of extra terms in the Lane-Emden equation [107–114]. This has several physical consequences for the structure of non-relativistic stars, with some observational discriminators attached to them. For instance, for white dwarfs, many such models modify the Chandrashekar $1.40M_{\odot}$ limit of GR [115], including scalar-tensor theories and their Horndeski extensions and beyond [112, 116–119], allowing us to place constraints on some of these theories. In particular, this feature may allow us to generate the so-called Super-Chandrashekar white dwarfs, with masses as high as $2.8M_{\odot}$, to meet some recent controversial observations [120, 121].

Another aspect of non-relativistic stars affected by modified theories of gravity is their luminosity, as demonstrated in [110, 122]. Moreover, the modified Lane-Emden equation in this case also has a direct impact in the minimum mass required for a star to burn sufficiently stable fuel to compensate for photospheric losses, that

is, to belong to the main sequence. Using a crude but surprisingly accurate analytic model, GR yields an estimate of roughly $\sim 0.09M_{\odot}$ [123, 124] for this minimum main sequence mass (MMSM), which is just less than $\sim 10\%$ smaller than the one obtained via numerical simulations. For three theories of modified gravity, namely, scalar-tensor [125], DHOST [119], and metric-affine $f(\mathcal{R}) = \mathcal{R} + \alpha\mathcal{R}^2$ [122], this same calculation has been carried out, yielding constraints upon the parameters of each theory resulting from the comparison with the least massive star ever observed, Gl 866 C, with $M_{MMSM} \approx 0.0930 \pm 0.0008M_{\odot}$ [126]. Observations of the radii of low-mass brown dwarfs are another possibility to constrain theories of gravity, as provided by the future mission GAIA [127], since for such objects the theoretical models given by the (modified) Lane-Emden equation are mass-independent [114, 125, 128]. Moreover, some modified theories of gravity shift the stability bound of GR (with a critical value of the polytropic index $n = 3$), allowing for a wider range of the polytropic index n , and at the same time providing an additional dependence on the theory's parameter [10, 129, 130].

It turns out that modified gravity has also impact on evolution of stellar objects: the main sequence and red giant stars in modified gravity framework were studied in [131–133] while low-mass stellar objects in [134], where it was demonstrated that Hayashi tracks and radiative core development are gravity model dependent phenomena. It was also argued that the upper mass limit of fully convective stars on the main sequence might be different than the one provided by numerical simulations whose codes are based on Newtonian equations. Moreover, due to the fact that one does not observe any stars in the so-called Hayashi forbidden zone, studying Hayashi tracks may provide a tool for constraining gravitational theories [134].

Another important problem that needs to be deeper examined is the age of the stellar objects. One of the methods to determine the clusters' age, as well as the age of their individual stars and white dwarfs, uses lithium abundance in low-mass stars. The lithium depletion method has been believed so far to be the most reliable technique for young globular clusters' age determination, and this is why this procedure is utilized to calibrate other techniques used for the age estimation.

An additional use of lithium abundance is to distinguish brown dwarfs from Main Sequence stars, because the true low-mass stars burn out lithium before they reach the Main Sequence, while in the brown dwarf's atmosphere this light element is observed. It was however demonstrated [135] that the lithium abundance in low-mass stellar objects depends on the gravitational model, introducing an additional uncertainty to age determination techniques, if they rely on the light element depletion method. This causes a significant shortening of the early stellar evolution phases, having the following consequences: it will contribute to the explanation of "too old" white dwarfs, as for example the one in the binary system KIC 8145411 [136, 137]. Furthermore, one also deals with the changes in the number of stars in the pre- and main sequence phases, giving different impact to the distant galaxies brightness in comparison to the GR prediction [132]. Moreover, the lithium abundance may also be a tool to test theories of gravity: theories which prominently prolong the low-mass stars' lifetimes, in comparison to the current accepted models, would rise doubts on those that introduce such an effect.

In summary, stars represent yet another suitable scenario to test the predictions of modified theories of gravity. Using both relativistic and non-relativistic stars, the combination of the predictions of any theory for both such types of stars may allow us to narrow down the range of observationally viable values of the corresponding parameters, as has been proven in the case of some scalar-tensor theories [43]. In addition, such constraints can be connected with others coming from gravitational wave astronomy and cosmological tests (such as inflationary and dark energy models). It thus represents a promising avenue in which to explore the strong field regime of our gravitational theories.

References

1. J.M. Lattimer, M. Prakash, The physics of neutron stars. *Science* **304**, 536–542 (2004). [arxiv:astro-ph/0405262](#)
2. G.J. Olmo, D. Rubiera-Garcia, A. Wojnar, *Stellar Structure Models in Modified Theories of Gravity: Lessons and Challenges*. [arXiv:1912.05202](#)
3. G.J. Olmo, Palatini approach to modified gravity: $f(R)$ theories and beyond. *Int. J. Mod. Phys. D* **20**, 413–462 (2011). [arXiv:1101.3864](#)
4. T. Chiba, 1/R gravity and scalar–tensor gravity. *Phys. Lett. B* **575**, 1–3 (2003). [arxiv:astro-ph/0307338](#)
5. A.L. Erickcek, T.L. Smith, M. Kamionkowski, Solar System tests do rule out 1/R gravity. *Phys. Rev. D* **74**, 121501 (2006). [arxiv:astro-ph/0610483](#)
6. K. Kainulainen, J. Piilonen, V. Reijonen, D. Sunhede, Spherically symmetric spacetimes in $f(R)$ gravity theories. *Phys. Rev. D* **76**, 024020 (2007). [arXiv:0704.2729](#)
7. T. Faulkner, M. Tegmark, E.F. Bunn, Y. Mao, Constraining $f(R)$ gravity as a scalar tensor theory. *Phys. Rev. D* **76**, 063505 (2007). [arxiv:astro-ph/0612569](#)
8. T. Multamaki, I. Vilja, Static spherically symmetric perfect fluid solutions in $f(R)$ theories of gravity. *Phys. Rev. D* **76**, 064021 (2007). [arxiv:astro-ph/0612775](#)
9. K. Henttunen, T. Multamaki, I. Vilja, Stellar configurations in $f(R)$ theories of gravity. *Phys. Rev. D* **77**, 024040 (2008). [arXiv:0705.2683](#)
10. P. Pani, V. Cardoso, T. Delsate, Compact stars in Eddington inspired gravity. *Phys. Rev. Lett.* **107**, 031101 (2011). [arXiv:1106.3569](#)
11. E. Barausse, T.P. Sotiriou, J.C. Miller, A No-go theorem for polytropic spheres in Palatini $f(R)$ gravity. *Class. Quant. Grav.* **25**, 062001 (2008). [arxiv:gr-qc/0703132](#)
12. E. Barausse, T.P. Sotiriou, J.C. Miller, Curvature singularities, tidal forces and the viability of Palatini $f(R)$ gravity. *Class. Quant. Grav.* **25**, 105008 (2008). [arXiv:0712.1141](#)
13. G.J. Olmo, Re-examination of Polytropic Spheres in Palatini $f(R)$ Gravity. *Phys. Rev. D* **78**, 104026 (2008). [arXiv:0810.3593](#)
14. J.M. Lattimer, M. Prakash, Neutron star observations: prognosis for equation of state constraints. *Phys. Rept.* **442**, 109–165 (2007). [arxiv:astro-ph/0612440](#)
15. F.J. Llanes-Estrada, E. Lope-Oter, Hadron matter in neutron stars in view of gravitational wave observations. *Prog. Part. Nucl. Phys.* **109**, 103715 (2019). [arXiv:1907.12760](#)
16. L. Shao, Degeneracy in studying the supranuclear equation of state and modified gravity with neutron stars. *AIP Conf. Proc.* **2127**(1), 020016 (2019). [arXiv:1901.07546](#)
17. J. Antoniadis et al., A massive pulsar in a compact relativistic binary. *Science* **340**, 6131 (2013). [arXiv:1304.6875](#)
18. F. Crawford, M.S.E. Roberts, J.W.T. Hessels, S.M. Ransom, M. Livingstone, C.R. Tam, V.M. Kaspi, A survey of 56 Mid-latitude EGRET error boxes for radio pulsars. *Astrophys. J.* **652**, 1499–1507 (2006). [arxiv:astro-ph/0608225](#)

19. M. Linares, T. Shahbaz, J. Casares, Peering into the dark side: magnesium lines establish a massive neutron star in PSR J2215+5135. *Astrophys. J.* **859**(1), 54 (2018). [arXiv:1805.08799](#)
20. H.C. Collaboration et al., Relativistic Shapiro delay measurements of an extremely massive millisecond pulsar. *Nat. Astron.* **4**(1), 72–76 (2019). [arXiv:1904.06759](#)
21. M. Aparicio Resco, Á. de la Cruz-Dombriz, F.J. Llanes Estrada, V. Zapatero Castrillo, On neutron stars in $f(R)$ theories: small radii, large masses and large energy emitted in a merger. *Phys. Dark Univ.* **13**, 147–161 (2016). [arXiv:1602.03880](#)
22. A. Cooney, S. DeDeo, D. Psaltis, Neutron stars in $f(R)$ gravity with perturbative constraints. *Phys. Rev. D* **82**, 064033 (2010). [arXiv:0910.5480](#)
23. M. Orellana, F. Garcia, F.A. Teppa Pannia, G..E.. Romero, Structure of neutron stars in R -squared gravity. *Gen. Rel. Grav.* **45**, 771–783 (2013). [arXiv:1301.5189](#)
24. S.S. Yazadjiev, D.D. Doneva, K.D. Kokkotas, K.V. Staykov, Non-perturbative and self-consistent models of neutron stars in R -squared gravity. *JCAP* **1406**, 003 (2014). [arXiv:1402.4469](#)
25. A.V. Astashenok, S.D. Odintsov, A. de la Cruz-Dombriz, The realistic models of relativistic stars in $f(R) = R + \alpha R^2$ gravity. *Class. Quant. Grav.* **34**(20), 205008 (2017). [arXiv:1704.08311](#)
26. A.V. Astashenok, A.S. Baigashov, S.A. Lapin, Neutron stars in frames of R^2 -gravity and gravitational waves. *Int. J. Geom. Meth. Mod. Phys.* **16**(01), 1950004 (2018). [arXiv:1812.10439](#)
27. V. Folomeev, Anisotropic neutron stars in R^2 gravity. *Phys. Rev. D* **97**(12), 124009 (2018). [arXiv:1802.01801](#)
28. S. Capozziello, M. De Laurentis, R. Farinelli, S.D. Odintsov, Mass-radius relation for neutron stars in $f(R)$ gravity. *Phys. Rev. D* **93**(2), 023501 (2016). [arXiv:1509.04163](#)
29. G. Cognola, E. Elizalde, S. Nojiri, S.D. Odintsov, L. Sebastiani, S. Zerbini, A Class of viable modified $f(R)$ gravities describing inflation and the onset of accelerated expansion. *Phys. Rev. D* **77**, 046009 (2008). [arXiv:0712.4017](#)
30. A.V. Astashenok, S. Capozziello, S.D. Odintsov, Further stable neutron star models from $f(R)$ gravity. *JCAP* **1312**, 040 (2013). [arXiv:1309.1978](#)
31. H. Alavirad, J.M. Weller, Modified gravity with logarithmic curvature corrections and the structure of relativistic stars. *Phys. Rev. D* **88**(12), 124034 (2013). [arXiv:1307.7977](#)
32. M. De Laurentis, Noether's stars in $f(\mathcal{R})$ gravity. *Phys. Lett. B* **780**, 205–210 (2018). [arXiv:1802.09073](#)
33. R. Kase, S. Tsujikawa, Neutron stars in $f(R)$ gravity and scalar-tensor theories. *JCAP* **1909**(09), 054 (2019). [arXiv:1906.08954](#)
34. A.V. Astashenok, S. Capozziello, S.D. Odintsov, Maximal neutron star mass and the resolution of the hyperon puzzle in modified gravity. *Phys. Rev. D* **89**(10), 103509 (2014). [arXiv:1401.4546](#)
35. M.W. Horbatsch, C.P. Burgess, Semi-analytic stellar structure in scalar-tensor gravity. *JCAP* **1108**, 027 (2011). [arXiv:1006.4411](#)
36. A. Cisterna, T. Delsate, M. Rinaldi, Neutron stars in general second order scalar-tensor theory: the case of nonminimal derivative coupling. *Phys. Rev. D* **92**(4), 044050 (2015). [arXiv:1504.05189](#)
37. A. Wojnar, H. Velten, Equilibrium and stability of relativistic stars in extended theories of gravity. *Eur. Phys. J. C* **76**(12), 697 (2016). [arXiv:1604.04257](#)
38. H. Sotani, K.D. Kokkotas, Maximum mass limit of neutron stars in scalar-tensor gravity. *Phys. Rev. D* **95**(4), 044032 (2017). [arXiv:1702.00874](#)
39. H.O. Silva, H. Sotani, E. Berti, M. Horbatsch, Torsional oscillations of neutron stars in scalar-tensor theory of gravity. *Phys. Rev. D* **90**(12), 124044 (2014). [arXiv:1410.2511](#)
40. M. Horbatsch, H.O. Silva, D. Gerosa, P. Pani, E. Berti, L. Gualtieri, U. Sperhake, Tensor-multi-scalar theories: relativistic stars and $3 + 1$ decomposition. *Class. Quant. Grav.* **32**(20), 204001 (2015). [arXiv:1505.07462](#)
41. J. Novak, Spherical neutron star collapse in tensor–scalar theory of gravity. *Phys. Rev. D* **57**, 4789–4801 (1998). [arxiv:gr-qc/9707041](#)

42. M. Crisostomi, K. Koyama, Self-accelerating universe in scalar-tensor theories after GW170817. *Phys. Rev. D* **97**(8), 084004 (2018). [arXiv:1712.06556](#)
43. E. Babichev, K. Koyama, D. Langlois, R. Saito, J. Sakstein, Relativistic stars in Beyond Horndeski Theories. *Class. Quant. Grav.* **33**(23), 235014 (2016). [arXiv:1606.06627](#)
44. J. Chagoya, G. Tasinato, Compact objects in scalar-tensor theories after GW170817. *JCAP* **1808**(08), 006 (2018). [arXiv:1803.07476](#)
45. R. Kase, M. Minamitsuji, S. Tsujikawa, Relativistic stars in vector-tensor theories. *Phys. Rev. D* **97**(8), 084009 (2018). [arXiv:1711.08713](#)
46. P. Pani, E. Berti, V. Cardoso, J. Read, Compact stars in alternative theories of gravity. Einstein-Dilaton-Gauss-Bonnet gravity. *Phys. Rev. D* **84**, 104035 (2011). [arXiv:1109.0928](#)
47. G. Panotopoulos, Á. Rincón, Relativistic strange quark stars in Lovelock gravity. *Eur. Phys. J. Plus* **134**(9), 472 (2019). [arXiv:1907.03545](#)
48. H.O. Silva, J. Sakstein, L. Gualtieri, T.P. Sotiriou, E. Berti, Spontaneous scalarization of black holes and compact stars from a Gauss-Bonnet coupling. *Phys. Rev. Lett.* **120**(13), 131104. [arXiv:1711.02080](#)
49. D.D. Doneva, S.S. Yazadjiev, Neutron star solutions with curvature induced scalarization in the extended Gauss-Bonnet scalar-tensor theories. *JCAP* **1804**(04), 011 (2018). [arXiv:1712.03715](#)
50. J.L. Blazquez-Salcedo, L.M. Gonzalez-Romero, J. Kunz, S. Mojica, F. Navarro-Lerida, Axial quasinormal modes of Einstein-Gauss-Bonnet-dilaton neutron stars. *Phys. Rev. D* **93**(2), 024052 (2016). [arXiv:1511.03960](#)
51. T. Katuragawa, S. Nojiri, S.D. Odintsov, M. Yamazaki, Relativistic stars in de Rham-Gabadadze-Tolley massive gravity. *Phys. Rev. D* **93**, 124013 (2016). [arXiv:1512.00660](#)
52. P. Kareeso, P. Burikham, T. Harko, Mass-radius ratio bounds for compact objects in Lorentz-violating dRGT massive gravity theory. *Eur. Phys. J. C* **78**(11), 941 (2018). [arXiv:1802.01017](#)
53. S.H. Hendi, G.H. Bordbar, B. Eslam Panah, S. Panahiyan, Neutron stars structure in the context of massive gravity. *JCAP* **1707**, 004 (2017). [arXiv:1701.01039](#)
54. J. Enander, E. Mortsell, On stars, galaxies and black holes in massive bigravity. *JCAP* **1511**(11), 023 (2015). [arXiv:1507.00912](#)
55. K. Aoki, K.-I. Maeda, M. Tanabe, Relativistic stars in bigravity theory. *Phys. Rev. D* **93**(6), 064054 (2016). [arXiv:1602.02227](#)
56. S.H. Hendi, G.H. Bordbar, B.E. Panah, S. Panahiyan, Modified TOV in gravity's rainbow: properties of neutron stars and dynamical stability conditions. *JCAP* **1609**(09), 013 (2016). [arXiv:1509.05145](#)
57. S. Ilijic, M. Sossich, Compact stars in $f(T)$ extended theory of gravity. *Phys. Rev. D* **98**(6), 064047 (2018). [arXiv:1807.03068](#)
58. A. DeBenedictis, S. Ilijic, *Spherically Symmetric Vacuum in Covariant $F(T) = T + \frac{\alpha}{2}T^2 + \mathcal{O}(T^\gamma)$ Gravity Theory*
59. D. Deb, S. Ghosh, S.K. Maurya, M. Khlopov, S. Ray, *Anisotropic Compact Stars in $f(T)$ Gravity Under Karmarkar Condition*. [arXiv:1811.11797](#)
60. A.V. Astashenok, S.D. Odintsov, From neutron stars to quark stars in mimetic gravity. *Phys. Rev. D* **94**(6), 063008 (2016). [arXiv:1512.07279](#)
61. J.C. Fabris, H. Velten, A. Wojnar, Existence of static spherically-symmetric objects in action-dependent Lagrangian theories. *Phys. Rev. D* **99**(12), 124031 (2019). [arXiv:1903.12193](#)
62. R. Xu, J. Zhao, L. Shao, *Neutron Star Structure in the Minimal Gravitational Standard-Model Extension and the Implication to Continuous Gravitational Waves*. [arXiv:1909.10372](#)
63. K. Kim, J.J. Oh, C. Park, E.J. Son, *Neutron Star Structure in Hořava-Lifshitz Gravity*. [arXiv:1810.07497](#)
64. C. Eling, T. Jacobson, M. Coleman Miller, Neutron stars in Einstein-Aether theory. *Phys. Rev. D* **76**, 042003 (2009). [arXiv:0705.1565](#). Erratum: *Phys. Rev. D* **80**, 129906 (2009)
65. E. Barausse, Neutron star sensitivities in Horava gravity after GW170817. *Phys. Rev. D* **100**(8), 084053 (2019). [arXiv:1907.05958](#)
66. P.H.R.S. Moraes, J.D.V. Arbañil, M. Malheiro, Stellar equilibrium configurations of compact stars in $f(R, T)$ gravity. *JCAP* **1606**, 005 (2016). [arXiv:1511.06282](#)

67. A. Das, F. Rahaman, B.K. Guha, S. Ray, Compact stars in $f(R, T)$ gravity. *Eur. Phys. J. C* **76**(12), 654 (2016). [arXiv:1608.00566](#)
68. D. Deb, S.V. Ketov, M. Khlopov, S. Ray, Study on charged strange stars in $f(R, T)$ gravity. *JCAP* **1910**(10), 070 (2019). [arXiv:1812.11736](#)
69. S.K. Maurya, F. Tello-Ortiz, *Charged Anisotropic Compact Star in $f(R, T)$ Gravity: A Minimal Geometric Deformation Gravitational Decoupling Approach*. [arXiv:1905.13519](#)
70. S.K. Maurya, A. Errehymy, D. Deb, F. Tello-Ortiz, M. Daoud, Study of anisotropic strange stars in $f(R, T)$ gravity: an embedding approach under the simplest linear functional of the matter-geometry coupling. *Phys. Rev. D* **100**(4), 044014 (2019). [arXiv:1907.10149](#)
71. G.A. Carvalho, S.I.D. Santos, P.H.R.S. Moraes, M. Malheiro, *Strange Stars in Energy-Momentum-Conserved $f(R, T)$ Gravity*. [arXiv:1911.02484](#)
72. A.M. Oliveira, H.E.S. Velten, J.C. Fabris, L. Casarini, Neutron stars in rastall gravity. *Phys. Rev. D* **92**(4), 044020 (2015). [arXiv:1506.00567](#)
73. S. Hansraj, A. Banerjee, *Equilibrium Stellar Configurations in Rastall Theory and Linear Equation of State*. [arXiv:1807.00812](#)
74. K. Kainulainen, V. Reijonen, D. Sunhede, The Interior spacetimes of stars in Palatini $f(R)$ gravity. *Phys. Rev. D* **76**, 043503 (2007). [arxiv:gr-qc/0611132](#)
75. F.A. Teppa Pannia, F. Garcia, S.E. Perez Bergliaffa, M. Orellana, G.E. Romero, Structure of compact stars in R-squared Palatini gravity. *Gen. Rel. Grav.* **49**(2), 25 (2017). [arXiv:1607.03508](#)
76. G. Panotopoulos, Strange stars in $f(R)$ theories of gravity in the Palatini formalism. *Gen. Rel. Grav.* **49**(5), 69 (2017). [arXiv:1704.04961](#)
77. A. Wojnar, On stability of a neutron star system in Palatini gravity. *Eur. Phys. J. C* **78**(5), 421 (2018). [arXiv:1712.01943](#)
78. C.M. Will, The confrontation between general relativity and experiment. *Living Rev. Rel.* **17**, 4 (2014). [arXiv:1403.7377](#)
79. P. Bull et al., Beyond Λ CDM: problems, solutions, and the road ahead. *Phys. Dark Univ.* **12**, 56–99 (2016). [arXiv:1512.05356](#)
80. E. Berti et al., Testing general relativity with present and future astrophysical observations. *Class. Quant. Grav.* **32**, 243001 (2015). [arXiv:1501.07274](#)
81. N. Stergioulas, Rotating stars in relativity. *Living Rev. Rel.* **6**, 3 (2003). [arxiv:gr-qc/0302034](#)
82. K.V. Staykov, D.D. Doneva, S.S. Yazadjiev, K.D. Kokkotas, Slowly rotating neutron and strange stars in R^2 gravity. *JCAP* **1410**(10), 006 (2014). [arXiv:1407.2180](#)
83. K.V. Staykov, D.D. Doneva, S.S. Yazadjiev, Orbital and epicyclic frequencies around neutron and strange stars in R^2 gravity. *Eur. Phys. J. C* **75**(12), 607 (2015). [arXiv:1508.07790](#)
84. K.V. Staykov, D.D. Doneva, S.S. Yazadjiev, K.D. Kokkotas, Gravitational wave asteroseismology of neutron and strange stars in R^2 gravity. *Phys. Rev. D* **92**(4), 043009 (2015). [arXiv:1503.04711](#)
85. H.O. Silva, N. Yunes, Neutron star pulse profiles in scalar-tensor theories of gravity. *Phys. Rev. D* **99**(4), 044034 (2019). [arXiv:1808.04391](#)
86. K. Staykov, K.Y. Ekşi, S.S. Yazadjiev, M.M. Türkoğlu, A.S. Arapoğlu, Moment of inertia of neutron star crust in alternative and modified theories of gravity. *Phys. Rev. D* **94**(2), 024056 (2016). [arXiv:1507.05878](#)
87. D. Popchev, K.V. Staykov, D.D. Doneva, S.S. Yazadjiev, Moment of inertia-mass universal relations for neutron stars in scalar-tensor theory with self-interacting massive scalar field. *Eur. Phys. J. C* **79**(2), 178 (2019). [arXiv:1812.00347](#)
88. K.V. Staykov, D. Popchev, D.D. Doneva, S.S. Yazadjiev, Static and slowly rotating neutron stars in scalar-tensor theory with self-interacting massive scalar field. *Eur. Phys. J. C* **78**(7), 586 (2018). [arXiv:1805.07818](#)
89. H.O. Silva, A. Maselli, M. Minamitsuji, E. Berti, Compact objects in Horndeski gravity. *Int. J. Mod. Phys. D* **25**(09), 1641006 (2016). [arXiv:1602.05997](#)
90. A. Cisterna, T. Delsate, L. Ducobu, M. Rinaldi, Slowly rotating neutron stars in the nonminimal derivative coupling sector of Horndeski gravity. *Phys. Rev. D* **93**(8), 084046 (2016). [arXiv:1602.06939](#)

91. A. Maselli, H.O. Silva, M. Minamitsuji, E. Berti, Neutron stars in Horndeski gravity. *Phys. Rev. D* **93**(12), 124056 (2016). [arXiv:1603.04876](#)
92. A. Sullivan, N. Yunes, Slowly-Rotating neutron stars in massive bigravity. *Class. Quant. Grav.* **35**(4), 045003 (2018). [arXiv:1709.03311](#)
93. H.O. Silva, C.F.B. Macedo, E. Berti, L.C.B. Crispino, Slowly rotating anisotropic neutron stars in general relativity and scalar-tensor theory. *Class. Quant. Grav.* **32**, 145008 (2015). [arXiv:1411.6286](#)
94. J.B. Hartle, Slowly rotating relativistic stars. 1. Equations of structure. *Astrophys. J.* **150**, 1005–1029 (1967)
95. D.D. Doneva, S.S. Yazadjiev, N. Stergioulas, K.D. Kokkotas, Rapidly rotating neutron stars in scalar-tensor theories of gravity. *Phys. Rev. D* **88**(8), 084060 (2013). [arXiv:1309.0605](#)
96. S.S. Yazadjiev, D.D. Doneva, K.D. Kokkotas, Rapidly rotating neutron stars in R-squared gravity. *Phys. Rev. D* **91**(8), 084018 (2015). [arXiv:1501.04591](#)
97. S.S. Yazadjiev, D.D. Doneva, K.D. Kokkotas, Oscillation modes of rapidly rotating neutron stars in scalar-tensor theories of gravity. *Phys. Rev. D* **96**(6), 064002 (2017). [arXiv:1705.06984](#)
98. B. Kleihaus, J. Kunz, S. Mojica, M. Zagermann, Rapidly Rotating Neutron Stars in Dilatonic Einstein-Gauss-Bonnet Theory. *Phys. Rev. D* **93**(6), 064077 (2016). [arXiv:1601.05583](#)
99. D.D. Doneva, S.S. Yazadjiev, N. Stergioulas, K.D. Kokkotas, Differentially rotating neutron stars in scalar-tensor theories of gravity. *Phys. Rev. D* **98**(10), 104039 (2018). [arXiv:1807.05449](#)
100. P. Pani, E. Berti, Slowly rotating neutron stars in scalar-tensor theories. *Phys. Rev. D* **90**(2), 24025 (2014). [arXiv:1405.4547](#)
101. E. Barausse, C. Palenzuela, M. Ponce, L. Lehner, Neutron-star mergers in scalar-tensor theories of gravity. *Phys. Rev. D* **87**, 081506 (2013). [arXiv:1212.5053](#)
102. K. Yagi, L.C. Stein, N. Yunes, T. Tanaka, Isolated and binary neutron stars in dynamical Chern-Simons gravity. *Phys. Rev. D* **87**, 084058 (2013). [arXiv:1302.1918](#). Erratum: *Phys. Rev. D* **93**, no. 8, 089909 (2016)
103. M. Okounkova, L.C. Stein, M.A. Scheel, S.A. Teukolsky, Numerical binary black hole collisions in dynamical Chern-Simons gravity. *Phys. Rev. D* **100**(10), 104026 (2019). [arXiv:1906.08789](#)
104. Z. Carson, B.C. Seymour, K. Yagi, *Future Prospects for Probing Scalar-Tensor Theories with Gravitational Waves from Mixed Binaries*. [arXiv:1907.03897](#)
105. C. Zhang, X. Zhao, A. Wang, B. Wang, K. Yagi, N. Yunes, W. Zhao, T. Zhu, *Gravitational Waves from the Quasi-Circular Inspiral of Compact Binaries in Einstein-Aether Theory*. [arXiv:1911.10278](#)
106. X. Zhao et al., Gravitational waveforms and radiation powers of the triple system PSR J0337+1715 in modified theories of gravity. *Phys. Rev. D* **100**(8), 083012 (2019). [arXiv:1903.09865](#)
107. S. Capozziello, M. De Laurentis, S.D. Odintsov, A. Stabile, Hydrostatic equilibrium and stellar structure in $f(R)$ -gravity. *Phys. Rev. D* **83**, 064004 (2011). [arXiv:1101.0219](#)
108. R. Farinelli, M. De Laurentis, S. Capozziello, S.D. Odintsov, Numerical solutions of the modified Lane-Emden equation in $f(R)$ -gravity. *Mon. Not. Roy. Astron. Soc.* **440**, 2909–2915 (2014). [arXiv:1311.2744](#)
109. R. André, G.M. Kremer, Stellar structure model in hydrostatic equilibrium in the context of $f(\mathcal{R})$ -gravity. *Res. Astron. Astrophys.* **17**(12), 122 (2017). [arXiv:1707.07675](#)
110. K. Koyama, J. Sakstein, Astrophysical Probes of the Vainshtein mechanism: stars and galaxies. *Phys. Rev. D* **91**, 124066 (2015). [arXiv:1502.06872](#)
111. R. Saito, D. Yamauchi, S. Mizuno, J. Gleyzes, D. Langlois, Modified gravity inside astrophysical bodies. *JCAP* **1506**, 008 (2015). [arXiv:1503.01448](#)
112. C. Wibisono, A. Sulaksono, Information-entropic method for studying the stability bound of nonrelativistic polytropic stars within modified gravity theories. *Int. J. Mod. Phys. D* **27**(05), 1850051 (2018). [arXiv:1712.07587](#)
113. A. Wojnar, Polytropic stars in Palatini gravity. *Eur. Phys. J. C* **79**(1), 51 (2019). [arXiv:1808.04188](#)

114. A. Sergyeyev, A. Wojnar, *The Palatini Star: Exact Solutions of the Modified Lane-Emden Equation*. [arXiv:1901.10448](#)
115. S. Chandrasekhar, The highly collapsed configurations of a stellar mass (Second paper). *Mon. Not. Roy. Astron. Soc.* **95**, 207–225 (1935)
116. R.K. Jain, C. Kouvaris, N.G. Nielsen, White dwarf critical tests for modified gravity. *Phys. Rev. Lett.* **116**(15), 151103 (2016). [arXiv:1512.05946](#)
117. S. Chowdhury, T. Sarkar, *Small Anisotropy in Stellar Objects in Modified Theories of Gravity*. [arXiv:1811.07685](#)
118. G.A. Carvalho, R.V. Lobato, P.H.R.S. Moraes, J.D.V. Arbañil, R.M. Marinho, E. Otoniel, M. Malheiro, Stellar equilibrium configurations of white dwarfs in the $f(R, T)$ gravity. *Eur. Phys. J. C* **77**(12), 871 (2017). [arXiv:1706.03596](#)
119. M. Crisostomi, M. Lewandowski, F. Vernizzi, Vainshtein regime in scalar-tensor gravity: Constraints on degenerate higher-order scalar-tensor theories. *Phys. Rev. D* **100**(2), 024025 (2019). [arXiv:1903.11591](#)
120. S. Kalita, B. Mukhopadhyay, T.R. Govindarajan, *Violation of Chandrasekhar Mass-limit in Noncommutative Geometry: a Strong Possible Explanation for the Super-Chandrasekhar Limiting Mass White Dwarfs*. [arXiv:1912.00900](#)
121. S. Banerjee, S. Shankar, T.P. Singh, Constraints on modified gravity models from white dwarfs. *JCAP* **1710**(10), 004 (2017). [arXiv:1705.01048](#)
122. G.J. Olmo, D. Rubiera-García, A. Wojnar, Minimum main sequence mass in quadratic Palatini $f(R)$ gravity. *Phys. Rev. D* **100**(4), 044020 (2019). [arXiv:1906.04629](#)
123. S. Jumar, The structure of stars of very low mass. *Astrophys. J.* **137**, 1121 (1963)
124. A. Burrows, J. Liebert, The Science of brown dwarfs. *Rev. Mod. Phys.* **65**, 301–336 (1993)
125. J. Sakstein, Hydrogen burning in low mass stars constrains scalar-tensor theories of gravity. *Phys. Rev. Lett.* **115**, 201101 (2015). [arXiv:1510.05964](#)
126. D. Segransan, X. Delfosse, T. Forveille, J.L. Beuzit, S. Udry, C. Perrier, M. Mayor, Accurate masses of very low mass stars. 3. 16 New or improved masses. *Astron. Astrophys.* **364**, 665 (2000). [arxiv:astro-ph/0010585](#)
127. Gaia Collaboration, A.G.A. Brown et al., Gaia data release 2. *Astron. Astrophys.* **616**, A1 (2018). [arXiv:1804.09365](#)
128. D. Saumon, W.B. Hubbard, A. Burrows, T. Guillot, J.I. Lunine, G. Chabrier, A Theory of extrasolar giant planets. *Astrophys. J.* **460**, 993–1018 (1996). [arxiv:astro-ph/9510046](#)
129. P. Pani, T. Delsate, V. Cardoso, Eddington-inspired Born-Infeld gravity. Phenomenology of non-linear gravity-matter coupling. *Phys. Rev.* **85**, 084020 (2012). [arXiv:1201.2814](#)
130. A. Wojnar, Stability of polytropic stars in Palatini gravity. *In preparation* (2020)
131. P. Chang, L. Hui, Stellar structure and tests of modified gravity. *Astrophys. J.* **732**(1), 25 (2011)
132. A.-C. Davis, E.A. Lim, J. Sakstein, D.J. Shaw, Modified gravity makes galaxies brighter. *Phys. Rev. D* **85**(12), 123006 (2012)
133. S. Chowdhury, T. Sarkar, *Modified Gravity in the Interior of Population II Stars*. [arXiv:2008.12264](#)
134. A. Wojnar, Early evolutionary tracks of low-mass stellar objects in modified gravity. *Phys. Rev. D* **102**, 124045 (2020). [arXiv:2007.13451](#)
135. A. Wojnar, *Lithium Abundance is a Gravitational Model Dependent Quantity*. [arXiv:2009.10983](#)
136. K. Masuda, H. Kawahara, D.W. Latham, A. Bieryla, M. Kunitomo, M. MacLeod, W. Aoki, Self-lensing discovery of a 0.2 m_{\odot} white dwarf in an unusually wide orbit around a sun-like star. *Astrophys. J.* **881**, L3 (2019)
137. G. Laughlin, P. Bodenheimer, F.C. Adams, The end of the main sequence. *Astrophys. J.* **482**, 420–432 (1997)

Chapter 23

Compact Objects in General Relativity and Beyond



Jose Luis Blázquez-Salcedo, Burkhard Kleihaus, and Jutta Kunz

Recent years have seen tremendous progress in gravitation and the astrophysics of compact objects. The new window of gravitational wave (GW) multimessenger astronomy opened by the LIGO/VIRGO observations has provided us with the first glimpses of the cataclysmic events of stellar type black hole (BH) mergers [1–5] as well as the merger of neutron stars (NSs) [6]. In particular, the latter event has been associated with numerous observations in the electromagnetic spectrum [7–10], allowing far-reaching conclusions concerning our understanding of NSs on the one hand and gravity on the other. Moreover, the EHT collaboration has recently presented the first observation of a BH shadow, giving us an amazing image of the central supermassive BH of M87 [11–13].

Depending on the mass of the progenitor star, NSs or BHs arise after stellar core collapse. From the observational side, exploiting a large variety of techniques from radio and X-ray observations to GWs, much progress has been made in recent years in extracting basic properties of neutron stars, such as their masses and radii [10, 14–16]. From the theoretical side, however, the still unknown equation of state (EOS) of the nuclear matter under the extreme conditions present in NSs allows for a multitude of NS models, all satisfying the observational constraints. Here, substantial progress will be possible, when in the analysis of future observations the so-called *universal relations* will be exploited [17, 18]. These represent rather accurate relations between

J. L. Blázquez-Salcedo (✉)

Departamento de Física Teórica and IPARCOS, Universidad Complutense de Madrid,
E-28040 Madrid, Spain
e-mail: jlblaz01@ucm.es

B. Kleihaus · J. Kunz

Institut für Physik, Universität Oldenburg, Postfach 2503, D-26111 Oldenburg, Germany
e-mail: b.kleihaus@uni-oldenburg.de

J. Kunz

e-mail: jutta.kunz@uni-oldenburg.de

various appropriately scaled NS properties, including their ringdown frequencies, that are to a large extent EOS-independent.

Due to their extreme compactness, BHs and NSs represent ideal laboratories to test GR and alternative theories of gravity [19–21]. Alternative gravitational theories introduce additional degrees of freedom, and most prominently a gravitational scalar field. Depending on the theory, the resulting compact objects may then differ significantly from their GR counterparts [19–21]. NSs and BHs may be scalarized, as discussed below, and the GW spectrum will get much richer, allowing, for instance, for scalar radiation. The presence of these new degrees of freedom must be consistent with present and future observations, and thus strong constraints on the parameters of the theories can arise.

23.1 Neutron Stars

23.1.1 Neutron Stars in General Relativity

To obtain NSs, the Tolman-Oppenheimer-Volkoff (TOV) equations of GR need to be supplemented by an equation of state (EOS) describing the dense strongly interacting NS matter (see, e.g., the reviews [14–16]). In particular, in the NS core, the EOS is largely unknown, and depending on the assumptions on its decomposition and the hadronic interactions, very diverse EOSs result, leading to very diverse NS properties. While observations of high mass NSs with $M \sim 2$ solar masses (M_{\odot}) [22–24] have been able to rule out various EOSs, there still remains a plethora of viable EOSs, and thus the challenge to find the appropriate theoretical models to describe highly dense nuclear matter. The mass-radius relation for static NSs is demonstrated in Fig. 23.1 for various EOSs.

If we are to exploit NSs as astrophysical labs to not only learn about nuclear and particle physics, but also about gravity, we need to eliminate, or at least strongly reduce, the EOS dependence of the observables. Interestingly, this can indeed be done by considering appropriately scaled (typically) dimensionless quantities, that allow us to extract so-called *universal relations* for the NSs (see, e.g., the reviews [17, 18]). These *universal relations* not only concern NS properties like the moment of inertia I , the rotational quadrupole moment Q and the tidal quadrupole moment λ or Love number, which form the famous I -Love- Q relations [29–31], but also concern asteroseismology and thus the quasi-normal modes (QNMs) describing the ringdown of NSs [21, 32, 33]. The key point is then, that gravity theories beyond GR may also yield *universal relations* which, however, could be distinctly different from those of GR, thus allowing us to put bounds on the parameters of the respective theories.

Let us begin by briefly recalling the *universal relations* in GR. The mass M and the radius R of the NSs yield the compactness $C = M/R$, which is dimensionless in geometric units, and thus a good candidate for considering *universal relations*. For

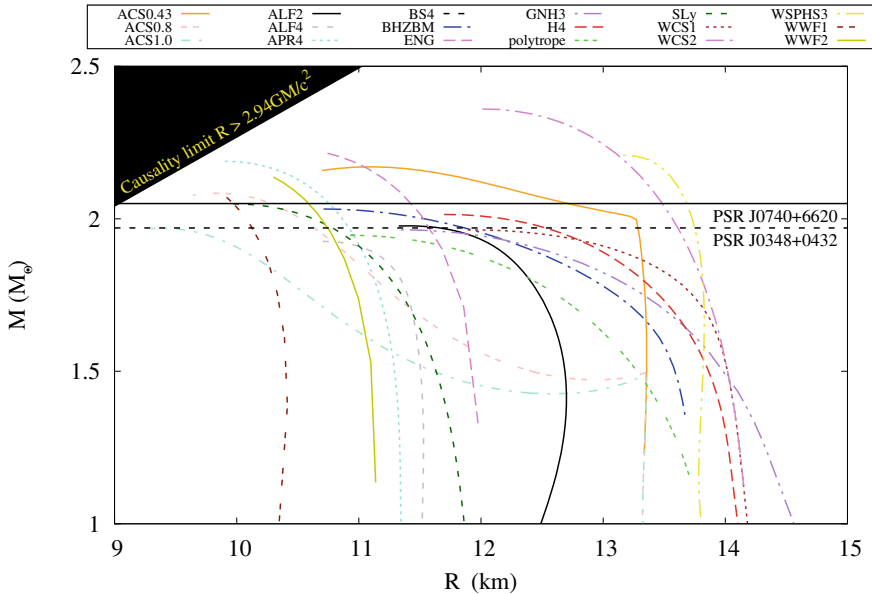


Fig. 23.1 NS mass M (in solar masses M_{\odot}) versus radius R (in km) for a variety of EOSs (see, e.g., [25–28]). Additionally, we show the high mass pulsars [22–24] and the causality limit for NSs

a Schwarzschild BH the compactness is maximal, $C = 0.5$, while for a NS it mostly resides in the range $0.1 < C < 0.3$. The moment of inertia $I = J/\Omega$ is obtained from the angular momentum J and the rotational velocity Ω of the fluid. Its dimensionless counterpart for the *universal relations* is $\bar{I} = I/M^3$.

In general the star will carry also higher multipole moments, the mass moments M_{2l} and the current moments S_{2l+1} . The mass and the angular momentum may then be viewed as its lowest multipole moments, $M = M_0$ and $J = S_1$. The higher moments can be obtained following the procedures of Geroch and Hansen [34, 35] (see also [36, 37]) or Thorne [38]. The rotational quadrupole moment then corresponds to the second mass moment $Q = M_2$, with its dimensionless counterpart for the *universal relations* $\bar{Q} = QM/J^2$.

The tidally induced quadrupole moment corresponds to the tidal deformability or Love number λ_2 [39, 40]. Its dimensionless counterpart for the *universal relations* is given by $\bar{\lambda}_2 = \lambda_2/M^5$. However, the response of NSs to external tidal fields may also yield the corresponding higher tidal mass and current moments λ_n [41], i.e., the higher Love numbers, which need to be appropriately scaled for their use in the *universal relations*.

When evaluating the I -Love and Q -Love relations, Yagi and Yunes [17, 29] found remarkably little dependence of the corresponding scaled quantities \bar{I} , $\bar{\lambda}_2$, \bar{Q} on the EOS, exhibiting deviations below 1% from a best fit of the type

$$\ln y_i = a_i + b_i \ln x_i + c_i (\ln x_i)^2 + d_i (\ln x_i)^3 + e_i (\ln x_i)^4,$$

with coefficients shown in Table I [17, 29]:

y_i	x_i	a_i	b_i	c_i	d_i	e_i
\bar{I}	$\bar{\lambda}_2$	1.496	0.05951	0.02238	-6.953×10^{-4}	8.345×10^{-6}
\bar{I}	\bar{Q}	1.393	0.5471	0.03028	0.01926	4.434×10^{-4}
\bar{Q}	$\bar{\lambda}_2$	0.1940	0.09163	0.04812	-4.283×10^{-3}	1.245×10^{-4}

Interestingly, these relations are much better than the previously considered relations of these scaled quantities versus the compactness [17]. When going to higher multipole moments, the so-called *three hair relations* emerge [17, 42]. These are no more as well satisfied as the I -Love- Q relations, but still exhibit considerable EOS independence. As examples we give the universal \bar{S}_3 - \bar{Q} and \bar{M}_4 - \bar{Q} relations in Table II [17, 42]:

y_i	x_i	a_i	b_i	c_i	d_i	e_i
\bar{S}_3	\bar{Q}	3.131×10^{-3}	2.071	-0.7152	0.2458	-0.03309
\bar{M}_4	\bar{Q}	-0.02287	3.849	-1.540	0.5863	-8.337×10^{-2}

where universality holds to 4% and 10%, respectively. While the accuracy of the universal relations deteriorates with increasing l , they would still be highly useful to determine the lower moments within good accuracy [17, 42].

The name *three hair relations* results from a generalization of the *no-hair* or *two hair relation* of black holes in GR, since uncharged rotating black holes are fully described by only two numbers, their mass and their spin. For neutron stars it turns out, that besides their mass and their spin, a third number is needed, their quadrupole moment, to approximately describe them [17, 42]. In a Newtonian setting, the three hair relations can be understood by making the elliptical isodensity approximation, assuming that stellar isodensity surfaces are self-similar ellipsoids with a fixed stellar eccentricity, and the density as a function of the isodensity radius for a rotating configuration matches the one of a non-rotating configuration with the same volume [17, 42]. The *three hair relations* also remain valid in the fully relativistic regime. As discussed in [17, 31], an emergent approximate symmetry—*isodensity self-similarity*—seems to be the (most probable) cause of these universal relations for compact stars.

Whereas most known NSs are well described in the perturbative limit of slow rotation, rapidly rotating NSs require the full solution of the rotating generalization of the TOV equations (see, e.g., [43]). The domain of existence of rotating NSs is delimited by the NSs rotating at the Kepler limit, the NSs along the secular instability line, and the static NSs. The domain thus forms a two-dimensional surface and not a single line, as in the static/slow rotation limit. Accordingly, when rapid rotation is considered, the universal relations generalize from lines to surfaces in a three-dimensional space, where the third axis is, e.g., represented by the scaled dimensionless angular momentum $\bar{J} = J/M^2$ [31, 44–47].

Asteroseismology is the second area where universal relations have received much attention in recent years, since they arise in NS QNMs, and QNMs emitted during the ringdown phase of merger events should be quite well discernible by future GW detectors. QNMs of NSs come in various types [21, 32, 33]. The general pulsations are usually described in terms of radial and non-radial pulsations, where the non-radial ones are decomposed into parity-even (polar) and parity-odd (axial) QNMs. The axial modes decouple from the nuclear matter, and thus represent pure space-time modes of oscillation, called w -modes. The polar modes couple to the nuclear matter, and thus to the fluid oscillations. All Newtonian fluid modes find their analogues in GR, yielding in particular the fundamental f -mode, and the excited p -modes. However, there are also polar w -modes, that are without Newtonian counterparts [48]. Since in GR no gravitational monopolar or dipolar radiation exists, the ringdown spectrum of neutron stars is expected to be dominated by the quadrupolar f -, p - and w -modes.

To obtain the QNM spectrum one employs perturbation theory, involving metric and fluid perturbations [21, 32, 33]. Decomposing these in terms of tensor spherical harmonics, and performing a Laplace transformation, one is left with an eigenvalue problem for a complex spectral parameter $\omega = \omega_R + i\omega_I$. The real part ω_R corresponds to the ringdown frequency of the mode, while the imaginary part ω_I determines whether the mode is stable ($\omega_I > 0$) or unstable ($\omega_I < 0$). For stable modes, ω_I is the damping rate, and its inverse is the decay time $\tau = 1/\omega_I$.

Generically, the QNM spectrum is quite EOS-dependent, but as noticed by Anderson and Kokkotas [32, 49] early on, the oscillation frequency ω_R , the damping rate ω_I of the f -mode and the first w -mode exhibit some EOS independence and thus universal behavior. This observation has been followed up by a number of further QNM studies in GR [25, 26, 50–55]. Figures 23.2a and b illustrate the strong EOS dependence for the f -mode frequency and decay time for a variety of EOSs, while Figs. 23.2c and d demonstrate approximate EOS independence for the scaled frequency and scaled decay rate versus compactness (we note that for quark stars a slightly different set of universal relations holds for the f -mode). As in the case of the I -Love- Q relations, compactness C turned out to be not the best parametrization for the universal relations. Instead, a parametrization in terms of the scaled moment of inertia $\bar{I} = I/M^3$ proved to work rather well (on the 1–2% level), yielding for instance for the f -mode the relations [54]

$$M\omega_R = -0.0047 + 0.133\eta + 0.575\eta^2, \quad M\omega_I = 0.00694\eta^4 - 0.0256\eta^6,$$

where $\eta = \bar{I}^{-1/2}$ has been called the effective compactness. Other promising universal relations obtained in [25, 26] represent relations between the scaled frequency of a mode and the scaled damping rate.

In the above discussion of the QNMs, only non-rotating NSs have been addressed. The presence of rotation in a star complicates the mode analysis tremendously. Most studies have therefore employed the so-called Cowling approximation, where the space-time is frozen [56]. The presence of rotation leads to a splitting of co- and counter-rotating perturbations, which for slow rotation will simply be a shift propor-

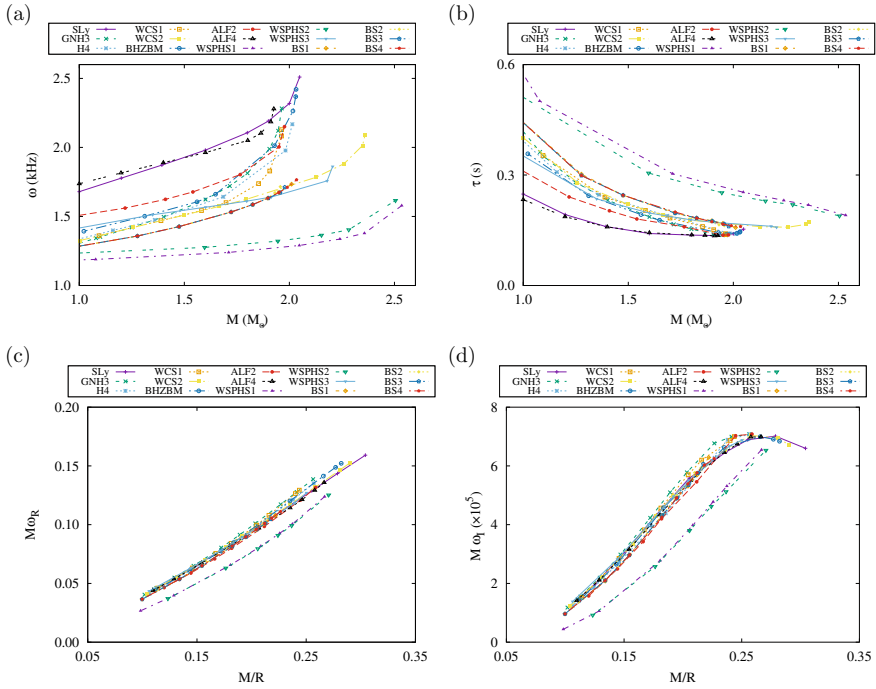


Fig. 23.2 NS f -mode for a variety of EOSs (see, e.g., [25–28]). **a** Frequency ω_R (in kHz) versus mass M (in M_\odot). **b** Decay time τ (in s) vs mass M (in M_\odot); a set of universal relations for the f -mode. **c** Scaled frequency $M\omega_R$ vs compactness M/R . **d** Scaled decay rate $M\omega_I$ vs compactness M/R . Note the different universal relations for quark matter (lower curves)

tional to the rotation frequency Ω of the star. Only recently has a full calculation of the f -mode of rapidly rotating NSs been reported [57], providing also a universal relation for the f -mode frequency

$$M\omega_R = (c_1 + c_2\bar{\Omega} + c_3\bar{\Omega}^2) + (d_1 + d_3\bar{\Omega}^2)\eta,$$

where $\bar{\Omega} = M\Omega$, and the coefficients c_i and d_i differ for co- and counter-rotation [57].

Addressing briefly the usefulness of the *universal relations* in terms of a few examples within GR, we note that the relations can be employed to gain additional information on NS properties. For instance, a measurement of any of the three quantities constituting the I -Love- Q relations will automatically yield the remaining two quantities [17]. Invoking the three-hair-relations, a measurement of the mass, rotation period and moment of inertia would allow to obtain the seven lowest moments within an accuracy of 10% [42]. If an axial or polar mode would be measured, we could use the relation between the frequency and the effective compactness ($M\omega_R$ - η), together with the relation between the damping rate and the effective compactness ($M\omega_I$ - η)

to determine the mass M and the moment of inertia I of the star [54]. Moreover, we might then extract the radius R and obtain valuable information on the EOS (obtaining information about the EOS from macroscopic data is sometimes called the inverse stellar structure problem [50]).

23.1.2 Neutron Stars in Generalized Theories of Gravity

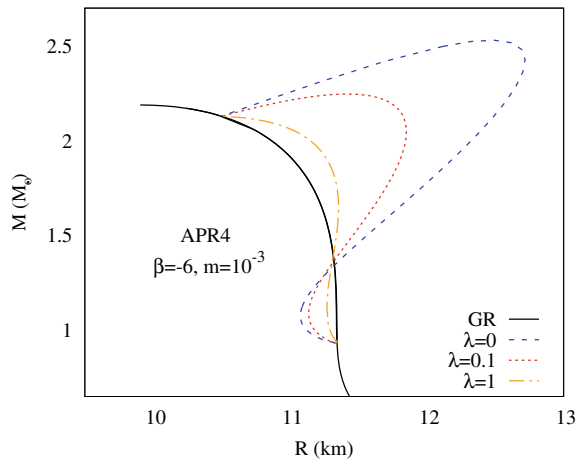
Generalized theories of gravity can affect the properties of neutron stars considerably, the most well-known and well-studied effect being their scalarization in the presence of gravitational scalar fields, discovered by Damour and Esposito-Farese [58]. In scalar-tensor theories (STTs) [59–61] the physical action is given in the Jordan frame, where the scalar field does not couple directly to the matter fields. The transformation to the Einstein frame then involves a coupling function $A(\varphi)$ relating the metric in both frames, $\tilde{g}_{\mu\nu} = A^2(\varphi)g_{\mu\nu}$ (the tilde referring to the Jordan frame), with φ representing the scalar field in the Einstein frame. The Einstein equations in the Einstein frame then contain a stress-energy tensor with appropriate powers of the coupling function $A(\varphi)$. At the same time, an equation for the scalar field is obtained

$$\nabla^\mu \nabla_\mu \varphi = -4\pi k(\varphi)T,$$

where T is the trace of the stress-energy tensor and $k(\varphi) = \frac{d \ln(A(\varphi))}{d\varphi}$ is the logarithmic derivative of the coupling function $A(\varphi)$. Examples for the mass-radius relation of scalarized NSs are shown in Fig. 23.3 and compared with the respective GR relation.

Let us consider choices of the coupling function $A(\varphi)$, which allow for GR NS solutions, i.e., solutions with $\varphi = 0$ reproducing the GR solutions. The phenomenon of matter-induced spontaneous scalarization then arises, when it becomes energeti-

Fig. 23.3 NS mass M (in solar masses M_\odot) versus radius R (in km) for a viable nuclear matter EOS (see, e.g., [28]) for GR and for STT with “Gaussian” coupling function parameter β , scalar mass m and several values of the quartic self-interaction coupling constant λ



cally favorable for a NS to acquire a non-zero value for the scalar field inside the star [58]. A branch of spontaneously scalarized NSs then bifurcates from the GR branch, when the coupling and the compactness are sufficiently strong [27, 58, 62–74]. In particular, in [27] it could be shown, that the onset of scalarization depends in a universal, i.e., almost EOS-independent, way on the gravitational potential at the center of the star.

Depending on the chosen coupling function, the NS properties, like their mass M , radius R , moment of inertia I , quadrupole moment Q , etc., can change distinctively, in principle, when the NSs get scalarized. This concerns, in particular, the rapidly rotating case, where for a given coupling function the effect of scalarization is significantly enhanced [70, 71]. Clearly, an investigation of the universal I -Love- Q relations of NSs in STT is called for [67, 71]. However, the spontaneously scalarized NSs possess universal I -Love- Q relations, that differ from those in GR only a little (i.e., within less than a few percent) [67], when the present observational constraints on the coupling functions are taken into account [22, 75, 76]. Thus these I -Love- Q relations cannot serve to discriminate between GR and the respective STTs. This also holds for the three hair relations involving the higher multipole moments, holding in GR as well as for scalarized NSs [77].

While the observational constraints on the coupling functions have been getting quite strong in recent years [22, 75, 76], the presence of a mass term can evade these constraints. In fact, the scalar field becomes short-ranged, i.e., the effect of the mass is to suppress the scalar field exponentially at distances on the order of its Compton wavelength (which should be smaller than the separation of NSs in a binary system precisely to evade the constraints) [74, 78]. Thus a much broader range of parameters is allowed than in the massless case. From the universal I -Love- Q relations, mainly the I - Q relation has been considered [74], showing that relatively large deviations from the GR relation can occur. Thus massive STT could be tested with these I -Love- Q relations.

Turning to the QNMs of NSs in STTs, we note that QNMs of nonrotating NSs were first considered in [79], where the polar f and p modes were obtained in the Cowling approximation, i.e., the perturbations of the space-time and the scalar field were frozen. Subsequently, also the gravitational axial w modes were studied [80]. In the axial case, there is, however, no coupling to the fluid and the scalar field to begin with. The exact results for the QNMs are therefore obtained in a considerably simpler way. Consequently, also the universal relations have been investigated for axial QNMs [81]. Whereas, in general, the frequency and the damping time of the modes are higher in GR than in STT, the STT universal relations do not deviate significantly from the respective GR relations, either for a massless scalar field [81] or for a massive scalar field with self-interaction [28], as illustrated in Fig. 23.4. Exploratory studies of the polar modes for the rapidly rotating case have again been performed in the Cowling approximation [82]. Going beyond the Cowling approximation would allow for qualitatively new types of polar modes, since scalar radiation would be produced. This would represent an important probe, if detectable. So far, their presence has only been studied in the sector of radial NS oscillations [83].

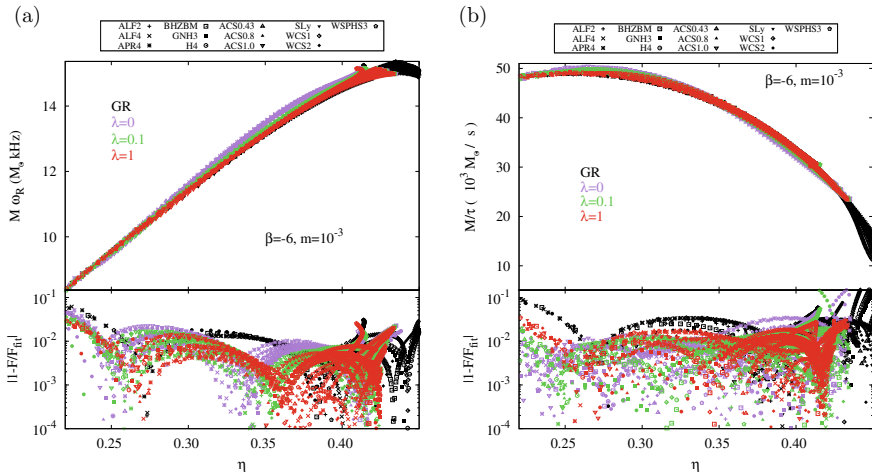


Fig. 23.4 Universal relations for NS fundamental axial mode for GR and for STT with “Gaussian” coupling function parameter β , scalar mass m and several values of the quartic self-interaction coupling constant λ (see, e.g., [28]). **a** Scaled frequency $M\omega_R$ versus generalized compactness η . **b** Scaled decay rate $M\omega_I$ versus generalized compactness η . Note the same universal relations for quark matter

We next consider $f(R)$ theories [84–86], which can be reformulated in terms of STTs. Here, in particular, R^2 gravity has received much attention, which is based on the Lagrangian $f(R) = R + aR^2$, and has been reformulated and studied in the Einstein frame [72, 87–93]. The resulting scalar field potential leads to a mass of the scalar field, $m_\varphi \sim a^{-1/2}$. For $a \rightarrow 0$ the GR limit is recovered, whereas for $a \rightarrow \infty$ a certain Brans-Dicke theory is approached. Various properties of NSs have been studied in detail, both for slowly and rapidly rotating NSs [72, 87–93]. As in STTs, also in R^2 gravity, faster rotation implies larger deviations from GR. The universal I - Q relations are retained in R^2 gravity, but deviations from the GR relations can become large ($>20\%$) and will thus possibly allow for observational constraints on the theory [90].

Axial QNMs for NSs in R^2 gravity have been considered in [94, 95]. As compared to GR, the frequencies and the damping times decrease in R^2 gravity, when the parameter a is increased. But whereas the frequencies typically deviate significantly from the GR values, the damping times differ significantly only for large scalar mass. The universal relations in R^2 gravity exhibit some qualitative differences with respect to the GR ones, which increase with increasing parameter a [94, 95].

Recently, the full polar QNMs of NSs in R^2 gravity have been studied without use of the Cowling approximation [96]. It was shown that the spectrum of these stars includes ultra-long lived modes in the radial sector, and that it is enriched by a family of scalar modes. The analysis was also done for a particular type of massive STT with very similar results. The analysis of the universal relations in this context is currently under way.

NSs have also been considered in more general theories involving scalar fields. These theories are particularly attractive, when they give rise to second order equations and do not contain ghosts, as discussed long ago by Horndeski [97–100]. Horndeski theories in fact comprise a wide variety of theories. A subset of Horndeski theories is known as the *Fab Four* [101, 102]. They are motivated largely by cosmology, since they allow for a *dynamical self-tuning mechanism*. The *Fab Four* comprise: (i) General Relativity (“George”), (ii) Einstein-dilaton-Gauss-Bonnet gravity (“Ringo”), (iii) theories with a non-minimal coupling with the Einstein tensor (“John”), (iv) and theories involving the double-dual of the Riemann tensor (“Paul”). Whereas all combinations were considered in [103], let us first focus on the combination of (i) and (iii), yielding spherically symmetric NSs with a time-dependent scalar field $\varphi(r, t) = Qt + F(r)$, where Q is a constant. Such a time-dependence is allowed because of the shift symmetry of the action.

For the resulting NSs [103–107] the external metric is simply the Schwarzschild metric, thus the stars pass all Solar System tests, but the structure of the NSs is considerably different from GR. The axial QNMs possess different frequencies and damping times compared to GR. The QNMs exhibit still the same type of universal relations as present in GR, which do, however, differ strongly from those of GR, as seen in Fig. 23.5 [104].

Let us focus next on Einstein-dilaton-Gauss-Bonnet (EdGB) theory, i.e., considering (i) and (ii), which is motivated by string theory [108, 109]. In this case the scalar dilaton field couples with coupling function $A(\varphi) = \exp(-\gamma\varphi)$ to the higher-order curvature Gauss-Bonnet (GB) term. Without a coupling function, the GB term would not contribute to the field equations. For this specific coupling function the NSs are

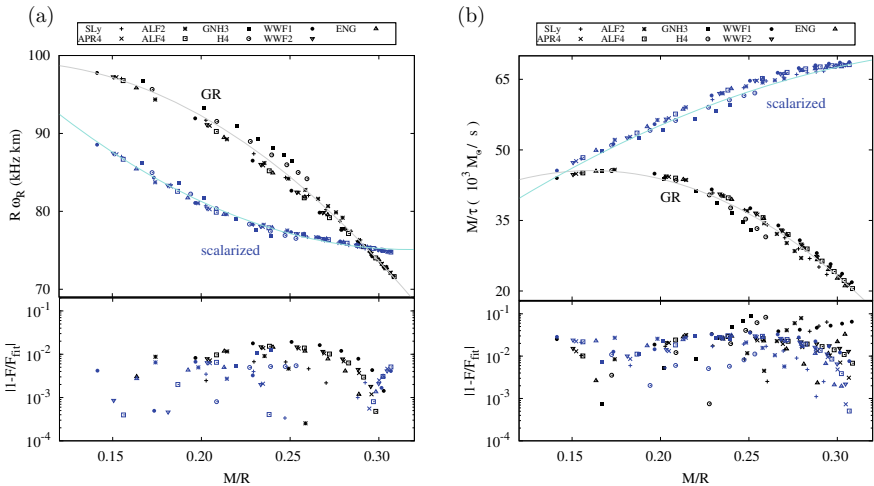


Fig. 23.5 Universal relations for NS fundamental axial mode for GR and for Horndeski theory (i) and (iii) [104] with parameter $Q = 0$. **a** Scaled frequency $M\omega_R$ versus compactness M/R . **b** Scaled decay rate $M\tau_c$ vs compactness M/R

always scalarized, but the scalarization is not spontaneous. In fact, the GR solutions are not solutions of the EdGB field equations.

The theory then involves two coupling constants, the GB coupling constant α in front of the GB term and the coupling constant γ in the exponential coupling function. As noted in [110], in the small scalar field limit, the solutions depend only on the combination $\alpha\gamma$. Requiring that the scalar field be real leads to constraints on the parameters, since NSs then exist only for a certain range of values [110–112]. Static and slowly rotating NSs have been studied in [110], whereas the full domain of existence of rotating NSs has been explored in [111, 112]. Here the universal I - Q relations were also considered, showing that the GR relations remain basically valid for EdGB NSs.

Axial QNMs have also been investigated in EdGB theory [113]. The frequency of the modes increases distinctively in the presence of the GB coupling, whereas the damping time varies only slightly. The respective universal relations of GR still hold in EdGB theory [113].

EdGB theory can be considered a particular case of Einstein-scalar-Gauss-Bonnet (EsGB) theory [114–116], where the dilatonic coupling function is generalized to some arbitrary coupling function. In this case the coupling function can allow for spontaneous scalarization, when the first derivative of the coupling function vanishes for vanishing scalar field, and at the same time, the second derivative is positive. The GR solutions then remain solutions, while the GB term serves as a source for the scalar field, yielding curvature-induced scalarized NSs [114, 117]. As in the EdGB case, neutron star solutions cannot exist for arbitrary values of the parameters of the coupling function, since the scalar field should be real. Also, NSs have been found where the scalar field has one or more zeros, representing radially excited NSs [117].

As our final example let us consider dynamical Chern-Simons (dCS) gravity, which involves third-order equations and introduces parity-violation into gravity [118]. The static NS solutions in dCS gravity are the same as in GR. Therefore, one has to consider rotation, to see effects of the Chern-Simons (CS) term. In the slow rotation limit, the moment of inertia and the quadrupole moment were first calculated in [119–121]. While these differ from GR, the electric-type tidal deformability and thus the Love number agrees with GR [122]. The I -Love- Q relations have been studied in dCS gravity in [17, 29, 30, 123]. Since the dCS relations can deviate considerably from the GR ones, this will allow to place strong constraints on dCS gravity with future observations,

Concluding this section, we note that, whereas there is a large degeneracy with respect to the EOSs and the generalized models of gravity, the universal relations represent excellent (largely) EOS-independent tests, that may be used to constrain gravity models, whenever they possess distinctly different universal relations from GR.

23.2 Black Holes

23.2.1 Black Holes in General Relativity

The existence of BHs is a genuine prediction of GR; however, their properties are highly constrained. Leaving aside electric (and magnetic) charge, since astrophysical BHs are expected to be basically uncharged, black holes in GR are described by the Kerr family of rotating BHs, and in the static limit, by the Schwarzschild BHs. These asymptotically flat BH solutions of the vacuum Einstein equations are uniquely characterized by their global charges, the mass M and the angular momentum J (see, e.g. [124]), thus they carry *no hair*. Their multipole moments are completely determined by these two quantities [34, 35]

$$M_l + i S_l = M \left(i \frac{J}{M} \right)^l,$$

where $M_0 = M$, $S_1 = J$, and the odd mass moments M_l and the even current moments S_l are identically zero. The Kerr BHs are subject to the angular momentum bound, $j = \frac{J}{M^2} \leq 1$, which is saturated by extremal BHs. Beyond this bound only naked singularities reside. The *no-hair* hypothesis will be testable in various future experiments [125].

The QNMs of Schwarzschild and Kerr BHs are well studied [33, 126–129]. As in the case of NSs, the QNMs of BHs are of utmost importance in the ringdown phase after merger events, and thus represent crucial observables. All Schwarzschild QNMs possess positive imaginary parts, and therefore represent damped modes, showing that Schwarzschild BHs are linearly stable. The Kerr BHs are linearly stable as well [130]. The Schwarzschild and Kerr QNMs are called *isospectral*, since the polar and axial perturbations possess identical complex eigenvalues ω . Of course, the Kerr QNMs again feature splitting of the QNM frequencies due to rotation. Intuitive understanding of the modes is known in the high-overtone limit, where the frequencies can be related to the surface gravity of the horizon [131], and in the eikonal limit, where they can be described in terms of the Keplerian frequency of the circular photon orbit and the Lyapunov exponent of the orbit [132, 133].

Also of tremendous observational significance is the shadow of a BH. It represents the region around a BH, where any light from background stars will be captured, making this region appear dark. For Schwarzschild black holes this region is spherical and determined by the photon ring, i.e., the unstable photon orbit at a radius of $3M$. Calculated first by Synge [134], the angle α determining the size of the shadow of a Schwarzschild black hole is

$$\sin^2 \alpha = \frac{27}{4} \frac{(\rho_0 - 1)}{\rho_0^3},$$

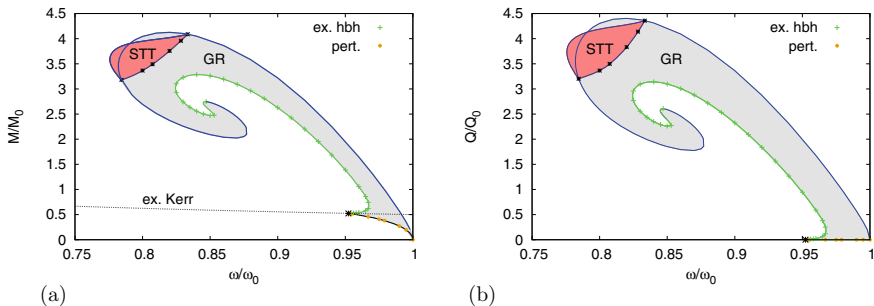


Fig. 23.6 Domain of existence of fundamental rotating BHs with complex scalar hair for GR (grey) and with additional scalarization for STT (red). **a** Normalized mass M . **b** Normalized scalar charge Q versus normalized parameter ω (of the harmonic time dependence) [145]. Moreover, in (a) we indicate the domain of Kerr BHs

where $\rho_0 = r/(2m)$ represents the observer coordinate. For Kerr BHs one has to distinguish co-rotating and counter-rotating orbits, and a photon region results. The shadow is then no longer spherical, unless viewed from the rotation axis, and its deviation from a circle is a measure for the BH spin [135–137].

The *no-hair* theorem of GR can be evaded in a number of ways. For instance, when including non-Abelian gauge and scalar fields (see, e.g., [138, 139]), or rotating complex scalar and Proca fields [140–142]. In particular, the latter case has drawn considerable interest, and various physical properties of these rotating hairy BHs have been addressed and compared to their pure Kerr counterparts [140, 143–147]. For instance, they can exceed the Kerr bound, $J/M^2 > 1$, they can possess a quadrupole moment larger than the Kerr value J^2/M , or even multiple disconnected shadows may arise.

23.2.2 Black Holes in Generalized Theories of Gravity

Addressing BHs in the same set of gravity theories discussed above in the context of NSs, we first note that the STTs which give rise to matter-induced spontaneous scalarization of NSs, possess only the Schwarzschild and Kerr BH solutions, but no additional scalarized branches of BHs. In fact, the *no-hair* theorems do not allow for scalar hair in these STTs, when only a single real scalar field is present. For massive complex scalars, on the other hand, besides the Kerr BHs the rotating hairy BHs [140, 141] are also recovered. Also, rotating hairy BHs with additional scalarization are possible [145], as demonstrated in Fig. 23.6, where their domain of existence is shown for the fundamental scalarized BHs. Since $f(R)$ theories may be considered special cases of STTs, the Schwarzschild and Kerr BHs are also recovered there.

Turning to Horndeski theories, we note that, depending on the chosen action, hairy BHs may arise (see, e.g., [148] for a review). The *no-hair* theorem can, for instance,

be evaded by allowing for a time-dependent scalar field in the combination (i) and (iii) of the *Fab Four* [149, 150]. But even when within the Horndeski theories the Schwarzschild BHs is recovered, the presence of additional degrees of freedom can lead to non-GR signatures in the QNM spectrum [151–154].

Considering next the case of curvature-induced scalarization, we note that the *no-hair* theorem is evaded in the presence of the GB term. The field equations now possess an *effective* energy momentum tensor containing the higher curvature terms. EdGB BHs possess distinctive features as compared to Schwarzschild and Kerr BHs. Since there are no known closed form solutions, static BHs have first been constructed perturbatively [155, 156] and numerically [157–159]. As in the case of NSs discussed above, there arises a condition for the EdGB BHs from the requirement that the dilaton field should be real [157]. For given coupling constants α and γ of the theory, this translates into a lower bound on the mass of these dilatonic BHs. The minimum mass solution is often referred to as the critical solution. In fact, for larger values of γ (including $\gamma = 1$) there are two branches of BH solutions: the fundamental branch, which extends from the minimum mass to infinity, and a short secondary branch, which extends from the minimum mass to a naked singularity [157–159]. For a given mass, the EdGB BHs have a smaller size than the Schwarzschild BHs. For large masses, the fundamental branch of EdGB BHs approaches the branch of Schwarzschild BHs from below. But mass and radius are not proportional. Therefore, the scaled horizon area A_H/M^2 is not constant as for Schwarzschild.

For fixed coupling constants, the slowly [160–163] and fast [111, 164–166] rotating EdGB BHs possess a domain of existence, that is limited by the static EdGB BHs, the critical EdGB BHs, the extremal EdGB BHs, and the Kerr BHs, as shown in Fig. 23.7a, where the scaled area is shown versus the scaled angular momentum. Interestingly, the Kerr bound can be slightly exceeded by fast rotating EdGB BHs (see Fig. 23.7a). The EdGB quadrupole moment can differ considerably from the Kerr case (see Fig. 23.7b), where $QM/J^2 = 1$ [111, 165]. The shadow of EdGB BHs is always smaller than the shadow of the comparable Kerr BHs; however, the deviations are always smaller than a few percent [167]. Let us note, that area and entropy differ in the presence of the GB coupling, since the entropy receives a contribution from the GB term [168]. Since the entropy of EdGB BHs is larger than for Kerr BHs, this indicates stability of these solutions.

Mode stability of EdGB BHs has been investigated in the static case, where the QNMs have been obtained and analyzed [160, 169–174]. All modes except for the $l = 0$ mode on the short secondary branch are stable. Because of the scalar field, there is monopolar and dipolar radiation, not present in GR. The axial modes are pure space-time modes. Here the geodesic correspondence of the eikonal approximation works quite well, except for the parameter region, where the critical solution is approached. The polar modes are coupled to the dilaton. Here we need to distinguish scalar-led and gravitational-led modes, which in the GR limit reduce to the QNMs of Schwarzschild BHs. The deviations of the polar modes from GR modes are larger than for axial modes. Not surprisingly, the presence of the dilaton breaks the isospectrality of the GR BHs. This is illustrated in Fig. 23.8, where the fundamental axial modes and polar gravitational-led and scalar-led modes are shown. While there would be scalar

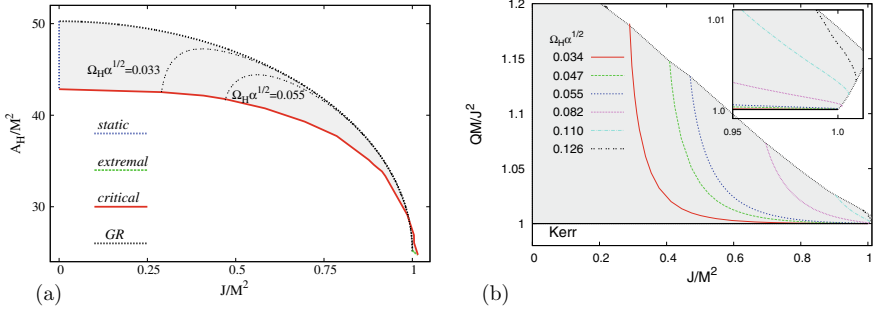


Fig. 23.7 Domain of existence of rotating BHs with dilaton hair in EdGB theory. **a** Scaled horizon area A_H/M^2 . **b** Scaled quadrupole moment QM/J^2 vs scaled angular momentum J/M^2 . Furthermore, we present families of solutions with fixed scaled horizon angular velocities [165]. The Kerr BHs form part of the boundary (black)

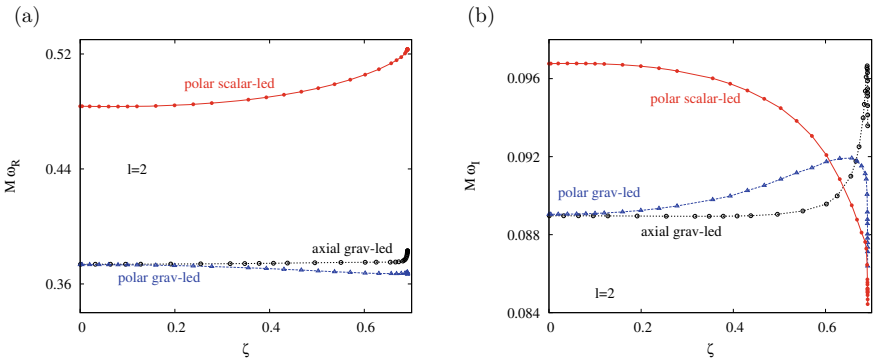


Fig. 23.8 QNMs of EdGB BHs. **a** Scaled frequency $M\omega_R$. **b** Scaled decay rate $M\omega_I$ versus scaled GB coupling constant $\zeta = \alpha/M^2$ (for $\gamma = 1$) for the fundamental axial, polar gravitational-led, and polar scalar-led modes [171]

radiation from EdGB BHs, its detection would depend on the coupling of the dilaton to matter.

We next turn to the BHs of EsGB theory with a coupling function chosen such, as to allow for curvature-induced spontaneous scalarization [114–116, 175–181]. Then, scalarized BHs arise for a certain range of the coupling constant, i.e., at certain values, branches of scalarized BHs bifurcate from the Schwarzschild solution. These branches represent the fundamental solutions and their excitations (see Fig. 23.9). QNMs of static EsGB black holes have received much interest [175, 178, 182–184]. The fundamental scalarized solutions can be stable (in part of their domain of existence), depending on the choice of coupling function. This is, for instance, the case for a “Gaussian” coupling function [114, 175]. Stability under spherical perturbations can also be achieved, when a mass term and a potential for the scalar are included [180]. The analysis of the non-radial perturbations of the fundamental

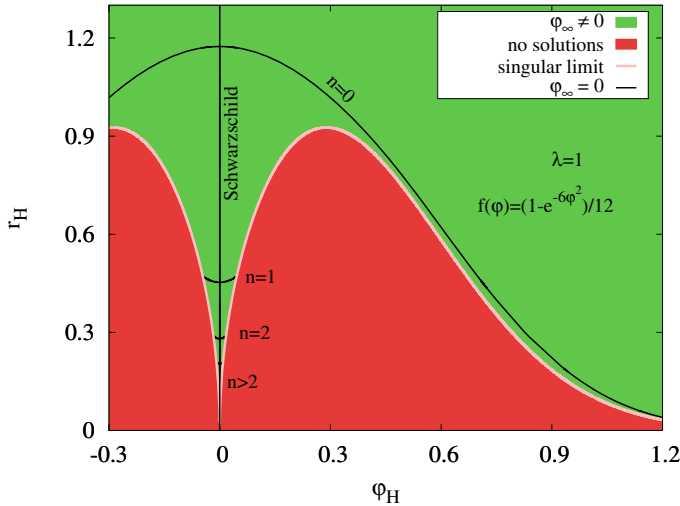


Fig. 23.9 Domain of existence of static scalarized EsGB BHs: horizon radius r_H versus the horizon scalar field ϕ_H [175]. The fundamental spontaneously scalarized BHs are labeled by $n = 0, n \geq 1$ labels radially excited BHs. Additionally, we indicate the Schwarzschild BHs

scalarized solutions of the case with a “Gaussian” coupling function was recently performed for the axial channel [183] and polar channel [184], showing stability of this branch under these higher multipole perturbations (except for the region where hyperbolicity is lost).

The fundamental as well as excited rapidly rotating scalarized BHs have been investigated recently for “Gaussian” and quadratic coupling functions [179, 181]. In the Gaussian case the domain of existence of the fundamental BHs is quite broad for small rotation rates, but becomes narrower for faster rotation. Interestingly, this can be exploited to obtain bounds on the coupling constant of the theory, by studying the shadow of these rotating scalarized BHs. For slowly rotating BHs, the deviations in the shadow size between EsGB and Kerr BHs can be large, e.g., in the (stable) static limit above 40% [179]. Considering the shadow of M87, observations suggest that the deviation from Kerr should be below 10%, allowing to obtain a (weak) bound on the coupling constant [179]. Moreover, the phenomenon of spin-induced spontaneous scalarization of sufficiently fast rotating BHs has been observed [185–189].

Finally, in dCS theory, static BHs are given by the Schwarzschild metric. They have been shown to be mode stable [190–192]. However, rotating dCS BHs carry scalar hair. Slowly rotating BHs have been obtained in [193–195], where the dCS correction to the quadrupole moment was calculated, and rapidly rotating BHs were obtained in [196], employing a linear coupling function. Appropriately chosen coupling functions may allow for spontaneously scalarized rotating dCS BHs.

23.3 Conclusions

Here we have addressed the properties of NSs and BHs in GR and generalized theories of gravity. For NSs we have highlighted the power of the EOS-independent, *universal relations*, which may differ significantly from their GR counterparts [17, 18]. Non-rotating and slowly rotating compact objects and their QNMs have been studied already for numerous gravity theories. However, much less is known about rapidly rotating NSs and BHs and their QNMs in generalized theories of gravity. Here, theoretical progress will be valuable and timely, to provide predictions and templates for future highly precise observations. These will then allow us to put stronger bounds on these generalized theories [197–206].

Bounds must, however, be employed with caution. Consider, for example, the joint observation of GW170817 in gravitational waves and in the electromagnetic spectrum, allowing to constrain the speed of gravitational waves. This observation has been interpreted to rule out a large number of alternative theories of gravity [207–209]. Closer inspection revealed that when viewing these generalized theories as effective field theories, subtleties arise, that challenge these conclusions [210]. Moreover, generalized theories of gravity may remain viable in the context of compact objects, when they are not required to resolve the cosmological issues at the same time [170, 211–213].

References

1. LIGO Scientific, Virgo Collaboration, B.P. Abbott et al., Observation of Gravitational Waves from a Binary Black Hole Merger. *Phys. Rev. Lett.* **116**(6), 061102 (2016) ([arXiv:1602.03837](#))
2. LIGO Scientific, Virgo Collaboration, B.P. Abbott et al., GW151226: Observation of Gravitational Waves from a 22-Solar-Mass Binary Black Hole Coalescence. *Phys. Rev. Lett.* **116**(24), 241103 (2016) ([arXiv:1606.04855](#))
3. LIGO Scientific, Virgo Collaboration, B.P. Abbott et al., GW170814: A Three-Detector Observation of Gravitational Waves from a Binary Black Hole Coalescence. *Phys. Rev. Lett.* **119**(14), 141101 (2017) ([arXiv:1709.09660](#))
4. LIGO Scientific, VIRGO Collaboration, B.P. Abbott et al., GW170104: Observation of a 50-Solar-Mass Binary Black Hole Coalescence at Redshift 0.2. *Phys. Rev. Lett.* **118**(22), 221101 (2017) ([arXiv:1706.01812](#)). [Erratum: *Phys. Rev. Lett.* 121, no.12, 129901(2018)]
5. LIGO Scientific, Virgo Collaboration, B.P. Abbott et al., GWTC-1: A Gravitational-Wave Transient Catalog of Compact Binary Mergers Observed by LIGO and Virgo during the First and Second Observing Runs. [arXiv:1811.12907](#)
6. LIGO Scientific, Virgo Collaboration, B.P. Abbott et al., GW170817: Implications for the Stochastic Gravitational-Wave Background from Compact Binary Coalescences. *Phys. Rev. Lett.* **120**(9), 091101 (2018) ([arXiv:1710.05837](#))
7. D.A. Coulter et al., Swope Supernova Survey 2017a (SSS17a), the Optical Counterpart to a Gravitational Wave Source. *Science* (2017) ([arXiv:1710.05452](#)). [Science358,1556(2017)]
8. LIGO Scientific, Virgo Collaboration, B. P. Abbott et al., *GW170817: Observation of Gravitational Waves from a Binary Neutron Star Inspiral*, *Phys. Rev. Lett.* **119** (2017), no. 16 161101, [arXiv:1710.05832](#)
9. LIGO Scientific, Virgo, Fermi GBM, INTEGRAL, IceCube, AstroSat Cadmium Zinc Telluride Imager Team, IPN, Insight-Hxmt, ANTARES, Swift, AGILE Team, 1M2H Team,

- Dark Energy Camera GW-EM, DES, DLT40, GRAWITA, Fermi-LAT, ATCA, ASKAP, Las Cumbres Observatory Group, OzGrav, DWF (Deeper Wider Faster Program), AST3, CAASTRO, VINROUGE, MASTER, J-GEM, GROWTH, JAGWAR, CaltechNRAO, TTU-NRAO, NuSTAR, Pan-STARRS, MAXI Team, TZAC Consortium, KU, Nordic Optical Telescope, ePESSTO, GROND, Texas Tech University, SALT Group, TOROS, BOOTES, MWA, CALET, IKI-GW Follow-up, H.E.S.S., LOFAR, LWA, HAWC, Pierre Auger, ALMA, Euro VLBI Team, Pi of Sky, Chandra Team at McGill University, DFN, ATLAS Telescopes, High Time Resolution Universe Survey, RIMAS, RATIR, SKA South Africa/MeerKAT Collaboration, B. P. Abbott et al., Multi-messenger Observations of a Binary Neutron Star Merger. *Astrophys. J.* **848** (2017), no. 2 L12, [arXiv:1710.05833](#)
10. LIGO Scientific, Virgo Collaboration, B.P. Abbott et al., Properties of the binary neutron star merger GW170817. *Phys. Rev.* **X9** (2019), no. 1 011001, [arXiv:1805.11579](#)
 11. Event Horizon Telescope Collaboration, K. Akiyama et al., *First M87 Event Horizon Telescope Results. I. The Shadow of the Supermassive Black Hole*, *Astrophys. J.* **875** (2019), no. 1 L1, [arXiv:1906.11238](#)
 12. Event Horizon Telescope Collaboration, K. Akiyama et al., First M87 Event Horizon Telescope Results. V. Physical Origin of the Asymmetric Ring. *Astrophys. J.* **875** (2019), no. 1 L5, [arXiv:1906.11242](#)
 13. Event Horizon Telescope Collaboration, K. Akiyama et al., First M87 Event Horizon Telescope Results. VI. The Shadow and Mass of the Central Black Hole. *Astrophys. J.* **875** (2019), no. 1 L6, [arXiv:1906.11243](#)
 14. J.M. Lattimer, The nuclear equation of state and neutron star masses. *Ann. Rev. Nucl. Part. Sci.* **62**, 485–515 (2012). ([arXiv:1305.3510](#))
 15. F. Ozel and P. Freire, *Masses, Radii, and the Equation of State of Neutron Stars*, *Ann. Rev. Astron. Astrophys.* **54** (2016) 401–440, [arXiv:1603.02698](#)
 16. G. Baym, T. Hatsuda, T. Kojo, P. D. Powell, Y. Song, and T. Takatsuka, *From hadrons to quarks in neutron stars: a review*, *Rept. Prog. Phys.* **81** (2018), no. 5 056902, [arXiv:1707.04966](#)
 17. K. Yagi and N. Yunes, *Approximate Universal Relations for Neutron Stars and Quark Stars*, *Phys. Rept.* **681** (2017) 1–72, [arXiv:1608.02582](#)
 18. D. D. Doneva and G. Pappas, *Universal Relations and Alternative Gravity Theories*, *Astrophys. Space Sci. Libr.* **457** (2018) 737–806, [arXiv:1709.08046](#)
 19. C.M. Will, The Confrontation between general relativity and experiment. *Living Rev. Rel.* **9**, 3 (2006). ([gr-qc/0510072](#))
 20. V. Faraoni, S. Capozziello, *Beyond Einstein Gravity*, vol. 170 (Springer, Dordrecht, 2011)
 21. E. Berti et al., Testing General Relativity with Present and Future Astrophysical Observations. *Class. Quant. Grav.* **32**, 243001 (2015). ([arXiv:1501.07274](#))
 22. P. Demorest, T. Pennucci, S. Ransom, M. Roberts, J. Hessels, Shapiro Delay Measurement of A Two Solar Mass Neutron Star. *Nature* **467**, 1081–1083 (2010). ([arXiv:1010.5788](#))
 23. J. Antoniadis et al., A Massive Pulsar in a Compact Relativistic Binary. *Science* **340**, 6131 (2013). ([arXiv:1304.6875](#))
 24. NANOGrav Collaboration, H. Cromartie et al., Relativistic Shapiro delay measurements of an extremely massive millisecond pulsar. *Nature Astron.* **4** (2019), no. 1 72–76, [arXiv:1904.06759](#)
 25. J. L. Blázquez-Salcedo, L. M. Gonzalez-Romero, and F. Navarro-Lerida, *Phenomenological relations for axial quasinormal modes of neutron stars with realistic equations of state*, *Phys. Rev.* **D87** (2013), no. 10 104042, [arXiv:1207.4651](#)
 26. J. L. Blázquez-Salcedo, L. M. Gonzalez-Romero, and F. Navarro-Lerida, *Polar quasi-normal modes of neutron stars with equations of state satisfying the $2M_{\odot}$ constraint*, *Phys. Rev.* **D89** (2014), no. 4 044006, [arXiv:1307.1063](#)
 27. Z. Altaha Motahar, J. L. Blázquez-Salcedo, B. Kleihaus, and J. Kunz, *Scalarization of neutron stars with realistic equations of state*, *Phys. Rev.* **D96** (2017), no. 6 064046, [arXiv:1707.05280](#)
 28. Z. Altaha Motahar, J. L. Blázquez-Salcedo, D. D. Doneva, J. Kunz, and S. S. Yazadjiev, *Axial quasinormal modes of scalarized neutron stars with massive self-interacting scalar field*, *Phys. Rev.* **D99** (2019), no. 10 104006, [arXiv:1902.01277](#)

29. K. Yagi, N. Yunes, I-Love-Q. *Science* **341**, 365–368 (2013). ([arXiv:1302.4499](#))
30. K. Yagi and N. Yunes, *I-Love-Q Relations in Neutron Stars and their Applications to Astrophysics, Gravitational Waves and Fundamental Physics*, *Phys. Rev.* **D88** (2013), no. 2 023009, [arXiv:1303.1528](#)
31. K. Yagi, L. C. Stein, G. Pappas, N. Yunes, and T. A. Apostolatos, *Why I-Love-Q: Explaining why universality emerges in compact objects*, *Phys. Rev.* **D90** (2014), no. 6 063010, [arXiv:1406.7587](#)
32. N. Andersson, K.D. Kokkotas, Towards gravitational wave asteroseismology. *Mon. Not. Roy. Astron. Soc.* **299**, 1059–1068 (1998). (gr-qc/9711088)
33. K.D. Kokkotas, B.G. Schmidt, Quasinormal modes of stars and black holes. *Living Rev. Rel.* **2**, 2 (1999). (gr-qc/9909058)
34. R. P. Gerch, *Multipole moments. II. Curved space*, *J. Math. Phys.* **11** (1970) 2580–2588
35. R.O. Hansen, Multipole moments of stationary space-times. *J. Math. Phys.* **15**, 46–52 (1974)
36. C. Hoenselaers, Z. Perjes, Remarks on the Robinson-Trautman solutions. *Class. Quant. Grav.* **10**, 375–384 (1993)
37. T.P. Sotiriou, T.A. Apostolatos, Corrected multipole moments of axisymmetric electrovacuum spacetimes. *Class. Quant. Grav.* **21**, 5727–5733 (2004). (gr-qc/0407064)
38. K.S. Thorne, Multipole Expansions of Gravitational Radiation. *Rev. Mod. Phys.* **52**, 299–339 (1980)
39. E.E. Flanagan, T. Hinderer, Constraining neutron star tidal Love numbers with gravitational wave detectors. *Phys. Rev. D* **77**, 021502 (2008). ([arXiv:0709.1915](#))
40. T. Hinderer, Tidal Love numbers of neutron stars. *Astrophys. J.* **677**, 1216–1220 (2008). ([arXiv:0711.2420](#))
41. T. Damour, A. Nagar, Relativistic tidal properties of neutron stars. *Phys. Rev. D* **80**, 084035 (2009). ([arXiv:0906.0096](#))
42. L.C. Stein, K. Yagi, N. Yunes, Three-Hair Relations for Rotating Stars: Nonrelativistic Limit. *Astrophys. J.* **788**, 15 (2014). ([arXiv:1312.4532](#))
43. N. Stergioulas, Rotating Stars in Relativity. *Living Rev. Rel.* **6**, 3 (2003). (gr-qc/0302034)
44. D.D. Doneva, S.S. Yazadjiev, N. Stergioulas, K.D. Kokkotas, Breakdown of I-Love-Q universality in rapidly rotating relativistic stars. *Astrophys. J.* **781**, L6 (2013). ([arXiv:1310.7436](#))
45. G. Pappas, T.A. Apostolatos, Effectively universal behavior of rotating neutron stars in general relativity makes them even simpler than their Newtonian counterparts. *Phys. Rev. Lett.* **112**, 121101 (2014). ([arXiv:1311.5508](#))
46. S. Chakrabarti, T. Delsate, N. Gurlbebeck, J. Steinhoff, I-Q relation for rapidly rotating neutron stars. *Phys. Rev. Lett.* **112**, 201102 (2014). ([arXiv:1311.6509](#))
47. K. Yagi, K. Kyutoku, G. Pappas, N. Yunes, and T. A. Apostolatos, *Effective No-Hair Relations for Neutron Stars and Quark Stars: Relativistic Results*, *Phys. Rev.* **D89** (2014), no. 12 124013, [arXiv:1403.6243](#)
48. K.D. Kokkotas, B.F. Schutz, W-modes: A New family of normal modes of pulsating relativistic stars. *Mon. Not. Roy. Astron. Soc.* **255**, 119 (1992)
49. N. Andersson, K.D. Kokkotas, Gravitational waves and pulsating stars: What can we learn from future observations? *Phys. Rev. Lett.* **77**, 4134–4137 (1996). (gr-qc/9610035)
50. K.D. Kokkotas, T.A. Apostolatos, N. Andersson, The Inverse problem for pulsating neutron stars: A “Fingerprint analysis” for the supranuclear equation of state. *Mon. Not. Roy. Astron. Soc.* **320**, 307–315 (2001). (gr-qc/9901072)
51. O. Benhar, E. Berti, and V. Ferrari, *The Imprint of the equation of state on the axial w modes of oscillating neutron stars*, *Mon. Not. Roy. Astron. Soc.* **310** (1999) 797–803, gr-qc/9901037. [ICTP Lect. Notes Ser.3,35(2001)]
52. O. Benhar, V. Ferrari, L. Gualtieri, Gravitational wave asteroseismology revisited. *Phys. Rev. D* **70**, 124015 (2004). (astro-ph/0407529)
53. L.K. Tsui, P.T. Leung, Universality in quasi-normal modes of neutron stars. *Mon. Not. Roy. Astron. Soc.* **357**, 1029–1037 (2005). (gr-qc/0412024)
54. H.K. Lau, P.T. Leung, L.M. Lin, Inferring physical parameters of compact stars from their f-mode gravitational wave signals. *Astrophys. J.* **714**, 1234–1238 (2010). ([arXiv:0911.0131](#))

55. C. Chirenti, G. H. de Souza, and W. Kastaun, *Fundamental oscillation modes of neutron stars: validity of universal relations*, *Phys. Rev. D* **D91** (2015), no. 4 044034, [arXiv:1501.02970](#)
56. E. Gaertig, K.D. Kokkotas, Gravitational wave asteroseismology with fast rotating neutron stars. *Phys. Rev. D* **83**, 064031 (2011). ([arXiv:1005.5228](#))
57. C. Krüger and K. Kokkotas, *Fast Rotating Relativistic Stars: Spectra and Stability without Approximation*, *Phys. Rev. Lett.* **125** (2020), no. 11 111106, [arXiv:1910.08370](#)
58. T. Damour, G. Esposito-Farese, Nonperturbative strong field effects in tensor - scalar theories of gravitation. *Phys. Rev. Lett.* **70**, 2220–2223 (1993)
59. C. Brans and R. H. Dicke, *Mach's principle and a relativistic theory of gravitation*, *Phys. Rev.* **124** (1961) 925–935. [,142(1961)]
60. T. Damour, G. Esposito-Farese, Tensor multiscalar theories of gravitation. *Class. Quant. Grav.* **9**, 2093–2176 (1992)
61. Y. Fujii, K. Maeda, *The scalar-tensor theory of gravitation* (Cambridge University Press, Cambridge Monographs on Mathematical Physics, 2007)
62. T. Damour, G. Esposito-Farese, Tensor - scalar gravity and binary pulsar experiments. *Phys. Rev. D* **54**, 1474–1491 (1996). (gr-qc/9602056)
63. T. Harada, Neutron stars in scalar tensor theories of gravity and catastrophe theory. *Phys. Rev. D* **57**, 4802–4811 (1998). (gr-qc/9801049)
64. T. Harada, Stability analysis of spherically symmetric star in scalar - tensor theories of gravity. *Prog. Theor. Phys.* **98**, 359–379 (1997). (gr-qc/9706014)
65. M. Salgado, D. Sudarsky, U. Nucamendi, On spontaneous scalarization. *Phys. Rev. D* **58**, 124003 (1998). (gr-qc/9806070)
66. H. Sotani, Slowly Rotating Relativistic Stars in Scalar-Tensor Gravity. *Phys. Rev. D* **86**, 124036 (2012). ([arXiv:1211.6986](#))
67. P. Pani and E. Berti, *Slowly rotating neutron stars in scalar-tensor theories*, *Phys. Rev. D* **D90** (2014), no. 2 024025, [arXiv:1405.4547](#)
68. H.O. Silva, C.F.B. Macedo, E. Berti, L.C.B. Crispino, Slowly rotating anisotropic neutron stars in general relativity and scalar-tensor theory. *Class. Quant. Grav.* **32**, 145008 (2015). ([arXiv:1411.6286](#))
69. H. Sotani and K. D. Kokkotas, *Maximum mass limit of neutron stars in scalar-tensor gravity*, *Phys. Rev. D* **D95** (2017), no. 4 044032, [arXiv:1702.00874](#)
70. D. D. Doneva, S. S. Yazadjiev, N. Stergioulas, and K. D. Kokkotas, *Rapidly rotating neutron stars in scalar-tensor theories of gravity*, *Phys. Rev. D* **D88** (2013), no. 8 084060, [arXiv:1309.0605](#)
71. D. D. Doneva, S. S. Yazadjiev, K. V. Staykov, and K. D. Kokkotas, *Universal I-Q relations for rapidly rotating neutron and strange stars in scalar-tensor theories*, *Phys. Rev. D* **D90** (2014), no. 10 104021, [arXiv:1408.1641](#)
72. K. V. Staykov, D. D. Doneva, and S. S. Yazadjiev, *Moment-of-inertia–compactness universal relations in scalar-tensor theories and \mathcal{R}^2 gravity*, *Phys. Rev. D* **D93** (2016), no. 8 084010, [arXiv:1602.00504](#)
73. S. S. Yazadjiev, D. D. Doneva, and D. Popchev, *Slowly rotating neutron stars in scalar-tensor theories with a massive scalar field*, *Phys. Rev. D* **D93** (2016), no. 8 084038, [arXiv:1602.04766](#)
74. D. D. Doneva and S. S. Yazadjiev, *Rapidly rotating neutron stars with a massive scalar field—structure and universal relations*, *JCAP* **1611** (2016), no. 11 019, [arXiv:1607.03299](#)
75. P. C. C. Freire, N. Wex, G. Esposito-Farese, J. P. W. Verbiest, M. Bailes, B. A. Jacoby, M. Kramer, I. H. Stairs, J. Antoniadis, and G. H. Janssen, *The relativistic pulsar-white dwarf binary PSR J1738+0333 II. The most stringent test of scalar-tensor gravity*, *Mon. Not. Roy. Astron. Soc.* **423** (2012) 3328, [arXiv:1205.1450](#)
76. A. M. Archibald, N. V. Gusinskaia, J. W. T. Hessels, A. T. Deller, D. L. Kaplan, D. R. Lorimer, R. S. Lynch, S. M. Ransom, and I. H. Stairs, *Universality of free fall from the orbital motion of a pulsar in a stellar triple system*, *Nature* **559** (2018), no. 7712 73–76, [arXiv:1807.02059](#)
77. G. Pappas, D. D. Doneva, T. P. Sotiriou, S. S. Yazadjiev, and K. D. Kokkotas, *Multipole moments and universal relations for scalarized neutron stars*, *Phys. Rev. D* **D99** (2019), no. 10 104014, [arXiv:1812.01117](#)

78. V. I. Danchev and D. D. Doneva, *Constraining the equation of state in modified gravity via universal relations*, *Phys. Rev. D* **103** (2021), no. 2 024049, [arXiv:2010.07392](#)
79. H. Sotani, K.D. Kokkotas, Probing strong-field scalar-tensor gravity with gravitational wave asteroseismology. *Phys. Rev. D* **70**, 084026 (2004). (gr-qc/0409066)
80. H. Sotani, K.D. Kokkotas, Stellar oscillations in scalar-tensor theory of gravity. *Phys. Rev. D* **71**, 124038 (2005). (gr-qc/0506060)
81. Z. Althaha Motahar, J. L. Blazquez-Salcedo, B. Kleihaus, and J. Kunz, *Axial quasinormal modes of scalarized neutron stars with realistic equations of state*, *Phys. Rev. D* **98** (2018), no. 4 044032, [arXiv:1807.02598](#)
82. S. S. Yazadjiev, D. D. Doneva, and K. D. Kokkotas, *Oscillation modes of rapidly rotating neutron stars in scalar-tensor theories of gravity*, *Phys. Rev. D* **96** (2017), no. 6 064002, [arXiv:1705.06984](#)
83. R. F. P. Mendes and N. Ortiz, *New class of quasinormal modes of neutron stars in scalar-tensor gravity*, *Phys. Rev. Lett.* **120** (2018), no. 20 201104, [arXiv:1802.07847](#)
84. T.P. Sotiriou, V. Faraoni, *f(R) Theories Of Gravity*. *Rev. Mod. Phys.* **82**, 451–497 (2010). ([arXiv:0805.1726](#))
85. A. De Felice, S. Tsujikawa, *f(R) theories*. *Living Rev. Rel.* **13**, 3 (2010). ([arXiv:1002.4928](#))
86. S. Capozziello, M. De Laurentis, *Extended Theories of Gravity*. *Phys. Rept.* **509**, 167–321 (2011). ([arXiv:1108.6266](#))
87. S.S. Yazadjiev, D.D. Doneva, K.D. Kokkotas, K.V. Staykov, Non-perturbative and self-consistent models of neutron stars in R-squared gravity. *JCAP* **1406**, 003 (2014). ([arXiv:1402.4469](#))
88. K. V. Staykov, D. D. Doneva, S. S. Yazadjiev, and K. D. Kokkotas, *Slowly rotating neutron and strange stars in R^2 gravity*, *JCAP* **1410** (2014), no. 10 006, [arXiv:1407.2180](#)
89. S. S. Yazadjiev, D. D. Doneva, and K. D. Kokkotas, *Rapidly rotating neutron stars in R-squared gravity*, *Phys. Rev. D* **91** (2015), no. 8 084018, [arXiv:1501.04591](#)
90. D. D. Doneva, S. S. Yazadjiev, and K. D. Kokkotas, *The I-Q relations for rapidly rotating neutron stars in f(R) gravity*, *Phys. Rev. D* **92** (2015), no. 6 064015, [arXiv:1507.00378](#)
91. K. V. Staykov, D. D. Doneva, and S. S. Yazadjiev, *Orbital and epicyclic frequencies around neutron and strange stars in R^2 gravity*, *Eur. Phys. J.* **C75** (2015), no. 12 607, [arXiv:1508.07790](#)
92. S. S. Yazadjiev, D. D. Doneva, and K. D. Kokkotas, *Tidal Love numbers of neutron stars in f(R) gravity*, *Eur. Phys. J.* **C78** (2018), no. 10 818, [arXiv:1803.09534](#)
93. A. V. Astashenok, S. D. Odintsov, and A. de la Cruz-Dombriz, *The realistic models of relativistic stars in f(R) = R + αR^2 gravity*, *Class. Quant. Grav.* **34** (2017), no. 20 205008, [arXiv:1704.08311](#)
94. J. L. Blazquez-Salcedo, D. D. Doneva, J. Kunz, K. V. Staykov, and S. S. Yazadjiev, *Axial quasinormal modes of neutron stars in R^2 gravity*, *Phys. Rev. D* **98** (2018), no. 10 104047, [arXiv:1804.04060](#)
95. J. L. Blazquez-Salcedo, Z. Althaha Motahar, D. D. Doneva, F. S. Khoo, J. Kunz, S. Mojica, K. V. Staykov, and S. S. Yazadjiev, *Quasinormal modes of compact objects in alternative theories of gravity*, *Eur. Phys. J. Plus* **134** (2019), no. 1 46, [arXiv:1810.09432](#)
96. J. L. Blázquez-Salcedo, F. Scen Khoo, and J. Kunz, *Ultra-long-lived quasi-normal modes of neutron stars in massive scalar-tensor gravity*, *EPL* **130** (2020), no. 5 50002, [arXiv:2001.09117](#)
97. G.W. Horndeski, Second-order scalar-tensor field equations in a four-dimensional space. *Int. J. Theor. Phys.* **10**, 363–384 (1974)
98. A. Nicolis, R. Rattazzi, E. Trincherini, The Galileon as a local modification of gravity. *Phys. Rev. D* **79**, 064036 (2009). ([arXiv:0811.2197](#))
99. T. Kobayashi, M. Yamaguchi, J. Yokoyama, Generalized G-inflation: Inflation with the most general second-order field equations. *Prog. Theor. Phys.* **126**, 511–529 (2011). ([arXiv:1105.5723](#))
100. T. Kobayashi, *Horndeski theory and beyond: a review*, [arXiv:1901.07183](#)

101. C. Charmousis, E.J. Copeland, A. Padilla, P.M. Saffin, General second order scalar-tensor theory, self tuning, and the Fab Four. *Phys. Rev. Lett.* **108**, 051101 (2012). ([arXiv:1106.2000](#))
102. C. Charmousis, E.J. Copeland, A. Padilla, P.M. Saffin, Self-tuning and the derivation of a class of scalar-tensor theories. *Phys. Rev. D* **85**, 104040 (2012). ([arXiv:1112.4866](#))
103. A. Maselli, H. O. Silva, M. Minamitsuji, and E. Berti, *Neutron stars in Horndeski gravity*, *Phys. Rev.* **D93** (2016), no. 12 124056, [arXiv:1603.04876](#)
104. J. L. Blázquez-Salcedo and K. Eickhoff, *Axial quasinormal modes of static neutron stars in the nonminimal derivative coupling sector of Horndeski gravity: spectrum and universal relations for realistic equations of state*, *Phys. Rev.* **D97** (2018), no. 10 104002, [arXiv:1803.01655](#)
105. A. Cisterna, T. Delsate, and M. Rinaldi, *Neutron stars in general second order scalar-tensor theory: The case of nonminimal derivative coupling*, *Phys. Rev.* **D92** (2015), no. 4 044050, [arXiv:1504.05189](#)
106. A. Cisterna, T. Delsate, L. Ducobu, and M. Rinaldi, *Slowly rotating neutron stars in the nonminimal derivative coupling sector of Horndeski gravity*, *Phys. Rev.* **D93** (2016), no. 8 084046, [arXiv:1602.06939](#)
107. E. Babichev, K. Koyama, D. Langlois, R. Saito, and J. Sakstein, *Relativistic Stars in Beyond Horndeski Theories*, *Class. Quant. Grav.* **33** (2016), no. 23 235014, [arXiv:1606.06627](#)
108. D.J. Gross, J.H. Sloan, The Quartic Effective Action for the Heterotic String. *Nucl. Phys. B* **291**, 41–89 (1987)
109. R.R. Metsaev, A.A. Tseytlin, Order alpha-prime (Two Loop) Equivalence of the String Equations of Motion and the Sigma Model Weyl Invariance Conditions: Dependence on the Dilaton and the Antisymmetric Tensor. *Nucl. Phys. B* **293**, 385–419 (1987)
110. P. Pani, E. Berti, V. Cardoso, and J. Read, *Compact stars in alternative theories of gravity. Einstein-Dilaton-Gauss-Bonnet gravity*, *Phys. Rev.* **D84** (2011) 104035, [arXiv:1109.0928](#)
111. B. Kleihaus, J. Kunz, and S. Mojica, *Quadrupole Moments of Rapidly Rotating Compact Objects in Dilatonic Einstein-Gauss-Bonnet Theory*, *Phys. Rev.* **D90** (2014), no. 6 061501, [arXiv:1407.6884](#)
112. B. Kleihaus, J. Kunz, S. Mojica, and M. Zagermann, *Rapidly Rotating Neutron Stars in Dilatonic Einstein-Gauss-Bonnet Theory*, *Phys. Rev.* **D93** (2016), no. 6 064077, [arXiv:1601.05583](#)
113. J. L. Blázquez-Salcedo, L. M. Gonzalez-Romero, J. Kunz, S. Mojica, and F. Navarro-Lerida, *Axial quasinormal modes of Einstein-Gauss-Bonnet-dilaton neutron stars*, *Phys. Rev.* **D93** (2016), no. 2 024052, [arXiv:1511.03960](#)
114. D. D. Doneva and S. S. Yazadjiev, *New Gauss-Bonnet Black Holes with Curvature-Induced Scalarization in Extended Scalar-Tensor Theories*, *Phys. Rev. Lett.* **120** (2018), no. 13 131103, [arXiv:1711.01187](#)
115. H. O. Silva, J. Sakstein, L. Gualtieri, T. P. Sotiriou, and E. Berti, *Spontaneous scalarization of black holes and compact stars from a Gauss-Bonnet coupling*, *Phys. Rev. Lett.* **120** (2018), no. 13 131104, [arXiv:1711.02080](#)
116. G. Antoniou, A. Bakopoulos, and P. Kanti, *Evasion of No-Hair Theorems and Novel Black-Hole Solutions in Gauss-Bonnet Theories*, *Phys. Rev. Lett.* **120** (2018), no. 13 131102, [arXiv:1711.03390](#)
117. D. D. Doneva and S. S. Yazadjiev, *Neutron star solutions with curvature induced scalarization in the extended Gauss-Bonnet scalar-tensor theories*, *JCAP* **1804** (2018), no. 04 011, [arXiv:1712.03715](#)
118. S. Alexander, N. Yunes, Chern-Simons Modified General Relativity. *Phys. Rept.* **480**, 1–55 (2009). ([arXiv:0907.2562](#))
119. N. Yunes, D. Psaltis, F. Ozel, A. Loeb, Constraining Parity Violation in Gravity with Measurements of Neutron-Star Moments of Inertia. *Phys. Rev. D* **81**, 064020 (2010). ([arXiv:0912.2736](#))
120. Y. Ali-Haïmoud, Y. Chen, Slowly-rotating stars and black holes in dynamical Chern-Simons gravity. *Phys. Rev. D* **84**, 124033 (2011). ([arXiv:1110.5329](#))
121. K. Yagi, L.C. Stein, N. Yunes, T. Tanaka, Isolated and Binary Neutron Stars in Dynamical Chern-Simons Gravity. *Phys. Rev. D* **87**, 084058 (2013). ([arXiv:1302.1918](#). [Erratum: *Phys. Rev. D*93, no.8,089909(2016)])

122. K. Yagi, L.C. Stein, N. Yunes, T. Tanaka, Post-Newtonian, Quasi-Circular Binary Inspirals in Quadratic Modified Gravity. *Phys. Rev. D* **85**, 064022 (2012). ([arXiv:1110.5950](#)). [Erratum: *Phys. Rev. D* **93**, no.2,029902(2016)]
123. T. Gupta, B. Majumder, K. Yagi, and N. Yunes, *I-Love-Q Relations for Neutron Stars in dynamical Chern Simons Gravity*, *Class. Quant. Grav.* **35** (2018), no. 2 025009, [arXiv:1710.07862](#)
124. P. T. Chrusciel, J. Lopes Costa, and M. Heusler, *Stationary Black Holes: Uniqueness and Beyond*, *Living Rev. Rel.* **15** (2012) 7, [arXiv:1205.6112](#)
125. V. Cardoso and L. Gualtieri, *Testing the black hole ‘no-hair’ hypothesis*, *Class. Quant. Grav.* **33** (2016), no. 17 174001, [arXiv:1607.03133](#)
126. H.-P. Nollert, TOPICAL REVIEW: Quasinormal modes: the characteristic ‘sound’ of black holes and neutron stars. *Class. Quant. Grav.* **16**, R159–R216 (1999)
127. L. Rezzolla, Gravitational waves from perturbed black holes and relativistic stars. ICTP Lect. Notes Ser. **14**, 255–316 (2003). (gr-qc/0302025)
128. E. Berti, V. Cardoso, A.O. Starinets, Quasinormal modes of black holes and black branes. *Class. Quant. Grav.* **26**, 163001 (2009). ([arXiv:0905.2975](#))
129. R.A. Konoplya, A. Zhidenko, Quasinormal modes of black holes: From astrophysics to string theory. *Rev. Mod. Phys.* **83**, 793–836 (2011). ([arXiv:1102.4014](#))
130. B.F. Whiting, Mode Stability of the Kerr Black Hole. *J. Math. Phys.* **30**, 1301 (1989)
131. H.-P. Nollert, Quasinormal modes of Schwarzschild black holes: The determination of quasinormal frequencies with very large imaginary parts. *Phys. Rev. D* **47**, 5253–5258 (1993)
132. V. Ferrari, B. Mashhoon, New approach to the quasinormal modes of a black hole. *Phys. Rev. D* **30**, 295–304 (1984)
133. H. Yang, D.A. Nichols, F. Zhang, A. Zimmerman, Z. Zhang, Y. Chen, Quasinormal-mode spectrum of Kerr black holes and its geometric interpretation. *Phys. Rev. D* **86**, 104006 (2012). ([arXiv:1207.4253](#))
134. J.L. Synge, The Escape of Photons from Gravitationally Intense Stars. *Mon. Not. Roy. Astron. Soc.* **131**(3), 463–466 (1966)
135. J. Bardeen, *Timelike and null geodesics in the Kerr metric*, in *Black Holes* (C. DeWitt and B. DeWitt, eds.), p. 215. Gordon and Breach, New York, 1973
136. V. Perlick, Gravitational lensing from a spacetime perspective. *Living Rev. Rel.* **7**, 9 (2004)
137. A. Grenzebach, V. Perlick, and C. Lammerzahl, *Photon Regions and Shadows of Kerr-Newman-NUT Black Holes with a Cosmological Constant*, *Phys. Rev.* **D89** (2014), no. 12 124004, [arXiv:1403.5234](#)
138. M.S. Volkov, D.V. Gal’tsov, Gravitating nonAbelian solitons and black holes with Yang-Mills fields. *Phys. Rept.* **319**, 1–83 (1999). (hep-th/9810070)
139. B. Kleihaus, J. Kunz, and F. Navarro-Lerida, *Rotating black holes with non-Abelian hair*, *Class. Quant. Grav.* **33** (2016), no. 23 234002, [arXiv:1609.07357](#)
140. C.A.R. Herdeiro, E. Radu, Kerr black holes with scalar hair. *Phys. Rev. Lett.* **112**, 221101 (2014). ([arXiv:1403.2757](#))
141. C. A. R. Herdeiro and E. Radu, *Asymptotically flat black holes with scalar hair: a review*, *Int. J. Mod. Phys.* **D24** (2015), no. 09 1542014, [arXiv:1504.08209](#)
142. R. Brito, V. Cardoso, C. A. R. Herdeiro, and E. Radu, *Proca stars: Gravitating Bose–Einstein condensates of massive spin 1 particles*, *Phys. Lett.* **B752** (2016) 291–295, [arXiv:1508.05395](#)
143. C. Herdeiro and E. Radu, *Ergosurfaces for Kerr black holes with scalar hair*, *Phys. Rev.* **D89** (2014), no. 12 124018, [arXiv:1406.1225](#)
144. C. Herdeiro and E. Radu, *Construction and physical properties of Kerr black holes with scalar hair*, *Class. Quant. Grav.* **32** (2015), no. 14 144001, [arXiv:1501.04319](#)
145. B. Kleihaus, J. Kunz, and S. Yazadjiev, *Scalarized Hairy Black Holes*, *Phys. Lett.* **B744** (2015) 406–412, [arXiv:1503.01672](#)
146. P. V. P. Cunha, C. A. R. Herdeiro, E. Radu, and H. F. Runarsson, *Shadows of Kerr black holes with scalar hair*, *Phys. Rev. Lett.* **115** (2015), no. 21 211102, [arXiv:1509.00021](#)
147. T. Shen, M. Zhou, C. Bambi, C.A.R. Herdeiro, E. Radu, Iron $K\alpha$ line of Proca stars. *JCAP* **1708**, 014 (2017). ([arXiv:1701.00192](#))

148. E. Babichev, C. Charmousis, and A. Lehébel, *Asymptotically flat black holes in Horndeski theory and beyond*, *JCAP* **1704** (2017), no. 04 027, [arXiv:1702.01938](#)
149. E. Babichev, C. Charmousis, Dressing a black hole with a time-dependent Galileon. *JHEP* **08**, 106 (2014). ([arXiv:1312.3204](#))
150. T. Kobayashi and N. Tanahashi, *Exact black hole solutions in shift symmetric scalar–tensor theories*, *PTEP* **2014** (2014) 073E02, [arXiv:1403.4364](#)
151. O. J. Tattersall, P. G. Ferreira, and M. Lagos, *General theories of linear gravitational perturbations to a Schwarzschild Black Hole*, *Phys. Rev.* **D97** (2018), no. 4 044021, [arXiv:1711.01992](#)
152. O. J. Tattersall and P. G. Ferreira, *Quasinormal modes of black holes in Horndeski gravity*, *Phys. Rev.* **D97** (2018), no. 10 104047, [arXiv:1804.08950](#)
153. O. J. Tattersall and P. G. Ferreira, *Forecasts for Low Spin Black Hole Spectroscopy in Horndeski Gravity*, *Phys. Rev.* **D99** (2019), no. 10 104082, [arXiv:1904.05112](#)
154. O. J. Tattersall, *Quasi-Normal Modes of Hairy Scalar Tensor Black Holes: Odd Parity*, *Class. Quant. Grav.* **37** (2020), no. 11 115007, [arXiv:1911.07593](#)
155. S. Mignemi, N.R. Stewart, Charged black holes in effective string theory. *Phys. Rev. D* **47**, 5259–5269 (1993). (hep-th/9212146)
156. S. Mignemi, Dyonic black holes in effective string theory. *Phys. Rev. D* **51**, 934–937 (1995). (hep-th/9303102)
157. P. Kanti, N.E. Mavromatos, J. Rizos, K. Tamvakis, E. Winstanley, Dilatonic black holes in higher curvature string gravity. *Phys. Rev. D* **54**, 5049–5058 (1996). (hep-th/9511071)
158. T. Torii, H. Yajima, K.-I. Maeda, Dilatonic black holes with Gauss-Bonnet term. *Phys. Rev. D* **55**, 739–753 (1997). (gr-qc/9606034)
159. Z.-K. Guo, N. Ohta, and T. Torii, *Black Holes in the Dilatonic Einstein-Gauss-Bonnet Theory in Various Dimensions. I. Asymptotically Flat Black Holes*, *Prog. Theor. Phys.* **120** (2008) 581–607, [arXiv:0806.2481](#)
160. P. Pani, V. Cardoso, Are black holes in alternative theories serious astrophysical candidates? The Case for Einstein-Dilaton-Gauss-Bonnet black holes. *Phys. Rev. D* **79**, 084031 (2009). ([arXiv:0902.1569](#))
161. P. Pani, C.F.B. Macedo, L.C.B. Crispino, V. Cardoso, Slowly rotating black holes in alternative theories of gravity. *Phys. Rev. D* **84**, 087501 (2011). ([arXiv:1109.3996](#))
162. D. Ayzenberg, N. Yunes, Slowly-Rotating Black Holes in Einstein-Dilaton-Gauss-Bonnet Gravity: Quadratic Order in Spin Solutions. *Phys. Rev. D* **90**, 044066 (2014). ([arXiv:1405.2133](#). [Erratum: *Phys. Rev. D*91, no.6,069905(2015)])
163. A. Maselli, P. Pani, L. Gualtieri, and V. Ferrari, *Rotating black holes in Einstein-Dilaton-Gauss-Bonnet gravity with finite coupling*, *Phys. Rev.* **D92** (2015), no. 8 083014, [arXiv:1507.00680](#)
164. B. Kleihaus, J. Kunz, E. Radu, Rotating Black Holes in Dilatonic Einstein-Gauss-Bonnet Theory. *Phys. Rev. Lett.* **106**, 151104 (2011). ([arXiv:1101.2868](#))
165. B. Kleihaus, J. Kunz, S. Mojica, and E. Radu, *Spinning black holes in Einstein–Gauss-Bonnet–dilaton theory: Nonperturbative solutions*, *Phys. Rev.* **D93** (2016), no. 4 044047, [arXiv:1511.05513](#)
166. B. Chen and L. C. Stein, *Deformation of extremal black holes from stringy interactions*, *Phys. Rev.* **D97** (2018), no. 8 084012, [arXiv:1802.02159](#)
167. P. V. P. Cunha, C. A. R. Herdeiro, B. Kleihaus, J. Kunz, and E. Radu, *Shadows of Einstein–dilaton–Gauss–Bonnet black holes*, *Phys. Lett.* **B768** (2017) 373–379, [arXiv:1701.00079](#)
168. R.M. Wald, Black hole entropy is the Noether charge. *Phys. Rev. D* **48**(8), R3427–R3431 (1993). (gr-qc/9307038)
169. P. Kanti, N. E. Mavromatos, J. Rizos, K. Tamvakis, and E. Winstanley, *Dilatonic black holes in higher curvature string gravity. 2: Linear stability*, *Phys. Rev.* **D57** (1998) 6255–6264, hep-th/9703192
170. D. Ayzenberg, K. Yagi, and N. Yunes, *Linear Stability Analysis of Dynamical Quadratic Gravity*, *Phys. Rev.* **D89** (2014), no. 4 044023, [arXiv:1310.6392](#)

171. J. L. Blazquez-Salcedo, C. F. B. Macedo, V. Cardoso, V. Ferrari, L. Gualtieri, F. S. Khoo, J. Kunz, and P. Pani, *Perturbed black holes in Einstein-dilaton-Gauss-Bonnet gravity: Stability, ringdown, and gravitational-wave emission*, *Phys. Rev.* **D94** (2016), no. 10 104024, [arXiv:1609.01286](#)
172. J. L. Blazquez-Salcedo, F. S. Khoo, and J. Kunz, *Quasinormal modes of Einstein-Gauss-Bonnet-dilaton black holes*, *Phys. Rev.* **D96** (2017), no. 6 064008, [arXiv:1706.03262](#)
173. R. A. Konoplya, A. F. Zinhailo, and Z. Stuchlík, *Quasinormal modes, scattering, and Hawking radiation in the vicinity of an Einstein-dilaton-Gauss-Bonnet black hole*, *Phys. Rev.* **D99** (2019), no. 12 124042, [arXiv:1903.03483](#)
174. A. F. Zinhailo, *Quasinormal modes of Dirac field in the Einstein–Dilaton–Gauss–Bonnet and Einstein–Weyl gravities*, *Eur. Phys. J.* **C79** (2019), no. 11 912, [arXiv:1909.12664](#)
175. J. L. Blazquez-Salcedo, D. D. Doneva, J. Kunz, and S. S. Yazadjiev, *Radial perturbations of the scalarized Einstein-Gauss-Bonnet black holes*, *Phys. Rev.* **D98** (2018), no. 8 084011, [arXiv:1805.05755](#)
176. G. Antoniou, A. Bakopoulos, and P. Kanti, *Black-Hole Solutions with Scalar Hair in Einstein-Scalar-Gauss-Bonnet Theories*, *Phys. Rev.* **D97** (2018), no. 8 084037, [arXiv:1711.07431](#)
177. D. D. Doneva, S. Kiorpelidi, P. G. Nedkova, E. Papantonopoulos, and S. S. Yazadjiev, *Charged Gauss-Bonnet black holes with curvature induced scalarization in the extended scalar-tensor theories*, *Phys. Rev.* **D98** (2018), no. 10 104056, [arXiv:1809.00844](#)
178. H. O. Silva, C. F. B. Macedo, T. P. Sotiriou, L. Gualtieri, J. Sakstein, and E. Berti, *Stability of scalarized black hole solutions in scalar-Gauss-Bonnet gravity*, *Phys. Rev.* **D99** (2019), no. 6 064011, [arXiv:1812.05590](#)
179. P. V. P. Cunha, C. A. R. Herdeiro, and E. Radu, *Spontaneously Scalarized Kerr Black Holes in Extended Scalar-Tensor–Gauss-Bonnet Gravity*, *Phys. Rev. Lett.* **123** (2019), no. 1 011101, [arXiv:1904.09997](#)
180. C. F. B. Macedo, J. Sakstein, E. Berti, L. Gualtieri, H. O. Silva, and T. P. Sotiriou, *Self-interactions and Spontaneous Black Hole Scalarization*, *Phys. Rev.* **D99** (2019), no. 10 104041, [arXiv:1903.06784](#)
181. L. G. Collodel, B. Kleihaus, J. Kunz, and E. Berti, *Spinning and excited black holes in Einstein-scalar-Gauss–Bonnet theory*, *Class. Quant. Grav.* **37** (2020), no. 7 075018, [arXiv:1912.05382](#)
182. C. F. Macedo, *Scalar modes, spontaneous scalarization and circular null-geodesics of black holes in scalar-Gauss–Bonnet gravity*, *Int. J. Mod. Phys. D* **29** (2020), no. 11 2041006, [arXiv:2002.12719](#)
183. J. L. Blázquez-Salcedo, D. D. Doneva, S. Kahlen, J. Kunz, P. Nedkova, and S. S. Yazadjiev, *Axial perturbations of the scalarized Einstein-Gauss-Bonnet black holes*, *Phys. Rev. D* **101** (2020), no. 10 104006, [arXiv:2003.02862](#)
184. J. L. Blázquez-Salcedo, D. D. Doneva, S. Kahlen, J. Kunz, P. Nedkova, and S. S. Yazadjiev, *Polar quasinormal modes of the scalarized Einstein-Gauss-Bonnet black holes*, *Phys. Rev. D* **102** (2020), no. 2 024086, [arXiv:2006.06006](#)
185. A. Dima, E. Barausse, N. Franchini, and T. P. Sotiriou, *Spin-induced black hole spontaneous scalarization*, *Phys. Rev. Lett.* **125** (2020), no. 23 231101, [arXiv:2006.03095](#)
186. S. Hod, *Onset of spontaneous scalarization in spinning Gauss-Bonnet black holes*, *Phys. Rev. D* **102** (2020), no. 8 084060, [arXiv:2006.09399](#)
187. D. D. Doneva, L. G. Collodel, C. J. Krüger, and S. S. Yazadjiev, *Black hole scalarization induced by the spin: 2+1 time evolution*, *Phys. Rev. D* **102** (2020), no. 10 104027, [arXiv:2008.07391](#)
188. C. A. R. Herdeiro, E. Radu, H. O. Silva, T. P. Sotiriou, and N. Yunes, *Spin-induced scalarized black holes*, *Phys. Rev. Lett.* **126** (2021), no. 1 011103, [arXiv:2009.03904](#)
189. E. Berti, L. G. Collodel, B. Kleihaus, and J. Kunz, *Spin-induced black-hole scalarization in Einstein-scalar-Gauss-Bonnet theory*, *Phys. Rev. Lett.* **126** (2021), no. 1 011104, [arXiv:2009.03905](#)
190. V. Cardoso, L. Gualtieri, *Perturbations of Schwarzschild black holes in Dynamical Chern-Simons modified gravity*. *Phys. Rev. D* **80**, 064008 (2009). ([arXiv:0907.5008](#). [Erratum: *Phys. Rev. D* **81**, 089903(2010)])

191. C. Molina, P. Pani, V. Cardoso, L. Gualtieri, Gravitational signature of Schwarzschild black holes in dynamical Chern-Simons gravity. *Phys. Rev. D* **81**, 124021 (2010). ([arXiv:1004.4007](#))
192. M. Kimura, *Stability analysis of Schwarzschild black holes in dynamical Chern-Simons gravity*, *Phys. Rev. D* **98** (2018), no. 2 024048, [arXiv:1807.05029](#)
193. N. Yunes and F. Pretorius, *Dynamical Chern-Simons Modified Gravity. I. Spinning Black Holes in the Slow-Rotation Approximation*, *Phys. Rev. D* **79** (2009) 084043, [arXiv:0902.4669](#)
194. K. Konno, T. Matsuyama, S. Tanda, Rotating black hole in extended Chern-Simons modified gravity. *Prog. Theor. Phys.* **122**, 561–568 (2009). ([arXiv:0902.4767](#))
195. K. Yagi, N. Yunes, T. Tanaka, Slowly Rotating Black Holes in Dynamical Chern-Simons Gravity: Deformation Quadratic in the Spin. *Phys. Rev. D* **86**, 044037 (2012). ([arXiv:1206.6130](#). [Erratum: *Phys. Rev. D* 89,049902(2014)])
196. T. Delsate, C. Herdeiro, and E. Radu, *Non-perturbative spinning black holes in dynamical Chern–Simons gravity*, *Phys. Lett.* **B787** (2018) 8–15, [arXiv:1806.06700](#)
197. E. Barausse, C. Palenzuela, M. Ponce, L. Lehner, Neutron-star mergers in scalar-tensor theories of gravity. *Phys. Rev. D* **87**, 081506 (2013). ([arXiv:1212.5053](#))
198. M. Shibata, K. Taniguchi, H. Okawa, and A. Buonanno, *Coalescence of binary neutron stars in a scalar-tensor theory of gravity*, *Phys. Rev. D* **89** (2014), no. 8 084005, [arXiv:1310.0627](#)
199. K. Taniguchi, M. Shibata, and A. Buonanno, *Quasiequilibrium sequences of binary neutron stars undergoing dynamical scalarization*, *Phys. Rev. D* **91** (2015), no. 2 024033, [arXiv:1410.0738](#)
200. N. Sennett and A. Buonanno, *Modeling dynamical scalarization with a resummed post-Newtonian expansion*, *Phys. Rev. D* **93** (2016), no. 12 124004, [arXiv:1603.03300](#)
201. M. Ponce, C. Palenzuela, E. Barausse, and L. Lehner, *Electromagnetic outflows in a class of scalar-tensor theories: Binary neutron star coalescence*, *Phys. Rev. D* **91** (2015), no. 8 084038, [arXiv:1410.0638](#)
202. N. Sennett, L. Shao, and J. Steinhoff, *Effective action model of dynamically scalarizing binary neutron stars*, *Phys. Rev. D* **96** (2017), no. 8 084019, [arXiv:1708.08285](#)
203. L. Sagunski, J. Zhang, M. C. Johnson, L. Lehner, M. Sakellariadou, S. L. Liebling, C. Palenzuela, and D. Neilsen, *Neutron star mergers as a probe of modifications of general relativity with finite-range scalar forces*, *Phys. Rev. D* **97** (2018), no. 6 064016, [arXiv:1709.06634](#)
204. E. Berti, K. Yagi, and N. Yunes, *Extreme Gravity Tests with Gravitational Waves from Compact Binary Coalescences: (I) Inspiral-Merger*, *Gen. Rel. Grav.* **50** (2018), no. 4 46, [arXiv:1801.03208](#)
205. E. Berti, K. Yagi, H. Yang, and N. Yunes, *Extreme Gravity Tests with Gravitational Waves from Compact Binary Coalescences: (II) Ringdown*, *Gen. Rel. Grav.* **50** (2018), no. 5 49, [arXiv:1801.03587](#)
206. F. Hernandez Vivanco, R. Smith, E. Thrane, P. D. Lasky, C. Talbot, and V. Raymond, *Measuring the neutron star equation of state with gravitational waves: The first forty binary neutron star merger observations*, *Phys. Rev. D* **100** (2019), no. 10 103009, [arXiv:1909.02698](#)
207. T. Baker, E. Bellini, P. G. Ferreira, M. Lagos, J. Noller, and I. Sawicki, *Strong constraints on cosmological gravity from GW170817 and GRB 170817A*, *Phys. Rev. Lett.* **119** (2017), no. 25 251301, [arXiv:1710.06394](#)
208. J. M. Ezquiaga and M. Zumalacárregui, *Dark Energy After GW170817: Dead Ends and the Road Ahead*, *Phys. Rev. Lett.* **119** (2017), no. 25 251304, [arXiv:1710.05901](#)
209. J. Sakstein and B. Jain, *Implications of the Neutron Star Merger GW170817 for Cosmological Scalar-Tensor Theories*, *Phys. Rev. Lett.* **119** (2017), no. 25 251303, [arXiv:1710.05893](#)
210. C. de Rham and S. Melville, *Gravitational Rainbows: LIGO and Dark Energy at its Cutoff*, *Phys. Rev. Lett.* **121** (2018), no. 22 221101, [arXiv:1806.09417](#)
211. T. Kobayashi, H. Motohashi, T. Suyama, Black hole perturbation in the most general scalar-tensor theory with second-order field equations I: the odd-parity sector. *Phys. Rev. D* **85**, 084025 (2012). ([arXiv:1202.4893](#). [Erratum: *Phys. Rev. D* 96, 109903 (2017)])
212. T. Kobayashi, H. Motohashi, and T. Suyama, *Black hole perturbation in the most general scalar-tensor theory with second-order field equations II: the even-parity sector*, *Phys. Rev. D* **89** (2014), no. 8 084042, [arXiv:1402.6740](#)

213. G. Antoniou, A. Bakopoulos, P. Kanti, B. Kleihaus, and J. Kunz, *Novel Einstein–scalar–Gauss–Bonnet wormholes without exotic matter*, *Phys. Rev. D* **101** (2020), no. 2 024033, [arXiv:1904.13091](https://arxiv.org/abs/1904.13091)

Chapter 24

Parametrized Post-Newtonian Formalism



Manuel Hohmann

24.1 Historical Remarks

In order to assess the viability of different gravity theories and compare their predictions to a large number of observations, several frameworks have been developed. The common idea behind these frameworks is to characterise each gravity theory by a number of certain parameters, which can then be compared to a corresponding set of observations. The parameters introduced as an intermediate step in these formalisms serve as an abstraction both to the observations and to the theories under consideration, and thus allow us to divide testing gravity theories into two parts: deriving a fixed set of predicted values of the parameters from any given gravity theory, and comparing these to their experimentally determined values.

An early example of such a formalism is the Eddington-Robertson-Schiff formalism for tests of post-Newtonian gravity in the Solar System [1–3]. It is based on the assumption that the Sun is a point-like, non-rotating mass generating a spherically symmetric gravitational field, which is described by a metric tensor, while the planets are test bodies moving along the geodesics of this metric. The Eddington-Robertson-Schiff metric contains two free parameters, β and γ , which are determined by solving the field equations of a given (metric) gravity theory for a point-like source mass. This theoretical prediction of the two parameters is complemented by their experimental measurement, as they describe, among other observables, the light deflection angle and perihelion precession of mercury. The advantage in using the Eddington-Robertson-Schiff formalism lies in the fact that instead of calculating the trajectories of light and mercury (and potentially other observables) for any given gravity theory, it suffices to calculate only two parameters, whose values can be compared to different observations. This advantage comes with the drawback that the formalism may

M. Hohmann (✉)

Laboratory of Theoretical Physics, Institute of Physics, University of Tartu,
W. Ostwaldi 1, 50411 Tartu, Estonia
e-mail: manuel.hohmann@ut.ee

be applied only to theories satisfying a particular set of assumptions—in this case metric gravity theories, whose metric takes a particular form for a point-like source.

Further developments led to a generalisation of the Eddington-Robertson-Schiff formalism, first by relaxing the assumption of a static point mass as the gravitational source. These generalisations are allowed to include rotation to describe the Lense-Thirring effect [3], as well as a simple extension to fluids [4]. A system of several gravitating point masses was assumed in [5, 6], and the formalism was subsequently extended to a full perfect fluid description [7–9]. The modern form of the parametrized post-Newtonian (PPN) formalism was then developed from combining these preceding approaches into a single formalism [10, 11], and complementing it with another extension in order to also describe preferred location effects occurring in a particular class of gravity theories [12]. This is the formalism we will discuss in the following section.

24.2 Parametrized Post-Newtonian Formalism

The central ingredient of the parametrized post-Newtonian formalism [13] is a perturbative expansion of the metric tensor around a flat Minkowski background,

$$g_{\mu\nu} = \eta_{\mu\nu} + h_{\mu\nu}, \quad (24.1)$$

where the perturbation $h_{\mu\nu}$ is due to a localised source matter distribution, which vanishes asymptotically far away from the source. This matter source is described by the energy-momentum tensor of a perfect fluid,

$$T^{\mu\nu} = (\rho + \rho\Pi + p)u^\mu u^\nu + pg^{\mu\nu}, \quad (24.2)$$

with density ρ , pressure p , specific internal energy Π and four-velocity u^μ , normalised by the metric to $g_{\mu\nu}u^\mu u^\nu = -1$. It is further assumed that the velocity $v^i = u^i/u^0$ of the source matter in a given frame of reference, in which the expansion (24.1) is valid, is small compared to the speed of light, $|\vec{v}| \ll c \equiv 1$. Based on this assumption, we promote the velocity to a perturbation parameter, and assigns so-called velocity orders $\mathcal{O}(n) \propto |\vec{v}|^n$ to all quantities present in the theory under investigation, based on their orders of magnitude in the Solar System. For the matter variables, velocity orders of $\mathcal{O}(2)$ are used for ρ and Π and $\mathcal{O}(4)$ for p . The metric perturbation is expanded in the form

$$h_{\mu\nu} = \overset{1}{h}_{\mu\nu} + \overset{2}{h}_{\mu\nu} + \overset{3}{h}_{\mu\nu} + \overset{4}{h}_{\mu\nu} + \mathcal{O}(5), \quad (24.3)$$

where we used overscripts to denote the velocity orders $\overset{n}{h}_{\mu\nu} \sim \mathcal{O}(n)$. Finally, it is assumed that the gravitational field is quasi-static, i.e., its time evolution is governed

entirely by the motion of the localised sources. This assumption justifies assigning an additional velocity order to time derivatives, $\partial_0 \sim \mathcal{O}(1)$.

In order to determine which terms in the expansion (24.3) are relevant, one considers the action

$$S[\gamma] = -m \int \sqrt{-g_{\mu\nu} \dot{\gamma}^\mu \dot{\gamma}^\nu} dt = -m \int \sqrt{-g_{00} - 2g_{0i} \dot{\gamma}^i - g_{ij} \dot{\gamma}^i \dot{\gamma}^j} dt \quad (24.4)$$

of a test particle of mass m moving along a trajectory $\gamma^\mu = (t, \vec{x})$, which we chose to parametrise by the coordinate time t . Here one assumes that the velocity of the test particle is of the same order $|\dot{\gamma}| \sim \mathcal{O}(1)$ as that of the source matter. Expanding the action (24.4) into velocity orders, we find that the second velocity order corresponds to the Newtonian limit, with ${}^2\bar{h}_{00} = 2U$ given by the Newtonian potential, while the post-Newtonian limit appears as the fourth velocity order, thus containing the metric components ${}^2\bar{h}_{ij}$, ${}^3\bar{h}_{0i}$, ${}^4\bar{h}_{00}$. Odd velocity orders do not appear, since they are antisymmetric under time reversal, and thus correspond to dissipative processes. These are prohibited by energy-momentum conservation: conservation of rest mass prohibits terms of the first velocity order, while the third velocity order is prohibited by Newtonian energy conservation.

In order to determine the aforementioned components of the metric perturbations, it is assumed that they are expressed in a generic form

$${}^2\bar{h}_{00} = 2U, \quad (24.5a)$$

$${}^2\bar{h}_{ij} = 2\gamma U \delta_{ij}, \quad (24.5b)$$

$${}^3\bar{h}_{0i} = -\frac{1}{2}(3 + 4\gamma + \alpha_1 - \alpha_2 + \zeta_1 - 2\xi)V_i - \frac{1}{2}(1 + \alpha_2 - \zeta_1 + 2\xi)W_i, \quad (24.5c)$$

$${}^4\bar{h}_{00} = -2\beta U^2 + (2 + 2\gamma + \alpha_3 + \zeta_1 - 2\xi)\Phi_1 + 2(1 + 3\gamma - 2\beta + \zeta_2 + \xi)\Phi_2 + 2(1 + \zeta_3)\Phi_3 + 2(3\gamma + 3\zeta_4 - 2\xi)\Phi_4 - (\zeta_1 - 2\xi)A - 2\xi\Phi_W, \quad (24.5d)$$

where a number of post-Newtonian potentials are introduced, which are defined as Poisson-like integrals over the source matter distribution. In particular, they are given by the Newtonian potentials at the second velocity order

$$U(t, \vec{x}) = \int \frac{\rho(t, \vec{x}')}{|\vec{x} - \vec{x}'|} d^3x', \quad U_{ij}(t, \vec{x}) = \int \frac{\rho(t, \vec{x}')(x_i - x'_i)(x_j - x'_j)}{|\vec{x} - \vec{x}'|^3} d^3x', \quad (24.6)$$

the third-order vector potentials

$$V_i(t, \vec{x}) = \int \frac{\rho(t, \vec{x}')v_i(t, \vec{x}')}{|\vec{x} - \vec{x}'|} d^3x', \quad W_i(t, \vec{x}) = \int \frac{\rho(t, \vec{x}')v_j(t, \vec{x}')(x_i - x'_i)(x_j - x'_j)}{|\vec{x} - \vec{x}'|^3} d^3x', \quad (24.7)$$

as well as the fourth-order scalar potentials

$$\begin{aligned}
\Phi_1(t, \vec{x}) &= \int \frac{\rho(t, \vec{x}') v^2(t, \vec{x}')}{|\vec{x} - \vec{x}'|} d^3 x', & \Phi_2(t, \vec{x}) &= \int \frac{\rho(t, \vec{x}') U(t, \vec{x}')}{|\vec{x} - \vec{x}'|} d^3 x', \\
\Phi_3(t, \vec{x}) &= \int \frac{\rho(t, \vec{x}') \Pi(t, \vec{x}')}{|\vec{x} - \vec{x}'|} d^3 x', & \Phi_4(t, \vec{x}) &= \int \frac{p(t, \vec{x}')}{|\vec{x} - \vec{x}'|} d^3 x', \\
A(t, \vec{x}) &= \int \frac{\rho(t, \vec{x}') [v_i(t, \vec{x}') (x_i - x'_i)]^2}{|\vec{x} - \vec{x}'|^3} d^3 x', & B(t, \vec{x}) &= \int \frac{\rho(t, \vec{x}')}{|\vec{x} - \vec{x}'|} (x_i - x'_i) \frac{dv_i(t, \vec{x}')}{dt} d^3 x'. \\
\Phi_W(t, \vec{x}) &= \int \rho(t, \vec{x}') \rho(t, \vec{x}'') \frac{x_i - x'_i}{|\vec{x} - \vec{x}'|^3} \left(\frac{x'_i - x''_i}{|\vec{x} - \vec{x}''|} - \frac{x_i - x''_i}{|\vec{x}' - \vec{x}''|} \right) d^3 x' d^3 x''. \quad (24.8)
\end{aligned}$$

Here we have also included the PPN potentials U_{ij} and B , which do not appear in the standard PPN metric (24.5), but must be included to describe theories with broken diffeomorphism invariance, as mentioned in Sect. 24.4.2. The coefficients $\gamma, \beta, \alpha_1, \alpha_2, \alpha_3, \zeta_1, \zeta_2, \zeta_3, \zeta_4, \xi$ are the PPN parameters, which characterise the particular gravity theory under consideration, and which are determined by solving the gravitational field equations using the generic metric (24.5). They are usually assumed to be constant, but this assumption may be relaxed, as discussed in Sect. 24.4.

24.3 Comparison to Observations

The specific form of the PPN parameters in the metric (24.5) is chosen such that they can be given a physical interpretation, which is closely linked to the observational properties of the gravity theory under consideration:

1. γ measures the amount of spatial curvature produced by unit rest mass.
2. β measures the non-linearity in the gravitational superposition law.
3. $\alpha_1, \alpha_2, \alpha_3$ measure the violation of local Lorentz invariance, i.e., the presence of preferred-frame effects.
4. $\alpha_3, \zeta_1, \zeta_2, \zeta_3, \zeta_4$ measure the violation of total energy-momentum conservation.
5. ξ measures the violating of local position invariance, i.e., the presence of preferred-location effects.

Further, they are normalised such that for General Relativity they take the values $\beta = \gamma = 1$, while all other parameters vanish due to the absence of the corresponding effects. Finally, they are chosen such that they are linked to observations either in the Solar System or in other compact gravitating systems, such as stellar or neutron star binaries. Numerous bounds on the parameters have been obtained from such observations; see Table 24.1 for an overview.

In the table we have also included the Nordtvedt parameter [5, 6]

$$\eta_N = 4\beta - \gamma - 3 - \frac{10}{3}\xi - \alpha_1 + \frac{2}{3}\alpha_2 - \frac{2}{3}\zeta_1 - \frac{1}{3}\zeta_2, \quad (24.9)$$

Table 24.1 Current bounds on the PPN parameters according to [21], unless otherwise indicated

Par.	Bound	Effects	Experiment
$2^*\gamma - 1$	$2.3 \cdot 10^{-5}$	Time delay	Cassini tracking [14]
	$2 \cdot 10^{-4}$	Light deflection	VLBI [15]
$\beta - 1$	$8 \cdot 10^{-5}$	Perihelion shift	Solar System ephemeris [16–18]
ξ	$4 \cdot 10^{-9}$	Spin precession	Millisecond pulsars
$2^*\alpha_1$	10^{-4}	2^* orbital polarisation	Lunar laser ranging
	$4 \cdot 10^{-5}$		PSR J1738+0333
α_2	$2 \cdot 10^{-9}$	Spin precession	Millisecond pulsars
α_3	$4 \cdot 10^{-20}$	Self-acceleration	Pulsar spin-down statistics
η_N	$9 \cdot 10^{-4}$	Nordtvedt effect	Lunar laser ranging
ζ_1	0.02	Combined PPN bounds	–
ζ_2	$4 \cdot 10^{-5}$	Binary pulsar acceleration	PSR 1913+16
ζ_3	10^{-8}	Newton’s 3rd law	Lunar acceleration
ζ_4	0.006	–	Kreuzer experiment [19]

since this particular combination is closely related to the Nordtvedt effect, which can be tested separately by using lunar laser ranging¹.

24.4 Extensions and Modifications

Although the standard PPN formalism as described in Sect. 24.2 is suitable to describe the post-Newtonian limits of a large class of gravity theories, it still allows for numerous extensions to include further physical effects or adapt it to gravity theories which are not covered by the standard PPN formalism. In the following, we list a few such extensions and modifications.

24.4.1 Invariant Density Formulation

In a more recent adaptation of the PPN formalism [22], the density variable ρ appearing in the definition of the post-Newtonian potentials is replaced by a conserved quantity $\rho^* = \rho\sqrt{-gu^0}$, which satisfies the continuity equation

$$\partial_0\rho^* + \partial_i(\rho^*v_i) = 0. \tag{24.10}$$

¹ Assuming $6\zeta_4 = 3\alpha_3 + 2\zeta_1 - 3\zeta_3$ [20].

The advantage of this modification is that it allows for simpler transformation rules between potentials, since the continuity equation (24.10) together with integration by parts yields

$$\partial_0 \int \rho^*(t, \vec{x}) f(t, \vec{x}) d^3x = \int \rho^*(t, \vec{x}) \frac{df}{dt}(t, \vec{x}) d^3x \quad (24.11)$$

for any function f . Note, however, that by using this modified definition, several of the formulas mentioned in Sect. 24.2 change [22].

24.4.2 Broken Diffeomorphism Invariance

In order to achieve the standard form (24.5) of the post-Newtonian metric, certain PPN potentials, which would otherwise appear in the most general post-Newtonian metric, have been eliminated by applying a specific coordinate transformation. This is possible only if the theory under investigation is invariant under the full diffeomorphism group, and does not exhibit any preferred coordinate system. If diffeomorphism invariance is (partially) broken, additional potentials, together with corresponding PPN parameters, remain in the PPN metric. This is the case, for example, in Hořava-Lifshitz gravity [23], where the broken invariance under changes of the time coordinate leads to the presence of the PPN potential B in the fourth order metric component h_{00}^4 , together with a PPN parameter ζ_B [24–26]. Similarly, breaking of spatial diffeomorphism invariance would require introducing a term proportional to the potential U_{ij} in the second-order metric component h_{ij}^2 .

24.4.3 Yukawa-Type Couplings

For the standard PPN formalism it is assumed that the metric perturbations, as well as perturbations of other relevant fields, appear in the gravitational field equations in terms of second total derivative order, i.e., either as second-order derivatives of the fields or as products of two first-order derivatives. In this case the field equations are of Poisson type and can be solved by the PPN potentials introduced in Sect. 24.2. This corresponds to the physical interpretation that these fields are massless. However, if mass terms are present in the field equations, which carry no derivatives, one must introduce Yukawa-type potentials in order to solve the field equations. Such an extension of the PPN formalism has been developed in the context of scalar-tensor gravity in [27, 28].

24.4.4 Higher Derivative Orders

The opposite situation, compared to the previous case, is the appearance of terms in the perturbative field equations with higher than second derivative order, i.e., either higher than second-order derivatives acting on the perturbations, or products of terms such that their total number of derivatives exceeds two. Such terms require the introduction of additional PPN potentials that contain derivatives of the matter variables. PPN potentials of this form have been introduced in the context of Poincaré gauge theory in [29].

24.4.5 Parity-Violating Terms

As discussed in Sect. 24.2, the PPN potentials are defined as solutions to a set of Poisson-like equations, and as such are of even parity. In order to solve the field equations on theories involving parity-violating terms, additional, parity-odd potentials must be introduced. An example is given by Chern-Simons gravity, which features the parity-violating term $*RR = \frac{1}{2}\epsilon^{\mu\nu\rho\sigma} R^\alpha{}_{\beta\mu\nu} R^\beta{}_{\alpha\rho\sigma}$, which requires the introduction of a new potential $\epsilon^{ijk}\partial_j V_k$ in the metric component h_{0i} , together with a corresponding PPN parameter [30–32].

24.4.6 Screening Mechanisms

An important assumption of the PPN formalism is the validity of the linear and quadratic order perturbation theory around the asymptotically flat Minkowski background. While this assumption holds for most theories, there are also counterexamples, such as Horndeski or bimetric gravity, in which strong coupling effects are present and lead to a screening on Solar System scales [33, 34]. Such effects may be included into the PPN formalism by introducing the characteristic scale of the screening effect, known as the Vainshtein radius, as another perturbation parameter [35].

A different kind of screening is present in the so-called chameleon theory. In this case the scalar field is suppressed inside matter, and so only a thin shell, forming the outer layer of the source mass, contributes to the post-Newtonian scalar field [36–40]. General screening effects are discussed in [41].

24.4.7 *Cosmological Background Evolution*

In the standard PPN formalism it is assumed that the background around which the perturbation is performed is given by a Minkowski spacetime, and thus in particular stationary, i.e., invariant under time translation. As a consequence, the values of the post-Newtonian parameters are constant in time. In [42] this assumption has been dropped and an evolving cosmological background assumed, which leads to a possible time dependence of the PPN parameters.

24.4.8 *Multiple Metrics*

Another assumption of the standard PPN formalism, whose footing is the validity of the Einstein equivalence principle, is the existence of a single, dynamical metric, which governs the behaviour of physical systems within a gravitational field. Note that this assumption does not exclude theories with an additional, non-dynamical metric, such as Rosen's theory [43], whose PPN parameters agree with General Relativity except for α_2 [44], or massive gravity [45, 46], provided that one allows for Yukawa-type terms.

Including another, dynamical metric, however, requires an extension of the standard PPN formalism, which features additional PPN potentials and in which both metrics are treated perturbatively [47–49].

24.4.9 *Tetrad Formulation*

The aforementioned approaches have a common feature that the fundamental field which carries the gravitational interaction, and which is thus expanded in the post-Newtonian perturbation orders, is the metric (or one of several metrics). However, there are also gravity theories in which one considers a tetrad as the fundamental field variable, so that the metric becomes a dependent quantity. For such theories one must therefore perform a perturbative expansion of the tetrad. Such a post-Newtonian expansion has been developed in the context of Poincaré gauge theory in [50], and in the case of translation gauge theory in [51]. An adaptation for a scalar-tetrad theory of gravity has been developed in [52]. For the covariant formulation of teleparallel gravity, it has been developed in [53].

24.4.10 *Gauge-Invariant Approach*

An important assumption of the PPN formalism is the existence of a particular gauge, or choice of coordinates, in which the post-Newtonian metric takes the stan-

dard form (24.5). Determining the post-Newtonian limit of a given theory of gravity conventionally involves solving the perturbative field equations either in this particular gauge, or choosing a gauge in which the equations become possibly simpler, and then transforming the resulting solution into the standard PPN gauge. Either method may turn out to be cumbersome, since in general there is no canonical gauge choice that simplifies the field equations, and even if such a gauge is found, the equations may still exhibit a highly non-trivial coupling between the tensor components of the metric and other fields. In cosmology, such difficulties are overcome by making use of a gauge-invariant approach [54–57]. Using the same mathematical footing, which requires the use of second-order perturbations [58, 59], a similar approach to the PPN formalism has been developed [60].

24.5 Post-Newtonian Limit of Particular Theories

The PPN formalism has been applied to a vast number of gravitational theories, some of which we mentioned in Sect. 24.4 in the context of extensions of the formalism. Here we list further results on the post-Newtonian limit for selected classes of gravity theories, which belong to the most relevant and most actively studied modified gravity theories.

24.5.1 Scalar-Tensor and $f(R)$ Theories

An important class of gravity theories is described by the general scalar-tensor action [61]

$$S = \frac{1}{2\kappa^2} \int \left[\mathcal{A}(\phi)R - \mathcal{B}(\phi)g^{\mu\nu} \partial_\mu \phi \partial_\nu \phi - 2\kappa^2 \mathcal{V}(\phi) \right] \sqrt{-g} d^4x + S_m[\chi, e^{2\alpha(\phi)} g_{\mu\nu}]. \quad (24.12)$$

Here, χ collectively denotes any set of matter fields, while \mathcal{A} , \mathcal{B} , \mathcal{V} , α are free functions of the scalar field. This class of theories has the property that by a redefinition of the scalar field and a conformal transformation of the metric, equivalent theories can be related to each other, which are described by different choices of the free functions in the action. This allows us to represent such an equivalence class of theories in different conformal frames and representations. Making use of this freedom, the PPN parameters for different subclasses of these theories have been calculated, mostly choosing to work in the Jordan frame $\alpha(\phi) \equiv 0$, using the scalar field parameterisation $\mathcal{A}(\phi) \equiv \phi$ and redefining the kinetic term as $\mathcal{B}(\phi) \equiv \omega(\phi)/\phi$. The only non-trivial parameters for this case are γ and β :

1. For an arbitrary function ω , but vanishing potential \mathcal{V} , the PPN parameters are given by

$$\gamma = \frac{\omega_0 + 1}{\omega_0 + 2}, \quad \beta = 1 + \frac{\omega_1 \Phi}{(2\omega_0 + 3)(2\omega_0 + 4)^2}, \quad (24.13)$$

where $\omega_0 = \omega(\Phi)$, $\omega_1 = \omega'(\Phi)$ and Φ is the cosmological background value of the scalar field [62]. Light propagation in the Solar System at the post-Newtonian level has been studied for this class of theories in [63, 64].

2. In [65–67] the PPN parameter γ for constant ω and non-vanishing potential \mathcal{V} has been derived.
3. For general free functions ω and \mathcal{V} , the post-Newtonian field equations have been derived in [68]. The PPN parameters β and γ for this class of theories have been calculated under the assumption of a static point mass source in the Jordan frame $\alpha(\phi) \equiv 0$ [69] as well as the Einstein frame $\mathcal{A}(\phi) \equiv 1$ [38]. A frame-independent calculation in terms of conformal invariants is shown in [70]. The result has been extended to a homogeneous sphere replacing the point mass source [71].
4. Non-standard kinetic terms and matter couplings of the scalar field have been considered in [72–75] for the calculation of γ .
5. Screening mechanisms in the context of the post-Newtonian approximation of scalar-tensor theories have been discussed in [76, 77].

The obtained results have also been applied to obtain the post-Newtonian limit of $f(R)$ type gravity theories, through their dynamical equivalence with scalar-tensor gravity [78–85].

Care must be taken when the resulting PPN parameters for the case of a massive scalar field and a point mass source are to be interpreted physically, since the former leads to non-constant values of the PPN parameters, which contrasts the standard assumption of constant PPN parameters [38, 69], while the latter is only a very coarse approximation of the Sun, neglecting its gravitational self-energy [71]. This influences, for example, the derivation of the light deflection by the S2un, so that in general a full calculation of light trajectories in the post-Newtonian solution of the spacetime geometry must be performed [86, 87].

24.5.2 Multi-scalar-Tensor Theories

A straightforward generalisation of the scalar-tensor theories discussed above is to include multiple scalar fields [88, 89]. For the case of a vanishing potential, the PPN parameters have been obtained in the Einstein frame in [88] and in the Jordan frame for a diagonal kinetic term in [89], and a general kinetic term in [90]. For an arbitrary frame, they have been expressed in terms of invariant quantities in [91]. For the general case including a potential, the PPN parameter γ has been calculated in [92].

Various gravity theories can be reformulated as particular multi-scalar-tensor gravity theories, and also for such classes of theories the post-Newtonian limit has been considered: for C-theory with a vanishing potential [93], as well as for non-local gravity both in the biscalar representation [94] and independent thereof [95].

24.5.3 *Horndeski Gravity*

Another generalisation of the scalar-tensor action (24.12) is given by the Horndeski class of gravity theories [96–98]. Their post-Newtonian limit has been derived in [99] for the case of negligible Vainshtein screening. An alternative approach using an effective energy-momentum tensor including gravitational waves is presented in [100]. In general, however, also screening effects must also be taken into account [101].

24.5.4 *Bimetric and Multimetric Gravity*

Since their development about a decade ago, theories of massive gravity [102] and bimetric gravity [103, 104], being the unique ghost-free theories of these types, have received growing attention; see [45, 46, 105] for a number of reviews. One interesting aspect of these theories is the possibility to include a dark matter sector that is only coupled gravitationally to ordinary matter. The post-Newtonian parameter γ is calculated under this assumption, and the deflection of light by visible and dark matter sources is obtained in [106].

24.5.5 *Teleparallel Gravity*

Another large class of theories, which has gained growing interest during the last decade, is based on the framework of teleparallel gravity [107, 108]. The most simple contender theory in this class is the Teleparallel Equivalent of General Relativity [109], which constitutes one of the three physically equivalent, but geometrically distinct formulations of General Relativity [110]. Due to this equivalence, its PPN parameters agree with that of General Relativity.

Modifications of TEGR, however, differ also in their phenomenology from analogous modifications of the standard Einstein-Hilbert formulation of General Relativity in terms of curvature. A prominent example is given by $f(\mathbb{T})$ theories [111, 112], whose PPN parameters are identical to those of General Relativity [53], while $f(R)$ type modifications lead to a deviation of the PPN parameters, as discussed in Sect. 24.5.1.

Another class of modified teleparallel gravity theories is based on New General Relativity [113]. Using the Eddington-Robertson-Schiff formalism, it has been found that their PPN parameters β and γ are of the form $\beta = 1 - \epsilon/2$ and $\gamma = 1 - 2\epsilon$, with a theory-dependent constant parameter ϵ . This result has later been generalised to a larger class of theories [114], which is based on a covariant formulation of teleparallel gravity [115, 116], and using a tetrad-based framework to derive the full set of PPN parameters [53]. The result has shown that also in this larger class of theories the

PPN parameters β and γ are of the same form as in New General Relativity, while all other PPN parameters vanish. An interesting consequence of this result is the fact that the Nordtvedt parameter (24.9) vanishes identically, even for those theories whose individual PPN parameters differ from that of General Relativity. This means that such theories lead to different predictions, e.g., for the deflection of light or the precession of the Mercury orbit, but are indistinguishable by lunar laser ranging experiments.

In analogy to scalar-tensor theories of gravity (which could also more precisely be called scalar-curvature theories), as described in Sect. 24.5.1, also a large class of scalar extensions to teleparallel gravity has also been studied, which are summarised under the term scalar-torsion gravity [117–120]. In the most simple cases, in which the scalar field is minimally coupled to torsion, the PPN parameters are identical to those of General Relativity [121, 122]. However, this degeneracy is broken if a coupling between the scalar field and the teleparallel boundary term is considered [123]. Equivalently, one could study a kinetic coupling of the scalar field to the vector part of the torsion, and also in this case an effect on the PPN parameters β and γ is found for both massive and massless scalar fields [124, 125].

References

1. A.S. Eddington, *The Mathematical Theory of Relativity* (Cambridge University Press, Cambridge, 1922)
2. H.P. Robertson, Relativity and cosmology, in *Space Age Astronomy*, ed. by A.J. Deutsch, W.B. Klemperer (1962), p. 228
3. L.I. Schiff, Comparison of theory and observation in general relativity, in *Relativity Theory and Astrophysics. Vol. 1: Relativity and Cosmology*, ed. by J. Ehlers (1967), p. 105
4. R. Baierlein, Testing general relativity with laser ranging to the moon. *Phys. Rev.* **162**, 1275–1288 (1967)
5. K. Nordtvedt, Equivalence principle for massive bodies. 1. Phenomenology. *Phys. Rev.* **169**, 1014–1016 (1968)
6. K. Nordtvedt, Equivalence principle for massive bodies. 2. Theory. *Phys. Rev.* **169**, 1017–1025 (1968)
7. K.S. Thorne, C.M. Will, Theoretical frameworks for testing relativistic gravity. I. Foundations. *Astrophys. J.* **163**, 595–610 (1971)
8. C.M. Will, Theoretical frameworks for testing relativistic gravity. 2. Parametrized post-newtonian hydrodynamics, and the Nordtvedt effect. *Astrophys. J.* **163**, 611–627 (1971)
9. C.M. Will, Theoretical frameworks for testing relativistic gravity. 3. Conservation laws, Lorentz invariance and values of the PPN parameters. *Astrophys. J.* **169**, 125–140 (1971)
10. C.M. Will, K. Nordtvedt Jr., Conservation laws and preferred frames in relativistic gravity. I. Preferred-frame theories and an extended PPN formalism. *Astrophys. J.* **177**, 757 (1972)
11. K.J. Nordtvedt, C.M. Will, Conservation laws and preferred frames in relativistic gravity. II. Experimental evidence to rule out preferred-frame theories of gravity. *Astrophys. J.* **177**, 775–792 (1972)
12. C.M. Will, Relativistic gravity in the solar system. III. Experimental disproof of a class of linear theories of gravitation. *Astrophys. J.* **185**, 31–42 (1973)
13. C.M. Will, *Theory and Experiment in Gravitational Physics* (1993)
14. B. Bertotti, L. Iess, P. Tortora, A test of general relativity using radio links with the Cassini spacecraft. *Nature* **425**, 374–376 (2003)

15. E. Fomalont, S. Kopeikin, G. Lanyi, J. Benson, Progress in measurements of the gravitational bending of radio waves using the VLBA. *Astrophys. J.* **699**, 1395–1402 (2009). [arXiv:0904.3992](#)
16. A. Verma, A. Fienga, J. Laskar, H. Manche, M. Gastineau, Use of MESSENGER radioscience data to improve planetary ephemeris and to test general relativity. *Astron. Astrophys.* **561**, A115 (2014). [arXiv:1306.5569](#)
17. V. Viswanathan, A. Fienga, M. Gastineau, J. Laskar, *INPOP17a planetary ephemerides, Notes Scientifiques et Techniques de l'Institut de Mecanique Celeste* **108** (2017)
18. V. Viswanathan, A. Fienga, O. Minazzoli, L. Bernus, J. Laskar, M. Gastineau, The new lunar ephemeris INPOP17a and its application to fundamental physics. *Mon. Not. Roy. Astron. Soc.* **476**(2), 1877–1888 (2018). [arXiv:1710.09167](#)
19. L.B. Kreuzer, Experimental measurement of the equivalence of active and passive gravitational mass. *Phys. Rev.* **169**, 1007–1012 (1968)
20. C.M. Will, Active mass in relativistic gravity - theoretical interpretation of the Kreuzer experiment. *Astrophys. J.* **204**, 224–234 (1976)
21. C.M. Will, The confrontation between general relativity and experiment. *Living Rev. Rel.* **17**, 4 (2014). [arXiv:1403.7377](#)
22. C.M. Will, *Theory and Experiment in Gravitational Physics* (Cambridge University Press, Cambridge, 2018)
23. P. Horava, Quantum gravity at a Lifshitz point. *Phys. Rev. D* **79**, 084008 (2009). [arXiv:0901.3775](#)
24. K. Lin, S. Mukohyama, A. Wang, Solar system tests and interpretation of gauge field and Newtonian prepotential in general covariant Hořava-Lifshitz gravity. *Phys. Rev. D* **86**, 104024 (2012). [arXiv:1206.1338](#)
25. K. Lin, A. Wang, Static post-Newtonian limits in nonprojectable Hořava-Lifshitz gravity with an extra U(1) symmetry. *Phys. Rev. D* **87**(8), 084041 (2013). [arXiv:1212.6794](#)
26. K. Lin, S. Mukohyama, A. Wang, T. Zhu, Post-Newtonian approximations in the Hořava-Lifshitz gravity with extra U(1) symmetry. *Phys. Rev. D* **89**(8), 084022 (2014). [arXiv:1310.6666](#)
27. H.W. Zaglauer, *Phenomenological aspects of scalar fields in astrophysics, cosmology and particle physics*. Ph.D. thesis, Washington U., St. Louis (1990)
28. T. Helbig, Gravitational effects of light scalar particles. *Astrophys. J.* **382**, 223–232 (1991)
29. M.S. Gladchenko, V.N. Ponomarev, V.V. Zhytnikov, PPN metric and PPN torsion in the quadratic Poincare gauge theory of gravity. *Phys. Lett. B* **241**, 67–69 (1990)
30. S. Alexander, N. Yunes, A New PPN parameter to test Chern-Simons gravity. *Phys. Rev. Lett.* **99**, 241101 (2007). [arxiv:hep-th/0703265](#)
31. S. Alexander, N. Yunes, Parametrized post-Newtonian expansion of Chern-Simons gravity. *Phys. Rev. D* **75**, 124022 (2007). [arXiv:0704.0299](#)
32. S. Alexander, N. Yunes, Chern-Simons modified general relativity. *Phys. Rept.* **480**, 1–55 (2009)
33. A. Vainshtein, To the problem of nonvanishing gravitation mass. *Phys. Lett. B* **39**, 393–394 (1972)
34. E. Babichev, C. Deffayet, An introduction to the Vainshtein mechanism. *Class. Quant. Grav.* **30**, 184001 (2013). [arXiv:1304.7240](#)
35. A. Avilez-Lopez, A. Padilla, P.M. Saffin, C. Skordis, The parametrized post-Newtonian-Vainshteinian formalism. *JCAP* **1506**(06), 044 (2015). [arXiv:1501.01985](#)
36. J. Khoury, A. Weltman, Chameleon fields: awaiting surprises for tests of gravity in space. *Phys. Rev. Lett.* **93**, 171104 (2004). [arxiv:astro-ph/0309300](#)
37. A. Hees, A. Fuzfa, Combined cosmological and solar system constraints on chameleon mechanism. *Phys. Rev. D* **85**, 103005 (2012). [arXiv:1111.4784](#)
38. A. Schäfer, R. Angéilil, R. Bondarescu, P. Jetzer, A. Lundgren, Testing scalar-tensor theories and parametrized post-Newtonian parameters in Earth orbit. *Phys. Rev. D* **90**(12), 123005 (2014). [arXiv:1410.7914](#)

39. C. Burrage, J. Sakstein, A compendium of chameleon constraints. *JCAP* **1611**(11), 045 (2016). [arXiv:1609.01192](#)
40. C. Burrage, J. Sakstein, Tests of chameleon gravity. *Living Rev. Rel.* **21**(1), 1 (2018). [arXiv:1709.09071](#)
41. R. McManus, L. Lombriser, J. Peñarrubia, Parameterised post-Newtonian expansion in screened regions. *JCAP* **1712**(12), 031 (2017). [arXiv:1705.05324](#)
42. V.A.A. Sanghai, T. Clifton, Parameterized post-Newtonian cosmology. *Class. Quant. Grav.* **34**(6), 065003 (2017). [arXiv:1610.08039](#)
43. N. Rosen, A theory of gravitation. *Ann. Phys.* **84**, 455–473 (1974)
44. D.L. Lee, C.M. Caves, W.-T. Ni, C.M. Will, Theoretical frameworks for testing relativistic gravity. 5. Post Newtonian limit of Rosen’s theory. *Astrophys. J.* **206**, 555–558 (1976)
45. K. Hinterbichler, Theoretical aspects of massive gravity. *Rev. Mod. Phys.* **84**, 671–710 (2012). [arXiv:1105.3735](#)
46. C. de Rham, Massive gravity. *Living Rev. Rel.* **17**, 7 (2014). [arXiv:1401.4173](#)
47. T. Clifton, M. Banados, C. Skordis, The parameterised post-Newtonian limit of bimetric theories of gravity. *Class. Quant. Grav.* **27**, 235020 (2010). [arXiv:1006.5619](#)
48. M. Hohmann, M.N.R. Wohlfarth, Multimetric extension of the PPN formalism: experimental consistency of repulsive gravity. *Phys. Rev. D* **82**, 084028 (2010). [arXiv:1007.4945](#)
49. M. Hohmann, Parameterized post-Newtonian formalism for multimetric gravity. *Class. Quant. Grav.* **31**, 135003 (2014). [arXiv:1309.7787](#)
50. L.L. Smalley, Postnewtonian approximation of the Poincare gauge theory of gravitation. *Phys. Rev. D* **21**, 328–331 (1980)
51. J. Nitsch, F.W. Hehl, Translational Gauge theory of gravity: post Newtonian approximation and spin precession. *Phys. Lett.* **90B**, 98–102 (1980)
52. J. Hayward, Scalar tetrad theories of gravity. *Gen. Rel. Grav.* **13**, 43–55 (1981)
53. U. Ualikhanova, M. Hohmann, *Parameterized post-Newtonian limit of general teleparallel gravity theories*. [arXiv:1907.08178](#)
54. J.M. Bardeen, Gauge invariant cosmological perturbations. *Phys. Rev. D* **22**, 1882–1905 (1980)
55. H. Kodama, M. Sasaki, Cosmological perturbation theory. *Prog. Theor. Phys. Suppl.* **78**, 1–166 (1984)
56. V.F. Mukhanov, H.A. Feldman, R.H. Brandenberger, Theory of cosmological perturbations. Part 1. Classical perturbations. Part 2. Quantum theory of perturbations. Part 3. Extensions. *Phys. Rept.* **215**, 203–333 (1992)
57. K.A. Malik, D. Wands, Cosmological perturbations. *Phys. Rept.* **475**, 1–51 (2009). [arXiv:0809.4944](#)
58. K. Nakamura, Second-order gauge invariant cosmological perturbation theory: Einstein equations in terms of gauge invariant variables. *Prog. Theor. Phys.* **117**, 17–74 (2007). [arxiv:gr-qc/0605108](#)
59. K. Nakamura, Gauge-invariant formulation of the second-order cosmological perturbations. *Phys. Rev. D* **74**, 101301 (2006). [arxiv:gr-qc/0605107](#)
60. M. Hohmann, Gauge-invariant approach to the parametrized post-Newtonian formalism. *Phys. Rev. D* **101**(2), 024061 (2020). [arXiv:1910.09245](#)
61. E.E. Flanagan, The Conformal frame freedom in theories of gravitation. *Class. Quant. Grav.* **21**, 3817 (2004). [arxiv:gr-qc/0403063](#)
62. K. Nordvedt Jr., Post-Newtonian metric for a general class of scalar tensor gravitational theories and observational consequences. *Astrophys. J.* **161**, 1059–1067 (1970)
63. O. Minazzoli, B. Chauvineau, Scalar-tensor propagation of light in the inner solar system at the millimetric level. *Class. Quant. Grav.* **28**, 085010 (2011). [arXiv:1007.3942](#)
64. X.-M. Deng, Y. Xie, Two-post-Newtonian light propagation in the scalar-tensor theory: an N -point-masses case. *Phys. Rev. D* **86**, 044007 (2012). [arXiv:1207.3138](#)
65. G.J. Olmo, The Gravity Lagrangian according to solar system experiments. *Phys. Rev. Lett.* **95**, 261102 (2005). [arxiv:gr-qc/0505101](#)

66. G.J. Olmo, Post-Newtonian constraints on $f(R)$ cosmologies in metric and Palatini formalism. *Phys. Rev. D* **72**, 083505 (2005). [arxiv:gr-qc/0505135](#)
67. L. Perivolaropoulos, PPN parameter γ and solar system constraints of massive Brans-Dicke theories. *Phys. Rev. D* **81**, 047501 (2010). [arXiv:0911.3401](#)
68. Y. Xie, W.-T. Ni, P. Dong, T.-Y. Huang, Second post-Newtonian approximation of scalar-tensor theory of gravity. *Adv. Space Res.* **43**, 171–180 (2009). [arXiv:0704.2991](#)
69. M. Hohmann, L. Jarv, P. Kuusk, E. Randla, Post-Newtonian parameters γ and β of scalar-tensor gravity with a general potential. *Phys. Rev. D* **88**(8), 084054 (2013). [arXiv:1309.0031](#). Erratum: *Phys. Rev. D* **89**(6), 069901 (2014)
70. L. Järvi, P. Kuusk, M. Saal, O. Vilson, Invariant quantities in the scalar-tensor theories of gravitation. *Phys. Rev. D* **91**(2), 024041 (2015). [arXiv:1411.1947](#)
71. M. Hohmann, A. Schäfer, Post-Newtonian parameters γ and β of scalar-tensor gravity for a homogeneous gravitating sphere. *Phys. Rev. D* **96**(10), 104026 (2017). [arXiv:1708.07851](#)
72. J.W. Moffat, V.T. Toth, Modified Jordan-Brans-Dicke theory with scalar current and the Eddington-Robertson γ -parameter. *Int. J. Mod. Phys. D* **21**, 1250084 (2012). [arXiv:1001.1564](#)
73. K. Saaidi, A. Mohammadi, H. Sheikahmadi, γ parameter and solar system constraint in Chameleon Brans Dick theory. *Phys. Rev. D* **83**, 104019 (2011). [arXiv:1201.0271](#)
74. O. Minazzoli, γ parameter and solar system constraint in scalar-tensor theory with a power law potential and universal scalar/matter coupling. [arXiv:1208.2372](#)
75. N.C. Devi, S. Panda, A.A. Sen, Solar system constraints on scalar tensor theories with non-standard action. *Phys. Rev. D* **84**, 063521 (2011). [arXiv:1104.0152](#)
76. M. Roshan, F. Shojai, Notes on the post-Newtonian limit of massive Brans-Dicke theory. *Class. Quant. Grav.* **28**, 145012 (2011). [arXiv:1106.1264](#)
77. O. Minazzoli, A. Hees, Intrinsic solar system decoupling of a scalar-tensor theory with a universal coupling between the scalar field and the matter Lagrangian. *Phys. Rev. D* **88**(4), 041504 (2013). [arXiv:1308.2770](#)
78. S. Capozziello, A. Troisi, PPN-limit of fourth order gravity inspired by scalar-tensor gravity. *Phys. Rev. D* **72**, 044022 (2005). [arxiv:astro-ph/0507545](#)
79. S. Capozziello, A. Stabile, A. Troisi, Fourth-order gravity and experimental constraints on Eddington parameters. *Mod. Phys. Lett. A* **21**, 2291–2301 (2006). [arxiv:gr-qc/0603071](#)
80. S. Capozziello, A. Stabile, A. Troisi, The Newtonian limit of $f(R)$ gravity. *Phys. Rev. D* **76**, 104019 (2007). [arXiv:0708.0723](#)
81. S. Capozziello, A. Stabile, A. Troisi, Comparing scalar-tensor gravity and $f(R)$ -gravity in the Newtonian limit. *Phys. Lett. B* **686**, 79–83 (2010). [arXiv:1002.1364](#)
82. T. Clifton, The parameterised post-Newtonian limit of fourth-order theories of gravity. *Phys. Rev. D* **77**, 024041 (2008). [arXiv:0801.0983](#)
83. M. Capone, M.L. Ruggiero, Jumping from metric $f(R)$ to scalar-tensor theories and the relations between their post-Newtonian Parameters. *Class. Quant. Grav.* **27**, 125006 (2010). [arXiv:0910.0434](#)
84. S. Capozziello, A. Stabile, The weak field limit of fourth order gravity, in *Classical and Quantum Gravity: Theory and Applications* Chapter 2*, ed. by *R. Frignanni, Vincent (2010). [arXiv:1009.3441](#)
85. T. Harko, T.S. Koivisto, F.S.N. Lobo, G.J. Olmo, Metric-Palatini gravity unifying local constraints and late-time cosmic acceleration. *Phys. Rev. D* **85**, 084016 (2012). [arXiv:1110.1049](#)
86. X.-M. Deng, Y. Xie, Solar System tests of a scalar-tensor gravity with a general potential: insensitivity of light deflection and Cassini tracking. *Phys. Rev. D* **93**(4), 044013 (2016)
87. X. Zhang, W. Zhao, H. Huang, Y. Cai, Post-Newtonian parameters and cosmological constant of screened modified gravity. *Phys. Rev. D* **93**(12), 124003 (2016). [arXiv:1603.09450](#)
88. T. Damour, G. Esposito-Farese, Tensor multiscalar theories of gravitation. *Class. Quant. Grav.* **9**, 2093–2176 (1992)
89. A.L. Berkin, R.W. Hellings, Multiple field scalar - tensor theories of gravity and cosmology. *Phys. Rev. D* **49**, 6442–6449 (1994). [arxiv:gr-qc/9401033](#)
90. E. Randla, PPN parameters for multiscalar-tensor gravity without a potential. *J. Phys. Conf. Ser.* **532**, 012024 (2014)

91. P. Kuusk, L. Jarv, O. Vilson, Invariant quantities in the multiscalar-tensor theories of gravitation. *Int. J. Mod. Phys. A* **31**(02n03), 1641003 (2016). [arXiv:1509.02903](#)
92. M. Hohmann, L. Jarv, P. Kuusk, E. Randla, O. Vilson, Post-Newtonian parameter γ for multiscalar-tensor gravity with a general potential. *Phys. Rev. D* **94**(12), 124015 (2016). [arXiv:1607.02356](#)
93. T.S. Koivisto, The post-Newtonian limit in C-theories of gravitation. *Phys. Rev. D* **84**, 121502 (2011). [arXiv:1109.4585](#)
94. T.S. Koivisto, Newtonian limit of nonlocal cosmology. *Phys. Rev. D* **78**, 123505 (2008). [arXiv:0807.3778](#)
95. A. Conroy, T. Koivisto, A. Mazumdar, A. Teimouri, Generalized quadratic curvature, non-local infrared modifications of gravity and Newtonian potentials. *Class. Quant. Grav.* **32**(1), 015024 (2015). [arXiv:1406.4998](#)
96. G.W. Horndeski, Second-order scalar-tensor field equations in a four-dimensional space. *Int. J. Theor. Phys.* **10**, 363–384 (1974)
97. C. Deffayet, X. Gao, D. Steer, G. Zahariade, From k-essence to generalised Galileons. *Phys. Rev. D* **84**, 064039 (2011). [arXiv:1103.3260](#)
98. T. Kobayashi, M. Yamaguchi, J. Yokoyama, Generalized G-inflation: inflation with the most general second-order field equations. *Prog. Theor. Phys.* **126**, 511–529 (2011). [arXiv:1105.5723](#)
99. M. Hohmann, Parametrized post-Newtonian limit of Horndeski's gravity theory. *Phys. Rev. D* **92**(6), 064019 (2015). [arXiv:1506.04253](#)
100. S. Hou, Y. Gong, Constraints on Horndeski theory using the observations of Nordtvedt effect, Shapiro time delay and binary pulsars. *Eur. Phys. J. C* **78**(3), 247 (2018). [arXiv:1711.05034](#)
101. R. Kase, S. Tsujikawa, Screening the fifth force in the Horndeski's most general scalar-tensor theories. *JCAP* **1308**, 054 (2013). [arXiv:1306.6401](#)
102. C. de Rham, G. Gabadadze, A.J. Tolley, Resummation of massive gravity. *Phys. Rev. Lett.* **106**, 231101 (2011). [arXiv:1011.1232](#)
103. S. Hassan, R.A. Rosen, Bimetric gravity from ghost-free massive gravity. *JHEP* **1202**, 126 (2012). [arXiv:1109.3515](#)
104. K. Hinterbichler, R.A. Rosen, Interacting spin-2 fields. *JHEP* **1207**, 047 (2012). [arXiv:1203.5783](#)
105. A. Schmidt-May, M. von Strauss, Recent developments in bimetric theory. *J. Phys. A* **49**(18), 183001 (2016). [arXiv:1512.00021](#)
106. M. Hohmann, Post-Newtonian parameter γ and the deflection of light in ghost-free massive bimetric gravity. *Phys. Rev. D* **95**(12), 124049 (2017). [arXiv:1701.07700](#)
107. A. Einstein, Riemann-Geometrie mit Aufrechterhaltung des Begriffes des Fernparallelismus. *Sitzber Preuss Akad Wiss* **17**, 217–221 (1928)
108. R. Aldrovandi, J.G. Pereira, *Teleparallel Gravity*, vol. 173 (Springer, Dordrecht, 2013)
109. J.W. Maluf, The teleparallel equivalent of general relativity. *Ann. Phys.* **525**, 339–357 (2013). [arXiv:1303.3897](#)
110. J.B. Jiménez, L. Heisenberg, T.S. Koivisto, The geometrical trinity of gravity. *Universe* **5**(7), 173 (2019). [arXiv:1903.06830](#)
111. G.R. Bengochea, R. Ferraro, Dark torsion as the cosmic speed-up. *Phys. Rev. D* **79**, 124019 (2009). [arXiv:0812.1205](#)
112. E.V. Linder, Einstein's other gravity and the acceleration of the universe. *Phys. Rev. D* **81**, 127301 (2010). [arXiv:1005.3039](#). Erratum: *Phys. Rev. D* **82**, 109902 (2010)
113. K. Hayashi, T. Shirafuji, New general relativity. *Phys. Rev. D* **19**, 3524–3553 (1979). (409 (1979))
114. S. Bahamonde, C.G. Böhrer, M. Krššák, New classes of modified teleparallel gravity models. *Phys. Lett. B* **775**, 37–43 (2017). [arXiv:1706.04920](#)
115. M. Krššák, E.N. Saridakis, The covariant formulation of f(T) gravity. *Class. Quant. Grav.* **33**(11), 115009 (2016). [arXiv:1510.08432](#)
116. M. Krssak, R.J. van den Hoogen, J.G. Pereira, C.G. Böhrer, A.A. Coley, Teleparallel theories of gravity: illuminating a fully invariant approach. *Class. Quant. Grav.* **36**(18), 183001 (2019). [arXiv:1810.12932](#)

117. M. Hohmann, L. Järv, U. Ualikhanova, Covariant formulation of scalar-torsion gravity. *Phys. Rev. D* **97**(10), 104011 (2018). [arXiv:1801.05786](#)
118. M. Hohmann, Scalar-torsion theories of gravity I: general formalism and conformal transformations. *Phys. Rev. D* **98**(6), 064002 (2018). [arXiv:1801.06528](#)
119. M. Hohmann, C. Pfeifer, Scalar-torsion theories of gravity II: $L(T, X, Y, \phi)$ theory. *Phys. Rev. D* **98**(6), 064003 (2018). [arXiv:1801.06536](#)
120. M. Hohmann, Scalar-torsion theories of gravity III: analogue of scalar-tensor gravity and conformal invariants. *Phys. Rev. D* **98**(6), 064004 (2018). [arXiv:1801.06531](#)
121. J.-T. Li, Y.-P. Wu, C.-Q. Geng, Parametrized post-Newtonian limit of the teleparallel dark energy model. *Phys. Rev. D* **89**(4), 044040 (2014). [arXiv:1312.4332](#)
122. Z.-C. Chen, Y. Wu, H. Wei, Post-Newtonian approximation of teleparallel gravity coupled with a scalar field. *Nucl. Phys. B* **894**, 422–438 (2015). [arXiv:1410.7715](#)
123. H. Mohseni Sadj, Parameterized post-Newtonian approximation in a teleparallel model of dark energy with a boundary term. *Eur. Phys. J. C* **77**(3), 191 (2017). [arXiv:1606.04362](#)
124. E.D. Emtsova, M. Hohmann, Post-Newtonian limit of scalar-torsion theories of gravity as analogue to scalar-curvature theories. *Phys. Rev. D* **101**(2), 024017 (2020). [arXiv:1909.09355](#)
125. K. Flathmann, M. Hohmann, Post-Newtonian limit of generalized scalar-torsion theories of gravity. *Phys. Rev. D* **101**(2), 024005 (2020). [arXiv:1910.01023](#)

Chapter 25

Gravitational Waves



Mairi Sakellariadou

The direct detection of gravitational-waves from the LIGO and Virgo collaborations [1–3] opened a new window into the Universe, offering a novel and powerful way to test not only astrophysical models about compact objects [4], but also cosmological models [5–7], particle physics beyond the Standard Model [7–12], General Relativity [13–16], modified gravity [17, 18], and even quantum gravity proposals [15, 19, 20].

25.1 Tests of General Relativity

Einstein's theory of General Relativity (GR) allows for the existence of only two gravitational-wave polarisations (the tensor plus and cross modes), and predicts a massless graviton propagating at the speed of light. On the contrary, any general metric theory of gravity may allow for up to four additional polarisations: two vector modes (helicity ± 1), and two scalar (helicity 0)—the breathing and longitudinal—modes. The detection of any such additional polarisation modes would imply violation of General Relativity, while a non-detection may constrain any extended theory of gravity.

Interferometers with different orientations will respond differently to GW signals emitted from a given sky location as a function of their polarisation. When allowing for all six polarisation modes, a network of at least five detectors is required in order to uniquely determine the polarisation of transient gravitational-wave signals, like the ones detected from compact binary coalescences (CBC). This is because our

M. Sakellariadou (✉)

Theoretical Particle Physics and Cosmology Group, Department of Physics, King's College London, University of London, Strand, London WC2R 2LS, UK
e-mail: mairi.sakellariadou@kcl.ac.uk

detectors are only sensitive to the traceless scalar mode, and hence we expect to be able to distinguish only five polarisations.

In addition to the gravitational-waves from CBC, one expects an astrophysical gravitational-wave background (GWB) formed by the superposition of many weak or distant, independent and unresolved sources. The isotropic GWB can be described in terms of the energy density per logarithmic frequency interval f as

$$\Omega_{\text{GW}} = \frac{f}{\rho_c} \frac{d\rho_{\text{GW}}}{df}, \quad (25.1)$$

where $d\rho_{\text{GW}}$ stands for the energy density in GW in the frequency interval between f and $f + df$, and ρ_c denotes the critical energy density. The GWB from compact binaries is well approximated by the power law

$$\Omega_{\text{GW}} = \Omega_{\text{ref}} \left(\frac{f}{f_{\text{ref}}} \right)^{2/3}, \quad (25.2)$$

where Ω_{ref} denotes the background's amplitude at a reference frequency f_{ref} , usually chosen to be equal 25 Hz.

Considering a GWB of astrophysical origin, in [14] a Bayesian approach allowing for full parameter estimation on the GWB, assuming a power-law model for the GW energy density in each polarisation mode, was proposed. This method can be applied not only within the context of simple cases of purely tensor, vector or scalar-polarised backgrounds, but also in the situations appearing in alternative theories of gravity that predict a mixed background of multiple polarisation modes.

Utilising this Bayesian method, it was demonstrated [14] that one may detect and identify, with the existing detectors, an GWB containing any combination of GW polarisation modes. In particular, it was shown that after three years of observation at design sensitivity, Advanced LIGO will be able to impose upper bounds to the amplitudes of tensor, vector, and scalar polarisation to respectively, $\Omega_{\text{ref}}^{\text{T}} < 1.6 \times 10^{-10}$, $\Omega_{\text{ref}}^{\text{V}} < 2.0 \times 10^{-10}$ and $\Omega_{\text{ref}}^{\text{S}} < 5.0 \times 10^{-10}$, at 95% credibility [14].

Let us use the currently available compact binary signals observed by Advanced LIGO and Advanced Virgo during the first two observing runs of the advanced detector era (O1 and O2), assuming either a log uniform or a uniform prior on the reference GW amplitude Ω_{ref} for each polarisation mode, and considering the presence of tensor, vector and scalar backgrounds. Applying the Bayesian method of [14] and marginalising over the spectral indices and the amplitudes for the three different polarisation modes, we obtain [21] the following upper limits on tensor, vector and scalar polarisations, respectively:

$$\Omega_{\text{ref}}^{\text{T}} < 8.2 \times 10^{-8}, \quad \Omega_{\text{ref}}^{\text{V}} < 1.2 \times 10^{-7}, \quad \Omega_{\text{ref}}^{\text{S}} < 4.2 \times 10^{-7},$$

for uniform prior, and

$$\Omega_{\text{ref}}^{\text{T}} < 3.2 \times 10^{-8}, \quad \Omega_{\text{ref}}^{\text{V}} < 2.9 \times 10^{-8}, \quad \Omega_{\text{ref}}^{\text{S}} < 6.1 \times 10^{-8},$$

for log-uniform.

For compact binary coalescences we can also investigate deviations from GR by introducing separate modifications to the emitted gravitational-wave waveform and its propagation. The former corresponds to GR modifications in the strong-field region close to the compact binary, and the latter to the weak-field region away from the emitting source. For instance, deviations from GR may introduce modifications of the dynamics of compact binaries, hence leading to modifications of the orbital phase which consequently imply shifts in the GW phase coefficients as a function of the intrinsic parameters of the compact binaries.

Introducing a phenomenological (but well-motivated) parametrised deviation in the waveform model for binary black holes, including the post-Newtonian coefficients, it was shown using data from the catalogue [3], as detected by the Advanced LIGO and Advanced Virgo during the first two runs of these detectors, that these deviations are consistent with their GR value of zero [16].

Introducing a phenomenological modification of the GW dispersion relation

$$E^2 = p^2 c^2 + A_\alpha p^\alpha c^\alpha, \quad (25.3)$$

in terms of the phenomenological parameters A_α , α , where E , p , c are the energy and momentum of GWs and the speed of light, respectively, one can use GWs data in order to test GR, where the additional power-law term in momentum is absent. Considering α values from 0 to 4 in steps of 0.5, and utilising data from the catalogue [3], 90% credible upper bound on the absolute value of the parameter A_α and the mass of the graviton m_g were imposed [16]. In particular, it was found that

$$m_g \leq 5.0 \times 10^{-23} \text{ eV}/c^2,$$

at 90% credible limit.

The first detection of a GW signal from a neutron star merger, the GW170817 event, accompanied by a short-duration gamma-ray burst (SGRB), the GRB 170817A, with an observed time delay of $(+1.74 \pm 0.05)\text{s}$, offered a powerful tool to test General Relativity [22] and constrain alternative theories of gravity.

Coupling the standard electromagnetic theory with General Relativity, gravitational and electromagnetic waves propagate at the same speed. Consequently, the temporal offset of $(+1.74 \pm 0.05)\text{s}$ can be used to constrain theories that predict a deviation of the speed of gravity from the speed of light, or on theories leading to Lorentz violation. Also, it can be used to test the equivalence principle [22].

Assuming that the SGRB signal was emitted 10s after the GW signal, and knowing the travel distance the temporal offset can be used to set a conservative bound on the fractional speed difference $\Delta v/v_{\text{EM}}$, where $\Delta v = v_{\text{GW}} - v_{\text{EM}}$, with v_{GW} the speed of gravitational and v_{EM} the speed of electromagnetic waves. This conservative constraint on the fractional speed difference is [22]

$$-3 \times 10^{-15} \leq \frac{\Delta v}{v_{\text{EM}}} \leq 7 \times 10^{-16}. \quad (25.4)$$

Lorentz symmetry is a cornerstone of both the standard model (SM) of particle physics and Einstein's theory of General Relativity. However, particle physics beyond the SM or modified gravity may lead to Lorentz symmetry violation. Consequently, an observation of Lorentz violation would be an indicator of new physics.

Let us consider the gravitational Standard-Model Extension (SME) [23], an effective field-theory based framework for studying Lorentz symmetry. The Lagrange density of the SME contains the SM and GR, along with all possible Lorentz-violating terms constructed by coupling observer vector or tensor coefficients for Lorentz violation to SM operators. Each Lorentz-violating term is the coordinate-independent product of a coefficient for Lorentz violation with a Lorentz-violating operator. Hence, the Lorentz-violating process associated with any operator is dictated by the corresponding coefficient, implying that any experimental signal for Lorentz violation can be expressed in terms of one or more of these coefficients. The full SME includes an infinite number of SM operators of increasing mass dimension. A limiting case is the minimal SME, a restriction of the SME to include only Lorentz-violating operators of mass dimensions of four or less.

The difference Δv in group velocities between EM and GWs, in the minimal SME case, reads

$$\Delta v = - \sum_{\ell m, \ell \leq 2} Y_{\ell m}(\hat{n}) \left[\frac{1}{2} (-1)^{1+\ell} \bar{s}_{\ell m}^{(4)} - c_{(I)\ell m}^{(4)} \right], \quad (25.5)$$

where $Y_{\ell m}$ are spherical harmonics, \hat{n} denotes the sky position and $\bar{s}_{\ell m}^{(4)}$, $c_{(I)\ell m}^{(4)}$ are spherical-basis coefficients for Lorentz violation in the gravitational and electromagnetic sectors, respectively.

Using the GW170817 binary neutron star merger, accompanied by gamma-ray burst (GRB), namely the GRB 170817A event, constraints have been imposed [22] on the gravity sector coefficients $\bar{s}_{\ell m}^{(4)}$, by considering such coefficients one at a time, while setting all other coefficients, including those from the electromagnetic sector, equal to zero. It is worth noting that the isotropic ($\ell = 0$) upper bound on $\bar{s}_{00}^{(4)}$ was improved by more than 10 orders of magnitude, with the current upper bound reaching 5×10^{-15} .

An attempt can also be made to use GWs followed by EM radiation in order to test the equivalence principle through the Shapiro effect. The Shapiro effect predicts the difference between the propagation time of massless particles in curved spacetime, with respect to that in a flat background; the former being slightly higher. However, as has been recently pointed out [24], the Shapiro delay is not an observable in General Relativity, and is computed by comparing it with a fiducial Euclidean distance. Moreover, the Shapiro delay calculated in the usual way, namely by taking

the Newtonian potential to vanish at infinity, diverges as one incorporates many far-away sources. Thus, a conservative lower bound to the Shapiro delay cannot be obtained by just considering a subset of the sources of the gravitational field.

25.2 Modified Gravity

The Universe is at present in a phase of accelerated expansion, and several theoretical, and often phenomenological, proposals have been made in order to account for such a late-time evolution.

Considering the propagation of tensor perturbations in an FLRW universe, in the context of GR, we have

$$h''_A + 2\mathcal{H}[1 - \delta(\eta)]h'_A + k^2 h_A = \Pi_A, \quad (25.6)$$

where A denotes the two (plus and cross) polarisations and prime stands for conformal time; Π_A is the source term related to the anisotropic stress tensor.

In a modified gravity model the above equation becomes

$$h''_A + 2[1 - \delta(\eta)]\mathcal{H}h'_A + [c_T^2(\eta)k^2 + m_T^2(\eta)]h_A = \Pi_A, \quad (25.7)$$

where $\delta(\eta)$, c_T , m_T are functions that can in principle be constrained from GW data.

The function $\delta(\eta)$ modifies the friction term in the propagation equation and can therefore affect the amplitude of GWs propagating across cosmological distances, introducing the so-called *GW luminosity distance*, which can be probed by LISA standard sirens.

Following a phenomenological approach, let us write [25]

$$\Xi(z) \equiv \frac{d_L^{\text{GW}}(z)}{d_L^{\text{EM}}(z)} = \Xi_0 + \frac{1 - \Xi_0}{(1+z)^n}, \quad (25.8)$$

where Ξ_0 , n denote the two parameters of the phenomenological model.

The value $\Xi_0 = 1$ corresponds to GR, while for large redshifts $\Xi(z \gg 1) = \Xi_0$, constant. This simple expression smoothly interpolates between these asymptotic values with a power-law determined by the index n . Following this two-parameter parametrisation approach, we can first construct simulated catalogues of LISA massive black hole binaries with electromagnetic counterparts, and consequently use them in order to constrain modified gravity models [18].

The important ingredients in order to build these mock catalogues are the initial mass function of the massive black hole seeds, and the delays between galaxy and massive black hole mergers. In Ref. [18] two distinct seeding models were used: a light seed scenario in which the massive black holes evolve from the remnants of population III stars (with remnant masses $\sim 10^2 M_{\text{Sun}}$) at high redshifts $z \geq 15$; and

a heavy seed scenario in which the black hole seeds form from bar instabilities of protogalactic disks, with seed masses $\sim 10^5 M_{\text{Sun}}$, again at $z \geq 15$.

Regarding delay times, the model used in Ref. [18] followed the evolution of dark matter halos driven by dynamical friction, from the moment when they first touch to the final halo/galaxy merger, including any environmental effects.

Investigating LISA forecasts, it was consequently shown that LISA will be able to measure the parameter Ξ_0 to an accuracy that reaches 1.1%, and in the worst scenario will still be 4.4% [18]. Since the parameters Ξ_0, n are related to parameters of different modified gravity models, by using data from LISA we will be able to constrain modified gravity models at a high level of accuracy.

25.3 Quantum Gravity

Quantum Gravity (QG) can affect the generation of gravitational waves and modify their propagation. In what follows, we will briefly describe modifications of the propagation of GWs in different QG theories.

Within the context of brane theories with extra dimensions, we may wonder whether there is damping of the waveform due to gravitational leaking into the extra dimensions. In such theories there is a high dimensional bulk within which there are embedded branes of any dimensionality (not only three) allowed from the particular string theory under consideration. Damping of the waveform may be expected, since gravitons can escape into the bulk, whereas matter fields are trapped on the branes. Therefore, sources of gravitational waves with electromagnetic counterparts may provide a test of spacetime dimensionality.

In the context of GR the luminosity distance d_L is related to the amplitude of gravitational waves through

$$h_{\text{GR}} \propto d_L^{-1}, \quad (25.9)$$

where the electromagnetic luminosity distance reads

$$d_L^{\text{EM}} \simeq \frac{z(1+z)}{H_0} \simeq \frac{z}{H_0} \text{ for } z \ll 1. \quad (25.10)$$

Any deviation from the above GR estimation depends on the number of spacetime dimensions D ; in particular, we may expect a systematic overestimation of the electromagnetic luminosity distance inferred from GW data.

Assuming that light and matter propagate in a four-dimensional spacetime, we have

$$h \propto \frac{1}{d_L^{\text{GR}}} = \frac{1}{d_L^{\text{EM}}} \left[1 + \left(\frac{d_L^{\text{EM}}}{R_c} \right)^n \right]^{-(D-4)/(2n)}, \quad (25.11)$$

where R_c and n stand respectively for the distance scale of the screening and the transition steepness, and have different values for different string theory models.

In the above equation d_L^{GR} is obtained from the strain measured in a GW interferometer, whereas d_L^{EM} is the luminosity distance measured for the optical counterpart of the standard siren. Performing a Bayesian analysis from the joint posterior probability for D , d_L^{GW} , d_L^{EM} , given the two statistically independent measurements of electromagnetic and gravitational-wave data from GW170817, constraints were imposed on the number of spacetime dimensions [15]. The results of the analysis have shown consistency with the GR prediction of $D = 4$.

We may then wonder whether sources of gravitational waves with an electromagnetic counterpart could also be used to constrain non-perturbative approaches to quantum gravity. Most quantum gravity theories exhibit a long-range non-perturbative mechanism, known as dimensional flow, with important consequences for the propagation of GWs over cosmological distances. Quantisation of spacetime geometry leads to an anomalous spacetime measure $\delta\rho(x)$ and a kinetic operator $\mathcal{K}(\vartheta)$; the former represents how volumes scale and the latter encodes modified dispersion relations.

Consider a spin-2 perturbation $h_{\mu\nu}$, described by two polarisations, over a background metric $g_{\mu\nu}^{(0)} = g_{\mu\nu} - h_{\mu\nu}$. The perturbed action reads [19, 20]

$$S = \frac{1}{2\ell_*^{2\Gamma}} \int d\varrho \sqrt{-g^{(0)}} [h_{\mu\nu} \mathcal{K} h^{\mu\nu} + \mathcal{O}(h_{\mu\nu}^2) + \mathcal{J}^{\mu\nu} h_{\mu\nu}], \quad (25.12)$$

where \mathcal{J} denotes a source and ℓ_* , Γ define respectively a characteristic scale of geometry and a scaling parameter. Note that there are two limits of Γ ; the Γ_{UV} corresponding for QG corrections, which are important, and the Γ_{meso} corresponding to contributions to GR, which are small but cannot be neglected.

Specifying a spacetime measure ρ , a kinetic operator \mathcal{K} , and a source \mathcal{J} , the strain of the emitted gravitational waves is determined by the convolution $h \propto \int d\rho \mathcal{J} G$ of the source with the retarded Green's function.

In radial coordinates and in the local wave zone, the amplitude of GWs becomes the product of a dimensionless function f_h that depends on the source, and a power-law distance behaviour [19, 20]

$$h(t, r) \sim f_h(t, r) (\ell_*/r)^\Gamma, \quad [f_h] = 0. \quad (25.13)$$

For GWs propagating over cosmological distances, the relation between the luminosity distance, as measured in a GW interferometer through the strain and the luminosity distance measured for the counterpart of the standard siren, is [19, 20]

$$h \propto \frac{1}{d_L^{\text{GW}}}, \quad \frac{d_L^{\text{GW}}}{d_L^{\text{EM}}} = 1 + \epsilon \left(\frac{d_L^{\text{EM}}}{\ell_*} \right)^{\gamma-1}, \quad (25.14)$$

with $\epsilon = \pm(\gamma - 1)$, and $\gamma \neq 0$.

The above equation is exact in the presence of only one fundamental length scale $\ell_\star = \mathcal{O}(l_{\text{Pl}})$ and then $\gamma = \Gamma_{\text{UV}}$, with a specific value for a given quantum gravity theory. Conversely, this equation is valid only near the IR regime if ℓ_\star is a mesoscopic scale, and in this case $\gamma = \Gamma_{\text{meso}} \approx 1$.

Constraints can then be placed on the parameters ℓ_\star and γ in a model-independent way, by constraining the ratio $d_L^{\text{GW}}(z)/d_L^{\text{EM}}(z)$ as a function of the redshift z of the source.

Using the neutron star merger GW170817 and a simulated $z = 2$ supermassive black hole merger within LISA detectability, it was shown [19, 20] that the only quantum gravity theories that can be constrained in this way are those with $\Gamma_{\text{meso}} > 1 > \gamma_{\text{UV}}$, and such theories are only group field theory, spin foams and loop quantum gravity.

The constraint reads [19, 20]

$$0 < \Gamma_{\text{meso}} - 1 < 0.02. \quad (25.15)$$

Complementary constraints can be certainly found, which can be tighter than the one above, using for instance solar system tests, nevertheless such constraints require additional assumptions and therefore are not model-independent.

References

1. LIGO Scientific, Virgo Collaboration, B.P. Abbott et al., Observation of gravitational waves from a binary black hole merger. *Phys. Rev. Lett.* **116**(6), 061102 (2016). [arXiv:1602.03837](#)
2. LIGO Scientific, Virgo Collaboration, B.P. Abbott et al., GW170817: Observation of Gravitational Waves from a Binary Neutron Star Inspiral. *Phys. Rev. Lett.* **119**(16), 161101 (2017). [arXiv:1710.05832](#)
3. LIGO Scientific, Virgo Collaboration, B.P. Abbott et al., *GWTC-1: A Gravitational-Wave Transient Catalog of Compact Binary Mergers Observed by LIGO and Virgo during the First and Second Observing Runs*. [arXiv:1811.12907](#)
4. LIGO Scientific, Virgo Collaboration, B.P. Abbott et al., Astrophysical implications of the Binary Black-Hole Merger GW150914. *Astrophys. J.* **818**(2), L22 (2016). [arXiv:1602.03846](#)
5. R. Caldwell et al., *Astro2020 Science White Paper: Cosmology with a Space-Based Gravitational Wave Observatory*. [arXiv:1903.04657](#)
6. B.S. Sathyaprakash et al., *Cosmology and the Early Universe*. [arXiv:1903.09260](#)
7. P. Auclair et al., *Probing the Gravitational Wave Background from Cosmic Strings with LISA*. [arXiv:1909.00819](#)
8. C. Ringeval, T. Suyama, Stochastic gravitational waves from cosmic string loops in scaling. *JCAP* **1712**(12), 027 (2017). [arXiv:1709.03845](#)
9. LIGO Scientific, Virgo Collaboration, B.P. Abbott et al., Constraints on cosmic strings using data from the first Advanced LIGO observing run. *Phys. Rev. D* **97**(10), 102002 (2018). [arXiv:1712.01168](#)
10. A.C. Jenkins, M. Sakellariadou, Anisotropies in the stochastic gravitational-wave background: formalism and the cosmic string case. *Phys. Rev. D* **98**(6), 063509 (2018). [arXiv:1802.06046](#)
11. V. Brdar, A.J. Helmboldt, J. Kubo, Gravitational Waves from first-order phase transitions: LIGO as a window to Unexplored Seesaw Scales. *JCAP* **1902**, 021 (2019). [arXiv:1810.12306](#)
12. C. Caprini et al., *Detecting Gravitational Waves from Cosmological Phase Transitions with LISA: an Update*. [arXiv:1910.13125](#)

13. LIGO Scientific, Virgo Collaboration, B.P. Abbott et al., Tests of general relativity with GW150914. *Phys. Rev. Lett.* **116**(22), 221101 (2016). [arXiv:1602.03841](#). Erratum: *Phys. Rev. Lett.* 121, no. 12, 129902 (2018)
14. T. Callister, A.S. Biscoveanu, N. Christensen, M. Isi, A. Matas, O. Minazzoli, T. Regimbau, M. Sakellariadou, J. Tasson, E. Thrane, Polarization-based Tests of Gravity with the Stochastic Gravitational-Wave Background. *Phys. Rev. X* **7**(4), 041058 (2017). [arXiv:1704.08373](#)
15. LIGO Scientific, Virgo Collaboration, B.P. Abbott et al., Tests of general relativity with GW170817. *Phys. Rev. Lett.* **123**(1), 011102 (2019). [arXiv:1811.00364](#)
16. LIGO Scientific, Virgo Collaboration, B.P. Abbott et al., Tests of general relativity with the Binary Black Hole Signals from the LIGO-Virgo Catalog GWTC-1. *Phys. Rev. D* **100**(10), 104036 (2019). [arXiv:1903.04467](#)
17. E. Berti et al., *Tests of General Relativity and Fundamental Physics with Space-based Gravitational Wave Detectors*. [arXiv:1903.02781](#)
18. LISA Cosmology Working Group Collaboration, E. Belgacem et al., Testing modified gravity at cosmological distances with LISA standard sirens. *JCAP* **1907**(07), 024 (2019). [arXiv:1906.01593](#)
19. G. Calcagni, S. Kuroyanagi, S. Marsat, M. Sakellariadou, N. Tamanini, G. Tasinato, Gravitational-wave luminosity distance in quantum gravity. *Phys. Lett. B* **798**, 135000 (2019). [arXiv:1904.00384](#)
20. G. Calcagni, S. Kuroyanagi, S. Marsat, M. Sakellariadou, N. Tamanini, G. Tasinato, Quantum gravity and gravitational-wave astronomy. *JCAP* **1910**(10), 012 (2019). [arXiv:1907.02489](#)
21. LIGO Scientific, Virgo Collaboration, B.P. Abbott et al., Search for the isotropic stochastic background using data from Advanced LIGO's second observing run. *Phys. Rev. D* **100**(6), 061101 (2019). [arXiv:1903.02886](#)
22. LIGO Scientific, Virgo, Fermi-GBM, INTEGRAL Collaboration, B.P. Abbott et al., Gravitational Waves and Gamma-rays from a Binary Neutron Star Merger: GW170817 and GRB 170817A. *Astrophys. J.* **848**(2), L13 (2017). [arXiv:1710.05834](#)
23. D. Colladay, V.A. Kostelecky, Lorentz violating extension of the standard model. *Phys. Rev. D* **58**, 116002 (1998). [arxiv:hep-ph/9809521](#)
24. O. Minazzoli, N.K. Johnson-McDaniel, M. Sakellariadou, Shortcomings of Shapiro delay-based tests of the equivalence principle on cosmological scales. *Phys. Rev. D* **100**(10), 104047 (2019). [arXiv:1907.12453](#)
25. E. Belgacem, Y. Dirian, S. Foffa, M. Maggiore, Modified gravitational-wave propagation and standard sirens. *Phys. Rev. D* **98**(2), 023510 (2018). [arXiv:1805.08731](#)

Chapter 26

Gravitational Lensing



László Á. Gergely

26.1 Deflection of Light in Schwarzschild Geometry

One of the first verified predictions of General Relativity was the deflection of light when it passes close to massive objects. Its value is twice the one estimated through Newtonian reasoning by Soldner in 1801 [1] (equivalent to applying the Equivalence Principle, as Einstein proved in 2011). This half of the correct result can be understood as arising from the weak-field and slow-motion limit of General Relativity, giving the metric component $g_{tt} = -1 - 2\phi(r)/c^2$ in terms of the Newtonian gravitational potential $\phi(r) = -G_N M/r$, with G_N the Newton's constant (note that here, obviously, for the moment we keep the light speed in our calculations, setting it to 1 in the next subsection and onward). This modification of the Minkowski metric induces a gravitational blueshift, as verified by the Pound-Rebka experiment [2].

Due to the Equivalence Principle, gravitational effects can be replaced locally by acceleration. Hence, there is a system where they locally cancel, with the proper time τ (defined as $ds^2 = -c^2 d\tau^2$) related to the coordinate time t (this being the proper time of another observer at infinity, where the metric is flat) as $d\tau = (-g_{00})^{1/2} dt$. The distant observer would not only see a severely redshifted spectrum of a source, but also an apparent light velocity

$$c(r) = \frac{dr}{dt} = c \left(1 + \frac{2\phi(r)}{c^2} \right)^{1/2}, \quad (26.1)$$

where $c = dr/d\tau$ is the invariant speed of light. Hence an effective index of refraction emerges as [3]:

L. Á. Gergely (✉)
Institute of Physics, University of Szeged, Dóm tér 9, Szeged 6720, Hungary

$$n(r) = \frac{c}{c(r)} = \left(1 + \frac{2\phi(r)}{c^2}\right)^{-1/2} \approx 1 - \frac{\phi(r)}{c^2}. \quad (26.2)$$

Light appears to be both redshifted and slowed down through the gravitational pull of a mass, as seen by a distant observer.

A radius-dependent index of refraction is not unencountered in nature; in this respect it bears similarities to gradient-index (GRIN) lenses, which model both the lens of the eye and the varying temperature and density layers above a hot road, causing the mirage. The analogy, however, stops here: the GRIN-lens eye ideally has almost no aberration at both short and low distances. The relaxed eye has the focal point at infinity, but flexing the eye muscles can accommodate for close focal points. The gravitational lens, however, has no focal point at all. Instead it has a focal line.

The other half of the deflection angle comes from the fact that not only time but also space is affected by gravity. Indeed, from the Schwarzschild solution

$$ds^2 = -c^2 \left(1 + \frac{2\phi(r)}{c^2}\right) dt^2 + \left(1 + \frac{2\phi(r)}{c^2}\right)^{-1} dr^2 + r^2 d\Omega^2, \quad (26.3)$$

as seen by an observer at infinity, the radially moving ($d\Omega^2 = 0$) photon ($ds^2 = 0$) has the apparent velocity

$$c(r) = \frac{dr}{dt} = \pm c \left(1 + \frac{2\phi(r)}{c^2}\right), \quad (26.4)$$

the plus (minus) sign referring to outward (inward) movement. The corresponding effective index of refraction becomes

$$n(r) = \frac{c}{|c(r)|} = \left(1 + \frac{2\phi(r)}{c^2}\right)^{-1} \approx 1 - \frac{2\phi(r)}{c^2}. \quad (26.5)$$

The factor of two appeared by taking into account the contribution of g_{rr} , which is mandatory as long as the motion is not slow, in particular for light.

This varying index of refraction yields the elementary bending $d\delta$ of a planar wavefront travelling in the \hat{x} direction (which subtends an angle $\pi/2 + \alpha$ with the gradient of the gravitational field, the \hat{r} direction) through the Huygens construction. Let y be the coordinate perpendicular to x , such that $r^2 = x^2 + y^2$ (see the magnified region of Fig. 26.1), then

$$\begin{aligned} d\delta &\approx \tan d\delta = \frac{c(x, y + dy) dt - c(x, y) dt}{dy} \\ &= \frac{\partial c(r)}{\partial r} \frac{\partial (r(x, y))}{\partial y} \left(\frac{dx}{c}\right) \\ &= \frac{2}{c^2} \frac{\partial \phi(r)}{\partial r} \frac{y}{r} dx = \frac{2G_N M}{c^2} \frac{y}{r^3} dx. \end{aligned}$$

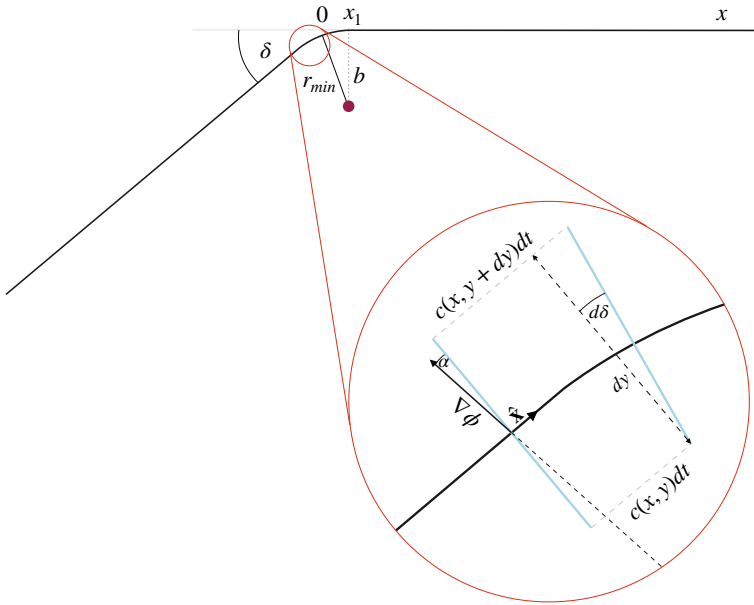


Fig. 26.1 Light deflection through the Huygens construction

The full deflection angle is found by integration over the trajectory (Fig. 26.1):

$$\delta \approx \frac{2G_N M}{c^2} \int_{-\infty}^{\infty} \frac{y dx}{r^3} = \frac{4G_N M}{c^2} \int_0^{\infty} \frac{y dx}{(y^2 + x^2)^{3/2}}.$$

For the second equality we explored that the orbit is symmetric on the two sides of the point of closest approach. The coordinate line x bends together with the trajectory; however, at large distances the potential goes to zero, hence the bending becomes negligible for large x (say $x > x_1$) and y can be chosen as the impact parameter. To zeroth order that can be approximated by the distance of the closest approach, r_{\min} . When x is small, in order to have x running along the orbit, at each point one can rotate the system of reference by an angle $\gamma(r)$ of the order $\mathcal{O}(\gamma) = \mathcal{O}(\delta)$. As the bending angle is small, to first order $y = y' + \gamma x'$ and $x = -\gamma y' + x'$, also $dx = -\gamma dy' + dx'$. To leading order one can also replace $y' = r_{\min}$, getting the same integrand as for large x . Hence

$$\delta \approx \frac{4G_N M}{c^2} \int_0^{\infty} \frac{r_{\min} dx}{(r_{\min}^2 + x^2)^{3/2}} = \frac{4G_N M}{c^2 r_{\min}}. \tag{26.6}$$

This gives $\delta = 1.75$ arcseconds for the deflection of light rays grazing the Sun, the prediction being first verified by Eddington and Dyson in 1919 [4] and confirmed several times since.

The effect increases with gravity, thus with curvature. While in the Solar System the deflection angles are small, for compact objects the values can be significantly larger. In the strong lensing regime the deflection angle can be extreme.

Deflection of light, however, is not the only effect pertinent to the realm of gravitational lensing. The multiplication of images of a bright source, the light of which is overpassing a gravitational lens is given by a lens equation. The number of its solutions depends on the geometry of the problem. The number of images and their angular separation are observables. Gravitational lensing, however, also magnifies the source image. The ratio of the magnifications of two images is another variable, depending on the particular geometry. We will discuss these in a specific example in what follows.

26.2 Deflection of Light by Spherically Symmetric, Static Tidal Charged Brane Black Holes

Considering non-vacuum solutions or a modified gravity theory, the generic, spherically symmetric, static line element reads

$$ds^2 = -f(r) dt^2 + h(r) dr^2 + r^2 (d\theta^2 + \sin^2\theta d\varphi^2), \quad (26.7)$$

where from now on we follow the usual convention of this manuscript and we set the light speed to $c = 1$. The more special case

$$f(r) = h^{-1}(r) = 1 - \frac{2m}{r} + \frac{q}{r^2} - \Lambda r^2, \quad (26.8)$$

beyond the Schwarzschild vacuum solution ($q = 0 = \Lambda$), also incorporates other metrics. For $\Lambda = 0$ and $q = Q^2$ (with Q the central electric charge) it represents the Reissner-Nordström black hole, which for $Q \leq m$ has horizons at $r_h = m \pm \sqrt{(m^2 - Q^2)}$, while for $Q > 0$ it encompasses a naked singularity of the Einstein-Maxwell system. A generic q leads to the interpretation of a tidal charged brane black hole [5] embedded in a higher dimensional spacetime, with its Weyl curvature generating the tidal charge q . This solution of the effective Einstein equation [6–8] on the brane has a similar horizon structure, a black hole for positive $q \leq m^2$ and a naked singularity above, while for negative q it has only one horizon at $r_h = m + \sqrt{(m^2 + |q|)}$, gravity being strengthened by the tidal charge in this case. For $m = 0 = q$ and a positive (negative) cosmological constant Λ the metric (26.7)–(26.8) describes the de Sitter (anti-de Sitter) spacetime. Rindler and Ishak proved that contrary to previous claims, although by a small amount, the cosmological constant affects the deflection angle generated by a concentrated spherically symmetric mass in a Schwarzschild-de Sitter geometry [9].

In what follows, we illustrate how to derive the deflection of light when more than one black hole parameter is present, and to higher order in these parameters on the example of the tidal charged black hole metric.

The deflection angle of light rays caused by brane black holes with tidal charge has been studied in Refs. [10, 11], to first order in the lensing parameters. Second order gravielectric contributions were derived in Ref. [12] in both m and q from the Lagrangian given by $2\mathcal{L} = (ds^2/d\lambda^2)$, where λ is a parameter of the null geodesic curve (a dot will denote the derivative with respect to λ). Hence,

$$0 = 2\mathcal{L} = -f(r)\dot{t}^2 + f^{-1}(r)\dot{r}^2 + r^2\dot{\varphi}^2, \quad (26.9)$$

and the cyclic variables t and φ lead to the constants of motion

$$E \equiv -p_t = f\dot{t}, \quad L \equiv p_\varphi = r^2\dot{\varphi}. \quad (26.10)$$

Then, Eq. (26.9) can be rewritten (in terms of the reciprocal radial variable $u = 1/r$ and the dependent variable φ) as

$$(u')^2 = \frac{E^2}{L^2} - u^2 f(u), \quad (26.11)$$

where a prime denotes differentiation with respect to φ . Differentiating this leads to

$$u'' = -uf - \frac{u^2}{2} \frac{df}{du}. \quad (26.12)$$

For the flat metric $f = 1$, this simplifies to $u'' + u = 0$, with solution $u = u_0 = b^{-1} \cos \varphi$, with $b = L/E$ the impact parameter and the polar angle φ measured from the line indicating the point of closest approach. For the tidal charged black hole, Eq. (26.12) gives

$$u'' + u = 3mu^2 - 2qu^3. \quad (26.13)$$

A perturbative solution in the small parameters

$$\varepsilon = mb^{-1}, \quad \eta = qb^{-2} \quad (26.14)$$

was sought for in the second-order accuracy form

$$u = b^{-1} \cos \varphi + \varepsilon u_1 + \eta v_1 + \varepsilon^2 u_2 + \eta^2 v_2 + \varepsilon \eta w_2 + \mathcal{O}(\varepsilon^3, \eta^3, \varepsilon \eta^2, \varepsilon^2 \eta), \quad (26.15)$$

generating differential equations for the unknown functions u_1 , u_2 , v_1 , v_2 and w_2 , solved for

$$\begin{aligned}
bu &= \cos \varphi + \frac{\varepsilon}{2} (3 - \cos 2\varphi) \\
&\quad - \frac{\eta}{16} (9 \cos \varphi - \cos 3\varphi + 12\varphi \sin \varphi) \\
&\quad + \frac{\varepsilon\eta}{16} (-87 + 40 \cos 2\varphi - \cos 4\varphi + 12\varphi \sin 2\varphi) \\
&\quad + \frac{\varepsilon^2}{16} (37 \cos \varphi + 3 \cos 3\varphi + 60\varphi \sin \varphi) \\
&\quad + \frac{\eta^2}{256} (271 \cos \varphi - 48 \cos 3\varphi + \cos 5\varphi \\
&\quad + 384\varphi \sin \varphi - 36\varphi \sin 3\varphi - 72\varphi^2 \cos \varphi) . \tag{26.16}
\end{aligned}$$

At infinities $u = 0$ and $\varphi = \pm\pi/2 \pm \delta/2$, with δ representing the light deflection by the lensing object with mass m and tidal charge q . To second-order:

$$\delta = 4\varepsilon - \frac{3\pi}{4}\eta + \frac{15\pi}{4}\varepsilon^2 + \frac{105\pi}{64}\eta^2 - 16\varepsilon\eta . \tag{26.17}$$

This can also be expressed in terms of the distance of minimal approach (thus for $u = 1/r_{\min}$ and $\varphi = 0$):

$$r_{\min} = b \left(1 - \varepsilon + \frac{1}{2}\eta - \frac{3}{2}\varepsilon^2 - \frac{5}{8}\eta^2 + 2\varepsilon\eta \right) , \tag{26.18}$$

as

$$\begin{aligned}
\delta &= \frac{4m}{r_{\min}} - \frac{3\pi q}{4r_{\min}^2} + \frac{(15\pi - 16)m^2}{4r_{\min}^2} \\
&\quad + \frac{57\pi q^2}{64r_{\min}^4} + \frac{(3\pi - 28)mq}{2r_{\min}^3} . \tag{26.19}
\end{aligned}$$

While the first-order solutions were in agreement with the results of Ref. [13] (when $q = Q^2$), the second-order contributions did not agree with the result of Ref. [14], obtained by a Hamilton-Jacobi approach. By carefully employing the eikonal method, the Lagrangian result was reproduced in Ref. [15], re-establishing the unicity of the expression for light deflection. This result was used to impose upper limits on the tidal charge from Solar System measurements.

26.3 The Lens Equation

Due to light deflection and the common perception of assuming that images lie in the direction from which light arrives to the observer (O), the light source (S) may appear in one or more different locations. As rays passing both above and below

the lensing object (L) arrive at O , in general, two images (I) appear. We denote the angular positions of the source and image as $\beta = \widehat{SOL}$ (chosen positive, e.g., S is above the optical axis, defined by L and O) and $\theta = \widehat{IOL}$ (with $s = \text{sgn } \theta$), respectively.

A lens equation for generic curved spacetimes was presented in Ref. [16]. However, we employ the exact lens equation for a spherically symmetric lens, derived in Ref. [17] by trigonometric considerations only (no approximations applied)

$$0 = \frac{2D_l}{D_s} \cos\left(\frac{\delta}{2} - |\theta|\right) \cos|\theta| \sin\frac{\delta}{2} + \cos(\delta - |\theta|) (\sin|\theta| - s \cos|\theta| \tan\beta) - \sin\delta. \quad (26.20)$$

Here, δ is the deflection angle, with the convention that $\delta > 0$ whenever the light is bent towards the optical axis and $\delta < 0$ otherwise, cf. Ref. [18], while D_l and D_s are the distances of O from L and from the projection of S to the optical axis, respectively.

Whenever S lies on the optical axis (such that $\beta = 0$), Eq. (26.20) simplifies as

$$0 = D_l \sin|\theta| + (D_s - D_l) \sin(|\theta| - \delta), \quad (26.21)$$

and the two images degenerate into the Einstein ring

$$|\theta| = \arctan \frac{(D_s - D_l) \sin\delta}{D_s \cos\delta}. \quad (26.22)$$

As shown in Ref. [17], a first-order expansion of Eq. (26.20) in the parameter $\epsilon := \delta - 2|\theta|$, representing the deviation from perfect alignment of the system, gives the Virbhadra-Ellis lens equation [19]

$$0 = \tan|\theta| - \tan(s\beta) - \frac{D_s - D_l}{D_s} [\tan|\theta| + \tan(\delta - |\theta|)]. \quad (26.23)$$

A similar approximate lens equation has been derived by Dabrowski and Schunck [20]. The zeroth order approximation, explored in Ref. [21], yields to an even simpler equation

$$|\theta| - s\beta - \frac{D_s - D_l}{D_s} \delta = 0. \quad (26.24)$$

Differences among the predictions of these lensing equations are in general of the order of microarcseconds, hence a proper selection should be made once instruments capable of resolving angular differences on the order of microarcseconds will be available.

26.4 Image Positions

In terms of the more convenient set of small parameters

$$\bar{\varepsilon} = \frac{m}{L}, \quad \bar{\eta} = \frac{q}{L^2}, \quad (26.25)$$

with $L = D_s D_l / (D_s - D_l)$, to second-order Eq. (26.20) formally decomposes as [17]:

$$0 = L_0 + \bar{\varepsilon} L_{10} + \bar{\eta} L_{01} + \bar{\varepsilon}^2 L_{20} + \bar{\varepsilon} \bar{\eta} L_{11} + \bar{\eta}^2 L_{02}. \quad (26.26)$$

If the mass term dominates, standard Schwarzschild lensing arises as a solution of the equation

$$0 = \cos |\theta| [\cos |\theta| (\tan |\theta| - s \tan \beta) - 4\bar{\varepsilon} \left(\cot |\theta| + s \frac{L}{D_l} \tan \beta \right)], \quad (26.27)$$

which, to leading order yields

$$0 = \theta^2 - \beta\theta - 4\bar{\varepsilon} \equiv S, \quad (26.28)$$

with the image positions

$$\theta_{1,2} = \frac{\beta \pm \sqrt{\beta^2 + 16\bar{\varepsilon}}}{2}. \quad (26.29)$$

With perfect alignment of S , L and O the Einstein ring with radius $\theta_E = 2\bar{\varepsilon}^{1/2}$ emerges.

If, by contrast, the tidal charge term dominates, then a similar analysis will give different results depending on its sign. For negative tidal charge one image appears above, the other below the optical axis, similar to Schwarzschild lensing, although the location of the images is distinctly different, as summarised in Fig. 4 of Ref. [17].

A positive tidal charge, however, generates a negative deflection angle—in other words, a scattering behaviour—similar to a negative mass [22]. There is also an upper limit $\bar{\eta}_{\max}$, above which no such scattered images could emerge.

Other cases and second-order corrections were discussed in Ref. [17]. For mass-dominated weak lensing, the position of the images is similar to the Reissner-Nordström black hole lensing [23], however a sensible tidal charge qualitatively modifies the image properties.

The lensing effect of boson stars has also been studied. Neutral boson stars are transparent, charged ones opaque, but they deflect light in the same way as the Schwarzschild or Reissner-Nordström black holes [20]. In the neutral case, however, beside the two images a third, much dimmer one may appear, due to the transparency of the lens.

26.5 Magnification Ratios

The magnification factor is defined as the ratio of the solid angle subtended by the image, divided by the solid angle subtended by the source. For a lens with axial symmetry it is given as [24, 25]

$$\mu = \left| \frac{\theta}{\beta} \frac{d\theta}{d\beta} \right|, \quad (26.30)$$

with both θ and β small. For the images (26.29) obtained in the case of Schwarzschild lensing the magnification factors are

$$\mu_{1,2} = \frac{1}{4} \left(\frac{1}{\beta} \sqrt{\beta^2 + 4\theta_E^2} + \frac{\beta}{\sqrt{\beta^2 + 4\theta_E^2}} \pm 2 \right). \quad (26.31)$$

For a collinear configuration both magnifications diverge as $\mu_{1,2} = \theta_E/2\beta$, however their ratio (the flux ratio) goes to unity.

The magnifications in the tidal charge dominated regime are given by more cumbersome expressions. Comparing the ratio of the magnifications for the various sub-cases transpired to be instructive. This ratio μ_1/μ_2 shows significant deviations from the Schwarzschild case even when the tidal charge is a second-order correction [17].

Moreover, by plotting the magnification ratio (flux ratio, brightness ratio) as a function of the image separation in the case of tidal charged black holes yields a power-law relation, which is significantly different from that for Schwarzschild black holes. This might be interpreted as a smoking gun for detecting the underlying black hole structure with precision observations, provided they are not blurred by environmental noise.

26.6 Strong Lensing by Spherically Symmetric, Static Tidal Charged Black Holes

At a closer approach to the gravitational centre, with lower values of the impact parameter, the deflection angle ceases to be small, and increases to finite values. If it passes over 2π , for all numbers of exact windings, relativistic images are formed on both sides of the lens, in an infinite sequence. Analytic methods for studying strong gravitational lensing in spherically symmetric geometries have been developed in Refs. [26, 27] for the case of almost perfect collinearity of the source, lens and observer, a configuration allowing for series expansion. It has been found that the deflection angle diverges logarithmically at a minimal impact parameter.

The above formalism has been applied to Schwarzschild, Reissner-Nordström, and Janis-Newman-Winicour black holes, for which the position and the magnification

of the relativistic images could be distinguished. If the mass and the distance of the lens is known by other methods and observations, then the position of the relativistic images could distinguish among these geometries. The optical resolution needed to investigate the strong field behaviour of light in the vicinity of the black hole at the centre of our galaxy through its relativistic images has been estimated.

The investigation of the lensed images of stars orbiting close to Sgr A* with a possible tidal charge was advanced in Ref. [28], in the regime between the weak and strong field lensing. It has been conjectured, that with the next generation of instruments, the detection of secondary images will place constraints on the size of the tidal charge. Strong gravitational lensing has also been discussed in Ref. [29], where an upper bound for the tidal charge of the supermassive black hole in the centre of our galaxy is derived, based on the margin of error of the detecting instrument in the measurements of the radius of the first (also of the second) relativistic Einstein ring, due to strong lensing. With constraints from the designed sensitivity of GRAVITY [30], a four-telescope beam combiner instrument for NIR interferometry with the Very Large Telescope Interferometer (VLTI), the supermassive black hole could be allowed to have a much larger tidal charge than derived for the Sun or neutron stars.

26.7 Gravitational Lensing by Other Spherically Symmetric, Static Brane Black Holes

The gravitational lensing of spherically symmetric, static brane black holes has been extensively studied. Such black holes include the tidal charged brane black hole [5], although the five-dimensional spacetime encompassing it has not been found.

Another possibility is the Garriga-Tanaka black hole [31], embedded in a five-dimensional AdS spacetime with curvature radius l and five-dimensional cosmological constant $\tilde{\Lambda} = -6l^{-2}$. The weak-field limit of the Schwarzschild metric on the brane receives corrections from the Kaluza-Klein modes of the five-dimensional AdS spacetime:

$$\begin{aligned} f(r) &= 1 - \frac{2m}{r} \left(1 - \frac{4}{\tilde{\Lambda} r^2} \right), \\ h(r) &= 1 + \frac{2m}{r} \left(1 - \frac{2}{\tilde{\Lambda} r^2} \right). \end{aligned} \quad (26.32)$$

The third-order corrections fade away with r^{-3} . Reference [10] calculated the bending of null geodesics by both the tidal charged and Garriga-Tanaka spherically symmetric, static brane black holes.

Brane-world black hole (both tidal charged and Garriga-Tanaka) lensing has also been studied in Ref. [32] by numerical techniques. Image magnifications of such braneworld primordial black holes were found to be significantly increased comparing to their four-dimensional analogues.

Reference [11] has calculated light deflection in the weak-field limit of yet another braneworld black hole [33], representing the near horizon approximation of the five-dimensional Schwarzschild geometry:

$$f(r) = h^{-1}(r) = 1 - \frac{r_0^2}{r^2}, \quad (26.33)$$

where r_0 is the radius of the five-dimensional black hole horizon, assumed much smaller than the size of the AdS radius. The bending angle of a light ray emerges as the result given in Eq. (26.6) is multiplied by $2l/r_{\min}$, indicating a more prominent effect for small impact parameters. Strong field images were analysed in Ref. [34].

Reference [11] also addressed the modifications of the Einstein ring radius and magnification for a point light source. It was shown that the radius of the Einstein ring decreases by a factor of $(l/2D_l)^{1/2}$, where D_l is the distance of the lens from the observer. The magnification of the Schwarzschild black hole is corrected by several factors, as given by their Eq. (27). Brane black holes of type (26.33) of our galactic halo, could be dimmed by the extra dimensional extension of gravity by as much as six orders of magnitude, which would make them extremely difficult to detect by gravitational lensing. That is an interesting scenario in the quest to explain dark matter.

Strong lensing brane black holes could have significantly different observational signatures compared to the Schwarzschild black holes, as discussed in Ref. [35]. This work investigated the tidal charged black hole and another black hole that has been originally proposed in Ref. [36] in the area gauge as

$$\begin{aligned} f(r) &= \left[(1 + \epsilon) \left(1 - \frac{2m}{r} \right)^{1/2} - \epsilon \right]^2, \\ h(r) &= \left(1 - \frac{2m}{r} \right)^{-1}. \end{aligned} \quad (26.34)$$

The parameter $\epsilon > 0$ scales with the difference of the horizon radius and a turning point in the area function. It is also related through $1 + \epsilon = (1 + \eta)^{-1}$ to the parameter η of Ref. [36], measuring the difference between the gravitational and inertial masses. The gravitational mass is given by $f(r)$ with $m(1 + \epsilon)$, where m is the ADM mass, the asymptotic limit of the Misner-Sharp mass, appearing in $h(r)$. This metric is singular at $r_0 = 2m$ and $r_h = 2m(1 + \epsilon)^2 / (1 + 2\epsilon)$, which is larger than r_0 , but only by a second-order contribution in ϵ . The event horizon at r_h is singular. Most notably, the radius of the photon sphere in this geometry is modified, being pulled inwards or pushed outwards together with the inwards/outwards shifted horizon relative to the Schwarzschild case. With black hole shadow imaging already a reality through the Event Horizon Telescope very-long-baseline interferometry (VLBI) measurements, this may turn out to be another test of General Relativity in the future.

Lensing properties of brane black holes are also discussed in the review [37]. It is argued that Myers-Perry black holes [38] (the projection onto the brane of the five-dimensional Schwarzschild solution given by the Myers-Perry metric) residing in the galactic halo would be difficult to detect by their weak lensing features, as their magnification is reduced in comparison to the Schwarzschild case.

Based on a formalism with two gravitational potentials, Ref. [39] investigated gravitational lensing, obtaining general expressions for the time delay, deflection angle, Einstein ring, image positions, magnification and critical curves (the loci of image points in the lens plane with infinite magnification).

26.8 Gravitational Lensing in Hořava-Lifshitz Gravity

A decade ago, Hořava proposed a renormalisable field theoretical model that can be interpreted as a complete theory of gravity [40, 41] (see also the review [42]). At low energies it reduces to Einstein gravity with a non-vanishing cosmological constant. At the ultraviolet energy scales, however, it exhibits an anisotropic Lifshitz scaling between time and space given by $x^i \rightarrow lx^i$ and $t \rightarrow l^z t$, with z the scaling exponent.

Hořava-Lifshitz gravity admits the Kehagias-Sfetsos asymptotically flat solution [43], given by

$$f(r) = h^{-1}(r) = 1 + \omega r^2 \left[1 - \left(1 + \frac{4G_N m}{\omega r^3} \right)^{1/2} \right], \quad (26.35)$$

where m is the total mass of the black hole and ω is the Hořava-Lifshitz parameter. The origin represents a curvature singularity, while

$$r_{\pm} = G_N m \left(1 \pm \sqrt{1 - \frac{1}{2G_N^2 m^2 \omega}} \right) \quad (26.36)$$

are coordinate singularities, disappearing in Eddington-Finkelstein coordinates. The outer apparent horizon r_+ is an event horizon that goes to the Schwarzschild radius in the limit $\omega \rightarrow \infty$ (in the same limit, the inner horizon degenerates into the central singularity).

The deflection angle of light can be calculated based on the result that light follows null geodesics (although massive particles do not). Image locations and the radius of the Einstein ring emerge by a similar procedure as described before.

For every ω there is a maximal deflection angle δ_{\max} , corresponding to certain r_{crit} , and light rays passing both above and below r_{crit} will experience less deflection than δ_{\max} [44], a feature inexistent in Schwarzschild weak lensing. The critical distance r_{crit} decreases with increasing ω , so when approaching the Schwarzschild limit, r_{crit} is confined below the horizon (goes to 0 when $\omega \rightarrow \infty$), generating the expected

decreasing $\delta(r_{\min})$ function out of the horizon, also producing two images, as in the Schwarzschild lensing.

Far from the Schwarzschild regime, however, the Kehagias-Sfetsos spacetime approaches flatness, therefore there is only one undeflected and unmagnified image. In the intermediate range only the upper focused image is produced, due to the existence of the maximal deflection angle δ_{\max} .

Concerning the Einstein rings, it has been found that for a given mass and lensing geometry, the Einstein angles in the Kehagias-Sfetsos spacetime are always smaller than their Schwarzschild counterpart. In the strong lensing regime the detection of the first two relativistic Einstein rings could constrain the parameter range of the the Kehagias-Sfetsos spacetime [44]. Their observation with the 10^{-5} arcsec expected accuracy of future instruments [45] would set the strongest observational constraint on the Hořava-Lifshitz parameter.

26.9 Gravitational Lensing in $f(R)$ Gravity

In the quest to explain dark matter and dark energy, higher-order theories of gravity were advanced, both in metric and Palatini (see the review [46]) approaches. In the action describing such theories in the metric formulation, the curvature scalar R of the Einstein-Hilbert action is replaced by an arbitrary function $f(R)$. It is known that this can be transformed to a particular form of Brans-Dicke scalar-tensor theory, with the Brans-Dicke parameter ω_0 vanishing (a massive dilaton gravity model).

It has been proven in Ref. [47] that the Schwarzschild solution is the unique spherically symmetric, asymptotically flat vacuum black hole solution for a scalar field of a generalised Brans-Dicke class with linear kinetic term, with the energy-momentum tensor of the scalar field obeying the weak energy condition in the Einstein frame.

Nevertheless, for $f = R^n$ a weak-field solution has been found in Ref. [48] as

$$f(r) = h^{-1}(r) = 1 - \frac{G_N m}{r} \left[1 + \left(\frac{r}{r_c} \right)^\sigma \right], \quad (26.37)$$

with a characteristic distance r_c (much larger than the Schwarzschild radius) and a strength parameter

$$\sigma = \frac{12n^2 - 7n - 1 - \sqrt{36n^4 + 12n^3 - 83n^2 + 50n + 1}}{6n^2 - 4n + 2} < 1$$

monotonically increasing with n . The Schwarzschild solution is recovered for $\sigma = 0$ ($n = 1$). This solution evades the conditions of the unicity theorem [47], as the deviation from General Relativity can be formulated in terms of an effective energy-momentum tensor, which violates all energy conditions [49]. This solution can be

considered as an approximation of a compact object, whose parameters fall outside the conditions of the above theorem.

Weak lensing characteristics in this geometry are as follows. Above (below) r_c , gravity is strengthened (weakened), and as a consequence, weak lensing features are modified compared to the Schwarzschild case. There is a critical impact parameter (depending upon r_c) for which the behaviour of the deflection angle changes. In Ref. [21] the effects on the amplification of the images and the Paczynski curve in microlensing experiments were estimated.

Image positions, Einstein ring radii, magnification factors and the magnification ratio have been computed [49]. Most importantly it was found that the magnification ratio as a function of image separation obeys a power-law depending on the parameter σ , with a double degeneracy. No $\sigma \neq 0$ value gives the same power as the one characterizing Schwarzschild black holes. As the magnification ratio and the image separation are the lensing quantities most conveniently determined by direct measurements, future lensing surveys will be able to constrain the parameter σ based on this prediction.

26.10 Gravitational Lensing in Scalar-Tensor Theories

The Janis-Newman-Winicour black hole [50] represents a spherically symmetric solution of the Einstein–massless scalar field equations, with a point singularity replacing the Schwarzschild horizon. It has been discussed in a more general context by Gautreau [51], rediscovered by Wyman [52], as shown in Ref. [53]. The strong lensing features were analysed by Bozza [27] and the effects of the scalar charge $q < m$ of the black hole (expressed through a parameter $\gamma = m/\sqrt{m^2 + q^2}$) on image positions and magnifications quantified. Such effects could in principle be measurable by VLBI techniques, provided the relativistic images survive environmental noise.

Gravitational lensing has been studied for the case of a static and circularly symmetric lens, characterised by both mass and scalar charge parameters [54]. With increasing scalar charge parameter, the deviations from Schwarzschild lensing become important, manifested in either the disposition or the emergence of two Einstein rings. The number and position of images may also vary.

Recently, the strong gravitational lensing by a Kiselev black hole [55] has been investigated. This black hole [56] arises under the assumption of spherical symmetry and it has quintessence ($p = w_q \rho$, $-1 < w_q < -1/3$) hair. For these parameters it has the asymptotics of de Sitter spacetime. The position and total magnification of relativistic images were computed and compared with the case of the Schwarzschild black hole. A possible observational signature was identified in the bending angle, being larger than for the Schwarzschild black hole with the same mass parameter.

26.11 Gravitational Lensing in Teleparallel Gravity

In the Teleparallel Equivalent of General Relativity (TEGR) the torsion T or in its symmetric counterpart (TEGR) the non-metricity Q generate forces representing gravity, causing the deflection of trajectories from the straight lines of the flat metric. In the equivalent general relativistic picture there is a curved metric, which exhibits these trajectories as its geodesics. Hence the description of weak and strong lensing, developed in terms of this metric, can be unequivocally rewritten in the language of torsion or non-metricity, with no new physical effects to be expected.

However, in the generalised $f(T)$ and $f(Q)$ theories the lensing properties could be different and are worth studying in order to derive effects and predictions that could either support or falsify these theories when confronted with high-sensitivity observations.

26.12 Gravitational Lensing, Galaxies and Cosmology

The baryonic (luminous) mass of the galaxies, although plagued by the uncertainties in the mass-to-light ratio, is assessed by observations on their luminosity. Realistic mass-to-light models, however, do not in general provide enough baryonic mass to explain the behaviour of galactic rotation curves, observed spectroscopically. The flatness of these curves is one indication for the existence of galactic dark matter halos. Many dark matter models compatible with galactic rotation curves have been proposed. They may differ, especially in the outer regions of the galaxies, where no spectroscopic information is available.

Gravitational lensing observations, however, are able to assess the combined baryonic and dark mass of the galaxy at distances far exceeding the validity of the galactic rotation curves. Hence, lensing surveys of galaxies and galactic clusters may distinguish from among the dark matter models. These surveys measure the convergence (magnification) and shear deformation of the objects, and are equally important for cosmological considerations. Notable examples are the first-year shear catalogue of the Subaru Hyper Suprime-Cam Subaru Strategic Program Survey [57] and the Kilo-Degree Survey (KiDS) [58], carried out with the VLT Survey Telescope (VST) and OmegaCAM camera, which is able to map the large-scale matter distribution in the Universe and constrain the equation-of-state of Dark Energy.

In a cosmological setting the perturbed Friedmann metric reads

$$ds^2 = -(1 + 2\Psi) dt^2 + a^2 (1 - 2\Phi) d\mathbf{x}^2, \quad (26.38)$$

with a being the scale factor. Lensing properties are sensitive to $\nabla^2(\Phi + \Psi)$ along the line of sight. The Poisson equation, on the other hand, contains $\nabla^2\Phi$, sourced by the fractional overdensity δ_o . In General Relativity $\Psi = \Phi$ (provided there are no anisotropic stresses), thus lensing is intimately related to δ_o along the line of

sight. By contrast, in alternative theories of gravity this relation is modified. Reference [59] proposed to determine the matter overdensity at a given redshift by measuring the velocity field, rather than from galaxy overdensities, and discussed the differences among the cold dark matter model with a cosmological constant, the Dvali-Gabadadze-Porrati, the TeVeS, and $f(R)$ gravity theories.

As an example of another lensing feature that could be tested by these methods, we mention again brane-world models. The higher-dimensional Weyl curvature induces a new source of gravity on the brane. In the spherically symmetric, static configuration it reduces to dark radiation and dark pressure components. These are able to modify spacetime geometry around galaxies consistently, with the flatness of galactic rotation curves [60–64]. Gravitational lensing could provide a test to discern between this geometrical model and other dark matter models. Indeed, in the asymptotic regions, light deflection is enhanced, as compared to dark matter halo predictions. For a linear equation of state of the Weyl fluid, there is a critical radius below which braneworld effects reduce, while above it they amplify the deflection of light [65]. This is in contrast to other dark matter models, in which the deflection angle increases due to dark matter at any radius.

26.13 Concluding Remarks

All results discussed above refer to the geometrical optics or high frequency approximation of light. In a gravitational theory this means that the wavelength of the light is much smaller than the gravitational curvature radius. This is an approximation, which always holds in flat spacetime and most of the time in weak gravity sectors as well. Information about the polarisation of the electromagnetic waves is not contained in the geometrical optics approximation. It has been argued that high-frequency wave propagation is insensitive to compositions of certain conformal, Kerr-Schild, and related transformations of the background metric, while the inclusion of the polarisation information breaks some of the degeneracy [66].

In the geometrical optics approximation we have seen that the occurrence of light deflection depends on the underlying geometry. While the general relativistic mass term of the Schwarzschild solution is expected to dominate gravitational lensing in most of the spherically symmetric cases, other charges of a hairy black hole could modify the deflection value in an essential way, leading to modified image positions. Moreover, the magnification or brightness of the images will also be affected.

For weak gravitational lensing, testing the power-law relation obeyed by the brightness ratio as a function of the image separation (both being observable quantities) could unequivocally distinguish between Schwarzschild lensing or hairy characteristics. For strong lensing, the detection of the positions of the relativistic images would provide information about the possible types of hair. Future precision measurements, able to penetrate the environmental noise, are expected to shed more light on these features, confirming or falsifying hairy features and thus the underlying gravitational theories.

References

1. J.G.V. Soldner, On the deflection of a light ray from its rectilinear motion, by the attraction of a celestial body at which it nearly passes by. *Phys. Rev. Lett.* **3**, 439–441 (1959)
2. R.V. Pound, G.A. Rebka, *Gravitational Red-Shift in Nuclear Resonance, Berliner Astronomisches Jahrbuch*
3. T.-P. Cheng, *Relativity, Gravitation and Cosmology, A Basic Introduction* (Oxford University Press, Oxford, 2010)
4. F.W. Dyson, A.S. Eddington, C. Davidson, A determination of the deflection of light by the sun's gravitational field, from observations made at the total Eclipse of 29 May 1919. *Phil. Trans. Roy. Soc. Lond. A* **220**, 291–333 (1920)
5. N. Dadhich, R. Maartens, P. Papadopoulos, V. Rezanian, Black holes on the brane. *Phys. Lett. B* **487**, 1–6 (2000). [arxiv:hep-th/0003061](https://arxiv.org/abs/hep-th/0003061)
6. T. Shiromizu, K.-I. Maeda, M. Sasaki, The Einstein equation on the 3-brane world. *Phys. Rev. D* **62**, 024012 (2000). [arxiv:gr-qc/9910076](https://arxiv.org/abs/gr-qc/9910076)
7. L.A. Gergely, Generalized Friedmann branes. *Phys. Rev. D* **68**, 124011 (2003). [arxiv:gr-qc/0308072](https://arxiv.org/abs/gr-qc/0308072)
8. L.A. Gergely, Friedmann branes with variable tension. *Phys. Rev. D* **78**, 084006 (2008). [arXiv:0806.3857](https://arxiv.org/abs/0806.3857)
9. W. Rindler, M. Ishak, Contribution of the cosmological constant to the relativistic bending of light revisited. *Phys. Rev. D* **76**, 043006 (2007). [arXiv:0709.2948](https://arxiv.org/abs/0709.2948)
10. S. Kar, M. Sinha, Bending of light and gravitational signals in certain on-brane and bulk geometries. *Gen. Rel. Grav.* **35**, 1775–1784 (2003)
11. A.S. Majumdar, N. Mukherjee, Gravitational lensing in the weak field limit by a braneworld black hole. *Mod. Phys. Lett. A* **20**, 2487–2496 (2005). [arxiv:astro-ph/0403405](https://arxiv.org/abs/astro-ph/0403405)
12. L.A. Gergely, B. Darazs, Weak gravitational lensing in brane-worlds. *Publ. Astron. Dep. Eotvos Univ.* **17**, 213–219 (2006). [arxiv:astro-ph/0602427](https://arxiv.org/abs/astro-ph/0602427)
13. J. Briet, D. Hobill, *Determining the Dimensionality of Spacetime by Gravitational Lensing*. [arXiv:0801.3859](https://arxiv.org/abs/0801.3859)
14. C.G. Boehmer, T. Harko, F.S.N. Lobo, Solar system tests of brane world models. *Class. Quant. Grav.* **25**, 045015 (2008). [arXiv:0801.1375](https://arxiv.org/abs/0801.1375)
15. L.A. Gergely, Z. Keresztes, M. Dwornik, Second-order light deflection by tidal charged black holes. *Class. Quant. Grav.* **26**, 145002 (2009). [arXiv:0903.1558](https://arxiv.org/abs/0903.1558)
16. S. Frittelli, E.T. Newman, An Exact universal gravitational lensing equation. *Phys. Rev. D* **59**, 124001 (1999). [arxiv:gr-qc/9810017](https://arxiv.org/abs/gr-qc/9810017)
17. Z. Horvath, L.A. Gergely, D. Hobill, Image formation in weak gravitational lensing by tidal charged black holes. *Class. Quant. Grav.* **27**, 235006 (2010). [arXiv:1005.2286](https://arxiv.org/abs/1005.2286)
18. K.S. Virbhadra, Relativistic images of Schwarzschild black hole lensing. *Phys. Rev. D* **79**, 083004 (2009). [arXiv:0810.2109](https://arxiv.org/abs/0810.2109)
19. K.S. Virbhadra, G.F.R. Ellis, Schwarzschild black hole lensing. *Phys. Rev. D* **62**, 084003 (2000). [arxiv:astro-ph/9904193](https://arxiv.org/abs/astro-ph/9904193)
20. M.P. Dabrowski, F.E. Schunck, Boson stars as gravitational lenses. *Astrophys. J.* **535**, 316–324 (2000). [arxiv:astro-ph/9807039](https://arxiv.org/abs/astro-ph/9807039)
21. S. Capozziello, V.F. Cardone, A. Troisi, Gravitational lensing in fourth order gravity. *Phys. Rev. D* **73**, 104019 (2006). [arxiv:astro-ph/0604435](https://arxiv.org/abs/astro-ph/0604435)
22. J.G. Cramer, R.L. Forward, M.S. Morris, M. Visser, G. Benford, G.A. Landis, Natural wormholes as gravitational lenses. *Phys. Rev. D* **51**, 3117–3120 (1995). [arxiv:astro-ph/9409051](https://arxiv.org/abs/astro-ph/9409051)
23. M. Sereno, Weak field limit of Reissner-Nordstrom black hole lensing. *Phys. Rev. D* **69**, 023002 (2004). [arxiv:gr-qc/0310063](https://arxiv.org/abs/gr-qc/0310063)
24. P. Schneider, The amplification caused by gravitational bending of light. *Astr. Ap.* **140**, 119 (1984)
25. R. Blandford, R. Narayan, Fermat's principle, caustics, and the classification of gravitational lens images. *Astroph. J.* **310**, 568 (1986)

26. V. Bozza, S. Capozziello, G. Iovane, G. Scarpetta, Strong field limit of black hole gravitational lensing. *Gen. Rel. Grav.* **33**, 1535–1548 (2001). [arXiv:gr-qc/0102068](#)
27. V. Bozza, Gravitational lensing in the strong field limit. *Phys. Rev. D* **66**, 103001 (2002). [arXiv:gr-qc/0208075](#)
28. A.Y. Bin-Nun, Lensing By Sgr A* as a probe of modified gravity. *Phys. Rev. D* **82**, 064009 (2010). [arXiv:1004.0379](#)
29. Z. Horvath, L.A. Gergely, Black hole tidal charge constrained by strong gravitational lensing. *Astron. Nachr.* **334**, 1047–1050 (2013). [arXiv:1203.6576](#)
30. S. Gillessen et al., GRAVITY: a four-telescope beam combiner instrument for the VLTI. *Proc. SPIE Int. Soc. Opt. Eng.* **7734**, 77340Y (2010). [arXiv:1007.1612](#)
31. J. Garriga, T. Tanaka, Gravity in the brane world. *Phys. Rev. Lett.* **84**, 2778–2781 (2000). [arXiv:hep-th/9911055](#)
32. A.Y. Bin-Nun, Relativistic images in randall-sundrum II Braneworld Lensing. *Phys. Rev. D* **81**, 123011 (2010). [arXiv:0912.2081](#)
33. R. Guedens, D. Clancy, A.R. Liddle, Primordial black holes in braneworld cosmologies: formation, cosmological evolution and evaporation. *Phys. Rev. D* **66**, 043513 (2002). [arXiv:astro-ph/0205149](#)
34. E.F. Eiroa, A Braneworld black hole gravitational lens: Strong field limit analysis. *Phys. Rev. D* **71**, 083010 (2005). [arXiv:gr-qc/0410128](#)
35. R. Whisker, Strong gravitational lensing by braneworld black holes. *Phys. Rev. D* **71**, 064004 (2005). [arXiv:astro-ph/0411786](#)
36. R. Casadio, A. Fabbri, L. Mazzacurati, New black holes in the brane world? *Phys. Rev. D* **65**, 084040 (2002). [arXiv:gr-qc/0111072](#)
37. A.S. Majumdar, N. Mukherjee, Braneworld black holes in cosmology and astrophysics. *Int. J. Mod. Phys. D* **14**, 1095 (2005). [arXiv:astro-ph/0503473](#)
38. R.C. Myers, M.J. Perry, Black holes in higher dimensional space-times. *Ann. Phys.* **172**, 304 (1986)
39. S. Pal, S. Kar, Gravitational lensing in braneworld gravity: Formalism and applications. *Class. Quant. Grav.* **25**, 045003 (2008). [arXiv:0707.0223](#)
40. P. Horava, Membranes at quantum criticality. *JHEP* **03**, 020 (2009). [arXiv:0812.4287](#)
41. P. Horava, Quantum gravity at a Lifshitz point. *Phys. Rev. D* **79**, 084008 (2009). [arXiv:0901.3775](#)
42. M. Visser, Status of Horava gravity: a personal perspective. *J. Phys. Conf. Ser.* **314**, 012002 (2011). [arXiv:1103.5587](#)
43. A. Kehagias, K. Sfetsos, The Black hole and FRW geometries of non-relativistic gravity. *Phys. Lett. B* **678**, 123–126 (2009). [arXiv:0905.0477](#)
44. Z. Horvath, L.A. Gergely, Z. Keresztes, T. Harko, F.S.N. Lobo, Constraining Hořava-Lifshitz gravity by weak and strong gravitational lensing. *Phys. Rev. D* **84**, 083006 (2011). [arXiv:1105.0765](#)
45. S. Trippe, R. Davies, F. Eisenhauer, N.M.F. Schreiber, T.K. Fritz, R. Genzel, High precision astrometry with MICADO at the European extremely large telescope. *Mon. Not. Roy. Astron. Soc.* **402**, 1126 (2010). [arXiv:0910.5114](#)
46. A. De Felice, S. Tsujikawa, $f(R)$ theories. *Living Rev. Rel.* **13**, 3 (2010). [arXiv:1002.4928](#)
47. T.P. Sotiriou, V. Faraoni, Black holes in scalar-tensor gravity. *Phys. Rev. Lett.* **108**, 081103 (2012). [arXiv:1109.6324](#)
48. S. Capozziello, V.F. Cardone, A. Troisi, Low surface brightness galaxies rotation curves in the low energy limit of r^{*n} gravity: no need for dark matter? *Mon. Not. Roy. Astron. Soc.* **375**, 1423–1440 (2007). [arXiv:astro-ph/0603522](#)
49. Z. Horvath, L.A. Gergely, D. Hobill, S. Capozziello, M. De Laurentis, Weak gravitational lensing by compact objects in fourth order gravity. *Phys. Rev. D* **88**(6), 063009 (2013). [arXiv:1207.1823](#)
50. A.I. Janis, E.T. Newman, J. Winicour, Reality of the Schwarzschild singularity. *Phys. Rev. Lett.* **20**, 878–880 (1968)
51. R. Gautreau, Gautreau, coupled Weyl gravitational and zero-rest-mass scalar fields. *Nuovo Cimento B* **62**, 360–370 (1969)

52. M. Wyman, Static spherically symmetric scalar fields in general relativity. *Phys. Rev. D* **24**, 839–841 (1981)
53. K.S. Virbhadra, Janis-Newman-Winicour and Wyman solutions are the same. *Int. J. Mod. Phys. A* **12**, 4831–4836 (1997). [arXiv:gr-qc/9701021](#)
54. K.S. Virbhadra, D. Narasimha, S.M. Chitre, Role of the scalar field in gravitational lensing. *Astron. Astrophys.* **337**, 1–8 (1998). [arXiv:astro-ph/9801174](#)
55. A. Younas, S. Hussain, M. Jamil, S. Bahamonde, Strong gravitational lensing by Kiselev black hole. *Phys. Rev. D* **92**(8), 084042 (2015). [arXiv:1502.01676](#)
56. V.V. Kiselev, Quintessence and black holes. *Class. Quant. Grav.* **20**, 1187–1198 (2003). [arXiv:gr-qc/0210040](#)
57. R. Mandelbaum et al., *The first-year shear catalog of the Subaru Hyper Suprime-Cam SSP Survey*. [arXiv:1705.06745](#)
58. Astro-WISE, KiDS Collaboration, J.T.A. de Jong, G.A.V. Kleijn, K.H. Kuijken, E.A. Valentijn, KiDS, The kilo-degree survey. *Exper. Astron.* **35**, 25–44 (2013). [arXiv:1206.1254](#)
59. P. Zhang, M. Liguori, R. Bean, S. Dodelson, Probing gravity at cosmological scales by measurements which test the relationship between gravitational lensing and matter overdensity. *Phys. Rev. Lett.* **99**, 141302 (2007). [arXiv:0704.1932](#)
60. M.K. Mak, T. Harko, Can the galactic rotation curves be explained in brane world models? *Phys. Rev. D* **70**, 024010 (2004). [arXiv:gr-qc/0404104](#)
61. T. Harko, M.K. Mak, Conformally symmetric vacuum solutions of the gravitational field equations in the brane-world models. *Annals Phys.* **319**, 471–492 (2005). [arXiv:gr-qc/0503072](#)
62. T. Harko, K.S. Cheng, Galactic metric, dark radiation, dark pressure and gravitational lensing in brane world models. *Astrophys. J.* **636**, 8–20 (2005). [arXiv:astro-ph/0509576](#)
63. C.G. Boehmer, T. Harko, Galactic dark matter as a bulk effect on the brane. *Class. Quant. Grav.* **24**, 3191–3210 (2007). [arXiv:0705.2496](#)
64. L.A. Gergely, T. Harko, M. Dwornik, G. Kupi, Z. Keresztes, Galactic rotation curves in brane world models. *Mon. Not. Roy. Astron. Soc.* **415**, 3275–3290 (2011). [arXiv:1105.0159](#)
65. K.C. Wong, T. Harko, K.S. Cheng, L.A. Gergely, Weyl fluid dark matter model tested on the galactic scale by weak gravitational lensing. *Phys. Rev. D* **86**, 044038 (2012). [arXiv:1207.3167](#)
66. A.I. Harte, Gravitational lensing beyond geometric optics: II. Metric independence. *Gen. Rel. Grav.* **51**(12), 160 (2019). [arXiv:1906.10708](#)

beyond which the quantum nature of gravity cannot be neglected (for a review, see Ref. [2]).

Hawking figured out that, in order to describe the innermost regions of a black hole, we cannot really forget about quantum effects. We could then wonder whether this quantum region should be treated as a source localised deep inside the horizon. To put this idea to the test, we could employ, for instance, the *horizon quantum mechanics* (HQM) formalism (see, e.g., [3–13]). Let us consider a quantum particle of mass m described by a Gaussian wave-packet of typical spatial extension $\sigma = \lambda_m \simeq \hbar/m$, namely

$$\Psi_S(r) = \left(\frac{1}{\pi \lambda_m^2} \right)^{3/4} \exp \left(-\frac{r^2}{2 \lambda_m^2} \right), \quad (27.2)$$

with $r = |\mathbf{x}|$. Taking the Fourier transform of $\Psi_S(r)$, we obtain

$$\tilde{\Psi}_S(\mathbf{p}) = \left(\frac{1}{\pi m^2} \right)^{3/4} \exp \left(-\frac{|\mathbf{p}|^2}{2 m^2} \right). \quad (27.3)$$

If we now assume the validity of the flat mass–shell relation, $E^2 = |\mathbf{p}|^2 + m^2$, the momentum–space representation of Ψ_S yields the spectral decomposition of the system,

$$\Psi_S(\mathbf{x}) \sim \int d^3 p e^{i\mathbf{p}\cdot\mathbf{x}} \tilde{\Psi}_S(\mathbf{p}) \sim \int dE \varphi_E(\mathbf{x}) C_S(E), \quad (27.4)$$

with $C_S(E) \sim \tilde{\Psi}_S(|\mathbf{p}|^2 = E^2 - m^2)$ and $\varphi_E(\mathbf{x})$ the eigenfunctions of an appropriate Hamiltonian operator. Interpreting the Schwarzschild expression $R_H = 2 G_N M$, with G_N Newton’s constant, as a kind of Gupta–Bleuler condition for the admissible physical states, from (27.3) we can compute the *horizon wave–function*

$$\Psi_H(r_H) = \mathcal{N}_H \Theta(r_H - R_H) \exp \left(-\frac{M_{Pl}^2 r_H^2}{8 m^2 \ell_{Pl}^2} \right), \quad (27.5)$$

which determines the size of the gravitational radius ($r_H = 2 G_N E$) at the quantum level (see [5] for details). From here, we can compute the probability for a quantum system to lie inside its own event horizon as

$$P_{BH} = \int_0^\infty \mathcal{P}_S(r < r_H) \mathcal{P}_H(r_H) dr_H, \quad (27.6)$$

with $\mathcal{P}_H(r_H) = 4\pi r_H^2 |\Psi_H(r_H)|^2$ and

$$\mathcal{P}_S(r < r_H) = 4\pi \int_0^{r_H} \bar{r}^2 |\Psi_H(\bar{r})|^2 d\bar{r}. \quad (27.7)$$

Computing P_{BH} for the case (27.5), we find that $P_{\text{BH}}(m) \ll 1$ for $m \ll M_{\text{Pl}}$, while it quickly approaches unity as $m \simeq M_{\text{Pl}}$, with M_{Pl} denoting the Planck mass. This result is consistent with the standard semi-classical expectation however, if we compute the corresponding quantum fluctuations ΔR_{H} for the size of the horizon, we find that

$$\Delta R_{\text{H}}^2 = \langle R_{\text{H}}^2 \rangle_{\Psi_{\text{H}}} - \langle R_{\text{H}} \rangle_{\Psi_{\text{H}}}^2 \sim (2 G_N m)^2 \equiv R_{\text{H}}^2. \quad (27.8)$$

In other words, for such a localised object the quantum fluctuations of the horizon scale as the size of the horizon itself, i.e., $\Delta R_{\text{H}} \sim R_{\text{H}}$. This is, definitely, rather unreasonable, since one expects that the bigger a black hole, the more classical it will appear. This conclusion thus seems to suggest that modelling the interior of a black hole in terms of very localised quantum objects might not be a viable option.

27.2 Corpuscular Gravity

Corpuscular gravity (see, e.g., [14–20] for a review of the topic) offers a way to effectively describe the interior of black holes as extended objects. Specifically, in this picture, black holes are treated as self-sustained [21] marginally bound states constituted of a very large number of soft and off-shell gravitons with typical wavelength $\lambda_{\text{G}} \simeq R_{\text{H}}$. It is worth noting that this picture of gravity in the strong coupling regime represents a possible implementation of a much more general scheme, known as *classicalisation*, whose scope is to provide an alternative to the standard Wilsonian UV-completion of non-renormalisable theories [22]. Denoting $\epsilon_{\text{G}} = \hbar/\lambda_{\text{G}}$, the typical energy of these constituent gravitons, and introducing the effective (dimensionless) gravitational coupling $\alpha_{\text{G}} = \epsilon_{\text{G}}^2/M_{\text{Pl}}^2$, we find that these gravitons satisfy an energy balance that reads

$$K + U \simeq 0, \quad (27.9)$$

with $K \simeq \epsilon_{\text{G}}$ denoting the “kinetic energy” of each constituent graviton and $U \simeq -\alpha_{\text{G}} N \hbar/\lambda_{\text{G}}$ representing a first rough approximation of the binding potential felt by each of the $N \gg 1$ constituents. This condition then implies

$$\alpha_{\text{G}} N \simeq 1. \quad (27.10)$$

As a consequence, the softness of the constituents will be measured by the multiplicity of the collective state, since

$$\epsilon_{\text{G}} = M_{\text{Pl}} \sqrt{\alpha_{\text{G}}} \simeq \frac{M_{\text{Pl}}}{\sqrt{N}}. \quad (27.11)$$

Furthermore, since $\lambda_{\text{G}} \simeq R_{\text{H}}$, it is easy to see that

$$R_{\text{H}} \simeq \lambda_{\text{G}} \simeq \frac{\hbar}{\epsilon_{\text{G}}} \simeq \sqrt{N} \ell_{\text{Pl}}, \quad (27.12)$$

which also suggests that the mass of the black hole should scale as

$$M \simeq \sqrt{N} M_{\text{Pl}}, \quad (27.13)$$

or equivalently $M \simeq N \epsilon_{\text{G}}$.

From the perspective of condensed matter physics, the quantity $g = \alpha_{\text{G}} N$ represents the collective coupling of the system. Hence, the condition (27.10) tells us that, whereas the constituents of the bound state interact very weakly with each other through the coupling $\alpha_{\text{G}} \simeq 1/N \ll 1$, the collective interaction $g \simeq 1$ is indeed strong. The system is therefore at its quantum *critical point*, meaning that its constituents will tend to leak out because of (however small) quantum fluctuations. The peculiar feature of this leaking of gravitons out of the black hole is that the system still remains at the critical point throughout the whole depletion process (at least until the gravitational interaction is no longer able to overcome the internal quantum pressure generated by the confined matter [23]). This description therefore offers a way to produce the Hawking process [24] as the result of the quantum depletion [16–18, 25] rather than a pure vacuum effect. In detail, let us focus on a tree-level $2 \rightarrow 2$ scattering between two gravitons within the marginally bound state. Assuming that one of them gains enough energy to escape the ground state, we can then naively estimate the decay rate of the system as

$$\Gamma \sim \alpha_{\text{G}}^2 N(N-1) \frac{\epsilon_{\text{G}}}{\hbar}, \quad (27.14)$$

where α_{G}^2 comes from the two vertices of the scattering process, $N(N-1)$ is a combinatorial factor that accounts for the fact that each constituent interacts with the remaining $N-1$ gravitons in the bound state, and ϵ_{G} is the scale of the momentum transfer. From the criticality condition (27.10) and the scaling of ϵ_{G} in (27.11), we find

$$\Gamma \simeq \frac{1}{\sqrt{N} \ell_{\text{Pl}}} + \mathcal{O}\left(\frac{1}{N^{3/2} \ell_{\text{Pl}}}\right), \quad (27.15)$$

which leads to the master equation for the quantum depletion

$$\dot{N} \simeq -\Gamma \simeq -\frac{1}{\sqrt{N} \ell_{\text{Pl}}} + \mathcal{O}\left(\frac{1}{N^{3/2} \ell_{\text{Pl}}}\right). \quad (27.16)$$

As discussed above, the quantum criticality of the system also relates the total mass of a black hole to the number of constituents of the bound state. Hence, from (27.13), we can rephrase the depletion law (27.16) in terms of the mass M , which yields

$$\dot{M} \sim -\frac{M_{Pl}^3}{\ell_{Pl} M^2} \sim -\frac{T_H^2}{\hbar}, \quad (27.17)$$

with $T_H \simeq \hbar/G_N M \simeq \epsilon_G$. In other words, the quantum depletion acts as a corpuscular precursor of the Hawking process and it reduces to the latter in the semi-classical limit (i.e., for $N \rightarrow \infty$, $\ell_{Pl} \rightarrow 0$, and $\sqrt{N}\ell_{Pl} = \text{constant}$).

Applying the HQM to this model, we finds that the expectation value of the gravitational radius is very close to the classical one and that the fluctuations are suppressed according to $\Delta R_H/R_H \sim 1/N$. Indeed, let us consider, for the sake of simplicity, a collection of N marginally bound scalar particles acting as ‘‘toy gravitons’’. The marginally bound condition can be implemented at the level of the single-particle Hilbert space by requiring that each particle’s spectrum contain: i) a ground state $|\epsilon\rangle$ of energy $\epsilon = M_{Pl}/\sqrt{N}$; ii) a continuous part of quasi-gapless excitations $|\omega_i\rangle$, meant to model the depleted states. Then, since the collective state sources the deformation of the spacetime, the single-particle wave-function for each constituent toy graviton reads

$$|\Psi_S^{(i)}\rangle = \frac{|\epsilon\rangle + \gamma |\psi_c^{(i)}\rangle}{\sqrt{1 + \gamma^2}}, \quad (27.18)$$

with

$$|\psi_c^{(i)}\rangle = \int_{\epsilon}^{\infty} d\omega_i f_i(\omega_i|\epsilon) |\omega_i\rangle, \quad (27.19)$$

where $f_i(\omega_i|\epsilon)$ represents the energy distribution function for the states in the continuous part of the spectrum and $\gamma \geq 0$ denotes the likelihood of a constituent to be in the continuum. The N -particle wave-function of the system is given by the symmetrised tensor product

$$|\Psi_S\rangle = \bigotimes_{i=1, \dots, N}^S |\Psi_S^{(i)}\rangle. \quad (27.20)$$

The total Hamiltonian \widehat{H} will correspondingly have a spectrum that can be split into a discrete part $|M\rangle = \otimes^S |\epsilon\rangle$, such that $\widehat{H}|M\rangle = M|M\rangle = N\epsilon|M\rangle$, and a continuous part $|E\rangle$, with $\widehat{H}|E\rangle = E|E\rangle$ and $E > M$. If we then model $f_i(\omega_i|\epsilon)$ with a thermal spectrum at a temperature $T \simeq \epsilon$, we find that

$$\frac{\Delta R_H}{R_H} \sim \frac{1}{N}, \quad (27.21)$$

which means that for a black hole of large mass $M \simeq \sqrt{N} M_{Pl} \gg M_{Pl}$ the quantum corrections to the classical results are suppressed by a very small factor of order $1/N$.

27.3 Gravitational Collapse

A more precise derivation of (27.10), based on the Hamiltonian formulation of gravity, was provided in [26], where the Newtonian potential was explicitly described as a coherent state of many soft virtual gravitons [27]. More precisely, let us consider a spherically symmetric distribution of matter of radius R and total mass M . In General Relativity we know that the Hamiltonian constraint for an asymptotically flat spacetime reads

$$H = H_G + H_m = M , \quad (27.22)$$

with H_G and H_m representing the (super-)Hamiltonian of gravity and matter, respectively. Since we are interested in the gravitational collapse, let us prepare the distribution of matter in such a way that, in its initial configuration, all the components are infinitely far apart from each other. In other words, in the initial configuration the gravitational interaction is negligible and $H_{in} \simeq M$. As the system shrinks down to the size R , assuming we can neglect the contribution of any emission of radiation, the total energy in the final configuration reads

$$H(R) \simeq M + K_m(R) + U_{\text{Grav}}(R) + U_P(R) , \quad (27.23)$$

with $K_m(R)$ the total kinetic energy of the matter content, $U_{\text{Grav}}(R) \leq 0$ accounts for the gravitational interaction, and $U_P(R) \geq 0$ describes any non-gravitational repulsive effects (e.g., Pauli exclusion principle). At the corpuscular level we can split $U_{\text{Grav}}(R)$ into two contributions

$$U_{\text{Grav}}(R) = U_G(R) + U_{\text{GG}}(R) , \quad (27.24)$$

with $U_G(R)$ keeping track of the gravitational interaction among the matter constituents mediated by gravitons and $U_{\text{GG}}(R)$ representing the energy content due to the gravitons self-interactions. At leading order, we can approximate $U_G(R)$ with the Newtonian potential energy

$$U_G(R) \simeq M V_N(R) \simeq -\frac{G_N M^2}{R} . \quad (27.25)$$

From a field-theoretic perspective, the Newtonian potential can be understood as a coherent state of $N \simeq M^2/M_{\text{Pl}}^2$ soft virtual gravitons with typical size $\lambda_G \simeq R$. Hence, in this picture $U_G(R) \simeq -N \epsilon_G$. Since gravitons self-interact, we can then estimate $U_{\text{GG}}(R)$ as the energy due to the interaction between each constituent graviton with the collective state,

$$U_{\text{GG}}(R) \simeq N(-\epsilon_G(R))V_N(R) \simeq \frac{G_N^2 M^3}{R^2} , \quad (27.26)$$

which clearly resembles a *post-Newtonian correction*. Taking the limit $R \rightarrow R_H$, we obtain

$$U_{GG}(R_H) \simeq -U_G(R_H) \simeq M, \quad (27.27)$$

which implies the quantum criticality condition (27.10) and the scaling of the typical momenta of the constituent gravitons (27.11).

27.4 Bootstrapping Newton

A refinement of this study was then presented in [28], where an effective theory for the gravitational potential of a static spherically symmetric distribution of matter was investigated with the addition of a term accounting for the interaction of each graviton with the collective state. Specifically, we can start from the Einstein–Hilbert action for some minimally coupled matter fields

$$S = \int d^4x \sqrt{-g} \left[-\frac{R}{16\pi G_N} + \mathcal{L}_m \right]. \quad (27.28)$$

Linearising the action and considering static, non-relativistic, and spherically symmetric matter profiles characterised by an energy density $\rho = \rho(r)$, we find a Lagrangian of the form

$$L_N[V_N] \simeq -4\pi \int_0^\infty r^2 dr \left[\frac{(\partial_r V_N)^2}{8\pi G_N} + \rho V_N \right], \quad (27.29)$$

which clearly leads to the Poisson equation and

$$H_N[V_N]|_{\text{on-shell}} = -L_N[V_N]|_{\text{on-shell}} \sim \int_0^R r^2 dr \rho(r) V_N(r), \quad (27.30)$$

as expected. This allows us to make the identification $U_G(R) \sim H_N[V_N]|_{\text{on-shell}}$ at the leading order of the approximation. At the next-to-leading order, we acquire

$$\begin{aligned} L_{\text{NLO}}[V] &\simeq -4\pi \int_0^\infty r^2 dr \left[\frac{(\partial_r V)^2}{8\pi G_N} (1 - 4V) + \rho V (1 - 2V) \right] \\ &\simeq L_N[V] - 4\pi \int_0^\infty r^2 dr [J_V V + J_\rho \rho], \end{aligned} \quad (27.31)$$

with $J_V = -(\partial_r V)^2/(2\pi G_N)$ denoting the gravitational current and $J_\rho = -2V^2$ representing the higher-order correction to the matter part. Note that the self-sourcing feature, at the heart of the corpuscular model, manifests itself through $J_V \sim (\partial_r V)^2$.

The corresponding field equation then reads

$$\Delta V = 4\pi G_N \rho + \frac{2(\partial_r V)^2}{1 - 4V}, \quad (27.32)$$

and the corresponding next-to-leading-order expansion of the Hamiltonian functional, computed on-shell, is therefore given by

$$H_{\text{NLO}}[V]|_{\text{on-shell}} \sim \int_0^\infty r^2 dr \left[\rho V(1 - 4V) - \frac{3(\partial_r V)^2 V}{2\pi G_N} \right]. \quad (27.33)$$

The first term in the square brackets contains information about ρ and can be understood as the gravitational energy of the matter constituents mediated by gravitons,

$$U_G(R) \sim \int_0^R r^2 dr \rho V(1 - 4V), \quad (27.34)$$

whereas the second term keeps track of the self-sourcing and can be interpreted as the energy associated with the gravitons self-interaction, namely

$$U_{GG}(R) \sim -\frac{3}{2\pi G_N} \int_0^R r^2 dr (\partial_r V)^2 V. \quad (27.35)$$

The classical analogue of the criticality condition (27.27) is recovered for $H_{\text{NLO}}[V]|_{\text{on-shell}} \simeq 0$, that for some well-behaved matter distributions leads to $R \sim R_H$.

From a quantum-mechanical perspective, denoting by $\Phi = V/\sqrt{G_N}$ and $J_m = 4\pi\sqrt{G_N}\rho$, (27.31) leads to an effective scalar field theory defined by the Lagrangian

$$L[\Phi] = 4\pi \int_0^\infty r^2 dr \left[\frac{1}{2} \Phi \square \Phi - J_m \Phi(1 - 2\sqrt{G_N}\Phi) + 4\pi\sqrt{G_N}(\partial_\mu \Phi)^2 \Phi \right]. \quad (27.36)$$

Considering the linear order and recalling that $\Phi = \Phi(r)$, we then obtain the classical field equation

$$\Delta \Phi = J_m, \quad (27.37)$$

as mentioned above. Then, we can construct a *coherent state* $|g\rangle$ such that

$$\langle g | \widehat{\Phi} | g \rangle = \Phi(r), \quad (27.38)$$

namely a state that reproduces the classical behaviour, and is defined by

$$\widehat{a}_k |g\rangle = e^{i\gamma_k(t)} g_k |g\rangle, \quad g_k = -\frac{\widetilde{J}_m(k)}{\sqrt{2\hbar k^3}}. \quad (27.39)$$

We can easily infer the total occupation number for such a state, which reads

$$N \simeq \int_0^\infty \frac{k^2 dk}{2\pi^2} |g_k|^2 \sim \frac{M^2}{M_{Pl}^2} \log\left(\frac{R_\infty}{R}\right), \quad (27.40)$$

where we considered the case of a source of mass M and spatial extension R , while R_∞ denotes an infrared cut-off related to the size of the Universe. In other words, we have shown that the Newtonian potential can be recovered from a coherent state of scalar toy gravitons and that the occupation number of this state scales holographically with the size of the horizon. This justifies the naive arguments in the previous section.

It is then interesting to consider what sort of modification of this coherent state would allow us to also reproduce the post-Newtonian correction, that is

$$\sqrt{G_N} \langle g' | \hat{\Phi} | g' \rangle = V_N(r) + V_{PN}(r), \quad (27.41)$$

with $|g'\rangle \simeq \mathcal{N}(|g\rangle + |\delta g\rangle)$ such that $\hat{a}_k |g\rangle = g_k |g\rangle + \delta g_k |\delta g\rangle$. It turns out that, assuming that most of the toy gravitons belong to one mode $\bar{k} \simeq R$, we find

$$\delta g_k \sim \delta g_{\bar{k}} \sim -\ell_{Pl} \bar{k}^{5/2} |g_{\bar{k}}|^2, \quad (27.42)$$

with $\bar{k} \sim 1/R$.

A further improvement of this model was then carried out in [29, 30], with the aim of understanding the effects of the matter pressure in this simplified setting. This last approach was termed *bootstrapped Newtonian gravity* and can be understood as an explicit effective implementation for investigating the classicalisation of the gravitational interaction. In more detail, if we are interested in describing general compact objects, the sole energy density ρ of a non-relativistic matter distribution is not enough to give a substantial insight on the fundamental physics governing the gravitational collapse. The simplest way to go beyond this restriction consist of introducing a pressure term in the model. To this aim, we can replace the Lagrangian (27.31) with

$$L_{BN}[V] \simeq L_N[V] - 4\pi \int_0^\infty r^2 dr [J_V V + J_\rho (\rho + p)], \quad (27.43)$$

where we replaced $\rho \rightarrow \rho + p$ in order to add a pressure p that satisfies $\partial_r p = -(\partial_r V)(\rho + p)$. Most notably, for this model it was found that a finite value of the pressure can support sources of arbitrarily large compactness $\mathcal{C} \equiv G_N M/R$, thus concluding that there is no equivalent of the Buchdahl limit in this effective model. Note that, even though the strong energy condition is preserved in the limit $\mathcal{C} \gg 1$, the dominant energy condition is violated in this regime. This is rather consistent with the idea that a high-compactness configuration should be sourced by a system in a fully quantum regime.

27.5 Quantum Compositeness of Gravity at Cosmological Scales

Similar arguments to the one presented for black holes can be applied to cosmological spaces [20, 31]. Indeed, as argued in [32], this can be achieved by recalling that the Friedmann equation provides the Hamiltonian constraint for cosmology, allowing us to extend the arguments in [26] to such spaces. More precisely, the Friedmann equation

$$H^2 = \left(\frac{\dot{a}}{a}\right)^2 = \frac{8\pi G_N}{3} \rho_m \quad (27.44)$$

implements the Hamiltonian constraint for Robertson-Walker geometries, namely it corresponds to

$$\mathcal{H} = \mathcal{H}_G + \mathcal{H}_m = 0, \quad (27.45)$$

where the total Hamiltonian $H_{\text{Tot}} \sim \mathcal{N}(t) \mathcal{H}$, with $\mathcal{N}(t)$ the lapse function.

Now, considering the de Sitter solution of the Einstein field equations with a cosmological constant Λ , we find

$$H^2 = \left(\frac{\dot{a}}{a}\right)^2 = \frac{8\pi G_N}{3} \rho_\Lambda, \quad \rho_\Lambda = \frac{\Lambda}{8\pi G_N}, \quad (27.46)$$

which corresponds to an exponentially growing scale factor leading to a spacetime with an horizon at

$$L_\Lambda = \sqrt{\frac{3}{\Lambda}}. \quad (27.47)$$

Upon integrating (27.46) over the volume inside L_Λ , we obtain

$$L_\Lambda \simeq G_N L_\Lambda^3 \rho_\Lambda \simeq G_N M_\Lambda, \quad (27.48)$$

with $M_\Lambda \simeq L_\Lambda^3 \rho_\Lambda$ denoting the fraction of dark energy contained within this volume. This last expression is akin to the one for the gravitational radius for a Schwarzschild black hole. Thus, we are tempted to try and extend the same Hamiltonian analysis carried out for black holes and compact objects to the case of cosmological spaces. To this aim, let us consider a universe filled only with dark energy (considered as a purely gravitational effect), i.e., $\mathcal{H}_m = 0$. Then, we are left with the constraint

$$\mathcal{H} = \mathcal{H}_G \simeq 0. \quad (27.49)$$

In the corpuscular picture we can split \mathcal{H}_G into two contributions:

(i) the energy associated with the coherent state of N marginally bound gravitons,

$$U_G \simeq -N\epsilon_G \simeq -N \frac{\hbar}{L_\Lambda}; \quad (27.50)$$

(ii) the energy due to the gravitational interaction of each constituent with the collective (Newtonian) potential generated by the remaining $N - 1$ quanta,

$$U_{GG} \simeq -N\epsilon_G V_N(L_\Lambda) \simeq N^{3/2} \frac{\hbar \ell_{Pl}}{L_\Lambda^2}. \quad (27.51)$$

Hence, the Hamiltonian constraint reads

$$\mathcal{H} = \mathcal{H}_G \simeq U_G + U_{GG} \simeq 0, \quad (27.52)$$

and yields

$$L_\Lambda \simeq \sqrt{N} \ell_{Pl}. \quad (27.53)$$

This also implies the criticality condition (27.10), since

$$\epsilon_\Lambda \simeq \frac{\hbar}{L_\Lambda} \simeq \frac{M_{Pl}}{\sqrt{N}}, \quad (27.54)$$

hence $\alpha_G = \epsilon_G^2/M_{Pl}^2 \simeq 1/N$, as in the case of black holes. This allows interpretation of the de Sitter space and, in general, any cosmological spacetime as the result of a bound state of a large number of soft virtual gravitons. The peculiarity of the (quasi) de Sitter case is that gravitons in it should be at a critical point.

Along this line of reasoning, if we assume that the quasi-de Sitter state, which is usually employed to model the inflationary phase of the Universe, is the result of a marginally bound configuration of a large number of soft off-shell gravitons, it is possible to show that the Starobinsky model [33, 34] naturally emerges from the corpuscular picture without the need of an inflaton field [32, 35]. Besides, if one also takes into account the effect of the quantum depletion, it turns out that the pure de Sitter space is excluded at the quantum mechanical level [32, 36, 37]. On a different note, if one applies the corpuscular theory to model the late-time large scale structure of the Universe, some of the phenomena, usually explained by assuming the existence of *dark matter*, can be simply understood as the response of a cosmological reservoir of gravitons, responsible for the accelerated expansion, to the presence of local impurities, namely baryonic matter [38–40].

27.6 Outlook

There are three main directions of development for the above project, respectively, regarding:

- (a) compact astrophysical sources and black holes;
- (b) cosmological models of the early and present Universe, and
- (c) the fundamental classicalisation of the gravitational interaction.

First of all, the bootstrapped Newtonian model of compact sources appears amenable to further investigate the quantum corpuscular nature of very compact astrophysical sources and their transition to black hole states. From the more theoretical point of view, we expect to deepen our understanding of the nature of real black holes by continuing to refine the quantum description of the bootstrapped potential generated by static sources in the form of coherent states of gravitons. On the more phenomenological side, we expect that the implementation of specific equations of state to describe the matter source will lead to differences with respect to the predictions of General Relativity.

From the cosmological point of view, the effective dark matter phenomenology obtained as a reaction of the cosmological (quasi) de Sitter condensate to the presence of localised matter sources will benefit from a more detailed description of the latter. *Vice versa*, the unified description of the bootstrapped potential for local sources in terms of a coherent state built out of gravitons in the cosmological condensate might shed more light on the nature of both dark matter and black holes.

Finally, pushing the model of compact sources to their quantum limit, roughly defined as states with a small number of gravitons in the bootstrapped gravitational potential, should provide an explicit construction of the classicalisation process and the final stages of black hole evaporation, as well as a way to clarify the role played by the matter.

References

1. S.W. Hawking, R. Penrose, The singularities of gravitational collapse and cosmology. *Proc. Roy. Soc. Lond. A* **314**, 529–548 (1970)
2. S. Hossenfelder, Minimal length scale scenarios for quantum gravity. *Living Rev. Rel.* **16**, 2 (2013). [arXiv:1203.6191](#)
3. R. Casadio, *Localised Particles and Fuzzy Horizons: A Tool for Probing Quantum Black Holes*. [arXiv:1305.3195](#)
4. R. Casadio, F. Scardigli, Horizon wave-function for single localized particles: GUP and quantum black hole decay. *Eur. Phys. J. C* **74**(1), 2685 (2014). [arXiv:1306.5298](#)
5. R. Casadio, A. Giugno, O. Micu, Horizon quantum mechanics: A hitchhiker’s guide to quantum black holes. *Int. J. Mod. Phys. D* **25**(02), 1630006 (2016). [arXiv:1512.04071](#)
6. R. Casadio, A. Giugno, A. Giusti, Global and local horizon quantum mechanics. *Gen. Rel. Grav.* **49**(2), 32 (2017). [arXiv:1605.06617](#)
7. R. Casadio, O. Micu, F. Scardigli, Quantum hoop conjecture: black hole formation by particle collisions. *Phys. Lett. B* **732**, 105–109 (2014). [arXiv:1311.5698](#)

8. R. Casadio, O. Micu, D. Stojkovic, Horizon wave-function and the quantum cosmic censorship. *Phys. Lett. B* **747**, 68–72 (2015). [arXiv:1503.02858](#)
9. R. Casadio, O. Micu, D. Stojkovic, Inner horizon of the quantum Reissner-Nordström black holes. *JHEP* **05**, 096 (2015). [arXiv:1503.01888](#)
10. R. Casadio, A. Giugno, A. Giusti, O. Micu, Horizon quantum mechanics of rotating black holes. *Eur. Phys. J. C* **77**(5), 322 (2017). [arXiv:1701.05778](#)
11. A. Giugno, A. Giusti, A. Helou, Horizon quantum fuzziness for non-singular black holes. *Eur. Phys. J. C* **78**(3), 208 (2018). [arXiv:1711.06209](#)
12. R. Casadio, A. Giugno, A. Giusti, M. Lenzi, Quantum formation of primordial black holes. *Gen. Rel. Grav.* **51**(8), 103 (2019). [arXiv:1810.05185](#)
13. R. Casadio, O. Micu, Horizon quantum mechanics of collapsing shells. *Eur. Phys. J. C* **78**(10), 852 (2018). [arXiv:1806.05944](#)
14. G. Dvali, C. Gomez, Black hole’s quantum N-portrait. *Fortsch. Phys.* **61**, 742–767 (2013). [arXiv:1112.3359](#)
15. G. Dvali, C. Gomez, Black hole’s 1/N hair. *Phys. Lett. B* **719**, 419–423 (2013). [arXiv:1203.6575](#)
16. G. Dvali, C. Gomez, Black holes as critical point of quantum phase transition. *Eur. Phys. J. C* **74**, 2752 (2014). [arXiv:1207.4059](#)
17. R. Casadio, A. Giugno, A. Orlandi, Thermal corpuscular black holes. *Phys. Rev. D* **91**(12), 124069 (2015). [arXiv:1504.05356](#)
18. R. Casadio, A. Giugno, O. Micu, A. Orlandi, Thermal BEC black holes. *Entropy* **17**, 6893–6924 (2015). [arXiv:1511.01279](#)
19. R. Casadio, A. Giusti, J. Mureika, Lower dimensional corpuscular gravity and the end of black hole evaporation. *Mod. Phys. Lett. A* **34**(22), 1950174 (2019). [arXiv:1805.10444](#)
20. A. Giusti, On the corpuscular theory of gravity. *Int. J. Geom. Meth. Mod. Phys.* **16**(03), 1930001 (2019)
21. R. Casadio, A. Giugno, O. Micu, A. Orlandi, Black holes as self-sustained quantum states, and Hawking radiation. *Phys. Rev. D* **90**(8), 084040 (2014). [arXiv:1405.4192](#)
22. G. Dvali, G.F. Giudice, C. Gomez, A. Kehagias, UV-completion by classicalization. *JHEP* **08**, 108 (2011). [arXiv:1010.1415](#)
23. R. Casadio, A. Giusti, The role of collapsed matter in the decay of black holes. *Phys. Lett. B* **797**, 134915 (2019). [arXiv:1904.12663](#)
24. S.W. Hawking, Particle creation by black holes. *Commun. Math. Phys.* **43**(167), 199–220 (1975)
25. W. Mück, Hawking radiation is corpuscular. *Eur. Phys. J. C* **76**(7), 374 (2016). [arXiv:1606.01790](#)
26. R. Casadio, A. Giugno, A. Giusti, Matter and gravitons in the gravitational collapse. *Phys. Lett. B* **763**, 337–340 (2016). [arXiv:1606.04744](#)
27. W. Mück, On the number of soft quanta in classical field configurations. *Can. J. Phys.* **92**(9), 973–975 (2014). [arXiv:1306.6245](#)
28. R. Casadio, A. Giugno, A. Giusti, M. Lenzi, Quantum corpuscular corrections to the Newtonian potential. *Phys. Rev. D* **96**(4), 044010 (2017). [arXiv:1702.05918](#)
29. R. Casadio, M. Lenzi, O. Micu, Bootstrapping Newtonian gravity. *Phys. Rev. D* **98**(10), 104016 (2018). [arXiv:1806.07639](#)
30. R. Casadio, M. Lenzi, O. Micu, Bootstrapped Newtonian stars and black holes. *Eur. Phys. J. C* **79**(11), 894 (2019). [arXiv:1904.06752](#)
31. G. Dvali, C. Gomez, Quantum compositeness of gravity: black holes. *JCAP* **1401**, 023 (2014). [arXiv:1312.4795](#)
32. R. Casadio, A. Giugno, A. Giusti, Corpuscular slow-roll inflation. *Phys. Rev. D* **97**(2), 024041 (2018). [arXiv:1708.09736](#)
33. A.A. Starobinsky, A new type of Isotropic Cosmological models without singularity. *Adv. Ser. Astrophys. Cosmol.* **3**, 130–133 (1987)
34. A.A. Starobinsky, Spectrum of relict gravitational radiation and the early state of the universe. *JETP Lett.* **30**, 682–685 (1979). (*Pisma Zh. Eksp. Teor. Fiz.* **30**, 719 (1979); 767 (1979))

35. A. Giugno, A. Giusti, Domestic corpuscular inflaton. *Int. J. Geom. Meth. Mod. Phys.* **16**(07), 1950108 (2019). [arXiv:1806.11168](https://arxiv.org/abs/1806.11168)
36. G. Dvali, C. Gomez, On exclusion of positive cosmological constant. *Fortsch. Phys.* **67**(1–2), 1800092 (2019). [arXiv:1806.10877](https://arxiv.org/abs/1806.10877)
37. R. Casadio, A. Giugno, A. Giusti, V. Faraoni, Is de Sitter space always excluded in semiclassical $f(R)$ gravity? *JCAP* **1906**(06), 005 (2019). [arXiv:1903.07685](https://arxiv.org/abs/1903.07685)
38. M. Cadoni, R. Casadio, A. Giusti, W. Mück, M. Tuveri, Effective fluid description of the dark universe. *Phys. Lett. B* **776**, 242–248 (2018). [arXiv:1707.09945](https://arxiv.org/abs/1707.09945)
39. M. Cadoni, R. Casadio, A. Giusti, M. Tuveri, Emergence of a dark force in corpuscular gravity. *Phys. Rev. D* **97**(4), 044047 (2018). [arXiv:1801.10374](https://arxiv.org/abs/1801.10374)
40. M. Tuveri, M. Cadoni, Galactic dynamics and long-range quantum gravity. *Phys. Rev. D* **100**(2), 024029 (2019). [arXiv:1904.11835](https://arxiv.org/abs/1904.11835)

Part III
Cosmology and Observational
Discriminators

Chapter 28

Introduction to Part III



Ruth Lazkoz and Vincenzo Salzano

The contributions that can be found in this section are aimed to characterise what has been the main nature of the Working Group 3 (WG3) within the CANTATA Cost Action: a “cross-group”, a link between members and participants from all working groups. Although the main footprint of the WG3 has always been strictly connected to the *direct* use of observations, the interplay and the close synergy with WG1 and WG2 has characterised the hybrid nature of its scientific outcomes, where theory and data analysis have never gone on separate roads, but have been always interconnected.

The contributions from this chapter are no exception to this rule. We have decided to select those scientists whose research trajectory might somehow summarise part of the scientific investigation that has been performed under CANTATA coverage, who have explored new interesting ways to test gravity, and who could outline a sort of road map to follow in the very near future, which looks very promising for observational cosmology. In forthcoming years we expect many terrestrial and space-based advanced surveys to be launched and/or become fully operative (among them, *Euclid* and SKA), throwing us directly into a new highly-upgraded era of *precision cosmology*. All of them will provide us with data of unprecedented precision about the large-scale structure, giving us the possibility for very accurate tests of gravity (and modified gravity theories, specifically) on scales spanning many orders of magnitude. A *phenomenological* summary of all the possible insights we can gain from using these data will be provided in Chap. 29. One of the main outputs of the above mentioned surveys will be, among other things, data related to the clustering of

R. Lazkoz (✉)

Department of Theoretical Physics, University of the Basque Country UPV/EHU,
P.O. Box 644, 48080 Leioa, Spain

V. Salzano

Institute of Physics, University of Szczecin, Wielkopolska 15, 70-451 Szczecin, Poland
e-mail: vincenzo.salzano@usz.edu.pl

galaxies. In Chap. 30, we have left our contributor to explore some more subtle effects, which might influence those data, i.e., *relativistic effects* on the number counts, which emerge as powerful complementary tool, to be used in addition to more standard and well-established ones.

A further distinctive element that has characterised the activity of this WG is the research performed on the numerical and computational side. In Chap. 31 we have a clear example of the entanglement between theory and numerics: the contributors introduce a theoretical framework, the Effective Field Theory, which has become very fruitful in recent years by providing interesting and stringent constraints on both (standard) dark energy models and modified gravity theories, thanks mainly to some numerical codes (now widely used in the cosmological community), which have been developed and improved by the same members of CANTATA, and which have helped to optimise the calculation of the most important quantities that are needed to apply such framework to real data in particular, cosmological perturbations.

Sticking more closely to the observational arena, we have to point out that the cosmological debate nowadays is particularly heated up by the so-called *observational tensions*, namely, statistically-grounded conflicts between different, complementary probes. The most (in)famous is the H_0 *tension*, based on a discrepancy between the measurement of the expansion rate of our Universe performed locally (by means of Cepheids and Type Ia Supernovae) and the same quantity inferred from cosmological analysis using high redshift/early times data (the Cosmic Microwave Background radiation as measured by the most update project in that field, the *Planck* telescope). This topic is dealt with in Chap. 32. The other less frequently reported tension, but equally controversial and decisive, is the so-called σ_8 *tension*: again, a statistically significant discordance is found when comparing the estimation of this parameter (related to matter density fluctuations, thus, to the evolution of cosmological perturbations) from *Planck* with low redshift data from galaxy clustering. This problem is discussed more closely in Chap. 33.

A special role in this series of contributions has been necessarily devoted to a field which, although old in its theoretical background and in its practical design, has reached full maturity only in the most recent years, eventually accomplishing extraordinary results (the Physics Nobel Prize in 2017): *gravitational wave astronomy*. A full section, Chap. 34, is devoted to the enormous implications that this field has on constraining alternative theories of gravity and on the future role played by gravitational waves astronomy in our understanding of how gravity works. Another kind of observational data that seems to be very promising in this perspective is *cosmological weak lensing*. Although not as new as the previous one, this is a very sensitive and hard-to-retrieve probe, which will become crucial in the near future, thanks to some of the surveys we have introduced above, which will be accurate enough, and will observe such a huge amount of galaxies as to make it feasible at unique levels. A discussion about weak lensing will be found on Chap. 35.

Finally, our two last contributions will focus not on cosmological scales, nor on the statistical properties of the gravitational structures, but will describe which constraints or information about modifications of gravity can be derived from analysing clusters of galaxies and galaxies as single objects. In Chap. 36, the focus of the atten-

tion is galaxy clusters, the largest clearly-observable self-gravitating structures for which we can retrieve multi-messenger astronomical data covering a wide range of wavelengths and complementary information. Instead, in Chap. 37, we will mainly use numerical simulations to study possible characteristic features that should be imprinted in galaxies and clusters of galaxies by modified gravity theories, and which could help to eventually discriminate among General Relativity and alternative gravities.

Chapter 29

Phenomenological Tests of Gravity on Cosmological Scales



Yashar Akrami  and Matteo Martinelli 

29.1 Cosmological Tests of Gravity

The late-time accelerated expansion of the Universe [1, 2] (see Refs. [3–6] for recent comprehensive reviews on the subject) is still a mystery and needs to be addressed by theoretical physics. This cosmic acceleration could be driven by the cosmological constant or some dynamical dark energy, or could be a consequence of deviations from General Relativity (GR); see, e.g., Refs. [7–11] for reviews.

There are reasons to believe that GR may not be the ultimate theory of gravity on large scales, and despite its striking and continued observational successes, there is a persistent interest in extending GR at cosmological scales. The need for unknown ingredients of dark matter and dark energy to explain the observed cosmic evolution, and the unsolved and related *problem of the cosmological constant* [12, 13], all suggest that gravity might be different in the infrared (IR), as it should be in the ultraviolet (UV) in the quest for a theory of quantum gravity. More importantly, GR has been verified only over a surprisingly small range of scales, and there is no reason to presume its validity on all scales; the theory *has* to be tested in all regimes in order to avoid unjustified extrapolation. Finally, if GR is “the” theory of gravity on large scales, we want to know what makes it so special, why gravity is described by only massless spin-2 particles, and why other degrees of freedom are forbidden in the gravitational sector.

Several alternative (or modified) theories of gravity on the cosmological scales have been proposed, some of which are able to explain cosmic acceleration [7–11]. While the efforts for building new models continue and the existing cosmological

Y. Akrami (✉)

Département de Physique, École Normale Supérieure, 24 Rue Lhomond, 75005 Paris, France
e-mail: akrami@ens.fr

M. Martinelli

Instituto de Física Teórica, Cátedra de Física Teórica UAM-CSI, Campus de Cantoblanco, E-28049 Madrid, Spain
e-mail: matteo.martinelli@uam.es

© The Author(s), under exclusive license to Springer Nature Switzerland AG 2021
E. N. Saridakis et al. (eds.) *Modified Gravity and Cosmology*,
https://doi.org/10.1007/978-3-030-83715-0_29

425

surveys have already provided us with important constraints on modified theories of gravity, several upcoming surveys are expected to eventually pin down the nature of gravity. There have been remarkable efforts in performing systematic studies of gravity beyond GR on large scales, and various techniques have been developed for testing the models in different regimes in connection with the wealth of information that is expected to be provided by the upcoming surveys, especially those observing the large-scale structure (LSS) of the Universe.

We are all excited by the recent milestones that observations of gravitational waves (GWs) [14, 15] and black-hole images have marked for physics, especially their strong implications for theories of gravity, many of which are now significantly disfavoured or constrained by GWs [16–34] (see also Refs. [35–39])—this is perhaps a call to go back to the basics, and rethink the justifications behind the models of gravity that we have constructed over the past two decades. The incredible knowledge that GWs have provided and will continue to provide will, however, need to be complemented by the precision measurements of the LSS, as one undoubtedly leading cosmological probe in coming years, in order to achieve a full understanding of gravity.

Cosmological surveys probe gravitational interactions in a large range of scales and in different regimes; the larger the scale of interest, the more linear the evolution and growth of the cosmological structure. We can therefore define four regimes of cosmological interest that can be probed by LSS surveys: *ultra-large scales*, i.e., scales that are comparable to the size of the horizon with the structure that can be treated linearly, *intermediate scales* that are well inside the horizon but are still linear, subhorizon scales that are *mildly nonlinear*, and very small scales where the structure is *fully nonlinear*, i.e., the regime in which linear perturbation theory breaks down completely. In the next subsections, we focus on the first two regimes, where the cosmological structure is studied through the theory of linear perturbations. We then briefly discuss the mildly and fully nonlinear regimes in Sect. 29.1.4.

29.1.1 *Large Scales and the Linear Regime: Phenomenological Departures from GR*

On sufficiently large scales, we can apply the theory of linear cosmological perturbations to the large-scale structure of the Universe. This can be done by perturbing the Friedman-Lemaître-Robertson-Walker (FLRW) metric as (in the Newtonian gauge)

$$g_{\mu\nu} = \text{diag}[-(1 + 2\Psi), a^2(1 - 2\Phi)\delta_{ij}], \quad (29.1)$$

where Φ and Ψ are the so-called gravitational (or Bardeen) potentials and a is the scale factor of the Universe. The energy densities and pressures of different components X are also perturbed,

$$\rho_X = \bar{\rho}_X(1 + \delta_X) \quad \text{and} \quad p_X = \bar{p}_X(1 + \delta_X^p), \quad (29.2)$$

where $\bar{\rho}_X$ and \bar{p}_X are, respectively, the background density and pressure for the component X . In GR, we can combine the 00 and 0*i* components of the linearised Einstein equations to obtain the so-called (cosmological) *Poisson equation* for a mode k in Fourier space,

$$-k^2 \Psi = \frac{\kappa^2}{2} \delta^* \rho, \quad (29.3)$$

where

$$\delta^* \rho = \sum_X \bar{\rho}_X \left[\delta_X + 3(1 + w_X) \frac{H}{a} \frac{\theta_X}{k^2} \right], \quad (29.4)$$

with $\kappa^2 = 8\pi G$ the gravitational constant, H the Hubble parameter, and $\theta_X = \nabla \cdot \mathbf{v}_X$, where \mathbf{v}_X is the peculiar velocity for the component X with the equation of state parameter w_X . The traceless, transverse component of the Einstein equations yields the so-called *slip relation*,

$$\Phi - \Psi = 0. \quad (29.5)$$

Equations (29.3) and (29.5), together with the perturbed conservation equations for the components X , fully describe the cosmological evolution at the linear level in standard cosmology.

In theories of gravity beyond GR, the forms of Eqs. (29.3) and (29.5) are modified in general, as new degrees of freedom enter the perturbation equations. In order to study the evolution of structure in modified gravity, one can derive similar linearised equations for any models of interest and use those equations to constrain the models by observations. One can also work with theoretically motivated parameterisations of deviations from GR, e.g., through the effective field theory (EFT) of dark energy and modified gravity [40–44] or covariant parameterisations such as in Horndeski theory and beyond [45]. Here, however, we focus on a popular phenomenological parameterisation directly at the level of the linearised Einstein equations, i.e., the Poisson equation and the slip relation, Eqs. (29.3) and (29.5). We later discuss the advantages and disadvantages of this approach.

Let us start with subhorizon and linear perturbations, where the so-called *quasi-static approximation* is valid. This regime covers a large fraction of the scales probed by current and future LSS surveys. In this subhorizon, quasi-static regime, for any perturbative quantity X in the equations we assume

$$\ddot{X} \sim H\dot{X} \sim H^2 X \ll k^2 X, \quad (29.6)$$

where k is the wavenumber of the mode under consideration and an overdot denotes a derivative with respect to time. This approximation dramatically simplifies the equations and has been shown to hold for almost all popular theories of gravity. One can then remove the extra degrees of freedom (which usually appear in extensions to GR) from the linearised Einstein equations and replace their effects by two functions

of space and time, $\mu(a, k)$ and $\eta(a, k)$, in the Poisson equation (29.3) and the slip relation (29.5), respectively, to obtain

$$-k^2\Psi = \frac{\kappa^2}{2}\mu(a, k)\delta^*\rho, \quad (29.7)$$

$$\Phi = \eta(a, k)\Psi. \quad (29.8)$$

Here, μ quantifies the modification to the effective Newton's constant and η is called the gravitational slip [38, 46–48]. The two quasi-static parameters are generally functions of both time and scale. The scale dependence, however, becomes important typically on very small scales, i.e., deeply in the nonlinear regime, or on scales close to the horizon. Therefore, for the intermediate scales, as we defined above, μ and η can be considered as functions of time only. While the parameter μ sources the growth rate of structure, it is the combination of μ and η ,

$$\Sigma \equiv \frac{1}{2}\mu(1 + \eta), \quad (29.9)$$

that sources the weak gravitational lensing through the combination of the Poisson equations for Φ and Ψ , leading to

$$-k^2(\Phi + \Psi) = \kappa^2\Sigma(a, k)\delta^*\rho, \quad (29.10)$$

where the combination $\Phi + \Psi$ is known as the *Weyl potential*.

The parameterisation of departures from GR in terms of the quantities μ , η and Σ has the advantage of providing us with a simple, model-independent way of testing gravity on cosmological scales. On the one hand, any deviations from $\mu = 1$ and $\eta = 1$ at any time or scale are signatures of violations of GR, and this therefore gives a direct way of testing the standard theory. On the other hand, any model of modified gravity provides particular forms for these functions in terms of k and a , which can then be used in constraining the model with observational data. The forms of μ and η can be obtained for any modified gravity models of interest.

There are, however, issues with this phenomenological approach. First of all, the functional forms of μ and η , especially in terms of k , are typically the same for most interesting theories of gravity [49], and there are therefore degeneracies between different theories. For example, the functions μ and η obtained for Horndeski models of scalar-tensor gravity have the general forms [50]

$$\begin{aligned} \mu &= \frac{a_1 + a_2k^2}{b_1 + b_2k^2}, \\ \eta &= \frac{b_1 + b_2k^2}{c_1 + c_2k^2}, \end{aligned} \quad (29.11)$$

where a_i , b_i and c_i are functions of background quantities and therefore of time. A similar structure has been obtained for bimetric theories of gravity [51, 52]. This means that if we find a favoured non-GR form for any of these functions from observations, it is not easy to uniquely identify the underlying theory. In addition, one needs to parameterise the forms of μ and η when constraining the functions observationally, and these parameterisations add extra levels of arbitrariness to the analysis. The improved constraining power of future data has, however, the potential to solve this issue, allowing us to constrain these free functions through reconstruction techniques without the need to assume any specific parameterisation (see, e.g., Ref. [53]). Finally, as we discussed before, the $\{\mu, \eta\}$ parameterisation of departures from GR is valid only for the quasi-static regime, which holds only for subhorizon modes.

Since most alternative theories of gravity in the IR aim at explaining cosmic acceleration, which corresponds to horizon-scale physics, they directly affect observables on ultra-large (horizon-size) scales. The fact that physics on such scales is linear makes them of particular interest. Even though the starting point for our phenomenological parameterisation of modified gravity was based on subhorizon scales where the quasi-static approximation is believed to be valid, there are arguments in the literature also justifying the use of a similar parameterisation for ultra-large-scale modes [54]. These modes, however, suffer from one particular complication, and that is the problem of *cosmic variance*, which generates intrinsic and relatively large uncertainties on the measured quantities because of the low number of available modes on such large scales. Combining the data from different large-angle surveys taken at different redshifts will, however, help us tackle cosmic variance and better constrain theories of gravity. In addition, *relativistic effects* are important on horizon-size scales and cannot be neglected. This adds an extra level of complication when working with those modes. Finally, various other approximations that we usually make in cosmological data analysis to reduce the computation time may introduce additional uncertainties to the results that are comparable with departures from GR and signatures of modified gravity on ultra-large scales [55].

In the next section, we review the cosmological data and various probes that are used to test GR on cosmological (and linear) scales, and to place constraints on alternative theories of gravity.

29.1.2 *Cosmological Observables and Phenomenological Constraints*

Deviations from the Theory of General Relativity have imprints on several cosmological observables, which may therefore be used to constrain both phenomenological departures from standard gravity and possible alternative theories. In this section, we focus on the signatures that modified theories of gravity would have on cosmological observables, especially those of interest to current and upcoming surveys. In particular, we discuss the impacts of modifying gravity on the observations of large-

scale structure, as well as their effects on the propagation of the cosmic microwave background photons.

29.1.2.1 Cosmic Microwave Background

The cosmic microwave background (CMB) is a relic radiation coming from the epoch of recombination, when the free electrons in the Universe reached a sufficiently low abundance to allow photons to travel freely; this point in time, when the photons decoupled from free electrons, is known as the *last scattering surface*. Although extremely homogeneous, the tiny differences in the temperature of CMB photons ($\Delta T/T_{\text{CMB}} \approx 10^{-5}$ K for an average temperature of $T_{\text{CMB}} \approx 2.726$ K) carry a significant amount of information. Before recombination, photons were coupled via Thomson scattering to the primordial plasma, and deviations from the average temperature T_{CMB} can therefore be connected to primordial perturbations of the homogeneous matter distribution. As the CMB is the observable that allows us to look furthest in the past, such information is crucial to reconstruct the initial conditions of our Universe.

The information brought by CMB anisotropies is encoded in the angular power spectrum

$$C^{TT}(\ell) \equiv \langle |a_{\ell m}|^2 \rangle, \quad (29.12)$$

where the $a_{\ell m}$ are the coefficients of the spherical harmonics expansion of temperature perturbations

$$\frac{\Delta T}{T}(\mathbf{x}, \tau) = \sum_{\ell=1}^{\infty} \sum_{m=-\ell}^{\ell} a_{\ell m}(\mathbf{x}, \tau) Y_{\ell m}(\hat{n}), \quad (29.13)$$

with $Y_{\ell m}$ the spherical harmonics, τ the conformal time, and ℓ and m conjugates of the direction of incoming photons \hat{n} . (...) in Eq. (29.12) is the average over different values of m .

Theories alternative to GR are usually only expected to give deviations from the standard behaviour at low redshifts, as they are introduced, in most cases, to explain the late-time accelerated expansion of the Universe. For that reason, modified theories of gravity are not expected in general to impact the physics of recombination, and therefore to affect the primary anisotropies of the CMB described above.

Nevertheless, CMB photons are influenced by a number of secondary effects in their propagation from the last scattering surface to the observer; in particular, two effects are relevant for investigation of alternative theories of gravity; the *integrated Sachs-Wolfe* effect (ISW) and gravitational lensing.

The ISW effect is the cumulative variation of photons' energy due to temporal changes of gravitational potentials along their path, which can add or subtract energy,

$$\frac{\Delta T}{T} = \int_{\tau_0}^{\tau} d\tau (\Phi' + \Psi'), \quad (29.14)$$

where primes denote derivatives with respect to τ . As this is an integrated effect, late-time deviations from the GR evolution of the Bardeen potentials Φ and Ψ are imprinted on the temperature anisotropies of the CMB at large scales, and such deviations can therefore be observed to constrain departures from GR.

The second effect of interest is the weak gravitational lensing of CMB photons; along their path, these photons are affected by the gravitational potentials generated by the distribution of matter in the Universe, which leads to deflections of their path. Such an effect impacts the baryon acoustic oscillations imprinted on the temperature power spectrum $C^{TT}(\ell)$, decreasing its amplitude. By observing the effects on CMB spectra induced by gravitational lensing, it is possible to reconstruct $C^{\phi\phi}(\ell)$ [56], the power spectrum of the lensing potential ϕ , which can then be used to constrain theories of gravity.

29.1.2.2 Galaxy Clustering and Redshift-Space Distortions

The evolution of matter distribution, from the primordial perturbations in the matter density until the current distribution, is driven by the laws of gravity, determining the collapse of overdensities into the structure observed in the Universe. The matter perturbation, indicated in Fourier space as $\delta_m(k, z) \equiv (\rho_m(k, z) - \bar{\rho}_m)/\bar{\rho}_m$, evolves in time in GR as

$$\ddot{\delta}_m(k, z) + 2H(z)\dot{\delta}_m(k, z) - \frac{3H_0^2\Omega_m^0(1+z)^3}{2}\delta_m(k, z) = 0, \quad (29.15)$$

where the label ‘m’ denotes non-relativistic matter with the present density parameter Ω_m^0 , H_0 is the present value of the Hubble parameter and z is redshift. As the evolution of δ_m is connected with the Poisson equation described in the previous section, by employing the parameterisation of deviations from GR introduced in Eq. (29.7), we can obtain a generalized form

$$\ddot{\delta}_m(k, z) + 2H(z)\dot{\delta}_m(k, z) - \frac{3H_0^2\Omega_m^0(1+z)^3}{2}\mu(k, z)\delta_m(k, z) = 0. \quad (29.16)$$

Modifications of gravity, therefore, enter this evolution through the phenomenological function $\mu(k, z)$, and additionally, through the modification of the background expansion rate $H(z)$.

Given a specific cosmological model, we can therefore obtain the matter power spectrum $P_m(k, z)$ defined as

$$P_m(k, z) \propto \langle \delta_m(k, z)\delta_m(k, z) \rangle. \quad (29.17)$$

From Eq. (29.16) it is clear how departing from GR affects the evolution of δ_m and, consequently, how it impacts $P_m(k, z)$. This quantity, however, refers to the evolution of the total matter density, including dark matter, and therefore cannot be

directly observed. Nevertheless, galaxy surveys provide observations of the distribution of galaxies, and can therefore obtain the observed power spectrum $P_{\text{obs}}(k, z)$, which can be used as a proxy to the total matter distribution. The relation between these two spectra contains several physical effects, which also carry cosmological information [57]:

- The galaxy bias $b(z)$, which relates the linear galaxy and matter power spectra as

$$P_g(k, z) = b^2(z)P_m(k, z). \quad (29.18)$$

This term comes from the fact that the galaxy distribution is a biased tracer of the underlying matter distribution; this bias term can in principle be obtained from models of galaxy evolution and dark matter halo collapse (see, e.g., Ref. [58] for an extensive review), thus it can in principle be affected by modifications of the standard theory of gravity.

- The non-cosmological contribution to galaxy redshifts due to their peculiar velocities. Assuming redshift to be due only to the cosmological expansion introduces distortions in the density field that imprint a specific pattern in the power spectrum, known as *redshift space distortions (RSD)*. However, peculiar velocities are sourced by the density fields and can therefore themselves provide cosmological information. These velocities depend on the growth rate $f(z)$, defined as

$$f(z) \equiv -\frac{d \ln D(z)}{d \ln(1+z)}, \quad (29.19)$$

with $D(z)$ the growth factor defined through $\delta_m(k, z)/\delta_m(k, z_i) = D(z)/D(z_i)$, where the label i denotes ‘initial values’.

In the linear regime, this allows us to define a redshift-space power spectrum, $P_{\text{rs}}(k, z)$ [59],

$$P_{\text{rs}}(k, \gamma; z) = [b(z)\sigma_8(z) + f(z)\sigma_8(z)\gamma^2]^2 \frac{P_m(k, z)}{\sigma_8^2(z)}, \quad (29.20)$$

where $\sigma_8(z)$ is the root mean square of linearly evolved density fluctuations in spheres of $8h^{-1}$ Mpc at redshift z with $h \equiv H_0/100$, while $\gamma = \cos \theta$, with θ the angle between the wave vector \mathbf{k} and the line-of-sight direction.

- The Alcock-Paczynski effect, arising from the fact that a measurement of the galaxy power spectrum requires the assumption of a reference cosmology in order to transform redshifts into distances. If this assumption does not correspond to the true underlying cosmology, it is necessary to rescale the wave vector components, k_{\parallel} and k_{\perp} , as

$$k_{\perp} = \frac{k_{\perp, \text{ref}}}{q_{\perp}} \quad \text{and} \quad k_{\parallel} = \frac{k_{\parallel, \text{ref}}}{q_{\parallel}}, \quad (29.21)$$

where the coefficients q_{\perp} and q_{\parallel} are given, respectively, by the ratios of the angular diameter distance D_A and expansion rate H to the corresponding quantities in the reference cosmology,

$$q_{\perp} = \frac{D_A(z)}{D_{A,\text{ref}}(z)} \quad \text{and} \quad q_{\parallel} = \frac{H_{\text{ref}}(z)}{H(z)}. \quad (29.22)$$

It can be shown that overall, the Alcock-Paczynski effect rescales the power spectrum by a factor of $(q_{\perp}^2 q_{\parallel})^{-1}$ [60].

At the linear level, the combination of these effects allows us to relate the observed galaxy power spectrum to the total matter one as [57]

$$P_{\text{obs}}(k, z) = \frac{1}{q_{\perp}^2 q_{\parallel}} P_{\text{rs,lin}}(k(k_{\text{ref}}, \gamma_{\text{ref}}), \gamma(\gamma_{\text{ref}}); z). \quad (29.23)$$

Therefore, by solving Eq. (29.16) using the phenomenological departures from GR described in Sect. 29.1.1, one can obtain theoretical predictions for the galaxy power spectrum and use observations to constrain deviations from standard gravity.

29.1.2.3 Weak Gravitational Lensing

Weak gravitational lensing does not affect only the CMB photons travelling from the last scattering surface, but also the light emitted by any cosmological sources due to the distribution of matter anisotropies along the line of sight. Using galaxy surveys, it is possible to measure the distortions in the shape of distant light sources, e.g., distant galaxies, and to infer through this the amplitude of the gravitational lensing that these have endured. Weak lensing is a particularly powerful probe for cosmology, since it measures simultaneously the growth of structure through the matter power spectrum and the geometry of the Universe. The reconstruction of the matter density field can be conducted by looking at the correlations of the image distortions. The observable we need to work with is, therefore, the shear angular power spectrum $C^{\gamma\gamma}(\ell)$, which can be obtained as (see, e.g., Ref. [57])

$$C_{ij}^{\gamma\gamma}(\ell) = \frac{c}{H_0} \int \frac{\hat{W}_i^{\gamma}(z) \hat{W}_j^{\gamma}(z)}{E(z)r^2(z)} P_{\Phi+\Psi}(k_{\ell}, z) dz, \quad (29.24)$$

where $E(z) \equiv H(z)/H_0$, $r(z)$ is the comoving distance, $P_{\Phi+\Psi}$ is the power spectrum of the Weyl potential $\Phi + \Psi$, and we have made use of the Limber approximation [61–66], which relates scales k to multipoles ℓ as $k_{\ell} = (\ell + 1/2)/r(z)$; see, e.g., Ref. [67] for the full computation. Notice that here we assume a tomographic weak lensing survey, with the indices i and j running on the redshift bins of the survey; such a tomographic reconstruction that is used by weak lensing surveys allows us

to obtain information on the evolution of the Weyl potential in time, thus carrying significant information for investigating the time evolution of the potential.

By defining the lensing kernel $\tilde{W}_i^\gamma(z)$, a purely geometrical quantity expressed as

$$\tilde{W}_i^\gamma(z) = \int_z^{z_{\max}} n_i(z') \frac{r(z' - z)}{r(z')} dz', \quad (29.25)$$

with $n_i(z)$ the normalised observed galaxy number density in the i th redshift bin, the quantity $\hat{W}_i^\gamma(z)$ in Eq. (29.24) is

$$\hat{W}_i^\gamma(z) = \frac{r(z)}{2} \tilde{W}_i^\gamma(z). \quad (29.26)$$

In Λ CDM cosmology, which relies on the assumption of GR, it is easy to relate the weak lensing power spectrum $P_{\Phi+\Psi}$ to the matter power spectrum P_m using the relation

$$P_{\Phi+\Psi}^{\text{GR}} = \left[3 \left(\frac{H_0}{c} \right)^2 \Omega_m^0 (1+z) \right]^2 P_m^{\text{GR}}, \quad (29.27)$$

which leads to

$$C_{ij}^{\gamma\gamma, \text{GR}}(\ell) = \frac{c}{H_0} \int \frac{W_i^{\gamma, \text{GR}}(z) W_j^{\gamma, \text{GR}}(z)}{E(z) r^2(z)} P_m^{\text{GR}}(k_\ell, z) dz, \quad (29.28)$$

with the window function $W_i^{\gamma, \text{GR}}(z)$ given by

$$W_i^{\gamma, \text{GR}}(z) = \left[3 \left(\frac{H_0}{c} \right)^2 \Omega_m^0 (1+z) \right] \frac{r(z)}{2} \tilde{W}_i^\gamma(z). \quad (29.29)$$

Equation (29.27), however, does not hold if we depart from GR, and one would therefore have to use the full expression (29.24) to obtain theoretical predictions on this observable. Using Eqs. (29.7), (29.8) and (29.10), it is possible to rewrite the window function as [68]

$$W_i^\gamma(z) = \left[3 \left(\frac{H_0}{c} \right)^2 \Omega_m^0 (1+z) \right] \left\{ \frac{\mu(k, z)[1 + \eta(k, z)]}{2} \right\} \frac{r(z)}{2} \tilde{W}_i^\gamma(z), \quad (29.30)$$

for modified theories of gravity, where we used the fact that in this parameterisation

$$P_{\Phi+\Psi} = \left[3 \left(\frac{H_0}{c} \right)^2 \Omega_m^0 (1+z) \Sigma(k, z) \right]^2 P_m, \quad (29.31)$$

with Σ given by Eq. (29.9).

Weak lensing is therefore sensitive to the modifications that an extended theory of gravity would bring to the evolution of perturbations through its effect on the Weyl potential, which is related to the matter power spectrum through Eq. (29.31). Notice that since weak lensing probes the dark matter power spectrum directly, this observable is not limited by any assumptions about the galaxy bias, which represents one of the main limitations of galaxy surveys.

29.1.3 Einstein-Boltzmann Codes: From Theoretical Predictions to Data Analysis

Having obtained the expressions for theoretical predictions of cosmological observables in Sect. 29.1.2, we can in principle compare these with observations and constrain the parameters that measure deviations from GR. In order to compute these predictions, however, one has to solve the equations for cosmological perturbations in the presence of the modified Poisson equations of Sect. 29.1.1. For this purpose, we can rely on the publicly available Einstein-Boltzmann solvers CAMB [69] and CLASS [70], which are able to compute the evolution of the cosmological background and perturbations from the early Universe to the present time.

These codes work in the standard Λ CDM/GR model and its simple extensions, but their modifications based on phenomenological parameterisations of modified gravity are also publicly available. One example of these codes is MGCAMB [71–73], which implements deviations from GR parameterised by the μ , η and Σ functions, as well as some specific models of modified gravity (e.g., the Hu-Sawicki $f(R)$ model [74]).

As an example, Fig. 29.1 shows predictions for the CMB temperature and lensing-potential spectra, using the parameterisation of Eqs. (29.7) and (29.8), obtained by the *Planck* collaboration using the MGCAMB code [75], with μ and η parameterized as

$$\begin{aligned}\mu(z) &= 1 + E_{11}\Omega_{\text{DE}}(z), \\ \eta(z) &= 1 + E_{22}\Omega_{\text{DE}}(z),\end{aligned}\tag{29.32}$$

where $\Omega_{\text{DE}}(z)$ is the dark energy density parameter, and E_{11} and E_{22} are free parameters.

Having Einstein-Boltzmann codes able to produce the quantities highlighted in Sect. 29.1.2, they can then be interfaced with codes for sampling cosmological parameter spaces (e.g., Cobaya,¹ CosmoMC [76], CosmoSIS [77] and MontePython [78]), enabling us to compare theoretical predictions to observational data. Such a pipeline, therefore, allows us to reconstruct the posterior probabilities of cosmological parameters and to obtain observational constraints on models and parameters.

¹ <https://github.com/CobayaSampler/cobaya>.

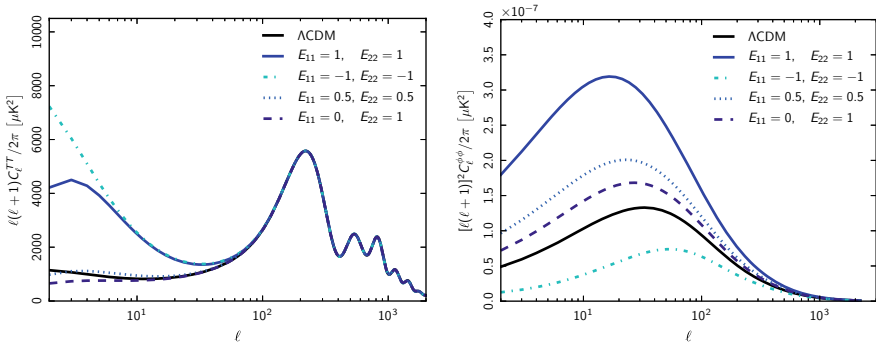


Fig. 29.1 Effects of modifications of gravity on CMB power spectra, demonstrated through the parameterisations given in Eqs. (29.32) for deviations from the standard Poisson equation and slip relation, taken from the results of the *Planck* collaboration [75]

29.1.4 Small Scales and Nonlinearities

Nonlinear structure formation is of extreme interest for testing gravity, as nonlinear observables are highly sensitive to the properties of gravitational interactions. In addition, the smaller the scales, the larger the statistical weight in the data, as more modes contribute to cosmological observables. Analysing the small scales is, however, much more complicated and computationally expensive, because on the one hand, the evolution of quantities is nonlinear, which on its own makes the numerical analysis complicated and slow, and on the other hand, the physics on small scales is considerably more complex than the linear and large scales because of the nonlinear gravitational collapse and the important roles that non-gravitational physics plays on such scales; this includes the Baryonic effects of gas, stars and highly energetic astrophysical processes such as supernova explosions and active galactic nuclei, which affect the evolution of the structure on sub-Megaparsec scales [79]. For these reasons, the computation of nonlinear observables usually relies on numerical simulations of the large-scale structure, which are computationally expensive and time-consuming, especially because of the variety of modified gravity models with several free parameters each. Recently, there has been considerable progress in developing numerical (N -body and hydrodynamic) simulations, as well as employing cutting-edge artificial intelligence (e.g., machine learning and deep learning) and inference techniques to tackle the complexity of the small and nonlinear scales for testing the standard model and beyond; see, e.g., Refs. [80–83] and references therein.

In addition to N -body simulations and numerical techniques, various analytical methods have also been developed, based on the frameworks of standard perturbation theory (SPT) [84, 85], Lagrangian perturbation theory (LPT) [86, 87], renormalised perturbation theory (RPT) [88], effective field theory (EFT) [89–93] and kinetic field theory (KFT) [94] (see also Refs. [58, 95] for reviews) for modelling the large-scale structure in the mildly nonlinear regime, where the theory of cosmological

perturbations can still be applied by going beyond linear orders. In particular, in the framework of the effective field theory of large-scale structure (EFTofLSS), one can capture interesting effects on scales smaller than the intermediate ones that we discussed in Sect. 29.1.1, while the perturbative regime is valid, computations are analytical, and physics is well understood and under control. In an EFT description of a system, all the physics relevant at a macroscopic scale of interest is captured by integrating out the short-distance physics, affecting long-distance modes only through a few parameters in a perturbative expansion. Since in our Universe, matter perturbations are strongly (weakly) coupled in the UV (IR), a perturbative EFT can be consistently applied to the formation of structure on a relatively wide range of cosmologically interesting scales, making precise analytical predictions possible. The mildly nonlinear regime studied by analytic, perturbative techniques such as EFTofLSS are particularly interesting from the point of view of cosmological modifications to gravity, as they can capture the onset of “GR to modified gravity” transition, which is central to modified gravity models.

Even though there has been considerable progress in developing numerical and analytic techniques to study the nonlinear regime and small scales, the level of accuracy needed for analysing the wealth of data provided by the upcoming and future cosmological surveys requires significantly more work in this direction in the coming years.

29.2 Existing Constraints and Tensions

In recent years, observational collaborations performing galaxy or CMB surveys have started to constrain possible alternative theories of gravity. A first example is the *Planck* 2015 release, which dedicated a paper to dark energy and modified gravity models, including phenomenological deviations from GR [75]. The analysis was further improved in the 2018 release of the *Planck* collaboration [96]. In this latest release, *Planck* constrained deviations from GR following the approach of Sect. 29.1.1, considering $\mu(z, k)$ and $\eta(z, k)$ as free functions and computing $\Sigma(z, k)$ as $\Sigma(z, k) = [1 + \eta(z, k)]\mu(z, k)/2$, while keeping the background expansion history to mimic that of a Λ CDM cosmology. Note that the *Planck* collaboration assumed no scale dependence for these functions.

In the upper panel of Fig. 29.2, the *Planck* results on the present values of the μ and η functions are shown, using only the CMB observables (both temperature and polarisation spectra, and CMB lensing reconstruction), as well as in combination with external data sets, i.e., measurements of the baryon acoustic oscillations (BAO) and redshift space distortions from the Sloan Digital Sky Survey (SDSS) and the Baryon Oscillation Spectroscopic Survey (BOSS) [97–99], the Pantheon supernovae catalogue [100] and the weak lensing data from the Dark Energy Survey (DES) [101].

These results show no significant preference towards deviations from GR, as the limit $\mu(z=0) = \eta(z=0) = 1$ is within $\sim 1\sigma$ confidence region. As discussed in Sect. 29.1.2.1, the CMB constrains modified gravity theories mainly through their

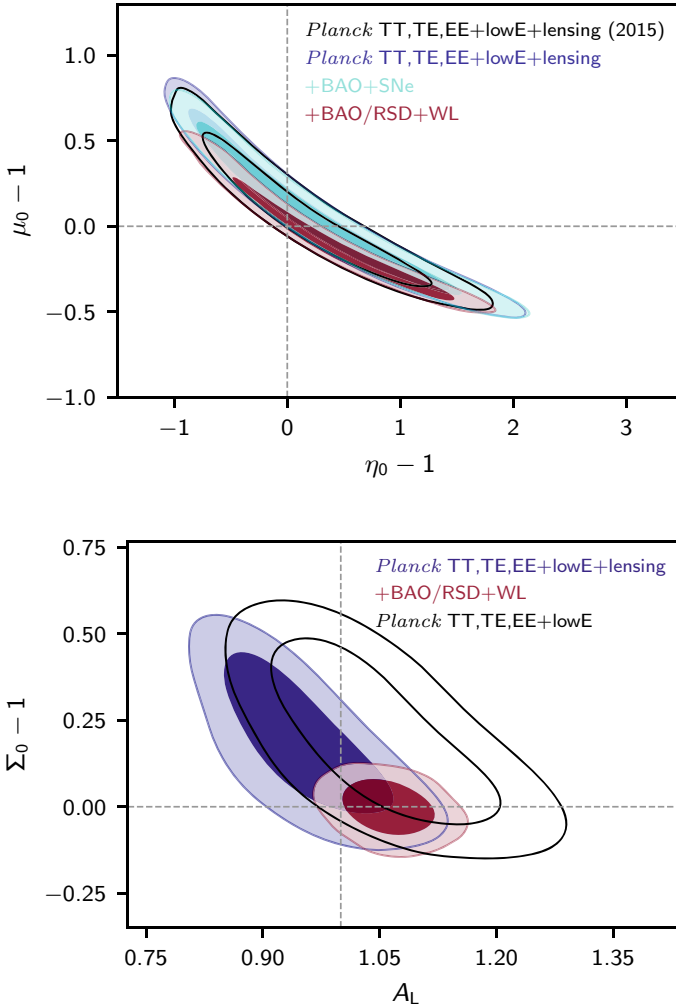


Fig. 29.2 Constraints on parameterised deviations from General Relativity obtained using *Planck* data [96]. The upper panel shows the contours for μ and η values at the present time, while the lower panel shows the degeneracy between the modified gravity lensing function Σ and the phenomenological lensing amplitude A_L . The figures are taken from Ref. [96]

effects on the ISW and CMB lensing; given that the constraining power of the former is severely limited by cosmic variance, CMB lensing contributes the most to these constraints. This, interestingly, connects the constraints on modified gravity to one of the open “curious” implications of the *Planck* results: assuming a Λ CDM cosmology but allowing for a phenomenological departure from its predicted lensing amplitude through the parameter A_L defined through

$$C^{\phi\phi}(\ell) = A_L C_{\Lambda\text{CDM}}^{\phi\phi}(\ell), \quad (29.33)$$

Planck finds a preference for $A_L > 1$ when analysing temperature and polarization spectra, while the value of A_L is shifted back towards the ΛCDM limit when the CMB lensing reconstruction is included [96]. In the lower panel of Fig. 29.2, we show the *Planck* results on the degeneracy between A_L and the modified gravity quantity $\Sigma_0 \equiv \Sigma(z=0)$, which encodes the effect of modified gravity on the Weyl potential $\Phi + \Psi$ affecting the lensing amplitude: the results show how, in order to recover $A_L = 1$, an approximately 1σ shift away from the GR limit $\Sigma_0 = 1$ is required when the CMB lensing reconstruction is not included; by adding this further observable the results are, however, consistent with GR within 1σ . This highlights how improving the lensing reconstruction, from both CMB and LSS surveys, is crucial in order to improve the constraints on modified gravity models.

Other phenomenological investigations of departures from GR have been performed by recent galaxy surveys, mainly the Kilo-Degree Survey (KiDS) [102] and DES [103]. The KiDS collaboration decided not to rely on a particular parameterisation of the μ and η functions (labelled Q and R , respectively, in their paper), but rather to constrain their values in 4 redshift and 4 scale bins. Note that given that no adequate prescriptions for computing the matter power spectrum on nonlinear scales are currently available for modified gravity theories, the KiDS collaboration provided results using both their standard range of scales (results labelled as FS) and limiting the analysis only to linear scales (results labelled as LS).

In Fig. 29.3, we show the results obtained by KiDS on the modified gravity functions, using their weak lensing data and comparing with CMB constraints. The upper panel compares the results to those obtained in ΛCDM in an attempt to ease the tension on the σ_8 parameter between *Planck* and KiDS measurements (at the level of $\sim 2\sigma$ in ΛCDM ; see, e.g., Ref. [104] for updates on the tension), highlighting how introducing eight modified gravity degrees of freedom, together with the conservative assumption about the scales used in the analysis, significantly washes out the constraining power of this survey. The lower panel shows instead the constraints on the modified gravity parameters, once again showing the impact of the assumptions on the analysis of nonlinear scales and, at the same time, showing how the KiDS survey is significantly more sensitive to Σ (obtained as a combination of $Q = \mu$ and $R = \eta$), which impacts the Weyl potential, rather than to Q , which is instead related to the clustering of matter.

The DES collaboration decided instead to constrain parameterised modified gravity functions with a parameterisation similar to the one adopted by *Planck* but using $\mu(z)$ and $\Sigma(z)$ as primary functions and constraining $\eta(z)$ as a derived function. In Fig. 29.4, they have compared, similarly to the KiDS approach, their results (blue contours) with those obtained from *Planck* together with BAO/RSD and supernovae data (yellow contours), as well as the combination of the two data sets (red contours). The left panel shows how, as for KiDS, the DES measurements are more sensitive to changes in the lensing equations (through Σ) rather than in the Poisson equation for non-relativistic particles (through μ), with no significant evidence for non-GR cosmologies. The right panel depicts instead how allowing for departures from GR

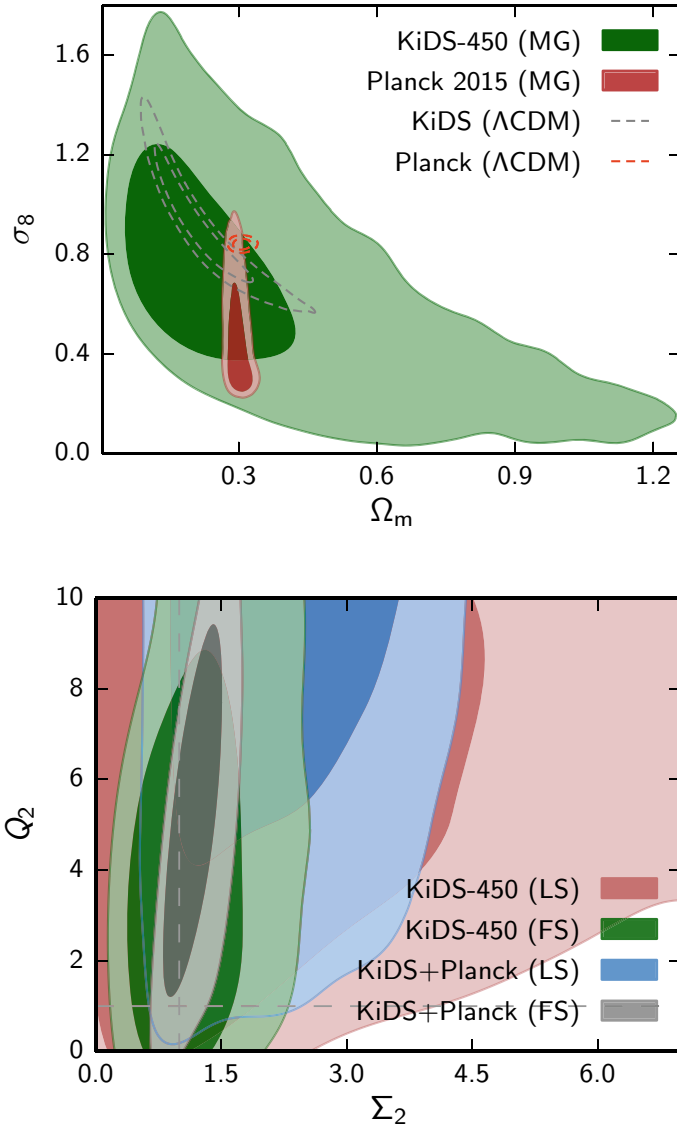


Fig. 29.3 Upper panel: Effect of allowing gravity to be modified on the contours of σ_8 and Ω_m (note that here Ω_m is the present value of the matter density parameter). These results are provided by the KiDS collaboration [102]. Lower panel: Constraints on the binned modified gravity functions $Q(=\mu)$ and Σ obtained using KiDS weak lensing data alone and combined with *Planck* CMB observations. The figures are taken from Ref. [102]

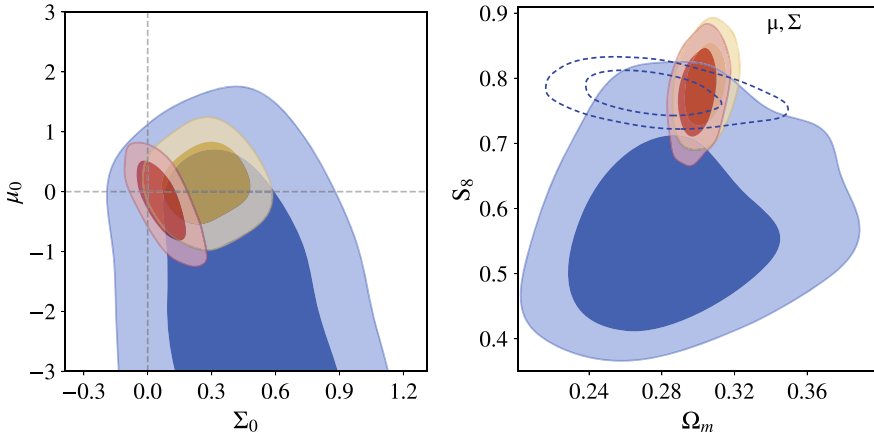


Fig. 29.4 The left panel depicts the constraints on the parameters μ_0 and Σ_0 for deviations from GR obtained by DES (blue contour), *Planck* and BAO/RSD/SNIa (yellow contours), as well as their combination (red contour). For the same data sets, the right panel shows the effect of allowing for departures from GR on the quantities $S_8 \equiv \sigma_8 \sqrt{\Omega_m^0/0.3}$ and Ω_m^0 (denoted as Ω_m in the figure). The figures are taken from Ref. [103]

significantly worsens and shifts the constraint on S_8 with respect to the Λ CDM case (dashed line), highlighting once again how future LSS surveys have the potential to improve the constraints on these theories.

Overall, the results from these current surveys do not show significant evidence for modified gravity. All the results are compatible with the Λ CDM limit, with small deviations ($\sim 1\sigma$) in the Σ function affecting the evolution of the lensing potential. Moreover, the results of these collaborations demonstrate how the constraints are significantly degraded with respect to the analyses involving other extensions of the Λ CDM model, showing how improvements in the near future in both the sensitivity of the surveys and the theoretical treatment of small scales are necessary to further investigate these non-standard cosmologies.

Nevertheless, allowing for modifications of gravity provides a promising way to ease the tension on the measured value of the $S_8 \equiv \sigma_8 \sqrt{\Omega_m^0/0.3}$ parameter between CMB and LSS observations (estimated to be $\sim 2\sigma$ for both KiDS and LSS data). However, as the results shown in this section highlight, allowing for deviations from GR and the necessity to cut out the measurements at small scales significantly lower the constraining power of the data; therefore it will be necessary to wait for more sensitive observations in the future to properly address the possibility that the S_8 tension might be a hint of modifications to the standard theory of gravity.

Finally, it is important to stress that here we did not discuss the (statistically) most significant tension between currently available data, i.e., the tension in the measured values of the Hubble constant H_0 (see, e.g., Ref. [105] for a review). For what concerns this parameter, the values inferred from high-redshift measurements through the CMB (and LSS), which assume a Λ CDM expansion of the Universe,

and those obtained through local, model-independent methods [106, 107] are in tension with $\sim 4.5\sigma$. Such a significant tension can be seen as a strong motivation to go beyond the Λ CDM model, and modifications of gravity might suggest ways to achieve this. However, the model-independent results presented in this section rely on the assumption of a background expansion which perfectly mimics that of Λ CDM and therefore do not significantly affect the constraints on H_0 . Such an assumption is necessary for two main reasons: on the one hand, the sensitivity of the current data is not sufficient for simultaneously constraining modifications of the background expansion and of the evolution of perturbations, while on the other hand, in order to test realistic theories of gravity, modifications of the two sectors must be connected to each other, which is unfeasible with the simple parameterisations presented here. While the first issue will be eased with the upcoming plethora of LSS data from future surveys (see Sect. 29.3), the second point is also currently under investigation and promising results have been achieved, although for more restricted classes of theoretical models rather than for fully general parameterisations [108].

29.3 Upcoming Surveys and the Road Ahead

As we discussed in the previous section, the current cosmological constraints on deviations from GR and on modified theories of gravity are relatively weak, and no significant deviations from Λ CDM can be inferred from the existing data, despite small tensions that are, to some extent, not even consistent. The situation may, however, change dramatically in the future, when the upcoming cosmological surveys with much higher levels of precision start to deliver data. Currently, the constraints on the modified gravity parameters μ , η and Σ are of $\mathcal{O}(1)$, which we expect to reduce to $\mathcal{O}(10^{-1}) - \mathcal{O}(10^{-2})$ in the next few years.

We expect an exciting time to come when the Stage IV LSS surveys are fully operational, providing a large amount of highly precise cosmological data. These surveys include several ground-based experiments such as the Dark Energy Spectroscopic Instrument (DESI) [109, 110], the Rubin Observatory Legacy Survey of Space and Time (LSST) [111–113], the Square Kilometre Array (SKA) [114–120], and the Subaru Hyper Suprime-Cam (HSC) and Prime Focus Spectrograph (PFS) surveys [121, 122], as well as the space-based experiments *Euclid* [57, 123, 124], the Nancy Grace Roman Space Telescope [125, 126], and the Spectro-Photometer for the History of the Universe, Epoch of Reionization, and Ices Explorer (SPHEREx) [127, 128]. In addition to these LSS surveys, future ground-based CMB experiments, such as CMB-S4 [129, 130], the Simons Observatory (SO) [131] and CMB-HD [132, 133], will provide extremely high-resolution CMB maps covering a large fraction of the sky, which can also help us test gravity and constrain modified gravity quantities.

Several forecast analyses for these experiments and surveys are currently being performed, and here we only present a few representative examples of the constraints we expect to achieve by using some of these surveys. Figure 29.5 shows the results of a Fisher matrix forecast analysis for *Euclid* and the SKA for the two phenomeno-

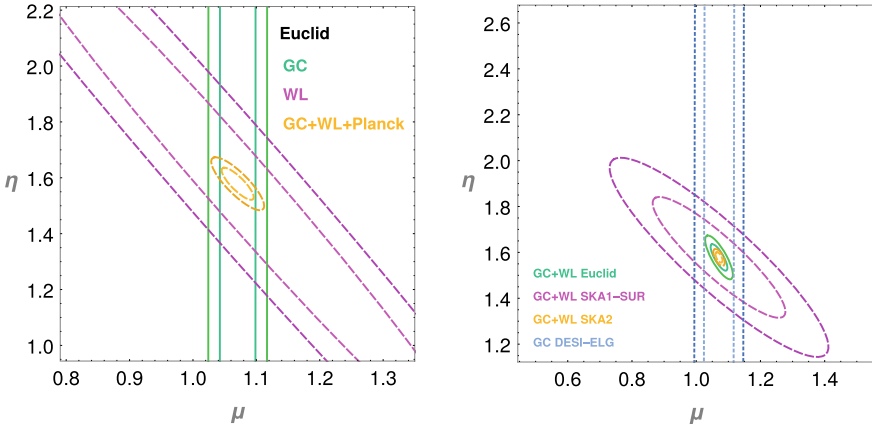


Fig. 29.5 Left panel: Results of a Fisher matrix forecast analysis for *Euclid* and for a late-time parameterisation of modified gravity functions μ and η where the amplitude of deviations from GR is assumed to be proportional to the dark energy density parameter $\Omega_{\text{DE}}(z)$. Linear and mildly nonlinear scales have been included and the contours show the predicted 1σ and 2σ confidence regions for galaxy clustering (GC) and weak lensing (WL) surveys, as well as their combination with the *Planck* constraints. Right panel: Fisher matrix forecast confidence regions for μ and η and for *Euclid* and two phases of the SKA, SKA1 and SKA2, when combinations of GC and WL have been considered. Constraints from DESI are also shown with only GC observables included. The figures are taken from Ref. [53]

logical modified gravity functions μ and η , when the late-time parameterisation of Eq. (29.32) has been used and linear and mildly nonlinear scales have been considered [53]. The constraints are based on galaxy clustering (GC) and weak lensing (WL) observables and their combinations. The left panel of the figure indicates that combining the *Euclid* GC and WL measurements with *Planck* breaks many degeneracies in the parameter space and provides extremely tight constraints on μ and η . On the other hand, the right panel of the figure presents the constraining power for the combination of GC and WL surveys for *Euclid* and phases 1 and 2 of the SKA, as well as GC only for DESI. Although all the constraints in the figure are parameterisation-dependent (i.e., they depend on how μ and η are parameterised in terms of time and scale), the contours prove a dramatic reduction in the uncertainties compared to the current constraints. In order to see this more clearly, we have provided in Fig. 29.6 the forecast constraints on the phenomenological modified gravity parameters $\mu_0 \equiv \mu(z=0)$ and $\gamma_0 = \eta_0 \equiv \eta(z=0)$, to be provided by the HI galaxy sample of the *Medium-Deep Band 2 Survey* for phase 1 of the SKA (SKA1), as defined in the SKA Red Book 2018 [120]. The figure includes also current constraints from *Planck* and DES (GC only) for comparison. The improvement from adding SKA1 is comparable to DES.

With the level of precision we expect to reach in the next few years, we will be able to strongly constrain departures from GR and test a large class of its interesting and theoretically well-motivated alternatives. In case the current tensions in cosmo-

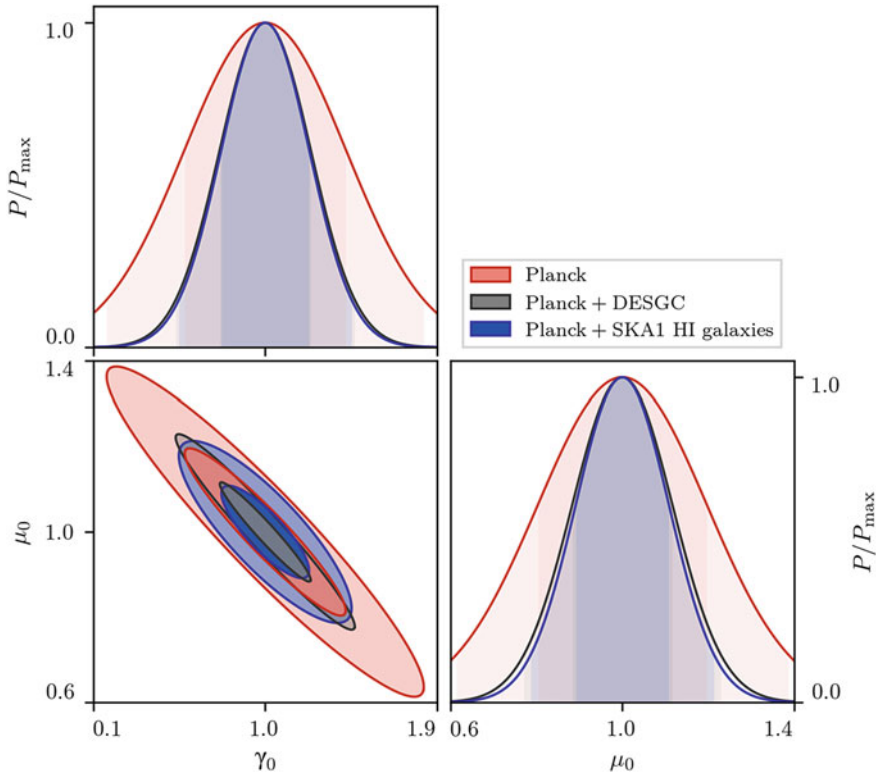


Fig. 29.6 Fisher matrix forecast constraints on the phenomenological modified gravity parameters $\mu_0 \equiv \mu(z=0)$ and $\gamma_0 = \eta_0 \equiv \eta(z=0)$ when the broadband shape of the power spectrum detected by the HI galaxy sample of the *Medium-Deep Band 2 Survey* is used for Phase 1 of the SKA (SKA1). Constraints from *Planck* and DES (galaxy clustering only) are also presented for comparison. The figure is taken from Ref. [120]

logical observations that seem to indicate preference for departures from standard gravity hold against the tide of various future high-quality data, they will then provide undeniable evidence for new physics in the gravitational sector.

References

1. A.G. Riess, Supernova Search Team, Collaboration et al., Observational evidence from supernovae for an accelerating universe and a cosmological constant. *Astron. J.* **116**, 1009–1038 (1998). [arXiv:astro-ph/9805201](https://arxiv.org/abs/astro-ph/9805201)
2. S. Perlmutter, Supernova Cosmology Project Collaboration et al., Measurements of and from 42 high redshift supernovae. *Astrophys. J.* **517**, 565–586 (1999). [arXiv:astro-ph/9812133](https://arxiv.org/abs/astro-ph/9812133)
3. R.R. Caldwell, M. Kamionkowski, The physics of cosmic acceleration. *Ann. Rev. Nucl. Part. Sci.* **59**, 397–429 (2009). [arXiv:0903.0866](https://arxiv.org/abs/0903.0866)

4. D.H. Weinberg, M.J. Mortonson, D.J. Eisenstein, C. Hirata, A.G. Riess, E. Rozo, Observational probes of cosmic acceleration. *Phys. Rept.* **530**, 87–255 (2013). [arXiv:1201.2434](#)
5. A. Joyce, B. Jain, J. Khoury, M. Trodden, Beyond the cosmological standard model. *Phys. Rept.* **568**, 1–98 (2015). [arXiv:1407.0059](#)
6. P. Bull et al., Beyond Λ CDM: problems, solutions, and the road ahead. *Phys. Dark Univ.* **12**, 56–99 (2016). [arXiv:1512.05356](#)
7. L. Amendola, S. Tsujikawa, *Dark Energy: Theory and Observations* (Cambridge University Press, Cambridge, 2010)
8. T. Clifton, P.G. Ferreira, A. Padilla, C. Skordis, Modified gravity and cosmology. *Phys. Rept.* **513**, 1–189 (2012). [arXiv:1106.2476](#)
9. K. Koyama, Cosmological tests of modified gravity. *Rept. Prog. Phys.* **79**(4), 046902 (2016). [arXiv:1504.04623](#)
10. M. Ishak, Testing general relativity in cosmology. *Living Rev. Rel.* **22**(1), 1 (2019). [arXiv:1806.10122](#)
11. P.G. Ferreira, Cosmological tests of gravity. *Ann. Rev. Astron. Astrophys.* **57**, 335–374 (2019). [arXiv:1902.10503](#)
12. S. Weinberg, The cosmological constant problem. *Rev. Mod. Phys.* **61**, 1–23 (1989)
13. J. Martin, Everything you always wanted to know about the cosmological constant problem (But were afraid to ask). *Comptes Rendus Phys.* **13**, 566–665 (2012). [arXiv:1205.3365](#)
14. B.P. Abbott, LIGO Scientific, Virgo, Collaboration et al., GW170817: observation of gravitational waves from a binary neutron star inspiral. *Phys. Rev. Lett.* **119**(16), 161101 (2017). [arXiv:1710.05832](#)
15. A. Goldstein et al., An ordinary short gamma-ray burst with extraordinary implications: fermi-GBM detection of GRB 170817A. *Astrophys. J.* **848**(2), L14 (2017). [arXiv:1710.05446](#)
16. P. Creminelli, F. Vernizzi, Dark energy after GW170817 and GRB170817A. *Phys. Rev. Lett.* **119**(25), 251302 (2017). [arXiv:1710.05877](#)
17. J. Sakstein, B. Jain, Implications of the neutron star merger GW170817 for cosmological scalar-tensor theories. *Phys. Rev. Lett.* **119**(25), 251303 (2017). [arXiv:1710.05893](#)
18. J.M. Ezquiaga, M. Zumalacárregui, Dark energy after GW170817: dead ends and the road ahead. *Phys. Rev. Lett.* **119**(25), 251304 (2017). [arXiv:1710.05901](#)
19. T. Baker, E. Bellini, P.G. Ferreira, M. Lagos, J. Noller, I. Sawicki, Strong constraints on cosmological gravity from GW170817 and GRB 170817A. *Phys. Rev. Lett.* **119**(25), 251301 (2017). [arXiv:1710.06394](#)
20. S. Nojiri, S.D. Odintsov, Cosmological bound from the neutron star merger GW170817 in modified gravity. [arXiv:1711.00492](#)
21. S. Boran, S. Desai, E.O. Kahya, R.P. Woodard, GW170817 falsifies dark matter emulators. *Phys. Rev. D* **97**(4), 041501 (2018). [arXiv:1710.06168](#)
22. L. Amendola, M. Kunz, I.D. Saltas, I. Sawicki, Fate of large-scale structure in modified gravity after GW170817 and GRB170817A. *Phys. Rev. Lett.* **120**(13), 131101 (2018). [arXiv:1711.04825](#)
23. M. Crisostomi, K. Koyama, Vainshtein mechanism after GW170817. *Phys. Rev. D* **97**(2), 021301 (2018)
24. D. Langlois, R. Saito, D. Yamauchi, K. Noui, Scalar-tensor theories and modified gravity in the wake of GW170817. *Phys. Rev. D* **97**(6), 061501 (2018). [arXiv:1711.07403](#)
25. A.E. Gumrukcuoglu, M. Saravani, T.P. Sotiriou, Hořava gravity after GW170817. *Phys. Rev. D* **97**(2), 024032 (2017). [arXiv:1711.08845](#)
26. L. Heisenberg, S. Tsujikawa, Dark energy survivals in massive gravity after GW170817: SO(3) invariant. *JCAP* **1801**(01), 044 (2017). [arXiv:1711.09430](#)
27. C.D. Kreisch, E. Komatsu, Cosmological constraints on horndeski gravity in light of GW170817. *JCAP* **1812**(12), 030 (2017). [arXiv:1712.02710](#)
28. A. Dima, F. Vernizzi, Vainshtein screening in scalar-tensor theories before and after GW170817: constraints on theories beyond horndeski. *Phys. Rev. D* **97**(10), 101302 (2018). [arXiv:1712.04731](#)

29. S. Peirone, K. Koyama, L. Pogosian, M. Raveri, A. Silvestri, Large-scale structure phenomenology of viable Horndeski theories. *Phys. Rev. D* **97**(4), 043519 (2018). [arXiv:1712.00444](#)
30. M. Crisostomi, K. Koyama, Self-accelerating universe in scalar-tensor theories after GW170817. *Phys. Rev. D* **97**(8), 084004 (2018). [arXiv:1712.06556](#)
31. E.V. Linder, No slip gravity. *JCAP* **1803**(03), 005 (2018). [arXiv:1801.01503](#)
32. R. Kase, S. Tsujikawa, Dark energy scenario consistent with GW170817 in theories beyond Horndeski gravity. *Phys. Rev. D* **97**(10), 103501 (2018). [arXiv:1802.02728](#)
33. R.A. Battye, F. Pace, D. Trinh, Gravitational wave constraints on dark sector models. *Phys. Rev. D* **98**(2), 023504 (2018). [arXiv:1802.09447](#)
34. Y. Akrami, P. Brax, A.-C. Davis, V. Vardanyan, Neutron star merger GW170817 strongly constrains doubly coupled bigravity. *Phys. Rev. D* **97**(12), 124010 (2018). [arXiv:1803.09726](#)
35. L. Lombriser, A. Taylor, Breaking a dark degeneracy with gravitational waves. *JCAP* **1603**(03), 031 (2016). [arXiv:1509.08458](#)
36. P. Brax, C. Burrage, A.-C. Davis, The speed of galileon gravity. *JCAP* **1603**(03), 004 (2016). [arXiv:1510.03701](#)
37. L. Lombriser, N.A. Lima, Challenges to self-acceleration in modified gravity from gravitational waves and large-scale structure. *Phys. Lett. B* **765**, 382–385 (2017). [arXiv:1602.07670](#)
38. L. Pogosian, A. Silvestri, What can cosmology tell us about gravity? constraining Horndeski gravity with Σ and μ . *Phys. Rev. D* **94**(10)(2016). [arXiv:1606.05339](#)
39. D. Bettoni, J.M. Ezquiaga, K. Hinterbichler, M. Zumalacregui, Speed of gravitational waves and the fate of scalar-tensor gravity. *Phys. Rev. D* **95**(8), 084029 (2017). [arXiv:1608.01982](#)
40. P. Creminelli, G. D’Amico, J. Norena, F. Vernizzi, The effective theory of quintessence: the $w < -1$ side unveiled. *JCAP* **0902**, 018 (2009). [arXiv:0811.0827](#)
41. G. Gubitosi, F. Piazza, F. Vernizzi, The effective field theory of dark energy. *JCAP* **1302**, 032 (2013). [arXiv:1210.0201](#)
42. J.K. Bloomfield, É.É. Flanagan, M. Park, S. Watson, Dark energy or modified gravity? an effective field theory approach. *JCAP* **1308**, 010 (2013). [arXiv:1211.7054](#)
43. J. Gleyzes, D. Langlois, F. Piazza, F. Vernizzi, Essential building blocks of dark energy. *JCAP* **1308**, 025 (2013). [arXiv:1304.4840](#)
44. J. Gleyzes, D. Langlois, F. Piazza, F. Vernizzi, Healthy theories beyond Horndeski. [arXiv:1404.6495](#)
45. E. Bellini, I. Sawicki, Maximal freedom at minimum cost: linear large-scale structure in general modifications of gravity. *JCAP* **1407**, 050 (2014). [arXiv:1404.3713](#)
46. W. Hu, I. Sawicki, A parameterized post-friedmann framework for modified gravity. *Phys. Rev. D* **76**, 104043 (2007). [arXiv:0708.1190](#)
47. E. Bertschinger, P. Zukin, Distinguishing modified gravity from dark energy. *Phys. Rev. D* **78**, 024015 (2008). [arXiv:0801.2431](#)
48. M.A. Amin, R.V. Wagoner, R.D. Blandford, A sub-horizon framework for probing the relationship between the cosmological matter distribution and metric perturbations. *Mon. Not. Roy. Astron. Soc.* **390**, 131–142 (2008). [arXiv:0708.1793](#)
49. T. Baker, P.G. Ferreira, C.D. Leonard, M. Motta, New gravitational scales in cosmological surveys. *Phys. Rev. D* **90**(12), 124030 (2014). [arXiv:1409.8284](#)
50. A. De Felice, T. Kobayashi, S. Tsujikawa, Effective gravitational couplings for cosmological perturbations in the most general scalar-tensor theories with second-order field equations. *Phys. Lett. B* **706**, 123–133 (2011). [arXiv:1108.4242](#)
51. A.R. Solomon, Y. Akrami, T.S. Koivisto, Linear growth of structure in massive bigravity. *JCAP* **1410**, 066 (2014). [arXiv:1404.4061](#)
52. F. Könnig, Y. Akrami, L. Amendola, M. Motta, A.R. Solomon, Stable and unstable cosmological models in bimetric massive gravity. *Phys. Rev. D* **90**, 124014 (2014). [arXiv:1407.4331](#)
53. S. Casas, M. Kunz, M. Martinelli, V. Pettorino, Linear and non-linear modified gravity forecasts with future surveys. *Phys. Dark Univ.* **18**, 73–104 (2017). [arXiv:1703.01271](#)
54. T. Baker, P. Bull, Observational signatures of modified gravity on ultra-large scales. *Astrophys. J.* **811**, 116 (2015). [arXiv:1506.00641](#)

55. M. Martinelli, R. Dalal, F. Majidi, Y. Akrami, S. Camera, E. Sellentin, Ultra-large-scale approximations and galaxy clustering: debiasing constraints on cosmological parameters. To appear (2021). [arXiv:2106.15604](#)
56. T. Okamoto, W. Hu, CMB lensing reconstruction on the full sky. *Phys. Rev. D* **67**, 083002 (2003)
57. Euclid, Collaboration, A. Blanchard et al., Euclid preparation: VII: forecast validation for Euclid cosmological probes. [arXiv:1910.09273](#)
58. V. Desjacques, D. Jeong, F. Schmidt, Large-scale galaxy bias. *Phys. Rept.* **733**, 1–193 (2018). [arXiv:1611.09787](#)
59. N. Kaiser, Clustering in real space and in redshift space. *Mon. Not. Roy. Astron. Soc.* **227**, 1–27 (1987)
60. W.E. Ballinger, J.A. Peacock, A.F. Heavens, Measuring the cosmological constant with redshift surveys. *Mon. Not. Roy. Astron. Soc.* **282**, 877–888 (1996). [arXiv:astro-ph/9605017](#)
61. N. Kaiser, Weak gravitational lensing of distant galaxies. *Astrophys. J.* **388**, 272 (1992)
62. M. LoVerde, N. Afshordi, Extended limber approximation. *Phys. Rev. D* **78**, 123506 (2008). [arXiv:0809.5112](#)
63. T. Giannantonio, C. Porciani, J. Carron, A. Amara, A. Pillepich, Constraining primordial non-Gaussianity with future galaxy surveys. *Mon. Not. Roy. Astron. Soc.* **422**, 2854–2877 (2012). [arXiv:1109.0958](#)
64. T.D. Kitching, J. Alsing, A.F. Heavens, R. Jimenez, J.D. McEwen, L. Verde, The limits of cosmic shear. *Mon. Not. Roy. Astron. Soc.* **469**(3), 2737–2749 (2017). [arXiv:1611.04954](#)
65. M. Kilbinger et al., Precision calculations of the cosmic shear power spectrum projection. *Mon. Not. Roy. Astron. Soc.* **472**(2), 2126–2141 (2017). [arXiv:1702.05301](#)
66. P. Lemos, A. Challinor, G. Efstathiou, The effect of Limber and flat-sky approximations on galaxy weak lensing. *JCAP* **05**, 014 (2017). [arXiv:1704.01054](#)
67. P.L. Taylor, T.D. Kitching, J.D. McEwen, T. Tram, Testing the cosmic shear spatially-flat universe approximation with generalized lensing and shear spectra. *Phys. Rev. D* **98**(2), 023522 (2018). [arXiv:1804.03668](#)
68. A. Spurio Mancini, F. Köhlinger, B. Joachimi, V. Pettorino, B.M. Schäfer, R. Reischke, S. Brieden, M. Archidiacono, J. Lesgourgues, KiDS+GAMA: constraints on Horndeski gravity from combined large-scale structure probes. [arXiv:1901.03686](#)
69. A. Lewis, A. Challinor, A. Lasenby, Efficient computation of CMB anisotropies in closed FRW models. *Astrophys. J.* **538**, 473–476 (2000). [arXiv:astro-ph/9911177](#)
70. D. Blas, J. Lesgourgues, T. Tram, The cosmic linear anisotropy solving system (CLASS) II: approximation schemes. *JCAP* **1107**, 034 (2011). [arXiv:1104.2933](#)
71. G.-B. Zhao, L. Pogosian, A. Silvestri, J. Zylberberg, Searching for modified growth patterns with tomographic surveys. *Phys. Rev. D* **79**, 083513 (2009). [arXiv:0809.3791](#)
72. A. Hojjati, L. Pogosian, G.-B. Zhao, Testing gravity with CAMB and CosmoMC. *JCAP* **1108**, 005 (2011). [arXiv:1106.4543](#)
73. A. Zucca, L. Pogosian, A. Silvestri, G.-B. Zhao, MGCAMB with massive neutrinos and dynamical dark energy. *JCAP* **2019**(05), 001 (2020). [arXiv:1901.05956](#)
74. W. Hu, I. Sawicki, Models of $f(R)$ cosmic acceleration that evade solar-system tests. *Phys. Rev. D* **76**, 064004 (2007). [arXiv:0705.1158](#)
75. P.A.R. Ade, Planck, Collaboration et al., Planck 2015 results. XIV: dark energy and modified gravity. *Astron. Astrophys.* **594**, A14 (2016). [arXiv:1502.01590](#)
76. A. Lewis, S. Bridle, Cosmological parameters from CMB and other data: a Monte Carlo approach. *Phys. Rev. D* **66**(2002). [arXiv:astro-ph/0205436](#)
77. J. Zuntz, M. Paterno, E. Jennings, D. Rudd, A. Manzotti, S. Dodelson, S. Bridle, S. Sehrish, J. Kowalkowski, CosmoSIS: modular cosmological parameter estimation. *Astron. Comput.* **12**, 45–59 (2015). [arXiv:1409.3409](#)
78. B. Audren, J. Lesgourgues, K. Benabed, S. Prunet, Conservative constraints on early cosmology: an illustration of the Monte Python cosmological parameter inference code. *JCAP* **1302**, 001 (2013). [arXiv:1210.7183](#)

79. N.E. Chisari, M.L.A. Richardson, J. Devriendt, Y. Dubois, A. Schneider, A.M.C. Le Brun, R.S. Beckmann, S. Peirani, A. Slyz, C. Pichon, The impact of baryons on the matter power spectrum from the Horizon-AGN cosmological hydrodynamical simulation. *Mon. Not. Roy. Astron. Soc.* **480**(3), 3962–3977 (2018). [arXiv:1801.08559](#)
80. J. Alsing, T. Charnock, S. Feeney, B. Wandelt, Fast likelihood-free cosmology with neural density estimators and active learning. *Mon. Not. Roy. Astron. Soc.* **488**(3), 4440–4458 (2019). [arXiv:1903.00007](#)
81. M. Ntampaka et al., The role of machine learning in the next decade of cosmology. *BAAS* **51**, 14 (2019). [arXiv:1902.10159](#)
82. S. He, Y. Li, Y. Feng, S. Ho, S. Ravanbakhsh, W. Chen, B. Póczos, Learning to predict the cosmological structure formation. *Proc. Nat. Acad. Sci.* **116**(28), 13825–13832 (2019). [arXiv:1811.06533](#)
83. N. Chartier, B. Wandelt, Y. Akrami, F. Villaescusa-Navarro, CARPool: fast, accurate computation of large-scale structure statistics by pairing costly and cheap cosmological simulations. *Mon. Not. Roy. Astron. Soc.* **503**(2), 1897–1914 (2021)
84. B. Jain, E. Bertschinger, Second order power spectrum and nonlinear evolution at high redshift. *Astrophys. J.* **431**, 495 (1994). [arXiv:astro-ph/9311070](#)
85. M.H. Goroff, B. Grinstein, S.J. Rey, M.B. Wise, Coupling of modes of cosmological mass density fluctuations. *Astroph. J.* **311**, 6–14 (1986)
86. F. Bouchet, S. Colombi, E. Hivon, R. Juszkiewicz, Perturbative Lagrangian approach to gravitational instability. *Astron. Astrophys.* **296**, 575 (1995). [arXiv:astro-ph/9406013](#)
87. T. Matsubara, Resumming cosmological perturbations via the lagrangian picture: one-loop results in real space and in redshift space. *Phys. Rev. D* **77**, 063530 (2008). [arXiv:0711.2521](#)
88. M. Crocce, R. Scoccimarro, Renormalized cosmological perturbation theory. *Phys. Rev. D* **73**, 063519 (2006). [arXiv:astro-ph/0509418](#)
89. J.J.M. Carrasco, M.P. Hertzberg, L. Senatore, The effective field theory of cosmological large scale structures. *JHEP* **09**, 082 (2012). [arXiv:1206.2926](#)
90. Z. Vlah, M. White, A. Aviles, A Lagrangian effective field theory. *JCAP* **09**, 014 (2015). [arXiv:1506.05264](#)
91. A. Perko, L. Senatore, E. Jennings, R.H. Wechsler, Biased tracers in redshift space in the EFT of large-scale structure (2016). [arXiv:1610.09321](#)
92. G. Cusin, M. Lewandowski, F. Vernizzi, Nonlinear effective theory of dark energy. *JCAP* **1804**(04), 061 (2018). [arXiv:1712.02782](#)
93. G. Cusin, M. Lewandowski, F. Vernizzi, Dark energy and modified gravity in the effective field theory of large-scale structure. *JCAP* **1804**(04), 005 (2018). [arXiv:1712.02783](#)
94. M. Bartelmann, E. Kozlikin, R. Lilow, C. Littek, F. Fabis, I. Kostyuk, C. Viermann, L. Heisenberg, S. Konrad, D. Geiss, Cosmic structure formation with kinetic field theory. [arXiv:1905.01179](#)
95. F. Bernardeau, S. Colombi, E. Gaztanaga, R. Scoccimarro, Large scale structure of the universe and cosmological perturbation theory. *Phys. Rept.* **367**, 1–248 (2002). [arXiv:astro-ph/0112551](#)
96. Planck, Collaboration, N. Aghanim et al., Planck 2018 results. VI: cosmological parameters. [arXiv:1807.06209](#)
97. F. Beutler, C. Blake, M. Colless, D.H. Jones, L. Staveley-Smith et al., The 6dF galaxy survey: baryon acoustic oscillations and the local Hubble constant. *Mon. Not. Roy. Astron. Soc.* **416**, 3017–3032 (2011). [arXiv:1106.3366](#)
98. A.J. Ross, L. Samushia, C. Howlett, W.J. Percival, A. Burden, M. Manera, The clustering of the SDSS DR7 main Galaxy sample-I: a 4 per cent distance measure at $z = 0.15$. *Mon. Not. Roy. Astron. Soc.* **449**(1), 835–847 (2015). [arXiv:1409.3242](#)
99. B.O.S.S. Collaboration, S. Alam et al., The clustering of galaxies in the completed SDSS-III baryon oscillation spectroscopic survey: cosmological analysis of the DR12 galaxy sample. *Mon. Not. Roy. Astron. Soc.* **470**(3), 2617–2652 (2017). [arXiv:1607.03155](#)
100. D.M. Scolnic et al., The complete light-curve sample of spectroscopically confirmed SNe Ia from Pan-STARRS1 and cosmological constraints from the combined pantheon sample. *Astrophys. J.* **859**(2), 101 (2018). [arXiv:1710.00845](#)

101. T.M.C. Abbott, DES, Collaboration et al., Dark energy Survey year 1 results: cosmological constraints from galaxy clustering and weak lensing. *Phys. Rev. D* **98**(4), 043526 (2018). [arXiv:1708.01530](#)
102. S. Joudaki et al., KiDS-450: testing extensions to the standard cosmological model. *Mon. Not. Roy. Astron. Soc.* **471**(2), 1259–1279 (2017). [arXiv:1610.04606](#)
103. D.E.S. Collaboration, T.M.C. Abbott et al., Dark energy survey year 1 results: constraints on extended cosmological models from galaxy clustering and weak lensing. *Phys. Rev. D* **99**(12)(2019). [arXiv:1810.02499](#)
104. KiDS, Collaboration, M. Asgari et al., KiDS-1000 cosmology: cosmic shear constraints and comparison between two point statistics. 7 (2020). [arXiv:2007.15633](#)
105. L. Verde, T. Treu, A.G. Riess, Tensions between the early and the late universe, in *Nature Astronomy 2019* (2019). [arXiv:1907.10625](#)
106. A.G. Riess, S. Casertano, W. Yuan, L.M. Macri, D. Scolnic, Large Magellanic Cloud Cepheid standards provide a 1% foundation for the determination of the Hubble constant and stronger evidence for physics beyond Λ CDM. *Astrophys. J.* **876**(1), 85 (2019). [arXiv:1903.07603](#)
107. K.C. Wong et al., H0LiCOW XIII. A 2.4% measurement of H_0 from lensed quasars: 5.3 σ tension between early and late-Universe probes. [arXiv:1907.04869](#)
108. J. Espejo, S. Peirone, M. Raveri, K. Koyama, L. Pogosian, A. Silvestri, Phenomenology of large scale structure in scalar-tensor theories: joint prior covariance of w_{DE} , Σ and μ in Horndeski. *Phys. Rev. D* **99**(2)(2018). [arXiv:1809.01121](#)
109. DESI, Collaboration, A. Aghamousa et al., The DESI experiment Part I: science, targeting, and survey design. [arXiv:1611.00036](#)
110. DESI, Collaboration, A. Aghamousa et al., The DESI experiment Part II: instrument design. [arXiv:1611.00037](#)
111. L.S.S.T. Collaboration, Z. Ivezić et al., LSST: from science drivers to reference design and anticipated data products. *Astrophys. J.* **873**(2), 111 (2019). [arXiv:0805.2366](#)
112. LSST Science, LSST Project, Collaboration, P.A. Abell et al., LSST science book, version 2.0. [arXiv:0912.0201](#)
113. LSST Dark Energy Science, Collaboration, D. Alonso et al., The LSST dark energy science collaboration (DESC) science requirements document. [arXiv:1809.01669](#)
114. P. Bull, P.G. Ferreira, P. Patel, M.G. Santos, Late-time cosmology with 21cm intensity mapping experiments. [arXiv:1405.1452](#)
115. M.J. Jarvis, D. Bacon, C. Blake, M.L. Brown, S.N. Lindsay, A. Raccanelli, M. Santos, D. Schwarz, Cosmology with SKA radio continuum surveys. [arXiv:1501.03825](#)
116. D. Bacon et al., Synergy between the large synoptic survey telescope and the square kilometre array. *PoS AASKA14*, 145 (2015). [arXiv:1501.03977](#)
117. T.D. Kitching, D. Bacon, M.L. Brown, P. Bull, J.D. McEwen, M. Oguri, R. Scaramella, K. Takahashi, K. Wu, D. Yamauchi, Euclid & SKA synergies. [arXiv:1501.03978](#)
118. S. Yahya, P. Bull, M.G. Santos, M. Silva, R. Maartens, P. Okouma, B. Bassett, Cosmological performance of SKA HI galaxy surveys. *Mon. Not. Roy. Astron. Soc.* **450**(3), 2251–2260 (2015). [arXiv:1412.4700](#)
119. M.G. Santos et al., Cosmology with a SKA HI intensity mapping survey. [arXiv:1501.03989](#)
120. SKA Collaboration, D.J. Bacon et al., Cosmology with phase 1 of the square kilometre array: red book 2018: technical specifications and performance forecasts. Submitted to: *Publ. Astron. Soc. Austral.* (2018). [arXiv:1811.02743](#)
121. H. Aihara et al., The hyper supprime-cam SSP survey: overview and survey design. *Publ. Astron. Soc. Jap.* **70**, S4 (2018). [arXiv:1704.05858](#)
122. N. Tamura et al., Prime focus spectrograph (PFS) for the Subaru telescope: overview, recent progress, and future perspectives. *Proc. SPIE Int. Soc. Opt. Eng.* **9908**, 99081M (2016). [arXiv:1608.01075](#)
123. EUCLID Collaboration, Collaboration, R. Laureijs et al., Euclid definition study report. [arXiv:1110.3193](#)
124. L. Amendola et al., Cosmology and fundamental physics with the Euclid satellite. *Living Rev. Rel.* **21**(1), 2 (2018). [arXiv:1606.00180](#)

125. D. Spergel et al., Wide-field infrared survey telescope-astrophysics focused telescope assets WFIRST-AFTA 2015 report. [arXiv:1503.03757](#)
126. R. Hounsell et al., Simulations of the WFIRST supernova survey and forecasts of cosmological constraints. *Astrophys. J.* **867**(1), 23 (2017). [arXiv:1702.01747](#)
127. O. Doré et al., Cosmology with the SPHEREX All-Sky spectral survey. [arXiv:1412.4872](#)
128. O. Doré et al., Science impacts of the SPHEREx all-sky optical to near-infrared spectral survey II: report of a community workshop on the scientific synergies between the SPHEREx survey and other astronomy observatories. [arXiv:1805.05489](#)
129. CMB-S4, Collaboration, K.N. Abazajian et al., *CMB-S4 Science Book* 1st edn. [arXiv:1610.02743](#)
130. CMB-S4, Collaboration, K. Abazajian et al., CMB-S4: forecasting constraints on primordial gravitational waves. [arXiv:2008.12619](#)
131. P. Ade, Simons Observatory, Collaboration et al., The Simons observatory: science goals and forecasts. *JCAP* **02**, 056 (2019). [arXiv:1808.07445](#)
132. N. Sehgal et al., CMB-HD: an ultra-deep, high-resolution millimeter-wave survey over half the sky. [arXiv:1906.10134](#)
133. N. Sehgal et al., CMB-HD: Astro2020 RFI response. [arXiv:2002.12714](#)

Chapter 30

Relativistic Effects



Camille Bonvin

The clustering of galaxies is highly sensitive to the theory of gravity and provides, therefore, a powerful way to test for deviations from General Relativity. The two dominant contributions to the galaxy number counts are density perturbations and redshift-space distortions (RSD). These contributions have been measured in surveys like BOSS [1] and WiggleZ [2] and used to test the consistency of General Relativity and place constraints on alternative models [3, 4]. Here we will show that other more subtle effects, called *relativistic effects*, contribute to the galaxy number counts [5–7]. We will see that these effects contain additional information with respect to density and RSD, and that they can therefore be used to place new constraints on the theory of gravity. In particular we will show how one of these effects, called gravitational redshift, can be used to test the equivalence principle for dark matter [8].

30.1 Number Counts

We start by deriving the general expression describing the clustering of galaxies. Maps of galaxies can be pixelised, i.e., separated in bins of solid angle and redshift. An observer can then count how many galaxies he detects in each pixel, $N(z, \mathbf{n})$, where z denotes the redshift of the pixel and \mathbf{n} its direction in the sky, and construct the galaxy fractional number overdensity

$$\Delta(z, \mathbf{n}) = \frac{N(z, \mathbf{n}) - \bar{N}(z)}{\bar{N}(z)}. \quad (30.1)$$

C. Bonvin (✉)
Department of Physics and Astronomy, University of Hawai'i, Watanabe Hall,
2505 Correa Road, Honolulu, HI 96822, USA

Here, $\bar{N}(z)$ is the mean number of galaxies per pixel at redshift z . The number of galaxies can be expressed in terms of the galaxy number density, ρ , and the volume of the pixel, \mathcal{V} , as $N(z, \mathbf{n}) = \rho(z, \mathbf{n})\mathcal{V}(z, \mathbf{n})$. Inserting this in (30.1), and keeping only terms at linear order in the perturbations we find [6]

$$\Delta(z, \mathbf{n}) = \delta_g(z, \mathbf{n}) - \frac{3 \delta z}{1 + \bar{z}} + \frac{\delta \mathcal{V}(z, \mathbf{n})}{\bar{\mathcal{V}}(\bar{z})}, \quad (30.2)$$

where $\delta_g(z, \mathbf{n})$ denotes the departure from the background number density of galaxies at the background redshift \bar{z}

$$\delta_g(z, \mathbf{n}) = \frac{\rho(z, \mathbf{n}) - \bar{\rho}(\bar{z})}{\bar{\rho}(\bar{z})}. \quad (30.3)$$

The perturbations in the redshift δz and the perturbations in the volume $\delta \mathcal{V}(z, \mathbf{n})$ can be calculated by solving the propagation of null geodesics in a perturbed Friedmann-Lemaître-Robertson-Walker Universe. At linear order in perturbation theory we find the relativistic expression for Δ [5–7]

$$\begin{aligned} \Delta(z, \mathbf{n}) = & b \cdot D - \frac{1}{\mathcal{H}} \partial_r (\mathbf{V} \cdot \mathbf{n}) \\ & + (5s - 2) \int_0^r dr' \frac{r - r'}{2rr'} \Delta_\Omega(\Phi + \Psi) \\ & + \left(1 - 5s - \frac{\dot{\mathcal{H}}}{\mathcal{H}^2} + \frac{5s - 2}{r\mathcal{H}} + f_{\text{evo}} \right) \mathbf{V} \cdot \mathbf{n} + \frac{1}{\mathcal{H}} \dot{\mathbf{V}} \cdot \mathbf{n} + \frac{1}{\mathcal{H}} \partial_r \Psi \\ & + \frac{2 - 5s}{r} \int_0^r dr' (\Phi + \Psi) + 3\mathcal{H} \nabla^{-2} (\nabla \mathbf{V}) + \Psi + (5s - 2) \Phi \\ & + \frac{1}{\mathcal{H}} \dot{\Phi} + \left(\frac{\dot{\mathcal{H}}}{\mathcal{H}^2} + \frac{2 - 5s}{r\mathcal{H}} + 5s - f_{\text{evo}} \right) \left[\Psi + \int_0^r dr' (\dot{\Phi} + \dot{\Psi}) \right], \quad (30.4) \end{aligned}$$

where ∂_r denotes a derivative along the line-of-sight, a dot is a derivative with respect to conformal time η , \mathcal{H} is the Hubble parameter in conformal time, $\mathcal{H} = \dot{a}/a$, b is the bias, s is the magnification bias, and f_{evo} denotes the evolution bias. The variable D is the gauge-invariant density perturbation in the comoving gauge, V denotes the gauge-invariant velocity potential in the Newtonian gauge, and Φ and Ψ are the two gauge-invariant Bardeen potentials.

The first line in (30.4) contains the density and redshift-space distortion (RSD) contributions, which we call hereafter the *standard terms*. These terms have been measured with great precision in past surveys [1, 2] and used to place constraints on modified theories of gravity [3, 4]. The second line contains the effect of *lensing magnification* (also called magnification bias). This effect is a combination of the fact that gravitational lensing increases the volume of observation, consequently diluting the number of galaxies that we observe, whereas at the same time it increases the

luminosity of galaxies, allowing us to see galaxies that would otherwise be fainter than the flux limit of our detector [9, 10]. Lensing magnification has been measured by cross-correlating background galaxies (or quasars) at high redshift, with foreground galaxies at low redshift [9, 11]. The last three lines contain the so-called *relativistic effects* [5–7]. These effects are neglected in current surveys, since they are suppressed by powers of \mathcal{H}/k with respect to the standard terms. Hereafter, we will see, however, that it is possible to construct an estimator to isolate some of the relativistic effects, which makes them detectable with the coming generation of surveys.

30.2 Correlation Function

30.2.1 Estimators

The standard strategy to extract information from the galaxy number counts is to measure the two-point correlation function of Δ . Various two-point estimators have been used in galaxy surveys. The estimator that is the closest to observations is the angular power spectrum, $C_\ell(z, z')$ [6, 7]. This is the estimator used in Cosmic Microwave Background analyses, since it is perfectly adapted to observations covering the whole sky. It has, furthermore, the advantage of being directly constructed from observable quantities, namely the angular separation between galaxies (which is directly translated into the multipole ℓ) and the redshifts z and z' . However, for spectroscopic surveys, the angular power spectrum has the disadvantage of requiring a very large number of redshift bins to recover all the available information [12] and of not providing a simple separation between density and redshift-space distortions, which is needed to test modified gravity in a model-independent way. As such, the angular power spectrum is most useful for photometric surveys and we will not use it here.

The second well-known estimator is the power spectrum, $P(k, \mu)$ (here μ represents the angle between the direction of observation \mathbf{n} and the vector \mathbf{k}), and more precisely its first three even multipoles: the monopole $P_0(k)$, the quadrupole $P_2(k)$ and the hexadecapole $P_4(k)$. The multipoles expansion has the advantage of allowing separate measurements of the bias b and the growth rate of structure f (more precisely, one measures the two combinations $b\sigma_8$ and $f\sigma_8$). Contrary to the angular power spectrum, the power spectrum requires the use of a fiducial cosmology to translate the measurements of angle and redshifts into cartesian coordinates, used to build the Fourier mode \mathbf{k} . However, this can be accounted for by introducing scaling parameters, which allow the true cosmology to differ from the fiducial one [13]. The true problem of the power spectrum is the fact that it is built on the flat-sky approximation, i.e., the approximation that the directions to the two pixels in the correlation are parallel. As such it is not well adapted to surveys with large sky coverage, like the coming generation of surveys.

In particular, since relativistic effects are expected to be of the same order of magnitude as wide-angle effects [14], the power spectrum cannot be consistently used to study relativistic effects. Methods have been proposed to overcome this problem, but they complicate significantly the measurement of the power spectrum [15]. The second more fundamental problem of the power spectrum is that it does not allow for a consistent calculation of the integrated terms in Eq. (30.4), in particular of the lensing magnification, which is important at high redshift [16]. The power spectrum indeed requires the knowledge of Δ on three-dimensional hypersurfaces of constant time, whereas lensing can only be calculated consistently on the past-light cone of the observer. The power spectrum is therefore badly adapted to the coming generation of surveys that will probe large scales and high redshifts.

The last two-point estimator that is widely used is the two-point correlation function in redshift space, $\xi(d, \sigma)$, where d represents the separation between pairs of galaxies, and σ denotes the angle between this separation and the direction of observation \mathbf{n} . As for the power spectrum, the first three even multipoles of the correlation function, $\xi_0(d)$, $\xi_2(d)$ and $\xi_4(d)$ are routinely measured in galaxy surveys. These multipoles provide a separate measurement of b and f . The correlation function also requires a fiducial cosmology to translate the measurement of angles and redshift into a measurement of d and σ , but as for the power spectrum, this can consistently be accounted for. The correlation function has, furthermore, the advantage over the power spectrum that it can be calculated in the full sky [14, 17]. One can then consistently expand around the flat-sky approximation and control the regime in which this approximation is valid. Moreover, lensing magnification can be included in the modelling of the correlation function and of its multipoles [16]. The correlation function is therefore ideally adapted to the coming generation of surveys. Its only disadvantage is that its covariance matrix is non-diagonal, which complicates the construction of the likelihood. In the following we will use the correlation function to extract relativistic effects.

30.2.2 *Even and Odd Multipoles*

Let us start by calculating the correlation function in General Relativity, i.e., using the continuity equation to relate the peculiar velocity V to the matter density D (in the standard terms), using the Euler equation to relate the gravitational potential Ψ to the peculiar velocity V (in the relativistic terms), and assuming no anisotropic stress and Poisson equation to relate the two metric potentials to the density D (in the lensing magnification term).

The full-sky expression for the correlation function from the standard terms (density and RSD) can be found in [14, 18]. This expression is valid at all scales. In the flat-sky approximation it reduces to the well-known expression

$$\begin{aligned} \xi^{\text{st}}(z, d, \sigma) = & \left[b^2 + \frac{2bf}{3} + \frac{f^2}{5} \right] \mu_0(d, z) - \left[\frac{4bf}{3} + \frac{4f^2}{7} \right] \mu_2(d, z) \cdot P_2(\cos \sigma) \\ & + \frac{8f^2}{35} \mu_4(d, z) \cdot P_4(\cos \sigma), \end{aligned} \quad (30.5)$$

where P_ℓ is the Legendre polynomial of degree ℓ , f is the growth rate of structure defined through $f = d \ln D_1 / d \ln a$, with D_1 the growth function and

$$\mu_\ell(d, z) = \frac{1}{2\pi^2} \int dk k^2 P(k, z) j_\ell(kd). \quad (30.6)$$

Here, P denotes the density matter power spectrum at present defined as

$$\langle D(\mathbf{k}, z) D(\mathbf{k}', z) \rangle = (2\pi)^3 P(k, z) \delta_D(\mathbf{k} + \mathbf{k}'), \quad (30.7)$$

where we have used the Fourier transform convention $f(\mathbf{x}, z) = \frac{1}{(2\pi)^3} \int d^3\mathbf{k} e^{-i\mathbf{k}\cdot\mathbf{x}} f(\mathbf{k}, z)$. The redshift z denotes the mean redshift of the pair, or the mean redshift of the bin in which we average the correlation function. In the flat-sky approximation we automatically neglect the evolution between the two galaxies in the pair.

The lensing magnification adds contributions to the correlation function. The full-sky and flat-sky expressions for the lensing can be found in [16]. The multipoles can then be numerically extracted using

$$\xi_\ell^{\text{lens}}(z, d) = \frac{2\ell + 1}{2} \int_{-1}^1 d\mu \xi^{\text{lens}}(z, d, \mu) P_\ell(\mu). \quad (30.8)$$

In this chapter, we will neglect the lensing magnification, since we will work at relatively small redshift ($z \leq 1.2$), where the lensing is strongly subdominant.

Finally, the relativistic effects also contribute to the correlation function. The dominant relativistic effects are due to the third line in Eq. (30.4), which contains one gradient of the potentials. As such they are suppressed by one power of \mathcal{H}/k with respect to the standard terms. However, these terms are anti-symmetric, which implies that their correlation with the density and RSD exactly vanishes. Hence their contribution to the correlation function comes from their auto-correlation, which is suppressed by $(\mathcal{H}/k)^2$ with respect to the standard terms. Due to this suppression, these terms become relevant only at very large separations, where cosmic variance is important. It is therefore very difficult to detect these terms in the monopole, quadrupole and hexadecapole of the correlation function. To overcome this difficulty, the following method has been proposed: if one splits the population of galaxies into two (or more) populations, then the correlation function can contain an anti-symmetric part. Consequently, the correlation between the standard terms and the relativistic effects does not vanish anymore, and it generates odd multipoles in the correlation function. By measuring these odd multipoles, one can therefore *isolate*

the contribution from relativistic effects. The full-sky expression for the relativistic correlation function can be found in [14].

In the flat-sky, cross-correlating two populations of galaxies, one bright and one faint population, we obtain

$$\begin{aligned} \xi^{\text{rel}}(z, d, \sigma) = & \frac{\mathcal{H}}{\mathcal{H}_0} \left\{ \left[(b_{\text{B}} - b_{\text{F}}) \left(\frac{2}{r\mathcal{H}} + \frac{\dot{\mathcal{H}}}{\mathcal{H}^2} \right) + 3(s_{\text{F}} - s_{\text{B}})f^2 \left(1 - \frac{1}{r\mathcal{H}} \right) \right. \right. \\ & + 5(b_{\text{B}}s_{\text{F}} - b_{\text{F}}s_{\text{B}})f \left(1 - \frac{1}{r\mathcal{H}} \right) \left. \left. \right] v_1(d, z) P_1(\cos \sigma) \right. \\ & \left. + 2 \left(1 - \frac{1}{r\mathcal{H}} \right) (s_{\text{B}} - s_{\text{F}})f v_3(d, z) P_3(\cos \sigma) \right\}, \end{aligned} \quad (30.9)$$

where b_{B} and s_{B} denotes the bias and magnification bias of the bright galaxies, b_{F} and s_{F} those of the faint galaxies, and

$$v_\ell(d, z) = \frac{1}{2\pi^2} \int dk k \mathcal{H}_0 P(k, z) j_\ell(kd). \quad (30.10)$$

In the flat-sky the standard terms do not contribute to the odd multipoles. However, because the standard terms are larger than the relativistic terms by one factor k/\mathcal{H} , their full-sky correction is of the same order of magnitude as the flat-sky relativistic effects. For consistency we therefore need to include this correction, which reads

$$\begin{aligned} \xi^{\text{st corr}}(z, d, \sigma) = & \left[- (b_{\text{B}} - b_{\text{F}}) \frac{2f}{5} \mu_2(d, z) + (b_{\text{B}} - b_{\text{F}}) \frac{rf'}{6} \left(\mu_0(d, z) \right. \right. \\ & - \frac{4}{5} \mu_2(d, z) \left. \left. \right) - \frac{rf}{6} (b'_{\text{B}} - b'_{\text{F}}) \left(\mu_0(d, z) - \frac{4}{5} \mu_2(d, z) \right) \right. \\ & \left. + \frac{r}{2} (b_{\text{B}} b'_{\text{F}} - b'_{\text{B}} b_{\text{F}}) \mu_0(d, z) \right] \frac{d}{r} P_1(\cos \sigma) + \left[(b_{\text{B}} - b_{\text{F}}) \frac{2f}{5} \right. \\ & \left. - (b_{\text{B}} - b_{\text{F}}) \frac{rf'}{5} + (b'_{\text{B}} - b'_{\text{F}}) \frac{rf}{5} \right] \mu_2(d, z) \frac{d}{r} P_3(\cos \sigma), \end{aligned} \quad (30.11)$$

where a prime denotes a derivative with respect to conformal distance r . The first term is a wide-angle correction, due to the fact that the line-of-sights to the two galaxies are not parallel. The other terms are evolution corrections, coming from the fact that the bias and the growth rate f are evolving between the two galaxies. As shown in [14], the evolution corrections are always much smaller than the relativistic contributions and we can safely neglect them. The wide-angle correction is, however, of the same order as the relativistic effects and we have to keep it.

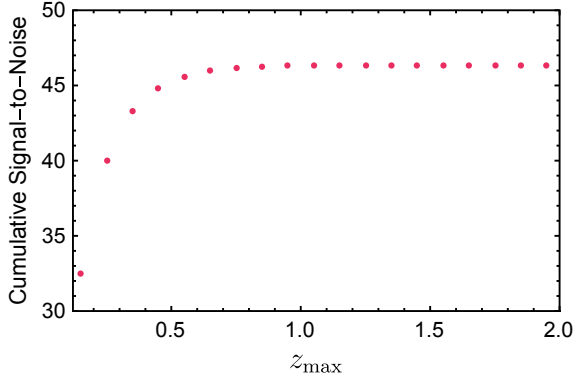
30.3 Test of the Equivalence Principle

Let us now explore how the monopole, quadrupole, hexadecapole and dipole can be used to test gravity. Note that the octupole is also non-zero, but its signal-to-noise is significantly lower than the one of the dipole, thus we prefer not to consider it here (see, e.g., [19] for a discussion about the octupole in theories with a screening mechanism). As explained above, the even multipoles are sensitive to density and RSD. A combined measurement of these quantities allows, therefore, to probe the density D and velocity V separately. They have been used to constrain modifications of gravity through their impact on the growth rate f . The dipole is sensitive to the time component of the metric Ψ , through the effect of gravitational redshift (the last term in the third line of (30.4)) and through the velocity via Doppler effects (the first two terms in the third line of (30.4)). The dipole therefore adds new information, via the measurement of Ψ , and can be used to test the Euler equation which relates Ψ to V . This provides a direct test of the equivalence principle for dark matter [8]. V is indeed the peculiar velocity of galaxies, which are mainly made of dark matter, and it tells us therefore how halos of dark matter fall inside a gravitational potential. Ψ , on the other hand, is measured from gravitational redshift, and tells us how light escapes from that same gravitational potential. The dipole therefore provides a way of testing the equivalence between the fall of light and the fall of dark matter. Any violation of this principle would leave an imprint on the dipole.

Note that such a test of the equivalence principle cannot be performed without the dipole. Lensing measurements indeed provide a measurement of the sum of the two metric potentials $\Phi + \Psi$. If one does not know the value of the anisotropic stress, this cannot be used to test the equivalence principle. Standard tests of gravity usually assume that the equivalence principle is valid, to translate measurements of V from RSD into measurements of Ψ , using the Euler equation. They then compare the Ψ obtained in this way with lensing measurements of $\Phi + \Psi$ to test for the presence of anisotropic stress. They also compare Φ with a measurement of the density D to test the validity of the Poisson equation. With this method, we see that if a non-zero anisotropic stress is detected, we cannot know if this anisotropic stress is real, or if it is a consequence of the fact that the Euler equation is not valid, and that the inferred Ψ is wrong. Similarly, any observed deviation in the Poisson equation could either be real, or due to the fact that Ψ is incorrect (leading to an incorrect Φ). Observing the dipole is therefore crucial for these tests, since it will break the degeneracies by providing a direct measurement of Ψ . Note that this method is highly complementary to the tests of the equivalence principle that have been proposed using consistency relations between the two-point and three-point correlation functions [20, 21]. These consistency relations indeed provide a test of the equivalence principle between baryons and dark matter, but they do not provide a measurement of the gravitational potential Ψ .

As discussed above, the dipole is a combination of relativistic effects (30.9) and wide-angle effects (the first term in (30.11)). To measure Ψ with the dipole, it is therefore necessary to remove the wide-angle effects. As shown in [14], the wide-

Fig. 30.1 Signal-to-noise for the dipole for a survey like SKA phase 2, cumulative over separations from $10 \leq d \leq 200 \text{ Mpc}/h$ and up to redshift z_{max} . We use pixels of size $\ell_{Pl} = 2 \text{ Mpc}/h$



angle effects are proportional to the difference between the quadrupole of the bright and of the faint populations. We can therefore remove the wide-angle effects by constructing the following estimator ¹ [22]

$$\begin{aligned} \hat{\xi}_1 = & \frac{3}{8\pi} \left(\frac{\ell_{Pl}}{d} \right)^2 \frac{\ell_{Pl}^3}{\mathcal{V}_z} \sum_{ij} [\Delta_B(\mathbf{x}_i)\Delta_F(\mathbf{x}_j) - \Delta_F(\mathbf{x}_i)\Delta_B(\mathbf{x}_j)] P_1(\cos \sigma_{ij}) \delta_K(d_{ij} - d) \\ & - \frac{3}{10} \frac{d}{r} \frac{5}{4\pi} \left(\frac{\ell_{Pl}}{d} \right)^2 \frac{\ell_{Pl}^3}{\mathcal{V}_z} \sum_{ij} [\Delta_B(\mathbf{x}_i)\Delta_B(\mathbf{x}_j) - \Delta_F(\mathbf{x}_i)\Delta_F(\mathbf{x}_j)] P_2(\cos \sigma_{ij}) \delta_K(d_{ij} - d), \end{aligned} \tag{30.12}$$

where ℓ_{Pl} denotes the size of the cubic pixels, and \mathcal{V}_z is the volume of the redshift bin in which we average the dipole.

To test the Euler equation, we modify it in the following way [8]

$$\dot{\mathbf{V}} \cdot \mathbf{n} + \mathcal{H}[1 + \Theta(z)]\mathbf{V} \cdot \mathbf{n} + [1 + \Gamma(z)]\partial_r \Psi = 0, \tag{30.13}$$

where $\Theta(z)$ and $\Gamma(z)$ are two free parameters, which vanish if the equivalence principle is valid. For simplicity we assume that these two parameters depend only on redshift and not on scale. This is the case in particular models, like scalar-tensor and vector-tensor theories, that are non-minimally coupled to dark matter (in the quasi-static approximation). The dipole is then modified in the following way by $\Theta(z)$ and $\Gamma(z)$

$$\begin{aligned} \xi_1 = \langle \hat{\xi}_1 \rangle = & \frac{\mathcal{H}}{\mathcal{H}_0} \left\{ (b_B - b_F) \left[\left(\frac{2}{r\mathcal{H}} + \frac{\dot{\mathcal{H}}}{\mathcal{H}^2} \right) f + \Upsilon(z) \right] + 3(s_F - s_B) f^2 \left(1 - \frac{1}{r\mathcal{H}} \right) \right. \\ & \left. + 5(b_B s_F - b_F s_B) f \left(1 - \frac{1}{r\mathcal{H}} \right) \right\} v_1(d, z), \end{aligned} \tag{30.14}$$

¹ Note that the sign in [8, 22] is incorrect, however this is a typo and the results are correct.

where

$$\Upsilon(z) \equiv \frac{\Theta - \Gamma}{1 + \Gamma} f - \frac{\Gamma}{1 + \Gamma} \left(\frac{\dot{\mathcal{H}}}{\mathcal{H}^2} f + f^2 + \frac{\dot{f}}{\mathcal{H}} \right). \quad (30.15)$$

We now forecast the precision with which future experiments, like DESI [23] and the SKA [24], will be able to constrain $\Theta(z)$ and $\Gamma(z)$. Details of the forecasts can be found in [8]. Here we summarise the results.

In Fig. 30.1 we show the cumulative signal-to-noise of the dipole for a survey like SKA phase 2, cumulative over separations (from $10 \leq d \leq 200 \text{ Mpc}/h$), and up to redshift z_{max} . We use the specifications of [25] for the number density, volume and bias. We split the populations of galaxies into two populations with the same number of galaxies, with bias $b_B = b + \Delta b/2$ and $b_F = b - \Delta b/2$, and we choose $\Delta b = 0.5$. The signal-to-noise is directly proportional to Δb . As an example, a bias difference of $\Delta b \simeq 1$ between the bright and faint populations of luminous red galaxies has been measured in BOSS [18]. For the HI galaxies targeted by the SKA, the expected bias difference is less well known, therefore we choose a conservative bias difference of $\Delta b = 0.5$. For simplicity we set here $s_B = s_F = 0$. From Fig. 30.1, we see that above $z \simeq 1 - 1.2$, there is no improvement of the signal-to-noise. This is due to the fact that the dipole decreases with redshift and is therefore more easily detectable at low redshift. We can therefore safely neglect the contribution from lensing magnification to the dipole, and also to the other even multipoles, since it is strongly subdominant below $z = 1.2$. The cumulative signal-to-noise over the whole range of redshift reaches 46.4, showing that the dipole will be robustly measured with the SKA.

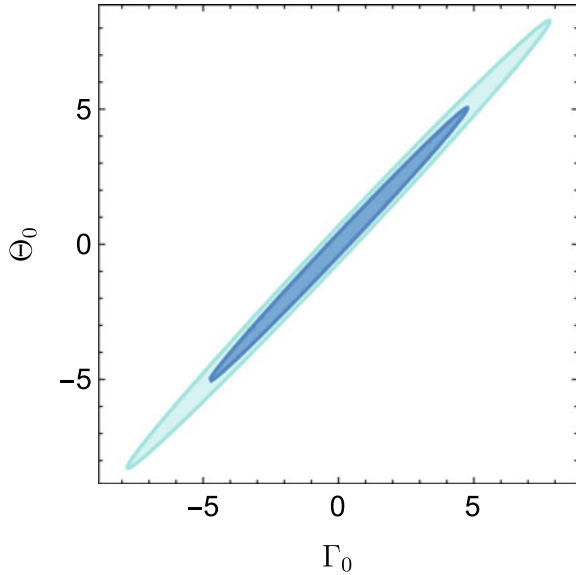
Following [26], we assume that the functions $\Theta(z)$ and $\Gamma(z)$ evolve as

$$\Theta(z) = \Theta_0 \frac{\Omega_\Lambda(z)}{\Omega_\Lambda(0)}, \quad (30.16)$$

and similarly for $\Gamma(z)$. This means that the breaking of the equivalence principle happens at late time, when dark energy or modified gravity are relevant. We forecast the constraints on Θ_0 and Γ_0 , using a Fisher matrix analysis. In Fig. 30.2 we show the 1σ and 2σ contours obtained by fixing all other cosmological parameters and the biases to their fiducial values, and assuming no other deviation from General Relativity. We see that the constraints are extremely degenerated. This can be understood from Eq. (30.15), which shows that the first term in Υ is sensitive to $\Theta - \Gamma$ (at lowest order in Θ and Γ the denominator reduces to 1). This first term dominates in Υ , which is therefore mainly sensitive to this combination. What we are therefore really interested in is rather the sensitivity of the dipole to Υ , or similarly to one of the parameters Θ or Γ , since our goal is to detect any generic violation of the equivalence principle.

In the following we therefore fix $\Theta = 0$, and we forecast the constraints on Γ_0 . We also include this time the monopole, quadrupole and hexadecapole in the forecasts. These terms are not sensitive to Γ_0 but they are sensitive to the biases, which we model in the following way [25]

Fig. 30.2 Joint 1σ and 2σ constraints on Θ_0 and Γ_0 obtained from the dipole for a survey like SKA phase 2. All other cosmological parameters and the biases are fixed to their fiducial values. Published in [8] (©OP Publishing Ltd and SISSA Medialab Srl. Reproduced by permission of IOP Publishing. All rights reserved)



$$b_B(z) = b_1 e^{b_2 z} + \frac{\Delta b}{2}, \tag{30.17}$$

$$b_F(z) = b_3 e^{b_4 z} - \frac{\Delta b}{2}, \tag{30.18}$$

where as before we fix the bias difference $\Delta b = b_B - b_F = 0.5$. We therefore have four additional free parameters b_1, b_2, b_3 and b_4 that we want to constrain. We choose their fiducial value as in [25] (see table 6): $b_1 = b_3 = 0.554$ and $b_2 = b_4 = 0.783$. In this way the bias of the bright and of the faint population are uncorrelated, but their difference is always 0.5. The even multipoles are also sensitive to any modification in the growth of structure. We model this by a function $\mu(z)$, which modifies the growth function

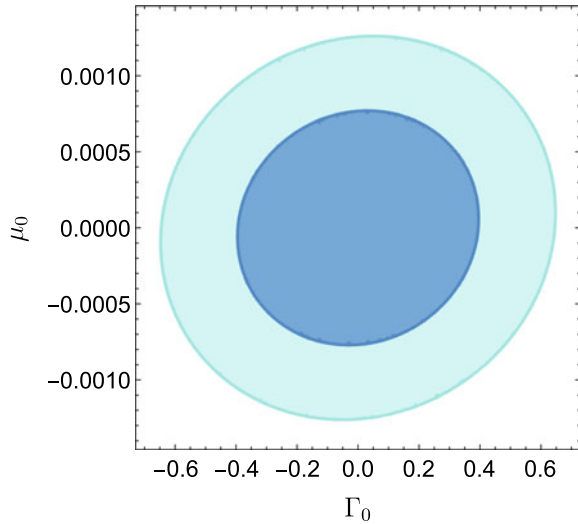
$$D_1(z) = \bar{D}_1(z)[1 + \mu(z)], \tag{30.19}$$

where \bar{D}_1 denotes the growth function in a Λ CDM universe, and we let $\mu(z)$ evolve as in Eq. (30.16). The growth rate can then be written as a function of μ_0

$$f(z) = \bar{f}(z) + 3\Omega_{m0}(1+z)^3 \left[\frac{1 - \Omega_m(z)}{1 - \Omega_{m0}} \right]^2 \mu_0, \tag{30.20}$$

where \bar{f} denotes the growth rate in a Λ CDM universe. The parameter μ_0 and the four bias parameters are constrained by the even multipoles and by the dipole, whereas Γ_0 is only constrained by the dipole. In Fig. 30.3 we show the 1σ and 2σ contours on Γ_0 and μ_0 , marginalised over the bias parameters. We see that the constraints on

Fig. 30.3 Joint 1σ and 2σ constraints on μ_0 and Γ_0 obtained from a combination of the dipole, monopole, quadrupole and hexadecapole for a survey like SKA phase 2. We marginalise over the biases of the bright and faint populations. Θ_0 is fixed to zero and all other cosmological parameters are fixed to their fiducial values. Published in [8] (©OP Publishing Ltd and SISSA Medialab Srl. Reproduced by permission of IOP Publishing. All rights reserved)



Γ_0 are much tighter, now that $\Theta_0 = 0$. This really shows the sensitivity of the dipole to a generic breaking of the equivalence principle. The constraints on μ_0 are tighter than the constraints on Γ_0 by two orders of magnitude. This simply reflects the fact that the even multipoles, which are sensitive to μ_0 , have a significantly larger signal-to-noise than the dipole, which is sensitive to Γ_0 . A constraint of $\sim 20\text{--}30\%$ on the validity of the equivalence principle is, however, a very significant constraints at low redshift, since standard RSD and lensing measurement are completely insensitive to this.

30.4 Conclusions

Galaxy clustering is a powerful probe of the theory of gravity. Here we have demonstrated that the relativistic effects in the galaxy number counts do carry additional information, which is complementary to the standard density and RSD contributions. In particular, one extremely interesting relativistic effect is gravitational redshift, which is sensitive to the time component of the metric, Ψ . We have shown that by splitting the population of galaxies into two populations, and by fitting for a dipole in the cross-correlation between these two populations, we can isolate the effect of gravitational redshift. We can then use this effect in conjunction with RSD to test the equivalence principle for dark matter. We have forecasted the precision with which a violation of the equivalence principle can be detected with a survey like SKA phase two and we have seen that it reaches $20\text{--}30\%$. This shows the interest of relativistic effects in galaxy clustering.

References

1. BOSS webpage. <http://www.sdss3.org/surveys/boss.php>
2. WiggleZ webpage. <http://wigglez.swin.edu.au/site/>
3. BOSS Collaboration, S. Alam et al., The clustering of galaxies in the completed SDSS-III baryon oscillation spectroscopic survey: cosmological analysis of the DR12 galaxy sample. *Mon. Not. Roy. Astron. Soc.* **470**, 2617–2652 (2017). [arXiv:1607.03155](https://arxiv.org/abs/1607.03155)
4. D. Parkinson, S. Riemer-Sørensen, C. Blake, G.B. Poole, T.M. Davis, S. Brough, M. Colless, C. Contreras, W. Couch, S. Couch et al., The wigglez dark energy survey: final data release and cosmological results. *Phys. Rev. D* **86** (2012)
5. J. Yoo, A.L. Fitzpatrick, M. Zaldarriaga, A new perspective on galaxy clustering as a cosmological probe: general relativistic effects. *Phys. Rev. D* **80** (2009). [arXiv:0907.0707](https://arxiv.org/abs/0907.0707)
6. C. Bonvin, R. Durrer, What galaxy surveys really measure. *Phys. Rev. D* **84**, 063505 (2011). [arXiv:1105.5280](https://arxiv.org/abs/1105.5280)
7. A. Challinor, A. Lewis, The linear power spectrum of observed source number counts. *Phys. Rev. D* **84**, 043516 (2011). [arXiv:1105.5292](https://arxiv.org/abs/1105.5292)
8. C. Bonvin, P. Fleury, Testing the equivalence principle on cosmological scales. *JCAP* **1805**(05), 061 (2018). [arXiv:1803.02771](https://arxiv.org/abs/1803.02771)
9. S.D.S.S. Collaboration, R. Scranton et al., Detection of cosmic magnification with the Sloan Digital Sky Survey. *Astrophys. J.* **633**, 589–602 (2005). [arxiv:astro-ph/0504510](https://arxiv.org/abs/astro-ph/0504510)
10. C. Duncan, B. Joachimi, A. Heavens, C. Heymans, H. Hildebrandt, On the complementarity of galaxy clustering with cosmic shear and flux magnification. *Mon. Not. Roy. Astron. Soc.* **437**(3), 2471–2487 (2014). [arXiv:1306.6870](https://arxiv.org/abs/1306.6870)
11. D.E.S. Collaboration, M. Garcia-Fernandez et al., Weak lensing magnification in the Dark Energy Survey Science Verification Data. *Mon. Not. Roy. Astron. Soc.* **476**(1), 1071–1085 (2018). [arXiv:1611.10326](https://arxiv.org/abs/1611.10326)
12. J. Asorey, M. Crocce, E. Gaztanaga, A. Lewis, Recovering 3D clustering information with angular correlations. *Mon. Not. Roy. Astron. Soc.* **427**, 1891 (2012). [arXiv:1207.6487](https://arxiv.org/abs/1207.6487)
13. X. Xu, A.J. Cuesta, N. Padmanabhan, D.J. Eisenstein, C.K. McBride, Measuring d_a and h at $z = 0.35$ from the SDSS dr7 LRGS using baryon acoustic oscillations. *Mon. Not. R. Astron. Soc.* **431**, 2834–2860 (2013)
14. C. Bonvin, L. Hui, E. Gaztañaga, Asymmetric galaxy correlation functions. *Phys. Rev. D* **89**(8), 083535 (2014). [arXiv:1309.1321](https://arxiv.org/abs/1309.1321)
15. K. Yamamoto, M. Nakamichi, A. Kamino, B.A. Bassett, H. Nishioka, A Measurement of the quadrupole power spectrum in the clustering of the 2dF QSO survey. *Publ. Astron. Soc. Jap.* **58**, 93–102 (2006). [arxiv:astro-ph/0505115](https://arxiv.org/abs/astro-ph/0505115)
16. V. Tansella, C. Bonvin, R. Durrer, B. Ghosh, E. Sellentin, *The full-sky relativistic correlation function and power spectrum of galaxy number counts: I. Theoretical aspects*. [arXiv:1708.00492](https://arxiv.org/abs/1708.00492)
17. P.H.F. Reimberg, F. Bernardeau, C. Pitrou, Redshift-space distortions with wide angular separations. *JCAP* **1601**(01), 048 (2016). [arXiv:1506.06596](https://arxiv.org/abs/1506.06596)
18. E. Gaztañaga, C. Bonvin, L. Hui, Measurement of the dipole in the cross-correlation function of galaxies. *JCAP* **1701**(01), 032 (2017). [arXiv:1512.03918](https://arxiv.org/abs/1512.03918)
19. D. Kodwani, H. Desmond, Screened fifth forces in parity-breaking correlation functions. *Phys. Rev. D* **100**(6), 064030 (2019). [arXiv:1904.12310](https://arxiv.org/abs/1904.12310)
20. A. Kehagias, J. Norena, H. Perrier, A. Riotto, Consequences of symmetries and consistency relations in the large-scale structure of the universe for non-local bias and modified gravity. *Nucl. Phys. B* **883**, 83–106 (2014). [arXiv:1311.0786](https://arxiv.org/abs/1311.0786)
21. P. Creminelli, J. Gleyzes, L. Hui, M. Simonović, Single-Field consistency relations of large scale structure. Part III: test of the equivalence principle. *JCAP* **1406**, 009 (2014). [arXiv:1312.6074](https://arxiv.org/abs/1312.6074)
22. A. Hall, C. Bonvin, Measuring cosmic velocities with 21 cm intensity mapping and galaxy redshift survey cross-correlation dipoles. *Phys. Rev. D* **95**(4), 043530 (2017). [arXiv:1609.09252](https://arxiv.org/abs/1609.09252)
23. DESI Collaboration, A. Aghamousa et al., *The DESI Experiment Part I: Science, Targeting, and Survey Design*. [arXiv:1611.00036](https://arxiv.org/abs/1611.00036)

24. SKA webpage. <https://www.skatelescope.org>
25. P. Bull, Extending cosmological tests of General Relativity with the Square Kilometre Array. *Astrophys. J.* **817**(1), 26 (2016). [arXiv:1509.07562](https://arxiv.org/abs/1509.07562)
26. J. Gleyzes, D. Langlois, F. Vernizzi, A unifying description of dark energy. *Int. J. Mod. Phys. D* **23**(13), 1443010 (2015). [arXiv:1411.3712](https://arxiv.org/abs/1411.3712)

Chapter 31

Cosmological Constraints from the Effective Field Theory of Dark Energy



Noemi Frusciante and Simone Peirone

31.1 The Effective Field Theory for Dark Energy in a Nutshell

The Effective Field Theory (EFT) framework for dark energy (DE) provides an effective description for cosmological perturbations of genuine departures from General Relativity (GR) [1–7]. It encompasses any dark energy and modified gravity (MG) models with one additional scalar degree of freedom (DoF) through a variety of geometrical operators compatible with the residual symmetries of unbroken spatial diffeomorphisms. The operators are organised in powers of the number of perturbations and spatial derivatives, and each of them multiplies a time-dependent function, called EFT function. The EFT action is constructed in the unitary gauge around a Friedmann-Lemaître-Robertson-Walker (FLRW) background, and up to second order in perturbations it reads [1]

$$S = \frac{1}{2} \int d^4x \sqrt{-g} \left[M_{\text{pl}}^2 f(t) R - 2\Lambda(t) - 2c(t)g^{00} + M_2^4(t)(\delta g^{00})^2 - \bar{m}_1^3(t) \delta g^{00} \delta K - \bar{M}_2^2(t) \delta K^2 - \bar{M}_3^2(t) \delta K_\mu{}^\nu \delta K^\mu{}_\nu + \mu_1^2(t) \delta g^{00} \delta R + m_2^2(t) h^{\mu\nu} \partial_\mu g^{00} \partial_\nu g^{00} + \dots \right] + S_m[g_{\mu\nu}, \chi_m], \quad (31.1)$$

N. Frusciante (✉)

Researcher, Instituto de Astrofísica e Ciências do Espaço, Faculdade de Ciências da Universidade de Lisboa, Edifício C8, Campo Grande, 1749016 Lisboa, Portugal
e-mail: nfrusciante@fc.ul.pt

S. Peirone

Institute Lorentz, Leiden University, PO Box 9506, Leiden 2300 RA, The Netherlands
e-mail: peirone@lorentz.leidenuniv.nl

where M_{pl}^2 is the Planck mass, $g^{00} = -1 + \delta g^{00}$ is the time-time component of the metric and δg^{00} its perturbation, g is the determinant of the metric, $g^{\mu\nu}$, $h_{\mu\nu} = g_{\mu\nu} + n_\mu n_\nu$ is the induced metric, with n_μ being the unit vector perpendicular to the time slicing, δR and $\delta R_{\mu\nu}$ are the perturbations of the Ricci scalar and tensor, and δK and δK_ν^μ are the perturbations of the extrinsic curvature scalar and tensor. \mathfrak{f} , Λ , c , M_i , m_i , \bar{M}_i , \bar{m}_i and μ_i are the EFT functions. We note that \mathfrak{f} , Λ , c are the sole EFT functions entering in both the background equations and linear perturbations, while the others affect only the perturbations. S_m is the matter action, with the metric $g_{\mu\nu}$ universally coupled to the matter fields χ_m . The ellipsis stand for possible extensions of the action in several directions to include: additional second order operators, e.g., $(\delta R)^2$ [3], or higher order terms in derivatives [8–10], direct gravitational interaction between the additional scalar DoF and the matter fields [11–14], theories with second-order derivative equations of motion with a vector or tensor additional field [15, 16], non-linear perturbative effects [17–22].

The EFT framework preserves a direct link between the model-independent approach of the EFT basis and specific DE/MG models, such as $f(R)$, Horndeski and others. It is indeed possible to obtain a mapping recipe, which allows us to write any EFT function in term of the free functions characterising a specific theory [1–3, 9, 10, 23, 24]. It follows that considering sub-sets of EFT functions, we can model specific classes of DE/MG models. For example, the sub-set of background EFT functions $\{\mathfrak{f}, \Lambda, c\}$ describes the Generalised Brans–Dicke class of theories (GBD), while imposing $\bar{M}_2^2 = -\bar{M}_3^2 = 2\mu_1^2$ (and $m_2^2 = 0$) restricts us to Horndeski theory [25, 26] and relaxing the latter condition to have $\bar{M}_2^2 = -\bar{M}_3^2$ (and $m_2^2 = 0$) we can construct scalar-tensor theories beyond Horndeski, the so called Gleyzes–Langlois–Piazza–Vernizzi (GLPV) theories [27]. Finally, Lorentz violating theories are characterised by $m_2^2 \neq 0$ [1, 9].

An alternative basis of the EFT action (31.1), called α -basis, was introduced in [28]. This basis encodes specific physical properties of the Horndeski theory in four time-dependent phenomenological functions, namely: the *running Planck mass* $\alpha_M(t)$, which defines the time variation of the *effective Planck mass* $M^2(t)$, the *braiding* $\alpha_B(t)$ accounting for the interaction between the extra DoF and the metric, the *kineticity* $\alpha_K(t)$, which is purely a kinetic function, and the *speed of tensor excess* $\alpha_T(t)$, describing any modification in the speed of propagation of tensor modes. The inclusion of GLPV models requires an extra function, $\alpha_H(t)$, defining the departure from Horndeski models [12, 24], and two additional functions are necessary to include Lorentz violation effects, $\alpha_{K_2}(t)$, $\alpha_B^{GLPV}(t)$ [10], respectively an extension of the *kineticity* and deviation from GLPV models. These functions can be identified in terms of the EFT basis as follows

$$\alpha_M = \frac{1}{H} \frac{d \ln M^2}{d \ln t}, \quad \alpha_B(t) = -\frac{M_{\text{pl}}^2 \dot{\mathfrak{f}} + \bar{m}_1^3}{H M^2},$$

$$\alpha_T(t) = \frac{\bar{M}_3^2}{M^2} \equiv c_t^2 - 1, \quad \alpha_K(t) = \frac{2c + 4M_2^4}{H^2 M^2},$$

$$\alpha_{K_2}(t) = \frac{8m_2^2}{M^2 H^2}, \quad \alpha_H(t) = \frac{2\mu_1^2 + \bar{M}_3^2}{M^2},$$

$$\alpha_B^{GLPV}(t) = \frac{\bar{M}_3^2 + \bar{M}_2^2}{M^2}, \quad (31.2)$$

where $M^2(t) = M_{\text{pl}}^2 - \bar{M}_3^2$, c_t is the speed of propagation of gravitational waves (GWs) (tensor modes) and $H = \frac{1}{a} \frac{da}{dt}$ is the Hubble function. While all the α functions enter into the linear scalar perturbation equations, only two of them impact the propagation of GWs, i.e., α_M , which modifies the friction term and α_T , which as previously mentioned, is the deviation in the speed of propagation of GWs.

The advantage of having at our disposal a framework to perform model-independent explorations of gravity models allowed to identifying clear patterns [2, 4, 11–13, 13, 14, 14, 17, 19, 29–42, 42–53] to be tested against cosmological data. In the following we will overview the state of the art about cosmological constraints obtained in the EFT context using present day measurements and forecasts from future missions.

31.2 Einstein Boltzmann Codes

The large number of DE/MG proposals introduces the challenge of being able to constrain them against observational data, such as the cosmic microwave background (CMB) radiation, galaxy clustering (GC), weak lensing (WL), redshift-space distortions (RSD), Supernovae Ia (SNIa) and baryon acoustic oscillations (BAO). To this purpose one needs to accurately compute a range of theoretical predictions for the considered cosmologies. This is possible thanks to Einstein-Boltzmann (EB) codes that numerically solve the linear evolution of relevant perturbed quantities (e.g., gravitational potentials, matter density fluctuations) on an expanding FLRW background.

For the standard Λ CDM scenario, many different EB codes exist [54–60]. Among these, the most widely used in the cosmological analyses are: CAMB [61] and CLASS [62]. EB codes based on the EFT framework have also been developed in order to test a broad class of DE/MG models. In such codes the linear perturbation equations are written in terms of the EFT functions preserving the model-independent approach of the EFT framework. The EFT functions can be then fixed according to two procedures:

- The *pure* EFT approach: each EFT function (or a sub-set) is directly parametrised, for example as a function of the scale factor, a , or the DE density parameter Ω_{DE} . In this case the background expansion has to be chosen as well, by fixing the DE equation of state w_{DE} ;
- The *mapping* approach: the EFT functions evolve according to a specific DE/MG model through the mapping recipe [1–3, 9, 10, 23, 24], and their behaviour is fixed after solving the background Friedmann equations for the chosen model.

As a first example of such codes, EFTCAMB [63, 64] (www.eftcamb.org) is an implementation of the EFT framework into CAMB. The code can compute cosmological observables for specific models (*designer* $f(R)$ -gravity [64], $f(R)$ Hu-Sawicki model [65], minimally coupled quintessence [5], low-energy Hořava gravity [9], covariant Galileon [66], K-mouflage [67], Galileon Ghost Condensate [68], beyond Horndeski model [69], generalised cubic covariant Galileon [70]) as well as for phenomenological parameterisations of the time dependence of the EFT functions and w_{DE} . The code is interfaced with a Markov Chain Monte-Carlo (MCMC) code, EFTCosmoMC [64], which allows constraints to be placed on specific MG models, see e.g. refs. [9, 64–69], to explore the interplay between massive neutrinos and DE [71], the tension between primary and weak lensing signal in CMB data [72], as well as the behaviour and impact of theoretical priors [37, 73, 74].

Among the same category, `hi_class` [47] (www.hiclass-code.net) implements in CLASS the evolution equations in terms of the α -basis defining Horndeski [47] and GLPV models [42]. `hi_class` is interfaced with `MontePython` [75, 76] to perform cosmological constraints. It has been used to place constraints on parameterisations of the $\alpha_i(\tau)$ with current CMB data [77], study relativistic effects on ultra-large scales [46], forecast constraints forecast with Stage 4 clustering, lensing and CMB data [78], and constraints on Brans-Dicke theory [78] and Covariant Galileon models [79].

Another example implementing the α -basis is COOP [80] (www.cita.utoronto.ca/~zqhuang). The code then outputs CMB power spectra by using the line of sight integral approach [57, 81], while the matter power spectra are computed via a gauge transformation from the Newtonian to the cold dark matter (CDM) rest frame in synchronous gauge. COOP includes the dynamics of the GLPV operator, and it has been used in order to study the signatures of a non-vanishing α_{H} on the matter power spectrum and on the primary and lensing CMB signals [14].

Finally, there is `EoS_class` [53] (<https://github.com/fpace>), which implements the equation of state approach [82] in CLASS, using the α -basis description of the Horndeski theory. As specific theory the code includes the *designer* $f(R)$ -model (CLASS_EOS_FR) [83].

The aforementioned codes have been validated [53, 84] by comparing the shapes of the CMB angular power spectra and of dark matter power spectrum, showing an excellent sub-percent agreement on the scales of interest for present and upcoming surveys.

A common feature of the above codes is that they have built-in modules to enforce stability conditions. Such conditions are derived in the EFT framework encompassing general classes of DE/MG models [2, 4, 8, 29] to ensure that the model under consideration is stable against ghosts, negative speeds of propagation and tachyonic instabilities. All of the above EB codes check for the no-ghost and positive speeds of propagation. EFTCAMB is the only one that includes the no-tachyonic condition [37]. Stability requirements, when used as priors in MCMC codes, reduce the viability space, these codes have to explore, and they can even dominate over the constraining power of observational data [4, 9, 37, 45, 64, 74, 74].

Another advantage in using such EB codes is that the set of linear perturbative equations are evolved without assuming any Quasi Static (QS) approximation. The latter considers the time derivatives of linear perturbations as sub-leading contributions compared to the spatial derivatives inside the sound horizon of the DE mode, i.e. $k/aH > c_s$ [50, 85], hence they are neglected. However, such approximation in some cases is not sufficient to exploit the full dynamics of the extra DoF. For example, in Horndeski theory, time derivatives revealed to modify the evolution of the linear gravitational potentials even within the sound horizon of the scalar field ($k < 0.001 \text{ h/Mpc}$) [34] and a semi-dynamical treatment of the linear perturbations at a pivot scale showed that the QS approximation is not sufficiently accurate for GLPV models [35].

31.3 Cosmological Constraints on Horndeski and GLPV Models

Modifications in the gravitational interaction can largely affect the shapes of the cosmological power spectra [86–90]. The EFT approach allows inspection of the DE/MG effects on these large scale observables in a model-independent fashion [14, 17, 19, 42, 44–53], i.e., no covariant theory is considered, while a pure EFT approach is adopted. In this case the effects of a specific operator in the EFT action can be easily investigated. Let us notice that although switching on/off a specific operator can introduce a modification in the observables, the magnitude of such modification strictly depends on the adopted parameterisation for the corresponding EFT function. For example, a positive braiding term, α_B , impacts both the lensing and matter power spectra that are enhanced compared to Λ CDM scenario, and depending on its magnitude can generate either a suppressed or an enhanced ISW (integrated Sachs-Wolfe) tail at low- ℓ in the temperature-temperature power spectrum [53]. A suppression in the lensing power spectrum and an enhanced TT power spectrum at low- ℓ with respect to Λ CDM scenario can be obtained for values of the effective Planck mass larger than M_{Pl} [45]. Furthermore, α_M also alters the amplitude of the GWs; in particular, if $\alpha_M < 0$, the GW amplitude is smaller than that predicted by Λ CDM scenario, and the opposite holds for positive values [91]. In this case, in the GWs and electromagnetic luminosity distance are different and can be then tested by GWs experiments and standard sirens [92–96].

Concerning the propagation of GWs, α_T changes the location of the inflationary peak of the BB spectrum [44]. α_H modulates the matter power spectrum, the lensing potential and the CMB TT power spectrum at low- ℓ [14, 42, 52]. Finally, the kineticity coupling, α_K , modifies the low- ℓ TT power spectrum due to the late-time ISW effect [50]. This coupling does not affect the constraints on the other model parameters regardless of the chosen parametrisation [50, 77, 97, 98], and it is hard to be constrained because its effect has been proven to be below the cosmic variance [50].

Nevertheless, it gives a non-negligible contribution to the viable parameter space of the theory and thus it cannot be neglected in cosmological analysis [50, 97].

In the following we discuss the cosmological constraints obtained in the *pure* EFT approach (we refer the reader to [99] for a review). Then one has to make a choice about the parametrisation to use for the EFT functions. Usually, such parameterisations are chosen in terms of the scale factor, a (e.g., linear, exponential, e-fold), the DE density parameter $\Omega_{\text{DE}}(a)$, or they are constants. As expected, the results of an analysis depend dramatically on the parametrisation adopted as well as on the choice for the background evolution: $w_{\text{DE}} = -1$ (Λ CDM), $w_{\text{DE}} = w_0$, where w_0 is a constant (wCDM) or $w_{\text{DE}} = w_0 + w_a(1 - a)$, where w_a is also a constant (CPL) [100, 101]. Nevertheless, one can identify some clear trends.

In the literature, the set of EFT functions largely considered is the one describing the Horndeski class of models or sub-classes, i.e. $\{\bar{m}_1^3, M_2^4, \bar{M}_2^2\}$ in the EFT basis and $\{\alpha_M, \alpha_K, \alpha_B, \alpha_T\}$ in the α -basis. The modifications induced by the running Planck mass function, α_M , have been constrained using different datasets. Planck CMB data (2015) and the H_0 prior by Riess et al. [102] constrain the free parameter in $\alpha_M = \alpha_{M,0}\Omega_{\text{DE}}(a)$ to be positive at 2σ [103]. Let us note that this model, if representative of a covariant theory, would lead to a ghost instability. Indeed the kinetic term in this case is vanishing, since both α_B and α_K are zero. Considering instead the relation $\alpha_M = -\alpha_B$ will avoid the presence of scalar ghosts, and additionally it mimics the dynamics of $f(R)$ [104, 105] and Brans-Dicke [106, 107] theories. In this case the amplitude of a power law parametrisation for α_M , is found to be < 0.097 at 95% C.L., using the combination of CMB+WL+BAO+RSD data [108] in agreement with the upper bound obtained using Planck13+WP+BAO+lensing (< 0.061 at 95% C.L.) [64]. The recent analysis by Planck 2018 shows that CMB data alone favour this parameter to be negative [109]. On the other hand, assuming $\alpha_M = -\alpha_B/2$, which is the case of the No Slip Gravity model [110], stability conditions force α_M to be positive if the background is Λ CDM, while a larger viability space, allowed by a CPL background, leads the combination of CMB+BAO+RSD+SNIa measurements to favour a negative amplitude for α_M (parametrised with the e-fold form) [111].

The complete class of Horndeski theory is investigated assuming a parameterisation for the four α -functions proportional to Ω_{DE} on a Λ CDM background [77]. Also in this case, a combination of CMB+BAO+RSD data and the shape of the power spectrum of galaxies from the WiggleZ survey favour a negative value for the amplitude of α_M at more than 2σ . Instead, when assuming luminal propagation of tensor modes ($\alpha_T = 0$), the MCMC analysis shows a preference for a positive value at 2σ using KiDS+GAMA datasets [112], while CMB, RSD, matter power spectrum from SDSS and BAO measurements do not particularly favour any sign for $\alpha_{M,0}$ ($= 0.20_{-0.82}^{+1.15}$ 95% C.L.) [113]. The latter combination of datasets, when used on a linear parametrisation in the scale factor, instead prefers a positive amplitude ($0.27_{-0.26}^{+0.54}$ 95% C.L.) [113]. Some of these results are summarised in Fig. 31.1.

Additionally, it has been shown that the constraints on α_M will improve considerably for Stage IV CMB experiments, even when considering a CPL parametrisation for the DE equation of state parameter [114]. Considering the propagation of tensor modes, α_M is degenerate with the tensor-to-scalar ratio r , as they both affect the

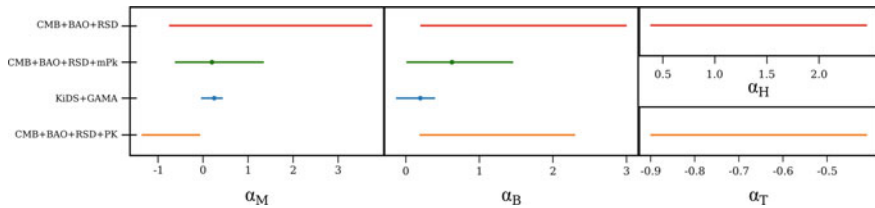


Fig. 31.1 Collection of cosmological constraints obtained on the linear DE-parametrisation, i.e. $\alpha_i(t) = \alpha_i \Omega_{DE}(a)$ on a Λ CDM background. This is the most commonly used parametrisation for which we can show more results and which covers different combinations of data sets. The α functions sharing the same colour are those switched on in the analysis. The constraints showed are at 95% C.L. The blue error bars are from Ref. [112], the green ones from ref. [113], the orange ones are from Ref. [77], and finally the red ones are from Ref. [42].

amplitude of the primordial peak. Demanding for r to be close to zero requires α_M to assume negative values according to BICEP2 data [115]. The sign of the amplitude of the braiding function, α_B , is favoured to be positive regardless of the parametrisation considered when tested against the combinations KiDS+GAMA ($\alpha_{B,0} = 0.20^{+0.20}_{-0.33}$ 95% C.L.) [112] and CMB+BAO+RSD with both the power spectrum of galaxies from the WiggleZ survey ($0.19 < \alpha_{B,0} < 2.30$ 95% C.L.) [77] and matter power spectrum from SDSS ($\alpha_{B,0} = 0.48^{+0.83}_{-0.46}$ 95% C.L.) [113]. However, when it shares a relation with α_M , as previously discussed, it might show a negative amplitude in the case where α_M is found to be positive.

Cosmological constraints on the amplitude of the parameter encoding the variation in the speed of GWs, $\alpha_{T,0}$, regardless of the parametrisation adopted, show that data (CMB, RSD, BAO) prefer sub-luminal propagation of GWs [45, 113]. Super-luminal propagation of GWs is instead possible when considering the B-modes data of the CMB in polarisation (Planck and BICEP2 datasets) [116]. The speed of propagation of GWs is further constrained by the detection of the GW170817/GRB170817A event that sets $\alpha_{T,0} \sim \mathcal{O}(10^{-15})$ [117] (see Sect. 31.4). In that case setting $\alpha_T = 0$ has the impact to improve the constraints on the parameters of the remaining α -functions and some investigations using present-day data and forecasts for next generation surveys have been performed with this prior [17, 50, 97, 113, 118].

Constraints on *pure* GLPV models with luminal propagation of tensor modes are derived using a combination of CMB, BAO and RSD datasets [42]. The beyond Horndeski parameter, α_H , is found to be degenerate with α_B and α_M . The data favour generally positive values of α_H and of order $\mathcal{O}(1)$. We note that a stringent constraint on the present-day value of α_H of the order $\mathcal{O}(10^{-6})$ is found when testing a specific model that extends the Galileon ghost condensate to the domain of beyond Horndeski theories [69], and the phenomenon of GWs decay into DE sets a bound of $\mathcal{O}(10^{-10})$ [119].

The original EFT formalism given by the action (31.1) assumes the validity of the weak equivalence principle (WEP) and the matter fields, χ_m , are hence minimally coupled to gravity through a unique metric $g_{\mu\nu}$. However, direct gravitational

interactions between the additional scalar DoF and the matter fields can also be considered, for example considering couplings between dark matter and neutrinos. In the latter case, observational constraints are indeed less severe than the case of baryons and photons [120, 121]. In the context of the EFT, framework couplings with matter fields have been investigated for Horndeski theory [11] and later generalised to GLPV theory [12–14]. In particular, a direct coupling between DE and dark matter has been investigated in the Horndeski case [122], with the coupling function of the form:

$$\gamma_c(t) = \frac{\beta_\gamma}{2\sqrt{2}} c_s(t) \sqrt{\alpha(t)}, \quad (31.3)$$

where β_γ is a constant and $c_s(t)$ and $\alpha(t)$ correspond respectively to the speed of propagation of the DE mode and kinetic function given by the following combination $\alpha_K + 3/2\alpha_B^2$. The forecast analysis based on spectroscopic and photometric surveys with specifications similar to Euclid gives the error on β_γ of the order $\sim 10^{-4}$ [11].

Improvements in the cosmological constraints of the EFT function parameters are obtained by considering specifications similar to those of future generation surveys. The constraints on the amplitude of the α -functions increased by a factor 5 [78] forecasting LSST [123], SKA [124] and CMB-S4 [125] experiments. Considering future CMB primaries, CMB lensing, GC and cosmic shear data, a variation of the effective Newtonian gravitational coupling larger than 10% is excluded and setting $c_t = 1$ constrains the remaining parameters at the 10% level [114]. Furthermore, for a Euclid-like experiment, the results of two cosmic shear methods have been compared using the parametrisation $\alpha_i = \alpha_{i,0}\Omega_{\text{DE}}$: the 3D analysis better constrains the model's parameters by about 20% compared to the tomographic approach [126].

Observational measurements of RSD, GC and WL show a tension with Planck CMB data in the estimation of σ_8 , by predicting a lower growth of structures [127–130]. Horndeski models have been investigated in the EFT framework by using large samples of models obtained with the Monte-Carlo approach. The results show that the models satisfying $M^2 > M_{\text{pl}}^2$ and with sub-luminal propagation of tensor modes can produce with respect to Λ CDM a lower growth of structure at low- z and a larger one at high- z [32]. An investigation on the growth index $\gamma(a)$ [131] shows that the majority of Horndeski models with the same expansion history as the standard cosmological statistically generate a growth rate of cosmic structures that is 12% smaller than Λ CDM one, and no viable theory has a larger leading order growth index γ_0 than that of Λ CDM [4]. A suppression of the matter power spectrum is also possible in GLPV models, thanks to the extra free function α_H [14, 42, 52], as discussed earlier. These aspects can be used to construct viable models able to ease the σ_8 tension.

The above constraints rely on a specific choice of the time evolution of EFT functions further specified through a certain number of free parameters. Such a choice should try to model realistically cosmological observables, with the aim of revealing the nature of cosmic acceleration. At the same time, it should not include too many free parameters, to avoid loosening the constraining power of data [45]. Smooth parameterizations that are acceptable to describe the theory space as cosmological

observables are only slightly sensitive to short time-scale variations [132]. Furthermore, one should be careful, because sometimes the selected forms of the EFT functions generate simplified shapes of relevant physical quantities such as $\mu(t, k)$ or $\Sigma(t, k)$, if compared to the complex behavior they show when specific covariant models are considered [133, 134]. The risk in this case might be to underestimate the modifications of the underlying gravity force or even miss its signatures. An alternative approach relies on data-driven analysis to reconstruct the EFT functions across cosmic times using cosmological data, from which one can then derive specific model properties [36, 135]. The reconstruction of *pure* Horndeski models from CMB+WL+BAO+SNIa+ H_0 shows that between $0.1 < a < 1$: the variation of the Planck mass and α_T are positive and α_B is mostly negative [135].

Despite the uncertainties in fixing the EFT functions, the EFT framework has already boosted our knowledge about the real nature of gravity force and helped in deriving novel predictions.

31.4 Astrophysical Constraints

Astrophysical constraints can be used to complement those obtained from measurements at cosmological scales. In particular, the parameter space identified by the EFT functions can be constrained using the bounds from the joint detection of the GWs event GW170817 and its electromagnetic counterpart GRB170817A and those from massive astrophysical bodies. In details:

- *GW170817 and GRB170817A*: the joint detection of the GWs event GW170817 from a binary neutron stars merger [136] and its gamma-ray burst GRB170817A [117] placed a strong constraint on the deviation of the speed of GW from the speed of light, c . It is estimated to be $-3 \times 10^{-15} \leq c_t - c \leq 7 \times 10^{-16}$ [117]. In the EFT formalism it implies $|\alpha_T| < 10^{-15}$, with a very tiny amount of room left for this kind of deviation in DE/MG models [137–139]. For example, assuming that this condition holds at any time and setting exactly $\alpha_T = 0$, we obtain

$$\begin{aligned} \bar{M}_3^2 &= -\bar{M}_2^2 = 0 \quad (\text{in GLPV}); \\ \bar{M}_3^2 &= -\bar{M}_2^2 = -2\mu_1^2 = 0 \quad (\text{in Hordenski}). \end{aligned} \tag{31.4}$$

For the Horndeski case the above relations imply that the quintic Horndeski Lagrangian is ruled out and the quartic Lagrangian reduces to $f(\phi)R$ where $f(\phi)$ is a function of the scalar field [137, 138]. Going beyond the Horndeski case and considering GLPV models culminates in the quintic GLPV vanish as well [137, 138]. As a consequence, some well-known MG models were ruled out [139], and we refer the reader to [140] for a review about viable models after GW170817. Additionally, the phenomenon of the decay of GWs into DE fluctuations is found to be driven by a coupling proportional to α_H [119]. A large decay rate of the GWs, which implies that no wave would reach the detector, is associated with $\alpha_H \neq 0$,

hence α_H is constrained to be of the order 10^{-10} . According to this result GLPV would be completely ruled out. However, one has also to consider that the bound on α_T should be imposed only at $z < 10^{-2}$ [39, 140], since the source of GWs is at redshift $z \simeq 0.009$.

Another source of debate about the applicability of the LIGO/Virgo bound on models that modify gravity at large scales concerns the LIGO/Virgo measured frequencies. Indeed, those are close to the cut-off scale of DE/MG models, and if ultra-violet effects come into play to recover the GR propagation of GWs around the frequency $f \sim 100$ Hz, the previous bounds on c_t and α_H cannot be applied [141]. In this regard, measurements at lower frequencies, e.g., those that will be provided by the future space-based mission LISA [142], would offer a proper testing ground. Further theoretical bounds [143], which follow the requirement $c_t^2 = 1$, were set on the braiding function α_B and α_H respectively within the Horndeski and GLPV models. It has been shown that GWs of large amplitude generated by binary systems can lead to ghost and gradient instabilities in the dark energy perturbations. This contingency is avoided for Horndeski models when $|\alpha_B| < 10^{-2}$ and for GLPV models when $|\alpha_H| < 10^{-20}$.

- *Massive astrophysical bodies:* MG theories are characterised by screening mechanisms that work to hide the fifth force on small scales or high density environments in order to recover GR [144]. Solar-System and astrophysical tests indeed constrain gravity in these cases to be that described by GR with high accuracy [145, 146]. The Vainshtein screening mechanism [147–150], which is generally characteristic of Horndeski and GLPV theories, exhibits a very peculiar feature in GLPV: a “partial breaking” inside astrophysical bodies where the fifth force is not completely screened while outside the object GR is restored [151]. In case the screening mechanism is fully operating, the Minkowski potentials $\phi(r)$, $\psi(r)$ inside an overdensity are equal. In GLPV theories the equations for these potentials can be written as [151, 152]

$$\frac{d\phi}{dr} = \frac{G_N \tilde{M}(r)}{r^2} + \frac{\Upsilon_1 G_N}{4} \frac{d^2 \tilde{M}(r)}{dr^2}, \quad (31.5)$$

$$\frac{d\psi}{dr} = \frac{G_N \tilde{M}(r)}{r^2} - \frac{5\Upsilon_2 G_N}{4r} \frac{d\tilde{M}(r)}{dr}, \quad (31.6)$$

where $\tilde{M}(r)$ is the mass inside the object and Υ_i are dimensionless constants, which in the EFT formulation read [153, 154]

$$\Upsilon_1 = \frac{4\alpha_H^2}{c_t^2(1 + \alpha_B) - \alpha_H - 1}, \quad (31.7)$$

$$\Upsilon_2 = \frac{4\alpha_H(\alpha_H - \alpha_B)}{5(c_t^2(1 + \alpha_B) - \alpha_H - 1)}. \quad (31.8)$$

Thus in models with $\alpha_H \neq 0$ the potentials are no longer equal because the screening is not fully efficient. Constraints on these parameters have been obtained using

dwarf, neutron, hyperon and quark stars and galaxy clusters [152–156]. The stringent constraint on Υ_1 and the first bound on Υ_2 are obtained at $0.1 < z < 1.2$, using X-ray and lensing profiles of galaxy clusters from XMM Cluster Survey [157] and CFHTLenS [158]. They are $\Upsilon_1 = -0.11_{-0.67}^{+0.93}$ and $\Upsilon_2 = -0.22_{-1.19}^{+1.22}$ at 2σ [152]. These bounds can be used to constrain the EFT functions from Eqs. (31.7)–(31.8). If on top of these bounds one also considers the GWs constraint on c_t [117], the EFT parameter space further reduces [159].

Another peculiar characteristic of the Vainshtein mechanism is the *piercing effect* [160], i.e., within screened environments, the gradient of the scalar field is not bound to vanish for shift symmetric models. It is possible to further bound α_T and α_H by combining the Hulse–Taylor pulsar constraint on the local value of c_t , which is of the order 10^{-2} [160] with the parameterised post-Newtonian constraint from the Cassini experiment on the screened gravitational slip parameter $\eta_{sc} - 1 = (2.3 \pm 2.1) \times 10^{-5}$ [161]. Finally, note that on super-Compton scales, η reduces to $\eta_{sc} = \frac{1}{1+\alpha_T}$ [31]. This is connected to the modification of gravity that remains in a screened environment.

References

1. G. Gubitosi, F. Piazza, F. Vernizzi, The effective field theory of dark energy. JCAP **1302**, 032 (2013). [arXiv:1210.0201](#). JCAP1302, 032 (2013)
2. J.K. Bloomfield, É.É. Flanagan, M. Park, S. Watson, Dark energy or modified gravity? An effective field theory approach. JCAP **1308**, 010 (2013). [arXiv:1211.7054](#)
3. J. Gleyzes, D. Langlois, F. Piazza, F. Vernizzi, Essential building blocks of dark energy. JCAP **1308**, 025 (2013). [arXiv:1304.4840](#)
4. F. Piazza, H. Steigerwald, C. Marinoni, Phenomenology of dark energy: exploring the space of theories with future redshift surveys. JCAP **1405**, 043 (2014). [arXiv:1312.6111](#)
5. B. Hu, M. Raveri, N. Frusciante, A. Silvestri, *EFTCAMB/EFTCosmoMC: Numerical Notes v2.0*. [arXiv:1405.3590](#)
6. S. Tsujikawa, The effective field theory of inflation/dark energy and the Horndeski theory. Lect. Notes Phys. **892**, 97–136 (2015). [arXiv:1404.2684](#)
7. C. Li, Y. Cai, Y.-F. Cai, E.N. Saridakis, The effective field theory approach of teleparallel gravity, f(T) gravity and beyond. JCAP **10**, 001 (2018). [arXiv:1803.09818](#)
8. R. Kase, S. Tsujikawa, Effective field theory approach to modified gravity including Horndeski theory and Horava Lifshitz gravity. Int. J. Mod. Phys. D **23**(13), 1443008 (2015). [arXiv:1409.1984](#)
9. N. Frusciante, M. Raveri, D. Vernieri, B. Hu, A. Silvestri, Horava gravity in the effective field theory formalism: from cosmology to observational constraints. Phys. Dark Univ. **13**, 7–24 (2016). [arXiv:1508.01787](#)
10. N. Frusciante, G. Papadomanolakis, A. Silvestri, An extended action for the effective field theory of dark energy: a stability analysis and a complete guide to the mapping at the basis of EFTCAMB. JCAP **1607**(07), 018 (2016). [arXiv:1601.04064](#)
11. J. Gleyzes, D. Langlois, M. Mancarella, F. Vernizzi, Effective theory of interacting dark energy. JCAP **1508**(08), 054 (2015). [arXiv:1504.05481](#)
12. J. Gleyzes, D. Langlois, F. Piazza, F. Vernizzi, *Exploring Gravitational Theories Beyond Horndeski*. [arXiv:1408.1952](#)

13. S. Tsujikawa, Cosmological disformal transformations to the Einstein frame and gravitational couplings with matter perturbations. *Phys. Rev. D* **92**(6), 064047 (2015). [arXiv:1506.08561](#)
14. G. D'Amico, Z. Huang, M. Mancarella, F. Vernizzi, Weakening gravity on redshift-survey scales with kinetic matter mixing. *JCAP* **1702**, 014 (2017). [arXiv:1609.01272](#)
15. M. Lagos, T. Baker, P.G. Ferreira, J. Noller, A general theory of linear cosmological perturbations: scalar-tensor and vector-tensor theories. *JCAP* **1608**(08), 007 (2016). [arXiv:1604.01396](#)
16. M. Lagos, E. Bellini, J. Noller, P.G. Ferreira, T. Baker, A general theory of linear cosmological perturbations: stability conditions, the quasistatic limit and dynamics. *JCAP* **1803**(03), 021 (2018). [arXiv:1711.09893](#)
17. E. Bellini, R. Jimenez, L. Verde, Signatures of horndeski gravity on the dark matter bispectrum. *JCAP* **1505**(05), 057 (2015). [arXiv:1504.04341](#)
18. N. Frusciante, G. Papadomanolakis, *Tackling Non-linearities with the Effective Field Theory of Dark Energy and Modified Gravity*. [arXiv:1706.02719](#)
19. D. Yamauchi, S. Yokoyama, H. Tashiro, Constraining modified theories of gravity with the galaxy bispectrum. *Phys. Rev. D* **96**(12), 123516 (2017). [arXiv:1709.03243](#)
20. G. Cusin, M. Lewandowski, F. Vernizzi, Nonlinear effective theory of dark energy. *JCAP* **04**, 061 (1804). [arXiv:1712.02782](#)
21. G. Cusin, M. Lewandowski, F. Vernizzi, Dark energy and modified gravity in the effective field theory of large-scale structure. *JCAP* **1804**(04), 005 (2018). [arXiv:1712.02783](#)
22. J. Kennedy, L. Lombriser, A. Taylor, *Screening and Degenerate Kinetic Self-acceleration from the Nonlinear Freedom of Reconstructed Horndeski Theories*. [arXiv:1902.09853](#)
23. J. Bloomfield, A simplified approach to general scalar-tensor theories. *JCAP* **1312**, 044 (2013). [arXiv:1304.6712](#)
24. J. Gleyzes, D. Langlois, F. Vernizzi, A unifying description of dark energy. *Int. J. Mod. Phys. D* **23**(13), 1443010 (2015). [arXiv:1411.3712](#)
25. G.W. Horndeski, Second-order scalar-tensor field equations in a four-dimensional space. *Int. J. Theor. Phys.* **10**, 363–384 (1974)
26. C. Deffayet, S. Deser, G. Esposito-Farese, Generalized Galileons: all scalar models whose curved background extensions maintain second-order field equations and stress-tensors. *Phys. Rev. D* **80**, 064015 (2009). [arXiv:0906.1967](#)
27. J. Gleyzes, D. Langlois, F. Piazza, F. Vernizzi, *Healthy Theories Beyond Horndeski*. [arXiv:1404.6495](#)
28. E. Bellini, I. Sawicki, Maximal freedom at minimum cost: linear large-scale structure in general modifications of gravity. *JCAP* **1407**, 050 (2014). [arXiv:1404.3713](#)
29. A. De Felice, N. Frusciante, G. Papadomanolakis, On the stability conditions for theories of modified gravity in the presence of matter fields. *JCAP* **1703**(03), 027 (2017). [arXiv:1609.03599](#)
30. A. De Felice, N. Frusciante, G. Papadomanolakis, *A de Sitter Limit Analysis for Dark Energy and Modified Gravity Models*. [arXiv:1705.01960](#)
31. L. Pogosian, A. Silvestri, What can cosmology tell us about gravity? Constraining Horndeski gravity with Σ and μ . *Phys. Rev. D* **94**(10), 104014 (2016). [arXiv:1606.05339](#)
32. L. Perenon, F. Piazza, C. Marinoni, L. Hui, Phenomenology of dark energy: general features of large-scale perturbations. *JCAP* **1511**(11), 029 (2015). [arXiv:1506.03047](#)
33. L. Perenon, C. Marinoni, F. Piazza, Diagnostic of horndeski theories. *JCAP* **1701**(01), 035 (2017). [arXiv:1609.09197](#)
34. S. Peirone, K. Koyama, L. Pogosian, M. Raveri, A. Silvestri, Large-scale structure phenomenology of viable Horndeski theories. *Phys. Rev. D* **97**(4), 043519 (2018). [arXiv:1712.00444](#)
35. L. Lombriser, A. Taylor, Semi-dynamical perturbations of unified dark energy. *JCAP* **1511**(11), 040 (2015). [arXiv:1505.05915](#)
36. J. Espejo, S. Peirone, M. Raveri, K. Koyama, L. Pogosian, A. Silvestri, Phenomenology of large scale structure in scalar-tensor theories: joint prior covariance of w_{DE} , Σ and μ in Horndeski. *Phys. Rev. D* **99**(2), 023512 (2018). [arXiv:1809.01121](#)

37. N. Frusciante, G. Papadomanolakis, S. Peirone, A. Silvestri, *The Role of the Tachyonic Instability in Horndeski Gravity*. [arXiv:1810.03461](#)
38. J. Kennedy, L. Lombriser, A. Taylor, Reconstructing Horndeski models from the effective field theory of dark energy. *Phys. Rev. D* **96**(8), 084051 (2017). [arXiv:1705.09290](#)
39. J. Kennedy, L. Lombriser, A. Taylor, Reconstructing Horndeski theories from phenomenological modified gravity and dark energy models on cosmological scales. *Phys. Rev. D* **98**(4), 044051 (2018). [arXiv:1804.04582](#)
40. L. Lombriser, C. Dalang, J. Kennedy, A. Taylor, *Inherently Stable Effective Field Theory for Dark Energy and Modified Gravity*. [arXiv:1810.05225](#)
41. S. Tsujikawa, Possibility of realizing weak gravity in redshift space distortion measurements. *Phys. Rev. D* **92**(4), 044029 (2015). [arXiv:1505.02459](#)
42. D. Traykova, E. Bellini, P.G. Ferreira, *The Phenomenology of Beyond Horndeski Gravity*. [arXiv:1902.10687](#)
43. E.V. Linder, *No Run Gravity*. [arXiv:1903.02010](#)
44. L. Amendola, G. Ballesteros, V. Pettorino, Effects of modified gravity on B-mode polarization. *Phys. Rev. D* **90**, 043009 (2014). [arXiv:1405.7004](#)
45. V. Salvatelli, F. Piazza, C. Marinoni, Constraints on modified gravity from Planck 2015: when the health of your theory makes the difference. *JCAP* **1609**(09), 027 (2016). [arXiv:1602.08283](#)
46. J. Renk, M. Zumalacárregui, F. Montanari, Gravity at the horizon: on relativistic effects, CMB-LSS correlations and ultra-large scales in Horndeski's theory. *JCAP* **1607**(07), 040 (2016). [arXiv:1604.03487](#)
47. M. Zumalacárregui, E. Bellini, I. Sawicki, J. Lesgourgues, P.G. Ferreira, *hi_ class: Horndeski in the cosmic linear anisotropy solving system*. *JCAP* **1708**(08), 019 (2017). [arXiv:1605.06102](#)
48. M. Brush, E.V. Linder, M. Zumalacárregui, *No Slip CMB*. [arXiv:1810.12337](#)
49. C. García-García, E.V. Linder, P. Ruff-Lapuente, M. Zumalacárregui, Dark energy from α -attractors: phenomenology and observational constraints. *JCAP* **1808**, 022 (2018). [arXiv:1803.00661](#)
50. N. Frusciante, S. Peirone, S. Casas, N.A. Lima, *The Road Ahead of Horndeski: Cosmology of Surviving Scalar-Tensor Theories*. [arXiv:1810.10521](#)
51. S. Hirano, T. Kobayashi, H. Tashiro, S. Yokoyama, Matter bispectrum beyond Horndeski theories. *Phys. Rev. D* **97**(10), 103517 (2018). [arXiv:1801.07885](#)
52. D. Duniya, T. Moloi, C. Clarkson, J. Larena, R. Maartens, B. Mwangi, A. Weltman, *Probing Beyond-Horndeski Gravity on Ultra-Large Scales*. [arXiv:1902.09919](#)
53. F. Pace, R.A. Battye, B. Bolliet, D. Trinh, *Dark Sector Evolution in Horndeski Models*. [arXiv:1905.06795](#)
54. P.J.E. Peebles, J.T. Yu, Primeval adiabatic perturbation in an expanding universe. *Astrophys. J.* **162**, 815–836 (1970)
55. M.L. Wilson, J. Silk, On the Anisotropy of the cosmological background matter and radiation distribution. I. The Radiation anisotropy in a spatially flat universe. *Astrophys. J.* **243**, 14–25 (1981)
56. C.-P. Ma, E. Bertschinger, Cosmological perturbation theory in the synchronous and conformal Newtonian gauges. *Astrophys. J.* **455**, 7–25 (1995). [arxiv:astro-ph/9506072](#)
57. U. Seljak, M. Zaldarriaga, A Line of sight integration approach to cosmic microwave background anisotropies. *Astrophys. J.* **469**, 437–444 (1996). [arxiv:astro-ph/9603033](#)
58. U. Seljak, N. Sugiyama, M.J. White, M. Zaldarriaga, A Comparison of cosmological Boltzmann codes: are we ready for high precision cosmology? *Phys. Rev. D* **68**, 083507 (2003). [arxiv:astro-ph/0306052](#)
59. M. Kaplinghat, L. Knox, C. Skordis, Rapid calculation of theoretical CMB angular power spectra. *Astrophys. J.* **578**, 665 (2002). [arxiv:astro-ph/0203413](#)
60. M. Doran, CMBEASY: an object oriented code for the cosmic microwave background. *JCAP* **0510**, 011 (2005). [arxiv:astro-ph/0302138](#)
61. A. Lewis, A. Challinor, A. Lasenby, Efficient computation of CMB anisotropies in closed FRW models. *Astrophys. J.* **538**, 473–476 (2000). [arxiv:astro-ph/9911177](#)

62. D. Blas, J. Lesgourgues, T. Tram, The cosmic linear anisotropy solving system (CLASS) II: approximation schemes. *JCAP* **1107**, 034 (2011). [arXiv:1104.2933](#)
63. B. Hu, M. Raveri, N. Frusciante, A. Silvestri, Effective field theory of cosmic acceleration: an implementation in CAMB. *Phys. Rev. D* **89**(10), 103530 (2014). [arXiv:1312.5742](#)
64. M. Raveri, B. Hu, N. Frusciante, A. Silvestri, Effective field theory of cosmic acceleration: constraining dark energy with CMB data. *Phys. Rev. D* **90**(4), 043513 (2014). [arXiv:1405.1022](#)
65. B. Hu, M. Raveri, M. Rizzato, A. Silvestri, Testing Hu & Sawicki $f(R)$ gravity with the effective field theory approach. *Mon. Not. Roy. Astron. Soc.* **459**(4), 3880–3889 (2016). [arXiv:1601.07536](#)
66. S. Peirone, N. Frusciante, B. Hu, M. Raveri, A. Silvestri, Do current cosmological observations rule out all Covariant Galileons? *Phys. Rev. D* **97**(6), 06 (2018). [arXiv:1711.04760](#)
67. G. Benevento, M. Raveri, A. Lazanu, N. Bartolo, M. Liguori, P. Brax, P. Valageas, *K-mouflage Imprints on Cosmological Observables and Data Constraints*. [arXiv:1809.09958](#)
68. S. Peirone, G. Benevento, N. Frusciante, S. Tsujikawa, Cosmological data favor Galileon ghost condensate over Λ CDM. [arXiv:1905.05166](#)
69. S. Peirone, G. Benevento, N. Frusciante, S. Tsujikawa, *First Cosmological Constraints and Phenomenology of a Beyond-Horndeski Model*. [arXiv:1905.11364](#)
70. N. Frusciante, S. Peirone, L. Atayde, A. De Felice, Phenomenology of the generalized cubic covariant Galileon model and cosmological bounds. *Phys. Rev. D* **101**(6), 064001 (2020). [arXiv:1912.07586](#)
71. B. Hu, M. Raveri, A. Silvestri, N. Frusciante, Exploring massive neutrinos in dark cosmologies with EFTCAMB/EFTCosmoMC. *Phys. Rev. D* **91**(6), 063524 (2015). [arXiv:1410.5807](#)
72. B. Hu, M. Raveri, Can modified gravity models reconcile the tension between the CMB anisotropy and lensing maps in Planck-like observations? *Phys. Rev. D* **91**(12), 123515 (2015). [arXiv:1502.06599](#)
73. M. Raveri, P. Bull, A. Silvestri, L. Pogosian, Priors on the effective Dark Energy equation of state in scalar-tensor theories. *Phys. Rev. D* **96**(8), 083509 (2017). [arXiv:1703.05297](#)
74. S. Peirone, M. Martinelli, M. Raveri, A. Silvestri, Impact of theoretical priors in cosmological analyses: the case of single field quintessence. *Phys. Rev. D* **96**(6), 063524 (2017). [arXiv:1702.06526](#)
75. B. Audren, J. Lesgourgues, K. Benabed, S. Prunet, Conservative constraints on early cosmology: an illustration of the monte python cosmological parameter inference code. *JCAP* **1302**, 001 (2013). [arXiv:1210.7183](#)
76. T. Brinckmann, J. Lesgourgues, *MontePython 3: Boosted MCMC Sampler and Other Features*. [arXiv:1804.07261](#)
77. E. Bellini, A.J. Cuesta, R. Jimenez, L. Verde, Constraints on deviations from Λ CDM within Horndeski gravity. *JCAP* **1602**(02), 053 (2016). [arXiv:1509.07816](#). Erratum: *JCAP*1606, no. 06, E01 (2016)
78. D. Alonso, E. Bellini, P.G. Ferreira, M. Zumalacárregui, Observational future of cosmological scalar-tensor theories. *Phys. Rev. D* **95**(6), 063502 (2017). [arXiv:1610.09290](#)
79. J. Renk, M. Zumalacárregui, F. Montanari, A. Barreira, Galileon gravity in light of ISW, CMB, BAO and H_0 data. *JCAP* **1710**(10), 020 (2017). [arXiv:1707.02263](#)
80. Z. Huang, A cosmology forecast Toolkit–CosmoLib. *JCAP* **1206**, 012 (2012). [arXiv:1201.5961](#)
81. W. Hu, M.J. White, CMB anisotropies: total angular momentum method. *Phys. Rev. D* **56**, 596–615 (1997). [arxiv:astro-ph/9702170](#)
82. R.A. Battye, J.A. Pearson, Parametrizing dark sector perturbations via equations of state. *Phys. Rev. D* **88**(6), 061301. [arXiv:1306.1175](#)
83. R.A. Battye, B. Bolliet, J.A. Pearson, $f(R)$ gravity as a dark energy fluid. *Phys. Rev. D* **93**(4), 044026 (2016). [arXiv:1508.04569](#)
84. E. Bellini et al., Comparison of Einstein-Boltzmann solvers for testing general relativity. *Phys. Rev. D* **97**(2), 023520 (2018). [arXiv:1709.09135](#)
85. I. Sawicki, E. Bellini, Limits of quasistatic approximation in modified-gravity cosmologies. *Phys. Rev. D* **92**(8), 084061 (2015). [arXiv:1503.06831](#)

86. R.K. Sachs, A.M. Wolfe, Perturbations of a cosmological model and angular variations of the microwave background. *Astrophys. J.* **147**, 73–90 (1967). (Gen. Rel. Grav. 39, 1929 (2007))
87. L. Kofman, A.A. Starobinsky, Effect of the cosmological constant on large scale anisotropies in the microwave background. *Sov. Astron. Lett.* **11**, 271–274 (1985). (*Pisma Astron. Zh.* 11, 643(1985))
88. W. Hu, M.J. White, Acoustic signatures in the cosmic microwave background. *Astrophys. J.* **471**, 30–51 (1996). [arxiv:astro-ph/9602019](https://arxiv.org/abs/astro-ph/9602019)
89. V. Acquaviva, C. Baccigalupi, Dark energy records in lensed cosmic microwave background. *Phys. Rev. D* **74**, 103510 (2006). [arxiv:astro-ph/0507644](https://arxiv.org/abs/astro-ph/0507644)
90. L. Amendola, V. Pettorino, C. Quercellini, A. Vollmer, Testing coupled dark energy with next-generation large-scale observations. *Phys. Rev. D* **85**, 103008 (2012). [arXiv:1111.1404](https://arxiv.org/abs/1111.1404)
91. R.C. Nunes, M.E.S. Alves, J.C.N. de Araujo, *Primordial Gravitational Waves in Horndeski Gravity*. [arXiv:1811.12760](https://arxiv.org/abs/1811.12760)
92. LIGO Scientific, Virgo, 1M2H, Dark Energy Camera GW-E, DES, DLT40, Las Cumbres Observatory, VINROUGE, MASTER Collaboration, B.P. Abbott et al., A gravitational-wave standard siren measurement of the Hubble constant. *Nature* **551**(7678), 85–88 (2017). [arXiv:1710.05835](https://arxiv.org/abs/1710.05835)
93. S. Nissanke, D.E. Holz, N. Dalal, S.A. Hughes, J.L. Sievers, C.M. Hirata, *Determining the Hubble Constant from Gravitational Wave Observations of Merging Compact Binaries*. [arXiv:1307.2638](https://arxiv.org/abs/1307.2638)
94. M. Lajos, M. Fishbach, P. Landry, D.E. Holz, Standard sirens with a running Planck mass. *Phys. Rev. D* **99**(8), 083504 (2019). [arXiv:1901.03321](https://arxiv.org/abs/1901.03321)
95. J.M. Ezquiaga, M. Zumalacregui, Dark Energy in light of Multi-Messenger Gravitational-Wave astronomy. *Front. Astron. Space Sci.* **5**, 44 (2018). [arXiv:1807.09241](https://arxiv.org/abs/1807.09241)
96. LISA Cosmology Working Group Collaboration, E. Belgacem et al., Testing modified gravity at cosmological distances with LISA standard sirens. *JCAP* **1907**(07), 024 (2019). [arXiv:1906.01593](https://arxiv.org/abs/1906.01593)
97. C.D. Kreisch, E. Komatsu, Cosmological constraints on Horndeski gravity in light of GW170817. *JCAP* **1812**(12), 030 (2018). [arXiv:1712.02710](https://arxiv.org/abs/1712.02710)
98. L. Perenon, J. Bel, R. Maartens, A. de la Cruz-Dombriz, *Optimising Growth of Structure Constraints on Modified Gravity*. [arXiv:1901.11063](https://arxiv.org/abs/1901.11063)
99. N. Frusciante, L. Perenon, *Effective Field Theory of Dark Energy: a Review*. [arXiv:1907.03150](https://arxiv.org/abs/1907.03150)
100. M. Chevallier, D. Polarski, Accelerating universes with scaling dark matter. *Int. J. Mod. Phys. D* **10**, 213–224 (2001). [arxiv:gr-qc/0009008](https://arxiv.org/abs/gr-qc/0009008)
101. E.V. Linder, Exploring the expansion history of the universe. *Phys. Rev. Lett.* **90**, 091301 (2003). [arxiv:astro-ph/0208512](https://arxiv.org/abs/astro-ph/0208512)
102. A.G. Riess, L. Macri, S. Casertano, H. Lampeitl, H.C. Ferguson, A.V. Filippenko, S.W. Jha, W. Li, R. Chornock, A 3% solution: determination of the Hubble constant with the Hubble space telescope and wide field camera 3. *Astrophys. J.* **730**, 119 (2011). [arXiv:1103.2976](https://arxiv.org/abs/1103.2976).
Erratum: *Astrophys. J.* 732, 129 (2011)
103. Z. Huang, Observational effects of a running Planck mass. *Phys. Rev. D* **93**(4), 043538 (2016). [arXiv:1511.02808](https://arxiv.org/abs/1511.02808)
104. T.P. Sotiriou, V. Faraoni, $f(R)$ theories of gravity. *Rev. Mod. Phys.* **82**, 451–497 (2010). [arXiv:0805.1726](https://arxiv.org/abs/0805.1726)
105. A. De Felice, S. Tsujikawa, $f(R)$ theories. *Living Rev. Rel.* **13**, 3 (2010). [arXiv:1002.4928](https://arxiv.org/abs/1002.4928)
106. C. Brans, R.H. Dicke, Mach’s principle and a relativistic theory of gravitation. *Phys. Rev.* **124**(142), 925–935 (1961)
107. B. Boisseau, G. Esposito-Farese, D. Polarski, A.A. Starobinsky, Reconstruction of a scalar tensor theory of gravity in an accelerating universe. *Phys. Rev. Lett.* **85**, 2236 (2000). [arxiv:gr-qc/0001066](https://arxiv.org/abs/gr-qc/0001066)
108. Planck Collaboration, P.A.R. Ade et al., Planck 2015 results. XIV. Dark energy and modified gravity. *Astron. Astrophys.* **594**, A14 (2016). [arXiv:1502.01590](https://arxiv.org/abs/1502.01590)
109. Planck Collaboration, N. Aghanim et al., *Planck 2018 Results. VI. Cosmological Parameters*. [arXiv:1807.06209](https://arxiv.org/abs/1807.06209)

110. E.V. Linder, No slip gravity. *JCAP* **1803**(03), 005 (2018). [arXiv:1801.01503](#)
111. G. Brando, F.T. Falciano, E.V. Linder, H.E.S. Velten, *Modified gravity away from a Λ CDM Background*. [arXiv:1904.12903](#)
112. A. Spurio Mancini, F. Köhlinger, B. Joachimi, V. Pettorino, B.M. SchSfer, R. Reischke, S. Brieden, M. Archidiacono, J. Lesgourgues, *KiDS+GAMA: Constraints on Horndeski Gravity from Combined Large-Scale Structure Probes*. [arXiv:1901.03686](#)
113. J. Noller, A. Nicola, *Cosmological Parameter Constraints for Horndeski Scalar-Tensor Gravity*. [arXiv:1811.12928](#)
114. R. Reischke, A. Spurio Mancini, B.M. Schfer, P.M. Merkel, *Investigating Scalar-Tensor Gravity with Statistics of the Cosmic Large-Scale Structure*. [arXiv:1804.02441](#)
115. V. Pettorino, L. Amendola, Friction in Gravitational Waves: a test for early-time modified gravity. *Phys. Lett. B* **742**, 353–357 (2015). [arXiv:1408.2224](#)
116. M. Raveri, C. Baccigalupi, A. Silvestri, S.-Y. Zhou, Measuring the speed of cosmological gravitational waves. *Phys. Rev. D* **91**(6), 061501 (2015). [arXiv:1405.7974](#)
117. LIGO Scientific, Virgo, Fermi-GBM, INTEGRAL Collaboration, B.P. Abbott et al., Gravitational Waves and Gamma-rays from a Binary Neutron Star Merger: GW170817 and GRB 170817A. *Astrophys. J.* **848**(2), L13 (2017). [arXiv:1710.05834](#)
118. L. Perenon, H. Velten, The effective field theory of dark energy diagnostic of linear Horndeski theories after GW170817 and GRB170817A. *Universe* **5**(6), 138 (2019). [arXiv:1903.08088](#)
119. P. Creminelli, M. Lewandowski, G. Tambalo, F. Vernizzi, Gravitational Wave Decay into Dark Energy. *JCAP* **1812**(12), 025 (2018). [arXiv:1809.03484](#)
120. L. Hui, A. Nicolis, C. Stubbs, Equivalence principle implications of modified gravity models. *Phys. Rev. D* **80**, 104002 (2009). [arXiv:0905.2966](#)
121. P. Creminelli, J. Gleyzes, L. Hui, M. Simonovi, F. Vernizzi, Single-Field consistency relations of large scale structure. Part III: test of the equivalence principle. *JCAP* **1406**, 009 (2014). [arXiv:1312.6074](#)
122. J. Gleyzes, D. Langlois, M. Mancarella, F. Vernizzi, Effective theory of dark energy at redshift survey scales. *JCAP* **1602**(02), 056 (2016). [arXiv:1509.02191](#)
123. LSST Science, LSST Project Collaboration, P.A. Abell et al., *LSST Science Book, Version 2.0*. [arXiv:0912.0201](#)
124. SKA Collaboration, D.J. Bacon et al., cosmology with Phase 1 of the Square Kilometre Array: Red Book 2018: Technical specifications and performance forecasts. Submitted to: *Publ. Astron. Soc. Austral.* (2018). [arXiv:1811.02743](#)
125. CMB-S4 Collaboration, K.N. Abazajian et al., *CMB-S4 Science Book*, 1st edn. [arXiv:1610.02743](#)
126. A.S. Mancini, R. Reischke, V. Pettorino, B.M. SchÄefer, M. ZumalacÄrregui, Testing (modified) gravity with 3D and tomographic cosmic shear. *Mon. Not. Roy. Astron. Soc.* **480**, 3725 (2018). [arXiv:1801.04251](#)
127. H. Hildebrandt et al., KiDS-450: cosmological parameter constraints from tomographic weak gravitational lensing. *Mon. Not. Roy. Astron. Soc.* **465**, 1454 (2017). [arXiv:1606.05338](#)
128. J.T.A. de Jong et al., The first and second data releases of the Kilo-Degree Survey. *Astron. Astrophys.* **582**, A62 (2015). [arXiv:1507.00742](#)
129. K. Kuijken et al., Gravitational lensing analysis of the kilo degree survey. *Mon. Not. Roy. Astron. Soc.* **454**(4), 3500–3532 (2015). [arXiv:1507.00738](#)
130. I. Fenech Conti, R. Herbonnet, H. Hoekstra, J. Merten, L. Miller, M. Viola, Calibration of weak-lensing shear in the Kilo-Degree Survey. *Mon. Not. Roy. Astron. Soc.* **467**(2), 1627–1651 (2017). [arXiv:1606.05337](#)
131. E.V. Linder, Cosmic growth history and expansion history. *Phys. Rev. D* **72**, 043529 (2005). [arxiv:astro-ph/0507263](#)
132. J. Gleyzes, Parametrizing modified gravity for cosmological surveys. *Phys. Rev. D* **96**(6), 063516 (2017). [arXiv:1705.04714](#)
133. E.V. Linder, G. Sengör, S. Watson, Is the effective field theory of dark energy effective? *JCAP* **1605**(05), 053 (2016). [arXiv:1512.06180](#)

134. E.V. Linder, Challenges in connecting modified gravity theory and observations. *Phys. Rev. D* **95**(2), 023518 (2017). [arXiv:1607.03113](#)
135. M. Raveri, *Reconstructing Gravity on Cosmological Scales*. [arXiv:1902.01366](#)
136. LIGO Scientific, Virgo Collaboration, B.P. Abbott et al., GW170817: observation of gravitational waves from a binary neutron star inspiral. *Phys. Rev. Lett.* **119**(16), 161101 (2017). [arXiv:1710.05832](#)
137. P. Creminelli, F. Vernizzi, Dark energy after GW170817 and GRB170817A. *Phys. Rev. Lett.* **119**(25), 251302 (2017). [arXiv:1710.05877](#)
138. T. Baker, E. Bellini, P.G. Ferreira, M. Lagos, J. Noller, I. Sawicki, Strong constraints on cosmological gravity from GW170817 and GRB 170817A. *Phys. Rev. Lett.* **119**(25), 251301 (2017). [arXiv:1710.06394](#)
139. J.M. Ezquiaga, M. Zumalacárregui, Dark energy after GW170817: dead ends and the road ahead. *Phys. Rev. Lett.* **119**(25), 251304 (2017). [arXiv:1710.05901](#)
140. R. Kase, S. Tsujikawa, *Dark Energy in Horndeski Theories After GW170817: A Review*. [arXiv:1809.08735](#)
141. C. de Rham, S. Melville, Gravitational rainbows: LIGO and dark energy at its cutoff. *Phys. Rev. Lett.* **121**(22), 221101 (2018). [arXiv:1806.09417](#)
142. LISA Collaboration, H. Audley et al., *Laser Interferometer Space Antenna*. [arXiv:1702.00786](#)
143. P. Creminelli, G. Tambalo, F. Vernizzi, V. Yingcharoenrat, *Dark-Energy Instabilities Induced by Gravitational Waves*. [arXiv:1910.14035](#)
144. A. Joyce, B. Jain, J. Khoury, M. Trodden, Beyond the cosmological standard model. *Phys. Rept.* **568**, 1–98 (2015). [arXiv:1407.0059](#)
145. J.-P. Uzan, Varying constants, gravitation and cosmology. *Living Rev. Relat.* **14**(2) (2011)
146. C.M. Will, The Confrontation between General Relativity and Experiment. *Living Rev. Rel.* **17**(4) (2014). [arXiv:1403.7377](#)
147. A. Vainshtein, To the problem of nonvanishing gravitation mass. *Phys. Lett. B* **39**, 393–394 (1972)
148. A. Nicolis, R. Rattazzi, E. Trincherini, The Galileon as a local modification of gravity. *Phys. Rev. D* **79**, 064036 (2009). [arXiv:0811.2197](#)
149. K. Koyama, G. Niz, G. Tasinato, Effective theory for the Vainshtein mechanism from the Horndeski action. *Phys. Rev. D* **88**, 021502 (2013). [arXiv:1305.0279](#)
150. R. Kimura, T. Kobayashi, K. Yamamoto, Vainshtein screening in a cosmological background in the most general second-order scalar-tensor theory. *Phys. Rev. D* **85**, 024023 (2012). [arXiv:1111.6749](#)
151. T. Kobayashi, Y. Watanabe, D. Yamauchi, Breaking of Vainshtein screening in scalar-tensor theories beyond Horndeski. *Phys. Rev. D* **91**(6), 064013 (2015). [arXiv:1411.4130](#)
152. J. Sakstein, H. Wilcox, D. Bacon, K. Koyama, R.C. Nichol, Testing gravity using galaxy clusters: new constraints on Beyond Horndeski Theories. *JCAP* **1607**(07), 019 (2016). [arXiv:1603.06368](#)
153. K. Koyama, J. Sakstein, Astrophysical Probes of the Vainshtein mechanism: stars and galaxies. *Phys. Rev. D* **91**, 124066 (2015). [arXiv:1502.06872](#)
154. R. Saito, D. Yamauchi, S. Mizuno, J. Gleyzes, D. Langlois, Modified gravity inside astrophysical bodies. *JCAP* **1506**, 008 (2015). [arXiv:1503.01448](#)
155. J. Sakstein, Hydrogen burning in low mass stars constrains scalar-tensor theories of gravity. *Phys. Rev. Lett.* **115**, 201101 (2015). [arXiv:1510.05964](#)
156. J. Sakstein, E. Babichev, K. Koyama, D. Langlois, R. Saito, Towards strong field tests of Beyond Horndeski Gravity Theories. *Phys. Rev. D* **95**(6), 064013 (2017). [arXiv:1612.04263](#)
157. A.K. Romer, P.T.P. Viana, A.R. Liddle, R.G. Mann, *A Serendipitous Galaxy Cluster Survey with XMM: Expected Catalogue Properties and Scientific Applications*. [arxiv:astro-ph/9911499](#)
158. C. Heymans et al., CFHTLenS: the Canada-France-Hawaii telescope lensing survey. *Mon. Not. Roy. Astron. Soc.* **427**, 146 (2012). [arXiv:1210.0032](#)
159. J. Sakstein, B. Jain, Implications of the Neutron Star Merger GW170817 for Cosmological Scalar-Tensor Theories. *Phys. Rev. Lett.* **119**(25), 251303 (2017). [arXiv:1710.05893](#)

160. J. Beltrá Jiménez, F. Piazza, H. Velten, Evading the Vainshtein Mechanism with Anomalous Gravitational Wave Speed: Constraints on Modified Gravity from Binary Pulsars. *Phys. Rev. Lett.* **116**(6), 061101 (2016). [arXiv:1507.05047](https://arxiv.org/abs/1507.05047)
161. B. Bertotti, L. Iess, P. Tortora, A test of general relativity using radio links with the Cassini spacecraft. *Nature* **425**, 374–376 (2003)

Chapter 32

The H_0 Tensions to Discriminate Among Concurring Models



Eleonora Di Valentino

The latest 2018 legacy release from the Planck satellite [1] of the Cosmic Microwave Background (CMB) temperature and polarization anisotropies power spectra, has provided a fantastic confirmation of the standard Λ Cold Dark Matter (Λ CDM) cosmological model. However, some anomalies and tensions between Planck and external cosmological probes, present above the three standard deviations, are becoming even more stronger, justifying possible extensions of the standard cosmological scenario. The most famous one is the so-called *Hubble constant H_0 tension* between the CMB estimation of H_0 , under the assumption of the Λ CDM model, and the direct local distance ladder measurements.

In particular, the Planck collaboration found $H_0 = 67.27 \pm 0.60$ km/s/Mpc at 68% CL for Planck TTTEEE + lowE 2018 [2] ($H_0 = 67.36 \pm 0.54$ km/s/Mpc at 68% CL for Planck TTTEEE + lowE + CMB lensing 2018), but this bound is model-dependent and affected by the degeneracy with the other parameters of the model. This constraint is in tension at about 3.3σ , with the 2.4% determination of the Hubble constant by Riess et al. in 2016 (R16) [3], $H_0 = 73.24 \pm 1.74$ km/s/Mpc at 68% CL, based on the analysis of the Hubble Space Telescope (HST) observations using four geometric distance calibrations of Cepheids. Moreover, the tension increases to 3.6σ if we consider the 2.3% 2018 Riess et al. (R18) [4] estimate of the Hubble constant $H_0 = 73.48 \pm 1.66$ km/s/Mpc at 68% CL, including parallax measurements of seven long-period Milky Way Cepheids. Finally, the tension arises to 4.4σ with the latest 2019 SH0ES collaboration (R19) constraint [5] on the Hubble constant $H_0 = 74.03 \pm 1.42$ km/s/Mpc at 68% CL, obtained using the HST observations of 70 long-period Cepheids in the Large Magellanic Cloud (LMC).

E. Di Valentino (✉)

Jodrell Bank Center for Astrophysics, School of Physics and Astronomy, University of Manchester, Oxford Road, Manchester M13 9PL, UK

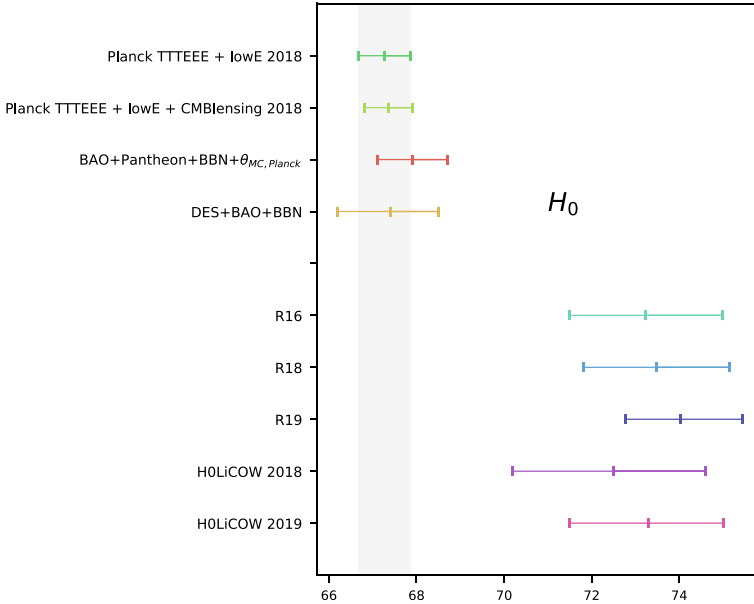


Fig. 32.1 Whisker plots showing the 68% CL constraint on the Hubble constant H_0 from different cosmological probes. The grey band is the 2018 Planck TTTEEE + lowE 68% CL bound on H_0

Actually, the Hubble constant tension is referring to two independent blocks, as we can see in Fig. 32.1. On the left side, preferring smaller values, we have estimates of H_0 as obtained by Planck 2018, and some combinations of data. In particular, we are showing two different combinations of Baryon Acoustic Oscillation (BAO) measurements [6–8], the first-year measurements of the Dark Energy Survey (DES) experiment [9–11], supernovae from the recent Pantheon catalogue [12] (Pantheon), a prior on the baryon density of $\Omega_b h^2 = 0.0222 \pm 0.005$ derived from measurements of primordial D [13] assuming Big Bang Nucleosynthesis (BBN), and a prior on θ_{MC} as obtained by Planck in a Λ CDM scenario. Namely, we have that BAO+Pantheon+BBN+ $\theta_{MC, Planck}$ gives $H_0 = 67.9 \pm 0.8$ km/s/Mpc at 68% CL, and DES+BAO+BBN find $H_0 = 67.4^{+1.1}_{-1.2}$ km/s/Mpc at 68% CL. On the right side, instead, preferring larger values, we find the late Universe measurements, as obtained by the SHOES collaboration and the H0LiCOW experiment, which is performing a cosmographic analysis of multiply-imaged quasars systems through the time-delay strong lensing. Therefore, we have the H0LiCOW 2018 [14] Hubble constant estimate $H_0 = 72.5^{+2.1}_{-2.3}$ km/s/Mpc at 68% CL and the 2.4% H0LiCOW 2019 [15] constraint $H_0 = 73.3^{+1.7}_{-1.8}$ km/s/Mpc at 68% CL. Therefore, the late Universe estimates (R19 and H0LiCOW 2019) combined together give $H_0 = 73.8 \pm 1.1$ km/s/Mpc at 68% CL, showing a 5.3σ tension with the early Universe values obtained in a Λ CDM model, and resulting in a Universe expanding faster at late times than one driven by the cosmological constant.

In addition, we have the re-analysis of the R16 Cepheid data by using Bayesian hyper-parameters (HPs) [16], which gives $H_0 = 73.75 \pm 2.11$ km/s/Mpc at 68% CL. Then, we have to mention the local determination of the Hubble constant [17] as obtained by considering the cosmographic expansion of the luminosity distance, i.e., $H_0 = 75.35 \pm 1.68$ km/s/Mpc at 68% CL, in agreement with R19, but in tension at about 4.5σ with Planck 2018. Moreover, there is the debated independent determination of the Hubble constant based on the Tip of the Red Giant Branch (TRGB). In fact, a first measurement made by [18] (F19), which gives $H_0 = 69.8 \pm 0.8(stat) \pm 1.7(sys)$ km/s/Mpc at 68% CL, has been followed by the re-analysis of [19] (Y19), which gives $H_0 = 72.4 \pm 2.0$ km/s/Mpc at 68% CL, contesting the F19 overestimate of the LMC extinction, and concluded by the revised measurement made by [20] (F20), which gives $H_0 = 69.6 \pm 0.8(stat) \pm 1.7(sys)$ km/s/Mpc at 68% CL, discussing the Y19 neglect of the correction for reddening. However, these H_0 measurements are not useful to discriminate between Planck and R19 because they are in agreement with both within 95% CL.

Finally, many others independent late Universe measurements point towards a larger value for the Hubble constant, like MIRAS (variable red giant stars) [21], STRIDES (STRong-lensing Insights into Dark Energy Survey) [22], water masers and the use of the Surface Brightness Fluctuations method [23]. If the late Universe measurements are averaged by excluding each time a different method or geometric calibration or team, these H_0 estimates will be in tension between 4.5σ and 6.3σ with the Planck one (see the recent review [24]).

However, since the CMB constraints are model-dependent, by changing the underlying cosmological scenario we can have completely different cosmological parameter constraints. Even if possible systematic effects can always be present in some (or all) of the cosmological experiments, there is a possibility of restoring the concordance between these measurements taken at a face value, considering the extended model beyond the Λ CDM one. For a list of recent works (from 2015 onwards) trying to solve or alleviate the H_0 tension, see, for example, [25–93].¹

In the following sections of the paper we will investigate some interesting departures from the Λ CDM model, starting from the most famous extensions, namely a neutrino effective number different from 3.046 in Sect. 32.1 or a dark energy equation of state different from the cosmological constant in Sect. 32.2, until the most recent proposed solutions. In particular, we will revise in Sect.32.3 a multi-parameters approach, in Sect. 32.4 an Early Dark Energy scenario, in Sect. 32.5 the Interacting Dark Energy model, in Sect. 32.6 the Modified Gravity solution, and in Sect. 32.7 a list of other specific models solving the H_0 tension. In Sect. 32.8 we will see which characteristic a model should have for alleviating the Hubble constant tension, and finally in Sect. 32.9 we will discuss which will be the constraints on H_0 expected in the near future.

¹ While the book was under review, many new H_0 measurements and new proposed solutions to the tension appear. For an updated perspective, see the letter submitted for SNOWMASS 2021 [94] about H_0 (and references therein). In particular, here a list of updated references about the solutions [95–195] and here about the measurements [196–234].

32.1 The Effective Number of Relativistic Degrees of Freedom

One of the most famous extensions considered in the literature for solving the H_0 tension is the possibility of having extra relativistic degrees of freedom at the recombination. We can parametrise the radiation density ρ_r as a function of the photon density ρ_γ in the following way:

$$\rho_r = \left[1 + \frac{7}{8} \left(\frac{4}{11} \right)^{4/3} N_{\text{eff}} \right] \rho_\gamma, \quad (32.1)$$

where $(4/11)^{1/3} = T_\nu/T_\gamma$ is the ratio between the background temperatures of neutrinos and photons derived under the approximation of an instantaneous neutrino decoupling. N_{eff} is expected to be equal to 3.046 for three active massless neutrino families [235, 236]. If we have more relativistic degrees of freedom, we then have more radiation and we can measure the effect on the CMB temperature power spectrum from the smearing and shifting of the acoustic peaks in the damping tail. More radiation also means a delay in the matter to radiation equivalence, producing an enhancement of the early Integrated Sachs Wolfe (eISW) effect, which peaks around the multipole $\ell \sim 200$ [237].

Letting the N_{eff} parameter free to vary, thanks to the well known degeneracy between H_0 and N_{eff} , could increase the H_0 value at the price of additional radiation at recombination, due to additional relativistic species, like, for example, sterile neutrinos or thermal axions [125, 126, 238–241]. With Planck 2015 TT+lowP we had in fact $N_{\text{eff}} = 3.13 \pm 0.32$ at 68% CL, corresponding to $H_0 = 68.0 \pm 2.8$ km/s/Mpc at 68% CL, solving the Hubble constant tension at 2.1σ . Now, with the inclusion of the Planck 2018 polarization data, which is insensitive to the eISW, we have help in breaking the degeneracy between the cosmological parameters. The improved constraint on $N_{\text{eff}} = 2.92 \pm 0.19$ at 68% CL from Planck 2018 TTTEEE + lowE corresponds to $H_0 = 64.4 \pm 1.4$ km/s/Mpc at 68% CL, in tension at about 3.8σ with R19. With the addition of the Planck polarization data and the new τ estimate, that shifts the mean value of N_{eff} towards smaller values because of their correlation, an extra dark radiation, producing a neutrino effective number different from the standard value 3.046, seems no more a suitable solution for solving the Hubble constant tension between Planck and R19.

32.2 Dark Energy Equation of State

The second most important extension considered in the H_0 tension discussion, is a dark energy component with an equation of state w different from -1, i.e., different from a cosmological constant. Varying w means to change the expansion rate of the Universe through the first Friedmann equation. From Planck 2018 TTTEEE + lowE

we have $w = -1.58^{+0.16}_{-0.35}$ at 68% CL, to which corresponds $H_0 > 69.9$ km/s/Mpc at 95% CL, which solves the H_0 tension within two standard deviations. The Hubble constant is in fact almost unconstrained in this model, because of the geometrical degeneracy present with the DE equation of state w , so it can be perfectly in agreement with R19 at the price of a phantom-like dark energy. Phantom dark energy has several theoretical problems and is expected to produce a Big Rip in the future of the Universe. Moreover, it violates the energy condition $\rho \geq |p|$, which means that the matter could move faster than light and a comoving observer could measure a negative energy density, and the Hamiltonian could have vacuum instabilities due to negative kinetic energy. Nevertheless, there exist models expecting an effective energy density with a phantom equation of state without showing the problems mentioned before, as - for example - the Parker Vacuum Metamorphosis [242–244].

Another possibility is allowing the DE equation of state varying with redshift. For example, we can consider the well-known Chevallier - Polarski - Linder parametrisation (CPL) [245, 246] of the DE equation of state $w(a)$ with two parameters:

$$w(a) = w_0 + (1 - a)w_a, \quad (32.2)$$

where a is the dimensionless cosmological scale factor normalized to unity today. Here, w_0 gives an idea of the behaviour of the DE equation of state today, while w_a of the evolution with time. If $w(a)$ is increasing with a we will have $w_a < 0$, while if $w(a)$ is become more negative with a we will have a positive w_a . In this scenario from Planck 2018 TTTEEE + lowE we have $w_0 = -1.21^{+0.33}_{-0.60}$ and $w_a < -0.85$ at 68% CL, and $H_0 > 63$ km/s/Mpc at 95% CL, solving the tension with R19 within 2σ .

32.3 Multi-parameters Extension

In order to understand which is the best extension preferred by the data for solving the H_0 tension, we can try to vary the cosmological parameters all together. In practice, instead of solving the H_0 tension with a specific mechanism, we look for a combination of parameters that can ameliorate it. In fact, even if the Λ CDM model provides a good fit of the data, some of the assumptions and simplifications made in this six parameters approach are no more fully justified. This simplification can be excessive and can hide some physical aspects driving the evolution of the Universe.

If we consider, for example, a multi-parameter space, we can understand where data wants us to go, avoiding biases due to the choice of the model. In [68] we see a multi-parameter approach varying 10, 11 or 12 parameters at the same time. In particular, in the 10 parameters space the extensions of the standard Λ CDM model under consideration are a running of the scalar spectral index α_s , a total neutrino mass Σm_ν , the effective number of relativistic degrees of freedom N_{eff} and a dark energy equation of state w . In the 11 parameters space there is the addition of the A_{lens} parameter [247], parametrising the lensing potential in the temperature power spectrum of the CMB. This phenomenological parameter is just a consistency check

that the Planck data fails, because it is different from the expected value at about 2.8σ in the last 2018 data release. Finally, in the 12 parameters approach the CPL parametrisation $w(a) = w_0 + (1 - a)w_a$ of the dark energy equation of state with redshift is taken under consideration.

The bottom line of this multi-parameters approach is that H_0 is almost unconstrained in these very extended scenarios, mainly because of the strong geometrical degeneracy present with the dark energy equation of state $w(a)$. For Planck 2018 TTTEEE + lowE in a 10 parameters scenario we have $H_0 > 65.2$ km/s/Mpc at 95% CL, in a 11 parameters space $H_0 = 73^{+10}_{-20}$ km/s/Mpc at 68% CL and in a 12 parameters approach $H_0 = 72 \pm 20$ km/s/Mpc at 68% CL. For this reason, a safe combination of Planck 2018 and R19 can be performed, and the new “concordance” model has N_{eff} exactly in agreement with the standard expectation, while the cosmological constant is ruled out at more than three standard deviations, in favour of a phantom-like dark energy. Unfortunately, this “concordance” model is strongly in tension with BAO and Pantheon data at more than 3σ , and the combination of Planck with these datasets restores the H_0 tension at high significance.

32.4 Early Dark Energy

Very important models, effective in reducing the H_0 tension, are Early Dark Energy (EDE) scenarios. In these models, the Dark Energy behaves like a cosmological constant at early times ($z \geq 3000$) and then decays away like radiation or faster at later times. For EDE scenarios, the sound horizon at decoupling is reduced, resulting in a larger value of the Hubble parameter H_0 inferred from the CMB.

In [48] the authors consider two physical models for the EDE:

- An oscillating scalar field with a potential $V(\phi) \propto (1 - \cos[\phi/f])^n$ [248]. At early times this field acts like a cosmological constant, but at a certain point it starts to oscillate, and behaves like a fluid with an equation of state $w_n = (n - 1)/(n + 1)$.
- A field that slowly rolls down a potential that is linear in ϕ at early times and reaches asymptotically zero at late times.

Depending on n , the homogeneous EDE density dilutes like matter ($n = 1$), radiation ($n = 2$) or faster than radiation ($n \geq 3$). For $n \sim \infty$ the energy density dilutes instead as a^{-6} . For Planck 2015 TTTEEE [249] + lowTEB + CMBlensing 2015 + R18 + BAO + Pantheon, the Hubble constant is $H_0 = 70.3 \pm 1.2$ km/s/Mpc at 68% CL for $n = 2$, $H_0 = 70.6 \pm 1.3$ km/s/Mpc at 68% CL for $n = 3$ and $H_0 = 69.9 \pm 1.1$ km/s/Mpc at 68% CL for $n = \infty$. Within these models, the H_0 tension with R19 is reduced at about 2σ , 1.8σ and 2.2σ respectively, with an improvement of the χ^2 of 9.5, 14.5 and 9.1 in fitting the data, with respect to the standard Λ CDM model. However, it is difficult to assess this result as a possible solutions of the Hubble constant tension because the authors of [48] are combining together R18 and BAO, which are potentially in tension with each other and can bias the final findings. A re-analysis with the Planck 2018

TTTEEE + lowE can be found in Ref. [155], that for $n = 3$ gives $H_0 = 68.3 \pm 1.0$ km/s/Mpc at 68% CL, in tension with R19 at 3.5σ .

A possibility for the realization of an EDE is that an axion could interact with a dilaton, as proposed by [250].

Moreover, EDE models suffer a fine-tuning problem (see, for example, [251]), because, in order to solve the Hubble tension, the early component of dark energy needs to become active around the time of matter-radiation equality, and these quantities are completely disconnected. However, in [129] the possibility that the EDE scalar couples to neutrinos, receiving a large injection of energy when neutrinos become non-relativistic, i.e., around the time of matter-radiation equality, is considered to solve the fine-tuning.

In addition, in [83] the authors investigate a first-order phase transition in a dark sector in the early Universe, before recombination. This will lead to a short phase of a New EDE component ameliorating the Hubble constant tension. For Planck 2015 TTTEEE + lowTEB + CMBlensing 2015 + R19 + BAO + Pantheon, the Hubble constant is $H_0 = 70.4^{+0.9}_{-1.0}$ km/s/Mpc at 68% CL, reducing the tension with R19 at 2.1σ . A re-analysis with the Planck 2018 TTTEEE + lowE + CMBlensing + BAO + Pantheon can be found in Ref. [117], which gives $H_0 = 69.6^{+1.0}_{-1.3}$ km/s/Mpc at 68% CL, reducing the Hubble constant tension at 2.5σ .

Finally, in [131] the authors studied a phenomenological EDE model with an Anti-de Sitter (*AdS*) vacua around recombination, obtaining for Planck 2018 + BAO + Pantheon + R19 $H_0 = 72.64^{+0.57}_{-0.64}$ km/s/Mpc at 68% CL, reducing the tension within one standard deviation.

32.5 Interacting Dark Energy

Another possibility is to consider an Interacting Dark Energy (IDE) scenario, where Dark Matter (DM) and Dark Energy (DE) share interactions other than gravitational. In this model the conservation equations for DM and DE can be modified with the introduction of an interaction rate $Q = \xi \mathcal{H} \rho_{DE}$, proportional to the comoving Hubble rate \mathcal{H} and the dark energy density ρ_{DE} via a negative dimensionless parameter ξ quantifying the strength of the coupling.

In the IDE scenario, as recently analysed in [69, 70], for Planck 2018 TTTEEE + lowE the Hubble constant is $H_0 = 72.8^{+3.0}_{-1.5}$ km/s/Mpc at 68% CL [69], solving the tension with R19 within one standard deviation. The ‘‘concordance’’ model obtained combining Planck 2018 + R19 gives a non-zero coupling ξ at more than five standard deviations, indicating a flux of energy from DM to DE. Planck 2018 TTTEEE + lowE + BAO data estimates instead $H_0 = 69.4^{+0.9}_{-1.5}$ km/s/Mpc at 68% CL [70], increasing the tension with R19 again at 2.5σ . However, the procedure that leads to the extraction of the BAO data is assuming a Λ CDM model (for a discussion about the BAO model dependence see, for example, [252]), so it might need to be revised when applied to extended DE cosmologies.

It is important to mention the following works [28–30, 41, 44, 53, 59, 97] pointing towards the same conclusions, i.e., the possibility that an IDE model could alleviate the Hubble constant tension with a coupling different from zero. However, these papers make use of the old Planck 2015 likelihood and need to be updated in light of the new released polarisation data.

32.6 Modified Gravity

An argument in favor of Modified Gravity models (see Ref. [253], and references therein) is the possibility of relieving the Hubble constant tension. In fact, if gravity is weaker at intermediate scales than expected in General Relativity (GR), then the H_0 estimate from CMB can have larger values.

In [84] is presented a data-driven reconstruction of gravitational theories and Dark Energy models on cosmological scales, making use of the Effective Field Theory (EFT) approach, which compresses the freedom in defining such models into a finite set of functions that can be reconstructed across cosmic times using cosmological data. Using the EFT approach, some of the models, in particular Scalar Horndeski (SH) and Full Horndeski (FH), can alleviate the present discrepancy in the determination of the Hubble constant between Planck and R19, and are statistically preferred against the standard Λ CDM model.

Moreover, in [86] the EFT approach is applied to the torsional gravity, finding the possibility of alleviating the H_0 tension. The use of the EFT formalism allows us to study systematically the evolution equations at the background and perturbation levels separately, in a model-independent way, examining the role of the coefficients in relaxing the Hubble constant tension. In [86] the authors focus on a well-known class of torsional gravity, namely the $f(T)$ gravity, where T is the torsion scalar. They find that, imposing initial conditions at the last scattering reproducing the Λ CDM scenario, and imposing the late times values preferred by local measurements, $f(T)$ models described by this parameterization:

$$f(T) = -T - 2\Lambda/M_P^2 + \alpha T^\beta, \quad (32.3)$$

can alleviate the Hubble constant tension. Moreover, using this information, extended models can be considered, like, for example, the $f(T, B)$ gravity, where B is the boundary term $B = -2\nabla_\mu T_\nu{}^\mu$. However, an actual fit of the data with these promising models is missing, and for this reason it is difficult to quantify how much they are effectively able in alleviating the H_0 tension between Planck and R19.

Finally, a promising class of theories, within the context of the Modified Gravity proposals solving the H_0 tension, are the Horndeski ones. On this topic we can find [141], where the authors studied a *generalized cubic covariant Galileon* (GCCG) model, obtaining for Planck 2015 TT + lowTEB $H_0 = 72_{-5}^{+8}$ km/s/Mpc at 95% CL, alleviating the tension with R19. However, in the paper the Planck high- ℓ polarization is not included and the tension with R19 is restored when Planck data are combined with external datasets.

32.7 More Specific Models

In the literature, we can find many more specific models that can relieve the Hubble constant tension, but at the moment most of them make use of the old Planck 2015 likelihood. Here we list just a few of them:

- In [32] the authors analyse the *Parker vacuum metamorphosis* (PVM) model, physically motivated by quantum gravitational effects and with the same number of parameters as Λ CDM, showing that it can remove the H_0 tension, and give an improved fit of the data. For Planck 2015 TTTEEE + lowTEB $H_0 = 78.61 \pm 0.38$ km/s/Mpc at 68% CL for the original PVM, reducing the tension with R19 at 2.2σ , while $H_0 = 71.6^{+2.8}_{-5.1}$ km/s/Mpc at 68% CL for the elaborated PVM, with one more degree of freedom, removing the H_0 tension within one standard deviation. An updated re-analysis for Planck 2018 TTTEEE + lowE can be found in Ref. [119], which gives $H_0 = 76.7^{+3.9}_{-2.6}$ km/s/Mpc at 68% CL for the elaborated PVM.
- In [34] the authors propose the $\ddot{u}\Lambda$ CDM, based on *über gravity*, to alleviate the H_0 tension. In this model, there is a sharp transition between Λ CDM to a phase in which the Ricci scalar is constant. For Planck 2015 TT + lowTEB + R16 + BAO $H_0 = 70.6^{+1.1}_{-1.3}$ km/s/Mpc at 68% CL, improving the agreement with R19 at 1.9σ . Again this bound is obtained by combining together the SHOES collaboration R16 constraint on H_0 with BAO measurements, and considering just the temperature power spectrum for the CMB at higher multipoles. However, as we can see from the figures in the paper [34], a Planck only constraint on H_0 is really relaxed within this model, so in agreement with R19 within one standard deviation, with only one additional free parameter.
- In [36] the authors show how the *Galileon Gravity* is able to alleviate the Hubble tension. Considering Planck 2015 TT + lowTEB + CMBlensing 2015 + BAO and varying the total neutrino mass too, for the Cubic Galileon $H_0 = 71.6 \pm 2.1$ km/s/Mpc at 95% CL, for the Quartic Galileon $H_0 = 72.4 \pm 2.0$ km/s/Mpc at 95% CL and for the Quintic Galileon $H_0 = 72.3 \pm 2.1$ km/s/Mpc at 95% CL, reducing, respectively, the tension between the CMB and R19 at 1.4σ , 0.9σ and 1σ .
- In [38] the authors analyse *Nonlocal Gravity*, and in particular the RR model, obtained by the requirement of providing a viable cosmological evolution severely and corresponding to a dynamical mass generation for the conformal mode. In this scenario, for Planck 2015 TTTEEE + lowTEB + BAO + JLA, $H_0 = 69.49^{+0.79}_{-0.80}$ km/s/Mpc at 68% CL, reducing the tension with R19 at 2.8σ .
- In [39] the authors investigate the *running vacuum model* (RVM), finding that in the dynamical quasi-vacuum models (w DVMs) with a varying dark energy equation of state can alleviate the tension if Large Scale Structure (LSS) data are not considered. In particular, for Planck 2015 TTTEEE + lowTEB + CMBlensing 2015 + BAO + R16 $H_0 = 71.0 \pm 1.5$ km/s/Mpc at 68% CL for w RVM, i.e., at 1.5σ tension with R19. However, this result is driven by the addition of the R16 prior on the Hubble constant and is mainly due to the phantom behaviour of the dark energy.

- In [40] the author proposes the *f(T) parallel telegravity* that performs in a fantastic way in removing the H_0 tension. For Planck 2015 TTTEEE + lowTEB + BAO $H_0 = 72.4^{+3.3}_{-4.1}$ km/s/Mpc at 68% CL, improving the agreement with R19 within 1σ , even in presence of the BAO data, which are difficult to put in agreement with a larger H_0 value. An updated re-analysis for Planck 2018 TTTEEE + lowE can be found in Ref. [112], which gives $H_0 = 66.51 \pm 3.65$ km/s/Mpc at 68% CL.
- In [47] the authors studied several DE equations of state varying with redshift, but with just one free parameter. All the models considered in the paper favour a phantom DE equation of state at the present time, while leading the H_0 values in fantastic agreement with the Hubble constant direct measurement R19 within one standard deviation, for Planck 2015 TTTEEE + lowTEB.
- In [49] the authors show that with a phase transition in the dark sector, based on a simplified model such that the cosmological constant has two values before a transition redshift and afterwards it becomes single-valued, the Hubble constant tension can be relieved. This model is called *double- Λ Cold Dark Matter* and using BAO volume distances listed in [49], R18 and a gaussian prior from the Planck 2015 value on Θ , i.e., the distance of the last scattering surface to us, $H_0 = 72.5^{+2.5}_{-3.0}$ km/s/Mpc at 68% CL with a χ^2 analysis. The tension with R19 is therefore solved within one standard deviation.
- In [50] the authors analysed a DE model based on *Ginzburg-Landau theory of phase transition* (GLTofDE). In the mean field approximation, a phase transition happens which causes a spontaneous symmetry breaking. Using a χ^2 analysis with BAO, R18 and quasars $H(z)$ data points as listed in [50], CMB distance data point and a prior on $\Omega_m h^2$ based on the Planck 2015 value, $H_0 = 71.89 \pm 0.93$ km/s/Mpc at 68% CL, i.e., in agreement with R19 at 1.3σ .
- In [52] the authors claim that delaying the onset of neutrino free-streaming until close to the matter-radiation equality epoch, introducing a neutrino self-interaction in presence of a total neutrino mass different from zero, H_0 can be larger than in the standard cosmological model. In the case of a strongly interacting neutrino cosmology for Planck 2015 TTTEEE + lowTEB the Hubble constant is $H_0 = 66.2^{+2.3}_{-1.9}$ km/s/Mpc at 68% CL, reducing the H_0 tension at 2.9σ .
- In [54] the authors analyse the effect of *two-body dark matter decays*, where the products of the decay include a massless and a massive particle. For Planck 2015 TTTEEE + lowTEB + CMB lensing 2015 + R18 + BAO $H_0 = 70^{+4}_{-3}$ km/s/Mpc at 68% CL, improving the agreement with R19 within 1σ . However, again the presence of the R18 prior in the data combination makes it difficult to assess how good the model is in solving the Hubble tension. An updated re-analysis for Planck 2018 TTTEEE + lowE + CMB lensing 2018 can be found in Ref. [114], which gives $H_0 = 67.31^{+0.53}_{-0.56}$ km/s/Mpc at 95% CL, consistent with the Λ CDM value.
- In [56] the authors consider a scenario with an evolving scalar field ϕ^{2n} , asymptotically *rocking and rolling*. For Planck 2015 TTTEEE + lowTEB + Pantheon + R18 + BAO $H_0 = 70.1^{+1.0}_{-1.2}$ km/s/Mpc at 68% CL, reducing the tension with R19 at 2.3σ , for the case in which $n = 2$. However, even in this analysis for the presence of the R18 prior on H_0 it is difficult to assess how much the model can solve the Hubble tension between the data.

- In [67] the authors analysed a *Phenomenologically Emergent Dark Energy* (PEDE) scenario, introduced in Ref. [144], finding that the H_0 tension with R19 is alleviated within one standard deviation without additional degrees of freedom with respect to the Λ CDM model. In fact, for Planck 2015 TTTEEE + lowTEB $H_0 = 72.58_{-0.80}^{+0.79}$ km/s/Mpc at 68% CL. An updated re-analysis for Planck 2018 TTTEEE + lowE can be found in Ref. [135], which finds $H_0 = 72.35_{-0.79}^{+0.78}$ km/s/Mpc at 68% CL, in agreement with R19.
- In [73] the authors investigate two *metastable dark energy models*: (I) a DE decaying exponentially and (II) a DE decaying into DM. For Pantheon + BAO $H_0 = 75.0_{-5.8}^{+4.7}$ km/s/Mpc at 68% CL for the model I, while $H_0 = 71.8_{-4.6}^{+4.7}$ km/s/Mpc at 68% CL for the model II, respectively. Unfortunately, when CMB distance priors from Planck 2018 are added to the analysis, the tension with R19 is restored at more than 3σ .
- In [79] the authors consider a *decaying dark matter* (DDM) model, where a fraction of dark matter density decays into dark radiation. For Planck 2015 TT + lowTEB + R18 $H_0 = 70.6_{-1.3}^{+1.1}$ km/s/Mpc at 68% CL, improving the agreement with R19 at 1.9σ . However this result is driven by the addition of the R18 prior on the Hubble constant, therefore it is difficult to quantify the ability of the model in solving the Hubble tension by itself. An updated re-analysis for Planck 2018 TTTEEE + lowE can be found in Ref. [168], which finds $H_0 = 67.7 \pm 1.2$ km/s/Mpc at 68% CL.
- In [81] the authors show that assuming a non-Gaussian covariance contribution from a primordial trispectrum (*super- Λ CDM*), H_0 is larger than in the classic Λ CDM model and the $\Delta\chi^2 = -7.8$ with the addition of just two degrees of freedom. In fact, for Planck 2015 TT + τ prior $H_0 = 68.4_{-2.3}^{+2.5}$ km/s/Mpc at 95% CL, reducing the tension with R19 at 2.9σ .
- In [82] the authors investigated a *self-interacting neutrino mode*. For Planck 2015 TT + lowTEB $H_0 = 70.4 \pm 1.3$ km/s/Mpc at 68% CL, alleviating the H_0 tension within 1.9σ . When the high- ℓ polarization is also considered, however, the tension increases again, but is alleviated at 2.8σ , giving $H_0 = 69.59_{-0.71}^{+0.74}$ km/s/Mpc at 68% CL.
- In [85] the authors propose a modification of the effective electron rest mass m_e during the cosmological recombination era, for ameliorating the Hubble constant tension. For Planck 2018 TTTEEE + lowE + BAO in this model $H_0 = 69.1 \pm 1.2$ km/s/Mpc at 68% CL, reducing the Hubble tension with R19 at 2.7σ , at the price of an indication for a larger electron rest mass $m_e = (1.0078 \pm 0.0067)m_{e,0}$ at 68% CL.

32.8 Requirements: Hubble Hunter's Guide

Guidance to model builders about where in redshift departures from Λ CDM are expected for solving the Hubble constant tension can be found in [78]. The estimation of H_0 from the CMB data can be done in three steps: determination of the sound horizon at the CMB last-scattering r_s^* from the baryon density and the matter density,

determination of the comoving angular diameter distance to last scattering $D_A^* = r_s^*/\theta_s^*$ from the position of the acoustic peaks, determination of $H(z)$ for all the redshift z from $D_A^* = \int_0^{z^*} dz/H(z)$ adjusting the last free density parameter.

The authors divide the models into post- and pre-recombination solutions. Since BAO constrains the product Hr_s , the Hubble tension can be seen also as a tension between a high and a low sound horizon, as preferred by Λ CDM and distance ladder, respectively. Therefore, to have an agreement between all the data, the authors conclude that the late-time solutions (for example a phantom DE) to the Hubble constant tension, which do not require a departure from the *CMB* prior to recombination, are unlikely to be a viable path, because they can change the Hubble constant estimate, leaving unaltered the sound horizon (and the tension with BAO data). The most likely solutions to the Hubble tension have instead to be found in the pre-recombination possibilities (for example an EDE). Moreover, within the pre-recombination solutions, those increasing $H(z)$ and decreasing r_s are the best. These should lead to features in the CMB power spectra that we could already see in Planck, like, for example, the excess of lensing in the temperature power spectrum of Planck ($A_{lens} > 1$ at 2.8σ).

Their findings are in agreement with a previous work [51], where the authors find that late-time dark energy explanations are slightly disfavoured, whereas a pre-CMB decoupling extra dark energy component is better in alleviating the Hubble constant tension. An updated view can instead be found in [254], where it is shown that the early solutions are promising but cannot solve completely the H_0 tension.

32.9 Standard Sirens

The next decade of experiments will be decisive in confirming or ruling out the scenarios listed in the previous sections. In fact, together with the next generation of CMB experiments, like the Simons Observatory or CMB-S4, and cosmic surveys, like Euclid and LSST, which are expected to reach an uncertainty of about a 1% in the H_0 estimate, an important role will play complementary probes like Standard Sirens [255, 256].

In fact, the observations of gravitational-wave and electromagnetic emission produced by the merger of the binary neutron-star system GW170817 have opened the possibility of using Standard Sirens, the gravitational-wave analogue of astronomical standard candles, to constrain the value of the Hubble constant. Indeed, in [257] a constraint of $H_0 = 70_{-8}^{+12}$ km/s/Mpc at 68% CL has been reported. While this constraint is significantly weaker than those derived from observations of Cepheid variables, it does not require any form of cosmic ‘distance ladder’ and can be considered, in principle, as more conservative. The GW170817 determination of H_0 is relatively poor and strongly non-Gaussian, but it is possible to investigate what is the impact on the Planck constraints in an extended parameter space in which the Planck data alone is unable to strongly constrain the Hubble constant [258].

At least more than 25 additional observations of Standard Sirens are needed for reaching a useful uncertainty on H_0 to discriminate between Planck and the SH0ES

collaboration value. Actually, an uncertainty of about 2% in the H_0 determination is expected in the early(mid)-2020s [259], for the analysis of Gravitational Waves events with electromagnetic counterparts. These H_0 estimates from bright Standard Sirens will be model-independent, oppositely to the measurements from CMB experiments.

References

1. Planck Collaboration, Y. Akrami et al., *Planck 2018 results. I. Overview and the cosmological legacy of Planck*. [arXiv:1807.06205](#)
2. Planck Collaboration, N. Aghanim et al., *Planck 2018 results. VI. Cosmological parameters*. [arXiv:1807.06209](#)
3. A..G. Riess et al., A 2.4% determination of the local value of the hubble constant. *Astrophys. J.* **826**(1), 56 (2016). [arXiv:1604.01424](#)
4. A.G. Riess et al., New parallaxes of galactic cepheids from spatially scanning the hubble space telescope: implications for the hubble constant. *Astrophys. J.* **855**(2), 136 (2018). [arXiv:1801.01120](#)
5. A.G. Riess, S. Casertano, W. Yuan, L.M. Macri, D. Scolnic, Large magellanic cloud cepheid standards provide a 1% foundation for the determination of the hubble constant and stronger evidence for physics beyond Λ CDM. *Astrophys. J.* **876**(1), 85 (2019). [arXiv:1903.07603](#)
6. F. Beutler, C. Blake, M. Colless, D.H. Jones, L. Staveley-Smith et al., The 6dF galaxy survey: baryon acoustic oscillations and the local hubble constant. *Mon. Not. Roy. Astron. Soc.* **416**, 3017–3032 (2011). [arXiv:1106.3366](#)
7. A..J. Ross, L. Samushia, C. Howlett, W..J. Percival, A. Burden, M. Manera, The clustering of the SDSS DR7 main Galaxy sample - I. A 4 per cent distance measure at $z = 0.15$. *Mon. Not. Roy. Astron. Soc.* **449**(1), 835–847 (2015). [arXiv:1409.3242](#)
8. B.O.S.S. Collaboration, S. Alam et al., The clustering of galaxies in the completed SDSS-III Baryon Oscillation Spectroscopic Survey: cosmological analysis of the DR12 galaxy sample. *Mon. Not. Roy. Astron. Soc.* **470**(3), 2617–2652 (2017). [arXiv:1607.03155](#)
9. D.E.S. Collaboration, M.A. Troxel et al., Dark energy survey year 1 results: cosmological constraints from cosmic shear. *Phys. Rev. D* **98**(4), 043528 (2018). [arXiv:1708.01538](#)
10. D.E.S. Collaboration, T.M.C. Abbott et al., Dark Energy Survey year 1 results: cosmological constraints from galaxy clustering and weak lensing. *Phys. Rev. D* **98**(4), 043526 (2018). [arXiv:1708.01530](#)
11. DES Collaboration, E. Krause et al., Dark energy survey year 1 results: multi-probe methodology and simulated likelihood analyses. Submitted to: *Phys. Rev. D* (2017). [arXiv:1706.09359](#)
12. D.M. Scolnic et al., The complete light-curve sample of spectroscopically confirmed SNe Ia from Pan-STARRS1 and cosmological constraints from the combined pantheon sample. *Astrophys. J.* **859**(2), 101 (2018). [arXiv:1710.00845](#)
13. R.J. Cooke, M. Pettini, C.C. Steidel, One percent determination of the primordial deuterium abundance. *Astrophys. J.* **855**(2), 102 (2018). [arXiv:1710.11129](#)
14. S. Birrer et al., H0LiCOW - IX. Cosmographic analysis of the doubly imaged quasar SDSS 1206+4332 and a new measurement of the Hubble constant. *Mon. Not. Roy. Astron. Soc.* **484**, 4726 (2019). [arXiv:1809.01274](#)
15. K.C. Wong et al., H0LiCOW XIII. A 2.4% measurement of H_0 from lensed quasars: 5.3 σ tension between early and late-Universe probes. [arXiv:1907.04869](#)
16. W. Cardona, M. Kunz, V. Pettorino, Determining H_0 with Bayesian hyper-parameters. *JCAP* **1703**(03), 056 (2017). [arXiv:1611.06088](#)
17. D. Camarena, V. Marra, Local determination of the Hubble constant and the deceleration parameter. [arXiv:1906.11814](#)
18. W.L. Freedman et al., The Carnegie-Chicago Hubble Program. VIII. An Independent Determination of the Hubble Constant Based on the Tip of the Red Giant Branch. [arXiv:1907.05922](#)

19. W. Yuan, A.G. Riess, L.M. Macri, S. Casertano, D. Scolnic, Consistent calibration of the tip of the red giant branch in the large magellanic cloud on the hubble space telescope photometric system and a re-determination of the hubble constant. *Astrophys. J.* **886**, 61 (2019). [arXiv:1908.00993](#)
20. W.L. Freedman, B.F. Madore, T. Hoyt, I.S. Jang, R. Beaton, M.G. Lee, A. Monson, J. Neeley, J. Rich, Calibration of the Tip of the Red Giant Branch (TRGB). [arXiv:2002.01550](#)
21. C.D. Huang, A.G. Riess, W. Yuan, L.M. Macri, N.L. Zakamska, S. Casertano, P.A. Whitelock, S.L. Hoffmann, A.V. Filippenko, D. Scolnic, Hubble Space Telescope Observations of Mira Variables in the Type Ia Supernova Host NGC 1559: An Alternative Candle to Measure the Hubble Constant. [arXiv:1908.10883](#)
22. DES Collaboration, A.J. Shajib et al., STRIDES: A 3.9 Per Cent Measurement of the Hubble Constant from the Strong Lens System DES J0408-5354. [arXiv:1910.06306](#)
23. L. Verde, T. Treu, A.G. Riess, Tensions between the Early and the Late Universe, in *Nature Astronomy 2019* (2019). [arXiv:1907.10625](#)
24. A.G. Riess, The expansion of the universe is faster than expected. *Nat. Rev. Phys.* **2**(1), 10–12 (2019). [arXiv:2001.03624](#)
25. E. Di Valentino, A. Melchiorri, J. Silk, Beyond six parameters: extending Λ CDM. *Phys. Rev. D* **92**(12), 121302 (2015). [arXiv:1507.06646](#)
26. E. Di Valentino, A. Melchiorri, J. Silk, Reconciling Planck with the local value of H_0 in extended parameter space. *Phys. Lett. B* **761**, 242–246 (2016). [arXiv:1606.00634](#)
27. J.L. Bernal, L. Verde, A.G. Riess, The trouble with H_0 . *JCAP* **1610**(10), 019 (2016). [arXiv:1607.05617](#)
28. S. Kumar, R.C. Nunes, Probing the interaction between dark matter and dark energy in the presence of massive neutrinos. *Phys. Rev. D* **94**(12), 123511 (2016). [arXiv:1608.02454](#)
29. S. Kumar, R.C. Nunes, Echo of interactions in the dark sector. *Phys. Rev. D* **96**(10), 103511 (2017). [arXiv:1702.02143](#)
30. E. Di Valentino, A. Melchiorri, O. Mena, Can interacting dark energy solve the H_0 tension? *Phys. Rev. D* **96**(4), 043503 (2017). [arXiv:1704.08342](#)
31. E. Di Valentino, C. Boehm, E. Hivon, F.R. Bouchet, Reducing the H_0 and σ_8 tensions with Dark Matter-neutrino interactions. *Phys. Rev. D* **97**(4), 043513 (2018). [arXiv:1710.02559](#)
32. E. Di Valentino, E.V. Linder, A. Melchiorri, Vacuum phase transition solves the H_0 tension. *Phys. Rev. D* **97**(4), 043528 (2018). [arXiv:1710.02153](#)
33. T. Binder, M. Gustafsson, A. Kamada, S.M.R. Sandner, M. Wiesner, Reannihilation of self-interacting dark matter. *Phys. Rev. D* **97**(12), 123004 (2018). [arXiv:1712.01246](#)
34. N. Khosravi, S. Baghran, N. Afshordi, N. Altamirano, H_0 tension as a hint for a transition in gravitational theory. *Phys. Rev. D* **99**(10), 103526 (2019). [arXiv:1710.09366](#)
35. E. Di Valentino, A. Melchiorri, E.V. Linder, J. Silk, Constraining dark energy dynamics in extended parameter space. *Phys. Rev. D* **96**(2), 023523 (2017). [arXiv:1704.00762](#)
36. J. Renk, M. Zumalacárregui, F. Montanari, A. Barreira, Galileon gravity in light of ISW, CMB, BAO and H_0 data. *JCAP* **1710**(10), 020 (2017). [arXiv:1707.02263](#)
37. E. Di Valentino, Crack in the cosmological paradigm. *Nat. Astron.* **1**(9), 569–570 (2017). [arXiv:1709.04046](#)
38. E. Belgacem, Y. Dirian, S. Foffa, M. Maggiore, Nonlocal gravity. Conceptual aspects and cosmological predictions. *JCAP* **1803**(03), 002 (2018). [arXiv:1712.07066](#)
39. J. Solá, A. Gómez-Valent, J. de Cruz Pérez, The H_0 tension in light of vacuum dynamics in the Universe. *Phys. Lett. B* **774**, 317–324 (2017). [arXiv:1705.06723](#)
40. R.C. Nunes, Structure formation in f(T) gravity and a solution for H_0 tension. [arXiv:1802.02281](#)
41. W. Yang, S. Pan, E. Di Valentino, R.C. Nunes, S. Vagnozzi, D.F. Mota, Tale of stable interacting dark energy, observational signatures, and the H_0 tension. *JCAP* **1809**(09), 019 (2018). [arXiv:1805.08252](#)
42. E.Ó. Colgáin, M.H.P.M. van Putten, H. Yavartanoo, de Sitter Swampland, H_0 tension & observation. *Phys. Lett. B* **793**, 126–129 (2019). [arXiv:1807.07451](#)

43. F. D'Eramo, R.Z. Ferreira, A. Notari, J.L. Bernal, Hot Axions and the H_0 tension. *JCAP* **1811**(11), 014 (2018). [arXiv:1808.07430](#)
44. W. Yang, A. Mukherjee, E. Di Valentino, S. Pan, Interacting dark energy with time varying equation of state and the H_0 tension. *Phys. Rev. D* **98**(12), 123527 (2018). [arXiv:1809.06883](#)
45. R.-Y. Guo, J.-F. Zhang, X. Zhang, Can the H_0 tension be resolved in extensions to Λ CDM cosmology? *JCAP* **1902**, 054 (2019). [arXiv:1809.02340](#)
46. M.-X. Lin, M. Raveri, W. Hu, Phenomenology of modified gravity at recombination. *Phys. Rev. D* **99**(4), 043514 (2019). [arXiv:1810.02333](#)
47. W. Yang, S. Pan, E. Di Valentino, E.N. Saridakis, S. Chakraborty, Observational constraints on one-parameter dynamical dark-energy parametrizations and the H_0 tension. *Phys. Rev. D* **99**(4), 043543 (2019). [arXiv:1810.05141](#)
48. V. Poulin, T.L. Smith, T. Karwal, M. Kamionkowski, Early dark energy can resolve the hubble tension. *Phys. Rev. Lett.* **122**(22), 221301 (2019). [arXiv:1811.04083](#)
49. A. Banihashemi, N. Khosravi, A.H. Shirazi, Ups and Downs in Dark Energy: phase transition in dark sector as a proposal to lessen cosmological tensions. [arXiv:1808.02472](#)
50. A. Banihashemi, N. Khosravi, A.H. Shirazi, Ginzburg-landau theory of dark energy: a framework to study both temporal and spatial cosmological tensions simultaneously. *Phys. Rev. D* **99**(8), 083509 (2019). [arXiv:1810.11007](#)
51. E. Mörtzell, S. Dhawan, Does the Hubble constant tension call for new physics? *JCAP* **1809**(09), 025 (2018). [arXiv:1801.07260](#)
52. C.D. Kreisch, F.-Y. Cyr-Racine, O. Doré, The Neutrino Puzzle: Anomalies, Interactions, and Cosmological Tensions. [arXiv:1902.00534](#)
53. M. Martinelli, N.B. Hogg, S. Peirone, M. Bruni, D. Wands, Constraints on the interacting vacuum-geodesic CDM scenario. *Mon. Not. Roy. Astron. Soc.* **488**(3), 3423–3438 (2019). [arXiv:1902.10694](#)
54. K. Vattis, S.M. Koushiappas, A. Loeb, Late universe decaying dark matter can relieve the H_0 tension. [arXiv:1903.06220](#)
55. S. Kumar, R.C. Nunes, S.K. Yadav, Dark sector interaction: a remedy of the tensions between CMB and LSS data. [arXiv:1903.04865](#)
56. P. Agrawal, F.-Y. Cyr-Racine, D. Pinner, L. Randall, Rock 'n' Roll Solutions to the Hubble Tension. [arXiv:1904.01016](#)
57. W. Yang, S. Pan, A. Paliathanasis, S. Ghosh, Y. Wu, Observational constraints of a new unified dark fluid and the H_0 tension. [arXiv:1904.10436](#)
58. W. Yang, S. Pan, E. Di Valentino, A. Paliathanasis, J. Lu, Challenging bulk viscous unified scenarios with cosmological observations. *Phys. Rev. D* **100**(10), 103518 (2019). [arXiv:1906.04162](#)
59. W. Yang, O. Mena, S. Pan, E. Di Valentino, Dark sectors with dynamical coupling. *Phys. Rev. D* **100**(8), 083509 (2019). [arXiv:1906.11697](#)
60. E. Di Valentino, R.Z. Ferreira, L. Visinelli, U. Danielsson, Late time transitions in the quintessence field and the H_0 tension. *Phys. Dark Univ.* **26**, 100385 (2019). [arXiv:1906.11255](#)
61. H. Desmond, B. Jain, J. Sakstein, Local resolution of the Hubble tension: The impact of screened fifth forces on the cosmic distance ladder. *Phys. Rev. D* **100**(4), 043537 (2019). [arXiv:1907.03778](#)
62. W. Yang, S. Pan, S. Vagnozzi, E. Di Valentino, D.F. Mota, S. Capozziello, Dawn of the dark: unified dark sectors and the EDGES Cosmic Dawn 21-cm signal. *JCAP* **1911**, 044 (2019). [arXiv:1907.05344](#)
63. S. Pan, W. Yang, E. Di Valentino, E.N. Saridakis, S. Chakraborty, Interacting scenarios with dynamical dark energy: observational constraints and alleviation of the H_0 tension. *Phys. Rev. D* **100**(10), 103520 (2019). [arXiv:1907.07540](#)
64. L. Visinelli, S. Vagnozzi, U. Danielsson, Revisiting a negative cosmological constant from low-redshift data. *Symmetry* **11**(8), 1035 (2019). [arXiv:1907.07953](#)
65. M. Martinelli, I. Tutusaus, CMB tensions with low-redshift H_0 and S_8 measurements: impact of a redshift-dependent type-Ia supernovae intrinsic luminosity. *Symmetry* **11**(8), 986 (2019). [arXiv:1906.09189](#)

66. Y.-F. Cai, M. Khurshudyan, E.N. Saridakis, Model-independent reconstruction of $f(T)$ gravity from Gaussian Processes. *Astrophys. J.* **888**, 62 (2020). [arXiv:1907.10813](#)
67. S. Pan, W. Yang, E. Di Valentino, A. Shafieloo, S. Chakraborty, Reconciling H_0 tension in a six parameter space?. [arXiv:1907.12551](#)
68. E. Di Valentino, A. Melchiorri, J. Silk, Cosmological constraints in extended parameter space from the Planck 2018 Legacy release. [arXiv:1908.01391](#)
69. E. Di Valentino, A. Melchiorri, O. Mena, S. Vagnozzi, Interacting dark energy after the latest Planck, DES, and H_0 measurements: an excellent solution to the H_0 and cosmic shear tensions. [arXiv:1908.04281](#)
70. E. Di Valentino, A. Melchiorri, O. Mena, S. Vagnozzi, Non-minimal dark sector physics and cosmological tensions. [arXiv:1910.09853](#)
71. N. Schöneberg, J. Lesgourgues, D.C. Hooper, The BAO+BBN take on the Hubble tension. *JCAP* **1910**(10), 029 (2019). [arXiv:1907.11594](#)
72. A. Shafieloo, D.K. Hazra, V. Sahni, A.A. Starobinsky, Metastable dark energy with radioactive-like decay. *Mon. Not. Roy. Astron. Soc.* **473**(2), 2760–2770 (2018). [arXiv:1610.05192](#)
73. X. Li, A. Shafieloo, V. Sahni, A.A. Starobinsky, Revisiting Metastable Dark Energy and Tensions in the Estimation of Cosmological Parameters. [arXiv:1904.03790](#)
74. A. Cuceu, J. Farr, P. Lemos, A. Font-Ribera, Baryon acoustic oscillations and the hubble constant: past, present and future. *JCAP* **1910**(10), 044 (2019). [arXiv:1906.11628](#)
75. E. Colgáin, H. Yavartanoo, Testing the Swampland: H_0 tension. *Phys. Lett. B* **797**, 134907 (2019). [arXiv:1905.02555](#)
76. S. Pan, W. Yang, C. Singha, E.N. Saridakis, Observational constraints on sign-changeable interaction models and alleviation of the H_0 tension. *Phys. Rev. D* **100**(8), 083539 (2019). [arXiv:1903.10969](#)
77. K.V. Berghaus, T. Karwal, Thermal Friction as a Solution to the Hubble Tension. [arXiv:1911.06281](#)
78. L. Knox, M. Millea, Hubble constant hunter’s guide. *Phys. Rev. D* **101**(4), 043533 (2020). [arXiv:1908.03663](#)
79. K.L. Pandey, T. Karwal, S. Das, Alleviating the H_0 and σ_8 anomalies with a decaying dark matter model. [arXiv:1902.10636](#)
80. S. Vagnozzi, New physics in light of the H_0 tension: an alternative view. [arXiv:1907.07569](#)
81. S. Adhikari, D. Huterer, Super-CMB fluctuations can resolve the Hubble tension. [arXiv:1905.02278](#)
82. L. Lancaster, F.-Y. Cyr-Racine, L. Knox, Z. Pan, A tale of two modes: neutrino free-streaming in the early universe. *JCAP* **1707**(07), 033 (2017). [arXiv:1704.06657](#)
83. F. Niedermann, M.S. Sloth, New Early Dark Energy. [arXiv:1910.10739](#)
84. M. Raveri, Reconstructing Gravity on Cosmological Scales. [arXiv:1902.01366](#)
85. L. Hart, J. Chluba, Updated fundamental constant constraints from Planck 2018 data and possible relations to the Hubble tension. [arXiv:1912.03986](#)
86. S.-F. Yan, P. Zhang, J.-W. Chen, X.-Z. Zhang, Y.-F. Cai, E.N. Saridakis, Interpreting cosmological tensions from the effective field theory of torsional gravity. *Phys. Rev. D* **101**(12), 121301 (2020). [arXiv:1909.06388](#)
87. S.K. Yadav, Constraints on dark matter-photon coupling in the presence of time-varying dark energy. *Mod. Phys. Lett. A* **33**, 1950358 (2019). [arXiv:1907.05886](#)
88. M. Kasai, T. Futamase, A possible solution to the Hubble constant discrepancy – Cosmology where the local volume expansion is driven by the domain average density. *PTEP* **2019**(7), 073E01 (2019). [arXiv:1904.09689](#)
89. H. Amirhashchi, A.K. Yadav, Interacting Dark Sectors in Anisotropic Universe: Observational Constraints and H_0 Tension. [arXiv:2001.03775](#)
90. A. Perez, D. Sudarsky, E. Wilson-Ewing, Resolving the H_0 tension with diffusion. [arXiv:2001.07536](#)
91. S. Pan, W. Yang, A. Paliathanasis, Non-linear interacting cosmological models after Planck 2018 legacy release and the H_0 tension. *Mon. Not. Roy. Astron. Soc.* **493**(3), 3114–3131 (2020). [arXiv:2002.03408](#)

92. R. D'Agostino, R.C. Nunes, Measurements of H_0 in modified gravity theories. [arXiv:2002.06381](#)
93. G. Benevento, W. Hu, M. Raveri, Can Late Dark Energy Transitions Raise the Hubble constant?. [arXiv:2002.11707](#)
94. E. Di Valentino et al., Cosmology Intertwined II: The Hubble Constant Tension. [arXiv:2008.11284](#)
95. T. Tram, R. Vallance, V. Vennin, Inflation model selection meets dark radiation. JCAP **01**, 046 (2017). [arXiv:1606.09199](#)
96. E. Di Valentino, L. Mersini-Houghton, Testing predictions of the quantum landscape multi-verse 2: the exponential inflationary potential. JCAP **03**, 020 (2017). [arXiv:1612.08334](#)
97. A. Gómez-Valent, V. Pettorino, L. Amendola, Update on coupled dark energy and the H_0 tension. Phys. Rev. D **101**(12), 123513 (2020). [arXiv:2004.00610](#)
98. M. Lucca, D.C. Hooper, Tensions in the dark: shedding light on Dark Matter-Dark Energy interactions. [arXiv:2002.06127](#)
99. C. Van De Bruck, J. Mifsud, Searching for dark matter - dark energy interactions: going beyond the conformal case. Phys. Rev. D **97**(2), 023506 (2018). [arXiv:1709.04882](#)
100. E. Di Valentino, A. Mukherjee, A.A. Sen, Dark Energy with Phantom Crossing and the H_0 tension. [arXiv:2005.12587](#)
101. R.E. Keeley, S. Joudaki, M. Kaplinghat, D. Kirkby, Implications of a transition in the dark energy equation of state for the H_0 and σ_8 tensions. JCAP **12**, 035 (2019). [arXiv:1905.10198](#)
102. W. Yang, S. Pan, E. Di Valentino, E.N. Saridakis, Observational constraints on dynamical dark energy with pivoting redshift. Universe **5**(11), 219 (2019). [arXiv:1811.06932](#)
103. T. Karwal, M. Kamionkowski, Dark energy at early times, the Hubble parameter, and the string axiverse. Phys. Rev. D **94**(10), 103523 (2016). [arXiv:1608.01309](#)
104. T.L. Smith, V. Poulin, M.A. Amin, Oscillating scalar fields and the Hubble tension: a resolution with novel signatures. Phys. Rev. D **101**(6), 063523 (2020). [arXiv:1908.06995](#)
105. M. Lucca, The role of CMB spectral distortions in the Hubble tension: a proof of principle. [arXiv:2008.01115](#)
106. M.-X. Lin, G. Benevento, W. Hu, M. Raveri, Acoustic dark energy: potential conversion of the Hubble tension. Phys. Rev. D **100**(6), 063542 (2019). [arXiv:1905.12618](#)
107. S. Kumar, R.C. Nunes, S.K. Yadav, Cosmological bounds on dark matter-photon coupling. Phys. Rev. D **98**(4), 043521 (2018). [arXiv:1803.10229](#)
108. W. Yang, E. Di Valentino, S. Pan, S. Basilakos, A. Paliathanasis, Metastable dark energy models in light of Planck 2018: Alleviating the H_0 tension. [arXiv:2001.04307](#)
109. S. Pan, G.S. Sharov, W. Yang, Field theoretic interpretations of interacting dark energy scenarios and recent observations. Phys. Rev. D **101**(10), 103533 (2020). [arXiv:2001.03120](#)
110. W.K. Wu, P. Motloch, W. Hu, M. Raveri, Hubble constant tension between CMB lensing and BAO measurements. [arXiv:2004.10207](#)
111. N. Blinov, G. Marques-Tavares, Interacting radiation after Planck and its implications for the Hubble Tension. [arXiv:2003.08387](#)
112. D. Wang, D. Mota, Can $f(T)$ gravity resolve the H_0 tension?. [arXiv:2003.10095](#)
113. G. Alestas, L. Kazantzidis, L. Perivolaropoulos, H_0 tension, phantom dark energy and cosmological parameter degeneracies. Phys. Rev. D **101**(12), 123516 (2020). [arXiv:2004.08363](#)
114. S.J. Clark, K. Vattis, S.M. Koushiappas, CMB constraints on late-universe decaying dark matter as a solution to the H_0 tension. [arXiv:2006.03678](#)
115. R.E. Keeley, A. Shafieloo, D.K. Hazra, T. Souradeep, Inflation Wars: A New Hope. [arXiv:2006.12710](#)
116. D.K. Hazra, A. Shafieloo, T. Souradeep, Parameter discordance in Planck CMB and low-redshift measurements: projection in the primordial power spectrum. JCAP **04**, 036 (2019). [arXiv:1810.08101](#)
117. F. Niedermann, M.S. Sloth, Resolving the Hubble Tension with New Early Dark Energy. [arXiv:2006.06686](#)
118. M. Archidiacono, S. Gariazzo, C. Giunti, S. Hannestad, T. Tram, Sterile neutrino self-interactions: H_0 tension and short-baseline anomalies. [arXiv:2006.12885](#)

119. E. Di Valentino, E.V. Linder, A. Melchiorri, H_0 Ex Machina: Vacuum Metamorphosis and Beyond H_0 . [arXiv:2006.16291](#)
120. S. Capozziello, M. Benetti, A.D. Spallicci, Addressing the cosmological H_0 tension by the Heisenberg uncertainty. [arXiv:2007.00462](#)
121. L.A. Anchordoqui, S.E. Perez Bergliaffa, Hot thermal universe endowed with massive dark vector fields and the Hubble tension. *Phys. Rev. D* **100**(12), 123525 (2019). [arXiv:1910.05860](#)
122. M.M. Ivanov, Y. Ali-Haïmoud, J. Lesgourgues, H_0 tension or T_0 tension?. [arXiv:2005.10656](#)
123. M. Gonzalez, M.P. Hertzberg, F. Rompineve, Ultralight Scalar Decay and the Hubble Tension. [arXiv:2006.13959](#)
124. A. Hryczuk, K. Jodłowski, Self-interacting dark matter from late decays and the H_0 tension. [arXiv:2006.16139](#)
125. S. Carneiro, P.C. de Holanda, C. Pigozzo, F. Sobreira, Is the H_0 tension suggesting a fourth neutrino generation? *Phys. Rev. D* **100**(2), 023505 (2019). [arXiv:1812.06064](#)
126. A. Paul, A. Ghoshal, A. Chatterjee, S. Pal, Inflation, (pre)heating and neutrino anomalies: production of sterile neutrinos with secret interactions. *Eur. Phys. J. C* **79**(10), 818 (2019). [arXiv:1808.09706](#)
127. G.B. Gelmini, A. Kusenko, V. Takhistov, Hints of Sterile Neutrinos in Recent Measurements of the Hubble Parameter. [arXiv:1906.10136](#)
128. L.A. Anchordoqui, Hubble Hullabaloo and String Cosmology, 5 (2020). [arXiv:2005.01217](#)
129. J. Sakstein, M. Trodden, Early dark energy from massive neutrinos as a natural resolution of the Hubble tension. *Phys. Rev. Lett.* **124**(16), 161301 (2020). [arXiv:1911.11760](#)
130. A. Gogoi, P. Chanda, S. Das, Dark matter nugget and new early dark energy from interacting neutrino: A promising solution to Hubble anomaly. [arXiv:2005.11889](#)
131. G. Ye, Y.-S. Piao, Is the Hubble tension a hint of AdS around recombination?. [arXiv:2001.02451](#)
132. L. Hart, J. Chluba, New constraints on time-dependent variations of fundamental constants using Planck data. *Mon. Not. Roy. Astron. Soc.* **474**(2), 1850–1861 (2018). [arXiv:1705.03925](#)
133. C.-T. Chiang, A.Z. Slosar, Inferences of H_0 in presence of a non-standard recombination. [arXiv:1811.03624](#)
134. K. Jedamzik, L. Pogosian, Relieving the Hubble tension with primordial magnetic fields. [arXiv:2004.09487](#)
135. W. Yang, E. Di Valentino, S. Pan, O. Mena, A complete model of Phenomenologically Emergent Dark Energy. [arXiv:2007.02927](#)
136. A. Chudaykin, D. Gorbunov, N. Nedelko, Exploring Early Dark Energy solution to the Hubble tension with Planck and SPTPol data. [arXiv:2011.04682](#)
137. T. Sekiguchi, T. Takahashi, Early recombination as a solution to the H_0 tension. [arXiv:2007.03381](#)
138. B. Bose, L. Lombriser, Easing cosmic tensions with an open and hotter universe. [arXiv:2006.16149](#)
139. P. Agrawal, G. Obied, C. Vafa, H_0 Tension, Swampland Conjectures and the Epoch of Fading Dark Matter. [arXiv:1906.08261](#)
140. L.A. Anchordoqui, I. Antoniadis, D. Lüst, J.F. Soriano, T.R. Taylor, H_0 tension and the String Swampland. *Phys. Rev. D* **101**, 083532 (2020). [arXiv:1912.00242](#)
141. N. Frusciante, S. Peirone, L. Atayde, A. De Felice, Phenomenology of the generalized cubic covariant Galileon model and cosmological bounds. *Phys. Rev. D* **101**(6), 064001 (2020). [arXiv:1912.07586](#)
142. M. Braglia, M. Ballardini, W.T. Emond, F. Finelli, A.E. Gumrukcuoglu, K. Koyama, D. Paoletti, A larger value for H_0 by an evolving gravitational constant. [arXiv:2004.11161](#)
143. M. Ballardini, M. Braglia, F. Finelli, D. Paoletti, A.A. Starobinsky, C. Umiltá, Scalar-tensor theories of gravity, neutrino physics, and the H_0 tension. [arXiv:2004.14349](#)
144. X. Li, A. Shafieloo, A Simple Phenomenological Emergent Dark Energy Model can Resolve the Hubble Tension. *Astrophys. J. Lett.* **883**(1), L3 (2019)
145. M. Rezaei, T. Naderi, M. Malekjani, A. Mehrabi, A Bayesian comparison between Λ CDM and phenomenologically emergent dark energy models. *Eur. Phys. J. C* **80**(5), 374 (2020). [arXiv:2004.08168](#)

146. X. Li, A. Shafieloo, Generalised Emergent Dark Energy Model: Confronting Λ and PEDE. [arXiv:2001.05103](#)
147. G. Choi, M. Suzuki, T.T. Yanagida, Quintessence axion dark energy and a solution to the Hubble tension. *Phys. Lett. B* **805**, 135408 (2020). [arXiv:1910.00459](#)
148. G. Choi, M. Suzuki, T.T. Yanagida, Degenerate sub-keV fermion dark matter from a solution to the Hubble tension. *Phys. Rev. D* **101**(7), 075031 (2020). [arXiv:2002.00036](#)
149. Z. Berezhiani, A. Dolgov, I. Tkachev, Reconciling Planck results with low redshift astronomical measurements. *Phys. Rev. D* **92**(6), 061303 (2015). [arXiv:1505.03644](#)
150. L.A. Anchordoqui, V. Barger, H. Goldberg, X. Huang, D. Marfatia, L.H.M. da Silva, T.J. Weiler, IceCube neutrinos, decaying dark matter, and the Hubble constant. *Phys. Rev. D* **92**(6), 061301 (2015). [arXiv:1506.08788](#). [Erratum: *Phys.Rev.D* 94, 069901 (2016)]
151. A. Desai, K.R. Dienes, B. Thomas, Constraining dark-matter ensembles with supernova data. *Phys. Rev. D* **101**(3), 035031 (2020). [arXiv:1909.07981](#)
152. J. Alcaniz, N. Bernal, A. Masiero, F.S. Queiroz, Light Dark Matter: A Common Solution to the Lithium and H_0 Problems. [arXiv:1912.05563](#)
153. A. Chudaykin, D. Gorbunov, I. Tkachev, Dark matter component decaying after recombination: lensing constraints with Planck data. *Phys. Rev. D* **94**, 023528 (2016). [arXiv:1602.08121](#)
154. A. Chudaykin, D. Gorbunov, I. Tkachev, Dark matter component decaying after recombination: sensitivity to baryon acoustic oscillation and redshift space distortion probes. *Phys. Rev. D* **97**(8), 083508 (2018). [arXiv:1711.06738](#)
155. J.C. Hill, E. McDonough, M.W. Toomey, S. Alexander, Early Dark Energy Does Not Restore Cosmological Concordance. [arXiv:2003.07355](#)
156. M.M. Ivanov, E. McDonough, J.C. Hill, M. Simonović, M.W. Toomey, S. Alexander, M. Zaldarriaga, Constraining Early Dark Energy with Large-Scale Structure. [arXiv:2006.11235](#)
157. M. Rezaei, S.P. Ojaghi, M. Malekjani, Cosmography approach to dark energy cosmologies: new constraints using the Hubble diagrams of supernovae, quasars and gamma-ray bursts. [arXiv:2008.03092](#)
158. D. Wang, Can $f(R)$ gravity relieve H_0 and σ_8 tensions?. [arXiv:2008.03966](#)
159. U. Leonhardt, D. Berechya, Observed Hubble constant is consistent with physics of the quantum vacuum. [arXiv:2008.04789](#)
160. G. Ballesteros, A. Notari, F. Rompineve, The H_0 tension: ΔG_N vs. ΔN_{eff} . [arXiv:2004.05049](#)
161. N. Blinov, K.J. Kelly, G.Z. Krnjaic, S.D. McDermott, Constraining the self-interacting neutrino interpretation of the Hubble tension. *Phys. Rev. Lett.* **123**(19), 191102 (2019). [arXiv:1905.02727](#)
162. A. Hernández-Almada, G. Leon, J. Magaña, M.A. García-Aspeitia, V. Motta, Generalized Emergent Dark Energy: observational Hubble data constraints and stability analysis. [arXiv:2002.12881](#)
163. S.M. Feeney, D.J. Mortlock, N. Dalmaso, Clarifying the Hubble constant tension with a Bayesian hierarchical model of the local distance ladder. *Mon. Not. Roy. Astron. Soc.* **476**(3), 3861–3882 (2018). [arXiv:1707.00007](#)
164. A. Banerjee, H. Cai, L. Heisenberg, E.O. Colgáin, M. Sheikh-Jabbari, T. Yang, Hubble Sinks In The Low-Redshift Swampland. [arXiv:2006.00244](#)
165. S.L. Adler, Implications of a frame dependent dark energy for the spacetime metric, cosmography, and effective Hubble constant. *Phys. Rev. D* **100**(12), 123503 (2019). [arXiv:1905.08228](#)
166. Y. Gu, M. Khlopov, L. Wu, J.M. Yang, B. Zhu, Light gravitino dark matter for Hubble tension and LHC. [arXiv:2006.09906](#)
167. Ö. Akarsu, S. Kumar, S. Sharma, L. Tedesco, Constraints on a Bianchi type I spacetime extension of the standard Λ CDM model. *Phys. Rev. D* **100**(2), 023532 (2019). [arXiv:1905.06949](#)
168. A. Nygaard, T. Tram, S. Hannestad, *Updated constraints on decaying cold dark matter*. [arXiv:2011.01632](#)
169. H. Benaoum, W. Yang, S. Pan, E. Di Valentino, *Modified Emergent Dark Energy and its Astronomical Constraints*. [arXiv:2008.09098](#)
170. C. Krishnan, E.O. Colgáin, M. Sheikh-Jabbari, T. Yang, *Running Hubble Tension and a H_0 Diagnostic*. [arXiv:2011.02858](#)

171. E. Di Valentino, *A (brave) combined analysis of the H_0 late time direct measurements and the impact on the Dark Energy sector*. [arXiv:2011.00246](#)
172. N. Kitazawa, *Polarizations of CMB and the Hubble tension*. [arXiv:2010.12164](#)
173. L.A. Anchordoqui, *Decaying dark matter, the H_0 tension, and the lithium problem*. [arXiv:2010.09715](#)
174. Y.-H. Yao, X.-H. Meng, *A new coupled three-form dark energy model and implications for the H_0 tension*. *Phys. Dark Univ.* **30**, 100729 (2020)
175. M. Artymowski, I. Ben-Dayan, U. Kumar, *Emergent dark energy from unparticles*. [arXiv:2010.02998](#)
176. K. Jedamzik, L. Pogosian, G.-B. Zhao, *Why reducing the cosmic sound horizon can not fully resolve the Hubble tension*. [arXiv:2010.04158](#)
177. T.L. Smith, V. Poulin, J.L. Bernal, K.K. Boddy, M. Kamionkowski, R. Murgia, *Early dark energy is not excluded by current large-scale structure data*. [arXiv:2009.10740](#)
178. R. Murgia, G.F. Abellán, V. Poulin, *The early dark energy resolution to the Hubble tension in light of weak lensing surveys and lensing anomalies*. [arXiv:2009.10733](#)
179. F.X. Linares Cedeño, U. Nucamendi, *Revisiting cosmological diffusion models in Unimodular Gravity and the H_0 tension*. [arXiv:2009.10268](#)
180. M.-X. Lin, W. Hu, M. Raveri, *Testing H_0 in Acoustic Dark Energy with Planck and ACT Polarization*. [arXiv:2009.08974](#)
181. A. De Felice, S. Mukohyama, M.C. Pookkillath, *Addressing H_0 tension by means of Λ CDM*. [arXiv:2009.08718](#)
182. P.D. Alvarez, B. Koch, C. Laporte, A. Rincon, *Can scale-dependent cosmology alleviate the H_0 tension?* [arXiv:2009.02311](#)
183. F. Arias-Aragon, E. Fernandez-Martinez, M. Gonzalez-Lopez, L. Merlo, *Neutrino Masses and Hubble Tension via a Majoron in MFV*. [arXiv:2009.01848](#)
184. H. Kameli, S. Baghram, *Merger history of dark matter halos in the light of H_0 tension*. [arXiv:2008.13175](#)
185. C. Ortiz, *Surface Tension: Accelerated Expansion, Coincidence Problem & Hubble Tension*. [arXiv:2011.02317](#)
186. S. Mandal, D. Wang, P. Sahoo, *Cosmography in $f(Q)$ gravity*. [arXiv:2011.00420](#)
187. M. Hashim, W. El Hanafy, A. Golovnev, A. El-Zant, *Toward a concordance teleparallel Cosmology I: Background Dynamics*. [arXiv:2010.14964](#)
188. M. Braglia, W.T. Emond, F. Finelli, A.E. Gumrukcuoglu, K. Koyama, *Unified framework for early dark energy from α -attractors*. *Phys. Rev. D* **102**(8), 083513 (2020). [arXiv:2005.14053](#)
189. R. Briffa, S. Capozziello, J. Levi Said, J. Mifsud, E.N. Saridakis, *Constraining Teleparallel Gravity through Gaussian Processes*. [arXiv:2009.14582](#)
190. A. Chudaykin, D. Gorbunov, N. Nedelko, *Combined analysis of Planck and SPTPol data favors the early dark energy models*. [arXiv:2004.13046](#)
191. S.D. Odintsov, D.S.-C. Gómez, G.S. Sharov, *Analyzing the H_0 tension in $F(R)$ gravity models*. [arXiv:2011.03957](#)
192. Y. Yao, X. Meng, *Relieve the H_0 tension with a new coupled generalized three-form dark energy model*. [arXiv:2011.09160](#)
193. N.J. Cruz, C. Escamilla-Rivera, *Late-time and Big Bang nucleosynthesis constraints for generic modify gravity surveys*. [arXiv:2011.09623](#)
194. W. da Silva, R. Silva, *Growth of matter perturbations in the extended viscous dark energy models*. [arXiv:2011.09516](#)
195. W. da Silva, R. Silva, *Cosmological Perturbations in the Tsallis Holographic Dark Energy Scenarios*. [arXiv:2011.09520](#)
196. S. Dhawan, D. Brout, D. Scolnic, A. Goobar, A. Riess, V. Miranda, *Cosmological model insensitivity of local H_0 from the Cepheid distance ladder*. *Astrophys. J.* **894**(1), 54 (2020). [arXiv:2001.09260](#)
197. W.M.A.P. Collaboration, G. Hinshaw et al., *Nine-Year Wilkinson microwave anisotropy probe (WMAP) observations: cosmological parameter results*. *Astrophys. J. Suppl.* **208**, 19 (2013). [arXiv:1212.5226](#)

198. S.P.T. Collaboration, J. Henning et al., Measurements of the temperature and e-mode polarization of the CMB from 500 square degrees of SPTpol data. *Astrophys. J.* **852**(2), 97 (2018). [arXiv:1707.09353](#)
199. ACT Collaboration, S. Aiola et al., *The Atacama Cosmology Telescope: DR4 Maps and Cosmological Parameters*. [arXiv:2007.07288](#)
200. M.M. Ivanov, M. Simonović, M. Zaldarriaga, Cosmological parameters from the BOSS galaxy power spectrum. *JCAP* **05**, 042 (2020). [arXiv:1909.05277](#)
201. G. D’Amico, J. Gleyzes, N. Kokron, D. Markovic, L. Senatore, P. Zhang, F. Beutler, H. Gil-Mar, The cosmological analysis of the SDSS/BOSS data from the effective field theory of large-scale structure. *JCAP* **05**, 005 (2020). [arXiv:1909.05271](#)
202. eBOSS Collaboration, S. Alam et al., *The Completed SDSS-IV extended Baryon Oscillation Spectroscopic Survey: Cosmological Implications from two Decades of Spectroscopic Surveys at the Apache Point observatory*. [arXiv:2007.08991](#)
203. X. Zhang, Q.-G. Huang, Constraints on H_0 from WMAP and BAO measurements. *Commun. Theor. Phys.* **71**(7), 826–830 (2019). (v)
204. L. Pogosian, G.-B. Zhao, K. Jedamzik, *Recombination-independent determination of the sound horizon and the Hubble constant from BAO*. [arXiv:2009.08455](#)
205. O.H. Philcox, B.D. Sherwin, G.S. Farren, E.J. Baxter, *Determining the Hubble Constant without the Sound Horizon: Measurements from Galaxy Surveys*. [arXiv:2008.08084](#)
206. M. Reid, D. Pesce, A. Riess, An improved distance to NGC 4258 and its implications for the Hubble constant. *Astrophys. J. Lett.* **886**(2), L27 (2019). [arXiv:1908.05625](#)
207. V. Bonvin et al., H0LiCOW – V. New COSMOGRAIL time delays of HE 0435–1223: H_0 to 3.8 per cent precision from strong lensing in a flat Λ CDM model. *Mon. Not. Roy. Astron. Soc.* **465**(4), 4914–4930 (2017). [arXiv:1607.01790](#)
208. S. Birrer et al., *TDCOSMO IV: Hierarchical time-delay cosmography – joint inference of the Hubble constant and galaxy density profiles*. [arXiv:2007.02941](#)
209. S. Birrer, T. Treu, *TDCOSMO V: strategies for precise and accurate measurements of the Hubble constant with strong lensing*. [arXiv:2008.06157](#)
210. S. Dhawan, S.W. Jha, B. Leibundgut, Measuring the Hubble constant with Type Ia supernovae as near-infrared standard candles. *Astron. Astrophys.* **609**, A72 (2018). [arXiv:1707.00715](#)
211. W.L. Freedman, B.F. Madore, V. Scowcroft, C. Burns, A. Monson, S.E. Persson, M. Seibert, J. Rigby, Carnegie Hubble program: a mid-infrared calibration of the Hubble constant. *Astrophys. J.* **758**, 24 (2012)
212. Y.J. Kim, J. Kang, M.G. Lee, I.S. Jang, *Determination of the Local Hubble Constant from Virgo Infall Using TRGB Distances*. [arXiv:2010.01364](#)
213. H. Yu, B. Ratra, F.-Y. Wang, Hubble parameter and baryon acoustic oscillation measurement constraints on the hubble constant, the deviation from the spatially flat LCDM model, the deceleration-acceleration transition redshift, and spatial curvature. *Astrophys. J.* **856**(1), 3 (2018). [arXiv:1711.03437](#)
214. A. Gómez-Valent, L. Amendola, H_0 from cosmic chronometers and Type Ia supernovae, with Gaussian processes and the weighted polynomial regression method, in *15th Marcel Grossmann Meeting on Recent Developments in Theoretical and Experimental General Relativity, Astrophysics, and Relativistic Field Theories*, 5 (2019). [arXiv:1905.04052](#)
215. B.S. Haridasu, V.V. Luković, M. Moresco, N. Vittorio, An improved model-independent assessment of the late-time cosmic expansion. *JCAP* **10**, 015 (2018). [arXiv:1805.03595](#)
216. K. Dutta, A. Roy Ruchika, A.A. Sen, M. Sheikh-Jabbari, Cosmology with low-redshift observations: no signal for new physics. *Phys. Rev. D* **100**(10), 103501 (2019). [arXiv:1908.07267](#)
217. R.C. Nunes, A. Bernui, θ_{BAO} estimates and the H_0 tension. [arXiv:2008.03259](#)
218. K. Liao, A. Shafieloo, R.E. Keeley, E.V. Linder, A model-independent determination of the Hubble constant from lensed quasars and supernovae using Gaussian process regression. *Astrophys. J. Lett.* **886**(1), L23 (2019). [arXiv:1908.04967](#)
219. K. Liao, A. Shafieloo, R.E. Keeley, E.V. Linder, *Determining H_0 Model-Independently and Consistency Tests*. [arXiv:2002.10605](#)

220. E. Kourkchi, R.B. Tully, G.S. Anand, H.M. Courtois, A. Dupuy, J.D. Neill, L. Rizzi, M. Seibert, Cosmicflows-4: the calibration of optical and infrared Tully-Fisher relations. *Astrophys. J.* **896**(1), 3 (2020). [arXiv:2004.14499](#)
221. J. Schombert, S. McGaugh, F. Lelli, Using the baryonic Tully-Fisher relation to measure H_0 . *Astron. J.* **160**(2), 71 (2020). [arXiv:2006.08615](#)
222. T. de Jaeger, B. Stahl, W. Zheng, A. Filippenko, A. Riess, L. Galbany, *A measurement of the Hubble constant from Type II supernovae*. [arXiv:2006.03412](#)
223. D. Fernández Arenas, E. Terlevich, R. Terlevich, J. Melnick, R. Chávez, F. Bresolin, E. Telles, M. Plionis, S. Basilakos, An independent determination of the local Hubble constant. *Mon. Not. Roy. Astron. Soc.* **474**(1), 1250–1276 (2018). [arXiv:1710.05951](#)
224. D. Pesce et al., The megamaser cosmology project. XIII. Combined Hubble constant constraints. *Astrophys. J. Lett.* **891**(1), L1 (2020). [arXiv:2001.09213](#)
225. J.-Z. Qi, J.-W. Zhao, S. Cao, M. Biesiada, Y. Liu, *Measurements of the Hubble constant and cosmic curvature with quasars: ultra-compact radio structure and strong gravitational lensing*. [arXiv:2011.00713](#)
226. E.J. Baxter, B.D. Sherwin, *Determining the Hubble Constant without the Sound Horizon Scale: Measurements from CMB Lensing*. [arXiv:2007.04007](#)
227. H.S.T. Collaboration, W. Freedman et al., Final results from the Hubble Space Telescope key project to measure the Hubble constant. *Astrophys. J.* **553**, 47–72 (2001). [arXiv:astro-ph/0012376](#)
228. V. Gayathri, J. Healy, J. Lange, B. O'Brien, M. Szczepanczyk, I. Bartos, M. Campanelli, S. Klimentko, C. Lousto, R. O'Shaughnessy, *Hubble Constant Measurement with GW190521 as an Eccentric Black Hole Merger*. [arXiv:2009.14247](#)
229. S. Mukherjee, A. Ghosh, M.J. Graham, C. Karathanasis, M.M. Kasliwal, I. Magaña Hernandez, S.M. Nissanke, A. Silvestri, B.D. Wandelt, *First measurement of the Hubble parameter from bright binary black hole GW190521*. [arXiv:2009.14199](#)
230. G. Ashton, K. Ackley, I.M.n. Hernandez, B. Piotrkowski, *Current observations are insufficient to confidently associate the binary black hole merger GW190521 with AGN J124942.3+344929*. [arXiv:2009.12346](#)
231. A. Bonilla, S. Kumar, R.C. Nunes, *Measurements of H_0 and reconstruction of the dark energy properties from a model-independent joint analysis*. [arXiv:2011.07140](#)
232. D. Harvey, *A 4% measurement of H_0 using the cumulative distribution of strong-lensing time delays in doubly-imaged quasars*. [arXiv:2011.09488](#)
233. F. Renzi, A. Silvestri, *A look at the Hubble speed from first principles*. [arXiv:2011.10559](#)
234. D. Wang, *Assessing the potential of cluster edges as a standard ruler*. [arXiv:2011.11924](#)
235. G. Mangano, G. Miele, S. Pastor, T. Pinto, O. Pisanti, P.D. Serpico, Relic neutrino decoupling including flavor oscillations. *Nucl. Phys. B* **729**, 221–234 (2005). [arXiv:hep-ph/0506164](#)
236. P.F. de Salas, S. Pastor, Relic neutrino decoupling with flavour oscillations revisited. *JCAP* **1607**(07), 051 (2016). [arXiv:1606.06986](#)
237. M. Archidiacono, E. Giusarma, S. Hannestad, O. Mena, Cosmic dark radiation and neutrinos. *Adv. High Energy Phys.* **2013**, 191047 (2013). [arXiv:1307.0637](#)
238. E. Di Valentino, E. Giusarma, O. Mena, A. Melchiorri, J. Silk, Cosmological limits on neutrino unknowns versus low redshift priors. *Phys. Rev. D* **93**(8), 083527 (2016). [arXiv:1511.00975](#)
239. D. Green et al., Messengers from the early Universe: cosmic neutrinos and other light relics. *Bull. Am. Astron. Soc.* **51**(7), 159 (2019). [arXiv:1903.04763](#)
240. R.Z. Ferreira, A. Notari, Observable windows for the QCD axion through the number of relativistic species. *Phys. Rev. Lett.* **120**(19), 191301 (2018). [arXiv:1801.06090](#)
241. E. Di Valentino, E. Giusarma, M. Lattanzi, O. Mena, A. Melchiorri, J. Silk, Cosmological Axion, neutrino mass constraints from Planck, temperature and polarization data. *Phys. Lett. B* **752**(2016), 182–185 (2015). [arXiv:1507.08665](#)
242. L. Parker, A. Raval, New quantum aspects of a vacuum dominated universe. *Phys. Rev. D* **62**, 083503 (2000). [arXiv:gr-qc/0003103](#). [Erratum: *Phys. Rev. D* **67**, 029903(2003)]
243. L. Parker, D.A.T. Vanzella, Acceleration of the universe, vacuum metamorphosis, and the large time asymptotic form of the heat kernel. *Phys. Rev. D* **69**, 104009 (2004). [arXiv:gr-qc/0312108](#)

244. R.R. Caldwell, W. Komp, L. Parker, D.A.T. Vanzella, A sudden gravitational transition. *Phys. Rev. D* **73**, 023513 (2006). [arXiv:astro-ph/0507622](#)
245. M. Chevallier, D. Polarski, Accelerating universes with scaling dark matter. *Int. J. Mod. Phys. D* **10**, 213–224 (2001). [arXiv:gr-qc/0009008](#)
246. E.V. Linder, Exploring the expansion history of the universe. *Phys. Rev. Lett.* **90**, 091301 (2003). [arXiv:astro-ph/0208512](#)
247. E. Calabrese, A. Slosar, A. Melchiorri, G.F. Smoot, O. Zahn, Cosmic Microwave Weak lensing data as a test for the dark universe. *Phys. Rev. D* **77**, 123531 (2008). [arXiv:0803.2309](#)
248. M. Kamionkowski, J. Pradler, D.G.E. Walker, Dark energy from the string axiverse. *Phys. Rev. Lett.* **113**(25), 251302 (2014). [arXiv:1409.0549](#)
249. Planck Collaboration, N. Aghanim et al., Planck 2015 results. XI. CMB power spectra, likelihoods, and robustness of parameters. *Astron. Astrophys. A* **594**, 11 (2016). [arXiv:1507.02704](#)
250. S. Alexander, E. McDonough, Axion-Dilaton destabilization and the Hubble tension. *Phys. Lett. B* **797**, 134830 (2019). [arXiv:1904.08912](#)
251. V. Pettorino, L. Amendola, C. Wetterich, How early is early dark energy? *Phys. Rev. D* **87**, 083009 (2013). [arXiv:1301.5279](#)
252. A. Heinesen, C. Blake, D.L. Wiltshire, Quantifying the accuracy of the Alcock-Paczynski scaling of baryon acoustic oscillation measurements. *JCAP* **2001**(01), 038 (2020). [arXiv:1908.11508](#)
253. Planck Collaboration, P.A.R. Ade et al., Planck 2015 results. XIV. Dark energy and modified gravity. *Astron. Astrophys. A5* **594**, 142 (2016). [arXiv:1502.01590](#)
254. N. Arendse et al., Cosmic dissonance: new physics or systematics behind a short sound horizon? *Astron. Astrophys. A* **639**, 57 (2020). [arXiv:1909.07986](#)
255. E. Di Valentino, D.E. Holz, A. Melchiorri, F. Renzi, *The cosmological impact of future constraints on H_0 from gravitational-wave standard sirens*. [arXiv:1806.07463](#)
256. A. Palmese et al., *Gravitational Wave Cosmology and Astrophysics with Large Spectroscopic Galaxy Surveys*. [arXiv:1903.04730](#)
257. LIGO Scientific, Virgo, 1M2H, Dark Energy Camera GW-E, DES, DLT40, Las Cumbres Observatory, VINROUGE, MASTER Collaboration, B. P. Abbott et al., A gravitational-wave standard siren measurement of the Hubble constant. *Nature* **551**(7678), 85–88 (2017). [arXiv:1710.05835](#)
258. E. Di Valentino, A. Melchiorri, First cosmological constraints combining Planck with the recent gravitational-wave standard siren measurement of the Hubble constant. *Phys. Rev. D* **97**(4), 041301 (2018). [arXiv:1710.06370](#)
259. H.-Y. Chen, M. Fishbach, D.E. Holz, A two per cent Hubble constant measurement from standard sirens within five years. *Nature* **562**(7728), 545–547 (2018). [arXiv:1712.06531](#)

Chapter 33

σ_8 Tension. Is Gravity Getting Weaker at Low z ? Observational Evidence and Theoretical Implications



Lavrentios Kazantzidis and Leandros Perivolaropoulos

The simplest model consistent with current cosmological observations is the Λ CDM model, which assumes the existence of a fine tuned cosmological constant that drives the accelerating expansion of the Universe [1]. A wide range of cosmological observations have imposed strong constraints on the six free parameters of the model. These observations include Type Ia supernovae (SnIa) used as distance indicators [2–5], the Cosmic Microwave Background (CMB) angular power spectrum [6–8], the Baryon Acoustic Oscillations (BAO) [9, 10], Cluster Counts (CC) [11–15], Weak Lensing (WL) [16–21] and Redshift Space Distortions (RSD) [22–26]. The first three of the above (SnIa, CMB power spectrum peak locations and BAO), act as cosmological distance indicators and directly probe the cosmic metric independent of the underlying theory of gravity. These are known as “geometric probes” [15, 27, 28]. The other three types of observations, probe simultaneously the cosmic metric and the growth rate of cosmological perturbations. They are sensitive to the dynamics of growth and thus to the type of the underlying theory of gravity. These are known as “dynamical probes” [15, 27, 28].

The consistency of the standard Λ CDM model with cosmological observations requires that the model passes two types of tests:

- The quality of fit of the model is acceptable in the context of each one of the above observational probes.
- The best fit values of the six free parameters of the model obtained with each individual probe are consistent with each other at a level of about $1 - 2\sigma$. If this is not the case, then we have a “tension” of Λ CDM.

The Λ CDM model appears to pass the first test in the context of practically all current observational probes. However, there seem to be some issues for Λ CDM

L. Kazantzidis · L. Perivolaropoulos (✉)
Department of Physics, University of Ioannina, 45110 Ioannina, Greece
e-mail: leandros@uoi.gr

L. Kazantzidis
e-mail: l.kazantzidis@uoi.gr

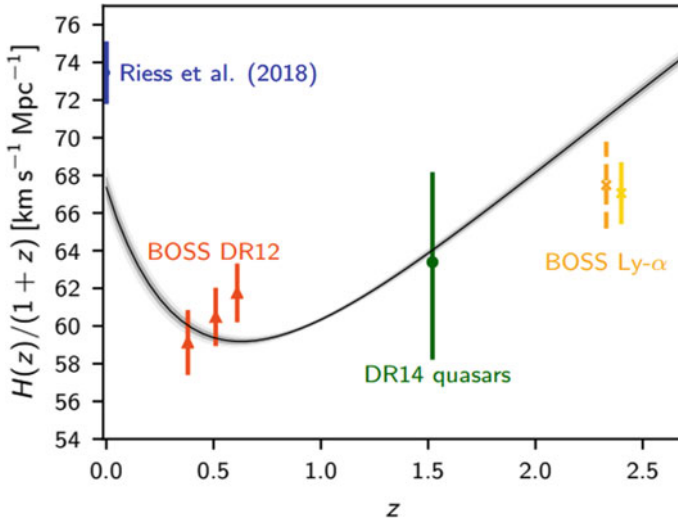


Fig. 33.1 The comoving Hubble parameter as a function of z superimposed with BAO data from BOSS DR12 [10] survey (orange points), BOSS DR14 quasar sample [34] (green point), SDSS DR12 Ly α sample [35] (yellow points) and the Hubble Space Telescope survey [36] (blue point). The black line corresponds to the best fit obtained from the Planck 18 CMB data under the assumption of a Λ CDM background, while the grey areas are the 1σ regions (from Ref. [8])

in the context of the second test [29]. In particular, two classes of tension have appeared to persist and amplify during the past decade. The first is the H_0 tension, where H_0 is the Hubble parameter. The Planck mission [7, 8] reports that $H_0 = 67.4 \pm 0.5 \text{ km s}^{-1} \text{ Mpc}^{-1}$ at the 1σ level, whereas local measurements mainly from Cepheid [30] and SNIa luminosity distance indicators [31, 32] report that $H_0 = 74.03 \pm 1.42 \text{ km s}^{-1} \text{ Mpc}^{-1}$ at the 1σ level, a value approximately 4σ away from the Planck reported one. This tension indicates that the local measurement of the Hubble parameter (at scales up to 400 Mpc) obtained mostly using SNIa, is higher than the global value obtained from the Hubble volume on scales of 10 Gpc [33] through an extrapolation of $H(z)$ from the last scattering surface to the present time in the context of Λ CDM scenario, as shown in Fig. 33.1.

Possible explanations of this tension include systematic errors of the CMB and/or the SNIa distance indicators. Alternatively this tension could be an early hint for physical deviations from the Λ CDM model (see, e.g., Ref. [37] for a recent review). The later possibility is more likely in view of the fact that other local cosmological observations, including other SNIa data analysis methods [38–40], gravitational lensing [41] and Tully-Fisher type calibration of SNIa [42], appear to be consistent with the SNIa measurement [31, 32]. In contrast, measurements involving BAO [9] and SNIa calibration using the tip of the red-giant branch distances [43] are consistent with the extrapolated global CMB measurements of H_0 .

A natural cause for this tension could be cosmic variance. If it happens that we live in a locally underdense region of the Universe we would locally measure a value of H_0 that would be higher than the mean value over the whole Universe. It has been shown, however [44, 45], that the required magnitude of such an underdensity on the required scales of 150 Mpc is very unlikely in a Λ CDM Universe. In such a Universe cosmic variance adds a 1σ error to the locally measured H_0 of only $\sigma_{H_0} = 0.31 \text{ km sec}^{-1} \text{ Mpc}^{-1}$, which is negligible compared to the $6 \text{ km s}^{-1} \text{ Mpc}^{-1}$ needed to resolve the H_0 tension.

Non-gravitational physical mechanisms that can reduce the H_0 tension include the following:

- Modifications of expansion rate at late times in the context of alternative dark energy models [46–49], decaying dark matter models [50, 51], or the presence of massive sterile neutrinos [52] that tend to amplify the accelerating expansion at late times. Such modifications could drive upwards the low z part of the $H(z)$ curve shown in Fig. 33.1, thus bringing the $z = 0$ prediction of the CMB closer to the H_0 result of the local measurements of Ref. [32].
- Inhomogeneous cosmologies [53] that would make a local deep underdensity more likely than in the case of Λ CDM.
- A new component of dark radiation [54] that would tend to decrease the sound horizon r_s at radiation drag, thus leading to a predicted increase of H_0 by shifting the whole curve of Fig. 33.1 upwards. This approach has the advantage of shifting, at the same time, the BAO points shown in Fig. 33.1.

The origin of these mechanisms is non-gravitational and the consensus is that since H_0 is a geometric parameter it can not be affected by modifications of GR. However, as discussed in more detail below, the physics of SnIa is heavily based on the assumption of validity of GR. For example, an evolving Newton’s constant at low redshifts would directly affect the absolute magnitude of SnIa, leading to a requirement for a new interpretation of the SnIa distance moduli. Therefore, even though the SnIa absolute magnitude is usually assumed constant and is marginalised as being a nuisance parameter, its possible evolution may carry useful information about the robustness of the determination of H_0 using SnIa and about possible modifications of GR. Two interesting questions, therefore arise:

- Are there indications for evolution of the SnIa absolute magnitude at low z ?
- What would be the implications of such evolution on the derived value of H_0 and on the possible evolution of the effective Newton’s constant?

These are among the questions discussed in what follows.

The second tension in the context of Λ CDM is the σ_8 tension, where σ_8 is the density rms matter fluctuations within spheres of radius $8h^{-1} \text{ Mpc}$ and is determined by the amplitude of the primordial fluctuations power spectrum and by the growth rate of cosmological fluctuations. In particular, dynamical probes, (mainly RSD [22, 25, 26, 55] WL [16, 17, 19, 20], and E_G data [56]), favour lower values of σ_8 and/or Ω_{0m} than the corresponding values reported by Planck [7, 8] at a $2 - 3\sigma$ level. This tension, if not due to systematics of the dynamical probes or CMB data, could be

Table 33.1 Planck18/ Λ CDM parameters values from Ref. [8], based on TT, TE, EE, lowE and lensing likelihoods

Parameter	Planck18/ Λ CDM [8]
$\Omega_b h^2$	0.02237 ± 0.00015
$\Omega_c h^2$	0.1200 ± 0.0012
n_s	0.9649 ± 0.0042
H_0	67.36 ± 0.54
Ω_{m0}	0.3153 ± 0.0073
w	-1
σ_8	0.8111 ± 0.0060

interpreted as an indication of a weaker gravitational growth of perturbations than the growth indicated by GR in the context of a Λ CDM model with the Planck18/ Λ CDM parameter values, which are shown in the following Table 33.1.

In addition to a possible evolution of the effective Newton constant discussed below, non-gravitational mechanisms can also reduce the σ_8 tension (see, e.g., Ref. [57] for a recent review). Such effects include the following:

- Interacting dark energy models, which modify the equation for the evolution of linear matter fluctuations in a given $H(z)$ cosmological background [58–60].
- Dynamical dark energy models [46, 59, 61–64] and running vacuum models [65, 66], which modify the cosmological background $H(z)$ to a form different from Λ CDM.
- Effects of massive neutrinos [64, 67]. Neutrinos are relativistic at early times (contribute to radiation) while at late times they become non-relativistic but with significant velocities (hot dark matter), while they constitute a non-negligible fraction of the dark matter of the Universe. The conversion of radiation to hot dark matter plays a role in the Hubble expansion. At the same time the residual streaming velocities are still large enough at late times to slow down the growth of structure. Thus, neutrinos affect both background expansion and the growth of cosmological perturbations in such a way as to slow down the growth as required by the RSD data. Their effects on easing the σ_8 tension coming from WL data has been questioned by the recent analysis of Ref. [68] (see also Fig. 33.2).

Besides these categories, alternative parameters beyond the standard ones, such as a running scalar spectral index, a modified matter expansion rate or a bulk viscosity coefficient may have the potential to ease the σ_8 tension [69].

In addition to these non-gravitational effects that can slow down growth at low redshifts, modified gravity theories can also contribute in the same direction in a manner that is more generic and fundamental. The feature required from this class of theories is a reduced effective Newton's constant G_{eff} at low redshifts. It turns out that this behaviour cannot be achieved in a Λ CDM background for most scalar-tensor and $f(R)$ theories [25, 70, 71]. However, it is possible in other less generic modi-

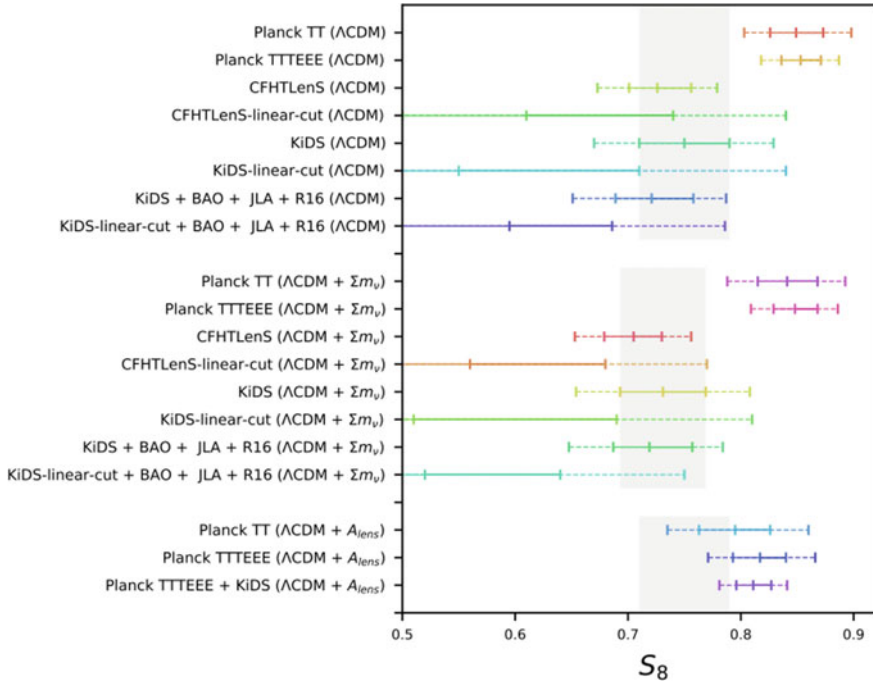


Fig. 33.2 $1 - 2\sigma$ constraints for $S_8 = \sigma_8 \sqrt{\frac{\Omega_{m0}}{0.3}}$ for various combinations of datasets and models superimposed with the Kilo Degree Survey (KiDS) [64] survey bounds (grey regions) for each cosmological model (adopted from Ref. [68]). In particular, the CFHTLenS linear cut model corresponds to the conservative cut of the cosmic shear data of the Canada-France-Hawaii Telescope Lensing (CFHTLenS) survey [112, 113] in order to reduce the non-linear scale contribution [87], the JLA acronym corresponds to the Supernovae Data from Ref. [4], the R16 stands for the H_0 measurement given in Ref. [32], the BAO data correspond to the data used in Ref. [7], while the KiDS linear cut model describes the conservative cut of Ref. [17] and $\sum m_\nu$ stands for the inclusion of massive neutrinos. Notice that only the introduction of the A_{lens} parameter, which is degenerate with the evolution of G_{eff} [86], can lead to a reduction of the tension between Planck and dynamical probes

fied gravity theories, including teleparallel theories of gravity [72, 73], Horndeski theories [74–76], or theories beyond Horndeski [77].

Clearly, a reduced (compared to GR) evolving effective Newton’s constant would have important signatures on low z cosmological observations. In particular:

- It would affect [25, 26] the low l CMB power spectrum through the Integrated Sachs-Wolfe (ISW) effect [78, 79].
- It would affect [25, 26] the growth rate of cosmological fluctuations as detected through the RSD [22–26], WL [16–21] and CC data [11–15].
- It would induce an evolution of the SnIa absolute magnitude, which depends on the magnitude of Newton’s constant [80–84]. Notice, however, that the value of the effective Newton’s constant here should be obtained from a strong gravity calcula-

tion in the context of a modified gravity theory and thus is not generally identical to the G_{eff} derived for the growth of cosmological perturbation that involves a perturbative calculation.

For a viable modified gravity mechanism there should be consistency with respect to the type and magnitude of Newton's constant evolution favoured by the above cosmological observations, keeping in mind the strong gravity effects involved in the SNIa physics. It will be seen in what follows that indeed all of the above probes mildly favour a reduced value of Newton's constant at low z . However, the favoured magnitude and statistical significance of such a reduction varies among the above observational probes.

A Newton's constant $G_{\text{eff}}(z)$ evolving with redshift, may be parametrised in the context of a wide range of parametrisations, including theoretically motivated [85–89] and model-independent [25, 26] forms, and leads to a modification of the linear growth of cosmological perturbations.

This modified growth equation is obtained by considering the perturbed Friedmann–Lemaître–Robertson–Walker (FLRW) metric in the Newtonian gauge, which is given by [90–92]

$$ds^2 = -(1 + 2\Psi)dt^2 + a^2(1 - 2\Phi)d\vec{x}^2, \quad (33.1)$$

where a is the scale factor that is connected to the redshift z through $a = 1/(1+z)$, and Ψ, Φ correspond to the Bardeen potentials in the Newtonian gauge [91]. Einstein's equations in Fourier space at linear order take the form [93–95]

$$k^2\Psi = -4\pi G_N \mu(a, k) a^2 \rho_m \Delta, \quad (33.2)$$

$$\Phi = \eta(a, k)\Psi, \quad (33.3)$$

$$k^2(\Phi + \Psi) = -8\pi G_N \Sigma(a, k) a^2 \rho_m \Delta, \quad (33.4)$$

where $\mu \equiv G_{\text{eff}}/G_N$ (G_N is Newton's constant as measured by local experiments and Solar System observations), Δ is the comoving density contrast defined as $\Delta \equiv \delta + 3aHu/k$. $\delta \equiv \frac{\delta\rho_m}{\rho_m}$ is the linear matter growth factor, u is the irrotational component potential of the peculiar velocity, ρ_m is the matter density of the background, η is the gravitational slip and $\Sigma \equiv G_L/G_N$ is the lensing normalized Newton constant.

In GR, G_{eff} , which is connected with the growth of matter perturbations and G_L , which is related with the lensing of light through the Weyl potential $\frac{\Phi_+}{2} = \Phi + \Psi$, coincide with G_N . The Weyl potential can be connected with lensing, since the cosmic convergence of null geodesics with respect to unperturbed geodesics is given by [96]

$$\kappa(r, \theta) = \frac{1}{4} \int_0^r dr' \left(\frac{r-r'}{r} \right) r' \nabla^2 \Phi_+(\theta, r'), \quad (33.5)$$

where r and θ are the comoving coordinates of the source. The parameters μ , η and Σ are connected as

$$\Sigma(a, k) = \frac{\mu(a, k) [1 + \eta(a, k)]}{2}, \quad (33.6)$$

and they are key parameters in detecting deviations from GR where their value coincides with unity.

In what follows we focus on the parameter μ . This parameter is associated with the linear matter growth factor through the growth equation [95]

$$\ddot{\delta} + 2H\dot{\delta} = \frac{3}{2} H^2 \Omega_m \mu \delta, \quad (33.7)$$

where the dot denotes differentiation with respect to cosmic time t . Equation (33.7) is derived using the conservation of the matter energy momentum tensor and the modified Poisson Eq. (33.2), assuming scales much smaller than the Hubble scale. For most modified gravity models the scale dependence of μ is very weak in scales much smaller than the Hubble scale. In addition, most growth data do not report scale dependence but only redshift dependence. Thus, we only parametrise the dependence of μ on the the scale factor, i.e. $\mu(a, k) = \mu(a)$, and we obtain the growth equation in redshift space as

$$\delta'' + \left(\frac{H'}{H} - \frac{1}{1+z} \right) \delta' = \frac{3}{2} \frac{\Omega_m}{(1+z)^2} \mu \delta, \quad (33.8)$$

where in Eq. (33.8), the prime denotes differentiation with respect to the redshift z . The equation for the growth rate $f(z) \equiv \frac{d \ln \delta}{d \ln a}$ may also be obtained from Eq. (33.8) as

$$(1+z) f' - f^2 + \left[(1+z) \frac{H'}{H} - 2 \right] f = -\frac{3}{2} \Omega_m \mu, \quad (33.9)$$

Fixing the background $H(z)$ and considering a specific parametrisation for μ , Eq. (33.9) can be solved (either numerically or analytically) with initial conditions deep in the matter era, where $\delta \sim a$ (assuming GR is restored at early times). Combining this solution with the rms density fluctuations on scales of 8 Mpc, σ_8 , which evolves as $\sigma_8(z) = \sigma_8(z=0) \frac{\delta(z)}{\delta(z=0)}$, we obtain theoretical prediction for the product $f\sigma_8$ given $\sigma_8(z=0) \equiv \sigma_8$, $H(z)$ and $\mu(z)$. In particular,

$$f\sigma_8(a) \equiv f(a) \cdot \sigma(a) = \frac{\sigma_8}{\delta(1)} a \delta'(a) \quad (33.10)$$

is reported by many surveys since 2006, leading to collections of data which can be used to simultaneously constrain $H(z)$ and $\mu(z)$.

On the other hand, $H(z)$ is usually parametrised as $wCDM$ i.e.

$$H^2(z) = H_0^2 \left[\Omega_{m0}(1+z)^3 + (1 - \Omega_{m0})(1+z)^{3(1+w)} \right], \quad (33.11)$$

which reduces to Λ CDM for an equation of state parameter $w = -1$, the effective Newton's constant parameter μ does not have a commonly accepted parametrisation. Some authors motivated from the predictions of scalar-tensor theories use a scale dependent parametrisation for μ and η as [85, 89]

$$\begin{aligned}\mu(a, k) &= \frac{1 + \beta_1 \lambda_1^2 k^2 a^s}{1 + \lambda_1^2 k^2 a^s}, \\ \eta(a, k) &= \frac{1 + \beta_2 \lambda_2^2 k^2 a^s}{1 + \lambda_2^2 k^2 a^s}.\end{aligned}\quad (33.12)$$

In the special case of $f(R)$ theories the parameters that appear in Eq. (33.12) are

$$\beta_1 = 4/3; \quad \beta_2 = 1/2; \quad \lambda_2^2/\lambda_1^2 = 4/3. \quad (33.13)$$

Clearly for $\beta_1 > 1$ (as is the case for $f(R)$ theories [97, 98] and in most scalar-tensor theories) we have $\mu > 1$ at low z , and thus gravity is stronger than in GR at low z in these classes of theories [71, 97–100].

Another parametrisation that has been studied in the literature is the parametrisation of no-slip gravity [75], a subclass of Horndeski theories which remains viable after the binary star collision GW170817 [101]. In this case μ takes the form [75]

$$\mu = \frac{2}{2 + b + b \tanh\left[\frac{\tau}{2} \log_{10}\left(\frac{a}{a_t}\right)\right]}, \quad (33.14)$$

where b , τ and a_t correspond to parameters that describe the amplitude, the rapidity and the scale factor at the time when μ shifts from unity in the early Universe to $\mu = 1 + b$.

An alternative scale-dependent class of parametrisations for μ and η is of the form [86, 87]

$$\mu(a, k) = 1 + f_1(a) \frac{1 + c_1(\lambda H/k)^2}{1 + (\lambda H/k)^2}; \quad (33.15)$$

$$\eta(a, k) = 1 + f_2(a) \frac{1 + c_2(\lambda H/k)^2}{1 + (\lambda H/k)^2}. \quad (33.16)$$

For sub-Hubble scales this parametrisation becomes scale-independent and has been expressed as [86]

$$\mu(a, k) = 1 + E_{11} \Omega_{\text{DE}}(a); \quad (33.17)$$

$$\eta(a, k) = 1 + E_{22} \Omega_{\text{DE}}(a). \quad (33.18)$$

where $\Omega_{\text{DE}}(a)$ is the density parameter of the dark energy. For $E_{11} < 0$, gravity is weaker compared to GR at low z , and indeed the best fit value obtained in Ref. [86]

when dynamical probes are taken into account is negative ($E_{11} = -0.21_{-0.45}^{+0.19}$ when CMB and WL data are taken into account).

A model and scale-independent parametrisation [25, 26] for μ , which reduces to the GR value at low and high z , while respecting the constraints from Solar Systems tests and from the nucleosynthesis [102, 103] is

$$\mu = 1 + g_a(1-a)^n - g_a(1-a)^{2n} = 1 + g_a \left(\frac{z}{1+z} \right)^n - g_a \left(\frac{z}{1+z} \right)^{2n}, \quad (33.19)$$

where g_a and n integer with $n \geq 2$ are parameters to be fit from data. A distinguishing feature of this parametrisation is that it naturally and generically respects Solar System and nucleosynthesis constraints ($\frac{d\mu}{dz}|_{z=0} = 0$, $\mu(z=0) = 1$, $\mu(z \rightarrow \infty) = 1$) [102–105].

An alternative approach for the parametrisation of deviations from GR is based directly on the growth rate f of density fluctuations. The growth rate f is usually parametrised using the “growth index” γ as

$$f(z) = \frac{d \ln \delta}{d \ln a} \approx \Omega_m(z)^\gamma, \quad (33.20)$$

where γ in most dark energy models based on GR is $\gamma \approx 0.55$. For many modified gravity theories this quantity is not constant and is parameterised instead as a function of the redshift z (see, e.g., Ref. [106], and for updated observational constraints of this parameter Refs. [71, 107–109]. In particular, recent observations indicate that $\gamma > 0.55$ (weaker growth rate) in contrast to the usual theoretical prediction of $\gamma < 0.55$ that is supported by many modified gravity models such as $f(R)$ theories [110] and indicates stronger gravity at low z . In what follows we focus on the parametrisation (33.19).

The μ parametrisation (33.19) has been extensively studied in Refs. [25, 26, 111], where it was shown that in the context of a wide range of different RSD datasets, a negative value of the parameter g_a is favoured in the context of Planck18/ Λ CDM background expansion rate $H(z)$ ($g_a = -0.68 \pm 0.18$), indicating weaker gravity than the GR prediction at low z .

This trend for weaker gravity at low z is also supported by WL data [16, 17, 19, 20, 68], even though in these references this trend was expressed as a trend for lower values of σ_8 and Ω_{0m} (or equivalently $S_8 \equiv \sigma_8 \sqrt{\Omega_{m0}/3}$) compared to the Planck18/ Λ CDM best fit, since μ was fixed to unity. This tension level which can not be released even by the inclusion of massive neutrinos, is demonstrated in Fig. 33.2. In Fig. 33.2 A_{lens} is an effective parameter that rescales the lensing amplitude in the CMB spectra. The extension of Λ CDM involving the parameter A_{lens} is degenerate with a modified gravity extension and can clearly decrease the σ_8 tension implied by the WL data, as shown in Fig. 33.2 [68]. In contrast, the introduction of massive sterile neutrinos appears to have little effect on the tension level.

As discussed above, an evolving μ can also affect the H_0 tension problem. Indeed, local measurements of H_0 are heavily based on SNIa as distance indicators

and on the assumption that after proper calibration the SnIa absolute magnitude M may be assumed to be constant. The peak luminosity of SnIa, is related to the gravitational constant as $L \propto G^{-3/2}$ [81], which leads to an absolute magnitude M that is associated with μ through [80, 81]

$$M - M_0 = \frac{15}{4} \log_{10}(\mu), \quad (33.21)$$

where M_0 is a reference asymptotic value of the absolute magnitude. A more detailed and accurate approach for determining the dependence of M of SnIa on the Newton's constant has been implemented in Ref. [83] through a semi-analytical method of light curve fitting that uses the standardised intrinsic luminosity L instead of the peak luminosity of individual events to find the dependence of M on the value of G . In this model the sign of the power index $-\frac{3}{2}$ appearing above, is indicated to be positive instead. This possibility will be discussed in a following publication [114]. Usually, M is considered to be a constant nuisance parameter and is marginalised. However, since dynamical probes favour a μ smaller than the GR value, similar trends (perhaps not of the same magnitude due to the strong gravitational fields involved) are expected for the absolute magnitude M . In what follows we present a short preliminary analysis attempting to address this issue and identify possible trends and constraints in the absolute M of the SnIa.

In the context of the above discussion, the following questions arise:

- What is the current level of the $f\sigma_8$ tension and what is the implied evolution of μ in the context of Λ CDM?
- Are there hints of a similar evolution of μ in the Pantheon SnIa dataset?
- What is the allowed evolution of μ from the low l CMB data?

These questions will be addressed in what follows.

The structure of this brief review is the following: In Sect. 33.1 we review the $f\sigma_8$ tension and the implications of a dynamical $\mu(z)$ for modified gravity theories. In Sect. 33.2 a tomographic analysis of the SnIa absolute magnitude of the Pantheon dataset is performed and the constraints on possible evolution at low z are specified. Finally, in Sect. 33.3 the constraints on an evolving μ from the low l angular CMB spectrum and the ISW effect are presented in the context of a Λ CDM background, while in Sect. 33.4 we outline and discuss our results.

33.1 The $f\sigma_8$ Tension and Modified Gravity

33.1.1 Observational Evidence

The solution of Eq. (33.8) with initial conditions deep in the matter era, a w CDM background (33.11) and an evolving parameter $\mu(z)$ of the form (33.19) with $n = 2$

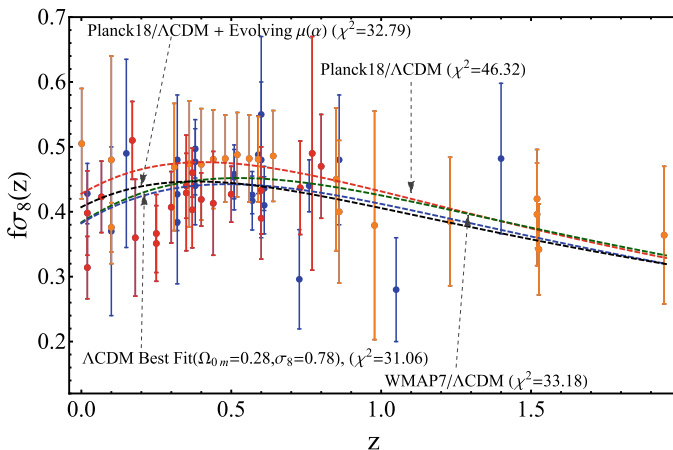


Fig. 33.3 Evolution of $f\sigma_8$ as a function of redshift. The red dashed line corresponds to the Planck18/ Λ CDM model ($\Omega_{m0} = 0.315 \pm 0.007$, $\sigma_8 = 0.811 \pm 0.006$), the green one to the WMAP7/ Λ CDM ($\Omega_{m0} = 0.266 \pm 0.025$, $\sigma_8 = 0.801 \pm 0.030$), the black one to an evolving μ with a Planck18/ Λ CDM background ($\Omega_{m0} = 0.315 \pm 0.007$, $\sigma_8 = 0.811 \pm 0.006$, $g_a = -0.681 \pm 0.177$), while the blue one describes the best fit Λ CDM coming from the 63 compilation of Ref. [26] ($\Omega_{m0} = 0.279 \pm 0.028$, $\sigma_8 = 0.775 \pm 0.018$). The orange points correspond to the 20 latest datapoints, while the red ones correspond to the 20 earliest of this compilation. The blue points account for the rest of the growth data

respects both nucleosynthesis constraints and Solar System constraints. The theoretical prediction for $f\sigma_8(z)$ obtained from such a solution using also Eq. (33.10) depends on the parameters Ω_{m0} , w and g_a and is shown in Fig. 33.3, along with a large compilation of corresponding datapoints [26] (the different colours correspond to early or more recent times of publication). Clearly, the parameter values $(\Omega_{m0}, w, \sigma_8, g_a) = (0.31, -1, 0.83, 0)$ corresponding to Planck18/ Λ CDM lead to larger growth ($f\sigma_8(z)$) than most data would imply, especially at redshifts $z < 1$ (red line).

The fit to the data may be improved either by modifying the background expansion rate $H(z)$ (e.g. lowering Ω_{m0}) and/or by lowering the strength of gravity at low z . Fixing the background $H(z)$ to Planck18/ Λ CDM and allowing g_a in Eq. (33.19) to vary we obtain [25, 26] a best fit value of $g_a = -0.68 \pm 0.18$ for $n = 2$ which is approximately 3.7σ away from the GR value $g_a = 0$.

The trend for weaker gravity at low redshifts is also evident in Fig. 33.4, which shows the best fit form of $\mu(a)$ as a function of the scale factor a for the best fit values of g_a coming from the robust RSD data compilation of Ref. [25] for different values of n . The required drop of $\mu(a)$ becomes stronger and localised to low z as n increases. As discussed in Sect. 33.3, however, such a large drop is not consistent with the low l CMB angular power spectrum and the ISW effect.

An interesting feature of the theoretical model predictions for $f\sigma_8(z)$ shown in Fig. 33.3 is the degeneracy among these predictions for $z > 1$. This degeneracy has

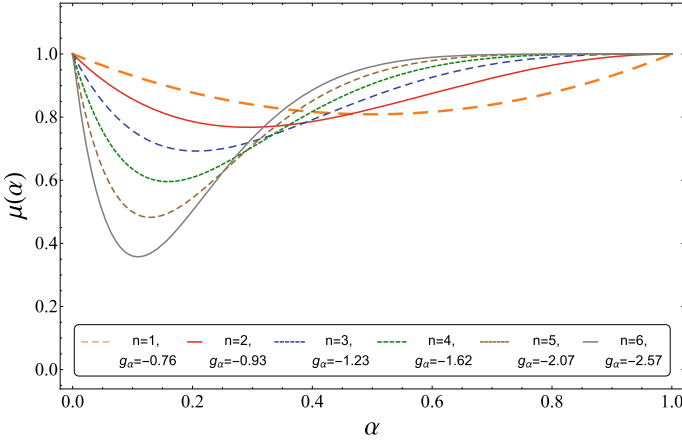


Fig. 33.4 Evolution of μ as a function of the scale factor a considering the best fit values for g_a and various values of n using the robust collection of Ref. [25]

been investigated in some detail in [115] for $f\sigma_8(z)$ and for other cosmological observables. It was found that there are blind redshift spots where observables are degenerate with respect to specific cosmological parameters. For $f\sigma_8(z)$ with respect to the parameter g_a there is a blind spot at $z \simeq 2.5$ and its constraining power is significantly reduced for $z > 1$. Thus $f\sigma_8(z)$ datapoints with $z < 1$ can constrain $\mu(z)$ (or equivalently g_a) much more efficiently than points at higher redshifts. This is demonstrated in Fig. 33.5, which shows the difference between the growth rate in the context of an evolving $f\sigma_8(z)$ from the Planck18/ Λ CDM $f\sigma_8(z)$ [115] for various values of g_a . This difference is defined as

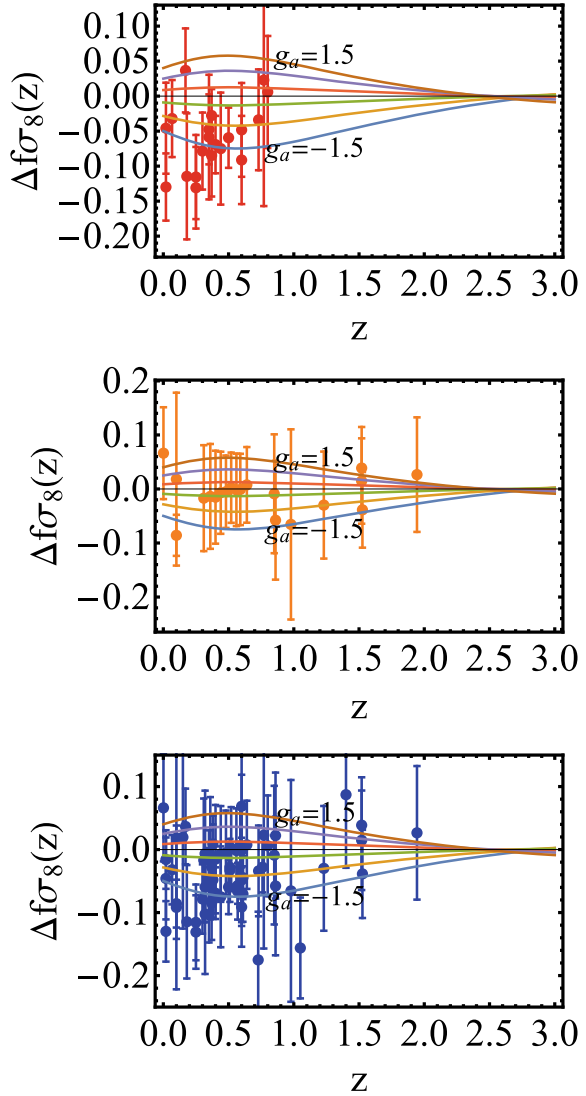
$$\Delta f\sigma_8 = f\sigma_8(z, \Omega_{m0}^{Planck18}, -1, g_a) - f\sigma_8(z, \Omega_{m0}^{Planck18}, -1, 0). \quad (33.22)$$

Clearly, early published datapoints that tend to have lower redshifts (right panel) have more constraining power than more recently published datapoints (middle panel), which have higher z and larger errorbars. The tension level comes mainly from early datapoints, which appear to favour $\Delta f\sigma_8 < 0$, i.e. weaker growth.¹

The trend for weaker growth of matter perturbation than the growth favoured by Planck18/ Λ CDM has been pointed out in a wide range of studies in the context of different dynamical probe data. One of the first analyses that pointed out the weak growth tension was that of Ref. [22], where it was pointed out that RSD measurements are consistently lower than the values expected from Planck in the context of Λ CDM

¹ The RSD datapoints of Fig. 33.5 include a 1 – 3% “fiducial cosmology” Alcock-Paczynski correction [22, 25, 26, 116], i.e. they have been multiplied by a factor $\frac{H(z)d_A(z)}{H_{fid}(z)d_{A,fid}(z)}$ where the subscript fid indicates the fiducial cosmology used in each survey to convert angles and redshift to distances for evaluating the correlation function and $H(z)$, $d_A(z)$ correspond to the Hubble parameter and the angular diameter distance of the true cosmology.

Fig. 33.5 Evolution of $\Delta f\sigma_8$ as a function of the redshift z for different values of g_a . These curves are superimposed with the 20 earliest datapoints (upper panel), the 20 latest (middle panel) and the full compilation (lower panel) of Ref. [26]. Notice that early lower z datapoints are much more efficient in detecting hints of modified gravity (a non-zero value of g_a)



cosmology. It was also pointed out that other dynamical probes like the Sunyaev-Zeldovich (SZ) cluster counts [117] also indicate weaker growth ($\sigma_8 = 0.77 \pm 0.02$, $\Omega_{m0} = 0.29 \pm 0.02$). Similar trends were found earlier, using the measurement of the galaxy cluster mass function in the redshift range $z \in [0, 0.9]$ [118], where lower values of Ω_{m0} and σ_8 were favoured. Later studies confirmed this trend by pointing out that best fit cosmological parameters like the matter density Ω_{m0} and the dark energy equation of state w differ at a level of $2 - 3\sigma$ between geometric probes (SNIa, BAO and CMB peak locations) and dynamical probes (RSD data, CC and

WL) [15, 119]. The dynamical probes of growth pointed consistently towards lower values of Ω_{m0} and thus weaker growth. It was also realised that in particular, WL data indicated consistently a $2 - 3\sigma$ tension with the Planck parameter values of $\Omega_{m0} - \sigma_8$ [7, 17, 68] (for updated constraints see also Fig. 33.2 adopted from Ref. [68]). For example, the Kilo-Degree Survey (KiDs-450) [17, 64] finds $S_8 \equiv \sigma_8 \sqrt{\Omega_{m0}/0.3} = 0.74 \pm 0.035$, which is smaller at a 2.6σ tension compared to the corresponding Planck best fit value $S_8 = 0.832 \pm 0.013$ [8]. More recent WL cosmic shear data from the Dark Energy Survey [18, 20] indicate $S_8 = 0.792 \pm 0.024$, i.e., a weaker tension with geometric probes and Planck (about $1 - 2\sigma$), albeit in the same direction of weaker growth and lower $\Omega_{m0} - \sigma_8$ (DES indicates that $\Omega_{m0} = 0.264^{+0.032}_{-0.019}$ [20] to be compared with Planck best fit $\Omega_{m0} = 0.315 \pm 0.007$ [8]. Reduced value of σ_8 ($\sigma_8 = 0.77 \pm 0.02$) is also indicated by high l measurements ($l > 2000$) of the E-mode angular auto-power spectrum (EE) and the temperature-E-mode cross-power spectrum (TE) taken with the SPTpol instrument [120].

The tension level between geometric and dynamical probes has recently been quantified by using specific statistics designed to probe the tension in a more efficient and quantitative manner [121–123]. These studies have verified the statistical significance of the tension between geometric and dynamical probes and demonstrated that even though the dynamical probes (RSD, WL and CC) are consistent with each other, pointing towards weaker growth than GR, they are in discordance with the geometric probes in the context of GR.

33.1.2 Theoretical Implications

The most generic approach to the “weak growth” tension is the modified gravity approach. If this tension is in fact due to a modification of GR on cosmological scales the following question arises: “What observationally viable modified gravity models can reproduce a weaker gravity than that predicted by GR at low redshifts?” A naive response to this question would indicate that any viable modified gravity model can lead to weaker gravity than GR at late times with proper choice of its parameters. However, it may be shown that this is not the case. Recent studies have addressed this question for $f(R)$ theories, for minimal scalar tensor theories [71, 111], for Horndeski theories [75, 124] and beyond Horndeski Gleyzes-Langlois-Piazza-Vernizzi (GLPV) theories [99].

We will consider $f(R)$ models with an action of the form

$$S = \int d^4x \sqrt{-g} \frac{f(R)}{2} + S_m, \quad (33.23)$$

where from now on we set $8\pi G_N = 1$. The predicted $\mu(z, k)$ is given as [70]

$$\mu(z, k) = \left(\frac{df}{dR} \right)^{-1} \left[\frac{1 + 4 \left(\frac{d^2 f}{dR^2} / \frac{df}{dR} \right) \cdot k^2 (1+z)^2}{1 + 3 \left(\frac{d^2 f}{dR^2} / \frac{df}{dR} \right) \cdot k^2 (1+z)^2} \right], \quad (33.24)$$

where in this case μ depends on both the redshift z and the scale k . In addition, the stability conditions

$$\begin{aligned} \frac{d^2 f}{dR^2} &> 0 \\ \frac{df}{dR} &> 0 \end{aligned} \quad (33.25)$$

should be satisfied [98]. Also in viable $f(R)$ models $\frac{df}{dR} \simeq 1$ at early times deep in the matter era (high R) [125]. Thus, since $\frac{d^2 f}{dR^2} > 0$ we must have $\frac{df}{dR} < 1$ at late times (low R). It follows that both factors of Eq. (33.24) are larger than unity and we have generically in $f(R)$ theories that $\mu(z) \geq 1$. This is a generic result independent of the background $H(z)$, indicating that $f(R)$ theories are unable to resolve the weak growth tension because they predict stronger gravity than GR.

A similar result is true for minimal scalar-tensor theories, provided that the expansion background is close to Λ CDM. The minimal scalar-tensor action has the form [126]

$$S = \int d^4x \sqrt{-g} \left[\frac{1}{2} F(\phi) R - \frac{1}{2} g^{\mu\nu} \partial_\mu \phi \partial_\nu \phi - U(\phi) \right] + S_m. \quad (33.26)$$

The dynamical equations obtained by variation of this action in the context of a flat FRW metric are of the form [92, 126]

$$3FH^2 = \rho_m + \frac{1}{2} \dot{\phi}^2 - 3H\dot{F} + U \quad (33.27)$$

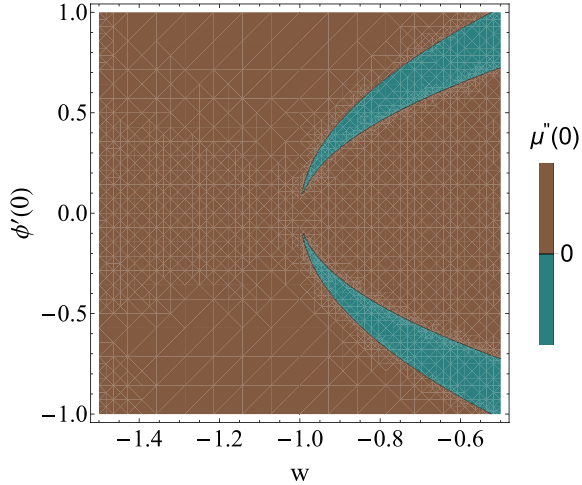
$$-2F\dot{H} = (\rho_m + p_m) + \dot{\phi}^2 + \ddot{F} - H\dot{F}, \quad (33.28)$$

where the dot represents differentiation with respect to cosmic time t . After rewriting the equations of motion in terms of the redshift, defining the rescaled square Hubble parameter as $q(z) = \frac{H^2(z)}{H_0^2}$ and eliminating the scalar field potential $U(\phi)$, we obtain a differential equation that associates the coupling function $F(\phi)$ and the scalar field ϕ as

$$F''(z) + \left[\frac{q'(z)}{2q(z)} - \frac{2}{1+z} \right] F'(z) - \frac{1}{(1+z)} \frac{q'(z)}{q(z)} F(z) + 3 \frac{1+z}{q(z)} \Omega_{m0} = -\phi'(z)^2, \quad (33.29)$$

where the prime stands for differentiation with respect to redshift z . In scalar tensor theories μ is expressed as [82, 92]

Fig. 33.6 The second derivative of $\mu(0)$ in the parametric space of $\phi'(0)$ and w . The brown region describes the parameter values for $\mu''(0) > 0$, while the blue region describes the parameter values for $\mu''(0) < 0$ (from Ref. [71])



$$\mu(z) = \frac{1}{F(z)} \frac{F(z) + 2F_{,\phi}^2}{F(z) + \frac{3}{2}F_{,\phi}^2}. \tag{33.30}$$

Using Eq. (33.30) in the differential equation (33.29) and expanding around $z = 0$, while using the Solar System constraint $\mu'(z = 0) = 0$ [102, 103], we find in the context of a w CDM background [71]

$$\mu''(0) = 9(1+w)(-1 + \Omega_{m0} + \frac{9(1+w)^2(-1 + \Omega_{m0}^2)}{\phi'(0)^2} + 2\phi'(0)^2). \tag{33.31}$$

For a Λ CDM background, Eq. (33.31) leads to the low z expansion

$$\mu(z) \approx \mu(0) + \frac{1}{2}\mu''(0)z^2 = 1 + \phi'(0)^2 z^2 + \dots, \tag{33.32}$$

which implies that $\mu(z)$ can only increase with redshift around $z = 0$ in the context of a Λ CDM background. In fact this result ($\mu''(0) > 0$) is also applicable for $w < -1$, as can be seen from Eq. (33.31), while for $w > -1$ it is possible to have $\mu''(0) < 0$, as shown in Fig. 33.6. Thus, the increasing nature of $\mu(z)$ in scalar tensor theories that respect the Solar System constraints has been demonstrated analytically in the context of a Λ CDM background around $z = 0$.

This result is also demonstrated numerically by using Eqs. (33.29), (33.30) in the context of the best fit parametrisation (33.19) obtained from the RSD growth data [25] ($g_a < 0$). Figure 33.7 shows the corresponding evolution of $\phi'(z)^2$, demonstrating that, as expected, for a decreasing $\mu(z) < 1$ we obtain $\phi'(z)^2 < 0$ (ghost instabilities) at least close to $z = 0$ when the Solar System constraints are respected (this does not include the $n = 1$ case). In the case of more general scalar-tensor theories (Horndeski and beyond Horndeski) it has been shown that weaker gravity may be possible,

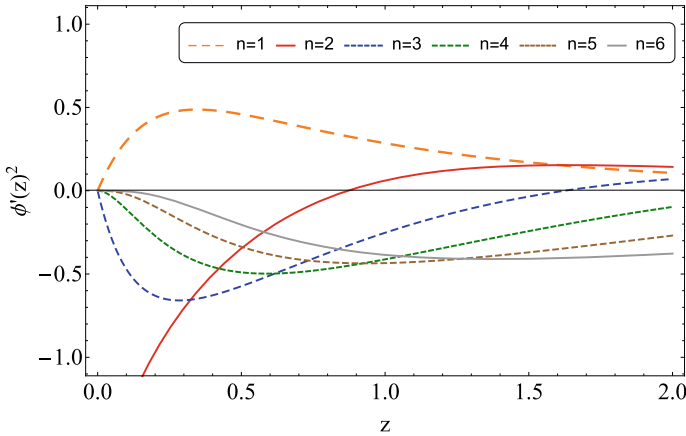


Fig. 33.7 Evolution of the scalar field ϕ as a function of redshift z corresponding to the best fit values of g_a and various values n using the robust compilation of Ref. [25]. Notice that the $n = 1$ case shows no ghost instabilities ($\phi'(z \simeq 0) > 0$) but it does not satisfy the Solar System constraint $\mu'(z = 0) = 0$ and thus Eq. (33.32 is not applicable for $n = 1$

provided specific constraints among the terms of the Lagrangian are applicable [75, 99].

We therefore conclude that from the theoretical point of view it is highly challenging to construct a viable theoretical model that allows for weaker gravity than GR at low redshifts while at the same time it respects solar system and other observational constraints with an $H(z)$ background close to Λ CDM. This challenge, however, may prove a useful discriminating tool among modified gravity models if the weak growth tension persists and gets verified by future cosmological data.

The issue of weak growth tension is expected to be clarified within the next decade due to a wide range of upcoming surveys. The surveys include Euclid [127, 128] (aiming at mapping the geometry of the Universe when dark energy leads to its accelerated expansion), Square Kilometer Array (SKA) [129, 130] (aiming at analysing radiosignals from various galactic sources), Large Synoptic Survey Telescope (LSST) [131] (aiming at mapping and cataloguing galaxies, in order to study their impact on the distortion of spacetime), Cosmic Origins Explorer (COre) (aiming at mapping the polarisation of the CMB) [132], Dark Energy Spectroscopic Instrument (DESI) [133, 134] (aiming at studying the effects of dark energy and obtaining the optical spectra of galaxies and quasars) and Wide Field Infrared Survey Telescope (WFIRST) [135, 136] (aiming at answering key questions in cosmology, probing BAO, WL and Supernovae data simultaneously). These surveys are expected to provide new and more detailed measurements of the dark energy probes BAO, SNIa, RSD, WL and CC extending to both dynamical and geometrical probes. They are expected to either confirm or eliminate the weak growth tension. In the first case, they will also provide a concrete discriminator among the modified gravity models

and non-gravitational models that constitute candidate extensions of the standard Λ CDM model and are motivated by the weak growth tension.

33.2 Evolving G_{eff} and the Pantheon SNIa Dataset

If the effective Newton's constant $\mu = G_{eff}/G_N$ is indeed evolving with redshift on cosmological timescales it is expected to lead to an evolution of the absolute luminosity and absolute magnitude of SNIa. In this section we present preliminary work searching for such evolution of the SNIa absolute magnitude with redshift. We use the Pantheon SNIa dataset [5], which is the latest compilation of SNIa. It consists of 1048 data points with redshifts spanning the region $z \in [0.01, 2.3]$. This dataset is a combined set of the PS1 SNIa dataset [137], which consists of 279 SNIa with redshifts spanned in the region $z \in [0.03, 0.68]$ along with probes of low redshifts ($z \in [0.01, 0.1]$), including the CfA1-CfA4 [138–141] and CSP surveys [142, 143], as well as high redshifts ($z > 0.1$), probed by SDSS [144, 145], SNLS [146, 147] and HST surveys [148, 149].

The measured apparent magnitude m for SNIa data is connected to cosmological parameters through the relation

$$m_{th}(z) = M + 5 \log_{10} \left[\frac{d_L(z)}{Mpc} \right] + 25, \quad (33.33)$$

where $d_L(z)$ is the luminosity distances and M is the absolute magnitude. The luminosity distance for a flat FLRW metric, is given by

$$d_L = c(1+z) \int_0^z \frac{dz'}{H(z')}. \quad (33.34)$$

The Pantheon dataset provides the apparent magnitude $m_{obs}(z_i)$ after corrections over the stretch, colour and possible biases from simulations [5]. Following the usual method of maximum likelihood [150] we can obtain the best fit parameters, minimising the quantity

$$\chi^2(M, \Omega_{m0}, w, h) = V_{Panth.}^i C_{ij}^{-1} V_{Panth.}^j, \quad (33.35)$$

where $V_{Panth.}^i \equiv m_{obs}(z_i) - m_{th}(z)$, C_{ij} provided in [5], is the covariance matrix and h is the dimensionless parameter of the Hubble constant, which is defined as $h \equiv H_0/100$ (km/s)/Mpc.

Usually, the absolute magnitude M is considered a nuisance parameter and is marginalised along with h , due to a clear degeneracy between the two parameters. However, in the context of modified gravity with an evolving Newton's constant the absolute magnitude is expected to evolve with redshift in accordance with Eq. (33.21) and may contain useful information on fundamental physics. In an effort to

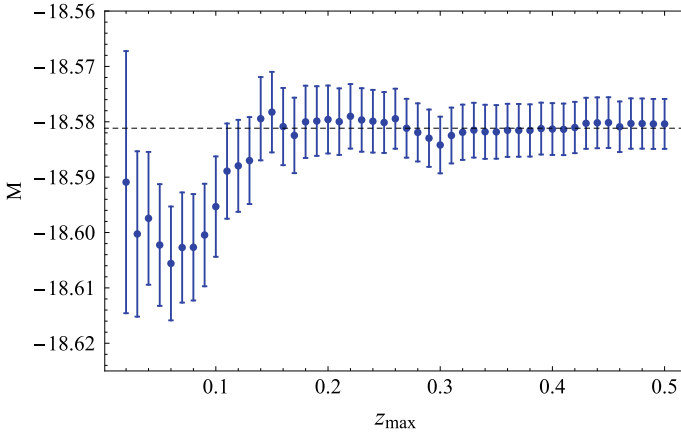


Fig. 33.8 Evolution of the absolute magnitude M as a function of the cutoff z_{max} . We have set $h = 1$ and thus the value of M is shifted compared to its usual value of $M = -19.3$

identify such evolution we minimise χ^2 with respect to the parameter M with fixed background corresponding to the best fit Λ CDM $H(z)$ as obtained from the full Pantheon dataset with M marginalization (we fix $w = -1$ and $\Omega_{m0} = 0.28$ [137] and set $h = 1$ for simplicity). In this context, we identify the best fit value and 1σ error of M for various subsets of the full Pantheon dataset. In Fig. 33.8 we show the best fit absolute magnitude M using subsamples of the Pantheon dataset in the redshift range $z \in [0.01, z_{max}]$. The 1σ range for the M parameter for various cutoffs z_{max} is also shown.

It is clear from Fig. 33.8 that low redshift data in the redshift range $z \in [0.01, 0.1]$ seem to favour a value M smaller than its best fit asymptotic value based on the full dataset ($z_{max} = 2.3$) at a level of about 2σ . At redshifts $z > 0.2$, M approaches its asymptotic value (dashed line). Our results are consistent with the analysis of Ref. [151], where the best fit parameters of Ω_{m0} and H_0 were investigated as a function of the redshift cutoff z_{max} . In agreement with our results it was found that the low z Pantheon data appear to have interesting features, which may indicate the presence of either systematics or new physics.

In Fig. 33.9 (left panel) we show the 100-point moving best fit value of M along with its 1σ errors. To construct this plot we rank the Pantheon datapoints from lowest to highest redshift. We start with the first 100 datapoints (lowest redshift points 1 to 100) and use them to obtain the best fit value of M (assuming the fixed Λ CDM background) with its 1σ error. The corresponding z coordinate of this point is the mean redshift of the first 100 points. The i th point is obtained by repeating the above procedure for the datapoints from i to $i + 100$.

Using the best fit value of M obtained from each 100-point subsample, we can calculate μ using Eq. (33.21) (right panel of Fig. 33.9 setting M_0 equal to the best fit value of M obtained from the full Pantheon dataset). Clearly, an oscillating effect is evident for the absolute magnitude M at low z , that is eased at high redshifts. The

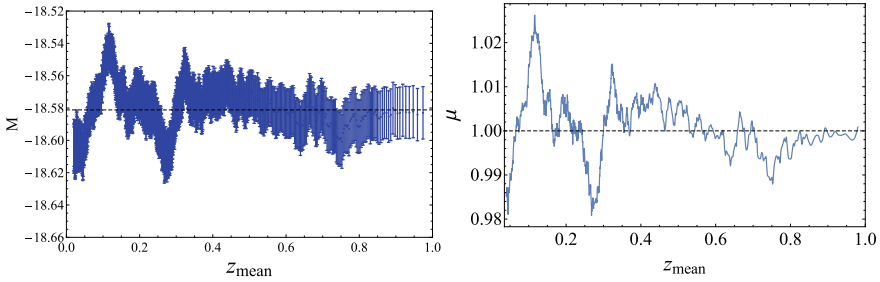


Fig. 33.9 Left Panel: Variation of the absolute magnitude M as a function of z_{mean} for 100 point Pantheon subsamples. Right Panel: The corresponding variation of μ as a function of z_{mean} for 100 datapoint Pantheon subsamples

same oscillating effect was also observed in Refs. [45, 84, 152], where a binning method was used instead.

The absolute magnitude M is degenerate with h . Therefore, the value of h obtained under the assumption of a constant M would not be the same as the value of h that would be obtained if M was allowed to evolve. In particular, using the “Hubble constant free” luminosity distance, that is defined as [153]

$$D_L(z) = \frac{H_0 d_L(z)}{c}, \quad (33.36)$$

we can rewrite Eq. (33.33) as [153]

$$m_{th}(z) = M + 5 \log_{10}(D_L(z)) + 5 \log_{10}\left(\frac{c/H_0}{1 \text{ Mpc}}\right) + 25. \quad (33.37)$$

In terms of h and taking into account the possible evolution of $\mu(z)$,² Eq. (33.37) takes the form

$$m_{th}(z) = M_0 + \frac{15}{4} \log_{10}(\mu(z)) + 5 \log_{10}(D_L(z)) - 5 \log_{10}(h) + 42.38. \quad (33.38)$$

Using Eq. (33.38) it is easy to show that a change of μ by a small amount $\Delta\mu$ around $\mu = 1$ is equivalent to a small change of h by

$$\Delta h = -\frac{3}{4} h \Delta\mu. \quad (33.39)$$

Thus, a decrease of μ at low z ($\Delta\mu < 0$) is equivalent to an increase of h by Δh compared to the true value of h . The value of $\Delta\mu \simeq -2 \times 10^{-2}$ indicated in Fig. 33.9

² The μ here is the evolving normalized Newton’s constant and should not be confused with the distance modulus.

could be interpreted as a shift of h by about 1.5% if μ was assumed fixed to 1. This artificial increase of h is in the right direction but does not appear to be enough to explain a tension of about 8% between the value indicated by the CMB and the value indicated by the SNIa sample. We stress, however, that the above analysis is heuristic and a more detailed analysis is required to include the possible effects of a varying μ in the derivation of H_0 from SNIa. In particular, the effects on Cepheid period-luminosity relation, used in the determination of H_0 have not been taken into account, the effects of strong gravity in the interior of the progenitor stars have been ignored and the background cosmology has been assumed fixed to Λ CDM. These effects should be taken into account in a more complete and detailed analysis.

33.3 Constraints on Evolving G_{eff} from Low l CMB Spectrum and the ISW Effect

As stated in the previous sections an evolving Newton's constant $\mu(z)$ would help resolve the weak growth and the H_0 tensions. However, such an evolution would also affect [154] other dynamical probes, and in particular the low l (large scale) CMB angular power spectrum through the Integrated-Sachs Wolfe (ISW) effect created as the CMB photons travel through time varying gravitational potential that would be modified by the evolving $\mu(z)$. Any such modification is constrained by the Planck data. The questions that we address in this section are the following:

- What are the constraints imposed by the Planck CMB TT power spectrum data on the parameter g_a of the parametrisation (33.19), assuming a fixed slip parameter to its GR value $\eta = 1$?
- Are these constraints consistent with the value of g_a required to resolve the weak growth tension?

In order to address these questions we use the 2019 version [155] of MGCAMB [156, 157], which is a modified version of the CAMB code [158], that it is designed to produce the CMB spectrum in the context of modified gravity theories with a given background model $H(z)$ and a given scale dependent evolution of μ and η . We fix $H(z)$ to Planck15/ Λ CDM, since the Planck18 likelihood chains that are implemented in COSMOMC and MGCOSMOMC are not yet publicly available, $\eta = 1$ and for $\mu(z)$ we use the parametrisation (33.19). The values of the parameters for the Planck15/ Λ CDM model are shown in Table 33.2.

The predicted form of the CMB angular power spectrum for various values of g_a is shown in Fig. 33.10 along with the corresponding Planck datapoints.

As we can see, the low- l Planck data do not allow significant variations in the parameter g_a and imply strong constraints on it. These constraints can be made precise using MGCOSMOMC [156, 157], the 2019 modified version [155] of the COSMOMC code [159]. Allowing variation of the parameters (Ω_{m0} , σ_8 , g_a) while fixing the rest to their Planck15/ Λ CDM values, we obtain the parameter contour constraints shown in Fig. 33.11.

Table 33.2 Planck15/ Λ CDM parameters values from Ref. [7] based on TT, TE, EE and lowP likelihoods. Notice that σ_8 is larger for the 2015 data release, which implies a stronger σ_8 tension that the Planck18/ Λ CDM best fit model

Parameter	Planck15/ Λ CDM [7]
$\Omega_b h^2$	0.02225 ± 0.00016
$\Omega_c h^2$	0.1198 ± 0.0015
n_s	0.9645 ± 0.0049
H_0	67.27 ± 0.66
Ω_{m0}	0.3156 ± 0.0091
w	-1
σ_8	0.831 ± 0.013

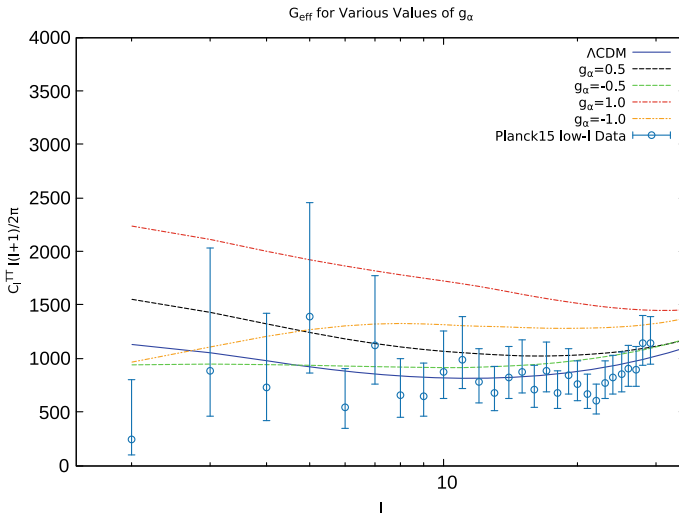


Fig. 33.10 The theoretically predicted form of the CMB power spectrum for a Planck15/ Λ CDM background in the context of a varying μ cosmology described by Eq. (33.19) for various values of g_a (obtained using MGCAMB)

Clearly, even though negative values of g_a are mildly favoured and are consistent with the small μ variation implied by the Pantheon SNIa data of the previous section, this parameter is constrained to be larger than -0.1 at a 3σ level. This range is barely overlapping with the 2σ range of g_a indicated by the compilation of the RSD growth data shown in Fig. 33.12. Thus, as pointed out also in previous studies [25], the low l CMB spectrum strongly constrains the evolution of μ in the context of the parametrisation (33.19) and implies that additional parameters and/or systematic effects are required for the resolution of the weak growth tension (e.g., the extension of the Λ CDM $H(z)$ to w CDM or the introduction of a sterile massive neutrino).

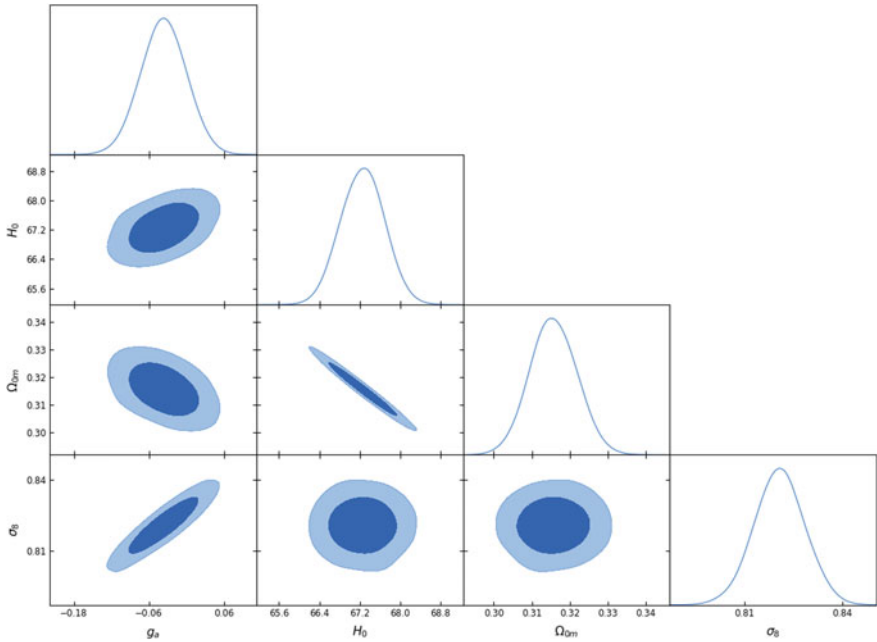


Fig. 33.11 The $1\sigma - 2\sigma$ contour ranges of cosmological parameters in the context of the parametrisation (33.19), using the Planck15/ Λ CDM data and setting $n = 2$

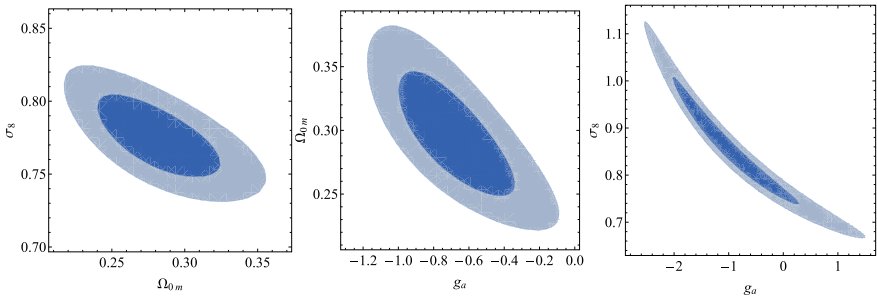


Fig. 33.12 The $1\sigma - 2\sigma$ parameter constraints in the context of an evolving μ described by the parametrisation (33.19) with $n = 2$. The full RSD data compilation of Ref. [26] was used. The third parameter in each plot was fixed to the corresponding Planck15/ Λ CDM. Notice the strong indication for weaker gravity at low z whose magnitude is marginally consistent with the corresponding indication from CMB data (Fig. 33.11)

33.4 Conclusions

Assuming a Planck/ Λ CDM background expansion $H(z)$ and fixing the slip parameter η to unity, we have investigated the constraints on a possible evolution of Newton’s constant expressed through the parameter μ using three observational probes: large

RSD data compilations, the Pantheon SNIa distance indicators and the TT CMB angular power spectrum from the Planck mission. We have shown that all three probes mildly favour a Newton's constant that is weaker at low z compared to GR. For RSD data this trend is at the $2 - 3\sigma$ level at $z < 0.3$, for SNIa it is at about 2σ at $z < 0.1$ and for the CMB it is at less than 1σ . In the case of RSD and CMB data we have assumed a specific parametrisation that respects the Solar System and nucleosynthesis constraints while reducing to GR at $z = 0$ and at high z . The magnitude of suggested and allowed variation of μ is much smaller for the SNIa and CMB data ($1 - 2\%$) compared to the corresponding magnitude suggested by the RSD data (about 50%). This inconsistency suggests that a variation of Newton's constant in the context of a modified gravity scenario for the parametrisation and the background considered may not by itself be able to explain the weak growth tension indicated by dynamical observational probes.

The simultaneous mild indication for weaker gravity at low z by independent probes suggests the more careful investigation of the scenario of an evolving Newton's constant in the context of different μ and η parametrisations, different $H(z)$ backgrounds and further dynamical observational probes. Such probes may include dynamical probes such as updated RSD data, WL and CC, as well as geometrical probes including CMB spectrum peaks, BAO and updated SNIa datasets.

The difficulty of viable modified gravity theories ($f(R)$ and scalar-tensor, Horndeski and beyond Horndeski) to provide a weaker gravity at low redshifts is an interesting point that may be used as a powerful discriminator among modified gravity theories.

References

1. S.M. Carroll, The Cosmological constant. *Living Rev. Rel.* **4**, 1 (2001). [arxiv:astro-ph/0004075](#)
2. Supernova Search Team Collaboration, A.G. Riess et al., Observational evidence from supernovae for an accelerating universe and a cosmological constant. *Astron. J.* **116**, 1009–1038 (1998). [arxiv:astro-ph/9805201](#)
3. Supernova Cosmology Project Collaboration, S. Perlmutter et al., Measurements of Ω and Λ from 42 high redshift supernovae. *Astrophys. J.* **517**, 565–586 (1999). [arxiv:astro-ph/9812133](#)
4. S.D.S.S. Collaboration, M. Betoule et al., Improved cosmological constraints from a joint analysis of the SDSS-II and SNLS supernova samples. *Astron. Astrophys.* **568**, A22 (2014). [arXiv:1401.4064](#)
5. D.M. Scolnic et al., The complete light-curve sample of spectroscopically confirmed SNIa from Pan-STARRS1 and cosmological constraints from the combined pantheon sample. *Astrophys. J.* **859**(2), 101 (2018). [arXiv:1710.00845](#)
6. W.M.A.P. Collaboration, G. Hinshaw et al., Nine-year Wilkinson microwave anisotropy probe (WMAP) observations: cosmological parameter results. *Astrophys. J. Suppl.* **208**, 19 (2013). [arXiv:1212.5226](#)
7. Planck Collaboration, P.A.R. Ade et al., Planck 2015 results. XIII. Cosmological parameters. *Astron. Astrophys.* **594**, A13 (2016). [arXiv:1502.01589](#)
8. Planck Collaboration, N. Aghanim et al., Planck 2018 results. VI. Cosmological parameters. [arXiv:1807.06209](#)

9. É. Aubourg et al., Cosmological implications of baryon acoustic oscillation measurements. *Phys. Rev. D* **92**(12), 123516 (2015). [arXiv:1411.1074](#)
10. BOSS Collaboration, S. Alam et al., The clustering of galaxies in the completed SDSS-III Baryon oscillation spectroscopic survey: cosmological analysis of the DR12 galaxy sample. *Mon. Not. Roy. Astron. Soc.* **470**(3), 2617–2652 (2017). [arXiv:1607.03155](#)
11. D.S.D.D. Collaboration, E. Rozo et al., Cosmological constraints from the SDSS maxBCG cluster catalog. *Astrophys. J.* **708**, 645–660 (2010). [arXiv:0902.3702](#)
12. D. Rapetti, S.W. Allen, A. Mantz, H. Ebeling, Constraints on modified gravity from the observed X-ray luminosity function of galaxy clusters. *Mon. Not. Roy. Astron. Soc.* **400**, 699 (2009). [arXiv:0812.2259](#)
13. Planck Collaboration, P.A.R. Ade et al., Planck 2015 results. XXIV. Cosmology from Sunyaev-Zeldovich cluster counts. *Astron. Astrophys.* **594**, A24 (2016). [arXiv:1502.01597](#)
14. S.P.T. Collaboration, S. Bocquet et al., Mass calibration and cosmological analysis of the SPT-SZ galaxy cluster sample using velocity dispersion σ_v and X-ray Y_X measurements. *Astrophys. J.* **799**(2), 214 (2015). [arXiv:1407.2942](#)
15. E.J. Ruiz, D. Huterer, Testing the dark energy consistency with geometry and growth. *Phys. Rev. D* **91**, 063009 (2015). [arXiv:1410.5832](#)
16. H. Hildebrandt et al., KiDS-450: cosmological parameter constraints from tomographic weak gravitational lensing. *Mon. Not. Roy. Astron. Soc.* **465**, 1454 (2017). [arXiv:1606.05338](#)
17. S. Joudaki et al., KiDS-450 + 2dFLenS: cosmological parameter constraints from weak gravitational lensing tomography and overlapping redshift-space galaxy clustering. *Mon. Not. Roy. Astron. Soc.* **474**(4), 4894–4924 (2018). [arXiv:1707.06627](#)
18. DES Collaboration, M.A. Troxel et al., Dark Energy Survey Year 1 results: Cosmological constraints from cosmic shear. *Phys. Rev. D* **98**(4), 043528 (2018). [arXiv:1708.01538](#)
19. F. Köhlinger et al., KiDS-450: the tomographic weak lensing power spectrum and constraints on cosmological parameters. *Mon. Not. Roy. Astron. Soc.* **471**(4), 4412–4435 (2017). [arXiv:1706.02892](#)
20. DES Collaboration, T.M.C. Abbott et al., Dark Energy Survey year 1 results: cosmological constraints from galaxy clustering and weak lensing. *Phys. Rev. D* **98**(4), 043526 (2018). [arXiv:1708.01530](#)
21. DES Collaboration, T.M.C. Abbott et al., Dark energy survey year 1 results: constraints on extended cosmological models from galaxy clustering and weak lensing. *Phys. Rev. D* **99**(12), 123505 (2019). [arXiv:1810.02499](#)
22. E. Macaulay, I.K. Wehus, H.K. Eriksen, Lower growth rate from recent redshift space distortion measurements than expected from Planck. *Phys. Rev. Lett.* **111**(16), 161301 (2013). [arXiv:1303.6583](#)
23. A. Johnson, C. Blake, J. Dossett, J. Koda, D. Parkinson, S. Joudaki, Searching for modified gravity: scale and redshift dependent constraints from galaxy peculiar velocities. *Mon. Not. Roy. Astron. Soc.* **458**(3), 2725–2744 (2016). [arXiv:1504.06885](#)
24. S. Basilakos, S. Nesseris, Testing Einstein’s gravity and dark energy with growth of matter perturbations: indications for new physics? *Phys. Rev. D* **94**(12), 123525 (2016). [arXiv:1610.00160](#)
25. S. Nesseris, G. Pantazis, L. Perivolaropoulos, Tension and constraints on modified gravity parametrizations of $G_{\text{eff}}(z)$ from growth rate and Planck data. *Phys. Rev. D* **96**(2), 023542 (2017). [arXiv:1703.10538](#)
26. L. Kazantzidis, L. Perivolaropoulos, Evolution of the $f\sigma_8$ tension with the Planck 15/Λ CDM determination and implications for modified gravity theories. *Phys. Rev. D* **97**(10), 103503 (2018). [arXiv:1803.01337](#)
27. S. Nesseris, L. Perivolaropoulos, Crossing the phantom divide: theoretical implications and observational status. *JCAP* **0701**, 018 (2007). [arxiv:astro-ph/0610092](#)
28. S. Basilakos, S. Nesseris, L. Perivolaropoulos, Observational constraints on viable $f(R)$ parametrizations with geometrical and dynamical probes. *Phys. Rev. D* **87**(12), 123529 (2013). [arXiv:1302.6051](#)

29. P. Bull et al., Beyond Λ CDM: problems, solutions, and the road ahead. *Phys. Dark Univ.* **12**, 56–99 (2016). [arXiv:1512.05356](#)
30. G.A. Tammann, A. Sandage, B. Reindl, The expansion field: the value of H_0 . *Astron. Astrophys. Rev.* **15**, 289–331 (2008). [arXiv:0806.3018](#)
31. A.G. Riess, S. Casertano, W. Yuan, L.M. Macri, D. Scolnic, Large magellanic cloud cepheid standards provide a 1% foundation for the determination of the hubble constant and stronger evidence for physics beyond Λ CDM. *Astrophys. J.* **876**(1), 85 (2019). [arXiv:1903.07603](#)
32. A.G. Riess et al., A 2.4% determination of the local value of the hubble constant. *Astrophys. J.* **826**(1), 56 (2016). [arXiv:1604.01424](#)
33. B. Margalef-Bentabol, J. Margalef-Bentabol, J. Cepa, Evolution of the cosmological horizons in a concordance universe. *JCAP* **1212**, 035 (2012). [arXiv:1302.1609](#)
34. P. Zarrouk et al., The clustering of the SDSS-IV extended Baryon oscillation spectroscopic survey DR14 quasar sample: measurement of the growth rate of structure from the anisotropic correlation function between redshift 0.8 and 2.2. *Mon. Not. Roy. Astron. Soc.* **477**(2), 1639–1663 (2018). [arXiv:1801.03062](#)
35. J.E. Bautista et al., Measurement of baryon acoustic oscillation correlations at $z = 2.3$ with SDSS DR12 Ly α -Forests. *Astron. Astrophys.* **603**, A12 (2017). [arXiv:1702.00176](#)
36. A.G. Riess et al., New parallaxes of galactic cepheids from spatially scanning the hubble space telescope: implications for the hubble constant. *Astrophys. J.* **855**(2), 136 (2018). [arXiv:1801.01120](#)
37. D. Huterer, D.L. Shafer, Dark energy two decades after: observables, probes, consistency tests. *Rept. Prog. Phys.* **81**(1), 016901 (2018). [arXiv:1709.01091](#)
38. G. Efstathiou, H0 revisited. *Mon. Not. Roy. Astron. Soc.* **440**(2), 1138–1152 (2014). [arXiv:1311.3461](#)
39. W. Cardona, M. Kunz, V. Pettorino, Determining H_0 with Bayesian hyper-parameters. *JCAP* **1703**(03), 056 (2017). [arXiv:1611.06088](#)
40. B.R. Zhang, M.J. Childress, T.M. Davis, N.V. Karpenka, C. Lidman, B.P. Schmidt, M. Smith, A blinded determination of H_0 from low-redshift Type Ia supernovae, calibrated by Cepheid variables. *Mon. Not. Roy. Astron. Soc.* **471**(2), 2254–2285 (2017). [arXiv:1706.07573](#)
41. S.H. Suyu et al., Two accurate time-delay distances from strong lensing: implications for cosmology. *Astrophys. J.* **766**, 70 (2013). [arXiv:1208.3311](#)
42. J.G. Sorce, R.B. Tully, H.M. Courtois, The mid-infrared tully-fisher relation: calibration of the type ia supernova scale and H_0 . *Astrophys. J.* **758**, L12 (2012)
43. G.A. Tammann, B. Reindl, The luminosity of supernovae of type Ia from TRGB distances and the value of H_0 . *Astron. Astrophys.* **549**, A136 (2013). [arXiv:1208.5054](#)
44. H.-Y. Wu, D. Huterer, Sample variance in the local measurements of the Hubble constant. *Mon. Not. Roy. Astron. Soc.* **471**(4), 4946–4955 (2017). [arXiv:1706.09723](#)
45. L. Kazantzidis, L. Perivolaropoulos, Hints of a local matter underdensity or modified gravity in the low z Pantheon data. *Phys. Rev. D* **102**(2), 023520 (2020). [arXiv:2004.02155](#)
46. W. Yang, S. Pan, E. Di Valentino, E.N. Saridakis, S. Chakraborty, Observational constraints on one-parameter dynamical dark-energy parametrizations and the H_0 tension. *Phys. Rev. D* **99**(4), 043543 (2019). [arXiv:1810.05141](#)
47. W. Yang, S. Pan, A. Paliathanasis, S. Ghosh, Y. Wu, Observational constraints of a new unified dark fluid and the H_0 tension. [arXiv:1904.10436](#)
48. E. Belgacem, Y. Dirian, S. Foffa, M. Maggiore, Nonlocal gravity. Conceptual aspects and cosmological predictions. *JCAP* **1803**(03), 002 (2018). [arXiv:1712.07066](#)
49. G. Alestas, L. Kazantzidis, L. Perivolaropoulos, H_0 tension, Phantom dark energy and cosmological parameter degeneracies. *Phys. Rev. D* **101**(12), 123516 (2020). [arXiv:2004.08363](#)
50. K.L. Pandey, T. Karwal, S. Das, Alleviating the H_0 and σ_8 anomalies with a decaying dark matter model. [arXiv:1902.10636](#)
51. K. Vattis, S.M. Koushiappas, A. Loeb, Late universe decaying dark matter can relieve the H_0 tension. [arXiv:1903.06220](#)
52. M.-M. Zhao, D.-Z. He, J.-F. Zhang, X. Zhang, Search for sterile neutrinos in holographic dark energy cosmology: reconciling Planck observation with the local measurement of the Hubble constant. *Phys. Rev. D* **96**(4), 043520 (2017). [arXiv:1703.08456](#)

53. V.V. Luković, B.S. Haridasu, N. Vittorio, Cosmological constraints from low-redshift data. *Found. Phys.* **48**(10), 1446–1485 (2018). [arXiv:1801.05765](#)
54. J.L. Bernal, L. Verde, A.G. Riess, The trouble with H_0 . *JCAP* **1610**(10), 019 (2016). [arXiv:1607.05617](#)
55. S. Basilakos, S. Nesseris, Conjoined constraints on modified gravity from the expansion history and cosmic growth. *Phys. Rev. D* **96**(6), 063517 (2017). [arXiv:1705.08797](#)
56. F. Skara, L. Perivolaropoulos, Tension of the E_G statistic and redshift space distortion data with the Planck - Λ CDM model and implications for weakening gravity. *Phys. Rev. D* **101**(6), 063521 (2020). [arXiv:1911.10609](#)
57. M. Ishak, Testing general relativity in cosmology. *Living Rev. Rel.* **22**(1), 1 (2019). [arXiv:1806.10122](#)
58. A. Pourtsidou, T. Tram, Reconciling CMB and structure growth measurements with dark energy interactions. *Phys. Rev. D* **94**(4), 43518 (2016). [arXiv:1604.04222](#)
59. B.J. Barros, L. Amendola, T. Barreiro, N.J. Nunes, Coupled quintessence with a Λ CDM background: removing the σ_8 tension. *JCAP* **1901**(01), 007 (2019). [arXiv:1802.09216](#)
60. S. Camera, M. Martinelli, D. Bertacca, Does quartessence ease cosmic tensions? *Phys. Dark Univ.* **23**, 100247 (2019). [arXiv:1704.06277](#)
61. F. Melia, The linear growth of structure in the $R_h = ct$ universe. *Mon. Not. Roy. Astron. Soc.* **464**(2), 1966–1976 (2017). [arXiv:1609.08576](#)
62. G. Lambiase, S. Mohanty, A. Narang, P. Parashari, Testing dark energy models in the light of σ_8 tension. *Eur. Phys. J. C* **79**(2), 141 (2019). [arXiv:1804.07154](#)
63. J. Ooba, B. Ratra, N. Sugiyama, Planck 2015 constraints on spatially-flat dynamical dark energy models. [arXiv:1802.05571](#)
64. S. Joudaki et al., KiDS-450: testing extensions to the standard cosmological model. *Mon. Not. Roy. Astron. Soc.* **471**(2), 1259–1279 (2017). [arXiv:1610.04606](#)
65. A. Gomez-Valent, J. Sola, Relaxing the σ_8 -tension through running vacuum in the Universe. *EPL* **120**(3), 39001 (2017). [arXiv:1711.00692](#)
66. A. Gómez-Valent, J. Solà Peracaula, Density perturbations for running vacuum: a successful approach to structure formation and to the σ_8 -tension. *Mon. Not. Roy. Astron. Soc.* **478**(1), 126–145 (2018). [arXiv:1801.08501](#)
67. A. Diaz Rivero, V. Miranda, C. Dvorkin, Observable predictions for massive-neutrino cosmologies with model-independent dark energy. [arXiv:1903.03125](#)
68. E. Di Valentino, S. Bridle, Exploring the tension between current cosmic microwave background and cosmic shear data. *Symmetry* **10**(11), 585 (2018)
69. D. Wang, Dark Energy Survey Year 1: Exploring New Physics Beyond the Standard Cosmology. [arXiv:1904.00657](#)
70. S. Tsujikawa, Matter density perturbations and effective gravitational constant in modified gravity models of dark energy. *Phys. Rev. D* **76**, 023514 (2007). [arXiv:0705.1032](#)
71. R. Gannouji, L. Kazantzidis, L. Perivolaropoulos, D. Polarski, Consistency of modified gravity with a decreasing $G_{\text{eff}}(z)$ in a Λ CDM background. *Phys. Rev. D* **98**(10), 104044 (2018). [arXiv:1809.07034](#)
72. R. D’Agostino, O. Luongo, Growth of matter perturbations in nonminimal teleparallel dark energy. *Phys. Rev. D* **98**(12), 124013 (2018). [arXiv:1807.10167](#)
73. M. Gonzalez-Espinoza, G. Otalora, J. Saavedra, N. Videla, Growth of matter overdensities in non-minimal torsion-matter coupling theories. *Eur. Phys. J. C* **78**(10), 799 (2018). [arXiv:1808.01941](#)
74. J. Kennedy, L. Lombriser, A. Taylor, Reconstructing Horndeski theories from phenomenological modified gravity and dark energy models on cosmological scales. *Phys. Rev. D* **98**(4), 044051 (2018). [arXiv:1804.04582](#)
75. E.V. Linder, No slip gravity. *JCAP* **1803**(03), 005 (2018). [arXiv:1801.01503](#)
76. R. Gannouji, L. Perivolaropoulos, D. Polarski, F. Skara, Weak gravity on a Λ CDM background. [arXiv:2011.01517](#)
77. G. D’Amico, Z. Huang, M. Mancarella, F. Vernizzi, Weakening gravity on redshift-survey scales with kinetic matter mixing. *JCAP* **1702**, 014 (2017). [arXiv:1609.01272](#)

78. L. Pogosian, P.S. Corasaniti, C. Stephan-Otto, R. Crittenden, R. Nichol, Tracking dark energy with the ISW effect: short and long-term predictions. *Phys. Rev. D* **72**, 103519 (2005). [arXiv:astro-ph/0506396](#)
79. S. Ho, C. Hirata, N. Padmanabhan, U. Seljak, N. Bahcall, Correlation of CMB with large-scale structure: I. ISW tomography and cosmological implications. *Phys. Rev. D* **78**, 043519 (2008). [arXiv:0801.0642](#)
80. L. Amendola, P.S. Corasaniti, F. Occhionero, Time variability of the gravitational constant and type Ia supernovae. [arXiv:astro-ph/9907222](#)
81. E. Gaztanaga, E. Garcia-Berro, J. Isern, E. Bravo, I. Dominguez, Bounds on the possible evolution of the gravitational constant from cosmological type Ia supernovae. *Phys. Rev. D* **65**, 023506 (2002). [arXiv:astro-ph/0109299](#)
82. S. Nesseris, L. Perivolaropoulos, Evolving newton's constant, extended gravity theories and snia data analysis. *Phys. Rev. D* **73**, 103511 (2006). [arXiv:astro-ph/0602053](#)
83. B.S. Wright, B. Li, Type Ia supernovae, standardizable candles, and gravity. *Phys. Rev. D* **97**(8), 083505 (2018). [arXiv:1710.07018](#)
84. D. Sapone, S. Nesseris, C.A. Bengaly, Is there any measurable redshift dependence on the SN Ia absolute magnitude? [arXiv:2006.05461](#)
85. E. Bertschinger, P. Zumin, Distinguishing modified gravity from dark energy. *Phys. Rev. D* **78**, 024015 (2008). [arXiv:0801.2431](#)
86. E. Di Valentino, A. Melchiorri, J. Silk, Cosmological hints of modified gravity? *Phys. Rev. D* **93**(2), 023513 (2016). [arXiv:1509.07501](#)
87. Planck Collaboration, P.A.R. Ade et al., Planck 2015 results. XIV. Dark energy and modified gravity. *Astron. Astrophys.* **594**, A14 (2016). [arXiv:1502.01590](#)
88. T. Baker, P.G. Ferreira, C.D. Leonard, M. Motta, New gravitational scales in cosmological surveys. *Phys. Rev. D* **90**(12), 124030 (2014). [arXiv:1409.8284](#)
89. J. Li, G.-B. Zhao, Cosmological tests of gravity with the latest observations. *Astrophys. J.* **871**(2), 196 (2019). [arXiv:1806.05022](#)
90. J.M. Bardeen, Gauge invariant cosmological perturbations. *Phys. Rev. D* **22**, 1882–1905 (1980)
91. C.-P. Ma, E. Bertschinger, Cosmological perturbation theory in the synchronous and conformal Newtonian gauges. *Astrophys. J.* **455**, 7–25 (1995). [arXiv:astro-ph/9506072](#)
92. G. Esposito-Farese, D. Polarski, Scalar tensor gravity in an accelerating universe. *Phys. Rev. D* **63**, 063504 (2001). [arXiv:gr-qc/0009034](#)
93. D. Huterer et al., Growth of cosmic structure: probing dark energy beyond expansion. *Astropart. Phys.* **63**, 23–41 (2015). [arXiv:1309.5385](#)
94. L. Pogosian, A. Silvestri, K. Koyama, G.-B. Zhao, How to optimally parametrize deviations from general relativity in the evolution of cosmological perturbations? *Phys. Rev. D* **81**, 104023 (2010). [arXiv:1002.2382](#)
95. L. Perenon, J. Bel, R. Maartens, A. de la Cruz-Dombriz, Optimising growth of structure constraints on modified gravity. [arXiv:1901.11063](#)
96. I. Tereno, E. Semboloni, T. Schrabback, COSMOS weak-lensing constraints on modified gravity. *Astron. Astrophys.* **530**, A68 (2011). [arXiv:1012.5854](#)
97. W. Hu, I. Sawicki, Models of $f(R)$ cosmic acceleration that evade solar-system tests. *Phys. Rev. D* **76**, 064004 (2007). [arXiv:0705.1158](#)
98. A.A. Starobinsky, Disappearing cosmological constant in $f(R)$ gravity. *JETP Lett.* **86**, 157–163 (2007). [arXiv:0706.2041](#)
99. S. Tsujikawa, Possibility of realizing weak gravity in redshift space distortion measurements. *Phys. Rev. D* **92**(4), 044029 (2015). [arXiv:1505.02459](#)
100. D. Polarski, A.A. Starobinsky, H. Giacomini, When is the growth index constant? *JCAP* **1612**(12), 037 (2016). [arXiv:1610.00363](#)
101. LIGO Scientific, Virgo Collaboration, B.P. Abbott et al., GW170817: observation of gravitational waves from a binary neutron star inspiral. *Phys. Rev. Lett.* **119**(16), 161101 (2017). [arXiv:1710.05832](#)

102. R. Gannouji, D. Polarski, A. Ranquet, A.A. Starobinsky, Scalar-tensor models of normal and phantom dark energy. *JCAP* **0609**, 016 (2006). [arXiv:astro-ph/0606287](#)
103. S. Nesseris, L. Perivolaropoulos, The limits of extended quintessence. *Phys. Rev. D* **75**, 023517 (2007). [arXiv:astro-ph/0611238](#)
104. J. Muller, J.G. Williams, S.G. Turyshev, Lunar laser ranging contributions to relativity and geodesy. *Astrophys. Space Sci. Libr.* **349**, 457–472 (2008). [arXiv:gr-qc/0509114](#)
105. E.V. Pitjeva, N.P. Pitjev, Relativistic effects and dark matter in the Solar system from observations of planets and spacecraft. *Mon. Not. Roy. Astron. Soc.* **432**, 3431 (2013). [arXiv:1306.3043](#)
106. R. Gannouji, B. Moraes, D. Polarski, The growth of matter perturbations in f(R) models. *JCAP* **0902**, 034 (2009). [arXiv:0809.3374](#)
107. A. Shafieloo, B. L’Huillier, A.A. Starobinsky, Falsifying Λ CDM: model-independent tests of the concordance model with eBOSS DR14Q and Pantheon. *Phys. Rev. D* **98**(8), 083526 (2018). [arXiv:1804.04320](#)
108. R. Gannouji, D. Polarski, Consistency of the expansion of the universe with density perturbations. *Phys. Rev. D* **98**(8), 083533 (2018). [arXiv:1805.08230](#)
109. S. Basilakos, F.K. Anagnostopoulos, Growth index of matter perturbations in the light of dark energy survey. [arXiv:1903.10758](#)
110. Z.-Y. Yin, H. Wei, Non-parametric reconstruction of growth index via Gaussian processes. *Sci. China Phys. Mech. Astron.* **62**(9), 999811 (2019). [arXiv:1808.00377](#)
111. L. Perivolaropoulos, L. Kazantzidis, Hints of modified gravity in cosmos and in the lab? *Int. J. Mod. Phys. D* **28**(05), 1942001 (2019). [arXiv:1904.09462](#)
112. C. Heymans et al., CFHTLenS: the Canada-France-Hawaii telescope lensing survey. *Mon. Not. Roy. Astron. Soc.* **427**, 146 (2012). [arXiv:1210.0032](#)
113. T. Erben et al., CFHTLenS: the Canada-France-Hawaii telescope lensing survey - imaging data and catalogue products. *Mon. Not. Roy. Astron. Soc.* **433**, 2545 (2013). [arXiv:1210.8156](#)
114. L. Kazantzidis, L. Perivolaropoulos, Work in progress
115. L. Kazantzidis, L. Perivolaropoulos, F. Skara, Constraining power of cosmological observables: blind redshift spots and optimal ranges. *Phys. Rev. D* **99**(6), 063537 (2019). [arXiv:1812.05356](#)
116. C. Alcock, B. Paczynski, An evolution free test for non-zero cosmological constant. *Nature* **281**, 358–359 (1979)
117. Planck Collaboration, P.A.R. Ade et al., Planck 2013 results. XX. Cosmology from Sunyaev–Zeldovich cluster counts. *Astron. Astrophys.* **571**, A20 (2014). [arXiv:1303.5080](#)
118. A. Vikhlinin et al., Chandra cluster cosmology project III: cosmological parameter constraints. *Astrophys. J.* **692**, 1060–1074 (2009). [arXiv:0812.2720](#)
119. J.L. Bernal, L. Verde, A.J. Cuesta, Parameter splitting in dark energy: is dark energy the same in the background and in the cosmic structures? *JCAP* **1602**(02), 059 (2016). [arXiv:1511.03049](#)
120. SPT Collaboration, J. Henning et al., Measurements of the temperature and E-mode polarization of the CMB from 500 square degrees of SPTpol data. *Astrophys. J.* **852**(2), 97 (2018). [arXiv:1707.09353](#)
121. M. Raveri, Are cosmological data sets consistent with each other within the Λ cold dark matter model? *Phys. Rev. D* **93**(4), 043522 (2016). [arXiv:1510.00688](#)
122. W. Lin, M. Ishak, Cosmological discordances: a new measure, marginalization effects, and application to geometry versus growth current data sets. *Phys. Rev. D* **96**(2), 023532 (2017). [arXiv:1705.05303](#)
123. B. Sagredo, J.S. Lefaurie, D. Sapone, Comparing dark energy models with hubble versus growth rate data. [arXiv:1808.05660](#)
124. R. Arjona, W. Cardona, S. Nesseris, Designing Horndeski and the effective fluid approach. [arXiv:1904.06294](#)
125. L. Amendola, R. Gannouji, D. Polarski, S. Tsujikawa, Conditions for the cosmological viability of f(R) dark energy models. *Phys. Rev. D* **75**, 083504 (2007). [arXiv:gr-qc/0612180](#)
126. B. Boisseau, G. Esposito-Farese, D. Polarski, A.A. Starobinsky, Reconstruction of a scalar tensor theory of gravity in an accelerating universe. *Phys. Rev. Lett.* **85**, 2236 (2000). [arXiv:gr-qc/0001066](#)

127. EUCLID Collaboration Collaboration, R. Laureijs et al., *Euclid Definition Study Report*. [arXiv:1110.3193](#)
128. L. Amendola et al., Cosmology and fundamental physics with the Euclid satellite. *Living Rev. Rel.* **21**(1), 2 (2018). [arXiv:1606.00180](#)
129. M.J. Jarvis, D. Bacon, C. Blake, M.L. Brown, S.N. Lindsay, A. Raccanelli, M. Santos, D. Schwarz, *Cosmology with SKA Radio Continuum Surveys*. [arXiv:1501.03825](#)
130. D. Bacon et al., Synergy between the large synoptic survey telescope and the square kilometre array. *PoS AASKA14*, 145 (2015). [arXiv:1501.03977](#)
131. LSST Collaboration, P. Marshall et al., *Science-Driven Optimization of the LSST Observing Strategy*. [arXiv:1708.04058](#)
132. F.R. Bouchet et al., *CORÉ: Cosmic Origins Explorer - A White Paper*
133. DESI Collaboration, A. Aghamousa et al., *The DESI Experiment Part I: Science, Targeting, and Survey Design*. [arXiv:1611.00036](#)
134. DESI Collaboration, A. Aghamousa et al., *The DESI Experiment Part II: Instrument Design*. [arXiv:1611.00037](#)
135. D. Spergel et al., *Wide-Field Infrared Survey Telescope-Astrophysics Focused Telescope Assets WFIRST-AFTA 2015 Report*. [arXiv:1503.03757](#)
136. R. Hounsell et al., Simulations of the WFIRST supernova survey and forecasts of cosmological constraints. *Astrophys. J.* **867**(1), 23 (2017). [arXiv:1702.01747](#)
137. D. Scolnic et al., Systematic uncertainties associated with the cosmological analysis of the first pan-STARRS1 type Ia supernova sample. *Astrophys. J.* **795**(1), 45 (2014). [arXiv:1310.3824](#)
138. A.G. Riess et al., BV RI light curves for 22 type Ia supernovae. *Astron. J.* **117**, 707–724 (1999). [arXiv:astro-ph/9810291](#)
139. S. Jha et al., Ubvri light curves of 44 type Ia supernovae. *Astron. J.* **131**, 527–554 (2006). [arXiv:astro-ph/0509234](#)
140. M. Hicken, P. Challis, S. Jha, R.P. Kirsher, T. Matheson, M. Modjaz, A. Rest, W.M. Wood-Vasey, CfA3: 185 type Ia supernova light curves from the CfA. *Astrophys. J.* **700**, 331–357 (2009). [arXiv:0901.4787](#)
141. M. Hicken et al., CfA4: light curves for 94 type Ia supernovae. *Astrophys. J. Suppl.* **200**, 12 (2012). [arXiv:1205.4493](#)
142. C. Contreras et al., The carnegie supernova project: first photometry data release of low-redshift type Ia supernovae. *Astron. J.* **139**, 519–539 (2010). [arXiv:0910.3330](#)
143. M.D. Stritzinger et al., The carnegie supernova project: second photometry data release of low-redshift type Ia supernovae. *Astron. J.* **142**, 156 (2011). [arXiv:1108.3108](#)
144. S.D.S.S. Collaboration, M. Sako et al., The data release of the sloan digital sky survey-II supernova survey. *Publ. Astron. Soc. Pac.* **130**(988), 064002 (2018). [arXiv:1401.3317](#)
145. R. Kessler et al., First-year sloan digital sky survey-II (SDSS-II) supernova results: hubble diagram and cosmological parameters. *Astrophys. J. Suppl.* **185**, 32–84 (2009). [arXiv:0908.4274](#)
146. S.N.L.S. Collaboration, M. Sullivan et al., SNLS3: constraints on dark energy combining the supernova legacy survey three year data with other probes. *Astrophys. J.* **737**, 102 (2011). [arXiv:1104.1444](#)
147. S.N.L.S. Collaboration, A. Conley et al., Supernova constraints and systematic uncertainties from the first 3 years of the supernova legacy survey. *Astrophys. J. Suppl.* **192**, 1 (2011). [arXiv:1104.1443](#)
148. A.G. Riess et al., New hubble space telescope discoveries of type Ia supernovae at $z > 1$ narrowing constraints on the early behavior of dark energy. *Astrophys. J.* **659**, 98–121 (2007). [arXiv:astro-ph/0611572](#)
149. N. Suzuki, D. Rubin, C. Lidman, G. Aldering, R. Amanullah et al., The hubble space telescope cluster supernova survey: V. Improving the dark energy constraints above $z > 1$ and building an early-type-hosted supernova sample. *Astrophys. J.* **746**, 85 (2012). [arXiv:1105.3470](#)
150. R. Arjona, W. Cardona, S. Nesseris, Unraveling the effective fluid approach for $f(R)$ models in the subhorizon approximation. *Phys. Rev. D* **99**(4), 043516 (2019). [arXiv:1811.02469](#)
151. E.Ó. Colgáin, A hint of matter underdensity at low z ? *JCAP* **1909**, 006 (2019). [arXiv:1903.11743](#)

152. L. Kazantzidis, H. Koo, S. Nesseris, L. Perivolaropoulos, A. Shafieloo, Hints for possible low redshift oscillation around the best fit Λ CDM model in the expansion history of the universe. [arXiv:2010.03491](#)
153. S. Nesseris, L. Perivolaropoulos, Comparison of the legacy and gold snia dataset constraints on dark energy models. *Phys. Rev. D* **72**, 123519 (2005). [arXiv:astro-ph/0511040](#)
154. T. Giannantonio, M. Martinelli, A. Silvestri, A. Melchiorri, New constraints on parametrised modified gravity from correlations of the CMB with large scale structure. *JCAP* **1004**, 030 (2010). [arXiv:0909.2045](#)
155. A. Zucca, L. Pogosian, A. Silvestri, G.-B. Zhao, MGCAMB with massive neutrinos and dynamical dark energy. *JCAP* **2019**(05), 001 (2020). [arXiv:1901.05956](#)
156. A. Hojjati, L. Pogosian, G.-B. Zhao, Testing gravity with CAMB and CosmoMC. *JCAP* **1108**, 005 (2011). [arXiv:1106.4543](#)
157. G.-B. Zhao, L. Pogosian, A. Silvestri, J. Zylberberg, Searching for modified growth patterns with tomographic surveys. *Phys. Rev. D* **79**, 083513 (2009). [arXiv:0809.3791](#)
158. A. Lewis, A. Challinor, A. Lasenby, Efficient computation of CMB anisotropies in closed FRW models. *Astrophys. J.* **538**, 473–476 (2000). [arXiv:astro-ph/9911177](#)
159. A. Lewis, S. Bridle, Cosmological parameters from CMB and other data: a Monte Carlo approach. *Phys. Rev. D* **66**, 103511 (2002). [arXiv:astro-ph/0205436](#)

Chapter 34

Testing Gravity with Standard Sirens: Challenges and Opportunities



Jose María Ezquiaga

34.1 Gravitational Wave Propagation Beyond General Relativity

Gravitational wave (GW) astronomy presents promising opportunities to test gravity at new scales and regimes. Theories beyond General Relativity (GR) generically modify the emission, propagation and detection of GWs with respect to Einstein's gravity [1]. These modifications can be imprinted either in the phase, amplitude or polarisation of the GW. Among the possible probes, we will focus on tests of the propagation of GWs because they are clean (compared to effects in the emission) and precise (since small modification accumulate over large travel distances). For the interested reader in modifications of the strong gravity regime close to the merger of a compact binary, we refer to the recent roadmap [2].

The propagation of GWs in gravity theories beyond GR depends on the number of additional fields and the background in which they propagate. We will restrict to cosmological environments respecting the symmetries of Friedmann–Robertson–Walker (FRW) metrics. Conveniently, at leading order in perturbations over FRW backgrounds, the tensor modes coupled to matter h_{ij} only interact with other tensor perturbations t_{ij} . Assuming first that there are only the transverse-traceless polarisations h_{ij} , we can parametrise the modified cosmological GW evolution by

$$h''_{ij} + (2 + \nu)\mathcal{H}h'_{ij} + (c_g^2 k^2 + m_g^2 a^2)h_{ij} = 0. \quad (34.1)$$

GR corresponds to the limit in which $\nu = m_g = 0$ and $c_g = c$, so that GWs propagate at the speed of light and they are only affected by the Hubble friction (we are timing in conformal time η). However, the additional friction ν , the anomalous speed c_g and the effective mass m_g generically alter the GR prediction h_{ij}^{GR} by

J. M. Ezquiaga (✉)

NASA Einstein Fellow, Kavli Institute for Cosmological Physics and Enrico Fermi Institute,
The University of Chicago, Chicago, IL 60637, USA

$$h_{ij} \sim h_{ij}^{\text{GR}} \underbrace{e^{-\frac{1}{2} \int \nu \mathcal{H} d\eta}}_{\text{Affects amplitude}} \underbrace{e^{ik \int (c_g^2 - 1 + a^2 m_g^2 / k^2)^{1/2} d\eta}}_{\text{Affects phase}}. \quad (34.2)$$

Mainly, the additional friction will modify the amplitude, which affects the inferred GW luminosity distance d_L^{GW} , while the anomalous speed and the effective mass change the phase. In analogy with optics, these effects could be interpreted as arising from a dia-gravitational medium for GWs [3]. Note that we are assuming that there is not a modification in the emission in order to take the GR signal as an initial condition. For a compact binary coalescence, the wave-form h^{GR} depends at leading order on the chirp mass \mathcal{M}_c , the frequency f , the redshift z , the cosmic expansion history $H(z)$, the polarisation $+$, \times and the inclination angle ι by [4]¹

$$h_+^{\text{GR}} = |h^{\text{GR}}| \frac{1 + \cos^2 \iota}{2} \cos \Phi \quad \text{and} \quad h_\times^{\text{GR}} = |h^{\text{GR}}| \cos \iota \sin \Phi, \quad (34.3)$$

where Φ is the phase that depends on the time to coalescence and the chirp mass. The chirp amplitude $|h^{\text{GR}}|$ is given by

$$|h^{\text{GR}}| = \frac{4}{d_L^{\text{GR}}} \left(\frac{G \mathcal{M}_z}{c^2} \right)^{5/3} \left(\frac{\pi f}{c} \right)^{2/3}, \quad (34.4)$$

where \mathcal{M}_z is the redshifted chirp mass, $\mathcal{M}_z = (1+z)\mathcal{M}_c$, and the GW luminosity distance in GR is equal to the standard electromagnetic (EM) one, which is determined by the Hubble parameter,

$$d_L^{\text{GR}} = d_L^{\text{em}} = (1+z) \int_0^z \frac{c}{H(z)} dz. \quad (34.5)$$

Therefore, within GR, a measurement of d_L^{GW} directly contains information of the cosmic expansion history.

Whenever there are additional tensor modes t_{ij} the phenomenology enriches because now there could be mixings with the tensor modes coupled to matter h_{ij} . In analogy with neutrino physics, this would induce GW oscillations along the propagation. For instance, in the case in which there are interactions in the friction and in the mass terms, the propagation equations can be parametrised by [5]

$$\left[\frac{d^2}{d\eta^2} + 2 \begin{pmatrix} \mathcal{H} & -\alpha \\ \alpha & \mathcal{H} + 2\Delta\nu \end{pmatrix} \frac{d}{d\eta} + c^2 k^2 + m_g^2 a^2 \begin{pmatrix} 1 & -1 \\ -\tan^{-2} \theta_g & \tan^{-2} \theta_g \end{pmatrix} \right] \begin{pmatrix} h_{ij} \\ t_{ij} \end{pmatrix} = 0, \quad (34.6)$$

¹ The signal at the detector $h(t)$ also depends on the orientation (defined by two angles θ and ϕ) when tacking into account the antenna pattern functions $F_{+,\times}$, i.e. $h(t) = h_+(t)F_+(\theta, \phi) + h_\times(t)F_\times(\theta, \phi)$.

which is similar to (34.1) but promoting ν and m_g to matrices. Nonetheless, there could also be mixings in the velocities or the $+$ and \times polarisations could be affected differently, which we are not covering here (see [5]). It is important to note that the additional tensor modes could arise from extra dynamical metric fields such as in bigravity [6, 7], but also from effective configurations of vector fields with an internal symmetry [8, 9].

In broad terms, modifications of the cosmological propagation of GWs can induce frequency and redshift dependent deviations w.r.t. GR. Frequency-dependent phenomena are, for instance, the modified dispersion relation of an effective mass [10] or the modulation of the wave-form when there is a mass mixing [6, 7]. Conversely, redshift-dependent phenomena are the time delay produced by an anomalous speed or the modified luminosity distance. Frequency-dependent modifications can be constrained with GWs alone, while redshift-dependent ones require an independent determination of z to break the degeneracy with the theory parameters. In this contribution we will concentrate on redshift-dependent modifications. We will first present how GWs can become standard sirens in Sect. 34.2. Then, we will discuss how to constrain gravity theories with the GW speed, the luminosity distance and GW oscillations in Sects. 34.3, 34.4 and 34.5 respectively. We will conclude with the future prospects in Sect. 34.6.

34.2 Standard Sirens

A GW becomes a standard siren when it probes the cosmological evolution of the luminosity distance [11, 12]. From the amplitude of the GW of a compact binary (see 34.3–34.4), it is clear that d_L^{GW} is degenerate with the inclination angle. Moreover, since in the detector frame only redshifted masses are measured, the cosmological evolution of d_L^{GW} is degenerate with the redshift of the source, which is unknown a priori. The distance-inclination degeneracy can in principle be broken if the $+$ and \times polarisations can be distinguished. This requires at least a three detector network and a good sky localisation. Regarding the redshift identification, there are two main methods:

- *EM counterpart*: the first method entails an EM counterpart of the GW. The redshift is then obtained from the EM signal itself or from the host galaxy. Binary neutron stars (BNS) produce a short gamma-ray burst (sGRB) after the merger. sGRB have a beaming angle θ_j typically expected to be $\theta_j \leq 30^\circ$. This implies that, given the random orientation of the sources, both GW and EM signals will only be detected in a small fraction of events. Observing a bright afterglow or kilonovae [13] could increase the chances of detecting a counterpart. Of course, the key parameter for an efficient search is the localisation in the sky provided by the GW signal itself. This improves with higher signal-to-noise ratios (SNR) and with a network of ground-based detectors. BNS will be the primary source of standard sirens for LIGO-Virgo [14], although black-hole neutron star mergers may be relevant too

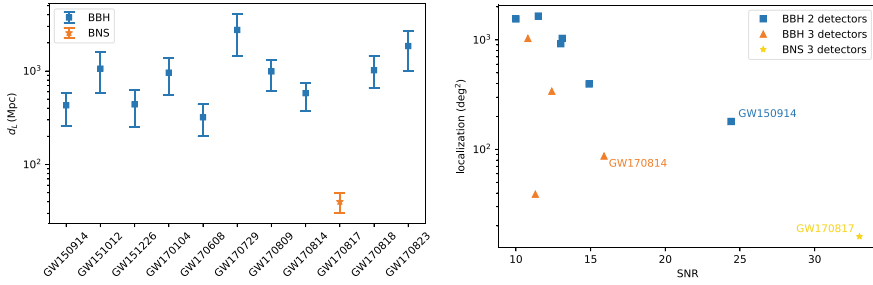


Fig. 34.1 On the left, luminosity distance d_L of the GW events reported by the LIGO-Virgo collaboration in runs O1-2 [26]. On the right, 90% credible localisation for the 11 events as a function of signal-to-noise ratio (SNR). We distinguish those events detected only with the two LIGO detectors and those that were found also by Virgo. For an updated list of all the candidate events in O3 not included in the figures see <https://gracedb.ligo.org/latest/>

[15]. Super massive black-holes (SMBHs) are thought to be good standard sirens for LISA [12].

- *Statistical method:* alternatively, we could associate every GW event with all the galaxies within the error box in the localisation and infer the cosmology [11, 16]. As more events accumulate, the true cosmology will statistically prevail. This method applies to all types of sources, including binary black-holes (BBH) which are the most common events and can be observed at further distances (see left panel of Fig. 34.1). BBH standard sirens are also known as dark sirens. For very loud events, there might be only few galaxies in the localisation box [17]. On the con side, this method relies on a complete galaxy catalogue.

When the binary involves neutron stars, there are also other possibilities to infer the redshift; see [18–20]. However, they entail a good knowledge of the population of neutron stars and their equation of state.

GW170817 has become the first GW event detected together with an EM counterpart [21]. The redshift, $z = 0.008^{+0.002}_{-0.003}$, was obtained identifying the host galaxy NGC4993 [22]. On the other hand, from the amplitude of the GW signal the luminosity distance was obtained, $d_L = 40^{+8}_{-14}$ Mpc. Assuming GR holds (34.5), the first standard siren measurement of the Hubble constant H_0 was performed [23]. The error was 14%, mainly caused by the uncertainty in the determination of the GW amplitude. Since the event had a large SNR with a precise localisation (see right panel of Fig. 34.1), the statistical method could be applied to obtain H_0 , although the error is significantly larger [24]. The statistical method has also been applied to a dark siren: GW170814, a three detector BBH event with good sky localisation [25].

34.3 The Speed of GWs

The speed of GWs is determined by the second-order action for the tensor perturbations, which depends on the underlying gravity theory and the background fields. The key quantity is the *effective metric* $\mathcal{G}^{\mu\nu}$ for the GWs, shaping the leading derivative interactions

$$\mathcal{L} \propto h_{\mu\nu} \mathcal{G}^{\alpha\beta} \nabla_\alpha \nabla_\beta h^{\mu\nu} = h_{\mu\nu} (\mathcal{C} \square + \mathcal{D}^{\alpha\beta} \nabla_\alpha \nabla_\beta) h^{\mu\nu}. \quad (34.7)$$

GR predicts that the effective metric for the GWs is equal to the background metric $g^{\mu\nu}$. Accordingly, the local speed of GWs is equal to the speed of light, $c_g = c$. Other gravity theories have different predictions. The effective metric $\mathcal{G}^{\mu\nu}$ can be decomposed in a part proportional to $g^{\mu\nu}$ and another that is not (see \mathcal{C} and $\mathcal{D}^{\alpha\beta}$ terms respectively in (34.7)). Whenever the two metrics are not conformally related, the *GW-cone* and the light-cone will not match inducing an anomalous propagation speed $c_g \neq c$ and a time delay between both signals.

In order to have a non-luminal GW speed, there must be terms in the action affecting the second derivative interactions of the metric and not vanishing in the given background. For instance, in scalar-tensor gravity, two conditions have to be fulfilled [27]:

- (i) There is a non-trivial scalar field configuration spontaneously breaking Lorentz invariance. In order to explain DE, one typically demands $\dot{\phi} \sim H_0$.
- (ii) There is a derivative coupling to the curvature. This highlights the presence of a modified gravity coupling leading to $\mathcal{D}^{\alpha\beta} \sim \partial^\alpha \phi \partial^\beta \phi$.

Whenever these two conditions are fulfilled, the GW and the EM signals will travel at different speeds. For example, 1% differences in the speed for sources at 100Mpc induce time delays of tens of millions of years, frustrating any multi-messenger detection.

34.3.1 Constraints After GW170817

GW170817 was followed by a sGRB only $\Delta t = 1.74 \pm 0.05$ s after [28]. Since the BNS was at $\mathcal{O}(40\text{Mpc})$, this event led to the impressive constraint on the speed of GWs

$$-3 \cdot 10^{-15} \leq c_g/c - 1 \leq 7 \cdot 10^{-16}. \quad (34.8)$$

This result has profound implications for many gravity theories and dark energy models (see [1] for a recent review). In particular, a large sector of the scalar-tensor dark energy models is now ruled out [29–32]. These include cosmologically viable models with screening and self-accelerating like the covariant Galileon [33, 34], or proposals to self-tune the cosmological constant like the Fab-Four [35]. For vector-tensor theories the situation is very similar. In order to describe DE and to pass

the GW test, some couplings of the theory have to be eliminated [9, 29, 31]. The implications of GW170817 extend to other gravity theories such as doubly-coupled bigravity [36], $f(T)$ gravity [37], Hořava gravity [38] or Born-Infeld models [39].

Nonetheless, it is important to remark possible caveats and ways to avoid these constraints:

- *Constraints apply to dark energy models:* constraints after GW170817 generically apply only to gravity theories in which the additional fields have a relevant role in cosmology. For instance, we could take as an example the case of Galileons. There, the tensor speed excess is proportional to [29]

$$(c_g^2 - 1) \propto \left(\frac{\dot{\phi}}{H_0} \right)^4. \quad (34.9)$$

Accordingly, for models in which the Galileon triggers the present expansion, $\dot{\phi} \sim H_0$, there are $\mathcal{O}(1)$ deviations in c_g . However, if we resign from this goal, Galileons could be in agreement with GW170817, simply choosing $\dot{\phi} < 10^{-4} H_0$. Definitely, this sector of the theory is less interesting a priori but serves to exemplify that, in most cases, GW170817 constrains DE models rather than gravity theories. Another example considered recently is scalar Gauss-Bonnet gravity [40], where it was shown that if the scalar does not have a dominant energy density, it passes the constraints on the speed.

- *Cosmological tuning of $c_g(z=0) = c$ is not viable:* although tuning by hand the parameters of the theory to pass GW170817 is not appealing, it is tempting to devise a dynamical mechanism that leads to this tuning. One could therefore think that a cosmological model with such mechanism could be viable. However, to avoid the constraint on the speed of GWs, one has to fix $c_g = c$ on arbitrary backgrounds [29]. This is because when the GW travels from the source to the observer, it will cross backgrounds deviating from FRW, e.g. when they cross the Milky Way or due to the large-scale structure. Therefore, delays between the GW and the EM radiation will be accumulated again. Given the strength of the GW170817 constraint, any small deviation from the cosmological background would kill the tuning mechanism. This reasoning has been applied lately to an interesting sector of Horndeski gravity in which the scalar EoM dynamically cancel the anomalous speed [41]. Nevertheless, large-scale inhomogeneities are sufficient to make the mechanism fail.
- *Constraints assume EFT validity:* when computing the speed of GWs or any other GW observable from a dark energy model, we are assuming that the effective field theory is valid. In other words, we are assuming that higher-order operators do not modify the action. However, the frequency of GW170817 was of the same order of the typical strong coupling scale of the EFT of DE

$$\Lambda_{\text{strong}} \sim (M_{\text{pl}} H_0^2)^{1/3} \sim 260 \text{ Hz}. \quad (34.10)$$

Taking the cut-off of the theory around the strong coupling scale $M_{\text{cutoff}} \sim \Lambda_{\text{strong}}$, higher dimensional operators could modify the dispersion relation. Nevertheless, one would not expect them to conspire to completely erase the anomalous speed at the level of $\mathcal{O}(10^{-15})$ [30]. On the contrary, when the cut-off scale is parametrically smaller, $M_{\text{cutoff}} \ll \Lambda_{\text{strong}}$, the situation could change [42]. Lorentz invariance in the ultra-violet (UV) imposes luminal GW propagation. Therefore, higher dimensional operators would tend to cancel any anomalous speed beyond the cut-off scale, which with these assumptions might already happen in the LIGO band. The computation of the speed of GWs beyond M_{cutoff} requires, however, knowledge of the UV completion. In any case, the possibility that $c_g(k_{\text{LIGO}}) = c$ could be tested detecting GWs at different frequencies, for example with LISA.

34.4 GW Luminosity Distance

Another powerful observable to constrain modifications in the GW propagation is the luminosity distance d_L^{gw} , which can be obtained from the inverse of the amplitude $|h_{+, \times}| \propto 1/d_L^{\text{gw}}$. GR predicts that GWs are only sensitive to the Hubble friction along the propagation so that the GW luminosity distance is equal to the EM one, cf. (34.5). However, in other theories of gravity, the cosmic medium could be, for instance, more absorptive. This would dim the received signal, which would be interpreted as the source being further apart. In other words, the GW luminosity distance d_L^{gw} would be larger than the EM luminosity distance d_L^{em} .

Following the propagation Eq. (34.1), in the case in which $c_g = c$,² the ratio of the GW and EM luminosity distance is given by

$$\frac{d_L^{\text{gw}}(z)}{d_L^{\text{em}}(z)} = \exp \left[\frac{1}{2} \int_0^z \frac{\nu(z')}{1+z'} dz' \right]. \quad (34.11)$$

For instance, in scalar-tensor gravity, the additional friction is equal to the effective Planck mass run rate α_M

$$\nu = \alpha_M = \frac{d \ln M_*^2}{d \ln a}, \quad (34.12)$$

where M_* is the local, effective Planck mass, i.e., the normalisation of the kinetic term of the tensor perturbations. Then, we arrive at

$$\frac{d_L^{\text{gw}}(z)}{d_L^{\text{em}}(z)} = \frac{M_*(0)}{M_*(z)}, \quad (34.13)$$

² For the general formula of luminosity distance ratio $d_L^{\text{gw}}/d_L^{\text{em}}$ when $c_g \neq c$ see Sect. 2.2.3 of Ref. [43].

where $M_*(0)$ and $M_*(z)$ are the effective Planck masses at the time of observation and emission respectively. Instead of fixing the theory, one could parametrise the friction term. One possibility is to assume that $\nu(z)$ scales with the DE [44], i.e.

$$\nu(z) = c_M \frac{\Omega_{DE}(z)}{\Omega_{DE}(0)}, \quad (34.14)$$

where c_M is constant. This is a reasonable parametrisation for modified gravity theories trying to explain the late-time cosmic acceleration. Assuming that the background cosmology is Λ CDM, we obtain

$$\frac{d_L^{\text{gw}}}{d_L^{\text{em}}} = \exp \left\{ \frac{1}{2} \frac{c_M}{\Omega_{DE}(0)} \log \left\{ \frac{1+z}{[\Omega_m(0)(1+z)^3 + \Omega_{DE}(0)]^{1/3}} \right\} \right\}. \quad (34.15)$$

For illustration, in Fig. 34.2 we depict how the ratio $d_L^{\text{gw}}(z)/d_L^{\text{em}}(z)$ varies for different values of c_M . Positive values of c_M make d_L^{gw} to be larger than d_L^{em} and vice versa. We compare the effects at low redshift (left panel) with high redshift (right panel) expected for ground-base and space-base interferometers respectively. Clearly, low redshift signals are less effective at constraining a modification in the propagation of GWs. In the case of scalar-tensor gravity, present cosmological surveys place constraints of order one on c_M , while future ones could reach $\mathcal{O}(0.1)$ [45].

An alternative possibility is to parametrise the ratio of luminosity distances, which is more directly linked to observations. A convenient choice is [46]

$$\frac{d_L^{\text{gw}}(z)}{d_L^{\text{em}}(z)} = \Xi_0 + \frac{1 - \Xi_0}{(1+z)^n}, \quad (34.16)$$

which resembles the usual (w_0, w_a) parametrisation of the equation of state of DE. This parametrisation interpolates between 1 at $z = 0$ and a constant value Ξ_0 at high redshift. From Fig. 34.2 one can already see that this is the expected behaviour when the modification follows the DE. Reference [43] studied in detail how this parametrisation adjusts to several modified gravity theories, including degenerate higher order scalar-tensor theories and non-local infrared modifications of gravity. It was found a good fit in most of the cases, specially at high redshift.

Present constraints on a modified GW luminosity distance are still very loose [46, 47]. This is because at the moment there is only one standard siren, GW170817. This is expected to change significantly in the coming years as more detections accumulate in the next observing runs of advanced LIGO-Virgo. Looking further to the future, using thousands of BNS standard sirens, the Einstein Telescope could reach a 1% measurement of Ξ_0 [46]. In the same manner, using SMBHs at $z \sim 2 - 5$ as standard sirens, LISA could constrain Ξ_0 to the 1 - 5% level [43].

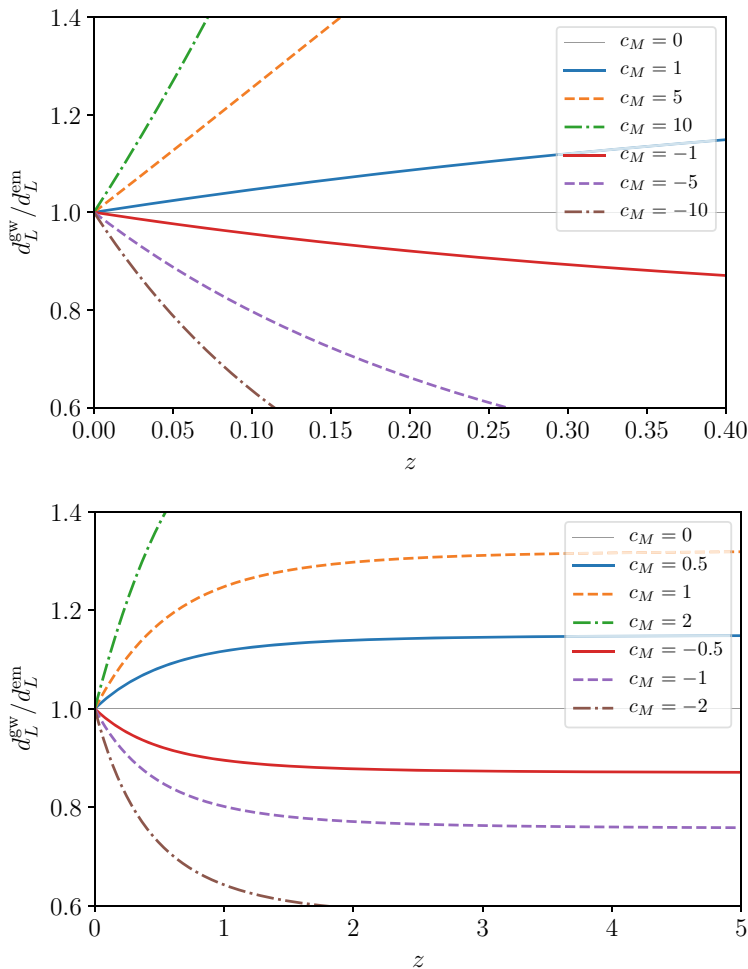


Fig. 34.2 Ratio between the GW and the EM luminosity distances due to an additional friction term in the propagation ν scaling with the DE, $\nu(z) = c_M \Omega_{DE}(z) / \Omega_{DE}(0)$. We compare low- (upper) and high-redshift (lower) signals expected for ground- and space-base GW detectors respectively

34.5 GW Oscillations

If GWs mix with other tensor modes t_{ij} along the propagation, there will be modifications of the GW luminosity distance. This is because GW detectors are only sensitive to h_{ij} . Therefore, if h_{ij} converts partially into t_{ij} , the amplitude detected will be lower and the inferred d_L^{GW} larger. If the conversion is complete, no GW would be detected, making d_L^{GW} effectively to diverge. A series of consecutive mixings imprints a characteristic oscillatory pattern in the GW luminosity distance that can be probed with standard sirens.

We can proceed as in the previous section and compute the ratio of the GW and EM luminosity distances. Considering only the mass mixing described in (34.6), which is characteristic of bigravity theory, it would be given by [5, 43]

$$\frac{d_L^{\text{gw}}}{d_L^{\text{em}}} = \frac{1}{\cos^2 \theta_g} \left\{ 1 + \tan^4 \theta_g + 2 \tan^2 \theta_g \cos \left[\frac{m_g^2}{2k} \int_0^z \frac{dz}{(1+z)^2 H(z)} \right] \right\}^{-1/2}. \quad (34.17)$$

The mixing angle θ_g controls the amount of conversion while the effective mass m_g determines the frequency of oscillation. The mixing angles range from 0 to $\pi/2$, having the maximum mixing at $\theta_g = \pi/4$ when a complete oscillation of h_{ij} into t_{ij} occurs. Note that the frequency of oscillation also depends on the frequency of the GW. For example, to have an $\mathcal{O}(1)$ frequency of oscillation at low redshift, $m_g^2/2k$ should be of the order of H_0 to compensate the Hubble parameter in the denominator. Since $H_0 \sim 10^{-33} \text{ eV} \sim 10^{-18} \text{ Hz}$, this means that present ground-based interferometer, $f_{\text{LIGO}} \sim 100 \text{ Hz}$, can test $m_g \sim 10^{-23} \text{ eV}$ through the oscillations of d_L^{gw} .

In the same manner, the future space-based detector LISA, $f_{\text{LISA}} \sim 10 \text{ mHz}$, will be sensitive to $m_g \sim 10^{-25} \text{ eV}$. In the upper panel of Fig. 34.3 we present how the GW luminosity distance varies with θ_g and m_g . As the mixing angle approaches to $\pi/4$, the amplitude of the oscillation increases. Similarly, the frequency of oscillation increases with m_g . The plot corresponds to the expected redshift range, $z \sim 2 - 6$, and sensitivity, $\Delta d_L/d_L \sim 10\%$, of LISA standard sirens. A recent analysis studied the capability of LISA to detect GW oscillations in d_L^{gw} [43], showing that LISA could probe masses of $m_g \gtrsim 2 \cdot 10^{-25} \text{ eV}$ with mixing angles $0.05\pi \lesssim \theta_g \lesssim 0.45\pi$.

Moving now to the friction mixing in (34.6), the ratio of the GW and EM luminosity distance reads [5]

$$\frac{d_L^{\text{gw}}}{d_L^{\text{em}}} = (1+z)^{\Delta\nu} \left\{ \cos [\omega_\nu \log(1+z)] + \frac{\Delta\nu}{\omega_\nu} \sin [\omega_\nu \log(1+z)] \right\}^{-1}. \quad (34.18)$$

This expression contains a first global friction term induced by $\Delta\nu$, the difference between the friction term of t_{ij} and h_{ij} . The oscillation rate is determined by $\omega_\nu = \sqrt{\alpha^2 - \Delta\nu^2}$, where α is the non-diagonal term producing the mixing. In the limit of no mixing, $\alpha \rightarrow 0$, one recovers $d_L^{\text{gw}}/d_L^{\text{em}} \rightarrow 1$. Moreover, there is always a complete conversion of h_{ij} into t_{ij} , implying that at certain redshifts there will be no GW events. This in turn translates into periodic divergences of $d_L^{\text{gw}}/d_L^{\text{em}}$ that makes this models easier to probe. This can be seen in the lower panel of Fig. 34.3, where we depict $d_L^{\text{gw}}/d_L^{\text{em}}$ for different values of $\Delta\nu$ and α . The global friction term $(1+z)^{\Delta\nu}$ makes the minimum values of $d_L^{\text{gw}}/d_L^{\text{em}}$ to increase away from 1 as $\Delta\nu$ increases. On the other hand, the mixing parameter α controls the frequency of oscillation. Future GW detectors could also probe this type of GW oscillations, which occur, for instance, in theories with cosmological gauge fields [8, 9].

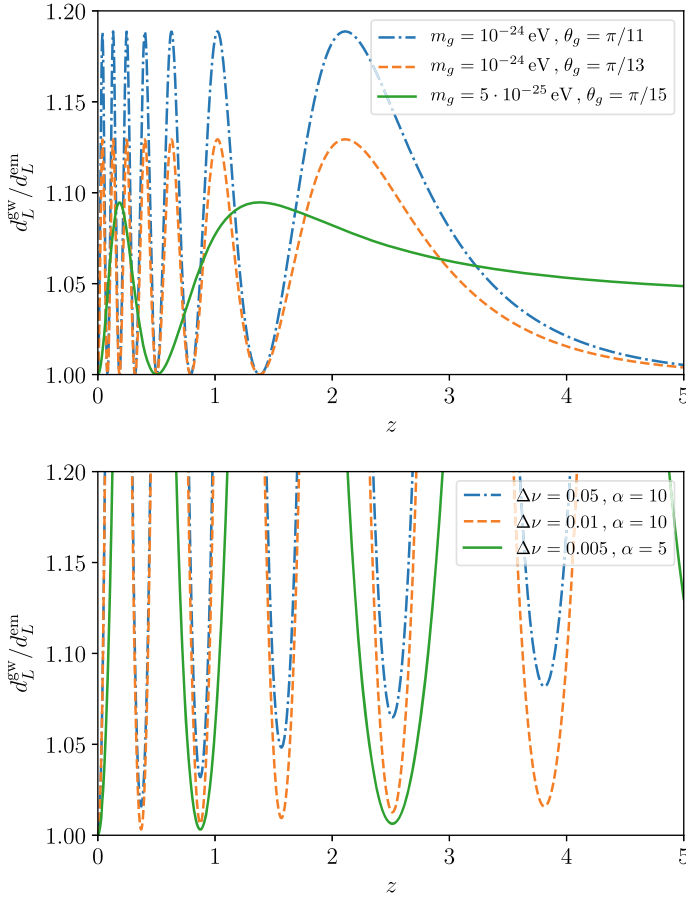


Fig. 34.3 Modified GW luminosity distance as a function of redshift for theories with a mass mixing (upper) or a friction mixing (lower). The ratio $d_L^{\text{gw}}/d_L^{\text{em}}$ is plotted for different values of the effective mass m_g and mixing angle θ_g ; and damping factor $\Delta\nu$ and friction mixing α . Figures reproduced from [5]

34.6 Future Prospects

In the last four years we have witnessed a vibrant beginning of GW astronomy: from the excitement of the first detection, to the routine of the following events and back to the euphoria of a multi-messenger historic achievement. BBH mergers have taught us not only about a population of heavy BHs [26] but also that their signals have served to strongly constrain the mass of the graviton [48]. More notoriously, GW170817, a BNS event, brought the first standard siren measurement of the Hubble constant (see Sect. 34.2) and an impressive bound on the speed of GWs, $|c_g/c - 1| \leq 10^{-15}$, that swept out many DE contenders (see Sect. 34.3).

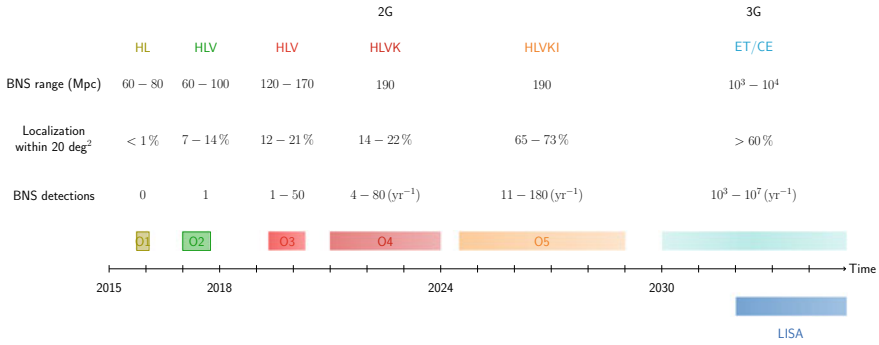


Fig. 34.4 Schematic multi-messenger GW astronomy timeline. The binary neutron star (BNS) rate, the localisation area in the sky, and the number of BNS detections are given for past and future observation runs. Second generation (2G) ground-based detectors organise in five runs (O1–O5) with a different number of detectors online (from 2 to 5) [49]. The nomenclature used is H=Hanford, L=Livingston, V=Virgo, K=KAGRA, I=IndIGO. Third generation (3G) detectors projected are Einstein Telescope (ET) [50] or Cosmic Explorer (CE) [51]. The localisation in 3G depends on the network of detectors, which is still uncertain [52]. For reference, we include the timeline space-based detector LISA [53]. The reader should note that these numbers correspond to present expectations. Figure updated from Ref. [1]

The following years are no less exciting, with observational improvements pointing in three main directions: number of detections, sky localisation and distance range (see Fig. 34.4). All of them will boost the constraining power of standard siren tests of gravity and cosmology. Moreover, any deviation of the ratio of luminosity distances $d_L^{\text{gw}}/d_L^{\text{em}}$ from being 1 would be a smoking gun of physics beyond GR and Λ CDM. However, these observational opportunities will also pose theoretical challenges, as we will be crossing both discovery and precision frontiers. In what comes next, we overview these challenges and opportunities, focusing on those related to unveil the nature of gravity and dark energy.

34.6.1 Theoretical Challenges

In this chapter we have focused on the cosmological propagation of GWs. However, modifications in the propagation are not restricted to cosmological backgrounds. For instance, when a GW crosses a screened region, the spatially dependent background might affect the GW signal. From a phenomenological perspective there are two possible GW observables beyond what we have considered here: additional polarisations and frequency dependent modifications.

Additional polarisations: on FRW backgrounds GWs can only mix with other tensor perturbations. Nevertheless, in more general spacetimes there could be an interplay between the scalar, vector and tensor polarisations. In particular, non-GR polarisations could be excited along the propagation even if they were not originally

produced. If those polarisations couple to matter, they could be detected with a network of ground-based detectors. This would be a clear indication of a modification of gravity. In addition, one could also probe if the two tensor polarisations have the same properties, constraining parity-violating gravity [54].

Frequency-dependent modifications: the propagation of GWs depends on space and time, but may also depend on the frequency of the wave. The simplest example is having a graviton mass, which modifies the dispersion relation. The advantage of this type of modification is that they can be probed with GWs alone and on single events, due to the chirping of the GW signal. Moreover, GW detectors are very sensitive to frequency-dependent modifications. These effects might be caused by the breaking of the EFT at the frequencies of GW detectors [42], or by the decay of GWs into DE [55]. It would be interesting to search further for these phenomena in the landscape of modified gravity.

Finally, a theoretical challenge across the different probes would be to understand possible degeneracies with astrophysics. Along the same lines, the separation between modifications in the emission and propagation might not be possible with the improved precision of future detectors.

34.6.2 Observational Opportunities

The future of gravitational wave astronomy is promising. With a larger catalogue of events, one could perform statistically significant studies at the same time of precision measurements from rare events with high SNR. Moreover, new frequencies will be opened, namely the mHz from space-based detectors, certainly leading to discoveries as well as enabling new techniques such as multi-band GW astronomy. Here we highlight how some of these observational opportunities could contribute to the quest of the dark side of the Universe.

2G detectors: second generation (2G) detectors are still on their way to their design sensitivity (see Fig. 34.4). Thus, merger rates are expected to increase in future observational runs. In fact, we are now witnessing one of such steps forward in O3 compared to the previous runs O1-2. Collecting statistics has implications for the study of the cosmic expansion, enlarging the number of multi-messenger events to be used as standard sirens or the number of BBHs to be used as dark sirens. This will improve the measurement of the Hubble constant (see Sect. 34.2) as well as the constraints on the propagation of GWs (see, for example, the upper panel of Fig. 34.2). Moreover, all of the planned 2G detectors are not yet online. KAGRA is expected to join by the end of O3 and IndIGO just in the last run (again, see Fig. 34.4). Having a large network of detectors is essential to test the number of polarisations, a fundamental property of each gravity theory. This will open new opportunities to test, for instance, chiral GWs.

3G detectors: third generation (3G) detectors will improve their predecessors in multiple ways [56]: observing more distant binaries, in a wider frequency range and with higher precision. All of these improvements will be relevant to test gravity.

Detecting mergers at high-redshift will serve to determine the evolution of the GW luminosity distance. Enlarging the frequency band will be interesting at both ends. At low frequencies, reaching down 1 Hz, 3G detectors will be sensitive to higher masses, possibly above $100M_{\odot}$. If some events have small mass ratios, precession effects could be observed. At high frequencies, reaching up to 5 kHz, the merger phase of BNS could be much better constrained, including tidal effects. As the sensitivity will improve significantly, 3G detectors could hear many orders of magnitude more events. This will ensure precision measurements of H_0 and the propagation of GWs beyond 2G capabilities. Moreover, it is expected that some signals will be strongly lensed [57]. This could be a perfect arena to test modifications of gravity.

Space-based detectors: a million kilometer interferometers in space could hear GWs in the mHz band. This is the goal of LISA, which will inaugurate a completely new channel to detect very massive BBHs, galactic binaries and possibly cosmological backgrounds. If identified with an EM counterpart, SMBH binaries would become standard sirens at cosmological scales, $z \sim 2 - 5$. LISA standard sirens could bound generic modifications of the GW luminosity distance (see the lower panel of Fig. 34.2) and GW oscillations (see Fig. 34.3). Extreme mass ratio inspirals and galactic binaries are also good candidates to test gravity [58].

Multi-band GW astronomy: the reach of GW astronomy can be enhanced if GW events are heard at different frequencies. Heavy BBHs like GW150914 could be detected months in advance by LISA [59]. This will again open new opportunities. For instance, with multi-band events one could combine the information that is better measured in space, such as eccentricities, with the inference on the mass and spin obtained at the merger. This could improve the source characterisation. Similarly, anticipating the detection of a signal from space will improve its localisation on Earth, making the search for an EM counterpart more effective. At the same time, multi-band events with precise localisation are perfect candidates to probe additional polarisations.

Synergies with cosmological surveys: GW observatories will not be alone in probing the dark universe. Cosmological surveys such as LSST, Euclid or WFIRST will have a fundamental role (see recent reviews of their science cases in [60–63] respectively). With respect to the theoretical challenges, they will constrain, among others, the DE equation of state and possible deviations of GR in the growth of structure [60, 62, 63]. These complementary observations could be useful in breaking degeneracies. From the observational side, a key task of future surveys will be to deliver complete and uniform galaxy catalogues. This is essential in order to properly identify the redshift of a GW signal with the statistical method (see Sect. 34.2). We expect that the most challenging questions about DE will only be addressed with a powerful synergy between GW astronomy and other cosmological probes.

References

1. J.M. Ezquiaga, M. Zumalacregui, Dark energy in light of multi-messenger gravitational-wave astronomy. *Front. Astron. Space Sci.* **5**, 44 (2018). [arXiv:1807.09241](#)
2. L. Barack et al., Black holes, gravitational waves and fundamental physics: a roadmap. [arXiv:1806.05195](#)
3. J.A.R. Cembranos, M. Coma Díaz, P. Martín-Moruno, Modified gravity as a diagravitational medium. *Phys. Lett. B* **788**, 336–340 (2019). [arXiv:1805.09629](#)
4. M. Maggiore, *Gravitational Waves: Volume 1: Theory and Experiments*, vol. 1 (Oxford university press, 2008)
5. J.B. Jiménez, J.M. Ezquiaga, L. Heisenberg, Probing cosmological fields with gravitational wave oscillations. [arXiv:1912.06104](#)
6. T. Narikawa, K. Ueno, H. Tagoshi, T. Tanaka, N. Kanda, T. Nakamura, Detectability of bigravity with graviton oscillations using gravitational wave observations. *Phys. Rev. D* **91**, 062007 (2015). [arXiv:1412.8074](#)
7. K. Max, M. Platscher, J. Smirnov, Gravitational wave oscillations in bigravity. *Phys. Rev. Lett.* **119**(11), 111101 (2017). [arXiv:1703.07785](#)
8. R.R. Caldwell, C. Devulder, N.A. Maksimova, Gravitational wave-Gauge field oscillations. *Phys. Rev. D* **94**(6), 063005 (2016). [arXiv:1604.08939](#)
9. J.B. Jimnez, L. Heisenberg, Non-trivial gravitational waves and structure formation phenomenology from dark energy. *JCAP* **1809**(09), 035 (2018). [arXiv:1806.01753](#)
10. C.M. Will, Bounding the mass of the graviton using gravitational wave observations of inspiralling compact binaries. *Phys. Rev. D* **57**, 2061–2068 (1998). [arXiv:gr-qc/9709011](#)
11. B.F. Schutz, Determining the Hubble constant from gravitational wave observations. *Nature* **323**, 310–311 (1986)
12. D.E. Holz, S.A. Hughes, Using gravitational-wave standard sirens. *Astrophys. J.* **629**, 15–22 (2005). [arXiv:astro-ph/0504616](#)
13. B.D. Metzger, Kilonovae. *Living Rev. Rel.* **20**, 3 (2017). [arXiv:1610.09381](#)
14. N. Dalal, D.E. Holz, S.A. Hughes, B. Jain, Short GRB and binary black hole standard sirens as a probe of dark energy. *Phys. Rev. D* **74**, 063006 (2006). [arXiv:astro-ph/0601275](#)
15. S. Vitale, H.-Y. Chen, Measuring the Hubble constant with neutron star black hole mergers. *Phys. Rev. Lett.* **121**(2), 021303 (2018). [arXiv:1804.07337](#)
16. W. Del Pozzo, Inference of the cosmological parameters from gravitational waves: application to second generation interferometers. *Phys. Rev. D* **86**, 043011 (2012). [arXiv:1108.1317](#)
17. H.-Y. Chen, D.E. Holz, Finding the one: identifying the host galaxies of gravitational-wave sources. [arXiv:1612.01471](#)
18. C. Messenger, J. Read, Measuring a cosmological distance-redshift relationship using only gravitational wave observations of binary neutron star coalescences. *Phys. Rev. Lett.* **108**, 091101 (2012). [arXiv:1107.5725](#)
19. S.R. Taylor, J.R. Gair, I. Mandel, Hubble without the Hubble: cosmology using advanced gravitational-wave detectors alone. *Phys. Rev. D* **85**, 023535 (2012). [arXiv:1108.5161](#)
20. C. Messenger, K. Takami, S. Gossan, L. Rezzolla, B.S. Sathyaprakash, Source Redshifts from gravitational-wave observations of binary neutron star mergers. *Phys. Rev. X* **4**(4), 041004 (2014). [arXiv:1312.1862](#)
21. B.P. Abbott, LIGO Scientific, Virgo, Collaboration et al., GW170817: observation of gravitational waves from a binary neutron star inspiral. *Phys. Rev. Lett.* **119**(16), 161101 (2017). [arXiv:1710.05832](#)
22. B.P. Abbott, LIGO Scientific, Virgo, Fermi GBM, INTEGRAL, IceCube, AstroSat Cadmium Zinc Telluride Imager Team, IPN, Insight-Hxmt, ANTARES, Swift, AGILE Team, 1M2H Team, Dark Energy Camera GW-EM, DES, DLT40, GRAWITA, Fermi-LAT, ATCA, ASKAP, Las Cumbres Observatory Group, OzGrav, DWF (Deeper Wider Faster Program), AST3, CAASTRO, VINROUGE, MASTER, J-GEM, GROWTH, JAGWAR, CaltechNRAO, TTU-NRAO, NuSTAR, Pan-STARRS, MAXI Team, TZAC Consortium, KU, Nordic Optical Telescope, ePESSTO, GROND, Texas Tech University, SALT Group, TOROS, BOOTES, MWA,

- CALET, IKI-GW Follow-up, H.E.S.S., LOFAR, LWA, HAWC, Pierre Auger, ALMA, Euro VLBI Team, Pi of Sky, Chandra Team at McGill University, DFN, ATLAS Telescopes, High Time Resolution Universe Survey, RIMAS, RATIR, SKA South Africa/MeerKAT, Collaboration et al., Multi-messenger observations of a binary neutron star merger. *Astrophys. J.* **848**(2), L12 (2017). [arXiv:1710.05833](https://arxiv.org/abs/1710.05833)
23. B.P. Abbott, LIGO Scientific, Virgo, 1M2H, Dark Energy Camera GW-E, DES, DLT40, Las Cumbres Observatory, VINROUGE, MASTER, Collaboration et al., A gravitational-wave standard siren measurement of the Hubble constant. *Nature* **551**(7678), 85–88 (2017). [arXiv:1710.05835](https://arxiv.org/abs/1710.05835)
 24. Virgo, members of the LIGO Scientific, Collaboration, M. Fishbach, R. Gray, I.M. Hernandez, H. Qi, A. Sur, A standard siren measurement of the Hubble constant from GW170817 without the electromagnetic counterpart. [arXiv:1807.05667](https://arxiv.org/abs/1807.05667)
 25. M. Soares-Santos, DES, LIGO Scientific, Virgo, Collaboration et al., First measurement of the Hubble constant from a dark standard siren using the dark energy survey galaxies and the LIGO/Virgo BinaryBlack-hole Merger GW170814. *Astrophys. J.* **876**(1), L7 (2019). [arXiv:1901.01540](https://arxiv.org/abs/1901.01540)
 26. LIGO Scientific, Virgo, Collaboration, B.P. Abbott et al., GWTC-1: a gravitational-wave transient catalog of compact binary mergers observed by LIGO and Virgo during the first and second observing runs. [arXiv:1811.12907](https://arxiv.org/abs/1811.12907)
 27. D. Bettoni, J.M. Ezquiaga, K. Hinterbichler, M. Zumalacárregui, Speed of gravitational waves and the fate of scalar-tensor gravity. *Phys. Rev. D* **95**(8), 084029 (2017). [arXiv:1608.01982](https://arxiv.org/abs/1608.01982)
 28. B.P. Abbott, LIGO Scientific, Virgo, Fermi-GBM, INTEGRAL, Collaboration et al., Gravitational waves and gamma-rays from a binary neutron star merger: GW170817 and GRB 170817A. *Astrophys. J.* **848**(2), L13 (2017). [arXiv:1710.05834](https://arxiv.org/abs/1710.05834)
 29. J.M. Ezquiaga, M. Zumalacárregui, Dark energy after GW170817: dead ends and the road ahead. *Phys. Rev. Lett.* **119**(25), 251304 (2017). [arXiv:1710.05901](https://arxiv.org/abs/1710.05901)
 30. P. Creminelli, F. Vernizzi, Dark Energy after GW170817 and GRB170817A. *Phys. Rev. Lett.* **119**(25), 251302 (2017). [arXiv:1710.05877](https://arxiv.org/abs/1710.05877)
 31. T. Baker, E. Bellini, P.G. Ferreira, M. Lagos, J. Noller, I. Sawicki, Strong constraints on cosmological gravity from GW170817 and GRB 170817A. *Phys. Rev. Lett.* **119**(25), 251301 (2017). [arXiv:1710.06394](https://arxiv.org/abs/1710.06394)
 32. J. Sakstein, B. Jain, Implications of the neutron star merger GW170817 for cosmological scalar-tensor theories. *Phys. Rev. Lett.* **119**(25), 251303 (2017). [arXiv:1710.05893](https://arxiv.org/abs/1710.05893)
 33. A. Nicolis, R. Rattazzi, E. Trincherini, The Galileon as a local modification of gravity. *Phys. Rev. D* **79**, 064036 (2009). [arXiv:0811.2197](https://arxiv.org/abs/0811.2197)
 34. C. Deffayet, G. Esposito-Farese, A. Vikman, Covariant Galileon. *Phys. Rev. D* **79**, 084003 (2009). [arXiv:0901.1314](https://arxiv.org/abs/0901.1314)
 35. C. Charmousis, E.J. Copeland, A. Padilla, P.M. Saffin, General second order scalar-tensor theory, self tuning, and the Fab Four. *Phys. Rev. Lett.* **108**, 051101 (2012). [arXiv:1106.2000](https://arxiv.org/abs/1106.2000)
 36. Y. Akrami, P. Brax, A.-C. Davis, V. Vardanyan, Neutron star merger GW170817 strongly constrains doubly coupled bigravity. *Phys. Rev. D* **97**(12), 124010 (2018). [arXiv:1803.09726](https://arxiv.org/abs/1803.09726)
 37. Y.-F. Cai, C. Li, E.N. Saridakis, L. Xue, $f(T)$ gravity after GW170817 and GRB170817A. [arXiv:1801.05827](https://arxiv.org/abs/1801.05827)
 38. A.E. Gumrukcuoglu, M. Saravani, T.P. Sotiriou, Hořava Gravity after GW170817. *Phys. Rev. D* **97**(2), 024032 (2017). [arXiv:1711.08845](https://arxiv.org/abs/1711.08845)
 39. S. Jana, G.K. Chakravarty, S. Mohanty, Constraints on Born-Infeld gravity from the speed of gravitational waves after GW170817 and GRB 170817A. *Phys. Rev. D* **97**(8), 084011 (2018). [arXiv:1711.04137](https://arxiv.org/abs/1711.04137)
 40. N. Franchini, T.P. Sotiriou, Cosmology with subdominant Horndeski scalar field. [arXiv:1903.05427](https://arxiv.org/abs/1903.05427)
 41. E.J. Copeland, M. Kopp, A. Padilla, P.M. Saffin, C. Skordis, Dark energy after GW170817, revisited. *Phys. Rev. Lett.* **122**(6), 061301 (2018). [arXiv:1810.08239](https://arxiv.org/abs/1810.08239)
 42. C. de Rham, S. Melville, Gravitational rainbows: LIGO and dark energy at its cutoff. *Phys. Rev. Lett.* **121**(22), 221101 (2018). [arXiv:1806.09417](https://arxiv.org/abs/1806.09417)

43. E. Belgacem, LISA Cosmology Working Group, Collaboration et al., Testing modified gravity at cosmological distances with LISA standard sirens. *JCAP* **1907**(07), 024 (2019)
44. M. Lagos, M. Fishbach, P. Landry, D.E. Holz, Standard sirens with a running Planck mass. *Phys. Rev. D* **99**(8), 083504 (2019). [arXiv:1901.03321](#)
45. D. Alonso, E. Bellini, P.G. Ferreira, M. Zumalacárregui, Observational future of cosmological scalar-tensor theories. *Phys. Rev. D* **95**(6), 063502 (2017). [arXiv:1610.09290](#)
46. E. Belgacem, Y. Dirian, S. Foffa, M. Maggiore, Modified gravitational-wave propagation and standard sirens. *Phys. Rev. D* **98**(2), 023510 (2018). [arXiv:1805.08731](#)
47. S. Arai, A. Nishizawa, Generalized framework for testing gravity with gravitational-wave propagation. II. Constraints on Horndeski theory. *Phys. Rev. D* **97**(10), 104038 (2018). [arXiv:1711.03776](#)
48. B.P. Abbott, LIGO Scientific, Virgo, Collaboration et al., Tests of general relativity with the binary black hole signals from the LIGO-virgo catalog GWTC-1. *Phys. Rev. D* **100**(10), 104036 (2019). [arXiv:1903.04467](#)
49. VIRGO, KAGRA, LIGO Scientific, Collaboration, B.P. Abbott et al., Prospects for observing and localizing gravitational-wave transients with advanced LIGO, advanced Virgo and KAGRA. *Living Rev. Rel.* **21**, 3 (2018). [arXiv:1304.0670](#). [*Living Rev. Rel.* **19**,1 (2016)]
50. B. Sathyaprakash et al., Scientific objectives of Einstein telescope. *Class. Quant. Grav.* **29**, 124013 (2012). [arXiv:1206.0331](#). [Erratum: *Class. Quant. Grav.* **30**, 079501 (2013)]
51. B.P. Abbott, LIGO Scientific, Collaboration et al., Exploring the sensitivity of next generation gravitational wave detectors. *Class. Quant. Grav.* **34**(4), 044001 (2017). [arXiv:1607.08697](#)
52. C. Mills, V. Tiwari, S. Fairhurst, Localization of binary neutron star mergers with second and third generation gravitational-wave detectors. *Phys. Rev. D* **97**(10), 104064 (2018). [arXiv:1708.00806](#)
53. P. Amaro-Seoane et al., eLISA/NGO: astrophysics and cosmology in the gravitational-wave millihertz regime. *GW Notes* **6**, 4–110 (2013). [arXiv:1201.3621](#)
54. A. Nishizawa, T. Kobayashi, Parity-violating gravity and GW170817. *Phys. Rev. D* **98**(12), 124018 (2018). [arXiv:1809.00815](#)
55. P. Creminelli, M. Lewandowski, G. Tambalo, F. Vernizzi, Gravitational wave decay into dark energy. *JCAP* **1812**(12), 025 (2018). [arXiv:1809.03484](#)
56. V. Kalogera et al., *Deeper, Wider, Sharper: Next-Generation Ground-Based Gravitational-Wave Observations of Binary Black Holes*. [arXiv:1903.09220](#)
57. A. Pirkowska, M. Biesiada, Z.-H. Zhu, Strong gravitational lensing of gravitational waves in Einstein Telescope. *JCAP* **1310**, 022 (2013). [arXiv:1309.5731](#)
58. J.R. Gair, M. Vallisneri, S.L. Larson, J.G. Baker, Testing general relativity with low-frequency, space-based gravitational-wave detectors. *Living Rev. Rel.* **16**, 7 (2013). [arXiv:1212.5575](#)
59. A. Sesana, The promise of multi-band gravitational wave astronomy. *Phys. Rev. Lett.* **116**(23), 231102 (2016). [arXiv:1602.06951](#)
60. M. Ishak et al., Modified gravity and dark energy models beyond $w(z)$ CDM testable by LSST. [arXiv:1905.09687](#)
61. K. Bechtol et al., Dark matter science in the Era of LSST. [arXiv:1903.04425](#)
62. L. Amendola et al., Cosmology and fundamental physics with the Euclid satellite. *Living Rev. Rel.* **21**(1), 2 (2018). [arXiv:1606.00180](#)
63. O. Dor et al., WFIRST: the essential cosmology space observatory for the coming decade. [arXiv:1904.01174](#)

Chapter 35

Testing the Dark Universe with Cosmic Shear



Valeria Pettorino and Alessio Spurio Mancini

Although a cosmological constant framework is still in agreement with current data, several other cosmological models in which gravity is modified are also still viable. There are several approaches that one can adopt in order to distinguish Λ CDM from modified gravity models. One can try to: (a) use or combine different probes, (b) get more data, (c) improve the analysis to extract more information from the available data. Below we focus on weak lensing, its different approaches and the impact of statistics we use on constraining or distinguishing cosmological models.

Weak lensing describes, in particular, small distortions in the observed image of galaxy shapes, induced by the presence of massive structures along the line of sight. Weak lensing can be typically described in terms of shear and convergence fields, quantifying anisotropic and isotropic distortions respectively. Convergence can be derived from shear, up to a constant, and both depend on the angular position θ on the sky. Given a convergence map $\kappa(\theta)$ for a particular realisation of a model, one can also compute the aperture mass map [1, 2] by applying a filter (see, for example, [3] for a review of different filters adopted in literature).

In Sect. 35.1 we will recall different weak lensing methodologies; in Sect. 35.2 we will describe how well we can use current and future probes (in particular including cross-correlations or combining with galaxy clustering) to test modified gravity models; in Sect. 35.3 we recall how higher order statistics, and in particular peak counts, can help in breaking degeneracies between parameters; finally in Sect. 35.4

V. Pettorino (✉)

AIM, CEA, CNRS, Université Paris-Saclay, Université Paris Diderot, Sorbonne Paris Cité,
91191 Gif-sur-Yvette, France
e-mail: valeria.pettorino@cea.fr

A. Spurio Mancini

Mullard Space Science Laboratory, University College London, Holmbury St. Mary, Dorking,
Surrey RH5 6NT, UK
e-mail: a.spuriomancini@ucl.ac.uk

we illustrate recent results using machine learning techniques to improve the discrimination efficiency between Λ CDM and alternative theories in which gravity is modified with respect to General Relativity.

35.1 2D, Tomographic and 3D Weak Lensing

Here we provide a mathematical description of cosmic shear in a general modified gravity context, similar to the one presented in [4]. We focus on two different formalisms commonly used to study the evolution in redshift of the lensing effect, so-called ‘tomography’ and ‘3D cosmic shear’. We assume spatial flatness throughout, and consider scalar linear perturbations on a Friedmann–Robertson–Walker metric, such that the line element in Newtonian gauge can be written as

$$ds^2 = -(1 + 2\Psi) dt^2 + a^2(t) (1 - 2\Phi) d\mathbf{x}^2, \quad (35.1)$$

with the scale factor $a(t)$ and the Bardeen potentials Ψ and Φ . In General Relativity $\Psi = \Phi$ in absence of anisotropic stress, but this is in general not true in a modified gravity theory. Poisson’s equation links one of the Bardeen potentials to the overdensity field $\delta(k, \chi)$,

$$\Psi(k, \chi) = -\frac{3}{2} \frac{\Omega_m}{(k\chi_H)^2} \frac{\delta(k, \chi)}{a(\chi)} \mu(k, a(\chi)), \quad (35.2)$$

with the Hubble radius $\chi_H \equiv 1/H_0$ and the function $\mu(k, a(\chi))$ parameterising variations from General Relativity, its value being 1 in standard gravity. We also define

$$\eta(k, a(\chi)) \equiv \frac{\Psi(k, a(\chi))}{\Phi(k, a(\chi))}, \quad (35.3)$$

as the ratio of the Bardeen potentials, again identically equal to 1 in General Relativity in absence of anisotropic stress. Other choices (such as Σ , defined in terms of the lensing potential $\Psi + \Phi$), of such two functions of time and scale are also possible, and may be more or less convenient; see [5] or [6] for a review.

A quantitative description of cosmic shear starts with the definition of the lensing potential

$$\Psi(\chi, \hat{\mathbf{n}}) = \int_0^\chi d\chi' \frac{\chi - \chi'}{\chi\chi'} [\Psi(\chi', \hat{\mathbf{n}}) + \Phi(\chi', \hat{\mathbf{n}})], \quad (35.4)$$

as a weighted projection of the sum of the Bardeen potentials along the line of sight. In Eq. 35.4, χ is the comoving distance and the normalised vector $\hat{\mathbf{n}}$ selects a direction in the sky. From its definition in Eq. 35.4 we notice that the lensing potential is sensitive to the growth of perturbations of the gravitational potentials, as well as to

the geometry of the Universe through the weighting factor $\frac{\chi - \chi'}{\chi\chi'}$. We will assume that the integration in Eq. 35.4 is carried out along the unperturbed light path, following the Born approximation. The lensing observables, i.e., convergence and shear, are derived from the lensing potential through linear relations, so that these three fields share the same statistical properties. Hence, cosmic shear is sensitive to structure growth and the geometry of the Universe.

The sensitivity of cosmic shear to the growth of structure is particularly important in studies of cosmic acceleration, as different dark energy and modified gravity models are endowed with different predictions for structure growth. As a consequence, it is crucial to include redshift information in a cosmic shear analysis, so that the effect of dark energy on structure growth can be studied in its evolution with redshift. A two-dimensional analysis (like the one carried out in [7], for example) can achieve this goal only to a limited extent, as it projects quantities along the line of sight; this implies loss of redshift information, due to the mixing of spatial scales and to the reduced sensitivity to those parameters that, entering the model in a nonlinear way, may produce different effects on the lensing signal at different redshifts [8].

To overcome the limitations of a purely two-dimensional analysis, a formalism was first introduced in [9], which assigns galaxies to different redshift bins according to their estimated (photometric) redshift, and calculates correlations of the lensing signal through redshift bins. This approach is commonly known as *tomography* and is the most common methodology to analyse a cosmic shear survey (as used, e.g., in [10]). The integration along the line of sight that characterises a two-dimensional analysis is here reduced to the width of the redshift bin; the correlation among different redshift bins provides information on the evolution in redshift of the lensing signal. Defining the matter power spectrum $P_\delta(k)$ as

$$\langle \delta(\mathbf{k}, z)\delta(\mathbf{k}', z) \rangle = (2\pi)^3 P_\delta(k, z)\delta^D(\mathbf{k} - \mathbf{k}'), \quad (35.5)$$

and making use of the Limber approximation [11–13], one can write down the flat-sky tomographic convergence power spectrum between tomographic bins i and j as

$$C_{ij}^\kappa(\ell) = \int \frac{d\chi}{\chi^2} W_i(\ell/\chi, \chi) W_j(\ell/\chi, \chi) P_\delta(\ell/\chi, \chi), \quad (35.6)$$

where the lensing efficiency function $W_i(\ell/\chi, \chi)$ is defined as

$$W_i(\ell/\chi, \chi) = \frac{3\Omega_m}{4\chi_H^2} \int_\chi^\infty d\chi' \frac{dz}{d\chi'} \frac{n_i(z(\chi'))}{a(\chi')} \left(\frac{\chi - \chi'}{\chi\chi'} \right) \left[1 + \frac{1}{\eta(\ell/\chi, \chi')} \right] \mu(\ell/\chi, \chi'), \quad (35.7)$$

with $n_i(z(\chi))$ the distribution of sources in the i -th bin, normalized to one, $\int d\chi n_i(z(\chi)) = 1$. Clearly, this approach still remains an approximation to a purely 3-dimensional treatment of the cosmic shear field, as it is still characterised by an averaging in redshift, which produces loss of information.

An alternative formalism, commonly known as *3D cosmic shear*, makes use of a spherical Fourier-Bessel decomposition of the cosmic shear field, to include all of the redshift information in the analysis. First introduced in [14] and subsequently refined in [15–17], this method has so far been applied to real data only in [18]. A code comparison between available codes and numerical challenges have been discussed in [19]. 3D cosmic shear is based on a decomposition of the cosmic shear field in a suitable basis of functions, given by a combination of spin-2 spherical harmonics ${}_2Y_{\ell m}(\hat{\mathbf{n}})$ for the angular components, and spherical Bessel functions for the radial coordinate $j_\ell(k\chi)$; together, these functions constitute the spherical Fourier-Bessel basis. The shear tensor $\gamma(\chi, \hat{\mathbf{n}})$ is defined as the second ∂ derivative of the lensing potential Ψ

$$\gamma(\chi, \hat{\mathbf{n}}) = \frac{1}{2} \partial \partial \Psi(\chi, \hat{\mathbf{n}}). \quad (35.8)$$

The shear γ can be expanded in the spherical Fourier-Bessel basis as

$$\gamma(\chi, \hat{\mathbf{n}}) = \sqrt{\frac{2}{\pi}} \sum_{\ell m} \int k^2 dk \gamma_{\ell m}(k) {}_2Y_{\ell m}(\hat{\mathbf{n}}) j_\ell(k\chi), \quad (35.9)$$

where the coefficients $\gamma_{\ell m}(k)$ are given by

$$\gamma_{\ell m}(k) = \sqrt{\frac{2}{\pi}} \int \chi^2 d\chi \int d\Omega \gamma(\chi, \hat{\mathbf{n}}) j_\ell(k\chi) {}_2Y_{\ell m}^*(\hat{\mathbf{n}}). \quad (35.10)$$

The covariance of shear modes can be related to the matter power spectrum [4, 19, 20],

$$\langle \tilde{\gamma}_{\ell m}(k) \tilde{\gamma}_{\ell' m'}^*(k') \rangle = \frac{9\Omega_m^2}{16\pi^4 \chi_H^4} \frac{(\ell+2)!}{(\ell-2)!} \int \frac{d\tilde{k}}{\tilde{k}^2} G_\ell(k, \tilde{k}) G_{\ell'}(k', \tilde{k}) \delta_{\ell\ell'}^K \delta_{mm'}^K.$$

where

$$G_\ell(k, k') = \int dz n_z(z) F_\ell(z, k) U_\ell(z, k'), \quad (35.11)$$

$$F_\ell(z, k) = \int dz_p p(z_p|z) j_\ell[k\chi^0(z_p)], \quad (35.12)$$

$$U_\ell(z, k) = \frac{1}{2} \int_0^{\chi(z)} \frac{d\chi'}{a(\chi')} \left(\frac{\chi - \chi'}{\chi\chi'} \right) j_\ell(k\chi') P_\delta^{1/2}(k, z(\chi)) \mu(k, a(\chi)) \left[1 + \frac{1}{\eta(k, a(\chi'))} \right]. \quad (35.13)$$

The estimates $\tilde{\gamma}$ of the pure cosmic shear field γ keep into account observational effects such as the redshift distribution $n_z(z)$ of the lensed galaxies and the conditional probability $p(z_p|z)$ of estimating the redshift z_p given the true redshift z . More recently, 3D cosmic shear was used in [4] to forecast modified gravity predictions, with a quantitative comparison with a tomographic analysis, whose results we recall below.

35.2 Current Data and Forecasts on Horndeski Gravity

The Horndeski Lagrangian [21] is the most general scalar-tensor theory of gravity with a scalar degree of freedom in addition to the metric, that respects the following conditions: it is four-dimensional, Lorentz-invariant, local and has equations of motion with derivatives not higher than second order. The latter condition guarantees that the theory is safe from Ostrogradski instabilities [22]. We will consider only universal coupling between the metric and the matter fields (collectively described by Φ_m and contained in the matter Lagrangian \mathcal{L}_m), which are therefore uncoupled to the scalar field. The Horndeski action can be written as follows:

$$S[g_{\mu\nu}, \Psi] = \int d^4x \sqrt{-g} \left[\sum_{i=2}^5 \frac{1}{8\mathbb{B}G_N} \mathcal{L}_i[g_{\mu\nu}, \Psi] + \mathcal{L}_m[g_{\mu\nu}, \Phi_M] \right], \quad (35.14)$$

$$\begin{aligned} \mathcal{L}_2 &= G_2(\Psi, X), \\ \mathcal{L}_3 &= -G_3(\Psi, X)\square\Psi, \\ \mathcal{L}_4 &= G_4(\Psi, X)R + G_{4X}(\Psi, X) [(\square\Psi)^2 - \Psi_{;\mu\nu}\Psi^{;\mu\nu}], \\ \mathcal{L}_5 &= G_5(\Psi, X)G_{\mu\nu}\Psi^{;\mu\nu} \\ &\quad - \frac{1}{6}G_{5X}(\Psi, X) [(\square\Psi)^3 + 2\Psi_{;\mu}{}^\nu\Psi_{;\nu}{}^\alpha\Psi_{;\alpha}{}^\mu - 3\Psi_{;\mu\nu}\Psi^{;\mu\nu}\square\Psi]. \end{aligned}$$

The subscripts Ψ, X denote partial derivatives, e.g. $G_{iX} = \frac{\partial G_i}{\partial X}$. The choice of the arbitrary functions $G_i(\Psi, X)$ of the scalar field Ψ and its kinetic term $X = -\frac{1}{2}\partial_\mu\Psi\partial^\mu\Psi$ determines the specific gravity model considered within this class. Several known models of dark energy and modified gravity are contained within this class, such as quintessence, $f(R)$ and Galileon models.

The evolution of linear perturbations in Horndeski gravity can be fully described by four functions of (conformal) time τ only [23, 24]:

- (i) α_K is the *kineticity* function, representing the kinetic energy of the scalar perturbations arising directly from the action;
- (ii) α_B is the *braiding* function, which describes mixing of the scalar field with the metric kinetic term;
- (iii) α_M is the *Planck mass run rate*, describing the rate of evolution of the effective Planck mass;
- (iv) α_T is the *tensor speed excess*, describing deviations of the propagation speed of gravitational waves from the speed of light. This function has recently been constrained to be very close to 0, its General Relativity value, by the detection of the binary neutron star merger GW170817 and the associated gamma ray burst GRB170817A [25, 26].

Constraints on these functions can be obtained from large-scale structure observations by choosing a time parametrization, such as the one that traces the evolution of the dark energy component $\Omega_{\text{DE}}(\tau)$:

$$\alpha_i(\tau) = \hat{\alpha}_i \Omega_{\text{DE}}(\tau) \quad i = K, B, M, T \quad (35.15)$$

and getting constraints on the proportionality coefficients $\hat{\alpha}_i$. All of these functions are identically vanishing in General Relativity, so that any detection of a value different from 0 would be a clear signal of deviations from Einstein's gravity. This is the idea developed in [4] and [27], using cosmic shear as the cosmological probe (alone and in cross-correlation with other observables) to constrain Horndeski gravity.

In [4], the authors present a Fisher matrix forecast for the Euclid survey, with the goal of quantitatively predicting its constraining power on Horndeski parameters as introduced above Eq. 35.2. The parameterization chosen for the evolution of the α functions is the one described by Eq. 35.15. The authors fix the values of α_K and α_T to 0, the former being largely uncorrelated with the other three functions and unconstrained by large-scale structure probes, the latter being strongly constrained by gravitational wave experiments. Moreover, they present a forecast comparing tomography and 3d cosmic shear, presenting expressions for both formalisms in a general modified gravity setting (similarly to the description provided in Sect. 35.1). They simultaneously place constraints on a set of cosmological parameters describing the evolution of the background (assumed to be well modelled by a Λ CDM model), as well as on the Horndeski parameters α_M and α_B , which act at the perturbation level. They find that a 3D analysis can constrain Horndeski theories better than a tomographic one, with a reduction of the errors of the order of 20% on the Horndeski parameters.

Despite performing a conservative cut in angular and radial scales and only using a linear matter power spectrum for the calculation of the covariance of the cosmic shear modes, 3D cosmic shear performs better than tomography in constraining both standard and Horndeski parameters (as shown in Fig. 35.1, taken from [4]). The two methods show similar degeneracies, despite being completely independent in their implementation and based on two different formalisms. To illustrate the importance of non-linear corrections, the authors produce constraints with 3D cosmic shear and a prescription for the non-linear matter power spectrum based on [28]; the resulting increase in sensitivity from the non-linear corrections calls for the development of nonlinear prescriptions for general dark energy models in view of applications to future datasets.

In [27], the authors present a cross-correlation analysis of cosmic shear, galaxy-galaxy lensing and galaxy clustering tomographic power spectra from $\sim 450 \text{ deg}^2$ of cosmic shear data from the Kilo Degree Survey (KiDS) and two overlapping spectroscopic samples from the GALaxy and Mass Assembly (GAMA) survey. The goal of this analysis is to provide the first constraints on Horndeski parameters achieved from currently available cosmic shear data (alone and in cross-correlation with the other two probes). The methodology followed to model the power spectra extends to a Horndeski gravity setting the analysis performed in [29], carried out in Λ CDM on the same power spectra dataset. The authors adopt the same parameterization for the Horndeski α_B, α_M functions chosen in [4] (and given by Eq. 35.15), finding values for $\hat{\alpha}_B$ and $\hat{\alpha}_M$ compatible with Λ CDM. Interestingly, the values found for $S_8 \equiv \sigma_8 \sqrt{\Omega_m/0.3}$ (a combination of the parameters Ω_m and σ_8 particularly well

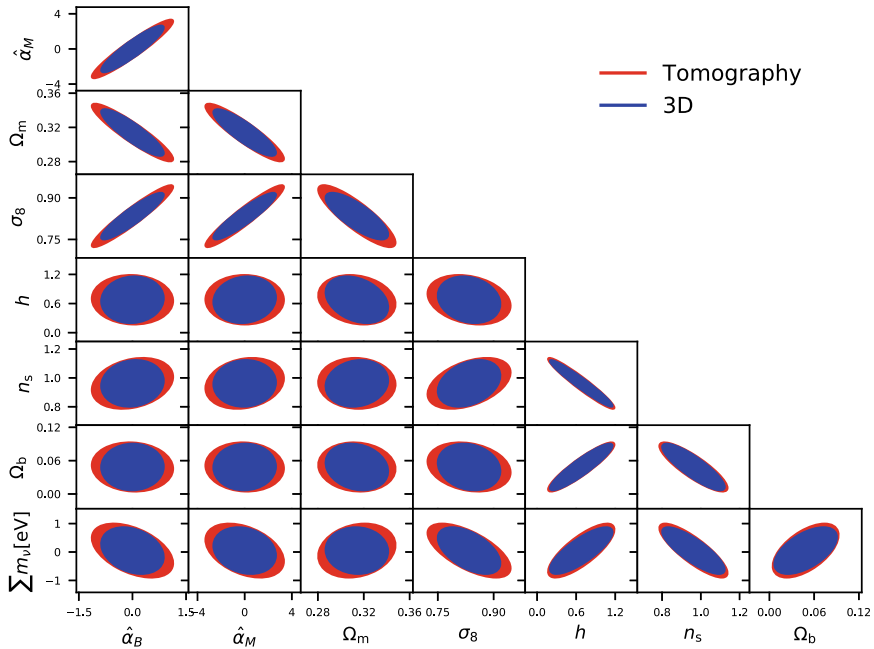


Fig. 35.1 1- σ Fisher forecast contours for Euclid-like survey, obtained with tomography (red) and 3D cosmic shear (blue). The parameters constrained are a set of standard cosmological parameters describing the evolution of the background and the Horndeski $\hat{\alpha}_B$ and $\hat{\alpha}_M$ parameters acting on the perturbations. As discussed in [4], a 3D analysis tightens constraints on all standard and Horndeski parameters of about 20% with respect to a tomographic analysis. The figure is taken from [4]

probed by lensing) are in better agreement with the Planck CMB values when the analysis is carried out in Horndeski gravity, rather than in Λ CDM; the tension in the $\Omega_m - \sigma_8$ plane between large-scale structure and CMB measurements is largely reduced in Horndeski gravity (see Fig. 35.2).

35.3 Higher-Order Statistics and Lensing Peak Counts

Using different statistics, beyond the second-order Gaussian power spectrum, can help to capture non Gaussian content and better discriminate among different cosmological models. An analysis of a variety of different statistics in weak lensing observables has been extensively presented in [3]. In particular, it is relevant to ask the following questions: if a non-standard gravity cosmology is mimicking a cosmological constant, can we distinguish the two scenarios using weak lensing? Which statistic best discriminates them? Massive neutrinos are degenerate with the strength of a fifth force gravitational interaction: higher values of the neutrino mass suppress

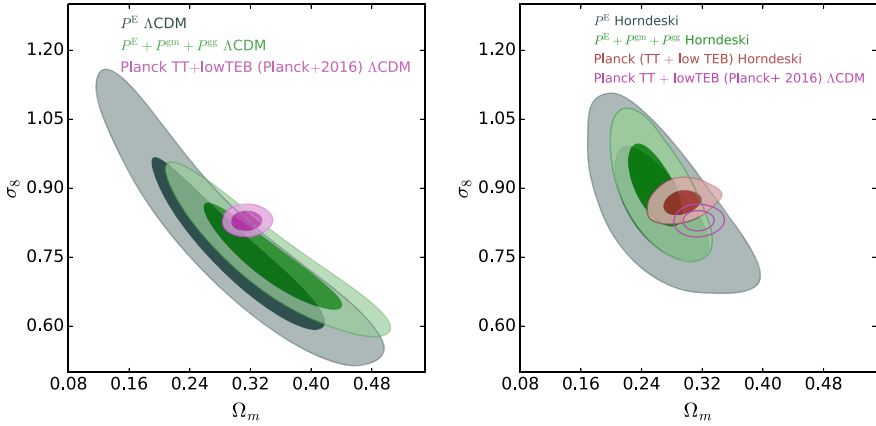


Fig. 35.2 68% and 95% contours on the cosmological parameters Ω_m and σ_8 . The grey contours are obtained considering $\sim 450 \text{ deg}^2$ of cosmic shear data from the KiDS survey; the green contours are obtained from a joint analysis of cosmic shear - galaxy-galaxy lensing and galaxy clustering from the same KiDS samples and two overlapping spectroscopic samples from the GAMA survey. In the left panel, large-scale structure and CMB probes are analysed assuming a ΛCDM model (the Planck contours in magenta are the same as in [30]). In the right panel, the large-scale structure constraints are obtained assuming Horndeski gravity; in brown we plot the Planck contours assuming Horndeski gravity, whereas in magenta the ΛCDM contours of [30] (the same as in the left panel) are reproduced for comparison

the growth of structure, and can therefore compensate higher values of the strength of the fifth force interaction, which would enhance the growth. For example, an $f(R)$ model with amplitude $f_{R0} \sim 10^{-5}$ and massive neutrinos of $m_\nu \sim 1.5 \text{ eV}$ can mimic the matter power spectrum of a cosmological constant model with a neutrino mass of 0.06 eV (as currently typically fixed in ΛCDM). Authors in [3] then used hydro simulations for ΛCDM and different $f(R)$ cosmologies (of the type Hu-Sawicki), built on purpose to be degenerate in their matter power spectra. They then compared different statistics in weak lensing observables, including variance, skewness, kurtosis and peak counts, i.e. the number count of lensing peaks in their aperture mass maps.

Results show that peak counts best capture non-Gaussian information and represent the statistic that has a higher chance to discriminate between $f(R)$ and ΛCDM models, with a discrimination efficiency that depends on redshift and angular scale of observation. Figure 35.3 from [3] nicely shows this effect for a specific filtering scale.

Peak counts are therefore a promising tool for future weak lensing surveys. In addition, as shown in forecasts presented in [31], combining peak counts with lensing power spectrum can improve the constraints on the sum of neutrino masses, on the relative matter density Ω_m , and on the primordial amplitude A_s by factors 39%, 32%, and 60% respectively, as compared to constraints derived from the power spectrum alone [32]. More recently, in [33] the authors proposed a new statistics that joins peaks and voids, and avoids the problem of defining what is a peak or what is a void.

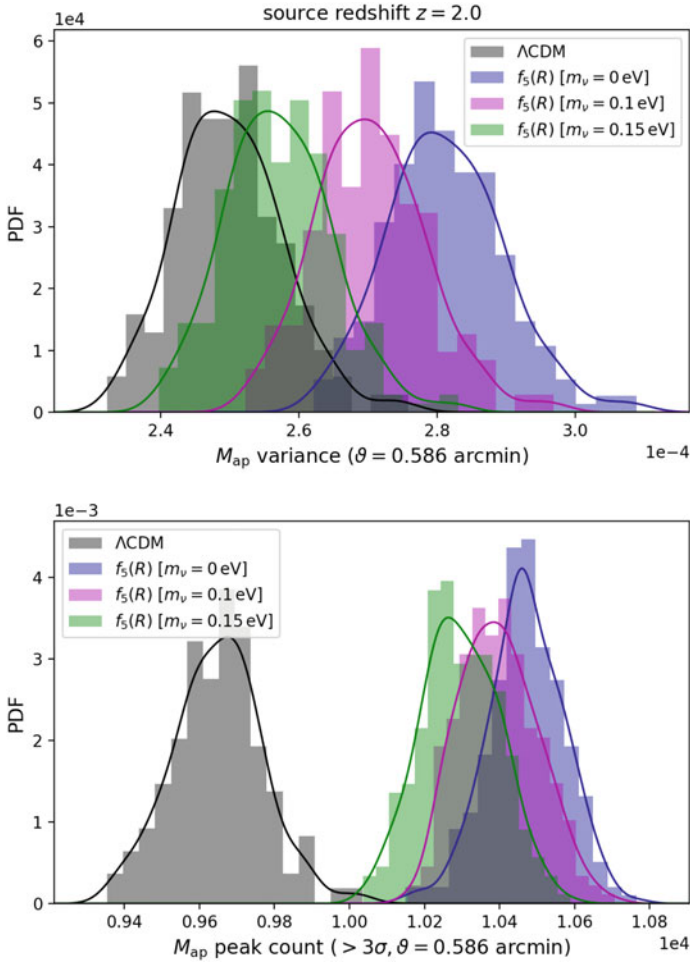


Fig. 35.3 Histograms of aperture mass statistics for Λ CDM and $f_5(R)$ models (i.e. Hu-Sawicki models with amplitude $f_{R0} = 10^{-5}$) and different values of the neutrino mass m_ν . Each histogram, with area normalised to one, comprises 256 samples of the statistic computed at a filtering scale of $\vartheta = 0.586'$ and for sources at redshift $z_s = 2.0$. Solid lines represent the result of smoothing the distribution by KDE (cf. Sect. 5.3 in [3]). Considering the most degenerate case with Λ CDM, $f_5(R)$ with $m_\nu = 0.15$ eV, second- and higher-order moments of M_{ap} do not appear able to distinguish the models. Peak counts, on the other hand, shown here for a 3σ threshold, cleanly separate the two distributions. It is interesting to note that peak counts separate all $f_5(R)$ cases from Λ CDM by approximately the same amount, independent of m_ν . The figure is taken from [3]

35.4 Machine Learning and the Dark Universe

Machine learning has recently seen an increase in applications in all fields, including cosmology for which new opportunities and challenges have been recently summarised in [34]. Convolutional Neural Networks (CNN) have been used in particular on weak lensing observables, trained on convergence maps, to discriminate models along the Ω_m, σ_8 degeneracy [35–37]. In [38] the authors also showed that the network can exploit information related to the steepness of local peaks, rather than to their amplitude. More recently, it was shown in [39] that CNN can break the degeneracy discussed above between neutrino masses and the dark universe, significantly outperforming all statistics, including peak counts.

We briefly recall here the main result developed in [39], as this directly compares with what discussed in Sect. 35.3 and the python code used in the analysis has been made publicly available: specifically, authors apply CNN to discriminating between Λ CDM cosmologies and $f(R)$ (Hu-Sawicki) models with massive neutrinos. The authors start from one simulation per model: this is possible for a classification problem, for which simulations are done on purpose for models which are degenerate at the level of the power spectrum. Convergence maps are then obtained with random reorientation in the same simulation run; furthermore, a compressed representation of the input is used, which reduces the dimensionality of the data and speeds up the training. As known, the network learning procedure consists in updating the parameters (weights) in the cost function via gradient descent and back-propagation in order to match the desired output. This learning (training) process is done on 75% of the available input data (for which labels are known) and tested on the remaining 25% of input data. Validation accuracy (i.e. the ratio of correct predictions to the total number of test observations) has been shown to go from 92% (for a noiseless case) down to 48% for a pessimistic noise level.

The results in [39] show that the CNN is able to discriminate Λ CDM from $f(R)$ gravity better than other statistics, including peak counts, for all choices of noise levels. For example, for an intermediate/optimistic noise level ($\sigma = 0.35$ standard deviation in Gaussian random noise), Λ CDM can be discriminated with 79% accuracy (against 30% maximum accuracy for peak count statistic, for the same redshift). Including all four source redshifts available $\{0.5, 1, 1.5, 2\}$ further increases CNN accuracy to 87% for the same noise level. With respect to peak count statistic, CNN also seems to be more efficient in discriminating among different neutrino masses, within $f(R)$ scenarios. Different types of machine learning techniques were also tested on the same simulations in [40], finding that CNN is the one that best performs, among the ones tested.

While the results are promising for classification problems, this proof of concept opens the path to new challenges. First, one may want to also address a regression problem, i.e. infer cosmological parameters from real data: in this case, one can expect many more simulations to be needed, and a different architecture to serve for regression. Second, one may expect weak lensing systematics to also play a role when dealing with real data, and it is not clear at this stage if machine learning will be robust to these systematics. This has to be investigated in the future.

References

1. P. Schneider, Detection of (dark) matter concentrations via weak gravitational lensing. *MNRAS* **283**, 837–853 (1996). [arXiv:astro-ph/9601039](#)
2. P. Schneider, L. van Waerbeke, B. Jain, G. Kruse, A new measure for cosmic shear. *MNRAS* **296**, 873–892 (1998). [arXiv:astro-ph/9708143](#)
3. A. Peel, V. Pettorino, C. Giocoli, J.-L. Starck, M. Baldi, Breaking degeneracies in modified gravity with higher (than 2nd) order weak-lensing statistics. *Astron. Astrophys. A* **619**, 38 (2018). [arXiv:1805.05146](#)
4. A. Spurio Mancini, R. Reischke, V. Pettorino, B.M. Schäfer, M. Zumalacárregui, Testing (modified) gravity with 3D and tomographic cosmic shear. *MNRAS* **480**, 3725–3738 (2018). [arXiv:1212.3338](#)
5. L. Amendola, M. Kunz, D. Sapone, Measuring the dark side (with weak lensing). *JCAP* **0804**, 013 (2008). [arXiv:0704.2421](#)
6. Planck Collaboration, P.A.R. Ade et al., Planck 2015 results. XIV. Dark energy and modified gravity. *Astron. Astrophys. A* **594**, 14 (2016)
7. M. Kilbinger, L. Fu, C. Heymans, F. Simpson, J. Benjamin, T. Erben, J. Harnois-Déraps, H. Hoekstra, H. Hildebrandt, T.D. Kitching, Y. Mellier, L. Miller, L. Van Waerbeke, K. Benabed, C. Bonnett, J. Coupon, M.J. Hudson, K. Kuijken, B. Rowe, T. Schrabback, E. Semboloni, S. Vafaei, M. Velander, CFHTLenS: combined probe cosmological model comparison using 2D weak gravitational lensing. *MNRAS* **430**, 2200–2220 (2013). [arXiv:1212.3338](#)
8. B.M. Schäfer, L. Heisenberg, Weak lensing tomography with orthogonal polynomials. *MNRAS* **423**, 3445–3457 (2012). [arXiv:1107.2213](#)
9. W. Hu, Power spectrum tomography with weak lensing. *Astrophys. J. Lett.* **522**, L21–L24 (1999). ([astro-ph/9904153](#))
10. J. Benjamin, L. Van Waerbeke, C. Heymans, M. Kilbinger, T. Erben, H. Hildebrandt, H. Hoekstra, T.D. Kitching, Y. Mellier, L. Miller, B. Rowe, T. Schrabback, F. Simpson, J. Coupon, L. Fu, J. Harnois-Déraps, M.J. Hudson, K. Kuijken, E. Semboloni, S. Vafaei, M. Velander, CFHTLenS tomographic weak lensing: quantifying accurate redshift distributions. *MNRAS* **431**, 1547–1564 (2013). [arXiv:1212.3327](#)
11. D.N. Limber, The Analysis of Counts of the Extragalactic Nebulae in Terms of a Fluctuating Density Field. *Astrophys J* **117**, 134 (1953)
12. N. Kaiser, Weak gravitational lensing of distant galaxies. *Astrophys J* **388**, 272–286 (1992)
13. M. LoVerde, N. Afshordi, Extended limber approximation. *Phys. Rev. D* **78**, 123506 (2008). [arXiv:0809.5112](#)
14. A. Heavens, 3D weak lensing. *MNRAS* **343**, 1327–1334 (2003). [arXiv:astro-ph/0304151](#)
15. P.G. Castro, A.F. Heavens, T.D. Kitching, Weak lensing analysis in three dimensions. *Phys. Rev. D* **72**, 023516 (2005). [arXiv:astro-ph/0503479](#)
16. A.F. Heavens, T.D. Kitching, A.N. Taylor, Measuring dark energy properties with 3D cosmic shear. *MNRAS* **373**, 105–120 (2006). ([astro-ph/0606568](#))
17. T.D. Kitching, A.F. Heavens, L. Miller, 3D photometric cosmic shear. *MNRAS* **413**, 2923–2934 (2011). [arXiv:1007.2953](#)
18. T.D. Kitching, A.F. Heavens, J. Alsing, T. Erben, C. Heymans, H. Hildebrandt, H. Hoekstra, A. Jaffe, A. Kiessling, Y. Mellier, L. Miller, L. van Waerbeke, J. Benjamin, J. Coupon, L. Fu, M.J. Hudson, M. Kilbinger, K. Kuijken, P. Rowe, T. Schrabback, E. Semboloni, M. Veland, 3D cosmic shear cosmology from CFHTLenS. *MNRAS* **442**, 1326–1349 (2014)
19. A. Spurio Mancini, P.L. Taylor, R. Reischke, T. Kitching, V. Pettorino, B.M. Schäfer, B. Zieser, P.M. Merkel, 3D cosmic shear: numerical challenges, 3D lensing random fields generation, and Minkowski functionals for cosmological inference. *Phys. Rev. D* **98**, 103507 (2018). [arXiv:1807.11461](#)
20. B. Zieser, P.M. Merkel, The cross-correlation between 3D cosmic shear and the integrated Sachs-Wolfe effect. *MNRAS* **459**, 1586–1595 (2016). [arXiv:1603.06406](#)
21. G.W. Horndeski, Second-order scalar-tensor field equations in a four-dimensional space. *Int. J. Theor. Phys.* **10**, 363–384 (1974)

22. R.P. Woodard, Avoiding dark energy with $1/r$ modifications of gravity. *Lect. Notes Phys.* **720**, 403–433 (2007). [arXiv:astro-ph/0601672](https://arxiv.org/abs/astro-ph/0601672)
23. J. Gleyzes, D. Langlois, F. Piazza, F. Vernizzi, Essential building blocks of dark energy. *JCAP* **1308**, 025 (2013). [arXiv:1304.4840](https://arxiv.org/abs/1304.4840)
24. E. Bellini, I. Sawicki, Maximal freedom at minimum cost: linear large-scale structure in general modifications of gravity. *JCAP* **1407**, 050 (2014). [arXiv:1404.3713](https://arxiv.org/abs/1404.3713)
25. LIGO Scientific, Virgo Collaboration, B.P. Abbott, R. Abbott, T.D. Abbott, F. Acernese, K. Ackley, C. Adams, T. Adams, P. Addesso, X. Adhikari, V.B. Adya et al., GW170817: observation of gravitational waves from a binary neutron star inspiral. *Phys. Rev. Lett.* **119**, 161101 (2017). [arXiv:1710.05832](https://arxiv.org/abs/1710.05832)
26. LIGO Scientific, Virgo, Fermi GBM, INTEGRAL, IceCube, AstroSat Cadmium Zinc Telluride Imager Team, IPN, Insight-Hxmt, ANTARES, Swift, AGILE Team, 1M2H Team, Dark Energy Camera GW-EM, DES, DLT40, GRAWITA, Fermi-LAT, ATCA, ASKAP, Las Cumbres Observatory Group, OzGrav, DWF (Deeper Wider Faster Program), AST3, CAASTRO, VINROUGE, MASTER, J-GEM, GROWTH, JAGWAR, CaltechNRAO, TTU-NRAO, NuSTAR, Pan-STARRS, MAXI Team, TZAC Consortium, KU, Nordic Optical Telescope, ePESSTO, GROND, Texas Tech University, SALT Group, TOROS, BOOTES, MWA, CALET, IKI-GW Follow-up, H.E.S.S., LOFAR, LWA, HAWC, Pierre Auger, ALMA, Euro VLBI Team, Pi of Sky, Chandra Team at McGill University, DFN, ATLAS Telescopes, High Time Resolution Universe Survey, RIMAS, RATIR, SKA South Africa/MeerKAT Collaboration, B.P. Abbott et al., Multi-messenger observations of a binary neutron star merger. *Astrophys. J.* **848**(2), L12 (2017). [arXiv:1710.05833](https://arxiv.org/abs/1710.05833)
27. A. Spurio Mancini, F. Köhlinger, B. Joachimi, V. Pettorino, B.M. Schäfer, R. Reischke, S. Brieden, M. Archidiacono, J. Lesgourgues, *KiDS+GAMA: Constraints on Horndeski gravity from combined large-scale structure probes* (2019). [arXiv:1901.03686](https://arxiv.org/abs/1901.03686)
28. A.J. Mead, J.A. Peacock, C. Heymans, S. Joudaki, A.F. Heavens, An accurate halo model for fitting non-linear cosmological power spectra and baryonic feedback models. *MNRAS* **454**, 1958–1975 (2015). [arXiv:1505.07833](https://arxiv.org/abs/1505.07833)
29. E. van Uitert, B. Joachimi, S. Joudaki, A. Amon, C. Heymans, F. Köhlinger, M. Asgari, C. Blake, A. Choi, T. Erben, D.J. Farrow, J. Harnois-Déraps, H. Hildebrandt, H. Hoekstra, T.D. Kitching, D. Klaes, K. Kuijken, J. Merten, L. Miller, R. Nakajima, P. Schneider, E. Valentijn, M. Viola, *KiDS+GAMA: cosmology constraints from a joint analysis of cosmic shear, galaxy-galaxy lensing, and angular clustering*. *MNRAS* **476**, 4662–4689 (2018). [arXiv:1706.05004](https://arxiv.org/abs/1706.05004)
30. Planck Collaboration, P.A.R. Ade, N. Aghanim, M. Arnaud, M. Ashdown, J. Aumont, C. Baccigalupi, A.J. Banday, R.B. Barreiro, J.G. Bartlett et al, Planck 2015 results. XIII. Cosmological parameters. *Astron. Astrophys. A* **594**, 13 (2016). [arXiv:1502.01589](https://arxiv.org/abs/1502.01589)
31. Z. Li, J. Liu, J.M.Z. Matilla, W.R. Coulton, Constraining neutrino mass with tomographic weak lensing peak counts. *Phys. Rev. D* **99**, 063527 (2019). [arXiv:1810.01781](https://arxiv.org/abs/1810.01781)
32. V. Ajani, A. Peel, V. Pettorino, J.-L. Starck, Z. Li, J. Liu, Constraining neutrino masses with weak-lensing multiscale peak counts. *Phys. Rev. D* **102**(10), 103531 (2020). [arXiv:2001.10993](https://arxiv.org/abs/2001.10993)
33. V. Ajani, J.-L. Starck, V. Pettorino, Starlet l1-norm for weak lensing cosmology. *Astron. Astrophys.* **645**, L11 (2021). [arXiv:2101.01542](https://arxiv.org/abs/2101.01542)
34. M. Ntampaka et al., The role of machine learning in the next decade of cosmology. *BAAS* **51**, 14 (2019). [arXiv:1902.10159](https://arxiv.org/abs/1902.10159)
35. J. Schmelzle, A. Lucchi, T. Kacprzak, A. Amara, R. Sgier, A. Réfrégier, T. Hofmann, *Cosmological model discrimination with Deep Learning* (2017). [arXiv:1707.05167](https://arxiv.org/abs/1707.05167)
36. A. Gupta, J.M.Z. Matilla, D. Hsu, Z. Haiman, Non-Gaussian information from weak lensing data via deep learning. *Phys. Rev. D* **97**, 103515 (2018). [arXiv:1802.01212](https://arxiv.org/abs/1802.01212)
37. J. Fluri, T. Kacprzak, A. Refregier, A. Amara, A. Lucchi, T. Hofmann, Cosmological constraints from noisy convergence maps through deep learning. *Phys. Rev. D* **98**, 123518 (2018). [arXiv:1807.08732](https://arxiv.org/abs/1807.08732)
38. D. Ribli, B.Á. Pataki, I. Csabai, An improved cosmological parameter inference scheme motivated by deep learning. *Nat. Astron.* **3**, 93–98 (2019). [arXiv:1806.05995](https://arxiv.org/abs/1806.05995)

39. A. Peel, F. Lalande, J.-L. Starck, V. Pettorino, J. Merten, C. Giocoli, M. Meneghetti, M. Baldi, Distinguishing standard and modified gravity cosmologies with machine learning. *Phys. Rev. D* **100**, 023508 (2019). [arXiv:1810.11030](https://arxiv.org/abs/1810.11030)
40. J. Merten, C. Giocoli, M. Baldi, M. Meneghetti, A. Peel, F. Lalande, J.-L. Starck, V. Pettorino, On the dissection of degenerate cosmologies with machine learning. *MNRAS* **487**, 104–122 (2019). [arXiv:1810.11027](https://arxiv.org/abs/1810.11027)

Chapter 36

Galaxy Clusters and Modified Gravity



Ippocratis D. Saltas and Lorenzo Pizzuti

36.1 What Makes Galaxy Clusters Interesting for Testing Gravity?

Put simply, a galaxy cluster is a self-gravitating system built out of dark matter, hot gas and baryonic tracers in the form of galaxies. What makes galaxy clusters attractive as tests of gravity is that they lie on the borderline between astrophysical and cosmological scales, allowing to test different aspects and predictions of gravity theories.

Traditionally, the combination of kinematical/dynamical measurements in a cluster with lensing observations allows to reconstruct the underlying mass distribution. In General Relativity (GR) the two are expected to be the same, however, this is no longer true within general families of theories beyond GR which predict that pressureless matter and light respond differently to gravity, in turn implying different predictions for the cluster's inferred dynamical/kinematical and lensing mass profiles. This idea has formed the basis for the construction of consistency checks studied predominantly within scalar-tensor theories such as $f(R)$, Brans–Dicke and (Beyond Horndeski) theories.

Disentangling genuine gravitational effects from the complicated astrophysical processes at cluster scales is, however, a subtle task and requires an adequate knowledge of the underlying systematics. In addition, since the bulk of the cluster's mass comes from dark matter, an adequate modelling of the dark matter density distribution is necessary, which proves challenging without knowledge of the actual physics

I. D. Saltas (✉)

CEICO, Institute of Physics of the Czech Academy of Sciences, Na Slovance 2,
182 21 Praha 8, Prague, Czechia

L. Pizzuti

Osservatorio Astronomico della Regione Autonoma Valle d'Aosta, Loc. Lignan 39,
I-11020 Nus, Italy
e-mail: pizzuti@oavda.it

© The Author(s), under exclusive license to Springer Nature Switzerland AG 2021

571

E. N. Saridakis et al. (eds.) *Modified Gravity and Cosmology*,

https://doi.org/10.1007/978-3-030-83715-0_36

of the dark sector. Therefore, the underlying assumptions for constraints on gravity in this regard have to be challenged and testes before conclusive statements are to be made.

Our goal here is to briefly review progress on the methods and constraints on theories beyond GR with the physics of galaxy clusters, along with a discussion on the associated hurdles from astrophysical and observational systematics.

36.2 Consistency Conditions Based on the Mass Profiles of Galaxy Clusters

36.2.1 Generalities

It is instructive to start with a recap of some useful concepts from cosmological perturbation theory. In galaxy clusters, matter collapses in a non-linear fashion, however, gravity remains linear implying that, the gravitational wells are sufficiently small for linear perturbation theory to hold. In this regard, the Poisson equation relates the Newtonian potential Ψ to the matter density as $\nabla^2\Psi = 8\pi G_N\rho_m$, while the gravitational slip parameter relates Ψ to the relativistic potential Φ through the gravitational slip parameter $\eta \equiv \Psi/\Phi$. The weak-lensing potential satisfies a Poisson-like equation as $\nabla^2(\Phi + \Psi) = 8\pi G_N\rho_{lens}$, where ρ_{lens} is the matter density inferred through lensing probes—we will get back to this later.

Hydrostatic equilibrium in a galaxy cluster is achieved through the balance between gravity and the gas pressure as

$$\frac{dP_{\text{tot.}}}{dr} = \rho_{\text{gas}} \frac{d\Psi}{dr}, \quad (36.1)$$

with the total pressure given by the sum of thermal and non-thermal pressure $P_{\text{tot.}} = P_{\text{therm.}} + P_{\text{non-therm.}}$. The thermal pressure comes predominantly from the hot gas, as $P_{\text{therm.}} = n_{\text{gas}}kT_{\text{gas}}$. Writing $d\Psi/dr = G_N M(r)/r^2$, Eq.(36.1) then provides a definition of the (non-)thermal mass profile. The bulk of the pressureless matter sourcing the potential Ψ comes from dark matter. The most popular density profile to model it is the Navarro–Frenk–White (NFW), which is a 2-parameter profile depending on a characteristic density and radius as

$$\rho_{\text{NFW}} = \frac{\rho_s}{(r/r_s)(1+r/r_s)^2}, \quad \rho_s \equiv \frac{1}{3} \cdot \frac{\rho_c(z)\Delta_{\text{vir}} \cdot c^3}{\log(1+c) - c(1+c)^{-1}}, \quad (36.2)$$

with $\rho_c \equiv 3H^2(z)/(8\pi G_N)$ corresponds to the critical density of the Universe. The concentration parameter, $c \equiv r_{\text{vir}}/r_s$, relates the viral radius with the scale r_s , with the former defining the region of the cluster that encloses a mean over density equal to $\rho_c\Delta_{\text{vir}}$. The popularity of the NFW profile relies in that it provides a good fit to

haloes within N-body simulations, and for large range of masses both in Newtonian and modified gravity. In particular, Ref. [1] showed that the NFW profile provides equally good fits to N-body simulations in $f(R)$ gravity as the standard Newtonian case, which was later confirmed by Ref. [2] considering the particular case of the Hu-Sawicki $f(R)$ model. Since here we will be mostly interested in constraints on the theory space of modified gravity, for more details on actual the halo modelling beyond GR we refer to [1–5].

36.2.2 Probes Based on Mass Profiles from Galaxy Kinematics and Lensing

Under the assumption of spherical symmetry, the Poisson equations for the potentials Ψ and $\Phi + \Psi$ allow us to derive the following expressions

$$\Psi(r) = G_N \int_{r_0}^r \frac{ds}{s^2} M_{\text{dyn}}(s), \quad (36.3)$$

$$\Phi(r) = G_N \int_{r_0}^r \frac{ds}{s^2} (2M_{\text{lens}} - M_{\text{dyn}}). \quad (36.4)$$

Equation (36.3) serves as a definition of the dynamical mass of the cluster, i.e the mass inferred from dynamical probes, while it is easy to see that for the lensing mass $M_{\text{lens}} = \frac{r^2}{2G} \frac{d}{dr} (\Phi + \Psi)$. Assuming that member galaxies are collision less tracers of the underlying gravitational field Ψ , their velocity dispersion field satisfies the Jeans equation

$$\frac{\partial(v\sigma_r^2)}{\partial t} + 2\beta(r) \frac{v\sigma_r^2}{r} = -v(r) \frac{\partial\Psi}{\partial r}, \quad (36.5)$$

where $v(r)$ is the number density of tracers, σ_r^2 the velocity dispersion along the radial direction and $\beta \equiv 1 - (\sigma_\theta^2 + \sigma_\phi^2)/2\sigma_r^2$ the velocity anisotropy profile. The latter, accounts for the neglected velocity component in along-the-light-of-sight observations, and it introduces an important source of uncertainty which has to be accounted for, as we will discuss in Sect. 36.3. In principle, the choice of $v(r)$ is also model dependent and its effect on any constraints needs to be investigated.

The combination of lensing and dynamics of a galaxy cluster can provide a powerful test based on the gravitational slip parameter η . Combining (36.3) and (36.4) we may derive an expression for the gravitational slip in terms of the dynamical and lensing mass profiles as

$$\eta(r) = \frac{\int_{r_0}^r \frac{ds}{s^2} [2M_{\text{lens}}(s) - M_{\text{dyn}}(s)]}{\int_{r_0}^r \frac{ds}{s^2} M_{\text{dyn}}(s)}. \quad (36.6)$$

Therefore, the existence of gravitational slip can be viewed as a consistency condition between the dynamical and lensing mass of the cluster—In GR, and in the presence of perfect fluid matter, it is $M_{dyn} = M_{lens}$ and $\eta = 1$, but this is not true anymore as soon as gravity is modified. In this view, the existence of new gravitational degrees of freedom will manifest itself as a tension in the mass profile inferred from kinematics and lensing.

The above idea formed the basis of Ref. [6] which combined kinematical and lensing observations of the relaxed cluster MACS J1206.2-0847 (hereafter MACS 1206), at redshift $z = 0.44$ (at redshift $z = 0.44$) from the CLASH¹ and CLASH-VLT² surveys to reconstruct the slip parameter η as a function of the distance from the cluster's center. In particular, it considered line-of-sight velocity measurements and projected positions for 592 member galaxies to perform a phase-space analysis using the code *MAMPOSSt* of Ref. [7], which solves the Jeans equation (36.5) to provide a maximum likelihood fit to the mass profile parameters. Assuming an NFW profile, a model for $\beta(r)$, and a Newtonian form for Ψ , combination of dynamics and lensing led to the constraint

$$\eta(r = 1.96\text{Mpc}) = 1.00_{-0.28}^{+0.31} \text{ (statistical)} \pm 0.35 \text{ (systematic)}. \quad (36.7)$$

The assumption of the NFW profile for the total matter distribution was challenged by repeating the analysis with an Hernquist and Burkert profile, where it was found that NFW provided the highest likelihood fit to the kinematic data. The same concept was followed in Ref. [8], which forecasted the ability of galaxy clusters to constraint η using the procedure outlined above. In particular, dynamical mass profiles were re-constructed from a set of 15 spherical mock clusters in equilibrium solving (36.5), followed by a maximum likelihood analysis for the NFW parameters (r_s, r_{200}) . Lensing information was simulated from the based on the observations of MACS 1206. Results showed that η can be constrained at the $\sim 9\%$ level (2σ) when assumed to be scale-independent, and at 21% when scale-dependence is accounted for.

Reference [9] implemented a similar combination of kinematics and lensing for MACS1206 with real data, but introducing the effect of the fifth-force in the gravitational potential within $f(R)$ gravity and a simplified approach for screening. Under the assumption of an NFW profile and the form of the anisotropy profile, it quoted the upper bound on the fifth force's Compton wavelength as

$$\lambda_{f(R)} \leq 1.61 \text{ (statistical)} + 0.30 \text{ (systematic)} \text{ Mpc}. \quad (36.8)$$

Notice that, $\lambda_{f(R)}$ is related to the mass of the scalar field as $\lambda_{f(R)} \sim 1/m_{f(R)}^2 \sim f_{RR}$.

We notice that, constraints on gravity from statistics of a sample of galaxy clusters should be in principle weighted over an appropriate mass function. In fact, the abundance of clusters in modified gravity have provided tight constraints on the allowed theory space of $f(R)$ scalar-tensor theories, since the fifth force modifies the collapse

¹ <http://www.stsci.edu/~postman/CLASH/>.

² <https://kyle.na.astro.it/CLASH-VLT/Public/index.html>.

of matter at large scales, leading to an enhancement of the mass function. This has been the topic of investigation in Refs. [10–16]. In particular, Ref. [12] combined geometrical probes with CMB and cluster abundance data to quote an upper bound on the parameter B related to the scalaron's Compton wavelength³ for the so-called designer $f(R)$ model as $B(z=0) < 1.1 \cdot 10^{-3}$ (95% C.L.). An updated analysis using a similar combination of observables and galaxy clusters up to $z \sim 0.5$ derived the tighter constraint $B(z=0) < 1.78 \cdot 10^{-4}$ (95.4% C.L.) [14]. It should be noticed that, the designer model does not assume a fixed, a priori functional form for $f(R)$, but rather fixes it implicitly by requiring that the predicted background evolution of the Universe matches with observations.

36.2.3 Probes Based on Thermal and Lensing Mass Profiles

An alternative route to test scalar-tensor theories with a conformal coupling between the scalar field and curvature, such as Brans–Dicke or $f(R)$ theories, can be followed through the construction of tests based on the cluster's thermal and lensing mass. In particular, the coupling between the scalar field and matter is expected to have a direct impact on the cluster's inferred thermal mass, but not on the lensing one, since photons travel on null geodesics. This is the main idea followed in [17], which considered the phenomenological implications of the coupling between the chameleon scalar field with the baryonic and dark matter component in the cluster.

The chameleon field is sourced by the scalar potential and matter density according to

$$\nabla^2 \phi = \frac{\partial V(\phi)}{\partial \phi} + \beta \sqrt{8\pi G_N} \rho e^{\beta \sqrt{8\pi G_N} \phi}, \quad (36.9)$$

with β a dimensionless coupling strength, and $\beta = 1/\sqrt{6}$ for the case of $f(R)$ gravity. Sufficiently deep within the cluster, $\nabla^2 \phi \approx 0$, and the scalar field acquires a minimum, ϕ_0 . In this region, the fifth-force is screened. Towards the outskirts of the cluster, a sizeable field gradient builds up, leading to a fifth-force effect with $F_\phi = -\beta \sqrt{8\pi G_N} \frac{d\phi}{dr}$. The contribution of the fifth-force to the r.h.s of the hydrostatic equilibrium (36.1) will in turn affect the gas and temperature profiles of the cluster. Typically, one assumes that outside the cluster the chameleon scalar acquires its ambient cosmological value, $\phi_{cosm.}$, which is the free, model parameter to be constrained. In the language of $f(R)$ gravity,

$$\frac{\partial f}{\partial R} \equiv f_R = -\sqrt{\frac{16\pi G_N}{3}} \phi. \quad (36.10)$$

³ $B \equiv \frac{f_{RR}}{1+f_R} R' \frac{H}{H'}$, with $' \equiv d/d \ln a$ where $a(t)$ is the scale factor and R the Ricci scalar.

Reference [17] started with a generalised NFW profile for dark matter, $\rho = \rho_s / [(r/r_s)(1 + r/r_s)]^b$, and a polytropic one for the gas. In the presence of the chameleon field, the gas distribution becomes steeper at the outskirts of the cluster (compared to GR), where the fifth force is operative. From an observational viewpoint, this in turn causes a decrease in the predicted X-ray surface brightness of the cluster at large radii. Using the X-ray temperature profile observations from the Hydra A cluster, Ref. [17] was able to derive the bound $\phi_{cosm.} < 10^{-4} / \sqrt{8\pi G_N}$ (at redshift $z = 0$) assuming $\beta = 1$. Notice that, this result is insensitive to the details of the potential $V(\phi)$.

The case of $f(R)$ gravity ($\beta = 1/\sqrt{6}$) was studied with a more thorough analysis in [18] adopting a conceptually similar strategy. The work reconstructed the 3-dimensional X-ray temperature and surface brightness profiles, as well as the expected Sunyaev–Zel’dovich (SZ) effect in the presence of the chameleon force under sufficiently general assumptions for the modeling of the gas temperature profile and pressure. With the aid of an MCMC analysis, and the observations of the Coma cluster, the best-fit values for the gas/dark-matter and modified gravity parameter space were inferred, leading to the 2σ constraints $\phi_{cosm.} \lesssim 7 \cdot 10^{-5} / \sqrt{8\pi G_N}$. Under (36.10) this translates to

$$f_{R_0} \lesssim 6 \cdot 10^{-5}. \quad (36.11)$$

In a similar context, Ref. [19] extended the analysis for multiple clusters, analysing 58 stacked cluster profiles observed within $0.1 < z < 1.2$, using X-ray and lensing data from the XMM Cluster Survey and the Canada France Hawaii Telescope Lensing Survey respectively. It is important that, the clusters were found to be living in unscreened environments, since otherwise the fifth force would be environmentally screened. The analysis concluded that, $f_{R_0} \lesssim 6 \cdot 10^{-5}$ at 2σ . The methodology of the latter works was further verified in [20], through the study of hydrodynamical simulations in $f(R)$ gravity. Most notably, it confirmed the validity of the NFW profile when modelling weak-lensing mass profiles in $f(R)$ gravity and the spherical symmetry of the stacked cluster profiles.

Galaxy clusters have been also employed to probe a broader part of the theory space of scalar-tensor theories, beyond a conformal coupling. In particular, the so-called Beyond Horndeski theories have been shown to exhibit an intriguing breaking of the Vainshtein mechanism within compact matter sources such as stars or galaxy clusters. A fundamental difference with conformally-coupled theories is that, here, lensing is directly affected by the fifth force. In particular, for the Beyond Horndeski theories exhibiting a breaking of the Vainshtein mechanism, the two scalar gravitational potentials *within* a compact object can be shown to be,

$$\frac{d\Psi(r)}{dr} = -\frac{G_N M(r)}{r^2} + \frac{Y_1 G_N}{4} \cdot \frac{d^2 M(r)}{dr^2}, \quad (36.12)$$

$$\frac{d\Phi(r)}{dr} = -\frac{G_N M(r)}{r^2} + \frac{5Y_2 G_N}{4r} \cdot \frac{dM(r)}{dr}, \quad (36.13)$$

where Y_1 and Y_2 are dimensionless couplings. For $Y_1 = 0 = Y_2$ the standard expressions are recovered. The gas in the cluster responds to Ψ , hence will be sensitive to Y_1 , whereas the lensing potential will probe both Y_1, Y_2 . Reference [21] used the same data and methodology of [19] for the modelling of the X-ray and lensing profiles to produce stacked profiles of 58 clusters. A simultaneous fit of the X-ray and lensing to the data with an MCMC analysis, lead to the following constraints for the fifth-force couplings,

$$Y_1 = -0.11_{-0.67}^{+0.93} \quad \text{and} \quad Y_2 = -0.22_{-1.19}^{+1.22}. \quad (36.14)$$

In the context of Beyond Horndeski theories it has been also investigated whether the fifth force associated with the breaking of Vainshtein mechanism could mimic the effect of dark matter in galaxy clusters. In particular, Ref. [22] considered a sample of galaxy clusters from the CLASH survey, and reconstructed their gas density from the observed X-ray profiles. It was then shown that for the particular sample of clusters, and assuming a Λ CDM background cosmology, the model can provide a good fit to the lensing of observations without the introduction of dark matter component. In a similar follow up analysis by the same authors, and assuming that $Y_1 = Y_2$, an upper bound at 2σ was derived as [23]

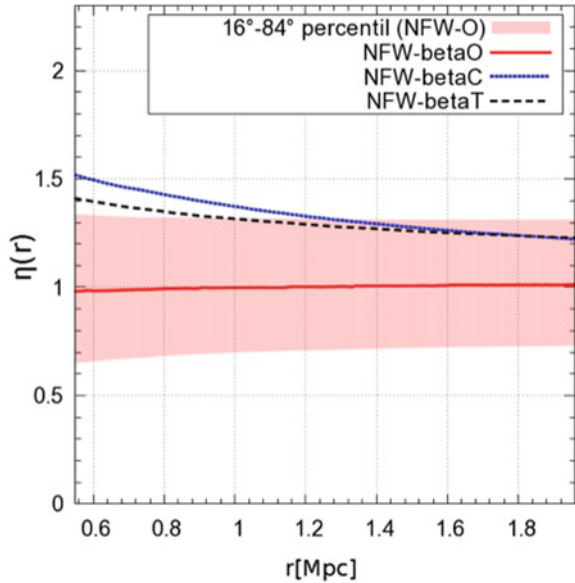
$$Y_1 \leq 0.16. \quad (36.15)$$

36.3 A Brief Discussion on Systematics

The previously discussed constraints rely on various simplifications regarding the modeling of the cluster, e.g the assumption of relaxation. Departures from these assumptions in realistic observations introduce systematics which need to be accounted for, if constraints need to be consistent and robust. Here, we will briefly discuss the impact of such systematics.

The Jean's equation is a powerful method to infer the local potential Φ in the cluster, however, applications of the method are limited by observational constraints, such as the fact that only the velocity dispersion along the line of sight σ_r^2 and the projected number density profile of galaxies can be measured directly. Tangential velocities are generally small and direct measurements of the velocity anisotropy are complicated. To infer $\beta(r)$ one can proceed parametrically, assuming a model for the anisotropy and determining the parameters of the profile along with the mass profile with a Maximum Likelihood fit to the data (see e.g. Ref. [24]). Nevertheless, some non-parametric techniques based on inverting the Jeans' equation can be found in literature (e.g., Refs. [25, 26]), but their application generally requires additional information and assumptions. From both observations of galaxy clusters (e.g., Ref. [27]) and analyses of halos in cosmological simulations (e.g., Refs. [28, 29]) it has been found that generally orbits tend to be isotropic in the center (i.e. $\beta = 0$) while the anisotropy grows with radius.

Fig. 36.1 From Fig. 3 of Ref. [30]: constraints on $\eta(r)$ obtained for the CLASH galaxy cluster MACS 1206 combining lensing and dynamics mass profile determinations. The mass profile is parametrized as a NFW model; different lines correspond to different ansatz in the velocity anisotropy parametrisation. The red shaded area indicates the region between the 16th and 84th percentile for the reference model, “O” profile



In Fig. 36.1 (right panel of Fig. 3 in Ref. [30]) we show the constraints on the gravitational slip, obtained by combining lensing and dynamics mass profiles of the cluster MACS 1206 by Ref. [30], changing the parametrisation of the velocity anisotropy profile in the dynamical analysis. All the three models used in the fit—the constant anisotropy “C”, the Tired model “T” of Ref. [31] and the Opposite model “O” of Ref. [24]—produce bounds on η in agreement within the 68% C.L. given the current uncertainties. However, with the expected precision achievable from future surveys (see below), these effects would become a relevant source of systematics.

A natural question arising when reconstructing mass profiles through a Jeans analysis is the dependence of the results on the number of tracers considered, since realistic observations typically come with a restricted number of spectroscopic velocity measurements. In addition, understanding of this may aid the optimisation of future cluster surveys. This question was investigated [8] in the context of forecasting constraints on η with future surveys, through a combination of simulated kinematical and lensing information. It was found that, keeping the NFW parameters fixed and assuming a scale-independent η , the effect on the forecasted errors is moderate when varying the tracers number between $100 \leq N_{\text{galaxies}} \leq 500$, while it becomes practically negligible for $N_{\text{galaxies}} > 500$.

Departures from dynamical relaxation and spherical symmetry produce a bias in the estimation of the mass profile, introducing systematics in the constraints of modified gravity parameters. In particular, this has been shown in Ref. [32], which performed a detailed study on cosmological N-body simulations showing a strong correlation between the constraints in modified gravity models and the effect of the aforementioned departures; the analysis further identified two observational criteria,

linked to the cluster's dynamical properties, to be used in the selection of those clusters suitable for the application of this kind of methods. Moreover the assumption of dynamical equilibrium limits the validity of the Jeans' equation out to the virial radius, which at $z = 0$ corresponds to the radius r_{200} . It is possible to employ other techniques which doesn't rely on the dynamical state of the cluster and thus they can be used to reconstruct the mass profile in more external regions $r > r_{200}$ (e.g., the Caustic method of Ref. [33]); nevertheless, these methods suffer different kinds of systematics, and the application can be more or less appropriate with respect to the Jeans' analysis depending on the case studied.

It is worth to notice that since both galaxies and the hot X-ray emitting gas of the Intra Cluster Medium (ICM) perceive the same gravitational potential, the two methods for reconstructing the mass profile are sensitive in the same way to modification of gravity. However, diffuse gas and galaxies dynamics suffer different systematics; for instance non-thermal pressure, e.g. associated with unthermalized gas motions, leads to a biased estimate of the cluster mass from X-ray analyses compared to other methods (see, e.g., Ref. [34] and references therein, Ref. [35]), especially in the cluster outskirts where the contribution of non-thermal pressure becomes large (e.g., Ref. [36]).

Moreover, analyses based on the dynamics of cluster member galaxies allow to constrain the gravitational potential out to the virial radius r_{200} (or beyond, as discussed above) while X-ray observations are generally limited to r_{500} ; in addition, gas clumping produces biased X-ray measurements in the outskirts of galaxy clusters (see, e.g., Ref. [37]). Clearly, combined X-ray and Jeans' analyses to infer the gravitational potential in the central region of relaxed clusters could in principle help in tightening the constraints on the inner shape of the mass profile and to break possible degeneracies between the dynamical parameters and additional degrees of freedom in non-standard theories of gravity.

Finally, as regards tests based on the slip parameter η , it is worth pointing out that $\eta = 1$ in GR only if relativistic corrections to the gravitational potentials Ψ and Φ can be neglected. In fact, future constraints of η based on galaxy cluster observations are expected to bring the statistical uncertainties down to few percents. At this level of precision, tiny departures from $\Psi = \Phi$ sourced by non-linear effects in GR, and not by a modification of gravity, are no more negligible and could constitute a severe limitation of the measurements of η . The contribution of these relativistic terms should be taken into account as systematic effect from future analyses.

36.4 Future Outlook

In the next years, new generation surveys will provide a significant amount of imaging and spectroscopic data covering a large portion of the sky, within a broad redshift range. Both ground-based (e.g., LSST and space-borne telescopes (e.g., Euclid are expected to observe several billions galaxies in different bands, aiming at probing the nature of dark energy and gravity at large scales. In particular, the forecasting

analysis of Ref. [38] showed that Euclid’s weak lensing measurements will be able to tighten the constraints on MG parameters placed by the Planck satellite mission by two orders of magnitude.

As for mass determinations of galaxy clusters, the combination of data from the aforementioned surveys with spectroscopic observations coming from next generation high-multiplexing spectrographs on 8m-class telescopes will provide joint dynamics and lensing mass reconstruction of thousands clusters. The signal-to-noise ratio will be much lower than what has been already achieved by current surveys such as the CLASH and CLASH-VLT. Therefore, a good understanding of systematic effects, as discussed in the previous section, is required in order to take full advantage of galaxy cluster analyses for testing gravity on cosmological scales.

Acknowledgements Ippocratis D. Saltas is supported by the Czech Science Foundation GAČR (Project: 21-16583M).

References

1. F. Schmidt, M.V. Lima, H. Oyaizu, W. Hu, Non-linear evolution of $f(R)$ cosmologies III: halo statistics. *Phys. Rev. D* **79**, 083518 (2009). [arXiv:0812.0545](#)
2. L. Lombriser, K. Koyama, G.-B. Zhao, B. Li, Chameleon $f(R)$ gravity in the virialized cluster. *Phys. Rev. D* **85**, 124054 (2012). [arXiv:1203.5125](#)
3. Y. Li, W. Hu, Chameleon halo modeling in $f(R)$ gravity. *Phys. Rev. D* **84**, 084033 (2011). [arXiv:1107.5120](#)
4. L. Lombriser, B. Li, K. Koyama, G.-B. Zhao, Modeling halo mass functions in chameleon $f(R)$ gravity. *Phys. Rev. D* **87**(12), 123511 (2013). [arXiv:1304.6395](#)
5. L. Lombriser, K. Koyama, B. Li, Halo modelling in chameleon theories. *JCAP* **1403**, 021 (2014). [arXiv:1312.1292](#)
6. L. Pizzuti et al., CLASH-VLT: testing the nature of gravity with galaxy cluster mass profiles. *JCAP* **1604**(04), 023 (2016). [arXiv:1602.03385](#)
7. G.A. Mamon, A. Biviano, G. Boué, MAMPOSSt: modelling anisotropy and mass profiles of observed spherical systems - I. Gaussian 3D velocities. *Mon. Not. Roy. Astron. Soc.* **429**, 3079–3098 (2013). [arXiv:1212.1455](#)
8. L. Pizzuti, I.D. Saltas, S. Casas, L. Amendola, A. Biviano, Future constraints on the gravitational slip with the mass profiles of galaxy clusters. *Mon. Not. Roy. Astron. Soc.* **486**(1), 596–607 (2019). [arXiv:1901.01961](#)
9. L. Pizzuti et al., CLASH-VLT: constraints on $f(R)$ gravity models with galaxy clusters using lensing and kinematic analyses. *JCAP* **1707**(07), 023 (2017). [arXiv:1705.05179](#)
10. F. Schmidt, A. Vikhlinin, W. Hu, Cluster constraints on $f(r)$ gravity. *Phys. Rev. D* **80**, 083505 (2009)
11. D. Rapetti, S.W. Allen, A. Mantz, H. Ebeling, The observed growth of massive galaxy clusters - III. Testing general relativity on cosmological scales. *Monthly Notices R. Astron. Soc.* **406**, 1796–1804 (2010)
12. L. Lombriser, A. Slosar, U. Seljak, W. Hu, Constraints on $f(R)$ gravity from probing the large-scale structure. *Phys. Rev. D* **85**, 124038 (2012). [arXiv:1003.3009](#)
13. D. Rapetti, S.W. Allen, A. Mantz, H. Ebeling, Testing general relativity on cosmic scales with the observed abundance of massive clusters. *Prog. Theor. Phys. Suppl.* **190**, 179–187 (2011)
14. M. Cataneo, D. Rapetti, F. Schmidt, A. Mantz, S. Allen, D. Applegate, P. Kelly, A. Von Der Linden, R. Morris, New constraints on $f(r)$ gravity from clusters of galaxies. *Phys. Rev. D - Part. Fields Grav. Cosmol.* **92** (2015)

15. S. Ferraro, F. Schmidt, W. Hu, Cluster abundance in $f(r)$ gravity models. *Phys. Rev. D* **83**, 063503 (2011)
16. M. Cataneo, D. Rapetti, L. Lombriser, B. Li, Cluster abundance in chameleon $f(R)$ gravity I: toward an accurate halo mass function prediction. *JCAP* **1612**(12), 024 (2016). [arXiv:1607.08788](#)
17. A. Terukina, K. Yamamoto, Gas density profile in dark matter halo in chameleon cosmology. *Phys. Rev. D* **86**, 103503 (2012)
18. A. Terukina, L. Lombriser, K. Yamamoto, D. Bacon, K. Koyama, R.C. Nichol, Testing chameleon gravity with the Coma cluster. *JCAP* **1404**, 013 (2014). [arXiv:1312.5083](#)
19. H. Wilcox et al., The XMM cluster survey: testing chameleon gravity using the profiles of clusters. *Mon. Not. Roy. Astron. Soc.* **452**(2), 1171–1183 (2015). [arXiv:1504.03937](#)
20. H. Wilcox, R.C. Nichol, G.-B. Zhao, D. Bacon, K. Koyama, A.K. Romer, Simulation tests of galaxy cluster constraints on chameleon gravity. *Mon. Not. Roy. Astron. Soc.* **462**(1), 715–725 (2016). [arXiv:1603.05911](#)
21. J. Sakstein, H. Wilcox, D. Bacon, K. Koyama, R.C. Nichol, Testing gravity using galaxy clusters: new constraints on beyond Horndeski theories. *JCAP* **1607**(07), 019 (2016). [arXiv:1603.06368](#)
22. V. Salzano, D.F. Mota, M.P. Dabrowski, S. Capozziello, No need for dark matter in galaxy clusters within Galileon theory. *JCAP* **1610**(10), 033 (2016). [arXiv:1607.02606](#)
23. V. Salzano, D.F. Mota, S. Capozziello, M. Donahue, Breaking the Vainshtein screening in clusters of galaxies. *Phys. Rev. D* **95**(4), 044038 (2017). [arXiv:1701.03517](#)
24. A. Biviano, P. Rosati, I. Balestra, A. Mercurio, M. Girardi, M. Nonino, C. Grillo, M. Scodreggio, D. Lemze, D. Kelson et al., CLASH-VLT: the mass, velocity-anisotropy, and pseudo-phase-space density profiles of the $z = 0.44$ galaxy cluster MACS J1206.2–0847. *Astron. Astrophys.* **558**, A1 (2013). [arXiv:1307.5867](#)
25. J. Binney, G.A. Mamon, M/L and velocity anisotropy from observations of spherical galaxies, or must M87 have a massive black hole. *Mon. Not. Roy. Astron. Soc.* **200**, 361–375 (1982)
26. O. Host, S.H. Hansen, R. Piffaretti, A. Morandi, S. Ettori, S.T. Kay, R. Valdarnini, Measurement of the dark matter velocity anisotropy in galaxy clusters. *Astrophys. J.* **690**, 358–366 (2009). [arXiv:0808.2049](#)
27. O. Host, Measurement of the dark matter velocity anisotropy profile in galaxy clusters. *Nucl. Phys. B Proc. Suppl.* **194**, 111–115 (2009). [arXiv:0810.3676](#)
28. S.H. Hansen, B. Moore, A universal density slope Velocity anisotropy relation for relaxed structures. *New Astron.* **11**, 333–338 (2006). [arXiv:astro-ph/0411473](#)
29. G.A. Mamon, A. Biviano, G. Murante, The universal distribution of halo interlopers in projected phase space. Bias in galaxy cluster concentration and velocity anisotropy? *Astron. Astrophys.* **520**, A30 (2010). [arXiv:1003.0033](#)
30. L. Pizzuti, B. Sartoris, S. Borgani, L. Amendola, K. Umetsu, A. Biviano, M. Girardi, P. Rosati, I. Balestra, G.B. Caminha, B. Frye, A. Koekemoer, C. Grillo, M. Lombardi, A. Mercurio, M. Nonino, CLASH-VLT: testing the nature of gravity with galaxy cluster mass profiles. *J. Cosmol. Astropart. Phys.* **2016**, 023 (2016). [arXiv:1602.03385](#)
31. O. Turet, F. Combes, G.W. Angus, B. Famaey, H.S. Zhao, Velocity dispersion around ellipticals in MOND. *A&A* **476**, L1–L4 (2007). [arXiv:0710.4070](#)
32. L. Pizzuti, B. Sartoris, S. Borgani, A. Biviano, Calibration of systematics in constraining modified gravity models with galaxy cluster mass profiles (2019). [arXiv:1912.09096](#)
33. A. Diaferio, M.J. Geller, Infall regions of galaxy clusters. *Astrophys. J.* **481**, 633–643 (1997). [arXiv:astro-ph/9701034](#)
34. S. Ettori, A. Donnarumma, E. Pointecouteau, T.H. Reiprich, S. Giodini, L. Lovisari, R.W. Schmidt, Mass profiles of galaxy clusters from X-ray analysis. *Space Sci. Rev.* **177**, 119–154 (2013). [arXiv:1303.3530](#)
35. V. Biffi, S. Borgani, G. Murante, E. Rasia, S. Planelles, G.L. Granato, C. Ragone-Figueroa, A.M. Beck, M. Gaspari, K. Dolag, On the nature of hydrostatic equilibrium in galaxy clusters. *Astrophys. J.* **827**, 112 (2016). [arXiv:1606.02293](#)

36. D. Martizzi, H. Agrusa, Mass modeling of galaxy clusters: quantifying hydrostatic bias and contribution from non-thermal pressure (2016). [arXiv:1608.04388](https://arxiv.org/abs/1608.04388)
37. D. Nagai, E.T. Lau, Gas clumping in the outskirts of Λ CDM clusters. *Astrophys. J.* **731**, L10 (2011). [arXiv:1103.0280](https://arxiv.org/abs/1103.0280)
38. M. Martinelli, E. Calabrese, F. De Bernardis, A. Melchiorri, L. Pagano, R. Scaramella, Constraining modified gravity with Euclid. *Phys. Rev. D* **83**, 023012 (2011). [arXiv:1010.5755](https://arxiv.org/abs/1010.5755)

Chapter 37

Probing Screening Modified Gravity with Non-linear Structure Formation



David F. Mota

Extended Theories of Gravity have considered a new paradigm to cure shortcomings of General Relativity at infrared and ultraviolet scales. They are an approach that, by preserving the undoubtedly positive results of Einstein's theory, is aimed to address problems recently emerged in astrophysics, cosmology and high energy physics [1]; in particular, problems like dark energy and dark matter. Several very good reviews have been written about the topic. Below I summarise some of them.

In Capozziello and De Laurentis [2] principles of such modifications are presented, focusing on specific classes of theories like $f(R)$ -gravity and scalar-tensor gravity in the metric and Palatini approaches. The special role of torsion is also discussed. The conceptual features of these theories are fully explored and attention is paid to the issues of dynamical and conformal equivalence between them considering also the initial value problem. A number of viability criteria are presented considering the post-Newtonian and the post-Minkowskian limits. In particular, the authors discuss the problems of neutrino oscillations and gravitational waves in Extended Gravity.

In Cai et al. [3] the role of torsion in gravity has been extensively investigated along the main direction of bringing gravity closer to its gauge formulation and incorporating spin in a geometric description. From teleparallel, to Einstein–Cartan, and metric-affine gauge theories, resulting in extending torsional gravity in the paradigm of $f(\mathbb{T})$ gravity, where $f(\mathbb{T})$ is an arbitrary function of the torsion scalar. Based on this theory, the authors review the corresponding cosmological and astrophysical applications. In particular, they study cosmological solutions arising from $f(\mathbb{T})$ gravity, both at the background and perturbation levels, in different eras along the cosmic expansion. The $f(\mathbb{T})$ gravity construction can provide a theoretical interpretation of the late-time universe acceleration, alternative to a cosmological constant, and it can easily accommodate with the regular thermal expanding history including the radiation and cold dark matter dominated phases. Furthermore, if one traces back

D. F. Mota (✉)

Institute of Theoretical Astrophysics, University of Oslo, P.O. Box 1029, 0315 Oslo, Blindern, Norway

e-mail: d.f.mota@astro.uio.no

to very early times, for a certain class of $f(\mathbb{T})$ models, a sufficiently long period of inflation can be achieved and hence can be investigated by cosmic microwave background observations? Or, alternatively, the Big Bang singularity can be avoided at even earlier moments due to the appearance of non-singular bounces. Various observational constraints, especially the bounds coming from the large-scale structure data in the case of $f(\mathbb{T})$ cosmology, as well as the behavior of gravitational waves, are described in detail. Moreover, the spherically symmetric and black hole solutions of the theory are reviewed. Additionally, the authors discuss various extensions of the $f(\mathbb{T})$ paradigm. Finally, we consider the relation with other modified gravitational theories, such as those based on curvature, like $f(R)$ gravity, trying to illuminate the subject of which formulation, or combination of formulations, might be more suitable for quantization ventures and cosmological applications.

While the above two review articles investigate modified gravity models as alternatives to dark energy, in Capozziello and De Laurentis [4], the authors review an alternative view to the dark matter puzzle that is represented by Extended Theories of Gravity. The approach consists in addressing issues like dark components from the point of view of gravitational field instead of requiring new material ingredients that, up to now, have not been detected at fundamental level. In this review paper, by extending the Hilbert-Einstein action of gravitational field to more general actions (e.g. $f(R)$ gravity), it is shown that several gravitating structures like stars, spiral galaxies, elliptical galaxies and clusters of galaxies can be self-consistently described without asking for dark matter. It is also shown that standard General Relativity tests and Equivalence Principle constraints can be evaded at Solar System scales.

Gravity theories beyond General Relativity may possibly explain several cosmological puzzles, specifically the present accelerated expansion of the Universe [1, 5–11]. Modified Gravity must, however, comply with strong requirements: One is that the model must have similar cosmological predictions to those of Λ CDM for the background evolution and the linear large scale structures [12]. Another condition is that the modifications to General Relativity are suppressed at small scales [13]. This requirement is assured through the so-called screening mechanisms [14].

Since different modified gravity theories can be degenerate with regard to both the background cosmology and the growth rate of linear perturbations, it is crucial to identify new probes that can be used to break these degeneracies. In this Chapter we study the effects of a class of screened modified gravity models in the nonlinear regime of structure formation. The aim is to predict possible smoking guns of modified gravity and of screening mechanisms at cluster of galaxy scales.

37.1 Theoretical Models

Scalar-tensor theories are an extension of General Relativity that add a scalar field φ to the standard Einstein-Hilbert Lagrangian. A general Lagrangian for the scalar field is

$$\mathcal{L} = -\frac{1}{2}\partial_\mu\varphi\partial_\nu\varphi - V(\varphi) + \beta(\varphi)T_\mu^\mu, \tag{37.1}$$

where $V(\varphi)$ is the self interacting potential, $\beta(\varphi)$ is a coupling function and T_μ^μ is the trace of the matter energy-momentum tensor. The scalar field gives rise to an additional *fifth force*, which can be quantified by $\gamma \equiv |\mathbf{F}_{\text{Fifth}}|/|\mathbf{F}_N|$, where \mathbf{F}_N is the Newtonian force. Experiments constrain $\gamma \ll 1$ in the Solar System. A screening mechanism with the aim to hide this field from local gravity experiments can be realised in two different ways.

Density dependent mass: If the mass of the field $m^2(\varphi)$ is large in dense environments, then the fifth force mediated by the scalar field is suppressed on scales above its Compton wavelength. On the other hand, in low density environments, the mass can be light and the scalar field mediates a long range fifth force. This is the so-called *Chameleon* screening [15].

Density dependent coupling: If the coupling to matter $\beta(\varphi)$ is small in the region of high density, the strength of the fifth force $\mathbf{F}_{\text{Fifth}}$ is weak and the modifications to gravity are suppressed. On the other hand, in low density environments, the size of the fifth force can be of the same order as standard gravity. This idea is the so-called *Symmetron* mechanism [16].

37.1.1 Chameleon- $f(R)$ Gravity

The Lagrangian for this theory is

$$S = \int d^4x \sqrt{-g} \frac{1}{16\pi G_N} (R + f(R)) + S_m(g_{\mu\nu}, \psi_i). \tag{37.2}$$

In the quasi-static and weak-field limits the equations of motion become

$$\nabla^2\Phi = \frac{16\pi G_N}{3} a^2 \delta\rho_m + \frac{1}{6} a^2 \delta R, \quad \nabla^2 f_R = -\frac{a^2}{3} [\delta R + 8\pi G_N \delta\rho_m], \tag{37.3}$$

where $\delta\rho_m = \rho_m - \bar{\rho}_m$ and $\delta R = R - \bar{R}$ are the density and Ricci scalar perturbations (overbars denote background quantities), and $f_R = df(R)/dR$. In this formulation, f_R plays the role of the scalar degree of freedom φ that determines the fifth force.

We choose the Hu-Sawicki model [17] as a working example, which is given by

$$f(R) = -m^2 \frac{c_1(R/m^2)^n}{c_2(R/m^2)^n + 1}, \tag{37.4}$$

where $m^2 = H_0^2\Omega_m$ is a mass scale and c_1, c_2 and n are model parameters. One recovers a Λ CDM expansion history by setting $c_1/c_2 = 6\Omega_\Lambda/\Omega_m$. In this paper

we consider $n = 1$, and we consider models with $|\bar{f}_{R0}| = 10^{-4}$, $|\bar{f}_{R0}| = 10^{-5}$ and $|\bar{f}_{R0}| = 10^{-6}$.

Notice that the modified Poisson equation, Eq. (37.3), can also be written as

$$\nabla^2 \Phi = \nabla^2 \Phi_N - \frac{1}{2} \nabla^2 f_R. \quad (37.5)$$

This makes explicit that in $f(R)$ models the total gravitational force is governed by a modified gravitational potential $\Phi = \Phi_N - \frac{1}{2} f_R$. It is the nonlinearity of $f(R)$ in Eq. (37.4) that gives rise to the Chameleon screening, and the screening of the fifth force is determined by the depth of the gravitational potential Φ_N .

37.1.2 Symmetron

The Symmetron model [16] action is given by

$$S = \int d^4x \sqrt{-g} \left[\frac{R}{16\pi G_N} - \frac{1}{2} (\partial\varphi)^2 - V(\varphi) \right] + S_m(\tilde{g}_{\mu\nu}, \psi). \quad (37.6)$$

The matter fields ψ couple to the Jordan frame metric $\tilde{g}_{\mu\nu}$, which relates to the Einstein frame metric $g_{\mu\nu}$ as $\tilde{g}_{\mu\nu} = A^2(\varphi)g_{\mu\nu}$. The coupling function $A(\varphi)$ is

$$A(\varphi) = 1 + \frac{1}{2} \left(\frac{\varphi}{M} \right)^2, \quad (37.7)$$

where M is a mass scale. The total force felt by matter is given by

$$\mathbf{F} = \nabla \left(\Phi_N + \frac{1}{2} \frac{\varphi^2}{M^2} \right) = \nabla \Phi_N + \frac{\varphi \nabla \varphi}{M^2}. \quad (37.8)$$

The potential is taken to be

$$V(\varphi) = V_0 - \frac{1}{2} \mu^2 \varphi^2 + \frac{1}{4} \lambda \varphi^4, \quad (37.9)$$

where the value of V_0 is determined by the condition that the model gives rise to the observed accelerated expansion of the Universe [18]. The field equation for φ reads

$$\square\varphi = V_{\text{eff},\varphi}, \quad (37.10)$$

where for nonrelativistic matter the effective potential is given by

$$V_{\text{eff}}(\varphi) = V_0 + \frac{1}{2} \left(\frac{\rho_m}{M^2} - \mu^2 \right) \varphi^2 + \frac{1}{4} \lambda \varphi^4. \quad (37.11)$$

In the quasi-static limit, Eq. (37.10) becomes

$$\nabla^2 \chi = \frac{a^2}{2\lambda_0^2} \left(\frac{\rho_m}{\rho_{\text{SSB}}} - 1 + \chi^2 \right) \chi, \quad (37.12)$$

where $\chi = \varphi/\varphi_0$.

Screening in the Symmetron model is very similar to the Chameleon- $f(R)$ case in the sense that the condition for screening is determined by the local gravitational potential. The important difference is that the coupling $\beta(\varphi) = \frac{\beta_0 \varphi}{\varphi_0}$, which is constant in $f(R)$ gravity, now depends on the local field value. In high density regions, $\rho_m > \rho_{\text{SSB}}$, the field falls into the minima $\varphi = 0$, and since the coupling is proportional to φ , the fifth force vanishes.

We define three physical parameters L , β and z_{SSB} which are the range of the field, the coupling strength to matter and the redshift of symmetry breaking:

$$L = \frac{\lambda_0}{\text{Mpc}/h} = \frac{3000H_0}{\sqrt{2}\mu}, \quad \beta = \frac{\phi_0 M_{\text{pl}}}{M^2} = \frac{\mu M_{\text{pl}}}{\sqrt{\lambda} M^2}, \quad (1 + z_{\text{SSB}})^3 = \frac{\mu^2 M^2}{\rho_{m0}}. \quad (37.13)$$

We simulate four symmetron models: `symm_A` ($z_{\text{SSB}} = 1$, $\beta = 1$, $L = 1$), `symm_B` ($z_{\text{SSB}} = 2$, $\beta = 1$, $L = 1$), `symm_C` ($z_{\text{SSB}} = 1$, $\beta = 2$, $L = 1$), and `symm_D` ($z_{\text{SSB}} = 3$, $\beta = 1$, $L = 1$).

37.2 Efficiency of Screening Mechanisms

The common feature to all the screening mechanisms proposed in the literature is that they are built, and their efficiency tested, assuming the so called quasi-static approximation for the field equations. For instance, in scalar-tensor theories, a scalar degree of freedom is introduced into the standard Einstein-Hilbert action. This field follows the Klein-Gordon equation of motion, which determines both its time and spatial variations. When constructing screening mechanisms to hide the scalar field within the accurately tested regimes, the quasi-static approximation is invariably applied to the equations of motion for the field. This simplifies the calculations by implying that the scalar field is at rest in the minimum of the local effective potential at all points in space and time. This reduces the equation of motion to a Poisson-like equation, which is readily solved to find the approximated scalar field value at any point.

Notice, however, that the full equation of motion for the scalar field is, in fact, a second order differential equation in time, more similar to a wave equation. Therefore, ignoring the time evolution of the field, via the quasi-static approximation, is to shortfall effects that are only possible to realize when considering the full equation of motion [19, 20].

37.2.1 Solar System Constraints

In order to test how screening mechanisms work in the Solar System, the community generally chooses a static, spherically symmetric matter distribution to mimic the Galaxy. We follow this approach and choose the Navarro-Frenk-White (NFW) density profile with the characteristics to represent the Milky Way Galaxy, specifically with a virial radius of $r_{\text{vir}} = 137 \text{ kpc}/h$ and concentration $c = 28$, resulting in a halo mass of $1.0 \times 10^{12} M_{\odot}$ and a circular velocity of 220 km/s at 8 kpc . The reason for the high value of the concentration is simply that we are modeling not only dark matter, but the total matter of the Milky Way, which is more concentrated than the pure dark matter halo. We also did the calculations with an Einasto profile with identical virial mass, and found that the results presented are not very sensitive to the choice of distribution. Because of limitations of spherical symmetry, we did not model a galactic disc.

One of the most precisely measured gravity parameters to probe deviations from general relativity is the parametrised post-Newtonian (PPN) parameter γ . It can be expressed as the ratio of the metric perturbations in the Jordan frame, Ψ_J and Φ_J . We find the expression for $\gamma - 1$ to be

$$\gamma - 1 = -\frac{\phi^2}{M^2} \frac{2}{\frac{\phi^2}{M^2} - 2\Psi_E - 2\Psi_E \frac{\phi^2}{M^2}}. \quad (37.14)$$

In general relativity, $\gamma = 1$ exactly. The strongest constraint to date, measured by the Cassini spacecraft [21], is $\gamma - 1 = (2.1 \pm 2.3) \times 10^{-5}$.

The screening mechanism of the symmetron model works by modifying the effective potential such that the field value is pushed towards zero in high density regions—like the inner regions of the Galaxy. This results in $\gamma - 1 \rightarrow 0$, such that the deviations from general relativity in the proximity of the Solar System are small. The same occurs for the fifth force F_{ϕ} associated to the scalar field.

We calculate the γ parameter arising from the smoothed matter distribution of the Milky Way. Note that, by using this method, we find an upper bound on the actual value of $|\gamma - 1|$ in the inner Solar System. This is because we do not include the presence of massive bodies like the Sun, which will increase the screening to some degree. Nevertheless, most of the screening is believed to come from the matter distribution of the Galaxy because, in the symmetron model, the Solar System cannot screen itself in vacuum, and therefore, the theory depends on a working screening from the Galaxy.

37.2.2 Simulations

Since the equation of motion is a hyperbolic partial differential equation, it can be solved as an initial value and boundary condition problem. The initial condition at

$t = 0$ is chosen to be the static solution of the nonlinear Klein-Gordon equation of motion. With a constant boundary condition, this would imply that the field will stay at rest forever. The boundary condition at the edge of the simulation at r_{\max} is chosen to emulate incoming sinusoidal waves in the scalar field, specifically $\chi(r_{\max}, t) = \chi_0(r_{\max}) + A \sin(\omega t)$. Possible sources of such waves will be discussed later.

We set up a radial grid, divided into linearly spaced steps Δr up to $r_{\max} = 4 \text{ Mpc}/h$. On each of the grid points we specify the matter density according to the NFW halo. Starting from the initial value and with the inclusion of incoming waves, we evolve Eq. (37.10) forward in time steps of size Δt , using the leapfrog algorithm for time integration in each grid point. Tests of this technique applied to the symmetron are presented in [22, 23]. We are only interested in events that happen during the last few megayears of cosmic time, meaning that we take the approximations $z \approx 0$ and $a \approx 1$ in all computations. Spatial derivatives are found using a finite difference method in spherical coordinates, assuming all derivatives in the tangential directions vanish. The code outputs the evolution of the scalar field and, more importantly, the value of $|\gamma - 1|$ at 8 kpc from the center—corresponding to the position of the Solar System in the Milky Way. Finally, we confirm that the values used for technical parameters of our solver give a stable solution by running convergence tests. These are performed by increasing the resolution in factors of two (both temporal and spatial resolution separately) until the resulting scalar field at some later time t_{\max} does not change significantly with resolution.

37.2.3 Results

We are interested in investigating how the PPN parameter γ changes when a wave enters the inner 100 kpc of the Milky Way. The modifications to gravity are initially screened very well in the regions around this position, with $|\gamma - 1| < 10^{-8}$. However, after the wave has arrived the scalar field is perturbed enough to breach the Solar System constraints, $|\gamma - 1| > 2 \times 10^{-5}$. In other words, the screening mechanism breaks down under these circumstances.

When measuring γ arising from a single sinusoidal wave with low frequency, there is a possibility that the local wave is between two extrema at the time of measurement. This could render this kind of detection difficult for several thousand years. Nevertheless, given that various astrophysical events—such as supernovae—can generate waves, the probability that one of the wavefronts would bring us away from the minima at the present time is not negligible.

Hence, it is possible to conclude that higher frequencies and amplitudes for the incoming scalar waves give larger deviations from the general relativity result (i.e., $\gamma = 1$). The limit where amplitude and frequency go to zero is equivalent to the quasi-static limit, where no waves are produced and their energy is zero. As one goes into the high frequency and amplitude regime, the waves carry more energy, and therefore, the PPN parameter γ starts deviating significantly from the quasi-static

limit. Note that, since in the symmetron model, the fifth force is $F_\phi \propto \nabla\phi^2/M^2$, these values can be immediately extrapolated to the impact of the waves on this quantity.

The dependence of the γ PPN parameter on the wave amplitude is straightforward to understand: When a wave propagates through the screened regions of the halo, a larger amplitude wave will lead to larger displacements of the field from the screening value $\phi \approx 0$. Therefore, $|\gamma - 1| \propto \phi^2$ will increase accordingly.

The frequency dependence of the γ parameter is a consequence of the following: The effective potential of the symmetron grows steeper and narrower in high density areas. In other words, the mass of the field increases towards the center of the halo. Therefore, it becomes more difficult to perturb the field away from the minimum, and a higher wave energy is needed to displace it. Specifically, if the energy of the external waves is small compared to the mass of the field, the field will not be perturbed and the γ parameter will not be affected.

The results obtained imply that if waves with sufficient amplitude or frequency can somehow be generated in a given model for modified gravity, they will have to be taken into account when constraining the model parameters. Cosmic tsunamis, resulting from extreme events, could even completely ruin the screening mechanisms in modified gravity by increasing the deviations from general relativity by several orders of magnitude compared to the quasi-static case. A subject that must be discussed now is the generation of such waves. Extreme events on small scales, such as collision of neutron stars, stellar, or super-massive black holes are obvious examples. Generation of waves by pulsating stars are another possibility.

In the specific case of the symmetron model, it is possible to obtain waves from events that occur on cosmological scales. First, the symmetron model undergoes a phase transition when the density falls below a specific threshold. This transition first occurs in voids when the expansion factor is close to a_{SSB} [22, 23]. When this happens, the scalar field receives a kick, which produces waves traveling from the center of the voids towards the dark matter halos. By doing postprocessing of simulations presented in [20], we find that, in a symmetron model with slightly different parameters, the amplitude of cosmological waves is typically smaller than 0.1 and the associated frequencies are of the order of 1/Myr. Note that these values depend on the model parameters and, hence, must be taken only as indicative. Scalar waves can also be created through the collapse of topological defects, which are known to exist in any model in which such phase transition occurs.

37.3 Distribution of Fifth Force in Dark Matter Haloes

To understand the main features of nonlinear structure formation within screened modified gravity, it is important to investigate the magnitude of the fifth force inside the dark matter haloes [24–27]. For that, we run N-body simulations for each model. The simulations were run with the code `ISIS` [28]. The background cosmology for all the models is $(\Omega_{m0}, \Omega_{\Lambda0}, H_0) = (0.267, 0.733, 71.9)$. The data sets are taken at $z = 0$, and all simulations were run with the same initial conditions.

The halos were identified using the spherical overdensity halo finder AHF [29]. For the analysis we used only halos consisting of at least 100 particles which limits the smallest halo we can probe to $M \sim 3 \times 10^{12} M_{\odot} h^{-1}$. In the high mass end the simulation-box limits the maximum halo-masses we can study and the largest halos in our simulations has mass $M \sim 2 - 3 \times 10^{15} M_{\odot} h^{-1}$. We have checked that the mass-function of our simulation agrees to $\sim 10\% - 20\%$ to simulations with larger box-size and also to the fit to the mass-function in the range $M \in [10^{13}, 8 \times 10^{14}] M_{\odot} h^{-1}$. The total number of halos in this mass-range in our simulations, which is what we used for the upcoming analysis, is ~ 8000 . In the $f(R)$ case, the maximum of the fifth force profile moves towards larger radii when increasing mass, and decreasing $|f_{R0}|$. This is a consequence of the screening that is activated in the centre of the haloes, and when decreasing $|f_{R0}|$. For the symmetron model, an increase of β or z_{SSB} leads to a stronger fifth force. A greater β value increases the $|\ddot{\chi}_{\text{Fifth}}|$ values by a constant factor, while altering z_{SSB} changes the shape of the fifth force profile in general. It is clear that the fifth force is screened in large massive haloes (since they have a higher density) while the force is active in the low mass range (where the density is lower).

The dependence of the symmetron fifth force on the redshift of symmetry breaking z_{SSB} is thus clear. The higher the symmetry breaking, the higher the masses that are unscreened and affected by the fifth force. The low mass end of the distribution is insensitive to changes in z_{SSB} , since in there the density is low and the force is unscreened. Differences in the models are also dependent of the strength of the coupling β .

37.4 The Matter and the Velocity Power Spectra

Due to the presence of the fifth force, it is expected in modified theories of gravity, that the acceleration felt by particles is in general higher than in General Relativity [27]. Therefore, a promising observable and probe of modified gravity is the measure of velocity distributions in galaxy clusters.

The global statistical properties of the velocity field are described by the velocity divergence power spectrum. Normalising the divergence of the velocity field $\nabla \cdot \mathbf{v}$ with the Hubble parameter gives the dimensionless expansion scalar $\theta = \frac{1}{H} \nabla \cdot \mathbf{v}$.

We compute the power-spectrum of θ from our simulations. To characterize this quantity, we study the relative particle velocity, which is simply defined as $v_{\text{rel}} = \sqrt{(\mathbf{v} - \mathbf{v}_{\mathcal{H}})^2}$, where \mathbf{v} and $\mathbf{v}_{\mathcal{H}}$ are the particle velocity and its halo velocity, respectively. For the latter, we use the core velocity of the halo. For our $f(R)$ simulations we find that the difference with respect to Λ CDM in the velocity divergence spectrum can be roughly two times as large as the difference in the matter power spectrum. For the Symmetron the difference can be much larger. For the `symm_C` model (which is the model with the largest value of the coupling strength β), we see that $(\Delta P/P)_m \approx 10\%$ at $k = 1h/Mpc$ while $(\Delta P/P)_{\theta} \approx 200\%$. The `symm_C`

model has a fifth force in unscreened regions four times that of the other Symmetron models and this is likely why we get this extreme signal.

The reason why generally we have $(\Delta P/P)_\theta \gtrsim (\Delta P/P)_m$ is that the velocity divergence field is not mass-weighted in any way. Hence, low-density regions (voids) will contribute a large part of the signal in the velocity divergence power-spectrum (since voids contribute a large part of the volume in the Universe), which is not the case for the matter power-spectrum. Now the fifth-force is generally not screened in low-density regions, so consequently velocities are boosted to significantly higher relative values (when compared with Λ CDM) in voids opposed to in clusters. This indicates that low-density regions like cosmic voids, as we would expect, is the place where the strongest signals of modified gravity can be found.

37.5 The Dynamical and Lensing Masses

A general prediction of Modified Gravity theories with screening mechanisms is violations of equivalence principle. The equivalence principle can be tested by observing differences between the gravitational mass and the inertial mass of objects, in cosmology through measurements of galaxy clusters masses. Astronomers infer the masses of galaxy clusters using lensing observations and dynamical methods. The former is a probe of the gravitational mass, while the later is a measure of the inertial mass. Differences between these two masses would be a smoking gun of modified gravity and screening mechanisms. In order to make predictions within the chameleon-f(R) and the symmetron gravity, we first need to compute the Bardeen potentials.

In the Jordan-frame we have

$$ds^2 = a^2(\eta) [-d\eta^2(1 + 2\Phi) + (1 - 2\Psi)d\mathbf{x}^2], \quad (37.15)$$

where $\Phi \simeq \Phi_N + \delta A(\phi)$, $\Psi \simeq \Phi_N - \delta A(\phi)$, with

$$\delta A(\phi) \equiv A(\phi) - 1 = \frac{1}{2} \left(\frac{\phi}{M} \right)^2. \quad (37.16)$$

The fifth-force potential is given by the difference in the above two potentials

$$\Phi_- = \frac{\Phi - \Psi}{2} = \delta A(\phi). \quad (37.17)$$

Lensing on the other hand is affected by the lensing potential

$$\Phi_+ = \frac{\Phi + \Psi}{2} = \Phi_N, \quad (37.18)$$

which satisfies the Poisson equation

$$\nabla^2 \Phi_+ = 4\pi G_N a^2 \delta \rho_m. \quad (37.19)$$

This is the same equation as in GR since it is conformally invariant and therefore photons are not affected by the fifth-force. The lensing mass is defined as

$$M_L = \frac{1}{4\pi G_N a^2} \int \nabla^2 \Phi_+ dV, \quad (37.20)$$

which is the gravitational mass of the halo. It is determined from the simulations by counting the number of particles within a given radius. For spherical symmetry, using the Stokes theorem, we have

$$M_L(r) \propto r^2 \frac{d\Phi_+}{dr}. \quad (37.21)$$

The dynamical mass $M_D(r)$ of a halo is defined as the mass contained within a radius r as inferred from the gravitational potential Φ , i.e.

$$M_D(r) = \frac{1}{4\pi G_N a^2} \int \nabla^2 \Phi dV, \quad (37.22)$$

where the integration is over the volume of the body out to radius r . For spherical symmetry, and using Stokes theorem, we find

$$M_D(r) \propto \int r^2 \frac{d\Phi(r)}{dr} = r^2 \left(\frac{d\Phi_N}{dr} + \frac{\phi}{M^2} \frac{d\phi}{dr} \right). \quad (37.23)$$

The terms in the brackets are recognised as the sum of the gravitational force and the fifth-force. Observationally, M_D can be determined from measurements of velocity dispersion of galaxies in clusters.

In GR the lensing mass is the same as the dynamical mass, but they can be significantly different in modified gravity. We follow [30] and define the relative difference

$$\Delta_M(r) = \frac{M_D}{M_L} - 1 = \frac{d\Phi_-/dr}{d\Phi_+/dr}. \quad (37.24)$$

This allows us to quantify the difference between the two masses in the simulations. In GR we have $\Delta_M \equiv 0$ while in the symmetron model Δ_M will vary depending on the mass of the halo and its environment. The theoretical maximum is achieved for small objects in a low-density environment where the screening is negligible and reads

$$\Delta_M^{\text{Max}}(r) = 2\beta^2. \quad (37.25)$$

For low-mass halos we obtain a significant dispersion of Δ_M from 0 to the maximum value obtained in low-density environments for the same mass ranges. This is because low-mass halos cannot efficiently screen themselves and must rely on the environment to get the screening. As expected, there is a clear trend that the small halos which are efficiently screened generally reside in high-density environments, while those which are less screened lie in low-density environments. Massive halos on the other hand can screen themselves efficiently and the environment only plays a small role in their total screening. Additionally, there is a large difference between large halos in dense environments and small halos in low density environments. The r -dependence of $\Delta_M(r)$ is shown to be rather weak in high density environments since the value of the scalar field inside the halo is mainly determined by the environment, while in low-density environments the value of the scalar field mainly depends on the mass of the halo, which leads to a stronger r -dependence. Finally, note also that the deviation from GR is stronger for higher symmetry-breaking redshift z_{SSB} , and for larger values of the coupling β , which implies a stronger fifth-force and therefore a stronger effect.

37.6 Thermal Versus Lensing Mass Measurements

In order to compare the lensing and thermal mass of the clusters we took measurements from [31, 32]. These two data-sets provide both thermal and lensing mass measurements and uncertainties for a total of 58 clusters in the mass range $M/M_\odot h^{-1} \in [5 \times 10^{13}, 3 \times 10^{15}]$ so there was no need to combine the mass estimates in a similar fashion as in the previous section. We divided the data for the thermal mass measurements by the data for the lensing mass measurements while properly propagating the error. As we're interested in a systematic deviation, we binned the data in six (lensing) mass bins which we stratified so that roughly the same number of halos are in each bin.

An important point to bear in mind when working with thermal mass estimates is the fact that the measured quantity in this case is the temperature of the intracluster gas. The conversion to a mass assumes hydrostatic-equilibrium [31, 32]. However, it has been shown that in reality the pressure of the intracluster medium will have a significant non-thermal component generated by random gas motions and turbulence. This means the inferred thermal mass given a temperature T will be slightly lower than the true mass of the cluster.

While empirical models exist in order to quantify the magnitude of this deviation (where the non-thermal component yield variations to the mass from 10 to 30%) we want to stress that these were calibrated against pure Λ CDM simulations, and thus their results cannot be taken into account when dealing with modified gravity. One has to consider instead that if gravity is truly enhanced, the temperature of the intracluster medium will be hotter and, thus, the inferred thermal mass will be greater (as shown in Sect. 37.4). This means the effect of any non-thermal physics (such as

cosmic rays) is degenerate with modified gravity and, consequently, at the present time thermal measurements cannot be used to constrain modified gravity [33–35].

Let us now compare the $M_{\text{therm}}/M_{\text{lens}}$ results of the Symmetron D model and our Λ CDM simulation to hypothetical measurements where we modelled the contribution of non-thermal pressure as

$$P_{\text{non-thermal}} = P_{\text{total}}\tilde{g}(M_{200}), \quad (37.26)$$

which resembles the functional forms fitted to Λ CDM simulations (see also Sect. 37.6.1). Thus, our proposed non-thermal contribution is not unreasonable. Modelling a non-thermal contribution as given by Eq. (37.26) while keeping the total pressure $P_{\text{total}} = P_{\text{therm}} + P_{\text{non-thermal}}$ (and, thus, the halo structure) constant is equivalent to rescaling the temperature as $T \rightarrow T(1 - \tilde{g})$ since naturally $P_{\text{therm}} \propto T$. In the case of a non-thermal contribution the M_{therm} measurement (which is carried out the same way as done by observations, i.e., assuming no non-thermal contribution) matches the lensing mass reasonably well *in the case of modified gravity*. We achieved this by choosing the functional form of \tilde{g} in Eq. (37.26) as

$$\tilde{g}(M) = \frac{1}{1 + \tilde{\alpha}M_{13}^{\tilde{\alpha}}}, \quad (37.27)$$

with $M_{13} \equiv M/(10^{13}M_{\odot}h^{-1})$ and $(\tilde{\alpha}, \tilde{\alpha}) = (3/4, 2/3)$. This serves as an example of how unknown non-thermal physics can cancel out any signal originating from modified gravity—which is a severe problem when trying to place constraints on the modifications of gravity using thermal measurements.

This problem will be alleviated once the contribution of non-thermal effects can be directly quantified using observational data (e.g., by measuring directly the intra-cluster turbulence). In the sequel of this subsection, we assume this has been done and it has been shown the contribution of the non-thermal components is negligible. We do this in order to show which constraints on modified gravity can be placed hypothetically using thermal mass estimates.

37.6.1 Including the Non-thermal Pressure Component

It is known that the pressure of the intracluster medium will have a significant non-thermal component generated by random gas motions and turbulence, so that the total pressure P_{Tot} of a cluster is

$$P_{\text{Tot}}(< r) = P_{\text{thermal}}(r) + P_{\text{non-thermal}}(r). \quad (37.28)$$

This results in the mass estimates [13] consist of a thermal and non-thermal component as well

$$M(< r) = M_{\text{thermal}}(r) + M_{\text{non-thermal}}(r) \quad (37.29)$$

where

$$M_{\text{thermal}}(r) = -\frac{r^2}{G_N \rho_{\text{gas}}(r)} \frac{dP_{\text{thermal}}(r)}{dr} \quad (37.30)$$

$$M_{\text{non-thermal}}(r) = -\frac{r^2}{G_N \rho_{\text{gas}}(r)} \frac{dP_{\text{non-thermal}}(r)}{dr}. \quad (37.31)$$

By using $P_{\text{thermal}} = kn_{\text{gas}}T_{\text{gas}}$, where $\rho_{\text{gas}} = \mu m_p n_{\text{gas}}$, we find that

$$\frac{dP_{\text{thermal}}}{dr} = \frac{kT_{\text{gas}}(r)}{\mu m_p} \left[\frac{d\rho_{\text{gas}}(r)}{dr} + \frac{\rho_{\text{gas}}(r)}{T_{\text{gas}}(r)} \frac{dT_{\text{gas}}(r)}{dr} \right], \quad (37.32)$$

and hence

$$M_{\text{therm}} = -\frac{k_B r^2 T_{\text{thermal}}(r)}{\mu m_p G_N} \left(\frac{d \ln \rho_{\text{thermal}}}{dr} + \frac{d \ln T_{\text{thermal}}}{dr} \right), \quad (37.33)$$

as show earlier in the paper.

Often, the non-thermal pressure is expressed as a fraction of the total pressure

$$P_{\text{non-thermal}}(r) = g(r)P_{\text{total}}(r) = \frac{g(r)}{1 - g(r)}P_{\text{thermal}}, \quad (37.34)$$

with the derivative

$$\frac{dP_{\text{non-thermal}}}{dr} = \frac{1}{1 - g(r)} \left[g(r) \frac{dP_{\text{thermal}}}{dr} + \frac{dg(r)}{dr} P_{\text{thermal}} + \frac{g(r)}{1 - g(r)} \frac{dg(r)}{dr} P_{\text{thermal}} \right]. \quad (37.35)$$

A fit to the g -function has been found from Λ CDM simulations to be

$$g(r) = \alpha_{\text{nt}}(1 + z)^{\beta_{\text{nt}}} \left(\frac{r}{r_{500}} \right)^{n_{\text{nt}}} \left(\frac{M_{200}}{3 \times 10^{14} M_{\odot}} \right)^{n_M}, \quad (37.36)$$

where the free variables have the Λ CDM best-fit values $\alpha_{\text{nt}} = 0.18$, $\beta_{\text{nt}} = 0.5$, $n_{\text{nt}} = 0.8$, and $n_M = 0.2$. The derivative of the g -factor is

$$\frac{dg(r)}{dr} = \frac{n_{\text{nt}}}{r} g(r). \quad (37.37)$$

Using the best fit we redo the analysis from before, now including the non-thermal pressure contribution. The results now differs: with the non-thermal pressure component having introduced a strong mass dependence. However, we want to stress

that this is just one particular example as the current expression of the non-thermal pressure contribution is derived from standard gravity simulations is strongly model dependent. Thus, we cannot simply use the expression as is for the modified gravity models.

In spite of this complication, we want to note that *in principle* it is possible to use the ratio between the thermal and lensing mass to constrain screened modified gravity theories, and also—when including the kinetic mass—to rule out certain combinations of non-universal coupling. All this, however, requires the contribution of the non-thermal pressure to be ‘under control’, i.e., the magnitude of the intra-cluster turbulence are at least limited by observations.

37.7 Modelling Void Abundance in Modified Gravity

Due to the fact that screening mechanisms are much less efficient in low density regions, then voids are clearly one of the most promising astrophysical objects to observe signatures of a strong and active fifth force, and, therefore, to probe possible deviations from General Relativity and evidence for Modified Gravity. In this section we review in detail how one can use voids statistics to perform such work.

37.7.1 Linear Power Spectrum

The spherical evolution model is usually the first step to investigate the abundance of virialized objects tracing the Universe structure, such as halos, and likewise it is a promising tool for voids [36]. It also offers a starting point to study the collapse of non-spherical structures and the parameters required to quantify the abundance of these objects within extended models.

The large scale structure of the Universe is well characterized by the evolution of dark matter, which interacts only gravitationally and can be approximated by a pressureless perfect fluid. The line element for a perturbed Friedmann-Lemaître-Robertson-Walker (FLRW) metric in the Newtonian gauge is given by

$$ds^2 = -a^2(1 + 2\Psi)d\tau^2 + a^2(1 - 2\Phi)dl^2, \quad (37.38)$$

where a is the scale factor, τ is the conformal time related to the physical time t by $ad\tau = dt$, dl^2 is the line element for the spatial metric in a homogeneous and isotropic Universe and Ψ and Φ are the gravitational potentials.

For a large class of modified gravity models, the perturbed fluid equations in Fourier space are given by

$$\dot{\delta} = -(1 + \delta)\theta, \quad (37.39)$$

$$\dot{\theta} + 2H\theta + \frac{1}{3}\theta^2 = k^2\Phi, \quad (37.40)$$

$$-k^2\Phi = 4\pi G_N \mu(k, a) \bar{\rho}_m \delta, \quad (37.41)$$

where $\delta = (\rho_m - \bar{\rho}_m)/\bar{\rho}_m$ is the matter density contrast, θ is the velocity divergence, $H = \dot{a}/a$ is the Hubble parameter and dots denote derivatives with respect to physical time t .

The first is the continuity equation, the second the Euler equation and the last is the modified Poisson equation, where modified gravity effects are incorporated within the function $\mu(a, k)$. In general this function depends on scale factor a as well as physical scale or wave number k in Fourier space.

Combining these equations we obtain an evolution equation for spherical perturbations in modified gravity given by

$$\delta'' + \left(\frac{3}{a} + \frac{E'}{E}\right)\delta' - \frac{4}{3} \frac{(\delta')^2}{1 + \delta} = \frac{3}{2} \frac{\Omega_m}{a^5 E^2} \mu(k, a) \delta (1 + \delta), \quad (37.42)$$

where primes denote derivatives with respect to the scale factor a , $E(a) = H(a)/H_0$, $H(a)$ is the Hubble parameter at a , H_0 is the Hubble constant and Ω_m is the present matter density relative to critical. Clearly the growth of perturbations is scale-dependent—a general feature of modified theories of gravity.

The linearized version of Eq. (37.42) is given by

$$\delta'' + \left(\frac{3}{a} + \frac{E'}{E}\right)\delta' = \frac{3}{2} \frac{\Omega_m}{a^5 E^2} \mu(k, a) \delta, \quad (37.43)$$

and can be used to determine linear quantities, such as the linear power spectrum. Notice that this matter linear equation is valid more generally and does not require spherical perturbations.

The function $\mu(k, a)$ above is given by

$$\mu(k, a) = \frac{(1 + 2\beta^2)k^2 + m^2 a^2}{k^2 + m^2 a^2}, \quad (37.44)$$

where β is the coupling between matter and the fifth force and m is the mass of the scalar field propagating the extra force.

It is important to stress that the parameterisation in Eq. (37.44) does not fully account for modified gravity perturbative effects, containing only effects of the background and linear perturbations for extra fields related to modified gravity. This is enough for the linearized Eq. (37.43), but is only an approximation in Eq. (37.42). For instance the parameterisation in Eq. (37.44) does not contain effects from the screening mechanisms, which would turn μ into a function not only of scale k , but of e.g. the local density or gravitational potential.

We start by defining the linear density contrast field $\delta(R)$ smoothed on a scale R around $\mathbf{x} = 0$ ¹

$$\delta(R) = \int \frac{d^3k}{(2\pi)^3} \tilde{\delta}(\mathbf{k}) \tilde{W}(k, R), \quad (37.45)$$

where tildes denote quantities in Fourier space and $W(\mathbf{x}, R)$ is the window function that smooths the original field $\delta(\mathbf{x})$ on scale R .

The variance $S(R) = \sigma^2(R)$ of the linear density field can be written as

$$S(R) = \langle |\delta(R)|^2 \rangle = \int \frac{dk}{2\pi^2} k^2 P(k) |\tilde{W}(k, R)|^2, \quad (37.46)$$

where $P(k)$ is the linear power spectrum defined via

$$\langle \tilde{\delta}(\mathbf{k}) \tilde{\delta}(\mathbf{k}') \rangle = (2\pi)^3 \delta_D(\mathbf{k} - \mathbf{k}') P(k), \quad (37.47)$$

and $\delta_D(\mathbf{k} - \mathbf{k}')$ is a Dirac delta function. Clearly the linear power spectrum will play a key role in describing the effects of modified gravity on void properties. For GR computations, we use CAMB to compute the linear power spectrum. For modified gravity, we may use MGCAMB, a modified version of CAMB which generates the linear spectrum for a number of alternative models, such as the Hu and Sawicki $f(R)$ model [17] and others. However it does not compute the linear spectrum for instance for the symmetron model. Therefore we also construct the linear power spectrum independently for an arbitrary gravity theory parametrized by Eqs. (37.43) and (37.44).

Our independent estimation of the spectrum is accomplished by evolving Eqs. (37.43) and (37.44) with parameters from specific gravity theories (e.g. for $f(R)$ and for symmetron models) for a set of initial conditions at matter domination. Since at sufficiently high redshifts viable gravity models reduce to GR, we take initial conditions given by CAMB at high redshifts ($z \approx 100$), when gravity is not yet modified and the Universe is deep into matter domination. We also compute initial conditions for δ numerically by using the Λ CDM power spectrum at two closeby redshifts, e.g. at $z = 99$ and $z = 100$.

Comparing the results of using this procedure with the results for the Hu & Sawicki model we can see that solving Eq. (37.43) for the power spectrum produces results nearly identical to the full solution from MGCAMB on all scales of interest. The percent level differences may be traced to the fact that the simplified equation solved does not contain information about photons and baryons, but only dark matter. For our purposes, this procedure can be used to compute the linear power spectrum for other modified gravity models that reduce to GR at high redshifts, such as the symmetron model. Additionally, the relative difference of $\sigma(R) = S(R)^{1/2}$ for the $f(R)$ model with respect to GR can be significant on the scales of interest ($1 \text{ Mpc}/h < R < 20$

¹ The choice $\mathbf{x} = 0$ is irrelevant because of translational invariance in a homogeneous Universe, and is used for simplicity here, as we are interested in the behaviour of δ as a function of scale R .

Mpc/h). Therefore we expect a similar impact on void properties derived from σ and the linear power spectrum.

37.7.2 Spherical Collapse

Because of the void-in-cloud effect, namely that voids inside halos are eventually swallowed and disappear, the linearly extrapolated density contrast δ_c for the formation of halos is important in describing the properties of voids as both are clearly connected. Within theoretical calculations of the void abundance using the excursion set formalism, δ_c corresponds to another absorbing barrier, whose equivalent is not present for halo abundance. Therefore calculating δ_c in the gravity theory of interest gives us important hints into the properties of both halos and voids.

The computation of δ_c is done similarly to that of the GR case, but using Eqs. (37.42) and (37.43) with the appropriate modified gravity parameterisation $\mu(k, a)$ (GR is recovered with $\mu(k, a) = 1$). We start with appropriate initial conditions² for δ and $\dot{\delta}$ and evolve the the linear Eq. (37.43) until a_c . The value of δ obtained is δ_c , the density contrast linearly extrapolated for halo formation at $a = a_c$. In this work, since we only study simulation outputs at $z = 0$, we take $a_c = 1$ in all calculations. The only modification introduced by a nontrivial parameterisation $\mu(k, a)$ is that the collapse parameters will depend on the scale k of the halo. As mentioned previously, the parameterisation of Eq. (37.44) only takes into account the evolution of the scalar field in the background, and does not account for the dependence of the collapse parameters on screening effects. Even though our calculation is approximated, it does approach the correct limits at sufficiently large and small scales.

For a Universe with only cold dark matter (CDM) under GR, the collapse equations can be solved analytically yielding $\delta_c = 1.686$. For a Λ CDM Universe, still within GR, δ_c changes to a slightly lower value, whereas for stronger gravity it becomes slightly larger. In particular, the value of δ_c starts at its Λ CDM value $\delta_c = 1.675$ on scales larger than the Compton scale ($k/a \ll m$; weak field limit where $\mu \approx 1$) and approaches the totally modified value $\delta_c = 1.693$ on smaller scales ($k/a \gg m$; strong field limit where $\mu \approx 1 + 2\beta^2 = 4/3$) where the modification to the strength of gravitational force is maximal. These values were computed at the background cosmology described in § 37.7.4. Note that δ_c reaches its strong field limit faster for larger values of $|f_{R0}|$ (value of the extra scalar field today), as expected. In the approximation of Eq. (37.42), δ_c varies with k less than in the full collapse, indicating that the no-screening approximation may not be sufficient. As a full exact calculation is beyond the scope of this work and given that δ_c does not change appreciably, in our abundance models we will fix δ_c to its Λ CDM value and encapsulate modified gravity effects on the linear power spectrum and on other model parameters.

² These initial conditions are actually determined by a shooting method, evolving the nonlinear Eq. (37.42) for multiple initial values and checking when collapse happens ($\delta \rightarrow \infty$) at $a = a_c$.

37.7.2.1 Spherical Expansion

We now compute δ_v , the analog of δ_c for voids, i.e. the density contrast linearly extrapolated to today for the formation of a void. We follow a procedure similar to spherical collapse, but in this case the initial values for δ_i are negative. We also set a criterium in the nonlinear field δ for the formation of a void to be $\delta_{sc} = -0.8$ or equivalently $\Delta_{sc} = 1 + \delta_{sc} = 0.2$. This quantity is somewhat the analogue for voids of the virial overdensity $\Delta_{vir} \approx 180$ for halo formation in an Einstein-de-Sitter (EdS) Universe. Despite the value of Δ_{vir} being only strictly appropriate for an EdS Universe, halos are often defined with this overdensity or other arbitrary values that may be more appropriate for specific observations. Similarly, $\delta_{sc} = -0.8$ is only strictly appropriate for shell-crossing in an EdS Universe. Here we will employ $\delta_{sc} = -0.8$, but we should keep in mind that this is an arbitrary definition of our spherical voids. When we fix this criterium for void formation we also fix the factor by which the void radius R expands with respect to its linear theory radius R_L . This factor is given by $R/R_L = (1 + \delta_{sc})^{-1/3} = 1.717$, and comes about from mass conservation throughout the expansion. Differently from halos, voids are not virialized structures and continue to expand faster than the background. Again environmental dependences are not incorporated in our computations as these values will depend only on scale factor a and the scale k or size of the void. Note that the behaviour of δ_v as a function of k , is very similar to that of δ_c . This is important when modelling the absorbing barriers used for evaluating the void abundance distribution function. Again the values of δ_v vary with k less than in the full calculation.

The spherical collapse and expansion calculations can be performed similarly for the symmetron model, with the appropriate change in the expression for the mass and coupling of the scalar field. For $f(R)$ gravity the change in parameters does not seem to be relevant and we fix these parameters to their Λ CDM values. In order to treat both gravity models in the same way, we do the same for the symmetron model. Therefore we do not show explicit calculations of δ_c and δ_v for symmetron.

37.7.3 Void Abundance Function

We now compute the void abundance distribution function as a function of void size using an extended Excursion Set formalism, which consists in solving the Fokker-Planck equation with appropriate boundary conditions. This procedure is valid when the barrier (boundary conditions) is linear in S and the random walk motion is Markovian.

Differently from the halo description, for voids it is necessary to use two boundary conditions, because of the void-in-cloud effect. In this case we use two Markovian stochastic barriers with linear dependence in the density variance S , which is a simple generalization from the conventional problem with a constant barrier. The barriers can be described statistically as

$$\begin{aligned}
\langle B_c(S) \rangle &= \delta_c + \beta_c S, \\
\langle B_c(S) B_c(S') \rangle &= D_c \min(S, S'), \\
\langle B_v(S) \rangle &= \delta_v + \beta_v S, \\
\langle B_v(S) B_v(S') \rangle &= D_v \min(S, S'),
\end{aligned} \tag{37.48}$$

where $B_c(S)$ is the barrier associated with halos and $B_v(S)$ the barrier associated with voids. Notice that the two barriers are uncorrelated, i.e. $\langle B_c(S) B_v(S') \rangle = 0$. Here β_c describes the linear relation between the mean barrier and the variance S , $\delta_{c,v}$ is the mean barrier as $S \rightarrow 0$ ($R \rightarrow \infty$), and $D_{c,v}$ describes the barrier diffusion coefficient.

As we consider different scales R , the smoothed density field $\delta(R)$ performs a random walk with respect to a *time coordinate* S , and we have

$$\begin{aligned}
\langle \delta(S) \rangle &= 0, \\
\langle \delta(S) \delta(S') \rangle &= \min(S, S').
\end{aligned} \tag{37.49}$$

We mention that this occurs when the window function in Eq. (37.45) S is sharp in k -space. For a window that is sharp in real space the motion of δ is not Markovian and the second equation in (37.49) is not true. In that case a more sophisticated method is necessary, and the solution presented above represents the zero-order approximation for the full solution.

The field δ satisfies a Langevin equation with white noise and therefore the probability density $\Pi(\delta, S)$ to find the value δ at variance S is a solution of the Fokker-Planck equation

$$\frac{\partial \Pi}{\partial S} = \frac{1}{2} \frac{\partial^2 \Pi}{\partial \delta^2}, \tag{37.50}$$

with boundary conditions

$$\Pi(\delta = B_c(S), S) = 0 \quad \text{and} \quad \Pi(\delta = B_v(S), S) = 0, \tag{37.51}$$

and initial condition

$$\Pi(\delta, S = 0) = \delta_D(\delta), \tag{37.52}$$

where δ_D is a Dirac delta function and notice that $S \rightarrow 0$ corresponds to void radius $R \rightarrow \infty$. In order to solve this problem, it is convenient to introduce the variable

$$Y(S) = B_v(S) - \delta(S). \tag{37.53}$$

Making the *simplifying* assumption that $\beta \equiv \beta_c = \beta_v$ ³ and using the fact that all variances can be added in quadrature, the Fokker-Planck Eq. (37.50) becomes

³ Notice that β here should not be confused with the coupling between matter and the extra scalar in Eq. (37.44).

$$\frac{\partial \Pi}{\partial S} = -\beta \frac{\partial \Pi}{\partial Y} + \frac{1+D}{2} \frac{\partial^2 \Pi}{\partial Y^2}, \tag{37.54}$$

where $D = D_v + D_c$.

We define $\delta_T = |\delta_v| + \delta_c$ and notice that $\delta(S) = B_v(S)$ implies $Y(S) = 0$, $\delta(S) = B_c(S)$ implies $Y(S) = -\delta_T$ (only occurs because we set $\beta_c = \beta_v$) and $\delta(0) = 0$ implies $Y(0) = \delta_v$. Therefore, the boundary conditions become

$$\Pi(Y = 0, S) = 0 \quad \text{and} \quad \Pi(Y = -\delta_T, S) = 0, \tag{37.55}$$

and the initial conditions

$$\Pi(Y, 0) = \delta_D(Y - \delta_v). \tag{37.56}$$

Rescaling the variable $Y \rightarrow \tilde{Y} = Y/\sqrt{1+D}$ and factoring the solution in the form $\Pi(\tilde{Y}, S) = U(\tilde{Y}, S) \exp[c(\tilde{Y} - cS/2 - \tilde{Y}_0)]$ where $c = \beta/\sqrt{1+D}$ and $\tilde{Y}_0 = \delta_v/\sqrt{1+D}$. The function $U(\tilde{Y}, S)$ obeys a Fokker-Planck equation like Eq. (37.50), for which the solution is known. Putting it all together the probability distribution function becomes

$$\begin{aligned} \Pi(Y, S) = \exp \left[\frac{\beta}{1+D} \left(Y - \frac{\beta S}{2} - \delta_v \right) \right] \\ \cdot \sum_{n=1}^{\infty} \frac{2}{\delta_T} \sin \left(\frac{n\pi \delta_v}{\delta_T} \right) \sin \left(\frac{n\pi}{\delta_T} Y \right) \exp \left[-\frac{n^2 \pi^2 (1+D)}{2\delta_T^2} S \right]. \end{aligned} \tag{37.57}$$

The ratio of walkers that cross the barrier $B_v(S)$ is then given by

$$\mathcal{F}(S) = \frac{\partial}{\partial S} \int_{\infty}^0 dY \Pi(Y, S) = \frac{1+D}{2} \frac{\partial \Pi}{\partial Y} \Big|_{Y=0}, \tag{37.58}$$

where we used the modified Fokker-Planck equation Eq. (37.54) and the first boundary condition from Eq. (37.55). The void abundance function, defined as $f(S) = 2S\mathcal{F}(S)$, for this model is then given by

$$\begin{aligned} f(S) = 2(1+D) \exp \left[-\frac{\beta^2 S}{2(1+D)} + \frac{\beta \delta_v}{(1+D)} \right] \\ \cdot \sum_{n=1}^{\infty} \frac{n\pi}{\delta_T^2} S \sin \left(\frac{n\pi \delta_v}{\delta_T} \right) \exp \left[-\frac{n^2 \pi^2 (1+D)}{2\delta_T^2} S \right]. \end{aligned} \tag{37.59}$$

There are four important limiting cases to consider:

- $D = \beta = 0$: This is the simplest case of two static barriers. It is given by

$$f_{D=\beta=0}(S) = 2 \sum_{n=1}^{\infty} \frac{n\pi}{\delta_T^2} S \sin \left(\frac{n\pi \delta_v}{\delta_T} \right) \times \exp \left(-\frac{n^2 \pi^2}{2\delta_T^2} S \right). \tag{37.60}$$

This is one of the functional forms tested in this work and the only case with no free parameters. We refer to this case as that of two static barriers (2SB).

- $D = 0$ and $\beta \neq 0$: This case considers that the barriers depend linearly on S but are not diffusive. In this case the expression is given by

$$f_{D=0}(S) = 2e^{-\frac{\beta^2 S}{2}} e^{\beta \delta_v} \sum_{n=1}^{\infty} \frac{n\pi}{\delta_T^2} S \sin\left(\frac{n\pi \delta_v}{\delta_T}\right) \times \exp\left(-\frac{n^2 \pi^2}{2\delta_T^2} S\right). \quad (37.61)$$

Note that these authors define the barrier with a negative slope, therefore our β is equal to their $-\beta$, but $\delta_v < 0$ in our case;

- $\beta = 0$ and $D \neq 0$: Here we have a barrier that does not depend on S but which is diffusive. In this case we have

$$f_{\beta=0}(S) = 2(1 + D) \sum_{n=1}^{\infty} \frac{n\pi}{\delta_T^2} S \sin\left(\frac{n\pi \delta_v}{\delta_T}\right) \cdot \exp\left[-\frac{n^2 \pi^2 (1 + D)}{2\delta_T^2} S\right] \quad (37.62)$$

- *Large void radius*: As discussed in [37, 38] and [39], for large radii R the void-in-cloud effect is not important as we do not expect to find big voids inside halos. In other words, when $S \rightarrow 0$ ($R \rightarrow \infty$) the abundance becomes equal to that of a one-barrier problem. Even though we do not attempt to properly consider the limit of Eq. (37.59) when $S \rightarrow 0$, this expression can be directly compared to the function of the problem with one linear diffusive barrier (1LDB), given by

$$f_{1\text{LDB}}(S) = \frac{|\delta_v|}{\sqrt{S(1 + D_v)}} \sqrt{\frac{2}{\pi}} \exp\left[-\frac{(|\delta_v| + \beta_v S)^2}{2S(1 + D_v)}\right]. \quad (37.63)$$

We can now compare the void abundance from multiple cases by taking their ratio with respect to the abundance of the 2SB model. The abundance of the model with $D \neq 0$ is substantially higher than 2SB, whereas that of the model with $\beta \neq 0$ is significantly lower. The cases with two linear diffusive barriers (2LDB) Eq. (37.59) and one linear diffusive barrier (1LDB) Eq. (37.63) are the main models considered in this work. The void abundance of the 1LDB and 2LDB models are nearly identical for $R > 4 \text{ Mpc}/h$, when the same values of β and D are used.

Given the ratio of walkers that cross the barrier $B_v(S)$ with a radius given by $S(R)$, the number density of voids with radius between R_L and $R_L + dR_L$ in linear theory is given by

$$\frac{dn_L}{d \ln R_L} = \frac{f(\sigma)}{V(R_L)} \frac{d \ln \sigma^{-1}}{d \ln R_L} \Big|_{R_L(R)}, \quad (37.64)$$

where the subscript L denotes linear theory quantities, $V(R_L)$ is the volume of the spherical void of linear radius R_L and recall $S = \sigma^2$.

Whereas for halos the number density in linear theory is equal to the final nonlinear number density, for voids this is not the case. In fact, Jennings et al. [39] shows that such criterion produces nonphysical void abundances, in which the volume

fraction of the Universe occupied by voids becomes larger than unity. Instead, to ensure that the void volume fraction is physical (less than unity) the authors of [39] impose that the volume density is the conserved quantity when going from the linear-theory calculation to the nonlinear abundance. Therefore, when a void expands from $R_L \rightarrow R$ it combines with its neighbours to conserve volume and not number. This assumption is quantified by the equation

$$V(R)dn = V(R_L)dn_L|_{R_L(R)} , \quad (37.65)$$

which implies

$$\frac{dn}{d \ln R} = \frac{f(\sigma)}{V(R)} \frac{d \ln \sigma^{-1}}{d \ln R_L} \frac{d \ln R_L}{d \ln R} \Big|_{R_L(R)} , \quad (37.66)$$

where recall in our case $R = (1 + \delta_{sc})^{-1/3} R_L = 1.717 R_L$ is the expansion factor for voids. Therefore we have trivially $d \ln R_L / d \ln R = 1$ above.

The expression in Eq. (37.66)—referred as the Vdn model—along with the function in Eq. (37.59) provide the theoretical prediction for the void abundance distribution in terms of void radius, which will be compared to the abundance of spherical voids found in N-body simulations of GR and modified gravity.

37.7.4 Voids from Simulations

We use the N-body simulations that were run with the Isis code [28] for Λ CDM, $f(R)$ Hu-Sawicki and symmetron cosmological models. For the $f(R)$ case we fixed $n = 1$ and considered $|f_{R0}| = 10^{-4}$, 10^{-5} and 10^{-6} . For symmetron, we fix $\beta_0 = 1$ and $L = 1$ and used simulations SymmA, SymmB, SymmD, which have $z_{SSB} = 1, 2, 3$ respectively. Each simulation has 512^3 particles in a box of size $256 \text{ Mpc}/h$, and cosmological parameters $(\Omega_b, \Omega_{dm}, \Omega_\Lambda, \Omega_\nu, h, T_{CMB}, n_s, \sigma_8) = (0.045, 0.222, 0.733, 0.0, 0.72, 2.726\text{K}, 1.0, 0.8)$. These represent the baryon density relative to critical, dark matter density, effective cosmological constant density, neutrino density, Hubble constant, CMB temperature, scalar spectrum index and spectrum normalization. The normalization is actually fixed at high redshifts, so that $\sigma_8 = 0.8$ is derived for the Λ CDM simulation, but is larger for the modified gravity simulations. In terms of spatial resolution, seven levels of refinement were employed on top of a uniform grid with 512 nodes per dimension. This gives an effective resolution of 32,678 nodes per dimension, which corresponds to $7.8 \text{ kpc}/h$. The particle mass is $9.26 \times 10^9 M_\odot/h$.

We ran the ZOBOV void-finder algorithm—based on Voronoi tessellation—on the simulation outputs at $z = 0$ in order to find underdense regions and define voids, and compared our findings to the Vdn model of Eq. (37.66) [39] with the various multiplicity functions $f(\sigma)$ proposed above (2SB, 1LDB and 2LDB models).

First, we used ZOBOV to determine the position of the density minima locations within the simulations and rank them by signal-to-noise S/N significance. Next, we started from the minimum density point of highest significance and grew a sphere around this point, adding one particle at a time in each step, until the overdensity $\Delta = 1 + \delta$ enclosed within the sphere was 0.2 times the mean background density of the simulation at $z = 0$. Therefore we defined *spherical* voids, which are more closely related to our theoretical predictions based on spherical expansion.

We also considered growing voids around the *center-of-volume* from the central Voronoi zones. The center-of-volume is defined similarly to the center-of-mass, but each particle position is weighted by the volume of the Voronoi cell enclosing the particle, instead of the particle mass. Using the center-of-volume produces results very similar to the previous prescription, so we only present results for the centers fixed at the density minima.

We can now compare the void abundance inferred from simulations for the three $f(R)$ and the three symmetron theories relative to the Λ CDM model. Since the differential abundance as a function of void radius is denoted by $dn/d \ln R$, we denote the relative difference between the $f(R)$ and Λ CDM abundances by $dn_{f(R)}/dn_{\Lambda\text{CDM}} - 1$ and show the results in terms of percent differences. In the $f(R)$ simulation this relative difference is around 100% at radii $R > 10 \text{ Mpc}/h$ (for the $|f_{R0}| = 10^{-4}$ case). In the symmetron simulation, the difference is around 40% (for the $z_{SSB} = 3$ case), for radii $R \sim 8 \text{ Mpc}/h$. This indicates that void abundance is a potentially powerful tool for constraining modified gravity parameters.

37.7.5 Results

37.7.5.1 Fitting β and D from Simulations

In order to use the theoretical expression in Eq. (37.59) to predict the void abundance we need values for the parameters β and D . The usual interpretation of β is that it encodes, at the linear level, the fact that the true barrier in real cases is not constant. In other words, the contrast density for the void (or halo) formation depends on its size/scale. This can occur because halos/voids are not perfectly spherical and/or because the expansion (or collapse) intrinsically depends on scale (Birkhoff's theorem is generally not valid in modified gravity). The scale dependency induced by modified gravity can be calculated using our model for spherical collapse (expansion), described in sections II.C and II.D, by fitting a linear relationship between δ_c (δ_v) or average barrier $\langle B_c \rangle$ ($\langle B_v \rangle$) as a function of the variance $S(R)$. Here we use $k = 2\pi/R$ to convert wave number to scale R .

Focusing on the average barriers $\langle B_c \rangle$, $\langle B_v \rangle$ as functions of variance S for multiple gravity theories, and empirical fits for the parameters δ_c , δ_v , β_c , β_v from Eqs. (37.48), we find that the corresponding fits indicate that the barriers depend weakly on scale in the range of interest. The values of δ_c , δ_v are nearly constant and those of β_c , β_v are of order 10^{-3} while the corresponding values for halos in Λ CDM are of order 10^{-1} .

Even though voids are quite spherical, the small values of β indicate that the main contribution to β may come from more general aspects of nonspherical evolution. The small fitted values of β can also be due to errors induced by the approximations in the nonlinear equation Eq. (37.42), which does not capture screening effects of modified gravity.

Given these issues, and as it is beyond the scope of this work to consider more general collapse models or study the exact modified gravity equations, we will instead keep the values of δ_c and δ_v fixed to their Λ CDM values and treat β as a free parameter to be fitted from the abundance of voids detected in the simulations.

Likewise, the usual interpretation of D is that it encodes stochastic effects of possible problems in our void (halo) finder [40], such as an intrinsic incompleteness or impurity of the void sample, or other peculiarities of the finder, which may even differ from one algorithm to another. Therefore D is also taken as a free parameter in our abundance models.

Focusing on the abundance of voids $dn/d \ln R$ as measured from simulations, as well as three theoretical models, namely the 2SB[39], 1LDB Eq. (37.63) and 2LDB Eq. (37.59) models, we can see that linear-diffusive-barrier models (1LDB and 2LDB) work best in all gravities, relative to the static barriers model (2SB). In fact, these two models describe the void abundance distribution within 10% precision for $R \lesssim 10 \text{ Mpc}/h$. We mention that the model with two linear diffusive barriers (2LDB) better describes the abundance of small voids ($R \lesssim 3 \text{ Mpc}/h$), due to the void-in-cloud effect, more relevant for small voids [37, 38].

As both parameters β and D have an explicit dependence on the modified gravity strength, next we fit a relationship between the abundance parameters β and D and the gravity parameters $\log_{10} |f_{R0}|$ and z_{SSB} . In these fits we set the value $\log_{10} |f_{R0}| = -8$ to represent the case of Λ CDM cosmology, as this is indeed nearly identical to Λ CDM for purposes of large-scale structure observables, i.e. $\log_{10} |f_{R0}| = -8 \simeq -\infty$.

As we expect β and D to depend monotonically on the modified gravity parameters, we fit for them using simple two-parameter functions. For β case we use a straight line, and for D a second order polynomial with maximum fixed by the Λ CDM value. Additionally, our values of β and D as a function of gravity parameters fluctuate considerably around the best fit. This occurs at least partially because we have used only one simulation for each gravity model, and we expect this oscillation to be reduced with a larger number of simulations. At present, the use of the fits is likely more robust than the use of exact values obtained for each parameter/case.

37.7.5.2 Constraining Modified Gravity

Given the discussion on β and D of the last subsection, we now check for the power of constraining modified gravity from the void distribution function in each of the three void abundance models considered, namely 2SB, 1LDB and 2LDB. We take the abundance of voids actually found in simulations (described in the §IV) to represent a hypothetical real measurement of voids and compare it to the model predictions, evaluating the posterior for $\log_{10} |f_{R0}|$ and z_{SSB} , thus assessing the constraining

power of each abundance model in each gravity theory. Obviously the constraints obtained in this comparison are optimistic—since we are taking as real data the same simulations used to fit for the abundance model parameters—but they provide us with idealized constraints similar in spirit to a Fisher analysis around a fiducial model. One can show that the 2SB model predicts values for the $f(R)$ parameter ($\log_{10} |f_{R0}|$), which are incorrect by more than 3σ for all cases. In fact, this model predicts incorrect values even for general relativity. This is not surprising given the bad χ^2 fits. Therefore we find this model to be highly inappropriate to describe the abundance of dark matter voids, and focus on models with linear diffusive barriers.

Both the 1LDB and 2LDB models predict correct values for the gravity parameters within 1σ in most cases. We find that the 1LDB model presents results similar to 2LDB, despite being a simpler model and providing a worse fit to the data (larger reduced χ^2). For Λ CDM both posteriors go to $\log_{10} |f_{R0}| = 10^{-8}$, which represents the GR case by assumption. This shows that within the $f(R)$ framework, we can also constrain GR with reasonable precision from void abundance, using one of these two abundance models with diffusive barriers (1LDB, 2LDB). Finally, for the symmetron model, the parameter z_{SSB} is also well constrained, similarly to f_{R0} in $f(R)$. Again the 2SB model has the worst result in all cases, and the 1LDB and 2LDB models produce similar results.

37.7.5.3 Voids in Galaxy Samples

In real observations it is much harder to have direct access to the dark matter density field. Instead we observe the galaxy field, a biased tracer of the dark matter. Therefore it is important to investigate the abundance of voids defined by galaxies and the possibility of constraining cosmology and modified gravity in this case.

We introduce galaxies in the original dark matter simulations using the Halo Occupation Distribution (HOD) model from [41]. In [42–44] the authors investigated similar void properties but did not consider spherical voids, using instead the direct outputs of the VIDE [45] void finder. In our implementation, first we find the dark matter halos in the simulations using the overdensities outputted by ZOBOV. We grow a sphere around each of the densest particles until its enclosed density is 200 times the mean density of the simulation. This process is the reverse analog of the spherical void finder described in § IV, the only difference being the criterium used to sort the list of potential halo centers. Here we sort them using the value of the point density, not a S/N significance, as the latter is not provided by ZOBOV in the case of halos.

We populate these halos with galaxies using the HOD model of [41]. This model consist of a mean occupation function of central galaxies given by

$$\langle N_{cen}(M) \rangle = \frac{1}{2} \left[1 + \operatorname{erf} \left(\frac{\log M - \log M_{min}}{\sigma_{\log M}} \right) \right], \quad (37.67)$$

with a nearest-integer distribution. The satellite galaxies follow a Poisson distribution with mean given by

$$\langle N_{sat}(M) \rangle = \langle N_{cen}(M) \rangle \left(\frac{M - M_0}{M'_1} \right)^\alpha. \quad (37.68)$$

Central galaxies are put in the center of halo, and the satellite galaxies are distributed following a Navarro Frenk and White profile.

We use parameter values representing the sample *Main 1* of [42–44], namely: $(\log M_{min}, \sigma_{\log M}, \log M_0, \log M'_1, \alpha) = (12.14, 0.17, 11.62, 13.43, 1.15)$. These parameters give a mock galaxy catalogue with galaxy bias $b_g = 1.3$ and mean galaxy density $\bar{n}_g = 5.55 \times 10^{-3} (h/\text{Mpc})^3$ in ΛCDM .

We then find voids in this galaxy catalogue using the same algorithm applied to the dark matter catalogue (described in § IV). We use the same criterium that a void is a spherical, non-overlapping structure with overdensity equal to 0.2 times the background galaxy density. However, as the galaxies are a biased tracer of the dark matter field, if we find galaxy voids with 0.2 times the mean density, we are really finding regions which are denser in the dark matter field. In fact, if $\delta_g = b_g \delta$ is the galaxy overdensity, with galaxy bias b_g and δ is the dark matter overdensity we have

$$\Delta = 1 + \delta = 1 + \frac{\delta_g}{b_g}. \quad (37.69)$$

Therefore, if we find voids with $\delta_g = -0.8$ and $b_g = 1.3$ we have $\Delta = 0.38$, i.e. the galaxy voids enclose a region of density 0.38 times the mean density of the dark matter field. Therefore it is this value that must be used in the previous theoretical predictions. Using this value, the relation between linear and nonlinear radii is $R = 1.37R_L$, and the density parameter for the spherical void formation—calculated using the spherical expansion equations (§ II.D)—is $\delta_v = -1.33$. We insert these new values into the theoretical predictions and compare to the measured galaxy void abundance. We mention that both original models, 2SB and 2LDB (blue curves), with $R = 1.71R_L$ and $\delta_v = -2.788$, provide incorrect predictions for the abundance of galaxy voids. However when corrected for the galaxy bias (red curves), these models are in good agreement with the data. We also see that the 2LDB provides a slightly better fit, which is not significant given the error bars.

The main problem of our galaxy catalogues is the low number density of objects. Larger box sizes (or a galaxy population intrinsically denser) might help decrease the error bars sufficiently in order to constrain modified gravity parameters. Focusing on the relative difference between the abundance for the three modified gravity models and GR as inferred from our simulations, we see that it is not possible to constrain the gravity model using the abundance of galaxy voids, as extracted from mock galaxy catalogues of the size considered here, due to limited statistics. Further investigations using larger or multiple boxes, or else considering a galaxy population with larger

intrinsic number density should decrease Poisson errors significantly, allowing for a better investigation of void abundance in the large data sets expected for current and upcoming surveys, such as the SDSS-IV, DES, DESI, Euclid and LSST.

37.8 Conclusions and Perspectives

In this chapter we briefly review gravity theories beyond General Relativity which may possibly explain several cosmological puzzles, specifically the present accelerated expansion of the Universe [1]. Modified Gravity must comply with strong requirements: One is that the model must have similar cosmological predictions to those of Λ CDM for the background evolution and the linear large scale structures [12]. Another condition is that the modifications to General Relativity are suppressed at small scales [13]. This requirement is assured through the so-called screening mechanisms [14]. Since different modified gravity theories can be degenerate with regard to both the background cosmology and the growth rate of linear perturbations, it is crucial to identify new probes that can be used to break these degeneracies. In this paper we study the effects of a class of screened modified gravity models in the nonlinear regime of structure formation. The aim is to predict possible smoking guns of modified gravity and of screening mechanisms at cluster of galaxy scales.

The rise of a fifth force in modified gravity theories leads to a stronger clustering of matter. Therefore, the matter power spectra has in general a higher amplitude than in GR. In screened modified gravity theories, the range of the fifth force at cosmological scales is around Mpc (in order to avoid the strong local gravity constraints); therefore, the linear power spectra is similar to Λ CDM, and the differences occur in the small scales of the nonlinear regime.

Overall, we find that halo velocity profiles are an excellent direct tracer of the fifth force: large deviations in the relative velocity of particles are found. Moreover, we find that the velocity field in modified gravity simulations is more affected by the presence of the fifth force than the density field for $f(R)$ -gravity. For the Symmetron model we found this to be even more apparent. A particular striking example of this is the *Symm_C* model, with boosts of up to $(\Delta P/P)_\theta \gtrsim 3$, whereas $(\Delta P/P)_m \sim 0.1$.

In order to find smoking guns of screening mechanisms, we studied the environmental dependence of the masses of dark matter halos in the symmetron modified gravity scenario. The potential governing the dynamics of the matter fields ($\Phi_- + \Phi_+$) can differ significantly from the lensing potential Φ_+ in this model, which leads to a clear difference between the mass of the halo as obtained from dynamical measurements and that obtained from gravitational lensing. Such an effect found in the symmetron model can be significantly stronger than in $f(R)$ gravity. This signature, which is unique to modified gravity, can in practice be measured by combining dynamical (e.g., velocity dispersion) and lensing mass measurements of clusters of galaxies or even single galaxies. We find that the environmental dependence is strongest for small halos as very large halos are sufficiently massive to be able to screen themselves.

This discovered feature of environmental dependence also allows us, in principle, to distinguish between different modified gravity scenarios such as $f(R)$, more general chameleons, and the symmetron. In $f(R)$ the maximum fraction of the fifth-force to the Newtonian force in halos are around 30% while in chameleon/symmetron scenarios this fraction can be either smaller or larger, depending on the value of the coupling strength β .

Although the theoretical nature of screening mechanisms is different, we find common features in both the matter and the velocity properties. In particular, our findings suggest that one can classify screening mechanisms into three general categories: (1) the fully screened regime where GR is recovered, (2) an unscreened regime where the strength of the fifth force is large, and, (3) a partially screened regime where screening occurs in the inner part of a halo, but the fifth force is active at larger radii. Any observable sensitive to this regimes and environments can be a future probe of screening mechanisms and modified gravity theories beyond General Relativity.

While the above results concerned modified gravity models which could be an alternative to a dark energy fluid, there are similar astrophysical probes which could also indicate that an extended theory of gravity could be an alternative to a dark matter particle.

For instance, in Salzano et al. [46], motivated by chameleon, symmetron and $f(R)$ gravity models, it was studied a phenomenological scenario where the scalar field has both a mass (i.e. interaction length) and a coupling constant to the ordinary matter which scale with the local properties of the considered astrophysical system. The authors analysed the feasibility of this scenario using the modified gravitational potential obtained in its context and applied it to the galactic and hot gas/stellar dynamics in galaxy clusters and elliptical/spiral galaxies respectively.

The main results are: 1. The velocity dispersion of elliptical galaxies can be fitted remarkably well by the suggested scalar field, with model significance similar to a classical Navarro-Frenk-White dark halo profile; 2. The analysis of the stellar dynamics and the gas equilibrium in elliptical galaxies has shown that the scalar field can couple with ordinary matter with different strengths (different coupling constants) producing and/or depending on the different clustering state of matter components; 3. Elliptical and spiral galaxies, combined with clusters of galaxies, show evident correlations among theory parameters which suggest the general validity of our results at all scales and a way toward a possible unification of the theory for all types of gravitational systems we considered.

All these results demonstrate that the proposed scalar field scenario can work fairly well as an alternative to dark matter. Moreover, Salzano et al. [47, 48] investigate an extension of covariant Galileon models in the so-called “beyond Horndeski” scenario, where a breaking of the Vainshtein mechanism is possible inside large astrophysical objects, thus having possibly detectable observational signatures. It is found that for those clusters which are very close to be relaxed, and thus less perturbed by possible astrophysical local processes, the Galileon model gives a quite good fit to both x-ray and lensing observations. When these models are applied to a sample of clusters of galaxies observed under the CLASH survey, using both new data from gravitational

lensing events and archival data from X-ray intra-cluster hot gas observations, one finds that the assumption of having only gas and no Dark Matter at all in the clusters is able to match observations. In particular, the authors find that, the general relativity limit is excluded at 2σ confidence level, thus making the this type of Galileon model clearly statistically different and competitive with respect to general relativity.

References

1. T. Clifton, P.G. Ferreira, A. Padilla, C. Skordis, Modified gravity and cosmology. *Phys. Rept.* **513**, 1–189 (2012). [arXiv:1106.2476](#)
2. S. Capozziello, M. De Laurentis, Extended theories of gravity. *Phys. Rept.* **509**, 167–321 (2011). [arXiv:1108.6266](#)
3. Y.-F. Cai, S. Capozziello, M. De Laurentis, E.N. Saridakis, $f(T)$ teleparallel gravity and cosmology. *Rept. Prog. Phys.* **79**(10), 106901 (2016). [arXiv:1511.07586](#)
4. S. Capozziello, M. De Laurentis, The dark matter problem from $f(R)$ gravity viewpoint. *Annalen Phys.* **524**, 545–578 (2012)
5. T. Koivisto, D.F. Mota, Vector field models of inflation and dark energy. *JCAP* **0808**, 021 (2008). [arXiv:0805.4229](#)
6. T.S. Koivisto, D.F. Mota, M. Zumalacárregui, Screening modifications of gravity through disformally coupled fields. *Phys. Rev. Lett.* **109**, 241102 (2012). [arXiv:1205.3167](#)
7. Y. Akrami, T.S. Koivisto, D.F. Mota, M. Sandstad, Bimetric gravity doubly coupled to matter: theory and cosmological implications. *JCAP* **1310**, 046 (2013). [arXiv:1306.0004](#)
8. M. Thorsrud, D.F. Mota, S. Hervik, Cosmology of a scalar field coupled to matter and an isotropy-violating maxwell field. *JHEP* **10**, 066 (2012). [arXiv:1205.6261](#)
9. J.D. Barrow, D.F. Mota, Gauge invariant perturbations of varying alpha cosmologies. *Class. Quant. Grav.* **20**, 2045–2062 (2003). [arxiv:gr-qc/0212032](#)
10. A. De Felice, D.F. Mota, S. Tsujikawa, Matter instabilities in general Gauss-Bonnet gravity. *Phys. Rev. D* **81**, 023532 (2010). [arXiv:0911.1811](#)
11. B. Li, D.F. Mota, D.J. Shaw, Microscopic and macroscopic behaviors of palatini modified gravity theories. *Phys. Rev. D* **78**, 064018 (2008). [arXiv:0805.3428](#)
12. Planck P.A.R.A. Collaboration, et al., Planck 2015 results. XIV. Dark energy and modified gravity. *Astron. Astrophys. A* **594**, 14 (2016). [arXiv:1502.01590](#)
13. C.M. Will, The confrontation between general relativity and experiment. *Living Rev. Rel.* **17**, 4 (2014). [arXiv:1403.7377](#)
14. P. Brax, Screened modified gravity. *Acta Phys. Polon. B* **43**, 2307–2329 (2012). [arXiv:1211.5237](#)
15. J. Khoury, A. Weltman, Chameleon fields: awaiting surprises for tests of gravity in space. *Phys. Rev. Lett.* **93**, 171104 (2004). [arXiv:astro-ph/0309300](#)
16. K. Hinterbichler, J. Khoury, Symmetron fields: screening long-range forces through local symmetry restoration. *Phys. Rev. Lett.* **104**, 231301 (2010). [arXiv:1001.4525](#)
17. W. Hu, I. Sawicki, Models of $f(R)$ cosmic acceleration that evade solar-system tests. *Phys. Rev. D* **76**, 064004 (2007). [arXiv:0705.1158](#)
18. A.-C. Davis, B. Li, D.F. Mota, H.A. Winther, Structure formation in the symmetron model. *Astrophys. J.* **748**, 61 (2012). [arXiv:1108.3081](#)
19. R. Hagala, C. Llinares, D.F. Mota, *Cosmic Tsunamis in Modified Gravity: Scalar Waves Disrupting Screening Mechanisms*. [arXiv:1607.02600](#)
20. R. Hagala, C. Llinares, D.F. Mota, Cosmological simulations with disformally coupled symmetron fields. *Astron. Astrophys.* **585**, A37 (2016). [arXiv:1504.07142](#)
21. B. Bertotti, L. Iess, P. Tortora, A test of general relativity using radio links with the Cassini spacecraft. *Nature* **425**, 374–376 (2003)

22. C. Llinares, D. Mota, Releasing scalar fields: cosmological simulations of scalar-tensor theories for gravity beyond the static approximation. *Phys. Rev. Lett.* **110**(16), 161101 (2013). [arXiv:1302.1774](#)
23. C. Llinares, D.F. Mota, Cosmological simulations of screened modified gravity out of the static approximation: effects on matter distribution. *Phys. Rev. D* **89**, 084023 (2014). [arXiv:1312.6016](#)
24. M.B. Gronke, C. Llinares, D.F. Mota, Gravitational redshift profiles in the $f(R)$ and symmetron models. *Astron. Astrophys.* **562**, A9 (2014). [arXiv:1307.6994](#)
25. M. Gronke, A. Hammami, D.F. Mota, H.A. Winther, Estimates of cluster masses in screened modified gravity. *Astron. Astrophys.* **595**, A78 (2016). [arXiv:1609.02937](#)
26. M. Gronke, D.F. Mota, H.A. Winther, Universal predictions of screened modified gravity on cluster scales. *Astron. Astrophys.* **583**, A123 (2015). [arXiv:1505.07129](#)
27. M. Gronke, C. Llinares, D.F. Mota, H.A. Winther, Halo velocity profiles in screened modified gravity theories. *Mon. Not. Roy. Astron. Soc.* **449**(3), 2837–2844 (2015). [arXiv:1412.0066](#)
28. C. Llinares, D.F. Mota, H.A. Winther, ISIS: a new N-body cosmological code with scalar fields based on RAMSES. Code presentation and application to the shapes of clusters. *Astron. Astrophys.* **562**, A78 (2014). [arXiv:1307.6748](#)
29. S.R. Knollmann, A. Knebe, Ahf: Amiga’s Halo finder. *Astrophys. J. Suppl.* **182**, 608–624 (2009). [arXiv:0904.3662](#)
30. H.A. Winther, D.F. Mota, B. Li, Environment dependence of dark matter halos in symmetron modified gravity. *Astrophys. J.* **756**, 166 (2012). [arXiv:1110.6438](#)
31. Y.-Y. Zhang et al., LoCuSS: a comparison of cluster mass measurements from XMM-Newton and Subaru—testing deviation from hydrostatic equilibrium and non-thermal pressure support. *Astrophys. J.* **711**, 1033–1043 (2010). [arXiv:1001.0780](#)
32. A. Mahdavi, H. Hoekstra, A. Babul, C. Bildfell, T. Jeltema, J.P. Henry, Joint analysis of cluster observations: II. Chandra/XMM-Newton X-ray and weak lensing scaling relations for a sample of 50 rich clusters of galaxies. *Astrophys. J.* **767**(2), 116 (2013). [arXiv:1210.3689](#)
33. A. Hammami, D.F. Mota, Cosmological simulations with hydrodynamics of screened scalar-tensor gravity with non-universal coupling. *Astron. Astrophys.* **584**, A57 (2015). [arXiv:1505.06803](#)
34. A. Hammami, D.F. Mota, Probing modified gravity via the mass-temperature relation of galaxy clusters. *Astron. Astrophys.* **598**, A132 (2017). [arXiv:1603.08662](#)
35. A. Hammami, C. Llinares, D.F. Mota, H.A. Winther, Hydrodynamic effects in the symmetron and $f(R)$ -gravity models. *Mon. Not. Roy. Astron. Soc.* **449**(4), 3635–3644 (2015). [arXiv:1503.02004](#)
36. R. Voivodic, M. Lima, C. Llinares, D.F. Mota, Modelling void abundance in modified gravity. *Phys. Rev. D* **95**(2), 024018 (2017). [arXiv:1609.02544](#)
37. R.K. Sheth, H.J. Mo, G. Tormen, Ellipsoidal collapse and an improved model for the number and spatial distribution of dark matter haloes. *Mon. Not. Roy. Astron. Soc.* **323**, 1 (2001). [arxiv:astro-ph/9907024](#)
38. R.K. Sheth, R. van de Weygaert, A hierarchy of voids: much ado about nothing. *Mon. Not. Roy. Astron. Soc.* **350**, 517 (2004). [arxiv:astro-ph/0311260](#)
39. E. Jennings, Y. Li, W. Hu, The abundance of voids and the excursion set formalism. *Mon. Not. Roy. Astron. Soc.* **434**, 2167 (2013). [arXiv:1304.6087](#)
40. M. Maggiore, A. Riotto, The Halo mass function from excursion set theory. II. The diffusing barrier. *Astrophys. J.* **717**, 515–525 (2010). [arXiv:0903.1250](#)
41. Z. Zheng, A.L. Coil, I. Zehavi, Galaxy evolution from halo occupation distribution modeling of DEEP2 and SDSS galaxy clustering. *Astrophys. J.* **667**, 760–779 (2007). [arxiv:astro-ph/0703457](#)
42. S. Nadathur, S. Hotchkiss, The nature of voids—I. Watershed void finders and their connection with theoretical models. *Mon. Not. Roy. Astron. Soc.* **454**(2), 2228–2241 (2015). [arXiv:1504.06510](#)
43. S. Nadathur, S. Hotchkiss, The nature of voids—II. Tracing underdensities with biased galaxies. *Mon. Not. Roy. Astron. Soc.* **454**(1), 889–901 (2015). [arXiv:1507.00197](#)

44. S. Nadathur, S. Hotchkiss, J.M. Diego, I.T. Iliev, S. Gottlöber, W.A. Watson, G. Yepes, Universal void density profiles from simulation and SDSS. *IAU Symp.* **308**, 542–545 (2014). [arXiv:1412.8372](#)
45. P.M. Sutter, G. Lavaux, N. Hamaus, A. Pisani, B.D. Wandelt, M.S. Warren, F. Villaescusa-Navarro, P. Zivick, Q. Mao, B.B. Thompson, VIDE: the void identification and examination toolkit. *Astron. Comput.* **9**, 1–9 (2015). [arXiv:1406.1191](#)
46. V. Salzano, S. Capozziello, N.R. Napolitano, D.F. Mota, Unifying static analysis of gravitational structures with a scale-dependent scalar field gravity as an alternative to dark matter. *Astron. Astrophys.* **561**, A131 (2014). [arXiv:1211.1019](#)
47. V. Salzano, D.F. Mota, S. Capozziello, M. Donahue, Breaking the Vainshtein screening in clusters of galaxies. *Phys. Rev. D* **95**(4), 044038 (2017). [arXiv:1701.03517](#)
48. V. Salzano, D.F. Mota, M.P. Dabrowski, S. Capozziello, No need for dark matter in galaxy clusters within Galileon theory. *JCAP* **1610**(10), 033 (2016). [arXiv:1607.02606](#)

Part IV

Conclusion

Chapter 38

The End of the Beginning



Emmanuel N. Saridakis

Once upon a time there was a concrete, holistic, self-consistent and perfect cosmological paradigm in agreement with all observations, a model so successful that became the most long-lived scientific system in history. This model was introduced by Aristotle (incorporating previous considerations) around 340 BC [1] and took its final form after the works of Autolycus, Eudoxus, Callippus, Apollonius, Conon, Hipparchus, Sosigenes and other Greek astronomers, and in particular of Claudios Ptolemy [2].

In the Aristotelian-Ptolemaic cosmological and physical paradigm the Earth is spherical and exists in the center of the universe (geocentrism), it does not revolve around anything else neither it rotates around its own axis. It is composed of four elements and their combinations: Earth, Water, Fire and Air. It is surrounded by ten concentric spheres made of a perfectly transparent substance known as “quintessence” (the “fifth” element). These spheres revolve around the earth, carrying the other celestial bodies. The first is the sphere of the Moon (Lunae), the second of the Mercury (Mercurii), the third of the Venus (Veneris), the fourth is the Sun (Solis), the fifth of the Mars (Martis), the sixth of the Jupiter (Iovis), the seventh of the Saturn (Saturni), and spheres eight, nine and ten hold the “fixed stars”. The fixed stars were given their name since they do not move relative to each other, unlike the planets, which move among and independently of the fixed stars (the Greek word planet means exactly that: wanderer). Even the subtle and puzzling observation of the “retrograde

E. N. Saridakis (✉)

National Observatory of Athens, Athens, Greece

Key Laboratory for Researches in Galaxies and Cosmology, Department of Astronomy,
University of Science and Technology of China, Hefei 230026, Anhui, P.R. China

School of Astronomy, School of Physical Sciences, University of Science and Technology
of China, Hefei 230026, P.R. China

e-mail: msaridak@noa.gr

© The Author(s), under exclusive license to Springer Nature Switzerland AG 2021

617

E. N. Saridakis et al. (eds.) *Modified Gravity and Cosmology*,

https://doi.org/10.1007/978-3-030-83715-0_38

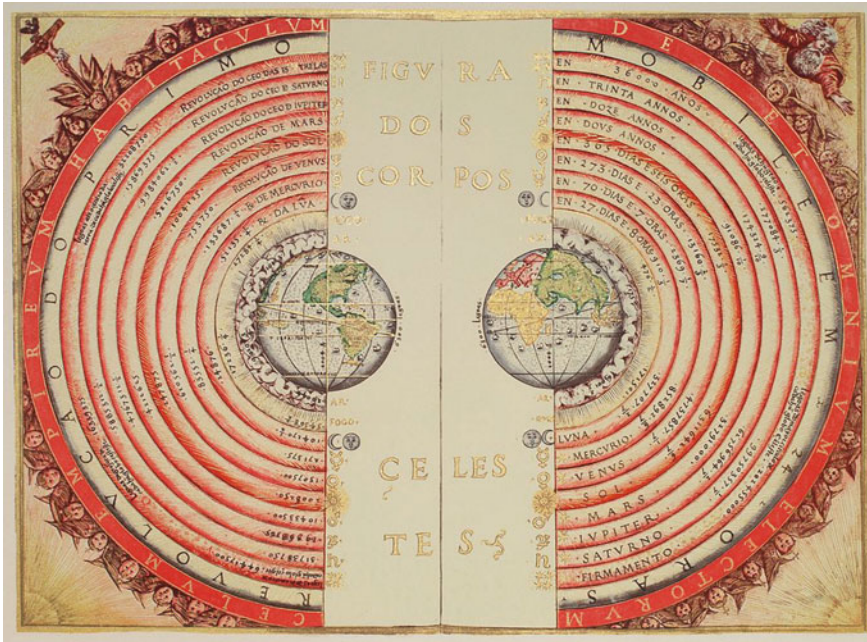


Fig. 38.1 An illustration of the Aristotelian-Ptolemaic geocentric system of 1568 by Portuguese cosmographer and cartographer Bartolomeu Velho (Bibliothèque Nationale, Paris)

motion” was incorporated in the model by Ptolemy through the epicycles modification. Finally, the Universe is spherical, finite and eternal. A Renaissance illustration of the Aristotelian-Ptolemaic cosmological paradigm can be seen in Fig. 38.1.

The Aristotelian-Ptolemaic system was remarkably plausible and powerful as a scientific theory, intuitively explaining all observations and being consistent with the main philosophical considerations. Hence, despite the existence of alternative models, and in particular of the Earth-rotational model of Heraclides Ponticos (4th century BC), and of the heliocentric model of Aristarchos of Samos (3rd century BC) and Seleucus of Seleucia (2nd century BC), the Aristotelian-Ptolemaic paradigm remained the absolute cosmological model for more than one thousand five hundred years.

It was only after the 11th century AD, where various Arab and Persian scholars such as Alhazen, Al-Zarkali, Fakhr al-Din al-Razi, Al-Tusi and Ibn al-Shatir, first through philosophical considerations and thinking and then incorporating observations performed in Maragha observatory, started putting into doubt the details of Aristotelian-Ptolemaic model such as the epicycles and the Earth’s non-rotation [3], although never actually disputing geocentrism [4]. The actual “paradigm shift” to heliocentrism was initialized by Copernicus in 1543 [5] (the influence of the Islamic, and in particular of Maragha, school on Copernicus remains speculative [6], however

it has been verified that Copernicus had read in detail pieces of Aristarchos of Samos [7]¹).

We stress here that the Aristotelian-Ptolemaic system was still the standard cosmological paradigm for many years after Copernicus, as at the time the Copernican system, which still used circular orbits, did not offer better predictions than the geocentric system, and it posed problems for both natural philosophy and Christian scripture. It was only after many decades, where detailed observations made by Tycho Brahe, Johannes Kepler, and Galileo Galilei postulated elliptical orbits and established heliocentrism [9] (although still not completely accepted, as Giordano Bruno's fate revealed).

Finally, the theoretical justification for the above "paradigm shift" was offered one century later by Isaac Newton, since for the first time he offered a physical theory as the underlying foundation of the cosmological model, namely the theory of gravitation [10]. In order to achieve this, Newton had first to use the detailed results of gravitation experiments made by Galileo, which allowed him to dispute the Aristotelian ideas on gravity (bodies do not fall towards Earth in order to come back to their "initial state" but due to the attraction between masses), as well as the detailed astronomical observations of Brahe and Kepler which allowed him to conclude that it is the same force that makes the celestial bodies to move and the bodies on Earth to fall. As he himself wrote: "If I have seen further it is by standing on the shoulders of Giants" [11].

Newtonian gravity and the Newtonian-Keplerian astronomical model was very successful in explaining observations. Nevertheless, theoretical investigation and progress in the fields of mechanics and especially in the novel field of electromagnetism [12], as well as the technological advance that allowed for radical increase in experimental capabilities (e.g. the Michelson–Morley experiment [13]) and in observational accuracy (e.g. observation of the precession of Mercury's perihelion [14]), started putting it into doubt. Despite the fact that some of the findings could be explained without a changing in the foundations of the Newtonian system² the complete and self-consistent incorporation of both theoretical research and all experimental and observational data led Einstein to construct a new gravitational theory. The theory of General Relativity, had different foundations, physical interpretation and mathematical structure from Newtonian gravity, nevertheless at the level of predictions it was served as its modification, exhibiting the latter as a particular limit

¹ Just before Copernicus sent his manuscript to be published in 1543, afraid of reactions he removed two pages from the submitted manuscript that acknowledged his indebtedness to the ancient Greek astronomers. However, he kept the two pages in his own personal copy, which was not discovered until 300 years later, towards the end of the 19th century [8].

² Urbain Le Verrier was able to describe the discrepancies with Uranus's orbit by predicting through purely theoretical calculations the existence and current position of a new planet, namely Neptune, which was indeed discovered by Johann Gottfried Galle in 1846 at exactly the predicted coordinates. This astonishing validation of celestial Newtonian mechanics led Verrier in 1859 to propose that the precession of Mercury's orbit was a result of another extra planet between Mercury and Sun, namely the Vulcan, or even of a series of smaller "corpuscules" [15].

and offering corrections that were larger at scales that had just then started to become accessible by technological advance.

The shift in the description of gravity soon started having effects in the description of astronomy, since from Newton times it was established that astronomical behavior was the result of gravitational interactions. Additionally, many people, amongst them Einstein [16], realized that an understanding of gravity offered the way to understand not only astronomy (the “laws of stars”) but also quantitatively describe the behavior of the universe as a whole and thus bringing cosmology (“laws of cosmos”) from the sphere of philosophy, to which it belonged for thousands of years, to the sphere of natural sciences.

The following decades were characterized by a significant advance in the quality and quantity of observations, leading to corrections and improvements in the new cosmological paradigm. The discovery of extra galaxies beyond the Milky Way, that are moreover moving away from each other [17], established the framework of an expanding and cooling universe originating from a primordial super-dense and super-hot state. Although this “Big Bang” theory offered verified quantitative predictions (e.g. the abundance of primordial elements and the cosmic microwave background radiation) and was able to describe all observations, theoretical investigation revealed that it might have some theoretical “problems” (or at least issues whose explanation was not “natural”), such as the horizon, the flatness and the magnetic monopole ones. Hence, after 1980 the phase of inflation [18–20] was established as a necessary ingredient of the cosmological paradigm at its early stages.³ Finally, the last decades the cosmological paradigm underwent through another modification, in order to incorporate the “indirect observation” of the dark matter sector, as well as the direct observation of accelerated expansion. Hence, the concordance model, the paradigm of Λ CDM cosmology, is now well established. Namely, a universe filled with the Standard Model particles plus the dark matter sector, which is governed by the gravitational theory of General Relativity with the addition of the cosmological constant, and which has originated from an inflationary Big Bang.

As one can see, exhaustive and diligent observations in various areas, in a dialectical relation with pure theoretical thinking and investigation, led to a series of paradigm shifts, each time offering a better and deeper description of Nature. As a result, the concrete, holistic, self-consistent and perfect Aristotelian-Ptolemaic cosmological and physical paradigm, in agreement with all observations and theoretical considerations for more than one and a half thousand years, gave its place to the concrete, holistic, self-consistent and perfect cosmological and physical paradigm of Λ CDM cosmology and General Relativity, in agreement with all observations and theoretical considerations for many decades.

A question thus arises naturally: Since accumulated observational, experimental and theoretical research and results are able (after a period of challenge of validity and dispute) to transmute viable and established theories, scenarios and paradigms

³ We will not enter here into the discussion of whether inflation is an over-predictable, non-falsifiable theory, and whether it completely satisfies the criteria of being a successful physical theory. The reader could see [21] and references therein.

into non-viable ones, which are then forced to give their place to new paradigms that are able to share the successes of their ancestors without sharing their failures, what will be the future of Λ CDM cosmology and General Relativity? Are these the final theories that will remain valid perpetually? They are not the final theories but for the moment there is no theoretical or observational need for their shift? They are not the final theories and we have already entered the phase of their challenge of validity and dispute? Has the paradigm shift already happened?

General Relativity and Λ CDM cosmology are remarkably powerful and successful in describing Nature. From the experimental point of view they have been completely verified in every experiment made. From the observational point of view they are to a large extent (if not completely) in agreement with observations. From the theoretical point of view, they are on an acceptable level, though presenting various disadvantages. Nevertheless, intense theoretical investigation over the last 50 years, as well as the radical improvement and advance in astronomical, astrophysical and cosmological observations over the last 25 years, has raised various questions.

Some of the theoretical questions are the following: (i) General Relativity is non-renormalizable and hence it cannot get quantized with standard approaches. Definitely, there is not any fundamental principle that gravity should be quantum, however it is almost a consensus in theoretical physics community that the fact that the other three fundamental interactions are, offers a strong indication that gravity should have a quantum nature too.⁴ (ii) The cosmological constant problem, namely what is the cosmological constant, what is its microscopic nature, and more importantly why is its observed value is many orders of magnitude smaller than the result of any field theoretical calculation. (iii) What is the microscopic nature of dark matter. (iv) What is the exact mechanism/scenario that leads to the successful inflationary realization.

Some of the observational issues (unless these are wrong due to unknown systematics) may include: (i) The H_0 tension: The direct measurements of the present value of the Hubble parameter give a value that is larger ($\sim 5\sigma$) than the one estimated by the Planck Probe through the CMB spectrum in the context of Λ CDM cosmology. (ii) The σ_8 tension: possible deviation was noticed between measurements of CMB and LSS surveys. (iii) The cuspy halo problem, the dwarf galaxy problem, and other clustering-related problems that seem to puzzle standard collisionless dark matter.

Even if the above observational issues, as well as others of less significance, will be proven to be wrong and Λ CDM cosmology with General Relativity will remain in perfect agreement with observations, still the theoretical issues are quite strong and seem to suggest that some kind of modification is still needed. In principle, the community follows two main roads to alleviate them. The first is to remain in the framework of General Relativity and modify the content of the universe, namely to consider extra fields and sectors, such as the inflaton, quintessence etc, or other particles beyond the Standard Model of particles physics. The second direction is to

⁴ Note that the AdS/CFT correspondence [22] revealed the possibility that the quantum behavior could be of effective nature arising from classical foundations. Although in this specific framework this did not turn out to be the case (at the “gravity side” gravity still needs to be quantum) it offered us the idea that “quantum” may be more complex than current knowledge suggests.

extend/modify the gravitational theory itself, namely construct gravitational theories which possess General Relativity as a particular limit, but which in general provide the extra degree(s) of freedom that could incorporate the aforementioned issues. Definitely, one may follow combinations of both main directions.

As one may see, the first direction, even if it successfully solved all observational and cosmology-related theoretical issues it cannot offer a solution to the theoretical issues related to General Relativity itself, since it leaves the gravitational theory unchanged. On the other hand, the ultimate goal of the second direction is to provide a complete and coherent solution to all open issues, namely both to cosmological as well as to purely theoretical ones.

If the modifications remain in the first direction, strictly speaking it will not constitute a paradigm shift, but rather an improvement of the existing paradigm (in the same lines that the discovery of extra particles in the framework of Standard Model, e.g. the top quark or the tau neutrino, is considered as its modification/completion and not as a paradigm shift). On the other hand, in the case of a novel gravitational theory, and depending on the amount of deviation from General Relativity in terms of foundations, physical interpretation and mathematical structure, a paradigm shift might seem secured. The reader must have already noticed the interesting similarity with the explanation of the perihelion shift of Mercury, where the paradigm shift of the new gravitation theory of General Relativity was proved to be the case instead of the existence of an extra planet, unseen till then and thus “dark”, in the framework of Newtonian gravity.

In the previous chapters of this Review we presented in detail the state of the art of gravitational modifications and extensions, as well as their cosmological and astrophysical implications, a topic that was the main field of interest of CANTATA Collaboration. In particular, we tried to provide the classification and definition of theoretical and phenomenological aspects of gravitational interaction that cannot be enclosed in the concordance model but might be considered as signs of alternative theories of gravity, to present the confrontation of the theoretical predictions with observations at both the background and the perturbation levels, and to examine how extended and modified theories of gravity could emerge from quantum field theory. We hope that the reader has obtained a clear picture of the motivations, the mathematical structure, the resulting physical behavior, and their advantages and disadvantages.

As we saw, the theories of gravitational extension and modification that are efficient in incorporating observations on an advanced level, and that attract the interest of the cosmological community, do not seem to alter the foundations of General Relativity. Gravity is still classical, it is related to the geometry of spacetime (even if this geometry is different or richer than the Riemannian one), and its Lagrangian is constructed by various invariants and fields. On the other hand, gravitational theories of radical difference from General Relativity, with novel foundations, mathematical structure, and physical interpretation, like string theory [23], loop quantum gravity [24], and supergravity [25], which attract the interest of the theoretical-physics community, although efficient in solving the theoretical problems of General Relativity, for the moment seem to be far away from providing better explanations and pre-

dictions for the high-accuracy near-future observations and experiments comparing to Λ CDM cosmology and General Relativity. Elaborating these progresses, and, in addition, knowing the structure of the previous scientific revolutions, we may deduce that the construction of the gravitational theory that could replace General Relativity will be a complex procedure that would require the superposition of argumentation and ideas from geometry, quantum field theory, statistical physics, complexity theory, known unknowns, as well as unknown unknowns.

So what can we say about the previously raised question? What is the future of Λ CDM cosmology and General Relativity? Clearly, there has not been any paradigm shift, and they remain the widely accepted lore system for the description of Nature. Additionally, still we have not entered into the phase of their challenge of validity and dispute, since their predictions are in general the best amongst various alternative theories and scenarios. Nevertheless, pieces of observational evidences, as well as diligent theoretical investigation, seem to have opened the door towards such a phase. The fact that we still lack robust and successful alternative paradigms is definitely an inhibitory and suspending factor, however the relevant discussion attracts a considerable part of the cosmological community.

If we were to use historical appositions with the Aristotelian-Ptolemaic paradigm, Newton has not appeared. The detailed observations of Brahe and Kepler and the experiments of Galileo have not appeared either. Copernicus ideas and proposition might or might not have appeared, it is too early to conclude on that. However, the argumentation and early observations of the Arab and Islamic school have definitely appeared.

From these it is revealed that we are not in the end. We are not in the beginning of the end either. It is better to say that we are in the end of the beginning. The investigation of Nature as a whole, and not only of specific parts of it, in order to reveal the truth, namely the physical laws that govern objective reality, is a hard and arduous procedure. A procedure that is not a solitary or instant play but it demands the collective work of scientific community in many generations. Nature is out there, it is knowable, and the physical laws, the first principles and the highest causes, are waiting to be discovered. It is up to us to accept the challenge.

The investigation of the truth is in one way hard, in another easy. An indication of this is found in the fact that no one is able to attain the truth adequately, while, on the other hand, no one fails entirely, but everyone says something true about the nature of things. And while individually they contribute little or nothing to the truth, by the union of all a considerable amount is amassed. Therefore, since the truth seems to be like the proverbial door, which no one can fail to hit, in this respect it is easy, but the fact that we can have a whole truth and not the particular part we aim at, shows the difficulty of it. Perhaps, too, as difficulties are of two kinds, the cause of the present difficulty is not in the facts but in us [26].

There is a science which investigates being as being and the attributes which belong to this in virtue of its own nature. This is not the same as any of the so-called special sciences; for none of these treats universally of being as being. They cut off a part of being and investigate the attribute of this part. Now since we are seeking the first principles and the highest causes, clearly there must be some thing to which these belong in virtue of its own nature. If then those who sought the elements of existing things were seeking these same principles, it is

necessary that the elements must be elements of being not by accident but just because it is being. Therefore it is of being as being that we also must grasp the first causes [27]. Aristotle, in *Metaphysics*.

References

1. Aristotle, *On the Heavens*. Volume VI, Aristotle in twenty-three volumes, Loeb classical library, translated by W. K. C. Guthrie (Harvard University Press, Cambridge, 1939)
2. P. Almagest, *Translated and Annotated by Gerald J. Toomer* (Princeton University Press, New Jersey, 1984)
3. G. Saliba, *History of Arabic Astronomy: Planetary Theories During the Golden Age of Islam* (New York University Press, New York, 1994)
4. T.E. Huff, *The Rise of Early Modern Science: Islam, China and the West* (Cambridge University Press, Cambridge, 2003)
5. N. Copernicus, *De Revolutionibus Orbium Coelestium*. Latin and English Edition, Translated by Edward Rosen (Octavo Publishing, New York, 1999)
6. N.K. Singh, M. Zaki Kirmani, *Encyclopaedia of Islamic Science and Scientists* (Global Vision Publishing House, New Delhi, 2005)
7. T. Heath, *Aristarchus of Samos: The Ancient Copernicus* (Clarendon Press, Oxford, 1913)
8. E. Rosen, Aristarchus of samos and copernicus. *Bull. Amer. Soc. Papyrolog.* **15**(1/2), 85–93 (1978)
9. J. Kepler, *Astronomia Nova*. Translated by W.H. Donahue (Green Lion Press, Michigan, 2015)
10. I. Newton, *Philosophiae Naturalis Principia Mathematica*, 3rd edn. (1726), in eds. by A. Koyré, I.B. Cohen (Cambridge University Press, Cambridge, 1972)
11. I. Newton, *Letter from Sir Isaac Newton to Robert Hooke, February 5, 1675*. Historical Society of Pennsylvania. Accessed 7 June 2018
12. H.A. Lorentz, La Théorie Électromagnétique de Maxwell et Son Application Aux Corps Mouvants. *Archives néerlandaises des Sciences exactes et naturelles*, vol. 451 (1892)
13. A.A. Michelson, E.W. Morley, On the relative motion of the Earth and the luminiferous ether. *Amer. J. Sci.* **34**, 333–345 (1887)
14. F. Tisserand, Les travaux de Le Verrier. *Annales de l’Observatoire de Paris* **15**, 23–43 (1880)
15. J.-P. Hsu, D. Fine, *100 Years of Gravity and Accelerated Frames*. Advanced Series on Theoretical Physical Science (2005)
16. A. Einstein, Kosmologische Betrachtungen zur allgemeinen Relativitätstheorie, pp. 142–152. *Sitzungsberichte der Königlich Preußischen Akademie der Wissenschaften*, Berlin (1917)
17. E. Hubble, A relation between distance and radial velocity among extra-galactic nebulae. *Proc. Nat. Acad. Sci.* **15**, 168–173 (1929)
18. D. Kazanas, Dynamics of the universe and spontaneous symmetry breaking. *Astrophys. J.* **241**, L59–L63 (1980)
19. A.H. Guth, The inflationary universe: a possible solution to the horizon and flatness problems. *Adv. Ser. Astrophys. Cosmol.* **3**, 139–148 (1987)
20. A.D. Linde, A new inflationary universe scenario: a possible solution of the horizon, flatness, homogeneity, isotropy and primordial monopole problems. *Phys. Lett. B* **108**, 389–393 (1982)
21. A. Ijjas, P.J. Steinhardt, A. Loeb, Inflationary schism. *Phys. Lett. B* **736**, 142–146 (2014). [arXiv:1402.6980](https://arxiv.org/abs/1402.6980)
22. J.M. Maldacena, The Large N limit of superconformal field theories and supergravity. *Int. J. Theor. Phys.* **38**, 1113–1133 (1999). [arXiv:hep-th/9711200](https://arxiv.org/abs/hep-th/9711200). [*Adv. Theor. Math. Phys.* **2**, 231 (1998)]
23. O. Aharony, S.S. Gubser, J.M. Maldacena, H. Ooguri, Y. Oz, Large N field theories, string theory and gravity. *Phys. Rept.* **323**, 183–386 (2000). [arXiv:hep-th/9905111](https://arxiv.org/abs/hep-th/9905111)

24. C. Rovelli, Loop quantum gravity. *Living Rev. Rel.* **1**, 1 (1998). [arXiv:gr-qc/9710008](https://arxiv.org/abs/gr-qc/9710008)
25. H.P. Nilles, Supersymmetry, supergravity and particle physics. *Phys. Rept.* **110**, 1–162 (1984)
26. Aristotle, *Metaphysics*. Volume I, Book B. Translated by W.D. Ross (Oxford University Press, Oxford, 1924)
27. Aristotle, *Metaphysics*. Volume I, Book Γ. Translated by W.D. Ross (Oxford University Press, Oxford, 1924)

Correction to: Modified Gravity and Cosmology



Emmanuel N. Saridakis, Ruth Lazkoz, Vincenzo Salzano,
Paulo Vargas Moniz, Salvatore Capozziello, Jose Beltrán Jiménez,
Mariafelicia De Laurentis, and Gonzalo J. Olmo

Correction to:

E. N. Saridakis et al. (eds.) *Modified Gravity and Cosmology*,
<https://doi.org/10.1007/978-3-030-83715-0>

The original version of this book was revised. The affiliations of the authors Álvaro de la Cruz-Dombriz in chapter 5, Francisco S. N. Lobo in chapter 13 and Sebastian Bahamonde, Konstantinos F. Dialektopoulos, Manuel Hohmann, Jackson Levi Said in chapter 14 have been updated. The incorrect equation (9.13) in chapter 9 has also been updated. Errors in reference linking have been corrected in all the chapters. The print edition of this book has also been updated with these changes.

The updated version of the book can be found at

<https://doi.org/10.1007/978-3-030-83715-0>

https://doi.org/10.1007/978-3-030-83715-0_5

https://doi.org/10.1007/978-3-030-83715-0_9

https://doi.org/10.1007/978-3-030-83715-0_13

https://doi.org/10.1007/978-3-030-83715-0_14

Index

A

Affine connection, 28, 29, 129, 130, 144, 177
 α -basis, 466
Aristotelian-Ptolemaic cosmology, 617
Atom interferometry, 285
Autoparallel curves, 28, 29
Averaged conservation laws, 256

B

Beyond Horndeski theories, 74, 319, 471, 520, 576, 577
Bianchi identities, 19
Bigravity, 90, 91, 367
Black hole, 20, 112, 151, 226, 306, 329, 377, 388, 393, 398, 408, 416
Black hole hair, 398
Bounce cosmology, 114, 165, 226
Braneworld cosmology, 98
Brans-Dicke theory, 47, 79, 180, 397, 466, 575

C

Casimir effect, 287
Chameleon mechanism/models, 54, 284, 294, 363, 575, 585
Classicalizing gravity, 405
Compact objects, 294, 329, 413, 576
Corpuscular gravity, 407
Cosmic Microwave Background (CMB), 168, 213, 430, 468, 483, 493, 494, 507, 511, 517, 527, 563
Cosmic shear, 472, 558
Cosmological data analysis, 429
Cosmological paradigm, 617
Cosmological surveys, 426, 442

Cross-correlations of cosmological probes, 562

D

Dark matter halo, 432, 590, 610
Deflection of light, 385, 389
Dipole moment tests, 288
Dwarf stars, 320
Dynamical system approach, 71, 218

E

Early dark energy, 485
Eddington-inspired Born-Infeld gravity, 165, 306
Effective field theory of dark energy, 465, 544
Effective Newton's constant, 188, 210, 510, 524
Effective theories, 99
Einstein-Boltzmann codes for dark energy and modified gravity, 467
Einstein frame, 163, 178, 284, 304, 335, 366, 397
Einstein-Hilbert action, 18, 30
Energy-momentum tensor, 18, 137, 151
Eöt-Wash, 287
Equivalence principle, 46, 79, 203, 229, 364, 377, 385, 471, 592
test of, 457
Extra dimensions, 97

F

Fifth force, 48, 288, 474, 563, 575, 585, 590
Finsler gravity, 243

Finsler Ricci scalar, 251
 Finsler spacetimes, 245
 Forecast constraints, 443, 561
 $f(\mathbb{Q})$ gravity, 158
 $f(R)$ gravity, 50, 165, 179, 303, 468, 511, 514, 575, 585
 Friedmann–Lemaître–Robertson–Walker (FLRW) metrics, 20
 $f(\mathbb{T})$ gravity, 37, 199, 367

G

Galaxy clustering, 443, 467, 557, 571
 Gauge theory of gravity, 130, 193
 Generalized Galileons, 80
 General relativity, 17, 27
 Geodesic deviation
 in Finsler gravity, 251
 in $f(R)$ gravity, 68
 in $f(\mathbb{T})$ gravity, 226
 in symmetric teleparallel equivalent of general relativity, 148
 Geodesics, 28, 147
 Geometrical optics approximation, 400
 Geometrical trinity, 145
 Gleyzes–Langlois–Piazza–Vernizzi (GLPV) theories, 466
 Gravitational collapse, 410, 600
 Gravitational wave anomalous speed, 543
 Gravitational wave oscillations, 547
 Gravitational waves, 85, 115, 164, 205, 230, 375, 467, 539
 Gravity’s rainbow, 261
 Growth factor, 509
 in teleparallel gravity, 211

H

Helicity, 91
 Higher order statistics, 557
 Hořava–Lifshitz, 269, 362, 396
 Horndeski theory, 80, 367, 466, 561
 H_0 tension, 213, 483, 515, 621
 Hubble constant, 213, 441, 483
 Hybrid metric–Palatini gravity, 177
 Hyperfluids, 140

I

Image separation, 393
 Inflation, 166, 217
 Integrated Sachs–Wolfe effect (ISW), 430, 469, 486, 527
 Interacting dark energy, 485

J

Jordan frame, 46, 178, 284, 293, 335, 586

K

Kinetic gas, 245

L

Laboratory constraints, 283, 296
 Lane–Emden equation, 320
 Large-scale structure, 59, 169, 491, 561, 584, 607
 Late-time solutions, 167
 Lens equation, 390
 Lensing, strong, 388, 398, 484
 Lensing, weak, 392, 435, 467, 558, 563, 572
 LIGO/Virgo, 297, 329, 375, 474, 541
 Limiting mass, 321
 LISA, 115, 379, 548
 Local Lorentz invariance/violation, 89, 150, 196, 307, 360, 377, 466, 543
 Lovelock’s theorem, 23

M

Machine learning, 566
 Magnification ratio, 393
 Massive gravity, 90
 Mass profiles, 573
 Mass-radius relations, 318
 Matter couplings, 30, 154
 Metric-affine gravity, 31, 137, 143, 177
 Model-independent constraints, 213, 382, 453, 466, 490, 512
 Modified luminosity distance, 545
 Multipoles, 433, 453

N

Neutron stars, 295, 307, 318, 330, 377, 473, 541, 550, 561, 590
 Noether symmetry approach, 222
 No hair theorem, 341
 Non-local gravity, 109
 in torsional theories, 203
 Non-metricity, 32, 132, 144, 300
 Non-Riemannian geometry, 130, 299
 Number counts, 451

O

Observational tensions, 442, 483, 507
 Observer space, 252

1-particle distribution function, 252
 1+3 formalism, 61

P
 Palatini formalism, 31, 50, 163, 177, 303
 Paradigm shift, 618
 Parametrized post-Newtonian formalism, 357
 Parity-violating terms, 201, 339, 363
 Peak counts, 564
 Phenomenological constraints, 416, 425, 468, 489, 550

Q
 Quantum effects, 296, 412, 414
 Quantum gravity, 153, 276, 381
 Quantum metric gravity, 276
 Quantum Palatini gravity, 277
 Quasi-normal mode, 330

R
 Relativistic effects, 451
 Riemann tensor, 17, 33

S
 Scalarization, 335
 Scalar perturbations, 59, 85, 180, 211, 359, 512, 598
 Scalar-tensor theories, 45, 81, 335, 366, 561
 Schwarzschild metric, 19
 Screening mechanisms, 293, 363, 576, 583
 Semiclassical gravity, 405
 Shift-symmetric theories, 83
 σ_8 Tension, 507
 σ_8 tension, 214, 432, 439, 472, 562, 605, 621
 Singularities
 black hole, 112
 cosmological, 164
 Small-scale effects, 299

Solar system constraints, 20, 49, 184, 207, 230, 293, 357, 390, 515, 588
 Standard sirens, 379, 469, 494, 541
 Stellar structure, 317
 Sturm-Liouville problem, 262
 Symmetron models, 586

T
 Tangent bundle, 245
 Teleparallel cosmology, 207
 Teleparallel covariance, 196
 Teleparallel dark energy, 207
 Teleparallel Equivalent of General Relativity (TEGR), 197
 Teleparallel gravity, 191, 367
 Teleparallel gravity with higher-order derivatives, 202
 Teleparallel Horndeski gravity, 204
 Tensor perturbations, 85, 165, 381
 Tests of general relativity, 377, 429
 Three hair relation, 332
 Tolman-Oppenheimer-Volkoff (TOV) equations, 318
 Torsion, 33, 133, 144, 192, 307
 Torsion gravity, 34, 133, 192

U
 Universal relation, 329

V
 Voids, 605

W
 Wheeler-DeWitt equation, 166, 261, 275

Z
 Zero point energy, 261